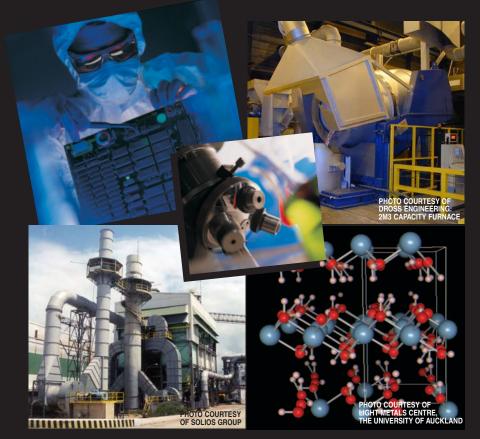


# **133rd Annual Meeting & Exhibition**

The Minerals, Metals & Materials Society welcomes you to the TECHNICAL PROGRAM for the 133<sup>rd</sup> TMS Annual Meeting & Exhibition, to be held March 14–18, 2004, in Charlotte, North Carolina.



## For your convenience, we have also included details on

- Meeting Activities and Registration
- Conference Proceedings
- Our Exhibition
- TMS Membership
- Additional On-line Resources that You May Utilize

All designed to help you prepare for and optimally benefit from one of the world's premier metals and materials events.

# This document comprises THE COMPLETE TECHNICAL PROGRAM

Including fully text-searchable paper titles, abstracts, and author names with affiliations

# **See you in Charlotte!**





http://www.tms.org/ AnnualMeeting.html

# The Improved Web Resource for Every TMS Publication...

# The New On-Line TMS Document Center

Customized to meet your unique needs and now upgraded to provide faster service and easier navigation, the On-Line TMS Document Center provides detailed information and on-line purchasing opportunities for TMS proceedings volumes, textbooks, journals, software programs, video series, and reports. If you need information, you've got to try the new TMS Document Center.

Check out these great new features:



## Find, Select, and Check Out the Products You Want FAST

The new TMS Document Center provides easier navigation and faster service for an overall improved shopping experience.



## Sample Articles Before You Buy

Not sure if a particular article is the one you need? Click on the PDF icon to view the first page of the article and know that you will be satisfied with your purchase.

## TMS Members: View JOM On-Line Free of Charge

TMS members can view the journal for free through the new TMS Document Center. Simply log in and articles from past and current issues are instantly at your fingertips to browse, read, and print out, free of charge!

## Purchase Download Suites

Purchase downloads in sets of 10, 25, 50, or 100, and use them to download any files in the TMS Document Center (for less than it would cost to download that many papers individually!). Download suites can be used all at once, over a series of visits to the site, or to create your own custom publication.



## **Create Your Own Custom Publication**

Gather individual papers and articles from TMS proceedings volumes, *JOM*, *Journal of Electronic Materials*, and *Metallurgical and Materials Transactions A* and *B* to create a one-of-a-kind publication that meets your needs. TMS will compile them in either a softcover book or on a CD-ROM—it's your choice.

## Coming in 2004: TMS Letters

*TMS Letters* is a peer-reviewed, on-line-only journal featuring technical updates of hitherto unpublished research presented at TMS meetings. Available free-of-charge to TMS members (and by subscription to nonmembers), the journal comprises two-page technical updates, including text and graphics. Visit the TMS Document Center for additional information about *TMS Letters*!

See it for yourself! Visit the new TMS Document Center today.

# http://doc.tms.org

## AN INTERNATIONAL EVENT IN SCIENCE AND ENGINEERING

During the week of March 14–18, the 2004 TMS Annual Meeting & Exhibition will host approximately 4,000 science and engineering professionals, representing more than 70 different countries. They are convening at the Charlotte Convention Center to attend a field-spanning array of metals and materials symposia containing more than 200 sessions and 1,900 individual technical presentations.

#### This year's meeting will feature programming by

- TMS Electronic, Magnetic & Photonic Materials Division
- TMS Extraction & Processing Division
- TMS Light Metals Division
- TMS Materials Processing & Manufacturing Division
- TMS Structural Materials Division
- TMS Education Committee
- TMS Young Leaders Committee
- ASM International's Materials Science Critical Technologies Sector
- International Titanium Association
- International Magnesium Association
- National Science Foundation
- TMS Public & Governmental Affairs Committee

# In addition to the technical programming featured on the following pages, attendees will have the opportunity to

- Tour the Exhibition of more than 160 Companies Displaying New Products and Services
- Attend Special Lectures and Tutorials
- Participate in Short Courses on Metal Matrix Composites, Introduction to Nanomanufacturing and Nanotechnology, Technology Transfer Seminar, Smelter Grade Alumina from the Smelting Perspective and Computational Modelling for the Materials Professional
- Enjoy Special Luncheons, Dinners, and Social Functions, including events honoring Didier de Fontaine, R.J. Arsenault, A.L. Roytburd and Roger D. Doherty
- Network Extensively
- **Experience** the Charm and Amenities of Charlotte

#### Extensive details about these and all conference-related activities can be found on the 2004 TMS Annual Meeting Web Site.

## WANT TO BE PART OF THE ACTION?

#### Registration is easy.

Just complete and mail or fax the Annual Meeting Registration Form that appears in this document. Or, visit the meeting web site to register immediately (and securely) on-line.

To register in advance, your submission must reach TMS not later than **February 16, 2004.** After this date, it will be necessary to register at the meeting site.

The **Westin Charlotte Hotel** is the TMS headquarters hotel. Special conference rates have been contracted with this hotel and others in the area surrounding the **Charlotte Convention Center.** To receive special rates, use the TMS 2004 Housing Reservation Form that appears in this document and that can be found on the meeting web site.

**Special Opportunity for TMS Nonmember Registrants:** All nonmember registrants automatically receive a one-year introductory associate membership in TMS for 2004. Membership benefits include a subscription to *JOM* (print and on-line versions) and significant discounts on TMS products and services.

More on the benefits of membership appears on the <u>TMS Membership Web Pages</u>.

## INTERESTED IN BUSINESS OPPORTUNITIES?

The 2004 TMS Annual Meeting & Exhibition presents businesses, universities, institutions, agencies, consultants, and others with myriad opportunities to partner in effective marketing communication. Such opportunities to reach thousands of meeting attendees include:

- Placing a **Booth** in the Exhibition
- Placing an Ad in the Official Conference Publication and At-Meeting Program: JOM
- Sponsoring High-Profile Attendee Services, such as the CyberCenter, Coffee Breaks, Signage, and Prize Drawings.
- Hosting a Hospitality Suite

More information on these opportunities is available on the 2004 TMS Annual Meeting Sponsorship Web Pages.

CONFERENCE PROCEEDINGS: THE **RECORDS OF EVENTS** 

The technical program of each TMS Annual Meeting yields numerous conference proceedings that document many presentations delivered in session rooms. Such publications can be ordered both before and after the meeting via the meeting registration form and/or the TMS Document Center.

The following symposium proceedings will be available in tandem with the meeting:

#### ADVANCED MATERIALS FOR ENERGY CONVERSION II

Dhanesh Chandra, Renato G. Bautista, and Louis Schlapbach, editors ISBN 0-87339-574-3 • Approx. 560 pp., illus., index, softcover Order No. 04-5743 • Weight 3 lbs M \$112 + S \$89 + L \$160

#### ADVANCES IN SUPERPLASTICITY AND

SUPERPLASTIC FORMING

Eric M. Taleff, Paul E. Krajewski, and Peter A. Friedman, editors ISBN 0-87339-564-6 • Approx. 436 pp., illus., index, softcover Order No. 04-5646 • Weight 2 lbs M \$115 + S \$91 + L \$164

#### **BULK METALLIC GLASSES**

Peter K. Liaw and Raymond A. Buchanan, editors ISBN 0-87339-573-5 • Approx. 256 pp., illus., index, softcover Order No. 04-5735 • Weight 2 lbs M \$125 + S \$99 + L \$179

#### **EPD CONGRESS 2004**

Mark Schlesinger, editor

Includes the proceedings from the following symposia: Electrochemical Mea-surements and Processing of Materials, General Pyrometallurgy, Materials Processing Fundamentals, Solid and Aqueous Wastes, Sustainable Development session of Recent Advances in Non-Ferrous Metals Processing, and General Recycling session of Recycling.

ISBN 0-87339-565-4 • Approx. 1,020 pp., CD-ROM Order No. 04-5654-CD • Weight 1 lb M \$71 + S \$56 + L \$101

LATERITE NICKEL SYMPOSIUM 2004 D.M. Lane and W.P. Imrie, editors ISBN 0-87339-550-6 • Approx. 1,144 pp., illus., index, hardcover Order No. 04-5506 • Weight 4 lbs M \$119 + S \$94 + L \$170

#### **LIGHT METALS 2004**

A.T. Tabereaux, editor

Includes the proceedings from the following symposia Alumina & Bauxite, Aluminum Can Recycling, Aluminum Reduction Technology, Carbon Technol-ogy, Cast House Technology, Reactive Metals session of Recent Advances in Non-Ferrous Metals Processing, Aluminum and Aluminum Dross Processing

sessions of Recycling. ISBN 0-87339-567-0 • Approx. 1,150 pp., illus., hardcover & CD-ROM Order No. 04-5670-G • Weight 7 lbs M \$150 + S \$125 + Ľ \$225

#### **MAGNESIUM TECHNOLOGY 2004**

Alan A. Luo, editor

ISBN 0-87339-568-9 • Approx. 436 pp., illus., hardcover & CD-ROM Order No. 04-5689-G • Weight 3 lbs M \$101 + S \$80 + L \$144

#### SOLIDIFICATION OF ALUMINUM ALLOYS

Men G. Chu, Douglas A. Granger, and Qingyou Han, editors ISBN 0-87339-569-7 • Approx. 440 pp., illus., softcover Order No. 04-5697 • Weight 2 lbs M \$118 + S \$93 + L \$168

#### **MULTIPHASE PHENOMENA AND CFD MODELING AND** SIMULATION IN MATERIALS PROCESSES L. Nastac and B. Li. editors

Includes the proceedings from the following symposia: Multiphase Phenomena in Materials Processing and CFD Modeling and Simulation of Engineering Processes.

ISBN 0-87339-570-0 • Approx. 760 pp., illus., softcover Order No. 04-5700 • Weight 4 lbs M \$132 + \$ \$105 + L \$189

#### SOLIDIFICATION PROCESSES AND MICROSTRUCTURES: A SYMPOSIUM IN HONOR OF PROF. W. KURZ

M. Rappaz, C. Beckermann, and R. Trivedi, editors ISBN 0-87339-572-7 • Approx. 432 pp., softcover Order No. 04-5727 • Weight 2 lbs M \$112 + S \$88 + L \$159

#### THE FIFTH GLOBAL INNOVATIONS SYMPOSIUM ON **MATERIALS PROCESSING AND MANUFACTURING:** SURFACES AND INTERFACES IN NANOSTRUCTURED MATERIALS AND TRENDS IN LIGA, MINIATURIZATION, AND NANOSCALE MATERIALS

Sharmila M. Mukhopadhyay, John Smugeresky, Sudipta Seal, Narendra B. Dahotre, and Arvind Agarwal, editors

Includes the proceedings from the following symposia: Surfaces and Interfaces in Nanostructured Materials and the Fifth Global Innovations Symposium on Materials Processing and Manufacturing: Trends in LIGA, Miniaturization, and Nanoscale Materials

ISBN 0-87339-566-2 • Approx. 720 pp., illus., softcover Order No. 04-5662 • Weight 4 lbs M \$118 + S \$93 + L \$168

#### **ULTRAFINE GRAINED MATERIALS III**

Yuntian Theodore Zhu, Terence G. Langdon, and Ruslan Z. Valiev, editors ISBN 0-87339-571-9 • Approx. 824 pp., illus., index, softcover Order No. 04-5719 • Weight 4 lbs M \$124 + S \$98 + L \$177

#### M /Member + S / Student + L / List

The following proceedings are planned for publication in TMS journals after the meeting:

#### In the Journal of Electronic Materials

Challenges in Advanced Thin Films: Microstructures. Interfaces. and Reactions

Lead-Free Solders and Processing Issues Relevant to Microelectronic Packaging

Phase Stability, Phase Transformation, and Reactive Phase Formation in Electronic Materials III

#### In Metallurgical and Materials Transactions

**Beyond Nickel-Base Superalloys** 

Hume-Rothery Symposium: Structural and Diffusional Growth Phase Transformations and Deformation in Magnesium Alloys

#### In TMS Letters

Processing and Properties of Powder-Based Materials

Other symposia eligible for TMS Letters:

Cost-Affordable Titanium

Dislocations

Educational Issues in Transport Phenomena in Materials Processing **General Abstracts** 

General Poster Session

Internal Stresses and Thermo-Mechanical Behavior in Multi-Component Materials Systems

Roytburd Symposium on Polydomain Stryctures

Symposium in Honor of Prof. Roger D. Doherty

The Didier de Fontaine Symposium on the Thermodynamics of Alloys The Role of Grain Boundaries in Material Design

Detailed information about these publications, and many others, can be found in the TMS Document Center.

## ADDITIONAL RESOURCES

On-line answers to any of your 2003 TMS Annual Meeting & Exhibition questions can be found at

- 2003 TMS Annual Meeting & Exhibition Web Site: Get up-to-the-minute meeting details and complete registration materials at http://www.tms.org/AnnualMeeting.html
- TMS Personal Conference Scheduler: Review the most-up-to-date version of the technical program, examine the calendar of events, and create your own personalized itinerary by visiting <u>http://pcs.tms.org</u>

- TMS Document Center: Review the complete tables of contents for conference proceedings and order publications by visiting <u>http://doc.tms.org</u>
- TMS Membership: Learn more about the benefits of membership by touring <u>http://www.tms.org/Society/membership.html</u>
- TMS Business-to-Business Partnering: Learn how TMS can help your organization maximize its impact by viewing <u>http://www.tms.org/Meetings/Annual-04/Exhibit2004/Annual04-exhibit-home.html</u>

#### If you want to contact a person, more details are available at

TMS Meetings Department The Minerals, Metals & Materials Society 184 Thorn Hill Road, Warrendale, PA 15086 USA Telephone: 1-800-759-4867 (in the U.S. and Canada) or (724) 776-9000, ext. 243 Fax: (724) 776-3770

# TMSLETTERS

#### A valuable new resource for members

#### A distinguished publication venue for authors

Timely, relevant, and rigorously reviewed, *TMS Letters* is a unique technical journal that presents cutting-edge research in succinct, informative technical updates.

The peer-reviewed journal will be available exclusively in on-line format through the TMS Document Center (*doc.tms.org*) and will be accessible free-of-charge to all TMS members as a benefit of membership. *TMS Letters* will be composed entirely of two-page technical updates, including text and graphics, of research presented at TMS meetings that are not published in any other book or journal.

The first issue of *TMS Letters* will consist exclusively of technical updates presented at the 2004 TMS Annual Meeting, to be held March 14–18, 2004. Presenters at the 2004 TMS Annual Meeting, whose work will not be published in any other book or journal, may submit their work for publication in the inaugural issue of *TMS Letters*.

To learn more about *TMS Letters* or to submit a technical update, contact: Dan Thoma Editor, *TMS Letters* c/o TMS 184 Thorn Hill Road, Warrendale, PA 15086 E-mail: tmsletters@tms.org Web: www.tms.org/tmsletters.html

www.tms.org/tmsletters.html

Visit this web site often, as more details will be made available throughout the year, including author instructions for submitting papers to the journal and non-member subscription information.

March 14-18, 2004 • Charlotte, N				Figure 16, 2004         Payment must accompany form.         AMC           Forms received past this date will be processed at the on-site         Forms received past this date will be processed at the on-site         Forms received past this date will be processed at the on-site         Forms received past this date will be processed at the on-site         Forms received past this date will be processed at the on-site         Forms received past this date will be processed at the on-site         Forms received past this date will be processed at the on-site         Forms received past this date will be processed at the on-site         Forms received past this date will be processed at the on-site         Forms received past this date will be processed at the on-site         Forms received past this date will be processed at the on-site         Forms received past this date will be processed at the on-site         Forms received past this date will be processed at the on-site         Forms received past this date will be processed at the on-site         Forms received past this date will be processed at the on-site         Forms received past this date will be processed at the on-site         Forma received past this date will be processed at the on-site         Forma received past this date will be processed at the on-site         Forma received past this date will be processed at the on-site         Forma received past this date will be processed at the on-site         Forma received past this date will be processed at the on-site         Forma received past this date will be processed at the on-site         Forma received past this date will be processed at the on-site         Forma received past this date will be proces the past the past t	04-TECH
http://www.tms.org	<b>1.</b> P	Member of: rof.	: TMS	AIST SME SPE Member Number:	
Web registration requires credit card payment.	Mr. M	Irs. 🗌 Ms	Last Name	First Name Middle	e Initial
<b>USA:</b> 724-776-3770	Informal First Na	ame to Appear	on Badge:	Date of Birth:	
Fax registration requires				Title:	
credit card payment.					
<b>Return with</b> TMS, Meeting Services				te/Province:Zip/Postal Code:Country:	
payment to: 184 Thorn Hill Road Warrendale, PA 15086	lelephone:			Fax:E-Mail:	
				Guests do not receive admission to technical se	essions.
2. Registration Fees: unti	Advance Fees il February 16, 2004	On-Site after Februar	v 16. 2004	3. Social Function Tickets: Fee Quantity Total	FD
Member Non-member Author*				Bigg Didier de Fontaine Honorary Dinner       \$60       \$         Bigg Sc R.J. Arsenalt Honorary Dinner       \$60       \$         Roger Doherty Honorary Dinner       \$60       \$	JD
Non-member *	\$550 NM	\$650	NML	Roger Doherty Honorary Dinner\$60 \$	DD
Student Member ##	\$0 STU \$25 STUN	\$0 \$ \$25 \$	STUL	TMS-AIME Banguet\$60 \$	AD
TMS Senior Member	\$250 RM	\$250 I	RML	Tables of 8 \$480 \$	AD8
Exhibit Booth Personnel	\$0 E	\$0 H	EL	Provide Sign to Read	
			EOL	المجارة         <	_ EP EP8
Registration TOTAL \$ _				Table Sign to Read	0
* Includes TMS membership for 2004	aal'a atudant idantifiaatia	n oord		t	LM
## Students must attach a copy of their sch		n calu.		<b>§</b> Eight Medias Division Educateon	_ LM8
<b>4. Tutorial Luncheon Tickets:</b> Monday 3/15/04	Fee	Quantity	Total	률도 Table Sign to Read	RD
The Young Leader Tutorial Lecture is free. You may purchase the optional box lunch for	\$25		\$ EM		_
			·	Social Function TOTAL \$	
5. Publication Orders: All order Order Number Title	ers that are not indicated	for shipment o	n this form mu	Shipping Subtotal At-Meeting List Subt	total ice
04-5654-CD EPD Congress 2004 (CD-R	OM)				
04-5506 Laterite Nickel 2004	,				
04-5670-G Light Metals 2004 (Book and	d CD-ROM Set)				
04-5689-G Magnesium Technology 200					
04-5743 Advanced Materials for Ene					
04-5662 Fifth Global Symposium on in Nanostructured Materials	Materials Processing an and Trends in LIGA Mir	id Manutacturin	ig: Surfaces a nd Nanoscale	nd Interfaces Materials 4 \$118 \$168 \$	
04-5719 Ultrafine Grained Materials					
04-5727 Solidification Processes and					
04-5697 Solidification of Aluminum A					
04-5735 Bulk Metallic Glasses					
04-5646 Advances in Superplasticity 04-5700 Multiphase Phenomena and					
	ND ZONE CHART			Subtotal \$	
Weight USA Canada Mexico	Western J. A. NZ Europe	EE, C/S Am, Pac. Rim,	Middle East, Africa	If books are to be shipped, please complete the following.	
1 \$4.50 \$4.00 \$5.00 2 \$5.00 \$7.50 \$9.50	\$4.50 \$5.00 \$8.50 \$9.50	\$5.50 \$10.50	\$7.50 \$14.50		
3 \$5.50 \$11.00 \$14.00 4 \$6.00 \$14.50 \$18.50	\$12.50 \$14.00 \$16.50 \$18.50	\$15.50 \$20.50	\$21.50 \$28.50	Total Weight Calculate shipping fees from the chart (at left) \$	
5 \$6.50 \$18.00 \$23.00	\$20.50 \$23.00 \$24.50 \$27.50	\$25.50 \$30.50	\$35.50 \$42.50	One-time \$5 handling fee per order shipped \$	
6 \$7.00 \$21.50 \$27.50 7 \$7.50 \$25.00 \$32.00 8 \$8.00 \$28.50 \$36.50	\$28.50 \$32.00 \$32.50 \$36.50	\$35.50 \$40.50	\$49.50 \$56.50	NOTE: If your order exceeds 12 pounds, add the amount	
9 \$8.50 \$32.00 \$41.00	\$36.50 \$41.00 \$40.50 \$45.50	\$45.50	\$63.50	that it is over from the chart (at the left) to reach the total weight of your order. [Example: 16 lbs. (delivered in U.S.A.)	
10 \$9.00 \$35.50 \$45.50 11 \$9.50 \$39.00 \$50.00 12 \$10.00 \$42.50 \$54.50	\$40.50 \$44.50 \$50.00 \$48.50 \$54.50	\$50.50 \$55.50 \$60.50	\$70.50 \$77.50 \$84.50	would be 12 lbs. (\$10.00) + 4 lbs (\$6.00) = 16 lbs. (\$16.00)] Publications TOTAL \$	
6. Continuing Education Short (	Courses: Sunday, Mar Advance Fees	ch 14, 2004 On-Site	Fees	7. 2004 Membership Dues: For current TMS members only Full Member	FM
	til February 16, 2004 ember Non-member	after Februa Member No		□ Sunor Member	ST
1. Metal Matrix Composites		\$525	\$610	8. Payment enclosed:	
2. Introduction to	. UOC\$ C1+4	φ020	φυτυ	Check, Bank Draft, Money Order	
Nanomanufacturing and	¢475 ¢500	¢EOE	<b>0010</b>	Make checks payable to TMS. Payment shall be made in USA dollars drawn on a USA bank.	
Nanotechnology	\$475 \$560	\$525	\$610	Credit Card Expiration Date:	
3. Technology Transfer Seminar	\$475 \$560	\$525	\$610	Card No.:	
4. Smelter Grade Alumina from				□ Visa □ MasterCard □ Diners Club □ American Express	
the Smelting Perspective	\$475 \$560	\$525	\$610	Cardholder Name:	
the Materials Professionals	\$475 \$560	\$525	\$610	Signature:	
				9. TOTAL FEES PAID	

Short Course TOTAL \$ \_\_\_\_\_ \$ \_\_\_\_\_

Refund policy: Writer requests must be mailed to TMS, post-marked no later than February 16, 2004. A \$50 processing fee will be charged for all cancellations. No refunds will be processed after February 16, 2004.



#### **133rd Annual International Meeting & Exhibition** March 14-18, 2004 • Charlotte, North Carolina, USA

Making your reservation is easier than ever through Travel Planners' real-time Internet reservation system! Just log on to www.tms.org, and follow the link to Travel Planners. You will be able to view actual

## **HOUSING RESERVATION FORM**

Mail or fax this housing form to: Travel Planners, Inc., 381 Park Ave. South, New York, NY 10016 FAX: 212-779-6128 • PHONE: 800-221-3531 (in 212, 718, 516, 914, 631 or international call 212-532-1660) (CHOOSE ONLY ONE OPTION)

availability, learn about your hotel's features and services, and obtain local city and sightseeing information. Most importantly, you will receive instant confirmation of your reservation!

#### Reservations must be received at Travel Planners by: Monday, February 16, 2004

Indicate 1st, 2nd, & 3rd hotel choice:       Type of Accomodations: (check one)       Image: Single 1 person/1bed □ Double 2 people/1bed □ Twin 2 people/2 beds       at the headquarters hotel, More with ear the headquarters hotel, More with Head and as with Head Head wachead housing ear the head hear ward wary acc	Arrival Date	Departure Date	
Street	ast Name	First Name	MI
City	Company		
Daytime Phone	Street	Address	
Additional Room Occupants	City	State/CountyZip/Postal Code	Country
<ul> <li>E-nail</li></ul>	Daytime Phone	Fax	
Non-Smoking Room Requested	Additional Room Occupants		
Indicate 1st, 2nd, & 3rd hotel choice:          Type of Accomadations: (check one)         [_]	E-mail		(confirmation will be sent via e-mail if address is provided
Indicate 1st, 2nd, & 3rd hotel choice:          Type of Accomodations: (check one)         Single 1 person/tbed □ Double 2 people/tbed □ Twin 2 people/2 beds         The 9 people/2	Non-Smoking Room Requested	Special Needs	
<ul> <li>HEADQUARTERS</li> <li>Westin Charlotte Hotel \$179/single • \$194/double</li> <li>Hilton Charlotte Hotel \$154/single • \$174/double</li> <li>Milton Charlotte Hotel \$154/single • \$174/double</li> <li>Minito Charlotte Hotel \$129/single • \$174/double</li> <li>Mariot Elized under the second state of the second state of</li></ul>		☐ Single 1 person/1bed ☐ Double 2 people/1bed ☐ Twin 2 peo ☐ Triple 3 people/2 beds ☐ Quad 4 people/2 beds If all three (3) requested hotels are unavailable, please process t	a financial liability for any and al rooms in that block that are no reserved. You are strongly encour aged to reserve your room(s) at the hotels listed to limit our financial liabil ity. Please help TMS achieve overal success with the 133rd TMS Annua
W. First St. E. First St. CHARLOTTE CONVENTION CENTER anajor credit card or deposit of one night and tax payable to Travel Planners, Inc.	<ol> <li>Westin Charlotte Hotel \$179/single • \$194/double</li> <li>Hilton Charlotte Hotel \$154/single • \$174/double</li> <li>Omni Hotel \$129/single • \$129/double</li> <li>Adams Mark Hotel \$125/single • \$125/double</li> <li>Holiday Inn Center City \$115/single • \$115/double</li> <li>Marriott City Center Hotel</li> </ol>	W. Trade St. E. Tride St. W. Fourth St. W. Fourth St. W. First St. W. First St. E. First St. W. First St. E. First St.	<ul> <li>reservation at one of the listed hotels prior to the advance housing deadline Thank you.</li> <li>Confirmations: Confirmations will be e-mailed faxed or mailed to you from Travel Planners, Inc.</li> <li>Changes/Cancellations: All changes and cancellations in hotel reservations must be madwith Travel Planners, Inc.</li> <li>Changes/Cancellations: All changes and cancellations in hotel reservations must be madwith Travel Planners, Inc.</li> <li>Changes/Cancellations: All changes and cancellations in hotel reservations must be madwith Travel Planners, Inc.</li> <li>Changes/Cancellations: All changes and cancellations in hotel reservations must be madwith Travel Planners, Inc. up until 3 business day prior to arrival and are subject to the individue hotel's cancellation policies. Cancellations and changes within 3 days of arrival MUST be madwith your hotel directly. Many hotels are now imposing fees for early departure. This rate is set by each hotel and may vary accordingly Please reconfirm your departure date at the time</li> </ul>

Deposit Payment: Check American Express MasterCard VISA Discover Diners

Account Number \_

Card Holder Name \_\_\_

\_\_ Expiration Date \_

form per com required. Make additional copies if needed.

\_\_\_\_ Authorized Signature \_\_\_\_

Monday	March 15	Tuesday-	GRID March 16	Wednesda	v-March 17	Thursday-March 18	
AM	PM	AM	PM	AM	PM	AM	
					Materials Analysis: Understanding the Columbia Disaster		
Dislocations: Modeling and Simulation Fundamentals	Dislocations: Simulation and Observation of Fundamental Mechanisms	Dislocations: Dislocation Structures and Patterning	Dislocations: Novel Experimental Methods	Dislocations: Plasticity, Voids, and Fracture	Dislocations: Dislocations in Complex Materials		
	Advances in Superplasticity and Superplastic Forming: Dvlp. of Advanced Superplastic Forming Processes	Advances in Superplasticity and Superplastic Forming: Advances in Superplastic Al-Mg Materials	Advances in Superplasticity and Superplastic Forming: Advances in Superplastic Forming of Light Alloys	Advances in Superplasticity and Superplastic Forming: Advd. Superplastic Matls. & the Sci. of Superplasticity	Advances in Superplasticity and Superplastic Forming: Modeling of Superplas- tic Forming Processes and Materials	General Abstracts: Session IX	-
Computational Thermodynamics and Phase Transformations: Grain Growth and Particle Coarsening	Computational Thermodynamics and Phase Transformations: Interfaces and Grain Boundaries	Computational Thermodynamics and Phase Transformations: Phase Field Modeling I	Computational Thermodynamics and Phase Transformations: Phase Field Modeling II	Computational Thermodynamics and Phase Transformations: Phase Equilibria and Thermodynamic Assessments	Computational Thermodynamics and Phase Transformations: Thermodynamics and Phase Transformation		
General Pyrometallurgy: Session I	5th Global Innovations Symposium: Plenary: Trends: Past, Present, and Future	5th Global Innovations Symposium: Small Volume Deformation	5th Global Innovations Symposium: Properties & Characterization of Matls. for Microsys./ LIGA Applications	5th Global Innovations Symposium: Properties, Processes, and Modeling	5th Global Innovations Symposium: Manufacturing and Evaluation of Layered Nano-Scale Materials		
Advanced Materials for Energy Conversion II: Energy Issues & Metal Hydrides I	Advanced Materials for Energy Conversion II: Metal Hydrides II	Advanced Materials for Energy Conversion II: Complex Hydrides I	Advanced Materials for Energy Conversion II: Complex Hydrides II	Advanced Materials for Energy Conversion II: Metal Hydrides III	Advanced Materials for Energy Conversion II: Metal Hydrides IV- Dynamics of Metal Hydrides &Tritium Gettering	Advanced Materials for Energy Conversion II: Thermoelectrics, Superconductors, and Piezoelectrics Materials	Т
Magnesium Technology 2004: Automotive Applications/Welding	Magnesium Technology 2004: Wrought Magnesium Alloys I	Magnesium Technology 2004: Wrought Magnesium Alloys II/Corrosion and Coatings	Magnesium Technology 2004: Primary Processing and Environmental Issues	Magnesium Technology 2004: Casting Processes and Properties	Magnesium Technology 2004: Fundamental Research	Magnesium Technology 2004: Alloy Development	
General Abstracts: Session I	General Abstracts: Session II	General Abstracts: Session IV	General Abstracts: Session V	Advanced Materials for Energy Conversion II: Thermodynamics, Superconductors & Batteries	Advanced Materials for Energy Conversion II: Magnetic Materials & Hydrogen Permeation	Advd. Matls. for Energy Conversion II: Metal Hydrides V-Thermal Energy Storage & Containment Matls.	У
Recent Advances in Non-Ferrous Metals Processing: Reactive Metals	Recent Advances in Non-Ferrous Metals Processing: Sustainable Development	Phase Transformations and Deformation in Mg Alloys: Solidification and Precipitation	Phase Transformations and Deformation in Mg Alloys: Plastic Deformation and Texture	Phase Transformations and Deformation in Mg Alloys: Creep Deformation	Phase Transformations and Deformation in Mg Alloys: Deformation and Strengthening		_
CFD Modeling and Simulation of Engineering Processes: Advanced Casting and Solidification Processes I	CFD Modeling and Simulation of Engineering Processes: Remelt Processes	CFD Modeling and Simulation of Engineering Processes: MEMS/ Microfluidics	CFD Modeling and Simulation of Engineering Processes: Advanced Casting and Solidification Processes II	CFD Modeling and Simulation of Engineering Processes: Process Modeling I	CFD Modeling and Simulation of Engineering Processes: Process Modeling II		
Cost-Affordable Titanium Symposium Dedicated to Prof. Harvey Flower: Overview and Innovative Processes	Cost-Affordable Titanium Symposium Dedicated to Prof. Harvey Flower: Break Through Technologies	Cost-Affordable Titanium Symposium Dedicated to Prof. Harvey Flower: Titanium Economics	Cost-Affordable Titanium Symposium Dedicated to Prof. Harvey Flower: Creative Processing	Cost-Affordable Titanium Symposium Dedicated to Prof. Harvey Flower: Creative Fabrication	Cost-Affordable Titanium Symposium Dedicated to Prof. Harvey Flower: Low Cost Titanium	Cost-Affordable Titanium Symposium Dedicated to Prof. Harvey Flower: Property Enhancement	
Third International Symposium on Ultrafine Grained Aterials: Processing I: Fundamentals and Technology	Third International Symposium on Ultrafine Grained Materials: Processing II: Structural Evolution	Third International Symposium on Ultrafine Grained Materials: UFG Material Fundamentals	Third International Symposium on Ultrafine Grained Materials: Microstruc- ture and Properties	Third International Symposium on Ultrafine Grained Materials: Mechanical Properties	Third International Symposium on Ultrafine Grained Materials: Superplas- ticity, Creep & Thermal Stability		
Materials Issues in Fuel Cells: State-of-the-Art	Materials Issues in Fuel Cells: Materials Challenges	Solidification of Aluminum Alloys: Microstructural Evolution I	Solidification of Aluminum Alloys: Microstructural Evolution II	Solidification of Aluminum Alloys: Solidification Cracking/ Mechanical Properties	Solidification of Aluminum Alloys: Gas Porosity/Micro- Macro Segregation	Solidification of Aluminum Alloys: Special Effects	

GRID							
	Monday-		Tuesday-		Wednesda	-	Thursday-March 18
	AM	PM	AM	PM	AM	PM	AM
207D	Solidification Processes and Microstructures: A Symp. in Honor of Prof. W. Kurtz: Processes	Solidification Processes and Microstructures: A Symp. in Honor of Prof. W. Kurtz: Mushy Zone Dynamics	Solidification Processes and Microstructures: A Symp. in Honor of Prof. W. Kurtz: Microstructures	Solidification Processes and Microstructures: A Symp. in Honor of Prof. W. Kurtz: Rapid Solidification	Solidification Processes and Microstructures: A Symp. in Honor of Prof. W. Kurtz: Phase Field	General Abstracts: Session VIII	
208A	Hume Rothery Symp.: Struct. & Diffusional Growth Mechanisms of Irrational Interphase Boundaries: Session I	Hume Rothery Symp.: Struct. & Diffusional Growth Mechanisms of Irrational Interphase Boundaries: Session II	Hume Rothery Symp.: Struct. & Diffusional Growth Mechanisms of Irrational Interphase Boundaries: Session III	Hume Rothery Symp.: Struct. & Diffusional Growth Mechanisms of Irrational Interphase Boundaries: Session IV	Hume Rothery Symp.: Struct. & Diffusional Growth Mechanisms of Irrational Interphase Boundaries: Session V	Hume Rothery Symp.: Struct. & Diffusional Growth Mechanisms of Irrational Interphase Boundaries: Session VI	
208B		Processing, Microstructure and Properties of Powder- Based Materials: Session I	Processing, Microstructure and Properties of Powder- Based Materials: Session II	Processing, Microstructure and Properties of Powder- Based Materials: Session III	General Abstracts: Session VI	General Abstracts Session VII	
209A	Bulk Metallic Glasses: Processing I	Bulk Metallic Glasses: Processing II	Bulk Metallic Glasses: Fatigue and Fracture	Bulk Metallic Glasses: Theoretical Modeling and Shear Bands	Bulk Metallic Glasses: Bio, Corrosion, and Fracture Behavior	Bulk Metallic Glasses: Phase Transformation and Alloy Design	Bulk Metallic Glasses: Mechanical Behavior
209B	Internal Stresses & Thermo-Mech. Behavior in Multi-Component Matls. Sys.: Electronic Thin Films & Pkgg. Matls. I	Internal Stresses & Thermo-Mech. Behavior in Multi-Component Matls. Sys.: Electronic Thin Films & Pkgg. Matls. II	Internal Stresses & Thermo-Mech. Behavior in Multi-Component Matls. Sys.: Creep and Plasticity I	in Multi-Component		Educational Issues in Transport Phenomena in Materials Processing: Presentations and Panel Discussion	
210A	Automotive Alloys 2004: Session I	Automotive Alloys 2004: Session II	Automotive Alloys 2004: Session III	Automotive Alloys 2004: Session IV	High Risk Technologies in Metallurgy with Commercial Potential: Session I	High Risk Technologies in Metallurgy with Commercial Potential: Session II	
210B	Materials by Design: Atoms to Applications: Materials Chemistry and Alloy Design	Materials by Design: Atoms to Applications: Materials Character- ization and Microstruc- tural Modeling	Computational and	Materials by Design: Atoms to Applications: Designing Nanostructures	Materials by Design: Atoms to Applications: Design for Mechanical Functionality I	Materials by Design: Atoms to Applications: Design for Mechanical Functionality II	
211A	R.J. Arsenault Symposium on Materials Testing and Evaluation: Session I	R.J. Arsenault Symposium on Materials Testing and Evaluation: Session II	R.J. Arsenault Symposium on Materials Testing and Evaluation: Session III	R.J. Arsenault Symposium on Materials Testing and Evaluation: Session IV	Failure of Structural Materials: Fundamentals	Failure of Structural Materials: Fatigue	Failure of Structural Materials: General
211B	Beyond Ni-Base Superalloys: Superalloys and Niobium Silicides	Beyond Ni-Base Superalloys: Molybdenum Silicides I	Beyond Ni-Base Superalloys: Precious Metal Alloys	Beyond Ni-Base Superalloys: Molybdenum Silicides II	Beyond Ni-Base Superalloys: Niobium Silicides	Beyond Ni-Base Superalloys: Other Systems and Physical Properties of Silicides	
212A		General Abstracts: Session III	Electrochemical Measurements and Processing of Materials: Electrodepo- sition Processes	Electrochemical Measurements and Processing of Materials: Electro- chemical Refining	Electrochemical Measurements and Processing of Materials: Electro- chemical Metal Production	Electrochemical Measurements and Processing of Materials: Electro- chemical Sensors and Measurements	
212B	Materials Processing Fundamentals: Solidification and Casting	Materials Processing Fundamentals: Deformation Processing	Materials Processing Fundamentals: Liquid Metal Processing	Materials Processing Fundamentals: Smelting and Refining	Materials Processing Fundamentals: Aqueous Processing	Materials Processing Fundamentals: Powders, Composites, Coatings and Measurements	
213A	Carbon Technology: Cathode Material and Corrosion	Carbon Technology: Anode Raw Materials	Carbon Technology: Green Anodes and Soderberg Paste	Carbon Technology: Anode Baking	Carbon Technology: Anode Quality and Performance	Aluminum Reduction Technology: Materials and Fundamentals	
213B/C	Cast Shop Technology: Melting and Refractories	Cast Shop Technology: Modeling of Casting Processes	Cast Shop Technology: Casting	Cast Shop Technology: Metal Treatment	Cast Shop Technology: Alloying and Furnace Processing	Cast Shop Technology: Grain Refining	Cast Shop Technology: Foundry
Ц				450			

GRID								
Monday-I AM	March 15 PM	Tuesday-I AM	March 16 PM	Wednesday AM	r-March 17 PM	Thursday-March 18 AM		
Aluminum Reduction - Potroom Improvements	Aluminum Reduction Technology: Cell Development and Operations	Aluminum Reduction Technology: Pot Control	Aluminum Reduction Technology: Modeling - Industry Trends	Aluminum Reduction Technology: Emerging Technologies	Aluminum Reduction Technology: Environmental	Aluminum Reduction Technology: Modeling	213D	
Phase Stability, Phase Transformation, and Reactive Phase Formation in Electronic Materials III Session I	Phase Stability, Phase Transformation, and Reactive Phase Formation in Electronic Materials III Session II	Phase Stability, Phase Transformation, and Reactive Phase Formation in Electronic Materials III Session III	Phase Stability, Phase Transformation, and Reactive Phase Formation in Electronic Materials III Session IV	Phase Stability, Phase Transformation, and Reactive Phase Formation in Electronic Materials III Session V	Solid and Aqueous Wastes from Non- Ferrous Metals Industry: Session I	Solid and Aqueous Wastes from Non- Ferrous Metals Industry: Session II	214	
Nanostructured Magnetic Matls.: Recent Progress in Magnetic Nanostructures	Nanostructured Mag- netic Matls.: Synthesis & Characterization of Nanostructured Magnetic Matls.	Nanostructured Mag- netic Matls.: Magnetic Tunnel Junctions and Semiconductor Spintronics	Nanostructured Magnetic Matls.: Self Assembly and Patterned Nanostructures	Metals for the Future: Structural Materials	Metals for the Future: Functional Materials	Metals for the Future: Processing and Bio- Materials	215	
Symp. on Microstruc- tural Stability in Honor of Prof. Roger D. Doherty: Microstruc- tural Stability: Recrystallization	Symp. on Microstruc- tural Stability in Honor of Prof. Roger D. Doherty: Microstruc- tural Stability: Texture Development	Symp. on Microstruc- tural Stability in Honor of Prof. Roger D. Doherty: Microstruc- tural Stability: Plastic Deformation	Symp. on Microstruc- tural Stability in Honor of Prof. Roger D. Doherty: Microstructl. Stability: Precipitation & Other Topics	Roytburd Symposium on Polydomain Structures: Elastic Domains in Structural Materials	Roytburd Symposium on Polydomain Structures: Domains in Ferroelectrics and Magnetics		216A	
The Didier de Fontaine Symp. on the Thermo- dynamics of Alloys: Fundamentals of Alloy Theory	The Didier de Fontaine Symp. on the Thermo- dynamics of Alloys: Experimental Techniques	The Didier de Fontaine Symp. on the Thermo- dynamics of Alloys: First Principle Calcul- ations & Cluster Expansion Techniques	The Didier de Fontaine Symp. on the Thermo- dynamics of Alloys: Interatomic Potentials and Cluster Expansion Techniques	The Didier de Fontaine Symp. on the Thermo- dynamics of Alloys: Jt. Session w/Computatl. Thermodynamics & Phase Transformations I	The Didier de Fontaine Symp. on the Thermo- dynamics of Alloys: Jt. Session w/Computatl. Thermodynamics & Phase Transformations II		216B	
		Surfaces & Interfaces in Nanostructured Matls.: General Phenomena & Processes	Surfaces & Interfaces in Nanostructured Matls.: Grain & Phase Boundaries	Surfaces & Interfaces in Nanostructured Matls.: Synthesis & Processing	Surfaces & Interfaces in Nanostructured Matls.: Coatings and Surface Modification	Surfaces & Interfaces in Nanostructured Matls.: Self-Organized & Biological Materials		
International Laterite Nickel Symposium - 2004: Economics and Project Assessment	International Laterite Nickel Symposium - 2004: Mineralogy and Geometallurgy/Panel Discussion	International Laterite Nickel Symposium - 2004: Pressure Acid Leaching	International Laterite Nickel Symposium - 2004: Process Development for Prospective Projects	International Laterite Nickel Symposium - 2004: Process and Operational Lessons Learned - Part I	International Laterite Nickel Symposium - 2004: Process and Operational Lessons Learned - Part II	International Laterite Nickel Symposium - 2004: Atmospheric Leaching/Slurry Rheology, Solution Extraction and Other	217B/C	
Recycling: General Recycling	Recycling: Aluminum and Aluminum Dross Processing	Aluminum Can Recycling: Session I	International Laterite Nickel Symposium - 2004: Roasting and Smelting	Materials Education to Revitalize the Workforce: Session I	Materials Education to Revitalize the Workforce: Session II		217D	
Alumina and Bauxite: Bayer Plant Operations: Red Side	Alumina and Bauxite: Process Modeling and Control	Alumina and Bauxite: Bayer Plant Operations: White Side	Alumina and Bauxite: Technology and Future Trends	The Role of Grain Boundaries in Material Design: Grain Boundary Character	The Role of Grain Boundaries in Material Design: Grain Boundary Segregation, Diffusion, Damage	The Role of Grain Boundaries in Material Design: Simulation of Grain Boundary Effects of Properties	218A	
Challenges in Advd. Thin Films: Microstruc- tures, Interfaces & Reactions: Advances in Photonic & Opto- elect. Matls. & Proc.	Challenges in Advd. Thin Films: Microstruct., Interfaces & Reactions: Microstruct., Prop. & Reliability of Microelec. Devices	Challenges in Advd. Thin Films: Microstruc- tures, Interfaces and Reactions: Modifica- tion, Characterization, and Modeling	Challenges in Advd. Thin Films: Micro- struct., Interfaces & Reactions: Design, Proc. & Property Control	Multiphase Phenomena in Materials Processing: Session I	Multiphase Phenomena in Materials Processing: Session II	Multiphase Phenomena in Materials Processing Session III	218B	
Nanostructured Materials for Biomedical Applications: Session I	Nanostructured Materials for Biomedical Applications: Session II	Nanostructured Materials for Biomedical Applications: Session III	Nanostructured Materials for Biomedical Applications: Session IV	Nanostructured Materials for Biomedical Applications: Session V	Nanostructured Materials for Biomedical Applications: Session VI	Nanostructured Materials for Biomedical Applications: Session VII	219A	
Lead-Free Solders & Procg. Issues Rele- vant to Microelectronic Pkgg.: Fundamentals, Phases, Wetting & Solidification	Lead-Free Solders & Procg. Issues Relevant to Microelect. Pkgg.: Envionmental & Matls. Issues for Lead-Free	Lead-Free Solders & Procg. Issues Relevant to Microelect. Pkgg.: Mechanical Properties & Fatigue Behavior	Lead-Free Solders & Procg. Issues Relevant to Microelect. Pkgg.: Electromigration and Creep in Leadfree Solders	Lead-Free Solders & Procg. Issues Relevant to Microelect. Pkgg.: Interfacial Interactions, Intermetallics & Substrates	Lead-Free Solders & Procg. Issues Relevant to Microelect. Pkgg.: Microstructural Characterization & Evolution		219B	
		1			1	1		

# Table of Contents

(In Order By Technical Track)

SESSION TITLE	ROOM	DAY	PAGE
Hot-Topic Track: Building MSE Synergies			
High Risk Technologies in Metallurgy with Commercial Potential: Session I	210A	Wed-AM	369
High Risk Technologies in Metallurgy with Commercial Potential: Session II	210A	Wed-PM	414
Materials Analysis: Understanding the Columbia Disaster	Ballroom B	Wed-PM	418
Materials by Design: Atoms to Applications: Materials Chemistry and Alloy Design	210B	Mon-AM	192
Materials by Design: Atoms to Applications: Materials Characterization and Microstructural Modeling	210B	Mon-PM	234
Materials by Design: Atoms to Applications: Computational and Experimental Strategies	210B	Tues-AM	288
Materials by Design: Atoms to Applications: Designing Nanostructures	210B	Tues-PM	334
Materials by Design: Atoms to Applications: Design for Mechanical Functionality I	210B	Wed-AM	376
Materials by Design: Atoms to Applications: Design for Mechanical Functionality II	210B	Wed-PM	419
Materials Education to Revitalize the Workforce: Session I	217D	Wed-AM	377
Materials Education to Revitalize the Workforce: Session II	217D	Wed-PM	420
Materials Issues in Fuel Cells: State-of-the-Art	207B/C	Mon-AM	193
Materials Issues in Fuel Cell: Materials Challenges	207B/C	Mon-PM	235
Metals for the Future: Structural Materials	215	Wed-AM	379
Metals for the Future: Functional Materials	215	Wed-PM	422
Metals for the Future: Processing and Bio-Materials	215	Thurs-AM	445
Advanced Materials			
Advanced Materials for Energy Conversion II: Energy Issues & Metal Hydrides I	203A	Mon-AM	169
Advanced Materials for Energy Conversion II: Metal Hydrides II	203A	Mon-PM	210
Advanced Materials for Energy Conversion II: Complex Hydrides I	203A	Tues-AM	262
Advanced Materials for Energy Conversion II: Complex Hydrides II	203A	Tues-PM	309
Advanced Materials for Energy Conversion II: Metal Hydrides III	203A	Wed-AM	353
Advanced Materials for Energy Conversion II: Thermodynamics, Superconductors & Batteries	204	Wed-AM	354
Advanced Materials for Energy Conversion II: Metal Hydrides IV - Dynamics of Metal Hydrides, and Tritium Gettering	203A	Wed-PM	395
Advanced Materials for Energy Conversion II: Magnetic Materials & Hydrogen Permeation	204	Wed-PM	396
Advanced Materials for Energy Conversion II: Thermoelectrics, Superconductors, and Piezoelectric Materials	203A	Thurs-AM	435
Advanced Materials for Energy Conversion II: Metal Hydrides V, Thermal Energy Storage and Containment Materials	204	Thurs-AM	436
Beyond Nickel-Base Superalloys: Superalloys and Niobium Silicides	211B	Mon-AM	174
Beyond Nickel-Base Superalloys: Molybdenum Silicides I	211B	Mon-PM	215

SESSION TITLE	ROOM	DAY	PAGE
Advanced Materials continued			
Beyond Nickel-Base Superalloys: Precious Metal Alloys	211B	Tues-AM	269
Beyond Nickel-Base Superalloys: Molybdenum Silicides II	211B	Tues-PM	315
Beyond Nickel-Base Superalloys: Niobium Silicides	211B	Wed-AM	357
Beyond Nickel-Base Superalloys: Other Systems and Physical Properties of Silicides	211B	Wed-PM	400
Bulk Metallic Glasses: Processing I	209A	Mon-AM	175
Bulk Metallic Glasses: Processing II	209A	Mon-PM	216
Bulk Metallic Glasses: Fatigue and Fracture	209A	Tues-AM	270
Bulk Metallic Glasses: Theoretical Modeling and Shear Bands	209A	Tues-PM	316
Bulk Metallic Glasses: Bio, Corrosion, and Fracture Behavior	209A	Wed-AM	359
Bulk Metallic Glasses: Phase Transformation and Alloy Design	209A	Wed-PM	402
Bulk Metallic Glasses: Mechanical Behavior	209A	Thurs-AM	438
Processing, Microstructure and Properties of Powder-Based Materials: Session I	208B	Mon-PM	242
Processing, Microstructure and Properties of Powder-Based Materials: Session II	208B	Tues-AM	295
Processing, Microstructure and Properties of Powder-Based Materials: Session III	208B	Tues-PM	340
Roytburd Symposium on Polydomain Structures: Elastic Domains in Structural Materials	216A	Wed-AM	384
Roytburd Symposium on Polydomain Structures: Domains in Ferroelectrics and Magnetics	216A	Wed-PM	425
Electronic Materials			
Challenges in Advanced Thin Films: Microstructures, Interfaces, and Reactions: Advances in Photonic and Optoelectronic Materials and Processes	218B	Mon-AM	179
Challenges in Advanced Thin Films: Microstructures, Interfaces, and Reactions: Microstructures, Properties, and Reliability of Microelectronic Devices	218B	Mon-PM	220
Challenges in Advanced Thin Films: Microstructures, Interfaces, and Reactions: Modification, Characterization, and Modeling	218B	Tues-AM	274
Challenges in Advanced Thin Films: Microstructures, Interfaces, and Reactions: Design, Process, and Property Control of Functional and Structural Thin-Films	218B	Tues-PM	320
Lead-Free Solders and Processing Issues Relevant to Microelectronic Packaging: Fundamentals, Phases, Wetting and Solidification	219B	Mon-AM	189
Lead-Free Solders and Processing Issues Relevant to Microelectronic Packaging: Environmental and Materials Issues for Lead-Free	219B	Mon-PM	231
Lead-Free Solders and Processing Issues Relevant to Microelectronic Packaging: Mechanical Properties and Fatigue Behavior	219B	Tues-AM	285
Lead-Free Solders and Processing Issues Relevant to Microelectronic Packaging: Electromigration and Creep in Leadfree Solders	219B	Tues-PM	331
Lead-Free Solders and Processing Issues Relevant to Microelectronic Packaging: Interfacial Interactions, Intermetallics and Substrates	219B	Wed-AM	373
Lead-Free Solders and Processing Issues Relevant to Microelectronic Packaging: Microstructural Characterization and Evolution	219B	Wed-PM	416
Phase Stability, Phase Transformation, and Reactive Phase Formation in Electronic Materials III: Session I	214	Mon-AM	198
Phase Stability, Phase Transformation, and Reactive Phase Formation in Electronic Materials III: Session II	214	Mon-PM	240

SESSION TITLE	ROOM	DAY	PAGE
Electronic Materials continued			
Phase Stability, Phase Transformation, and Reactive Phase Formation in Electronic Materials III: Session III	214	Tues-AM	293
Phase Stability, Phase Transformation, and Reactive Phase Formation in Electronic Materials III: Session IV	214	Tues-PM	338
Phase Stability, Phase Transformation, and Reactive Phase Formation in Electronic Materials III: Session V	214	Wed-AM	382
Extraction and Processing			
Educational Issues in Transport Phenomena in Materials Processing: Presentations and Panel Discussion	209B	Wed-PM	408
General Pyrometallurgy: Session I	202B	Mon-AM	185
International Laterite Nickel Symposium - 2004: Economics and Project Assessment	217B/C	Mon-AM	188
International Laterite Nickel Symposium - 2004: Mineralogy and Geometallurgy	217B/C	Mon-PM	230
International Laterite Nickel Symposium - 2004: Panel Discussion	217B/C	Mon-PM	231
International Laterite Nickel Symposium - 2004: Pressure Acid Leaching	217B/C	Tues-AM	284
International Laterite Nickel Symposium - 2004: Process Development for Prospective Projects	217B/C	Tues-PM	328
International Laterite Nickel Symposium - 2004: Roasting and Smelting	217D	Tues-PM	330
International Laterite Nickel Symposium - 2004: Process and Operational Lessons Learned - Part I	217B/C	Wed-AM	372
International Laterite Nickel Symposium - 2004: Process and Operational Lessons Learned - Part II	217B/C	Wed-PM	415
International Laterite Nickel Symposium - 2004: Atmospheric Leaching	217B/C	Thurs-AM	443
International Laterite Nickel Symposium - 2004: Slurry Rheology, Solution Extraction and Other	217B/C	Thurs-AM	443
Materials Processing Fundamentals: Solidification and Casting	212B	Mon-AM	194
Materials Processing Fundamentals: Deformation Processing	212B	Mon-PM	236
Materials Processing Fundamentals: Liquid Metal Processing	212B	Tues-AM	289
Materials Processing Fundamentals: Smelting and Refining	212B	Tues-PM	335
Materials Processing Fundamentals: Aqueous Processing	212B	Wed-AM	378
Materials Processing Fundamentals: Powders, Composites, Coatings and Measurements	. 212B	Wed-PM	420
Recent Advances in Non-Ferrous Metals Processing: Reactive Metals	205	Mon-AM	199
Recent Advances in Non-Ferrous Metals Processing: Sustainable Development	205	Mon-PM	244
Recycling: General Recycling	217D	Mon-AM	200
Recycling: Aluminum and Aluminum Dross Processing	217D	Mon-PM	244
Solid and Aqueous Wastes from Non-Ferrous Metal Industry: Session I	214	Wed-PM	426
Solid and Aqueous Wastes from Non-Ferrous Metal Industry: Session II	214	Thurs-AM	448
Light Metals			
Alumina and Bauxite: Bayer Plant Operations: Red Side	218A	Mon-AM	170
Alumina and Bauxite: Process Modeling and Control	218A	Mon-PM	212

SESSION TITLE	ROOM	DAY	PAGE
Light Metals continued			
Alumina and Bauxite: Bayer Plant Operations: White Side	218A	Tues-AM	265
Alumina and Bauxite: Technology and Future Trends	218A	Tues-PM	311
Aluminum Can Recycling: Session I	217D	Tues-AM	266
Aluminum Reduction - Potroom Improvements	213D	Mon-AM	171
Aluminum Reduction Technology: Cell Development and Operations	213D	Mon-PM	212
Aluminum Reduction Technology: Pot Control	213D	Tues-AM	267
Aluminum Reduction Technology: Modeling - Industry Trends	213D	Tues-PM	312
Aluminum Reduction Technology: Emerging Technologies	213D	Wed-AM	356
Aluminum Reduction Technology: Environmental	213D	Wed-PM	398
Aluminum Reduction Technology: Materials and Fundamentals	213A	Wed-PM	399
Aluminum Reduction Technology: Modeling	213D	Thurs-AM	437
Automotive Alloys 2004: Session I	210A	Mon-AM	172
Automotive Alloys 2004: Session II	210A	Mon-PM	213
Automotive Alloys 2004: Session III	210A	Tues-AM	268
Automotive Alloys 2004: Session IV	210A	Tues-PM	313
Carbon Technology: Cathode Material and Corrosion	213A	Mon-AM	176
Carbon Technology: Anode Raw Materials	213A	Mon-PM	217
Carbon Technology: Green Anodes and Soderberg Paste	213A	Tues-AM	272
Carbon Technology: Anode Baking	213A	Tues-PM	317
Carbon Technology: Anode Quality and Performance	213A	Wed-AM	360
Cast Shop Technology: Melting and Refractories	213B/C	Mon-AM	177
Cast Shop Technology: Modeling of Casting Processes	213B/C	Mon-PM	218
Cast Shop Technology: Casting	213B/C	Tues-AM	272
Cast Shop Technology: Metal Treatment	213B/C	Tues-PM	318
Cast Shop Technology: Alloying and Furnace Processing	213B/C	Wed-AM	361
Cast Shop Technology: Grain Refining	213B/C	Wed-PM	403
Cast Shop Technology: Foundry	213B/C	Thurs-AM	439
Cost-Affordable Titanium Symposium Dedicated to Prof. Harvey Flower: Overview and Innovative Processes.	206B	Mon-AM	182
Cost-Affordable Titanium Symposium Dedicated to Prof. Harvey Flower: Break Through Technologies	206B	Mon-PM	223
Cost-Affordable Titanium Symposium Dedicated to Prof. Harvey Flower: Titanium Economics	206B	Tues-AM	278
Cost-Affordable Titanium Symposium Dedicated to Prof. Harvey Flower: Creative Processing	206B	Tues-PM	323
Cost-Affordable Titanium Symposium Dedicated to Prof. Harvey Flower: Creative Fabrication	206B	Wed-AM	364

SESSION TITLE	ROOM	DAY	PAGE
Light Metals continued			
Cost-Affordable Titanium Symposium Dedicated to Prof. Harvey Flower: Low Cost Titanium	206B	Wed-PM	406
Cost-Affordable Titanium Symposium Dedicated to Prof. Harvey Flower: Property Enhancement	206B	Thurs-AM	440
Magnesium Technology 2004: Automotive Applications/Welding	203B	Mon-AM	191
Magnesium Technology 2004: Wrought Magnesium Alloys I	203B	Mon-PM	233
Magnesium Technology 2004: Wrought Magnesium Alloys II/Corrosion and Coatings	203B	Tues-AM	287
Magnesium Technology 2004: Primary Processing and Environmental Issues	203B	Tues-PM	332
Magnesium Technology 2004: Casting Processes and Properties	203B	Wed-AM	375
Magnesium Technology 2004: Fundamental Research	203B	Wed-PM	417
Magnesium Technology 2004: Alloy Development	203B	Thurs-AM	444
Phase Transformations and Deformation in Magnesium Alloys: Solidification and Precipitation	205	Tues-AM	294
Phase Transformations and Deformation in Magnesium Alloys: Plastic Deformation and Texture	205	Tues-PM	339
Phase Transformations and Deformation in Magnesium Alloys: Creep Deformation	205	Wed-AM	383
Phase Transformations and Deformation in Magnesium Alloys: Deformation and Strengthening	205	Wed-PM	425
Solidification of Aluminum Alloys: Microstructural Evolution I	207B/C	Tues-AM	298
Solidification of Aluminum Alloys: Microstructural Evolution II	207B/C	Tues-PM	343
Solidification of Aluminum Alloys: Solidification Cracking/Mechanical Properties	207B/C	Wed-AM	385
Solidification of Aluminum Alloys: Gas Porosity/Micro-Macro Segregation	207B/C	Wed-PM	427
Solidification of Aluminum Alloys: Special Effects	207B/C	Thurs-AM	449
Micro- and Nanoscale Technologies			
5th Global Innovations Symposium: Trends in LIGA, Miniaturization, and Nano-Scale Materials, Devices and Technologies: Plenary: Trends: Past, Present, and Future	202B	Mon-PM	209
5th Global Innovations Symposium: Trends in LIGA, Miniaturization, and Nano-Scale Materials, Devices and Technologies: Small Volume Deformation	202B	Tues-AM	261
5th Global Innovations Symposium: Trends in LIGA, Miniaturization, and Nano-Scale Materials, Devices and Technologies: Properties and Characterization of Materials for Microsystem/LIGA Applications	202B	Tues-PM	308
5th Global Innovations Symposium: Trends in LIGA, Miniaturization, and Nano-Scale Materials, Devices and Technologies: Properties, Processes, and Modeling	202B	Wed-AM	352
5th Global Innovations Symposium: Trends in LIGA, Miniaturization, and Nano-Scale Materials, Devices and Technologies: Manufacturing and Evaluation of Layered Nano-Scale Materials	202B	Wed-PM	394
Nanostructured Magnetic Materials: Recent Progress in Magnetic Nanostructures	215	Mon-AM	195
Nanostructured Magnetic Materials: Synthesis and Characterization of Nanostructured Magnetic Materials	t	Mon-PM	237
Nanostructured Magnetic Materials: Magnetic Tunnel Junctions and Semiconductor Spintronics		Tues-AM	290
Nanostructured Magnetic Materials: Self Assembly and Patterned Nanostructures	215	Tues-PM	336
Nanostructured Materials for Biomedical Applications: Session I	219A	Mon-AM	197

SESSION TITLE F	ROOM	DAY	PAGE
Micro- and Nanoscale Technologies continued			
Nanostructured Materials for Biomedical Applications: Session II	219A	Mon-PM	239
Nanostructured Materials for Biomedical Applications: Session III	219A	Tues-AM	291
Nanostructured Materials for Biomedical Applications: Session IV	219A	Tues-PM	337
Nanostructured Materials for Biomedical Applications: Session V	219A	Wed-AM	381
Nanostructured Materials for Biomedical Applications: Session VI	219A	Wed-PM	424
Nanostructured Materials for Biomedical Applications: Session VII	219A	Thurs-AM	447
Surfaces and Interfaces in Nanostructured Materials: General Phenomena & Processes	217A	Tues-AM	301
Surfaces and Interfaces in Nanostructured Materials: Grain & Phase Boundaries	217A	Tues-PM	346
Surfaces and Interfaces in Nanostructured Materials: Synthesis & Processing	217A	Wed-AM	388
Surfaces and Interfaces in Nanostructured Materials: Coatings and Surface Modification	. 217A	Wed-PM	428
Surfaces and Interfaces in Nanostructured Materials: Self-Organized and Biological Materials	2174	Thurs-AM	450
	2178	THUIS-AW	430
Third International Symposium on Ultrafine Grained Materials: Processing I: Fundamentals and Technology	207A	Mon-AM	206
Third International Symposium on Ultrafine Grained Materials: Processing II: Structural Evolution	207A	Mon-PM	251
Third International Symposium on Ultrafine Grained Materials: Posters	207A	Mon-PM/Tue/Wed	253
Third International Symposium on Ultrafine Grained Materials: UFG Material Fundamentals	207A	Tues-AM	305
Third International Symposium on Ultrafine Grained Materials: Microstructure and Properties	207A	Tues-PM	349
Third International Symposium on Ultrafine Grained Materials: Mechanical Properties	207A	Wed-AM	391
Third International Symposium on Ultrafine Grained Materials: Superplasticity, Creep & Thermal Stability	207A	Wed-PM	432
Physical Metallurgy			
Advances in Superplasticity and Superplastic Forming: Development of Advanced Superplastic Forming Processes	201B	Mon-PM	211
Advances in Superplasticity and Superplastic Forming: Advances in Superplastic Al-Mg Materials	201B	Tues-AM	264
Advances in Superplasticity and Superplastic Forming: Advances in Superplastic			
Forming of Light Alloys	2018	Tues-PM	310
Advances in Superplasticity and Superplastic Forming: Advanced Superplastic Materials and the Science of Superplasticity	201B	Wed-AM	355
Advances in Superplasticity and Superplastic Forming: Modeling of Superplastic Forming Processes and Materials	201B	Wed-PM	397
CFD Modeling and Simulation of Engineering Processes: Advanced Casting and Solidification Processes I	206A	Mon-AM	178
CFD Modeling and Simulation of Engineering Processes: Remelt Processes	206A	Mon-PM	219
CFD Modeling and Simulation of Engineering Processes: MEMS/Microfluidics	206A	Tues-AM	273
CFD Modeling and Simulation of Engineering Processes: Advanced Casting and Solidification Processes II	206A	Tues-PM	319
CFD Modeling and Simulation of Engineering Processes: Process Modeling I	206A	Wed-AM	362
CFD Modeling and Simulation of Engineering Processes: Process Modeling II	206A	Wed-PM	404

SESSION TITLE	ROOM	DAY	PAGE
Physical Metallurgy continued			
Computational Thermodynamics and Phase Transformations: Grain Growth and Particle Coarsening	202A	Mon-AM	180
Computational Thermodynamics and Phase Transformations: Interfaces and Grain Boundaries	202A	Mon-PM	222
Computational Thermodynamics and Phase Transformations: Phase Field Modeling I	202A	Tues-AM	276
Computational Thermodynamics and Phase Transformations: Phase Field Modeling II	202A	Tues-PM	322
Computational Thermodynamics and Phase Transformations: Phase Equilibria and Thermodynamic Assessments	202A	Wed-AM	363
Computational Thermodynamics and Phase Transformations: Joint Session with The Didier de Fontaine Symposium on the Thermodynamics of Alloys I	216B	Wed-AM	389
Computational Thermodynamics and Phase Transformations: Thermodynamics and Phase Transformations	202A	Wed-PM	405
Computational Thermodynamics and Phase Transformations: Joint Session with The Didier de Fontaine Symposium on the Thermodynamics of Alloys II	216B	Wed-PM	430
Dislocations: Modeling and Simulation Fundamentals	201A	Mon-AM	182
Dislocations: Simulation and Observation of Fundamental Mechanisms	201A	Mon-PM	224
Dislocations: Dislocation Structures and Patterning	201A	Tues-AM	278
Dislocations: Novel Experimental Methods	201A	Tues-PM	324
Dislocations: Plasticity, Voids, and Fracture	201A	Wed-AM	365
Dislocations: Dislocations in Complex Materials	201A	Wed-PM	407
Electrochemical Measurements and Processing of Materials: Electrodeposition Processes	212A	Tues-AM	280
Electrochemical Measurements and Processing of Materials: Electrochemical Refining	212A	Tues-PM	325
Electrochemical Measurements and Processing of Materials: Electrochemical Metal Production	212A	Wed-AM	366
Electrochemical Measurements and Processing of Materials: Electrochemical Sensors and Measurements	212A	Wed-PM	409
Failure of Structural Materials: Fundamentals	211A	Wed-AM	367
Failure of Structural Materials: Fatigue	211A	Wed-PM	410
Failure of Structural Materials: General	211A	Thurs-AM	441
Hume Rothery Symposium: Structure and Diffusional Growth Mechanisms of Irrational Interphase Boundaries: Session I	208A	Mon-AM	186
Hume Rothery Symposium: Structure and Diffusional Growth Mechanisms of Irrational Interphase Boundaries: Session II	208A	Mon-PM	228
Hume Rothery Symposium: Structure and Diffusional Growth Mechanisms of Irrational Interphase Boundaries: Session III	208A	Tues-AM	282
Hume Rothery Symposium: Structure and Diffusional Growth Mechanisms of Irrational Interphase Boundaries: Session IV	208A	Tues-PM	327
Hume Rothery Symposium: Structure and Diffusional Growth Mechanisms of Irrational Interphase Boundaries: Session V	208A	Wed-AM	370
Hume Rothery Symposium: Structure and Diffusional Growth Mechanisms of Irrational Interphase Boundaries: Session VI	208A	Wed-PM	415

SESSION TITLE	ROOM	DAY	PAGE
Physical Metallurgy continued			
Internal Stresses and Thermo-Mechanical Behavior in Multi-Component Materials Systems: Electronic Thin Films and Packaging Materials I	209B	Mon-AM	187
Internal Stresses and Thermo-Mechanical Behavior in Multi-Component Materials Systems: Electronic Thin Films and Packagaing Materials II	209B	Mon-PM	229
Internal Stresses and Thermo-Mechanical Behavior in Multi-Component Materials Systems: Creep and Plasticity I	209B	Tues-AM	283
Internal Stresses and Thermo-Mechanical Behavior in Multi-Component Materials Systems: Creep and Plasticity II	209B	Tues-PM	327
Internal Stresses and Thermo-Mechanical Behavior in Multi-Component Materials Systems: Anisotropy and Residual Stresses	209B	Wed-AM	371
Multiphase Phenomena in Materials Processing: Session I	218B	Wed-AM	379
Multiphase Phenomena in Materials Processing: Session II	218B	Wed-PM	423
Multiphase Phenomena in Materials Processing: Session III	218B	Thurs-AM	446
R.J. Arsenault Symposium on Materials Testing and Evaluation: Session I	211A	Mon-AM	201
R.J. Arsenault Symposium on Materials Testing and Evaluation: Session II	211A	Mon-PM	246
R.J. Arsenault Symposium on Materials Testing and Evaluation: Session III	211A	Tues-AM	296
R.J. Arsenault Symposium on Materials Testing and Evaluation: Session IV	211A	Tues-PM	342
Solidification Processes and Microstructures: A Symposium in Honor of Prof. W. Kurz: Processes	207D	Mon-AM	202
Solidification Processes and Microstructures: A Symposium in Honor of Prof. W. Kurz: Mushy Zone Dynamics	207D	Mon-PM	247
Solidification Processes and Microstructures: A Symposium in Honor of Prof. W. Kurz: Microstructures	207D	Tues-AM	299
Solidification Processes and Microstructures: A Symposium in Honor of Prof. W. Kurz: Rapid Solidification	207D	Tues-PM	344
Solidification Processes and Microstructures: A Symposium in Honor of Prof. W. Kurz: Phase Field	207D	Wed-AM	386
Symposium on Microstructural Stability in Honor of Prof. Roger D. Doherty: Microstructural Stability: Recrystallization	216A	Mon-AM	204
Symposium on Microstructural Stability in Honor of Prof. Roger D. Doherty: Microstructural Stability: Texture Development	216A	Mon-PM	249
Symposium on Microstructural Stability in Honor of Prof. Roger D. Doherty: Microstructural Stability: Plastic Deformation	216A	Tues-AM	302
Symposium on Microstructural Stability in Honor of Prof. Roger D. Doherty: Microstructural Stability: Precipitation and Other Topics	216A	Tues-PM	347
The Didier de Fontaine Symposium on the Thermodynamics of Alloys: Fundamentals of Alloy Theory	216B	Mon-AM	205
The Didier de Fontaine Symposium on the Thermodynamics of Alloys: Experimental Techniques	216B	Mon-PM	250
The Didier de Fontaine Symposium on the Thermodynamics of Alloys: First Principle Calculations and Cluster Expansion Techniques	216B	Tues-AM	304
The Didier de Fontaine Symposium on the Thermodynamics of Alloys: Interatomic Potentials and Cluster Expansion Techniques	216B	Tues-PM	348
The Didier de Fontaine Symposium on the Thermodynamics of Alloys: Joint Session with Computational Thermodynamics and Phase Transformations I	216B	Wed-AM	389

SESSION TITLE	ROOM	DAY	PAGE
Physical Metallurgy continued			
The Didier de Fontaine Symposium on the Thermodynamics of Alloys: Joint Session with Computational Thermodynamics and Phase Transformations II	216B	Wed-PM	430
The Role of Grain Boundaries in Material Design: Grain Boundary Character	218A	Wed-AM	390
The Role of Grain Boundaries in Material Design: Grain Boundary Segregation, Diffusion, Damage	218A	Wed-PM	431
The Role of Grain Boundaries in Material Design: Simulation of Grain Boundary Effects of Properties	218A	Thurs-AM	451
General Abstracts			
General Abstracts: Session I	204	Mon-AM	184
General Abstracts: Session II	204	Mon-PM	225
General Abstracts: Session III	212A	Mon-PM	226
General Abstracts: Session IV	204	Tues-AM	281
General Abstracts: Session V	204	Tues-PM	326
General Abstracts: Session VI	208B	Wed-AM	368
General Abstracts: Session VII	208B	Wed-PM	411
General Abstracts: Session VIII	207D	Wed-PM	412
General Abstracts: Session IX	201B	Thurs-AM	441
General Poster Session			
General Poster Session	Ballroom Foyer	MonPM-WedPM	453

# **Table of Contents**

## (Alphabetical Order)

SESSION TITLE	ROOM	DAY	PAGE
5th Global Innovations Symposium: Trends in LIGA, Miniaturization, and Nano-Scale Materials, Devices and Technologies: Plenary: Trends: Past, Present, and Future	202B	Mon-PM	209
5th Global Innovations Symposium: Trends in LIGA, Miniaturization, and Nano-Scale Materials, Devices and Technologies: Small Volume Deformation	202B	Tues-AM	261
5th Global Innovations Symposium: Trends in LIGA, Miniaturization, and Nano-Scale Materials, Devices and Technologies: Properties and Characterization of Materials for Microsystem/LIGA Applications	202B	Tues-PM	308
5th Global Innovations Symposium: Trends in LIGA, Miniaturization, and Nano-Scale Materials, Devices and Technologies: Properties, Processes, and Modeling	202B	Wed-AM	352
5th Global Innovations Symposium: Trends in LIGA, Miniaturization, and Nano-Scale Materials, Devices and Technologies: Manufacturing and Evaluation of Layered Nano-Scale Materials	202B	Wed-PM	394
		Mon-AM	
Advanced Materials for Energy Conversion II: Energy Issues & Metal Hydrides I			169
Advanced Materials for Energy Conversion II: Metal Hydrides II		Mon-PM	210
Advanced Materials for Energy Conversion II: Complex Hydrides I	203A	Tues-AM	262
Advanced Materials for Energy Conversion II: Complex Hydrides II	203A	Tues-PM	309
Advanced Materials for Energy Conversion II: Metal Hydrides III	203A	Wed-AM	353
Advanced Materials for Energy Conversion II: Thermodynamics, Superconductors & Batteries	204	Wed-AM	354
Advanced Materials for Energy Conversion II: Metal Hydrides IV - Dynamics of Metal Hydrides, and Tritium Gettering	203A	Wed-PM	395
Advanced Materials for Energy Conversion II: Magnetic Materials & Hydrogen Permeation	204	Wed-PM	396
Advanced Materials for Energy Conversion II: Thermoelectrics, Superconductors, and Piezoelectric Materials		Thurs-AM	435
Advanced Materials for Energy Conversion II: Metal Hydrides V, Thermal Energy Storage and Containment Materials	204	Thurs-AM	436
Advances in Superplasticity and Superplastic Forming: Development of Advanced Superplastic Forming Processes	201B	Mon-PM	211
Advances in Superplasticity and Superplastic Forming: Advances in Superplastic Al-Mg Materials	201B	Tues-AM	264
Advances in Superplasticity and Superplastic Forming: Advances in Superplastic Forming of Light Alloys	201B	Tues-PM	310
Advances in Superplasticity and Superplastic Forming: Advanced Superplastic Materials and the Science of Superplasticity	201B	Wed-AM	355
Advances in Superplasticity and Superplastic Forming: Modeling of Superplastic Forming Processes and Materials	201B	Wed-PM	397
Alumina and Bauxite: Bayer Plant Operations: Red Side	218A	Mon-AM	170
Alumina and Bauxite: Process Modeling and Control	218A	Mon-PM	212
Alumina and Bauxite: Bayer Plant Operations: White Side	218A	Tues-AM	265
Alumina and Bauxite: Technology and Future Trends		Tues-PM	311

SESSION TITLE	ROOM	DAY	PAGE
Aluminum Can Recycling: Session I	217D	Tues-AM	266
Aluminum Reduction - Potroom Improvements	213D	Mon-AM	171
Aluminum Reduction Technology: Cell Development and Operations	213D	Mon-PM	212
Aluminum Reduction Technology: Pot Control	213D	Tues-AM	267
Aluminum Reduction Technology: Modeling - Industry Trends	213D	Tues-PM	312
Aluminum Reduction Technology: Emerging Technologies	213D	Wed-AM	356
Aluminum Reduction Technology: Environmental	213D	Wed-PM	398
Aluminum Reduction Technology: Materials and Fundamentals	213A	Wed-PM	399
Aluminum Reduction Technology: Modeling	213D	Thurs-AM	437
Automotive Alloys 2004: Session I	210A	Mon-AM	172
Automotive Alloys 2004: Session II	210A	Mon-PM	213
Automotive Alloys 2004: Session III	210A	Tues-AM	268
Automotive Alloys 2004: Session IV	210A	Tues-PM	313
Beyond Nickel-Base Superalloys: Superalloys and Niobium Silicides	211B	Mon-AM	174
Beyond Nickel-Base Superalloys: Molybdenum Silicides I	211B	Mon-PM	215
Beyond Nickel-Base Superalloys: Precious Metal Alloys	211B	Tues-AM	269
Beyond Nickel-Base Superalloys: Molybdenum Silicides II	211B	Tues-PM	315
Beyond Nickel-Base Superalloys: Niobium Silicides	211B	Wed-AM	357
Beyond Nickel-Base Superalloys: Other Systems and Physical Properties of Silicides	211B	Wed-PM	400
Bulk Metallic Glasses: Processing I	209A	Mon-AM	175
Bulk Metallic Glasses: Processing II	209A	Mon-PM	216
Bulk Metallic Glasses: Fatigue and Fracture	209A	Tues-AM	270
Bulk Metallic Glasses: Theoretical Modeling and Shear Bands	209A	Tues-PM	316
Bulk Metallic Glasses: Bio, Corrosion, and Fracture Behavior	209A	Wed-AM	359
Bulk Metallic Glasses: Phase Transformation and Alloy Design	209A	Wed-PM	402
Bulk Metallic Glasses: Mechanical Behavior	209A	Thurs-AM	438
Carbon Technology: Cathode Material and Corrosion	213A	Mon-AM	176
Carbon Technology: Anode Raw Materials	213A	Mon-PM	217
Carbon Technology: Green Anodes and Soderberg Paste	213A	Tues-AM	272
Carbon Technology: Anode Baking	213A	Tues-PM	317
Carbon Technology: Anode Quality and Performance	213A	Wed-AM	360
Cast Shop Technology: Melting and Refractories	213B/C	Mon-AM	177
Cast Shop Technology: Modeling of Casting Processes	213B/C	Mon-PM	218
Cast Shop Technology: Casting	213B/C	Tues-AM	272
Cast Shop Technology: Metal Treatment	213B/C	Tues-PM	318
Cast Shop Technology: Alloying and Furnace Processing	213B/C	Wed-AM	361

SESSION TITLE	ROOM	DAY	PAGE
Cast Shop Technology: Grain Refining	213B/C	Wed-PM	403
Cast Shop Technology: Foundry	213B/C	Thurs-AM	439
CFD Modeling and Simulation of Engineering Processes: Advanced Casting and Solidification Processes I	. 206A	Mon-AM	178
CFD Modeling and Simulation of Engineering Processes: Remelt Processes	. 206A	Mon-PM	219
CFD Modeling and Simulation of Engineering Processes: MEMS/Microfluidics	206A	Tues-AM	273
CFD Modeling and Simulation of Engineering Processes: Advanced Casting and Solidification Processes II	. 206A	Tues-PM	319
CFD Modeling and Simulation of Engineering Processes: Process Modeling I	206A	Wed-AM	362
CFD Modeling and Simulation of Engineering Processes: Process Modeling II	206A	Wed-PM	404
Challenges in Advanced Thin Films: Microstructures, Interfaces, and Reactions: Advances in Photonic and Optoelectronic Materials and Processes	. 218B	Mon-AM	179
Challenges in Advanced Thin Films: Microstructures, Interfaces, and Reactions: Microstructures, Properties, and Reliability of Microelectronic Devices	. 218B	Mon-PM	220
Challenges in Advanced Thin Films: Microstructures, Interfaces, and Reactions: Modification, Characterization, and Modeling	218B	Tues-AM	274
Challenges in Advanced Thin Films: Microstructures, Interfaces, and Reactions: Design, Process, and Property Control of Functional and Structural Thin-Films	218B	Tues-PM	320
Computational Thermodynamics and Phase Transformations: Grain Growth and Particle Coarsening	. 202A	Mon-AM	180
Computational Thermodynamics and Phase Transformations: Interfaces and Grain Boundaries	202A	Mon-PM	222
Computational Thermodynamics and Phase Transformations: Phase Field Modeling I	. 202A	Tues-AM	276
Computational Thermodynamics and Phase Transformations: Phase Field Modeling II	. 202A	Tues-PM	322
Computational Thermodynamics and Phase Transformations: Phase Equilibria and Thermodynamic Assessments	202A	Wed-AM	363
Computational Thermodynamics and Phase Transformations: Joint Session with The Didier de Fontaine Symposium on the Thermodynamics of Alloys I	216B	Wed-AM	389
Computational Thermodynamics and Phase Transformations: Thermodynamics and Phase Transformations	. 202A	Wed-PM	405
Computational Thermodynamics and Phase Transformations: Joint Session with The Didier de Fontaine Symposium on the Thermodynamics of Alloys II	216B	Wed-PM	430
Cost-Affordable Titanium Symposium Dedicated to Prof. Harvey Flower: Overview and Innovative Processes.	206B	Mon-AM	182
Cost-Affordable Titanium Symposium Dedicated to Prof. Harvey Flower: Break Through Technologies	206B	Mon-PM	223
Cost-Affordable Titanium Symposium Dedicated to Prof. Harvey Flower: Titanium Economics	206B	Tues-AM	278
Cost-Affordable Titanium Symposium Dedicated to Prof. Harvey Flower: Creative Processing	206B	Tues-PM	323
Cost-Affordable Titanium Symposium Dedicated to Prof. Harvey Flower: Creative Fabrication	206B	Wed-AM	364
Cost-Affordable Titanium Symposium Dedicated to Prof. Harvey Flower: Low Cost Titanium	206B	Wed-PM	406
Cost-Affordable Titanium Symposium Dedicated to Prof. Harvey Flower: Property Enhancement	. 206B	Thurs-AM	440

SESSION TITLE	ROOM	DAY	PAGE
Dislocations: Modeling and Simulation Fundamentals	201A	Mon-AM	182
Dislocations: Simulation and Observation of Fundamental Mechanisms	201A	Mon-PM	224
Dislocations: Dislocation Structures and Patterning	201A	Tues-AM	278
Dislocations: Novel Experimental Methods	201A	Tues-PM	324
Dislocations: Plasticity, Voids, and Fracture	201A	Wed-AM	365
Dislocations: Dislocations in Complex Materials	201A	Wed-PM	407
Educational Issues in Transport Phenomena in Materials Processing: Presentations and Panel Discussion	209B	Wed-PM	408
Electrochemical Measurements and Processing of Materials: Electrodeposition Processes	212A	Tues-AM	280
Electrochemical Measurements and Processing of Materials: Electrochemical Refining	212A	Tues-PM	325
Electrochemical Measurements and Processing of Materials: Electrochemical Metal Production	212A	Wed-AM	366
Electrochemical Measurements and Processing of Materials: Electrochemical Sensors and Measurements	212A	Wed-PM	409
Failure of Structural Materials: Fundamentals	211A	Wed-AM	367
Failure of Structural Materials: Fatigue	211A	Wed-PM	410
Failure of Structural Materials: General	211A	Thurs-AM	441
General Abstracts: Session I	204	Mon-AM	184
General Abstracts: Session II	204	Mon-PM	225
General Abstracts: Session III	212A	Mon-PM	226
General Abstracts: Session IV	204	Tues-AM	281
General Abstracts: Session V	204	Tues-PM	326
General Abstracts: Session VI	208B	Wed-AM	368
General Abstracts: Session VII	208B	Wed-PM	411
General Abstracts: Session VIII	207D	Wed-PM	412
General Abstracts: Session IX	201B	Thurs-AM	441
General Poster Session	Ballroom Foyer	MonPM-WedPM	453
General Pyrometallurgy: Session I	202B	Mon-AM	185
High Risk Technologies in Metallurgy with Commercial Potential: Session I	210A	Wed-AM	369
High Risk Technologies in Metallurgy with Commercial Potential: Session II	210A	Wed-PM	414
Hume Rothery Symposium: Structure and Diffusional Growth Mechanisms of Irrational Interphase Boundaries: Session I	208A	Mon-AM	186
Hume Rothery Symposium: Structure and Diffusional Growth Mechanisms of Irrational Interphase Boundaries: Session II	208A	Mon-PM	228
Hume Rothery Symposium: Structure and Diffusional Growth Mechanisms of Irrational Interphase Boundaries: Session III	208A	Tues-AM	282
Hume Rothery Symposium: Structure and Diffusional Growth Mechanisms of Irrational Interphase Boundaries: Session IV	208A	Tues-PM	327
Hume Rothery Symposium: Structure and Diffusional Growth Mechanisms of Irrational Interphase Boundaries: Session V	208A	Wed-AM	370

SESSION TITLE	ROOM	DAY	PAGE
Hume Rothery Symposium: Structure and Diffusional Growth Mechanisms of Irrational Interphase Boundaries: Session VI	208A	Wed-PM	415
Internal Stresses and Thermo-Mechanical Behavior in Multi-Component Materials Systems: Electronic Thin Films and Packaging Materials I	209B	Mon-AM	187
Internal Stresses and Thermo-Mechanical Behavior in Multi-Component Materials Systems: Electronic Thin Films and Packagaing Materials II	209B	Mon-PM	229
Internal Stresses and Thermo-Mechanical Behavior in Multi-Component Materials Systems: Creep and Plasticity I	209B	Tues-AM	283
Internal Stresses and Thermo-Mechanical Behavior in Multi-Component Materials Systems: Creep and Plasticity II	209B	Tues-PM	327
Internal Stresses and Thermo-Mechanical Behavior in Multi-Component Materials Systems: Anisotropy and Residual Stresses	209B	Wed-AM	371
International Laterite Nickel Symposium - 2004: Economics and Project Assessment	217B/C	Mon-AM	188
International Laterite Nickel Symposium - 2004: Mineralogy and Geometallurgy	217B/C	Mon-PM	230
International Laterite Nickel Symposium - 2004: Panel Discussion	217B/C	Mon-PM	231
International Laterite Nickel Symposium - 2004: Pressure Acid Leaching	217B/C	Tues-AM	284
International Laterite Nickel Symposium - 2004: Process Development for Prospective Projects	217B/C	Tues-PM	328
International Laterite Nickel Symposium - 2004: Roasting and Smelting	217D	Tues-PM	330
International Laterite Nickel Symposium - 2004: Process and Operational Lessons Learned - Part I	217B/C	Wed-AM	372
International Laterite Nickel Symposium - 2004: Process and Operational Lessons Learned - Part II	217B/C	Wed-PM	415
International Laterite Nickel Symposium - 2004: Atmospheric Leaching	217B/C	Thurs-AM	443
International Laterite Nickel Symposium - 2004: Slurry Rheology, Solution Extraction and Other	217B/C	Thurs-AM	443
Lead-Free Solders and Processing Issues Relevant to Microelectronic Packaging: Fundamentals, Phases, Wetting and Solidification	219B	Mon-AM	189
Lead-Free Solders and Processing Issues Relevant to Microelectronic Packaging: Environmental and Materials Issues for Lead-Free	219B	Mon-PM	231
Lead-Free Solders and Processing Issues Relevant to Microelectronic Packaging: Mechanical Properties and Fatigue Behavior	219B	Tues-AM	285
Lead-Free Solders and Processing Issues Relevant to Microelectronic Packaging: Electromigration and Creep in Leadfree Solders	219B	Tues-PM	331
Lead-Free Solders and Processing Issues Relevant to Microelectronic Packaging: Interfacial Interactions, Intermetallics and Substrates	219B	Wed-AM	373
Lead-Free Solders and Processing Issues Relevant to Microelectronic Packaging: Microstructural Characterization and Evolution	219B	Wed-PM	416
Magnesium Technology 2004: Automotive Applications/Welding	203B	Mon-AM	191
Magnesium Technology 2004: Wrought Magnesium Alloys I	203B	Mon-PM	233
Magnesium Technology 2004: Wrought Magnesium Alloys II/Corrosion and Coatings	203B	Tues-AM	287
Magnesium Technology 2004: Primary Processing and Environmental Issues	203B	Tues-PM	332
Magnesium Technology 2004: Casting Processes and Properties	203B	Wed-AM	375
Magnesium Technology 2004: Fundamental Research	203B	Wed-PM	417
Magnesium Technology 2004: Alloy Development	203B	Thurs-AM	444

SESSION TITLE	ROOM	DAY	PAGE
Materials Analysis: Understanding the Columbia Disaster	Ballroom B	Wed-PM	418
Materials by Design: Atoms to Applications: Materials Chemistry and Alloy Design	210B	Mon-AM	192
Materials by Design: Atoms to Applications: Materials Characterization and Microstructural Modeling	210B	Mon-PM	234
Materials by Design: Atoms to Applications: Computational and Experimental Strategies	210B	Tues-AM	288
Materials by Design: Atoms to Applications: Designing Nanostructures	210B	Tues-PM	334
Materials by Design: Atoms to Applications: Design for Mechanical Functionality I	210B	Wed-AM	376
Materials by Design: Atoms to Applications: Design for Mechanical Functionality II	210B	Wed-PM	419
Materials Education to Revitalize the Workforce: Session I	217D	Wed-AM	377
Materials Education to Revitalize the Workforce: Session II	217D	Wed-PM	420
Materials Issues in Fuel Cells: State-of-the-Art	207B/C	Mon-AM	193
Materials Issues in Fuel Cell: Materials Challenges	207B/C	Mon-PM	235
Materials Processing Fundamentals: Solidification and Casting		Mon-AM	194
Materials Processing Fundamentals: Deformation Processing	212B	Mon-PM	236
Materials Processing Fundamentals: Liquid Metal Processing		Tues-AM	289
Materials Processing Fundamentals: Smelting and Refining		Tues-PM	335
Materials Processing Fundamentals: Aqueous Processing		Wed-AM	378
Materials Processing Fundamentals: Powders, Composites, Coatings and Measurement		Wed-PM	420
Metals for the Future: Structural Materials		Wed-AM	379
Metals for the Future: Functional Materials		Wed-PM	422
Metals for the Future: Processing and Bio-Materials		Thurs-AM	445
Multiphase Phenomena in Materials Processing: Session I		Wed-AM	379
Multiphase Phenomena in Materials Processing: Session II		Wed-AM	423
Multiphase Phenomena in Materials Processing: Session III		Thurs-AM	446
Nanostructured Magnetic Materials: Recent Progress in Magnetic Nanostructures	215	Mon-AM	195
Nanostructured Magnetic Materials: Synthesis and Characterization of Nanostructured Magnetic Materials	215	Mon-PM	237
Nanostructured Magnetic Materials: Magnetic Tunnel Junctions and Semiconductor Spintronics	215	Tues-AM	290
Nanostructured Magnetic Materials: Self Assembly and Patterned Nanostructures	215	Tues-PM	336
Nanostructured Materials for Biomedical Applications: Session I	219A	Mon-AM	197
Nanostructured Materials for Biomedical Applications: Session II	219A	Mon-PM	239
Nanostructured Materials for Biomedical Applications: Session III	219A	Tues-AM	291
Nanostructured Materials for Biomedical Applications: Session IV	219A	Tues-PM	337
Nanostructured Materials for Biomedical Applications: Session V	219A	Wed-AM	381
Nanostructured Materials for Biomedical Applications: Session VI	219A	Wed-PM	424
Nanostructured Materials for Biomedical Applications: Session VII	219A	Thurs-AM	447
Phase Stability, Phase Transformation, and Reactive Phase Formation in Electronic Materials III: Session I	214	Mon-AM	198

SESSION TITLE	ROOM	DAY	PAGE
Phase Stability, Phase Transformation, and Reactive Phase Formation in Electronic Materials III: Session II	214	Mon-PM	240
Phase Stability, Phase Transformation, and Reactive Phase Formation in Electronic Materials III: Session III	214	Tues-AM	293
Phase Stability, Phase Transformation, and Reactive Phase Formation in Electronic Materials III: Session IV	214	Tues-PM	338
Phase Stability, Phase Transformation, and Reactive Phase Formation in Electronic Materials III: Session V	214	Wed-AM	382
Phase Transformations and Deformation in Magnesium Alloys: Solidification and Precipitation	205	Tues-AM	294
Phase Transformations and Deformation in Magnesium Alloys: Plastic Deformation and Texture	205	Tues-PM	339
Phase Transformations and Deformation in Magnesium Alloys: Creep Deformation	205	Wed-AM	383
Phase Transformations and Deformation in Magnesium Alloys: Deformation and Strengthening	205	Wed-PM	425
Processing, Microstructure and Properties of Powder-Based Materials: Session I	208B	Mon-PM	242
Processing, Microstructure and Properties of Powder-Based Materials: Session II	208B	Tues-AM	295
Processing, Microstructure and Properties of Powder-Based Materials: Session III	208B	Tues-PM	340
Recent Advances in Non-Ferrous Metals Processing: Reactive Metals	205	Mon-AM	199
Recent Advances in Non-Ferrous Metals Processing: Sustainable Development	205	Mon-PM	244
Recycling: General Recycling	217D	Mon-AM	200
Recycling: Aluminum and Aluminum Dross Processing	217D	Mon-PM	244
Roytburd Symposium on Polydomain Structures: Elastic Domains in Structural Materials .	216A	Wed-AM	384
Roytburd Symposium on Polydomain Structures: Domains in Ferroelectrics and Magnetic	cs 216A	Wed-PM	425
R.J. Arsenault Symposium on Materials Testing and Evaluation: Session I	211A	Mon-AM	201
R.J. Arsenault Symposium on Materials Testing and Evaluation: Session II	211A	Mon-PM	246
R.J. Arsenault Symposium on Materials Testing and Evaluation: Session III	211A	Tues-AM	296
R.J. Arsenault Symposium on Materials Testing and Evaluation: Session IV	211A	Tues-PM	342
Solid and Aqueous Wastes from Non-Ferrous Metal Industry: Session I	214	Wed-PM	426
Solid and Aqueous Wastes from Non-Ferrous Metal Industry: Session II	214	Thurs-AM	448
Solidification of Aluminum Alloys: Microstructural Evolution I	207B/C	Tues-AM	298
Solidification of Aluminum Alloys: Microstructural Evolution II	207B/C	Tues-PM	343
Solidification of Aluminum Alloys: Solidification Cracking/Mechanical Properties	207B/C	Wed-AM	385
Solidification of Aluminum Alloys: Gas Porosity/Micro-Macro Segregation	207B/C	Wed-PM	427
Solidification of Aluminum Alloys: Special Effects	207B/C	Thurs-AM	449
Solidification Processes and Microstructures: A Symposium in Honor of Prof. W. Kurz: Processes	207D	Mon-AM	202
Solidification Processes and Microstructures: A Symposium in Honor of Prof. W. Kurz: Mushy Zone Dynamics	207D	Mon-PM	247
Solidification Processes and Microstructures: A Symposium in Honor of Prof. W. Kurz: Microstructures	207D	Tues-AM	299

SESSION TITLE	ROOM	DAY	PAGE
Solidification Processes and Microstructures: A Symposium in Honor of Prof. W. Kurz: Rapid Solidification	207D	Tues-PM	344
Solidification Processes and Microstructures: A Symposium in Honor of Prof. W. Kurz: Phase Field	207D	Wed-AM	386
Surfaces and Interfaces in Nanostructured Materials: General Phenomena & Processes	217A	Tues-AM	301
Surfaces and Interfaces in Nanostructured Materials: Grain & Phase Boundaries	217A	Tues-PM	346
Surfaces and Interfaces in Nanostructured Materials: Synthesis & Processing	217A	Wed-AM	388
Surfaces and Interfaces in Nanostructured Materials: Coatings and Surface Modification	. 217A	Wed-PM	428
Surfaces and Interfaces in Nanostructured Materials: Self-Organized and Biological Materials	217A	Thurs-AM	450
Symposium on Microstructural Stability in Honor of Prof. Roger D. Doherty: Microstructural Stability: Recrystallization	216A	Mon-AM	204
Symposium on Microstructural Stability in Honor of Prof. Roger D. Doherty: Microstructural Stability: Texture Development	216A	Mon-PM	249
Symposium on Microstructural Stability in Honor of Prof. Roger D. Doherty: Microstructural Stability: Plastic Deformation	216A	Tues-AM	302
Symposium on Microstructural Stability in Honor of Prof. Roger D. Doherty: Microstructural Stability: Precipitation and Other Topics	216A	Tues-PM	347
The Didier de Fontaine Symposium on the Thermodynamics of Alloys: Fundamentals of Alloy Theory	216B	Mon-AM	205
The Didier de Fontaine Symposium on the Thermodynamics of Alloys: Experimental Techniques	216B	Mon-PM	250
The Didier de Fontaine Symposium on the Thermodynamics of Alloys: First Principle Calculations and Cluster Expansion Techniques	216B	Tues-AM	304
The Didier de Fontaine Symposium on the Thermodynamics of Alloys: Interatomic Potentials and Cluster Expansion Techniques	216B	Tues-PM	348
The Didier de Fontaine Symposium on the Thermodynamics of Alloys: Joint Session with Computational Thermodynamics and Phase Transformations I	216B	Wed-AM	389
The Didier de Fontaine Symposium on the Thermodynamics of Alloys: Joint Session with Computational Thermodynamics and Phase Transformations II	216B	Wed-PM	430
The Role of Grain Boundaries in Material Design: Grain Boundary Character	218A	Wed-AM	390
The Role of Grain Boundaries in Material Design: Grain Boundary Segregation, Diffusion, Damage	218A	Wed-PM	431
The Role of Grain Boundaries in Material Design: Simulation of Grain Boundary Effects of Properties	218A	Thurs-AM	451
Third International Symposium on Ultrafine Grained Materials: Processing I: Fundamentals and Technology	207A	Mon-AM	206
Third International Symposium on Ultrafine Grained Materials: Processing II: Structural Evolution	207A	Mon-PM	251
Third International Symposium on Ultrafine Grained Materials: Posters	207A	Mon-PM/Tue/Wed	253
Third International Symposium on Ultrafine Grained Materials: UFG Material Fundamentals	207A	Tues-AM	305
Third International Symposium on Ultrafine Grained Materials: Microstructure and Properties	207A	Tues-PM	349
Third International Symposium on Ultrafine Grained Materials: Mechanical Properties	207A	Wed-AM	391
Third International Symposium on Ultrafine Grained Materials: Superplasticity, Creep & Thermal Stability	207A	Wed-PM	432

# **TECHNICAL PROGRAM**

Charlotte Convention Center; Charlotte, North Carolina USA; March 14-18, 2004

# MONDAY

#### Advanced Materials for Energy Conversion II: Energy Issues & Metal Hydrides I

Sponsored by: Light Metals Division, LMD-Reactive Metals Committee

*Program Organizers:* Dhanesh Chandra, University of Nevada, Metallurgical & Materials Engineering, Reno, NV 89557 USA; Renato G. Bautista, University of Nevada, Metallurgical and Materials Engineering, Reno, NV 89557-0136 USA; Louis Schlapbach, EMPA Swiss Federal, Laboratory for Materials Testing and Research, Duebendorf CH-8600 Switzerland

Monday AM	Room: 203A
March 15, 2004	Location: Charlotte Convention Center

Session Chairs: Renato G. Bautista, University of Nevada, Matls. & Metalurgl. Engrg., Reno, NV 89557 USA; Dhanesh Chandra, University of Nevada, Metallurgl. & Matls. Engrg., Reno, NV 89557 USA; Louis Schlapbach, EMPA, Swiss Federal Lab for Matls. Testing & Rsch., Duebendorf Switzerland

#### 8:30 AM Plenary

**Overview of Advanced Materials for Energy Conversion II Symposium**: *Dhanesh Chandra*<sup>1</sup>; Renato G. Bautista<sup>1</sup>; Louis Schlapbach<sup>2</sup>; <sup>1</sup>University of Nevada, Metallurgl. & Matls. Engrg., MS 388, Coll. of Engrg., Reno, NV 89557 USA; <sup>2</sup>EMPA, Swiss Federal Lab. for Matls. Testing & Rsch., Duebendorf Switerzland

An overview of Advanced Materials For Energy Conversion II Symposium, that includes storage will be presented. In this symposium we emphasize fields of materials related to energy conversion, fundamentals as well as applied research and industrial practices. Recent advances in methodology used in neutron scattering to characterize the hydrides, such as in-situ type experiments. The symposium sessions will include Hydrogen and Tritium Storage in intermetallics, alantes, and other hydrides, Batteries, Fuel Cells, Superconductors, Magnets, Membrane Materials, Thermal Energy Storage Materials, Photovoltaics and others. Several advances have been made in fuel cell materials, and we will highlight some of the key advances. Several adavnces have been made in hydrogen and tritum storage materials, we will empahsize light weight Alanate hydrides; Li based hydrides seem to be promising materials for storage. In addition Uranium hydride kinteics and other issues will be presented in thsi sympsoium. Fundamental understanding of the hydriding mechanisms will be discussed. We also have sessions devoted to materials for other Thermal Energy Storage Materials such as solid state organic phase change materials, photovoltaics, and thermoelectric materials will be be presented.

#### 8:45 AM Plenary

Energy Crisis - Fact or Fiction: *Bhakta B. Rath*<sup>1</sup>; <sup>1</sup>Naval Research Laboratory, Matls. Sci. & Component Tech. Direct., Code 6000, Washington, DC 20375-5341 USA

Global consumption of energy is staggering. The U.S. Department of Energy projects the total world consumption to rise by 59% between 1999 and 2020, from 382 to 607 quads per year (one quad being defined as 1015 BTU and equivalent to more than 7 billion gallons of petroleum). The same report predicts a 20% increase of carbon dioxide equivalent to approximately ten billion metric pounds of carbon. Another complication in the energy equation is that global population will increase from 6.0 to 7.5 billion. The impact of these projections may have long-range and profound implications. In the United States, hydrocarbon-based fuel use is twice that of coal or natural gas consumption and four times greater than the use of nuclear energy or renewable energy resources. Virtually the entire existing energy related infrastructure for the United States relies on fossil fuels. Undoubtedly, we will remain dependent on hydrocarbon combustion for the foreseeable future. As such, the country can not afford to ignore the long-term impacts of continued hydrocarbon combustion. It is essential to develop a long-term plan to deal with the use of alternative energy sources.

#### 9:15 AM Plenary

Advanced Materials Research in Photovoltaics: Progress and Challenges: *Thomas Surek*<sup>1</sup>; <sup>1</sup>National Renewable Energy Laboratory, Golden, CO 80401 USA

Photovoltaics (PV) is solar electric power - a semiconductor-based technology that converts sunlight to electricity. Three decades of research has led to the discovery of new materials and devices and new processing techniques for low-cost manufacturing. This has resulted in improved sunlight-to-electricity conversion efficiencies, improved outdoor reliability, and lower module and system costs. The manufacture and sale of PV has grown into a \$4 billion industry worldwide, with more than 560 megawatts of PV modules shipped in 2002. This paper reviews the most significant advances in PV materials and devices research over the past 30 years and examines the research challenges to reach the ultimate potential of current-generation (crystalline silicon), next-generation (thin films), and future-generation PV technologies. The latter include innovative materials and device concepts that hold the promise of significantly higher conversion efficiencies and/or much lower costs.

#### 9:45 AM Plenary

Advances in Fuel Cell Materials: Solid Electrolytes, Anodes and Cathodes, for Distributed and Portable Power: G. Jeffrey Snyder<sup>1</sup>; <sup>1</sup>Caltech/JPL, MS 277-207, Pasadena, CA 91109 USA

Fuel cells have emerged as the most promising alternative to the combustion engine to reduce the environmental impact and dependence on fossil fuels. Fuel cells directly convert the chemical energy of fuels to electrical energy with high efficiency. Many types of fuels can be used with hydrogen most widely considered. The primary components of a fuel cell are an ion conducting electrolyte, a cathode, and an anode. Advances in the materials that make up these components are of fundamental importance for improving fuel cell performance and are a focus of research at Caltech. The solid acid and solid oxide electrolytes are ideal for elevated temperature, high efficiency fuel cells. Improved power densities are achieved with microstructure engineered cathode and anode materials. With advanced thermal management techniques, single chamber fuel cells have been demonstrated that are small enough for hand-held electronics.

#### 10:15 AM Break

#### 10:30 AM Keynote

A New Means of Chemical Energy Conversion by Semiconductors: *V. V. Styrov*<sup>1</sup>; A. E. Kabansky<sup>1</sup>; <sup>1</sup>Priazovsky State Technical University, Dept. of Physics, University Str. 7, Mariupol, Donetsky Reg. 87500 Ukraine

The reaction of recombination of hydrogen atoms from the gas phase on solid surfaces (the energy release up to 4,48eV) leads to generation of electron-hole pairs in solids (Ge, CdS, ZnSe, ZnS). Thus one can observe during the surface chemical reaction all the effects known under optical excitation (chemoluminescence, longitudinal chemovoltaic effect on p-n junction, transversal chemovoltaic effect and so on). We have found the gas-solid system (atomic hydrogen+germanium) with extremely high efficiency of e-p pairs generation approaching unity per recombination. This system is perspective for chemical-to-electric energy conversion on Ge-based p-n junctions. The efficiency of chemical-to-light conversion in the system of atomic hydrogen+ZnS-Tm reaches one quantum (478,5nm) per 100 recombination. A solid-state laser can be designed under certain conditions with "chemical pumping". One more group of chemoeffects consists in electron emission stimulated by the surface reaction. The solids with the negative electron affinity are promising for chemical-to-electric energy conversion.

#### 10:55 AM Keynote

#### Hydrogen Storage-A Critical Challenge for the Hydrogen Economy: Russell H. Jones<sup>1</sup>; <sup>1</sup>Pacific Northwest National Laboratory, Matls. Scis., PO Box 999, Richland, WA 99352 USA

Vehicle range on a single tank of hydrogen is critical for the economic viability of hydrogen fueled vehicles. A range of 500 kilometers is projected for economic viability and this requires the storage of 4 kg of H2. Hydrogen storage concepts being considered and evaluated include: 1) compressed H2, 2) liquid H2, 3) bulk storage in hydrides, 4) surface adsorption on carbon and boron nitride nanotubes and 5) generation by chemical reaction of a hydride with water. Compressed H2 tanks with a capacity of about 2 kg of H2 stored at 350 bar of pressure have been certified while tanks with higher capacity stored at 700 bar are being developed. Liquidified H2 tanks can store more H2 in a vehicle than compressed H2 but liquifying H2 requires considerable energy and boil-off of the liquid H2 is a concern, especially in enclosed spaces. Storage of H2 in bulk hydrides or on the surface of carbon or boron nitride nanotubes are attractive because of the low pressures involved. Recent studies have shown that NaAlH4 can be reversibly charged and discharged with H2 100's of times but the capacity of this hydride material is only about 1/2 of that needed. Storage of H2 on the surfaces of carbon nanotubes has shown great promise but verification of the storage capacities has not occurred. However, carbon nanotubes have the potential to store about 80% of the desired quantity of H2 so it remains a viable storage material. Generation of H2 by chemical reaction of a hydride such as LiH with water to produce H2 is also attractive because of the significant amounts of H2 that can be generated by this process. The key issues for this process of generating H2 is the need to reprocess the reaction products and the cost associated with transportation and reprocessing this product. There are several options for storing hydrogen on-board a vehicle but as summarized above considerable development work is needed before the hydrogen economy can be realized. Critical materials issues associated with H2 storage will be presented.

#### 11:20 AM Keynote

International Hydrogen Storage R&D in IEA Task 17: Gary Sandrock<sup>1</sup>; <sup>1</sup>SunaTech, Inc., IEA Task 17 Operating Agent, 113 Kraft Pl., Ringwood, NJ 07456 USA

The International Energy Agency Agreement on the Production and Utilization of Hydrogen is marking its 25th anniversary. This presentation summarizes the R&D activities in currently active Annex 17 - Solid and Liquid State Hydrogen Storage Materials. Task 17 was chartered in 2001 and sets as its main target the development of reversible hydrogen storage media capable of delivering 5 wt.% H at less than 80°C. Nine countries are official participants: Canada, Japan, Lithuania, Norway, Spain, Sweden, Switzerland, the United Kingdom and the United States. The nine national participations are represented by 28 research centers representing universities, national laboratories and industries. Internationally collaborative R&D are being performed under 28 projects divided into three categories of H-storage media: hydrides, carbon and combined hydrides plus carbon. Included in the Task 17 activities is the IEA/DOE/SNL Hydride Information Center, an extensive series of online databases of hydride properties and applications.

#### 11:45 AM Invited

Nanoscale Selective, Highly Efficient Doped and Metal Atom Seeded Visible Light Tunable Nanoparticles: Application to Sensors, Microreactors, and Solar Cells: James L. Gole<sup>1</sup>; John Stout<sup>1</sup>; Clemens Burda<sup>2</sup>; <sup>1</sup>Georgia Institute of Technology, Sch. of Physics, 837 State St., Atlanta, GA 30332-0430 USA; <sup>2</sup>Case Western Reserve, Dept. of Chmst., Cleveland, OH USA

An exciting aspect of research at the nanoscale results as nanostructures hold the potential to display an enhanced and unexpected reactivity relative to that at the micron scale and bulk phase. Further, their formation and interaction may be accompanied by phase transformations not commonly observed in bulk systems. These factors can lead to unusual surface oxidation states, routes for highly efficient metallization, and the potential use of metastable phases as they apply to catalysis and energy conversion in environmentally benign systems. We have used a modified-flow tube furnace configuration carefully calibrated for temperature, temperature gradients, entrainment gas flow rate, and total pressure, and variable Si/SiO2 mixtures to generate silica (SiOx) nanospheres which are found to display enhanced catalytic activity and unexpected oxidation state distributions and reactivity. These structures can be agglomerated to wire-like configurations subsequently providing a means to grow silica nanotubes. Layered Sn/SnO mixtures to generate SnOx nanostructures at pressures of a few hundred Torr, display a phase coexistence between rutile and orthohombic crystal structures normally observed at pressures in excess of 150 kbar in the bulk. These observations have suggested a nanoscale exclusive synthesis route. In seconds, at room temperature, we produce nitrogen doped, stable, and environmentally benign TiO2xNx photocatalysts whose optical response can be tuned across the entire visible region. This synthesis, which can be simultaneously accompanied by metal atom seeding, can be accomplished through the direct nitration of anatase TiO2 nanostructures with alkyl ammonium salts. Tunability throughout the visible depends on the degree of TiO2 nanoparticle agglomeration and the influence of metal seeding. The introduction of a small quantity of palladium in the form of the acetate, chloride, or nitrate catalyzes further nitrogen uptake, appears to lead to a partial phase transformation, displays a counterion effect, and produces a material absorbing well into the near infrared. Silver introduced as the nitrate into a TiO2 or TiO2-xNx nanostructure framework, forms seeded AgxO - TiO2 or TiO2-xNx nanostructure mixtures which can be induced to self-assemble to agglomerate nanoneedle and planar arrays using select metals. Surprisingly, no organics are incorporated into the final TiO2-xNx products. These visible light absorbing photocatalysts readily photodegrade methylene blue and gaseous acetaldehyde. They can be transformed from liquids to gels and placed on the surfaces of sensor and microreactor based configurations to 1) produce an improved photocatalytically induced solar based sensor response, and 2) facilitate catalytically induced disinfection of airborne pathogens. In contrast to a nitration process which is facile at the nanoscale, we find little or no direct nitridation of micrometer sized anatase or rutile TiO2 powders at room temperature. Thus, we demonstrate an example of how a traversal to the nanoscale can vastly improve the efficiency for producing important submicron particles.

# Alumina and Bauxite: Bayer Plant Operations: Red Side

Sponsored by: Light Metals Division, LMD-Aluminum Committee Program Organizers: Travis Galloway, Century Aluminum, Hawesville, KY 42348 USA; David Kirkpatrick, Kaiser Aluminum & Chemical Group, Gramercy, LA 70052-3370 USA; Alton T. Tabereaux, Alcoa Inc., Process Technology, Muscle Shoals, AL 35661 USA

Monday AM	Room: 2	18A		
March 15, 2004	Location:	Charlotte	Convention	Center

Session Chair: Fred S. Williams, CMIS Corporation, Victoria, TX 77904 USA

#### 8:30 AM

Wollastonite as a Substitute for Lime in Phosphorus Control During Digestion and as Precoat or Filter-Aid for Pregnant Liquor Filtration in the Bayer Process: *Guy Forté*<sup>1</sup>; <sup>1</sup>Alcan International Ltd., Arvida R&D Ctr., 1955 Blvd. Mellon, PO Box 1250, Jonquiere, Quebec G7S 4K8 Canada

The use of wollastonite, a calcium silicate, was considered as a substitute for lime to control phosphorus in Bayer digestion and as precoat or filter-aid in the Bayer filtration process. Its stability in Bayer liquor and efficiency to control phosphorus was studied and will be reported. Bayer liquor filtration rate against wollastonite dosage will be presented and compared to standard lime precoat or filter-aid.

#### 8:55 AM

Effect of Pre-Desilication and Digestion Conditions on Silica Level in Bayer Liquor: *Eric Tizon*<sup>1</sup>; Philippe Clerin<sup>1</sup>; Benoît Cristol<sup>1</sup>; <sup>1</sup>Aluminium Pechiney, Direction de la Recherche et du Développement, BP- 54, Gardanne 13541 France

Controlling silica level in Bayer liquor is critical in order to prevent scaling or alumina quality issues. Experiments carried out in industrial liquor with metasilicate and kaolin were undertaken to simulate silica metabolism during pre-desilication and digestion operations. Effects of factors such as pre-desilication residence time, alumina and caustic concentration and digestion temperature have been studied. Depending on pre-desilication and digestion conditions, silica solubilisation during digestion has been attributed to kaolin, unstable zeolite or even sodalite dissolution for high caustic and alumina concentrations. The percentage of kaolin to DSP conversion often has the greatest influence on silica solubilisation during digestion. This can be limited by lack of residence time or accessibility of the kaolin in bauxite. It has been found that other factors, including the degree of maturation of the DSP from zeolite A to sodalite and its solubility in the digestion conditions, can also influence silica solubilisation in the digestion process.

#### 9:20 AM

#### Combination of Hydroxamate and Polyacrylamide Based Flocculents for Settler Performance Improvement in ADG Alumina Refinery: Jean-Marc Rousseaux<sup>1</sup>; B. Cristol<sup>1</sup>; S. Torsiello<sup>2</sup>; <sup>1</sup>Aluminium Pechiney, BP 54, 13541 Gardanne France; <sup>2</sup>Aluminium De Grèce, Paralia Distomou, 32003 Beotia Greece

HX® is a well-known settler flocculent, which has proven its efficiency in many alumina refineries. It has been found that a judicious combination of a well-chosen PAM with HX can significantly reduce the dosage without detrimental effects on settling rate, clarification and mud compaction. Three key parameters are to be considered to achieve the PAM + HX combination. Firstly, the right PAM anionicity and molecular weight should be determined. Besides the caustic level of the liquor (with respect to anionicity), chemical mud characteristics play a major role in the choice of the two PAM properties. Secondly, the choice of the respective PAM and HX proportions will have a significant effect on flocculation performances. Finally, for optimal results, it is necessary to pre-mix the PAM and HX flocculants before addition in feed-line and feed-well. Lab test results and industrial application in ADG refinery are detailed in this paper.

#### 9:45 AM

Continued Efforts on the Development of Salicylic Acid Containing Red Mud Flocculants: Everett C. Phillips<sup>1</sup>; <sup>1</sup>Ondeo Nalco Co., Mining & Mineral Process Chem., One Ondeo Nalco Ctr., Naperville, IL 60563-1198 USA

New digestion and process technology (such as high rate and pressure decantation) and the desire to increase liquor productivity, even while processing cheaper and lower grade bauxite ores, continues to increase demands on the red mud clarification process. As previously reported in 2003, Ondeo Nalco Co. has developed a range of new high molecular weight flocculants containing salicylic acid chemistry that promise substantial improvements for the clarification of red mud slurries when used alone or in combination with other chemistries. This paper summarizes further progress in this area. Efforts to explore the benefits of these new flocculants relative to those currently used in the industry and applications strategies to maximize their performance in combination with other flocculants will be discussed. The results of several plant evaluations will also be summarized.

#### 10:10 AM Break

#### 10:20 AM

Adsorption of Calcium on Red Mud and Gibbsite in the Bayer Process: Marie Raty<sup>1</sup>; *Kenneth T. Stanton*<sup>1</sup>; B. K. Hodnett<sup>1</sup>; M. Loan<sup>1</sup>; <sup>1</sup>University of Limerick, Matl. Sci. & Tech. Dept., Plassey Technological Park, Limerick Ireland

There is some evidence that calcium can be added to Bayer liquor in order to prevent scaling and losses of product in the mud circuit as calcium seems to modify gibbsite (Al2O3.3H2O) crystallisation. Calcium carbonate (CaCO3) was determined to have a solubility equilibrium from 5 to 30 ppm of Ca2+ in solutions of different causticity. Calcium adsorption on red mud and gibbsite surface was investigated. Results showed that Ca2+ adsorbed to a small degree on red mud surface (0.02 mg/g at equilibrium) and that the adsorption is at least ten times higher on gibbsite is similar to the dissolution rate of CaCO3 in the caustic solution at 70°C. This study shows that gibbsite has a pronounced affinity for calcium adsorption compared to red mud, although it is unclear at this stage how Ca2+ affects its growth rate.

#### 10:45 AM

Benefits of the Utilization of Cleaning Liquor in Red Side of CVG-Bauxilum: *Ricardo Alfredo Galarraga*<sup>1</sup>; Rodolfo José Díaz<sup>1</sup>; <sup>1</sup>CVG-Bauxilum, Gerencia de Producción, Zona Industrial Matanzas, Puerto Ordaz, Bolivar 8015 Venezuela

CVG-Bauxilum, in trying to reduce the maintenance costs and the cleaning time of equipment, has made changes to the original cleaning system with the purpose of obtaining a more versatile chemical cleaning system with caustic liquor to pipes and equipment with incrustations. The revised system has the possibility of making at least ten individuals circuits. The present work approaches mainly three topics: 1. comparison of costs between manual cleaning, cleaning with high pressure water and cleaning pipes with caustic liquor; 2. main circuits used to guarantee scale removal, higher levels of production and cur-

rent reliability of equipment; 3. previous analysis made in the laboratory to optimize and to guarantee results. The exact knowledge of the characteristics of material to remove, the magnitude of the incrustations in each one of the cases and the appropriate conditions of liquor for the effective accomplishment of the removal constitute essentially the beginning of this work.

#### 11:10 AM

Mechanochemistry and the Bayer Process of Alumina Production: Rakesh Kumar<sup>1</sup>; T. C. Alex<sup>1</sup>; M. K. Jha<sup>1</sup>; Z. H. Khan<sup>1</sup>; S. P. Mahapatra<sup>2</sup>; C. R. Mishra<sup>2</sup>; <sup>1</sup>National Metallurgical Laboratory, Nonferrous Process Div., Burmamines, Jamshedpur, Jharkhand 831007 India; <sup>2</sup>National Aluminium Company, P1, Nayapali, Bhubaneswar, Orissa 761013 India

The concept of mechanical activation has been applied to the traditional Bayer process of alumina production. The basic idea has been to achieve moderation in process conditions, reduce alumina and soda losses in the red mud, and alter the rheological character of red mud to improve its settling behaviour. The research pursued has primarily focussed on: (a) the particle breakage and structural changes in bauxite due to attrition milling; and (b) alumina recovery in simultaneous milling and leaching experiments. Particle breakage dominates during the initial stage (3-5 min) of the milling. Both XRD and TEM studies have indicated that the gibbsite present in the bauxite undergoes structural changes due to the milling. In typical 'simultaneous milling and leaching' experiments, it is found that almost all the alumina can be dissolved in alkali at 90°C after 15 minutes. Unlike the plant red mud, that was found to contain gibbsite as the dominant mineral, the solid residue produced in the laboratory experiments contained hematite as the dominant mineral.

#### 11:35 AM

**Preheators and Digestors in the Bayer Digestion Process:** Songqing Gu<sup>1</sup>; Zhonglin Yin<sup>1</sup>; <sup>1</sup>Zhengzhou Light Metal Research Institute, Chalco, No. 82 Jiyuan Rd., Shangjie Dist., Zhengzhou, Henan 450041 China

The existing preheaters and digesters applied in Bayer digestion processes are classified and investigated in this paper. The characteristics and mineral compositions of bauxite to be treated have great effects on the performance and operational efficiency of the preheaters and digesters. Therefore, the design concept and selection principle of Bayer digestion facilities and whole systems should be considered thoroughly on the basis of analysis of chemical and mineral compositions of bauxites and the results of studying behaviors of the minerals in bauxites in the preheating and digestion process.

#### **Aluminum Reduction - Potroom Improvements**

Sponsored by: Light Metals Division, LMD-Aluminum Committee Program Organizers: Alton T. Tabereaux, Alcoa Inc., Process Technology, Muscle Shoals, AL 35661 USA; Tom Alcorn, Noranda Aluminum Inc., New Madrid, MO 63869 USA

Monday AM	Room: 213D
March 15, 2004	Location: Charlotte Convention Center

Session Chair: Tom Alcorn, Noranda Aluminum Inc., New Madrid, MO 63869 USA

#### 8:30 AM

N

Automated Positioning of Prebaked Anodes in Electrolysis Cells, Part 1: Jean-Pierre Gagne<sup>1</sup>; Marc-Andre Thibault<sup>1</sup>; Robin Boulianne<sup>1</sup>; Gilles Dufour<sup>2</sup>; Gauthier Claude<sup>3</sup>; <sup>1</sup>Societe de Technologies de l'Aluminium STAS, 1846 rue outarde, Chicoutimi, Quebec Canada; <sup>2</sup>Alcoa Canada, 1 Place Ville Marie, Montreal, Quebec Canada; <sup>3</sup>Alcoa Canada, Aluminerie Deschambault, 1 Blvd. des Sources, Deschambault, Quebec Canada

During the production of aluminum in smelters, the anodes used in the electrolysis cells need to be frequently replaced. At the present time this is done manually, which not only is a most labour intensive task but also is subject to human error. Even though the operations are highly mechanized, human intervention is essential to ensure proper positioning of the anodes upon replacement (anode gaging). Even with the best trained operating crew, such an operation is prone to variability and lack of consistency given the number of people involved and the methods used. For the last two years, STAS and Alcoa Canada, have been working on the development of an automated system aimed at the vertical positioning of the carbon anodes upon their replacement on electrolysis cells. The control system is based on a precise measurement of the anodes and anode butts within the anode replacement cycle. The measurement system is relying upon the use of artificial vision. This paper will present the system developed by STAS and installed and tested on a pot tending machine at Alcoa Deschambault, Québec.

#### 8:55 AM

**Tomago Aluminum AP22 Project**: *Claude Vanvoren*<sup>1</sup>; Laurent Fiot<sup>2</sup>; Nigel Backhouse<sup>2</sup>; Chris Jamey<sup>2</sup>; <sup>1</sup>Aluminium Pechiney, Rsch. Ctr. LRF, BP 114, 73300 Saint Jean de Maurienne France; <sup>2</sup>Tomago Aluminum Company Pty Limited, Tomago Rd., Raymond Terrace, NSW 2325 Australia

Late April 2002, Tomago Aluminium announced the expansion of its production capacity by 70 000 tpy. This project is based on the AP22 Pechiney reduction cell technology, developped late 90's as reengineered technology for the well known AP18 cell. The project entered in its active phase early 2003 with the start up of a 20 pots trial section. Over and above the fine tuning of final operating setpoint, the purpose of this trial section is to pilot anode and anode assemblies transition phase, which, in such a large plant (3 potlines, 840 cells), requires to master both logistic and transient cell operating target. Progressive production increase will take place from 2004 and full production (530 000 tpy) is planned to be achieved in 2007 after lining turnover completion. Project progress, technical performance of the trial section as well as technical options on the cell and its surrounding will be discussed.

#### 9:20 AM

#### **Summer Potroom Efficiency Improvements**: Craig Anthony Lightle<sup>1</sup>; Mike Muncy<sup>1</sup>; Lon Ramsey<sup>1</sup>; John Browning<sup>1</sup>; Tom Saunders<sup>1</sup>; Chuck Tommey<sup>1</sup>; <sup>1</sup>Century Aluminum Corp, Ravenswood Reduction Plant, PO Box 98, Ravenswood, WV 26164 USA

In order for older U.S. reduction plants to remain in a competitive position, they must implement continuous improvement programs. At Century Aluminum of West Virginia, one program that has proven to be very successful and critical to making our operating plan has been "Victory Over Summer". Achieving monthly production and efficiency goals throughout the summer has always been difficult at the Ravenswood Facility due to excessively hot and humid conditions. Month goals have become tighter over the years and more critical to meet or exceed. As a result, a joint team of Potroom Operations and Potroom Technical personnel proposed a summer "campaign" focusing on maintaining and exceeding standard practices through increased monitoring and auditing, while also emphasizing early detection of operational concerns. This campaign due to measurable results has become a part of summer operation at the Ravenswood Facility. This presentation will outline the procedures utilized and the level of improvement attained.

#### 9:45 AM

**Exhaustion, Pneumatic Conveyor and Storage of Carbonaceous Waste Materials**: *Paulo Douglas S. de Vasconcelos*<sup>1</sup>; <sup>1</sup>Albras Alumínio Brasileiro S/A, Barcarena, Pará - Brazil, Rod. Pa 483 Km 21 - 68447-000

In smelters that use prebaked anodes, operations such as butt cleaning, butt and anode reject crushing and grinding, handling of coke packing material in the bake furnace, floor sweeping and discharge of dust from bake furnace cranes cause significant problems with the high generation of carbon dust and consequent environmental pollution. To control the dust pollution is a very difficult task. Another problem, meanwhile, is how to convey and store the dust collected. This paper presents the problem existing in the carbon plant of Albras, describing the pneumatic conveyor system developed by the Carbon Plant Engineering department, and the storage of the dust collected in the carbon plant. Examples of application of the system are the sale of carbon dust to the cement industry, or to generate steam for our alumina And/ or carbon plant in the future.

#### 10:10 AM Break

#### 10:20 AM

Experience with Power Saving in the Soderberg Lines at Hydro Aluminium Karmøy: *Knut A. Paulsen*<sup>1</sup>; Egil Furu<sup>1</sup>; Kristian Rolland<sup>1</sup>; *Ola Tratteberg*<sup>1</sup>; Marvin Bugge<sup>2</sup>; <sup>1</sup>Hydro Aluminium, Karmøy Plant, N-4265 Håvik Norway; <sup>2</sup>Norsk Hydro a.s, Rsch. Ctr., N-3901 Porsgrunn Norway

Due to very little rainfall during the fall of 2002, the water power production was severely reduced in Norway during the winter 2002/2003. The aluminium plants were asked to reduce their consumption. This paper describes the experiences gained in the Soderberg lines at Hydro Aluminium Karmøy when the line current was lowered from 135 kA and kept at 120 kA for a four months period. In order to save

additional energy the bath chemistry was adjusted to less surplus aluminiumfluoride and the cell voltage lowered considerably. Several challenges were initiated as the cells adjusted to the new heat balance situation. An immediate response from the cells was that the number of cathode failures/leakages and red-hot cathodeshieldspots dropped to zero. The side ledge thickness increased, particularly in the upper part. The super heat was lower, causing alumina dissolution problems and building up of heaps at the point feeding positions. This affected the anode effect frequency. Due to the adjusted bath chemistry with less aluminiumfluoride the temperature increased from 960-965 up to about 970°C, and above. A considerable decrease in dust and fluoride emissions was observed. Also, a decrease in the iron content in the metal produced was observed. The sodium content in the metal produced increased by 30% as the cell performance stabilized with low bath acidity. In the paper the experiences gained and the actions taken to cope with the operational challenges are discussed. During such an energy saving period, there are positive and negative effects observed. All three periods, the lowering of the current and energy input, the low energy period and the period bringing the cell lines back to normal current and production have their own challenges.

#### 10:45 AM

**Process Improvements to Raise the Line Current at Albras**: *Guilherme Epifânio da Mota*<sup>1</sup>; José Eduardo Macedo Blasques<sup>1</sup>; <sup>1</sup>ALBRAS - Alumínio Brasileiro S.A., Estrada PA 483 Km 21- Vila Murucupi, Barcarena, Pará 68447-000 Brasil

After the cut back made during the power-rationing period that occurred in Brazil in 2001, the Albras potlines were given current increases of up to 26 kA to reestablish and further increase metal production. During the ramping up period, problems with some equipments and process limitations were encountered. The dry scrubbers exhaustion rate reached the limit and the cell ACDs needed adjustment. With the line tending to heat up it was necessary to make key changes very quickly. Amongst these changes were a reduction in anode cover and a new audit practice in order to guarantee a better cover homogeneity, which would not compromise the anode consumption and the metal purity. Another implementation was the use of bath cavity cleaners during anode changes to facilitate reaching new ACD targets. This paper presents how the main process variables responded to the current increases and the new operational practices.

#### 11:10 AM

Experience with Booster Pots in the Prebake Line at Hydro Aluminium Karmøy: *Jørn Tonheim*<sup>1</sup>; Ove Kobbeltvedt<sup>1</sup>; Knut Arne Paulsen<sup>1</sup>; Marvin Bugge<sup>2</sup>; Sara Thornblad Mathisen<sup>2</sup>; <sup>1</sup>Hydro Aluminium Karmøy, N-4265 Håvik Norway; <sup>2</sup>Hydro Aluminium Porsgrunn, N-3901 Porsgrunn Norway

In September 1999 five booster pots were introduced in the Karmøy prebake line. These pots have been operated with 5.5 to 17.5 kA extra amperage, and are currently (June 2003) operated at 210 kA (which is +15.5 kA). The anode size and the stub size have been increased. Anodes with slots have been tested at both 204.5 kA and 210 kA. The pots were operated to 200 kA without modifications of the cathode lining. During September to November 2001 three pots were relined, and the cathode lining were modified. In January 2002 the current was increased to 210 kA. Two of the pots are still operated with the original cathode lining. The sideledge thickness has decreased in the test pots with old cathode lining. Operational performance has been good.

#### Automotive Alloys 2004: Session I

Sponsored by: Light Metals Division, LMD-Aluminum Committee Program Organizer: Subodh K. Das, Secat, Inc., Coldstream Research Campus, Lexington, KY 40511 USA

Monday AM	Room: 210A
March 15, 2004	Location: Charlotte Convention Center

Session Chair: Subodh K. Das, Secat Inc., Coldstream Rsch. Campus, Lexington, KY 40511 USA

#### 8:30 AM

Assuring Continued Recyclability of Automotive Aluminum Alloys: Chemical-Composition—Based Batching of Wrought Alloy Compositions from Al Scrap Shred Recovered from Nonmagnetic Shredder Fraction and AIVs: Adam Jan Gesing<sup>1</sup>; Benjamin AuBuchon<sup>1</sup>; Paul Torek<sup>1</sup>; Ron Dalton<sup>1</sup>; Richard Wolanski<sup>1</sup>; <sup>1</sup>Huron Valley Steel Corporation, 41000 Huron River Dr., Belleville, MI 48111 USA

There is continuing development at HVSC of recycling technologies needed to assure continued, high-value recyclability of all present and future automotive alloys - particularly wrought alloys as the use of these increases in the aluminum intensive vehicle (AIV). Here we add to our series of papers presenting the sort results from a prototype industrial sorter that uses laser induced breakdown spectroscopy (LIBS) to chemically analyze and sort each shredded scrap particle. This time we concentrate on the results that demonstrate the quality of the composition and the product recoveries that are achievable by the current prototype sorter sorting the Al shred recovered from both commercially available nonmagnetic shredder fraction and from the shredded AIVs.

#### 9:00 AM

Assuring Continued Recyclability of Automotive Aluminum Alloys: X-Ray-Absorption-Based Grouping of Light Metal Shredded Scrap: Adam Jan Gesing<sup>1</sup>; Tako P.R. de Jong<sup>2</sup>; Wijnand L. Dalmijn<sup>3</sup>; Richard Wolanski<sup>1</sup>; <sup>1</sup>Huron Valley Steel Corporation, 41000 Huron River Dr., Belleville, MI 48111 USA; <sup>2</sup>Delft University of Technology, Fac. of Civil Engrg. & Geoscis., Mijnbouwstraat 120, 2628 RX, Delft The Netherlands; <sup>3</sup>Delft University of Technology, Fac. of Mining & Petroleum Engrg., Mijnbouwstraat 120, 2628 RX, Delft The Netherlands

As the proportion of light metals used in automobile construction increases, so does the economic incentive to separate and group Al and Mg scrap recovered from shredded auto hulks into value-added alloy groupings. Dual-wavelength x-ray absorption imaging improved our ability to resolve small differences in material density, thickness and average atomic number. It is routinely applied to bone density scan measurements and to airport luggage inspection. In this paper we demonstrate the capability of the dual wavelength x-ray imaging technique to resolve differences between different light metal alloys in shredded metal scrap.

#### 9:30 AM

Processing and Properties of Ti-38-644 Alloy for Titanium Automotive Suspension Springs: Victor R. Jablokov<sup>1</sup>; J. Randolph Wood<sup>1</sup>; Brian G. Drummond<sup>2</sup>; <sup>1</sup>ATI Allvac, R&D, 2020 Ashcraft Ave., PO Box 5030, Monroe, NC 28111 USA; <sup>2</sup>ATI Allvac, Business Dvlp., 2020 Ashcraft Ave., PO Box 5030, Monroe, NC 28111 USA

The metastable beta titanium alloy Ti-38-644 has a long history of use for aerospace springs and fasteners. A vast range of mechanical properties is attainable for this alloy by manipulating the processing parameters and adjusting subsequent thermal treatments. The present work focuses on adjusting the thermomechanical processing procedures of Ti-38-644 to improve its viability and cost for the automotive suspension spring market. Particular attention has been given to cold drawing after the hot rolling process and conducting thermal aging treatments on the order of 30 minutes to 6 hours. Short aging times are less disruptive to the manufacturing cycle and offer the potential for elimination of post-process pickling procedures which are common for aerospace titanium spring parts. It is anticipated that the improved processing and associated cost reduction of Ti-38-644 will be beneficial for near-future automotive vehicle applications.

#### 9:55 AM

Synthesis of Closed-Cell Aluminum Microfoams: Halil Berberoglu<sup>1</sup>; Hélène Ruckebusch<sup>1</sup>; Jonathan Chang<sup>1</sup>; Aram Agrapetian<sup>1</sup>; Laurent Pilon<sup>1</sup>; <sup>1</sup>University of California, Mech. & Aeros. Engrg. Dept., 37-132 Engineering IV - Box 951597, Los Angeles, CA 90095-1597 USA

Aluminum foams have been identified as potential lightweight materials with adequate mechanical, thermal, and non-corroding properties to be used in various applications such as crash energy absorber, noise control, machine construction, sporting equipment, and biomedical applications. Aluminum foams should have controllable, homogeneous, and uniform morphology. However, current processes do not repeatedly produce metal foams with the desired characteristics. A novel technique for making closed-cell aluminum microfoams is presented. The process consists of stirring molten aluminum at highspeed in an inert atmosphere. During spinning, the inert gas is drawn into the aluminum melt and is broken into microscopic bubbles. These bubbles get trapped in the bulk in an orderly fashion as the melt solidifies.

#### 10:20 AM

Fatigue Life Prediction of Cast A356 Automotive Components: Jianzhang Yi<sup>1</sup>; Yunxin Gao<sup>1</sup>; Peter D. Lee<sup>1</sup>; Daan M. Maijer<sup>2</sup>; Harvey M. Flower<sup>1</sup>; Trevor C. Lindley<sup>1</sup>; <sup>1</sup>Imperial College London, Dept. of Matls., Prince Consort Rd., London SW7 2BP UK; <sup>2</sup>University of British Columbia, Dept. of Metals & Matls. Engrg., Frank Forward Bldg., 309-6350 Stores Rd., Vancouver V6T 1Z4 Canada

The fatigue design of cast components has traditionally been based on an extensive material property database together with experience from in-service performance. However, such an approach requires a significant amount of fatigue S-N testing in view of the complex shapes of cast components and the corresponding large variation in microstructures and defect populations. Also, this approach does not incorporate the flexibility necessary for product design optimisation. In the present study, a new methodology is proposed which allows prediction of fatigue life of automotive components made from cast aluminium-silicon alloys. Experimentally, a wide range of microstructure (secondary dendrite arm spacing) and defects (pores, inter-metallic particles) were introduced in a cast A356 aluminium-silicon alloy by using a wedge cast mould and carefully controlling the casting conditions and eutectic modifier addition. Analysis of experimental results and finite element analysis were used to identify the crack initiating defect and to characterise the development of fatigue damage including interactions between the different defect types. A fatigue life prediction model has been developed which relates porosity, eutectic modification and secondary dendrite arm spacing to fatigue life. This model was used in conjunction with finite element stress analysis to predict the fatigue life of a cast A356 brake calliper with reasonable correlation to experimental results.

#### 10:45 AM

Improvement in Bake Hardening Response of a Twin Roll Cast Al-Mg-Si Sheet: Yucel Birol<sup>1</sup>; Canan Inel<sup>2</sup>; <sup>1</sup>Marmara Research Center, Matls. & Chem. Tech. Rsch. Inst., Gebze, Kocaeli 41470 Turkey; <sup>2</sup>Assan Aluminum, Quality Sys. Lab., E-5 Karayolu 32. Km Tuzla, Istanbul Turkey

Body panel sheet is expected to have a low and stable yield strength in the as-delivered condition for easy stamping and a high yield strength after the paint bake cycle for high dent resistance required in service. The heat-treatable Al-Mg-Si aluminum alloys are increasingly used for automotive body panel applications owing to their ability to meet in large part, these conflicting demands. The age hardening potential of these alloys, however, can not be fully exploited in paint bake cycles at automobile plants due to the low temperatures and short times involved. Hence, the microstructure in the conventional T4 condition must be modified after the solution heat treatment so as to improve the aging kinetics and the paint bake response. The present work was undertaken to improve the paint bake response of a twin roll cast 6016 sheet. Different pre-aging treatments were employed and the critical process parameters were identified.

#### 11:10 AM

Aluminum High-Speed Train: Aureliu Panaitescu<sup>1</sup>; Augustin Moraru<sup>1</sup>; Alexandru Ionescu<sup>2</sup>; *Ileana Panaitescu*<sup>3</sup>; <sup>1</sup>"Politehnica" University of Bucharest, Elect. Engrg. Dept., Splaiul Independentei 313, Bucharest 060032 Romania; <sup>2</sup>Iveco Fiat, Torino Italy; <sup>3</sup>Isvor Fiat, Engrg. Processes & ICT, Corso Dante 103, Turin 10126 Italy

This paper distinguishes itself by focusing on a new high-speed public transportation system and not on the aluminum alloys used for its construction. There are many regions around world where the transportation problem between far urban locations might be solved with high-speed trains (v > 190-250 mph) safe in operation and non-polluting. The expectations for the linear motor trains with magnetic levitation didn't prevail commercially even in recent days. The vehicle here presented may become, we believe, a very convenient solution because its constructive simplicity and the acceptable investments needed for its construction; should be of great interest for both the aluminum alloys producers and the engineers involved within the ground transportation. There are presented the main operation characteristics and compared with the French high speed train characteristics (TGV).

#### 11:35 AM

Infrared Imaging Investigation of Foam Removal Mechanism in Lost Foam Aluminum Process: *Qi Zhao*<sup>1</sup>; *Thomas W. Gustafson*<sup>2</sup>; <sup>1</sup>Metal Casting Technology, 127 Old Wilton Rd., Milford, NH 03055 USA; <sup>2</sup>General Motors, GM Powertrain/CDVC, 1629 N. Washington Ave., Saginaw, MI 48605-5073 USA

A high-speed infrared camera was used to measure and record variations in thermal profile across the surfaces of ceramic coating coated foam plates during the lost foam aluminum casting. The real time images were analyzed to gain the insight of the process fundamentals. The results were compared with the observations in the past vacuumassisted foundry experiments. The process kinetics information acquired from the real time IR imaging verified that foam removal in the lost foam aluminum casting, regardless vacuum-assisted or gravity

# Beyond Nickel-Base Superalloys: Superalloys and Niobium Silicides

Sponsored by: Structural Materials Division, SMD-Corrosion and Environmental Effects Committee-(Jt. ASM-MSCTS), SMD-High Temperature Alloys Committee, SMD-Mechanical Behavior of Materials-(Jt. ASM-MSCTS), SMD-Refractory Metals Committee *Program Organizers*: Joachim H. Schneibel, Oak Ridge National Laboratory, Oak Ridge, TN 37831-6115 USA; David A. Alven, Lockheed Martin - KAPL, Inc., Schenectady, NY 12301-1072 USA; David U. Furrer, Ladish Company, Cudahy, WI 53110 USA; Dallis A. Hardwick, Air Force Research Laboratory, AFTL/MLLM, Wright-Patterson AFB, OH 45433 USA; Martin Janousek, Plansee AG Technology Center, Reutte, Tyrol A-6600; Yoshinao Mishima, Tokyo Institute of Technology, Precision and Intelligence Laboratory, Yokohama, Kanagawa 226 Japan; John A. Shields, HC Stark, Cleveland, OH 44117 USA; Peter F. Tortorelli, Oak Ridge National Laboratory, Oak Ridge, TN 37831-6156 USA

 Monday AM
 Room: 211B

 March 15, 2004
 Location: Charlotte Convention Center

Session Chairs: Yoshinao Mishima, Tokyo Institute of Technology, Dept. of Matls. Sci. & Engrg., Yokohama, Kanagawa 226-8502 Japan; Peter F. Tortorelli, Oak Ridge National Laboratory, Metals & Ceram. Div., Oak Ridge, TN 37831 USA

## 8:30 AM Introduction - by Joachim H. Schneibel

#### 8:45 AM Invited

Superalloys: Evolution and Revolution for the Future: *Hiroshi Harada*<sup>1</sup>; 'NIMS, High Temp. Matls. 21 Project, Sengen 1-2-1, Tsukuba Science City, Ibaraki 305-0047 Japan

The temperature capability of Ni-base superalloys has been improved by more than 300C since the invention in early 1940's. Despite a view that the superalloy has reached its limitation in temperature capability, recent efforts of alloy development are again lifting up the temperature capability, e.g., fourth generation superalloys with platinum group metals (Ru or Ir) additions capable up to 1100C, suggesting further evolutions in future. Also, platinum group metals base superalloys, namely, refractory superalloys, proposed by the author and some of his group members have resulted in revolutionary improvements in temperature capability, reaching 1800C. This paper describes the present status of the superalloy developments and tries to provide a view of the future possibilities.

#### 9:15 AM

Effect of Ru on Elemental Partitioning Behaviour and Phase Stability of Ni-Based Superalloys: An-Chou Yeh<sup>1</sup>; Sammy Tin<sup>1</sup>; <sup>1</sup>University of Cambridge, Rolls-Royce Univ. Tech. Ctr., Dept. of Matls., New Museum Site, Pembroke St., Cambridge UK

Nickel-base single crystal superalloys are predominately used as materials for turbine blades in aero-engines because of its excellent mechanical properties at elevated temperatures. Due to the elevated levels of refractory alloying additions, precipitation of intermetallic Topologically-Close-Packed (TCP) phases that eventually degrade the mechanical properties occurs after prolonged exposure at elevated temperatures. Recent studies have shown that additions of the platinum group metal; ruthenium offers the possibility to increase the stability of the microstructure and creep resistance of this class of alloys at high temperatures. The present investigation carefully details the influence of Ru on the stability and elemental partitioning behaviour of Ni-base superalloys. Microstructures in both as-cast and solution-treated conditions were carefully characterized, and Electron-Probe Micro-Analysis was performed to study the elemental segregation behaviour in as-cast samples. Compositional differences between the g-g' phases were quantified using a variety of chemical analysis techniques. The long-term phase stability of the alloys was investigated over a wide range of thermal exposures and TEM analysis was performed to identify the various TCP phases present in Ru-containing alloys. Underlying mechanisms of how ruthenium addition improves the properties of Ni-based superalloys are discussed.

#### 9:30 AM

Microstructures and Mechanical Properties in Ni<sub>3</sub>Al-Ni<sub>3</sub>Ti-Ni<sub>3</sub>V-Based Multi-Intermetallic Alloys: *Takayuki Takasugi*<sup>1</sup>; Yoshinari Nunomura<sup>1</sup>; Yasuyuki Kaneno<sup>1</sup>; <sup>1</sup>Osaka Prefecture University, Dept. of Metall. & Matls. Sci., 1-1 Gakuen-cho, Sakai, Osaka 599-8531 Japan

The phase relation, microstructures, high-temperature deformation and oxidation behavior of intermetallic alloys based on Ni<sub>3</sub>Al-Ni<sub>3</sub>Ti-Ni<sub>3</sub>V pseudo-ternary alloy system were investigated. As the constituent intermetallic phases, L12(Ni3Al), D024(Ni3Ti), D022(Ni3V) and hcp(Ni<sub>3</sub>Ti<sub>0.65</sub>V<sub>0.35</sub>) were identified at 1273K, and then their phase fields were discussed, based on the electrical and geometrical factors of constituent atoms. Among four intermetallic phases, five kinds of twophase relations and two kinds of three-phase relations were found to exist. Also, D024(Ni3Ti) phase extended up to concentration field in which a majority of constituent Ti elements were replaced by Al and V elements. The prepared alloys exhibited widely different microstructures, depending on the number and the kind of the constituent intermetallic phases, and also heat trea tment. Particularly, the alloys which contain low Ti content and have bi-modal three-phase fine microstructures composed of L12(Ni3Al), D024(Ni3Ti) and D022(Ni3V) showed extremely superior high-temperature strength and ductility, and also reasonable corrosion and oxidation properties.

#### 9:45 AM

**Oxidation Resistance - One Barrier to Moving Beyond Ni-Base Alloys:** *Bruce A. Pint*<sup>1</sup>; Ian G. Wright<sup>1</sup>; <sup>1</sup>Oak Ridge National Laboratory, Metals & Ceram., 1 Bethel Valley Rd., MS 6156, Oak Ridge, TN 37831-6156 USA

The implementation of new high-temperature materials is often hampered by their lack of oxidation or environmental resistance. In fact, this failing is one of the strongest barriers to moving beyond Nibase superalloys. In practice, high-temperature alloys have at least reasonable, inherent oxidation resistance. In the case of the current generation of superalloys, these alloys have sufficient oxidation resistance to provide limited protection but, for reliable maximum-temperature operation, they are coated with an oxidation-resistant metallic coating and an outer ceramic thermal barrier layer. In the materials development process, the considerations of microstructural and compositional demands to provide increased high-temperature strength are paramount, and result in the needs for oxidation resistance, along with other realities, being given minor attention. The assumption made is that an oxidation-resistant coating will be available to protect these substrates. For many systems, this assumption is seriously flawed as interactions with the substrate or mechanical degradation of the coating lead to insufficient reliability for critical components. Examples are given for currently-used materials and materials classes with critical oxidation resistance problems.

#### 10:00 AM Break

#### 10:30 AM

**Computational Design of Oxidation Resistant Niobium Alloys**: John E. Morral<sup>1</sup>; Yunzhi Wang<sup>1</sup>; <sup>1</sup>Ohio State University, Matls. Sci. & Engrg., 2041 College Rd., Columbus, OH 43210 USA

Computer software is now available that can predict the microstructural evolution that accompanies gas-solid reactions. Accordingly, with the proper databases the software could predict whether or not an alloy will form a protective oxide film on the surface of an alloy. Using the niobium system as an example, it will be shown how calculated phase diagrams, diffusion constants and the assumptions of "local equilibrium" and "zero stress" can be combined to screen which combination of two, three, or more elements in niobium is likely to form a protective alumina scale. Further screening is possible via phase field modeling in which both non-equilibrium and the formation of residual stresses can be considered.

#### 10:45 AM

Influence of Microstructure on High Temperature Oxidation in Multicomponent Nb Alloys: Sarath K. Menon<sup>1</sup>; Triplicane A. Parthasarathy<sup>1</sup>; Madan G. Mendiratta<sup>1</sup>; <sup>1</sup>UES Inc., Matl. Procg. Div., 4401 Dayton-Xenia Rd., Dayton, OH 45432-1894 USA

Nb-based metal/silicide alloys (Nb-Ti-Si-Cr-Al-Hf-Sn) are being explored to extend the temperature capability of the current Ni-based superalloys in jet engines. One of the serious concerns in the application of Nb based alloys is their poor oxidation resistance at elevated temperatures. In this paper an overview of the high temperature oxidation resistance of these multiphase alloys will be provided. These alloys contain a distribution of the Nb<sub>5</sub>Si<sub>3</sub> phase in  $\beta$  matrix. The Nb-Si phase diagram is characterized by a high temperature eutectoid reaction, Nb<sub>3</sub>Si >  $\beta$  + Nb<sub>5</sub>Si<sub>3</sub>, however the reaction has been found to be extremely sluggish. Our studies on ternary Nb-Si-Ti alloys have shown that this eutectoid reaction had occurred to completion in some ternary alloys indicating that the extremely sluggish eutectoid reaction had been considerably accelerated with the addition of Ti. The eutec-

#### 11:00 AM

Chlorination of Mo-Nb-Si-B intermetallic Alloys to Improve Oxidation Resistance: Vikas Behrani<sup>1</sup>; Andrew J. Thom<sup>1</sup>; Matthew J. Kramer<sup>1</sup>; Mufit Akinc<sup>1</sup>; <sup>1</sup>Iowa State University, Ames Lab., Matls. Chmst./Dept. of Matls. Sci. & Engrg., Spedding Hall, Ames, IA 50011 USA

Recent studies showed that quaternary Mo-Nb-Si-B system is not oxidation resistant. The difference in oxidation resistance between Mo-Si-B and Mo-Nb-Si-B may be interpreted in terms of the volatility of the oxide. Chlorination is a novel processing technique to selectively remove Nb2O5 from the scale as volatile NbCl5. This work studied the chlorination of oxidized Mo-Nb-Si-B alloy of nominal composition 63(Nb,Mo)-30Si-7B;Nb/Mo=1 (at%) comprised of three phase microstructure of (Nb,Mo)5Si3Bx(T1)-(Nb,Mo)5(Si,B)3(T2)-(Nb,Mo)5Si3Bx(D88). Oxidation behavior of these alloys in air has been studied before and after chlorination. Results show that Nb2O5 can be selectively removed from scale leaving a borosilicate rich scale. Linear oxidation rate of the chlorinated alloys were reduced by up to ~3 times no-treated alloy under identical conditions. Chlorination will form a dense scale after heat treatment at 1000°C in argon. Microstructure analysis shows that borosilicate glass reflowed to fill voids created by v olatilized Nb2O5, thus reducing oxidation rate.

#### 11:15 AM

Oxidation Behavior of the Multi Component Nb-Si-Ti-Al-Cr-X Alloys for High Temperature Aeroengine Applications: *Raghvendra Tewari*<sup>1</sup>; Hyojin Song<sup>1</sup>; Amit Chatterjee<sup>2</sup>; P. I. Rosales<sup>1</sup>; Vijay K. Vasudevan<sup>1</sup>; <sup>1</sup>University of Cincinnati, Dept. of Chem. & Matls. Engrg., Cincinnati, OH 45221-0012 USA; <sup>2</sup>Rolls-Royce Corporation, 2001 S. Tibbs Ave., Indianapolis, IN 46241 USA

Nb-based silicides possess a good combination of properties which make them potential materials for high temperature applications. However, these silicides exhibit poor oxidation at elevated temperatures. Present paper reports the oxidation behavior of the multi-component Nb-Si-Ti-Al-Cr-X alloys. The as cast specimens which have been oxidized at different temperatures, showed the presence of two types of oxides under cyclic as well as static conditions. The chemical composition and in depth profile analysis of the oxide layer have shown presence of different oxides scales. Cross sectional examination of oxides has revealed cracks in the oxide layer and deep penetration of oxygen in to the matrix phase. Elemental mapping of these oxides have clearly revealed that many elements, like Cr, Si, do not constitute substantially into the oxide layer. XPS results showed different oxidation states of the Ti and Al elements indicating a complex nature of the oxide. Based on these observations, a possible mechanism of oxidation of these alloys has been proposed.

#### 11:30 AM

Study of the Effects of Cr, Al and Ta Additions on the Microstructure and Oxidation Behaviour of Nb-Silicide Based In Situ Composites: Kostas Zelenitsas<sup>1</sup>; Panayiotis Tsakiropoulos<sup>1</sup>; <sup>1</sup>University of Surrey, Sch. of Engrg., Mech. & Aeros. Engrg., Metall. Rsch. Grp., Guildford, Surrey GU2 7XH England

Niobium silicide based in situ composites have been designed to study the synergistic effects of Cr, Al and Ta on phase selection in Nb-Ti-Si alloys in the as solidified condition and after heat treatment. The alloys were prepared using clean melting and casting in water-cooled copper crucibles/moulds. Tantalum offers solid solution strengthening and Cr and Al play important roles in phase selection and oxidation behaviour. In our study particular attention has been paid to segregation phenomena in ingots and on phase equilibria involving the Nbss and the Nb3Si, Nb5Si3 and Laves phases. Selected alloys have also been evaluated for their oxidation behaviour using isothermal oxidation tests that cover the whole range from pest, to intermediate to high temperature oxidation. The results of microstructural characterization using XRD, EPMA and TEM will be presented and discussed together with preliminary results of our oxidation studies.

#### 11:45 AM

Applicability of Mo(Si,Al)2-Base Oxidation Resistant Coating Onto Nb-Base Structural Materials: *Tatsuo Tabaru*<sup>1</sup>; Jin-Hak Kim<sup>1</sup>; Kazuhisa Shobu<sup>1</sup>; Michiru Sakamoto<sup>1</sup>; Hisatoshi Hirai<sup>1</sup>; Shuji Hanada<sup>2</sup>; <sup>1</sup>National Institute of Advanced Industrial Science and Technology, Inst. for Structural & Engrg. Matls., 807-1 Shuku, Tosu, Saga 841-0052 Japan; <sup>2</sup>Tohoku University, Inst. for Matls. Rsch., 2-1-1 Katahira, Aoba, Sendai, Miyagi 980-8577 Japan

Applicability of Mo(Si,Al)<sub>2</sub>-base oxidation resistant coating for Nb-base materials were investigated focusing on the oxidation resistance, thermal expansion behavior and interfacial stability with Nb. Mo(Si,Al)<sub>2</sub> with various substitution ratios of Al for Si exhibit a good oxidation resistance due to a protective alumina scale formation at temperatures up to 1673 K, and the parabolic rate constants are an order lower than that for NiAl. Average coefficients of thermal expansion (CTEs) between 298 and 1723 K are (9.2~10.5) x 10<sup>-6</sup> /K, while those for some Nb alloys are (8.2~8.7) x 10<sup>-6</sup> /K. The satisfactory oxidation resistance and small CTE mismatch with Nb suggest that Mo(Si,Al)<sub>2</sub> is a promising candidate for the oxidation resistant coating on Nb-base materials. Joining of Mo(Si,Al)<sub>2</sub> and Nb-base alloys, however, forms an diffusion-reaction layer consisting of Nb<sub>5</sub>Si<sub>3</sub> and Mo<sub>5</sub>Si<sub>3</sub>. Effect of an interlayer to suppress such reaction-layer formation is also described.

#### Bulk Metallic Glasses: Processing I

Sponsored by: Structural Materials Division, ASM International: Materials Science Critical Technology Sector, SMD-Mechanical Behavior of Materials-(Jt. ASM-MSCTS) Program Organizers: Peter K. Liaw, University of Tennessee,

Department of Materials Science and Engineering, Knoxville, TN 37996-2200 USA; Raymond A. Buchanan, University of Tennessee, Department of Materials Science and Engineering, Knoxville, TN 37996-2200 USA

Monday AM	Room: 209A
March 15, 2004	Location: Charlotte Convention Center

Session Chairs: Raymond A. Buchanan, University of Tennessee, Matls. Sci. & Engrg., Knoxville, TN 37996-2200 USA; Daniel Miracle, Air Force Research Laboratory, Matls. & Mfg. Direct., Wright-Patterson AFB, OH 45433 USA

#### 8:30 AM Invited

Principles for the Constitution, Structure and Stability of Metallic Glasses: Daniel Miracle<sup>1</sup>; Oleg Senkov<sup>2</sup>; Stephane Gorsse<sup>3</sup>; Wynn S. Sanders<sup>1</sup>; Kevin Kendig<sup>1</sup>; <sup>1</sup>Air Force Research Laboratory, Matls. & Mfg. Direct., 2230 Tenth St., Wright-Patterson AFB, OH 45433 USA; <sup>2</sup>UES, Inc., 4401 Dayton-Xenia Rd., Dayton, OH USA; <sup>3</sup>University of Bordeaux, ICMCB, Bordeaux France

The current understanding of the stability of metallic glasses relies heavily upon empirical ideas such as electron-to-atom ratio and the number of constituents, or upon isolated models based on features such as atom size, enthalpy of mixing, or reduced glass transition temperature. There is at present no clear rationale for determining the relative importance of these models, or for providing a credible link between these separate concepts. The objective of this presentation will be to highlight recent developments in the understanding of principles that influence the constitution, structure and stability of metallic glasses, and to describe an approach to unify these ideas into a single conceptual framework. Modification of an earlier model based on atomic level lattice strains will be combined with the more recent principle of efficient atomic packing to provide specific insight into the composition and local atomic structure of metallic glasses. Although earlier efforts to relate thermodynamic quantities to glass formability via simple relationships have been shown to be inadequate, a new methodology will be developed that provides a direct quantitative link between traditional thermodynamic quantities and atomic size. Together, the principles of atomic level strains, efficient atomic packing and thermodynamic modeling will be shown to provide a unified framework to more clearly understand the constitution, structure and stability of metallic glasses.

#### 8:55 AM Invited

A Guide to Optimum Compositions for Bulk Metallic Glass Formation: Z. P. Lu<sup>1</sup>; C. T. Liu<sup>1</sup>; 'Oak Ridge National Laboratory, Metals & Ceram. Div., Oak Ridge, TN 37831 USA

In the development of new bulk metallic glasses (BMGs) and other non-crystalline materials, it is vitally important for us to understand the nature of glass formation and know how to locate optimum compositions for glass formation. Considerable efforts have been devoted to this area; however, no reliable approaches have been developed to analyze the glass-forming ability (GFA) for various materials. In this study, a comprehensive expression to predict glass forming ability for various glass-forming systems,  $\lambda = T_x/(T_g+T_l)$ , has been derived from characteristic features of TTT (time-temperature-transformation) curves with considerations of all transformation kinetics, wherein  $T_{\star}$  is the crystallization temperature, Tg is the glass transition temperature and  $T_1$  is the liquidus temperature. This approach is not only verified by Fe-based glass-forming alloys developed recently but also strongly supported by the experimental data reported by other groups for various metallic glass systems. The current physical metallurgy approach will also help us attain a comprehensive understanding of the nature of glass formation from a basic science standpoint, and paves a new avenue in synthesizing novel bulk metallic glasses.

#### 9:20 AM

**Thermal Tempering of Bulk Metallic Glasses - I: Modeling:** *Cahit C. Aydiner*<sup>1</sup>; Ersan Ustundag<sup>1</sup>; <sup>1</sup>Caltech, Matls. Sci., MC 138-78, Pasadena, CA 91125 USA

Recently developed bulk metallic glasses (BMGs) possess exceptional glass formation ability and can be processed into large dimensions. This, however, can generate large residual stresses. The BMG processing typically involves casting an alloy into a thin-walled mold followed by severe quenching. This procedure leads to large thermal gradients due to the low thermal conductivity of BMG. In addition, the alloy experiences large changes in its viscosity within a small temperature range during glass transition. All of these parameters lead to 'thermal tempering' which generates compressive surface residual stresses balanced with mid-tension. We have modeled the development of these stresses using several approaches: (i) instant freezing model; (ii) viscoelastic model; and (iii) structural model. The results show that significant surface residual stresses approaching several hundred MPa can be generated in typical BMG specimens. The predictions of these models will be compared with each other and with experimental data.

#### 9:45 AM

Thermal Tempering of Bulk Metallic Glasses - II: Residual Stress Measurements: Cahit C. Aydiner<sup>1</sup>; Ersan Ustundag<sup>1</sup>; <sup>1</sup>Caltech, Matls. Sci., MC 138-78, Pasadena, CA 91125 USA

Bulk metallic glasses (BMGs) can be processed into large dimensions by casting into a thin-walled mold followed by severe quenching. This procedure leads to large thermal gradients due to the low thermal conductivity of BMG. In addition, the alloy experiences large changes in its viscosity within a small temperature range during glass transition. All of these lead to 'thermal tempering' which generates compressive surface residual stresses balanced with mid-tension. Since neither photoelasticity nor diffraction can be applied to BMGs, we employed a mechanical relaxation method, the crack compliance (slitting) technique which yielded excellent accuracy and spatial resolution. It will be shown that surface compression in excess of 300 MPa can be generated in BMGs under certain processing conditions. Then, results from bending experiments will be discussed about the effects of such high residual stresses on the mechanical properties of BMGs. The results will also be compared to modeling predictions.

#### 10:10 AM

Stability of Ni-Based Bulk Metallic Glasses: *Michelle L. Tokarz*<sup>1</sup>; Scott Speakman<sup>2</sup>; E. Andrew Payzant<sup>2</sup>; Wallace Porter<sup>2</sup>; John C. Bilello<sup>1</sup>; <sup>1</sup>University of Michigan, Matls. Sci. & Engrg., 3062 H H Dow Bldg., Ann Arbor, MI 48109 USA; <sup>2</sup>Oak Ridge National Laboratory, High Temp. Matls. Lab., PO Box 2008, MS6064, Oak Ridge, TN 37831-6064 USA

Ni-based bulk metallic glasses of varying concentrations were studied in order to understand their stability at elevated temperatures. The x-ray scattering patterns of several of these metallic glasses showed evidence of intermediate range order, which is atypical. This study explores the connection between this order and the subsequent phase transformations that occur at elevated temperatures. DSC scans provided glass transition temperatures, which were used as a reference. A number of x-ray diffraction patterns were obtained at constant temperatures below Tg, (for times from 5 to 36 hours). These showed the appearance and growth of crystalline peaks. Additionally, the characteristics of the amorphous scattering signal changes, during an isothermal hold, were tracked. Further experiments were performed on polished samples to distinguish any potential surface effects. Finally, these data are compared to those obtained from Vitreloy-106 (a well characterized traditional bulk metallic glass) such that differences can be identified and understood.

#### 10:35 AM

Glass Forming Ability and Thermal Stability of a Ti Containing Zr-Based Bulk Amorphous Alloy: Jun Shen<sup>1</sup>; <sup>1</sup>University of Sydney, CAMT, Sch. of Aeros., Mech. & Mechatronic Engrg., Sydney, NSW 2006 Australia

The apparent activation energies for crystallization of bulk Zr59Cu18Ni13A110 and Zr56.6Cu17.3Ni12.5Al9.6Ti4 alloys are Ec??295.6kJ/mol and Ec??248.5kJ/mol?Crespectively. The crystallization kinetics of bulk Zr56.6Cu17.3Ni12.5Al9.6Ti4 amorphous alloy is composed of two stages, in each stage the Avrami exponent is around 1.0?'2.5, indicating that the crystallization is controlled by limit nucleation and steady growth process. While the activation energy for nucleation and growth for bulk Zr56.6Cu17.3Ni12.5Al9.6Ti4 alloy are 364.8kJ/mol and254.6kJ/mol, respectively. It can be therefore concluded that the addition of Ti to bulk Zr-Cu-Ni-Al amorphous alloy has a role of suppressing the nucleation process on one hand, which is in favor of promoting GFA. On the other hand, the crystallization process is accelerated by Ti addition and consequently resulting in lowering of the stability of the amorphous phase.

#### 11:00 AM

The Thermal Stability of Zr-Cu-Ni-Ti-Be-Y Bulk Metallic Glasses: *Chun Huei Tsau*<sup>1</sup>; <sup>1</sup>Chinese Culture University, Inst. of Matls. Sci. & Mfg., 1, No, 55 Hwa Kang Rd., Yang Ming Shan, Taipei Taiwan

Five compositions of Zr-Cu-Ni-Ti-Be-Y amorphous alloys with 3 mm in thickness were made by arc-melting and die-casting processes. The thermal properties and mechanical properties of these alloys were examined and calculated their transformation temperature and activation energies. Results revealed that the increasing of content of Be could increase both of the Tx and ?'T (?'T=Tx-Tg). These exhibited that increasing the content of Be resulted in increasing the glass formability of the alloys in the present study. The hardness of these alloys at amorphous and crystallizing states was about 500 DPH and 450DPH, respectively. Compositions had no significantly effect on the hardness of these alloys. In addition, the alloys with the content of Be more than 20 at.% would crystallize while they annealed at elevated temperature for several hours, even though the annealing temperature was below the Tx point.

#### 11:25 AM Invited

Mg-Based Bulk Metallic Glass Composites with Plasticity and High Strength: Jian Xu<sup>1</sup>; Han Ma<sup>1</sup>; Evan Ma<sup>2</sup>; <sup>1</sup>Chinese Academy of Sciences, Inst. of Metal Rsch., Shenyang Natl. Lab. for Matls. Sci., 72 Wenhua Rd., Shenyang, Liaoning 110016 China; <sup>2</sup>Johns Hopkins University, Dept. of Matls. Sci. & Engrg., Baltimore, MD 21218 USA

Composite alloys of  $(Mg_{0.65}Cu_{0.075}Ni_{0.075}Zn_{0.05}Ag_{0.05}Y_{0.1})_{100-x}Fe_x(x=9,13)$ have been produced through copper mold casting, based on a good bulk metallic glass former and a new composite design scheme. Upon cooling the melt, an  $\alpha$ -Fe solid solution precipitates uniformly with sizes in the 1 to 8  $\mu$ m range while the remaining melt undergoes a glass transition to yield the in situ composite. Compressive strength of the composite approaches 1 GPa, a factor of 1.6 higher than the single-phase metallic glass. In contrast to all the previous Mg-based monolithic glasses that always fail in the elastic regime, a plastic strain to failure of the order of 1% was obtained for the composite. We used a new BMG composite design scheme that takes advantage of the immiscibility of the components. It is the first time that the very brittle Mgbased BMGs have ever exhibited usable plasticity.

## Carbon Technology: Cathode Material and Corrosion

Sponsored by: Light Metals Division, LMD-Aluminum Committee Program Organizers: Markus Meier, R&D Carbon, Sierre CH 3960 Switzerland; Amir A. Mirchi, Alcan Inc., Arvida Research and Development Centre, Jonquiere, QC G7S 4K8 Canada; Alton T. Tabereaux, Alcoa Inc., Process Technology, Muscle Shoals, AL 35661 USA

Monday AM	Room: 213A
March 15, 2004	Location: Charlotte Convention Center

Session Chair: Stefan A. Vogt, Alcoa Aluminio Espanol, San Ciprian (Lugo) 27890 Spain

#### NOTE: Session begins at 10:20 AM

10:20 AM

<sup>3-</sup>D Modelling of Thermal and Sodium Expansion in Soderberg Aluminium Reduction Cells: Yang Sun<sup>1</sup>; Karl G. Forslund<sup>2</sup>; Morten

**MONDAY AM** 

Sørlie<sup>3</sup>; Harald Oye<sup>1</sup>; <sup>1</sup>Norwegian University of Science and Technology, Dept. of Matls. Tech., Trondheim 7491 Norway; <sup>2</sup>Elkem Aluminium ANS Lista, PO Box 128, Farsund N-4551 Norway; <sup>3</sup>ELKEM ASA Aluminium Research, PO Box 8040, Vagsbygd 4675 Norway

A three dimensional transient mathematical model of a Soderberg aluminium reduction cell was developed to study cathode changes during heat up and early operation by using the ANSYS program. In this nonlinear finite element model, material non-linearity and the influence of temperature on the material's mechanical properties were taken into account. First thermal field distribution and sodium concentration distribution in the cathode carbon block with time were calculated, and then the stress distribution and deformation were calculated and analyzed. Points where the construction should be strengthened and area of high stress are pointed out. It is also shown that thermal excursions and sodium expansion can cause a gap under the cathode carbon block, allowing bath to fill the void and reacting with the refractory to crystalline compounds, result in a push-up of the cathode carbon block that may result in a permanent bottom heave over time.

#### 10:45 AM

Cathode Quality Improvement by Application of an Intensive Homogenizer for Green Mix Preparation: Frank Hiltmann<sup>1</sup>; Johann Daimer<sup>1</sup>; Berthold Hohl<sup>2</sup>; Roman Nowak<sup>3</sup>; Janusz Tomala<sup>3</sup>; <sup>1</sup>SGL Carbon GmbH, Griesheim Plant, Frankfurt 65933 Germany; <sup>2</sup>Maschinenfabrik Gustav Eirich, Hardheim 74732 Germany; <sup>3</sup>ZEW S.A., a member of SGL Carbon Group, Raciborz 47-400 Poland

As a part of the continuous quality improvement program of SGL CARBON's Racibórz facility, the process unit steps in the green shop were analysed and a potential for further process efficiency and product homogeneity improvement attributed to the existing green mix buffer silo. ZEW has successfully commissioned a batchwise-operated EIRICH mixer DW 29/4 as a homogenizer, downstream of the existing sigma-blade kneading mixers. As the homogenizer allows to control feeding of the vibrocompacting mould as well, the existing intermediate silo could be replaced. After an installation period of only four weeks, the redesigned paste mixing line came into operation. Compared to the original situation, the green plant now shows a significantly better performance in terms of stability of green production process and product characteristics. This paper presents the technical solution and the operational results before and after the start-up of the new equipment.

#### 11:10 AM

**Erosion Rate Testing of Graphite Cathode Materials**: *Siegfried Wilkening*<sup>1</sup>; Pierre Reny<sup>2</sup>; <sup>1</sup>Hydro Aluminium T & P, PO Box 2468, Bonn 53014 Germany; <sup>2</sup>Aluminery Alouette Inc., Case postale 1650, Sept Iles (Quebec) G4R5M9 Canada

The operational advantages of graphite cathode blocks in highamperage aluminium reduction cells are accompanied by an increased and uneven wear phenomenon. By means of a laboratory testing method it could be shown that the graphite erosion rate depends on the AIF3 content of the electrolytic melt and the current density. A decrease in the erosion rate can be achieved by the intercalation of durable and densifying coke residues from pitch and resin impregnation in the open pore structure of the graphite blocks. The deposition of some finely dispersed TiO2 in the graphite pores reduces the erosion rate significantly.

#### 11:35 AM

Variable Resistivity Cathode Against Graphite Erosion: Jean Michel Dreyfus<sup>1</sup>; Loig Rivoaland<sup>1</sup>; Serge Lacroix<sup>1</sup>; <sup>1</sup>Carbone Savoie-LRE, BP 16, Venissieux Cedex 69631 France

Pre-baked electrolysis cells equipped with graphite cathodes exhibit a reduction in lifetime compared to cells built with graphitic grades. This limitation is clearly related today to a wear mechanism induced by an electrochemical reaction. The importance of the current density peak on the wear celerity has been highlighted and led to the development of new concepts aimed at a better balance of the current density in the cell. The variable resistivity graphite cathode is one of the most promising ways, which can be offered by the cathode supplier. The actual technology development, resistivity pattern, current peak balance and erosion rate improvements are discussed through simulation models, products properties and in situ erosion measurements.

#### Cast Shop Technology: Melting and Refractories

Sponsored by: Light Metals Division, LMD-Aluminum Committee Program Organizers: Corleen Chesonis, Alcoa Inc., Alcoa Technical Center, Alcoa Center, PA 15069 USA; Jean-Pierre Martin, Aluminum Technologies Centre, c/o Industrial Materials Institute, Boucherville, QC J4B 6Y4 Canada; Alton T. Tabereaux, Alcoa Inc., Process Technology, Muscle Shoals, AL 35661 USA

Monday AM	Room: 213B/C
March 15, 2004	Location: Charlotte Convention Center

*Session Chairs:* Pierre Proulx, Universite de Sherbrooke, Chem. Engrg., Sherbrooke, Quebec J1K 2R1 Canada; Chris Bickert, Pechiney Group, Neuilly Sur Seine 92200 France

#### NOTE: Session begins at 8:55 AM

#### 8:55 AM

Energy Efficiency Tests in Aluminum Combination Melting and Holding Furnaces: Cynthia K. Belt<sup>1</sup>; <sup>1</sup>Commonwealth Aluminum, 7319 Newport Rd. SE, Uhrichsville, OH 44683 USA

Natural gas efficiency is extremely important in reverbatory furnaces. Most efforts are made to reduce gas usage in pure melting furnaces while holding and combination furnaces have been largely ignored. Tests were run during production to improve the energy efficiency of the aluminum combination melting and holding furnaces located at the Newport facility of Commonwealth Aluminum. These tests included idle modes, reduced excess air, reduced fire rate, reduced flue temperature, pilot relight burners, and reduced flue size. The variables stressed are less expensive process, control, and equipment changes that can be easily cost justified. The testing ran for over two years. Results of these real-world tests will be discussed.

#### 9:20 AM

**Corrosion Kinetics of Refractory by Molten Aluminium**: Jingguo Gao<sup>1</sup>; Saïed Afshar<sup>1</sup>; *Claude Allaire*<sup>1</sup>; <sup>1</sup>Ecole Polytechnique of Montreal, 8475 Christophe Colomb St., Montreal, Quebec H2M 2N9 Canada

Alumino-silicate refractories for aluminum cast-house applications are exposed to severe corrosion conditions in service. This research work was performed with a new set of samples issued from an improved formulation technique. To predict the service life of refractory material and to improve the properties, the corrosion kinetics of aluminosilicate materials was first studied under static conditions in Al-5wt.%Mg. It is suggested that the silica content inside refractories has little influence on the incubation time prior to the chemical attack. The latter appeared to be controlled by diffusion process. To verify the dynamic solicitation influence on the corrosion, special cylinder shape alumino-silicate refractory castables were submitted to the same above alloy, under both static and dynamic testing conditions. These tests were performed under protective gas such as argon or nitrogen.

#### 9:45 AM

High Temperature Confinement Composite Refractories: Jean-Benoît Pineault<sup>2</sup>; Claude Allaire<sup>1</sup>; <sup>1</sup>Ecole Polytechnique of Montreal, 8475 Christophe Colomb Rd., Montreal, Quebec H2M 2N9 Canada; <sup>2</sup>Groupe Refraco Inc., 1207 Antonio-Lemaire, Chicoutimi, Quebec G7K 1J2 Canada

In many high temperature industrial applications, such as primary aluminum treatment furnaces and launders, composite refractories with varying properties between their hot and cold faces would be beneficial. Such composites with varying mechanical, thermal and chemical properties along their thickness have recently been developed according to an improved technique. Examples of such materials as well as their properties are presented in this paper.

#### 10:10 AM Break

#### 10:45 AM

Room and High Temperature Measurement of the Elastic Properties of Refractories Using a New Apparatus and Set-Up: Claude Allaire<sup>1</sup>; *Jonathan Allaire*<sup>1</sup>; Alain Carbonneau<sup>1</sup>; <sup>1</sup>Ecole Polytechnique of Montreal, 8475 Christophe Colomb St., Montreal, Quebec H2M 2N9 Canada

Knowing the elastic properties of materials is of prime importance. These properties do not only reflect the extent of bonding in the material, but also permit to characterize its behavior under stress. For refractories, the measurement of such properties may be difficult due to their heterogeneous nature. This paper presents a new apparatus and set-up allowing the measurement of the Elastic and Shear Modulus, as well as the Poisson's ratio of refractories, at room and high temperature, according to a non destructive acoustic technique. Examples of results obtained from different types of refractory castables, suitable for the lining of aluminum treatment furnaces and/ or launders, are presented. The effects of the material pre-firing temperature and composition, as well as the sample's dimensions are discussed. Finally, the results obtained at room temperature with the new apparatus and set-up are compared to those obtained using the Grindo Sonic apparatus, as a reference.

## 11:10 AM

Refractories for Aluminium Melting and Holding Furnaces: The Importance of Materials Testing: Marcel Hogenboom<sup>1</sup>; Marcel Spreij<sup>1</sup>; <sup>1</sup>Corus Research Development & Technology, Ceram. Rsch. Ctr., PO Box 10.000, IJmuiden 1970 CA The Netherlands

Refractory lining lifetime of melting and holding furnaces and downtime due to refractory re-linings, are important parameters for increasing the aluminium output of casthouses and decreasing costs. When optimising the refractory linings to value for money, performance and downtime, testing of refractory materials plays an important role. Since process installation are not devised for revealing information on refractory performance, laboratory testing is essential. Failure risk can be decreased significantly by using relevant laboratory testing as a basis for materials selection. The importance of refractory materials testing is illustrated by examples of improvements made in refractory lining concepts, introduction of alternative materials, quality control and evaluation of new developments.

#### 11:35 AM

Effect of Corrosion by Molten Al-5wt%Mg on Mechanical and Physical Properties of Aluminosilicate Refractories: N. Ntakaburimvo<sup>1</sup>; *Claude Allaire*<sup>1</sup>; <sup>1</sup>Ecole Polytechnique of Montreal, 8475 Christophe Colomb St., Montreal, Quebec H2M 2N9 Canada

In addition to refractory corrosion classification based on the traditional criteria which are depth penetration, discoloration aspect and/ or cracking and friability level, the present work focussed on the aluminosilicate refractories properties modification due to corrosion by molten Al-5% Mg alloy. After corrosion, samples were cooled inside the furnace to avoid the effect of thermal shock on residual properties. The measured material properties before and after corrosion were the strength, the elastic modulus, the apparent porosity, as well as the apparent and bulk density. The material strength was measured at room temperature and at 900°C for both cases. The obtained results showed that the residual mechanical properties are much more improved in case of most corroded materials. However, the residual hot modulus of rupture was reduced in the case of two castables, and this may be attributed to the nature of formed phases during corrosion process. Considering together the overall tested materials, the relative porosity was reduced within 21% to 38%, while the relative bulk density was increased by 5% to 9%. This suggests the necessity of the combination of the traditional experimental refractory corrosion resistance criteria and the measurement of the material's strength after corrosion in its nearly service conditions.

# CFD Modeling and Simulation of Engineering Processes: Advanced Casting and Solidification Processes I

Sponsored by: Materials Processing & Manufacturing Division, ASM/MSCTS-Materials & Processing, MPMD/EPD-Process Modeling Analysis & Control Committee, MPMD-Solidification Committee, MPMD-Computational Materials Science & Engineering-(Jt. ASM-MSCTS)

*Program Organizers:* Laurentiu Nastac, Concurrent Technologies Corporation, Pittsburgh, PA 15219-1819 USA; Shekhar Bhansali, University of South Florida, Electrical Engineering, Tampa, FL 33620 USA; Adrian Vasile Catalina, BAE Systems, SD46 NASA-MSFC, Huntsville, AL 35812 USA

 Monday AM
 Room: 206A

 March 15, 2004
 Location: Charlotte Convention Center

*Session Chairs:* Laurentiu Nastac, Concurrent Technologies Corporation, Pittsburgh, PA 15219-1819 USA; Andreas Ludwig, University of Leoben, Dept. of Ferrous Metall., Leoben A-8700 Austria

8:30 AM Opening Remarks - Laurentiu Nastac

#### 8:35 AM Invited

Programs and Opportunities at ATP Focusing on Modeling and Simulation of Engineering Processes: *Dilip Kumar Banerjee*<sup>1</sup>; <sup>1</sup>National Institute of Standards and Technology (NIST), Advd. Tech. Prog. (ATP), 100 Bureau Dr., MS 4730, Gaithersburg, MD 20899-4730 USA

This paper will discuss ATP's contribution over the last decade to the development and use of process modeling as a tool to address some of the challenges faced by the US metal casting industries. Particular attention will be given to highlight how process modeling can be used to improve the manufacturability of components needed for high performance and critical applications. The challenges associated with the design and production of thin walled cast parts with intricate and complex internal geometries will be discussed. Modeling issues associated with the control of the final grain structure in the solidified parts will also be addressed. This paper will discuss the advantages of using appropriate mathematical models for designing new alloys for use in various applications. Finally, the author would discuss the role of ATP over the last decade in uplifting the US technological base by forming useful partnership with various industries to fund high-risk research in order to bring to market new and improved products for the broader benefit of the nation.

#### 9:10 AM Invited

A 3D-FEM Solver for Non-Steady State Navier-Stokes Equations With Free Surface: Application to Mold Filling Simulation in Casting Processes: *Michel Bellet*<sup>1</sup>; Estelle Saez<sup>1</sup>; Olivier Jaouen<sup>2</sup>; Thierry Coupez<sup>1</sup>; <sup>1</sup>Ecole des Mines de Paris, CEMEF, BP 207, Sophia Antipolis F-06904 France; <sup>2</sup>Transvalor S.A., 694 Ave. du Dr. Maurice Donat, Mougins F-06255 France

The paper presents a 3D finite element solver for non steady state fluid flow. The thermomechanical simulation package REM3D® has been initially developed to model Stokes-flow for polymer injection. The mechanical module is based on a Eulerian velocity-pressure formulation. The spatial discretization uses P1+/P1 tetrahedral elements. The front tracking module consists of the resolution of a transport equation, thanks to an original space-time discontinuous Galerkin formulation. It includes mesh adaptation, which permits a dynamic refinement at the fluid interface, thus controling the numerical diffusion. The same approach is used to solve heat transfer. In this paper, we focus on the specific adaptations done to treat Navier-Stokes flow in casting. The treatment of inertia terms is detailed, as well as the implementation of sliding conditions at mould surface, using conservative normals. Validation examples and application to industrial mold filling cases are presented.

#### 9:40 AM Invited

Application of CFD Technique for Modeling of Globular Equiaxed Solidification in Binary and Decomposition in Monotectic Alloys: Andreas Ludwig<sup>1</sup>; Menghuai Wu<sup>1</sup>; <sup>1</sup>University of Leoben, Dept. of Metall., Franz-Josef-Str. 18, Leoben Austria

Phase separation is frequently occurring during solidification accompanied by phenomena like melt convection, sedimentation or with two liquids Marangoni driven motion. In order to describe these phase separation phenomena a two-phase volume averaging model was designed specially for globular equiaxed solidification of binary alloys and decomposition and solidification of hyper-monotectic alloys. The model considers nucleation and growth of equiaxed grains or second phase droplets, motion and sedimentation of grains or droplet, feeding flow and solute transport by diffusion and convection. It allows the prediction of macrosegregations and the distributions of grain size or droplet size. Evaluations were made by comparing the predictions gained with simulation with experimental results. For example it is shown that the numerically predicted grain size distribution in a plate casting (Al-4wt%Cu) agrees reasonably well with the experimental analyses.

# 10:10 AM Break

#### 10:30 AM

Melt Flow and its Effect on Interface Curvature in a Horizontal Unidirectional Solidification System: *Taiming Guo*<sup>1</sup>; Hongmin Li<sup>1</sup>; M. J. Braun<sup>1</sup>; G-X. Wang<sup>1</sup>; <sup>1</sup>The University of Akron, Dept. of Mech. Engrg., Akron, OH 44325-3903 USA

This paper presents an experimental and numerical investigation on natural convection and melt flow near the solid/liquid interface during horizontal unidirectional solidification. In particular, the analysis is focusing on the melt flow near the solid/liquid interface under various channel heights (H) and temperature differences across the hot and cold ends (DT) of the samples and their effects on the interface shape. One horizontal unidirectional solidification system with succinonitrile is constructed so that interface shape and melt flow near the interface can be observed from the top through the microscope and from the side through the telescope at the same time. Experiments on samples with channel height of 1, 3.2 and 5 mm, respectively, have been conducted under various temperature differences across the hot and cold ends. The fluid velocity and interface shape are then quantified. Experimental observations show that the interface shape is significantly influenced by the channel height and temperature difference, both of which strongly affect the melt flow near the interface. Curved interfaces are observed for large channel height and high temperature difference, while an almost flat vertical interface is observed when the channel height is pretty small. A two-dimensional numerical simulation has been performed using the commercial CFD package, Fluent. The enthalpy-porosity solidification model is used to track the phase change between the liquid and solid. The effects of channel height and temperature difference on interface shape and melt flow are analyzed through variation of Rayleigh number (RaH). Good agreements between the numerical predictions and the experimental measurements have been achieved.

# 11:00 AM

**Directional Solidification of a Silicon Ingot: Modeling and Experimental Validation**: *Harald Laux*<sup>1</sup>; <sup>1</sup>SINTEF Materials Technology, Flow Tech., Alfred Getz vei 2, Trondheim 7465 Norway

The industrial production of wafers for solar cells is mostly based on multi-crystalline silicon produced by directional solidification in specialized furnaces. Today there is still room for considerable improvements of the quality of cast ingots, and small improvements may already result in large cost reductions for the final product. One means of improving the average ingot quality is to optimize solidification and furnace operation parameters. In this respect controlled experiments and process simulation by means of CFD will help to understand the fundamentals of the process and to improve it accordingly. This work presents first results of the modeling activities in a five-year research programme. Among others, one goal of the programme is to develop and validate a mathematical model that can simulate industrial furnaces for production of silicon ingots and that is complex enough to assess the final ingot quality from the CFD results for a given set of solidification and furnace operation parameters. At this early stage the process will be simulated using a standard enthalpyporosity method, and the CFD results will be validated against temperature measurements in controlled in-house experiments. The evolution of the temperature distribution in the furnace, the solidification front and residual stresses will be computed with the model. The validation will show if the chosen model is sufficient accurate and useful for future extension to model also the distribution of solutes and the precipitation of particle phases.

# 11:30 AM

Numerical Calculation of the Drag Force Acting on a Solid Particle Pushed by a Solid/Liquid Interface: Adrian Vasile Catalina<sup>1</sup>; Doru Michael Stefanescu<sup>2</sup>; Subhayu Sen<sup>1</sup>; <sup>1</sup>BAE SYSTEMS Analytical Solutions, SD46 NASA Marshall Space Flight Ctr., Huntsville, AL 35812 USA; <sup>2</sup>University of Alabama, Metallurgl. & Matls. Engrg., Tuscaloosa, AL 35487 USA

The distribution of insoluble particles in metal castings depends on the interaction of the particles with the advancing solid/liquid (SL) interface. The balance of the forces acting on a particle determines whether it is engulfed or pushed by the solidification front. An important component of this force balance is the drag force, FD, generated by the particle motion in front of the SL interface. Previous mathematical models for particle/interface interaction made use of steadystate solutions of FD provided by the lubrication theory. However, as recently demonstrated by both theoretical and experimental work, a dynamic analysis of the process is more appropriate. In this paper we report a numerical investigation on FD acting on a spherical particle undergoing an accelerated motion in front of SL interface. We account for a non-planar interface due to the particle/liquid thermal conductivity mismatch and assume a microgravity environment to eliminate the influence of natural convection.

# Challenges in Advanced Thin Films: Microstructures, Interfaces, and Reactions: Advances in Photonic and Optoelectronic Materials and Processes

Sponsored by: Electronic, Magnetic & Photonic Materials Division, EMPMD-Thin Films & Interfaces Committee *Program Organizers:* N. M. (Ravi) Ravindra, New Jersey Institute of Technology, Department of Physics, Newark, NJ 07102 USA; Seung H. Kang, Agere Systems, Device and Module R&D, Allentown, PA 18109 USA; Choong-Un Kim, University of Texas, Materials Science and Engineering, Arlington, TX 76019 USA; Jud Ready, Georgia Tech Research Institute - EOEML, Atlanta, GA 30332-0826 USA; Anis Zribi, General Electric Global Research Center, Niskayuna, NY 12309 USA

Monday AM	Room: 218B
March 15, 2004	Location: Charlotte Convention Center

Session Chairs: Anis Zribi, General Electric, Global Rsch. Ctr., Niskayuna, NY 12309 USA; Seung H. Kang, Agere Systems, IC Device Tech., Allentown, PA 18109 USA; N. M. (Ravi) Ravindra, New Jersey Institute of Technology, Dept. of Physics, Newark, NJ 07102 USA

# 8:30 AM Opening Remarks by Ravindra et al.

# 8:40 AM Invited

Photonic Crystals and Nano-Plasmonics: Enabling New Technology Through Materials Engineering: Matthew C. Nielsen<sup>1</sup>; Xiaolei Shi<sup>1</sup>; Ivan Celanovic<sup>1</sup>; Min-Yi Shih<sup>1</sup>; <sup>1</sup>General Electric, Global Rsch. Ctr., Niskayuna, NY 12309 USA

Data storage and transmission fuels many aspects of the world's economy. For example, 75% of IT spending in 2003 for large corporations is expected to be on data storage. In this paper, novel material structures will be presented that could dramatically change the way light interacts with materials, effecting how we store and transport data. Recent advances being made in the area of photonic crystals will first be presented. By building materials with a highly ordered structure, it is possible to create optical bands. Use of the band structure has been demonstrated for optical waveguides, filters, and lighting applications. While the promise exists for radical innovations in optical devices using the photonic crystals, we will present some of their limitations, mainly arising from current manufacturing processes. Another exciting area of photonics and materials research is nanoplasmonics. We will also describe how the interaction of light with materials can be controlled with plasmonics on the nano-scale, mainly for applications in data storage.

# 9:05 AM Invited

**Optical Nanostructures**: *Gernot S. Pomrenke*<sup>1</sup>; <sup>1</sup>Air Force Office of Scientific Research, Arlington, VA USA

Advances in understanding fundamental physics and engineering on the nanoscale are viewed as critical to the development of next generation devices and systems. Progress in nanotechnology is enabled by the remarkable success in semiconductor materials growth, nanoscale patterning, device fabrication, polymers and coating technology. It is now possible to fabricate, literally atom-by-atom, semiconductor materials that do not exist in nature and with properties that are near ideal for application in electronics, optics and magnetics. Nanotechnology as applied to optoelectronics offers an area ripe with opportunities and challenges. In one area the convergence of nanotechnology, material processing, tools, and applications is driving the realization of integrated photonics and the all photonics chip. Part of this approach is photonic crystals. Building these crystals requires creating periodic structures from dielectric materials that repeat themselves exactly and at regular intervals. If the matrix is made precisely, the resulting structure may have a photonic bandgap (PBG), a range of forbidden frequencies within which a particular wavelength may be blocked, and the electromagnetic radiation is reflected. Photonic bandgap structures and the associated nanofabrication allows photonics to advance optoelectronic miniaturization, light localization, and highly integrated optical devices and components. Integrated 3-D photonic crystal structures form the basis for the fabrication of a photonic chip utilizing the important 1.5 micron wavelength associated with micro-photonic circuits, computers, optical interconnects, micronets, and communication systems.

# 9:30 AM

**Optical Properties of Novel Glasses**: *Sufian Abedrabbo*<sup>1</sup>; D. Arafah<sup>1</sup>; N. M. Ravindra<sup>2</sup>; <sup>1</sup>University of Jordan, Dept. of Physics, Amman 11942 Jordan; <sup>2</sup>New Jersey Institute of Technology, Dept. of Physics, Newark, NJ 07102 USA

Ion-exchange methods have been deployed to form glasses with desired optical properties. The objective of this study is to utilize these glasses for optics and optical communication applications. We will address, specifically, areas such as imaging diagnostics, charge-coupled devices and optical fibers.

#### 9:45 AM Break

# 10:00 AM Invited

GaN Device Performance Based on Thin Film/Substrate Interface for Heterojunction and Homojunction Structures: Danielle Merfeld<sup>1</sup>; <sup>1</sup>GE Global Research, 1 Rsch. Cir., Bldg. KW-C1325, Niskayuna, NY 12309 USA

GaN material has been the subject of intense research over the last decade due to it's unique properties, which are particularly beneficial in optoelectronic and high-power microwave applications. Thin film properties of epitaxially grown GaN and other III-N compounds are highly dependent on the interface at the substrate, and commonly a buffer layer is incorporated into the growth recipe to assist in optimizing the initial island growth conditions as well as to reduce defects brought on by the lattice mismatch between GaN and the substrate. An analysis of various optoelectonic and high-power microwave devices explore the dependence of device performance and reliability on interface properties as measured by various analytical techniques (eg. TEM, SEM, X-ray topography). A comparison between the various methods of reducing the dislocations in the epitaxial III-N films is explored, including growth on bulk GaN substrates. Lastly, the potential benefit of homoepitaxial structures on device performance is analyzed.

#### 10:25 AM

Radiative Properties of Wide Bandgap Materials: N. M. Ravindra<sup>1</sup>; Anthony T. Fiory<sup>1</sup>; <sup>1</sup>New Jersey Institute of Technology, Dept. of Physics, Newark, NJ 07102 USA

A spectral emissometer operating in the wavelength range of 1 to 20 microns and temperature range of 30 to 2000°C has been utilized to measure the reflectance, transmittance and emittance of AlN, Diamond Like Carbon, Erbium Oxide and Sapphire. Interpretation of the measured data has been sought from bandstructure calculations.

#### 10:40 AM

Cold Welding of Organic Light Emitting Devices: Modeling and Reliability: Y. Cao<sup>1</sup>; C. Kim<sup>2</sup>; S. Sethiaraj<sup>3</sup>; O. Akogwu<sup>1</sup>; S. Forrest<sup>2</sup>; *Winston O. Soboyejo*<sup>1</sup>; <sup>1</sup>Princeton University, MAE, D404 Engrg. Quad., Olden St., Princeton, NJ 08544 USA; <sup>2</sup>Princeton University, Dept. of Elect. Engrg., Princeton, NJ 08544 USA; <sup>3</sup>University of Botswana, Dept. of Physics, Gaborone, Botswana Africa

This paper presents the results of a combined experimental and computational study of cold welding. Numerical finite element methods are used to study the effects of dust particle size and holding time on cold welding. These utilize material property measurements that are obtained from nano-indentation experiments. An interfacial fracture mechanics approach is then used to characterize the reliability of Au/Au cold welds. The interfacial fracture toughness of such welds is shown to depend on mode mixity and welding parameters. The implications of the results are also discussed for the reliability testing of organic light emitting devices that are fabricated using cold welding techniques.

# 10:55 AM Invited

**Some Si Based Heterostructures for Optical Applications**: *Magnus Willander*<sup>1</sup>; <sup>1</sup>Chalmers University of Technology and Gothenburg University, Lab. of Phys. Elect. & Photonics, Physics & Engrg. Physics, Dept. of Physics & Engrg. Physics, SE-412 96, Gothenburg Sweden

In this invited talk we will present our research on the growth and characterization of Si based heterostructures for optical and photonic devices. The heterostructures to be included are thin films as well as low dimensional heterostructures. The performance and functionality extension of Si technology due to the development of such heterostructures will be presented and discussed. The heterostructures include strained as well as poly-crystalline-Si1-xGex in addition to ZnO nano-wires and thin films all grown on Si and SiO2 substrates. We will present our growth and characterization for both heterostructures. We will concentrate on structural and optical characterization results in connection to device properties. The structural characterization includes x-ray diffraction for assessment of the crystallinity and the

stress in the films as well as secondary ion mass spectrometery for chemical analysis. In addition, results using photoluminescence as an optical characterization tool will be shown. The device application of these then films includes detectors, lasers, and other light emitting devices. Some of the Si-based heteorstructures to be presented are to include devices emitting and detecting up to the blue-green and violet wave lengths.

#### 11:20 AM Invited

Light-Emitting Composite SiOx/Si Films Produced by Vacuum Evaporation: I. Z. Indutnyy<sup>1</sup>; I. P. Lisovskyy<sup>1</sup>; D. O. Mazunov<sup>1</sup>; *Galyna Yurivna Rudko*<sup>1</sup>; P. E. Shepelyavyj<sup>1</sup>; V. A. Dan'ko<sup>1</sup>; <sup>1</sup>NAS of Ukraine, Inst. of Semiconductor Physics, 41, Nauky prosp., Kyiv 03028 Ukraine

Silicon oxide films with nanocrystalline silicon inclusions are a perspective optoelectronic material compatible with integrated circuit technology. Among the variety of methods used for their production the vacuum thermal evaporation of silicon monoxide is a promising one due to high mechanical and chemical stability of the films and to possibility of large-area Si-based displays fabrication. SiOx/Si films were deposited by evaporating SiO (Cerac Inc.) of 99.9% purity in vacuum at the residual pressure of 2.10-3 Pa and annealed in argon atmosphere. The analysis of the content of Si<sup>-</sup>COy<sup>-</sup>CSi4<sup>-</sup>Cy(1  $\stackrel{.}{i}$ Ú y $\stackrel{.}{i}$ Ú 4) molecular complexes in the structural network of the SiOx matrix by infrared transmission showed that the films consist of SiO2 with Si inclusions surrounded by SiOx interface layers. The photoluminescence spectra exhibit a broad band that ranges from 600 nm to beyond 980 nm.

# 11:45 AM

**Modeling of Photovoltaic Devices Based on Organic Materials**: *Dejan Karabasevic*<sup>1</sup>; Rifat Ramovic<sup>2</sup>; <sup>1</sup>Copper Institute Bor, 19210 Bor Serbia; <sup>2</sup>Faculty of Electrical Engineering, 11000 Belgrade Serbia

Optoelectronic devices based on organic materials have made very rapid progress in the last several years. With field-effect mobility and current on/off ratio values comparable to amorphous silicon, organic optoelectronic devices will find use in broad area optoelectronics applications. Further improvements of devices performances are possible in several areas such as improving device reliability and uniformity and in developing low-cost fabrication processes. It is also important to develop accurate analytical/numerical models that can be used to simulate devices and circuits. While analytical models are useful in understanding basic device operation, numerical simulation is often essential to understand the subtrashold characteristics, and to be able to design more complicated device structures. In this paper analytical model for organic photovoltaic devices based on a model used for a silicon thin-film transistors (TFT's) is proposed. One of the main problems of describing charge transport in molecular system by a semiconductor device simulation tool is mobility which is taken to be an energy and temperature dependent parameter just like in silicon, with the understanding that the underlying physics of transport that gives rise to these mobilities is totally different. On base of this model, simulation was made for pentacene organic TFT, and some of results such as current on/off response and trashold voltage characteristics, when the device is carried into the light beam, are presented.

# Computational Thermodynamics and Phase Transformations: Grain Growth and Particle Coarsening

Sponsored by: ASM International: Materials Science Critical Technology Sector, Electronic, Magnetic & Photonic Materials Division, Materials Processing & Manufacturing Division, Structural Materials Division, MPMD-Computational Materials Science & Engineering-(Jt. ASM-MSCTS), EMPMD/SMD-Chemistry & Physics of Materials Committee

Program Organizer: Jeffrey J. Hoyt, Sandia National Laboratories, Materials & Process Modeling, Albuquerque, NM 87122 USA

Monday AM	Room:	202A		
March 15, 2004	Location	: Charlotte	e Convention	Center

Session Chair: TBA

#### 8:30 AM Invited

Asynchronous Parallelization of the n-Fold Way Algorithm for Simulation of Grain Growth in 2D: Anthony D. Rollett<sup>1</sup>; Priya A. Manohar<sup>1</sup>; <sup>1</sup>Carnegie Mellon University, Matls. Sci. & Engrg., 4315 Wean Hall, 5000 Forbes Ave., Pittsburgh, PA 15206 USA This work describes an implementation of the Potts model for simulation of grain growth in 2D on a distributed-memory parallel architecture. The simulation scheme utilizes continuous-time, asynchronous parallel version of the n-fold way algorithm. Each Processing Element (PE) carries a piece of the global simulation domain while the virtual topology of the PEs is in the form of a square grid in 2D and Torus in 3D. Different PEs have different local simulated times. Interprocessor communication is facilitated by the Message Passing Interface (MPI) routines. Sample results for grain growth simulation in 2D are presented for 840 x 840 global domain size distributed over 16 PEs. The grain growth kinetics obtained in the simulation of pure, isotropic systems demonstrates a close agreement with the analytical models. Grain size distribution obtained in the parallel simulation is well described by the expected lognormal distribution, thus validating the simulation procedure.

## 9:00 AM Invited

Grain Growth in Deformed Materials: Corbett C. Battaile<sup>1</sup>; <sup>1</sup>Sandia National Laboratories, Matls. & Process Modlg., PO Box 5800, MS 1411, Albuquerque, NM 87185-1411 USA

The thermomechanical processing of materials can induce deformation and modify microstructure. Both the deformation and the microstructure evolution affect the properties of the material, and are generally interdependent. Recrystallization from dislocation substructures can dramatically affect the microstructure, but whether or not recrystallization occurs, internal stresses and strains in a deformed material can drive grain boundaries to move abnormally. We will present coupled simulations of deformation and grain evolution in purelyelastic and elastic-plastic polycrystals. Finite element calculations provide the local mechanical state data necessary to model the spatially nonuniform interface pressures that drive grain boundary motion in a front tracking approach. The coupled simulation method will be described in detail, and results for elastic and plastic polycrystals presented. Particular attention will be paid to the role of nonuniform internal stresses in promoting irregular interface migration, and to the treatment of plastic deformation in an evolving microstructure.

#### 9:30 AM

Effect of Grain Boundaries on Spinodal Decomposition: Ramanarayan Hariharaputran<sup>1</sup>; Thennathur A. Abinandanan<sup>2</sup>; <sup>1</sup>Brown University, Div. of Engrg., Providence, RI 02906 USA; <sup>2</sup>Indian Institutute of Science, Dept. of Metall., Bangalore, Karnataka 560 012 India

Through our phase field study of polycrystalline alloys undergoing spinodal decomposition (SD), we describe a new grain boundary (GB) effect namely 'discontinuous SD'. Discontinuous SD is exhibited by systems in which both GB-enhanced atomic mobility and intrinsic GB mobility( $M_g$  and  $L_g$ , respectively) are high: transformation front is formed due to a fast decomposition along the GB.The migration of the transformation front results in alternating A-rich and B-rich lamellae behind the front. We formulate a phenomenological theory (for large ( $L_g / M_g$ ) regime) to explain the characteristics of front migration: lamellar spacing, front velocity and the degree of decomposition within the lamellae.

# 9:50 AM

Modeling Microstructure Evolution and Mechanical Properties of Alloys Based on First-Principles Energetics: *Jianwei Wang*<sup>1</sup>; Chris Wolverton<sup>2</sup>; Stefan Müller<sup>3</sup>; Zi-kui Liu<sup>1</sup>; Long-Qing Chen<sup>1</sup>; <sup>1</sup>Pennsylvania State University, Dept. of Matls. Sci. & Engrg., 106 Steidle Bldg., Univ. Park, State College, PA 16802 USA; <sup>2</sup>Ford Research Laboratory, MD 3028/SRL, Dearborn, MI 48121-2053 USA; <sup>3</sup>Universität Erlangen-Nürnberg, Lehrstuhl für Festkörperphysik, Staudtstrasse 7, Erlangen 91058 Germany

We demonstrate a coupling of state-of-the-art atomistic, statistical and continuum approaches aimed at predicting the microstructure evolution and mechanical properties of alloys. This integrated method includes (1) first-principles calculations of total energies of various configurations, (2) a mixed-space cluster expansion approach for the energetics of complex coherently constrained configurations, (3) a kinetic Monte Carlo technique, and (4) a mechanistic strengthening model. As a case study, first-principles total energies of Al-Cu configurations are fitted to a mixed-space cluster expansion, yielding an expression that can describe the energetics of complex ~250,000-atom coherently constrained configurations with the accuracy of first-principles calculations. Combining this expansion with a kinetic Monte Carlo approach as well as a strengthening model allows one to quantitatively predict the growth and coarsening kinetics of GP zones as well as the effect of the predicted GP zone morphologies on age hardening of Al-Cu alloys.

# 10:10 AM Break

# 10:20 AM Invited

Analysis and Application of a Subgrain Model for Strain-Free Grain Nucleation During Recrystallization: Elizabeth A. Holm<sup>1</sup>; Mark A. Miodownik<sup>2</sup>; <sup>1</sup>Sandia National Laboratories, Dept. 1834, PO Box 5800, MS 1411, Albuquerque, NM 87185-1411 USA; <sup>2</sup>King's College, Dept. of Mech. Engrg., Strand, London WC2R 2LS UK

During or after plastic deformation, dislocations may organize into compact structures such as cell walls in a process termed recovery. If sufficient stored energy remains, the material may recrystallize by nucleating and propagating dislocation-free grains. How a recovered dislocation structure generates growing, strain-free grains has been debated for decades. We suggest a subgrain growth model that incorporates subgrain topology, boundary distribution and boundary properties to predict a nucleation frequency and recrystallization texture. The nucleation event is the mobility-driven discontinuous growth of certain subgrains, and the crystallographic orientations of favored subgrains dictate the recrystallization texture. We test the model on subgrain structures in plastically deformed aluminum, obtaining excellent phenomenological agreement between the model and experiments. This nucleation model is also applied to larger-scale process models of recrystallization in steel and copper, which incorporate the nucleation model into a continuum mechanics framework.

# 10:50 AM Invited

Kinetics of 3-D Grain Growth: Martin E. Glicksman<sup>1</sup>; <sup>1</sup>Rensselaer Polytechnic Institute, Matls. Sci. & Engrg., CII-9111, 110 8th St., Troy, NY 12180-3590 USA

The kinetics of grain growth in 3-D isotropic polycrystals is predicted by representing grains with N neighbors, as "average N-hedra." Average N-hedra satisfy space-filling and thermodynamic equilibria at quadrajunctions and triple lines. The analysis, based on symmetry and space filling, yields growth laws for the volumetric and areal rates of change for grains as a function of N. The results extend to 3-D the half-century old von Neumann-Mullins topological grain growth law that provides the 'n - 6' relationship in 2-D. Analytic kinetic laws may prove useful for constructing more accurate kinetic models of grain growth, and help clarify several long-standing issues on microstructures. The availability of exact topological formulas could be used to provide benchmarks to test numerical simulations, to guide further quantitative experiments on network dynamics, and to assist in deriving important statistical measures for polycrystalline materials.

#### 11:20 AM

An Accurate Yet Simple von Neumann-Mullins Relation for Grain Growth in 3D: David T. Wu<sup>1</sup>; Carl E. Krill<sup>2</sup>; <sup>1</sup>Yale University, Dept. of Mech. Engrg., PO Box 208284, New Haven, CT 06520-8284 USA; <sup>2</sup>Universität des Saarlandes, FR 7.3 Technische Physik, Postfach 151150, Geb. 43, Saarbrücken D-66041 Germany

Von Neumann-Mullin's Law is central to our understanding of grain growth in 2D. Since the 1950's, efforts to extend this relation to 3D have been stymied by topological complexities. By treating the number of grain edges as the fundamental topological parameter characterizing a given grain, we have derived a simple statistical expression for the growth rate in any dimension. The exact result of von Neumann-Mullins is recovered in 2D, and excellent agreement is obtained with phase-field simulations in 3D.

#### 11:40 AM

Structure and Stability of Al-Mg-Si-(Cu) Precipitates: A First-Principles Study: Ravi Chinnappan<sup>1</sup>; Wolverton Christopher<sup>1</sup>; <sup>1</sup>Ford Motor Company, Phys. & Environml. Scis., Scientific Rsch. Lab., 2101 Village Rd., REC R, Rm. 1525, Dearborn, MI 48124 USA

Precipitation in Al-Mg-Si-(Cu) alloys has been extensively studied, since this quaternary forms the basis of a wide variety of commercial alloys (e.g., 6xxx series alloys). The observed precipitation sequence is complex and involves a wide variety of metastable phases (e.g., GP zones, beta", beta"). Calculations of metastable phase equilibria in these alloys are hampered by the lack of quantitative information on the thermodynamics of these precipitate phases. We have undertaken an extensive first-principles study of energetics of all the reported precipitate phases of Al-Mg-Si-(Cu) alloys, using both local density approximation (LDA) and generalized gradient approximation (GGA). Our calculations provide a clear and consistent picture of the energetics of the precipitate phases, and in certain cases, provide insight into the compositional changes of precipitates during aging. In addition to energetics, we also examine the relative volumes of the various phases, and find no significant deviations from that of the solid solution phases. Thus, we predict no significant dimensional stability issues should arise during aging of commercial Al-Mg-Si-(Cu) alloys. By combining our first-principles energetics with computational thermodynamics approaches, we provide predictions of metastable phase equilibriua and precipitate volume fractions in a variety of 6xxx series alloys.

# Cost-Affordable Titanium Symposium Dedicated to Prof. Harvey Flower: Overview and Innovative Processes

Sponsored by: Structural Materials Division, SMD-Titanium Committee

*Program Organizers:* M. Ashraf Imam, Naval Research Laboratory, Washington, DC 20375-5343 USA; Derek J. Fray, University of Cambridge, Department of Materials Science and Metallurgy, Cambridge CB2 3Q2 UK; F. H. (Sam) Froes, University of Idaho, Institute of Materials and Advanced Processes, Moscow, ID 83844-3026 USA

Monday AM	Room: 2	06B
March 15, 2004	Location:	Charlotte Convention Center

Session Chair: Derek J. Fray, University of Cambridge, Dept. of Matls. Sci. & Metall., Cambridge CB2 3Q2 UK

# 8:30 AM

**Cost Affordable Titanium** — Is it Possible?: *F. H. (Sam) Froes*<sup>1</sup>; M. Ashraf Imam<sup>2</sup>; Derek J. Fray<sup>3</sup>; <sup>1</sup>University of Idaho, Inst. for Matls. & Advd. Processes, McClure Bldg., Rm. 437, Moscow, ID 83844 USA; <sup>2</sup>Naval Research Laboratory, 4555 Overlook Ave. S.W., Washington, DC 20375-5343 USA; <sup>3</sup>University of Cambridge, Dept. of Matls. Sci. & Metall., Pembroke St., Cambridge CB2 3QZ UK

Titanium is the "wonder" metal, which makes sense as the material of choice for a wide variety of applications. However, because of its relatively high price - a result of extraction and processing costs - it is used basically only when it is the only choice with the caveat that titanium has a bright "image". This can lead to use even when the economics are unfavorable. This paper will overview the potential areas which are amenable to cost reduction for titanium products. This will emphasize all steps in component fabrication from extraction and processing to fabrication of final parts.

# 9:15 AM

Breakthrough Technologies in Titanium Refinement Methods: L. Christodoulou<sup>1</sup>; W. S. DeRosset<sup>2</sup>; J. Christodoulou<sup>3</sup>; P. L. Martin<sup>4</sup>; <sup>1</sup>DARPA/DSO, 3701 N. Fairfax Dr., Arlington, VA 22203 USA; <sup>2</sup>AMSRL-WM-MD, Aberdeen Proving Ground, MD 21005-5066 USA; <sup>3</sup>Office of Naval Research, Matls. Div., Code 332, 800 N. Quincy St., Arlington, VA 22217-5660 USA; <sup>4</sup>AFRL/MLLMD, Wright-Patterson AFB, OH 45433-7817 USA

Recent advances in novel processing approaches for the production of titanium metal have attracted worldwide interest. Affordable methods to replace the Kroll Process for the production of Ti sponge have been sought for decades. In the early 20th century, Al was transformed from a "precious metal" to a "commodity" through the development of an efficient electrochemical refinement process. If a similar breakthrough can be devised for Ti, it would find applications in many systems where specific properties are being recognized as enabling; for example advanced armored vehicles, corrosion resistant marine systems as well as the usual aerospace platforms. This presentation will provide an overview of the emerging chemical and moltensalt electrochemical methods being pursued under DARPA sponsorship. The objectives of these studies will be related to the potential benefits for structural applications in future defense systems.

#### 9:45 AM

#### Extraction of Titanium from Solid Titanium Dioxide in Molten Salts: Derek J. Fray<sup>1</sup>; George Z. Chen<sup>1</sup>; <sup>1</sup>University of Cambridge, Dept. of Matls. Sci. & Metall., Pembroke St., Cambridge CB2 3QZ UK

The search for a cheaper replacement of the Kroll Process has continued ever since titanium was first produced commercially. In 2000, the authors reported that it was possible to reduce titanium and other metal oxides directly to metals by making the oxide the cathode in a bath of molten calcium chloride. Since that time, our understanding of the process has increased and it has been found that it is possible to produce many alloys by the direct electro-deoxidation. This paper will review the understanding of the process and present the latest developments.

#### 10:15 AM

**Developing Applications for Titanium**: *F. H. (Sam) Froes*<sup>1</sup>; Oscar Yu<sup>2</sup>; Takashi Nishimura<sup>3</sup>; <sup>1</sup>University of Idaho, Inst. for Matls. &

Advd. Processes (IMAP), McClure Bldg., Rm. 437, Moscow, ID 83844 USA; <sup>2</sup>RMI Titanium Company, 1000 Warren Ave., Niles, OH 44446-0269 USA; <sup>3</sup>NTC Corporation, 4-15-11 Mikage-Ishimachi, Higashinada-Ku, Kobe 658-0045 Japan

One of the ways to make titanium products more cost affordable is to increase the number of applications for titanium. This paper will review near term and far term applications for titanium, with emphasis on activities in the USA and Japan; both parallel and contrasting efforts. Applications will include both expanding aerospace use and developing non-aerospace applications.

#### 10:45 AM

Economic Analysis of the Application of Emerging Reduction Technologies to Mill Products Production: Edwin H. Kraft<sup>1</sup>; <sup>1</sup>EHKTechnologies, 10917 SE Burlington Dr., Vancouver, WA 98664 USA

The search for lower cost manufacturing approaches has continued since the beginning of the titanium industry in the mid 20th century. Within the past few years, over a dozen new reduction technologies have emerged, with many proceeding to serious development. It is still unclear, however, whether many of these will be economically viable or actually provide product meeting technical requirements. These emerging reduction technologies will be briefly reviewed. Since commercial success would appear to require integration of such processes into the mill products production stream, the economics of current production and markets will be reviewed and analyzed. The Decisive Analysis methodology will then be applied to economic analysis of the production of mill products incorporating the new reduction processes. The methodology will be described and applied using assumed process routes, business factors and cost factor probability distributions. Resulting economic scenarios will be presented.

#### 11:15 AM

**P/M Titanium for Aeroengine Components**: *David Rugg*<sup>1</sup>; <sup>1</sup>Rolls Royce, Derby DE248BJ UK

The advent of new material production processes and improved control/prediction of powder consolidation offers the potential for reducing gas turbine life cycle costs. End user requirements in terms of product manufacture and certification will be reviewed with respect to requirements and potential for optimised raw material input morphology and cleanliness. Examples of components where nett shape or near nett shape technology could be applied will be reviewed along with current production and repair practice. This will include electrolytic deoxidation powder routes and metal addition processes for titanium alloys.

# Dislocations: Modeling and Simulation Fundamentals

Sponsored by: ASM International: Materials Science Critical Technology Sector, Electronic, Magnetic & Photonic Materials Division, Materials Processing & Manufacturing Division, Structural Materials Division, EMPMD/SMD-Chemistry & Physics of Materials Committee, MPMD-Computational Materials Science & Engineering-(Jt. ASM-MSCTS) *Program Organizers:* Elizabeth A. Holm, Sandia National Laboratories, Albuquerque, NM 87185-1411 USA; Richard A. LeSar, Los Alamos National Laboratory, Theoretical Division, Los Alamos, NM 87545 USA; Yunzhi Wang, The Ohio State University, Department of Materials Science and Engineering, Columbus, OH 43210 USA

Monday AM	Room:	201A		
March 15, 2004	Location	: Charlotte	Convention	Center

Session Chair: TBA

# 8:30 AM Invited

Level-Set Simulation of Dislocation Dynamics in the Presence of Particles: David J. Srolovitz<sup>1</sup>; Yang Xiang<sup>1</sup>; Li-Tien Cheng<sup>2</sup>; E. Weinan<sup>3</sup>; <sup>1</sup>Princeton University, Princeton Matls. Inst., 320 Bowen Hall, 70 Prospect Ave., Princeton, NJ 08540-5211 USA; <sup>2</sup>University of California, Dept. of Math., La Jolla, CA 92039 USA; <sup>3</sup>Princeton University, Dept. of Math., Princeton, NJ 08544 USA

We present a new method for modeling dislocation dynamics within a level-set framework. This method naturally accounts for dislocation topology change, glide and climb with arbitrary mobilities, cross-slip, and interactions with arbitrary microstructural elements. Examples applications include the expansion of dislocation loops by glide, climb and cross-slip, dislocation intersections, and the operation of a Freak-Read source. The method is applied to edges and screws bypassing arrays of particles (impenetrable or penetrable, misfitting or not) with a focus on understanding bypass mechanisms. In addition to classical particle cutting and the formation of Orowan loops, a wide variety of new bypass mechanisms are observed. Depending on dislocation type and the nature of the misfit, dislocation loops can be produced lying in the slip plane or perpendicular to it - in front of and/or behind the particle, on the sides of the particle, or around the particle (but orthogonal to an Orowan loop).

# 9:05 AM

# First Principles Evaluation of Re Solid-Solution Softening in BCC Mo: Christopher Woodward<sup>1</sup>; Satish Rao<sup>1</sup>; <sup>1</sup>Air Force Research Laboratory, Wright Patterson AFB, OH 45433-7817 USA

Solid solution softening observed in the group VA and group VIA transition metals has traditionally been attributed to either extrinsic or intrinsic effects. Extrinsic effects include the scavenging of interstitial impurities by substitutional solid-solutions while intrinsic effects assume a direct solute-dislocation interaction that lowers the Peierls barrier. We have applied first principles methods to evaluate possible intrinsic solid-solution-softening in the group VI BCC transition metals. First, we calculated the magnitude of size and modulus misfit parameters of several solid solutions in Mo as suggested by the work of Fleischer. Second, we calculated the change in the primary Peierls barrier when Re solid solutions are introduced along a straight a/ 2<111> screw dislocation in Mo. Here the local strain field associated with the dislocation core is self-consistently coupled to the long-range elastic field using the recently developed lattice Greens Function Boundary Condition method. The dislocation is contained in a very small simulation cell making it possible to directly simulate the solute-dislocation interaction. Results from these two methods will be contrasted and compared to available experimental results.

# 9:25 AM

Ab-Initio Based Classical Potential for Molydenum Predicts Line: *Richard G. Hennig*<sup>1</sup>; Thomas J. Lenosky<sup>2</sup>; Dallas R. Trinkle<sup>1</sup>; Sven P. Rudin<sup>3</sup>; Christopher F. Woodward<sup>4</sup>; John W. Wilkins<sup>1</sup>; <sup>1</sup>Ohio State University, Dept. of Physics, 174 W. 18th Ave., Columbus, OH 43210 USA; <sup>2</sup>Finisar Corporation, Sunnyvale, CA 94089 USA; <sup>3</sup>Los Alamos National Laboratory, Theoretical Div., Los Alamos, NM 87545 USA; <sup>4</sup>Air Force Research Laboratory, Matls. & Mfg. Direct., Wright Patterson AFB, Dayton, OH 45433 USA

A classical potential for molybdenum is developed which accurately predicts defect energies, phonon dispersion, melting point, surface energy, and ideal shear strength of the bcc phase. The potential form is given by the modified embedded atom method and the potential parameters are optimized using ab-initio energies, lattice parameters, forces and elastic constants. The classical potential determines the line energies, core structures and Peierls stresses of the screw and edge dislocations in bcc molybdenum.

# 9:45 AM

Atomistic Simulation of Dislocation Interactions: Brian D. Wirth<sup>1</sup>; Jennifer A. Young<sup>2</sup>; Jaime Marian<sup>2</sup>; Joshua Robach<sup>3</sup>; Ian M. Robertson<sup>3</sup>; <sup>1</sup>University of California, Dept. of Nucl. Engrg., MC 1730, Berkeley, CA 94720-1730 USA; <sup>2</sup>Lawrence Livermore National Laboratory, Chmst. & Matls. Sci. Direct., PO Box 808, Livermore, CA 94550 USA; <sup>3</sup>University of Illinois, Matls. Sci., IL USA

The mechanisms of dislocation motion and dislocation-obstacle interactions are of practical importance to developing quantitative structure-property relations, mechanistic understanding of plastic flow localization, predictive models of mechanical behavior in irradiated metals and the dynamic response of materials to shock loading. Molecular dynamics simulations directly account for core interactions through semi-empirical interatomic potentials and provide fundamental insight into dislocation migration and material deformation mechanisms. However, MD simulations are practically limited to interactions occuring at high-strain rate. In this presentation, we describe our recent results to investigate the motion of screw and edge dislocations and their interaction with a variety of obstacles, including radiation produced dislocation loops, stacking fault tetrahedra and helium bubbles, as well as nanometer coherent and incoherent precipitates. Finally, we will discuss the experimental validation of these results through comparisons to in-situ straining observations in transmission electron microscopy.

## 10:05 AM Break

# 10:20 AM Invited

Phase Field Microelasticity Theory and Model of Dislocations, and its Further Developments: Yu U. Wang<sup>1</sup>; Yongmei M. Jin<sup>1</sup>; Armen G. Khachaturyan<sup>1</sup>; <sup>1</sup>Rutgers University, Ceram. & Matls. Engrg., 607 Taylor Rd., Piscataway, NJ 08854 USA

The application of Phase Field method to dislocation modeling and its further advances are discussed. Phase Field method provides a natural mesoscale description of dislocation structures without explicitly tracking individual segments. The long-range elastic interactions between individual dislocations are numerically solved in Phase Field Microelasticity formalism. The "short-range" dislocation reactions, such as multiplication, annihilation and formation of various metastable configurations, are automatically taken into consideration through Landau-type "chemical" energy, gradient energy and elastic energy functional. No ad hoc assumptions are made on possible dislocation patterns during evolution. The model is extended to dislocation dynamics near free surfaces and in deposited thin films driven by relaxation of epitaxial stress. The effect of image forces on dislocation motions is consistently taken into account. Examples of 3D simulations are presented. The theory and model is further extended to multi-crack system. A further development to surface roughening of heteroepitaxial films is also made.

# 10:55 AM

Phase Field Modeling of Dislocation Networks and Dislocation Core Structures: Chen Shen<sup>1</sup>; Yunzhi Wang<sup>1</sup>; <sup>1</sup>Ohio State University, Dept. of Matls. Sci. & Engrg., 2041 College Rd., Columbus, OH 43210 USA

Phase field method has become an attractive alternative to study dislocations of arbitrary configurations and dislocation-precipitate interactions. Recently the model has been extended to describe dislocation nodal reactions and network formation, as well as dissociation of various dislocation configurations into Shockley partials. The extensions are necessary steps towards advanced applications of the phase field method to dislocation substructure formation and coarsening. By incorporating gamma surface data from ab initio calculations into the crystalline energy of the phase field model, quantitative analysis of dislocation core structures is made possible. We present various example applications of the method to dislocation-precipitate interaction (looping and shearing of ordered intermetallic precipitates).

## 11:15 AM

A Model for Simulating the Motion of Line Defects in Twin Boundaries in the HCP Metals: Anna Serra<sup>1</sup>; David J. Bacon<sup>2</sup>; Yuri N. Osetsky<sup>3</sup>; <sup>1</sup>Universitat Politecnica de Catalunya, Dept. de Matematica Aplicada III, Jordi Girona 1-3 modul C-2, Barcelona 08034 Spain; <sup>2</sup>The University of Liverpool, Matls. Sci. & Engrg.. Dept. of Engrg., Brownlow Hill, Liverpool L69 3GH UK; <sup>3</sup>Oak Ridge National Laboratory, Computer Sci. & Math. Div., PO Box 2008, Oak Ridge, TN 37831-6158 USA

In previous studies we have used computer simulation to investigate the atomic structure of twin boundaries and defects such as twinning dislocations in the HCP metals (e.g. Phil.Mag.A, 73 (1996) 333). The models employed used conventional periodic boundary conditions along the dislocation line and fixed conditions in the other two directions, so that extensive defect motion could not be considered. A method has now been developed to simulate a twin boundary containing a step with dislocation character, with full periodicity in the boundary plane. It may be used for investigating either the static or dynamic properties of such interfaces as the defects in them move over large distances. In the present work, we first demonstrate the nature of the method and apply the statics variant (T=0K) to determine the Peierls stress for motion of twinning dislocations in {10-12}, {11-21}, {10-11} and {11-12} boundaries. Except for the {11-21} twin, shuffles are required for dislocation glide and hence boundary movement. We also consider the dynamics of defect motion at T>0K.

# 11:35 AM

**Dynamical Scaling in a Simple 1D Model of Dislocation Activity**: *Jack Deslippe*<sup>1</sup>; Murray Daw<sup>1</sup>; Daryl Chrzan<sup>2</sup>; Mike J. Mills<sup>3</sup>; Neeraj Thirumalai<sup>4</sup>; <sup>1</sup>Clemson University, Physics & Astron., Clemson, SC 29634 USA; <sup>2</sup>University of California, Mat. Sci. & Engrg., Berkeley, CA USA; <sup>3</sup>Ohio State University, Matl. Sci. & Engrg., Columbus, OH USA; <sup>4</sup>OSU/Exxon USA

We study a simple 1D model of dislocation creation and motion. The dislocation source operates under a simple stress criterion. The dislocations move, overdamped, under an external force and mutual interactions with the other dislocations. The simple numerical simulations are examined for dynamical scaling, where the dislocation distribution function would obey the form  $n(x,t) = t^{\alpha} g(x/t^{\alpha})$ . The existence of scaling is confirmed by detailed analysis of the evolution equation and the (discrete) operation of the source. The analysis shows that b=1 and a approaches 0 from below, and that the dislocation

density asymptotically approaches a step function and decreases logarithmically in time. The approach to the asymptotic form is also logarithmic in time, which means that the numerical simulations only slowly converge to the asymptotic form.

#### 11:55 AM

Atomic-Level Study of Void Hardening in fcc Metals: Yury N. Osetsky<sup>1</sup>; David J. Bacon<sup>2</sup>; <sup>1</sup>Oak Ridge National Laboratory, Computer Scis. & Math., 4500 S. MS G138, Oak Ridge, TN 37831-6138 USA; <sup>2</sup>The University of Liverpool, Matls. Sci. & Engrg., Brownlow Hill, Liverpool L69 3GH UK

Voids are strong obstacles for moving dislocations and cause a significant hardening of metals subjected to irradiation with high energy particles at high temperatures. In this paper we present results of atomic-scale modelling of interaction between edge and screw dislocations and voids in Cu. Simulations were performed using a recently developed model based on a periodic array of dislocations. Interaction with voids of up to 4nm diameter was studied over the temperature range from 0 to 600K in crystals containing up to about 7 million atoms. Strong temperature dependence of the critical resolved shear stress and specific mechanisms related to dissociated dislocations were observed. The results obtained are compared with those obtained by dislocation dynamics at the continuum level.

# **General Abstracts: Session I**

#### Sponsored by: TMS

*Program Organizers:* Adrian C. Deneys, Praxair, Inc., Tarrytown, NY 10591-6717 USA; John J. Chen, University of Auckland, Department of Chemical & Materials Engineering, Auckland 00160 New Zealand; Eric M. Taleff, University of Texas, Mechanical Engineering Department, Austin, TX 78712-1063 USA

Monday AM	Room:	204		
March 15, 2004	Location	: Charlotte	Convention	Center

Session Chair: Joel Kapusta, Air Liquide Canada, Boucherville, QC J4B 1V6 Canada

#### 8:30 AM

On the Identification of Dislocation Types and Dislocation Morphorlogies in 316 LN Stainless Steel: Hongbo Tian<sup>1</sup>; Joseph A. Horton<sup>2</sup>; Peter K. Liaw<sup>1</sup>; Alexandru D. Stoica<sup>3</sup>; Xunli Wang<sup>3</sup>; Yandong Wang<sup>3</sup>; James W. Richardson<sup>4</sup>; <sup>1</sup>University of Tennessee, Matls. Sci. & Engrg., Knoxville, TN 37996 USA; <sup>2</sup>Oak Ridge National Laboratory, Metals & Ceram. Div., Oak Ridge, TN 37831 USA; <sup>3</sup>Oak Ridge National Laboratory, Spallation Neutron Source, Metals & Ceram. Div., Oak Ridge, TN 37831 USA; <sup>4</sup>Argonne National Laboratory, Intense Pulsed Neutron Source, Argonne, IL 60439 USA

Fatigue tests under fully reversed stresses were performed at 0.2 Hz, and microstructures of the specimens were carefully studied. Transmission-Electron Microscopy (TEM) was employed to analyze dislocations in Type 316 low-carbon nitrogen-added (LN) stainless steel (SS) samples with the intention to investigate the dislocation types, and change of dislocation structures with the fatigue process and grain orientation. The dislocations in 316 LN SS after fatigue at 0.2 Hz with a R ratio of -1 were found to be mostly edge type, which was also substantiated by studies using neutron diffraction.

#### 8:55 AM

Semi-Qualitative Relation Between Creep Curve and Metallurgical Observation During Creep of Ferritic Steel: Manabu Tamura<sup>1</sup>; Hideo Sakasegawa<sup>2</sup>; Akira Kohyama<sup>3</sup>; Kei Shinozuka<sup>1</sup>; Hisao Esaka<sup>1</sup>; <sup>1</sup>National Defense Academy, Dept. Matls. Sci. & Engrg., 1-10-20 Hashirimizu, Yokosuka 2398686 Japan; <sup>2</sup>Kyoto University, Grad. Sch. of Energy Sci., Gokasho, Uji, Kyoto 611-0011 Japan; <sup>3</sup>Kyoto University, Inst. of Advd. Energy, Gokasho, Uji, Kyoto 611-0011 Japan

Creep test was performed at around 650°C on three ferritic steels, iron, ultra low carbon steel containing small amount of TaN particles with 20nm in diameter and tempered martensitic steel, Fe-8%Cr-2%W-0.2%V-0.04%Ta steel. Hardness and integrated breadth of X-ray diffraction peak were measured for the crept specimens. The thin films were also observed under TEM. Two parameters, equivalent obstacle spacing (EOS) and dislocation density parameter (C) were calculated from only creep curves applying a dislocation model for creep deformation. Up to minimum creep, the above parameters are consistent with the metallurgical observations. In an accelerated creep range, the metallurgical observations of Fe and tempered martensitic steel correspond to the changes in EOS and/or C. However, in TaN particle hardening steel accelerated creep is observed, though there is little change in hardness and EOS. Absolute values of EOS are roughly equal to the TEM observations.

#### 9:20 AM

Flexure Strength and Shear Strength of Silicon Carbide Joints (SiC/SiC) Fabricated by a Molybdenum Diffusion Bonding Technique: Brian V. Cockeram<sup>1</sup>; <sup>1</sup>Bechtel Bettis Laboratory, PO Box 79, W. Mifflin, PA 15122-0079 USA

The capability to form robust SiC to SiC joints is needed to enable the fabrication of more complex SiC-based mechanical structures. In this work molybdenum foils are used to develop a diffusion bond with SiC during a vacuum heat treatment. Fracture strength data for SiC joined using a molybdenum foil diffusion bond are compared with results for monolithic Chemical Vapor Deposited (CVD) SiC using a standard 4-point flexural test method (ASTM C1161) from roomtemperature to 1100C. Shear Strength results obtained using a doublenotched specimen are also compared for the joined and monolithic specimens. The average shear strength values for the monolithic and joined specimens were typically lower than the flexural strength data, as observed for other ceramic materials. Differences in elastic properties and coefficient of thermal expansion between SiC and the phases that are produced in the molybdenum foil bond region result in the formation of slightly larger flaws in the SiC near the joint region. These flaws are shown to be fracture initiation sites that result in a lower range of flexural strength values for molybdenum bonded SiC (263 to 50 MPa) compared to monolithic SiC (443 to 197 MPa). However, the shear strength values for the molybdenum-joined SiC (264 to 61 MPa) are found to be within the data scatter of the monolithic material (397 to 31 MPa). These results indicate that a molybdenum diffusion bonding technique can be used to produce joints that have only slightly lower flexural strength than monolithic SiC, but the molybdenum diffusion bonds are as strong as monolithic SiC in shear.

#### 9:45 AM

Hardness and Electrical Resistivity of Molybdenum in the Post-Irradiated and Annealed Conditions: Brian V. Cockeram<sup>1</sup>; <sup>1</sup>Bechtel Bettis Laboratory, PO Box 79, W. Mifflin, PA 15122-0079 USA

Hardness and electrical resistivity are two indirect measures of the defect density of a metal. Hardness and electrical resistivity data were measured for sheet forms of Low Carbon Arc Cast (LCAC) molybdenum to provide a basic assessment of the influence of irradiation on the defect density. Irradiation of molybdenum in the High Flux Isotope Reactor (HFIR) at temperatures ranging from 270C to 1100C and to neutron fluence levels ranging from 10.5 to 64.4 X 10^20 n/  $cm^2$  (E > 0.1 MeV) was shown to result in a small increase in the electrical resistivity of molybdenum. Hardness was shown to be a more sensitive measure of the irradiated defect density than electrical resistivity, with increases in hardness on the order of 100% for irradiation at temperatures < 605C. Annealing was performed at temperatures between 300C and 1250C, and the kinetics for the recovery of the hardness and electrical resistivity were compared. Recovery of the initial hardness and electrical resistivity for LCAC molybdenum irradiated at 270C and 605C was observed at 970C and 1100C using 1-hour isochronel anneals. Irradiation at temperatures > 935C resulted in little change in hardness or electrical resistivity, and little change in these values was resolved after annealing to temperatures as high as 1250C

# 10:10 AM Break

#### 10:20 AM

A Comparison of the Properties of AA-6061 Processed by Different Methods of Severe Plastic Deformation (SPD): Bala Cherukuri<sup>1</sup>; Teodora Nedkova<sup>1</sup>; Raghavan Srinivasan<sup>1</sup>; <sup>1</sup>Wright State University, Mech. & Matls. Engrg., 3640 Col. Glenn Hwy., Dayton, OH 45435 USA

Severe Plastic Deformation (SPD) has been emerged as a promising approach to refine the grain size of a metal, increase strain rate sensitivity and formability at higher temperatures. This paper will present the results of a study on AA-6061-O, which was subject to SPD processing by Equal Channel Angular Extrusion (ECAE), Multi Axial Compression and Accumulative Roll Bonding (ARB) at room temperature. Over-aged samples of AA6061 were deformed to approximately the same accumulated strain. Results will include the as-processed microstructure, the stability of the microstructure at elevated temperatures, and the flow behavior of the different materials determined through tension and compression tests at different strain rates and temperatures. Hardness and Electrical Resistivity Measurement of Fe22.5Ni77.5 Permalloy as a Function of Annealing in a Magnetic Field: *A. Gali*<sup>1</sup>; C. J. Sparks<sup>2</sup>; R. K. Williams<sup>2</sup>; E. P. George<sup>2</sup>; <sup>1</sup>University of Tennessee, Matls. Sci. & Engrg., 434 Dougherty Engrg. Bldg., Knoxville, TN 37996 USA; <sup>2</sup>Oak Ridge National Laboratory, Metals & Ceram. Div., 1 Bethel Valley Rd., Oak Ridge, TN 37831 USA

We are interested in developing more rapid survey measurements of the effects of annealing on ferromagnetic alloys. Previous work has shown that both the electrical resistivity and hardness can be correlated with changes in the short range order. Diffuse X-ray scattering measurements have shown preference for Fe-Ni first neighbor pairs and their correlation lengths provides us with a better understanding of the effect of local atomic arrangements on these properties. The direction of the applied magnetic field was along [100], [110] and [111] crystallographic directions to determine orientation dependence of the applied field on the resistivity and hardness measurements. We will discuss the effects of the crystallographic dependence of the applied field on the measured properties of the Fe-Ni alloys. Also we plan to apply a tensile load to the Fe22.5Ni77.5 alloy below the elastic limit and anneal at temperature where diffusion can occur. This will provide us with information on the atomic pair alignments under stress.

## 11:10 AM

Surface Properties and Mechanical Behavior of Foam Electro Plasma Cleaned Steels: *Pankaj Gupta*<sup>1</sup>; Greg Tenhundfeld<sup>1</sup>; Edward O. Daigle<sup>1</sup>; <sup>1</sup>CAP Technologies, LLC, Louisiana Business & Tech. Ctr., S. Stadium Dr., Baton Rouge, LA 70803-6100 USA

Foam electro plasma process (FEPP) is a novel tool for cleaning and coating of conductive materials. FEPP is environmentally friendly exhibiting improved surface characteristics and corrosion resistance. This technology exhibits a great promise in various industrial applications. The present study involves cleaning of various grades of steels using FEPP. Microstructural analysis of cross-section of steel was analysed. Surface profile and morphology of the cleaned steel was studied by optical profilometer and SEM, respectively. The composition analysis and hydrogen profiling was performed by RBS and NRA, respectively. Surface analysis also described the level of cleaning. Microhardness studies were conducted to study the effect of process on hardness of the material. Microhardness tests were conducted on surface and cross section of the cleaned steel specimens. The results were compared to the steel cleaned by conventional industrial processes. An attempt has been made to develop an overall understanding of the processing-structure-property relationship of the cleaned steel.

# 11:35 AM

Effect of Boron and Carbon on the Mechanical Properties of Fe-Co-V Magnetic Alloys: Saurabh Kabra<sup>1</sup>; Easo P. George<sup>2</sup>; <sup>1</sup>University of Tennessee, Matls. Sci. & Engrg., Knoxville, TN 37996-2200 USA; <sup>2</sup>Oak Ridge National Laboratory, Metals & Ceram. Div., 1 Bethel Valley Rd., Oak Ridge, TN 37831-6093 USA

The Fe-Co system is well known for its excellent magnetic properties. But it exhibits brittle fracture both in the ordered and the disordered states. Vanadium additions (~2%) have been shown to improve ductility, more so in the disordered state than the ordered state. In an earlier study it was shown that small additions of boron and carbon can significantly improve the ductility of FeCo-2V. In this study, we have investigated the effects of higher levels of boron and carbon additions, and the role of changes in the vanadium concentration on the mechanical properties of ordered Fe-Co alloys. The effects of borides and carbides on slip refinement are investigated as well as the role of environment on ductility and fracture behavior. Research sponsored by the Division of Materials Sciences and Engineering, Office of Basic Energy Sciences, U. S. Department of Energy, under Contract DE-AC05-00OR22725 with UT-Battelle, LLC.

# General Pyrometallurgy: Session I

Sponsored by: Extraction & Processing Division, EPD-Pyrometallurgy Committee

Program Organizer: Thomas P. Battle, DuPont Titanium Technologies, Wilmington, DE 19880-0352 USA

Monday AM	Room: 202B
March 15, 2004	Location: Charlotte Convention Center

Session Chairs: Thomas P. Battle, DuPont Titanium Technologies, Wilmington, DE 19880-0352 USA; Florian Kongoli, FLOGEN Technologies Inc., Montreal H3S 2C3 Canada

# 8:30 AM

Study of Smelting Parameters in the Production of Silicomanganese from Denizli-Tavas Manganese Ores of Turkey: Ahmet Geveci<sup>1</sup>; Ender Keskinkilic<sup>1</sup>; <sup>1</sup>Middle East Technical University, Metallurgl. & Matls. Engrg. Dept., METU (ODTU), Ankara 06531 Turkey

Smelting of silicomanganese from Denizli-Tavas Mn ore (31%Mn) has been studied. Mixtures of calcined ore, active carbon, calcium oxide and quartz were smelted in graphite crucibles by using an electronically controlled muffle furnace. Temperature, time, charge basicity, active carbon/ore wt. ratio were determined as smelting parameters. Silicomanganese production necessitated higher temperatures compared to ferromanganese smelting since considerable amount of Si should be present in the final product. Oxides of iron and manganese were reduced faster, whereas sufficient time should be allowed for the system for desired reduction of SiO2. Determination of optimum charge basicity was crucial for silicomanganese production. Increase in quantity of active carbon led to increase in both Mn and Si recoveries. However, presence of excessive active carbon resulted in formation of carbides. Addition of high-manganese Brazilian sinter (53% Mn) to the domestic ore has also been studied in relation to both ferromanganese and silicomanganese smelting.

#### 8:55 AM

**Optimization, Control and Automation of Pyrometallurgical Processes:** *F. Kongoli*<sup>1</sup>; I. McBow<sup>1</sup>; S. Llubani<sup>1</sup>; <sup>1</sup>FLOGEN Technologies, Inc., 5757 Decelles Ave., Ste. 511, Montreal, Quebec H3S 2C3 Canada

The optimization of various non-ferrous smelting and converting processes as well as iron and steel making processes has been classically viewed and carried out in a classical static way. It has been always attempted to find the best unique set of conditions where the smelting, converting or iron and steel making processes could run smoothly. However this is associated with natural difficulties and some times has proven impossible due to the inherent characteristics of the raw materials and the new smelting technologies. In this work a new approach of the optimization of these processes has been exposed. This not only allows a continuous optimization of the smelting process but at the same time can serve as an adequate means of control and automation of any specific process. The advantages of this new approach have been discussed.

# 9:20 AM

**Modeling of Sulfide Capacities of Binary Titanate Slags**: *Bora C. Derin*<sup>1</sup>; Onuralp Yücel<sup>1</sup>; Ramana G. Reddy<sup>2</sup>; <sup>1</sup>Istanbul Technical University, Metallurgl. & Matls. Engrg. Dept., Maslak, Istanbul 34469 Turkey; <sup>2</sup>University of Alabama, Dept. of Metallurgl. & Matls. Engrg., Tuscaloosa, AL 35487-0202 USA

In this paper, the Reddy-Blander Model for sulfide capacity calculations has been applied to TiO2 containing binary slags. The sulfide capacities of FeO-TiO2 and MnO-TiO2 slag systems at 1500°C were calculated and compared with the experimental data. An excellent agreement between the model calculated Cs data and experimental data was observed.

# 9:45 AM

**Production of High-Grade Ferronickel from Low-Grade Oxide Nickel Ores:** V. M. Paretsky<sup>1</sup>; A. V. Tarasov<sup>1</sup>; I. D. Reznik<sup>1</sup>; <sup>1</sup>State Research Center of Russian Federation, State Rsch. Inst. of Nonferrous Metals, 13, Acad. Korolyov St., 129515 Moscow Russia

Production of commercial-grade nickel-containing products, and in particular ferronickel with a nickel content of at least 20% from low-grade oxide ores is a very important issue for Russia, because Russia has immense reserves of oxide nickel ores with a nickel content of less than 1.2%. In practice, the process of electric smelting with slags containing over 13% FeO inevitably results in uncontrolled frothing of the melt and its spillage from the furnace. A method has been developed in the Gintsvetmet Institute for production of high-grade ferronickel by oxidizing low-grade ferronickel with ore in an electric furnace; the gas emission and frothing are eliminated due to a low carbon content of the melt in this process. A flow diagram has been proposed with two parallel streams of ore treated in continuous mode in two electric smelting furnaces. To verify the proposed flowsheet, laboratory tests have been carried out, which have demonstrated the feasibility of production of commercial-grade ferronickel with a content of 26.6% Ni and 1.83% Co from ores containing 1.08-1.1% Ni, 0.08-0.12% Co and up to 30.7% Fe. This technology is now in the process of preparation for commercial introduction at the Buruktalsky nickel smelter (South Urals, Russia).

# 10:10 AM

# 10:20 AM

Intensification of Reduction of Oxide Nickel Ores: A. V. Tarasov<sup>1</sup>; P. A. Kovgan<sup>1</sup>; V. M. Paretsky<sup>1</sup>; <sup>1</sup>State Research Center of Russian Federation, State Rsch. Inst. of Nonferrous Metals, 13, Acad. Korolyov St., 129515 Moscow Russia

Laboratory studies into reduction of oxide nickel ores with cast iron in sparged melt were carried out in crucibles at 1500C. Argon blowing at a rate of 0.9 to 1.1 m3/m2s through a vertical lance submerged into the melt down to the iron/ore interface permitted production of discard slag with 0.03% to 0.05% Ni and 0.01 Co. Bench-scale investigations of metallothermic reduction of oxide nickel ores were carried out in a plasma-arc furnace in intermittent mode. Ore containing 1.0% Ni and 0.08% Co was fed to the furnace along with 15% of calcium oxide as fluxing agent. Coke fines were fed over the melt at a rate of 1% of the weight of the ore to reduce iron in the ore to wuestite and prevent "boiling-up" of the melt. The ferronickel obtained contained 15.2% Ni, 1.75% Co, 0.35% Si and 0.43% Cr. The nickel and cobalt contents in "discard" slags after blowing were on average 0.045 and 0.015%, respectively. The reduction process can be intensified by changing the position of the blowing lances in the bath and the depth of their submersion. The nickel and cobalt contents of ferronickel can be increased by periodical carbonization of cast iron.

#### 10:45 AM Cancelled

# Melting Zone Evaluation in New Hot Metal Processes – An Innovative Approach

#### 11:10 AM

Mineralogical Changes Occurring During the Roasting of Zinc Sulphide Concentrates: Tzong T. Chen<sup>1</sup>; *Yoo-Hyun Sung*<sup>2</sup>; John E. Dutrizac<sup>1</sup>; <sup>1</sup>CANMET, 555 Booth St., Ottawa, Ontario K1A 0G1 Canada; <sup>2</sup>Korea Resources Corporation, Tech. Rsch. Inst., 686-48, Shindaebang-dong, Dongjak-gu, Seoul 156-706 Korea

Zinc concentrates and fluid-bed roaster calcines from CEZinc were studied. The Zinc concentrates consist of sphalerite and minor to trace amounts of pyrite, chalcopyrite, anglesite, galena, pyrrhotite, ankerite, gysum and silicates. During roasting of the concentrates, the S in the sphalerite (Zn,Fe)S diffuses out of the particle, whereas the associated Zn and Fe react in situ to form (Zn,Fe)O. The Fe from the (Zn,Fe)O phase migrates towards the peripheries of the particles, forming ZnFe2O4. The resulting "ZnO+ZnFe2O4" particles further agglomerate to form large, porous, spherical masses. A relatively compact ZnO-rich shell subsequently develops on the surface of the agglomerates and the development continues inwards; eventually, the particles become compact. Rhythmic bands are often present in the agglomerated masses. However, a small number of the particles remain as tiny un-agglomerated grains. The calcines consist of spherically agglomerated particles, and fragments of agglomerated particles, of ZnO and ZnFe2O4, as well as traces of Zn2SiO4, Pb oxide/oxysulphate and silicates. The ZnO, ZnFe2O4, Zn2SiO4 and Pb oxide/oxysulphate often form intimate intergrowths in the rhythmic bands. The ZnO and Zn2SiO4 phases contain minor amounts of Fe; most of the Cu in the calcine is present in the ZnO and ZnFe2O4 phases.

#### 11:35 AM

**Decomposition Kinetics of Flash Smelting Flue Dust Sulphates:** *Elli Nurminen*<sup>1</sup>; Heikki Jalkanen<sup>2</sup>; Kim Fagerlund<sup>3</sup>; Tiina Ranki-Kilpinen<sup>4</sup>; <sup>1</sup>Helsinki University of Technology, Matls. Procg. & Powder Metall., Vuorimiehentie 2 K, Espoo FIN-02150 Finland; <sup>2</sup>Helsinki University of Technology, Metall., Vuorimiehentie 2 K, Espoo 02150 Finland; <sup>3</sup>Outokumpu Research, Pyrometall./Sulphide Smelting, PO Box 60, Pori FIN-28330 Finland; <sup>4</sup>Outokumpu Technology, PO Box 86, Espoo FIN-02201 Finland

Sulphate decomposition was studied in the conditions of a typical copper flash smelting heat recovery boiler. The aim was to determine

the kinetics of the copper sulphate decomposition reactions and to find out if they are likely to take place in the process conditions prevailing in an industrial HRB. The information is essential in CFDmodelling of the reactions taking place in the boiler and for optimising the process. Thermal decomposition of sulphates was studied by thermogravimetry. The experiments were conducted with a commercial copper sulphate, a partially sulphated copper oxide and an industrial process flue dust. The main variables studied were temperature and gas composition of a N2-O2-SO2-mixture. The samples were characterized with SEM, optical microscope and XRD. Temperature affected the decomposition rate strongly but the gas composition had a minor effect on the kinetics. The decomposition was fastest in the partly sulphated oxide and slowest in commercial copper sulphate.

# Hume Rothery Symposium: Structure and Diffusional Growth Mechanisms of Irrational Interphase Boundaries: Session I

Sponsored by: Electronic, Magnetic & Photonic Materials Division, Structural Materials Division, EMPMD/SMD-Alloy Phases Committee, MPMD-Phase Transformation Committee-(Jt. ASM-MSCTS)

*Program Organizer:* H. I. Aaronson, Carnegie Mellon University, Department of Materials Science and Engineering, Pittsburgh, PA 15213 USA

Monday AM	Room: 208A	
March 15, 2004	Location: Charlotte Convention	Center

Session Chair: Gary R. Purdy, McMaster University, Dept. of Matls. Sci. & Engrg., Hamilton, Ontario L8S 4L7 Canada

#### 8:30 AM Invited

Low Energy and Low Mobility Structures at Irrational Interphase Boundaries, and Compliance With Nucleation Theory: *Hubert I. Aaronson*<sup>1</sup>; <sup>1</sup>Carnegie Mellon University, Dept. of Matls. Sci. & Engrg., 5000 Forbes Ave., Wean Hall 2313, Pittsburgh, PA 15213-3890 USA

Nucleation theory has led to predictions that partially coherent interfacial structures should develop during diffusional growth even at irrational planar boundaries (ALK, 1968). This prediction is now tested in alloy systems that appear to be successively less metallic in character. In both a massively transformed Ag-26% Al alloy and during precipitation at grain boundaries in Ti-Cr and Ni-Cr, nearly all interphase boundaries are indeed partially coherent. However in the massive transformations in near-TiAl and in MnAl(+2% C) alloys partially coherent structures are largely absent (Vasudevan et al, Soffa et al., 2002). Nie and Muddle (NM, 2002) and Howe, Reynolds and Vasudevan (HRV, 2002) reported a preference for edge-to-edge (Kelly and Zhang, 1999) rather than plane-to-plane matching of certain low index planes in both lattices at facets in a Ti-46.54% alloy. Recently Reynolds et al (2003) have shown with 3-D, NCS modeling that planar facets whose highly irrational crystallography was accurately determined by NM and HRV correspond physically to dense parallel rows of atoms intermingled in no obvious sequence but perhaps displaceable only with Moire ledges. Li et al will report in this symposium planar ZrN:alpha Zr-N facets whose structures cannot be rationalized by edgeto-edge matching. This implies that other type(s) of irrational interfacial structure capable of impeding growth remain to be discovered. Al:Xe(solid) interfaces, at which {111}Al and {100}Al facets are present despite a misfit of ca. 50% (Howe), suggest shallow minima in the polar gamma-plot that affect only nucleation. This spectrum of observations indicates that a marked difference in bond strength and character in the matrix and the product phases can cause the two phases to play unequal roles in determining the crystallography and structure of low energy and low mobility boundaries.

# 9:10 AM Invited

Calculation of Alpha/Gamma Interfacial Energy in Iron in the Presence of Irrational Crystallography: Takatoshi Nagano<sup>1</sup>; *Masato Enomoto*<sup>1</sup>; <sup>1</sup>Ibaraki University, Dept. of Matls. Sci., 4-12-1, Nakanarusawa, Hitachi 316-8511 Japan

The interfacial energies between alpha and gamma iron crystals, not only K-S (or N-W), but also irrationally oriented, were calculated at various interface orientations using the EAM potential. Blocks of alpha and gamma iron  $(10x10x5 \text{ nm}^3)$  were joined and relaxed by Monte Carlo Method under the condition that atom positions are fixed at the outer surface of the blocks. Whereas the polar plot of

MONDAY AM

calculated interfacial energy exhibited a number of small and large cusps for K-S (or N-W) relationship, a smoother and irregular energy surface was obtained for irrational OR. The three-dimensional Wulff plot is made for equilibrium shape of intragranular ferrite idiomorphs that are K-S (or N-W) and irrationally oriented with the austenite matrix. The energy of austenite grain boundaries is calculated using the same potential. The equilibrium shape of grain boundary ferrite allotriomorphs will be calculated at some boundary misorientations.

# 9:50 AM Invited

Edge-to-Edge Matching as a Criterion for Interphase Interfaces of Low Energy: Gary R. Purdy<sup>1</sup>; <sup>1</sup>McMaster University, Dept. of Matls. Sci. & Engrg., 1280 Main St. W., Hamilton, Ontario L8S4L7 Canada

As demonstrated by Aaronson and his co-workers over some five decades, the structure, energy and dynamic response of interphase boundaries are strongly mutually correlated; it has also become clear that very few, if any, solid-solid transformation interfaces can seriously be considered "incoherent". In recent attempts to rationalize these observations, many descriptions of less-rational interphase boundaries have focused on considerations of matching between atomic planes, lying parallel to the interface in the parent and product crystals. After reviewing several simple boundaries, their structure, energetics and (in some cases) their migration mechanisms, the role of edge-to-edge matching is examined. It is noted that many cases of habit plane matching are also cases where other sets of densely populated atomic planes meet edgewise at the interface. Some recent observations of boundary faceting where edge-to-edge matching is not accompanied by facet plane matching are examined, and their significance is discussed.

# 10:30 AM Break

# 10:45 AM Invited

Crystallography and Growth Mechanisms of Interphase Boundaries: Jian-Feng Nie<sup>1</sup>; <sup>1</sup>Monash University, Sch. of Physics & Matls. Engrg., Victoria 3800 Australia

In this paper a Moire plane model is used to examine the orientation, structure and migration mechanism of irrational, planar interphase boundaries in phase transformations. In contrast to existing approaches of structural ledges, disconnections and invariant lines/ planes that are based essentially on matching of atoms or lattice sites within two parallel, or close to parallel, closely-packed planes in the two lattices, the present model involves consideration of matching of a pair of non-parallel, closely-packed lattice planes that are related by a correspondence. It will be demonstrated that irrationally-oriented, planar interphase boundaries are defined by the Moire plane resulting from the intersection of these two lattice planes, and that such boundaries migrate in their normal directions by successive nucleation and lateral movement, within the macroscopic interface planes, of interfacial defects that have the form of Moire ledges. A comparison will be provided between the Moire plane model and approaches of structural ledges, disconnections and invariant lines/planes.

#### 11:25 AM Invited

Structures in Irrational Singular Interfaces: Wen-Zheng Zhang<sup>1</sup>; Xiaopeng Yang<sup>1</sup>; <sup>1</sup>Tsinghua University, Dept. of Matls. Sci. & Engrg., Beijing 100084 China

Reproducible facets or habit planes in irrational orientations suggest that they should be singular interfaces associated with local energy minima. When it is singular with respect to the orientation relationship (OR) and the interface orientation (IO), an irrational interface usually contains periodical good matching regions, extended along an invariant line (or a quasi-invariant line when the lattice misfit is large) and alternated with dislocations. The corresponding OR can be described by parallelism of at least two measurable  $\Delta g$  vectors for a system of either small or larger lattice misfit. The singular irrational interface must lie along the common moiré planes normal to the  $\Delta g$ 's. The edge-to-edge matching can be realized in this interface for different sets of planes. An irrational interface singular with respect only to IO is normal to one  $\Delta g$ . The relationship between the  $\Delta g$  description and the interfacial structures is explained in the framework of the O-lattice/CSL/DSCL.

# Internal Stresses and Thermo-Mechanical Behavior in Multi-Component Materials Systems: Electronic Thin Films and Packaging Materials I

Sponsored by: Electronic, Magnetic & Photonic Materials Division, Structural Materials Division, EMPMD-Electronic Packaging and Interconnection Materials Committee, EMPMD-Thin Films & Interfaces Committee, SMD-Composite Materials Committee-Jt. ASM-MSCTS

*Program Organizers:* Indranath Dutta, Naval Postgraduate School, Department of Mechanical Engineering, Monterey, CA 93943 USA; Bhaskar S. Majumdar, New Mexico Tech, Department of Materials Science and Engineering, Socorro, NM 87801 USA; Mark A.M. Bourke, Los Alamos National Laboratory, Neutron Science Center, Los Alamos, NM 87545 USA; Darrel R. Frear, Motorola, Tempe, AZ 85284 USA; John E. Sanchez, Advanced Micro Devices, Sunnyvale, CA 94088 USA

Monday AM	Room:	209B
March 15, 2004	Location	: Charlotte Convention Center

Session Chairs: K. N. Subramanian, Michigan State University, E. Lansing, MI 488824 USA; John Sanchez, Unity Semiconductor, Matls. Sci., Santa Clara, CA 95050 USA; Vijay Sarihan, Motorola, Final Mfg. Tech. Ctr., Tempe, AZ 85284 USA

## 8:30 AM Keynote

**Stress Induced by Electromigration in VLSI Interconnects**: *King-Ning Tu*<sup>1</sup>; <sup>1</sup>University of California, Dept. of Matls. Sci. & Engrg., Los Angeles, CA 90095 USA

Multi-leveled thin film interconnects in microelectronic devices are 3-D in structure and are confined in a dielectric layer. Electromigration and the confinement produce mechanical stresses in the interconnect. The stress can enhance or retard electromigration. The 3-D structure also produces current crowding wherever the interconnect turns. The current crowding can lead to stress concentration and inhomogeneous stress distribution. The analysis of stress induced by electromigration will be presented. In the beginning of the talk, a brief introduction of the multi-leveled interconnect structure and memory devices based on field-effect transistors will be given.

#### 9:00 AM Invited

Role of Film Intrinsic Stress in Packaging of Multi-Layer Micro-Electronics and MEMS Structures: Vijay Sarihan<sup>1</sup>; <sup>1</sup>Motorola, Final Mfg. Tech. Ctr., 2100 E. Elliot Rd., MD EL725, Tempe, AZ 85284 USA

Internal stress due to material CTE and Young's modulus mismatch plays havoc in microelectronics and MEMS structures but is well understood and controllable. However the film intrinsic stress develops as a function of processing. The level of stress and how it changes with additional processing or environmental exposure is still not well understood. This stress is typically neglected in response prediction as value, behavior and response impact are not well known. Film intrinsic stress can play a substantial role in enhancing or degrading the response of multi-layer structures. Intrinsic stress can cause failures or can be mitigating to situations that would have otherwise resulted in disaster. Thin film intrinsic stress is processing related so, it can be controlled by modifying processing parameters provided we know what is the outcome of the process changes and the desired requirement. These requirements point to a need for a measurement capability and a response prediction capability. In addition to processing parameters there is also a size and thickness link. Thus the measurement capability should be capable of addressing the typical size and thickness seen in actual devices and MEMS structures. This paper will present the impact of intrinsic stress in response prediction of micro-electronic structures. Special emphasis will be given to the role of internal stress in packaging of micro-electronic devices and MEMS structures. A variety of examples delineating the impact of thermo-mechanical stress and intrinsic stress will be covered. This will include device interconnects, special via structures in compound semiconductor devices, wafer level packages and MEMS. It will also present innovative techniques for measuring intrinsic stress, techniques that take size into consideration and relate the measurements to the actual size of interconnects. Since the sample preparation follows the processing witnessed by the actual device the technique is also capable of accounting for the effect of microstructure change.

# 9:25 AM Invited

Cyclic Deformation and Fatigue in Thin Metal Films: O. Kraft<sup>1</sup>; R. Monig<sup>2</sup>; G. P. Zhang<sup>2</sup>; C. A. Volkert<sup>1</sup>; <sup>1</sup>Research Center and University of Karlsruhe Germany; <sup>2</sup>Max-Planck-Institute for Metals Research Stuttgart, Stuttgart Germany

Continuous and patterned metal thin films are widely used in microelectronic and micro-electro-mechanical systems (MEMS). In these applications, temperature changes of up to several  $100^{\circ}$ C may occur, and, as a result of thermal mismatch between film and substrate materials, large mechanical stresses arises, which have been the subject of many detailed studies in the last decade. However, only little attention has been paid to fatigue, i.e. the effect of repeated cyclic loading, on the integrity of thin films. We have found that fatigue failure of mechanically or thermomechanically strained thin films is associated with the formation of extrusions and voids. Details of the damage morphology have been observed to depend sensitively on film thickness and grain size. In particular, fatigue in metal films with thickness and/or grain size of less than approximately 500 nm appears to be controlled by diffusive rather than by dislocation mechanisms.

#### 9:50 AM Invited

Ultra High-Cycle Fatigue in Pure Al Thin Films and Line Structures: C. Eberl<sup>1</sup>; R. Spolenak<sup>2</sup>; O. Kraft<sup>3</sup>; F. Kubat<sup>4</sup>; A. Leidl<sup>3</sup>; W. Ruile<sup>3</sup>; E. Arzt<sup>1</sup>; <sup>1</sup>Institut für Metallkunde der Universität Stuttgart, Stuttgart Germany; <sup>2</sup>Max-Planck Institut für Metallforschung; <sup>3</sup>Forschungszentrum Karlsruhe Germany; <sup>4</sup>Clausthal University of Technology Germany

The requirements of mechanical devices (MEMS and Surface Acoustic Wave (SAW)) increase due to shrinking size, rising frequencies and driving power. We focus on novel fatigue mechanisms stemming from the combination of small dimensions (100 nm) and ultrahigh frequencies (GHz). Tailored SAW test devices have been developed for improved stress and temperature control. Quantitative post test analysis as a function of testing time, power density and temperature revealed a direct correlation between void/extrusion density and device performance. In-situ measurements of the characteristic damage formation revealed an extrusion mechanism that operates on a short time scale. We have developed sophisticated models relating the device power to the mechanical stress state. Combined with thermal stresses measured in the device, these allowed the complete stress tensor to be determined. This mechanistic insight provides the physical understanding for improved life-time models and lead to the development of high power durable metallizations.

#### 10:15 AM Invited

Internal Stresses on the Thermomechanical Behavior of Sn-Based Solder Joints: J. G. Lee<sup>1</sup>; H. Rhee<sup>1</sup>; K. N. Subramanian<sup>1</sup>; <sup>1</sup>Michigan State University, Dept. of Chem. Engrg. & Matls. Sci., E. Lansing, MI 48824-1226 USA

Solder joints consist of various entities such as in a typical multicomponent system. When such a joint is subjected to temperature excursions during service, large stresses can arise due to different coefficients of thermal expansion (CTE) of components that make up the joint. The magnitude of stresses that can develop not only depends on the temperature differences encountered, but also on rates at which such changes are imposed. Microstructural constituents present in the solder joint also play significant roles in the development of these stresses. Acknowledgement: Work supported by the National Science Foundation under grant NSF DMR-0081796.

#### 10:40 AM Invited

Assessment of Stress-Induced Mechanical Properties and Microstructural Changes in Pb-Free Solder-Joint Interconnects: James P. Lucas<sup>1</sup>; A. U. Telang<sup>1</sup>; J. G. Lee<sup>1</sup>; H. Rhee<sup>1</sup>; T. R. Bieler<sup>1</sup>; K. N. Subramanian<sup>1</sup>; <sup>1</sup>Michigan State University, Chem. Engrg. & Matl. Sci., 3526 Engrg. Bldg., E. Lansing, MI 48824-1226 USA

Solder joints represent multi-component materials systems that are subjected to rather complex stress states in operation. As a primary interconnect in microelectronic packaging not only must the solder joint function reliably as an electrical interconnect, it must perform mechanically as a structural unit, as well. Due to coefficient of thermal expansion (CTE) mismatch, stress and strain develop in the solder joint interconnect. Stresses and strains developed in the joint resulting from thermo-mechanical fatigue (TMF) cycling can be particular detrimental. Residual stress built up during TMF affects microstructure evolution in the joint long after TMF cycling ceases. Nanoindentation testing (NIT) along with scanning probe microscopy (SPM) will be used to investigate the mechanical properties and internal stress behavior in Sn-based eutectic and near-eutectic Pb-free solder joints. Orientation imaging microscopy (OIM) will also be used in the assessment of internal stress effects.

### 11:05 AM

Double Shear Thermomechanical Fatigue (TMF) Response of a Lead-Free Solder Reinforced with SMA Fiber: Z. X. Wang<sup>1</sup>; I. Dutta<sup>2</sup>; B. S. Majumdar<sup>1</sup>; <sup>1</sup>New Mexico Tech, Matls. Dept., Socorro, NM 87801 USA; <sup>2</sup>Naval Postgraduate School, Mech. Engrg. Dept., Monterey, CA 93943 USA

Failure of microelectronic solders usually occurs through accumulation and localization of large shear strain under TMF loading. Here we present results of a novel approach utilizing the active characteristics of shape memory alloy (SMA) reinforcements. The premise is that a reverse strain of the SMA associated with martensite (M) to austenite (A) transformation during heating would induce active backstress on the matrix. In order to test the feasibility of this approach, we have conducted double-shear tests of a long-fiber composite wire, composed of a Sn3Ag matrix reinforced with a NiTi wire. Under TMF at constant load, the composite wire exhibited a sudden decrease in the shear creep rate on reaching the transformation temperature. Correspondingly, a bare NiTi wire showed a reverse local displacement at the transformation temperature, consistent with an M to A transformation. Preliminary modeling of internal stresses will be presented. This research was supported by ARO.

# International Laterite Nickel Symposium - 2004: Economics and Project Assessment

Sponsored by: Extraction & Processing Division, EPD-Aqueous Processing Committee, EPD-Copper, Nickel, Cobalt Committee, EPD-Process Fundamentals Committee, EPD-Process Mineralogy Committee, EPD-Pyrometallurgy Committee, EPD-Waste Treatment & Minimization Committee *Program Organizer:* William P. Imrie, Bechtel Corporation, Mining and Metals, Englewood, CO 80111 USA

Monday AM	Room: 2	17B/C	
March 15, 2004	Location:	Charlotte	Convention Center

Session Chairs: Steve C.C. Barnett, VP HSEQC Stainless Steel Materials, BHP-Billiton, London SW1V 1BH UK; James A. Murray, Snr Principle Engineer, Bechtel Corp. Mining & Metals, San Francisco, CA 94119 USA

# 8:30 AM

Nickel Market Dynamics: Santo Ranieri<sup>1</sup>; <sup>1</sup>Noranda Inc./ Falconbridge Ltd., Mkt. Rsch., Queen's Quay Terminal, 207 Queen's Quay W., Ste. 800, Toronto, Ontario M5J 1A7 Canada

We will briefly review the nickel market in 2003 and look forward to the supply demand balance for the next few years focusing in on the key factors influencing future price dynamics. On the supply side, we will examine slated brownfield and greenfield expansions including the Norilsk factor and the small to mid-range 'supply creep'. We will also review the cost side of the industry and what to expect going forward. On the demand side, we will discuss the stainless steel and non-stainless demand, the China factor and the stainless steel scrap supply cycle. We will conclude by pinpointing where the market is on the current price cycle, and where we believe the mid-term direction is headed.

#### 9:00 AM

**Past and Future of Nickel Laterite Projects**: Ashok D. Dalvi<sup>1</sup>; *W. Gordon Bacon*<sup>1</sup>; Robert C. Osborne<sup>1</sup>; <sup>1</sup>Inco Limited, 2060 Flavelle Blvd., Sheridan Park, Mississauga, Ontario L6M 1V1 Canada

Production of nickel from laterite ores has occurred for over 100 years beginning with processing of garnieritic ores from New Caledonia. However, until now the world nickel supply has been predominantly from sulfide sources. Going forward, the authors project that the production of nickel from sulfide ores will remain more or less constant. Most of the expansion in nickel production capacity over the next ten years will come from processing of laterite ores. Thus the capital and operating costs of new laterite projects will have significant impact on the nickel supply and therefore price. The authors have reviewed the history and capital and operating costs of these projects and those "on the drawing board". The authors have also evaluated the risk associated with such projects. The paper will discuss the impact of this and the recent history on the future development of laterite nickel projects.

# 9:30 AM

Start Up and Reliability of Nickel Laterite Plants: Finlay Campbell<sup>1</sup>; Ed McConaghy<sup>1</sup>; William Vardill<sup>1</sup>; <sup>1</sup>Dynatec Corporation,

Metallurgl. Tech. Div., 8301 - 113 St., Ft. Saskatchewan, Alberta T8L 4K7 Canada

Nickel laterite pressure acid leach plants and reduction roast plants have had a chequered history in terms of engineering, construction, start-up and operational reliability. Many potential projects have been the subject of detailed studies over the last thirty to forty years. Four reduction roast plants are currently operating, an additional one was partially constructed but never completed and one more was started up in 1974 and shutdown after 12 years operation. Three acid leach plants have been built and commissioned in the last five years trying to follow the example of the Moa Nickel plant in Cuba. An additional acid leach project is currently on hold, following limited construction work, its future subject to review by the owner because of potential cost over-runs. The paper will discuss difficulties that may be encountered as a project is developed and will address factors which may affect production ramp-up schedule, long term production performance and overall project success. Comparisons are made with rampup performance at other large metallurgical plants that employ some comparable unit operations.

# 10:00 AM Break

# 10:10 AM

The Importance of Life-Cycle Assessment Approach to the Evaluation of Environmental Impacts Associated with the Pressure Acid Leach Treatment of Nickel Laterite Ores: *William James Middleton*<sup>1</sup>; Matthew Searles<sup>2</sup>; <sup>1</sup>Inco Limited, Corp., Gen. Engrg. Bldg. (ITSL Sec.), Copper Cliff, Ontario POM 1N0 Canada; <sup>2</sup>BHPBilliton Newcastle Technology

The life-cycle assessment (LCA) approach can be an important tool for the quantification and evaluation of environmental impacts associated with metal production systems. At the conceptual phase of a new metals development project, LCA can: · Aid project decision making by evaluating the environmental consequences of design decisions; · Support project permitting and reinforce site/process environmental impact assessment; · Allow environmental impact comparisons between alternate flow sheets. This paper discusses the life-cycle assessment methodology, and its application as a supportive tool for environmental decision-making in process design and for site environmental impact assessment and permitting. Selected examples from a recent LCA performed on the Pressure Acid Leach Process for treating nickel Laterite ores are employed to demonstrate the usefulness of the tool.

#### 10:40 AM

The Implications of Sustainability in Developing a Nickel Laterite Project: Denis J. Kemp<sup>1</sup>; Mark Wiseman<sup>1</sup>; <sup>1</sup>Noranda Inc-Falconbridge Limited, Queen's Quay Terminal, 207 Queen's Quay W., Ste. 800, Toronto, Ontario M5J 1A7 Canada

Laterite projects are found in the tropical and sub-tropical regions of the world. As a result severe meteorological situations accompany such projects, often in regions of high seismic activity and political uncertainty. Frequently, socio-economic development supported by political interest is a major driver for development, while environmental protection imposes numerous stresses on the project. This paper will review and examine the many social, environmental, technical and financial issues that a mining and extraction process is subject to during development. The options that must be evaluated will be discussed in the context of sustainable development. Issues of project standards and cultural impact through to long term issues such as greenhouse gasses and climate change will be assessed in redirecting project environmental norms. Although a rationale for sustainable project can be developed many long term uncertainties around issues remain.

#### 11:10 AM

Beating US\$10 Per Pound of Installed Capacity for a Laterite Nickel Plant: *David S. Dolan*<sup>1</sup>; Roger M. Nendick<sup>2</sup>; <sup>1</sup>Fluor Australia Pty Ltd., GPO Box 1320L, Melbourne, Victoria 3001 Australia; <sup>2</sup>Fluor Mining and Minerals, 1075 W. Georgia St, Ste. 700, Vancouver, BC V6E 4M7 Canada

To beat capital costs of US\$10 per pound of installed capacity has appeared as a major hurdle for the "third" generation laterite nickel plants. Forecast costs are escalating. Where can savings come from? Ore beneficiation can reduce the tonnage rate to be processed. High pressure acid leach options include use of indirect slurry heating and higher operating temperatures to reduce flow rates and residence time. Progress has been reported in atmospheric leaching. High counter current decantation circuit settling rates and high underflow densities reduce CCD costs. Metal recovery options include direct from leach solution to metal production as used by Bulong and espoused by Goro and indirect recovery as used by Moa Bay, Murrin Murrin and Cawse. Plant location impacts on the costs of tailings disposal. Finally nickel and cobalt metal production routes are electrowinning, hydrogen reduction or some innovative routes being proposed for Goro. This paper reviews the status in these developments, with particular reference to equipment and processes that offer lower capital costs.

#### 11:40 AM

An Alternative Nickel Laterite Project Development Model: David A. Neudorf<sup>1</sup>; David A. Huggins<sup>2</sup>; <sup>1</sup>Hatch Associates, 2800 Speakman Dr., Mississauga, Ontario L5K 2R7 Canada; <sup>2</sup>Consultant, 4 Steele Ave., Annapolis, MD 21401 USA

Known resources of nickel laterites considerably exceed nickel sulfide resources and there is a growing consensus that most new nickel production will be sourced from laterites. The development of nickel laterite projects is very capital intensive due to inherently low grades, inability to concentrate ore prior to processing, complex processing technology and typically large infrastructure requirements. This has resulted in most recently proposed projects being "mega-projects," to achieve economy of scale. However, this may result in unacceptable project risk in many cases. Furthermore, many known laterite resources are not large enough to support a mega-project. This paper describes an alternative model for nickel laterite project development that allows smaller scale and reduces capital exposure. The requirements of this model in terms of process technology, infrastructure and commercial innovation are described.

# Lead-Free Solders and Processing Issues Relevant to Microelectronic Packaging: Fundamentals, Phases, Wetting and Solidification

*Sponsored by:* Electronic, Magnetic & Photonic Materials Division, EMPMD-Electronic Packaging and Interconnection Materials Committee

Program Organizers: Laura J. Turbini, University of Toronto, Center for Microelectronic Assembly & Packaging, Toronto, ON MSS 3E4 Canada; Srinivas Chada, Jabil Circuit, Inc., FAR Lab/ Advanced Manufacturing Technology, St. Petersburg, FL 33716 USA; Sung K. Kang, IBM, T. J. Watson Research Center, Yorktown Heights, NY 10598 USA; Kwang-Lung Lin, National Cheng Kung University, Department of Materials Science and Engineering, Tainan 70101 Taiwan; Michael R. Notis, Lehigh University, Department of Materials Science and Engineering, Bethlehem, PA 18015 USA; Jin Yu, Korea Advanced Institute of Science and Technology, Center for Electronic Packaging Materials, Department of Materials Science & Engineering, Daejeon 305-701 Korea

Monday AM	Room: 219B	
March 15, 2004	Location: Charlotte Convention Center	

Session Chairs: Laura J. Turbini, University of Toronto, Ctr. for Microelect. Assembly & Pkgg., Toronto, Ontario M5S 3E4 Canada; Sung K. Kang, IBM, T. J. Watson Rsch. Ctr., Yorktown Heights, NY 10598 USA

# 8:30 AM Invited

**Controlling Ag3Sn Plate Formation in Near-Ternary-Eutectic Sn-Ag-Cu Solders by Minor Zn Alloying Addition**: *Sung K. Kang*<sup>1</sup>; Da-Yuan Shih<sup>1</sup>; Donovan Leonard<sup>1</sup>; Donald W. Henderson<sup>2</sup>; Timothy A. Gosselin<sup>2</sup>; Sungil Cho<sup>3</sup>; Won Kyoung Choi<sup>4</sup>; <sup>1</sup>IBM, T.J. Watson Rsch. Ctr., Yorktown Heights, NY 10598 USA; <sup>2</sup>IBM Microelectronics, Endicott, NY USA; <sup>3</sup>KAIST, Matls. Sci. & Engrg., Daejon Korea; <sup>4</sup>Samsung Advanced Institute of Technology, Suwon 440-600 Korea

As a result of extensive search, near-ternary-eutectic Sn-Ag-Cu alloys have been identified as the leading Pb-free solder candidate to replace Pb-bearing solders for microelectronic applications. However, recent studies on the processing behaviors and solder joints reliability assessment have revealed several potential reliability risk factors associated with the alloy system. The formation of large Ag3Sn plates in solder joints, especially solidified in a relatively slow cooling rate, is one issue of concern. In the previous studies, the implication of large Ag3Sn plates on solder joint performance has been reported in addition to several methods to control the formation of large Ag3Sn plates. In this study, the effects of minor Zn alloying addition are investigated to control the formation of large Ag3Sn plates. The minor Zn addition has found to reduce the amount of undercooling required for the solidification and thereby to suppress the formation of large Ag3Sn plates. The Zn addition has also caused the changes in the microstructure in bulk as well as the interfacial reaction. The interaction of Zn with other alloying elements in the solder has also been

investigated to understand the role of Zn during the solidification of the near-ternary-eutectic alloys.

# 8:55 AM

Contact Angle Measurements of Sn-Ag and Sn-Cu Lead-Free Solders on Copper Substrates: *Mario F. Arenas*<sup>1</sup>; Viola L. Acoff<sup>1</sup>; <sup>1</sup>The University of Alabama, Metallurgl. & Matls. Engrg., PO Box 870202, Tuscaloosa, AL 35487 USA

Due to environmental concerns, a variety of Pb-free solder alloys have been proposed to replace the conventional Pb-37Sn as a general use solder. Eutectic solders of compositions Sn-3.5Ag (wt%) and Sn-0.7Cu (wt%) are strong candidates for that purpose. Implementation of those solder alloys requires detailed knowledge of the wettability of the new alloys on copper substrates. Since wettability is generally described by the contact wetting angle, its determination is of particular interest. In this study, the contact angles of various lead-free solders, belonging to the eutectic systems mentioned above, were measured on copper substrates to investigate the wetting behavior. Measurements were performed using the sessile-drop method under constant temperature in combination with a photographic technique that produced precise results. The effects of the addition of Bi and Cu to the Sn-Ag alloy and the type of flux were also investigated. The microstructures obtained during the wetting process were analyzed by scanning electron microscopy with energy dispersive X-ray spectroscopy. Results were compared against the conventional Pb-Sn alloy.

#### 9:15 AM

Effect of Cu Concentration on Morphology of Sn-Ag-Cu Solders by Mechanical Alloying: *Szu Tsung Kao*<sup>1</sup>; Jenq Gong Duh<sup>1</sup>; <sup>1</sup>National Tsing Hua University, Dept. of Matls. Sci. & Engrg., 101, Sect. 2 Kuang Fu Rd., Hsinchu 300 Taiwan

Cu contents in the solder alloy have recently been found to affect the intermetallic compound (IMC) formation mechanism in Sn-Ag and Sn-Ag-Cu solder system when reacted with Ni under bump metallization (UBM) after reflow. In this study, the effect of Cu concentration in the ternary Sn-3.5Ag-xCu (x=0.2, 0.7, and 1) solder alloy by mechanical alloying (MA) was investigated. The (Cu, Sn) solid solution was precipitated as Cu6Sn5 IMC which distributed non-uniformly through the microstructure. The IMCs, which exists at high Cu composition, cause the as-milled MA particle to fracture to a smaller size. Appreciable distinction on morphology of as-milled MA powders with different Cu concentration was revealed. When the Cu concentration was low (x=0.2), MA particle aggregated to a spherical ingot with large particle size. For high Cu concentration (x=0.7 and x=1), MA particle turned to flakes with smaller particle size. In addition to morphological difference, the microstructure and thermal behavior with various milling time for Sn-Ag-Cu alloy was also evaluated.

#### 9:35 AM

Effect of Silver on the Grain Boundary Pinning and Grain Growth in Bulk Tin and Bulk Eutectic Tin Silver Solder: Adwait U. Telang<sup>1</sup>; Thomas R. Bieler<sup>1</sup>; K. N. Subramanian<sup>1</sup>; <sup>1</sup>Michigan State University, Chem. Engrg. & Matl. Sci., 2527 Engrg. Bldg., E. Lansing, MI 48824 USA

Bulk specimens using 99.99% pure tin and eutectic Sn-3.5wt.%Ag were cast into a ceramic crucible in air. The specimens were metallographically polished and the microstructure was characterized over a 1000x1000  $\mu$   $^{2}$  area using orientation imaging microscopy (OIM). The initial microstructure of the pure tin showed 100-200 µ polycrystalline grains with a wide variety of misorientations in the as cast condition. After aging at 150°C for 200 hours, grain growth occurred to 250-1000  $\mu$ , and there were only two highly preferred high angle misorientations. During heating, aging, and cooling, ledges developed at grain boundaries, marking the position of most of the grain boundaries at the beginning of aging, and at the end of aging. In contrast, the OIM investigation of the bulk eutectic specimen showed 10-20  $\mu$  tin cells in a dendritic microstructure having two dominant crystal orientations with strongly preferred misorientations of <10° and 60° in a similarly sized region. Aging did not alter the eutectic microtexture but some additional high angle misorientation peaks developed. There was no ledge formation after this isothermal aging treatment. Aging caused sharpening of low angle boundaries within tin cells, and some boundaries were evident within the Ag3Sn precipitation regions. The role of Ag<sub>3</sub>Sn precipitates and the anisotropy of the thermal expansion coefficient of tin on microstructural evolution, grain boundary sliding, and ledge development is discussed.

#### 9:55 AM

Development of New Lead-Free Solder Containing Nano Sized Particles: Keun-Soo Kim<sup>1</sup>; Katsuaki Suganuma<sup>1</sup>; Minoru Ueshima<sup>2</sup>; <sup>1</sup>Osaka University, ISIR, 8-1 Mihogaoka, Ibaraki, Osaka 567-0047 Japan; <sup>2</sup>Senju Metal, Hashido 23, Adachi, Tokyo 120-8555 Japan

Controlling solidification behavior becomes one of the key factors because the formation of solidification defects must be prevented in order to accomplish stable and reliable assembling. It is expected that the addition of some solidification nuclei for Sn-Ag-Cu solder can refine the solidification microstructure and will suppress undercooling. In this study, the effects of small addition, of the nano sized metal and ceramic particles, on solidification aspects, and solderabilities of Sn-3Ag-0.5Cu lead-free solder were investigated. The solidification process of solder fillets of Sn-3Ag-0.5Cu-X joint has been examined by using in situ observation system and the solidification simulation. The useful effects of preventing solidification defect and improving solder structure can be obtained by the addition of Ni, Co or ceramic nano particles. The addition of fourth elements to Sn-3Ag-0.5Cu alloy significantly reduced the solidification defect and suppressed undercooling by being nucleation sites for solidification.

# 10:15 AM Break

#### 10:25 AM Invited

Solidification Phenomenon in CSP Soldering with Sn-Ag-Cu Lead-Free Alloy Using In Situ Observation System with Computer Simulation: Katsuaki Suganuma<sup>1</sup>; Keun-Soo Kim<sup>1</sup>; Chi-Won Hwang<sup>1</sup>; <sup>1</sup>Osaka University, ISIR, 8-1 Mihogaoka, Ibaraki, Osaka 567-0047 Japan

The formation of solidification defects in lead-free solders is greatly influenced by material factors as well as a design of circuit assemblies. The sensitivity of Sn-Ag-Cu solder microstructure to various types of circuit assemblies must be understood systematically in order to establish sound joint structures. In the present study, the solidification process of solder balls on circuit boards with a chip scale package (CSP) soldered with Sn-3wt%Ag-0.5wt%Cu has been examined primarily by using in situ observation system and the solidification simulation. Microstructural observations were carried out on soldered joints by using metallography. The solidification of solder ball on a CSP propagated from the near top region to the base chip. The solidification rate of solder balls in CSP joint is inhomogeneous and locally time dependent. The solidification simulation of CSP joint showed the solidification sequence and predicted location of soldification defects. The experimental results correlated with the simulation.

#### 10:50 AM

A Study of Solidification and Microstructure Development in Reflow of Nickel-Reinforced Nano-Composite Lead-Free Solder Paste: D. C. Lin<sup>1</sup>; T. S. Srivatsan<sup>1</sup>; G.-X. Wang<sup>1</sup>; M. Petraroli<sup>2</sup>; <sup>1</sup>University of Akron, Mech. Engrg., 302 E. Buchtel Mall, Akron, OH 44325-3903 USA; <sup>2</sup>The Timken Company, Timken Rsch., 1835 S.W. Dueber Ave., Canton, OH 44706-0930 USA

The increasing use of electronic devices in automobile and spacerelated applications puts a stringent requirement on mechanical strength and fatigue endurance capabilities of solder joints. This engineered efforts for new and improved high-strength, lead-free solders. Recent developments in nano-technology have made available a spectrum of nano-sized particles. Potential attempts have been made to form nanocomposites by using nano-particles as the reinforcing agents. A series of recent experiments have convincingly demonstrated that addition of trace amounts of nano-sized particles does significantly improve properties of the material. In this study, the base material used was the eutectic Sn-3.5%Ag alloy, and the nanoparticle was pure nickel. Nanocomposite solder pastes mixed with varying percentages of nanoparticle have been developed. Reflow experiments were performed under various cooling conditions. It was observed that addition of trace amounts of nickel nano-particles does significantly alter the solidification kinetics of the solder while concurrently influencing the intrinsic microstructural features, i.e., microstructural development and phase formation in the solidified end product. The nano-composite solders revealed appreciable increase in microhardness, up to as high as 20%.

# 11:10 AM

Can Thermodynamic Data Help Us to Develop New Solder Materials?: *Sabine Knott*<sup>1</sup>; Adolf Mikula<sup>1</sup>; <sup>1</sup>University of Vienna, Inst. of Inorganic Chmst., Währingerstraße 42, Vienna 1090 Austria

In Europe lead containing solders must be replaced by July 2006 with lead free materials. Therefore an intensive research to develop some new solder to replace Pb-Sn is going on. For the development of these new materials information of the phase diagrams, the phase equilibria and the melting behaviour is necessary. Some of these properties, like the melting temperature, the solidification path and the surface properties, must be measured. To calculate some properties like wetting and surface tension, various models can be used. For all these calculations the knowledge of the thermodynamic properties is necessary. We will show how the thermodynamic properties of the Cu-In-Zn and the Al-Sn-Zn systems are determined and how we can calculate the wetting and surface tension of these new solder materials.

# 11:30 AM

Experimental Investigation and Thermodynamic Calculation of the Phase Equilibria in the Sn-Au-Ni System: Xing Jun Liu<sup>1</sup>; Makoto Kinaka<sup>1</sup>; Yoshikazu Takaku<sup>1</sup>; Ikuo Ohnuma<sup>1</sup>; Ryosuke Kainuma<sup>1</sup>; Kiyohito Ishida<sup>1</sup>; <sup>1</sup>Tohoku University, Dept. of Matls. Sci., Grad. Sch. of Engrg., Sendai, Miyagi 980-8579 Japan

The phase equilibria in the Sn-Au-Ni system are of importance for understanding interfacial reaction between Sn base solders and Cu substrate coated by Au and Ni. In the present work, the phase equilibria of the Sn-Au-Ni system were investigated by means of differential scanning calorimetry and metallography. Six isothermal section diagrams in the Sn-rich portion at 200-600C, as well as three vertical sections at Au:Ni=1:1, 50 wt.%Sn and 40 wt.%Sn were determined. Some experimental results were obtained as follows: (1) there exists a ternary compound, SnAuNi2, which is stable up to about 400C, (2) there are very large solubilities of Au in the Ni3Sn2 in the Sn-Ni system, and of Sn in the AuSn compound in the Au-Sn system, and (3) there exists the phase equilibrium between Ni3Sn2 and AuSn compounds at 400C, rather than the continuous phase region from Ni3Sn2 to AuSn phases reported previously. Thermodynamic assessment of the Sn-Au-Ni system was also carried out using the CALPHAD method, in which the Gibbs energies of the liquid, fcc and bcc phases are described by the subregular solution model and that of compounds, including a ternary compounds, are represented by the sublattice model. The thermodynamic parameters for describing the phase equilibria were optimized, and agreement between the calculated and experimental results was obtained.

### 11:50 AM

Wetting/Spreading in the Au-Sn System: *Timothy J. Singler*<sup>1</sup>; Liang Yin<sup>1</sup>; Stephan J. Meschter<sup>2</sup>; <sup>1</sup>SUNY Binghamton, Dept. of Mech. Engrg., Binghamton, NY 13902-6000 USA; <sup>2</sup>BAE System, Failure Analy. Lab., 600 Main St., Johnson City, NY 13790 USA

Sn drops spreading isothermally on Au substrates in a gaseous flux atmosphere were used to characterize wetting/spreading in the Au-Sn system. The narrow temperature range 250<T<430°C was explored and revealed a wide variation in dynamic liquid/solid phase behavior, including partial and complete solutal freezing and the appearance of an extremely short-lived (e.g., 350 ms) transient solid phase. Contact line mobility and the roles of dissolution and formation of specific intermetallic compounds ( $\eta$  (AuSn<sub>4</sub>),  $\varepsilon$  (AuSn<sub>2</sub>),  $\delta$  (AuSn),  $\zeta$ ) in wetting are discussed.

# Magnesium Technology 2004: Automotive Applications/Welding

Sponsored by: Light Metals Division, LMD-Magnesium Committee Program Organizer: Alan A. Luo, General Motors, Materials and Processes Laboratory, Warren, MI 48090-9055 USA

Monday AM	Room: 203B
March 15, 2004	Location: Charlotte Convention Center

Session Chairs: John E. Allison, Ford Motor Company, Dearborn, MI 48124-2053 USA; Allen Schultz, Hatch Associates, Mississauga, ON L5K 2R7 Canada

# 8:30 AM

The Magnesium Powertrain Cast Components Project: Part I -Accomplishments of Phase I and the Objectives and Plans for Testing the Magnesium Engine in Phase II: Bob R. Powell<sup>1</sup>; Larry J. Ouimet<sup>1</sup>; Joy A. Hines<sup>2</sup>; John E. Allison<sup>2</sup>; Randy S. Beals<sup>3</sup>; Lawrence Kopka<sup>3</sup>; Peter P. Ried<sup>4</sup>; <sup>1</sup>General Motors Corporation, Warren, MI 48090-9055 USA; <sup>2</sup>Ford Motor Company, Dearborn, MI USA; <sup>3</sup>DaimlerChrysler Corporation, Auburn Hills, MI USA; <sup>4</sup>Ried and Associates, Portage, MI USA

The US Automotive Materials Partnership (USAMP) and the US Department of Energy launched the Magnesium Powertrain Cast Components Project in 2001 to determine the feasibility and desirability of producing a magnesium-intensive engine; a V6 engine with a magnesium block, bedplate, and structural oil pan. The Project completed the first two of five project goals: (1) evaluation of the best available low-cost, creep-resistant magnesium alloys and (2) design of the engine components. The Phase II goals of the project are: (3) casting and dynamometer- or vehicle-testing the magnesium components in

assembled powertrains, (4) developing a powertrain magnesium alloy design database and common alloy specification for magnesium powertrain alloys, and (5) promoting the building of the scientific infrastructure for magnesium in North America to enable even more advanced powertrain applications in the future. This presentation provides an overview of the Project.

# 8:50 AM

The USAMP Magnesium Powertrain Cast Components Project: Part II - Properties of Several New Creep-Resistant Magnesium Alloys: Joy A. Hines<sup>1</sup>; Robert C. McCune<sup>1</sup>; John E. Allison<sup>1</sup>; Bob R. Powell<sup>2</sup>; Larry J. Ouimet<sup>2</sup>; Randy S. Beals<sup>4</sup>; Lawrence Kopka<sup>4</sup>; Peter P. Ried<sup>3</sup>; <sup>1</sup>Ford Motor Company, Dearborn, MI USA; <sup>2</sup>General Motors Corporation, Warren, MI USA; <sup>3</sup>Ried and Associates, Portage, MI USA; <sup>4</sup>DaimlerChrylser Corporation, Auburn Hills, MI USA

As automotive companies try to reduce weight in vehicles to improve fuel economy, magnesium alloys have increasingly become an attractive replacement material for many components. However, the lack of high temperature creep resistance in the established Mg alloys such as AZ91 or AM60 has precluded their use in powertrain applications such as engine blocks. Recently, a number of new alloys have been introduced to address the lack of creep resistance at a reasonable cost. USAMP is in the third year of a five year project aimed at determining the feasibility of several new Mg alloys for use in certain powertrain components including engine blocks, low crank cases, oil pans, and front covers. The Magnesium Powertrain Cast Components (MPCC) project has examined six die casting and three sand casting alloys for their mechanical properties, corrosion resistance and castability. This talk will present some of the preliminary results of this investigation.

# 9:10 AM

The USAMP Magnesium Powertrain Cast Components Project: Part III - Fundamental Scientific Needs for Magnesium Utilization in the Powertrain Environment: Randy S. Beals<sup>1</sup>; Lawrence Kopka<sup>1</sup>; Joy A. Hines<sup>2</sup>; Robert C. McCune<sup>2</sup>; John E. Allison<sup>2</sup>; Alan A. Luo<sup>3</sup>; Bob R. Powell<sup>3</sup>; Larry J. Ouimet<sup>3</sup>; Peter P. Ried<sup>4</sup>; <sup>1</sup>DaimlerChrysler Corporation, Auburn Hills, MI USA; <sup>2</sup>Ford Motor Company, Dearborn, MI USA; <sup>3</sup>General Motors Corporation, Warren, MI USA; <sup>4</sup>Ried and Associates, Portage, MI USA

The Magnesium Powertrain Cast Components Project is a jointly sponsored effort (by the US Department of Energy and the US Council for Automotive Research) to determine the feasibility and desirability of producing a magnesium-intensive engine. Through FEA design activities and extensive alloy testing, the Project seeks to determine the technical requirements of a V-engine and which of several newly developed, high temperature magnesium alloys meet those requirements. An additional objective of the Project is to identify the fundamental scientific challenges of using magnesium alloys and casting processes in powertrain components, both within the current Project and for more advanced powertrain components, including transmission cases. The areas thus identified, such as creep and fatigue deformation mechanisms of magnesium alloys, thermodynamic and phase equilibrium databases, and predictive models of casting, manufacturing, and performance behavior will be presented and discussed. The Project program to promote new, and strengthen existing, magnesium scientific research in the North America will be described.

# 9:30 AM

Friction Stir Welding of Magnesium AM60 Alloy: *Naiyi Li*<sup>1</sup>; Tsung-Yu Pan<sup>1</sup>; Ronald P. Cooper<sup>1</sup>; Dan Q. Houston<sup>1</sup>; Zhili Feng<sup>2</sup>; Michael L. Santella<sup>2</sup>; <sup>1</sup>Ford Motor Company, Mfg. & Processes, 2101 Village Rd. MD3135, Dearborn, MI 48124 USA; <sup>2</sup>Oak Ridge National Laboratory, Metals & Ceramics, PO Box 2008, Oak Ridge, TN 37831 USA

An investigation has been carried out on the friction stir welding of magnesium alloy, AM60. Casting samples of various thickness have each been welded and their mechanical properties were presented. The microstructure and defect formation were conducted by optical and scanning electron microscopes. More attention was paid to failure mode of welded pieces near joined area or so-called thermo-mechanical affected zone under tension and voids formed during friction stir welding. In addition, the effect of FSW processing parameters and casting thickness on the mechanical properties will be presented. At the end, a cost analysis using friction stir welding for magnesium application on the Ford GT vehicles will be presented.

# 9:50 AM Break

# 10:20 AM

Friction Stir Welding of Magnesium Die Castings: Jan Ivar Skar<sup>1</sup>; Haavard Gjestland<sup>2</sup>; Ljiljana Djapic Oosterkamp<sup>3</sup>; Darryl Albright<sup>4</sup>; <sup>1</sup>Norsk Hydro ASA, Corp. Rsch. Ctr., PO Box 2560, Porsgrunn N- 3907 Norway; <sup>2</sup>Hydro Aluminium, Magnesium Competence Ctr., PO Box 2560, Porsgrunn N-3907 Norway; <sup>3</sup>Hydro Aluminium, R&D Matls. Tech., Karmøy, Haavik N-4265 Norway; <sup>4</sup>Hydro Magnesium, Mkt. Dvlp., 39209 Six Mile Rd., Ste. 200, Livonia, MI 48152 USA

Friction stir welding (FSW), being a solid-state process, is an attractive method for joining magnesium die castings. In this study, FSW of AZ91D and AM50A plates was performed on the individual alloys and to join them together. The welds were sound and free from defects, except for small surface cracks in AM50A; a fine microstructure characterized the weld zones. The mechanical properties of specimens transverse to the weld zone were measured, as were the corrosion properties. The mechanical properties were somewhat lower than the base metal, with the largest percentage decrease found in the elongation of AM50A, perhaps due to the surface cracking. The corrosion resistance of the weld zone was relatively poor, most likely due to iron contamination from wearing of the tool. Further optimization of the FSW tool design and process parameters must take place to improve the reliability of FSW for magnesium die castings.

#### 10:40 AM

Fundamental Studies of the Friction-Stir Welding of Dissimilar Magnesium Alloys and Magnesium Alloys to 6061 Aluminum: Anand C. Somasekharan<sup>1</sup>; Lawrence E. Murr<sup>1</sup>; <sup>1</sup>University of Texas, Dept. of Metallurgl. & Matls. Engrg., 500 W. Univ. Ave., El Paso, TX 79968 USA

This study involved the friction-stir welding (FSW) of various dissimilar magnesium (Mg) alloys to themselves and to 6061 aluminum (Al). This paper describes the specificities of the process used for the FSW of the Mg alloys to themselves and to Al6061, as well as the analysis of the resultant welds. The various Mg alloys used were hotrolled alloy AZ31B-H24 and semi-solid-cast alloys AZ91D (primary solid fractions of ~3% and ~20%) and AM60 (primary solid fractions of ~3% and ~20%). Dissimilar Mg alloy systems included the FSW of AZ91D with AM60, and the FSW of AZ91D with AZ31B-H24. Both Mg AZ91D and AZ31B-H24 alloys were welded to Al 6061. Numerous welds were made with the Mg alloys and Al 6061 in the advancing and retreating sides. Optical metallography was used to observe and confirm the weld zone characteristics unique to dissimilar welds. Dynamic recrystallization was observed in the weld region as well as in the transition region (HAZ), with a clear decrease in the grain size from the base material through the transition zone and into the FSW zone. The welds were free of porosities. The dissimilar Mg alloy welds revealed a homogenous, equi-axed, fine-grain structure in the FSW zone, with complex intercalated microstructures in the FSW zone. Vickers microhardness testing on the dissimilar Mg alloy systems revealed no degradation of residual microhardness of the material in the FSW zone or the transition zone. The FSW zone in the welds of Mg alloys to Al6061 showed unique dissimilar-weld characteristics such as complex intercalated microstructures with bands of recrystallized Mg inside Al and vice versa. Elemental data analysis (EDAX) was performed on the weld region to gauge the distribution of either material. Bands with equal parts of Mg and Al, as well as unique recrystallized bands with predominance of either material were observed. Vickers microhardness testing was performed on the weld cross-sections to obtain microhardness profiles that revealed the compensation of the usual degradation of Al6061 in the HAZ. TEM studies were also undertaken to further the understanding of these welds.

#### 11:00 AM

Magnesium-Lithium Alloy Weldability: A Microstructural and Property Characterization: Garrett J. Atkins<sup>1</sup>; David L. Olson<sup>1</sup>; Dan Eliezer<sup>2</sup>; <sup>1</sup>Colorado School of Mines, Matls. & Metallurgl. Engrg., 1500 S. Illinois St., Hill Hall, Golden, CO 80401 USA; <sup>2</sup>Ben Gurion University of the Negev, Dept. of Matls. Engrg., Beer Sheva 84105 Israel

Magnesium with over 10-wt % Lithium alloy addition exhibits a BCC crystal structure. This situation often offers a significant improvement in formability when compared to HCP magnesium alloys. Magnesium is commonly used as a cast alloy. However, a magnesium alloy with acceptable weldability and improved formability offers an economical advantage by allowing the use of formed wrought material along with acceptable welding procedures to fabricate welded technical assemblies. In this research the weld microstructure and properties were characterized for two magnesium-lithium alloys. With 7.5-wt% Li the first alloy is an alpha+beta alloy. The other alloy contained 10.2-wt% Li making it a fully bcc (beta) alloy. These materials were welded using the GTAW process and specific microstructures were file and characterized. Corrosion susceptibility and hardness profiles were measured and compared to a traditional magnesium alloy.

# 11:20 AM

Laser Welding of AM60 Magnesium Alloy: A. Dasgupta<sup>1</sup>; J. Mazumder<sup>1</sup>; <sup>1</sup>University of Michigan, Ctr. for Laser Aided Intelligent Mfg., Ann Arbor, MI USA

Due to limited fossil fuel reserves and stringent emission regulations, automotive companies today are keen on finding out ways to reduce fuel consumption and emission of vehicles. As a result, there has been an increased focus on lighter metals like aluminum and magnesium for auto fabrication. While much research has been done on the use of aluminum, there are lots of unanswered questions as far as use of magnesium is concerned. In this paper we have discussed the feasibility of laser welding of die-cast magnesium alloy AM60 for automotive applications. Porosity, mechanical strength and material characteristics of welds are presented. Techniques for reducing porosity are also discussed.

# Materials by Design: Atoms to Applications: Materials Chemistry and Alloy Design

Sponsored by: Electronic, Magnetic & Photonic Materials Division, EMPMD/SMD-Chemistry & Physics of Materials Committee

*Program Organizers:* Krishna Rajan, Rensselaer Polytechnic Institute, Department of Materials Science and Engineering, Troy, NY 12180-3590 USA; Krishnan K. Sankaran, The Boeing Company, Phantom Works, St. Louis, MO 63166-0516 USA

Monday AM	Room: 210B
March 15, 2004	Location: Charlotte Convention Center

Session Chair: Krishna Rajan, Rensselaer Polytechnic Institute, Dept. of Matls. Sci. & Engrg., Troy, NY 12180-3590 USA

# 8:30 AM Symposium Introduction: K. Rajan and K. K. Sankaran 8:45 AM

First Principles Multi-Scale Materials Design: William A. Goddard, III<sup>1</sup>; <sup>1</sup>California Institute of Technology, Pasadena, CA 91125 USA

Advances in theory are making it practical to consider fully first principles (de novo) predictions of the performance of materials and functional devices for many important systems and processes. In order for such de novo atomistic simulations to fully impact industrial design applications, it is necessary to develop strategies for linking the time and length scales from electrons to manufacturing. We will describe some of the advances in the atomistic methods plus the strategies in developing mesoscale descriptions of that provide fully first principles (de novo) predictions of the fundamental properties and processes for such systems. Overlapping these levels allows a bottoms-up strategy for getting a first principles description at the continuum level. We will illustrate some of the recent progress in Multi Scale Materials Design with applications to various problems in materials ranging from metals and oxides to semiconductors and polymers to nucleic acids and proteins.

# 9:15 AM

Noburnium: A 1300C Cyberalloy: Gregory B. Olson<sup>1</sup>; <sup>1</sup>Northwestern University, Dept. of Matls. Sci. & Engrg., 2220 Campus Dr., Evanston, IL 60208 USA

Under the Air Force MEANS initiative, a multi-institutional, multidisciplinary project addresses optimal integration of computational design and efficient experimentation for the accelerated design and development of high performance materials using the example of Nb-based superalloys combining oxidation resistance, creep strength and ductility for aeroturbine applications operating at 1300C and above. Integrated within a systems engineering framework, the effort tests the limits of ab-initio quantum mechanical methods to accelerate assessment of thermodynamic and kinetic databases enabling comprehensive predictive design of multicomponent multiphase microstructures as dynamic systems. Based on established principles underlying Ni base superalloys, the central microstructural concept is a dispersion strengthened system in which coherent cubic aluminide phases provide both creep strengthening and a source of Al for Al2O3 passivation enabled by a Nb-based BCC alloy matrix with required transport and oxygen solubility behaviors.

#### 9:45 AM

Interfacing Ab Initio Results to Phenomenological Alloy Thermodynamics: Patrice E.A. Turchi<sup>1</sup>; Vaclav Drchal<sup>2</sup>; Josef Kudrnovsky<sup>2</sup>; Zi-Kui Liu<sup>3</sup>; Larry Kaufman<sup>4</sup>; <sup>1</sup>Lawrence Livermore National Laboratory, C.&M.S. (L-353), PO Box 808, Livermore, CA 94551 USA; <sup>2</sup>Institute of Physics, Acad. of Scis. of the Czech Republic, Na Slovance 2, Prague 8 CZ 182-21 Czech Republic; <sup>3</sup>Pennsylvania State University, Dept. of Matls. Sci. & Engrg., University Park, PA 16803 USA; <sup>4</sup>Massachusetts Institute of Technology, Dept. of Matls. Sci. & Engrg., Cambridge, MA 02139 USA

First-principles results of alloy energetics and phase diagrams can appropriately supplement thermodynamic databases that are used within the phenomenological CALPHAD approach for predicting the stability properties of complex multi-component alloys. Routine energy minimization of alloys stability within ab initio methodology provides input to CALPHAD in terms of heats of formation and transformation for alloys exhibiting various crystalline structures, and any chemical configuration. Additionally, ab initio energetics combined with a statistical treatment provide the necessary thermodynamic information for subsequent assessments similar to those performed with experimental data within CALPHAD. Following a brief overview of the firstprinciples and phenomenological methodologies, examples of both aspects of the interfacing will be presented with applications to multicomponent alloys. Finally, validity of this interfacing and its relevance to alloy design will be discus sed. Work performed under the auspices of the U.S. Department of Energy by the University of California Lawrence Livermore National Laboratory under Contract W-7405-ENG-48.

#### 10:15 AM Break

#### 10:30 AM

**Design of Electronic Materials**: Subhash Mahajan<sup>1</sup>; <sup>1</sup>Arizona State University, Chem. & Matls. Engrg., Tempe, AZ 85287 USA

Abstract not available.

# 11:00 AM

Materials-by-Design: Direct and Inverse Methods Using Multi-Objective Stochastic Optimization: George S. Dulikravich<sup>1</sup>; <sup>1</sup>Florida International University, Dept. of Mech. & Matls. Engrg., Miami, FL 33199 USA

Alloy design for critical aero engine components such as turbine blades and discs is a difficult, time-consuming and expensive process. We propose to use and adapt an advanced semi-stochastic algorithm for constrained multi-objective optimization and combine it with experimental testing and verification to determine optimum concentrations of alloying elements in heat-resistant and corrosion-resistant stainless steel alloys that will simultaneously maximize a number of alloy's mechanical properties. The proposed research will result in a rigorous and efficient tool for the design of high-strength heat-resistant and corrosion-resistant steels unattainable by any means existing at the present time. The proposed methodologies will be applicable for the optimization of the composition of arbitrary alloys tailored to several physical properties. Inversely, for a desired set of physical properties objectives this algorithm will be able to determinate a corresponding set of candidate alloy compositions that will be able to create these specified properties.

## 11:30 AM

Experimental Phase Relations and Thermodynamics of Ultra-High Temperature Metals and Alloys: Surendra Saxena<sup>1</sup>; <sup>1</sup>Florida International University, Ctr. for the Study of Matter Under Extreme Conditions, Miami, FL 33199 USA

We may conduct phase equilibrium experiments to temperatures reaching ~4000 K. For many binary systems, only calculated data are available at such high temperatures and at other temperatures the products are poorly characterized and in-situ characterization coupled with ex-situ studies of quenched systems (e.g. high resolution transmission electron microscopy and microanalysis of phase stability) is totally missing. A detailed experimental study of phase stability at a variety of length scales coupled to the characterization of the phase transformations using electron microscopy, X-ray and Raman should establish a comprehensive basis for the design of new material microstructures and chemistries. Examples of such systems are many: W with several other metals e.g. W-Cr (1500-3400 K), W- Mo (solidmelt relation from 2600 to 3500 K), and similar binary systems with rhenium, and hafnium-based materials, silicides and binary refractory oxides such as Bi2O3-Sc2O3. The techniques are quite suitable to explore the synthesis of new alloys and intermetallics at high temperatures and also involve pressure if need be. The experimental data will be coupled to computational studies based on the use of large-scale thermochemical and crystallographic databases for the calculation and prediction of phase stability.

# Materials Issues in Fuel Cells: State-of-the-Art

Sponsored by: TMS

*Program Organizers:* Brajendra Mishra, Colorado School of Mines, Kroll Institute for Extractive Metals, Golden, CO 80401-1887 USA; John M. Parsey, ATMI, Mesa, AZ 85210-6000 USA

Monday AM	Room: 207B/C
March 15, 2004	Location: Charlotte Convention Center

Session Chairs: Brajendra Mishra, Colorado School of Mines, Metallurgl. Engrg., Golden, CO 80401 USA; Z. Gary Yang, Pacific Northwest National Laboratory, Matls. Sci. Div., Richland, WA 99352 USA

#### 8:30 AM Keynote

The Hydrogen Economy: Opportunities of Materials and Nanomaterials to Address Some Grand Challenges: M. S. Dresselhaus<sup>1</sup>; <sup>1</sup>Massachusetts Institute of Technology, Depts. of Elect. Engrg. & Computer Sci., & Dept. of Physics, Cambridge, MA 02139 USA

One of the Grand Challenges of the 21st Century is to achieve a sustainable energy supply. The 20th Century has seen remarkable advances in Science and Technology, resulting in expectations for a higher standard of living. This has required large increases in per capita energy consumption. Projections of per capita energy needs for the 21st Century indicate that new technologies for sustainable energy production, storage, and use will need to be developed in the next 50 years. The so-called hydrogen economy is one such proposal that is presently being considered worldwide. In this talk the requirements of a hydrogen economy will be discussed in the context of the recent DOE report on "Basic Research Needs for the Hydrogen Economy". Hydrogen production, storage and utilization, will be discussed with emphasis given to the large gap between present science/technology knowhow and the requirements in efficiency/cost for a sustainable hydrogen economy. Opportunities for materials and nanomaterials to narrow this gap will be discussed.

# 9:10 AM Invited

Materials Issues in Fuel Cell Development and Manufacturing: Dennis W. Readey<sup>1</sup>; <sup>1</sup>Colorado School of Mines, Dept. of Metallurgl. & Matls. Engrg., 1500 Illinois St., Golden, CO 80401 USA

At present, there is considerable interest in making fuel cells commercially viable because of their promise of more efficient utilization of fuels and, in some cases, lower emissions. Fuel cells are conceptually simple but the range of applications, fuels, types, and system integration generate many materials issues. Fuel cells are currently being considered as large power sources for stationary power plants, as power sources requiring power and temperature cycling for automobiles and other vehicles, and as small energy sources to replace batteries in laptop computers and hand-held electronic devices. In addition, although there is a current emphasis on hydrogen as a fuel, there is a need to have fuel cells that can operate on hydrocarbons such as methane and renewable fuels such as methanol. Finally, there are different approaches to fuel cells depending on the nature of the ionconducting electrolyte with the current interest focused on hydrogen conducting polymer electrolytes and either oxygen or hydrogen conducting oxides. Materials issues range from the ionic conductivity of the electrolyte to the manufacturability of cell components. Critical materials issues for fuel cells are identified and their status and potential analyzed.

# 9:40 AM Invited

SOFC and PEM Materials Challenges and Development at Ford Motor Company: Alexander Bogicevic<sup>1</sup>; <sup>1</sup>Ford Motor Company, Rsch. & Advd. Engrg., 2101 Village Rd., Scientific Rsch. Labs., MD 3083, Dearborn, MI 48188 USA

Ford Motor Company is devoting significant research resources to the development of mobile and stationary fuel cell applications based on SOFC and PEM fuel cell technology. These include fuel cells for powertrain applications, auxiliary power units, and emissions abatement systems at automotive manufacturing plants. This presentation will focus on principal materials development challenges that underpin the technology progress in each of these applications. A broad perspective on how these are addressed within corporate, government, and university institutions will be given, and further development needs discussed.

10:10 AM Break

# 10:20 AM

**Thermodynamic Modeling of the LaCoO3-ä**: *Mei Yang*<sup>1</sup>; Zi-Kui Liu<sup>2</sup>; <sup>1</sup>Pennsylvania State University, Dept. Matls. Sci. & Engrg., 304 Steidle Bldg., University Park, State College, PA 16802 USA; <sup>2</sup>Pennsylvania State University, Dept. Matls. Sci. & Engrg., 209 Steidle Bldg., University Park, State College, PA 16802 USA

The perovskite-type binary oxide LaCoO3 has many possible applications in different fields, such as heterogeneous catalysis, oxygen sensors, solid oxide fuel cells and magnetic media. This oxide has a wide range of oxygen deficiency depending on temperature and oxygen partial pressure, which greatly affects its stability under service environment. It is thus desirable to establish a procedure to develop thermodynamic properties of this perovskite so its stability can be predicted. In the present work, the thermodynamic modeling and the first-principles calculations will be combined to obtain the Gibbs energy of LaCoO3-ä as a function of temperature and oxygen deficiency. As a solution phase, LaCoO3-ä was described by a three sublattice model (La)1(Co)1(O,Va)3. (La)1(Co)1(O)3 and (La)1(Co)1(Va)3 are two end-members of this LaCoO3-LaCoVa3 pseudo-binary system. The First-Principles calculations were performed using the computer code: VASP based on the pseudo-potentials and a plane wave basis set. The ground state total energies of the pure La, Co and O, and the both end-members of LaCoO3-ä were calculated at 0 K. The enthalpies of formation of the both end-members were obtained accordingly and used as a supplement in Thermo-Calc to evaluate the optimized Gibbs energy functions for LaCoO3-ä. Good agreement with experimental data is obtained by this combined Computational thermodynamics/ First-Principles calculations novel approach.

# 10:45 AM

Bismuth Substituted Dysprosium Iron Garnets for Magento-Optic Devices: *Pragati Mukhopadhyay*<sup>1</sup>; *Gautam Mukhopadhyay*<sup>2</sup>; <sup>1</sup>Indian Institute of Technology-Bombay, Advd. Ctr. for Rsch. in Elect., Powai, Mumbai, Maharashtra 400076 India; <sup>2</sup>Indian Institute of Technology-Bombay, Dept. of Physics, Powai, Mumbai, Maharashtra 400076 India

Bismuth substituted iron garnet (Bi DyIG) films are potential materials for magneto-optic devices. Efforts are being made world over to make films by various methods to enhance magneto-optic properties and make low cost viable devices. We have grown and reported many different rare earth substituted bismuth iron garnet films by LPE (Liquid Phase Epiptaxy) with enhanced magneto-optic properties but not of low cost. We report here the preparation and characterization of bismuth substituted dysprosium iron garnet films by an inexpensive sol gel method utilizing a modified chelating agent. By this method single phase garnet films can be grown with ease on larger surfaces on variety of substrates.

# 11:10 AM

Preparation of Ti-Fe-O Thin Films by Pulsed Laser Deposition: *Tsuneo Suzuki*<sup>1</sup>; Shuntaro Suzuki<sup>1</sup>; Satoko Ogata<sup>1</sup>; Makoto Hirai<sup>1</sup>; Hisayuki Suematsu<sup>1</sup>; Weihua Jiang<sup>1</sup>; Kiyoshi Yatsui<sup>1</sup>; <sup>1</sup>Nagaoka University of Technology, Extreme Energy-Density Rsch. Inst., 1603-1, Nagaoka, Niigata 940-2188 Japan

An intermetallic compound of TiFe is known as one of the reversible hydrogen storage alloys. Ti-Fe thin films have been prepared by Pulsed laser deposition. Although, the thin film prepared by the PLD method consisted of TiFe phase, the thin film contained the oxygen of 23 at. %. Although, the thin film prepared by the PLD method consisted of TiFe phase, the thin film contained the oxygen of 23 at. %. In previous work, by changing the titanium and iron contents in the Ti-Fe-O thin films, the thin films were observed to become from b-Ti phase dissolving iron atoms of 35% to TiFe one. In order to reveal the phase transition from b-Ti to TiFe phase in Ti-Fe-O thin film, we have changed the composition of the thin film by changing the surface area ratio of the targets (Ti and Fe plates).

# 11:35 AM

The Application of Planetary Ball Mill "Activator" for Fuel Cells Materials Synthesis in Industry Scale: Belyaev Eugene Yurievich<sup>1</sup>; <sup>1</sup>Activator Corporation, Musy Dzhalilya, 25, Novosibirsk, Novosibirsk reg 630055 Russia

The "Activator" mill predestinated for chemical synthesis under reactants intensive mechanical treatment. We were developing ones for synthesis nanostructures materials with the productivity 3-5 kg/h. The "Activator" advantages are: rotation speed 1200 rpm (balls acceleration up to 2000 m/sec2); smart balls moving by software control; active jars cooling by water; 4 or 6 jars (1 liter volume each). The process examples: preparing nanocomposite materials for solid oxide fuel cells (SOFC) - metal/YSZ or oxide/YSZ composites, solid state synthesis of perovskite structure materials (La1-XSrXMnO3, La1-XSrXFe1-YCoYO3). The mixing, preliminary annealing and grinding are the main part of ceramics technology. The mechanochemical advances are the steps diminishing and cost optimizing. The carbon nanostructures for fuel cells elements are easy produced by carbon treatment and controlled crystallization ones. By intensive milling, graphite structure was deformed and became amorphous. By recrystallization during annealing, the structure fragments is conversed to nanostructures - nanotubes or onion-like carbon. The advances are in low energy consumption and high productivity. We were optimizing chemical processes in jars by controls of balls moving and treatment regimes: impact (for grinding) - vortex (for mixing) - impact and shift (for synthesis). These regimes are programming by software because the central axis and planetary rotation separated by mechanics and controls by inverters.

# Materials Processing Fundamentals: Solidification and Casting

Sponsored by: Extraction & Processing Division, Materials Processing & Manufacturing Division, EPD-Process Fundamentals Committee, MPMD/EPD-Process Modeling Analysis & Control Committee

*Program Organizers:* Adam C. Powell, Massachusetts Institute of Technology, Department of Materials Science and Engineering, Cambridge, MA 02139-4307 USA; Princewill N. Anyalebechi, Grand Valley State University, L. V. Eberhard Center, Grand Rapids, MI 49504-6495 USA

Monday AM	Room: 2	12B		
March 15, 2004	Location:	Charlotte	Convention	Center

Session Chair: TBA

# 8:30 AM Invited

Technical Issues Impeding the Proliferation of Continuous Casting Processes in the Aluminum Industry: Prince N. Anyalebechi<sup>1</sup>; <sup>1</sup>Grand Valley State University, Padnos Sch. of Engrg., L. V. Eberhard Ctr., Ste. 718, Grand Rapids, MI 49504-6495 USA

In the past 35 years, the use of continuous casting in the Aluminum Industry has been mostly confined to "common alloy products" such as foils, electric conductor rods, building products, selected food packaging alloys, etc. Development of surface sensitive, high formability and drawability products, such as beverage can stock and automotive sheet continues to be technically challenging. This is ascribed to: (a) our insufficient understanding of the complex and dynamic phenomena that occur at the mold/metal interface during solidification and the constraints they place on productivity, product surface quality, range of "castable" aluminum alloy compositions, and cast microstructure; and (b) the lack of appropriate downstream process technology to take advantage of the unique metallurgical characteristics of continuously cast products. These and other reported technical problems encountered in the continuous casting of higher strength aluminum alloys and their attendant effects on the metallurgical characteristics of the final products are discussed.

# 9:00 AM

Effects of Alloying Elements on the Empirical Relationships Between Dendrite Arm Spacing and Solidification Processing Conditions in Aluminum Alloys: *Prince N. Anyalebechi*<sup>1</sup>; <sup>1</sup>Grand Valley State University, Padnos Sch. of Engrg., L. V. Eberhard Ctr., Ste. 718, Grand Rapids, MI 49504-6495 USA

Published and unpublished experimentally determined values of dendrite cell size and arm spacing in aluminum alloys as a function of solidification conditions and alloy composition have been critically reviewed and collated. Functional empirical models for predicting the effects of alloying elements, solidification rate, and local solidification time on dendrite arm spacing in binary and multicomponent aluminum alloys have been developed. Results of the study indicate that secondary dendrite arm spacing (or cell size) in aluminum alloys generally decrease with increase in solidification rate and by addition of titanium, copper, iron and silicon. Conversely, secondary dendrite arm spacing (or cell size) in cast aluminum products increases with increase in local solidification time and by addition of zinc. Magnesium, the most widely used alloying element in the aluminum industry, does not have any statistically significant effect on dendrite coarsening in commercial aluminum alloys.

# 9:20 AM Cancelled

Evaluation of the Reactivity of Gamma Titanium Aluminides with Multi-Layered, Yttria Face Coat, Investment Casting Shells

## 9:40 AM

**Control of a Die Casting Simulation Using an Industrial Adaptive Model-Based Predictive Controller**: *Richard Vetter*<sup>2</sup>; Daan M. Maijer<sup>1</sup>; Mihai Huzmezan<sup>2</sup>; Duncan Meade<sup>3</sup>; <sup>1</sup>University of British Columbia, Dept. of Metals & Matls. Engrg., 309 - 6350 Stores Rd., Vancouver, BC V6T 1Z4 Canada; <sup>2</sup>University of British Columbia, Dept. of Elect. & Compu. Engrg., 2356 Main Mall, Vancouver, BC V6T 1Z4 Canada; <sup>3</sup>Universal Dynamics Technologies Inc., 100-13700 International Place, Richmond, BC V6V 2X8 Canada

Mathematical modeling and simulation is a common technique to improve and optimize industrial processes. Complex models of casting processes are available to describe the evolution of process variables such as temperature and pressure, and can be used to reliably predict defect formation. Similarly, advances in control theory have lead to widespread use of online control for the majority of industrial processes. A multivariable control scheme has been developed to control a 2-D axisymmetric model of an industrial low-pressure wheel die casting process for use in assessing predictive control strategies to reduce defect formation. Temperatures at various locations within the die are controlled to predefined set points based on the cyclic steady state temperature profile. The volume flow rates of cooling media in multiple channels are used as control variables. The incoming molten aluminum temperature and die open time are used as a measured disturbance variables for the controller. The commercial adaptive predictive controller, BrainWave, which uses Laguerre basis functions to build its control models, has been used to control this virtual process.

#### 10:00 AM Break

#### 10:20 AM

Examination of Liquid-Tin Assisted Directional Solidification for Large Ni-Base Superalloy Castings: Andrew J. Elliott<sup>1</sup>; Graeme B. Karney<sup>2</sup>; Tresa M. Pollock<sup>1</sup>; Michael F.X. Gigliotti<sup>3</sup>; Warren T. King<sup>4</sup>; <sup>1</sup>University of Michigan, Matls. Sci. & Engrg., 2300 Hayward St., Ann Arbor, MI 48109-2136 USA; <sup>2</sup>Oxford University, Matls. Sci., Parks Rd., Oxford OX1 3PH UK; <sup>3</sup>GE, Corp. R&D, Niskayuna, NY 21309 USA; <sup>4</sup>GE, Power Sys., Greenville, SC 29602 USA

The liquid metal cooling (LMC) process has been used to directionally solidify large stepped cross-section Ni-base superalloy castings with significantly enhanced thermal gradients and increased withdrawal rates compared to the conventional radiation cooling process. The improved LMC process capabilities resulted in considerably enhanced cooling rates, refined microstructure, and reduced occurrence of casting defects, including elimination of freckle-type defects. Experiments designed to isolate individual process variables including withdrawal rate, superheat, and baffle thickness have been carried out in order to better understand the LMC process and how to optimize the casting process with particular emphasis on the solid-liquid interface location and shape. Relationships between process conditions and primary and secondary dendrite arm spacing are also investigated.

#### 10:50 AM

Columnar to Equiaxed Transition Analysis During Directional Solidification of Different Alloy Systems: Alicia Esther Ares<sup>2</sup>; Rubens Caram<sup>3</sup>; *Carlos Enrique Schvezov*<sup>1</sup>; <sup>1</sup>University of Misiones, 1552 Félix de Azara St., Posadas-Misiones 3300 Argentina; <sup>2</sup>CONICET, 1552 Félix de Azara St., Posadas-Misiones 3300 Argentina; <sup>3</sup>University of Campinas, CP 6122, Campinas-Sao Paulo CP 6122 Brazil

Experiments were carried out in which the conditions of columnar to equiaxed transition (CET) in directional solidification of dendritic alloys are known, in alloy systems such as Al-Cu, Al-Mg, Al-Zn, Al-Li, Al-Si, Al-Si-Cu, Cu-Zn, Pb-Sn, Sn-Pb and stainless steel. These experiments allow determine that two interfaces are defined, assumed to be macroscopically flat. The transition does not occur in abrupt form in the samples and is presented when the gradient in the liquid ahead of the columnar dendrites reaches critical and minimum values, being negative in most of cases. Finally, the own experimental results are compared with the reported in the literature by other authors, such as, Kisakurek in Pb-Sn alloys, Mahapatra and Weinberg in Sn-Pb alloys, Flood and Hunt, Ziv and Weinberg, Fredriksson and Olsson and Wang and Beckermann in Al-Cu alloys, Gandin in Al-Si alloys, and Poole and Weinberg in stainless steel.

#### 11:20 AM

Microstructure Analysis of ZA Alloy Rod Directionally Solidified by Heated Mold Continuous Casting: Ying Ma<sup>1</sup>; Yuan Hao<sup>1</sup>; Feng Yun Yan<sup>1</sup>; Hong Jun Liu<sup>1</sup>; <sup>1</sup>Lanzhou University of Science & Technology, State Key Lab of Advd. Non-Ferrous Matls., 85 Langongping Rd., Lanzhou, Gansu 730050 China

The as-cast and heat treatment microstructure of ZA alloy rod directionally solidified by continuous casting has been analyzed. The results show that the microstructure of the ZA alloy line is the parallel directional dendritic columnar crystal. Each dendritic crystal of eutectic alloy ZA5 is composed of many layer eutectic âandçphases. The microstructure of hyper eutectic ZA alloys is primary dendritic crystal and interdendritic eutectic structure. The primary phase of ZA8 and ZA12 is âphase, while the primary phase of ZA22 and ZA27 is á phase.

#### 11:40 AM

The Solidification of Ceramic-Reinforced Superalloy: *Rui Shao*<sup>1</sup>; Matthew J.M. Krane<sup>1</sup>; Kevin P. Trumble<sup>1</sup>; <sup>1</sup>Purdue University, Sch. of Matls. Engrg., 501 Northwestern Ave., W. Lafayette, IN 47907-2036 USA

Abrasive blade tips are sometimes used on turbine blades to increase turbine engine efficiency by decreasing gas leakage at the blade tips. This research studied a potential method for producing ABT in situ in the blade casting processing. A porous ceramic preform was infiltrated with liquid Ni-based superalloy under a gas pressure of about 1 atm, and then the alloy was solidified directionally at different rates through the preform, producing a metal-matrix composite. Single crystals were achieved at cooling rates  $\leq 15$  K/min. Laue X-ray diffraction showed that the orientation of the metallic grains were unaffected by the preform and no strange grains were nucleated there. Solidification and heat transfer were modeled using a commercial control-volume based code. The model predicted that the temperature gradient in the composite is higher than in the alloy without a preform, and so it is possible that the presence of the preform can suppress heterogeneous nucleation.

# Nanostructured Magnetic Materials: Recent Progress in Magnetic Nanostructures

Sponsored by: Electronic, Magnetic & Photonic Materials Division, EMPMD-Superconducting and Magnetic Materials Committee, EMPMD-Nanomaterials Committee Program Organizers: Ashutosh Tiwari, North Carolina State University, Department of Materials Science & Engineering, Raleigh, NC 27695-7916 USA; Rasmi R. Das, University of Wisconsin, Applied Superconductivity Center, Materials Science and Engineering Department, Madison, WI 53706-1609 USA; Ramamoorthy Ramesh, University of Maryland, Department of Materials and Nuclear Engineering, College Park, MD 20742 USA

londay AM	Room: 2	15
larch 15, 2004	Location:	Charlotte Convention Center

Session Chair: TBA

Μ

Μ

### 8:30 AM Introductory Remarks

#### 8:40 AM Invited

**Magnified Magnetocaloric Effects in Magnetic Nanocomposites:** *R. D. Shull*<sup>1</sup>; V. Provenzano<sup>1</sup>; <sup>1</sup>National Institute of Standards and Technology, Magnetic Matls. Grp., Gaithersburg, MD USA

Upon the removal of a magnetic field from a material, the resulting reduction in magnetic spin alignment represents an increase in the material's spin entropy ( $\Delta$  S). If the field reduction is performed adiabatically so that the total entropy change is zero, then the increased spin entropy is offset by an equal decrease in lattice entropy, as reflected by a decrease in the temperature of the material. This  $\Delta T$  is called the magnetocaloric effect, and it is a property of the material and its magnetic state. The magnetocaloric effect, upon which the technology of magnetic refrigeration depends, may be enhanced in certain field and temperature regimes by finely dividing and grouping a ferromagnetic species in a nonmagnetic or weakly magnetic matrix, as in a magnetic nanocomposite. Here the basis for this enhancement will be reviewed and experimental data measured on several magnetic nanocomposites will be presented in proof of the earlier predictions of this effect. In particular, experimental verification of cluster calculations will be provided by experimental data for a new magnetic nanocomposite,  $Gd_3Ga_{5-x}Fe_xO_{12}$  (GGIG), that is superparamagnetic and possesses magnetocaloric effects 3-4 times larger than those of the presently preferred low-temperature paramagnetic refrigerant, gadolinium gallium garnet (GGG). This new material possesses the potential for both increasing the operating temperature of magnetic refrigerators and lowering the magnetic fields required for their operation.

Magnetic refrigerators could then be substantially reduced in size, made much more efficient, and enable cooling to much higher temperatures.

# 9:10 AM Invited

# Understanding Nanomagnetism Via In-Situ Magnetization and Induction Mapping of Lithographically Patterned Arrays: Y. Zhu<sup>1</sup>; <sup>1</sup>Brookhaven National Laboratory, Upton, NY 11973 USA

Understanding spin dynamics, configuration and nano-scale magnetization process is crucial to the development of novel magnetic materials, especially for recording media and data storage applications. Here, modern electron microscopy plays an indispensable role in revealing time-resolved magnetic structural behavior. We report our in-situ studies of magnetic domain evolution of Ni, Co and permalloy islands and arrays on non-magnetic film matrix during magnetization and demagnetization process using electron holography and Lorentz phase microscopy. We develop quantitative procedures for phase retrieval in conjunction with preparing the assemblies that have well controlled geometry via electron beam lithography to separate magnetic potential from electrostatic potential. We focus our attention on the local induction distribution and magnetic interaction of the individual magnetic elements as a function of their size, shape and distance. Experimentally observed vortex-spin configurations are compared with calculations including micromagnetics simulation. Collaborations with V. Volkov, M. Schofield, M. Beleggia, J. Lau, M. De Graef and M. Malac are acknowledged. Work supported by US DOE, No. DE-AC02-98CH10886.

# 9:40 AM Invited

# Nanostructured Magnetic Materials for Electronic and Bio Applications: Sungho Jin<sup>1</sup>; <sup>1</sup>University of California, Dept. of Mech. & Aeros. Engrg., 9500 Gilman Dr., La Jolla, CA 92093-0411 USA

The properties and use of modern magnetic materials depend much on their nano-scale microstructure. In Fe-Cr-Co spinodal type permanent magnetic materials, the control of the dimension and shape of the microstructure is crucial. By making the (Fe, Co)-rich ferromagnetic phase elongated in nanoscale dimension within a matrix of Crrich non-magnetic phase, superior magnetic properties are achieved because of the shape anisotropy of the ferromagnetic phase introduced by microstructural control. Magnetic field heat treating process or deformation aging process can be utilized to produce desirable anisotropic two-phase microstructure. One examplary application of such a material is the magnetically tunable optical fiber grating device useful for telecom channel switching. In magnetically switchable materials such as phase-decomposed microduplex Fe-6% Ni alloys, the control of size, shape and twist of each of the phases can produce fast and abrupt magnetization reversal and voltage impulse signals which may be useful for sensor or actuator functions in electronic or bio applications.

# 10:10 AM Invited

# Field-Tuned Collapse of an Orbital Ordered and Spin-Polarized State: Colossal Magnetoresistance in Bilayered Ruthenate: G. Cao<sup>1</sup>; <sup>1</sup>University of Kentucky, Dept. of Physics & Astron., Lexington, KY 40506 USA

The bilayered  $Ca_3Ru_2O_7$  with a Mott-like transition at 48 K features different in-plane anisotropies of magnetization and magnetoresistance. Applying magnetic field along the magnetic easy-axis precipitates a spin-polarized state via a first-order metamagnetic transition, but does not lead to a full suppression of the Mott state, whereas applying magnetic field along the magnetic hard axis does, causing a resistivity reduction of three orders of magnitude. The novelty of this bilayered  $Ca_3Ru_2O_7$  is that the colossal magnetoresistivity is a result of the collapse of the orbital ordered state that is realized by demolishing the spin-polarized state. This new phenomenon is striking in that the spin-polarization, which is a fundamental driving force for all other magnetoresistive systems, is detrimental to the colossal magnetoresistence in this 4d-based electron system! Evidence for a density wave is also presented. This work was supported by a NSF grant DMR-0240813.

# 10:40 AM

# Magnetocaloric Effect in Nanoscale Ferromagnetic Composites: Alex Umantsev<sup>1</sup>; <sup>1</sup>University of North Carolina, Natural Scis., 1200 Murchison Rd., Lyons Scis. Bldg., Fayetteville, NC 28301 USA

Magnetic refrigeration is an efficient cooling technology due to the magnetocaloric effect of some materials. Upon the adiabatic removal of a magnetic field from the materials, increased spin entropy is offset by an equal decrease in lattice entropy, as reflected by a decrease in the temperature of the material. This temperature decrease is called the magnetocaloric effect, and it is a property of the material and its magnetic state. The crux of the problem presented here is that nanoscale particles stabilize unusual magnetic phases that are completely unstable in the bulk. I will present a theory of a refrigeration cycle that employs such unusual magnetic phases and discuss a possibility of using such cycles at room temperatures. Although there has been significant progress made recently in the area of magnetic refrigeration in nanoscale ferromagnetic composites, the effect that will be discussed here has not been address yet.

#### 11:00 AM

Enhancement of Ferromagnetism and Metallicity of the Ru Doped Two Dimensional Layered Manganite  $La_{1,2}Ba_{1,8}Mn_2$ ,  $_{x}Ru_{x}O_7$  (x = 0, 0.1, 0.5, and 1.0): Nori Sudhakar<sup>1</sup>; K. P. Rajeev<sup>1</sup>; A. K. Nigam<sup>2</sup>; <sup>1</sup>Indian Institute of Technology, Dept. of Physics, Kanpur, Uttar Pradesh 208016 India; <sup>2</sup>Tata Institute of Fundamental Research, Homi Bhabha Rd., Colaba, Mumbai, Maharashtra 400005 India

The electrical transport and magnetic studies of the Ru doped 2D layered manganite system  $La_{1,2}Ba_{1,8}Mn_{2,x}Ru_xO_7$  (x=0,0.1,0.5,1.0) have been carried out in the temperature range of 5 to 320 K and in the presence of magnetic fields up to 7 T in order to investigate the low temperature magnetic state of the system. The electrical resistivity ( $\rho$ ) curves show a peak at high temperatures and well defined minima at low temperatures akin to the colossal magnetoresistive (CMR) materials. Ru doping has increased the ferro-para transition temperature ( $T_c$ ), saturation magnetization and the hysteresis up to x=0.5. We expect that the mixed valency of Ru (Ru<sup>4+</sup>/ Ru<sup>5+</sup>) and Mn (Mn<sup>3+</sup>/ Mn<sup>4+</sup>) will lead to interesting results because of the possibility of Mn-O-Ru superexchange in addition to the usual Mn-O-Mn conduction channels already present in the system. We hitherto report rather high  $T_c$  values (> 310 K) obtained for the layered manganites.

#### 11:20 AM

A Novel MRAM Design Using Square Ring Elements for the Hard Layer: Dwarakanath N. Geerpuram<sup>1</sup>; Anand S. Mani<sup>1</sup>; <sup>1</sup>University of Illinois, Dept. of Elect. & Compu. Engrg., 851 S. Morgan M/C 154, Rm. 1020 SEO, Chicago, IL 60607 USA

Previous MRAM designs use structures where the switching phenomenon and the switching field strengths are constrained by the imperfections introduced in the fabrication process. We propose to use onion states in square rings for data storage in the MRAM. The onion state corresponds to each half of the square ring, on either side of the diagonal, having the same magnetization orientation and forming head-to-head and tail-to-tail domain walls. We have experimentally verified, for  $2\mu$ m permalloy rings, using Magnetic Force Microscopy that the onion state is stable at remanence. The switching between two onion states is nucleation free and occurs through the formation of a unique state called the horseshoe by domain wall movement. We have also verified that this unique switching mechanism is reproducible over an array of rings. Moreover, it is not affected by fabrication imperfections. In fact, switching can be controlled by specifically induced asymmetries in the rings.

#### 11:40 AM

Magnetic Interactions Between Nano Particles of Arbitrary Shape: A Fourier Space Approach: Shakul Tandon<sup>1</sup>; Marco Beleggia<sup>2</sup>; Yimei Zhu<sup>2</sup>; *Marc De Graef*<sup>1</sup>; <sup>1</sup>Carnegie Mellon University, Matls. Sci. & Engrg., 5000 Forbes Ave., Pittsburgh, PA 15213-3890 USA; <sup>2</sup>Brookhaven National Laboratory, Matls. Dept., Upton, NY 11973 USA

A new formalism has been developed to describe the demagnetization field around a particle of arbitrary shape and uniform or nonuniform magnetization state. The formalism relies on a Fourier Space description of particle shape, through the so-called shape amplitude. We will present examples of the computation of the demagnetization tensor field for several particle shapes, including the cylinder and facetted particles. We will introduce a formalism for the computation of the magnetostatic interaction energy between arbitrarily shaped particles. We will focus in particular on the interactions between cylindrical disks, and describe the interactions for in-plane and perpendicular magnetization states. Analytical computations are possible for systems with a small number of interacting disks, and we will show that the symmetric three-disk system undergoes a discontinuous phase transition from a regular vortex state with zero net magnetization to a dipolar ferromagnetic state described by a magnetic order parameter.

# Nanostructured Materials for Biomedical Applications: Session I

Sponsored by: Electronic, Magnetic & Photonic Materials Division, EMPMD-Thin Films & Interfaces Committee Program Organizers: Roger J. Narayan, Georgia Tech, School of Materials Science and Engineering, Atlanta, GA 30332-0245 USA; J. Michael Rigsbee, North Carolina State University, Department of Materials Science and Engineering, Raleigh, NC 27695-7907 USA; Xinghang Zhang, Los Alamos National Laboratory, Los Alamos, NM 87545 USA

Monday AM	Room: 2	219A
March 15, 2004	Location:	Charlotte Convention Center

Session Chairs: Buddy D. Ratner, University of Washington, Dept. of Bioengrg. & Chem. Engrg., Seattle, WA 98195-1720 USA; Sungho Jin, University of California, Mech. & Aeros. Engrg., La Jolla, CA 92093-0411 USA

# 8:30 AM Introductory Comments: Nanostructured Materials for Medical Applications

# 8:50 AM Invited

**Nanostructure Processing of Advanced Biomaterials**: *Jackie Y. Ying*<sup>1</sup>; <sup>1</sup>Institute of Bioengineering and Nanotechnology, 51 Sci. Park Rd. 01-01/10, The Aries, Science Park II, Singapore 117586 Singapore

Nanostructured materials are of interest for a variety of applications. This talk describes the synthesis and properties of nanostructured materials that are made up of crystallites or particles of ~10 nm. They may be generated by various physical and chemical approaches with ultrahigh surface reactivity. Through controlled synthesis in reverse microemulsions, my laboratory has achieved polymeric nanoparticles for the glucose-sensitive delivery of insulin. Through chemical precipitation and additive dispersion, we have also attained nanocomposite systems as highly selective and sensitive semiconductor sensors, bioactive ceramic orthopedic implants, and efficient gene delivery vectors.

# 9:20 AM Invited

Multiscale Materials Processing and Characterization for Tomorrow's Biomaterials: Adrian B. Mann<sup>1</sup>; Richard E. Riman<sup>1</sup>; <sup>1</sup>Rutgers University, Ceram. & Matls. Engrg., 607 Taylor Rd., Piscataway, NJ 08854-8065 USA

Materials research has recently directed its focus towards biomaterials. Our perspective on biomaterials design and processing relies heavily on an understanding of natural materials. Using dental enamel as an example of a hard tissue, we will review the multi-scale structure and mechanical properties of natural biomaterials, and the limitations that lead to their failure. These will be contrasted with the limitations of current biomaterials. Our observations of existing technologies have led us to envision future biomaterials with optimized physical and chemical characteristics for hard tissue replacement. Using the power of advanced materials processing and characterization, we are developing new replacement materials that closely mimic the properties of natural tissues. As an example, natural apatites are defective and non-stoichiometric, by mechanochemical-hydrothermal methods we can dope nanostructured hydroxyapatite with ions such as carbonate, sodium, magnesium and non-stoichiometric calcium to give a material closely resembling the composition of the surrounding hard tissue.

# 9:50 AM Invited

**Bio-Nanotechnology: The Use of Nanostructured Materials as Improved Tissue Engineering Materials**: *Thomas Jay Webster*<sup>1</sup>; <sup>1</sup>Purdue University, Biomed. Engrg., 1296 Potter Bldg., W. Lafayette, IN 47907-1296 USA

Although many advanced properties for materials with constituent particle sizes less than 100 nm have been observed for traditional engineering applications, few advantages for the use of these materials in tissue-engineering have been explored. However, nanophase materials may give researchers control over interactions with biological entities in ways previously unimaginable with conventional materials. This is because organs of the body are nanostructures and, thus, cells in the body are accustomed to interacting with materials that have nanostructured features. Work will be presented that provides evidence that nanophase materials can be designed to control interactions with proteins and subsequently mammalian cells for more efficient tissue regeneration. This has been demonstrated for a wide range of nanophase material chemistries including ceramics, polymers, composites thereof, and more recently metals. Such investigations are leading to the design of a number of more successful tissue-engineering materials for orthopedic/dental, vascular, neural, bladder, and cartilage applications.

# 10:20 AM Invited

Artificial Microvasculature: The Current and the Future: Yadong Wang<sup>1</sup>; <sup>1</sup>Massachusetts Institute of Technology, Chem. Engrg., E25-342, 45 Carleton St., Cambridge, MA 02142 USA

Vital organs are highly vascularized. One of the biggest challenges in tissue engineering (TE) is the vascularization of engineered organs. To fabricate metabolically demanding organs, engineered vasculature at the micron level has to be developed. Two general strategies are employed to meet the challenge: 1. induce neovascularization by growth factors or synthetic substances in vivo; 2. microfabricate polymer scaffolds in vitro. The advantages and disadvantages of both approaches will be illustrated. The focus of this talk will be on the microfabrication approach, and I will try to speculate the direction of research in this exciting field.

# 10:50 AM Invited

Atmospheric Plasma Treatment for Surface Adhesion– Nanostructure and Chemistry: Marian G. McCord<sup>1</sup>; Suzanne R. Matthews<sup>1</sup>; Megan A. Christie<sup>1</sup>; Mohamed Bourham<sup>1</sup>; Yoon J. Hwang<sup>1</sup>; <sup>1</sup>North Carolina State University, Biomed. Engrg. Dept., Box 8301, Raleigh, NC 27695-8301 USA

PET films were subjected to atmospheric plasma treatment with He and He/O<sub>2</sub> gas plasmas. The surface chemistry and morphology of the films were extensively characterized. XPS revealed that for short treatment durations (1 - 2 min. or less), plasma treatment resulted in a decrease in surface carbon content, with a concurrent increase in surface oxygen content, and small increment in surface nitrogen content. For longer treatment durations (>2 min.), the effect began to reverse. C<sub>1s</sub> deconvolution analysis showed that C-C bonds decreased up to 1 min. in the He/Air plasma and up to 2 min. for the O<sub>2</sub> plasma, then increased again corresponding to C<sub>1s</sub> results for both gases. This increase in C-C bonds is thought to be due to sub-surface cross-linking between benzene rings as a result of UV radiation during plasma treatment. This may be attributed to an abundance of UV radiation in plasma bulk when using helium. Chain scissions by active particles in the plasma bulk and subsequent chemical reactions between molecules and active species resulted in other changes in surface chemistry. AFM showed that surface nanoscale roughness increased after plasma treatment. The surface roughness increased up to 3 min. exposure time and then decreased again for both gases. This may be the result of a deposition of nanoparticles on the PET film surface.

Preliminary work shows porcine keratinocyte proliferation increases for the plasma treated films as compared to controls. The effect of surface chemical and structural modifications on the adhesion of keratinocytes is currently being investigated. Plasma treated films with increasing nanoscale roughness will be placed in tissue culture dishes and plated with porcine epithelial cells. Cell count, adhesion, and metabolic activity will be characterized immediately following plating via fluorescent assay and centrifugation, and then every day for one week, and will be correlated with surface chemical and nanostructural features as determined by XPS and AFM. Similar experiments will be performed with a series of ECM proteins, in order to determine the effects of surface nanostructure on protein binding.

# 11:20 AM Invited

Novel Laser Fabrication of Materials: Electronic Devices to Engineered Tissue Constructs: *Douglas B. Chrisey*<sup>1</sup>; <sup>1</sup>US Naval Research Laboratory, Code 6372, 4555 Overlook Ave., Washington, DC 20375-5345 USA

At the US Naval Research Laboratory (NRL), we have used pulsed lasers to process thin films and multilayers of almost all classes of materials from electronic ceramics for microwave devices to engineered tissue constructs. The novelty of processing materials this way starts with a fundamental understanding of the laser-material interaction and energy relaxation pathways and then exploiting the unique properties of lasers and materials to produce a vapor unobtainable by conventional physical or chemical methods. Recently, we have developed a new CAD/CAM technique for the soft laser forward transfer of a very large variety of materials called MAPLE DW for Matrix Assisted Pulsed Laser Evaporation Direct Write. The novelty in this approach is found in the laser-matrix interaction that results in a highly focused and soft material transfer. For electronic materials, this quality allows MAPLE DW to be able to transfer reproducible voxels of micron-size powders, nanoparticles, and organometallic precursors. The transfers take place at room temperature and in ambient air and we have demonstrated the mesoscopic scale (10 mm - 1 cm) fabrication of simple passive electronic devices (conductors, dielectrics, and resistors) and small sub-systems (x-band band pass filter) at low temperatures on plastic substrates (kapton). The electrical transport properties of all these component devices were comparable to more conventional thick film techniques such as screen-printing. Because of MAPLE DW's gentle nature this technique was also found to be successful in depositing patterns of viable biomaterials such as proteins, bacteria, and mammalian cells. When transferred as single layers, the cells spread out and multiply, but when deposited on top of one another they assemble and grow slowly together behaving more like natural tissue. The fabrication of three-dimensional tissue constructs that more closely replicates the heterogeneous structure of natural tissue may now be envisioned. This presentation will give an overview of the novel laser processing work being done at NRL and the fundamental science and engineering questions being answered as well as specific examples of technology being transferred to address next generation military and commercial applications.

# Phase Stability, Phase Transformation, and Reactive Phase Formation in Electronic Materials III: Session I

Sponsored by: Electronic, Magnetic & Photonic Materials Division, Structural Materials Division, EMPMD/SMD-Alloy Phases Committee

*Program Organizers:* C. Robert Kao, National Central University, Department of Chemical and Materials Engineering, Chungli City 32054 Taiwan; Sinn-Wen Chen, National Tsing-Hua University, Department of Chemical Engineering, Hsinchu 300 Taiwan; Hyuck Mo Lee, Korea Advanced Institute of Science & Technology, Department of Materials Science & Engineering, Taejon 305-701 Korea; Suzanne E. Mohney, Pennsylvania State University, Department of Materials Science & Engineering, University Park, PA 16802 USA; Michael R. Notis, Lehigh University, Department of Materials Science and Engineering, Bethlehem, PA 18015 USA; Douglas J. Swenson, Michigan Technological University, Department of Materials Science & Engineering, Houghton, MI 49931 USA

Monday AM	Room: 214
March 15, 2004	Location: Charlotte Convention Center

Session Chairs: C. Robert Kao, National Central University, Dept. of Chem. & Matls. Engrg., Chungli City Taiwan; Suzanne E. Mohney, Pennsylvania State University, Dept. of Matls. Sci. & Engrg., University Park, PA 16802 USA

# 8:30 AM Opening Remarks

#### 8:35 AM Invited

Instability of Immiscible Co/Cu Multilayered Thin-Film Structures: P. F. Ladwig<sup>1</sup>; J. D. Olson<sup>2</sup>; J. H. Bunton<sup>2</sup>; D. J. Larson<sup>3</sup>; R. M. Ulfig<sup>2</sup>; R. L. Martens<sup>2</sup>; E. Oltman<sup>2</sup>; M. C. Bonsager<sup>3</sup>; T. T. Gribb<sup>2</sup>; T. F. Kelly<sup>2</sup>; A. E. Schultz<sup>3</sup>; B. B. Pant<sup>3</sup>; Y. A. Chang<sup>1</sup>; <sup>1</sup>University of Wisconsin, Dept. of Matls. Sci. & Engrg., 1509 Univ. Ave., Madison, WI 53706 USA; <sup>2</sup>Imago Scientific Instruments Corp., Madison, WI USA; <sup>3</sup>Seagate Technology, Bloomington, MN USA

We will first present experimental evidence obtained by threedimensional atom probe (3DAP), TEM, x-ray diffraction, and DSC to show that multilayered thin-film structures of Cu/Co undergo intermixing when subjected to a thermal treatment from ambient to about 410°C. We will then provide a thermodynamic rationalization for the observed phenomena.

#### 9:00 AM Invited

Reliability Investigation and Interfacial Reaction on Lead-Free Sn-Cu/Ni BGA Package: *Seung-Boo Jung*<sup>1</sup>; Jeong-Won Yoon<sup>1</sup>; Sang-Won Kim<sup>1</sup>; <sup>1</sup>Sungkyunkwan University, Dept. of Advd. Matls. Engrg., 300 Chunchun-dong, Changan-gu, Suwon, Kyounggi-do 440-746 Korea

Among various Pb-free solders, Sn-Cu is one of the most promising Pb-free solders. Also, recent research on lead-free solders for flip-chip interconnection indicated that the Sn-0.7wt%Cu alloy had the best thermo-mechanical fatigue behavior among the lead-free alloys evaluated and could be the optimal solder alloy for such applications. The alternative materials and the possible risk of the reliability problems for the Pb-free products have been a major concern for the industries. In this paper, the growths kinetic of intermetallic compound layers

formed between Sn-3wt% Cu BGA solder and Au/Ni plated Cu substrate by solid-state isothermal aging were examined. Aging was performed for time periods of 1-100days and at temperatures of 70-170°. Also, ball shear strength values were measured to evaluate the effect of the interfacial IMC reactions on the mechanical reliability of solder bumps as a function of reflow numbers and aging. The Sn-0.7wt%Cu/Au/Ni/Cu couples provided the baseline.

# 9:25 AM Invited

Thermal and Electrical Instability of Ultra Fine Copper Interconnects Integrated with Low-k Dielectrics: Seung H. Kang<sup>1</sup>; <sup>1</sup>IC Device Technology, Agere Systems, 555 Union Blvd., Allentown, PA 18109 USA

As integrated-circuit technologies have scaled down to sub-100 nm range, its desirable circuit performance cannot be accomplished without incorporating reliable high-performance interconnects that utilize various types of metallic and dielectric films. Achieving sufficient reliability of these ultra-fine electronic interconnects has become increasingly challenging, primarily, due to revolutionary changes in materials (Cu/low-k system). Conventional electromigration and stress migration failure modes are still investigated as primary reliability issues. However, a relatively unfamiliar failure mode has emerged in relation to thermally and/or mechanically driven Cu diffusion into low-k, leading to a void in Cu (causing an open circuit) and a Cu extrusion or island in low-k (causing a short circuit). In general, this phenomenon is not observed for a silicon oxide based dielectric material. This paper investigates this failure mode at various electrical and thermal stress conditions. In particular, this paper attempts to separate this phenomenon from the conventional electromigration failure mechanism since electrical signals caused by Cu out-diffusion or extrusion to low-k may often be misunderstood as an indication of electromigration-induced damage. This paper also addresses that the integrity of Cu diffusion barrier and the microstructural quality of thin-film interfaces play a key role in the kinetics of this failure mode.

#### 9:45 AM

Compositional Shift of Alloy Semiconductors Beneath Contact Metallizations: Brett A. Hull<sup>1</sup>; Suzanne E. Mohney<sup>1</sup>; <sup>1</sup>Pennsylvania State University, Dept. of Matls. Sci. & Engrg., 206A Steidle Bldg., University Park, PA 16802 USA

Researchers have long recognized the opportunity to engineer contacts to compound semiconductors by annealing well-designed contact metallizations. For example, it is possible to exchange Ga for Al immediately beneath certain Al-bearing contacts to GaAs, leading to the formation of an alloy of AlAs and GaAs, along with an enhanced Schottky barrier height on the n-type semiconductor. We have recently found that when metal contacts are annealed on alloy semiconductors, similar compositional shifts can occur, even if no group III or V element is present in the contact metallization. Instead, preferential reaction of one component of the alloy semiconductor can take place, leaving an alloy semiconductor enriched in the other component. In this presentation, we discuss the results of experiments on this type of reaction as it occurs in late transition metal contacts to group III nitride semiconductor alloys.

#### 10:00 AM

Shallow Pd/W/Au Ohmic Contacts for Heterojunction Bipolar Transistors: Sammy H. Wang<sup>1</sup>; Eric M. Lysczek<sup>1</sup>; Joshua A. Robinson<sup>1</sup>; Suzanne E. Mohney<sup>1</sup>; <sup>1</sup>Pennsylvania State University, Dept. of Matls. Sci. & Engrg., 206A Steidle Bldg., University Park, PA 16803 USA

Very shallow ohmic contacts to p-InGa<sub>0.25</sub>Sb<sub>0.75</sub> and p-InAs base layers are required for low power heterojunction bipolar transistors under development today. We previously reported that a Pd/W/Au (5/ 50/145 nm) contact to p-InGaSb can exhibit a specific contact resistance less than 3 x 10<sup>-7</sup> Ohm cm<sup>2</sup>. Palladium makes intimate contact to the p-InGaSb, a W barrier protects the semiconductor from reaction with Au, and Au reduces the metal sheet resistance. In this presentation, we describe the long-term electrical and metallurgical stability of the contacts and the use of surface passivation to improve the performance of the shallowest contacts. For p-InAs, we have found that the Pd/W/Au contact provides a specific contact resistance approximately a factor of 2 lower than that of conventional Ti/Pt/Au contacts following very mild anneals. Materials characterization using TEM and AES will also be presented.

# 10:15 AM Break

10:30 AM Invited Improving the Barrier Integrity of Ultra-Thin Metallic Films by Tailoring Their Structure: The Case of Electroless Deposited Co-Based Alloys: Moshe Eizenberg<sup>1</sup>; Amit Kohn<sup>1</sup>; <sup>1</sup>Technion - Israel Institute of Technology, Dept. of Matls. Engrg., Technion City, Haifa 32000 Israel

The transition to copper metallization in ULSI devices requires ultra-thin conductive diffusion barriers. This research examines how the structure of metallic films can be modified in order to reduce copper diffusion via fast paths such as grain boundaries. A model system was chosen of electroless deposited cobalt-based films alloyed with phosphorus and tungsten. These elements have very limited solubility both in cobalt and copper. However, electroless deposition enables to incorporate them in the cobalt film at concentrations considerably larger than their equilibrium solubility. Following thermal annealing, the excess phosphorus and tungsten enrich the grain boundaries. We correlate between barrier integrity, structure, and copper diffusivity through the Co(P,W) films. Thus, we show that Co(P -8 at.%, W -2 at.%) and Co(P -10 at.%) films are effective barriers, considerably better than pure cobalt, because copper grain boundary diffusion is hindered due to occupation of boundary sites by the alloying elements.

#### 10:55 AM Invited

Reliability of Cu/Barrier Structure in Nanometer Interconnect Lines: Junichi Koike<sup>1</sup>; <sup>1</sup>Tohoku University, Matls. Sci., 02 Aoba, Aramaki, Aoba-ku, Sendai, Miyagi 980-8579 Japan

Interconnect lines in advanced integrated circuits has been reduced to a width of less than 100 nm. Further reduction is required in order to keep increasing device speed and cell density. The increased performance by decreasing the interconnect line width may become possible based on design-oriented expectations. However, there exist numerous material problems to meet the expectations. The major problems related to Cu/barrier interconnect lines include the reliability of an extremely thin barrier layer and the resistance to stress- and electromigration of Cu lines. These problems have thier origins to the Cu/ barrier interface properties. In the presentation, the current status of the reliability issues will be reviewed and the future direction will be presented based on our recent work on Cu/barrier interface adhesion strength and its relation to stress- and electro-migration resistance.

#### 11:15 AM

Semiconductor-to-Metallic Phase Transition of VO<sub>2</sub> by Laser Excitation: *Huimin Liu*<sup>1</sup>; Omar Vasquez<sup>1</sup>; Victor R. Santiago<sup>1</sup>; Luz Diaz<sup>1</sup>; Felix E. Fernandez<sup>1</sup>; <sup>1</sup>University of Puerto Rico, Physics, PO Box 5023, Mayaguez, PR 00681-5023 USA

VO<sub>2</sub> thin films deposited on fused quartz substrate were prepared by pulsed laser deposition technique. It shows phase transition (PT) from monoclinic semiconductor phase to a metallic tetragonal rutile structure when the sample temperature is above 68°C. The observed PT thermochromic effect was ultrafast and passive. Ultrafast PT was also observed when optically pumped by laser excitation. It was not thermally initiated in this case. An interest in understanding the mechanism was therefore motivated. In this paper we report the study of transient holography using degenerate-four-wave-mixing (DFWM) measurement to identify the PT mechanism. A Nd:YAG pulsed laser with pulse duration of 30 psec operating at 532 nm was employed as the coherent light source. It showed that the observed transient holography in VO2 thin film is associated with the excited state dynamical process which essentially causes the structural change, or so-called optically induced-PT. The observed extremely large polarizability is believed to relate with large offset in their potential well minimum between the ground state and excited state. Through an unidentified intermediate state the transient lattice distortion trigged to structural change.

#### 11:30 AM

The Relationship Between Phase Stability and High Temperature Thermoelectric Properties of La Filled IrSb3 Based Skutterudite Compounds: Sung Wng Kim<sup>1</sup>; Yoshisato Kimura<sup>1</sup>; Yoshinao Mishima<sup>1</sup>; <sup>1</sup>Tokyo Institute of Technology, Interdisplinary Grad. Sch. of Sci. & Engrg., Dept. Matls. Sci. & Engrg., 4259 Nagatsuta Midori-ku, Yokohama, Kanagawa 226-8502 Japan

We previously reported that IrSb<sub>3</sub> based ternary compounds have showed good electrical properties and the relatively high thermal conductivity prevented the enhancement of the efficiency of these compounds. Recently, we have investigated the high temperature thermoelectric properties of La filled IrSb<sub>3</sub> based skutterudite compounds from the viewpoint of decrease of lattice thermal conductivity. The relationship between phase stability and high temperature thermoelectric properties has been investigated for compounds which the adjustment of valence electron count (VEC) by Ge charge compensation in La filled compounds was conducted. It has been confirmed from the Rietveld analysis that the La atoms were placed in structural vacancies in Ge charge compensated  $La_x Ir_4 Ge_{3x} Sb_{12-3x}$  compounds and the amount was lower than purposed amount. Owing to the rattling effect of La atoms in vacancies, the Ge charge compensated  $La_xIr_4Ge_{3x}Sb_{12:3x}$  compounds exhibited the tremendously decreased lattice thermal conductivity, 1.8W/mK from 10.2W/mK of binary IrSb<sub>3</sub>.

#### 11:45 AM

**Controlling the Microstructure from the Gold-Tin Reactions**: J. Y. Tsai<sup>1</sup>; C. W. Chang<sup>1</sup>; W. C. Luo<sup>1</sup>; Y. C. Shieh<sup>1</sup>; C. Robert Kao<sup>1</sup>; <sup>1</sup>National Central University, Dept. of Chem. & Matls. Engrg., Chungli City 320 Taiwan

For bonding applications in microelectronic and optoelectronic packages, the Au-Sn alloys have the advantages of having higher thermal conductivities, lowest melting temperature, and better mechanical properties compared to the Au-Si and Au-Ge alloys. The Au-Sn eutectic alloy with the 80%Au-20%Sn (Au20Sn, wt.%) composition is one of the most important Au-Sn alloys for these applications. The microstructure of the Au-Sn bond inevitably has a major impact on the strength of the bonding. In this study, we show that the microstructure of the Au-Sn bond can be controlled by the bonding parameters.

# Recent Advances in Non-Ferrous Metals Processing: Reactive Metals

Sponsored by: Light Metals Division, LMD-Reactive Metals Committee, EPD-Waste Treatment & Minimization Committee Program Organizers: Brajendra Mishra, Colorado School of Mines, Kroll Institute for Extractive Metals, Golden, CO 80401-1887 USA; John N. Hryn, Argonne National Laboratory, Argonne, IL 60439-4815 USA; V. I. Lakshmanan, Ortech Corporation, Mississauga, Ontario L5K1B3k Canada; V. Ramachandran, Scottsdale, AZ 85262-1352 USA; Alton T. Tabereaux, Alcoa Inc., Process Technology, Muscle Shoals, AL 35661 USA

Monday AM	Room:	205		
March 15, 2004	Locatior	: Charlotte	Convention	Center

*Session Chairs:* Brajendra Mishra, Colorado School of Mines, Kroll Inst. for Extractive Metals, Golden, CO 80401-1887 USA; John N. Hryn, Argonne National Laboratory, Argonne, IL 60439-4815 USA

# 8:30 AM Opening Remarks

#### 8:35 AM

Understanding the Electro-Reduction of Metal Oxides in Molten Salts: George Zheng Chen<sup>1</sup>; Derek J. Fray<sup>2</sup>; <sup>1</sup>University of Nottingham, Sch. of Chem., Environmental & Mining Engrg., Univ. Park, Nottingham NG7 2RD UK; <sup>2</sup>University of Cambridge, Dept. of Matls. Sci. & Metall., Pembroke St., Cambridge CB2 3QZ UK

Recent work has demonstrated that solid metal oxides can be directly electro-reduced to the respective metals or alloys in molten salts. Typically, for the electrolysis of Cr2O3, less than 0.2 wt % oxygen could be achieved in the produced metal powder with the current efficiency and energy consumption being 75% and 5 kWh/kg, respectively. However, the electrolysis of TiO2 was found to be less efficient. Based on experimental observations and hypothetical models, this paper illustrates various possible steps of the reduction mechanism, including (1) separated electron and oxygen transfer at the three phase interline (boundary), (2) metal atom aggregation and oxide surface renewal, (3) consecutive metallisation of oxide particles, (4) three-phase interline propagation and oxide cathode surface metallisation, (5) intercalation of calcium into the metal oxide cathode, (6) oxygen transport in the solid and liquid phases, and (7) interactions between molten salt and cathode before and after reduction.

#### 9:05 AM Cancelled

Hot Consolidation of Cu-Li Powders Alloys: A First Approach to Characterization

# 9:35 AM

An Overview of the Effect of Quench Rate, Pre-Age Stretch, and Artificial Aging for the Al-Li-Cu-X AF/C-458 Alloy: Aladar A. Csontos<sup>1</sup>; Brian M. Gable<sup>2</sup>; Edgar A. Starke<sup>2</sup>; <sup>1</sup>U.S. Nuclear Regulatory Commission, Office of Nucl. Matl. Safety & Safeguards, Two White Flint N., MS T7F3, 11545 Rockville Pike, Rockville, MD 20852-2738 USA; <sup>2</sup>University of Virginia, Dept. of Matls. Sci. & Engrg., 116 Engineer's Way, PO Box 400745, Charlottesville, VA 22904-4745 USA

Many Al-Li-X alloys have been investigated, however, few have gained widespread implementation into commercial aerospace applications. The recent USAF development of an isotropic Al-Li-Cu-X

alloy designated AF/C-458 has renewed interest in these low-density alloys. This talk will provide an overview of our experimental results demonstrating the effect of quench rate, pre-age plastic deformation, and artificial aging time and temperature on the AF/C-458 microstructural evolution and mechanical properties. Cooling rates of 1.8°C/sec, 68°C/sec, and 290°C/sec were used from the solutionizing anneal while the amount of pre-age stretch ranged from a 0% non-stretched condition to 8% plastic deformation. The subsequent single, duplex, and triple near-peak aged heat treatments resulted in similar mechanical properties indicating a large processing window for this alloy.

10:05 AM Break

10:20 AM Cancelled

Kennecott Utah Copper Smelter Maintenance Initiative

# 10:50 AM

The Role of Slip Length on the Ductility and Fracture Behavior of Isotropic Al-Li-Cu-X Alloys: *Aladar A. Csontos*<sup>1</sup>; Edgar A. Starke<sup>2</sup>; <sup>1</sup>U.S. Nuclear Regulatory Commission, Office of Nucl. Matl. Safety & Safeguards, Two White Flint N., MS T7F3, 11545 Rockville Pike, Rockville, MD 20852-2738 USA; <sup>2</sup>University of Virginia, Dept. of Matls. Sci. & Engrg., 116 Engineer's Way, PO Box 400745, Charlottesville, VA 22904-4745 USA

Widespread implementation of Al-Li-Cu-X alloys for aerospace applications has been hindered due in part to their characteristic anisotropic mechanical and fracture behaviors. The USAF recently developed two isotropic Al-Li-X alloys designated AF/C-489 (2.1Li wt.%) and AF/C-458 (1.8Li wt.%) with  $\varepsilon_f$  of 5% and 10%, respectively. Our study examines the role of alloy composition, grain structure, and microstructure on the slip, deformation, and fracture behaviors of these alloys. Planar slip intensities were predicted through slip intensity calculations utilizing precipitate density measurements, dislocation-particle interactions, and grain boundary misorientation-slip continuity statistics. The slip intensity predictions were then correlated to AFM slip height measurements. Our results suggest that the low ductility and coarse intergranular fracture behavior of AF/C-489 in comparison to the higher ductility and transgranular fracture behavior of AF/C-458 is most strongly attributed to the ~3 times greater slip length and to a much lesser extent on the higher Li content for AF/C-489.

# **Recycling: General Recycling**

Sponsored by: Light Metals Division, Extraction & Processing Division, LMD/EPD-Recycling Committee *Program Organizer:* Gregory K. Krumdick, Argonne National Laboratory, Argonne, IL 60439 USA

Monday AM	Room: 2	17D
March 15, 2004	Location:	Charlotte Convention Center

Session Chairs: Gregory K. Krumdick, Argonne National Laboratory, Argonne, IL 60439 USA; John M. Rapkoch, Process Metallurgy Consultant, Western Springs, IL 60558 USA

# 8:30 AM

Calculation of Recycling Rates - Fable or Truth: Markus Andreas Reuter<sup>1</sup>; Antoinette Van Schaik<sup>1</sup>; <sup>1</sup>Delft University of Technology, 120 Mijnbouwstraat, Delft The Netherlands

This paper discussed the definition and calculation of recycling rates based on the combination of dynamic modeling and the modeling of recycling systems. It is demonstrated with suitable examples from the car recycling industry how recycling rates should be calculated taking into consideration all distributed properties of the product, design, life cycle, the metallurgy and physical processing, etc. This paper will therefore give a good indication how recycling rates are being and could be determined; and if recycling quotas can be reached or not. Especially important is the fact that recycling rate should be placed within a statistical framework i.e. a recycling rate should be eassociated with a standard deviation determined by all steps within the life cycle of a car. This paper discusses the recycling of cars, but the developed methods are equally valid for any modern consumer product.

#### 8:55 AM

Statistical Study of Mo Recovery from Molybdenum Waste Catalyst: Seham Nagib Tawfic<sup>1</sup>; <sup>1</sup>Academy of Specific Study, Tech. Dvlp. Dept., Worker University, El-Darrasa, El-Tarabishi St., Cairo Egypt

Dissolution of molybdenum from molybdenum waste catalyst (MWC) that contain wt %: 42.79 Mo, 9.54 Fe, 4.9 Al, 8.68 SiO2, 6

Na, and 1.5 Cr using different leaching agents such as H2SO4, HCl, and NaOH was carried out. It was found that, NaOH is the best leaching agent because it has the highest Mo recovery in combined with the lower Fe and Al dissolution than the HCl. Factorial design of experiments and application of statistical analysis on the results of leaching studies using NaOH were carried out. A regression equation for the dissolution of Mo was developed as a function of NaOH stoichiometric (S), L/S ratio (C, ml/g), and temperature (T, oC). All parameters were varied at two levels for designing experiments to estimate error.

## 9:20 AM

Quasi-Stationary Analysis on the Chlorination and Vaporization Reaction of Pb-Oxychloride in Ash and Dust Recycling: Nan Wang<sup>1</sup>; Yoshiki WaKimoto<sup>1</sup>; Yokiko Oyama<sup>1</sup>; Shu Yamaguchi<sup>1</sup>; <sup>1</sup>University of Tokyo, Dept. of Matls. Sci. & Engrg., Sch. of Engrg., 7-3-1 Hongo, Bunkyo Ward, Tokyo 113-8656 Japan

A quasi-stationary analysis on chlorination-vaporization reaction of Pb-oxychloride in pyrometallurgical processing of ash and dust has been made, with the goals of clarification of reaction mechanism, estimation of rate-limiting step and establishment of rate-controlling equation. A molten salt layer composed of PbO-PbCl2 was considered to be formed dependent on the relative magnitude of evaporation rate of PbCl2 to its formation one, and the corresponding bulk diffusion of components throughout the formed molten salt layer was estimated to be the rate-limiting step for the overall reactions. Based upon the theoretical treatment of phenomenological mass transport equations, simulation calculation for the relative chemical potential, molar fraction and mass flux of the related components throughout molten salt layer have been performed under quasi-steady state, which can be used to evaluate the effects of treatment temperature and Cl-potential in atmosphere on the chlorination-vaporization reaction. Furthermore, the possibility of the corresponding diffusion of combined oxygenion as rate-limiting step was also proposed.

#### 9:45 AM

**Slags from Secondary Lead Processing**: *A. V. Tarasov*<sup>1</sup>; A. D. Besser<sup>1</sup>; V. M. Paretsky<sup>1</sup>; <sup>1</sup>State Research Center of Russian Federation, State Rsch. Inst. of Nonferrous Metals, 13, Acad. Korolyov St., 129515 Moscow Russia

The technology developed in the Gintsvetmet Institute for treating battery scrap and other lead-containing wastes on the basis of electrothermal smelting permits production of secondary lead with minimum amounts of slag generated (by 3 to 5 times less than in case of conventional technologies) and a reduction in the process gas volumes by 2 to 3 times. The proposed technology permits to minimize the cost of off-gas treatment due to smaller volumes as well. Electric smelting slags contain after in-furnace cleaning about 1.0% to 1.7% of lead in insoluble compounds. Such slags are rated as Class IV of toxic substances and are acceptable for utilization, e.g., in road construction. It should be noted that when treating spent batteries, mechanized dismantling and separation of individual battery components into separate fractions minimizes the content of slag-forming constituents in the charge fed to electric smelting. In combination with the use of a low-ash reductant (coke fines) this makes it possible to operate the unit for an extended period of time without replacing the slag layer in the electric furnace. In practice, the excess of slag is discharged from a full-scale electric furnace once every 10 to 15 days.

#### 10:10 AM

The Cooling and Heat Releasing Behavior of Reductive Slag During its Oxidizing: *Yuanchi Dong*<sup>1</sup>; Liaosha Li<sup>1</sup>; Zhitong Sui<sup>2</sup>; <sup>1</sup>Anhui University of Technology, Anhui Key Lab. of Metallurgl. Engrg. & Resources Recycling, Ma an shan, An hui 243002 China; <sup>2</sup>Northeastern University, Metall. Dept., Shenyang, Liaoning 110006 China

The cooling behavior of melted slag of blast furnace with oxygen blowing was studied on the foundation of experiments. The results are as following: (1) A great deal of heat will be released during slag oxidizing that resulted in the slag temperature going up. Excepting for the heat compensation of radiation losing, the released heat could bring on 300 K increment of temperature. It means that the released heat is sufficient to meet the slag re-composition having no use for added fuel. (2) The cooling rate of slag will decreased as the increasing of slag amount obviously. The rate went down below 3 K/min with 1000 kg slag and below 2 K/min with 10000 kg slag. So that it is important to control proper temperature level being benefit of the precipitation and grain growing of minerals with reasonable oxygen blowing and slag amount.

# 10:45 AM

The Spent Consumer Battery Recycling Situation in Taiwan: Esher Hsu<sup>1</sup>; *Chen-Ming Kuo*<sup>2</sup>; <sup>1</sup>National Taipei University, Dept. of Statistics, 67 Sect. 3, Min-Sheng E. Rd., Taipei 104 Taiwan; <sup>2</sup>I-Shou University, Dept. of Mech. Engrg., 1, Sec. 1, Hsueh-Cheng Rd., Ta-Hsu, Kaohsiung 84008 Taiwan

On November 11, 1999, all spent consumer batteries are proclaimed to be collected in Taiwan. Under current recycling system, all producers and importers of consumer batteries have to pay a collection/recycling fee to the Recycling Management Fund (RMF) of EPA based upon the rate approved by EPA. Collectors and recycling plants receive subsidies from RMF according to the collected and treated amounts audited by an independent auditing organization. Collected spent consumer batteries only reached 700T per year equivalent to 7% of the total quantity since 2000. How to increase collection efficiency of used batteries becomes an important issue for EPA in Taiwan. The objective of this study is to explore current recycling system of spent consumer battery in increasing collection efficiency. Results provide some suggestions to Taiwan EPA regarding recycling route, recycling system, recycling rates, and recycling subsidies.

#### 11:10 AM

The Auditing Functions in Taiwan Recycling System: Esher Hsu<sup>1</sup>; Hung-Wen Shen<sup>1</sup>; Chen-Ming Kuo<sup>2</sup>; <sup>1</sup>National Taipei University, Dept. of Statistics, 67 Sect. 3, Min-Sheng E. Rd., Taipei 104 Taiwan; <sup>2</sup>I-Shou University, Dept. of Mech. Engrg., 1, Sec. 1, Hsueh-Cheng Rd., Ta-Hsu, Kaohsiung 84008 Taiwan

In 1997, Taiwanese Environmental Protection Administration (TEPA) established a new recycling system, which is managed by government directly. In the new system, manufacturers and importers have to pay recycling fees to the TEPA Recycling Management Fund (RMF), and TEPA uses this Fund as economic incentives to encourage involvements of private companies in public sorting and recycling activities. To prevent cheating problems, TEPA also entrusts auditing companies to check the sorting and recycling amounts and qualities, and based on the reports from auditing companies, TEPA available the TEPA trial and error experience in the past five years (from 1997-2003) on the auditing operations in plastic containers recycling. Based on this case, this paper also will discuss the advantages and problems in such auditing functions in a public managed recycling system.

# R.J. Arsenault Symposium on Materials Testing and Evaluation: Session I

Sponsored by: Structural Materials Division, SMD-Mechanical Behavior of Materials-(Jt. ASM-MSCTS), SMD-Nuclear Materials Committee-(Jt. ASM-MSCTS)

*Program Organizers:* Raj Vaidyanathan, University of Central Florida, AMPAC MMAE, Orlando, FL 32816-2455 USA; Peter K. Liaw, University of Tennessee, Department of Materials Science and Engineering, Knoxville, TN 37996-2200 USA; K. Linga Murty, North Carolina State University, Raleigh, NC 27695-7909 USA

Monday AM	Room: 2	211A
March 15, 2004	Location:	Charlotte Convention Center

Session Chairs: P. K. Liaw, University of Tennessee, Matls. Sci. & Engrg., Knoxville, TN 37996-2200 USA; K. Linga Murty, North Carolina State University, Coll. of Engrg., Raleigh, NC 27695-7909 USA

# 8:30 AM Invited

Constant Stress Component Contours for Mode III Crack in Power Law Hardening Solid: Johannes Weertman<sup>1</sup>; <sup>1</sup>Northwestern University, Matls. Sci., 2220 Campus Dr., Evanston, IL 60208 USA

We found earlier a solution for the mode III crack in a power law hardening solid for full scale yielding (J. Weertman, submitted for publication). The solution consists of determining for the mode III crack problem the appropriate "space" potential in stress space (the analogue of finding the stress potential in real space). From this solution for the space potential we obtained, in real space, constant stress magnitude  $\sigma$  contours plots for various values of the power law stress exponent m ( $0 < m \le 1$ ). Here  $\sigma^2 = \sigma^2_{yz} + \sigma^2_{zx}$  where  $\sigma_{yz}$  and  $\sigma_{zx}$  are the stress components. In this paper our solution is developed further by finding, in real space and for various values of m, constant stress contours for the individual stress components  $\sigma_{yz}$  and  $\sigma_{zx}$ .

# 9:00 AM Invited

Design of Ferromagnetic Shape Memory Alloy and Composites for Fast Responsive and Robust Actuators: *Minoru Taya*<sup>1</sup>; <sup>1</sup>University of Washington, Ctr. for Intelligent Matls. & Sys., Dept. of Mech. Engrg., Seattle, WA 98195-2600 USA

The large strains in ferromagnetic shape memory alloys (SMA) such as NiMnGa induced by the applied magnetic field are the results of rearrangement of martensite variants in the ferromagnetic SMA observed at temperature T≤M<sub>f</sub>. The flow stress level of the ferromagnetic SMA, NiMnGa is as low as several MPa. To design a robust yet compact actuator with large load bearing capacity at room temperature range, we proposed a new actuation mechanism for a ferromagnetic SMA, which provides a faster responsive yet powerful actuation, "hybrid mechanism", which is based on a sequence of chain reactions: First, applied magnetic field H or flux density B with large gradient, inducing large stress field in a ferromagnetic actuator material, prompting stress-induced martensite phase change (A to M phase), thus, the elastic properties change from stiff (austensite phase) to softer (martensite phase), resulting in larger displacement. This talk will discuss the design of such ferromagnetic SMA and its applications to several types of actuators.

#### 9:30 AM

Characterization of Laser-Driven Shocked NiAl Monocrystals and Bicrystals: Pedro D. Peralta<sup>1</sup>; Damian Swift<sup>2</sup>; Chyi-Hwang Lim<sup>1</sup>; Eric Loomis<sup>1</sup>; Ken J. McClellan<sup>3</sup>; <sup>1</sup>Arizona State University, Dept. of Mech. & Aeros. Engrg., Engrg. Ctr., G Wing, Rm. 346, Tempe, AZ 85287-6106 USA; <sup>2</sup>Los Alamos National Laboratory, Physics Div., P-24, MS E526, Los Alamos, NM 87545 USA; <sup>3</sup>Los Alamos National Laboratory, Matls. Sci. & Tech. Div., MST-8, MS G755, Los Alamos, NM 87545 USA

Disks of oriented single crystals and bicrystals of NiAl were tested under direct laser-driven shocks. Specimens were recovered and characterized to study cracking and slip behavior. In addition, the crystallographic orientation of the tested samples was studied using Orientation Imaging Microscopy. Results indicate that direct laser-driven shocks in monocrystals induce cracking on {110} planes, with a high crack density for <100> samples and a low crack density for <110> and <111> specimens. In one bicrystal, a Grain Boundary Affected Zone was observed close to the boundary in only one grain, where both cracking and slip were present. Specimens developed gradients of orientation due to bowing of the foil caused by the impact. Furthermore, changes in the speed of sound across the inclined interface correlated with the cracking mode, i.e., a shock propagating from a "slow" to a "fast" grain resulted in intergranular cracks, whereas the reverse resulted in transgranular cracks.

#### 9:50 AM Break

#### 10:30 AM

Comparison of Recrystallization During and After Hot Working in FCC Metals: *Hugh J. McQueen*<sup>1</sup>; John J. Jonas<sup>2</sup>; <sup>1</sup>Concordia University, Mech. Engrg., 1455 Maisonneuve Blvd. W., Montreal, Quebec H3G 1M8 Canada; <sup>2</sup>McGill University, Matls. Engrg., Montreal, Quebec H3A 2B2 Canada

The recrystallization responses of face-centered cubic (FCC) metals to hot deformation at similar strain rates 10-2 to 10+2 s-1 and homologous temperatures (>0.55T<sub>m</sub>) are strongly dependent on stacking fault energy (SFE). Discontinuous dynamic recrystallization occurs readily in all the metals, except Al, in which it is only observed at purities > 99.999% or when particle stimulated nucleation is taking place. After hot deformation, static recrystallization (SRX) occurs rapidly above 0.65 T<sub>m</sub>, even after low strains (20-50% rolling reduction) and is employed for grain refinement in the initial high temperature stages of industrial rolling. However in Al alloys, SRX is selectively induced by increasing the accumulated strain and the length of certain interpass intervals. The presence of solutes and particles, as well as the SFE, affect the recrystallization behavior through their influence on dynamic recovery, which controls the characteristics of the dislocation substructure; alloying also influences the grain boundary mobility through both solute drag and particle pinning effects.

#### 10:50 AM

Static Recrystallization of Tool Steels: *Clement A.C. Imbert*<sup>2</sup>; Hugh J. McQueen<sup>1</sup>; <sup>1</sup>Concordia University, Mech. Engrg., Montreal, Quebec H3G 1M 8 Canada; <sup>2</sup>University of the West Indies, Mech. Engrg., St. Augustine W1 Trinidad

Double-twist torsion tests were used to determine static softening in the hot working range of three tool steels: W1, a carbon steel (1.03% carbon plus 0.8% other elements), A2 and D2, a medium and a high alloy steel, containing 8.45% and 14.82% alloying elements respectively. The carbon steel, which was single-phase austenite in the hot-working range, experienced rapid static recrystalli-zation (SRX) due to increase in diffusion rate of iron, caused by carbon in hot austenite, very little alloying solute and no carbides. SRX of the alloy tool steels was compared with austenitic stainless steels, with similar strengths but much greater alloying content, and with microalloyed steels, as well as with the dynamic recrystallization kinetics. Carbides in alloy tool steels, which exist throughout the hot-working range, retard recrystallization but are responsible for enhancing initiation due to formation of nuclei at the strain concentration at the particle/ matrix interface.

#### 11:10 AM

Enhanced Mechanical Properties in Bulk Ultrafine-Grained Copper: S. Xie<sup>1</sup>; P. K. Liaw<sup>1</sup>; H. Choo<sup>1</sup>; D. E. Fielden<sup>1</sup>; G. Wang<sup>1</sup>; Y. Sun<sup>1</sup>; <sup>1</sup>University of Tennessee, Dept. of Matls. Sci. & Engrg., Knoxville, TN 37996 USA

Ultrafine-grained (UFG) pure copper has been prepared by rolling the commercial coarse-grained (CG) copper, with liquid nitrogen cooling of the samples between consecutive rolling passes. The microstructures of these materials have been characterized using x-ray diffraction (XRD) and transmission-electron microscopy (TEM). It is found that low-angle subgrain boundaries transform to high-angle grain boundaries, and the grain size is refined from 100  $\sim$  200 mm to 0.1  $\sim$ 0.5 mm following rolling at low temperatures. The yield strength and hardness have been measured by tensile tests and micro-hardness tests, respectively. The results show that the strength has been enhanced about two times and micro-hardness has been increased more than 100%, compared with the commercial CG copper. The mechanism leading to the significantly enhanced mechanical properties has been discussed. Furthermore, the cold-rolled UFG copper was annealed at elevated temperatures in an attempt to create a bimodal distribution in grain sizes. The mechanical behavior of the heat-treated UFG copper is compared to that of the as-rolled copper. The present work is supported by the NSF International Materials Institutes (IMI) Program under DMR-0231320, with Dr. Carmen Huber as the Program Director.

#### 11:30 AM

A Study of the Surface Nanocrystallization and Hardening Process for Improved Fatigue Resistance of C-2000: *W. Yuan*<sup>1</sup>; P. K. Liaw<sup>1</sup>; C. Stephens<sup>1</sup>; R. McDanice<sup>1</sup>; H. Tian<sup>1</sup>; D. E. Fielden<sup>1</sup>; J. C. Villegas<sup>2</sup>; L. L. Shaw<sup>2</sup>; D. L. Klarstion<sup>3</sup>; <sup>1</sup>University of Tennessee, Matls. Sci. & Engrg., Knoxville, TN 37996 USA; <sup>2</sup>University of Connecticut, Metall. & Matls. Engrg., Storrs, CT 06269 USA; <sup>3</sup>Haynes International, Inc., Kokomo, IN 46904 USA

The nanostructured layer on the surface has high resistance to the fatigue- crack initiation, and the coarse grain below the surface can retard the growth of fatigue cracks. By means of the surface nanocrystallization and hardening process (SNH), a nanostructured layer was formed on the surface of the Haynes C-2000 Superalloy disk, and the coarse grain below the surface was not changed. Microstructural features of cross section near and below the surface were investigated using X-ray diffraction (XRD), scanning-electron microscope (SEM), and transmission-electron microscopy (TEM). The microhardness of the cross section from the surface was measured by nanoindentation, and the residual stress was determined by XRD. A grain-size gradient from the nano-layer to coarse grain, the micro-hardness gradient, and the residual-stress distribution from the compressive stress to the tension stress were introduced through the cross section of a C-2000 disk. Four-point-bend tests were employed to study the fatigue behavior of the SNH-treated specimens, relative to the untreated specimens. When the surface defects introduced by the SNH treatment are removed, the fatigue life of the treated specimens can be improved. The present work is supported by National Science Foundation under DMR-0207729 with Dr. K. L. Murty as the contract monitor.

# Solidification Processes and Microstructures: A Symposium in Honor of Prof. W. Kurz: Processes

Sponsored by: Materials Processing & Manufacturing Division, MPMD-Solidification Committee

*Program Organizers:* Michel Rappaz, Ecole Polytechnique Fédérale de Lausanne, MXG, Lausanne Switzerland; Christoph Beckermann, University of Iowa, Department of Mechanical Engineering, Iowa City, IA 52242 USA; R. K. Trivedi, Iowa State University, Ames, IA 50011 USA

Monday AM	Room:	207D		
March 15, 2004	Location	: Charlotte	Convention	Center

Session Chair: Michel Rappaz, Ecole Polytechnique Federa, MXG, Lausanne Switzerland

# 8:30 AM Introduction and Welcome Michel Rappaz

#### 8:45 AM Invited

Semi-Solid Forming: Our Understanding Today and its Implication for Improved Processes: Merton C. Flemings<sup>1</sup>; James Yurko<sup>2</sup>; Raul A. Martinez<sup>1</sup>; <sup>1</sup>Massachusetts Institute of Technology, Dept. of Matls. Sci. & Engrg., Rm. 4-415, Cambridge, MA 02139 USA; <sup>2</sup>IdraPrince, New Product Dvlp., 670 Windcrest Dr., Holland, MI 49423 USA

During the careers of Professor Wilfried Kurtz and the senior author of this paper, a wide range of new processes have been developed for aluminum alloy casting. Some of these are designed primarily to achieve economic net shape parts. Others achieve improved cleanliness or freedom from dissolved gas. Still others are designed primarily to improve properties through microstructure control. Semi-solid forming of aluminum is finding its main niche today in its ability to 1) control metal viscosity and hence mold filling behavior, 2) reduce die casting cycle time, 3) improve die life, and 4) improve casting soundness. This paper will review the understanding of semi-solid forming achieved progressively over the last 30 years and focus on recent fundamental and applied developments. Recent studies have extended our knowledge of the viscosity behavior of semi-solid alloys up to the shear rates obtained in die casting and are elucidating the overriding importance of cooling rate and convection at precisely the time of first solid formation. Industrial developments include new processes designed to improve process economics and product quality.

#### 9:15 AM Invited

Contribution to the Knowledge of the Formation of the Skin in Continuous Casting of Steel: *G. Lesoult*<sup>1</sup>; L. Ladeuille<sup>2</sup>; C.-A. Gandin<sup>1</sup>; <sup>1</sup>Ecole des Mines, UMR-CNRS 7584, Nancy F-54042 France; <sup>2</sup>Thyssenkrupp, UGO-BP23, Isbergues F-62330 France

In several continuous casting processes, metal is extracted through a withdrawal-stop sequence instead of a constant withdrawal speed. In this case, the solid skin forms according to two modes of solidification, during two main steps. In the first step, the liquid metal coming into contact with the upper part of the mold wall, as the already solidified shell is extracted, solidifies as a fine continuous solid film. It adheres to the mold and is thus separated from the moving shell. Therefore, two phenomena have to be studied: the solidification of the "static shell"  $\mathbf{S}_{\mathrm{s}},$  as opposed to the solidification of the extracted "dynamic shell" S<sub>d</sub>. In the second step, when the speed of the dynamic shell with respect to the mold decreases, then becomes zero and reverses, the lips of the two shells enter into contact and become welded. When extraction starts again, the upper static shell is removed with the former dynamic shell, i.e., becomes dynamic, and a new static skin starts to form. The first hundreds of microns of the skin are likely formed during the first step. Therefore, there is a particular interest in studying the formation of microstructure and microsegregation during the solidification of the static shell. An experimental device has been built at the laboratory scale to reproduce the local thermal conditions of the initial solidification of the static shell. Droplets of liquid steel fall on a copper substrate instrumented with a Si-photodiode. Measurements performed with the photodiode are used to estimate the evolution of the thermal conditions (temperature gradient and growth rate) during the solidification of the first 500 µm in the droplets. The growth rate is of the order of 1 to 2 cm s<sup>-1</sup> at the very beginning; it decreases down to 3 mm s<sup>-1</sup> after about 200 ms. The temperature gradient in the solid varies from 106 to 2.105 Km<sup>-1</sup> in the same time. The temperature gradient in the liquid is much smaller (about 10<sup>4</sup> Km<sup>-</sup> 1); it may be negative in the very early stages if the nucleation undercooling is large enough. Two types of microstructures are observed: cells and dendrites. The comparison between predicted and calculated microstructures leads to conclusions related to nucleation conditions of the first shell and to its mechanical behavior.

# 9:45 AM Invited

Introducing Casting Simulation in Industry: The Steps Towards Success: Marco Gremaud<sup>1</sup>; <sup>1</sup>Calcom ESI, Parc Scientifique EPFL, Lausanne CH-1015 Switzerland

The industrial world is moving towards the "digital factory" - a prototype-less automated production environment based on virtual engineering. In terms of productivity, quality and innovation, the expected benefits of this transition are spectacular. In this "digital factory", manufacturers, their suppliers and partners simultaneously work on the same numerical prototype, allowing for continuous improvement in design and immediate decision-making. This "extended enterprise" marks a revolutionary departure from the time-consuming, costly trial and error processes of physical prototyping. Casting simulation is one small piece of that new technology. However, the introduction of a casting modeling package in a foundry is not a simple task and often the result is mitigated by the challenges of implemenation. The author will try to identify what are the key parameters ensuring success when introducing a casting simulation software in a foundry and why more than 90% of casting foundries are still not using simulation.

# 10:15 AM Break

# 10:45 AM

Simulation of Stress, Strain, and Shrinkage of Solidifying Steel Shells with Different Carbon Contents: Chunsheng Li<sup>1</sup>; Ya Meng<sup>1</sup>; *Brian G. Thomas*<sup>1</sup>; <sup>1</sup>University of Illinois, Mech. & Industrial Engrg., 138 Mech. Engrg. Bldg., 1206 W. Green St., Urbana, IL 61801 USA

Thermal-mechanical behavior of the solidifying shell is important for design of taper and understanding crack formation and other defects during continuous casting of steel. A two-dimensional finiteelement model, CON2D, has been developed to simulate the evolution of temperature, stress and strain in the solidifying shell during this process. The model features unified elastic-viscoplastic constitutive models for austenite, ferrite, mushy, and liquid steel. A simple microsegregation model is adopted to track the volume fractions of each phase. The model was validated by simulating an SSCT experiment similar to that of Kurz. CON2D was then applied to investigate the effect of steel grade on thermo-mechanical behavior of a slice domain under realistic heat flux conditions. The shrinkage predicted by CON2D was compared with simpler methods, such as that of Dippanaar. The simple methods are found to over-estimate the shrinkage of low carbon steels, where a substantial fraction of soft delta-ferrite exists, but matches reasonably for high carbon steel, containing strong austenite. Implications of the stress and strain profiles in the solidifying steel are also discussed.

#### 11:00 AM

A 3D-FEM Model Solving Thermomechanics and Macrosegregation in Binary Alloys Solidification: Michel Bellet<sup>1</sup>; Victor Daniel Fachinotti<sup>1</sup>; Sylvain Gouttebroze<sup>1</sup>; <sup>1</sup>Ecole des Mines de Paris, CEMEF, BP 207, Sophia Antipolis F-06904 France

The paper presents a three-dimensional coupled numerical solution of momentum, energy and solute conservation equations, for binary alloys solidification. The interdendritic flow in the mushy zone is assumed to obey the Darcy's law. Thermal and solutal buoyancy forces are taken into account by means of the Boussinesq's model. Microsegregation is governed either by lever rule or Scheil models, assuming local equilibrium at phase interfaces. The resulting solute transport equation is solved using the Streamline-Upwind Petrov/ Galerkin method. Momentum, energy and solute equations are discretised in space using tetrahedral finite elements and are coupled by a simple staggered scheme at each time step. The full algorithm was implemented the 3D code THERCAST. Two applications are given: a comparison with a 2D finite volume code in a 2D case (Fe-C alloy in a square cavity), and a comparison with experiment in a 3D case (Pb-Sn in a parallelepipedic cavity).

# 11:15 AM

Effect of Casting Speed on Structure Formation and Hot Tearing During Direct-Chill Casting of Al-Cu Alloys: X. Suyitno<sup>1</sup>; D. Eskin<sup>2</sup>; L. Katgerman<sup>1</sup>; <sup>1</sup>Delft University of Technology, Lab. of Matls., Rotterdamseweg 137, Delft 2628 AL The Netherlands; <sup>2</sup>Netherlands Institute for Metals Research, Rotterdamseweg 137, Delft 2628 AL The Netherlands

Professor W. Kurz recently suggested Solidification Structure-Processing Maps as a useful tool for controlling commercial solidification technologies. As a development of this idea we studied the effect of casting speed on the structure formation and hot tearing during directchill (DC) casting of binary Al-Cu alloys. Several binary alloys were cast in our laboratory scale DC casting that allowed an automatically controlled change of the casting speed during casting. The microstructure of billets was analyzed by optical microscope and computer image analysis, and hot tears were measured directly on the crack sites. Besides that a finite element simulation was performed. Hot tearing susceptibilities are computed using five different hot tearing criteria. Clear relationships between the structure parameters and hot tearing on one side and the casting speed and composition on the other side were found. The outcome of this research will be a Composition-Casting Speed-Hot Tearing process chart.

# 11:30 AM

Simulation of Solidification and Precipitation in Continuous Casting of Micro Alloyed Steels: *Mohammad Safi*<sup>1</sup>; Heikel Hamadou<sup>1</sup>; Dieter Senk<sup>1</sup>; <sup>1</sup>RWTH-Aachen University, IEHK, Intze Str., Aachen, NRW 52056 Germany

There is a large demand in industry to produce steel with particular mechanical properties, e.g. simultaneous high strength and high toughness. Two main possibilities to improve the final mechanical properties of steel semi products during production are control of chemical composition and micro-structure. To simulate solidification and developement of micro-structure during continuous casting, the temperature field of a strand shell was calculated. The results were used as a basis of other subprograms to calculate dendritic structure, micro-segregation and precipitation. Influences of casting flux on micro-structure and subsrface precipitations were experimentally examined. Micro-segregation and subsequent interdendritic precipitation of titanium nitride in subsurface regions during solidification are discussed.

## 11:45 AM

Stray Grain Formation in Nickel-Base Superalloy Single-Crystal Welds: John M. Vitek<sup>1</sup>; Suresh S. Babu<sup>1</sup>; Jin-Woo Park<sup>1</sup>; Stan A. David<sup>1</sup>; <sup>1</sup>Oak Ridge National Laboratory, Metals & Ceram. Div., PO Box 2008, MS 6096; Bldg. 4508, Oak Ridge, TN 37831-6096 USA

During the welding of nickel-base superalloys, it is desirable to maintain the single crystal nature of the base material in the weldments. Stray grain formation during solidification destroys the single crystal structure and compromises properties. In addition, weld cracks form more easily along stray grain boundaries. Kurz and Gaumann studied the stray grain formation tendencies in terms of the degree of constitutional supercooling ahead of the growing dendrites during weld solidification. Using the same ideas, the present work investigated the stray grain formation tendencies and cracking behavior in welds of Rene N5, a nickel-base single-crystal superalloy. The thermal behavior during welding was modeled and the extent of constitutional supercooling ahead of the growing interface was quantitatively evaluated. In addition, the dendrite orientation with respect to the moving solid-liquid interface was also taken into account. The results supported the mechanism proposed by Kurz for stray grain formation. The analysis provides insight into the conditions needed in order to minimize stray grain formation during welding of nickel superalloys. This research was sponsored by the Office of Fossil Energy, DOE National Energy Technology Laboratory, under contract DE-AC05-00OR22725 with UT-Battelle, LLC.

# 12:00 PM

New Features in Microstructure Control During E-LMF: Selim Mokadem<sup>1</sup>; Cyrille Bezençon<sup>1</sup>; Jean-Marie Drezet<sup>2</sup>; Alain Jacot<sup>2</sup>; Jean-Daniel Wagnière<sup>1</sup>; Wilfried Kurz<sup>1</sup>; <sup>1</sup>Ecole Polytechnique Fédérale de Lausanne, Matl. Sci. & Engrg. Inst., Lab. de simulation des matériaux, MXG, Ecublens, Lausanne, Vaud 1015 Switzerland; <sup>2</sup>Calcom ESI, Parc Scientifique - EPFL, Lausanne, Vaud 1015 Switzerland

The Laser Metal Forming (LMF) process where metal powder is injected into a molten pool formed by controlled laser heating is a near net shape process applied to rapid prototyping or repair engineering. The LMF process has been further developed and applied to the repair of SX HPT (single crystal High Pressure and Temperature) blades of gas turbines through the deposition of an epitaxial and SX layer onto SX superalloy substrates (Epitaxial-Laser Metal Forming : E-LMF). SX repair using E-LMF requires controlled solidification conditions such as to prevent the formation of stray crystals ahead of the columnar front i.e. to ensure epitaxial growth and to avoid the columnar to equiaxed transition (CET) during solidification. The aim of this work is to present the development of new strategies for microstructure control during Epitaxial Laser Metal Forming through the consideration of dendritic growth orientation, growth competition mechanism, loss of epitaxy related to branching mechanism and liquid convection in the melt pool. Control of these phenomena is of major importance for an effective industrial application of the E-LMF process. For this purpose modelling facilities have been developed and used in association with extended experimental observation to predict the expected solidification morphology for a given set of laser processing parameters. New microstructure features such as Oriented-to-Misoriented Transition (OMT) and Loss of Epitaxy in the critical branching zone are presented and measures to be taken for avoiding the formation of spurious grains within the repaired area are discussed.

# 12:15 PM

Microstructure and Mechanical Behavior of Liquid Metal Directionally Solidified GTD-444: Steve J. Balsone<sup>1</sup>; Ganjiang Feng<sup>1</sup>; Lance Peterson<sup>1</sup>; Jon C. Schaeffer<sup>1</sup>; <sup>1</sup>GE Power Systems, 300 Garlington Rd., Greenville, SC 29615 USA

GTD-444 is a precipitation-strengthened nickel-base superalloy developed and patented by GE for advanced large power generation gas turbine components. Most components are made by directional solidification (DS) investment casting. The increased firing temperature and the growing size of advanced turbine components creates a strong demand on manufacturing sound casting with homogeneous microstructure and improved mechanical properties. Extensive R&D in high gradient casting process shows that liquid metal cooling (LMC) directional solidification is one of the most promising technologies to produce high-performance castings. In the present study, microstructure and mechanical properties of LMC DS and conventional DS GTD-444 castings were compared. Microstructure features like dendrite arm spacing, phase segregation, carbide and gamma prime morphology were analyzed. The effect of the microstructure on mechanical behavior and fracture mode will be presented.

# Symposium on Microstructural Stability in Honor of Prof. Roger D. Doherty: Microstructural Stability: Recrystallization

Sponsored by: Aluminum Association, Materials Processing and Manufacturing Division, Structural Materials Division, MPMD-Solidification Committee, SMD-Physical Metallurgy Committee *Program Organizer:* Anthony D. Rollett, Carnegie Mellon University, Department of Materials Science & Engineering, Pittsburgh, PA 15213-3918 USA

Monday AM	Room: 2	216A
March 15, 2004	Location:	Charlotte Convention Center

Session Chair: Anthony D. Rollett, Carnegie Mellon University, Dept. of Matls. Sci. & Engrg., Pittsburgh, PA 15213-3918 USA

# 8:30 AM

Unsolved Problems in Physical Metallurgy of Structural Alloys: Roger D. Doherty<sup>1</sup>; <sup>1</sup>Drexel University, Dept. of Matls. Sci. & Engrg., Philadelphia, PA 19104 USA

For a symposium in my name that two of my colleagues have organized I feel that it might be of interest to give an outline of some of what I feel are important unsolved problems in the field in which I have spent my career. I would very much like to learn of solutions that might satisfy me and which I could use for students taking my classes at Drexel. In the area of microstructure development and stability the topics in which I know I do not understand include: abnormal grain coarsening seen in many, but not all cases, of normal grain coarsening pinned by a low volume fraction of particles. In the topic of precipitation the usual model for heterogeneous nucleation at grain boundaries and at dislocations seem to occur under conditions of low supersaturation in which the standard models predict that the sites do not have sufficient energy to act as catalysts. The problem of heterogeneous nucleation in solidification seems experimentally too difficult even to know if there is a problem or not. A further problem is the nucleation of growth ledges at the impingement point of plate like precipitates on different habit planes. Theories of coarsening, and many experiments, indicate that as the volume fraction of precipitates increases and the diffusion distance between particles becomes smaller, the coarsening rate accelerates. But in the Ni-Ni<sub>3</sub>Al system as Alan Ardell has clearly shown, there is, for some unexplained reason, no significant acceleration of coarsening in that alloy system. Somewhat further from my main area of research are some important problems that I do not understand, though that may reflect lack of knowledge of recent relevant studies. Amongst these topics are what is the mechanism and thus what determines the value of the proportionality constant, k<sub>v</sub>, in the Hall-Petch equation for grain size strengthening? Perhaps more surprising is the lack of our ability to predict the

strength of most Aluminum based precipitation hardened alloys even when the microstructure is fully characterized. Here the strengthening precipitate phases have a different crystal structures from the matrix and so they form plate or rod like precipitates. The text book account of peak strength - as occurring at the transition from underaged precipitates that are sheared by the dislocations to overaged precipitates that are by-passed works well for spherical GP zones but seems to fail for plate-like precipitates. The problems may be related as both concern the difficulty of dislocations passing from one crystal to another at an interface in which the slip plane and direction both change. In these two mechanical areas there is recently some work being done. However in the structural area that does not seem to be the case even when the precipitates may have nanometer sizes.

#### 9:05 AM

Static and Directional Recrystallization of Cold-Rolled Nickel: *I. Baker*<sup>1</sup>; J. Li<sup>1</sup>; H. J. Frost<sup>1</sup>; <sup>1</sup>Dartmouth College, Thayer Sch. of Engrg., 8000 Cummings Hall, Hanover, NH 03755 USA

The microstructures of both statically annealed and directionally recrystallized 90% cold-rolled polycrystalline nickel were investigated using both electron back-scattered patterns on a scanning electron microscope and optical microscopy. The statically annealed nickel showed a {100}<001> texture and small grains after primary recrystallization at low temperature (~700 K), but a {124}<21-1> texture and large grains after secondary recrystallization at higher temperatures (>1000 K). The effects of hot zone velocity during directional annealing at 1273 K were investigated. Some cold-rolled specimens were first statically recrystallized at 643 K prior to directional recrystallization at 1273K in order to examine whether directional recrystallization at 1273 K was by primary or secondary recrystallization. It was shown that directional recrystallization to columnar grains or, under optimum conditions, a single crystal was always by secondary recrystallization. Columnar grains could be produced over a wide range of hot zone velocities. Research supported by AFOSR grant F49620-00-1-0076 and NSF grants DMI 9976509 and DMI 0217565.

#### 9:35 AM

Increasing Grain Size in Electrical Steels by Light Reduction Followed by Annealing: *Fernando J.G. Landgraf*<sup>1</sup>; Taeko Yonamine<sup>1</sup>; Marcos Flavio de Campos<sup>2</sup>; Ivan G.S. Falleiros<sup>3</sup>; <sup>1</sup>IPT-Institute for Technological Research, Metall. Div., Av. Prof Almeida Prado 532, Sao Paulo, SP 05508-901 Brazil; <sup>2</sup>Universidade Federal Fluminense, EEIMVR, Volta Redonda, RJ Brazil; <sup>3</sup>Universidade de Sao Paulo, Depto. Engrg. Metalurgica e Materiais, Sao Paulo, SP 05508-901 Brazil

Approximately half of the annual 6 million tons of non-oriented electrical steels sheets attain the necessary large grain size (150µm) by light deformation (4 to 8% area reduction) followed by annealing at 760°C. This paper addresses the taxonomy debate (is it primary recrystallization or strain induced abnormal grain growth?), discusses the inhomogeneous microstructural evolution along the sheet and describes the texture evolution in some circumstances. Evidences will be shown in favour of the primary recrystallization concept, as it follows the Burke and Turnbull recrystallization rules: the grain size-deformation relationship is monotonic whether producing grain size refinement or increase, annealing temperature has no effect on the final grain size and the lower the deformation, the longer the incubation period and longer it takes to recrystallize. Partial recrystallization investigation indicates that recrystallization starts at the surface of the 0.5mm thick sheets, although there is very little hardness gradient. The extent of the inward growth varies along RD and TD, making very difficult for a recrystallization kinetics study. Texture evolution of samples with different histories will be compared, including a new process developed with Professor Doherty's help when visiting Brazil in 2002.

# 10:05 AM

Growth Aspects of Recrystallization: Dorte Juul Jensen<sup>1</sup>; Erik M. Lauridsen<sup>1</sup>; Soren Schmidt<sup>1</sup>; Roy A. Vandermeer<sup>1</sup>; <sup>1</sup>Riso National Laboratory, Ctr. for Fundamental Rsch., Metal Structures in 4-D, Roskilde Denmark

A much debated issue is if "oriented growth" is an important mechanism in recrystallization. This is adressed by presenting growt rate data obtained by EBSP measurements for both cold and hot deformed aluminium. It is shown that oriented growth is significant in several cold deformed samples while it is not for the hot deformed sample. This is discussed and possible mechanisms which may contribute to oriented growth are examined. The results reported in this first part of the talk refer to mean growth rates averaged over a large number of individual grains. In the second part, growth rates for individual grains obtained by 3 Dimensional X-Ray Diffraction using high energy synchrotron radiation are reported. It is shown that there is a very large variability between the grains even within texturecomponents, and simulations are finally presented which illustrate how such variability may affect the overall recrystallization kinetics.

# 10:40 AM

Effect of Annealing Temperature on the Development of Twin Boundaries: D. R. Waryoba<sup>1</sup>; P. N. Kalu<sup>1</sup>; <sup>1</sup>FAMU-FSU College of Engineering and National High Magnetic Field Laboratory, Tallahassee, FL 32310 USA

The development of twin boundaries has been monitored in heavily drawn oxygen free high conducting (OFHC) copper wires, which were subsequently annealed at different temperatures. Samples of the wires deformed to true strains of 1.69, 2.31 and 3.56, were isothermally annealed at temperatures between 150°C and 750°C for one-hour in an argon-filled environment, and characterized using Orientation Imaging Microscopy. Analyses of the microtexture results revealed that the densities (number/ $\mu$ m2) of the Sigma-3 and Sigma-9 twin boundaries peaked just prior to the onset of recrystallization, and most of the recrystallized grains were bounded by these twin boundaries. Secondary recrystallization occurred when the wires were annealed at high temperatures, and the twin boundaries were found to be largely associated with annealing twins, which developed under this condition. Higher order twin boundaries (Sigma-27a and Sigma-27b) were virtually negligible.

# 11:10 AM

The Critical Strain for Dynamic Recrystallization: John J. Jonas<sup>1</sup>; <sup>1</sup>McGill University, Metallurgl. Engrg., 3610 Univ. St., Wong Bldg., Montreal, Quebec H3A 2B2 Canada

Under conditions of dynamic recrystallization, an inflection point is observed in the plot of work hardening rate vs. flow stress. This is shown to be associated with the initiation of an additional dynamic softening mechanism, in this case the migration of high angle boundaries. A normalization procedure is introduced according to which such inflection points can be defined and predicted, even under conditions of decreasing temperature and increasing strain rate, as in hot strip mills. The data obtained on thirteen steels indicate that the ratio of the critical strain for the initiation of dynamic recrystallization to that of the peak strain falls in the range 0.5 to 0.6 and increases with the concentration of alloying elements present. An extension of the normalization technique is shown to apply to the softening that takes place between roll passes as well. Both of these methods are useful in modelling the loads developed and the microstructural changes taking place in rolling mills.

#### 11:40 AM

The 40°<111> Orientation Relationship in the Nucleation of Recrystallisation in Aluminium: *Erik Nes*<sup>1</sup>; <sup>1</sup>Norwegian University of Science and Technology (NTNU), Dept. of Matls. Tech., Trondheim N-7491 Norway

The 40° <111> orientation relationship has a central role in the discussion of recrystallisation textures. This orientation relationship has traditionally been associated with the oriented growth theory, but recent experimental observations clearly demonstrate a link also to oriented nucleation. In this presentation the importance and understanding of the 40° <111> orientation relationship in is discussed in terms of recrystallization after both hot and cold deformation of aluminium and aluminium alloys. Special attention will be focused on the effect of stored energy and finely dispersed particles on the nucleation.

# The Didier de Fontaine Symposium on the Thermodynamics of Alloys: Fundamentals of Alloy Theory

Sponsored by: Materials Processing and Manufacturing Division, MPMD-Computational Materials Science & Engineering-(Jt. ASM-MSCTS)

*Program Organizers:* Diana Farkas, Virginia Polytechnic Institute and State University, Department of Materials Science and Engineering, Blacksburg, VA 24061 USA; Mark D. Asta, Northwestern University, Department of Materials Science and Engineering, Evanston, IL 60208-3108 USA; Gerbrand Ceder, Massachusetts Institute of Technology, Department of Materials Science and Engineering, Cambridge, MA 02139 USA; Christopher Mark Wolverton, Ford Motor Company, Scientific Research Laboratory, Dearborn, MI 48121-2053 USA

Monday AM	Room: 2	216B		
March 15, 2004	Location:	Charlotte	Convention	Center

Session Chair: TBA

# 8:30 AM Keynote

**Reflections on "Alloy Theory"**: *Didier R. De Fontaine*<sup>1</sup>; <sup>1</sup>University of California, Matls. Sci., 210 Hearst Mining Bldg., Berkeley, CA 94720-1760 USA

Classical Gibbsian Thermodynamics is as close as one gets to a perfect theory, formally that is. Unfortunately, little practical work can be done with it without numerical knowledge of the parameters that enter its equations. In the past, parameters were determined empirically, but now, at least in principle, the required numerical values can be determined ab initio by quantum mechanical means. Hence, today's "Alloy Theory" combines statistical thermodynamics and quantum mechanics into one integrated whole for which computer code packages are in fact being developed. In this talk I shall briefly outline some of the important steps which led to the new approach of the old problem.

#### 9:00 AM Invited

Using Thermodynamic Equations for Checking Self-Consistency of Theories, Models, and Experiments: John W. Cahn<sup>1</sup>; <sup>1</sup>National Institute of Science and Technology, MSEL, Gaithersburg, MD 20899-8555 USA

Thermodynamics gives exact relations among quantities which are precisely defined and often independently measurable. Failures in the relations outside of experimental error, computational uncertainties, or with quantities derived from theoretical models are strong indications that something is wrong and should be investigated. The Gibbs adsorption equation will be used with models of various interfaces to illustrate discrepancies between calculated temperature dependences of interfacial free energies and interfacial entropies, and how some have been resolved. Earlier discrepancies have pointed to diffuse or rough interfaces. The temperature dependence of the energy of dislocation boundaries through the temperature coefficient of elastic constants and the magnitude of the Burgers vector is an interesting example.

#### 9:30 AM Invited

Reliable First-Principle Alloy Thermodynamic Via Truncated Cluster Expansions: Duane D. Johnson<sup>1</sup>; <sup>1</sup>University of Illinois, Matls. Sci. & Engrg., 1304 W. Green St., Urbana, IL USA

Many major developments and applications of the cluster expansion (CE) have originated from Prof. de Fontaine's group. As such, the CE is increasingly used to combine electronic-structure calculations and Monte Carlo methods to predict alloy thermodynamic properties. The CE is a basis set expansion in terms of lattice clusters and effective cluster interactions, but is tractable only if truncated from its exact (infinite) form. Yet until now there was no well-defined procedure that could guarantee a reliable truncated CE. We present a method for an optimal truncation of the CE basis set that provides reliable thermodyamics, and exemplify its importance in fcc Ni3V. The new truncation procedure now provides excellent agreement to a range of measured quantities for fcc Ni3V, where previous use of CE failed. The results show that T=0K DFT results are not always pertinent to characterization measurements.

# 10:00 AM Invited

A Data Mining Approach to Crystal Structure Prediction: Dane Morgan<sup>1</sup>; Stefano Curtarolo<sup>1</sup>; Gerbrand Ceder<sup>1</sup>; <sup>1</sup>Massachusetts Institute of Technology, Dept. of Matls. Sci., 77 Mass. Ave., 13-4061, Cambridge, MA 02139 USA

Predicting crystal structures for a new alloy is one of the most fundamental problems in materials science. Total energy ab initio approaches have proven a powerful tool for crystal structure prediction, but how to choose the best structures to calculate is still an open problem. Traditionally, researchers have used a combination of experimental results, model Hamiltonians, optimization methods, and hard-won intuition to find good candidate structures for a new alloy. In this paper a new approach is proposed, called Data Mining of Quantum Calculations (DMQC), which uses statistical and data mining methods to mine existing ab initio and/or experimental data to predict likely structures for new alloys. When faced with a new alloy, DMQC makes optimal use of existing data on other alloys. Key data mining techniques for DMQC will be described, compared to other approaches, and tested on a database of over 10,000 ab initio energies. DMQC is shown to dramatically decrease the time needed to identify stable crystal structures.

# 10:30 AM Break

# 10:40 AM Invited

Long Range Order and Diffraction: Denis Gratias<sup>1</sup>; <sup>1</sup>LEM-CNRS/ ONERA, 29, Av de la Division Leclerc, Chatillon 92322 France

Bragg diffraction is well known to characterize long range crystalline order. Dany Shechtman's discovery in 1984 of quasicrystals exhibiting sharp diffraction peaks with no periodic order has broken this paradigm and opened a more general question "What distribution of matter diffracts?". The present talk is a didactical attempt to summarize in an illustrative way some of the most important recent mathematical results on this apparently simple issue. It will shown through concrete examples and little mathematics that the problem is far from trivial and that Long Range Order is not necessarily associated to Bragg diffraction and vice versa.

# 11:10 AM Invited

Linking Structures Via Thermodynamics: Suzana G. Fries<sup>1</sup>; <sup>1</sup>AC-CESS e.V., RWTH-Aachen, Intzestrasse 5, Aachen D-52072 Germany

The combination of the knowledge about electronic, crystallographic, micro and macro structures of a material, using thermodynamics as media is a powerful approach. Some examples will be shown where pragmatic and theoretical methods are used in order to correlate that structures for real multicomponent materials.

#### 11:40 AM

Sources of Entropy in Solid-Solid Phase Transformations: Brent Fultz<sup>1</sup>; <sup>1</sup>California Institute of Technology, Matls. Sci., Mail 138-78, Pasadena, CA 91125 USA

Temperature drives the formation of antisite atoms, excitations of phonons, and excitations of electrons. In thermal equilibrium these configurational, vibrational, and electronic contributions to the entropy can be assessed if their energy spectra are known. Each of these phenomena can make significant and comparable contributions to the entropy of solid-state phase transformations. Their interactions at high temperature are another opportunity for future research. We have focused on inelastic neutron scattering experiments to measure the energy spectra of phonons, but we seek sources of entropy by combining results from other techniques. Some systematics are presented, such as the effect of solute mass and atomic size mismatch on phonon entropies of compound formation. Electronic entropy plays a big role in crystal structure transformations in cerium, uranium and plutonium. Overall, however, systematic correlations are at best semiquantitative. Understanding entropy in materials will require detailed analyses, rather than general rules of thumb.

# Third International Symposium on Ultrafine Grained Materials: Processing I: Fundamentals and Technology

Sponsored by: Materials Processing & Manufacturing Division, MPMD-Shaping and Forming Committee

Program Organizers: Yuntian Ted Zhu, Los Alamos National Laboratory, Materials Science and Technology Division, Los Alamos, NM 87545 USA; Terence G. Langdon, University of Southern California, Departments of Aerospace & Mechanical Engineering and Materials Engineering, Los Angeles, CA 90089-1453 USA; Terry C. Lowe, Metallicum, Santa Fe, NM 87501 USA; S. Lee Semiatin, Air Force Research Laboratory, Materials & Manufacturing Directorate, Wright Patterson AFB, OH 45433 USA; Dong H. Shin, Hanyang University, Department of Metallurgy and Material Science, Ansan, Kyunggi-Do 425-791 Korea; Ruslan Z. Valiev, Institute of Physics of Advanced Material, Ufa State Aviation Technology University, Ufa 450000 Russia

Monday AM	Room:	207A		
March 15, 2004	Location	: Charlotte	Convention	Center

Session Chairs: Ruslan Z. Valiev, Ufa State Aviation Technical University, Matls. Sci. & Tech. Div., Los Alamos, NM 87545 USA; Terry C. Lowe, Metallicum, Santa Fe, NM 87501 USA; Zenji Horita, Kyushu University, Dept. Matls. Sci. & Engrg., Fukuoka 812-8581 Japan

# 8:30 AM Introductory Remarks

#### 8:35 AM Invited

Application of Equal-Channel Angular Pressing for Grain Refinement of Plate Samples: Masakazu Kamachi<sup>1</sup>; Minoru Furukawa<sup>2</sup>; Zenji Horita<sup>1</sup>; Terence G. Langdon<sup>3</sup>; <sup>1</sup>Kyushu University, Fac. of Engrg., Dept. of Matls. Sci. & Engrg., 6-10-1 Hakozaki, Higashi-ku, Fukuoka, Fukuoka 812-8581 Japan; <sup>2</sup>Fukuoka University of Education, Dept. of Tech., Munakata, Fukuoka 811-4192 Japan; <sup>3</sup>University of Southern California, Depts. of Aeros. & Mech. Engrg. & Matls. Sci., Los Angeles, CA 90089-1453 USA

Equal-channel angular pressing (ECAP) was applied to plate samples of high-purity aluminum for grain refinement. The plate sample was rotated by 90° in the same sense about the plate normal between each pass, which was designated in this study route  $B_{\text{CZ}}$ . Samples were subjected to a total of 4 passes, equivalent to an imposed strain of ~4. The microstructures were examined using optical microscopy and transmission electron microscopy. It was found that the microstructure consisted of equiaxed grains and elongated grains with the former having area fractions of ~70 to 80%. The average grain size in the equiaxed grain area was ~0.9 µm. The Vickers microhardness was measured on the three orthogonal sections and there was no significant difference throughout each section and between the sections. Tensile tests were conducted at room temperature and the tensile behavior was found to be independent of the direction of the specimen gauge lengths which were taken parallel to the two orthogonal planes perpendicular to the plate normal.

#### 8:55 AM

Continuous ECAE (Conshearing) Process of Aluminum and Steel Strips: *Hiroshi Utsunomiya*<sup>1</sup>; Ken-ichi Hatsuda<sup>2</sup>; Yoshiaki Okamura<sup>2</sup>; Tetsuo Sakai<sup>2</sup>; Yoshihiro Saito<sup>3</sup>; <sup>1</sup>University of Cambridge, Dept. of Engrg., Trumpington St., Cambridge, Cambridgeshire CB2 1PZ UK; <sup>2</sup>Osaka University, Dept. of Matls. Sci. & Engrg., 2-1 Yamadaoka, Suita 565-0871 Japan; <sup>3</sup>Osaka University, 4-1-12-613, Yamadanishi, Suita, Osaka 565-0824 Japan

The authors developed the 'Conshearing' process as a continuous version of ECAE. In this study, the process was applied to 2mm-thick low carbon (0.044%C) steel and AA1100 aluminum alloy strips at room temperature. In the case of the low carbon steel, Goss {110}<001> orientation develops after 2 passes. In addition to Goss, {110}<112>, {111> and {112}<110> components are found after several passes. The tensile strength increases from 380MPa to 700MPa. Lamelar dislocation cells or subgrains are formed in grains. In the case of AA1100 strips, the <111>||ND shear texture showed maximum intensity after two passes, the mean thickness and the length of the grains are 0.42mm and 1.4mm, respectively. The obtained material shows a tensile strength of 170MPa and an elongation of 23%. The continuous ultra grain refinement of the aluminum strip coils is feasible at room temperature.

# 9:10 AM

Mechanical Properties and Microstructures of High-Purity Copper Processed by Equal Channel Angular Extrusion: David J. Alexander<sup>1</sup>; <sup>1</sup>Los Alamos National Laboratory, MST-6 G770, Los Alamos, NM 87545 USA

High-purity oxygen-free electronic copper (C10100) has been processed by equal channel angular extrusion with up to 16 passes at room temperature (90° tooling, route Bc). Small tensile specimens (gage section 1.3 by 2.5 by 5.1 mm) were sectioned along the length of the billet by electrodischarge machining, as well as compression cubes. The samples were tested in the as-processed condition, and also after various heat treatments. The microstructures and mechanical properties will be presented and discussed.

# 9:25 AM

Ausforming of NiTi Shape Memory Alloys Using Equal Channel Angular Extrusion: Ajay V. Kulkarni<sup>1</sup>; *Ibrahim Karaman*<sup>1</sup>; Zhiping Luo<sup>2</sup>; <sup>1</sup>Texas A&M University, Dept. of Mech. Engrg., MS 3123, College Sta., TX 77843 USA; <sup>2</sup>Texas A&M University, Microscopy & Imaging Ctr., College Sta., TX 77843 USA

In this study, thermomechanical properties of severely deformed Ti-50.8 at% Ni alloy using Equal Channel Angular Extrusion (ECAE) are investigated. Solutionized NiTi bars were deformed at different temperatures, i.e. room temperature which is above the austenite finish temperature (Af) and 450 C. The aim was to investigate the effects of ausforming (deformation above Af) on shape memory characteristics of NiTi such as superelasticity, transformation temperatures and fatigue properties. DSC was used to explore the effects of heat treatment temperature and time on the as-received, solutionized and asdeformed materials in terms of transformation temperatures, R-phase formation, and change in thermal hysteresis. TEM was utilized to reveal the changes in microstructure and formation of nanograins by in-situ heating and cooling experiment. Cyclic deformation tests are done on the as received, solutionized and as-deformed samples before and after some selected heat treatments. In this presentation improvement in thermal and mechanical properties with severe ausforming and subsequent annealing will be demonstrated. Stable cyclic response, pseudoelastic strain, change in transformation temperatures, formation of R-phase and nanograins, effects of precipitates will be rationalized with the observations on microstructures and possible deformation mechanisms.

# 9:40 AM Invited

# Fabrication of Bulk Nanostructured Materials by ARB (Accumulative Roll-Bonding) Process: Nobuhiro Tsuji<sup>1</sup>; <sup>1</sup>Osaka University, Dept. Adaptive Machine Sys., 2-1 Yamadaoka, Suit, Osaka 565-0871 Japan

Accumulative Roll-Bonding (ARB) is a severe plastic deformation (SPD) process applicable to bulky materials. In the ARB process, the rolled material is cut, stacked to be the initial dimension, and then rollbonded again. Because this procedure can be repeated limitlessly, huge amount of total plastic strain can be applied to materials. Ultrafine grained structures with mean grain sizes about 100 nm have successfully formed in various kinds of metallic materials after several cycles of ARB. Because bulky specimens with various ultrafine grain sizes can be fabricated by the ARB process followed by annealing, various properties of the ultrafine grained materials are systematically clarified. Furthermore, it would be possible to fabricate novel nanostructured materials, such as bulk amorphous sheet, in certain systems by SPD using the ARB. All these features of the ARB process, and structures and properties of the fabricated nanostructured materials will be introduced in the present paper.

# 10:00 AM

Large Scale Manufacturing of Ultrafine-Grained Materials: Kevin P. Trumble<sup>1</sup>; W. Dale Compton<sup>2</sup>; Srinivasan Chandrasekar<sup>2</sup>; Srinivasan Swaminathan<sup>2</sup>; Travis L. Brown<sup>2</sup>; <sup>1</sup>Purdue University, Sch. of Matls. Engrg., 501 Northwestern Ave., W. Lafayette, IN 47907-2036 USA; <sup>2</sup>Purdue University, Sch. of Industrial Engrg., 315 N. Grant St., W. Lafayette, IN 47907-2023 USA

It has been known for some time that ultrafine-grained materials have interesting mechanical properties making them attractive for use in the discrete products sector. It is shown here that by subjecting a material to large scale deformation using machining, very fine-grained structures can be produced in a variety of metals and alloys. The chips produced during lathe machining of pure metals, steels, and other alloys are shown to be ultrafine-grained with crystal sizes between 50 and 800 nm. The hardness of the chips is found to be significantly greater than that of the bulk material. The manufacture of ultrafinegrained metals by machining, when combined with powder and composite processing methods can be expected to lead to the development of a number of advanced materials and bulk forms having new and interesting combinations of properties. The possibility exists that this approach can overcome many of the limitations pertaining to cost and material types that are generally associated with the commonly used methods for making ultrafine-grained materials.

# 10:15 AM

Strain Accommodation in Pearlite Lamellae of a High Carbon Steel During Equal Channel Angular Pressing: Jingtao Wang<sup>1</sup>; Xiaofang Cao<sup>2</sup>; ZhongZe Du<sup>2</sup>; Zheng Zhang<sup>2</sup>; Xicheng Zhao<sup>2</sup>; <sup>1</sup>Nanjing University of Science and Technology, Dept. of Matls. Sci. & Engr., No. 200, Xiaolingwei, Nanjing 210094 China; <sup>2</sup>Xi'an University of Architecture and Technology, Sch. of Metallurgl. Engrg., Yanta Rd. No 13, Xi'an 710055 China

Equal channel angular pressing (ECAP) was successfully applied on pearlite lamellae structure of a high carbon steel 65Mn (Fe-0.65%C-0.90%Mn) at 650°C via route C up to 5 passes. Strain accommodation of lamellae structure and structure evolution were investigated. Intensive strain during ECAP was accommodated by the formation of quasi-regular bamboo structure, continuous wavy bending structure, regular sharp shear up to an true strain of 1.9, and shear cutting of the cement lamellae and ultra-refinement of the matrix ferrite was observed in the subsequent ECAP passes, and finally a homogeneous submicro-grained ferrite matrix with a grain size of 0.3 micrometers even dispersed by spheroidized ultra-fine cementite particles was achieved.

10:30 AM Break

# 10:40 AM Invited

Ultrafine Grained Aluminum Alloys Via Friction Stir Processing: *Rajiv S. Mishra*<sup>1</sup>; Indrajit Charit<sup>1</sup>; <sup>1</sup>University of Missouri, Dept. of Metallurgl. Engrg., 1870 Miner Cir., Rolla, MO 65409 USA

Friction stir processing is a new technique to refine grain size in metallic materials. In this paper, a brief overview of the state-of-theart of friction stir processing for obtaining ultrafine grained microstructure in aluminum alloys will be presented. The current trends indicate that bulk ultrafine grained aluminum alloys can be obtained via friction stir processing. Results will be also presented for direct conversion of cast material to ultrafine grained material in one pass. An attractive feature of this process is the ability to refine microstructure in commercially available high strength aluminum alloys.

# 11:00 AM Invited

Theoretical and Experimental Investigation of Texture and Microstructural Evolution During ECAE: Irene J. Beyerlein<sup>1</sup>; Carlos N. Tome<sup>1</sup>; David J. Alexander<sup>2</sup>; Donald W. Brown<sup>2</sup>; Sven C. Vogel<sup>2</sup>; Saiyi Li<sup>2</sup>; Mark A. Bourke<sup>2</sup>; <sup>1</sup>Los Alamos National Laboratory, Theoretl. Div., MS B216, Los Alamos, NM 87544 USA; <sup>2</sup>Los Alamos National Laboratory, Matls. Sci. Div., Los Alamos, NM 87544 USA

We will present our current progress on the development of a predictive simulation tool, called SPAIN (Simulating Polycrystals for the Advancement and Implementation of Nanomaterials) for advancing understanding and optimal design of Severe Plastic Deformation (SPD) technologies. SPAIN will be designed to predict two relationships: the microstructural evolution from conventional metals to nanometals during SPD processing and the mechanical properties of the resulting nano-structured materials. For this talk, we selected Equal Channel Angular Pressing (ECAP) as our focus SPD technology. Our approach to developing SPAIN integrates both theoretical and experimental efforts on several length scales. The foundation of our modeling effort is the Visco-plastic self-consistent (VPSC) polycrystalline model, incorporating results from both larger scale FEM simulations and smaller scale substructure evolution models. Our experimental efforts advocate the use of state-of-the-art neutron diffraction and Orientation Imaging Microscopy (OIM) instruments and SPD processing capabilities at Los Alamos. We will present results of our comparative analyses of texture and microstructure of both single phase face-centered cubic FCC (Cu, Ni, and Al) and hexagonal close packed HCP (Be) polycrystals processed under multiple passes of different ECAP routes.

# 11:20 AM

FEM Simulation of the Continuous Combined Drawing and Rolling Pressing in Equal Channel Angular (CCDR-ECAP): Carmelo J. Luis Pérez<sup>1</sup>; Javier Leon Iriarte<sup>1</sup>; Ignacio Puertas Arbizu<sup>1</sup>; Pedro A. Gonzalez Crespo<sup>1</sup>; <sup>1</sup>Public University of Navarre, Mech. & Matls. Engrg. Dept., Campus de Arrosadia s/n, Pamplona, Navarra 31006 Spain

Equal channel angular processes are innovative methods used with the aim of improving properties of materials by severe plastic deformation. Depending on the processing route, microstructural characteristics may differ from one route to another. In spite of the great advantages that ECAE processes allow us to obtain, from the point of view of improving mechanical properties in materials, low industrial applications have been developed, which is mainly caused by mechanical limitations (buckling of the punch) and the low velocity of the process. Because of the limitations, previously mentioned, low industrial applications have been developed and few patents dealing with ECAP have been developed. In this work a new method is shown termed Continuous Combined Drawing and Rolling Pressing in Equal Channel Angular (CCDR-ECAP) allowing us to develop a continuous ECAP. Finite element simulations are included in order to show the advantages of this technique in relationship with the previous methods.

# 11:35 AM

Effect of Cryogenic Rolling on the Formation of Ultra-Fine Grains in 5052 Al Alloy: *Won Jong Nam*<sup>1</sup>; Young Bum Lee<sup>1</sup>; *Dong Hyuk Shin*<sup>2</sup>; <sup>1</sup>Kookmin University, Dept. Matl. Sci. & Engrg., 861-1 Chongnung-Dong, Sungbuk-Ku, Seoul 136-702 Korea; <sup>2</sup>Hanyang University, Dept. Metall. & Matl. Sci., Ansan, Kyunggi-Do 425-791 Korea

It has been known that ultra-fine grains less than 1µm in diameter can be obtained by severe plastic straining. In the present work, we have applied cryogenic rolling process to 5052 aluminum alloy and have achieved ultra-fine grains with less than 1µm in diameter showing high strength. Cryogenic rolling of fully annealed 5052 Al alloy plates with 10mm in thickness was performed at various strains, in comparison with cold rolling. To investigate the effect of annealing temperature on recrystallization, the sheets received 88% reduction were annealed at the temperature range of  $150 \sim 300^{\circ}$ C for an hour. Annealing of Al alloy deformed 88%, at  $200^{\circ}$ C for an hour, results in the considerable increase of tensile elongation without the great loss of strength and the occurrence of new polygonal grains less than 300nm in diameter.

# 11:50 AM Invited

Measuring 3D Strain and Particle Distribution in Equal Channel Angular Pressing: Hans J. Roven<sup>1</sup>; <sup>1</sup>The Norwegian University of Science and Technology, Dept. of Matls. Tech., 7491 Trondheim Norway

Equal Channel Angular Pressing (ECAP) has been known to the international community since the former USSR patent presented by V.M. Segal (1977). ECAP is an efficient process for (i) creating ultrafine grained materials, (ii) systematic studies of the relationship between shear deformation and deformation history, (iii) large shear strain accumulations and (iv) thermo-mechanical studies of microstructure and texture development without changing the size and shape of the work-piece. The present work is part of an extensive program on SPD processing of Al alloys. The current knowledge on strain distributions in ECAP is primarily based on FE- simulations and real measurements are very scarce in the open literature. In order to fill some of this lacking knowledge, measurements in sectioned billets are used to map the quasi- 3D strain distribution in route A of a 6082 AlMgSi alloy. An automated strain analyses unit and a rectangular grid are used for this purpose. Details of the strain distribution in the shear zone and towards the edges and corners are also followed. Further, the overall plastic flow in 1-3 passes of route A are measured and compared for two different cases (full friction and minimum friction). Also, different heat treatment conditions of the alloy before deformation are characterized as to study the influence on strain distribution. Another strain and plastic flow related process in ECAP is the micrometer sized particle break-up and distribution. This is characterized for the same alloy in passes 1-8 in route A and route Bc. The experimental results give strong evidence that the classical recrystallization mechanism related to particle stimulated nucleation (PSN) is not operating in SPD at room temperature. The creation of ultrafine grains is mechanistically linked to the local plastic strain and the corresponding severe lattice rotations.

#### 12:10 PM

Strengthening Mechanisms of Surface Nanocrystallization and Hardening Process: Juan C. Villegas<sup>1</sup>; Kun Dai<sup>1</sup>; Zachary Stone<sup>1</sup>; *Leon L. Shaw*<sup>1</sup>; Peter K. Liaw<sup>2</sup>; <sup>1</sup>University of Connecticut, Metall. & Matls. Engrg., Storrs, CT 06269 USA; <sup>2</sup>University of Tennessee, Matls. Sci. & Engrg., Knoxville, TN 37996 USA

Surface nanocrystallization and hardening (SNH) process is a surface severe-plastic-deformation (SPD) process. The strengthening mechanism of this process has been investigated in this study. Three engineering materials, Ni C-2000, Ti-6Al-4V and Al 5052, have been utilized as model materials for this purpose. A hardness increase of the order of 150% with respect to untreated samples is achieved for Ni C-2000, whereas little hardening is observed for Ti-6Al-4V and Al 5052 exhibits an intermediate behavior. The different responses from different materials to the SNH process have been discussed in terms of their work hardening capacities, microstructural evolution, and formation of nanograins. The implications of this study on the efficacies of the SNH process are discussed. This research is supported under U.S. NSF grant DMR-0207729.

# 12:25 PM

Microstructure, Mechanical Properties and Anysotropy of Pure Ti Processed by Twist Extrusion and Cold Rolling: *Dmitry Orlov*<sup>1</sup>; Vladimir Stolyarov<sup>2</sup>; Hamit Salimgareyev<sup>2</sup>; E. P. Soshnikova<sup>2</sup>; Alexey Reshetov<sup>1</sup>; Yan Beygelzimer<sup>1</sup>; Sergey Synkov<sup>1</sup>; Victor Varyukhin<sup>1</sup>; <sup>1</sup>Donetsk Phys. & Tech. Inst. of the National Academy of Sciences of Ukraine, Physics of High Pressure & Advd. Tech., 72 R. Luxemburg St., Donetsk 83114 Ukraine; <sup>2</sup>Ufa State Aviation Technical University, Inst. of Physics of Advd. Matls., 12 K. Marx St., Ufa 450000 Russia

It's investigated UFG structure formation in CPTi bulks processed by SPD (cold Twist Extrusion(TE), true strain e~5.1, with the following Cold Rolling(CR), true strain e~0.7). Evolution of microstructure and tensile mechanical properties in the CPTi were investigated under room temperature. After the TE, in transversal section it is formed structure fragments with size less 1µm. Strength increased on 80%; elongation was 3.4%. Following low-temperature annealing (300°C, 1hour) leaded to increasing in both strength and ductility properties. In longitudinal section, specimens' strength properties increased slightly. Elongation was about 6%. The following low-temperature annealing practically did not influence on the strength but improved elongation to 7.2%. The additional CR leaded to forming severe deformed structure. Average size of fragments was 50-500nm. It was observed elimination of anisotropy and equalization of strength. In both directions ultimate tensile strength became about 780-800MPa and ductility properties remained the same as in the original.

# 5th Global Innovations Symposium: Trends in LIGA, Miniaturization, and Nano-Scale Materials, Devices and Technologies: Plenary: Trends: Past, Present, and Future

Sponsored by: Materials Processing & Manufacturing Division, MPMD-Powder Materials Committee, MPMD-Phase Transformations Committee-(Jt. ASM-MSCTS), MPMD-Computational Materials Science & Engineering-(Jt. ASM-MSCTS), MPMD/EPD-Process Modeling Analysis & Control Committee, MPMD-Surface Engineering Committee, MPMD-Shaping and Forming Committee, MPMD-Solidification Committee

*Program Organizers:* John E. Smugeresky, Sandia National Laboratories, Department 8724, Livermore, CA 94551-0969 USA; Steven H. Goods, Sandia National Laboratories, Livermore, CA 94551-0969 USA; Sean J. Hearne, Sandia National Laboratories, Albuquerque, NM 87185-1415 USA; Neville R. Moody, Sandia National Laboratories, Livermore, CA 94551-0969 USA

Monday PM	Room:	20	)2B		
March 15, 2004	Locatior	<b>1</b> :	Charlotte	Convention	Center

Session Chairs: John E. Smugeresky, Sandia National Laboratories, Livermore, CA 94551 USA; Neville R. Moody, Sandia National Laboratories, Livermore, CA 94551 USA

# 2:00 PM Opening Remarks John E. Smugeresky

# 2:10 PM

Perspectives on Nanosciences and Nanotechnology: M. S. Dresselhaus<sup>1</sup>; <sup>1</sup>Massachusetts Institute of Technology, Cambridge, MA 02139 USA

Nanoscience research is now entering a new phase where the structure and properties of materials can be investigated, characterized and controlled at the nanoscale. New physical phenomena appear at the nanoscale, giving rise to unexpected materials properties, thus bringing new excitement to this research field. In this talk, special emphasis will be given to one-dimensional nanowires and nanotubes because they, in particular, exhibit unusual physical properties, due to their reduced dimensionality and their enhanced surface/volume ratio. These unusual properties have attracted interest in their potential for applications in novel electronic, optical, magnetic and thermoelectric devices. Some examples of research accomplishments and opportunities at the nanoscale will be described, with a view toward new interdisciplinary research programs now under development in the field of nanoscience and nanotechnology worldwide.

#### 2:40 PM

# Nanoceramics, Nanotubes and Nanocomposites Paving the Way for Nanotechnology Revolution – A Review of the Industry and Markets: *Thomas Abraham*<sup>1</sup>; <sup>1</sup>Business Communications Co., 25 Van Zant St., Norwalk, CT 06855 USA

With large-scale current and potential use of nanostructured materials (and nanotubes) in applications such as chemical mechanical polishing (CMP), magnetic recording and ferrofluids, sunscreens, catalysts, biodetection/labeling, conductive coatings, optical fibers, FEDs, chips and nanocomposites, the nanotechnology industry is taking off with commercial markets. The presentation provides an overview of the technologies, applications, industry structure and markets.

# 3:10 PM

The Difficult Transition From Technology to Commercialization- Lessons Learned Over the Past 50 Years: Keith A. Blakely<sup>1</sup>; 'NanoDynamics, Inc., 901 Fuhrmann Blvd., Buffalo, NY 14203 USA Abstract not available.

#### 3:40 PM Break

# 4:00 PM Plenary

### Materials Processing and Manufacturing at the Nanoscale: Fundamental Research and Commercialization Opportunities: Haris Doumanidis<sup>1</sup>; <sup>1</sup>National Science Foundation

This presentation overviews the philosophy and current portfolio of the new Nanomanufacturing Program at NSF. This is placed in the context of the global competition in nanotechnology, the National Nanotechnology Initiative and its promised impacts to society and everyday life. The Nanomanufacturing Program was established in 2001 to promote fundamental research and education in manufacturing at the nanoscale, and to transfer developments in nanoscience and nanotechnology discoveries from the laboratory to industrial applications. This presentation emphasizes issues related to nanomanufacturing research for technology transfer and commercialization of nanotechnology products. It stresses on the need for materials processing for scale-up of nanotechnology and high rate production, reliability, robustness, yield, efficiency and cost issues for manufacturing products and services. Nanomanufacturing capitalizes on the special material properties and processing capabilities at the nanoscale, and promotes integration of nanostructures to functional microdevices and meso/macroscale architectures and systems, as well as the interfacing issues across dimensional scales. Research in nanomanufacturing machines covers interdisciplinary areas and entails multi-functionality across all energetic domains, including mechanical, thermal, fluidic, chemical, biochemical, electromagnetic, optical etc. Nanomanufacturing focuses on a systems approach, encompassing nanoscale materials and structures, fabrication and integration processes, production equipment and characterization instrumentation, theory/modeling/simulation and control tools, learning from nature and biomimetic design, integration of multi-scale functional systems, and industrial application. The NSF program places special emphasis in education and training of the workforce, involvement of socioeconomic sciences, addressing the health, safety and environmental implications, development of manufacturing infrastructure, as well as outreach and synergy of the academic, industrial, federal and international community. Current NSF funded research at universities and small businesses, as well as present research challenges and support opportunities are also reviewed.

## 4:30 PM Plenary

Nanoscale Integrated Circuits and Future Materials Challenges: C. Michael Garner<sup>1</sup>; <sup>1</sup>Intel Corporation, Matls. Tech. Operation, SC11-230, 2191 Laurelwood Rd., Santa Clara, CA 95054-1514 USA

Continued scaling of integrated circuits will require the development of many new materials with properties and structure controlled at the nanometer scale. Integrated circuits have had minimum feature sizes less than 100nm since 2000, and many new materials are being integrated with each generation. As scaling continues, the materials comprising the dielectrics and conductors in the transistors, and the interconnects must have controllable electronic, electrical, nano-structural, and mechanical properties. The electrical performance of the MOS transistor depends on the electrical properties of the gate dielectric, gate electrode and stress state of the silicon. Interconnect performance depends on the resistance of the metal and capacitance of the interlevel dielectrics (ILD). Much work is being done to reduce the dielectric constant of the ILD through fabrication of porous dielectrics, but significant challenges remain to do this while maintaining mechanical strength of the ILD. Furthermore, as copper interconnects are scaled to smaller feature sizes, the diffusion barrier layer must be reduced in thickness while maintaining an effective diffusion barrier for the copper. Finally, the electrical resistivity of the copper interconnects must not be reduced significantly even though there is significant scattering due to surface, interface roughness, and grain scattering. These challenges offer opportunities for nano-materials in processing, advanced structural applications and devices in the future, but significant progress must be made in characterizing their electronic, electrical and chemical and mechanical properties.

# 5:00 PM Plenary

Nanostructured Ceramics: Processing, Applications and Commercialization: B. H. Kear<sup>1</sup>; <sup>1</sup>Rutgers University, Ctr. for Nanomatls. Rsch., 607 Taylor Rd., Piscataway, NJ 08854-8065 USA

Two methods have been devised for the production of nanostructured ceramics: one for single phase or nanocrystalline ceramics and the other for multiphase or nanocomposite ceramics. The first method makes use of a metastable nano-scale powder as starting material and pressure-assisted sintering to develop a nanocrystalline product. The second method utilizes a metastable micro-scale powder as starting material and pressure-assisted sintering to develop a nanocomposite product. Both methods depend for their success on control of a pressure-induced phase transformation to promote rapid densification without causing significant grain growth. Several examples will be given to illustrate the versatility of the transformation-assisted consolidation process. In addition, progress in near-net shape superplastic-like forming of nancomposite ceramics will be described. Applications include engine components, machine tools, and household items. A methodology for commercializing the new technologies will also be discussed.

# Advanced Materials for Energy Conversion II: Metal Hydrides II

Sponsored by: Light Metals Division, LMD-Reactive Metals Committee

*Program Organizers:* Dhanesh Chandra, University of Nevada, Metallurgical & Materials Engineering, Reno, NV 89557 USA; Renato G. Bautista, University of Nevada, Metallurgical and Materials Engineering, Reno, NV 89557-0136 USA; Louis Schlapbach, EMPA Swiss Federal, Laboratory for Materials Testing and Research, Duebendorf CH-8600 Switzerland

Monday PM	Room: 203A	
March 15, 2004	Location: Charlotte Convention	Center

Session Chairs: Jim C.F. Wang, Sandia National Laboratories, Livermore, CA 94550 USA; Bruce Clemens, Stanford University, Matls. Sci., Stanford, CA 94305 USA; Jean-Marc Joubert, CNRS, Thais Cedex F94320 France

# 2:00 PM Plenary

Solid State and Surface Phenomena in Energy Transformation Materials: Louis Schlapbach<sup>1</sup>; <sup>1</sup>EMPA, Swiss Federal Lab for Matls. Testing & Rsch., CH-8600, Duebendorf Switzerland

Solid state and surface phenomenon in energy transformation materials will discussed. Environmental issues related to the energy conversion systems; mainly production of carbon dioxide is an important issue. Clean hydrogen energy will have a signifcant impact on global issues related to energy in both stationary as well as mobile power generators. Fundamental understanding of hydrogen interactions with materials will allow development of new light weight hydrogen storage materials/systems. The use of hydrogen in fuel cells and engines for automobiles will have to be fully explored for clean energy conversion. In addition, energy loss prevention by using quasicrystalline coatings on materials will reduce tribology (energy loss). Heat transfer issues in gas turbines need to be also evaluated. Other systems such as thermoelectrics, photovoltaics, and others will also be discussed.

## 2:30 PM Invited

Novel Hydrides with [Al-H] Bonding Synthsized by Hydrogenation of Intermetallic Compounds: Etsuo Akiba<sup>1</sup>; Qing An Zhang<sup>2</sup>; Yumiko Nakamura<sup>1</sup>; <sup>1</sup>National Institute of Advanced Science and Technology, Energy Elect. Inst., Tsukuba Central 5, 1-1-1, Higashi, Tsukuba, Ibaraki 305-8565 Japan; <sup>2</sup>Anhui University of Technology, Sch. of Metall. & Matl., Maanshan, Anhui 243002 China

We successfully prepared novel hydrides by hydrogenation of intermetallics compounds that consisted of alkali earth metal (Mg, Ca, Sr and Ba) and Al. Starting from SrAl<sub>2</sub> Zintl phase alloy, two novel hydrides such as SrAl<sub>2</sub>H<sub>2</sub> Zintl hydride and Sr<sub>2</sub>AlH<sub>7</sub> alanate were synthesized. Alanates of BaAlH<sub>5</sub> and Ba<sub>2</sub>AlH<sub>7</sub> were synthesized from Ba<sub>7</sub>Al<sub>13</sub> intermetallic compound. Crystal structures of these novel hydrides were refined using powder neutron diffraction. Phase relations of pseudo binary alloys of (Sr, X)Al<sub>2</sub> (X=Ca and Ba) and Sr(Al, Mg)<sub>2</sub> were also investigated.

# 2:55 PM Invited

Intermetallic Compounds for Hydrogen Gas Storage: Jean-Marc Joubert<sup>1</sup>; V. Iosub<sup>2</sup>; M. Latroche<sup>2</sup>; A. Percheron-Guégan<sup>2</sup>; <sup>1</sup>CNRS, Lab. de Chimie Métallurgique des Terres Rares, 2-8 rue H. Dunant, Thiais Cedex F-94320 France; <sup>2</sup>CNRS, Lab. de Chimie Métallurgique des Terres Rares, 2-8 rue Henri Dunant, F-94320 Thiais Cedex France

Hydrogen gas is expected to play an important role in the future as an energy career according to its zero emission behaviour when used as a fuel. Many intermetallic compounds (e.g. LaNi5- or ZrMn2-type) react reversibly with hydrogen near atmospheric pressure and ambient temperature to form metal hydrides giving rise to dense and safe hydrogen storage possibility. Possible modifications of the storage properties (such as capacity, hydrogen pressure, aging, kinetics) by composition changes in order to suit a given application represent one of the main features of those compounds. Advantages and drawbacks of metal hydrides are presented and compared with other storage media. An example of application as a storage unit for a stationary fuel cell supply will be detailed.

# 3:20 PM Break

# 3:35 PM Invited

Low and High Pressure Hydrogen Storage in V-0.5 at.%C Alloy: Dhanesh Chandra<sup>1</sup>; Archana Sharma<sup>1</sup>; Joseph R. Wermer<sup>4</sup>; Willliam K. Cathey<sup>1</sup>; Robert C. Bowman<sup>2</sup>; Franklin E. Lynch<sup>3</sup>; <sup>1</sup>University of Nevada, Metallurgl. & Matls. Engrg., Mackay Sch. of Mines, Reno, NV 89557 USA; <sup>2</sup>NASA Jet Propulsion Laboratory, MS 79-24, Pasadena, CA 91109 USA; <sup>3</sup>Hydrogen Consultants, 12400 Dumont Way, Littleton, CO 80125 USA; <sup>4</sup>Los Alamos National Laboratory, Tritium Sci. & Engrg. Grp., MS C-348, Los Alamos, NM 87545 USA

Low and high pressure hydrding of cold-worked V-0.5 at.%C alloy, cycling of hydrides, thermodynamic and structural parameter aspects were investigated. Thermal cycling between beta and gamma phase hydrides increased the hysteresis but the desorption pressure did not significantly change. Prestraining this alloy also increased the hysteresis but the desorption pressure decreased slightly as compared to that of the unstrained alloy. Microstrains, <exp2>1/2, in the beta phase of the thermally cycled hydrides decreased after >700 cycles, whereas the domain sizes increased. However in the gamma phase, both the microstrains and the domain sizes decreased after thermal cycling. The dehydrogenated alpha phase after >700 thermal cycles showed residual microstrains in the lattice, similar those observed for the intermetallic hydrides. Thermodynamic aspects of alpha to beta phase transitions at low pressures will also be presented. The effects of thermal cycling and cold-work on absorption and desorption pressures, H/ M ratio, microstrains, long range strains and domain sizes in the beta and gamma phase hydrides of V-0.5 at.%C alloy are presented.

# 4:00 PM Invited

Neutron Metrology for the Hydrogen Economy: Terrence J. Udovic<sup>1</sup>; Taner Yildirim<sup>1</sup>; Charles F. Majkrzak<sup>1</sup>; Muhammad Arif<sup>1</sup>; David L. Jacobson<sup>1</sup>; <sup>1</sup>National Institute of Standards & Technology, Ctr. for Neutron Rsch., 100 Bureau Dr., MS 8562, Gaithersburg, MD 20899-8562 USA

Neutron scattering, transmission, and analysis techniques are particularly well-suited for studying materials of relevance to fuel-cell and hydrogen-storage technologies. The unusually large neutron scattering cross section for hydrogen (and deuterium) as well as the neutron's great penetrating power are routinely exploited in order to probe the amount, location, bonding states, and dynamics of hydrogen (and water) in a variety of technologically interesting materials. Developments over the past decade at the NIST Center for Neutron Research and elsewhere have greatly increased the sensitivity and dynamic range of neutron methods. In this talk, we will provide a flavor of the capabilities of modern neutron instrumentation for the study of energy systems and materials important for the hydrogen economy, from micron-scale imaging of working fuel-cell stacks and hydrogenstorage beds to atomic-scale characterization of hydrogen location, bonding, and transport mechanisms in fuel-cell membranes and hydrogen storage materials.

#### 4:25 PM Invited

Sensing of Hydrogen in Advanced Ni-MH Battery Materials: Brajendra Mishra<sup>1</sup>; David L. Olson<sup>1</sup>; <sup>1</sup>Colorado School of Mines, Metallurgl. Engrg., 920 15th St., Golden, CO 80401 USA

The AB5 type alloys, such as LaNi5, are used as hydrogen storage materials. Absorbed hydrogen provides electrons to the conduction band and also creates the hydride bonding band. Consequently, electrons change the magnetic and thermoelectric power properties of the AB5 hydrogen storage. Additionally, the linear relationship between the magnetic and thermoelectric power properties is discovered. This phenomenon is due to the reduction of the magnetic moment in B site of AB5 alloys and the partial filling of electrons from hydrogen in the conduction band of the alloys. Effect of absorbed hydrogen on the Seebeck coefficient of the studied alloys shows the similar pattern as the pressure composition isotherm. This behavior shows that Seebeck coefficient is a potential parameter to be used as an indicator of micro-structure or phase of AB5 alloys. Consequently, the magnetic susceptibility measurement is an important tool to be developed as a phase indicator for AB5 alloys.

# Advances in Superplasticity and Superplastic Forming: Development of Advanced Superplastic Forming Processes

Sponsored by: Materials Processing and Manufacturing Division,
Structural Materials Division, MPMD-Shaping and Forming
Committee, SMD-Mechanical Behavior of Materials-(Jt. ASM-MSCTS),
SMD-Structural Materials Committee
Program Organizers: Eric M. Taleff, University of Texas,
Mechanical Engineering Department, Austin, TX 78712-1063 USA;
P. A. Friedman, Ford Motor Company, Dearborn, MI 48124 USA;
Amit K. Ghosh, University of Michigan, Department of Materials
Science and Engineering, Ann Arbor, MI 48109-2136 USA; P. E.
Krajewski, General Motors R&D Center; Rajiv S. Mishra, University of Missouri, Metallurgical Engineering, Rolla, MO 65409-0340
USA; J. G. Schroth, General Motors, R&D Center, Materials and Processes Laboratory, Warren, MI 48090-9055 USA

Monday PM	Room: 2	201B
March 15, 2004	Location:	Charlotte Convention Center

Session Chairs: Eric M. Taleff, University of Texas, Dept. of Mech. Engrg., Austin, TX 78712-0292 USA; Paul E. Krajewski, General Motors, R&D Ctr., Warren, MI 48090-9055 USA

# 2:00 PM

The History and Current State-of-the-Art in Airframe Manufacturing Using Superplastic Forming Technologies: Daniel G. Sanders<sup>1</sup>; <sup>1</sup>Boeing, MR&D & Phantom Works, PO Box 3707 MS 5K-63, Seattle, WA 98124-2207 USA

This paper examines the progression of SPF in aerospace from the early days of hot forming to the state-of-the-art in current fabrication technologies. In the past fifteen years there has been a remarkable evolution of the Superplastic Forming (SPF) as an aerospace manufacturing process. The original aerospace applications and development of SPF were heavily influenced by military aircraft requirements for bomber and fighter projects such as the B-1, B-2, F-15E, and the F/A-18. Parts for these USAF airframes were hand-built in small lot sizes of one to three parts. At Boeing, the natural progression of SPF and hot forming methodology turned towards commercial aviation in the 1990?s, during the design of the B-777 and B-737-NG. It was during this timeframe that SPF production rates increased from one or two parts per month on the military side of the business to several hundred per month required for passenger jetliner manufacturing. The SPF process was thrust into the mass production mode, whereby highly automated presses were developed and brought on-line. New tooling innovations and part trimming methods were co-developed. Along with the advancements in SPF automation, there have been a number of material inventions that have accelerated the proliferation of parts. New aluminum alloys like 5083-SPF and 2195 have allowed designers to create large monolithic panels to replace built-up assemblies that used to require hundreds of fasteners and eliminate dozens of detail parts. Several titanium alloys, such as SP-700, 6-2-2-2, 6-2-4-2 and 15-3-3-3 have opened-up a wider range of part families that are subjected to high stresses, sonic vibration, corrosive environments and high operating temperatures. SPF advances have been made possible by concurrent advances in many other enabling technologies. Through the application of new alloys and clever engineering design, SPF implementations at Boeing have resulted part consolidation, weight reduction, faster through-put, inventory reduction, elimination of tooling families, simplified assembly and substantial cost savings. As we move further into the twenty-first century, the teaming and partnering of government institutions, industry partners and the universities is vital. Teaming of these organizations will be an essential element as SPF manufacturing moves into the mainstream automotive and domestic goods markets.

# 2:25 PM

General Motors' Quick Plastic Forming Process: James G. Schroth<sup>1</sup>; <sup>1</sup>General Motors, R&D Ctr., Matls. & Proc. Lab., MC 480-106-212, 30500 Mound Rd., Warren, MI 48090-9055 USA

General Motors has used hot blow forming processes for the production of aluminum closure panels for specific automotive applications. In the initial manifestation of GM's "Quick Plastic Forming" process, automated forming cells were built around traditional heatedplaten superplastic forming presses. Automotive volumes demand fast forming cycles and reproducible dimensions in hot-formed aluminum panels. The initial implementation of hot blow forming technology leveraged fully automated handling systems, novel sealing geometries and panel extraction methods, and an optimized tool material/coating/ lubricant system in conjunction with specialized cooling fixtures to produce dimensionally correct panels directly out of the forming cell. GM has continued to evolve its forming technology to facilitate shorter forming times, more complex panel geometries, and improved panel dimensions. Representative panel geometries produced with the system are described.

# 2:50 PM

Heating Aluminum Sheet to Enable High-Strain Forming: John E. Carsley<sup>1</sup>; *Richard H. Hammar*<sup>1</sup>; <sup>1</sup>General Motors Corporation, R&D & Planning/Matls. & Proc. Lab., MC 480-106-212, 30500 Mound Rd., Warren, MI 48090-9055 USA

Several novel technologies for shaping aluminum sheet into complex geometries call for elevated temperatures to improve formability. Some of these technologies include warm stamping, superplastic forming and hot hydroforming. Production cycles should not be limited by the speed at which the aluminum blanks are heated to the required temperatures. Several methods of heating aluminum sheet have been investigated and modeled in terms of the primary modes of heat transfer including conduction, convection and radiation. The paper describes the advantages of each method relative to the specifications of attaining a uniform, stable temperature in minimal time while preserving Class-A surface quality. Examples of each method are compared with respect to a blank temperature of approximately 850°F to 900°F, as needed for superplastic forming of AA5083.

# 3:10 PM

Tooling Materials for Superplastic Forming Processes: *M. David* Hanna<sup>1</sup>; 'General Motors, R&D Ctr., Matls. & Proc. Lab., MC 480-106-212, 30500 Mound Rd., Warren, MI 48090-9055 USA

Different steels and cast iron tools used for superplastic and hot forming operate at temperatures as high as 500°C and could be used in service for as long as five years. Experiments were conducted to determine if such tool materials soften (temper) during long-term, hightemperature exposure. Extrapolation from short-term tempering data indicated that no appreciable softening was observed in nodular cast iron or three different tool steels after five years at 480°C.

# 3:30 PM Break

# 3:50 PM

Mass Production of a Spare Tire Housing for an Automobile: Kuniaki Osada<sup>1</sup>; <sup>1</sup>Nippon Yakin Kogyo Co., Ltd, Project Planning & Dvlp. Div., 1-5-8 Kyobashi, Chuou-Ku, Tokyo Japan

Mass production of a spare tire housing made of 5083 Al alloy by superplastic forming was achieved. The housing is composed of two parts with different 3D geometries. Monthly number of the parts was approaching 4,000. In production, multiple forming operations in a single tool set, semi-automatic application of lubricants, and an effective layout of the whole process were key contributions to achieving production goals. In the multiple forming operations, the two pieces of the housing were expanded with a characteristic forming gas inlet mechanism at once. Owing to the mechanism used, it turned out to be possible to form four parts in as short as fifteen minutes. Application of two lubricants onto areas that require specific friction coefficients effectively worked with advantage of resistance to scratches. Because outside appearance of the housing is considerably important in a consumer product, surface treatments were carried out before shipment. In the presentation, key factors that lead to successful production will be summarized.

# 4:15 PM

**Evaluation of Die Coatings for Superplastic Forming Processes:** *Arianna T. Morales*<sup>1</sup>; <sup>1</sup>General Motors, R&D Ctr., Matls. & Proc. Lab., MC 480-106-212, Warren, MI 48090 USA

Typically, superplastically formed parts are made from fine-grained aluminum sheets blow formed into a sculptured ferrous die, which is heated to the proper forming temperature. Intimate contact between the die and the work piece enables the action of interatomic forces (adhesion, friction), and solid lubricants have to be used to prevent sticking and bonding of the aluminum to the ferrous dies. The use of tool coatings tailored for this process may enable the reduction and possible elimination of solid lubricants. The tool coatings can provide an optimal surface configuration for the forming process and significantly increase tool life. This paper will present results obtained from experiments with different coatings and surface treatments on superplastic forming dies.

# 4:35 PM

Certain classes of automotive body panels, such as deck lid outer panels, are preferably formed in two stages. The first stage, called the pre-forming stage, creates the necessary length of line and the thickness distribution that are needed for the second and final forming operation to produce wrinkle-free panels without excessive thinning. The first-stage forming can be accomplished either by gas pressure, i.e. QPF, or by stamping. Double-action QPF tools are special tools that combine two forming stages into one compact tool geometry. Doubleaction QPF offers many advantages over its single-action counterpart in terms of attainable panel shape complexity, production cycle time, improved use of limited press space, etc. This paper describes alternate types of double-action tools: one based on punch pre-forming and one utilizing air-pressure pre-forming.

# 4:55 PM

**SSR Fender Tool Development**: *Chongmin Kim*<sup>1</sup>; Mark G. Konopnicki<sup>2</sup>; Frank G. Lee<sup>3</sup>; <sup>1</sup>General Motors, R&D Ctr., Matls. & Proc. Lab., MC 480-106-212, 30500 Mound Rd., Warren, MI 48090-9055 USA; <sup>2</sup>General Motors, MC 480-106-212, 30500 Mound Rd., Warren, MI 48090-9055 USA; <sup>3</sup>General Motors, GMNA Engrg., Pontiac, MI USA

Math-based technology was effectively used to design a tool set for hot blow forming of large SSR fender panels with complex curvatures. The surface geometries of the forming tool set, consisting of a preform tool and a final form tool, were optimized during the tool design phase with extensive use of finite-element analysis of the forming process. The forming tool set produced both right and left fenders from one blank, resulting in good productivity and high material utilization. The forming tool set was fabricated in less than 20 weeks. This tool development exercise and the immediate success of the forming trial set a benchmark for rapid production of complex body panels.

# Alumina and Bauxite: Process Modeling and Control

Sponsored by: Light Metals Division, LMD-Aluminum Committee Program Organizers: Travis Galloway, Century Aluminum, Hawesville, KY 42348 USA; David Kirkpatrick, Kaiser Aluminum & Chemical Group, Gramercy, LA 70052-3370 USA; Alton T. Tabereaux, Alcoa Inc., Process Technology, Muscle Shoals, AL 35661 USA

Monday PM	Room: 2	18A	
March 15, 2004	Location:	Charlotte C	onvention Center

Session Chair: Benoit Cristol, Aluminium Pechiney, Alumina Tech., Gardanne Cedex 13541 France

# 2:00 PM

Application and Benefits of Advanced Control to Alumina Refining: *Robert K. Jonas*<sup>1</sup>; <sup>1</sup>Honeywell Industrial Solutions, Mining, Metals, & Minerals, 2500 W. Union Hills Dr., Phoenix, AZ 85053 USA

Substantial returns to alumina refineries can be realized through the use of control technology that utilizes existing infrastructure and requires minimal support staff. The globalization of markets and the consolidation of producers have created a more competitive environment that drives the need for optimal production and performance in alumina refineries. Throughout the Bayer process, advanced control is becoming a preferred tool to deliver return on capital employed. Primarily, this is being done using the prevailing control technology, multivariable predictive control. This paper will discuss the applications and benefits of this technology in the alumina industry. Increases in production, yield, and quality are being realized in many areas of the Bayer cycle using multivariable predictive control, most notably in the control of the bauxite digestion area. New benefits are being achieved by applying this control technology to evaporation and heatinterchange units. The technology is also proving to be suited to grinding, precipitation, and calcination. Improvements in production or yield of up to 1/2 to 4% are realizable.

#### 2:25 PM

The Effects of Changes in Liquor Temperature and Caustic Concentration on Seed Balance Parameters in Alumina Refinery Seed Classification Systems: *Walter Mason Bounds*<sup>1</sup>; <sup>1</sup>2583 Woodland Ridge Blvd., Baton Rouge, LA 70816 USA An important consideration in controlling alumina refinery seed classification systems is ensuring that seed produced matches quantity and particle size distribution with seed charged. When this condition is not satisfied, the system may not be stable, resulting in changing seed inventory quantities and particle size distribution. Previous papers have described methods for evaluating operating parameters for individual classification systems. In this paper, information from previous papers is utilized to simulate a classification system and determine the effects of changes in liquor temperature and caustic concentration on seed balance parameters, including mass balance and particle size distribution. Temperature and caustic concentration effects on out-ofbalance cases are also established to aid in illustrating consequences.

#### 2:50 PM

Perfomance Stability Criteria and Expert Control System of Rotary Sintering Kiln at "Achinsk Alumina Plant" PSC: Alexander I. Berezin<sup>1</sup>; Oleg O. Rodnov<sup>1</sup>; Vladislav V. Blinov<sup>2</sup>; Pavel D. Stont<sup>2</sup>; Oleg A. Chashchin<sup>3</sup>; Peter Ya. Hohlov<sup>3</sup>; Anatoliy M. Skoptsov<sup>3</sup>; <sup>1</sup>RUSAL Engineering & Technology Center, Pogranichnikov st. 37, Krasnoyarsk 660111 Russia; <sup>2</sup>Mayak PKF Ltd., Bograda st. 108, Krasnoyarsk 660021 Russia; <sup>3</sup>"Achinsk Alumina Plant" PSC, Achinsk 662150 Russia

Sintering of the charge in a rotary kiln is a complex non-steady physical-chemical process specified by numerous internal and external disturbing factors and highly dynamic changes of energy and material flows. To describe it criteria of thermal-physical similarity based on the second theorem of similarity theory have been defined. Values of criteria calculated for time periods when the conditions were steady are applicable for analysis of conditions on analogous kilns, the criteria being those of conditions stability. These criteria are used in an expert system capable of automatically controlling the sintering conditions by the rules based on experience and knowledge of expert specialists. Current process parameters form the basis to calculate stability criteria to define and set such control parameter values that provide for stabilization of optimum conditions.

#### 3:15 PM

Design and Training Improvements Through the Use of Dynamic Simulation: Robert K. Jonas<sup>1</sup>; <sup>1</sup>Honeywell Industrial Solutions, Mining, Metals, & Minerals, 2500 W. Union Hills Dr., Phoenix, AZ 85053 USA

Extensive use of dynamic process simulators is becoming the norm for many greenfield facilities in metals and mining, especially among alumina refineries. Dynamic simulation provides a means to validate process design to a greater degree than possible with typical process design tools that cannot handle the complexities of refineries and their interactions with operators and control systems. Many leading companies are benefiting from the use of dynamic simulation for control upgrades and greenfield projects because of the complexity of controls in the Bayer cycle. Dynamic simulation of both process and control systems provides for enhanced control validation and operator training. This paper discusses the current practices and benefits of dynamic simulation in alumina refining. Interactive and accurate simulation provides the mechanism to validate and improve new process and control designs. These improvements have proven to minimize design shortfalls that would negatively impact throughput, quality, and comm issioning times. By using dynamic simulation for operator training, further benefits can be attained by improved availability (minimization of lost production), safety, and environmental and safety certification.

# Aluminum Reduction Technology: Cell Development and Operations

Sponsored by: Light Metals Division, LMD-Aluminum Committee Program Organizers: Tom Alcorn, Noranda Aluminum Inc., New Madrid, MO 63869 USA; Jay Bruggeman, Alcoa Inc., Alcoa Center, PA 15069 USA; Alton T. Tabereaux, Alcoa Inc., Process Technology, Muscle Shoals, AL 35661 USA

Monday PM	Room: 2	213D
March 15, 2004	Location	Charlotte Convention Center

Session Chair: Craig Taylor, Noranda Inc., St. Jude Industrial Park, New Madrid, MO 63869 USA

2:00 PM

The Impact of Anode Cover Control and Anode Assembly Design on Reduction Cell Performance: Mark P. Taylor<sup>1</sup>; Greg L.

Reduction line amperages have been increasing around the world in recent years as companies seek to increase the return from existing assets. A key part of a smelter's asset base is its fleet of anode rods, which were designed to take a particular current range, and to carry the anode of the day with an acceptable voltage drop, and robustly enough to prevent drop off or wide-spread cracking of the carbon. Similarly the anode cover on reduction lines has been optimised or at least designed primarily to prevent air access to the anode surface - still a key design criterion for the cell. However the increase in heat generation within the anode, and within the bath as well in many smelters, as amperage has increased, has eventually brought these cell components to their temperature limits or beyond. The anode assembly design criterion which is now most critical for the stability of the cell is the dissipation of sufficient heat from the assembly and the cover to maintain component temperature and overall cell heat balance. This paper builds on earlier work regarding the thermochemical stability of cover and crust [1] to discuss the operating practice and assembly design issues which must be addressed at a smelter to meet the amperage challenge. Simple modelling of the assembly heat flows and the impact of anode cover on them is combined with plant results to demonstrate how the above issues can be addressed.

# 2:25 PM

The Influence of the Thermo-Electrical Characteristics of the Coke Bed on the Preheating of an Aluminium Reduction Cell: Carl Laberge<sup>1</sup>; László I. Kiss<sup>1</sup>; Martin Desilets<sup>2</sup>; <sup>1</sup>Université du Québec, 555 boul. de l'Université, Chicoutimi, Québec G7H 2B1 Canada; <sup>2</sup>Alcan International Limitée, 1955 boul. Mellon, Jonquière, Québec G7S 4K8 Canada

Coke beds are frequently used for the electrical preheating of aluminium electrolysis cells. Their electrical and thermal resistances have a strong influence on the rate of heat generation and on the uniformity of the temperature distribution during the warming-up. Both the electric and thermal transport processes have a complex nature inside granular materials. Material properties, bed thickness, pressure, granulometry, temperature level - all have an effect on the electric resistance and equivalent thermal conductivity. An experimental study was completed in order to analyze the mechanism of the transport processes and to supply constitutive laws for the mathematical modelling of the electrical preheating of an aluminium reduction cell. Results are presented to represent the most important tendencies of the electrical resistance and equivalent thermal conductivity as functions of temperature and bed thickness.

#### 2:50 PM

# Autopsy Procedures and Results at Century West Virginia: Marilou McClung<sup>1</sup>; Ron Zerkle<sup>1</sup>; <sup>1</sup>Century Aluminum of West Virginia, Techl., PO Box 98, Ravenswood, WV 26164 USA

Extending pot life can be a significant cost savings for any Reduction facility. The first step in Century Aluminum of West Virginia's pot life improvement program was to observe pot failure modes and conduct autopsies on a wide variety of pots to determine failure causes and mechanisms. A set of procedures was developed to enable us to conduct comprehensive autopsies and to standardize the information collected on all cells. This paper includes information on ur four levels of autopsy procedures, autopsy results and steps taken from the information gathered to improve pot life. Several examples of autopsy results are discussed in detail.

# 3:15 PM

**Busbar Modification of the End Pots of Potline 1 of Albras**: *Guilherme Epifanio Mota*<sup>1</sup>; Gilvando Jose Andrade<sup>1</sup>; <sup>1</sup>Albras - Aluminio Brasileiro S/A, Area de Redução/Fundição, Estrada Pa 483 KM 21 Vila Murucupi, Bracarena, Para 68447-000 Brasil

In The Albras Potlines the end pots have always presented inferior performance compared to the midle pots, giving high instability and voltage oscillation resulting, in low current efficiency. Even after the magnetic compensation of all the pots, such difference between those pots still remained. So, in order to eliminate this situation, and based on electromagnetic model simulations, it was proposed busbars modification at the end of the potroom, to improve the magnetic configuration by reduction of intensity and better symmetry of the vertical magnetic field components inside the end pots. This modification consisted of increasing the distance between the end busbars and end pots, reducing magnetic influence. With this, pot voltage oscillation decreased and increasing current efficiency. In addition, we expect an increase in pot life. This paper presents the average results of the end pots for the 6 months following the modification and the involved costs.

# 3:40 PM Break

# 3:50 PM

CVG Venalum - Line VI and VII: Lenin Dario Berrueta<sup>1</sup>; <sup>1</sup>C.V.G. Venalum, Presidencia, AV. Fuerzas Armadas, Edif. Corporativo, Puerto Ordaz, Bolivar 8050 Venezuela

The short and medium expansion plans of Venalum consider the construction of two reduction lines. This plan has been scheduled into two stages, each reduction line to be constructed along with its carbon plant and cast shop required to operate the pots fully independent from the previous Venalum infrastructure. During construction of the first expansion, the actual port facilities will be enhanced to cover the two new lines material handling requirements. Engineering of this expansion is based on the use of our own reduction technology, The V-350 Cell, therefore, investment cost can be kept close to 600 million dollars for Line VI, and lower for Line VII. The annual production capacity of each line will be in the order of 210.000 tonnes, hence, total annual output of Venalum after completion of the two lines will be over 850.000 tonnes, and sales in excess of a thousand million american dollars.

# 4:15 PM

**Brazil 2001 Energy Crisis - The Albras Approach**: *Handerson Penna Dias*<sup>1</sup>; <sup>1</sup>Albras - Aluminio Brasileiro SA, Est. PA 483 Km 21, Vila de Murucupi, Barcarena, PA 68447000 Brazil

Due to many causes Brazil has suffered a major energy shortage during the year of 2001. The Aluminum Industry has been heavily hit and forced to reduce its energy consumption. The paper describes the approach adopted by Albras to deal with the crisis and to get a fast return to normal operation at the beginning of 2002. The results are discussed regarding the low energy input operation and the impact on cell life.

## 4:40 PM

Henan Hong Kong Longquan Aluminum Co. Ltd. — Growing Up: Haibo She<sup>1</sup>; Shichang Chen<sup>2</sup>; Juanzhang Zhang<sup>3</sup>; <sup>1</sup>Shenyang Aluminium & Magnesium Engineering & Research Institute (SAMI), R&D, 184 Hepingbei St., Shenyang, Liaoning 110001 China; <sup>2</sup>Henan Hong Kong Longquan Aluminium Co. Ltd, Yichuan County, Luoyang 471713 China; <sup>3</sup>Luoyang Tiansong Carbon Co. Ltd, Yichuan County, Luoyang, Henan 471312 China

Henan Hong Kong Longquan Aluminum Co. Ltd. (LQAL) and Luoyang Tiansong Carbon Co. Ltd. (TSC) are located in Yichuan County, Luoyang, Henan Province, China. These companies are separately engaged in aluminum reduction and prebaked anode block production respectively. They are both owned by Yichuan Electrical Group. The 300 kA potline in LQAL is the first 300 kA potline and with the largest capacity per potline in operation so far in China. LQAL(200kt/ a) took twelve months to complete the construction of the first 300 kA potline, five months to successfully start-up the 256 pots, and six months to reach the designed operating targets. TSC (120kt/a) took twenty months to complete the construction of the plant. The two projects both are praised as "miracle" in the aluminum industry construction of China.

# Automotive Alloys 2004: Session II

Sponsored by: Light Metals Division, LMD-Aluminum Committee Program Organizer: Subodh K. Das, Secat, Inc., Coldstream Research Campus, Lexington, KY 40511 USA

Monday PM	Room: 27	10A
March 15, 2004	Location:	Charlotte Convention Center

Session Chair: Subodh K. Das, Secat Inc., Coldstream Rsch. Campus, Lexington, KY 40511 USA

#### 2:00 PM

Flanging of Aluminum Panels: Sergey F. Golovashchenko<sup>1</sup>; Andrey V. Vlassov<sup>2</sup>; <sup>1</sup>Ford Motor Company, Ford Rsch. & Advd. Engrg., MD 3135, 2101 Village Rd., Dearborn, MI 48124 USA; <sup>2</sup>Bauman Moscow State Technical University, Mech. Engrg. Tech., 5 2nd Baumanskaya St., Moscow 107005 Russia

Implementation of aluminum alloys for the production of automotive skin panels may create problems due to their lack of formability. In flanging and hemming operations, it may result in splits on the Aclass surface. In order to produce high-quality exterior panels, new technologies of flanging and hemming have to be developed. Employment of elastic materials instead of regular steel allows reduce the cost of stamping dies because only one side of the die has to be machined. In addition, ductility of aluminum alloys in flanging and hemming operations can be improved by applying normal pressure to the outer surface of the blank, where stretching of the material takes place. Application of the external pressure through compression of elastic material shifts the stress state from tensile to tension-compression and increases the mean stress. Experimental and numerical results illustrating flat hemming and sharp flanging of 6111-T4 prestrained sheet will be presented.

#### 2:30 PM

# Incremental Forming of Aluminum Alloys: Sergey F. Golovashchenko<sup>1</sup>; *Al R. Krause*<sup>1</sup>; <sup>1</sup>Ford Motor Company, Ford Rsch. & Advd. Engrg., MD 3135, 2101 Village Rd., Dearborn, MI 48124 USA

The lack of formability found in aluminum alloys is often an issue in the manufacturing of body components, particularly for complex forming operations. Traditionally this problem was addressed by stamping separate panels and joining them by spot welding or riveting adding cost. For components that have geometries just beyond traditional forming capabilities another option may be possible. The objective of this research was to investigate the potential of an intermediate heat treatment to extend the range of deformation possible with aluminum alloys. Times and temperature ranges for typical automotive aluminum alloys were investigated and their effects on tensile behavior analyzed. The effect of pre-heat treatment deformation on heat-treat times were also investigated.

#### 3:00 PM

# Formability Studies on Al Alloy 5754 for Manufacture of a Specific Automotive Component: *Gyan Jha*<sup>1</sup>; <sup>1</sup>Arco Aluminum Inc., 9960 Corporate Campus Dr., Ste. 3000, Louisville, KY 40223-4032 USA

This paper attempts to present the work done by ARCO Aluminum in the manufacture of AA 5754 Al alloy sheet material using different thickness and final processing conditions for the manufacture of a specific automotive component. Mechanical properties were evaluated for the sheet at various thickness and formability studies were carried out for all the sheets to determine the behavior of the sheet during forming in all three dimensions. These results were integrated with the CAD/CAM design of the component applicable to a specific hydraulic manufacturing press into proprietary software Autoform to predict the possibility of forming 2 different components by comparing the stresses raised at various locations under actual production conductions with the mechanical properties. A clear view of the stresses at various locations during sheet forming is obtained and when compared with the mechanical properties it is possible to determine safe and highly stressed areas and using an acceptance criteria for safety it is possible to highlight area of criticality in the component. This permits modification of the tooling design and loading conditions without investment in expensive tooling costs. Where necessary this permits development of the alloy to the correct specifications and subsequent modeling trials without investment in expensive tooling and development efforts.

#### 3:25 PM

Abnormal Grain Growth in Friction Stir Welded and Post Thermal-Mechanical Treated Al-2195: *Stanley M. Howard*<sup>1</sup>; Anthony Barajas<sup>2</sup>; Richard Wellnitz<sup>1</sup>; Anand Kaligotla<sup>1</sup>; <sup>1</sup>South Dakota School of Mines and Technology, Dept. of Matls. & Metallurgl. Engrg., 501 E. St. Joseph St., Rapid City, SD 57701 USA; <sup>2</sup>Oglala Lakota College, Kyle, SD 57752 USA

Samples from a fully annealed friction stir welded Al-2195 plate (0.084x0.61x0.10 m) were subjected to selected thermo-mechanical treatments to determine the effect on abnormal grain growth. Aswelded samples exhibited typical fine grain nugget microstructure. Treatments consisted of cold rolling reductions of 6, 20, 25, and 30% and hot rolling reductions of 10, 20, 30, and 40%. Samples were cut and rolled transverse to the weld. Samples, including control samples, were heated to 950°F (783 K) for 5 minutes to initiate possible grain growth and water quenched. Also, a sample was step heated at 50° F/h (22 K/h) from 750 to 950°F (672 to 783 K). Metallographic examination showed that all samples, except the cold-rolled ones, showed marked abnormal grain growth. Less growth occurred in the 6% cold-worked sample, and none was observed in the more severely cold-worked samples.

#### 3:50 PM

Anelastic Deformation After Unloading: *Jianfeng Wang*<sup>1</sup>; Richard Boger<sup>1</sup>; Robert H. Wagoner<sup>1</sup>; <sup>1</sup>Ohio State University, Dept. of Matls. Sci. & Engrg., 2041 College Rd., Columbus, OH 43210 USA

Previous draw-bend experiments showed springback continued to change for at least 2 years after forming for various aluminum alloys:

2008-T4, 5182-O, 6022-T4 and 6111-T4. DQSK and HSLA steels tested under same conditions showed no time-dependent springback, even after 7 years. In order to investigate a possible role of anelasticity in the measured response, special compression-tension tests of 6022-T4 and DQSK steel were conducted. The materials exhibited similar anelastic behavior following monotonic and reversed strain paths, with rapidly decreasing strain rates within the first hour. The similarity of the behavior of the two alloys and other characteristics of the anelastic deformation suggest that it is not the dominant cause of the time-dependent springback of aluminum alloys. In order to understand the features of anelasticity, tension-compression-unloading tests were also conducted for pure aluminum 1100-O and pure zinc (Alloy 101).

#### 4:15 PM

**Constitutive Behaviour of A356 During the Quenching Operation**: *Christina Michelle Estey*<sup>1</sup>; Steve Cockcroft<sup>1</sup>; Chris Hermesmann<sup>2</sup>; <sup>1</sup>University of British Columbia, Metals & Matls. Engrg., 309-6350 Stores Rd., Vancouver, BC V6T 1Z4 Canada; <sup>2</sup>Canadian Autoparts Toyota Inc., 7233 Progress Way, Delta, BC V4G 1E7 Canada

A collaborative effort is underway between the University of British Columbia and Canadian Autoparts Toyota Inc. to develop a mathematical model to predict the formation of residual stress, and hence the deformation, in A356 cast aluminum wheels during the quenching operation. In order to produce an accurate thermal stress model of the quenching operation, a detailed description of the constitutive behaviour of A356 is required in the solutionized condition. Unfortunately, most published constitutive data for A356 focuses on the final heat treated T6 condition. Therefore, an investigation was performed to determine the constitutive behaviour of A356 in the solution condition, prior to quenching and artificial aging. Uniaxial compression tests were performed over a range of temperatures (up to 500°C) and strain-rates (from 10-3 s-1 to 1 s-1) that are commonly experienced during the quenching operation at the wheel manufacturing plant.

#### 4:40 PM

Effect of Precipitation of Nb on High Temperature Strength of Automotive Ferritic Stainless Steel: Jae Cheon Ahn<sup>1</sup>; Gyu Man Sim<sup>2</sup>; Seung Chan Hong<sup>2</sup>; Chan Young So<sup>1</sup>; Kyung Sub Lee<sup>2</sup>; <sup>1</sup>INI Steel Corporation, R&D Dept., 1, Song hyun-dong, Dong-Ku, Incheon 401-712 Korea; <sup>2</sup>Hanyang University, Matls. Sci. & Engrg., 17 Haeng Dang-Dong, Sung Dong-Ku, Seoul 133-791 Korea

The effect of precipitation of Nb (0.45wt%) on high temperature strength of ferritic stainless steel for automotive manifold was investigated. Hot tensile tests were carried out at 700C with different stroke rate ranging from 1mm/min to 10mm/min. The strength was enhanced as the amount of solute Nb increased. It was thought that the strengthening mechanism was not only the solid solution strengthening but also the dynamic precipitation strengthening by Fe2Nb, since the Fe2Nb precipitates with a size of 20nm, which were not found before the tensile test, were observed at sub-grain boundaries by TEM. Also, the amount of dynamically precipitated Fe2Nb increased as the stroke rate was reduced. Thus, increment of the strength by Nb addition increased as the stroke rate decreased. However, coarse Fe2Nb precipitated by pre-aging at 700C remarkably reduced the strength. Therefore, size control of Fe2Nb was important factor in high temperature strength of ferritic stainless steel.

# 5:05 PM

Characteristics of Closed Cell Al and Al Alloys Foam Made by Pot Foaming Process: *Bo-Young Hur*<sup>1</sup>; *Zhekui Quan*<sup>1</sup>; Arai Hiroshi<sup>1</sup>; Sang-Youl Kim<sup>1</sup>; <sup>1</sup>Gyeongsang National University, Div. of Matls. Engrg., Kajoadong 900#, Chinju 660-701 S. Korea

Metallic foams were made by the pot foaming process. The matrix chosen are pro-alloyed Al-Si alloy (Al-2Si, Al-4Si) to investigate the affection of its good casting properties on the foaming behaviors and Pure Al as the reference. During the process a few process parameters such as: viscosity; surface tension and mixing temperature that affect the structure and the morphology of the closed cell foam are investigated. Herein the proper viscosity is effective to decrease the effect of drainage. The mixing temperature affects mainly the solidification of Al foam.

# Beyond Nickel-Base Superalloys: Molybdenum Silicides I

Sponsored by: Structural Materials Division, SMD-Corrosion and Environmental Effects Committee-(Jt. ASM-MSCTS), SMD-High Temperature Alloys Committee, SMD-Mechanical Behavior of Materials-(Jt. ASM-MSCTS), SMD-Refractory Metals Committee *Program Organizers:* Joachim H. Schneibel, Oak Ridge National Laboratory, Oak Ridge, TN 37831-6115 USA; David A. Alven, Lockheed Martin - KAPL, Inc., Schenectady, NY 12301-1072 USA; David U. Furrer, Ladish Company, Cudahy, WI 53110 USA; Dallis A. Hardwick, Air Force Research Laboratory, AFTL/MLLM, Wright-Patterson AFB, OH 45433 USA; Martin Janousek, Plansee AG Technology Center, Reutte, Tyrol A-6600 France; Yoshinao Mishima, Tokyo Institute of Technology, Precision and Intelligence Laboratory, Yokohama, Kanagawa 226 Japan; John A. Shields, HC Stark, Cleveland, OH 44117 USA; Peter F. Tortorelli, Oak Ridge National Laboratory, Oak Ridge, TN 37831-6156 USA

Monday PM	Room: 2	11B		
March 15, 2004	Location:	Charlotte	Convention	Center

Session Chairs: Matthew J. Kramer, Iowa State University, Ames Lab., Ames, IA 50011-3020 USA; Kyosuke Yoshimi, Tohoku University, Inst. for Matls. Rsch., Sendai, Miyagi 980-8577 Japan

# 2:00 PM Invited

**Oxidation of High Temperature Structural Molybdenum Borosilicides:** S. Woodard<sup>1</sup>; S. Vega<sup>1</sup>; D. Berczik<sup>1</sup>; <sup>1</sup>Pratt and Whitney, 400 Main St., MS 114-51, E. Hartford, CT 06040 USA

Historically, as high temperature structural materials molybdenum and molybdenum-based alloys have been limited to non-oxidizing environments in an uncoated condition due to the volatility of the primary oxide that forms on these alloys. In the early-1990's molybdenum borosilicides were identified as a new class of alloys that potentially possess adequate oxidation resistance in combination with the necessary mechanical properties to be utilized as a high temperature structural material in an oxidizing environment. Superior oxidation resistance is realized in molybdenum borosilicides that possess a high volume fraction of intermetallic phases, while mechanical properties such as impact resistance and ductility are more readily achieved in a material with a molybdenum matrix and a small volume fraction of intermetallic. Alloys near Mo-3Si-1B(wt%) are promising because they approach a balance between these competing material requirements. The oxidation resistance of such alloys will be reviewed across the 25°F-2200°F-temperature range, accompanied by a discussion of some key mechanical properties.

#### 2:30 PM

Scale Development on Bcc-Mo Bearing Mo-Si-B Alloys in Synthetic Combustion Gas Atmospheres: Andrew J. Thom<sup>1</sup>; Pranab Mandal<sup>1</sup>; Vikas Behrani<sup>1</sup>; Matthew J. Kramer<sup>1</sup>; Mufit Akine<sup>1</sup>; <sup>1</sup>Iowa State University, Ames Lab. & Dept. of Matls. Sci. & Engrg., Matls. Chmst., Spedding Hall, Ames, IA 50011 USA

Previous work showed that Si-rich Mo-Si-B alloys form protective scales on exposure to dry air to at least 1600°C. Alloys containing bcc-Mo also show reasonable resistance to dry air to about 1400°C. Exposures to wet air and simulated combustion gas (SCG) promote growth of thicker scales on the bcc-Mo alloy at much lower temperatures. Iso-thermal TGA measurements reveal the alloy undergoes a slow linear mass loss on the order of 1 x 10-3 mg/cm2/hr. The present paper discusses the development of the scale in the presence of water and SCG. Scale evolution involves the simultaneous processes of borosilicate scale formation, subscale formation of Mo and MoO2, slow transport and evolution of MoOx through the borosilicate scale, and volatility of boron and Si(OH)x-containing species from the borosilicate glass. Oxidation kinetics and scale microstructural analyses will be discussed to construct a thermochemical treatment of the oxidation process.

# 2:45 PM

The Behavior of Multiphase Mo-Si-B Alloys in High-Temperature Oxidizing and Sulfidizing Environments: Peter F. Tortorelli<sup>1</sup>; Joachim H. Schneibel<sup>1</sup>; Karren L. More<sup>1</sup>; Michael P. Brady<sup>1</sup>; <sup>1</sup>Oak Ridge National Laboratory, PO Box 2008, Oak Ridge, TN 37831 USA

The high-temperature corrosion behavior of Mo-Si-B alloys under various environmental conditions is being studied for possible use in advanced energy systems based on fossil fuels. Alloys of Mo-Mo5SiB2-Mo3Si with different compositions and phase morphologies were isothermally and cyclically oxidized in dry air or exposed to an H-2-H2S- H2O-Ar environment. Effects of the multiphase nature (composition, morphology) of the Mo-Si-B system on environmental resistance under these conditions were evaluated. Microstructural characterization indicated that the oxidation reactions resulted in cooperative behavior among the different phases while preliminary analyses suggested that sulfide formation mimicked the starting alloy microstructure. Quite low corrosion rates under sulfidizing conditions were observed. Implications of these findings for alloy design for oxidation and/or sulfidation resistance will be discussed. Research sponsored by the Advanced Research Materials Program, Office of Fossil Energy, U.S. Department of Energy, under contract DE-AC05-000R22725 with UT-Battelle, LLC.

# 3:00 PM

**Oxidation Behavior of Multiphase Mo-Si-B Alloys**: Voramon Supatarawanich<sup>1</sup>; David R. Johnson<sup>1</sup>; M. A. Dayananda<sup>1</sup>; <sup>1</sup>Purdue University, Sch. of Matls. Engrg., 501 Northwestern Ave., W. Lafayette, IN 47907-2044 USA

In this study multiphase Mo-Mo5SiB2(T2)-Mo3Si alloys with different compositions were examined for microstructure and oxidation behavior. The alloys were prepared by powder metallurgy and casting techniques and contained up to 50 vol.% bcc Mo solid solution. Cyclic oxidation tests were conducted at temperatures ranging from 800 to 1500°C in air. Upon oxidation at 800°C, alloys containing mostly the T2 phase formed an amorphous, adherent, and oxidation resistant silicate scale. However, the scale was not protective at 1500°C. Conversely, alloys with ~50%Mo (by vol.) exhibited lower weight loss when tested at 1500°C compared to tests performed at 1300°C. The oxidation behavior will be discussed in terms of the differences in microstructure for the hot-pressed, cast and heat treated specimens.

# 3:15 PM

Phase Stability and Oxidation of the T<sub>2</sub>/Mo<sub>ss</sub> Eutectic Alloy Pack-Cemented in a Si-Base Pack Mixture: Kazuhiro Ito<sup>1</sup>; Masato Yokobayashi<sup>1</sup>; Taisuke Hayashi<sup>1</sup>; Masaharu Yamaguchi<sup>1</sup>; <sup>1</sup>Kyoto University, Matls. Sci. & Engrg., Sakyo-ku, Kyoto 606-8501 Japan

The  $T_2/Mo_{ss}$  eutectic alloy in the Mo-Si-B system was pack-cemented in a Si-base pack mixture (Si:NaF:Al<sub>2</sub>O<sub>3</sub>=5:1:44(wt.%)) and its oxidation behavior was examined. The deposited layer of as-cemented substrate consists of MoSi<sub>2</sub>. Upon heating to temperatures at and above 1773K, the deposited layer is transformed into B-doped Mo<sub>5</sub>Si<sub>3</sub> through a reaction between the deposited layer and the matrix containing B. The B-doped Mo<sub>5</sub>Si<sub>3</sub> coating layer consists of columnar grains with the [001] orientation perpendicular to the coating surface. Steady-state oxidation was observed at 1573-1773K and the steady-state oxidation rates at 1573 and 1773K are almost equal to those of MoSi<sub>2</sub>. After formation of the B-doped Mo<sub>5</sub>Si<sub>3</sub> coating layer, no significant weight change was observed during 26 cycles of short-term cyclic oxidation at 1773K (1h x 26). However, the coating layer was completely oxidized after 2 cycles of long-term cyclic oxidation at 1773K (50h x 2).

# 3:30 PM Break

4:00 PM

Influence of Alloying Element on the Stability of Molybdenum Silicides: A First Principles Study: Yan Song<sup>1</sup>; Zheng Xiao Guo<sup>1</sup>; <sup>1</sup>Queen Mary, University of London, Dept. of Matls., Mile End Rd., London E1 4NS UK

Molybdenum silicides exhibit an attractive potential for structural application at elevated temperature. Mo5Si3 has a high melting point (2180°C) and excellent high temperature strength, but its high temperature oxidation resistance is very poor. Recently, B-doped Mo5Si3 has been found to have much better oxidation resistance than Mo5Si3, which attributed to the formation of the adherent and passivating borosilicate layer on the surface of the T2 phase during exposure at high temperature in air. In the present paper, first principles calculations of Mo5Si3 and Mo5SiB2 were carried out to identify the characteristics of electronic structure of these alloys. The total energy and electronic structure were calculated using a full potential linearized augmented plane wave method with the GGA approximation. Bulk modulus and theoretical strength of these alloys were estimated through the calculation of the total energy. The influence of alloying element on the stability of molybdenum silicides was discussed based on the electronic structures.

# 4:15 PM

Alloy Design and Solidification Microstructures for Mo-Si-B Alloys: *Ridwan Sakidja*<sup>1</sup>; Jeff Werner<sup>1</sup>; Sungtae Kim<sup>1</sup>; John H. Perepezko<sup>1</sup>; <sup>1</sup>University of Wisconsin, Dept. of Matls. Sci. & Engrg., 1509 Univ. Ave., Madison, WI 53706 USA

Alloys in the Mo-Si-B system are attractive as high temperature structural materials. In the current study, the effect of transition metal additions (Group IV-VII B elements) on the phase stability in the

ternary system and the solidification microstructures has been examined. The Mo<sub>3</sub>Si (A15) phase has limited soubility with most of transition metals which accordingly limits the extension of the BCC+A15 two-phase field in the ternary and higher order systems. In contrast, with most of the transition metals examined the borosilicide ternary-based T<sub>2</sub> phase shows almost a complete solid solution extension. The critical factor for the phase stability appears to be the existence of a unique feature of BCC-like transition metal arrangements within the T<sub>2</sub> lattice. The stability of the BCC+T<sub>2</sub> two-phase field consequently facilitates a variety of new high-temperature solidification microstructures in combinations of other silicide phases. The support of AFOSR (F49620-03-1-0033) is gratefully acknowledged.

#### 4:30 PM

Phase Equilibria in the Mo-Si-Ti System: Experimental Measurements and Thermodynamic Modeling: *Ying Yang*<sup>1</sup>; Y. A. Chang<sup>1</sup>; <sup>1</sup>University of Wisconsin, Matls. Sci. & Engrg., 1509 Univ. Ave., Madison, WI 53706 USA

Microstructures and phase equilibria of the alloys in the Mo-Si-Ti system were studied in as-cast and long-term annealed conditions by imaging with back scattered electrons (BSE) in a scanning electron microscope (SEM), electron probe microanalysis (EPMA) and X-ray diffraction (XRD) analysis. Isothermal sections were established to describe the solid state phase equilibria at 1600 and 1425°C. Using the CALPHAD (CALculation of PHAse Diagram) approach, a thermodynamic data set of the Mo-Si-Ti system was optimized by considering both the present experimental results and reliable literature data. This thermodynamic modeling can satisfactorily account for the available experimental data. The liquidus surface near the metal-rich end of the Mo-Si-Ti system calculated from the present thermodynamic modeling is in good agreement with experimental observation. Two type-II invariant four-phase reactions were determined in the metal-rich region of the Mo-Si-Ti system. One is L + Mo(Ti)5Si3® Ti(Mo)5Si3 + Mo(Ti)3Si, and the other is L + Mo(Ti)3Si - Ti(Mo)5Si3 + ?(Mo,Si,Ti).

#### 4:45 PM

An Experimental Study of Alloying Behaviour in the Mo-Si-Al System: Aris Arvanitis<sup>1</sup>; Spyros Diplas<sup>1</sup>; *Panayiotis Tsakiropoulos*<sup>1</sup>; Mark Whiting<sup>1</sup>; <sup>1</sup>University of Surrey, Sch. of Engrg., Mech. & Aeros. Engrg., Metall. Rsch. Grp., Guildford, Surrey GU2 7XH England

High energy X-ray photoelectron spectroscopy was used to measure the Auger parameters and plasmon loss structures of Mo, Si and Al in MoSi2 and MoSi2 + xAl (x=10 to 40 at% Al) alloys, where the microstructure changes from C11b to C40 to C54 with the Al addition. The variations of the Auger parameters and charge redistribution calculations in MoSi2 indicated a charge transfer at the Si sites very close to zero; this means that Mo and Si bond covalently, in agreement with theoretical predictions from ab-initio calculations. On introduction of Al into the MoSi2 compound there is a minor charge transfer away from the Al sites which bond strongly with Mo. The plasmon loss structures of the Si 1s and Al 1s peaks showed reduced intensity in the alloys relative to the pure metals. This is attributed to more strongly bound valence electrons. The study explains the silicon substitution by aluminium in the {110} close packed planes and the crystal structure modification from tetragonal C11b to hexagonal C40.

# **Bulk Metallic Glasses: Processing II**

Sponsored by: Structural Materials Division, ASM International: Materials Science Critical Technology Sector, SMD-Mechanical Behavior of Materials-(Jt. ASM-MSCTS)

*Program Organizers:* Peter K. Liaw, University of Tennessee, Department of Materials Science and Engineering, Knoxville, TN 37996-2200 USA; Raymond A. Buchanan, University of Tennessee, Department of Materials Science and Engineering, Knoxville, TN 37996-2200 USA

Monday PM	Room: 2	09A
March 15, 2004	Location:	Charlotte Convention Center

Session Chairs: Peter K. Liaw, University of Tennessee, Matls. Sci. & Engrg., Knoxville, TN 37996-2200 USA; Takeshi Egami, University of Tennessee, Matls. Sci. & Engrg., Knoxville, TN 37996-2200 USA

#### 2:00 PM Invited

Recent Progress in Bulk Glassy Alloys in Late Transition Metal Base Systems: Akihisa Inoue<sup>1</sup>; <sup>1</sup>Tohoku University, Inst. for Matls. Rsch., Sendai 980-8577 Japan

Since 1988, a number of bulk glassy alloys in Mg-, Zr-, Ti-, Hf- and lanthanide metal-based systems have been developed. However, their alloy systems had been limited to simple metal-, early transition metal-, lanthanide metal- and noble metal-based components. Very recently, we have succeeded in fabricating a number of bulk glassy alloys in late transition metal (LTM) base systems containing Fe, Co, Ni and Cu elements as a main component. These new bulk glassy alloys also satisfied the following three component rules for stabilization of supercooled liquid, i.e., (1) multi-component consisting of more than three elements, (2) atomic size mismatches above 12% among main three components, and (3) negative heats of mixing among their elements. We have also reported that the alloys with the three rules have a new liquid structure with highly dense packing, new local atomic configurations and long-range homogeneity. The new configuration is the origin for the high glass-forming ability even for the LTM base alloys. The new bulk glassy alloys can be produced by various casting processes and exhibit various useful properties, e.g., soft magnetic properties with extremely low coercive force, high permeability and low core losses, high electrical resistivity and high strength for Febased glassy alloys, high-frequency permeability, extremely high strength and high corrosion resistance for Co-based glassy alloys, high tensile strength, high corrosion resistance and high permeation ability of hydrogen for Ni-based glassy alloys, and high tensile strength, good ductility and high corrosion resistance for Cu-based glassy alloys. The Fe-based bulk glassy alloys have been commercialized as power-inductors for various portable electrical equipments and as high-strength materials for shot peening balls. In addition, when the Cu-based bulk glassy alloys include special elements such as Nb, Ta, Pd or Au leading to the deviation from the three component rules, we have found the formation of nanocrystalline and nanoquasicrystal-dispersed bulk glassy alloys with higher strength and ductility. These data indicate that the LTM base bulk glassy alloys may develop as a new type of functional materials.

#### 2:25 PM Invited

Why Certain Metallic Alloys Form Bulk Glasses: Takeshi Egami<sup>1</sup>; <sup>1</sup>University of Tennessee/ORNL, MSE/Physics, 208 S. College, Knoxville, TN 37996-1508 USA

For a long time bulk glasses were found only in complex nonmetallic solids. But now bulk metallic glasses with various compositions are formed and tested for applications. We discuss why certain alloy systems form bulk metallic glasses based uponm our elastic theory of glass formation and atomic transport in liquids. In our view glasses are formed primarily because the crystals are unstable because of elastic interactions due to the atomic size mismatch. In addition the topological and chemical complexity of certain liquid alloys results in lower viscosity and slower crystallization kinetics, allowing bulk glasses to form. Molecular dynamics simulations of model systems to support our theory will be presented.

#### 2:50 PM Invited

Formation and Properties of Iron-Based Bulk Amorphous Metals: Joseph Poon<sup>1</sup>; Gary J. Shiflet<sup>2</sup>; <sup>1</sup>University of Virginia, Physics, PO Box 400714, Charlottesville, VA 22904-4714 USA; <sup>2</sup>University of Virginia, Matls. Sci. & Engrg., Charlottesville, VA 22904-4745 USA

Bulk-solidifying iron-based metallic glasses have been synthesized and investigated as amorphous steel alloys. The design strategy of these amorphous alloy systems including their microstructures will be discussed. One type of amorphous steel alloys contains manganese and boron as the principal alloying components, another type contains manganese, molybdenum, and carbon as the principal alloying components. The tensile yield strengths and Vickers hardness of the present alloys are about two to three times those known in high-strength steels, while the elastic moduli are comparable to those reported for super austenitic steels. Some good corrosion resistance features are also observed. Devitrification studies have been performed to characterize the phase regions near the bulk glass forming compositions. The crystallized products and microstructures have been investigated in detail. The high glass formability, which correlates with the enhancement in the stability of the glassy phases, will be discussed in light of current ideas of glass formation.

#### 3:15 PM Invited

Consolidation of Blended Powders by Severe Plastic Deformation to Form Amorphous Metal Matrix Composites: K. Ted Hartwig<sup>1</sup>; Ibrahim Karaman<sup>1</sup>; Suveen N. Mathaudhu<sup>1</sup>; <sup>1</sup>Texas A&M University, Mech. Engrg., 319 Engr. Phys. Bldg., College Station, TX 77845-3123 USA

Because bulk amorphous metal can fail by shear localization, it is a potential environmentally friendly substitute material for depleted uranium in kinetic energy penetrators (KEPs). However, a deficiency of bulk amorphous metal alloys for the KEP application is their low density. The purpose of the work reported here is to fabricate a dense amorphous metal matrix composite. Warm equal channel angular extrusion (ECAE) was used to consolidate blended powders of amorphous Vitreloy 106a (Zr58.5Cu15.6Ni12.8A110.3Nb2.8) and crystalline tungsten. Severe plastic deformation processing was performed at temperatures above the Tg (400C) but below the Tx (465C) of the V106a. The effects of tungsten volume fraction, extrusion temperature, number of extrusion passes were investigated by metallographic examination, DSC, XRD, hardness and mechanical testing. Results show good infiltration of the amorphous phase in between W particles, retention of amorphous character in the glassy phase and substantial W-Vit106a interphase bond strength. Experimental results are presented which indicate that ECAE is a viable process for the preparation of bulk amorphous metal matrix composites from particulate precursors.

#### 3:40 PM

**Formation of Metallic Glassy Ingots Based on Yttrium**: *Faqiang Guo*<sup>1</sup>; Joseph Poon<sup>1</sup>; Gary J. Shiflet<sup>2</sup>; <sup>1</sup>University of Virginia, Dept. of Physics, Charlottesville, VA 22903 USA; <sup>2</sup>University of Virginia, Dept. of Matls. Sci. & Engrg., Charlottesville, VA 22903 USA

We report a family of yttrium metallic alloys that are able to form glassy ingots directly from the liquid, as well as forming bulk-sized amorphous rods with diameters over 2 cm by water cooling of the alloy melt sealed in quartz tubes. It is apparent that, in addition to the strong chemical interaction among the components, the simultaneous occurrence of well-distributed atom sizes and a strongly depressed liquidus temperature in multicomponent metallic alloys is responsible for the formation of glassy ingots.

# 4:05 PM Invited

**Glass Forming Ranges of Al-Fe(Ni)-Gd(Y): Thermodynamic Analysis**: *Aiwu Zhu*<sup>1</sup>; Gary J. Shiflet<sup>1</sup>; <sup>1</sup>University of Virginia, Matls. Scis., 116 Engineer's Way, Charlottesville, VA 22904 USA

Based on CALPHAD models of Al-Fe-Gd, Al-Ni-Gd and Al-Ni-Y alloys, this work reports a thermodynamic analysis of the chemical short range order (CSRO) of the undercooled liquid employing a quasichemical approximation. The driving forces and associated kinetics are calculated for the polymorphous transformation to crystals and for the primary crystallization of the relevant FCC and inter-metallic phases from the undercooled liquid.

#### 4:30 PM Cancelled

Amorphous Alloys by Cold Rolling

#### 4:55 PM

Bulk Glass Formation in Cu-Ti-Zr-(Ag,Ni) Alloys: E. S. Park<sup>1</sup>; H. J. Chang<sup>1</sup>; W. T. Kim<sup>2</sup>; D. H. Kim<sup>1</sup>; <sup>1</sup>Yonsei University, Dept. of Metallurgl. Engrg., Ctr. for Non-Crystalline Matls., 134 Shinchon-Dong, Seodaemun-gu, Seoul 120-749 Korea; <sup>2</sup>Chongju University, Dept. of Physics, Chongju 360-764 Korea

In the present study, Cu-based bulk amorphous alloys were developed through a systematic alloy design in the alloy system Cu-Ti-Zr. TEM analysis indicated that the as-melt-spun microstructure of the ternary Cu60Ti40-xZrx (x=0, 10, 20) alloys consisted of a nanocrystalline phase embedded in an amorphous matrix. Based on the results from the ternary alloys, effect of the addition of the fourth alloying elements on the glass forming ability was investigated. Partial replacements of Cu by Ag or Ni significantly improved the glass forming ability. For example, a fully amorphous Cu45Ti10Zr30Ag15 alloy rod of 5 mm in diameter was fabricated by an injection casting method. To illustrate the improved glass forming ability, the crystallization behaviors of the ternary and quaternary alloys were examined in detail by XRD, TEM and DSC analyses.

#### 5:20 PM Invited

Carbon-Nanotube-Reinforced Zr-Based Bulk Metallic Glass Composites and Their Properties: *Wei Hua Wang*<sup>1</sup>; Zan Bian<sup>1</sup>; Ru Ju Wang<sup>1</sup>; M. X. Pan<sup>1</sup>; D. Q. Zhao<sup>1</sup>; <sup>1</sup>Chinese Academy of Science, Inst. of Physics, Beijing 100080 China

We report the preparation of Carbon-nano tube (CNT)-reinforced Zr-based BMG composites. Physical properties and mechanical properties of the composites were investigated. Compressive testing shows that the composites still display high fracture strength. Investigation also shows that the composites have strong ultrasonic attenuation characteristics and excellent wave absorption ability. The strong wave absorption ability implies that CNT-reinforced Zr-based BMG composites, besides their excellent mechanical properties, may also have significant potential of application in shielding acoustic sound or environmental noise.

# Carbon Technology: Anode Raw Materials

Sponsored by: Light Metals Division, LMD-Aluminum Committee Program Organizers: Markus Meier, R&D Carbon, Sierre CH 3960 Switzerland; Amir A. Mirchi, Alcan Inc., Arvida Research and Development Centre, Jonquiere, QC G7S 4K8 Canada; Alton T. Tabereaux, Alcoa Inc., Process Technology, Muscle Shoals, AL 35661 USA

Monday PM	Room: 2	13A
March 15, 2004	Location:	Charlotte Convention Center

Session Chair: Todd W. Dixon, Conocophillips, Lake Charles Calcining Plant, Lake Charles, LA 70602-3187 USA

# 2:00 PM

Performance of Blended and Unblended Green Cokes During Calcination: Ravindra Narayan Narvekar<sup>1</sup>; Ajit Sambhaji Sardesai<sup>1</sup>; <sup>1</sup>Goa Carbon Limited, Production, St. Jose De Areal, Margao, Goa 403709 India

As anode grade green cokes get scarcer in quantity and inferior in quality, calciners are finding it necessary to blend two or more cokes to obtain specifications desired by end-users, particularly aluminium smelters. Ideally green cokes should be calcined singly, as the operating parameters need to be changed in keeping with the characteristics of each quality of green coke, particularly volatile matter, density and granulometry. Pre-calcination blending is generally preferred to post calcination blending, supposedly for the homogeneity of the product. We decided to compare, ascertain and establish the performances of individual green cokes as against blends of the same cokes during calcination. GCL conducted trials for six cokes individually as well as with their blends under similar operating conditions. The properties of the calcined cokes resulting from using a blend were compared with those calcined individually.

#### 2:25 PM

A Preview of Anode Coke Quality in 2007: *Franz Vogt*<sup>1</sup>; Robert T. Tonti<sup>1</sup>; Maia Hunt<sup>1</sup>; Les Edwards<sup>1</sup>; <sup>1</sup>CII Carbon, L.L.C., 1615 E. Judge Perez Dr., PO Box 1306, Chalmette, LA 70044 USA

Demand for petroleum coke for aluminum smelting anodes has reached about 10.4 million metric tons in 2003. This has created a coke calciner demand of 13.8 million metric tons of green coke suitable for making anodes. The green coke demand will increase to about 16.5 million metric tons by 2007. Although the oil refining industry will produce ample green coke to meet this demand, the quality will be quite different from that used in the past. During the last few years, the calcining industry has started using green cokes of a quality that would not have been considered suitable for anode use ten years ago. This paper surveys the available quality of green cokes worldwide, and makes projections on the quality of anode coke by 2007. The calcined coke of the future will be higher in sulphur and vanadium, higher in porosity and more isotropic. The change in structure could eventually lead to higher thermal shock sensitivity of anodes. Smelters will need to adapt by making process changes and improvements.

#### 2:50 PM

Characterization of the Surface Properties of Anode Raw Materials: Angelique N. Adams<sup>1</sup>; Harold H. Schobert<sup>2</sup>; <sup>1</sup>Alcoa Technical Center, Hall Process Improvement, 100 Technical Dr., Alcoa Ctr., PA 15069 USA; <sup>2</sup>The Energy Institute, C211 Coal Utilization Bldg., Univ. Park, PA 16802 USA

The interaction between filler and binder in anode green mix is of significant importance to anode properties. A better understanding of the physical and chemical interactions taking place during mixing could facilitate raw materials and processing decisions that improve anode properties. The aim of this work was to characterize the surface properties of anode raw materials and relate them to pitch penetration behavior. The type and quantity of oxygen functional groups on the surface, and the estimated surface tension, of petroleum coke and recycled anode butt material were determined using selective neutralization and film flotation techniques. The extent of pitch penetration into these materials was evaluated by image analysis of green mix from bench-scale electrodes and thermal analysis of pitch penetrated particles. The results indicate that pitch penetration is affected by the extent of oxidation of the surface of filler materials and the presence of bath constituents.

# 3:15 PM

Anthracene Oil Synthetic Pitch: A Novel Approach to Hybrid Pitches: Juan Jose Fernandez<sup>1</sup>; Francisco Alonso<sup>1</sup>; <sup>1</sup>Industrial Quimica del Nalon, S.A., R&D, Avda. Galicia, 31 bajo, Oviedo, Asturias E-33005 Spain

Because of the coal tar supply shortage, the pitch market is becoming very tight due to an increasing demand powered by the aluminum industry. Anthracene oil is the heaviest fraction coming from coal tar distillation with a quality consistency and known chemical composition (metal and QI free), guaranteed by the distilling technology applied on its production. The primary anthracene oil major application is carbon black feedstock. The high aromatic content suggests the potential for other end uses with a higher added value. This paper reports Industrial Quimica del Nalon pilot plant experience in the manufacture of synthetic pitches from anthracene oil. Pitches so obtained shows excellent rheological and wetting properties with minimized environmental and health impact because of its low PAHs concentration and reduced volatility.

#### 3:40 PM Break

# 3:50 PM

Hydrogen Transfer During Carbonization of Binder Pitches: Stian Madshus<sup>1</sup>; Trygve Foosnaes<sup>1</sup>; Margaret M. Hyland<sup>2</sup>; Harald Øye<sup>1</sup>; <sup>1</sup>Norwegian University of Science and Technology, Dept. of Matls. Tech., Sem Saelands v 12, Trondheim 7491 Norway; <sup>2</sup>University of Auckland, Sch. of Engrg., Private Bag 92019, Auckland 1 New Zealand

The hydrogen transfer properties of five coal-tar pitches and four petroleum pitches have been estimated from their ability to donate hydrogen (HDa) to anthracene and abstract hydrogen (HAa) from tetralin at 400°C. The ratio of hydrogen donor ability to acceptor ability, HDa/HAa, was used as a parameter to describe the hydrogen transfer properties of the pitch. A correlation between this parameter and the percentage of volatile matter released during the critical stages of carbonization was found for the coal-tar pitches. The texture of cokes obtained from carbonization of pitches to 600°C, was studied by cross-polarized light microscopy using an automatic computerized image analysis method. Cokes were further carbonized to 1050°C and analyzed by X-ray diffraction. The hydrogen transfer properties could partly explain the development of optical texture and microstructure in the pitch coke. The QI content of the coal-tar pitches was found to influence the pitch coke structure to a significant extent, reducing the size of the optical domains and lowering the optical domain anisotropy.

# Cast Shop Technology: Modeling of Casting Processes

Sponsored by: Light Metals Division, LMD-Aluminum Committee Program Organizers: Corleen Chesonis, Alcoa Inc., Alcoa Technical Center, Alcoa Center, PA 15069 USA; Jean-Pierre Martin, Aluminum Technologies Centre, c/o Industrial Materials Institute, Boucherville, QC J4B 6Y4 Canada; Alton T. Tabereaux, Alcoa Inc., Process Technology, Muscle Shoals, AL 35661 USA

Monday PM	Room:	213B/C		
March 15, 2004	Location	: Charlotte	Convention	Center

Session Chairs: Brian G. Thomas, University of Illinois, Mech. & Industrial Engrg. Dept., Urbana, IL 61801 USA; Steve L. Cockcroft, University of British Columbia, Dept. of Metals & Matls. Engrg., Vancouver, BC V6T 1Z4 Canada

#### 2:00 PM

Temperature Measurements and Modeling of Heat Losses in Molten Metal Distribution Systems: Jonny Kastebo<sup>1</sup>; Torbjörn Carlberg<sup>1</sup>; <sup>1</sup>Mid Sweden University, Engrg., Physics & Math., Holmgatan 10, Sundsvall 85170 Sweden

During casting of aluminium ingots the molten metal have to be transported from the furnace to the moulds. During the transport heat is lost both to the atmosphere and to the refractory launder system itself. As different dimensions of the cast ingots necessitate different design of the system the difference between the furnace temperature and the temperature in the metal, which enters the mould, can vary significantly. It is therefore of importance to have a good knowledge of the heat fluxes in the launder system and of how the temperature decreases during metal flow. In this work thorough measurements of the temperature have been made in casting tables of different design during casting of different ingot dimensions. Based on the experimental results an analytic model has been derived. Good correlation between calculated and measured temperature losses was obtained.

#### 2:25 PM

FEM Modeling of the Compressibility of Partially Solidified Al-Cu Alloys: Comparison with a Drained Compression Test: J.-M. Drezet<sup>1</sup>; O. Ludwig<sup>2</sup>; C. Martin<sup>2</sup>; M. M'Hamdi<sup>3</sup>; H.-G. Fjaer<sup>4</sup>; <sup>1</sup>Ecole Polytechnique Federale de Lausanne, LSMX, CH-1015 Lausanne Switzerland; <sup>2</sup>Institut National Polytechnique de Grenoble, GPM2, F-38402 Saint Martin d'Heres France; <sup>3</sup>Sintef, N-0314 Oslo Norway; <sup>4</sup>Institute for Energy Technology, PO Box 40, N-2027 Kjeller, Oslo Norway

In order to tackle the problem of hot tearing in aluminium alloys, a good description of the rheological behaviour of the mushy zone is a prerequisite. Although rheological testing of partially solidified aluminium alloys presents some large difficulties, three different tests, corresponding to three different types of stress state, tension, shear and compression, were used to determine a new rheological model. This model is a compressible constitutive model, it uses two internal variables and it was implemented in both Abaqus and Tearsim2D. In this paper, attention is given to the drained compression (oedometric) test, for which an analytical solution of the stress development and of the evolution of the two internal variables exists. The results obtained by Abaqus and Tearsim2D are compared to the experimental results and validated against the analytical solution. Finally, the influence of the liquid pressure is discussed. This particular study was carried out within the framework of the VIR[CAST] project in which a general thermo-mechanical model is built in order to predict hot tearing in DC cast billets or slabs.

# 2:50 PM

**Mathematical Modeling of Ingot Caster Filling Systems**: John F. Grandfield<sup>1</sup>; Paul J. Cleary<sup>2</sup>; Mahesh Prakash<sup>2</sup>; M. Sinnott<sup>2</sup>; K. Oswald<sup>3</sup>; V. Nguyen<sup>1</sup>; <sup>1</sup>CAST, CSIRO Mfg. Sci. & Tech., cnr Albert & Raglan Sts., Preston, Vic. 3072 Australia; <sup>2</sup>CRC for Cast Metals Manufacturing (CAST), CSIRO Math. & Info. Sci., Clayton, Vic Australia; <sup>3</sup>o.d.t. Engineering, Dandenong, Victoria Australia

Operators of chain conveyor ingot casters are interested in reducing dross generated during filling. This problem becomes more acute when steps are taken to increase ingot caster production rate and filling times are reduced. Another performance measure of a filling system is the variation in ingot weight. In order to optimise the design and examine possible low dross generating designs for ingot casting machines, mathematical models of the existing pouring wheel filling system were developed. Ingot casting machine filling systems present challenges to conventional flow modelling packages. Difficulties include the handling of multiple moving surfaces (fluid and solid) and prediction of oxide generation. Smooth particle hydrodynamic (SPH) modelling has a number of advantages in this regard and was applied to this problem. A new filling system design tailored to 30 tonne per hour production has been developed based on the modelling work. This design was tested on a full scale system.

#### 3:15 PM

Heat Transfer Boundary Conditions for the Numerical Simulation of the DC Casting Process: Adrian S. Sabau<sup>1</sup>; Kazunori Kuwana<sup>2</sup>; Srinath Viswanathan<sup>3</sup>; Kozo Saito<sup>2</sup>; Lee J. Davis<sup>4</sup>; <sup>1</sup>Oak Ridge National Laboratory, Metals & Ceram. Div., Bldg. 4508, MS 6083, Oak Ridge, TN 37831 USA; <sup>2</sup>University of Kentucky, Dept. of Mech. Engrg., 513 CRMS Bldg., Lexington, KY 40506-0108 USA; <sup>3</sup>Sandia National Laboratories, MS 1134, Dept. 1835, Albuquerque, NM 87185-1134 USA; <sup>4</sup>Wagstaff, Inc., 3910 N. Flora Rd., Spokane, WA 99216-1720 USA

The temperature evolution during the start-up phase of the Direct Chill (DC) casting process is critical to the prediction of strain-stress evolution during solidification. The start-up phase of DC casting is complex, as heat is extracted by the mold, starting block, and cooling water, while process parameters are ramped up to their steady state values. The modeling of DC casting involves making assumptions on the various heat transfer mechanisms, such as (a) direct contact of liquid metal-mold, (b) air gap between mold and ingot, (c) water cooling on rolling and end faces of the ingot, (d) ingot contact with the starting block, and (e) water intrusion between the starting block and ingot. The boundary conditions for the heat transfer analysis during the startup are discussed in detail. Numerical simulation results are presented for a typical casting run, including variable casting speed, metal head, and water flow rate.

# 3:40 PM Break

# 3:50 PM

Modelling of Microstructure Development During DC Casting of AA3103 Ingots - Application of Vircast Project Developments: Gerd-Ulrich Gruen<sup>1</sup>; Werner E. Droste<sup>1</sup>; <sup>1</sup>Hydro Aluminium Deutschland GmbH, R&D, Georg-von-Boeselager-Str. 21, Bonn 53117 Germany

The microstructure of DC cast ingots is influencing the following processing steps as well as the material properties of final products and cast houses are increasingly asked to deliver with tighter specifications. In order to fulfil these requirements a correct prediction of the microstructure evolution during casting is an ongoing challenge. In the European funded joint research project VIRCAST a related modelling toolset for multi-component multi-phase alloys has been developed within the last four years. During the final stage of this project this toolset has been applied to full scale DC and laboratory casting experiments of AA3103 alloys, which have been extensively monitored and where the final microstructure of the cast material has been evaluated. Within this paper calculated key microstructure parameters are compared with the related measurements and critically discussed.

#### 4:15 PM

**Prediction of Hot Tears in DC-Cast Aluminum Ingots**: Andre Phillion<sup>1</sup>; Steve Cockcroft<sup>1</sup>; <sup>1</sup>University of British Columbia, Metals & Matls. Engrg., 309-6350 Stores Rd., Vancouver, BC V6T 1Z4 Canada

Hot tearing is a major quality issue during DC casting of aluminium alloys. Often, even small cracks on the surface of the ingot will cause the ingot to be scrapped because of the potential for defects during the later stages of the process. It is well known that aluminium ingots are susceptible to cracking along the centre of the rolling face during the start-up phase or at high casting speeds. Thus, these alloys must be cast at lower speeds, reducing productivity. The present work aims to incorporate hot tearing into a thermo-mechanical finite element (FE) model of aluminium DC ingot casting. Hot tearing models proposed in literature will be implemented into an FE model and comparisons to industrial and published data will be performed. The effect of process variables, such as cast velocity and water flow-rate on hot tearing will also be discussed.

#### 4:40 PM

Numerical Simulation of DC Casting: Interpreting the Results of a Thermo-Mechanical Model: *Wim Boender*<sup>1</sup>; Jan Rabenberg<sup>1</sup>; Erik Paul van Klaveren<sup>1</sup>; André Burghardt<sup>1</sup>; <sup>1</sup>Corus, RD&T, PO Box 10,000, Wenckebachstraat 1, IJmuiden 1970 CA The Netherlands

A few problems impede the efficiency of DC casting. Cold cracking, which occurs when thermally induced stresses locally exceed the tensile strength, is one of these problems. Especially, hard alloys like AA2000 and AA7000 alloys are prone to cold cracking. To gain insight into the mechanical behaviour of an ingot during casting, Corus RD&T developed a thermo-mechanical model. This numerical model simulates the evolution of temperatures, stresses, and strains inside the ingot as a result of the casting parameters, the cooling conditions, and the alloy's properties. A tri-axial state of stress is shown to develop almost everywhere in the solid ingot. Interpreting these results, two approaches are reciprocally used to estimate the likelihood that a cold crack will form. In one approach, the principal stresses are assessed, yielding insight into the locations and directions of cracks. The other approach is based on energy, i.e. on the fracture toughness KIc. It provides insight into possible ways to avoid cold cracks, e.g. by pointing out that internal defects, like inclusions or pores, should be smaller than the critical crack length. The findings will be illustrated with results for the DC casting of an Al - 4.5% Cu alloy.

#### 5:05 PM

Application of Mathematical Models to Optimization of Cast Start Practice for DC Cast Extrusion Billets: J. F. Grandfield<sup>1</sup>; L. Wang<sup>1</sup>; <sup>1</sup>CRC for Cast Metals Manufacturing (CAST), CSIRO Mfg. & Infrastructure Tech., Preston, Victoria Australia

Producers of DC casting billets are interested in reducing scrap caused by hot tearing at the start of casting. This is the subject of large ongoing research programs within the industry. Using a relatively simple thermal model, predictions of pool depth versus cast length are made. Results compare favorably with published pool depth data. We illustrate how a such a model and current know-how could be applied to improve the cast start practice in terms of starting speed and ramp-up or dome height for a given alloy and product diameter in order to reduce cracking tendency. This type of model can be also used to examine the effect of other cast start variables such as dummy design, fill time and hold time.

# CFD Modeling and Simulation of Engineering Processes: Remelt Processes

Sponsored by: Materials Processing & Manufacturing Division, ASM/MSCTS-Materials & Processing, MPMD/EPD-Process Modeling Analysis & Control Committee, MPMD-Solidification Committee, MPMD-Computational Materials Science & Engineering-(Jt. ASM-MSCTS)

*Program Organizers:* Laurentiu Nastac, Concurrent Technologies Corporation, Pittsburgh, PA 15219-1819 USA; Shekhar Bhansali, University of South Florida, Electrical Engineering, Tampa, FL 33620 USA; Adrian Vasile Catalina, BAE Systems, SD46 NASA-MSFC, Huntsville, AL 35812 USA

Monday PM	Room: 206A
March 15, 2004	Location: Charlotte Convention Center

*Session Chairs:* Ramesh S. Minisandram, Allvac, Monroe, NC 28111 USA; Srinath Viswanathan, Sandia National Laboratories, Albuquerque, NM 87185-1134 USA; Ashish D. Patel, Carpenter Technology Corporation, Reading, PA 19601 USA

#### 2:00 PM Opening Remarks - Ramesh Minisandram

#### 2:05 PM Invited

The Effect of Electromagnetic Stirring on the Turbulent Flow of Liquid Metal in a Vacuum Arc Remelted Ingot: *Alain Jardy*<sup>1</sup>; Thibaut Quatravaux<sup>1</sup>; Denis Ablitzer<sup>1</sup>; <sup>1</sup>Ecole des Mines de Nancy, LSG2M - UMR 7584, Parc de Saurupt, Nancy Cedex 54042 France

A numerical model of the Vacuum Arc Remelting process has been developed and applied to simulate remelting of various metallic materials, such as specialty steels, titanium, nickel-based superalloys and zirconium alloys. In practice, electromagnetic stirring is sometimes used, resulting in a complex 3D molten metal flow. After having validated the numerical model for different remelting conditions, we can use it to study the effect of applying a continuous or alternated magnetic field on the thermohydrodynamic behaviour of the melt pool, as well as dispersion of inclusions in the bath. The intensity of flow turbulence, computed with a classical k-epsilon model, is shown to depend strongly on the nature of electromagnetic stirring.

#### 2:40 PM

Modelling the Electroslag Remelting of Ni-8 Cr-25 Mo Alloy: Shawn A. Cefalu<sup>1</sup>; Kent J. VanEvery<sup>1</sup>; Matthew J.M. Krane<sup>1</sup>; <sup>1</sup>Purdue University, Sch. of Matls. Engrg., 501 Northwestern Ave., W. Lafayette, IN 47907 USA

Segregation during electroslag remelting (ESR) of a nickel-chromium-molybdenum alloy (Ni-8 wt% Cr-25 wt% Mo) has been modeled. Features of the model include species transport, AC electromagnetic effects and an adapting grid coupled with fluid flow, heat transfer, and solidification. The effect of varying processing conditions, including power, ingot diameter and slag thickness, on macrosegregation patterns, local solidification time, local phase fractions, and liquid pool profiles obtained from this model are demonstrated.

#### 3:10 PM Invited

Computational Analysis of Metal Spray in the Nucleated Casting Process: Kanchan M. Kelkar<sup>1</sup>; Ramesh S. Minisandram<sup>2</sup>; Suhas V. Patankar<sup>1</sup>; Robin M. Forbes Jones<sup>2</sup>; William T. Carter<sup>3</sup>; <sup>1</sup>Innovative Research Inc., 3025 Harbor Ln. N., Ste. 300, Plymouth, MN 55447 USA; <sup>2</sup>Allvac An Allegheny Technologies Company, R&D, 2020 Ashcraft Ave., PO Box 5030, Monroe, NC 28110 USA; <sup>3</sup>GE Corporate R&D, Schenectady, NY 12301 USA

The nucleated casting process currently under development has the potential for production of Ni-based superalloy preforms with microstructure that is superior to product made by conventional casting processes. In this process, electroslag remelted (ESR) clean molten metal is conveyed via a water-cooled copper Cold-walled Induction Guide (CIG) to a gas atomizer. The spray of clean metal is then directly cast into a water-cooled crucible for ingot production. The microstructure of the resulting ingot preform is a function of the thermal state of the incoming metal droplets. This, in turn, depends on particle size, flight time and heat exchange with the gas phase. In the present study, a computational model is developed for the analysis of the flow and heat transfer processes in gas-metal spray system under axisymmetric and steady-state conditions. The gas-phase flow is analyzed using an Eulerian framework and turbulent mixing within the gas phase is modeled using the two-equation k-e model. The dynamics of the metal particles is analyzed using a Lagrangian framework which

involves calculation of the trajectories of the metal droplets. Thus, the motion of the metal droplets is influenced by the fluid drag and the heat transfer from the metal particles is governed by convective and radiative cooling at the surface of the particles. A two-way coupling is considered whereby the flow and heat transfer in the gas phase is also influenced by the drag induced by and heat transfer from the metal droplets. The model enables prediction of the profiles of mass and enthalpy fluxes and the liquid fraction of the metal spray at the ingot surface. The paper demonstrates how such a model is useful for both process design & optimization.

3:40 PM Break

# 4:00 PM Invited

**CFD Modeling and Simulation Applications for PAM-Assisted Casting of Ti-6Al-4V Ingots and Slabs**: *Laurentiu Nastac*<sup>1</sup>; Frank Spadafora<sup>2</sup>; Ernie M. Crist<sup>2</sup>; <sup>1</sup>Concurrent Technologies Corporation, Product & Process Analysis, 425 6th Ave., Regional Enterprise Tower, 28th Floor, Pittsburgh, PA 15219 USA; <sup>2</sup>RMI Titanium Company, 1000 Warren Ave., Niles, OH 44446 USA

This paper describes the modeling techniques and the experimental and computer results for two casting processes that are under development and optimization. These processes are described as follows: 1) Electromagnetic stirring (EMS) during casting of Ti-6Al-4V round ingots using the plasma arc cold hearth melting (PAM) process: The purpose of EMS is to establish a single-melt PAM process capable of consistently producing as-cast ingots without helium porosity and also having no need for surface conditioning prior to secondary processing. The modeling approach is based on the numerical solution of Maxwell's equations, fluid flow, and heat transfer equations, and mesoscopic modeling of the grain structure. 2) Casting of Ti-6Al-4V slabs using the single-melt PAM process: The purpose of slab casting is to eliminate an intermediate blooming step for converting round ingots for yield increase. The modeling approach is based on the numerical solution of fluid flow and heat transfer equations. The effects of pouring and mold temperatures on the pool and temperature profiles were studied. Also, the torch effects (such as the torch standoff and its traversing path) on the pool and temperature profiles were investigated and the best-case scenario was used in the experiments. Evaluation results at RMI showed that the plates made from the slabs met the mechanical properties and microstructure requirements. Acknowledgment. This work was conducted by the National Center for Excellence in Metalworking Technology (NCEMT) operated by Concurrent Technologies Corporation (CTC) under contract No. N00014-00-C-0544 to the U.S. Navy as part of the U.S. Navy Manufacturing Technology Program. E. J. Fasiska, F. R. Dax, Y. Pang, and D. Winterscheidt from CTC and K. O. Yu from RMI are acknowledged for their contribution to this work.

#### 4:30 PM

**Modeling of Vacuum Arc Remelting Process**: Ashish D. Patel<sup>1</sup>; Ramesh S. Minisandram<sup>2</sup>; <sup>1</sup>Carpenter Technology Corporation, 101 W. Bern St., Reading, PA 19601 USA; <sup>2</sup>Allvac, 2020 Ashcraft Ave., Monroe, NC 28111 USA

Vacuum Arc Remelting (VAR) is the final, and hence very critical, melting step for the production of a sound segregation fee ingot. The Specialty Metal Processing Consortium (SMPC) has developed a mathematical model for the VAR process. The model predicts the temperature distribution in the solidifying ingot, the flow in the molten metal pool and the electromagnetic field in the ingot. These predictions are used to estimate key solidification parameters, which dictate the likely hood of defect formation. In this talk, typical simulation results from different stages of VAR for both Nickel base superalloys and Titanium alloys will be presented and differences in the melt cycles for these alloys will be highlighted. The effect of pool profile on melting parameters will also be presented.

#### 5:00 PM

Modeling of Single-Roll Strip Casting of an Aluminum Alloy: Correlation of Strip Thickness, Solidification Zone Length and Puddle Shape: Suyitno<sup>1</sup>; E. N. Straatsma<sup>1</sup>; L. Katgerman<sup>1</sup>; <sup>1</sup>Delft University of Technology, Lab. of Matls., Rotterdamseweg 137, Delft 2628 AL The Netherlands

Single-roll strip casting process is studied using computational fluid dynamics which takes into account fluid flow, heat transfer and solidification. The computational model is based on the conservation laws of momentum, energy and continuity. Correlation of strip thickness, solidification zone length, and puddle shape on single-roll strip casting of AA3004 is explored. Some parameters: feeding pressure, roll speed, melt temperature, slit breadth and heat transfer in the contact surface are investigated. The strip thickness slightly increases with pressure, similarly the length of solidification zone. The variations of strip thickness and solidification zone length with roll speed show a sharp decline for strip thickness and slight decline for the length of solidification zone with increasing roll speed. The other parameters show a minor effect on the strip thickness and solidification zone length. Severe turbulence is observed on the free-jet flow.

# Challenges in Advanced Thin Films: Microstructures, Interfaces, and Reactions: Microstructures, Properties, and Reliability of Microelectronic Devices

Sponsored by: Electronic, Magnetic & Photonic Materials Division, EMPMD-Thin Films & Interfaces Committee *Program Organizers:* N. M. (Ravi) Ravindra, New Jersey Institute of Technology, Department of Physics, Newark, NJ 07102 USA; Seung H. Kang, Agere Systems, Device and Module R&D, Allentown, PA 18109 USA; Choong-Un Kim, University of Texas, Materials Science and Engineering, Arlington, TX 76019 USA; Jud Ready, Georgia Tech Research Institute - EOEML, Atlanta, GA 30332-0826 USA; Anis Zribi, General Electric Global Research Center, Niskayuna, NY 12309 USA

Monday PM	Room: 21	18B
March 15, 2004	Location:	Charlotte Convention Center

Session Chairs: Seung H. Kang, Agere Systems, IC Device Tech., Allentown, PA 18109 USA; Choong-Un Kim, University of Texas, Matls. Sci. & Engrg, Arlington, TX 76109 USA; David P. Field, Washington State University, Sch. of Mech. & Matls. Engrg., Pullman, WA 76019 USA

#### 2:00 PM Invited

Growth and Characterization of Si/SiGe Epitaxial Layers for Heterojunction FET Applications: *Douglas A. Webb*<sup>1</sup>; <sup>1</sup>ATMI, Epitaxial Services, 550 W. Juanita Ave., Mesa, AZ 85210 USA

Strained silicon, and silicon-germanium, epitaxial layer structures on silicon substrates have attracted considerable interest due to substantial carrier mobility enhancements that have been observed in field-effect transistors. Several companies have publicly announced plans for incorporating such "strained silicon" technology in advanced CMOS devices. There are a number of materials challenges that must be addressed with this technology. Using LPCVD, we have demonstrated threading dislocation densities of < 1E05/cm2, and surface roughness of ~1 nm for strained silicon on relaxed, compositionally graded Si0.8Ge0.2 "virtual substrates." X-ray diffraction analysis of these films indicates that the SiGe layer is fully relaxed, and is tilted slightly from the substrate. The evolution of surface roughness during the growth of the relaxed SiGe virtual substrate has been evaluated by atomic-force microscopy. It is found that roughness of graded layers increases significantly at compositions greater than ~5 atomic percent germanium. The resulting surface texture may complicate lithographic patterning and other fab processes. It may also contribute to inhomogeneities in the strain of subsequently grown silicon and silicon-germanium layers. Silicon layers grown on the relaxed SiGe layers were characterized by x-ray diffraction and Raman spectroscopy. The results indicate that the silicon growth is fully pseudomorphic. Layers grown beyond the critical thickness for formation of misfit dislocations still exhibit substantial residual strain.

#### 2:25 PM

Advanced Materials and Processes for Sub-100 nm Metallizations: Daniel Josell<sup>1</sup>; Thomas P. Moffat<sup>1</sup>; Daniel Wheeler<sup>1</sup>; <sup>1</sup>NIST, Metall. Div., MS 8555, 100 Bureau Dr., Gaithersburg, MD 20899 USA

I will discuss several advances in metallizations for integrated circuits. These include new processes for superconformal deposition of copper, now the standard for high conductivity, high-speed metallizations. Advanced fabrication processes will also be presented for superconformal deposition of silver, the only metal with a higher bulk electrical conductivity than copper. The use of ruthenium barriers for "seedless" copper feature filling will also be presented. The Curvature Enhanced Accelerator Coverage mechanism behind the superconformal, bottom-up "superfilling" will be summarized.

#### 2:40 PM

Oxidation Characteristics of Si by Using High-Concentration Ozone: Kunihiko Koike<sup>1</sup>; Koichi Izumi<sup>1</sup>; Akira Kurokawa<sup>2</sup>; Shingo Ichimura<sup>2</sup>; <sup>1</sup>Iwatani International Corporation, 4-5-1 Katsube, Moriyama, Shiga 524-0041 Japan; <sup>2</sup>National Institute of Advanced Industrial Science and Technology, 1-1-4 Umezono, Tsukuba, Ibaraki 305-8568 Japan

We investigated ozone oxidation characteristics on Si substrate with high-concentration (>20vol%) ozone gas. High-concentration ozone gas was supplied by a specially designed ozone generator system with ozone condensation unit. In the oxidation by ozone with the concentration of 25vol% under the temperature range from 340 to 625°C at 8Torr (1.1kPa), the formed oxide film thickness increased with oxidation time in accordance with parabolic laws, which suggests diffusion-controlled step. Parabolic constant at 625°C in ozone oxidation was estimated at 0.19 nm2/min. That value is smaller than 18.3 nm2/min. under the dry oxidation at 800°C, which was proposed by Deal and Grove. As we confirmed the parabolic constants were dependent on temperature, the activation energy in ozone oxidation was determined at 0.52 eV. It is also small, compared to 1.2 eV of the activation energy reported in oxidation by oxygen. Those results indicate the species of reaction in ozone oxidation is different from that in oxygen oxidation. However, the activation energy of 0.52 eV in ozone oxidation under diffusion-controlled step is almost the same as that in plasma oxidation reported previously. Judging from the comparison of activation energies, it might be said even if O(1D) or O(1S) in excited state generates in plasma state, they would convert to O(3P) in graoud state during diffusing in oxide film due to short life. We concluded that the oxidation using high-concentration ozone is in no way inferior to plasma oxidation. Moreover, the quality of ozone oxidation film was evaluated by means of estimation of amount of suboxides (Si3++Si2++Si+) using XPS analysis and compressive stress using FT-IR. The both of results showed that the quality of ozone oxide film at 500°C is equal to that of pyrogenic oxidation at 750°C.

#### 2:55 PM

Phase Stabilities in the Hf-O-Si System: Dongwon Shin<sup>1</sup>; Kyuhwan Chang<sup>2</sup>; Jerzy Ruzyllo<sup>2</sup>; Zi-Kui Liu<sup>1</sup>; <sup>1</sup>Pennsylvania State University, Dept. of Matls. Sci. & Engrg., University Park, PA 16802 USA; <sup>2</sup>Pennsylvania State University, Dept. of Elect. Engrg., University Park, PA 16802 USA

The gate oxide (SiO<sub>2</sub>) thickness in advanced complementary metaloxide semiconductor (CMOS) integrated circuits is continuously decreasing and is about to reach the level (about 1 nm) beyond which no further thinning will be possible. In order to continue growth of CMOS technology SiO<sub>2</sub> gate oxide will have to be replaced at this time with dielectric featuring dielectric constant significantly higher than 3.9. Currently, hafnium oxide and/or hafnium silicate attracts a lot of attention due to their sufficiently high dielectric constants and perceived compatibility with the Si-O system. To better control the thin film processing, the thermodynamic stability of phases in the Hf-O-Si system is investigated through the CALPHAD (CALculation PHAse Diagram) approach assisted by the first-principles calculations. The ionic model is used in the Hf-O and Si-O binary systems. Combining with the thermodynamic parameters of the Hf-Si binary system, the thermodynamic description of the ternary Hf-O-Si system is obtained, and the stability diagrams pertinent to the thin film processing are calculated.

#### 3:10 PM

The Prediction of Critical Thickness in Epitaxial Thin Films: *Joshua Robbins*<sup>2</sup>; Tariq A. Khraishi<sup>1</sup>; <sup>1</sup>University of New Mexico, Mech. Engrg. Dept., MSC01-1150, Albuquerque, NM 87131 USA; <sup>2</sup>Sandia National Laboratories, Computational Physics R&D, PO Box 5800, MS0819, Albuquerque, NM 87185-0819 USA

The current work models the strains and stresses in thin films grown by epitaxial growth processes on finite-thickness compliant substrates. It rigorously examines how these elastic fields influence the prediction of the critical film thickness. Some of the issues or parameters considered include the free surface effects, the strain partitioning model, the relative epilayer to substrate thickness, and the lattice and elastic constants. The work modifies some existing models for strain partitioning and critical thickness. Comparison between the different models is provided.

#### 3:25 PM

#### Assessment of Seal Integrity for Porous Low-k Dielectric Materials: Dongmei Meng<sup>1</sup>; Nancy L. Michael<sup>1</sup>; Choong-Un Kim<sup>1</sup>; <sup>1</sup>University of Texas, Matls. Sci. & Engrg., Arlington, TX 76019 USA

A number of processing and reliability challenges have emerged with the incorporation of ultralow dielectric constant (ULK) materials into IC metallization. In particular, the long-term reliability of Cu/ ULK is of great concern because contaminants from ambient may penetrate the open pore structure of the ULK and affect both interconnect and dielectric integrity. In attempts to protect the metallization structure, various seal strategies have been developed to close the two primary infiltration paths, cut die edges and bond pads. In this study, the effectiveness of the edge seal and bond pad structure in several ULK materials is investigated using an optical microscopy technique. Results indicate that diagnostic probing can damage the fragile structure and open the bond pad to ambient infiltration. Furthermore, the as-manufactured side seal often does not provide a complete seal or is easily compromised by thermal cycling. The data gathered in this study clearly indicate that current side seal and bond-pad structures used for ULK are inadequate to prevent contaminants from reaching Cu lines in packaged samples.

3:40 PM Break

#### 3:55 PM

Texture Investigation of Copper Interconnects With a Different Line Width: Jae-Young Cho<sup>1</sup>; Karbir Mirpuri<sup>1</sup>; Dong Nyung Lee<sup>2</sup>; Joong Kyu Ahn<sup>2</sup>; Jerzy A. Szpunar<sup>1</sup>; <sup>1</sup>McGill University, Metals & Matls. Engrg., 3610 Univ. St., Montreal, Quebec H3A 2B2 Canada; <sup>2</sup>Seoul National University, Sch. of Matls. Sci. & Engrg., Seoul 151-744 Korea

In order to understand the effect of line width on textural and microstructural evolution of Cu damascene interconnects, three Cu interconnects samples which have a different line width are investigated. According to x-ray diffraction results, (111) texture is developed in all investigated lines. Scattered {111}<112> and {111}<110> texture component are present in 0.18 ?Ým width interconnect lines, and {111}<110> texture was developed in 2?Ým width interconnect lines. The directional changes of (111) plane orientation with increase of the line width were investigated by x-ray diffraction method. In addition, microstructure and GBCD (grain boundary character distribution) of Cu interconnects were measured using OIM (orientation imaging microscopy). This measurement demonstrated that bamboo-like microstructure is developed in the narrow line and polygranular structure is developed in the wider line. The percentage of ?Ã3 boundaries is increased as the line width increases but it decreases in the blanket film. New interpretation of textural and microstructural evolution with an increase of line width in damascene interconnects lines is suggested, based on the state of stress in different interconnect lines.

#### 4:10 PM

**Grain Growth and Texture Formation in Cu Damascene Lines:** *David P. Field*<sup>1</sup>; <sup>1</sup>Washington State University, Mech. & Matls. Engrg., Box 642920, Pullman, WA 99164-2920 USA

Copper interconnect lines manufactured by the in-laid, or damascene, processing technique have been shown to result in a wide variety of microstructures. These structures necessarily affect the material performance, such as stress voiding, during further processing and ultimately control the manufacturability of the lines. This study examines the microstructures of in-laid Cu lines as a function of line width and other processing parameters. It is shown that crystallographic texture, grain size, and twin boundary fractions are all directly related to line width for fixed chemistry and barrier layers. These results are discussed from the standpoint of controlling mechanisms.

#### 4:25 PM Invited

Thermo-Mechanical Modeling of Thin Films and Metal Interconnects: Y.-L. Shen<sup>1</sup>; <sup>1</sup>University of New Mexico, Dept. of Mech. Engrg., MSC01 1150, Albuquerque, NM 87131 USA

An overview of recent advances in thermo-mechanical modeling of metal thin films and interconnects will be given. Attention is devoted to the employment of appropriate constitutive material behavior and the proper application and interpretation of numerical data. New modeling results will be presented on the copper interconnect/low-k dielectric systems. Several geometric and material parameters are investigated. The evolution of stresses and deformation pattern in the dual-damascene copper, barrier layers, the dielectrics and their interfaces is seen to have prominent influences in the structural integrity and reliability of contemporary and future-generation devices. Aside from the continuum-based modeling techniques, atomistic simulations of some fundamental mechanical features of thin films and their implications will be presented.

#### 4:50 PM

**Thermal Failure Mechanism of Cu Interconnects in Porous Dielectric**: *Nancy L. Michael*<sup>1</sup>; Dongmei Meng<sup>1</sup>; Choong-Un Kim<sup>1</sup>; <sup>1</sup>University of Texas, Matls. Sci. & Engrg., Arlington, TX 76019 USA

The integration of ultralow-k dielectrics (ULK) into IC metallization is central to continued improvement in advanced electronic device performance. Because ULK materials are highly porous, they are fundamentally different from previously used materials and bring an array of new challenges. One challenge is that with their open pore structure, ULK dielectrics provide a location for process gases to be trapped and a path for ambient to infiltrate deep into the structure and create chemical or physical instabilities. In this study, the thermal stability of Cu/ULK (k~2.2) structures is investigated using 0.25im Cu lines with several diffusion barrier arrangements. Baking tests (185°C-325°C) are conducted in both air and nitrogen ambient with intermittent resistance measurements using minimal current. Results indicate that regardless of diffusion barrier or ambient, Cu interconnects degrade and fail readily, even at the low temperatures used here. Resistance data show that the degradation process begins almost immediately and that the overall failure kinetics are dependent on the diffusion barrier. SEM and TEM images reveal that Cu has diffused through the barrier and resides in the pores of the ULK in the form of Cu2O.

# 5:05 PM Invited

Tribo-Mechanical Characterization of Interconnect Materials for Integration in Cu-Damascene Process: Ashok Kumar<sup>1</sup>; P. Zantye<sup>1</sup>; A. K. Sikder<sup>1</sup>; <sup>1</sup>University of South Florida, Dept. of Mech. Engrg., Nanomatls. & Nanomfg. Rsch. Ctr., Tampa, FL 33620 USA

Chemical mechanical planarization (CMP) has emerged as the most preferred method for achieving excellent global and local planarity and, as the feature sizes shrink, understanding the basics of CMP will be critical for successful implementation of this process in sub 0.35micron technology. Also it is important to understand the effects of mechanical and tribological properties of the interlayer coatings on the CMP process in order to successful evaluation and implementation of these materials. The constant push towards sub-micron miniaturization of device dimensions, increased density of devices, and faster processing power has led to the development of new interconnect technologies that use Copper and ultra low-k (k<2.2) polymer based dielectrics. Here we presented the polishing behavior of different interconnect materials (SiO2, SiC, low-k, Ta and Cu) and discuss the correlation of their mechanical properties with the polishing behavior. Mechanical properties were evaluated by the nanoindentation technique. A CMP tester was used to study the fundamental aspects of CMP process. The coefficient of friction (COF) and acoustic emission (AE) signals were monitored and analyzed for defect analysis, endpoint detection and online process characterization. Delamination and other defect generated during the CMP process shall also be addressed.

# Computational Thermodynamics and Phase Transformations: Interfaces and Grain Boundaries

Sponsored by: ASM International: Materials Science Critical Technology Sector, Electronic, Magnetic & Photonic Materials Division, Materials Processing & Manufacturing Division, Structural Materials Division, MPMD-Computational Materials Science & Engineering-(Jt. ASM-MSCTS), EMPMD/SMD-Chemistry & Physics of Materials Committee

Program Organizer: Jeffrey J. Hoyt, Sandia National Laboratories, Materials & Process Modeling, Albuquerque, NM 87122 USA

Monday PM	Room:	202A
March 15, 2004	Location	: Charlotte Convention Center

Session Chair: TBA

#### 2:00 PM Invited

Phase Transitions and Dynamical Behavior in Ferroelectrics by Atomic-Level Simulation: Simon Robert Phillpot<sup>1</sup>; <sup>1</sup>Argonne National Laboratory, Matls. Sci. Div., 9700 S. Cass Ave., Bldg. 212, Argonne, IL 60439 USA

We use molecular-dynamics simulation to characterize the phase transitions and dynamical behavior in perovksite ferroelectric,s such as KNbO<sub>c3></sub> and BaTio<sub>3</sub>, and in LiNbO<sub>3</sub>. We also characterize the microscopic processes that take place during polarization reversal in the tetragonal orthorhombic and rhomobohedral phases of monodomain KNbO<sub>3</sub>, an order-disorder perovskite ferroelectric. In the tetragonal phase, the polarization of each unit cell reorients from an [001] orientation to an [00] orientation through intermediate states with polarization parallel to [011] and [01]. For low electric field and low temperature, chains of polarization reverse in a spatially coherent manner, resulting in macroscopic intermediate states with orthorhombic symmetry. At high electric field and high temperature the process is completely incoherent and there is no well-defined macroscopic intermediate state.

#### 2:30 PM Invited

Vacancy Interaction With Anti-Phase Boundaries in Ni3Al: Raymond Tedstrom<sup>1</sup>; Murray Daw<sup>1</sup>; <sup>1</sup>Clemson University, Physics & Astron., Clemson, SC 29634 USA

We have investigated the interaction of a vacancy with anti-phase boundaries (APBs) in Ni3Al. The dynamics are investigated using hyperdynamics. On-the-fly kinetic Monte Carlo is accomplished using the Dimer Method to find the saddlepoints exiting a valley. Energetics are calculated with the Embedded Atom Method. The effects of stoichiometry are included through the segregation of anti-site defects to the APB. We study the binding of vacancies and the migration in and around the APB. In particular, we look for processes which can translate the APB perpendicular to itself. The authors acknowledge support from NASA (Aeropropulsion Base Research and Technology).

#### 3:00 PM

**Modelling the Solid-Liquid Interfacial Structure of Al**: James R. Morris<sup>1</sup>; Mikhail I. Mendelev<sup>2</sup>; Seungwu Han<sup>2</sup>; David J. Srolovitz<sup>2</sup>; Graeme J. Ackland<sup>3</sup>; <sup>1</sup>Metals & Ceramics Sciences, Ames Lab., Ames, IA 50011-3020 USA; <sup>2</sup>Princeton University, Dept. of Mech. & Aeros. Engrg., Princeton Matls. Inst., Princeton, NJ USA; <sup>3</sup>University of Edinburgh, Dept. of Physics & Astron., Edinburgh EH9 3JZ, Scotland UK

We have developed a new Embedded Atom-type potential for aluminum, specifically to provide good crystal, defect and liquid phase properties, including the melting temperature. We have calculated the anisotropic solid-liquid interfacial free energy for this and several other Al potentials, all of which have similar melting points. The average interfacial free energy and its anisotropy depends strongly on the potential. We compare the results to experimental values for both of these properties, including data from nucleation, grain boundary groove, and equilibrium shape measurements.

#### 3:20 PM

Phase Transformations at Interfaces in NiAl: Juan Anthony Brown<sup>1</sup>; Yuri Mishin<sup>1</sup>; <sup>1</sup>George Mason University, Sch. of Computational Scis., 4400 Univ. Dr., MSN 5C3, Fairfax, VA 22030 USA

NiAl is a technologically important material whose grain boundaries and surfaces have a significant impact on the mechanical behavior, oxidation resistance and other properties. The chemical composition and structure of these interfaces are studied depending on the bulk composition, temperature, and geometry using grand-canonical Monte Carlo methods and other simulation techniques in conjunction with embedded-atom potentials. NiAl surfaces tend to become Ni-rich by local antisite disorder. Al-terminated surfaces are unstable and are often eliminated by development of a terrace structure with stoichiometric or Ni-rich facets, or by injection of an anti-phase boundary into the bulk. Correlations are studied between the equilibrium surface structure, its orientation, energy and surface stresses. Grain boundaries in NiAl also tend to be Ni-rich. At increased bulk Ni concentration, some grain boundaries undergo structural transformations to structures containing more Ni atoms. The possible impact of these interfacial phase transformations on NiAl properties is discussed.

#### 3:40 PM Break

#### 3:50 PM Invited

Effects of Fe on Grain Boundaries in Al: *Mikhail I. Mendelev*<sup>1</sup>; Seungwu Han<sup>1</sup>; David J. Srolovitz<sup>1</sup>; James R. Morris<sup>2</sup>; Graeme J. Ackland<sup>3</sup>; <sup>1</sup>Princeton University, Dept. of Mech. & Aeros. Engrg., Princeton, NJ 08544 USA; <sup>2</sup>Ames Laboratory, A524 Physics, Ames, IA 50011-3020 USA; <sup>3</sup>University of Edinburgh, Dept. of Physics & Astron., Edinburgh, Scotland EH9 3JZ UK

Fe impurities profoundly affect the mobility of grain boundaries in Al and, hence, strongly modify microstructural evolution in Al alloys. We investigate the role of Fe impurities on grain boundary migration in Al. We develop a new set of Al-Fe interatomic potentials and use them in MD simulations to determine the most important properties that affect grain boundary migration. The interatomic potentials are of the EAM-type and are fit to a wide range of crystal, liquid and defect properties in the pure metals and Al-Fe alloys (obtained from first principles calculations and experiment). MD simulations performed with these potentials are used to determine the diffusivity of Fe in Al (bulk and grain boundary), the heat of segregation and segregation isotherms for several grain boundaries over a range of temperature. These data are used as input to predict the effect of Fe impurities on grain boundary migration in Al.

#### 4:20 PM Invited

Multi Phase Field Simulation Study of the Effect of Particle -Grain Boundary Interaction on Particle Ripening in Solids: Ingo Steinbach<sup>1</sup>; Markus Apel<sup>1</sup>; <sup>1</sup>Access e.V., Intzestr.5, Aachen 52072 Germany

Particles of secondary precipitates in a solid matrix act as pinning centres for grain boundary movement. This is well described by the Zener pinning model, which considers the reduction of grain boundary energy due to the particle-grain boundary interaction. In technical alloys this effect is used for the stabilization of grain boundary networks by particle inclusions. Dependent on the conditions during thermal treatment, however, the particle distribution and thereby the pinning effect is subjected to the effects of growth/dissolution and ripening. In this study the ripening of particles, colocated in a grain boundary network, is investigated on the lengthscale of the individual particles using the Multi Phase Field method. The particles are treated near thermodynamic equilibrium with the matrix grains. Considering distributions with particles in the bulk grain, at grain boundaries and at triple junctions the effect of particle-grain boundary interaction on the ripening behaviour of the particles is studied. Effects of grain boundary diffusion and grain boundary anisotropy are discussed shortly.

#### 4:50 PM

Stress and Capillarity Driven Grain Boundary Migration: A Molecular Dynamics Study: *Hao Zhang*<sup>1</sup>; Mikhail I. Mendelev<sup>1</sup>; David J. Srolovitz<sup>1</sup>; <sup>1</sup>Princeton University, Dept. of Mech. & Aeros. Engrg., Princeton, NJ 08540 USA

Grain boundary migration is key to a wide range of materials processing strategies. Quantitative boundary mobility data is difficult to obtain, yet important for quantitative prediction of microstructural evolution and understanding defect migration fundamentals. We present the results of a series of 3-d molecular dynamics simulations of grain boundary migration as a function of temperature and bicrystallography. In one study, stored elastic energy was used to drive the migration of nominally flat <001> tilt grain boundaries. In another, boundary migration was driven using a half-loop geometry. The boundary velocity was found to be a linear function of driving force. Simulations performed at different temperatures were used to extract the activation energy for boundary migration. Activation energies obtained in both studies were in reasonable agreement, yet are substantially smaller than found in experiment. These data are used to analyze whether boundary mobilities depend on the nature of the driving force.

# 5:10 PM

A Study of Horns in Diffusion Paths: *Hongwei Yang*<sup>1</sup>; <sup>1</sup>University of Connecticut, Dept. of Metall. & Matls. Engrg., 97 N. Eagleville Rd., Unit 3136, Storrs, CT 06269 USA

Interdiffusion behavior of diffusion couple in the ?×+?Ò region of the Al-Cr-Ni system at 1200°C is simulated by DICTRA software which uses the finite difference method. DICTRA simulations show sharp deviation from linear zigzag behavior in the diffusion path. The deviation appears i§horns" pointing either inward or outward, which depends on the relative position between composition vector and eigenvectors. A hypothetical ternary system is built up to study the occurrence of i§horns" and the corresponding characteristics by the comparison between DICTRA simulation and phase filed calculations. It is shown that the i§kirkendall" effect may create horns in diffusion paths.

# Cost-Affordable Titanium Symposium Dedicated to Prof. Harvey Flower: Break Through Technologies

Sponsored by: Structural Materials Division, SMD-Titanium Committee

*Program Organizers:* M. Ashraf Imam, Naval Research Laboratory, Washington, DC 20375-5343 USA; Derek J. Fray, University of Cambridge, Department of Materials Science and Metallurgy, Cambridge CB2 3Q2 UK; F. H. (Sam) Froes, University of Idaho, Institute of Materials and Advanced Processes, Moscow, ID 83844-3026 USA

Monday PM	Room: 2	06B
March 15, 2004	Location:	Charlotte Convention Center

Session Chair: F. H. (Sam) Froes, University of Idaho, Inst. for Matls. & Advd. Processes (IMAP), Moscow, ID 83844-3026 USA

#### 2:00 PM

**Co-Reduction of Titanium-Refractory Element Mixed Oxides**: *Kevin F. Dring*<sup>1</sup>; Martin Jackson<sup>1</sup>; Richard J. Dashwood<sup>1</sup>; Harvey M. Flower<sup>1</sup>; <sup>1</sup>Imperial College London, Matls., Royal Sch. of Mines, Prince Consort Rd., London SW7 2AZ England

Binary alloys of titanium-tungsten and titanium-tantalum were prepared by electrochemical deoxidation of mixed oxide ceramics via the Fray-Farthing-Chen (FFC) process. Material exhibiting less than 1500ppm oxygen was obtained by electrochemical reduction in molten calcium chloride at 950°C for 70-100 hours. The distribution of the both constituents was studied in deoxidised binary alloys containing a range of heavy metal additions. Microstructural and chemical analyses were conducted using scanning electron microscopy and x-ray energy dispersive spectrometry. A comparison with conventional methods of producing refractory element bearing titanium alloys is discussed.

#### 2:30 PM

A Coupled Thermal and Microstructure Model for Laser Metal Deposition of Ti-6Al-4V: S. M. Kelly<sup>1</sup>; S. S. Babu<sup>2</sup>; S. A. David<sup>2</sup>; T. Zacharia<sup>3</sup>; S. L. Kampe<sup>4</sup>; <sup>1</sup>Oak Ridge National Laboratory, Jt. Inst. for Computational Scis., PO Box 2008, MS6096, Oak Ridge, TN 37831-6096 USA; <sup>2</sup>Oak Ridge National Laboratory, Metals & Ceram. Div., PO Box 2008, MS6096, Oak Ridge, TN 37831-6096 USA; <sup>3</sup>Oak Ridge National Laboratory, Computing & Computational Scis., PO Box 2008, MS6232, Oak Ridge, TN 37831-6232 USA; <sup>4</sup>Virginia Tech, Matls. Sci. & Engrg. Dept., 213 Holden Hall (0237), Blacksburg, VA 24061-0237 USA

Near-net shape processes, such as laser metal deposition (LMD), offer a unique combination of process flexibility, time savings, and reduced cost in producing titanium alloy components. The current challenge in processing titanium alloys using LMD methods is understanding the complex microstructure evolution as a part is fabricated layer by layer. The microstructure is effected by the repeated thermal cycling that occurs during the deposition process. The current work focuses on the thermal and microstructural modeling of multilayered Ti-6Al-4V deposits. Prior work with LMD-Ti-6Al-4V has shown that a complex microstructure evolves consisting of a two-phase alpha+beta structure. Depending on the location within the part, the Widmanstatten alpha morphology may be colony (layer band) or basketweave. A thermal model has been developed using finite difference techniques to predict the thermal history of LMD processes. The characteristics of a thermal cycle are used to semi-quantitatively map the evolution of equilibrium and nonequilibrium phases in the deposit. The results of the thermal and microstructure models will be discussed in relation to the as-deposited microstructure.

# 3:00 PM

**MEM Titanium Production: Possibilities for Cost Reduction:** Yaroslav Yurievich Kompan<sup>1</sup>; Igor Victorovich Protokovilov<sup>1</sup>; <sup>1</sup>The Paton Electric Welding Institute, 11 Bozhenko St., Kiev 03680 Ukraine

Key differences of magnetically controllable electroslag melting (MEM) from VAR, EBR and other means of titanium melting are intensive directed motion of metallurgical melt and purification of metal by halogen flux. Utilization of the MEM technology assures homogeneity, fineness and high purity of metal ingot. Intensive heat and mass transfer in metallurgical pool creates a uniform temperature field of melt (T=1700-2000°C) and distribution of alloying elements throughout ingot volume, at the same time avoiding their burn during the melting process of a consumable electrode. Among reserves for cost reduction under MEM production of titanium and its alloys are: utilization of lower grade titanium sponge, less repeated remeltings, absence of expensive alloying elements burn, reduced share of scrap, low cost and higher reliability of melting equipment. Economic effectiveness of the MEM technology increases along with increasing number of alloying components in multicomponent alloys.

#### 3:30 PM

**Titanium Extraction by Molten Oxide Electrolysis**: *Donald R. Sadoway*<sup>1</sup>; <sup>1</sup>Massachusetts Institute of Technology, Dept. of Matls. Sci. & Engrg., 77 Mass. Ave., Rm. 8-203, Cambridge, MA 02139-4307 USA

Molten oxide electrolysis (MOE) is an extreme form of molten salt electrolysis, a technology that has been producing tonnage metal for over 100 years: aluminum, magnesium, lithium, sodium, and the rare-earth metals are all produced in this manner. MOE is distinguished by the avoidance of halide electrolytes and carbon anodes which enables the production of oxygen gas instead of halogens or  $CO_2$ . The viability of adaptation of MOE for the extraction of titanium by the direct electrolysis of a multicomponent oxide melt containing dissolved TiO<sub>2</sub> to produce liquid titanium and oxygen gas is assessed.

#### 4:00 PM

Improving Wear Resistance of Ti-6Al-4V Alloy: *Ibrahim Ucok*<sup>1</sup>; Kevin L. Klug<sup>1</sup>; Mehmet N. Gungor<sup>1</sup>; Joseph R. Pickens<sup>1</sup>; <sup>1</sup>Concurrent Technologies Corporation, 100 CTC Dr., Johnstown, PA 15904 USA

An objective of the Combat Vehicle Research (CVR) Program at Concurrent Technologies Corporation is to facilitate extensive use of titanium alloys in combat vehicle applications to take advantage of their high specific strength and excellent corrosion resistance in both wrought and cast forms. These properties make Ti alloys very attractive for replacing steel components to reduce the weight of combat vehicles, thereby improving vehicle mobility and facilitating air transport. However, the inferior wear resistance of Ti alloys compared to steels may be a limiting factor in certain high wear applications, especially when Ti replaces surface-hardened steel. In this study, Ti-6Al-4V substrates were subjected to commercially available surface treatments such as plasma nitriding, electro-spark alloying, electroless plating and thermal spray coatings. The engineered surfaces were evaluated by wear testing, hardness measurements and metallography. Composite diamond and WC-Co coatings were found to have the highest wear resistance under the test conditions employed.

# 4:30 PM

A New Novel Electrolytic Process to Produce Titanium: Jim C. Withers<sup>1</sup>; R. O. Loutfy<sup>1</sup>; <sup>1</sup>MER Corporation, Tucson, AZ 85706 USA

Considerable past effort has been devoted to the electrolytic extraction of titanium without commercial success. A novel new process that combines thermal reduction and electrolytic reduction of titanium from its oxide contained in a composite the anode has been demonstrated. As no solubility of the reduced oxide in the electrolyte is required, there is a large diversity of electrolytes and bath operating parameters including low temperature that can be utilized to produce titanium in a morphology of powder, flake and solid. Not only can CP titanium be produced, but also it is possible to utilize other oxides in the anode and produce alloys such as Ti-6A1-4V and other alloys. Rutile can be used as a feed to produce a very low cost titanium in a less purity than aerospace grade. Powder geometry and size can be controlled based on electrolysis parameters and other operating conditions such that the powders can be utilized directly in powder metallurgy processing to produce titanium components. Economic projections suggest titanium powder can be produced at substantially lower cost than the Kroll or Hunter processes. History and recent results will be discussed.

#### 5:00 PM

**Titanium Biocomposites through Powder Metallurgy**: *M. Karanjai*<sup>1</sup>; R. Sundaresan<sup>1</sup>; T. R. Rama Mohan<sup>2</sup>; B. P. Kashyap<sup>2</sup>; <sup>1</sup>International Advanced Research Centre for Powder Metallurgy and New Materials, Hyderabad 500 005 India; <sup>2</sup>Indian Institute of Technology Bombay, Mumbai 400 076 India

Apart from its well known applications as structural material, titanium finds a niche use as a biomaterial because of its excellent biocompatibility. However, titanium is a bio-inert material, and in implantology it is desirable to make it bioactive by addition of materials like hydroxyapatite (HA) or tri-calcium phosphate (TCP). These bioactive additives are generally very expensive. Composites with bioactive additives like HA and TCP-like phases in Ti matrix have been developed by in-situ formation from inexpensive precursors through PM processing. The starting materials are titanium powder produced by H-DH process and appropriate salts containing calcium and phosphorous. Results confirming formation of bioactive phases and mechanical properties of the composites are reported.

# Dislocations: Simulation and Observation of Fundamental Mechanisms

Sponsored by: ASM International: Materials Science Critical Technology Sector, Electronic, Magnetic & Photonic Materials Division, Materials Processing & Manufacturing Division, Structural Materials Division, EMPMD/SMD-Chemistry & Physics of Materials Committee, MPMD-Computational Materials Science & Engineering-(Jt. ASM-MSCTS)

*Program Organizers:* Elizabeth A. Holm, Sandia National Laboratories, Albuquerque, NM 87185-1411 USA; Richard A. LeSar, Los Alamos National Laboratory, Theoretical Division, Los Alamos, NM 87545 USA; Yunzhi Wang, The Ohio State University, Department of Materials Science and Engineering, Columbus, OH 43210 USA

Monday PM	Room:	20	)1A		
March 15, 2004	Location	ו:	Charlotte	Convention	Center

Session Chair: TBA

2:00 PM

Models of the Ductile-Brittle Transition (DBT) in Single and Polycrystals: N. M. Ghoniem<sup>1</sup>; J. Huang<sup>1</sup>; S. Noronha<sup>1</sup>; <sup>1</sup>University of California, Mech. & Aeros. Engrg. Dept., Los Angeles, CA 90095-1597 USA

In bcc single and polycrystal metals, a transition from a state of ductility at high temperature is suddenly changed to a state of low ductility at low temperature. A critical transition temperature, Tc, defines this universal behavior, where the fracture toughness increases dramatically once the operating temperature is above Tc. Below Tc, the mode of fracture is characterized as brittle and energy is dissipated mainly in the cleavage of atomic planes, while fracture occurs by ductile tearing above Tc. Similar behavior is also observed in covalentlybonded crystals, such as Si and SiC. We present here a new methodology for representation of 3-D cracks of arbitrary shape with parametric dislocation loop pileups. The conditions of nucleation and emission of small dislocation loops from 3-D crack tips are investigated in single crystal bcc metals. It is shown that the stress state ahead of crack tips cannot be described by 2-D elasticity methods due to the 3-D nature of the interaction between emitted loops and the crack surface. The increase in fracture toughness is shown to result from dislocation shielding, once emitted dislocation loops interconnect and form a continuous configuration, while regions of shielding/ anti-shielding are shown to occur when emitted loops have not yet connected. Modeling DBT in polycrystals involves the interaction between a main crack, micro-cracks at fractured precipitates or other weak sites, and emitted dislocations from the main crack and micro-cracks. The increase in fracture toughness at temperatures above Tc is shown to be a result of two mechanisms: (1) shielding the crack tip by emitted dislocations; (2) dissipation of energy in the production of dislocations by multiplication and source generation mechanisms.

#### 2:35 PM

Slip Step Evolution Around Indentations: *Kevin A. Nibur*<sup>1</sup>; David F. Bahr<sup>1</sup>; Brian P. Somerday<sup>2</sup>; <sup>1</sup>Washington State University, Mech. & Matls. Engrg., PO Box 642920, Pullman, WA 99164-2920 USA; <sup>2</sup>Sandia National Laboratory, Matls. & Engrg. Sci., 7011 E. Ave., Livermore, CA 94551 USA

Microscopic analysis of the evolution of slip steps is used to study dislocation activity around indentations in FCC metals. Nanoindentation, atomic force microscopy and orientation imaging microscopy are used to extract fundamental material behavior and identify specific slip planes associated with each slip step. Alloys with lower SFE have smaller, straighter and more closely spaced slip steps, whereas high SFE metals display wavy steps with a range of heights. In a low SFE stainless steel, average slip step heights increased with indentation load up to 200 mN. Beyond this load, a constant average step height of 17 nm was maintained even though pile-up heights increased due to an increased number of steps. Deformation evolves by the creation of additional slip steps around the indentation and not by the extension of existing steps as the indentation proceeds. The method is able to probe both bulk and local properties.

#### 2:55 PM

**Dislocation Mechanisms in Grain Boundary Sliding**: Diana Farkas<sup>1</sup>; Brian Hyde<sup>1</sup>; <sup>1</sup>Virginia Polytechnic Institute and State University, Matls. Sci. & Engrg., 201-A Holden Hall, Blacksburg, VA 24061 USA

Atomistic computer simulations were performed to investigate the mechanisms of grain boundary sliding in BCC Fe using the embedded atom method. For this study we have chosen the  $\Sigma=5$  [001] (310) symmetrical tilt boundary under shear deformation. The response of the boundary to shear loading was studied by molecular statics and dynamics. Sliding was determined to be governed by dislocation activity. The dislocations that are active during grain boundary sliding belong to the DSC lattice. The results show that, at least for special boundaries, the sliding process occurs by the motion of grain boundary dislocations. In this process, the sliding of the boundary under shear is accompanied by migration of the boundary parallel to itself. In analogy to the deformation of bulk materials, the deformation of special boundaries occurs by dislocations at shear stress values much lower than the theoretical strength of the boundary. We also analyze in detail the role of partial DSC grain boundary dislocations as they change the grain boundary's structure. The implications for the sliding behavior of more general boundaries are discussed.

# 3:15 PM

Drag on Dislocation Motion Due to Glissile Interstitial Loops: Zhouwen Rong<sup>1</sup>; David J. Bacon<sup>1</sup>; Yuri N. Osetsky<sup>2</sup>; <sup>1</sup>University of Liverpool, Dept. of Engrg., Brownlow Hill, Liverpool L69 3GH UK; <sup>2</sup>Oak Ridge National Laboratory, Computer Scis. & Math., PO Box 2008, Oak Ridge, TN 37831-6158 USA

Computer simulation has shown that self-interstitial atoms form clusters of closely-packed crowdion defects during radiation damage in metals and, depending on the crystal structure, are equivalent to nanosized dislocation loops with perfect Burgers vector. They can execute fast, thermally-activated glide along the crowdion orientation. Their interaction with dislocations and subsequent effect on slip is expected to be important for radiation hardening and yield phenomena. We report atomic-scale computer simulations of the interaction of a gliding edge dislocation with interstitial loops near the glide plane and its influence on the dislocation dynamics. The drag due to a loop is determined as a function of temperature and Burgers vector orientation for both iron and copper. The results are interpreted in terms of the diffusivity of loops and general conditions under which drag or dislocation breakaway should occur are predicted.

#### 3:35 PM Break

#### 3:50 PM

Dislocation Dynamics as a Path to Parameter-Free Prediction of Crystal Strength: Vasily V. Bulatov<sup>1</sup>; <sup>1</sup>University of California, Lawrence Livermore Natl. Lab., Livermore, CA 94551 USA

Massively-parallel Dislocation Dynamics (DD) simulations are widely recognized as the most direct and rigorous way to connect crystal plasticity with the underlying physics of dislocation motion and interactions. There are two major issues to be addressed for the DD approach to deliver on its promise. The first relates to one's ability to identify and accurately quantify key mechanisms of dislocation behavior on the atomic level. High quality of the atomistic input (local rules, mobility functions) is a pre-requisite of high fidelity of the DD approach. Second, to make DD simulations truly predictable and representative of crystal plasticity, very large ensembles of interacting dislocations must be evolved over long time intervals. The ability to compute large enough and long enough, i.e. computability, is the second important issue to resolve. We will overview the progress being made in the LLNL group in the development and implementation of Dislocation Dynamics on massively parallel computers.

#### 4:25 PM

TEM In-Situ Straining Experiments of FeAl (B2) Oriented Single Crystals Containing Boron and/or Nickel: Anna Fraczkiewicz<sup>1</sup>; David Colas<sup>1</sup>; Olivier Calonne<sup>1</sup>; Francois H. Louchet<sup>2</sup>; <sup>1</sup>ENSMSE, URA CNRS 1884, 158 Cours Fauriel, St-Etienne 42100 France; <sup>2</sup>ENSEEG, LTPCM, BP 75, St-Martin d'Heres 38 054 France

B2-ordered FeAl alloys currently exhibit a yield stress anomaly (YSA) at intermediate temperatures. The origins of YSA in FeAl are not clearly established; two major phenomena are mentioned in literature: (i), superdislocation decomposition (<111> -> <100> + <110>); (ii) vacancy-induced dislocation locking. In this work, Fe-40 % Al-100 ppm B single crystals, containing or not 3.8 at. % Ni, were in situ strained (along a <110> direction) in a TEM, at temperatures ranging between 300 and 700°C. Dislocation dynamics was observed and recorded; their identification was completed by post-mortem analysis in CTEM. In this talk, we report crucial dynamic observations of dislocation mechanisms during TEM in situ straining. Experimental evidence of dislocation decomposition and the presence of mobile anisotropic <110> loops bands are given, along with direct observations of superdislocation locking by APB tubes created by thermal vacancies. These results suggest that both elementary mechanisms are involved in the YSA of FeAl.

#### 4:45 PM

Dynamic Dislocation Multiplication and Propagation in bcc Metals: Luke L. Hsiung<sup>1</sup>; <sup>1</sup>Lawrence Livermore National Laboratory, Chmst. & Matls. Sci., 7000 E. Ave., PO Box 808, L-352, Livermore, CA 94551-9900 USA

Initial dislocation structures in as-annealed Mo and Ta crystals, and dislocation structures developed within the crystals compressed under different strain rates have been investigated using transmission electron microscopy (TEM). The purpose of this study is to understand and elucidate underlying mechanisms for the formation of dipoles (debris), the development of cross-grid dislocation arrays and patterning, and the occurrence of {0-11} anomalous slip (i.e. the Schmid's law violation) in bcc metals. Novel mechanisms based upon dynamic dislocation multiplication and propagation are proposed for the formation of dipoles, cross-grid dislocation pairs, dislocation entanglement, and the occurrence of anomalous slip. This work was performed under the auspices of the U. S. Department of Energy by the University of California, Lawrence Livermore National Laboratory under Contract No. W-7405-Eng-48.

#### 5:05 PM

First-Principles Electronic Structure of Screw Dislocations in Alpha-Fe: Murray Daw<sup>1</sup>; Daryl Chrzan<sup>2</sup>; <sup>1</sup>Clemson University, Phys-

ics & Astron., Clemson, SC USA; <sup>2</sup>University of California, LBNL, Berkeley, CA USA

We have performed first-principles calculations of the electronic structure of screw dislocations in alpha-Fe. The calculations are performed within the spin-polarized Generalized Gradient Approximation (GGA), using the Projector Augmented-wave Method (PAW). The calculations have been performed using the ab-initio total-energy and molecular-dynamics program VASP (Vienna ab-initio simulation program) developed at the Institut fur Materialphysik of the Universitat Wien.<sup>1-3</sup> The periodic supercell contains 96 atoms, two (opposite) screws, and the periodic vectors are chosen to form a quadrupolar array of dislocations. Both easy-core and hard-core structures have been determined and compared. The effects of magnetization are examined. 1G. Kresse and J. Hafner, Phys. Rev. B47, 558 (1993); ibid. B49, 14 251 (1994). 2G. Kresse and J. Furthmuller, Comput. Mat. Sci. v6, 15 (1996); ibid. Phys. Rev. B54, 11 169 (1996). 3G. Kresse and D. Joubert, Phys. Rev. B59, 1758 (1999). Supported by DOE, DOE/ EPSCOR and NERSC.

#### 5:25 PM

**Dislocations in Laves Phases:** *Sharvan Kumar*<sup>1</sup>; Matthew F. Chisholm<sup>2</sup>; Peter M. Hazzledine<sup>3</sup>; <sup>1</sup>Brown University, Div. of Engrg., 182 Hope St., Box D, Providence, RI 02912 USA; <sup>2</sup>Oak Ridge National Laboratory, Solid State Div., 1 Bethel Valley Rd., Oak Ridge, TN 37831 USA; <sup>3</sup>UES, Inc, 4401 Dayton-Xenia Rd., Dayton, OH 45432 USA

Slip, twinning and polytypic transformations in Laves phases are thought to occur by synchroshear. While a geometric description of these processes through the motion of "synchro-shockley" dislocations exists, little is known about the core structure of these synchroshockley dislocations and the structure of the faults they bound. Experimental results on polytypic transformations of Cr-based Laves phases have shown that in general, the transformations are extremely sluggish, and in the one case where it is rapid, the transformation rate appears to depend on ternary substitution. Reasons for the sluggishness or this chemical dependence of kinetics are not known but are probably connected to the core structure of the dislocations. This paper describes some observations of fault and core structures by Z contrast HREM. They are discussed in relation to the kinetics of transformations and to ductility in Laves phases.

# **General Abstracts: Session II**

Sponsored by: TMS

*Program Organizers:* Adrian C. Deneys, Praxair, Inc., Tarrytown, NY 10591-6717 USA; John J. Chen, University of Auckland, Department of Chemical & Materials Engineering, Auckland 00160 New Zealand; Eric M. Taleff, University of Texas, Mechanical Engineering Department, Austin, TX 78712-1063 USA

Monday PM	Room:	204		
March 15, 2004	Location	h: Charlotte	Convention	Center

Session Chair: Joy A. Hines, Ford Motor Company, Dearborn, MI 48123 USA

#### 2:00 PM

Numerical Study of the Solidification of a Pure Metal in a Rectangular Cavity: Beth Anne V. Bennett<sup>1</sup>; Jason Hsueh<sup>1</sup>; David T. Wu<sup>1</sup>; <sup>1</sup>Yale University, Dept. of Mech. Engrg., PO Box 208284, New Haven, CT 06520-8284 USA

Solidification of pure aluminum or gallium within a rectangular cavity is modeled numerically, and results are compared with published data. The model includes latent heat release, convection, conduction (with temperature-dependent variation in viscosity during phase change), and buoyancy. Microstructural development is modeled via a crystal size distribution function (SDF), which can be expressed in terms of nucleation and growth rates. The governing partial differential equations consist of conservation equations for mass, momentum, and energy, and evolution equations for the zeroth through third moments of the SDF. At each time step, these coupled, nonlinear equations are solved simultaneously at all grid points using Newton's method within the local rectangular refinement (LRR) solution-adaptive gridding method. The fully implicit LRR method automatically generates unstructured adaptive grids and incorporates multiple-scale finite differences, producing considerable computational savings without loss of accuracy, as compared to similar solution techniques on structured grids

Computer Simulations of Stress Corrosion Behavior of ZA-27/ Quartz Metal Matrix Composites: P. V. Krupakara<sup>1</sup>; <sup>1</sup>R. V. College of Engineering, Dept. of Chmst., Mysore Rd., Bangalore 560059 India

The stress corrosion resistance of ZA-27/Quartz metal matrix composites (MMCs) in high temperature acidic media has been evaluated using autoclave. Liquidmelt metallurgy technique using vortex method was used to fabricate MMC. Quartz particulates of size 50-80micro meters in size are added as reinforcement. ZA-27 containing 2,4,6 weight percentage of quartz were prepared. Stress corrosion test were conducted by weight loss method for different exposure time, normality and temperature of the acidic medium. The corrosion rate of composites were lower to that of matrix ZA-27 alloy under all condition.

# 2:50 PM

Electrochemical Modeling of Corrosion Inhibition Using Surfactants: Michael L. Free<sup>1</sup>; <sup>1</sup>University of Utah, 135 S. 1460 E., Rm. 416, Salt Lake City, UT 84112 USA

Equilibrium adsorption equations can be used in connection with mixed potential theory to model corrosion inhibition using surfactant molecules. This modeling approach utilizes surfactant hydrocarbon chain length and solution ionic strength data along with electrochemical principles and functional group adsorption properties to predict the rate of corrosion under a variety of conditions.

#### 3:15 PM

Oxygen Distribution in Yttria-Stabilized Zirconia Sintered by Pulsed Current Sintering: *Kimihiro Ozaki*<sup>1</sup>; <sup>1</sup>National Institute of Advanced Industrial Science and Technology, Inst. for Structural & Engrg. Matls., Anagahora 2266-98 Shimoshidami, Moriyama, Nagoya 463-8560 Japan

Pulsed current sintering is a way of sintering powders at a high heating rate and a high cooling rate by flowing electrical current in powder directly. An YSZ shows ionic conductivity at a high temperature. When an YSZ powder is put in a carbon die and is sintered by the pulsed current sintering, electrical current flows in the carbon die at a low temperature and flows in both of the carbon die and the YSZ powder at a high temperature. In the YSZ sintered in a vacuum, an oxygen deficiency occurred, and the oxygen concentration of the anode side was different from it of the cathode side. The deficiency increased with increase of yttria content, and the YSZ became blacker.

# 3:40 PM Break

#### 3:50 PM

Effective Activation Enthalpy for a Periodic Reaction Sequence: Application of the Escher Ring: *David T. Wu*<sup>1</sup>; <sup>1</sup>Yale University, Dept. of Mech. Engrg., PO Box 208284, New Haven, CT 06520-8284 USA

Many driven processes that reach steady state (e.g., interface motion in crystallization or solid phase epitaxy; grain boundary motion; and crack propagation) may be modeled as periodic sequences of firstorder reactions. Kinetically such a reaction sequence is mathematically equivalent to a biased random walk on an "Escher Ring." The overall rate has a simple general solution, and an effective activation enthalpy can be identified, which is bigger than or equal to that obtained from the so-called rate-limiting step.

#### 4:15 PM

**Characterization of Environment-Induced Degradation in Type 422 Stainless Steel:** Ajit K. Roy<sup>1</sup>; *Ramprashad Prabhakaran*<sup>1</sup>; <sup>1</sup>University of Nevada, Dept. of Mech. Engrg., 4505 Maryland Pkwy., Las Vegas, NV 89154-4027 USA

Globally significant efforts are ongoing to reduce the half-lives of spent nuclear fuels by a process known as transmutation. Martensitic Type 422 Stainless Steel is a candidate structural material to contain a target material used in this application. Extensive work has been performed to characterize the environment-induced degradation such as stress corrosion cracking and localized corrosion (pitting and crevice) of this material in aqueous environments of different pH values at ambient and elevated temperatures. This paper is focused on elucidating the results of this study, in particular, the effect of metallurgical and environmental variables on the susceptibility of this alloy to these degradation modes. The metallurgical and fractographic evaluations of this material as determined by optical microscopy and scanning electron microscopy will also be summarized. In essence, a mechanistic understanding of these degradations, based on the analyses of the available results will be presented in this paper.

#### 4:40 PM

High-Temperature Corrosion of Iron Aluminides in O2/Cl2/Ar Atmosphere: Gilsoo Han<sup>1</sup>; Weol D. Cho<sup>1</sup>; <sup>1</sup>University of Utah,

Metallurgl. Engrg., 135 S. 1460 E., Rm. 412, Salt Lake City, UT 84112 USA

The high-temperature corrosion of iron aluminde (Fe3Al) in environments containing chlorine has been investigated at 700°C using thermogravimetric method. The corrosion experiments were performed in Ar/0.5%Cl2 mixtures containing various levels of oxygen from trace amounts to 20% at temperature of 700°C. In general, the corrosion rate decreases with increasing oxygen content in the gas mixture. Several kinetic modes during the corrosion were observed depending on oxygen content. The microstructure of the corrosion scale was analyzed by using several analytical tools to identify the corrosion mechanism. In addition, a quasi stability diagram was developed for the Fe-Al-Cl2-O2 system to explain the corrosion mechanism. The corrosion study was extended to the corrosion of Y-doped Fe3Al in the same corrosive environments to investigate the effect of yttrium on the corrosion. The beneficial effects of yttrium on the corrosion were analyzed by corrosion kinetics and the microstructure of the corrosion scale formed on Y-doped Fe3Al.

#### 5:05 PM

Atomic-Level Interaction of Edge and Screw Dislocations With Stacking Fault Tetrahedra in fcc Metals: Yury N. Osetsky<sup>1</sup>; David J. Bacon<sup>2</sup>; <sup>1</sup>Oak Ridge National Laboratory, Computer Scis. & Math., 4500 S. MS G138, Oak Ridge, TN 37831-6138 USA; <sup>2</sup>The University of Liverpool, Matls. Sci. & Engrg., Brownlow Hill, Liverpool L69 3GH UK

Interaction between moving edge and screw dislocations and stacking fault tetrahedra (SFTs) was studied at atomic scale via molecular dynamics and statics. A recently developed technique based on a periodic array of dislocations has been used together with the empirical many-body potential fitted to reproduce elastic properties and point defects energies in fcc Cu. SFTs of size from 2.5nm to 4nm containing from 45 to 136 vacancies were simulated over the temperature range from 0 to 450K. It was observed that the critical resolved shear stress depends strongly on the position of the dislocation glide plane relative to the SFT's face. It also depends on crystal temperature. A specific mechanism have been observed by which a sheared SFT may recover its regular configuration. The results are compared with the experimental observations in quenched and irradiated fcc metals with low stacking fault energy.

# **General Abstracts: Session III**

Sponsored by: TMS

*Program Organizers:* Adrian C. Deneys, Praxair, Inc., Tarrytown, NY 10591-6717 USA; John J. Chen, University of Auckland, Department of Chemical & Materials Engineering, Auckland 00160 New Zealand; Eric M. Taleff, University of Texas, Mechanical Engineering Department, Austin, TX 78712-1063 USA

Monday PM	Room: 2	12A		
March 15, 2004	Location:	Charlotte	Convention	Center

Session Chair: Aladar A. Csontos, US Nuclear Regulatory Commission, Washington, DC 20555 USA

#### 2:00 PM

**Enhancement of Bending Limits in Thick Plate AA 6061-T6**: *M. P. Miles*<sup>1</sup>; C. Fuller<sup>2</sup>; M. Mahoney<sup>2</sup>; <sup>1</sup>Brigham Young University, Mfg. Engrg. Tech., 265 CTB, Provo, UT 84602 USA; <sup>2</sup>Rockwell Science Center, 1049 Camino dos Rios, Thousand Oaks, CA 91360 USA

Friction Stir Processing (FSP) is used to modify the surface microstructure of one inch thick 6061-T6 plate in order to enhance bending performance. The plate is approximately 25 mm thick and is processed to depths of 5.4 mm and 3.0 mm on the pre-tensile surface. Plane-strain bending experiments were performed on an unprocessed plate and on the plates processed to 5.4 and 3.0 mm of depth until cracks began to form on the plate surface. Finite Element Analysis (FEA) was used to simulate the bending experiments. The Latham-Cockroft failure criterion was used to predict the onset of cracking and the resulting bending limit in each case.

#### 2:25 PM

The Four-Point-Bending Fatigue Behavior of Several Superalloys: *Robert L. McDaniels*<sup>1</sup>; John Michael Cunningham<sup>1</sup>; Wei Yuan<sup>1</sup>; Hongbo Tian<sup>1</sup>; Gongyao Wang<sup>1</sup>; Peter K. Liaw<sup>1</sup>; Dwaine L. Klarstrom<sup>2</sup>; <sup>1</sup>University of Tennessee, Matls. Sci. & Engrg., 434 Dougherty Hall, Knoxville, TN 37996 USA; <sup>2</sup>Haynes International, Inc, 1020 W. Park Ave., PO Box 9013, Kokomo, IN 46904-9013 USA The four-point-bending fatigue testing was conducted on several superalloys under stress-controlled conditions. The testing was performed at room temperature in laboratory air at a frequency of 10 Hz. All tests were run to failure. At regular intervals, the tests were suspended, and replicas of the gage length were made, and subjected to scanning electron microscopy to establish the small crack growth behavior of the alloys. Fractography and metallography examinations were performed on selected specimens from each alloy. A mechanistic understanding of fatigue crack initiation behavior is provided.

#### 2:50 PM

Mechanical Behavior of a Closed-Cell Octet Structure: Wynn Steven Sanders<sup>1</sup>; <sup>1</sup>Air Force Research Laboratory, AFRL/MLLMD, 2230 Tenth St., Bldg. 655, Rm. 025, Wright-Patterson AFB, OH 45433 USA

Lattice- and truss-based materials have been investigated as alternatives to low-density, stochastic metallic foams. These materials exhibit significantly improved properties compared to stochastic foams. However, these "ideal" truss materials are open-cell structures; there may be applications where a closed-cell structure is desired. A relatively simple technique has been developed to construct a closed-cell version of the octet-truss lattice. Initial finite element modeling has shown that the relative modulus and relative strength of the closedcell octet structure is about twice that compared to the open-cell octet-truss lattice for relative densities below ten percent. In fact, the modulus is within twenty percent of the Hashin-Shtrikman upper bound for an isotropic porous material. Additionally, this structure is nearly isotropic. The closed-cell octet structure, which can be envisioned as a "three-dimensional honeycomb," may be a beneficial alternative to existing low-density metallic materials.

# 3:15 PM Cancelled

Plastic Strain and Grain Size Effects in the Surface Roughening of Aluminum Alloys

#### 3:40 PM Break

#### 3:50 PM

Improvement in Damping Capacity of Sintered Aluminum Alloy by Ceramic Dispersion: *Takuya Sakaguchi*<sup>1</sup>; Katsuhiro Nishiyama<sup>2</sup>; <sup>1</sup>Toyota Motor Corporation, Matl. Engrg. Div. 3, Misyuku 1200, Susono, Shizuoka Japan; <sup>2</sup>Tokyo University of Science, Suwa, Chino, Nagano Japan

Conventional aluminum alloys are not available for damping materials due to their low damping capacity. For improving damping capacity of aluminum alloy, it is known to be an effective way to disperse graphite in the aluminum alloy. However, addition of a considerable amount of graphite reduces the rigidity of the aluminum alloy because the rigidity of graphite is very low. In the present study, we have tried to disperse fine particles of NdNbO4, which is known to be a high damping ceramic, in aluminum alloy by powder metallurgy in order to raise both damping capacity and rigidity of the alloy.

#### 4:15 PM

Plastic Instability of Aluminum-Magnesium Alloy 5052: Chen-Ming Kuo<sup>1</sup>; Chi-Ho Tso<sup>2</sup>; <sup>1</sup>I-Shou University, Dept. of Mech. Engrg., 1, Sec. 1, Hsueh-Cheng Rd., Ta-Hsu, Kaohsiung 84008 Taiwan; <sup>2</sup>I-Shou University, Dept. of Matls. Sci. & Engrg., 1, Sec. 1, Hsueh-Cheng Rd., Ta-Hsu, Kaohsiung 84008 Taiwan

Plastic instability is observed during stress rate change test of aluminum-magnesium alloy 5052 at room temperature. In the stress rate change tests, strain retardation and plastic deformation instability are observed. During the stress rate change test, plastic strain is insignificant until the plastic instability occurs. If there is no unstable phenomenon, the plastic strain rate would practically have no changes from beginning to end. The occurrence of plastic instability is related to the applied stress rate and retention time. By the argument of dynamic strain ageing effect, the plastic instability could be justified as the interaction between solid solution element, magnesium, and dislocations. In order to model the plastic deformation, thermally activated kinetic flow theory coupled with structural evolution law has been employed. By changing the values of suitable parameters to simulate the microstructure change of instability, plastic instability could be modeled by the use of numerical method.

### 4:40 PM

Processing of Aluminum (AA6061) for Continuous Severe Plastic Deformation Using ECAE Technique: Shravan Kumar Indrakanti<sup>1</sup>; Yogesh Bhambri<sup>1</sup>; Raghavan Srinivasan<sup>1</sup>; Qingyou Han<sup>2</sup>; <sup>1</sup>Wright State University, Mech. & Matls. Engrg., 209 Russ Engrg. Ctr., 3640 Col. Glenn Hwy., Dayton, OH 45435 USA; <sup>2</sup>Oak Ridge National Laboratory, Metals & Ceram., PO Box-2008, MS-6083, Oak Ridge, TN 37831-6083 USA Studies prove that Equal channel angular extrusion (ECAE) can be applied as a Severe Plastic Deformation (SPD) method to produce ultra fine-grained materials. However this technique is a multi-step batch process that produces small cross-section, short length stock, which severely limits its commercialization. To overcome the limitations of ECAE, a new technology known as Continuous Severe Plastic Deformation (CSPD) was conceptualized. CSPD will be able to produce continuous long lengths of bulk ultra fine-grained materials. In this study ECAE concept was used to impart plastic strain in to a long length of aluminum AA6061 bar having ½ inch square cross section. AA6061 bars at various conditions were subjected to CSPD through a 135° ECAE die at room temperature. The experiment was repeated for multiple passes. Initial results indicate that CSPD process can be used to refine grain sizes. Results will be compared with that of the ECAE of batch process.

#### 5:05 PM

Variation in Poisson's Ratio With Other Elastic Constants: An Attempt Towards Rationalization of Elastic Constants for Isotropic Solid Materials: Anish Kumar<sup>1</sup>; T. Jayakumar<sup>1</sup>; Baldev Raj<sup>1</sup>; K. K. Ray<sup>2</sup>; <sup>1</sup>Indira Gandhi Centre for Atomic Research, Metall. & Matls. Grp., Kalpakkam 603102 India; <sup>2</sup>Indian Institute of Technology, Kharagpur 721302 India

A low symmetry crystal may have as many as 21 independent elastic constants. However the polycrystalline isotropic materials can be characterized by only two independent elastic constants. Hence, identification of any new relationship between the two independent elastic constants for isotropic solid materials would reduce the number of required independent elastic constants to one. A number of researchers have given the empirical relationships to relate shear modulus (G), Young's modulus (E) and bulk modulus (B) for various elements. The correlation of E and G shows a linear behaviour with deviation for the elements having higher elastic moduli. Higher moduli elements always show higher values of G as compared to that predicted by the correlation. From the basic elastic constant interrelationships, it can be deduced that the higher values of G indicates that is lower for elements having higher elastic moduli. In this direction, an attempt has been made to study the variation of Poisson's ratio with other elastic constants using the experiment data generated by the authors and also that collected from the literature for various isotropic solid materials, such as pure elements, ceramics, polymers and intermetallics. The analysis revealed that Poisson's ratio decreases with increase in other elastic constants. A linear correlation has been obtained between Poisson's ratio and ultrasonic shear wave velocity with almost constant slope for any given alloy system with different microstructures associated with various heat treatments, alloying elements, grain size, temperature effect etc. This observation brings out the possibility for rationalization of elastic constants at least for a group of alloy systems with different microstructural conditions. It has also been shown mathematically using the basic relationships among the elastic constants that the decrease in the Poisson's ratio with the shear wave velocity indicates that the shear wave velocity is affected more than ultrasonic longitudinal wave velocity for any change in the material condition. As the shear wave velocity is affected more and the error in the measurement is also less (due to larger time of flight for the same thickness), it is also deduced that shear wave velocity is a better parameter for material/microstructural characterization as compared to longitudinal wave velocity.

# Hume Rothery Symposium: Structure and Diffusional Growth Mechanisms of Irrational Interphase Boundaries: Session II

Sponsored by: Electronic, Magnetic & Photonic Materials Division, Structural Materials Division, EMPMD/SMD-Alloy Phases Committee, MPMD-Phase Transformation Committee-(Jt. ASM-MSCTS)

*Program Organizer:* H. I. Aaronson, Carnegie Mellon University, Department of Materials Science and Engineering, Pittsburgh, PA 15213 USA

Monday PM	Room: 208A
March 15, 2004	Location: Charlotte Convention Center

Session Chair: J.-F. Nie, Monash University, Sch. of Physics & Matls. Engrg., Victoria 3800 Australia

# 2:00 PM Invited

**Edge-to-Edge Matching - The Fundamentals**: *Patrick Manning Kelly*<sup>1</sup>; Ming-Xing Zhang<sup>1</sup>; <sup>1</sup>University of Queensland, Div. of Matls., Sch. of Engrg., Brisbane, Queensland 4072 Australia

The basis of the present authors' 'edge-to-edge matching' model for understanding the crystallography of partially coherent precipitates is the minimisation of the energy of the interface between the two phases. For relatively simple crystal structures this energy minimisation occurs when close-packed, or relatively close-packed, rows of atoms match across the interface. Hence, the fundamental principle behind 'edge-to-edge matching' is that the directions in each phase that correspond to the 'edges' of the planes that meet in the interface should be close-packed, or relatively close-packed, rows of atoms. A few of the recently reported applications of 'edge-to-edge matching' appear to ignore this fundamental principle. By comparing theoretical predictions with experimental data, the paper will explore the validity of this critical atom row coincidence condition, in situations where the two phases have relatively simple crystal structures and in those where the precipitate has a more complex structure.

#### 2:40 PM Invited

An Energy Minimization Principle Applied to Irrational Interphase Boundaries: Jan H. van der Merwe<sup>1</sup>; *Max W.H. Braun*<sup>2</sup>; Gary J. Shiflet<sup>3</sup>; <sup>1</sup>University of South Africa, Physics Dept., Pretoria S. Africa; <sup>2</sup>University of Pretoria, Physics Dept., Pretoria S. Africa; <sup>3</sup>University of Virginia, Matls. Sci. & Engrg., Charlottesville, VA 22904-4745 USA

Interphase boundaries with irrational habit planes and orientational relationships between phases are thought to be of high mobility most notably in the massive, pearlite and cellular solid-state phase transformations. Growing crystalline phases are often enclosed by facets which have been reported to show periodic interfacial fine structure. This suggests that the boundary formation is orientationally driven by minimization of interfacial energies. An analytical formulation of interfacial energies is constructed and relevant parameters are quantified to assess their impact on boundary formation. It is shown that energy minimization is accomplished by edge-to-edge matching of close packed (CP) or near CP atomic planes in accordance with a row-matching principle.

#### 3:20 PM Invited

Irrational Interface Structures and Orientation Relationships of Precipitates in a Duplex Stainless Steel: *Robert C. Pond*<sup>1</sup>; Huisheng Jiao<sup>2</sup>; Mark Aindow<sup>3</sup>; <sup>1</sup>University of Liverpool, Engrg. (Matls. Sci. & Engrg.), Liverpool, Merseyside L69 3BX UK; <sup>2</sup>University of Birmingham, Sch. of Metall. & Matls., Birmingham B15 2TT UK; <sup>3</sup>University of Connecticut, Metall. & Matls. Engrg., Storrs, CT 06269-3136 USA

Precipitation in a commercial duplex stainless steel, Zeron-100, has been investigated using electron microscopy. Acicular fcc precipitates of Ni-rich gamma phase formed in the Cr-rich alpha matrix by suitable heat treatment. The orientation relationships between a large number of particles and the matrix were distributed in a range between the Kurdjumov-Sachs and Pitsch relationships. Two irrational facets bounded each particle, and it was deduced that their structures were based on distinct reference structures with different orientation relationships between the precipitate and matrix. This orientational incompatibility,  $5.76^{\circ}$  about [~1-11]a/[~101]g, was accommodated by networks of crystal dislocations superimposed on the facets. These acted as tilt walls, but, although their combined angular tilt was always

observed to equal about  $5.7^\circ$ , this was not partitioned in a unique manner between the two facets. Such differential partitioning offers a natural explanation for the observed variation in particle orientation.

# 4:00 PM Break

## 4:20 PM Invited

Orientation Relationships Associated with Austenite Formation from Ferrite in a Coarse Grained Duplex Stainless Steel: *E. F. Monlevade*<sup>1</sup>; I.G.S. Falleiros<sup>2</sup>; <sup>1</sup>Nokia Institute of Technology, Rodovia Torquato Tapajós, 7200, Km 12 Tarumã, 69048-660 - Manaus, AM Brazil; <sup>2</sup>Escola Politécnica de Universidade de São Paulo, Dept. Engrg. Metalúrgica e de Materiais, Av. Prof. Mello Moraes 2462, Sao Paulo, SP 05508-900 Brazil

Studies on the morphology and crystallography of austenite precipitated from ferrite were performed in an Fe-22.5% Cr- 4.7%Ni - 3% Mo- duplex stainless steel. Samples were solution treated at 1325°C (yielding a grain size of ca. 2 mm), water quenched and then aged at temperatures ranging from 700 to 1100°C for times ranging from 5000 to 20000 secs. The morphology of grain boundary precipitates depends on the grain boundary segment at which the precipitates are formed, and may be adequately described by the Dubé classification system. Orientation relationships between austenite and the ferritic matrix were determined with EBSD analysis, employing graphic and algebraic methods. Grain boundary precipitates exhibited Kurdjumov-Sachs or Nishyiama-Wassermann O-Rs with at least one of the adjacent grains, and in some cases relationships intermediate between K-S and N-W appeared. In approximately 60% of the cases examined, grain boundary precipitates show a K-S and/or a N-W orientation relationships with both grains forming a boundary, though with small deviations (up to 5°) from the exact relationships.

#### 5:00 PM Invited

Morphology and Interfacial Structure of Mg<sub>17</sub>Al<sub>12</sub> Precipitates in Mg-Al Alloys: *Jian-Feng Nie*<sup>1</sup>; <sup>1</sup>Monash University, Sch. of Physics & Matls. Engrg., Victoria 3800 Australia

The precipitation process in Mg-Al alloys, during isothermal ageing at 200°C, involves solely the formation of the equilibrium precipitate phase Mg<sub>17</sub>Al<sub>12</sub> (body-centred cubic). In the present study, the morphology and the interfacial structure of Mg<sub>17</sub>Al<sub>12</sub> precipitates have been characterised in detail using high-resolution transmission electron microscopy and electron diffraction. Our observations indicate that most Mg<sub>17</sub>Al<sub>12</sub> precipitates have an irrational orientation relationship that approximates to the Burgers relationship, and a faceted lath morphology with habit plane parallel to  $(0001)_{\alpha}$ . The crosssection of the lath, viewed along the direction normal to the habit plane, has a shape of parallelogram. Both the major and the minor facets of this parallelogram are irrational with respect to both phases but are parallel to Moire planes. These experimental observations will be analysed using the Moire plane model that has recently been developed for accounting for the crystallography and migration mechanisms of irrationally-oriented, planar interphase boundaries.

# Internal Stresses and Thermo-Mechanical Behavior in Multi-Component Materials Systems: Electronic Thin Films and Packagaing Materials II

Sponsored by: Electronic, Magnetic & Photonic Materials Division, Structural Materials Division, EMPMD-Electronic Packaging and Interconnection Materials Committee, EMPMD-Thin Films & Interfaces Committee, SMD-Composite Materials Committee-Jt. ASM-MSCTS

*Program Organizers:* Indranath Dutta, Naval Postgraduate School, Department of Mechanical Engineering, Monterey, CA 93943 USA; Bhaskar S. Majumdar, New Mexico Tech, Department of Materials Science and Engineering, Socorro, NM 87801 USA; Mark A.M. Bourke, Los Alamos National Laboratory, Neutron Science Center, Los Alamos, NM 87545 USA; Darrel R. Frear, Motorola, Tempe, AZ 85284 USA; John E. Sanchez, Advanced Micro Devices, Sunnyvale, CA 94088 USA

Monday PM	Room: 20	09B
March 15, 2004	Location:	Charlotte Convention Center

*Session Chairs:* Darrel R. Frear, Motorola, Final Mfg. Tech. Ctr., Tempe, AZ 85284 USA; Indranath Dutta, Naval Postgraduate School, Monterey, CA 93943 USA

# 2:00 PM Invited

Mechanical and Fracture Behavior of Thin-Film Structures for Device Technologies: *Reinhold H. Dauskardt*<sup>1</sup>; <sup>1</sup>Stanford University, Dept. of Matls. Sci. & Engrg., Stanford, CA 94305-2205 USA

The mechanical and fracture properties of thin-film structures for device technologies will be examined. Adhesion and time- or loadingcycle dependent delamination of interfaces that effect mechanical integrity particularly during processing and device packaging are well known. Significant challenges evident for the reliability of emerging device technologies involve the introduction of new materials and the effect of decreasing length scales. Materials are nearly always optimized for other desired properties (e.g. dielectric properties or barrier diffusion resistance) and the resulting deleterious effect on mechanical performance can be significant. Decreasing length scales in device structures frequently result in high stress gradients and mechanical properties that differ significantly from the bulk. The effects of salient interface parameters and thin-film composition will be considered. In the case of highly porous films produced through nanotemplating processes, it will be demonstrated that remarkable increases in fracture resistance can be obtained. These are described in terms of molecular byproducts of the pore-creating process itself, specifically, porogen residual provide molecular bridging mechanisms to markedly effect fracture resistance. Multi-scale models are developed to explain the effect of a range of interface and adjacent layer properties on debonding behavior. These include interface morphology and chemistry, ductile metal or dielectric layer thickness, elastic properties and thickness of the barrier layer, and loading mode. Finally, the effect of more complex patterned thin-film structures are examined where length scales are restricted in more than one dimension.

# 2:25 PM Invited

Linking Dislocation-Based Plasticity to the Thermomechanical Behavior of Thin Films: T. John Balk<sup>1</sup>; Linda Sauter<sup>1</sup>; Tobias Schmidt<sup>1</sup>; Gerhard Dehm<sup>1</sup>; Eduard Arzt<sup>1</sup>; <sup>1</sup>Max-Planck-Institut für Metallforschung, Heisenbergstr. 3, 70569 Stuttgart Germany

The geometry and interface chemistry of metal thin films govern dislocation mechanisms and the resulting stress state. This talk will relate in-situ transmission electron microscope observations of dislocation motion to thermomechanical measurements of Cu and Au films. In addition, the effect of interlayer materials (Ta, Ag, Ti) on the plasticity of Cu thin films will be discussed. In unpassivated Cu films 270 nm or thinner, dislocations glide parallel to and very near the film/substrate interface, even though no resolved shear stress should exist on such glide planes. In thicker Cu films, threading dislocations move on inclined planes and deposit interfacial segments that disappear at elevated temperatures. However, a Ta interlayer stabilizes them, even at 500°C. During thermal cycling, significantly higher stresses evolve in Cu films on Ta than in Cu on silicon nitride. Other connections between dislocations and the thermomechanical behavior of metal thin films will also be drawn.

# 2:50 PM

Effect of Internal Stresses on Thermo-Mechanical Stability of Back-End Interconnect Structures in Microelectronic Devices:

*Indranath Dutta*<sup>1</sup>; Deng Pan<sup>1</sup>; Robert A. Marks<sup>1</sup>; Chanman Park<sup>1</sup>; Joseph B. Vella<sup>2</sup>; <sup>1</sup>Naval Postgraduate School, Ctr. for Matls. Sci. & Engrg., Monterey, CA 93943 USA; <sup>2</sup>Motorola, Proc. Matls. Characterization Lab., Tempe, AZ 85284 USA

Interconnect structures at the back-end of microelectronic devices can undergo significant deformation due to internal stresses which are thermo-mechanically induced during processing, or during service as part of a microelectronic package. These effects can have a pronounced effect on component reliability. Here, we present results of atomic force microscopy (AFM) studies on Cu-low K dielectric (LKD) back-end interconnect structures (BEIS) to demonstrate these effects, which include creep/plasticity of interconnect lines, and diffusionally accommodated sliding at Cu-LKD interfaces. These effects may result in in-plane (IP) changes in Cu line dimensions, cause strain incompatibilities between Cu and LKD in the out-of-plane (OOP) direction, and cause Cu lines to migrate or crawl under far-field shear stresses imposed by the package. We then present a shear-lag based approach, which incorporates a constitutive interfacial sliding law developed by us previously, to model Cu line deformation and interfacial sliding during back-end processing as well as during service after the chip is packaged.

# 3:15 PM Invited

Intrinsic Stresses and Microstructural Stability of Multilayered Structures at Elevated Temperatures: *Daniel Josell*<sup>1</sup>; <sup>1</sup>NIST, Metall. Div., MS 8555, 100 Burea Dr., Gaithersburg, MD 20878 USA

I will discuss the origins of equilibrium stresses and strains in fine multilayered materials when they are brought to elevated temperatures, including discussions of both interface stresses and interface free energies. This will lead directly into discussion of the capillary forces that destabilize polycrystalline multilayered structures. The discussions will include descriptions of the types of experiments used to quantify the underlying interfacial thermodynamic quantities as well as quantitative analysis and application to several experimental systems.

#### 3:40 PM Invited

The Effect of Thermal and Mechanical Load History on the Damage Accumulation During TMF in Dual Shear Specimens: *Thomas R. Bieler*<sup>1</sup>; A. U. Telang<sup>1</sup>; <sup>1</sup>Michigan State University, Chem. Engrg. & Matl. Sci., 2527 Engrg. Bldg., E. Lansing, MI 48824 USA

The intrinsic anisotropy of tin can play a significant role in the damage accumulation in an unloaded single shear lap solder joint, as seen in prior studies. To investigate the effect of external loads arising from differential thermal expansion between a substrate and a surface mount component, specimens with a nickel simulated surface mount component on a copper substrate having a 1 mm<sup>2</sup> joint area and solder thickness of about 100µ were prepared to induce extrinsic shear in joints undergoing TMF cycling. In one specimen, the joints were not connected at the substrate during solidification and cool down to room temperature, so they were not stressed. In the other specimen, a continuous copper substrate caused these joints to be strained such that the component was put in compression during cool down. Then they were cycled at -15°C for 3.5 hr, followed by 20 minutes at 150°C. The first specimen was clamped to a copper block to cause a significant reversal in sign of the shear imposed on the solder joint. In the second specimen, the existing compressive strain in the component at room temperature was further increased with cooling, but it was nearly unstressed at 150°C. It is expected that more damage would develop in the second specimen, due to a larger imposed shear at -15°C. The effect of these two strain histories on evolution of surface damage and microstructure will be compared using SEM and Orientation Imaging Microscopy.

# 4:05 PM Invited

A Combined Experimental and Analytical Approach for Interface Fracture Parameters Between Dissimilar Materials in Electronic Packages: N. R. Kay<sup>1</sup>; S. Ghosh<sup>1</sup>; I. Guven<sup>1</sup>; *E. Madenci*<sup>1</sup>; <sup>1</sup>The University of Arizona, Aeros. & Mech. Engrg., Tucson, AZ 85721-0119 USA

This study concerns the development of a combined experimental and analytical technique to determine the critical values of fracture parameters for interfaces between dissimilar materials in electronic packages. Failure of materials and interfaces are commonly linked to the fracture parameters such as the stress intensity factors and the energy release rate. However, there exists no experimental procedure for the direct measurement of these fracture parameters. This paper reports on the development of a new technique to obtain these parameters by testing specimens created from post-production electronic packages. The results from the experimental testing are then used as the input for an analytical model, which returns the desired parameters. Multiple techniques were developed for the preparation of test specimens from electronic packages. These methods involve different procedures of encapsulation for sectioning and techniques for the introduction of the crack to the interface. Another contribution from this work is the development of an analytical model to accurately model the region near the junction of two dissimilar materials (elastic or viscoelastic). The mean value of the interfacial strength compares favorably to published results.

# 4:30 PM

Validation of Residual Stresses Encountered in Brazed Metal/ Ceramic Joints: John J. Stephens<sup>1</sup>; Steven N. Burchett<sup>1</sup>; Michael K. Neilsen<sup>1</sup>; Charles A. Walker<sup>1</sup>; Evan Dudley<sup>1</sup>; Gerald Stoker<sup>1</sup>; <sup>1</sup>Sandia National Laboratories, Dept. 1833, PO Box 5800, MS0889, Albuquerque, NM 87185-0889 USA

This talk describes an ASCII/MAVEN project at SNL/NM aimed at validating the creep/plasticity constitutive models currently used for prediction of residual stresses in metal/ceramic braze joints. The test vehicle represents a generic Kovar/alumina ceramic braze joint, which uses a geometry that is amenable to measuring the displacement of the Kovar flange thru a furnace viewport during the braze thermal process cycle. The braze filler metal of interest is the 98Ag-2Zr active braze alloy, and we will present the results of uniaxial compression creep and stress-strain tests used to develop the creep-plasticity correlation used for the validation calculations. We will also discuss the special surface requirements needed to maximize the displacement signal output during the cooldown from the braze process cycle to room temperature. The effect of furnace cooldown rate on minimizing residual stresses in the ceramic will also be discussed. This work was conducted at Sandia National Laboratories, a multiprogram laboratory operated by Sandia Corporation, a Lockheed Martin Company, for the United States Department of Energy's National Nuclear Security Administration under Contract DE-AC04-94AL85000.

# International Laterite Nickel Symposium - 2004: Mineralogy and Geometallurgy

Sponsored by: Extraction & Processing Division, EPD-Aqueous Processing Committee, EPD-Copper, Nickel, Cobalt Committee, EPD-Process Fundamentals Committee, EPD-Process Mineralogy Committee, EPD-Pyrometallurgy Committee, EPD-Waste Treatment & Minimization Committee

*Program Organizer:* William P. Imrie, Bechtel Corporation, Mining and Metals, Englewood, CO 80111 USA

Monday PM	Room: 217B/C
March 15, 2004	Location: Charlotte Convention Center

Session Chairs: Vanessa de Macedo Torres, Companhia Vale do Rio Doce, Base Metals Projects Dept., Santa Luzia, MG 33030-970 Brazil; Robert C. Osborne, Inco Technical Services, Mississauga, Ontario L5K 1Z9 Canada

#### 2:00 PM

Mineralogical Characterization of Nickel Laterites from New Caledonia and Indonesia: *Tzong T. Chen*<sup>1</sup>; John E. Dutrizac<sup>1</sup>; Eberhard Krause<sup>2</sup>; R. C. Osborne<sup>2</sup>; <sup>1</sup>CANMET, 555 Booth St., Ottawa, Ontario K1A 0G1 Canada; <sup>2</sup>Inco Technical Services Ltd., 2060 Flavelle Blvd., Mississauga, Ontario L5K 1Z9 Canada

This mineralogical study is based on samples from typical "wet" nickel laterites of humid rain forests. An in-situ nickel laterite sample from Goro and a transported laterite sample from Plaine des Lacs, New Caledonia, are predominantly limonitic. Two-thirds of the particles in the Goro sample are <10 µm in size; they consist of skeletal goethite and serpentine, as well as minor amounts of talc, gibbsite, chlorite, quartz and clay minerals. The coarser grains are mainly Cr-spinel, serpentine, gibbsite and Mn oxide. Nickel occurs mainly in goethite, serpentine and Mn oxide; cobalt occurs in goethite and Mn oxide. The Plaine des Lacs sample is finer-grained and contains more Al and CO3, but less Mg and Si than the Goro material. The sample contains more kaolinite, chlorite, siderite and feldspar, but less serpentine and gibbsite than the Goro material. Nickel is detected mainly in goethite, serpentine, Fe-Mg silicate and Fe-Mn oxide. The Indonesian ore from Sorowako, as sampled from the reduction kiln feed containing some reverts, is predominantly saprolitic, with apparent particle sizes ranging from <100 µm to >1 cm. The sample of reduction kiln feed is rich in Mg silicates, Mg-Fe silicates and goethite, and exhibits complex alteration textures. The nickel contents vary from particle to particle. Nickel is present mainly in serpentine, olivine, chlorite and amphibole, and in subordinate amounts in goethite and Mn oxide. Cobalt is detected in the Mn oxide.

#### 2:25 PM

Vermelho Nickel Laterite - Geological Modelling and Resource Estimation Developments: *Marcio B. Fonseca*<sup>1</sup>; Divino Fernando R. Fleury<sup>1</sup>; Walter Riehl<sup>1</sup>; Marcos Aurélio A. Ferreira<sup>1</sup>; Márcio Roberto S. Rocha<sup>1</sup>; Marcelo A.C. Albuquerque<sup>1</sup>; <sup>1</sup>Companhia Vale do Rio Doce, Mineral Dvlp. Dept., BR 262 - Km 296, Santa Luzia, MG 33030-970 Brazil

Nickel-cobalt laterite deposits have become the focus of attention for hydrometallurgical processing. Following the lessons of the second generation high pressure acid leach (HPAL) projects in Western Australia other Ni-Co laterite projects are now evaluating potential HPAL projects with a rigorous integrated approach that begins with geological modeling, resource estimation and metallurgical studies. The Vermelho nickel-cobalt laterite deposit has been under exploration and study for several years with investigations of various metallurgical processes. Recent HPAL studies have indicated that the nickel and cobalt laterite at this deposit is amenable to upgrading by silica rejection followed by pressure leaching. These studies have required a detailed geological investigation to generate a new resource model. The recent development of a sophisticated geological model integrated with a multi-element resource estimation for this complex tropical nickel laterite deposit in northern Brazil provides an example of the contribution of geology at the critical project stage where process technology decisions are made on relatively small samples of the total resource.

#### 2:50 PM

**Ore Variability Influence on the Metallurgical Process**: *Nolberto Moreno Borjas*<sup>1</sup>; <sup>1</sup>Grupo Empresarial del Niquel, Punta Gorda, Carretera Moa – Baracoa km 5, CP83330, Moa, Holguín Cuba

This paper outlines the detrimental impact that unblended ore can have on the Ni and Co recoveries and the ore slurry density with real data from the Caron low-pressure ammonia leaching process for the Punta Gorda ore. The author briefly discusses the reason for the decrease in slurry density that the process experiences. The lower metal recoveries in the process that are caused by the unblended ore chemical characteristics and variations are shown with a data base statistical analysis drawn from the results obtained from a pilot test, designed with different ore bypassed from the normal process flow and a similar ore from a similar metallurgical treatment.

# 3:15 PM Break

#### 3:25 PM

Ravensthorpe Nickel Project Beneficiation Prediction MLR and Interpretation of Results: *Geoffrey W. Miller*<sup>1</sup>; Darryl Sampson<sup>1</sup>; John Fleay<sup>2</sup>; Jerome Conway-Mortimer<sup>3</sup>; <sup>1</sup>Ravensthorpe Nickel Operations Pty Ltd, Tech., PO Box 7763, Cloisters Sq., Perth, Western Australia Australia; <sup>2</sup>Hatch Minproc Ravensthorpe Joint Venture, 144 Stirling St., Perth, Western Australia 6805 Australia; <sup>3</sup>Geostats, 68 Watkins St., White Gum Valley, Western Australia 6162 Australia

The Ravensthorpe Nickel Project (RNP) flow sheet provides for the upgrading of Ni & Co in a size based beneficiation process prior to leaching. The upgrading effect on Ni and Co makes the beneficiation process a powerful addition to the flow sheet. Multiple linear regression (MLR) analysis based on 351 individual batch tests, 52 large scale composites and 21 pilot plant tests has been used to successfully model beneficiation product grade, recovery, upgrade and mass recovery. Statistically, 83% and 96% of the variability in nickel recovery and nickel product grade respectively was accounted for. Algorithms have been developed for Ni, Co, Mg, Al and Fe, which represents the revenue and operating cost factors for the process. The algorithms have subsequently been applied to the resource model, allowing prediction of elemental grade and recovery for the development of the mine schedules based upon these parameters and not head grades alone. This has allowed optimisation of the mine schedule for improvement to the project's NPV.

#### 3:50 PM

Sechol Nickel - Cobalt Lateritic Project. A Major New Nickel Cobalt Province in Guatemala: *Ricardo A. Valls*<sup>1</sup>; T. John Magee<sup>1</sup>; Bryn Harris<sup>1</sup>; <sup>1</sup>Jaguar Nickel Inc., Exploration, 55 Univ. Ave., Ste. 910, Toronto, Ontario M5J 2H7 Canada

The Sechol Project is located in east-central Guatemala, 140 km northeast from Guatemala City. In situ resources in the immediate area contain 133 million tonnes of mineralization, grading 1.51% nickel. The deposit is conformed of several large lateritic pockets, delimited by tectonic faults and hosted by ultramafic rocks from an ophiolitic complex that intruded a continental plate during the Early Cenozoic Era. Metal recovery from the deposit will be based on a recently patented atmospheric chloride process, followed by solution purification, production of an intermediate nickel/cobalt hydroxide, and fi-

MONDAY PM

nally acid and magnesia recovery by standard spray roasting technology. The AAL process will allow the exploitation of the whole lateritic profile to produce 20,000 Mt of nickel hydroxide and 800 Mt of cobalt hydroxide per year. The laterite potential of the Izabal Ultramafic Intrusive in particular and of the Guatemalan Ophiolitic Belt in general has not been completely explored.

# International Laterite Nickel Symposium - 2004: Panel Discussion

Sponsored by: Extraction & Processing Division, EPD-Copper, Nickel, Cobalt Committee Program Organizer: William P. Imrie, Bechtel Corporation,

Mining and Metals, Englewood, CO 80111 USA

Monday PM	Room: 217B/C	
March 15, 2004	Location: Charlotte Convention Ce	nter

Session Chairs: Bruce McKean, Director, Environmental Affairs, Nickel Development Institute, Toronto M5J 2H7, Canada

# From Feasibility to Sustainability - Questions Society Will Ask Lateritic Nickel Producers

An open forum on the questions other stakeholders – governments, environmentalists, communities, shareholders – will be asking lateritic nickel producers about their processes, their products and their impacts on the environment and on society. Four presenters will offer high-level views on how nickel production from laterites and the value-chain of nickel can be seen from the optic of sustainability. Short presentations followed by discussion by all attendees.

# 4:30 PM Introduction

#### 4:35 PM

Sustainability Looks at Nickel – The Criteria by Which Lateritic Nickel Will Be Judged: Bruce McKean<sup>1</sup>; <sup>1</sup>Director, Environmental Affairs, Nickel Development Institute, Toronto M5J 2H7, Canada

The environmental drivers are introduced: future generations (availability, recyclability, recycling), impacts (on nature, human health, human society). The reputation-based environmental perceptions are introduced: reputation of nickel, of nickel producers, of the mining industry. Collectively these add up to attributes that will affect how nickel from laterites is viewed: a contributor or a hindrance to the achievement of sustainability.

# 4:55 PM

The Nickel Value Chain - Linking to the Sustainability Drivers: Steve C.C. Barnett<sup>1</sup>; <sup>1</sup>VP HSEC Stainless Steel Materials, BHP Billiton, London, UK

The nickel industry is looking downstream – currently just at the European Union but eventually the entire OECD – to learn more about how the nickel flows and how the nickel is used. Comments will be made on two basic observations: nickel adds a great deal of value along the way – including employment and tax revenues – but nickel is also a major component in the environmental burdens associated with nickel's main customer: stainless steel.

#### 5:05 PM

Can There Be Sustainability Without Profitability? - The Economics of Nickel Laterites: Ashok D. Dalvi<sup>1</sup>; <sup>1</sup>Director, Process Engineering and Strategic Studies, Inco Limited, Mississauga, Ontario, L6M 1V1, Canada

Laterites, representing 70% of the nickel resource base, contribute only 40% of nickel production. That will need to change if future nickel supply is going to be assured. But the environmental and sustainability yardsticks being applied to greenfield developments come at a price, a price that cannot be paid at historic price levels. "Sustainability" for the nickel industry will be based on appropriate technical choices but will also require a change in what society has been used to be paying for nickel.

# 5:15 PM

Sustainability and Closure - Policies and Practices for Operators: Denis J. Kemp<sup>1</sup>; <sup>1</sup>Director, Environmental Development, Noranda Inc.-Falconbridge Limited, Toronto, Ontario M5J 1A7, Canada

Operators properly focus on everything that will allow an operating permit to be granted and that will also reassure communities of interest that their concerns and issues are being considered. Considerations of sustainability, however, keep stretching the boundaries of what influences permitting. An issue faced by mining operations – laterites are no exception – is the question of "what happens when the mine closes?" Who is responsible for the "sustainability" of resource-dependent communities that grow up around the mines?

5:25 PM Open Discussion

# Lead-Free Solders and Processing Issues Relevant to Microelectronic Packaging: Environmental and Materials Issues for Lead-Free

*Sponsored by:* Electronic, Magnetic & Photonic Materials Division, EMPMD-Electronic Packaging and Interconnection Materials Committee

Program Organizers: Laura J. Turbini, University of Toronto, Center for Microelectronic Assembly & Packaging, Toronto, ON M5S 3E4 Canada; Srinivas Chada, Jabil Circuit, Inc., FAR Lab/ Advanced Manufacturing Technology, St. Petersburg, FL 33716 USA; Sung K. Kang, IBM, T. J. Watson Research Center, Yorktown Heights, NY 10598 USA; Kwang-Lung Lin, National Cheng Kung University, Department of Materials Science and Engineering, Tainan 70101 Taiwan; Michael R. Notis, Lehigh University, Department of Materials Science and Engineering, Bethlehem, PA 18015 USA; Jin Yu, Korea Advanced Institute of Science and Technology, Center for Electronic Packaging Materials, Department of Materials Science & Engineering, Daejeon 305-701 Korea

Monday PM	Room: 219B
March 15, 2004	Location: Charlotte Convention Center

Session Chairs: Srinivas Chada, Jabil Circuit Inc., FAR Lab/Advd. Mfg. Tech., St. Petersburg, FL 33716 USA; King-Ning Tu, University of California, Matls. Sci. & Engrg., Los Angeles, CA 90095 USA

# 2:00 PM Invited

COST 531 - A European Action on Lead-Free Soldering: Herbert Ipser<sup>1</sup>; <sup>1</sup>University of Vienna, Inst. f. Anorganische Chemie, Waehringerstr. 42, Wien A-1090 Austria

A European Research Action on lead-free soldering has been initiated in 2002. Its goal is the establishment of a database that contains the relevant knowledge on possible lead-free solder materials and to provide the expertise for selecting particular materials for specific soldering purposes. By July 2003, 19 European countries have signed the corresponding Memorandum of Understanding, in addition, one Canadian research organization has been accepted as non-European partner. The Action is structured into four Working Groups: WG1 is responsible for experimental data on phase equilibria and thermochemical properties of possible lead-free solder materials and systems of relevance for joints with various substrates. WG2 carries out the theoretical modeling of the corresponding phase diagrams. WG3/4 investigates physical and chemical properties of candidate alloys, and WG5/6 is responsible for reliability as well as for processing and packaging issues. Currently nine Group Projects are active involving scientists from 38 participating research institutions in 15 European countries.

# 2:25 PM

V-Grooved Optical Fiber Array Packaged by Lead-Free Solder: Shengquan Ou<sup>1</sup>; Gu Xu<sup>1</sup>; Yuhuan Xu<sup>1</sup>; King-Ning Tu<sup>1</sup>; <sup>1</sup>University of California, Matls. Sci. & Engrg., 405 Hilgard Ave., Los Angeles, CA 90095 USA

Etched V-grooves along the [110] direction on (001) surface of Si wafers have been used in high precision alignment between fibers in opto-electronic devices. Nevertheless, bonding the fibers to the chips has been a challenging issue. Currently, the positioning of fibers using epoxy-bonding lacks precision as well as long-term stability. We proposed and conducted the novel technology of using metallic solder packaging instead of the organic epoxy-bonding. The study is of scientific significance because of the fact that solder does not wet SiO2 surface. To circumvent this problem, electron beam evaporation is used to deposit the multi-layered metallic coatings on the surfaces of fibers and V-grooved chips. Three types of multi-layered metallic film coatings were adopted, and they are Ti/Au, Ti/Cu/Au, and Ti/Ni/Au. The metallic film coating on the fiber from infrared noise interference. We utilized a low melting point Pb-free solder - eutectic 43Sn57Bi (in wt. %) with a

melting point of 139°C to bond the array of fibers to V-grooved chips. The mechanical and optical tests illustrated that we can realize the precise alignment of fibers by the soldering method and the bonding structure is strong at room temperature. The metallic solder bonding can be hermetic and it can isolate the optical device from ambient environment.

# 2:45 PM

#### Nanoindentation Investigation of Au-Sn Solder for Optoelectronic Applications: *Richard R. Chromik*<sup>1</sup>; Laura Limata<sup>1</sup>; Dongning Wang<sup>1</sup>; Richard P. Vinci<sup>1</sup>; Michael R. Notis<sup>1</sup>; <sup>1</sup>Lehigh University, Dept. of Matls. Sci. & Engrg., 5 E. Packer Ave., Bethlehem, PA 18015 USA

The optoelectronics industry requires solder alloys with enhanced creep resistance and long term reliability. One such candidate is eutectic Au-Sn solder. To address reliability concerns, nanoindentation has been used to characterize the mechanical properties of intermetallic phases in this system. By solid state annealing of diffusion couples, continuous layers of intermetallics are formed that provide both reliable test volumes for nanoindentation and relevant length scales to real solder joints. Both the elastic modulus and hardness are measured for Au-Sn intermetallics with results compared to previous measurements in the Cu-Sn and Ag-Sn systems. Nanoindentation creep measurements are also underway to examine the effect of time and temperature on deformation within the solder matrix.

#### 3:05 PM

Assembly and Reliability of Isotropic Conductive Adhesives for Fine Pitch Flip-Chip Applications: Stoyan Stoyanov<sup>1</sup>; Chris Bailey<sup>1</sup>; Robert Kay<sup>3</sup>; Rajkumar Durairaj<sup>2</sup>; Mike Hendriksen<sup>4</sup>; Marc Desmuilliez<sup>3</sup>; Ndy Ekere<sup>2</sup>; <sup>1</sup>University of Greenwich, Computing & Math. Scis., Greenwich Maritime Campus, Park Row, Greenwich, London SE10 9LS UK; <sup>2</sup>University of Greenwich, Sch. of Engrg., Chatham Maritime, Chatham, Kent ME4 4TB UK; <sup>3</sup>Heriot Watt University, Microsys. Engrg. Ctr., Edinburgh Scotland; <sup>4</sup>Celestica Limited, West Ave., Kidsgrove, Stoke on Trent, Staffordshire UK

Isotropic conductive adhesives (ICAs) are suitable for low temperature assembly, and have the added advantage that they are also an alternative to lead-free solders. This paper will present results from a highly interdisciplinary project into the formation and subsequent reliability of ICAs interconnects or flip-chip assembly at very fine pitch. Experimental results will be discussed that detail the performance of novel stencils and how, together with the rheology of a particular ICA, these impact the printing behaviour at these fine dimensions. Reliability modelling will also be discussed. These models, based on finite element analysis, provide predictions of stress due to the thermal mismatch in the materials (i.e. silicon chip, polymer underfill, ICA, organic substrate, etc). Results from these models coupled with optimisation analysis have helped identify process conditions that lead to longer joint life.

#### 3:25 PM

A Study of On-Board Reliability for BT Substrate Base Green CSP (Chip Scale Package): Chung Cho Liang<sup>1</sup>; T. B. Lu<sup>2</sup>; <sup>1</sup>I-SHOU University, Matls. Sci. & Engrg. Dept., #1, Sect. 1, hsueh-cheng Rd., ta-hsu hsiang, Kaohsiung 84008 Taiwan

In this paper, the study on the on-board reliability relationship between green assembly material characteristic and reliability failure mechanism in both 63Sn/37Pb and lead-free solder were reported. The failure criterion is base on the temperature cycle test (TCT). Besides, the paper discusses the influences of IR-reflow profile parameters and how it affects the solder material properties. For instance, package block warpage induced by halogen-free compounds and transition point of flux decompose rate effects on the result of on-board reliability. The thermal decomposing behavior of the lead-free type fluxes were analyzed by differential scanning calorimetry (DSC) and thermo gravimetric analysis (TGA). Combined with the relative X-ray inspection was show in Figure 1. Examining the above results, they were the important references for the lead-free IR-reflow profile design to avoid voids forming and improve TCT reliability. On-board reliability specimens were sectioned and analyzed by scanning electron microscope (SEM) and X-ray. The evolution of package warpage of two kind halogen-free compounds, during IR-reflow process, were monitored by special designed thermal mechanic analysis (TMA) experiments. The stress distribution of solder joins within the on-board samples was examined during TCT reliability. Results shown that poor IR-reflow profile design induced voids forming within solder joins and halogenfree compound with lower glass transition temperature reveal larger block warpage change during TCT, respectively. These conduct poor performances in TCT reliability test.

# 3:45 PM Break

#### 3:55 PM Invited

A Dynamic System Model to Assess the Environmental Impact of the Use of Lead Free Solder in Electronic Goods: Markus Andreas Reuter<sup>1</sup>; <sup>1</sup>Delft University of Technology, 120 Mijnbouwstraat, Delft The Netherlands

A dynamic model that interconnects more than ten metals will demonstrate the environmental impact of the use of lead free solder in electronic goods. Various case studies will show that care should be taken when banning metals, due to the complex inteconnected nature of the base metallurgical industry. This paper will clearly show that removing lead from the metal cycle could have severe consequences for the metallurgical ecosystem.

#### 4:20 PM

Effects of Load and Thermal Conditions on Lead Free Solder Joint Reliability: *Jin Liang*<sup>1</sup>; Dongkai Shangguan<sup>2</sup>; Stuart Downes<sup>1</sup>; <sup>1</sup>EMC Corp, 176 South St., Hopkinton, MA 01748 USA; <sup>2</sup>Flextronics, 2090 Fortune Dr., San Jose USA

Reliability of lead-free solder joints has been a hot topic widely debated in the electronic industry long before the European Union passed lead-free legislations. A recent survey conducted in Europe indicated that only 6% companies perceive the change to lead-free soldering from Sn-Pb eutectic solder is for technology benefit (none for process reasons). Those who think lead-free soldering has merits beyond environmental benefit also believe lead-free solder joints will be more reliable than the current Sn-Pb eutectic solder joints. Although some published data supports this claim, others also indicate otherwise. This created a state of confusion in the industry about the actual reliability of lead-free solder joints compared to joints produced with tin-lead eutectic solder. In reality, many mechanical, metallurgical and thermal factors affect the service reliability of solder joints. This paper tries to shed some light on the effects of mechanical loading and thermal conditions on solder joint reliability. These conditions are determined not only by external environments, but also by the solder alloy itself and its shape and geometry. Analyses both with first principles and finite element modeling are carried out on both areal array and peripheral packages, both leaded and lead-less joints and BGA solder balls. A general life assessment methodology is presented by taking into consideration solder joint geometry, thermal and mechanical characteristics of components and substrate materials, as well as application conditions. The theory also helps explain why lead-free solder joints may not be more reliable in certain application conditions as expected.

# 4:40 PM

Ethyl Alcohol Based Flux for Sn-3 Ag-1 Zn Lead Free Solder: Shih-Chin Chang<sup>1</sup>; Hui-Sheng Chiang<sup>1</sup>; <sup>1</sup>National Tsing-Hua University, Dept. of Matls. Sci. & Engrg., HsinChu, Taiwan 30043 Taiwan

Ethyl alcohol based flux was applied for the soldering of Sn-3 Ag-1 Zn lead free solder and Fe-42 Ni alloy (alloy 42). Perfect bonding was observed by using different fluxes with a range of different concentrations. The fracture path in peel test was observed to propagate inside the solder material by a void formation and connection process.

# 5:00 PM

Effect of Corrosion on Physical and Mechanical Properties of SnZn and SnPb Solders and Joints: *Zhidong Xia*<sup>1</sup>; Yaowu Shi<sup>1</sup>; Yongping Lei<sup>1</sup>; <sup>1</sup>Beijing University of Technology, The Key Lab. of Advd. Functional Matls. Ministry of Educ., 100, Ping Leyuan, Chaoyang Dist., Beijing 100022 China

Electric conductivity and mechanical properties of SnZn-based, SnPb solders and their soldered joints were tested in tap water and in 3% NaCl solution at room temperature. Corrosion affects slightly on the electric conductivity of the solder and the joint. Low corrosion potential of SnZn solder alloy and thus smaller joint resistance make the corrosion current larger through the joint. Adding bismuth element in SnZn alloy can increase the resistance of the solder. Tensile experiment of the solder shows that the strength and elongation of the solder decrease as the soaked time increases. Creep life of SnZn joint shortens in 3%NaCl solution, while in tap water, the life elongates distinctly. Tested results also show that a little insoluble corrosive product has no harm on the creep-resistance of the joint. Analysis of fractograph of corroded joint by SEM finds out that corrosion occurs along the grain boundaries.

#### 5:20 PM

Effect of Surface Treatment on Ceramics Bonding with Solder Glass Frit: Zheng Sun<sup>1</sup>; Dayou Pan<sup>1</sup>; Jun Wei<sup>1</sup>; Chee Khuen Wong<sup>1</sup>; <sup>1</sup>Singapore Institute of Manufacturing Technology, 71 Nanyang Dr., Singapore 638075 Singapore

Bonding of ceramics is becoming an increasingly important technology and has found wide applications in different engineering and electronic applications. In the present paper, furnace brazing of ceramics using glass frit filler material was investigated with emphasis on effects of surface treatment and processing parameters. Alumina (Al2O3) sheets and Schottglas GL1 G017-393 solder glass frit were used as the base and brazing materials, respectively. The alumina substrates were chemically (or physically) treated using various acids, as well as air plasma arc, respectively. In addition, effects of brazing parameters such as temperature, time and load were investigated. Tensile test for the brazed joints was conducted to assess the joint strengths. The results show that both surface roughness and contact angle of the substrates decrease after the surface treatments. Results from both tensile and metallographical tests show that sound brazed (or sealed) joints can be produced if appropriate parameters applied. The results indicate that relatively high surface roughness facilitates the joint strength due probably to the enhanced mechanical interlocking. It appears that the appropriate combination of the substrate surface roughness and the glass frit particle size plays dominant role in the joint strength. Furthermore, the study demonstrated that the mechanism of ceramics bonding using solder glass frit is fundamentally different from that of conventional brazing or soldering process. Bonding strength is not only related to surface contact angle, but also surface roughness. It is shown that with appropriate bonding conditions, high quality ceramics bonding or sealing can be achieved.

# Magnesium Technology 2004: Wrought Magnesium Alloys I

Sponsored by: Light Metals Division, LMD-Magnesium Committee Program Organizer: Alan A. Luo, General Motors, Materials and Processes Laboratory, Warren, MI 48090-9055 USA

Monday PM	Room: 2	03B
March 15, 2004	Location:	Charlotte Convention Center

Session Chairs: Alan A. Luo, General Motors, Matls. & Processes Lab., Warren, MI 48090-9055 USA; Sean R. Agnew, University of Virginia, Dept. of Matls. Sci. & Engrg., Charlottesville, VA 22904 USA

#### 2:00 PM

Thermal Forming of Magnesium Alloys: Processing and Simulation: Suhui Wang<sup>1</sup>; Ramnath K. Krishnamurthy<sup>1</sup>; Xin Wu<sup>1</sup>; Wuhua Yang<sup>2</sup>; Michael Wenner<sup>2</sup>; <sup>1</sup>Wayne State University, Mech. Engrg., 5050 Anthony Wayne Dr., Detroit, MI 48202 USA; <sup>2</sup>General Motors, R&D Ctr., Mfg. Sys. Rsch. Lab., 30500 Mound Rd., MC 480-106-359, Warren, MI 48090-9055 USA

Under thermally activated deformation conditions magnesium alloys exhibit greatly enhanced formability. It is of great interest to investigate the possibility of deformation processing for high-efficiency and low-cost manufacturing. In this study the elevated temperature deformation behaviors of AZ31B were investigated, first to determine the window of processing temperature and strain rate suitable for net-shape forming processes. The formability was evaluated under a biaxial loading condition using tube specimens and with internal gas pressure and axial loading. Then, the gas forming of tubes was studied, and the forming mechanics was analyzed. It was found that the deformed parts showed a strong crystallographic texture and anisotropic properties. The texture evolution was analyzed with a strain rate dependent crystal plasticity method, and the results are in good agreement with the experimental observations. A combined process design and texture design for optimal post-forming performance is discussed.

#### 2:20 PM

Mechanical Response of AZ31B Magnesium as a Function of Temperature, Strain Rate, and Orientation: Carl M. Cady<sup>1</sup>; George T. Gray<sup>1</sup>; Benjamin L. Henrie<sup>1</sup>; Ellen K. Cerreta<sup>1</sup>; Laura B. Addessio<sup>1</sup>; Micheal F. Lopez<sup>1</sup>; Shuh-Rong Chen<sup>1</sup>; David F. Teter<sup>2</sup>; Clarissa A. Yablinsky<sup>3</sup>; <sup>1</sup>Los Alamos National Laboratory, MST-8, MS G-755, Los Alamos, NM 87544 USA; <sup>2</sup>Los Alamos National Laboratory, MST 6, Los Alamos, NM 87545 USA; <sup>3</sup>Carnegie Mellon University, Pittsburgh, PA 15213 USA

Constitutive property studies have been conducted on a commercial magnesium alloy as a function of temperature  $(-75 e^{a}C \text{ to } 200 e^{a}C)$ , strain rate (0.001 s-1 to 2500 s-1), orientation, and stress state. Minimal influence of strain rate on the yield and flow stress of this material was seen over the range of strain rates from 0.001 to 2500 s-1. HowMONDAY PM

ever, a large variation in the mechanical response was observed related to both orientation with respect to rolling direction and stress-state. The yield stress in the through-thickness orientation is twice that of the in-plane direction for all strain rates. The flow stress for the inplane orientation is initially lower than that seen in the through-thickness direction but it intersects at ~12% strain. Varying the temperature also influences the through-thickness flow stress behavior significantly more than the in-plane behavior. These differences can be attributed to the dominant deformation mechanism activated for each orientation.

#### 2:40 PM

TEM Investigation of the Dislocations Activated Within Magnesium Alloy AZ31B Under Various Loading Conditions: Ozgur Duygulu<sup>1</sup>; Sean R. Agnew<sup>1</sup>; <sup>1</sup>University of Virginia, Dept. of Matls. Sci. & Engrg., 116 Engineer's Way, Charlottesville, VA 22904 USA

Recent experimental and simulation-based studies of the deformation mechanisms of wrought magnesium alloy AZ31B have stressed the importance of non-basal slip of dislocations having Burger's vectors of <a> type, as well as <c+a> type for determining the overall plastic response of the alloy. These mechanisms have been invoked to explain the strong in-plane anisotropy typical of cold-rolled sheet as well as the improved formability at elevated temperatures, respectively. These conclusions are critically evaluated in light of transmission electron microscopy analyses of the dislocations present at various temperatures and under different loading conditions. By examining grains of various orientations within a given sample, an assessment of the population of various dislocations is possible. The results of this study have implications for both sheet alloy and process development, as well as warm forming process development.

#### 3:00 PM

Heated Hydro Mechanical Deep Drawing of Magnesium Sheet Metal: Gerrit Kurz<sup>1</sup>; <sup>1</sup>Institute for Metal Forming and Metal Machine Tools, Sheet Metal Forming, Welfengarten 1A, Hannover 30167 Germany

In order to reduce fuel consumption efforts have been made to decrease the weight of automobile constructions by increasing the use of lightweight materials. In this field of application magnesium alloys are important because of their low density. A promising alternative to large surfaced and thin die casting parts has been observed in construction parts that are manufactured by sheet metal forming of magnesium. Magnesium alloys show a limited forming ability at room temperature. A considerable improvement of formability can be reached by heating the material. Formability increases above a temperature of approximately  $T = 225^{\circ}C$ . This paper will give an overview about the heated hydro-mechanical deep drawing process of magnesium sheet metal. It will further show how the process parameters temperature and fluid pressure influence the deep drawing process. Results of these deep drawing tests lead to the conclusion that it is possible to replace conventional steel workpieces and aluminum sheet workpieces by magnesium sheet workpieces.

#### 3:20 PM

Dynamic Recrystallization of AZ31 Magnesium Alloy During Torsion Deformation at Elevated Temperatures: W. J. Liu<sup>1</sup>; V. Kao<sup>1</sup>; E. Essadiqi<sup>1</sup>; S. Yue<sup>2</sup>; V. Verma<sup>3</sup>; <sup>1</sup>Natural Resources Canada, Matls. Tech. Lab., CANMET, 568 Booth St., Ottawa, Ontario K1A 0G1 Canada; <sup>2</sup>McGill University, Dept. of Metals & Matls. Engrg., 3610 Univ. St., Montreal, Que. H3A 2B2 Canada; <sup>3</sup>General Motors, Matls. & Processes Lab., Warren, MI 48090-9055 USA

It is believed that dynamic recrystallization is the mechanism responsible for grain structure refinement of magnesium alloys during elevated temperature deformation. In this study, isothermal torsion tests were carried out on an AZ31 alloy under constant strain rate conditions. Two critical values that characterize the dynamic recrystallization kinetics, namely the critical strain for recrystallization start (es) and the critical strain for recrystallization finish (ef), were determined from the measured flow curves and verified metallographically based on quenching samples interrupted during deformation. A kinetic model is developed which is capable of predicting recrystallization fractions from usual processing and material parameters such as temperature, strain, strain rate and original grain size.

# 3:40 PM Break

#### 3:50 PM

Mechanical Properties, Formability and Microstructure of Magnesium Alloy Tubes: *Alan A. Luo*<sup>1</sup>; Anil K. Sachdev<sup>1</sup>; <sup>1</sup>General Motors Corporation, Warren, MI USA

Magnesium alloys are being increasingly used in automotive industry for weight reduction and fuel economy improvement. Extruded tubular sections provide further opportunities in mass-efficient designs for automotive structural and interior applications. In this paper, some fundamental aspects of structural design using magnesium alloy tubes are discussed. Furthermore, mechanical properties, formability and microstructure of magnesium alloy tubes are examined at room and elevated temperatures. Deformation mechanisms and their implications on formability of magnesium alloys are also discussed.

#### 4:10 PM

#### **Pneumatic Bulging of Magnesium AZ31 Tubes and Sheet Metal at Elevated Temperatures**: *K. Siegert*<sup>1</sup>; S. Jäger<sup>1</sup>; <sup>1</sup>Stuttgart University, Inst. for Metal Forming Tech. Germany

This paper deals with pneumatic bulging of Magnesium AZ31 tubes and AZ31 sheet metal at elevated temperatures. In the following, flow-stress curves for AZ31 tubes and AZ31 sheet metal are presented, determined by pneumatic bulging. In addition to that forming limit curves for Magnesium AZ31 tubes and AZ31 sheet metal at different forming temperatures are presented as well. It can be shown that magnesium AZ31 is quite good formable at temperatures in the range of 250°C to 350°C. Outgoing from these fundamental investigations, an auto body sheet metal component was formed by pneumatic bulging at a temperature of about 300°C. Furthermore, the strains over the component were measured with an automated grid analysis. This analysis shows a nearly equal distribution of the strains over the component.

# 4:30 PM

Microstructure and Mechanical Properties of Mg-Al-Zn Alloys Processed by Different-Speeds-Rolling: *Tsunemichi Imai*<sup>1</sup>; Shangli Dong<sup>2</sup>; Naobumi Saito<sup>1</sup>; Ichinori Shigemastu<sup>1</sup>; <sup>1</sup>National Institute of Advanced Industrial Science and Technology, Inst. of Structural & Engrg. Matls., Nagoya Japan; <sup>2</sup>Harbin Institute of Technology, Harbin China

Rolling is an important process for sheet production of metals and their alloys, and high performance sheet is essential to extending application of Magnesium (Mg) alloys. A different-speeds-rolling (DSR) processing was carried out on Mg-Al-Zn based alloys in current investigation, aimed at enhacing metallurgy quality and mechanical property of Mg-Al-Zn alloys. The speed ratio of the upper roll and lower one of the mill was selected as 1.364, while the rolls temperature changed from ambient temperature to 573K. Preheating temperature of the rolled sample could also be varied within a wide range in order to obtain Mg sheet free of crack with the final thickness of 1.1 mm. The influence of rolling conditions on microstructure and mechanical property of the rolled Mg-Al-Zn sheet were carefully studied by several techniques, and the benefits of DSR to produce Mg sheet would be indicated.

# 4:50 PM

Effect of Thermoplastic ECAP on Mechanical Properties and Microstructures of AZ61 Mg Alloy: Yan Yinbiao<sup>1</sup>; <sup>1</sup>Nanjing University of Science & Technology, Dept. of Matl. Sci. & Engrg., 200 XiaoLingWei, Nanjing, Jiangsu 210094 China

The commercial AZ61 Mg alloy and its solution treated have been deformed in the temperature from 250C to 450C by the equal channel angular pressing(ECAP) their microstructures are observed with the metallographic microscope and mechanical properties are determined with tensile testing by AGS-10KND Machine. The results show that the effect of primal microstructures of AZ61 Mg alloys on their mechanical properties after thermoplastic ECAP is very small; The grain significantly are refined. specific elongation and yield strength of AZ61 Mg alloy notablely increase, but no change of tensile strength after the thermoplastic ECAP, it may be result from fabricability formating while ECAP; the effect of the deformation temperature on grain sizes and specific elongation and yield strength is more intensive than that of tensile strength; the tensile strength of AZ61 Mg alloy could not be improved by the thermoplastic ECA.

# Materials by Design: Atoms to Applications: Materials Characterization and Microstructural Modeling

*Sponsored by:* Electronic, Magnetic & Photonic Materials Division, EMPMD/SMD-Chemistry & Physics of Materials Committee

*Program Organizers:* Krishna Rajan, Rensselaer Polytechnic Institute, Department of Materials Science and Engineering, Troy, NY 12180-3590 USA; Krishnan K. Sankaran, The Boeing Company, Phantom Works, St. Louis, MO 63166-0516 USA

Monday PM	Room: 210B
March 15, 2004	Location: Charlotte Convention Center

Session Chair: Mutsuhiro Shima, Renssselaer Polytechnic Institute, Matls. Sci. & Engrg., Troy, NY 12180 USA

#### 2:00 PM

Microstructures by Design: Simulations of Nonequilibrium Processing: Alan C. Lund<sup>1</sup>; *Christopher A. Schuh*<sup>1</sup>; <sup>1</sup>Massachusetts Institute of Technology, Matls. Sci. & Engrg., 77 Mass. Ave., Cambridge, MA 02139 USA

With the growing interest in advanced metallic materials such as metallic glasses and nanocomposites, nonequilibrium processing methods such as mechanical alloying and ion-beam mixing are gaining prominence. Using simplified atomic-level models, we simulate these nonequilibrium processes, treating the intrinsic thermodynamic parameters of the material as tailorable. For hypothetical binary alloys with many different compositions, radius mismatches, and heats of mixing, we explore the development of the structural phase-space under extrinsic driving. We provide guidelines for the development of both crystalline and amorphous solid solutions, chemically ordered crystals and glasses, as well as nanocomposite materials. Connection with nonequilibrium thermodynamic theory is also made.

#### 2:30 PM

Mesoscale Response of an Austenitic Stainless Steel: Part I -EBSD and Three-Dimensional Microstructural Characterization: A. C. Lewis<sup>1</sup>; J. F. Bingert<sup>2</sup>; A. B. Geltmacher<sup>3</sup>; G. Spanos<sup>3</sup>; <sup>1</sup>National Research Council/Naval Research Laboratory, Code 6352, 4555 Overlook Ave. SW, Washington, DC 20375 USA; <sup>2</sup>Los Alamos National Laboratory, Los Alamos, NM 87545 USA; <sup>3</sup>Naval Research Laboratory, 4555 Overlook Ave., Washington, DC 20375 USA

Alloy steels will continue to be one of the main structural materials in Navy ships and boats in the foreseeable future, due to their relatively low cost, their good combination of mechanical properties, and the existing infrastructure for processing and fabrication. The ultimate goal of a Naval Materials by Design program is to allow a design engineer to specify performance criteria for a specific Naval structure, such as eliminating magnetic signature, optimizing corrosion resistance, and maximizing material strength. The Materials by Design framework will then determine enhanced/optimized alloy compositions and processing procedures that meet the specified criteria in a timely manner. As a significant part of a multidisciplinary Materials by Design program, three-dimensional characterization techniques have been developed and utilized to provide guidance to first-principles and atomistic simulations and realistic input for image-based finite element models for material response on the mesoscale. Automated electron backscatter diffraction (EBSD) has been used to characterize AL-6XN, a super-austenitic stainless steel with high Ni and Cr content and relatively low C. This technique is used to provide orientation and misorientation statistical distributions, and identify dominant coincident site lattice boundary planes. The presence of second phases such as s will also be investigated in this steel. An experimental methodology has been developed to combine EBSD with standard serial sectioning and focused ion beam sectioning to construct 3D microstructure sets incorporating orientation data.

#### 3:00 PM

Thermography Detection of Low-Cycle Fatigue: *Bing Yang*<sup>1</sup>; Peter K. Liaw<sup>1</sup>; J. Y. Huang<sup>2</sup>; R. C. Kuo<sup>2</sup>; J. G. Huang<sup>3</sup>; D. E. Fielden<sup>1</sup>; <sup>1</sup>University of Tennessee, Dept of Matls. Sci. & Engrg., Knoxville, TN 37996 USA; <sup>2</sup>Institute of Nuclear Energy Research (INER), PO Box 3-14, 1000 Wenhua Rd., Chiaan Village, Lungtan 325 Taiwan; <sup>3</sup>Taiwan Power Company, Taipei Taiwan

Two-dimensional thermography is a new technology that in-situ obtains the target surface temperature. Since mechanical-damaging

processes are always accompanied by heat-dissipation processes, thermography provides a convenient method to in-situ monitor the fatigue-damage processes. In the current research, thermography was used to "watch" temperature evolutions of reactor pressure vessel (RPV) steels "cycle by cycle" during low-cycle fatigue. Numerical analyses integrating thermodynamics and heat-conduction theories have been formulated to quantify the observed temperature evolutions. Stress amplitude, strain amplitude, plastic work, fatigue life, and cyclic-softening behavior have been predicted directly from the observed temperature evolutions, which provides an innovative method to quantify and control the fatigue behaviors of RPV steels. Furthermore, only one or no experiment is needed to determine the required up wide applications of thermography in studying in-situ mechanical damage of materials and components.

#### 3:30 PM Break

## 3:45 PM

#### The Digital Material - An Environment for Collaborative Material Design: *Matthew P. Miller*<sup>1</sup>; Paul R. Dawson<sup>1</sup>; <sup>1</sup>Cornell University, Mech. & Aeros. Engrg., 194 Rhodes Hall, Ithaca, NY 14853 USA

In spite of the many recent advances that have been made in simulations, material design and selection processes continue to be expensive and time consuming. Opportunities for insertion of alternative materials is hampered by not having basic property data available when critical design decisions must be made. The main reason for the empirical nature of alloy design is the crucial role played by the actual form of the microstructure in dictating alloy properties and behavior. Important are the phases, their spatial distribution, and the defects within them, all of which can vary widely even for the same composition. While much research has focused on the response of metals on many of the relevant size scales, there is still a general lack of quantitative understanding about how these processes interact. How do structural features on one size scale dictate the response of the material on a larger scale and, more importantly, how can one accurately represent these structure - property relationships? This pertains to such basic properties as the elastic moduli and strength. The fundamental goal of the research described here is to develop an accelerated materials insertion methodology - a framework capable of encompassing many types of models from multiple size scales that we refer to as the Digital Material. The hallmarks of the Digital Material are its model independence; researchers from many areas can contribute to the description, and its hybrid nature; both simulated and physically measured data are employed in the representation. Iron/Copper alloys have been developed as prototype material systems using the framework. The processes for instantiating, loading and probing virtual and physical specimens are described in this talk.

#### 4:15 PM

Mesoscale Response of an Austenitic Stainless Steel: Part II -Image-Based Finite Element Modeling: A. C. Lewis<sup>1</sup>; J. F. Bingert<sup>2</sup>; A. B. Geltmacher<sup>3</sup>; <sup>1</sup>National Research Council/Naval Research Laboratory, Code 6352, 4555 Overlook Ave. SW, Washington, DC 20375 USA; <sup>2</sup>Los Alamos National Laboratory, Los Alamos, NM 87545 USA; <sup>3</sup>Naval Research Laboratory, 4555 Overlook Ave., Washington, DC 20375 USA

The goal of a Materials by Design program is to develop the framework for a future computationally-based materials design and selection system. A critical component of such a program is the combination of computational techniques, from atomistic to continuum length scales, used to design a material to meet specific property requirements. A significant part of this multidisciplinary Materials by Design program is the development of three-dimensional image-based computational techniques to examine the role of microstructure on the mesoscale response of materials. Experimental data of three-dimensional microstructures in a super-austenitic stainless steel are used to generate mesoscale finite element models based on actual grain orientations, grain boundaries and second-phase particle locations. The constitutive relationships in these models include anisotropic elasticity and crystalline plasticity. These mesoscale models are used to examine the generation of local stress and strain states that will potentially cause local phase transformations, plasticity, damage and ultimately failure.

#### 4:45 PM

On the Synergy Between Classification of Textures and Process Sequence Selection: Shankar Ganapathysubramanian<sup>1</sup>; Nicholas Zabaras<sup>1</sup>; <sup>1</sup>Cornell University, Matls. Proc. Design & Control Lab., Sibley Sch. of Mech. & Aeros. Engrg., 188 Frank H. T. Rhodes Hall, Ithaca, NY 14853-3801 USA

The state of art in computational materials processing is based on a multi-length scale analysis incorporating polycrystalline plasticity, grain size, grain shape effects and effects due to phase distribution and grain boundaries. Considering the computational complexity involved in such multi-length scale formulations, innovative algorithms are needed towards the development of fast and efficient design methodologies. Such developments are crucial for the basis of futuristic ideas of real time control of properties during material processing. Our earlier efforts have shown that reduced-order models of microstructure (texture in particular) are a simple approach towards the development of fast and reliable design/control algorithms. In addition to this, such approaches have the added advantage of their ability to extend easily towards classification problems. This process of classification of texture will be addressed through this presentation. Our analysis incorporates Support Vector Machines algorithms that have been used widely in statistical machine learning tasks. Application of such techniques in texture classification will be demonstrated through a series of examples. Further, we will describe ways to discern data/modes from experimental pole figures, including real time analysis through 'Machine vision', and to use such information in predicting the deformation paths and processes. Comments will also be made on the nonunique nature of such paths. Finally, we will describe and discuss how such developments play an integral role in the development of multilength scale design methodologies.

# Materials Issues in Fuel Cells: Materials Challenges Sponsored by: TMS

*Program Organizers:* Brajendra Mishra, Colorado School of Mines, Kroll Institute for Extractive Metals, Golden, CO 80401-1887 USA; John M. Parsey, ATMI, Mesa, AZ 85210-6000 USA

Monday PM	Room: 207B/C
March 15, 2004	Location: Charlotte Convention Center

Session Chairs: John Michael Parsey Jr., ATMI, Mesa, AZ 85210-6000 USA; Jeanne Pavio, Motorola Labs., Tempe, AZ 85284 USA

#### 2:00 PM Cancelled

# The Facts Behind the Headlines of the Hydrogen Economy

#### 2:40 PM Invited

Application of Oxidation/Heat Resistant Alloys for SOFC Interconnects: Status and Challenges: Z. Gary Yang<sup>1</sup>; John S. Hardy<sup>1</sup>; Dean M. Paxton<sup>1</sup>; Prabhakar Singh<sup>1</sup>; Jeff W. Stevenson<sup>1</sup>; Matt S. Walker<sup>1</sup>; K. Scott Weil<sup>1</sup>; Gordon Xia<sup>1</sup>; <sup>1</sup>Pacific Northwest National Laboratory, 902 Battelle Blvd., MB K2-44, Richland, WA 99352 USA

Over the past several years, advances in the design and fabrication of planar SOFCs have led to a steady reduction in the temperatures necessary for their operation. Consequently, it appears more realistic now to use low cost oxidation and heat resistant alloys for interconnects in the intermediate-temperature (650-800°C) SOFC stacks. There are a large number of compositions developed in the past for a variety of traditional applications and recently a few of new alloys have been added specifically for the SOFC interconnect applications. To help define the suitability of these alloys, PNNL has carried out a systematical screening study and evaluated numerous selected alloys against a set of properties relative to the SOFC interconnect applications. Recently we have also focused on modifying the bulk alloy interconnect composition and engineering its surface for an improved performance. This paper will address status and issues of alloy interconnects for SOFC applications and present the details of our development efforts.

#### 3:10 PM

Portable Methanol-Based Micro Fuel Cells: System Design, Tradeoffs and Results: Jeanne Pavio<sup>1</sup>; <sup>1</sup>Motorola Labs, 2100 E. Elliot Rd., Tempe, AZ 85284 USA

Methanol-based fuel cells, both direct methanol (DMFCs) and reformed methanol (RHFC), are a promising technology for compact power applications because they possess the potential for very high energy density. Motorola Lab's Fuel Cell team has demonstrated a number of prototype portable power systems ranging from 100mW to 2W for low power (<20W), compact electronic applications. Low power systems require not only small sized fuel cell stacks, but also miniature and low power peripheral components. Initial target applications, such as two-way radios and PDAs, require that the fuel cell system have an energy density as good as, or better than, current rechargeable battery technology. Consequently, system power density must be greater than 200 Wh/L. Developing a high energy density fuel cell system requires a high energy density fuel source such as pure methanol (4780Whr/L, 6043Wh/kg), it demands miniaturization of the system for good volumetric and weight effectivity, and it demands long-term reliable performance. Compact 1W and 2W power sources are described for wireless communications and portable computing systems. Motorola's approach to a 20W power system based on a small fuel processor that reforms methanol to hydrogen is also described. System considerations and electronic controls will be reviewed along with basic technology and performance characteristics. Performance of a 2W prototype system will be discussed, along with projections for the 20W system.

# 3:35 PM

#### Extrusion of Stabilized Zirconias for Solid Oxide Fuel Cell Electrolytes: Kevin M. Hurysz<sup>1</sup>; Joe K. Cochran<sup>1</sup>; <sup>1</sup>Georgia Institute of Technology, Matls. Sci. & Engrg., 771 Ferst Dr. NW, Atlanta, GA 30332-0245 USA

Stabilized zirconias, particularly scandia stabilized zirconia (ScSZ), have been proven to be good materials for use as Solid Oxide Fuel Cell (SOFC) electrolytes. This paper will discuss the formation of stabilized zirconia pastes for extrusion into SOFC electrolytes. Paste constituents are characterized using microscopy, particle size, and surface area measurements. Paste properties are modeled using mathematical methods which are compared to experimental property data. The pastes are extruded into a geometry consistent with an operational SOFC. A variety of drying methods are investigated to reduce deformation of the green ceramic. Finally, extrudate behavior on firing is described and fired microstructures presented. Effort toward incorporation of the structure into a SOFC will be discussed.

#### 4:00 PM Break

#### 4:10 PM

Y2Zr2O7 (YZ) - Pyrochlore Based Oxide as an Electrolyte Material for Intermediate Temperature Solid Oxide Fuel Cells (ITSOFCs) - Influence of Mn Addition on YZ: *Kumar Manickam*<sup>1</sup>; I. Arul Raj<sup>1</sup>; R. Pattabiraman<sup>1</sup>; <sup>1</sup>Central Electrochemical Research Institute, Batteries & Fuel Cell Div., karaikudi, Tamilnadu 630006 India

Compositions in the pyrochlore system Y2Zr2O7 (YZ) and Y2Zr2xMnxO7- (YZM) (where x = 0.025, 0.05, 0.075 and 0.10) were examined as possible alternatives to stabilized zirconia solid oxide electrolyte in Intermediate Temperature Solid Oxide Fuel Cells (ITSOFCs). Such materials were prepared by glycine-nitrate combustion process. The prepared compounds were characterized by X-Ray Diffraction, Particle size, density measurement, Fourier Transform infrared spectroscopy, and Thermal analysis. Circular pellets were fabricated and annealed at different temperatures ranging from 1000 to 1400°C. The sintering behavior of YZ and YZM were investigated to obtain information on the densification factor, relative percentage shrinkage/ expansion in volume after heat treatment and apparent porosity value. The small doping level of Mn (?T10.0 wt. %) resulted in increased conductivity values. The key features, which make the YZ and YZM systems attractive as a fuel cell component, are discussed.

#### 4:35 PM

The Anomalous Oxidation Behavior of Oxidation Resistant Alloys Under SOFC Interconnect Dual Exposure Conditions: Z. Gary Yang<sup>1</sup>; Gordon Xia<sup>1</sup>; Matt S. Walker<sup>1</sup>; Prabhakar Singh<sup>1</sup>; Jeff W. Stevenson<sup>1</sup>; <sup>1</sup>Pacific Northwest National Laboratory, 902 Battelle Blvd., Mail Box K2-44, Richland, WA 99352 USA

The oxidation behavior of oxidation resistant alloys under varied environments has been widely investigated for a number of traditional applications, and recently several works have also focused on SOFC interconnect applications. These studies, however, were carried out using single atmosphere exposure conditions and were presumably based on the implicit assumption that the oxidation behavior as measured in either an oxidizing or reducing environment will be essentially identical to that occurring on the air or fuel side of the material when it experiences the dual atmosphere exposure conditions characteristic of the SOFC interconnect environment. However, our recent investigation clearly indicates that under dual exposures, the oxidation behavior on the airside can differ significantly from the behavior observed when the steels are exposed to air only. This paper will present details of this finding and discuss the results from our study on a number of selected alloys under the SOFC operating conditions.

#### 5:00 PM

Mechanochemical Synthesis of PbMoO4 Compound Oxide: Aghasi Razmik Torosyan<sup>1</sup>; Svetlana Ashot Barseghyan<sup>1</sup>; <sup>1</sup>NAS RA, 10 Arghutyan, 2 District, Yerevan 375051 Armenia

The present work the synthesis of compound oxide PbMoO4 under mechanical alloying conditions were investigated. The experiments were carried out in vibration ball mill at vial amplitude of 4 mm and frequency of 25 Hz for up to 10h. PbO and MoO3 with molecular ratio 1:1 were used in experiments of mechanochemical synthesis. The maximal yield of PbMoO4 was 95%. Longer milling times of powder blends didn't result in increase of product yield. The obtained products and the yields of reaction were determined employing X-ray diffraction analysis. In addition to the compound oxides and residues of starting oxides a small quantity metallic iron was found being a result of contamination during milling.Refinement of synthesized PbMoO4 from impurities was carried out by sequential flushing of the powder starting with 25% solution of ammonia to remove MoO3, and then with diluted solution of acetic acid to remove PbO and Fe. Such method of refining allowed to obtain rather pure compound oxide applicable for growing of PbMoO4 crystals. PbMoO4 compound oxide has a number of practical applications as crystal. In most of the important applications very fine grain size in submicron-nanoscale range is important to obtain the best properties. Mechanochemical processing of compound oxides carried out at ambient temperature may be advantageous compared to synthesis methods at high temperatures.

# Materials Processing Fundamentals: Deformation Processing

Sponsored by: Extraction & Processing Division, Materials Processing & Manufacturing Division, EPD-Process Fundamentals Committee, MPMD/EPD-Process Modeling Analysis & Control Committee

*Program Organizers:* Adam C. Powell, Massachusetts Institute of Technology, Department of Materials Science and Engineering, Cambridge, MA 02139-4307 USA; Princewill N. Anyalebechi, Grand Valley State University, L. V. Eberhard Center, Grand Rapids, MI 49504-6495 USA

Monday PM	Room:	21	2B		
March 15, 2004	Locatior	n:	Charlotte	Convention	Center

Session Chair: TBA

Ν

#### 2:00 PM Invited

Differences in the Microstructures of Continuous Cast-Rolled and Conventional Wrought Aluminum Alloy Products: Prince N. Anyalebechi<sup>1</sup>; <sup>1</sup>Grand Valley State University, Padnos Sch. of Engr., L. V. Eberhard Ctr., Ste. 718, Grand Rapids, MI 49504-6495 USA

The differences in the microstructures of wrought aluminum alloy products produced via the continuous casting-rolling and the conventional ingot casting-rolling routes have been investigated. Irrespective of alloy composition, the microstructures of the products produced via the continuous casting route consist of bands of eutectic colonies elongated and strung out in the rolling direction surrounded by regions depleted in second phases. In contrast, the microstructures of conventional wrought products consist of a uniform distribution of comparatively coarser constituent phase particles. Most importantly, wrought aluminum alloy products produced via the continuous casting-rolling route do not contain the matrix-strengthening dispersoids. The differences in microstructure are attributed to the different prevailing solidification conditions in ingot and continuous casting processes. They appear to explain the differences in the response of the two types of wrought products to post-casting processes and attendant properties and performance.

#### 2:30 PM Invited

Atomic Mismatch and Coherency Issues in the Theory of Driven Alloys: *Alan C. Lund*<sup>1</sup>; Christopher A. Schuh<sup>1</sup>; <sup>1</sup>Massachusetts Institute of Technology, Matls. Sci. & Engrg., 77 Mass. Ave., Cambridge, MA 02139 USA

Driven alloys evolve under competition of an extrinsic forcing (e.g., irradiation or plastic straining) and intrinsic thermodynamic parameters (e.g., thermal equilibration). The theoretical framework for these systems has explained many interesting experimental findings in non-equilibrium processing by irradiation, ion-beam mixing, or ball milling of powders, but has largely focused on systems with perfect crystalline coherency. Here we use computer simulations of driven 2-D alloys to expand the discussion to systems with significant atomic level stresses owing to a radius mismatch. These simulations show a significant effect of incoherency that is manifested primarily at low processing temperatures.

#### 3:00 PM

Prediction of the Shape Changes and Microstructural Evolution: Hoon-Jae Park<sup>1</sup>; K.-H. Na<sup>1</sup>; Y.-S. Lee<sup>2</sup>; <sup>1</sup>KITECH, Microforming,

MONDAY PM

35-3, HongChonRi, IbJangMyon, ChonAnSi, Choonchung-nam-do 330815 S. Korea; <sup>2</sup>Kookmin University, Mech. Engrg., 861-1 Chungneung-Dong, Sungbuk-Gu, Seoul 136-702 S. Korea

Main objectives of the forming processes are to form the products having the shape and mechanical properties as designed. To effectively predict the shape changes in steady state forming processes, an Eulerian analysis supplemented with a free surface correction algorithm and a stream line technique is addressed. Since the mechanical properties are related directly to the microstructures of the work piece, the prediction of microstructural changes must be included in the process model. In this work, anisotropy from deformation texture and deterioration of mechanical properties due to growth of micro voids are directly coupled into the virtual work expressions for the mass and momentum balances. The anisotropy and accumulated damage in the rolled sheet could be predicted. Applications to hydrostatic clad extrusion as well as shape rolling are given and the results are discussed in detail.

# 3:30 PM

On the Development of a Three-Dimensional Deformation Process Design Simulator: Swagato Acharjee<sup>1</sup>; Nicholas Zabaras<sup>1</sup>; 'Cornell University, Matls. Proc. Design & Control Lab., Sibley Sch. of Mech. & Aeros. Engrg., 188 Frank H. T. Rhodes Hall, Ithaca, NY 14853-3801 USA

A mathematically rigorous continuum sensitivity method (CSM) is developed and incorporated in a gradient optimization framework for process optimization and control in three-dimensional metal forming applications. CSM involves differentiation of the governing field equations of the direct problem (constitutive, contact and kinematic problems) with respect to the design variables and development of the weak forms for the corresponding sensitivity equations. This work is an extension of our earlier work where the problems were restricted to 2D and axisymmetric cases. Extension to 3D involves a novel approach to the formulation of the contact sensitivity problem. A number of industrially relevant multi-stage design problems related to preform and die design for desired properties in the final product are considered highlighting the features of the metal forming design simulator developed in-house. While emphasis is given to phenomenological state-variable based constitutive models, extension of the design simulator to incorporate multi-length scale polycrystal plasticity based constitutive models will also be discussed.

#### 3:50 PM Break

#### 4:10 PM

Investigation of Microstructural Evolution of Cold Roll Bonded and Annealed TiAl-Sheets: *Kazim Serin*<sup>1</sup>; Gajanan Chaudhari<sup>1</sup>; Viola L. Acoff<sup>1</sup>; <sup>1</sup>University of Alabama, Dept. of Metallurgl. & Matls. Engrg., Box 870202, Tuscaloosa, AL 35487 USA

In this study, the kinetics of the interfacial layer thickness growth of cold roll bonded and annealed titanium and aluminum sheets is investigated. Interrupted annealing experiments were performed for alloys with defined reduction levels at different temperatures between 600°C and 1200°C. The final microstructure depends on the reduction level of the initial foils, annealing temperature, and annealing time. The layer thickness was investigated by quantitative microstructural measurements using scanning electron microscopy (SEM) and transmission electron microscopy (TEM). The appropriate treatment for processing of TiAl-sheet materials was defined.

#### 4:30 PM

High Temperature Flow Behavior of an Austenitic Stainless Steel, ISO 5832-9, Used for Orthopedic Applications: Enrico José Giordani<sup>1</sup>; Oscar Balancin<sup>1</sup>; <sup>1</sup>Universidade Federal de São Carlos, Depto. de Engenharia de Materiais, Rodovia Washington Luiz, km 235, São Carlos, São Paulo 13565-905 Brazil

Knowing how a particular type of steel behaves at high temperature is essential for adequate thermomechanical processing aimed at producing high-performance hot-worked products that combine high strength and toughness. These properties can be attained through a recrystallized microstructure composed of fine grains, provided secondary recrystallization does not occur. An investigation was made of the stress-strain behavior of an austenitic stainless steel used as a biomaterial, ISO 5832-9, based on isothermic torsion tests over a temperature range of 900°C to 1300°C, at strain rates of 0.5 to 5.0s-1. The flow stress generally rises to a maximum at the onset of straining, before dropping to a steady-state level. This behavior is characteristic of materials that soften by dynamic recrystallization. The material showed high values of deformation at the onset of the steady-state and the high value of apparent activation energy (Q=703 kJ/mol), indicating that the material underwent an intense strain-induced Z-Phase precipitation.

# 4:50 PM

Streamline of Microstructure Evolution During Plastic Deformation: *Dongsheng Li*<sup>1</sup>; Hamid Garmestani<sup>1</sup>; <sup>1</sup>Georgia Institute of Technology, Sch. of Matls. Sci. & Engrg., 771 Ferst Dr., NW, Atlanta, GA 30332 USA

Modeling the microstructure evolution during mechanical deformation is essential in finding out how to achieve the preferred microstructure. Texture coefficients were used as a descriptor of the microstructure. A linear model is proposed in this study to describe the evolution of microstructure during thermalmechanical processing. Using this linear model, processing path function and streamline function are derived. From these functions, using known texture at several deformation points, processing path and streamlines were calculated to simulate the microstructure evolution in a microstructure space which is composed of texture coefficients. From these streamlines, an optimized processing method will be found out to achieve the desired microstructure.

#### 5:10 PM

Microhardness Testing as a Method of Understanding Bauschinger Phenomena in Cold Formed 301 Austenitic Stainless Steel Sheet: Chirayu Garud<sup>1</sup>; Philip Nash<sup>1</sup>; Sheldon Mostovoy<sup>1</sup>; Joseph C. Benedyk<sup>1</sup>; <sup>1</sup>Thermal Processing Technology Center, IIT, Chicago, IL USA

Microhardness distributions gave an indication of Bauschinger phenomena in the forming of heavily cold rolled and tempered 301 austenitic stainless steel sheet. Stainless steel sheet samples from different lots were cut longitudinal and transverse to the cold rolling direction in the as-received and tempered conditions, then bent to varying radii, and microhardness distribution obtained throughout the thickness in the principal section of the bend. Microhardness differences between the sections of the bend that underwent tensile and compressive strains were significantly different, indicative of a strong Bauschinger effect. The degree of softening due to the Bauschinger effect varied with bend radius, direction of rolling, and tempering conditions. Correlations were made of the Bauschinger effect with microstructure and texture of the sheet. The microhardness distribution method was useful in ascertaining the bariation in the Bauschinger effect between the two lots of steel and potential problems noted in dimensional control during the manufacture of precision formed automotive gaskets.

# Nanostructured Magnetic Materials: Synthesis and Characterization of Nanostructured Magnetic Materials

Sponsored by: Electronic, Magnetic & Photonic Materials Division, EMPMD-Superconducting and Magnetic Materials Committee, EMPMD-Nanomaterials Committee Program Organizers: Ashutosh Tiwari, North Carolina State University, Department of Materials Science & Engineering, Raleigh, NC 27695-7916 USA; Rasmi R. Das, University of Wisconsin, Applied Superconductivity Center, Materials Science and Engineering Department, Madison, WI 53706-1609 USA; Ramamoorthy Ramesh, University of Maryland, Department of Materials and Nuclear Engineering, College Park, MD 20742 USA

Monday PM	Room: 2	15	
March 15, 2004	Location:	Charlotte Convention Center	

Session Chair: TBA

Ν

# 2:00 PM Invited

Magnetic Nanostructures by Templated Electrodeposition: Giovanni Zangari<sup>1</sup>; Jie Gong<sup>2</sup>; <sup>1</sup>University of Virginia, Dept. of Matls. Sci. & Engrg. & CESE, Charlottesville, VA 22904 USA; <sup>2</sup>University of Alabama, MINT Ctr., Tuscaloosa, AL 35487-0209 USA

Electrochemical deposition into self-assembled porous structures provides a convenient method for the fabrication of ordered arrays of metallic or semiconductive nanostructures. The availability of such systems opens a wide range of opportunities for the fabrication and study of the behavior of nanoparticle or nanowire assemblies and for the inexpensive and precise production of devices. Our work is focused on the fabrication of nanoparticle or nanowire arrays of magnetic materials, with the objective to study the magnetic and magnetotransport properties of nanostructures and their interactions. Ordered aluminum oxide porous templates are fabricated by multiple anodization of high-purity Al sheets or of Al films sputtered onto Si. Long range order of the pore array, up to about 100 ?Ým2 can be achieved. The period of the array (60 ¡V 600 nm) and the pore size (15 ¡V 500 nm) can be varied in a wide range by control of the anodization chemistry and/or the anodization voltage. Magnetic metals, alloys and multilayers were electrodeposited into the closed pores or into open pores plugged by metallic films by ac and pulse reverse electrodeposition. The latter method in particular is capable to achieve an unprecedented uniformity in the dimensions and microstructure of the elements. Metal nanoparticles are polycrystalline and the crystalline grains exhibit a random orientation when grown into the closed pores; as a consequence, magnetic anisotropy is mainly determined by particle shape. A transition from in-plane to perpendicular anisotropy is observed at an aspect ratio (height/diameter) of about 1. Interparticle interactions are extremely important in highly packed arrays, inducing strong demagnetization fields and skew in the hysteresis loops. Cobalt nanoparticles with size above 50 nm switch their magnetization by incoherent processes. Thermal stability of the magnetization of nanoparticle assemblies is investigated, showing that 50 nm diameter particles exhibit high magnetic stability against thermal demagnetization. High quality multilayers Cu/magnetic alloy have been grown into the pores and their magnetic properties in the current-perpendicular-to-plane configuration have been investigated. An outlook on the utilization of anodic templates for the synthesis of novel materials and the investigation of novel phenomena will be provided.

#### 2:30 PM Invited

Synthesis and Characterization of FeCo Based Nanomagnetic Alloys: *Raju V. Ramanujan*<sup>1</sup>; Huafang Li<sup>1</sup>; <sup>1</sup>Nanyang Technological University, Sch. of Matls. Engrg., Blk. N4.1, Singapore 639798 Singapore

FeCo based nanomagnetic materials exhibit several attractive soft magnetic properties and are being considered for several new applications in high magnetic induction and high temperature devices. Such materials have been produced by crystallization from melt spun amorphous precursors, mechanical alloying from elemental powders as well as by chemical synthesis techniques. DSC, electrical resistivity measurement, XRD, SEM, TEM and VSM have been used to characterize the samples prepared by these techniques. The crystallization behavior and microstructural evolution of melt spun FeCo based amorphous precursor is discussed. The alloying process and microstructure of mechanical alloyed FeCo based alloys will also be reported and a comparison of the properties of alloys processed by the three techniques is provided.

#### 3:00 PM Invited

#### Group IV Element-Based Magnetic Semiconductors: Frank Tsui<sup>1</sup>; <sup>1</sup>University of North Carolina, Dept. of Physics & Astron., Chapel Hill, NC 27599 USA

The prospect of integrating electron charge and spin degrees of freedom has invigorated the field of spin-polarized electronics, 'spintronics'. To date, most activities are focused on Mn doped compounds of group III-V and II-VI families, where high quality but low TC ferromagnetic epitaxial films have been grown. But there is considerable interest in higher TC materials, particularly group IV elementbased magnetic semiconductors, owing to their potential compatibility with current Si-based processing technology. In order to achieve this, doping levels in access of several at. % and relatively high processing temperature would be some of the basic requirements. However, they also have been the main obstacles for the synthesis, since they tend to promote phase separation of dopant rich compounds, resulting in disordered and inhomogeneous materials. We describe combinatorial MBE synthesis of stable epitaxial films of doped Si and Ge using two or more dopants, and the resulting characteristic properties of the systems. In-situ RHEED experiments, and ex-situ x-ray diffraction, x-ray fluorescence spectroscopy and cross-sectional high resolution transmission electron microscopy measurements show that the presence of several dopants alters the local energetics and kinetics so that the tendency to phase separate can be controlled during non-equilibrium synthesis. The magnetic and transport properties of the systems exhibit high TC, large magnetoresistance effects, and shallow level conduction with low-temperature behavior dominated by variable range hoping, all of which can be controlled systematically by the doping concentration. The viability of these materials for spintronics has been demonstrated in heterojunction diodes made from these materials exhibiting large magnetization-dependent rectification effects.<sup>1</sup> <sup>1</sup>F. Tsui, L. Ma, L. He, Appl. Phys. Lett. 83 (5), Aug. 4, 2003.

#### 3:30 PM

Role of Altering the Primary Solidification Field on Tailored Pr9Fe91-xBx Nanocomposites: Y. Q. Wu<sup>1</sup>; *M. J. Kramer*<sup>1</sup>; *Z.* Chen<sup>2</sup>; B. M. Ma<sup>2</sup>; <sup>1</sup>Iowa State University, Ames Lab., Dept. of Matls. Sci. & Engrg., 37 Wilhelm Hall, Ames, IA 50011 USA; <sup>2</sup>Magnequench Technology Center, Research Triangle Park, NC 27709 USA Altering the primary solidification field is one means of controlling the nanostructure in rapidly solidified alloys. We investigated the effect of the B:Fe on  $Pr_9Fe_{91-x}B_x$  (x=5-12) nanocomposites. This composition range moves the primary solidifying phases from  $R_2Fe_{14}B/\alpha$ -Fe to  $R_2Fe_{14}B/Fe3B$  with minor  $Pr_2Fe_{23}B_3$ . Increasing B:Fe increases coercivity (H<sub>ci</sub>) but decreases remanence (B<sub>r</sub>) and energy product (BH)<sub>max</sub>. For instance alloys of  $Pr_9Fe_{86}B_5$  and  $Pr_9Fe_{79}B_{12}$  are 9.54 kG, 6.5 kO<sub>e</sub>, 14.4 MGO<sub>e</sub> and 7.06 kG, 7.1 kO<sub>e</sub>, 6.5 MGO<sub>e</sub>, respectively. TEM observations show that the  $Pr_9Fe_{86}B_5$  alloy has smallest grain size distribution (~ 13 nm for soft phase, ~35 nm for hard phase). The grain size of hard phase significantly increases when increasing the B content, especially for the alloys with more than 10 at% B. Besides X-ray analyses, EDS analyses further confirmed the formation of  $Pr_2Fe_{23}B_3$  phase in higher B content alloys (B=8.5~10.5 at.%).

#### 3:50 PM

Plasma Deposition of Ultrathin Films on Nanoparticles/ Nanotubes for Novel Engineering Applications: Donglu Shi<sup>1</sup>; He Peng<sup>1</sup>; Mark Schulz<sup>2</sup>; David Mast<sup>2</sup>; Wim Van Ooij<sup>1</sup>; <sup>1</sup>University of Cincinnati, Dept. of Chem. & Matls. Engrg., Cincinnati, OH 45221 USA; <sup>2</sup>University of Cincinnati, Dept. of Mech. Engrg., Cincinnati, OH 45211 USA; <sup>3</sup>University of Cincinnati, Dept. of Physics, Cincinnati, OH 45221 USA

The development of surface nanostructures will be one of the key engines that drive our technological society in the 21-century. This rapidly growing area focuses on tailoring a nanoparticle surface structure for specific and unique properties. The "nano-scale" engineering has produced such materials as layered composite semiconductors for high speed electronic devices, blue lasers and diodes and vertical cavity lasers that read and write our CDs, and highly conductive, but low loss thin films for panel displays. The broad range of these properties due to nano surface structures can include electro-magnetic conductivities, uniformity, index of refraction, high reflectance, low absorption, stress, and the adhesion of the film structure to the substrate. In these applications, the nanostructure involves an ultrathin film on the nanoparticle surface that can also be tailored into multilayers by our unique plasma technique. Both the substrate nanoparticle and the ultrathin film serve certain functionalities for specific applications. In this presentation, critical issues in the plasma deposition of thin films on various nanoparticles including carbon nanotubes will be discussed. In particular, a novel application in biosensor area will be presented with recent results on coating of nano magnetic particles. With a thin layer of polymer functional group on the nanoparticle surface, special bio films can be attached for detecting specific virus in food, serving as an effective tool for instant food test.

#### 4:10 PM

Characterization of Mechanically-Milled Nanocrystalline Powders of NiFe and FeCo: *Ian Baker*<sup>1</sup>; Elizabeth Parrish<sup>1</sup>; Basavaraju Shashishekar<sup>1</sup>; <sup>1</sup>Dartmouth College, Thayer Sch. of Engrg., 8000 Cummings Hall, Hanover, NH 03755 USA

Nanocrystalline powders of both NiFe and FeCo were prepared by mechanically alloying of elemental powders using a high energy ball mill. The microstructural evolution was studied as a function of milling time and subsequent annealing using X-ray diffractometry, transmission electron microscopy, scanning electron microscopy and differential scanning calorimtery. The magnetic behavior of the specimens was characterized using both a vibrating sample magnetometer and a magnetic force microscope. A reduction in grain size coupled with an increase in coercivity was observed as function of milling time. Interestingly a decrease in the coercivity below a grain size of 50-100nm, as noted in a number of other soft magnetic alloys by Herzer (G. Herzer, J. Magn. Magn. Mat., 112 258-262, (1992)) was not observed. This research was funded by NIST grant 60NANB2D0120 and NSF grant DMR-0139085.

#### 4:30 PM

Chemical Vapor Synthesis of Iron and Iron Oxide Nanoparticles: Vijay K. Vasudevan<sup>1</sup>; James M. Vetrone<sup>2</sup>; G. R. Bai<sup>2</sup>; Loren J. Thompson<sup>2</sup>; U. Welp<sup>2</sup>; Jeffrey A. Eastman<sup>2</sup>; <sup>1</sup>University of Cincinnati, Chem. & Matls. Engrg., Cincinnati, OH 45221-0012 USA; <sup>2</sup>Argonne National Laboratory, Matls. Sci. Div., Argonne, IL 60439 USA

Iron and iron oxide nanoparticles were synthesized by chemical vapor decomposition of n-butylferrocene precursor gas in a hot-walled deposition system. The effects of variations in reactor chamber pressure, temperature, precursor flow-rate, and oxygen:-nitrogen supply gas ratio on the structure, composition, size and size distribution of the particles were studied. The nanoparticles produced in the reactor chamber were dispersed directly into ethylene glycol without exposure to air, and then characterized by x-ray and electron diffraction, nanoprobe energy-dispersive x-ray spectroscopy, and HRTEM. The results indicate that nanoparticles with diameters ranging from 3 to 40 nm can be produced controllably. Of the different processing variables studied, oxygen content in the flow gas was observed to have the most dominant effect on the structure, composition, and size of the particles. Without oxygen,  $\gamma$ -iron nanoparticles with an fcc structure and diameters of 3-10 nm were observed. The presence of even a small amount of oxygen in the flow gas led to the formation of fcc Fe<sub>3</sub>O<sub>4</sub> (magnetite) nanoparticles, together with core-shell structures consisting of a yiron metallic core surrounded by a shell of iron oxide. With increasing oxygen flow, the nanoparticles were observed to increase in size. Concomitantly, for larger particles the metallic core was found to exhibit the bcc  $\alpha$ -iron structure. At still higher oxygen concentrations, coarse particles of β-Fe<sub>2</sub>O<sub>3</sub> particles were observed, followed by α-Fe<sub>2</sub>O<sub>3</sub> particles. Magnetic properties of nanoparticles synthesized under different conditions were measured. The mechanisms of the synthesis of the nanoparticles and their structure, composition, and magnetic properties will be discussed, as will the potential for self-assembly of these particles into functional architectures.

# 4:50 PM

Dependance of GMR on Film Thickness in Electrodeposited Nanogranular Cu-Co Thin Films: Gyana R. Pattanaik<sup>1</sup>; Steffen Melcher<sup>2</sup>; Ulrich K. Rossler<sup>2</sup>; K. Nenkov<sup>2</sup>; K.-H. Muller<sup>2</sup>; Subhash C. Kashyap<sup>1</sup>; Dinesh K. Pandya<sup>1</sup>; <sup>1</sup>Indian Institute of Technology, Dept. of Physics, Hauz Khas, New Delhi 110016 India; <sup>2</sup>IFW Dresden, Dresden 01171 Germany

Giant magneto-resistance (GMR) in granular thin films is believed to be largely dependent on the spin dependent scattering at the magnetic particle-nonmagentic host interface. At low film thickness, comparable to the spin dependent mean free path, the surface scattering is expected to influence the GMR. In this work we present our attempt to study the GMR and magnetic properties of Cu-Co thin films as a function of film thickness. We have used electrochemical deposition to grow good quality Cu-Co thin films of suitable thickness for the present study. The films were deposited onto Cu-coated (~10 nm) alumina substrates from a single sulfate bath. The thickness of the film was measured by optical as well as stylus techniques and was calibrated with the deposition time. The films were annealed at 425 C for 30 min to optimize the GMR. A maximum GMR of ~15 % was found in thicker film (~ 1 µm) at 10 K. The GMR was found to decrease with the film thickness and the decrease was more rapid for thickness below 100 nm. The ZFC-FC curves indicate that the magnetic particles in the nanogranular films have a range of blocking temperatures (corresponding to a range of sizes) which extends at least to room temperature for films thicker than 100 nm. A combined effect of interparticle interactions and growing magnetic particle size seems to be more likely. The average magnetic particle size estimated from the superparamagnetic behavior (without considering the interaction effects) of the films below a thickness of 100nm was in the range of 8-12 nm and that calculated from XRD line-widths was in the range of 7-9 nm.

# 5:10 PM

Electrical and Magnetoresistance Properties of Hexaferrite FeCo/Fe Nanocomposites Prepared by In Situ Solid-Gas Reduction: *C. Sudakar*<sup>1</sup>; G. N. Subbanna<sup>1</sup>; T. R. Narayanan Kutty<sup>1</sup>; <sup>1</sup>Indian Institute of Science, Matls. Rsch. Ctr., Sir C.V. Raman St., Bangalore, Karnataka 560012 India

Nanocomposites containing Fe or FeCo dispersed in hexaferrites (M, W and Y-phase) are realized by the heterogeneous solid-gas reduction under H2+N2. TEM studies reveal that metal nanoparticles precipitate coherently as thin flakes along the 'a-b' planes of hexaferrite lattice above the characteristic reduction temperature, TR >375°C. complex permittivity and permeability are enhanced with alloy content upto ~50 and ~1.2, respectively, in the broad frequency range of 4-18 GHz and renders these composites useful as broadband electromagnetic microwave absorbers. The electrical resistivity measurements reveal that the charge transport mechanism in the composite is by tunneling, whereas samples having higher fractions of alloy particles show metallic behavior due to percolation. Controlled reduction at TR leads to apparent metal-insulator changeover in r vs. T plot. This changeover persists even in presence of high magnetic field (7T) and is ascribed to the percolation of metal particles due to the difference in the coefficient of thermal expansion between the constituents. Further in the insulator regime, negative magnetoresistance of ~5-6% is observed. These nanocomposites also exhibit non-linearity in the Current-Voltage (I-V) characteristics with a ranging from 1.2 to 1.4 at different temperatures.

# 5:30 PM

 Sudhakar<sup>1</sup>; K. P. Rajeev<sup>1</sup>; <sup>1</sup>Indian Institute of Technology, Dept. of Physics, Kanpur, Uttar Pradesh 208016 India

We report here the interesting results of magneto-transport and electrical resistivity ( $\rho$ ) in the temperature range of 4.2 to 320 K and in the presence of magnetic fields up to 10 T on Ru-doped bilayered manganite system La<sub>1.2</sub>Ca<sub>1.8</sub>Mn<sub>2.x</sub>Ru<sub>x</sub>O<sub>7</sub> (0≤ x≤ 1.0). We find that the Ru-doping is found to affect the magneto-transport properties considerably. The magnetoresistance (MR), defined as [ $\rho$ (B)- $\rho$ (0)]/ $\rho$ (0) has been found to increase with Ru doping from 58% to 64% up to x = 0.1 and decreases marginally to 45% for the x = 1.0 sample. The  $\rho$  (B, T) data were analyzed by fitting the data to the both power law equation  $\rho = \rho_0$  - AB<sup>n</sup> and also to the exponential variations. The isothermal MR versus B curves taken up to ±10 T are highly symmetrical about the y-axis and their curvature changes from concave upwards-like behaviour to that of a parabolic-like one as the temperature increases.

# Nanostructured Materials for Biomedical Applications: Session II

Sponsored by: Electronic, Magnetic & Photonic Materials Division, EMPMD-Thin Films & Interfaces Committee *Program Organizers:* Roger J. Narayan, Georgia Tech, School of Materials Science and Engineering, Atlanta, GA 30332-0245 USA; J. Michael Rigsbee, North Carolina State University, Department of Materials Science and Engineering, Raleigh, NC 27695-7907 USA; Xinghang Zhang, Los Alamos National Laboratory, Los Alamos, NM 87545 USA

Monday PM	Room: 219A
March 15, 2004	Location: Charlotte Convention Center

Session Chairs: Douglas B. Chrisey, Naval Research Laboratory, Plasma Procg. Sect., Washington, DC 20375-5345 USA; J. Michael Rigsbee, North Carolina State University, Dept. of Matls. Sci. & Engrg., Raleigh, NC 27695-7907 USA

#### 2:00 PM Invited

Engineering the Nanobiointerface: The Route to 21st Century Biomaterials: Buddy D. Ratner<sup>1</sup>; <sup>1</sup>University of Washington, UWEB, Dept. of Bioengrg. & Chem. Engrg., Washington Rsch. Foundation, Seattle, WA 98195 USA

Implantable medical devices, and the biomaterials that comprise them, are measured on macro scales (centimeters). Yet the biocompatibility of such devices may be dictated by phenomena best described at nanometer dimensions. Biomedical implants and the NSFfunded University of Washington Engineered Biomaterials (UWEB) Engineering Research Center will be introduced. The classical definition of biocompatibility will be contrasted to a newer definition embracing nanomolecular concepts. Biological data on the in vivo healing responses of mammals to matricellular proteins such as osteopontin, thrombospondin 2 and SPARC will be presented with an emphasis on exploiting the special reactivity of such proteins. First, non-specific protein adsorption must be inhibited. Strategies to achieve this design parameter will be presented. Then methods to deliver the specific protein signals will be addressed. An imprinting approach and a selfassembly approach will be described. Finally, speculation on how such materials that precisely control interfacial biological reactions will be used in medicine will complete this lecture. Modern surface analysis techniques that can address the complexity of a functional nanobiointerface will be highlighted to define nanostructures and probe for order and organization.

#### 2:40 PM Invited

**Complex Behavior of Metal Ions Near Biological Polyelectrolytes**: *Gerard C.L. Wong*<sup>1</sup>; <sup>1</sup>University of Illinois, Matls. Sci. & Engrg., 1304 W. Green St., Urbana, IL 61801 USA

Electrostatics in aqueous media is commonly understood in terms of screened Coulomb interactions, where like-charged objects, such as polyelectrolytes, always repel. These intuitive expectations are based on mean field theories, such as the Poisson-Boltzmann formalism, which are routinely employed in colloid science and computational biology. Like-charge attractions, however, have been experimentally observed in a wide variety of systems. Intense theoretical scrutiny over the last 30 years has suggested that counterions play a central role, but no consensus exists for the precise mechanism. We have examined the organization of multivalent ions on actin filaments (a well-defined biological polyelectrolyte) using synchrotron x-ray diffraction, and discovered a new collective counterion mechanism. We will also present recent results on the influence of counterion valence and dynamics on polyelectrolyte self-organization, and along a more general compass, the implications of entropically controlled electrostatics for problems in biomineralization and biomedical applications.

## 3:20 PM Invited

Nanoshells: Tunable Plasmon-Resonant Nanoparticles With Biomedical Applications: Naomi Halas<sup>1</sup>; <sup>1</sup>Rice University, Elect. & Computer Engrg., MS 366, Houston, TX 77005 USA

Nanoshells are dielectric core-metal shell nanoparticles with a strong resonant optical absorption that can be tuned systematically across the spectrum by varying the relative size of the nanoparticle's core and shell layers. For biophotonic applications, the optical absorption of nanoshells can be tuned to the near infrared "water window", making them extremely strong absorber/scatterers of infrared light in a wavelength region where remarkably few optically active materials are available. When the outer metal layer is made of gold, the nanoparticles become highly biocompatible, and ideal for a wide range of biomedical applications. Together with Rice bioengineering collaborator Jennifer West, we have recently demonstrated a variety of such applications of nanoshells, including a near-instantaneous whole blood immunoassay, a photothermally triggerable drug delivery device, and a highly localized photothermal cancer therapy, which will be described.

#### 4:00 PM Invited

#### **Molecular Simulation of Protein-Surface Interactions**: *Robert A. Latour*<sup>1</sup>; <sup>1</sup>Clemson University, Dept. of Bioengrg., 501 Rhodes Rsch. Ctr., Clemson, SC 29634 USA

The ability to simulate protein-surface interactions provides enormous potential for nanoscale biomaterial surface design. Because of the size of the systems involved, molecular modeling of protein adsorption behavior must be approached using force field-based methods. Force fields, however, are designed for specific applications and they are generally not transferable. Accordingly, a force field designed to represent protein behavior in solution may not accurately represent the adsorption of proteins to surfaces. As a further complication, when it comes to protein adsorption, it is still unclear what molecular behavior a properly tuned force field should even predict. In order to address these complex issues, we are developing complementary experimental and computational methods using model peptide-surface systems to assess existing force fields and modify them if necessary to accurately simulate protein adsorption behavior. An overview of the issues involved and our approach for force field development will be presented.

#### 4:40 PM Invited

Surface Engineering Strategies to Control Cell Adhesion and Function in Biomaterial Applications: *Andres J. Garcia*<sup>1</sup>; <sup>1</sup>Georgia Institute of Technology, Mech. Engrg., 315 Ferst Dr., Atlanta, GA 30332-0363 USA

Cell adhesion to adsorbed proteins or adhesive sequences engineered on surfaces is critical to biomedical and biotechnological applications. Cell adhesion is primarily mediated by integrin receptors. In addition to anchoring cells, supporting cell spreading and migration, integrins provide signals that direct cell survival, proliferation, and differentiation. We have developed two biomolecular strategies for the engineering of surfaces to control integrin binding and cell adhesion in order to direct cell function. The first approach focuses on surfaces presenting well-defined chemistries that control protein adsorption to modulate integrin binding in order to potentiate cell adhesion and bone cell differentiation. In a second approach, we have engineered bioinspired surfaces presenting controlled ligand densities that promote the binding of specific integrin receptors and direct cell adhesive interactions. These surface engineering strategies provide a basis for the rational design of robust surfaces that tailor adhesive interactions.

#### 5:20 PM Invited

Mechanical Behavior of Human Stratum Corneum Tissue: Implications for Transdermal Drug Delivery Technologies: *Reinhold Horst Dauskardt*<sup>1</sup>; Kenneth Wu<sup>1</sup>; Marc Taub<sup>1</sup>; <sup>1</sup>Stanford University, Dept. of Matls. Sci. & Engrg., Bldg. 550, Stanford, CA 94305-2205 USA

The mechanical and fracture behavior of soft tissues is often crucial to their function, with the underlying cellular and extracellular structures being optimized for the required properties. These structures contain microstructural features at length scales ranging from microns to nanometer that profoundly effect their properties. The outermost layer of skin, or stratum corneum (SC), provides mechanical protection and a controlled permeable barrier to the external environment. The mechanical behavior of SC is also important for a range of emerging transdermal drug delivery technologies. For effective drug delivery, good initial and long-term adhesion to SC, clean removability, and skin and drug compatibility are required. However, an understanding of the mechanics and chemical determinants of adhesion to the soft dermal layer, together with quantitative and reproducible test methods for measuring adhesion, are lacking. We present a mechanics approach to study the delamination resistance and mechanical behavior of human SC tissue. The debond energy and cohesive strength characteristics of human SC are described in terms of the underlying cellular and intercellular lipid structures. The effects of hydration, temperature, and lipid-extraction upon SC tissue were explored, and the highly anisotropic nature of SC mechanical and fracture behavior will be discussed with reference to the underlying cellular structure. Implications for emerging transdermal drug delivery technologies is considered.

# Phase Stability, Phase Transformation, and Reactive Phase Formation in Electronic Materials III: Session II

Sponsored by: Electronic, Magnetic & Photonic Materials Division, Structural Materials Division, EMPMD/SMD-Alloy Phases Committee

Program Organizers: C. Robert Kao, National Central University, Department of Chemical and Materials Engineering, Chungli City 32054 Taiwan; Sinn-Wen Chen, National Tsing-Hua University, Department of Chemical Engineering, Hsinchu 300 Taiwan; Hyuck Mo Lee, Korea Advanced Institute of Science & Technology, Department of Materials Science & Engineering, Taejon 305-701 Korea; Suzanne E. Mohney, Pennsylvania State University, Department of Materials Science & Engineering, University Park, PA 16802 USA; Michael R. Notis, Lehigh University, Department of Materials Science and Engineering, Bethlehem, PA 18015 USA; Douglas J. Swenson, Michigan Technological University, Department of Materials Science & Engineering, Houghton, MI 49931 USA

Monday PM	Room: 2	14		
March 15, 2004	Location:	Charlotte	Convention	Center

Session Chairs: Doug Swenson, Michigan Technological University, Dept. of Matls. Sci. & Engrg., Houghton, MI 49931 USA; Rainer Schmid-Fetzer, Technical University of Clausthal, Inst. of Metall., Clausthal-Zellerfeld D-38678 Germany

#### 2:00 PM Invited

Thermodynamic Stability of Nitride Semiconductors (GaN, InN): Rainer Schmid-Fetzer<sup>1</sup>; Jochen Unland<sup>1</sup>; Boguslaw Onderka<sup>2</sup>; <sup>1</sup>Technical University of Clausthal, Inst. of Metall., Robert-Koch-Str. 42, Clausthal-Zellerfeld D-38678 Germany; <sup>2</sup>Polish Academy of Sciences, Inst. of Metall. & Matls. Sci., Reymonta 25, Krakow 30-059 Poland

The comparison of the thermodynamic phase stability of GaN and InN is in the focus of this presentation. Distinct differences are pointed out for these two materials, which are otherwise very similar, both crystallize in their stable form in the wurtzite (hexagonal) structure with P63mc space group. The decomposition of GaN and InN powder was studied experimentally using two different customized thermogravimetric methods, dynamic oscillation TGA, and isothermal stepping TGA for a higher resolution of the decomposition start. A reproducible mass gain at slightly lower temperature is only found for GaN, it suggests the equilibrium temperature to be at  $1110 \pm 10$  K under 1 bar of nitrogen. By contrast, decomposition start of InN was found consistently at 773  $\pm$  5 K, which is considered to be substantially higher than the equilibrium temperature based on our CALPHAD type thermodynamic analysis of all available phase equilibrium and thermodynamic data. This analysis includes the determination of the absolute entropies of GaN and InN based on a Debye- and Einstein-analysis of the experimental data on the heat capacity. An explicit equation for the fugacity-pressure relation of nitrogen, f(P), is developed. This is crucial because f can be several orders of magnitude higher than P for the high pressures encountered during GaN and InN decomposition. Based on the consistent thermodynamic descriptions various T-P-x phase diagrams are calculated. They indicate a good overall agreement between the different types of experimental data (calorimetric, vapor pressure, phase equilibrium) for Ga-N but not for In-N. The highpressure part of the decomposition pressure of GaN is actually predicted from the thermodynamic model in good agreement with the experimental data.

#### 2:20 PM Invited

Interface Reaction Between Ni and Amorphous SiC: Sungtae Kim<sup>1</sup>; J. H. Perepezko<sup>1</sup>; Z. F. Dong<sup>2</sup>; A. S. Edelstein<sup>3</sup>; <sup>1</sup>University of Wisconsin, Dept. of Matls. Sci. & Engrg., 1509 Univ. Ave., Madison, WI 53706 USA; <sup>2</sup>University of Alberta, Dept. of Elect. Engrg., Edmonton, AB T6G 2V4 Canada; <sup>3</sup>US Army Research Laboratory, Sensor Integration Branch, AMSRL-SE-SS, 2800 Powder Mill Rd., Adelphi, MD 20783 USA

Multilayered Ni/amorphous(a)-SiC samples prepared by ion-beam deposition with equal thicknesses of the Ni and a-SiC layers and a wavelength of 100 nm, have been examined to identify the controlling kinetics for reactive diffusion between Ni and a-SiC. In the initial stage of the reaction, a distinct amorphous layer adjacent to the original Ni/ a-SiC interface forms under metastable conditions. The Ni diffusion into the a-SiC layer results in formation of the distinct amorphous layer growing with parabolic growth kinetics. The diffusion of Si and C from the a-SiC phase results in formation of the NiSi phase as an intermediate phase within the original Ni layer. The examination of the amorphous phase stability, by a thermodynamic model for supercooled liquids, reveals a Ni and a-SiC two phase equilibrium at low temperature. The support of ONR (N00014-02-1-0004) is gratefully acknowledged.

# 2:40 PM Invited

**UBM Diffusion and Integrity Studies on Copper/Low-k Dielectrics**: *Seung Wook Yoon*<sup>1</sup>; Vaidyanathan Kripesh<sup>1</sup>; Wenyu Gao<sup>1</sup>; Yong Jie Jeffrey Su<sup>1</sup>; Mahadevan Krishna Iyer<sup>1</sup>; <sup>1</sup>IME, Singapore Sci. Park II, Singapore 1176685 Singapore

As the semiconductor speed increases continuously, more usage of new polymeric low-k dielectric materials to enhance the performance in Cu chip has taken place in last few years. The objective of this study is to investigate the UBM characterization with low-k dielectric material used in damascene copper integrated circuits. This paper focuses on electroless Ni/Au, Cu/Ta/Cu, Cu post and Ti/Ni/Cu/Au UBM fabrication on 8 inch dual damascene Cu wafers and flip chip package reliability with Pb-bearing and Pb-free solders. Diffusion study and bump shear test was carried out to evaluate the bump bonding and interfacial microstructure. In order to investigate the thermal stability of UBM system with various solders, multiple reflow and HTSTwere performed and their each interface between solder and UBM was observed with optical and electron microscopy (SEM and TEM), respectively. Failures observed and mechanisms will be reported in the full paper.

#### 3:00 PM Cancelled

#### Interfacial Reaction of Ni(Ti)/Si0.8Ge0.2 Films

# 3:15 PM

Bulk and Thin Film Studies of the Ni/GaP System: Wai Can Chan<sup>1</sup>; *Douglas J. Swenson*<sup>1</sup>; <sup>1</sup>Michigan Technological University, Dept. of Matls. Sci. & Engrg., 1400 Townsend Dr., Houghton, MI 49931 USA

Gallium phosphide has received interest as a potential material for high temperature microelectronics. It is well known that contact metallizations have a tendency to interact chemically with III-V semiconductors during device processing. Several studies of phase equilibria and chemical reactions between near noble metals and GaP have been reported in the literature; however, to date no such study has been conducted for the common metallization material Ni. In the present study, bulk phase equilibria and reactive thin film phase formation have been investigated in the Ga-Ni-P system. Phase equilibria have been established at 700°C, using X-ray diffraction and electron probe microanalysis. Ni (50 nm) films deposited on GaP(001) substrates were characterized using transmission electron microscopy and Auger electron spectroscopy depth profiling, subsequent to reaction temperatures and times ranging from 25-700°C and 30 seconds to 2 days. respectively. Equilibrium conditions (formation of NiGa and Ni<sub>2</sub>P) are reached after annealing at 500°C for 30 s. Both equilibrium reaction products exhibit orientation relationships with respect to the GaP substrate that are similar to those observed between isostructural metal-III and metal-V compounds and the III-V semiconductors. The diffusion paths exhibited by the Ni/GaP thin film couples are rationalized in terms of diffusion theory and the newly established Ga-Ni-P phase diagram.

#### 3:30 PM

Preparation and Characterization of Sputtered Copper Films Containing Immisicible Tungsten Carbide: Jinn P. Chu<sup>1</sup>; Yung Yen Hsieh<sup>1</sup>; C. H. Lin<sup>2</sup>; T. Mahalingam<sup>3</sup>; <sup>1</sup>National Taiwan Ocean University, Inst. of Matls. Engrg., 2, Pei-Ning Rd., Keelung 202 Taiwan; <sup>2</sup>Chin-Min College, Dept. of Elect. Matls., 110, Syuefu Rd., Toufen Twp., Miaoli 351 Taiwan; <sup>3</sup>Alagappa University, Dept. of Physics, Karaikudi-630 003 India

Since Cu and WC are mutually immiscible, copper films containing tungsten carbide is likely to be a noble material for applications. In this study, Cu-WC, films are prepared by R.F. magnetron sputter deposition technique on glass substrate and then annealed at 200°C, 400°C, 530°C and 650°C for 1 hr. With careful control of processing conditions, the tungsten and carbon concentrations in Cu films can be up to 12.2 and 7.4 at.%, respectively. Nonequlibrium supersaturated solid solutions of WC, in Cu with nanocrystalline microstructures are observed in asdeposited Cu-WC<sub>x</sub> films. Variations in lattice parameters for as-deposited and as-annealed Cu-WCx films evidenced by XRD again indicate that solute tungsten and carbon atoms are in the solid solution with copper. XRD results of Cu-WCx films indicate that Bragg peaks of copper shift to low angle side with increasing tungsten and carbon content. Microstructures of both as-deposited and as-annealed Cu-WCx films are examined by SEM and TEM. Microstructure reveal that finer film grains go with tungsten carbide content. Ultra-microhardness results show an increase in hardness with tungsten and carbon contents for both as-deposited and as-annealed films. Electrical resistivity measurements reveal that resistivity of as-deposited Cu-WC, films increase with tungsten carbide content and decrease with annealing temperature.

#### 3:45 PM Break

#### 4:00 PM Invited

Line Width Dependence of Grain Structure and Stress in Damascene Cu Lines: Young-Chang Joo<sup>1</sup>; Jong-Min Paik<sup>1</sup>; Jung-Kyu Jung<sup>1</sup>; Hyun Park<sup>2</sup>; <sup>1</sup>Seoul National University, Sch. of Matls. Sci. & Engrg., Rm. # 30-503, Seoul 151-744 S. Korea; <sup>2</sup>Seoul National University, Ctr. for Microstructure Sci. of Matls., Rm. #30-503, Seoul 151-744 S. Korea

In damascene Cu lines complicated grain structures were observed because of the grains grown from the bottom as well as the sidewall of the trenches. Furthermore, grain growth in damascene Cu, which confined by dielectric materials, causes a stress due to the annihilation of grain boundaries. Grain structure and stress in 0.13 to 2  $\mu$  damascene lines were analyzed using TEM, EBSD and XRD. For the sub-micron lines, the grain size at the top of trenches was larger than that of inner. It is because the overburden layer affects the grain growth within the trenches and this effect was confirmed by the grain growth simulation using Monte Carlo method. The stress increase as the line width and it is indicated that the stress is related to the microstructure. Through comparing results from experiment and finite element analysis, relationship between microstructure and stress and its dependence on process condition were quantified.

# 4:20 PM Invited

Thermal Stability Study of Sputtered Cu Films with Various Insoluble Elements: J. P. Chu<sup>1</sup>; Chon-Hsin Lin<sup>2</sup>; T. Mahalingam<sup>3</sup>; Y. Y. Hsieh<sup>1</sup>; S. F. Wang<sup>4</sup>; <sup>1</sup>National Taiwan Ocean University, Inst. of Matls. Engrg., No. 2, Pei-Ning Rd., Keelung 202 Taiwan; <sup>2</sup>Chin-Min College, Dept. of Elect. Matls., No. 110, Shyue-Fun Rd., Tou-Fen, Miao-Li 351 Taiwan; <sup>3</sup>Alagappa University, Dept. of Physics, Karaikudi 630 003 India; <sup>4</sup>National Taipei University of Technology, Dept. of Matls. & Minerals Resources Engrg., Taipei 106 Taiwan

Copper is an attractive material for metallization in microelectronics, owing to its low resistivity and high reliability against electromigration compared with Al and its alloys. However, Cu diffuses readily into Si and SiO<sub>2</sub>, resulting in the formation of copper silicide compounds at low temperatures. Doping the Cu with immiscible elements has been investigated in the present study in order to develop new interconnect materials for advanced metallization. The thermal annealing behavior of the insoluble binary Cu-W, Cu-Mo, Cu-C and Cu-Nb alloy films was studied and compared with that of a pure sputtered Cu film. Magnetron co-sputtered copper films deposited on Si substrates with insoluble solute concentration compositions in the range of 2.0-11.3 at% were annealed in vacuum at 200, 400, 530 and 800°C for 1 hr. Twins are observed and they are investigated by means of focused ion beam (FIB) and transmission electron microscopy (TEM) techniques. Thus, according to the FIB and TEM images of as-deposited and 400°C-annealed pure Cu film confirm the existance of twins and the formation of these twins are attributed to the intrinsic low stacking fault energy. Twins existed in pure Cu film and formed during the initial stage of annealing period may provide an additional diffusion path for copper silicide formation. Thermal annealing of Cu-W, Cu-Mo and Cu-Nb alloy films increases the stacking fault energy and results in a low twin density whereas the Cu-C films have no apparent influence on reducing the twin density. The effects of W, Mo, Nb and C on the thermal stability of Cu film were analyzed by X-ray diffraction, secondary ion mass spectroscopy and differential scanning calorimetry and the results are discussed.

# 4:40 PM Invited

Development of Cu-Zn-Al Alloy Sheets with Low Thermal-Expansion Due to Martensitic Transformation and Cold-Rolling: Jijie Wang<sup>2</sup>; Toshio Ohmori<sup>1</sup>; Yuji Sutou<sup>1</sup>; *Ryosuke Kainuma*<sup>1</sup>; Kiyohito Ishida<sup>1</sup>; <sup>1</sup>Tohoku University, Dept. Matls. Sci., Aoba-yama 02, Sendai, Miyagi 980-8579 Japan; <sup>2</sup>Northeastern University, Sch. of Matls. & Metall., Shenyang 110004 China

Recently, we reported that the control of stress-induced (SI) martensitic transformation due to cold working of the Cu-Zn-Al polycrystalline alloy results in low thermal expansion (LTE). This new type of LTE material is easily fabricated by conventional cold-rolling, and the coefficient of thermal expansion (CTE) in the range from about 0 to 32\*10-6 K-1 can be obtained by controlling the reduction ratio. In this paper, the effects of grain size, volume fraction of the  $\alpha$ (fcc) phase in the  $\beta$ (bcc) matrix and thermal stability on LTE properties of Cu-Zn-Al shape memory (SM) alloys induced by cold-rolling were investigated by dilatometry, optical microscopy, differential scanning calorimetry and electric conductivity measurements. The alloys with the larger grains showed a superior two-way memory (TWM) effect, wider LTE temperature intervals with excellent thermal stability under 80°C, and reproducibility. The  $\alpha+\beta$  two-phase alloys also exhibited a good combination of cold-workability and LTEproperties.

# 5:00 PM

#### Bromine and Chloride Induced Degradation of Gold-Aluminum Bonds: Ker-Chang Hsieh<sup>1</sup>; Min-Hsien Lue<sup>1</sup>; Chen-Town Huang<sup>1</sup>; Sheng-Tzung Huang<sup>1</sup>; <sup>1</sup>National Sun Yat-sen University, Inst. of Matls. Sci. & Engrg., Kaohsiung Taiwan

The presence of bromine in flame retardant epoxies accelerates the degradation of gold-aluminum wire bonds. In this study, 5wt% 2,6dibromophenol added in regular molding compound applied in the test samples. The thermal aging treatment was held at 175C and 205C respectively in oven for up to 1008 hours. The intermetallic degrading microstructure examined at different aging period. In order to examine the detail degrading microstructure, bulk AuAl4 and Au5Al2 phases were prepared and reacted with molding compound at 250C. This could help the understanding of degradation mechanism. The analysis of intermetallic phases were examined by the Jeol Superprobe JXA-8900R under WDS mode. A similar chloride degrading study performed by adding Tetrachlorobisphenol A in regular molding compound. The results show that bromine attacked Au4Al phase first and then Au5Al2 phase. The chloride reacted with Au4Al phase only.

#### 5:15 PM

Crystallization and Failure Behaviors of Ta-Ni Nanostructured/ Amorphous Diffusion Barriers for Copper Metallization: Jau Shiung Fang<sup>1</sup>; Giin Shan Chen<sup>2</sup>; 'National Huwei Institute of Technology, Dept. of Matls. Sci. & Engrg., 64 Wunhua Rd., Huwei, Yunlin 632 Taiwan; <sup>2</sup>Feng Chia University, Dept. of Matl. Sci., Taichung 400 Taiwan

This work examines the thin-film properties and diffusion barrier behaviors of thin Ta-Ni films, aiming at depositing highly crystallization-resistant and highly conductive diffusion barriers for Cu metallization. Structure analyzing indicates that the deposited Ta-Ni films indeed have a glassy structure and are free from highly resistive intermetallic compounds, thus giving a low resisitivity of 15.9 mW-cm. Examining Si/Ta-Ni(50nm)/Cu stacked samples by using 4-point probes and XRD reveals that thermally induced failure of amorphous Ta-Ni barriers are triggered by the barrier's crystallization at temperatures around 500°C. The failure temperature for 50 nm Ta-Ni thin film was 650°, which is higher than that of crystallization temperature. The effectiveness of the nanostructure/amorphous Ta-Ni thin film thus can be substantially enhanced by effectively blocking diffusion of copper towards the underlying silicon.

# Processing, Microstructure and Properties of Powder-Based Materials: Session I

Sponsored by: Materials Processing and Manufacturing Division, MPMD-Powder Materials Committee

*Program Organizers:* K. B. Morsi, San Diego State University, Department of Mechanical Engineering, San Diego, CA 92182 USA; James C. Foley, Los Alamos National Laboratory, Los Alamos, NM 87545 USA; Karl P. Staudhammer, Los Alamos National Laboratory, Nuclear Materials Technology Division, Los Alamos, NM 87545 USA

Monday PM	Room: 208B
March 15, 2004	Location: Charlotte Convention Center

Session Chair: Khaled B. Morsi, San Diego State University, Dept. of Mech. Engrg., San Diego, CA 92182 USA

#### 2:00 PM Invited

Modeling of Sintering at Multiple Length Scales: Anisotropy Phenomena: Eugene A. Olevsky<sup>1</sup>; Boris Kushnarev<sup>1</sup>; Veena Tikare<sup>2</sup>; <sup>1</sup>San Diego State University, Mech. Engrg., 5500 Campanile Dr., San Diego, CA 92182-1323 USA; <sup>2</sup>Sandia National Laboratories, Albuquerque, NM USA

Two major approaches in modeling of real sintering processes: (i) microscopic, physically-based, and (ii) macroscopic, phenomenological are combined in order to predict the evolution of realistic microstructures coupled with technologically important macroscopic analysis. Constitutive models of sintering used in finite element computer codes are refined taking into consideration peculiarities of real grain structures. Using the newly developed multi-scale theory of sintering, a new model capable of describing an anisotropic shrinkage under sintering is put forward. The model is based on the consideration of an oriented grain-pore meso-structure. Both grain-boundary and surface diffusion mechanisms of the mass transport are taken into consideration. Based on the model assumptions, the expressions for the effective anisotropic sintering stress and the anisotropic generalized viscosity are derived as functions of material and structure parameters. The obtained multi-scale solutions are compared to the experimental data on sintering of oxide ceramics.

#### 2:20 PM

**Microstructural Evolution During Sintering Nano-Alumina**: Lia A. Stanciu<sup>1</sup>; *Joanna R. Groza*<sup>1</sup>; <sup>1</sup>University of California, Matls. Sci., One Shields Ave., Davis, CA 95616 USA

A laser-flash technique (TOM) was used to evaluate the diameter of the sintering necks formed during the first stage of the consolidation process. The thermal diffusivity of nano-alumina was measured in-situ by the TOM device, in a temperature range between 20 and 1300°C, with a heating rate of 10°C/min. The plot of shrinkage and thermal diffusivity versus temperature was calculated. The increase in thermal diffusivity corresponds to the formation of the sintering necks. Interrupted sintering experiments were performed by Conventional, Microwave and Field Activated Sintering (FAST), followed by measurements of the thermal diffusivity. The growth rate of the sintering neck radius is the largest for the sintering under an electrical field and does not depend on the heating rate, for the heating rates used in this work.

#### 2:40 PM

A Novel Approach to Fabricating Sample Containment Assemblies for Microgravity Materials Processing: Michael Fiske<sup>2</sup>; Ken G. Cooper<sup>1</sup>; Glenn A. Williams<sup>1</sup>; Amir Mobasher<sup>3</sup>; <sup>1</sup>NASA, Marshall Space Flight Ctr., MS ED34, Huntsville, AL 35812 USA; <sup>2</sup>Morgan Research Corporation, Marshall Space Flight Ctr., 4811 A Bradford Dr., Huntsville, AL 35805 USA; <sup>3</sup>Alabama A&M University, Mech. Engrg., PO Box 404, Normal, AL 35762 USA

Over the course of the next decade, NASA has planned the deployment of the Materials Science Research Rack (MSRR), a multi-experiment facility for the International Space Station (ISS). This rack will consist of multiple experiments dedicated to various aspects of materials processing. To date, no requirements for geometrical commonality have been imposed on these furnace systems. Therefore, each of these configurations will require the development of unique Sample Containment Assemblies (SCA). These SCA's can be required to operate at up to 1600°C in inert or vacuum environments. It is very difficult to manufacture refractory metal cartridges with the required length/diameter aspect ratios. Laser Engineered Net Shaping (LENS<sup>TM</sup>) is a unique manufacturing process. The process uses additive fabrication techniques to deposit metal powders and form a fully dense object

**MONDAY PM** 

directly from computer-generated drawings. MSFC has one of these LENS<sup>™</sup> systems, and this paper discusses the status of a project to demonstrate that hermetic (non-porous) Sample Containment Assemblies of refractory metal alloys can be fabricated using Laser Engineered Net Shaping at a substantial time or cost savings over the currently employed techniques of Chemical Vapor Deposition (CVD) and Vacuum Plasma Spray (VPS).

#### 3:00 PM

#### Investigation of Laser-Clad W-Cu Composite Coating: Sheng-Hui Wang<sup>1</sup>; Lijue Xue<sup>1</sup>; <sup>1</sup>National Research Council of Canada, Integrated Mfg. Tech. Inst., 800 Collip Cir., London, Ontario N6G 4X8 Canada

Tungsten-copper composite is widely used as heavy-duty electrical contactors and discharging electrodes. Typically, the whole component is fabricated by P/M methods, such as liquid phase sintering and infiltration of liquid copper into a porous-sintered tungsten skeleton. In practice, however, only the surface layer of the component is often subjected to harsh working condition and, therefore, W-Cu composite surface coating may be more effective and economical. In other cases, damaged electrodes may be easily repaired by local deposition of the composite. This opens up a potential application for laser cladding process. In this study, the feasibility of fabricating W-Cu composite overlay is examined by laser cladding with blown powder technique. Nickel addition is used to increase the wettability between tungsten powders and copper melt during the deposition and, thus, the interfacial binding between tungsten particles and the copper substrate. The microstructure and properties, in particular, the abrasion resistance, of the composite coating are investigated and discussed.

#### 3:20 PM

Study of Process Induced Residual Stresses in Laser Clad IN-625 Superalloy and P20 Tool Steel: J.-Y. Chen<sup>1</sup>; L. Xue<sup>1</sup>; <sup>1</sup>Integrated Manufacturing Technologies Institute, National Research Council Canada, 800 Collip Cir., London, Ontario N6G 4X8 Canada

A blown powder laser cladding technique was used to deposit IN-625 superalloy on wrought IN-625 substrate and P20 tool steel on wrought P20 substrate. The former had no solid-state phase transformation during the cooling down while the latter experienced a martensitic transformation instead. Due to thermal and/or mechanical incompatibility between the clad layer and the substrate, significant amount of residual stresses could be introduced into the clad part by the process, which may adversely affect its mechanical properties and dimensional stability. A series of stress-relief heat treatments were performed on both clad specimens in order to change their characteristics of the residual stresses, which were evaluated using a hole-drilling method. The microstructure evolution in the laser clad IN-625 and P20 specimens after the heat treatments was also examined using optical microscope, SEM/EDS and XRD techniques. Moreover, their implications on the mechanical properties of the clad parts will also be addressed.

# 3:40 PM Break

#### 3:50 PM

#### Increased Toughness of High Temperature Aluminum Alloys: William J. Golumbfskie<sup>1</sup>; <sup>1</sup>Pennsylvania State University, Dept. of Matls. Sci. & Engrg., University Park, PA 16802 USA

The tensile properties and fracture toughness of two spray formed Al-Y-Ni-Co alloys were measured and correlated with their resultant microstructures. Significant differences in mechanical properties were observed with respect to microstructural by altering the secondary processing parameters and/or composition. The microstructure of the spray formed alloys consists of a large volume fraction of intermetallic particles distributed in an aluminum matrix. The information of the structure-property relationship has been coupled with a computational thermodynamic modeling of quaternary alloy system in an attempt to better determine a specific composition range and set of processing conditions to produce an improved toughness at room temperature while retaining high temperature strength.

#### 4:10 PM

In Situ Processing of TiC/TiN-Fe (Ti) Nanocomposites by Thermal Plasma: Lirong Tong<sup>1</sup>; Ramana G. Reddy<sup>1</sup>; <sup>1</sup>University of Alabama, Dept. of Metallurgl. & Matls. Engrg., PO Box 870202, Tuscaloosa, AL 35487 USA

A novel in situ processing technique of nanocomposite powders of Titanium Carbide/Titanium Nitride Iron (Titanium) alloys by thermal plasma was developed to investigate vaporization of raw materials, synthesis of TiC/TiN and solidification of TiC/TiN-Fe(Ti) nanocomposites from supersaturating vapor. A basic understanding of thermodynamics of synthesis of TiC/TiN, temperature profile and velocity distribution within reactor and vapor saturation of TiC/TiN is essential for quantitative predictions of characteristics of in situ synthesized TiC/TiN-Fe (Ti) nanocomposites. The paper presents thermodynamic analysis for predicting conditions of synthesis and recovery ratio of TiC/TiN. A mathematic model was developed for describing temperature profile and velocity distribution within the reactor. The model is applied to predict feeding rate, design in situ processing system of TiC/TiN-Fe(Ti) nanocomposites and calculate the final size of TiC/TiN-Fe(Ti) nanocomposite powder. The model predictions were found to be in reasonable agreement with experimental data for this system.

#### 4:30 PM Cancelled

#### Microstructure, Properties and Switching Behavior of Silver/ Graphite Electrical Contact Material Fabricated by Applying Nanotechnology

#### 4:50 PM

Effect of Rare Earth Oxide Concentrates on Oxidation Behavioir of AISI 304L Stainless Steel: Lalgudi V. Ramanathan<sup>1</sup>; Marina Fusser Pillis<sup>1</sup>; Edival D. de Araujo<sup>1</sup>; <sup>1</sup>Instituto de Pesquisas Energeticas e Nucleares-IPEN, Matls. Sci. & Tech. Ctr., Av. Prof. Lineu Prestes 2242, Cidade Universitaria, São Paulo 05508-000 Brazil

Rare earths are often added to chromia forming alloys to improve high temperature oxidation resistance. Rare earths can also be added as oxide dispersions to alloys, to enhance oxidation resistance. Significant cost reductions are possible if rare earth concentrates can be used instead of pure rare earth oxides, the former being a stage earlier in the process to obtain pure rare earth oxides. In this study the effect of adding pure rare earth oxides and rare earth concentrates to AISI 304L on its oxidation behavior has been evaluated. AISI 304L stainless steel powder compacts containing 2vol% of high purity rare earth oxides or a concentrate with lanthanum and yttrium oxides were prepared by mixing the different powders in a vibratory mill followed by pressing. The compacts thus obtained were sintered in a vacuum furnace. Isothermal oxidation measurements were carried out in air for up to 200h at 900°C. The parabolic oxidation rate constants were calculated. The reaction products were examined using various techniques such as SEM, EDS and XRD. The compacts with high purity rare earth oxides and those with the mixed rare earth concentrates exhibited similar oxidation rates.

#### 5:10 PM

The Influences of RE (Rare Earths) Oxides on Microhardness and Microstructure of Laser Cladding Layer of Co Based Powder: Jianjun Ding<sup>1</sup>; Feiqun Li<sup>1</sup>; Mon-Yu Wei<sup>2</sup>; <sup>1</sup>Shanghai Jiao Tong University, Coll. of Matls. Sci. & Engrg., 1954 Huashan Rd., Shanghai 200030 China; <sup>2</sup>Ta Hwa Institute of Technology, 1,Ta Hwa Rd., Chiung-Lin, Hsin-Chu Taiwan, China

In order to tap ulteriorly the potential of laser cladding layer in microstructure and property, the RE oxides were adopted by mixing with Co based powder as an addition in cladding materials. The experimental results indicate that the microhardness of laser cladding layers of Co based powder with 5wt% RE oxide Yb2O3 has an obvious enhancement and the corresponding microstructures are more fine compared with that without RE oxide addition under same laser processing conditions. Based on the above advantages come from RE oxide additions, it may lead to improving the properties of laser cladding layer in wearability and corrosion resistance and to decreasing microcracking trend of to a degree.

# MONDAY PM

# Recent Advances in Non-Ferrous Metals Processing: Sustainable Development

Sponsored by: Light Metals Division, LMD-Reactive Metals Committee, EPD-Waste Treatment & Minimization Committee Program Organizers: Brajendra Mishra, Colorado School of Mines, Kroll Institute for Extractive Metals, Golden, CO 80401-1887 USA; John N. Hryn, Argonne National Laboratory, Argonne, IL 60439-4815 USA; V. I. Lakshmanan, Ortech Corporation, Mississauga, Ontario L5K1B3k Canada; V. Ramachandran, Scottsdale, AZ 85262-1352 USA; Alton T. Tabereaux, Alcoa Inc., Process Technology, Muscle Shoals, AL 35661 USA

Monday PMRoom: 205March 15, 2004Location: Charlotte Convention Center

Session Chair: V. I. Lakshmanan, Process Research ORTECH Inc., Mississauga, ON L5K 1B3 Canada

# 2:00 PM Opening Remarks

# 2:05 PM

**Developing Sustainable Resource Recovery and Recycling**: *Michael Clapham*<sup>1</sup>; <sup>1</sup>Natural Resources Canada, Resource Recovery & Recycling, Minerals & Metals Sector, 580 Booth St., Ottawa, Ontario K1A 0E4 Canada

This paper will explore issues to be addressed in the development of resource recovery and recycling initiatives, which lead to significant increases in the recovery of products and materials at end-of-life. Taking a life cycle approach the paper will explore how issues such as design for environment, consumption patterns, sustainable markets for recovered products, infrastructure, policy mechanisms and technology can influence recovery rates. The benefits of increased recovery, such as materials and energy efficiencies, reduced burdens to land-fill, green house gas emissions and social implications will be discussed. Examples of Canadian activities within the resource recovery and recycling sector will be provided.

# 2:35 PM

The Environmental and Human Health Risk Communication Theory and Practice: B. R. Conard<sup>1</sup>; <sup>1</sup>INCO Limited, Environml. & Health Scis., 145 King St. W., Ste. 1500, Toronto, Ontario L5H 4B7 Canada

The framework of risk assessment and risk management for inorganic substances is steadily gaining ground in its ability to cost – effectively deal with judging the health outcome severity and probability of exposure to a hazardous material. The issue of the safe use of metals and their compounds is important to workers in production and downstream customer occupations, to neighbors of industrial facilities, and to general population of consumers of products. A critical but often marginalized component of risk assessment is risk communication. Communication between humans is fraught with challenges in any area, but is even more difficult when the subject is health risks that are scientifically and medically complex. Discussion will focus on common mistakes in this area by large corporations in the past and with real examples, indicate directions that have been successful in closing the gap between industry's performance and society's expectation.

#### 3:05 PM

**Technological Cycles of Metals: Are They Sustainable?**: *R. B. Gordon*<sup>1</sup>; T. E. Graedel<sup>1</sup>; B. Reck<sup>1</sup>; <sup>1</sup>Yale University, Kline Geology Lab., PO Box 208109, New Haven, CT 06520-8109 USA

Rate of use of most of the industrial metals increased dramatically in the last quarter of the 21st century. This trend cannot be sustained indefinitely without the utilization of metals in discarded products. We have completed the characterization of technological cycles of copper, silver and zinc at country, region and planetary spatial levels. We have also completed a study of the copper cycle in N. America for the entire 20th century, including stocks in use and discard and recycling rates. All of this allows us to determine rates of recycling and reuse for various discard streams - electronics, vehicles, industrial products and so forth. Of these three metals, silver has the highest recycling rate, reflecting both its intrinsic value and its predominant use in photographic films. Copper is also effectively recovered, especially from electrical and electronic equipment and from end of life vehicles. The recycling of zinc, being predominantly used as a sacrificial coating for steel, is problematic. Results will demonstrate differences in the metal cycles in different world regions and in different epochs.

# 3:35 PM Break

#### 3:50 PM

Sustainable Development – The Role of Waste Minimization and Recyclables: V. I. Lakshmanan<sup>1</sup>; R. Sridhar<sup>1</sup>; R. Ramchandran<sup>2</sup>; <sup>1</sup>Process Research ORTECH Inc., 2395 Speakman Dr., Mississauga, ON L5K 1B3 Canada; <sup>2</sup>RAM Consultants, 9650 E. Peregrine Place, Scottsdale, AZ 85262 USA

Sustainable industries continuously seek to obtain aggressive economic advantages together with environmental and resource conservation benefits. As a major player in the global resource industries sector, Canadian mining and metallurgical industries, provide opportunities for technology transfer in process and product development to treat recyclables and minimize waste generation. Integrated process developments with recyclables contribute to green house gas emission reductions. The paper with selected examples will discuss synergy between major mining and metallurgical industries with end users in the building materials, automotive and electronic industries.

# 4:20 PM

**Demonstrating Corporate Social Responsibility**: *Bob White*<sup>1</sup>; <sup>1</sup>BRI International Inc., 2570 Matheson Blvd. E., Ste. 110, Mississauga, ON L4W 4Z3 Canada

This paper will provide an overview of Corporate Sustainability and Social Responsibility (CSR) in terms of: · What it is? · Who and why private and public sector organizations are moving toward CSR? · A framework that will allow an organization to demonstrate commitment to CSR. The paper starts by providing a broad definition of CSR and the difference between CSR and corporate governance. This definition will provide an opportunity to understand just how complex CSR is and how difficult it is to achieve and sustain a process for CSR. The paper will also introduce information on the drivers for CSR, the threats and opportunities. The threat associated with increasing demands to demonstrate CSR, by people that have a significant influence over the organization. The opportunities related to using a framework for CSR to contribute to achieving sustainable development and competitive advantage in the face of increasing globalization and trade liberalization. It will explore the link among sustainable economic, social and environmental development; and CSR. The important benefits of CSR, including the economic, financial, market share, environmental and social aspects. Finally, the paper will describe how an integrated management system based on the best practices defined in international management system standards and models can be used to demonstrate commitment and obtain the sustainable benefits of CSR.

# Recycling: Aluminum and Aluminum Dross Processing

Sponsored by: Light Metals Division, Extraction & Processing Division, LMD/EPD-Recycling Committee Program Organizer: Gregory K. Krumdick, Argonne National Laboratory, Argonne, IL 60439 USA

Monday PM	Room: 2	217D
March 15, 2004	Location:	Charlotte Convention Center

Session Chairs: Ray Peterson, IMCO Recycling, Rockwood, TN 37854 USA; Angela Withers, IMCO Recycling, Rockwood, TN 37854 USA

# 2:00 PM

Worldwide Aluminum Scrap Supply and Environmental Impact Model: Paul R. Bruggink<sup>1</sup>; Kenneth J. Martchek<sup>2</sup>; <sup>1</sup>Alcoa Inc., Alcoa Tech., 100 Technical Dr., Alcoa Ctr., PA 15069-0001 USA; <sup>2</sup>Alcoa Inc., EHS Services, 201 Isabella St., Pittsburgh, PA 15212-5858 USA

A quantitative tool has been developed for the Global Aluminium Recycling Committee of the International Aluminium Institute to better describe the past and to better characterize the future mix of primary and recycled global aluminum metal supply. The model provides a better understanding of worldwide aluminum recycling flows by comparing annual regional and global statistics on primary and recycled aluminum processing with anticipated annual recycled aluminum supply predicted on the basis of regional and market product net shipments, average product lives, collection and recovery rates. Furthermore, the model permits investigations of the sensitivities of changes in scrap collection, recovery rates, and product lifetimes on the worldwide supply system. The model has also been used to identify gaps in recycling data and areas of greatest potential for increased recycling and reduced environmental effects. As an example, the paper will highlight the model's use for examining the potential impact of aluminum recycling and product lifetime assumptions on the greenhouse gas implications of the global aluminum industry through year 2010.

# 2:25 PM

# Modeling the Impact of Recycling on the Total U.S. Aluminum Supply and on the Industry's Energy Requirements: *William T. Choate*<sup>1</sup>; John A.S. Green<sup>2</sup>; Brian J. Copeland<sup>1</sup>; <sup>1</sup>BCS, Incorporated, 5550 Sterrett Place #306, Columbia, MD 21044 USA; <sup>2</sup>Aluminum Industry Consultant, 3712 Tustin Rd., Ellicott City, MD 21042 USA

The future availability of aluminum scrap will have an impact on the supply of recycled metal and the energy intensity of the aluminum industry. Recycled aluminum now accounts for nearly a third of the U.S. metal supply. The growth of recycling is due not only to economics but in part to a greater awareness of the energy savings and emission reductions associated with recycling aluminum. A model of the scrap metal supply has been built by the authors using the past 40 years of statistical data for the major aluminum markets. The model assigns life cycles assumptions to each product and then is used to evaluate the recycling metal supply through 2020. This paper discusses future trends in metal supply (surplus or shortfall) in the light of the model assumptions and results.

#### 2:50 PM

**Process Modelling of Aluminium Scraps Melting**: Bo Zhou<sup>1</sup>; Yongxiang Yang<sup>1</sup>; *Markus A. Reuter*<sup>1</sup>; <sup>1</sup>Delft University of Technology, Applied Earth Scis., Mijnbouwstraat 120, Delft 2628 RX The Netherlands

In a secondary aluminium recovery, aluminium scraps are melted and refined often in a rotary melting furnace. The feed is normally a complex combination of aluminium scraps with different sizes, shapes, compositions, paintings and other contaminations. During the process, the scraps are charged into the rotary furnace, passing through a molten salt layer, and melting in a bottom aluminium bath. Efficient melting of the scraps in the molten melt is a critical issue in the secondary aluminium industry. To study the scrap melting behavior, a furnace model has been developed based on a Computational Fluiddynamics (CFD) framework, coupled with user developed aluminium melting sub-model. The furnace model consists of a gas region with turbulent flow and combustion as well as radiative heat transfer in the upper part of the furnace, and a solid-liquid region of salt and aluminium metal in the lower part of the furnace. The aluminium melting model was developed for a single particle in the molten salt and aluminium melt based on the experimental study and heat transfer theory. In the melting model, solid aluminium melting, salt shell formation and re-melting on the metal solids were included. To represent the distributed nature of the scrap feed, aluminium scraps were classified into several groups depending on their properties, e.g. size of the scraps. The melting sub-model was subsequently modified from the numerical model for a single aluminium particle to the multi-particle system. Aluminium melting behavior was calculated with the exchange of information between the melting sub-model and the CFD combustion space. Heat sink due to scrap melting, was calculated by the submodel and fed back to the CFD combustion space model. Gas flow and temperature distribution in the top combustion space of CFD model were used to calculate the melting rate of aluminium scrap in the submodel.

# 3:15 PM

**Developments in Automatic Sorting and Quality Control of Scrap Metals**: Marian-Bogdan Mesina<sup>1</sup>; Tako P.R. de Jong<sup>1</sup>; *Wijnand L. Dalmijn*<sup>2</sup>; <sup>1</sup>Delft University of Technology, Resource Engrg., Mijnbouwstraat 120, Delft 2628 RX The Netherlands; <sup>2</sup>Delft University of Technology, Faculty of Design, Engrg. & Production, Mekelweg 2, Delft 2628 CD The Netherlands

Despite the advantages of mechanical systems and hand picking, which until today are extensively used for scrap metal sorting, the quality of the product can be considerably improved when sensor based systems are used. Advanced data processing and the combination of different sensors are expected to gain in importance in future applications, and increase the automation of sorting. At Delft University of Technology new methods using sensors have been investigated for sorting and quality control of scrap non-ferrous metals. A prototype system was developed for the identification and separation of scrap metals using electromagnetic and dual energy X-ray sensors. Recently developed actuator design enables sorting into more than three fractions of particles that are randomly orientated on a flat conveyer belt. The main parts of the automatic system and the experimental results are reported. In addition, the possibilities to integrate such sensors into an industrial plant are discussed.

# 3:40 PM Break

# 3:55 PM

**DROSRITE Extensive On-Site Hot Dross Treatment Tests**: *Michel G. Drouet*<sup>1</sup>; <sup>1</sup>Pyrogenesis Inc., 2000 William St., Ste. 200, Montréal H3J 1R4 Canada

DROSRITE is a salt-free process for the recovery of metal from dross. In addition to producing a salt-free residue, it does not produce any CO2 or Nox gases. The process is highly energy efficient, extracting heat from energy in the residue and, thus, it does not require any external heat source such as a plasma torch, an electric arc or a gas or an oil burner. A DROSRITE pilot unit built by Pyrogenesis was used, in early 2003, for a two months extensive series of fifty tests on the site of a large aluminum smelter in Europe. All the different types of dross produced at the site were tested. Hot dross, charged into the DROSRITE furnace, was treated without any external heat input. Results of this extensive industrial trial will be presented together with analysis of both the input dross and the output residue. The economic analysis will also be presented.

#### 4:20 PM

Formalization of Concerts of the Processes Occurring in Melting Aluminum Rejects at Rotor Furnaces: A. G. Zholnin<sup>1</sup>; S. B. Novichkov<sup>2</sup>; A. G. Stroganov<sup>1</sup>; <sup>1</sup>MOPM, city of Voskresensk Russia; <sup>2</sup>Russkiy Aluminiy, Prokatniy Div., Moscow Russia

The experience of re-melting aluminum at the rotor inclined furnaces (RIF) showed that the current level of understanding is not sufficient to explain the observed effects and control them deliberately. Certain uncontrolled losses of metal result from that. The attempts to optimize the economic parameters (to reduce the melting time, reduce the amount of the used fluxing agent) from relatively rich aluminum raw materials (50 and more percent of metal) sometimes result in nothing. In the language of metallurgists it is called the 100% melting loss. It is implied that all the metal has burned out, i.e. has passed into an oxide state. In fact it was found out in the studies of the refused slag that the most part of the metal is left in slag in the form of small spherical drops covered with the oxide film. Such effects made it necessary to pay more attention to the processes, occurring in this situation. The presented work is an attempt of further development of the concepts of processes of melting at the RIF, w hich were published earlier.<sup>1,2</sup> The phenomenological model proposed for consideration is the result of generalization of visual observation of the processes of re-melting different types of aluminum raw materials at the rotor inclined furnaces and the analysis of the results of the laboratory researches of the initial raw materials, refused slag and dust in the exhaust gases. The stated fact is mainly related to melting different types of aluminum rejects in the mode of «dry» melting with lower amount of the fluxing agent when secondary dross is in the loose dispersed state. In the process of melting in the environment of permanently mixed furnace feed the solid aluminum can pass into different states and simultaneously be in an oxide form, small tailing, drops, mess and swamp and be removed with the exhaust gases in the form of dust and volatile compounds formed in the result of chemical interaction of aluminum with the fluxing agents. In the model are considered certain possible reactions of transition of the metal from some states to other ones at different stages of melting for different types of raw materials. The reactions determining the process of melting of different types of raw materials were tabulated. The qualitative description of the processes occurring in the furnace feed during the process of melting aluminum raw materials at the rotor furnaces is the first step in the way of development of the theory of re-melting aluminum raw materials. The next stage should be a mathematical description of each reaction of the transition. It will require theoretical investigation, as well as experimental researches for refinement of the parameters or examination of certain aspects. <sup>1</sup>A.G. Zholnin, Ñ.B. Novichkov. A model of the physicochemical processes occurring in melting aluminum rejects in the rotor furnaces. Collection of Proceedings of the VII International conference "Aluminum of Siberia -2001", 10-12 September, Krasnoyarsk, 2002, p. 225-228. <sup>2</sup>A.G. Zholnin, Ñ.B. Novichkov. Mechanism of transition of aluminum from slag to «swamp» in the process of re-melting aluminum rejects at the rotor furnaces. Non-ferrous metallurgy, Moscow, 2003, .11, p. 22-27.

#### 4:45 PM

Peculiarities of Melting Aluminum Slag in a Laboratory Inclined Rotor Furnace: A. G. Zholnin<sup>1</sup>; A. E. Zakharov<sup>1</sup>; S. B. Novichkov<sup>2</sup>; A. G. Stroganov<sup>1</sup>; <sup>1</sup>MOPM, city of Voskresensk Russia; <sup>2</sup>Russkiy Aluminiy, Prokatniy Div., Moscow Russia

In this work are presented the results of melting aluminous dross at a laboratory rotor inclined furnace (LRIF) described in the work.<sup>1</sup> It was studied the impact on the melting process of the amount of the added fluxing agent, the fluxing agent composition, the furnace speed of rotation, the temperature of pouring, the content of dust in the slag and the impact of moisture and time of storing on the metal output. As the output parameters of the process, the weight of the poured out metal, the weight of the refused dross and the breakup of beads left in dross after pouring out the metal were controlled. All the beads with the diameter over 1mm were picked up. The smaller particles of aluminum have been left beyond our control. The screening of aluminous dross with the maximum size of particles of 20 mm and the metal content about 50% was used as a raw material. The mixtures based on sodium and potassium chlorides with the cryolite admixture. 1.5-2 kg of dross was loaded into each melting. The speed of rotation in most cases, excluding those, which were specially stipulated, was 2.5 rpm. It was established that there is a minimum amount of the fluxing agent, below which the molten pools are not formed. The metal is left in the dross in the form of beads. The influence of the proportion of sodium and potassium chlorides on the metal output is weak. The cryolite admixtures are efficient only for small amounts of the fluxing agent. The increase of the furnace speed of rotation under high content of the fluxing agent facilitates coalescence, and under low content of the same it strengthens the effect of breaking the drops. The isothermal soaking of the furnace feed before pouring out renders an ambiguous effect. The increase of the content of dust fraction in dross in the process of melting in the «dry fluxing agent» mode facilitates breaking of the beads and the decrease of the metal output. The content of magnesium in the alloy depends on the dross consistence, its decrease may be an indicator of quality of melting. The performed researches showed the efficiency of using laboratory furnaces for finding out the mechanisms of melting aluminum raw materials in RIF. It is natural that the obtained results cannot be automatically extended to the large dimension industrial furnaces because of the existence of the scale factor.2 But the found out mechanisms of melting permit to give certain specific recommendations and may be useful for the development of the technology of melting dross at the rotor inclined furnaces. <sup>1</sup>D.Ì. Zakharenko, A.G. Zholnin, Ñ.B. Novichkov, A.G. Stroganov. A laboratory rotor inclined furnace for re-melting the secondary aluminum raw materials. Nonferrous metallurgy, Moscow, 2003, 12, p. 26-33. <sup>2</sup>A.G. Zholnin, Ñ.B. Novichkov. The role of the scale factor in the process of re-melting the secondary aluminum raw materials at the rotor inclined furnaces. Nonferrous metallurgy, Moscow, 2002, 111, p. 28-31.

# R.J. Arsenault Symposium on Materials Testing and Evaluation: Session II

Sponsored by: Structural Materials Division, SMD-Mechanical Behavior of Materials-(Jt. ASM-MSCTS), SMD-Nuclear Materials Committee-(Jt. ASM-MSCTS)

*Program Organizers:* Raj Vaidyanathan, University of Central Florida, AMPAC MMAE, Orlando, FL 32816-2455 USA; Peter K. Liaw, University of Tennessee, Department of Materials Science and Engineering, Knoxville, TN 37996-2200 USA; K. Linga Murty, North Carolina State University, Raleigh, NC 27695-7909 USA

Monday PM	Room: 2	11A
March 15, 2004	Location:	Charlotte Convention Center

Session Chairs: K. Linga Murty, North Carolina State University, Coll. of Engrg., Raleigh, NC 27695-7909 USA; Raul B. Rebak, Lawrence Livermore National Laboratory, Chmst. & Matls. Sci., Livermore, CA 94550 USA

#### 2:00 PM Invited

#### Use of Multiple Material Characterization Techniques to Study Precipitation Kinetics of Copper in HSLA Steel: Chandra Shekhar Pande<sup>1</sup>; <sup>1</sup>Naval Research Lab, Code 6325, Washington DC USA

Precipitation kinetic of copper in a high strength low carbon ferrous alloy has been studied in the past by field ion microscopy. These precipitates being initially coherent with the matrix are difficult to detect by convention transmission electron microscopy (TEM). We have therefore used TEM in conjunction with small angle neutron scattering (SANS) to study copper precipitation. Direct measurement from TEM micrographs and integral transform of the SANS data was used to calculate the size distribution for a variety of aging conditions. Possible role of another electron optical technique viz electron energy loss imaging was also explored.

## 2:30 PM

Thermal Aging Studies on Mechanical and Fracture Characteristics of 1Cr1M00.25V Steel Using Ball Indentation, Ultrasonic Attenuation and Electrical Resistivity Techniques: Chang-Sung Seok<sup>1</sup>; Jeong-Pyo Kim<sup>1</sup>; Bong-Kook Bae<sup>1</sup>; K. L. Murty<sup>2</sup>; <sup>1</sup>Sungkyunkwan University, Sch. of Mech. Engrg., 300 Chunchun-dong, Jangan-gu, Suwon, Kyonggi-do 440-746 Korea; <sup>2</sup>North Carolina State University, PO Box 7909, Raleigh, NC 27695-7909 USA

Effect of thermal aging on mechanical and fracture characteristics of 1Cr-1Mo-0.25V steel was investigated following heat treatment at 630C (903K) for varied times up to 1820 hours (~75 days). Tensile and fracture (K1C) tests were performed at ambient before and following thermal aging that indicated decreased strength and fracture toughness (KQ) with corresponding increase in ductility. Microstructure of the aged material revealed coarsening of carbides and precipitates. Yield and tensile strengths derived from ball indentation tests on the as-received and aged samples were in close agreement with the tensile data. In addition, the indentation energy to fracture (IEF) revealed similar trends as per the fracture toughness although no one-to-one correlation was noted. Electrical resistivity determined using 4-point DC potential drop method, decreased with thermal aging very similar to the strength and hardness. A linear correlation was observed between the resistivity and strength while a parabolic curve was noted when it was compared with fracture toughness. Ultrasonic tests yielded results on the attenuation coefficient and nonlinear parameter that increased with aging time. While the ultrasonic data correlated linearly with the uniform strain, an inverse relation was observed with fracture toughness. These studies reveal the usefulness of ball indentation technique to inquire into aging characteristics of the steel thereby indicating the possible application for on-line interrogation of the steel structures. Both the resistivity and ultrasonic methods are shown to be applicable for non-destructive characterization and condition monitoring of the structures fabricated with this steel.

#### 2:50 PM

**Corrosion Testing of Nickel and Titanium Alloys**: Kenneth J. Evans<sup>1</sup>; Lana L. Wong<sup>1</sup>; *Raúl B. Rebak*<sup>1</sup>; <sup>1</sup>Lawrence Livermore National Laboratory, Chmst. & Matls. Sci., 7000 East Ave., L-631, Livermore, CA 94550 USA

Titanium (Ti) and Nickel (Ni) alloys are highly resistant to corrosion and are therefore extensively used in industrial applications such as in the chemical process industry. Both families of alloys also find important applications in the nuclear power generation and in the nuclear waste disposal. When Ti and Ni alloys are exposed to aggressive conditions, they may fail by the three major mechanisms of general corrosion, localized corrosion and environmentally assisted cracking. To assess each type of failure mode, a number of testing methods may be used. This review will compare corrosion testing methods used to assess the corrosion behavior of several Ti and Ni alloys in different types of environments including solution composition, temperature and applied potential.

## 3:10 PM

Non-Destructive and Microstructural Characterization of Thermal Barrier Coatings: Vimal Desai<sup>1</sup>; Y. H. Sohn<sup>1</sup>; <sup>1</sup>University of Central Florida, AMPAC, Box 162455, Orlando, FL 32816-2455 USA

The durability and reliability of thermal barrier coatings (TBCs) play an important role in the service reliability and durability of hotsection components in advanced turbine engines. Electrochemical impedance spectroscopy (EIS) and photostimulated luminescence spectroscopy (PSLS) are being concurrently developed as a complimentary non-destructive evaluation (NDE) techniques for quality control and life-remain assessment of TBCs. This talk will overview the relative changes in the impedance and luminescence examined in terms of resistance (or capacitance) of TBC constituents, residual stress and phase constituents in thermally grown oxide scale. Results from NDE by EIS and PSLS will be discussed in the light of microstructural development during high temperature oxidation, using a variety of micro-scopic techniques including focused ion beam in-situ lift-out (FIB-INLO) and scanning transmission electron microscopy (STEM).

#### 3:30 PM Break

#### 3:50 PM

Scanning Pyrometry from Digital Color Imaging: Nathan Rolander<sup>1</sup>; Douglas M. Matson<sup>1</sup>; <sup>1</sup>Tufts University, Mech. Engrg., 025 Anderson Hall, 200 College Ave., Medford, MA 02155 USA

High-speed color digital images are formed using Bayer demosaicking schemes to interpolate color from an array of filtered sensors. By

suppressing this data smoothing protocol, individual sensors within the color filter array can be used as one-color pyrometers and a generate a thermal scan to obtain temperature as a function of position within the camera view. Differential channel amplification (red-greenblue) can provide greater thermal resolution. A calculation of signalto-noise for each channel is used to measure the responsivity as a function of wavelength. Analyses of resultant thermal histograms shows a precision of +/-3 degrees in the investigation of rapid solidification behavior of metal alloys.

#### 4:10 PM Cancelled

#### Thermography and X-Ray Detection on the Evolutions of Lüders Bands During Mechanical Testing

#### 4:30 PM

Watching Stress-Strain Evolutions During Low-Cycle Fatigue by Thermography: *Bing Yang*<sup>1</sup>; Peter K. Liaw<sup>1</sup>; J. Y. Huang<sup>2</sup>; R. C. Kuo<sup>2</sup>; J. G. Huang<sup>3</sup>; <sup>1</sup>University of Tennessee, Dept. of Matls. Sci. & Engrg., Knoxville, TN 37996 USA; <sup>2</sup>Institute of Nuclear Energy Research (INER), PO Box 3-14, 1,000 Wenhua Rd., Chiaan Village, Lungtan, Taiwan 325 China; <sup>3</sup>Taiwan Power Company, Taipei Taiwan

Both elastic and plastic deformations affect material temperatures, but in different fashions. Consequently, temperature patterns could serve as fingerprints for stress-strain behaviors. A high-speed and highsensitivity thermographic-infrared (IR)-imaging system has been used to watch the temperature evolution cycle by cycle during 0.5 Hz lowcycle fatigue experiments. Numerical analyses integrating thermodynamics and heat-conduction theories have been formulated to calculate the stress amplitude, strain amplitude, and plastic work from the observed temperature evolutions. Cyclic softening behavior has been observed by thermography. A theoretical model has been developed to predict fatigue lives from the observed specimen temperatures. Furthermore, constitutive equations have been formulated to in-situ predict stress-strain variations from the measured temperatures. Thus, a new method has been developed to in-situ 'watch' material stressstrain evolutions during cyclic-loading conditions, which can open up wide applications of thermography in studying in-situ mechanical damage of materials and components.

#### 4:50 PM

# Assessment of Thermal Characteristics of YSZ Coating: *Kyongjun An*<sup>1</sup>; M. K. Han<sup>1</sup>; Joon-Kyun Lee<sup>1</sup>; <sup>1</sup>Korea Institute of Industrial Technology, 35-3, HongChonRi, IbJangMyun, ChonAnSi Korea

The approach is based on an experimental set-up in which one surface of the coating is exposed to a high temperature environment and heat is extracted from the other side by flowing air. This arrangement could be set-up in a laboratory. By measuring the overall thermal resistances of coatings of various thicknesses, it has been shown that the thermal conductivity of a segment of the coating can be determined by the differences in thermal resistances of two specimens with varying coating thicknesses. The objective of the present work is to extract the thermal conductivity of the thermal barrier coatings under conditions that are nearly the same as the actual application. It is also of interest to see if the thermal conductivity of coating can be affected by applying different coating thicknesses.

#### 5:10 PM

Dislocation Structure Evolution in Copper Crystals Under Cyclic and High Speed Loading: S. X.  $Li^{1}$ ; <sup>1</sup>Shenyang National Laboratory for Materials Science, Inst. of Metal Rsch., Shenyang 110016 China

The dislocation structure evolution of persistent slip bands (PSBs) and deformation bands of copper single crystals under cyclic straining and the annihilation of PSBs during annealing were investigated by a electron channeling contrast (ECC) technique. The structure of shear bands of copper single crystals under high rate straining were also studied by ECC. The dislocation structure evolution of PSBs and its internal and external stress fields were also computer simulated using dislocation dynamics and finite element methods. The results may provide further understanding of the plastic deformation localization of metals under either cyclic or high speed loading.

# Solidification Processes and Microstructures: A Symposium in Honor of Prof. W. Kurz: Mushy Zone Dynamics

Sponsored by: Materials Processing & Manufacturing Division, MPMD-Solidification Committee

*Program Organizers:* Michel Rappaz, Ecole Polytechnique Fédérale de Lausanne, MXG, Lausanne Switzerland; Christoph Beckermann, University of Iowa, Department of Mechanical Engineering, Iowa City, IA 52242 USA; R. K. Trivedi, Iowa State University, Ames, IA 50011 USA

Monday PM	Room: 207D
March 15, 2004	Location: Charlotte Convention Center

Session Chair: Christoph Beckermann, University of Iowa, Dept. of Mech. Engrg., Iowa City, IA 52242 USA

#### 2:00 PM Invited

Alloy Melting: *William J. Boettinger*<sup>1</sup>; Daniel Josell<sup>1</sup>; Deb Basak<sup>1</sup>; Sam R. Coriell<sup>1</sup>; <sup>1</sup>NIST, Metall. Div., Gaithersburg, MD 20899 USA

For practical reasons, melting receives less research attention than solidification. Yet partial melting may occur during joining or during casting with mushy zone macrosegregation. The modeling of these processes requires knowledge of the interface conditions, specifically the validity of the local equilibrium assumption. Existing research on this subject will be reviewed. In particular, experiments are presented that measure the effect of heating rate and grain size on the melting of Nb-47 mass%Ti. The method uses resistive self-heating of wire specimens at rates between 10<sup>2</sup> and 10<sup>4</sup> K/s and simultaneous measurement of radiance temperature and normal spectral emissivity as functions of time. The interpretation of the shapes of the temperature-time curves is supported by a model that includes diffusion in the solid coupled with a heat balance during the melting process. There is no evidence of loss of local equilibrium at the melt front during melting in these experiments.

# 2:30 PM Invited

About the Interactions Between Thermo-Solutal Convection, Shrinkage Flow and Grain Sedimentation: Andreas Ludwig<sup>1</sup>; Menghuai Wu<sup>1</sup>; <sup>1</sup>University of Leoben, Dept. of Metall., Franz-Josef-Str. 18, Leoben 8700 Austria

Based on a two-phase volume averaging model for globular equiaxed solidification detailed simulation results on the formation of macrosegregations in Al-4wt.% Cu die casting are presented. The model considers nucleation and growth of equiaxed grains, motion and sedimentation of grains, solute transport by diffusion and convection, feeding flow and thermo-solutal buoyancy driven flow. Special attention is paid on the interactions between thermo-solutal convection, shrinkage flow and grain sedimentation and the impact of these interactions on the formation of macrosegregation.

#### 3:00 PM

Direct Observation of Controlled Melting and Re-Solidification of Succinonitrile Mixtures in a Microgravity Environment: *Richard N. Grugel*<sup>1</sup>; A. V. Anilkumar<sup>2</sup>; C. P. Lee<sup>3</sup>; <sup>1</sup>Marshall Space Flight Center, MS-SD46, Huntsville, AL 35812 USA; <sup>2</sup>Vanderbilt University, Mech. Engrg., Box 1592, Sta. B, Nashville, TN 37235 USA; <sup>3</sup>ESI, Marshall Space Flight Ctr., Huntsville, AL 35812 USA

In support of the Pore Formation and Mobility Investigation (PFMI) direct observation of experiments on the controlled melting and subsequent re-solidification of succinonitrile were conducted in the glovebox facility (GBX) of the International Space Station (ISS). Samples were prepared on ground by filling glass tubes, 1 cm ID and approximately 30 cm in length, with pure succinonitrile (SCN) and SCN-Water mixtures under 450 millibar of nitrogen. Experimental processing parameters of temperature gradient and translation speed, as well as camera settings, were remotely monitored and manipulated from the ground Telescience Center (TSC) at the Marshall Space Flight Center. Sample temperatures are monitored by six in situ thermocouples. Real time visualization during melt back revealed bubbles of different sizes initiating at the solid/liquid interface, their release, interactions, and movement into the temperature field ahead of them. Subsequent resolidification examined planar interface breakdown and the transition to steady-state dendritic growth. A preliminary analysis of the observed phenomena and its implication to future microgravity experiments is presented and discussed.

MONDAY PM

Kinetics of Dendritic Mushy Zones: Microgravity Experiments: Afina Lupulescu<sup>1</sup>; Martin E. Glicksman<sup>1</sup>; <sup>1</sup>Rensselaer Polytechnic Institute, Dept. of Matls. Sci. & Engrg., Troy, NY 12180 USA

Kinetics of melting pivalic acid dendrites was observed under convection-free conditions on STS-87 as part of USMP-4, flown on shuttle Columbia in 1997. At low Stefan numbers, St«1, dendrites melt and shrink steadily toward extinction. Individual fragments follow a characteristic time-dependence derived using quasi-static theory based on conduction-limited melting under shape-preserving conditions. Agreement between analytic theory and experiments is found when the melting process occurs under shape-preserving conditions, as measured by the C/A ratio of the needle-like crystal fragments, approximated as prolate spheroids. In experiments where C/A varies, a "sectorizing" approach may be employed that divides the melting process into a series of steps, each approximated by a constant value of C/A. The sectorized approach allows prediction of the dendritic melting process even when neighbor interactions and fragmentation occur. Fragmentation of the dendrites is observed at higher initial supercoolings where the dendritic crystals are initially finer.

#### 3:30 PM

# Coarsening of Dendritic Microstructures: R. Mendoza<sup>1</sup>; D. Kammer<sup>1</sup>; P. W. Voorhees<sup>1</sup>; <sup>1</sup>Northwestern University, Matls. Sci. & Engrg., 2225 N. Campus Dr., Cook Hall, Evanston, IL 60208 USA

Wilfried Kurz has had a longstanding interest in the factors controlling the size scale of dendritic microstructures. We investigate the evolution of these microstructures during coarsening using three-dimensional digital reconstructions. The reconstructions allow quantitative measures of the microstructure to be obtained that have heretofore been impossible. For example, we have determined the probability of finding a patch of interface with a certain mean and Gaussian curvature, and the genus of the microstructure, all as a function of time during coarsening. We find that the directional solidification process used to create the samples induces a strong microstructural anisotropy that plays a major role in the evolution of the microstructure during coarsening. The dynamics of coarsening as a function of the volume fraction of solid will also be discussed.

#### 3:45 PM Break

#### 4:15 PM

**Coherency, Hot Cracking and Wilfried Kurz**: *Jai A. Sekhar*<sup>1</sup>; <sup>1</sup>University of Cincinnati, Dept. of Chem. & Matls. Engrg., 496 Rhodes Hall, Cincinnati, OH 45221-0012 USA

Professor Wilfried Kurz has extended several important ideas about coherency and deformation in the semi-solid state encountered during solidification. An article by him with co-authors Ackermann and Heinemann which appeared in the J. Mater. Sci. Eng. Vol. 75, pg.79, 1985, led to new understanding of the role of deformation at various temperatures in the semi-solid range. Subsequently, we were able to publish several articles from my group on the solidification cracking tendency and deformation studies of IC396M and Rene 108 alloys in the equiaxed state and the directionally solidified state. These studies led to the discovery of a crack free processing window for such alloys, giving rise to improved fatigue life for IC396M rotors. These and other studies are reviewed for results regarding the critical variables which influence the solidification cracking tendency in equiaxed microstructures, directionally solidified microstructures and also in faceted microstructures.

#### 4:30 PM

#### In-Situ Observations of Phenomena Related to Solidification of Ferrous Alloys: *Alan W. Cramb*<sup>1</sup>; *Sridhar Seetharaman*<sup>1</sup>; <sup>1</sup>Carnegie Mellon University, Matls. Sci., 5000 Forbes Ave., Pittsburgh, PA 15217 USA

There have been significant advances in the field of modeling solidification of metals, alloys and molten oxides through computational methods such as cellular automata and phase field. The ability to experimentally verify the predictions has however lagged behind due to difficulties posed by the high temperatures involved, containment of reactive molten metals and problems with radiation from the metal surfaces. This paper reviews recent experimental results from the Center for Iron and Steelmaking Research at Carnegie Mellon University on elucidating phenomena related to solidification and casting of ferrous alloys through in-situ observations using Confocal Scanning Laser Microscopy, High temperature Optical Microscopy and X-ray fluoroscopy and radioscopy. The phenomena that will be discussed includes: inclusion evolution during steel solidification, peritectic transformation and crystallization of industrial slags and fluxes.

## 4:45 PM

A Simple Microsegregation Model for Application in Macro Scale Solidification Calculations: Vaughan R. Voller<sup>1</sup>; <sup>1</sup>University of Minnesota, Civil Engrg., 500 Pillsbury Dr. SE, Minneapolis, MN 55455 USA

A major problem in computational modeling of physical processes is developing computational approaches that are able to bridge across length and time scales. This is a central issue in developing solidification models where the macro scale nodal field variables need to be consistent with phenomena occurring at the sub grid length scale of the solid-liquid interface, in particular the thermodynamics and local scale mass transport (microsegregation). In this paper a relatively simple microsegregation model, on the scale of a dendrite secondary arm space, is developed. The key features in this model are (i) domain variables obtained directly form macro-scale conservation equations, (ii) a thermodynamic treatment, for a multi-component alloy, that only requires calls to equilibrium calculations (i.e., the lever rule), and (iii) an accurate accounting for back-diffusion and coarsening at each time step, based on the current solid solute profiles. The application of model is illustrated by comparing its predictive performance, for several limit cases, with full numerical microsegregation solutions.

#### 5:00 PM

Network Modelling of Liquid Metal Transport in Solidifying Aluminium Alloys: W. O. Dijkstra<sup>1</sup>; C. Vuik<sup>2</sup>; A. J. Dammers<sup>3</sup>; L. Katgerman<sup>4</sup>; <sup>1</sup>Delft University of Technology, Lab. of Matls., Rotterdamseweg 137, Delft 2628 AL Netherlands; <sup>2</sup>Delft University of Technology, Dept. of Appl. Math. Analy., Melkeweg 4, Delft 2628 CD Netherlands; <sup>3</sup>Netherlands Institute for Metals Research, Delft 2628 AL Delft Netherlands; <sup>4</sup>Delft University of Technology, Lab. of Matls., Rotterdamseweg 137, Delft 2628 AL Netherlands

Development of fluid flow within the mushy zone of a DC-casting is important for the optimal control of many properties of the final cast material. We present a new numerical model based on a channel network. It allows to study flow effects at low liquid fractions within the mushy zone on a mesoscopic scale. Simulation of solidification within the channels together with mixing rules on their junctions describe the behaviour of the microstructure. In order to reduce the computational costs, the channels have to be represented by simple geometric objects like tubes. The collective behaviour of many channels within the network indicate the macroscopic effects as they occur in a small region of the underlying solidification process. The results of calculations for Al-4.5wt.%Cu alloy with and without inclusion of solidification shrinkage are presented.

#### 5:15 PM

Modeling of Macrosegregation and Solidification Grain Structures with a Coupled Cellular Automaton - Finite Element Method: Gildas Guillemot<sup>1</sup>; Charles-Andre Gandin<sup>1</sup>; Herve Combeau<sup>1</sup>; <sup>1</sup>LSG2M, UMR CNRS-INPL-UHP 7584, Ecole des Mines, Parc de Saurupt, Nancy 54042 France

Extension of a coupled Cellular Automaton (CA) - Finite Element (FE) method is presented for the prediction of solidification grain structures and macrosegregation. Following the validation procedure proposed by Ahmad et al. [Metallurgical and Materials Transactions 29A (1998) 617-630], application of the model to the experiments conducted by Hebditch and Hunt is proposed [Metallurgical Transactions 5 (1974) 1557-1564]. The algorithm and the numerical implementation of the coupling between the CA and FE methods are first validated by considering a columnar grain structure that develops with almost no undercooling. Such a calculation retrieves the solution of a purely FE calculation in which the grain structure is not accounted for. Several applications of the model are then presented in order to quantify the combined effects of the grain structure on the final macrosegregation map. In particular, the effect of the undercooling of the columnar growth, the presence of equiaxed grains nucleated in an undercooled liquid, as well as the transport and sedimentation of the equiaxed grains are investigated. Several improvements of the predicted segregation maps are clearly revealed when comparing with the experimental results.

#### 5:30 PM

A Mushy Zone Rayleigh Number to Describe Interdendritic Convection During Directional Solidification of Hypoeutectic Pb-Sb and Pb-Sn Alloys: Surendra N. Tewari<sup>1</sup>; R. Tiwari<sup>1</sup>; G. Magadi<sup>2</sup>; <sup>1</sup>Cleveland State University, Chem. Engrg. Dept., SH 464, Cleveland, OH 44115 USA; <sup>2</sup>American Bureau of Shipping, ABS Plaza, 16855 Northchase Dr., Houston, TX 77060 USA

Based on measurements of specific dendrite surface area ( $S_v$ ), fraction interdendritic liquid ( $\phi$ ) and primary dendrite spacing ( $\lambda_1$ ) on

transverse sections in a range of directionally solidified hypoeutectic Pb-Sb and Pb-Sn alloys that were grown at thermal gradients varying from 10 to 197 Kcm<sup>-1</sup> and growth speeds ranging from 2 to 157 µm s<sup>-</sup> <sup>1</sup> it is observed that  $S_v = \lambda_1^{-1} S^{*-0.33}(3.38 - 3.29\phi + 8.85\phi^2)$ , where  $S^* =$  $D_1G_{eff}/[V m_1 \text{ Co } (k-1)/k]$ , with  $D_1$  being solutal diffusivity in the melt, G<sub>eff</sub>, the effective thermal gradient, V, the growth speed, m<sub>l</sub>, the liquidus slope, Co, the solute content of the melt, and k the solute partition coefficient. This relationship has been used to define a mushy-zone permeability which accounts for the role of side-branching; other permeability relationships assume that it depends only upon  $\phi$  and  $\lambda_1$ . Incorporation of this permeability allows us to develop a mushy-zone Rayleigh number that quantitatively explains the following three experimental observations related to interdendritic convection: 1) Increasing convection results in reduced primary dendrite spacing. 2) Extent of longitudinal macrosegregation increases with increased mushy-zone convection. 3) On-set of channel-segregate (freckle) formation.

#### 5:45 PM

**Dynamics of Particle-Solidification Front Interactions**: Justin Wayne Garvin<sup>1</sup>; Yi Yang<sup>1</sup>; H. S. Udaykumar<sup>1</sup>; <sup>1</sup>University of Iowa, Mech. Engrg., 3131 Seamans Ctr., Iowa City, IA 52242 USA

A particle interacting with an advancing solidification front is studied using numerical simulations to couple phase change with particle motion. The particle is set in motion through the forces that act across the gap between the particle and the solidifying interface. A sharp-interface method is used to track both the phase boundary and the particle. Previous force expressions used in past literature are carefully scrutinized and found to inadaquately describe the nature of the forces in the gap. The effect of a premelted layer between the particle and the solidification front on the interaction dynamics is also studied through the coupling procedure. It is determined that the use of a premelted layer in the coupled model greatly effects the dynamics of the particle-front interaction. Both stable interfaces as well as dendritic interfaces are used in this study.

# Symposium on Microstructural Stability in Honor of Prof. Roger D. Doherty: Microstructural Stability: Texture Development

Sponsored by: Aluminum Association, Materials Processing and Manufacturing Division, Structural Materials Division, MPMD-Solidification Committee, SMD-Physical Metallurgy Committee *Program Organizer:* Anthony D. Rollett, Carnegie Mellon University, Department of Materials Science & Engineering, Pittsburgh, PA 15213-3918 USA

Monday PM	Room:	21	6A		
March 15, 2004	Location	1:	Charlotte	Convention	Center

Session Chair: Robert E. Sanders, Alcoa Inc, Alcoa Tech. Ctr., Alcoa Ctr., PA 15069 USA

#### 2:00 PM

Simulation of Development of Annealing Texture: Jerzy A. Szpunar<sup>1</sup>; <sup>1</sup>McGill University, Dept. of Metals & Matls. Engrg., 3610 Univ. St., Montreal Canada

This presentation is an overview of our research on transformation of microstructure and texture during annealing operations A model is presented that allows simulating texture and microstructure development at various stages of the annealing process. The model incorporates a description of the initial texture and microstructure, the anisotropy of stored energy of deformation, condition of nucleation and and differences in mobility of different grain boundaries. Several examples are presented to illustrate various factors that influence texture transformation. In particular texture transformation in IF and low carbon steels, aluminum alloys, Fe-Si steels and nanocrystalline Ni is discussed.

#### 2:35 PM

Quantitative Analysis of Texture Evolution for Cold Rolled DC and CC AA5052 and AA5182 Aluminum Alloys During Isothermal Annealing: Yumin Zhao<sup>1</sup>; James G. Morris<sup>1</sup>; <sup>1</sup>University of Kentucky, Dept. of Matls. Sci. & Engrg., 177 Anderson Hall, Lexington, KY 40506 USA

The as-received Direct Chill Cast (DC) and Continuous Cast (CC) AA5052 and AA5182 hot bands were preheated at 454°C for 4 hours followed by cold rolling to 80% reduction in thickness. The cold rolled AA5052 and AA5182 aluminum alloys were isothermally annealed at

three temperatures. Texture evolution during isothermal annealing was investigated by X-ray diffraction using the Schulz technique and ODF procedure. After the volume fractions for the various texture components were calculated employing an improved integration method, texture evolution during isothermal annealing was quantitatively analyzed using an Avrami type equation. At the same time the differences in recryatllization behaviors between AA5052 and AA5182 aluminum alloys and between DC and CC materials were compared. It was found that the texture evolutions could be well expressed by Avrami type equations. The cube recrystallization texture component was strong for AA5052 aluminum alloys and annealing temperature had little influence on the recrystallization texture of the AA5052 aluminum alloys. The recrystallization textures of AA5182 alloys were weak and varied with annealing temperature. In addition, DC AA5052 and DC AA5182 materials possessed stronger cube recrystallization textures than the corresponding CC materials. Furthermore, the n value in the Avrami type equation possessed different values for AA5052 versus AA5182 aluminum alloys and for DC versus CC materials. For AA5052 alloys, the n values increased with increase in annealing temperature. On the other hand, the n values for AA5182 alloys remained constant for the different annealing temperatures.

#### 3:10 PM

Nucleation and Growth of Orientations from Cold Rolled OFE Copper: Carl T. Necker<sup>1</sup>; <sup>1</sup>Los Alamos National Laboratory, MST-6, MS G770, Los Alamos, NM 87545 USA

The macroscopic strains imposed during cold rolling yield dramatic changes in the initially equiaxed microstructure and nearly random texture. It is primarily the rolling process that predetermines the development of new microstructures and textures during static annealing treatments. Although the presence of retained rolling textures and the formation of very strong cube textures during recrystallization is well documented, the highly complex microstructures and graded textures from which these recrystallization textures arise are only partially understood and are still worth investigating. Orientation Imaging Microscopy is used to explore both the deformed microstructure and texture as well as the incipient strain free grains that foreshadow conditions in the fully recrystallized state.

#### 3:45 PM

Texture Evolution During Grain Growth: Effect of Boundary Properties and Initial Microstructure: Ning Ma<sup>1</sup>; Suliman A. Dregia<sup>1</sup>; Yunzhi Wang<sup>1</sup>; <sup>1</sup>Ohio State University, Matls. Sci. & Engrg., 2041 College Rd., Columbus, OH 43210 USA

We incorporate the dependence of grain boundary energy and mobility on misorientation in three-dimension into the phase field model to investigate orientation selection during grain growth in systems consisting of a single cube component embedded in a matrix of randomly oriented grains in the initial microstructure. Starting from various fractions and spatial distributions of the cube component, we show that the effect of energy anisotropy on texture development differs drastically from that of mobility anisotropy. In all cases the fraction of the cube component increases if boundary energy is anisotropic, and decreases if boundary mobility is anisotropic while energy is isotropic. Similar to previous studies, when boundary energy is anisotriopic the misorientation distribution is no longer time-invariant and grain growth kinetics deviates from the behavior of isotropic grain growth. However, mobility anisotropy could also alter misorientation distribution and hence affect grain growth kinetics, which is different from the results obtained previously for systems of either random or singlecomponent texture. The initial spatial distribution of the texture component plays an important role in determining the time-evolution of the misorientation distribution and hence affects the overall kinetics of texture evolution and grain growth.

#### 4:20 PM

Growth of the Cube Component in FCC Deformation Textures: Simulation and Theory: Anthony D. Rollett<sup>1</sup>; <sup>1</sup>Carnegie Mellon University, Matls. Sci. & Engrg., Wean Hall 4315, 5000 Forbes Ave., Pittsburgh, PA 15213 USA

Prof. Doherty has devoted a substantial fraction of his career to advancing our understanding of the stability or lack of stability of microstructures. A notable example of such an issue is the appearance of minority texture components during annealing of deformed metals. Many theories have been advanced to explain the origins, for example, the cube component,  $\{001\}<100>$ , in fcc metals. One such theory concerns "microselection" whereby the cube component is favored during the early stages of recrystallization where coarsening takes place in the subgrain structure formed during recovery. To address this possibility, Monte Carlo simulation of grain growth is used to study the behavior of the cube component during grain growth in a

polycrystal for which the dominant texture is representative of rolling textures in fcc metals. The cube component was treated as a special texture component, inserted into the microstructure by assigning nearcube orientations to particular grains. A sensitivity analysis varied such parameters as initial cube volume fraction, the grain boundary energy and mobility functions, spatial correlation of the special component, and rotations of the special component away from the exact cube position. The results indicate a strong tendency for the cube component to grow provided that a moderate level of anisotropy exists in the grain boundary energy and mobility.

#### 4:55 PM

**3D** Simulations of Zener Drag: *Gael Couturier*<sup>1</sup>; Claire Maurice<sup>1</sup>; Roland Fortunier<sup>1</sup>; Roger Doherty<sup>2</sup>; Julian Driver<sup>1</sup>; <sup>1</sup>Ecole des Mines de Saint Etienne, Matls. Dept. France; <sup>2</sup>Drexel University, Dept. of Matls. Engrg., Philadelphia, PA USA

A 3D finite element model has been developed to simulate the interaction of a moving boundary with one or several second phase particles. The model is first applied to the case of curvature driven grain growth where a single boundary of varying dimension represents the average grain boundary radius during growth in a polycrystal containing particles. Compared with classical Zener predictions, it is shown that the restraining drag force exerted by each particle is less than expected but that an anchored boundary is in contact with 3 to 4 times the number of particles given by the rigid boundary assumption. Consequently the overall drag force is higher than derived from the basic Zener model and the limiting grain size is therefore smaller. Some preliminary results of Zener drag at a recrystallization boundary are also presented.

# The Didier de Fontaine Symposium on the Thermodynamics of Alloys: Experimental Techniques

Sponsored by: Materials Processing and Manufacturing Division, MPMD-Computational Materials Science & Engineering-(Jt. ASM-MSCTS)

*Program Organizers:* Diana Farkas, Virginia Polytechnic Institute and State University, Department of Materials Science and Engineering, Blacksburg, VA 24061 USA; Mark D. Asta, Northwestern University, Department of Materials Science and Engineering, Evanston, IL 60208-3108 USA; Gerbrand Ceder, Massachusetts Institute of Technology, Department of Materials Science and Engineering, Cambridge, MA 02139 USA; Christopher Mark Wolverton, Ford Motor Company, Scientific Research Laboratory, Dearborn, MI 48121-2053 USA

Monday PM	Room:	216B		
March 15, 2004	Location	: Charlott	e Convention	Center

Session Chair: TBA

#### 2:00 PM Invited

Nanoscale Modulations in Optimally Doped YBa2Cu3O6.92: X-Ray Evidence for Atomic Displacements in Higher Order ORTHO Phases: Z. Islam<sup>2</sup>; J. C. Lang<sup>2</sup>; D. Haskel<sup>2</sup>; D. R. Lee<sup>2</sup>; G. Srajer<sup>2</sup>; D. R. Haeffner<sup>2</sup>; U. Welp<sup>3</sup>; S. K Sinha<sup>4</sup>; S. C. Moss<sup>1</sup>; P. Wochner<sup>5</sup>; <sup>1</sup>University of Houston, Dept. of Physics, Houston, TX USA; <sup>2</sup>Argonne National Laboratory, Advd. Photon Source USA; <sup>3</sup>Argonne National Laboratory, Matls. Sci. Div. USA; <sup>4</sup>University of California, Dept. of Physics, San Diego, CA USA; <sup>3</sup>Max-Planck Institute fuer Metallforschung, Stuttgart Germany

Diffuse, strain-induced, superlattice peaks have been observed using synchrotron x-rays in a single domain crystal of YBa2Cu3O6.92 along the a-axis, i.e. normal to the filled oxygen chains. These broad satellite peaks correspond to a 4-unit cell modulation of the structure which is poorly correlated along both x-and y-axes, indicating a kinetically (diffusion) limited formation of the ORTHO phase(s) predicted by De Fontaine and co-workers. In addition, the separate satellites show a pronounced modulation along the z-axis whose Fourier transform can be well fit by a set of atomic displacements within a unit cell along z which are not the same for all atoms in the cell; i.e. this is not simply a x-y planar modulation. At room temperature the diffuse scattering about a normal Bragg peak is dominated by the one-phonon thermal diffuse scattering (TDS) as calculated from the measured phonon dispersion curves. At low temperature, however, there can be seen a familiar "bow-tie" diffuse scattering in the H-K plane which peaks along the <110> directions, in a manner earlier observed for Al-doped YBCO, which could be attributed to disorder among the oxygen chainplane sites. In the present case, the disorder underlying this Huang diffuse scattering (HDS), presumably arises from the inherent disorder associated with the short-range nature of the locally modulated structure. These results will be discussed in terms of the tendency of YBCO to assume a range of ORTHO phases.

#### 2:30 PM Invited

A Combined Kinetic Monte Carlo and Experimental Study of the Temporal: David N. Seidman<sup>1</sup>; <sup>1</sup>Northwestern University, Matls. Sci. & Engrg., Cook Hall, 2220 Campus Dr., Evanston, IL 60208-3108 USA

The temporal evolution of model Ni-Al-Cr superalloys is being studied, employing three-dimensional atom-probe (3DAP) and transmission electron microscopies, in parallel with kinetic Monte Carlo (KMC) simulations on the same alloys. The objectives are, employing these tools, to: (1) follow the kinetic pathways by which the gamma phase (fcc) decomposes into gamma (fcc) plus gamma-prime (L12 structure) phases; (2) to determine the chemistry of individual precipitates with subnanoscale resolution; (3) to distinguish between ordered gamma-prime precipitates and disordered ones; (4) to follow the temporal evolution of the concentration profiles of the precipitates; (5) to measure the time dependencies of the mean radius, number density and supersaturations of Al and Cr and to compare them with the Umantsev-Kuehmann-Voorhees model for coarsening of a ternary alloy; (6) to observe the process of coagulation of precipitates; (7) to examine the atomic mechanism of coarsening, that is, evaporationcondensation of single atoms versus the cluster-diffusion-coagulation mechanism.

#### 3:00 PM Invited

Nucleation and Coarsening of  $\gamma$  (Ni-Al) Precipitates in a  $\gamma$ ' (Ni<sub>3</sub>Al) Matrix: Yong Ma<sup>1</sup>; *Alan J. Ardell*<sup>1</sup>; <sup>1</sup>University of California, Dept. of Matls. Sci. & Engrg., 6531 Boelter Hall, Los Angeles, CA 90095-1595 USA

The morphology, spatial correlations and kinetics of coarsening of Ni<sub>3</sub>Al ( $\gamma$ ') precipitates have been thoroughly investigated, while precipitation of the disordered Ni-Al ( $\gamma$ ) solid solution from supersaturated  $\gamma$ ' has received relatively little attention. Since the  $\gamma$ - $\gamma$ ' interfacial free energy, lattice mismatch and elastic-constant mismatch are entirely independent of the majority phase, precipitation of  $\gamma$  from supersaturated  $\gamma$ ' might be a mirror image of the precipitation of  $\gamma$ ' from  $\gamma$ . This conjecture is completely belied by our preliminary results. For example: Nucleation of  $\gamma$ ' from supersaturated  $\gamma$  is extremely fast while nucleation of  $\gamma$  from  $\gamma$ ' is very slow; The coarsening rates of  $\gamma$  in  $\gamma$ ' increase strongly with f;  $\gamma$ ' precipitates coalesce with difficulty during coarsening while  $\gamma$  precipitates coalesce in the context of thermodynamics and kinetic processes in Ni-Al alloys.

#### 3:30 PM

Local Order or Local Decomposition in the Solid Solutions of Ni-Au and Pt-Rh?: *Bernd Schönfeld*<sup>1</sup>; Michael J. Portmann<sup>1</sup>; Christian Steiner<sup>1</sup>; Gernot Kostorz<sup>1</sup>; Felix Altorfer<sup>2</sup>; Joachim Kohlbrecher<sup>2</sup>; Angel Mazuelas<sup>3</sup>; Hartmut Metzger<sup>3</sup>; <sup>1</sup>ETH Zurich, Inst. of Appl. Physics, CH-8093 Zurich Switzerland; <sup>2</sup>PSI, CH-5232 Villigen Switzerland; <sup>3</sup>ESRF, F-38043 Grenoble France

For these two binary alloy systems exhibiting continuous solid solubility at elevated temperatures, there is an ongoing debate on the presence of short-range order and/or local clustering. Extensive measurements of diffuse scattering of neutrons and x-rays were thus performed to arrive at a conclusive characterization. Ni-Au single crystals containing 8.4 at.% and 60 at.% Au were studied in situ at temperatures above the miscibility gap, using small-angle and wide-angle neutron scattering. The incoherent scattering background was largely reduced by employing the Ni-58 isotope. An increase of coherent scattering towards small scattering vectors indicates local decomposition. A Pt-47 at.% Rh single crystal quenched from 920 K to room temperature, was investigated by laboratory X-rays, synchrotron radiation (enhanced scattering contrast at wavelengths close to the Rh K-edge) and neutrons. Weak maxima in diffuse scattering are found around 1 1/2 0 and 000, with local decomposition being more pronounced.

3:50 PM Break

# 4:00 PM Invited

Some Experimental Studies of Coherent Phase Separation in Binary Alloys: Gernot Kostorz<sup>1</sup>; <sup>1</sup>ETH Zurich, Appl. Physics, Zurich CH 8093 Switzerland On their way toward equilibrium, decomposing binary alloys often pass through intermediate, metastable states with coherent pre-precipitates. Small-angle scattering (of X-rays and neutrons) has been used to reveal microstructural features, especially early stages of decomposition in alloys, ideally studied as single crystals. Kinetic in-situ neutron scattering studies have been performed in newly developed high-temperature cells. A survey will be given on the early stages of phase separation in Ni-rich Ni-Ti where coherency strains and ordering of the precipitates affect the kinetics. A temporary slowing-down is observed in some cases. In Al-rich Al-Ag, coherency strains are small, but the decomposition also shows unexpectedly complex behavior. Here, the combined results of small-angle X-ray scattering, diffuse neutron scattering and high-resolution Z-contrast electron microscopy offer a consistent description of the microstructure starting with the very early stages of decomposition.

#### 4:30 PM Invited

**Diffuse Scattering Methods - A Critical Testbed for Alloy Theory:** *Harald Reichert*<sup>1</sup>; <sup>1</sup>MPI für Metallforschung, Heisenbergstrasse 3, Stuttgart 70569 Germany

Recently developed diffuse x-ray scattering methods enable us to retrieve effective pair interactions in k-space with unprecedented resolution and accuracy. In parallel, we have combined first-principles calculations of the alloy energetics with reciprocal space methods for the interpretation of the experimentally determined diffuse scattering maps. We have used this method to separate chemical and straininduced components in the effective pair interactions. In this presentation we will directly compare results from first-principles calculations for a series of model alloys (Cu-Au, Au-Ni,Ti-V) with diffuse scattering data. In all cases we find new features in the scattering maps with profound consequences for mechanisms such as the screening in alloys or phase separation kinetics.

#### 5:00 PM

Nanoscale Studies of the Temporal Evolution of the Early Stages of Decomposition and Coarsening in Model Ni-Al-Cr Superalloys: *Chantal K. Sudbrack*<sup>1</sup>; Kevin E. Yoon<sup>1</sup>; Jessica A. Weninger<sup>1</sup>; Ronald D. Noebe<sup>2</sup>; David N. Seidman<sup>1</sup>; <sup>1</sup>Northwestern University, Matls. Sci. & Engrg., 2220 Campus Dr., Evanston, IL 60208 USA; <sup>2</sup>NASA Glenn Research Center, 21000 Brookpark Rd., Cleveland, OH 44135 USA

Limited experimental data on decomposition pathways of ternary metallic alloys exists, and decomposition is not well understood due to complex interactions. We employ three-dimensional atom-probe (3DAP) and transmission electron microscopies to investigate gamma (fcc) to gamma (fcc) + gamma-prime (L1<sub>2</sub> structure) in Ni-5.2 Al-14.2 Cr and Ni-7.6 Al-8.6 Cr (at.%) aged at 600°C. For the times investigated (2 minutes to 1024 hours), these alloys exhibit a high number density (10<sup>24</sup> m<sup>-3</sup>) of spheroidal precipitates, 0.5-10 nm in radius. The reaction is identified as nucleation, growth and coarsening by the presence of solute-rich precipitates, exhibiting short-range order in the as-quenched state. Precipitate coagulation is present, and its influence on the power-law dependencies of the number density, mean radius, and supersaturations of Al and Cr, are discussed in light of parallel kinetic Monte Carlo simulations. This research is supported by the National Science Foundation and NASA Glenn HOTPC program.

#### 5:20 PM

The Role of Re on the Temporal Evolution of the Nanostructure of a Model Ternary Ni-Cr-Al Superalloy: Kevin Eylhan Yoon<sup>1</sup>; Ronald D. Noebe<sup>2</sup>; David N. Seidman<sup>1</sup>; <sup>1</sup>Northwestern University, Matls. Sci. & Engrg., 2220 N. Campus Dr., Evanston, IL 60208 USA; <sup>2</sup>NASA Glenn Research Center, Cleveland, OH 44135 USA

The temporal evolution of  $\gamma'$  (L1<sub>2</sub>) precipitates in a quaternary  $\gamma$  (fcc) Ni-Cr-Al-Re alloy, aged at 1073 K from 0.25 to 264 hours, is investigated by transmission electron and three-dimensional atomprobe (3DAP) microscopies. Rhenium (2 at.%) was added to a model Ni-8.5 at.% Cr-10 at.% Al superalloy to study its effects on the temporal evolution. The number density, mean radius, and volume fraction of  $\gamma'$  precipitates are measured, as well as the supersaturations of alloying elements as functions of time. The morphology of  $\gamma'$  precipitates is spheroidal, even for extended aging times. Rhenium delays the coarsening of  $\gamma'$  precipitates and stabilizes their morphology, in comparison to a model Ni-Cr-Al superalloy, aged at 1073 K. The coarsening kinetics do not obey the time dependencies predicted by LSW theory. The coalescence of precipitates is suggested to be a factor. This research is supported by the NSF and NASA Glenn HOTPC program.

# Third International Symposium on Ultrafine Grained Materials: Processing II: Structural Evolution

Sponsored by: Materials Processing & Manufacturing Division, MPMD-Shaping and Forming Committee Program Organizers: Yuntian Ted Zhu, Los Alamos National

Laboratory, Materials Science and Technology Division, Los Alamos, NM 87545 USA; Terence G. Langdon, University of Southern California, Departments of Aerospace & Mechanical Engineering and Materials Engineering, Los Angeles, CA 90089-1453 USA; Terry C. Lowe, Metallicum, Santa Fe, NM 87501 USA; S. Lee Semiatin, Air Force Research Laboratory, Materials & Manufacturing Directorate, Wright Patterson AFB, OH 45433 USA; Dong H. Shin, Hanyang University, Department of Metallurgy and Material Science, Ansan, Kyunggi-Do 425-791 Korea; Ruslan Z. Valiev, Institute of Physics of Advanced Material, Ufa State Aviation Technology University, Ufa 450000 Russia

Monday PM	Room:	207A		
March 15, 2004	Location	: Charlotte	Convention	Center

Session Chairs: Dong H. Shin, Hanyang University, Dept. Metall. Matls. Sci., Ansan Korea; Yuri Estrin, Clausthal University of Technology Germany; Jingtao Wang, Nanjing University of Science & Technology, Sch. of Matls. Sci. & Engrg., Nanjing 210094 China

#### 2:00 PM Invited

**Deformation Microstructures**: *Niels Hansen*<sup>1</sup>; Xiaoxu Huang<sup>1</sup>; Darcy A. Hughes<sup>2</sup>; <sup>1</sup>Risoe National Laboratory, Matls. Rsch. Dept., Ctr. for Fundamental Rsch., Metal Structures in 4-D, Roskilde DK-4000 Denmark; <sup>2</sup>Sandia National Laboratories, Ctr. for Matls. & Engrg. Scis., Livermore, CA 94550 USA

Microstructural characterisation and modelling have shown that a variety of metals deformed by different mechanical processes follow a general path of grain subdivision by dislocation boundaries and high angle boundaries. This general path has been demonstrated over length scales from the millimetre to the nanometre range by quantitative characterisation of microstructural parameters applying electron microscope techniques as transmission electron microscopy (TEM), Kikuchi pattern analysis and electron back scatter diffraction (EBSD). Studies on a finer scale by high resolution electron microscopy (HREM) have also been applied to characterise individual dislocations in the layers between boundaries. The microstructural characterisation has concentrated on metals as aluminium, copper, nickel and iron deformed by processes introducing strains up to about 5-10 (e.g., rolling, accumulative roll bonding and equal channel angular extrusion) and processes introducing strains of 100 or more (e.g., cyclic extrusion compression, high pressure torsion and friction). The structural parameters over many length scales have been analysed applying physical principles and mathematical procedures including scaling. This has led to improved understanding of the subdivision process and the relationships between processing and microstructure, and between microstructure and properties.

#### 2:20 PM

Principles of High-Pressure Torsion and Equal-Channel Angular Pressing: A Comparison of Microstructural Characteristics: Alexandre P. Zhilyaev<sup>1</sup>; Minoru Furukawa<sup>2</sup>; Zenji Horita<sup>3</sup>; *Terence G. Langdon*<sup>4</sup>; <sup>1</sup>Universitat Autonoma de Barcelona, Dept. de Fisica, Bellaterra 08193 Spain; <sup>2</sup>Fukuoka University of Education, Dept. of Tech., Munakata, Fukuoka 811-4192 Japan; <sup>3</sup>Kyushu University, Matls. Sci. & Engrg., Fac. of Engrg., Fukuoka 812-8581 Japan; <sup>4</sup>University of Southern California, Aeros. & Mech. Engrg. & Matls. Sci., Los Angeles, CA 90089-1453 USA

Two major procedures are currently in use for the production of ultrafine-grained materials: high-pressure torsion (HPT) in which a sample is subjected to a high pressure with concomitant torsional straining and equal-channel angular pressing (ECAP) where a sample is pressed through a die constrained within a channel that is bent through an abrupt angle. Both of these procedures lead to the imposition of a large imposed strain without any reduction in the cross-sectional dimensions of the work-piece. This paper examines these two procedures with special reference to the factors influencing the microstructural characteristics.

# MONDAY PM

#### 2:35 PM

**Evolution in Microstructural Parameters During High Pressure Torsion of Nickel**: *Xiaoxu Huang*<sup>1</sup>; A. Vorhauer<sup>2</sup>; Grethe Winther<sup>1</sup>; Niels Hansen<sup>1</sup>; R. Pippan<sup>2</sup>; M. Zehetbauer<sup>3</sup>; <sup>1</sup>Risoe National Laboratory, Matls. Rsch. Dept., Ctr. for Fundamental Rsch., Metal Structures in 4-D, Roskilde DK-4000 Denmark; <sup>2</sup>Austrian Academy of Sciences, Erich Schmid Institute Austria; <sup>3</sup>University of Vienna, Inst. of Matls. Physics Austria

High pressure torsion (HPT) is a well-developed deformation process which allows metal samples to be deformed to extremely high strains. In this work we apply HPT to deform nickel samples to strains above 10. At such high strains, the microstructural evolution has not been well understood. In this work, the microstructural evolution is characterized by transmission electron microscopy (TEM), with emphasis on the characterization of misorientation angles and their distribution. A semiautomatic TEM method is employed for orientation measurement to get a good statistics. The results showed that low misorientation angles dominate at low strains and that the fraction of low angle boundaries decreases with increasing strain. However, even at an effective strain of 34, there is still quite a large fraction of low angle dislocation boundaries existing in the structure that leads to a deviation of the misorientation distribution from that for a polycrystal with random orientations of grains.

# 2:50 PM Invited

**Development of Microstructure During Equi-Channel Angular Pressing of Pure Aluminum**: *Terry R. McNelley*<sup>1</sup>; Douglas L. Swisher<sup>1</sup>; Keiichiro Oh-ishi<sup>1</sup>; <sup>1</sup>Naval Postgraduate School, Dept. of Mech. Engrg., 700 Dyer Rd., Monterey, CA 93943-5146 USA

The evolution of microstructure and microtexture during repetitive equi-channel angular pressing (ECAP) of high-purity Al was examined by orientation imaging microscopy (OIM) and convergent beam electron diffraction (CBED) methods in transmission electron microscopy (TEM). Shear textures are apparent after an initial pressing pass but are very inhomogeneous. The texture and microstructure become more homogeneous and a highly refined, equiaxed deformation-induced microstructure evolves during repetive pressing operations. Nevertheless, after four ECAP passes a band-like arrangement may be resolved in both the OIM and TEM data. The bands align with shear plane and the interfaces between the bands are high-angle boundaries. Low angle boundaries separate equiaxed cells within the bands. After 12 ECAP passes the bands have become increasingly elongated such that there are only one or two cells across each band and the fraction of high-angle boundaries is increased. The mechanism of microstructure transformation will be discussed.

#### 3:10 PM Invited

Severe Plastic Deformation of Al: Effect of Strain Path: Ayman A. Salem<sup>1</sup>; S. L. Semiatin<sup>2</sup>; <sup>1</sup>Universal Technology Corporation, Dayton, OH 45432 USA; <sup>2</sup>Air Force Research Laboratory, Matls. & Mfg. Direct., Wright-Patterson AFB, OH 45433 USA

Microstructure evolution during severe plastic deformation of unalloyed aluminum (high purity and commercial-purity) was investigated to establish the effect of processing route and purity level on grain refinement and subgrain formation. Two lots of unalloyed aluminum with different purity levels (99.99%Al and 99%Al) were subjected to large plastic strains at room temperature. Four different deformation processes were used: equal channel angular extrusion, conventional conical-die extrusion, sheet rolling, and uniaxial compression. Orientation imaging microscopy was employed to characterize the developed microstructures. The various deformation routes yielded an ultrafine microstructure with a ~1.5 µm grain size in commercialpurity aluminum. For high-purity aluminum, however, the minimum grain size produced after the various deformation routes was  $\sim 20 \ \mu m$ , and there were indications of recrystallization. The high fraction of high-angle grain boundaries and the absence of subgrains/deformation bands in the final microstructure confirmed the occurrence of recrystallization of high-purity aluminum at large plastic strains.

#### 3:30 PM Invited

Formation of Defects During Equal Channel Angular Extrusion: *Rimma Lapovok*<sup>1</sup>; P. McKenzie<sup>1</sup>; <sup>1</sup>Monash University, Sch. of Physics & Matls. Engrg., Clayton, Vic 3800 Australia

The theoretical definition of damage imparted to a material by it's processing method, which is proportional to plastic deformation, unites several types of defects; such as that of grain-boundary voids and micro cavities formed by decochesion of hard particles from the surrounding matrix. As Equal Channel Angular Extrusion (ECAE) is a process of severe plastic deformation, the damage accumulated during processing of a material is significant. The intensity of damage accumulation depends on the route of extrusion taken and back-pressure

applied. In this paper, the damage accumulation-recovery model introduced in our previous works is proven experimentally. The initial distribution of cavities, the distribution in intermediate passes and after processing, and the development of defects due to plastic deformation during ECAE processing was studied by high resolution Field Emission Gun (FEG) Scanning Electron Microscopy (SEM) for different processing routes. It is shown, that Route A is the most favorable route for defect formation. Increasing the back-pressure was found to change the character of fracture in samples produced, because the decohesion of particles within the matrix and brittle fracture of hard particles is suppressed. The source of formation of voids during ECAE is therefore reduced.

#### 3:50 PM Break

#### 4:00 PM Invited

Microstructure and Texture Development in Cu and Al Under ECAP: New Experimental Results and Modeling: Yuri Estrin<sup>1</sup>; *Ralph Hellmig*<sup>1</sup>; Seung Chul Baik<sup>1</sup>; Hyoung Seop Kim<sup>2</sup>; Hans-Günter Brokmeier<sup>1</sup>; Aikaterini Zi<sup>1</sup>; <sup>1</sup>Clausthal University of Technology, Matls. Engrg. & Tech., Agricolastrasse 6, Clausthal-Zellerfeld 38678 Germany; <sup>2</sup>Chungnam National University, Dept. of Metallurgl. Engrg., Daejeon 305-764 Korea

Aluminum and copper were processed by equal channel angular pressing (ECAP) following the four standard routes. The effect of the ECAP route and the number of passes on strength and ductility as well as on the dislocation cell structure and texture was studied for both materials. To investigate the stress distribution in ECAP deformed workpieces, hardness maps with small imprint spacing were produced for various sections of the workpieces. The experimental results were compared with the simulations based on a phase-mixture model that combines a dislocation density evolution approach with crystal plasticity considerations. A good predictive capability of the model was confirmed.

#### 4:20 PM

**On the Mechanism of Grain Subdivision During Severe Plastic Deformation**: *A. E. Romanov*<sup>1</sup>; T. S. Orlova<sup>1</sup>; N. A. Enikeev<sup>2</sup>; A. A. Nazarov<sup>2</sup>; I. V. Alexandrov<sup>2</sup>; R. Z. Valiev<sup>2</sup>; <sup>1</sup>Ioffe Physico-Technical Institute, 26 Polytechnicheskaya, St. Petersburg 194021 Russia; <sup>2</sup>Ufa State Aviation Technology University, 12 K. Marx St., Ufa 450000 Russia

The problem of theoretical description of microstructure evolution at severe plastic deformation (SPD) is addressed. An energetic consideration for grain subdivision is developed in terms of disclination theory. The model assumes that larger grains split into a number of substructure elements in order to reduce the total latent energy stored in the material due to plastic deformation inhomogenities. The stored energy of a probe grain, which is constrained to a specific crystallographic orientation, is calculated using the disclination description. The grain is believed to be divided into a number of subgrains if the split configuration possessed lower energy than the initial one. Resulting structures are treated as disclination dipole and quadrupole configurations. The developed model demonstrates the typical features of substructure evolution at SPD: transformation of substructure into high angle grain boundaries and grain size refinement.

#### 4:35 PM

**Microstructures of Ferritic Warm Rolled Plain Carbon Steels**: *Gwenola Herman*<sup>1</sup>; Benoît Lechevalier<sup>2</sup>; Frank Montheillet<sup>2</sup>; Tarcisio Oliveira<sup>3</sup>; <sup>1</sup>Arcelor, R&D, CRDM, rue du comte Jean, Grande-Synthe BP2508, Dunkerque cedex 1 59381 France; <sup>2</sup>Ecole Nationale Supérieure des Mines de Saint-Etienne, CNRS URA 1884, Saint Etienne France; <sup>3</sup>ACESITA, Centro de Pesquisas, Praça 1° de Maio, 9, Timoteo - MG 35180-000 Brazil

Little work has been performed on ferritic warm deformation of plain carbon steels. By contrast, work on ferritic stainless steels has shown that intense hot deformation could lead to a fully dynamically recrystallised structure. This suggests that warm deformation in the ferritic region of steels could also lead to such microstructure, and therefore interesting prospects for the improvement of properties through grain size refinement. That is why the present prospective work focuses on warm rolling of plain carbon steels. Low carbon microalloyed steels (C<0.1%, 0.5%<Mn<1.5%, Si<0.4% + V) were intensively warm rolled (400-700°C) in the ferritic region after austenitic hot rolling on a laboratory rolling mill. This study shows that warm deformation in the ferritic region of plain carbon steels is indeed able to induce fragmentation of grains, although fragmentation remains partial. The EBSD analyses of microstructures suggest that in our case warm rolling induces continuous dynamic recrystallisation, although heterogeneous.

# 4:50 PM

Nano-Grained Steels Produced by Various Sever Plastic Deformation Processes: *Minoru Umemoto*<sup>1</sup>; *Yoshikazu Todaka*<sup>1</sup>; Koichi Tsuchiya<sup>1</sup>; <sup>1</sup>Toyohashi University of Technology, Production Sys. Engrg., 1-1 Hibarigaoka, Tempaku-cho, Toyohashi, Aichi 441-8580 Japan

The formation of nanocrystalline structure (NS) in steels by various severe plastic deformation processes, such as ball milling, a ball drop test, particle impact deformation and air blast shot peening are studied. Layered or equiaxed nanograined region appeared near the specimen surface and dislocated cell structured region appeared interior of specimens. The deformation induced nanograined regions have the following common specific characteristics: 1) with grains smaller than 100 nm and low dislocation density interior of grains, 2) extremely high hardness, 3) dissolution of cementite when it exist and 4) no recrystallization and slow grain growth by annealing. The deformation conditions to produce NS was discussed based on the available data in literatures. It was suggested that the most important condition is to impose a strain larger than about 7. High strain rates, low deformation temperature, multidirectional deformation, hydrostatic pressure are considered to be favorable conditions to produce NS.

#### 5:05 PM

Investigation Into the Effect on Grain Refinement of Developing a Strong Texture in an UFG Al-0.13% Mg Alloy Severely Deformed by ECAE: Christopher Paul Heason<sup>1</sup>; Philip B. Prangnell<sup>1</sup>; <sup>1</sup>UMIST, Manchester Matls. Sci. Ctr., Grosvenor St., Manchester M1 7HS UK

Much work has been done over the years in studying the production of UFG materials using equal channel angular extrusion (ECAE). Such materials are known to exhibit weak textures as a consequence of the repeated shear deformation. However, to date no investigation has been made into the effect of changing the deformation mode on such material. In this current study, a single phase Al-0.13% Mg alloy was severely deformed to a strain of ~10 at room temperature by ECAE, producing a submicron grain structure (>70% HAGB) and weak texture. Deformed billets were subsequently deformed by both conventional rolling and accumulative roll-bonding (ARB), producing sheet material with strong rolling textures and, in the case of ARB, an additional shear {001}<110> texture. It was found that, although initially the grain size decreased and HAGB fraction increased, as the rolling texture strengthened the HAGB fraction decreased to below 70% leading to an increase in grain size. This was associated with the appearance of coarse, unrefined banded regions, which were found to have very strong textures.

#### 5:20 PM

Structural Transformations in Metallic Multilayers During Intense Deformation: *Rainer J. Hebert*<sup>1</sup>; John H. Perepezko<sup>1</sup>; <sup>1</sup>University of Wisconsin, Dept. of Matls. Sci. & Engrg., 1509 Univ. Ave., Madison, WI 53706 USA

During repeated rolling and folding of metallic multilayers structural transformations occur that can include a refinement of the grainsize and the layer thickness to a nanometer level as well as atomicscale mixing and alloying reactions at the layer interfaces. The layer refinement is analyzed for Al-Pt and Al-Hf multilayers as a function of strain in terms of the relative specific interface area, the layer thickness distribution and the compass dimension of the layers. The analysis reveals a difference in the average layer thickness and the relative specific interface area between Al-Pt and Al-Hf multilayers that is approximately two orders of magnitude. The amorphization reaction at the Al-Pt interfaces during rolling is examined based on a TEM analysis. The results demonstrate the significance of the layer refinement for structural transformations in multi-phase materials during severe plastic deformation. The support of the ARO is gratefully acknowledged (DAAD 19-01-1-0486).

#### 5:35 PM

Structure Evolution During High Pressure Torsion of Ti-Ni-Based Shape Memory Alloys: Sergey Dmitriy Prokoshkin<sup>1</sup>; Irina Borisovna Trubitsyna<sup>1</sup>; Irina Yuriy Khemelevskaya<sup>1</sup>; Sergey Vladimir Dobatkin<sup>2</sup>; Evgeniy Vasiliy Tatyanin<sup>2</sup>; <sup>1</sup>Moscow State Steel and Alloys Institute, Leninsky prospekt 4, Moscow 119049 Russia; <sup>2</sup>Russian Academy of Science, Baikov Inst. of Metall. & Matl. Sci., Dept. of Phys.-Mech. Problems of Bulk Nanomatls., Leninsky prospekt 49, Moscow 119991 Russia

Ti-50.0at.%Ni (Ms = 68°C after quenching), Ti-50.7at.%Ni (Ms = -20°C) and Ti-47at.%Ni-3at.%Fe (Ms = -127°C) shape memory alloys subjected to a severe plastic deformation by high pressure torsion (HPT) have been studied using transmission electron microscopy, X  $_i$ V ray diffractometry and microhardness tests. True torsion strains var-

ied from 0 to 6.6, deformation temperatures from -196 to 200°C, and pressure from 4 to 8 GPa. A general sequence of structure formation with strain is from a strain-hardened dislocation substructure to a nanocrystalline structure and ultimately to an amorphized structure in all alloys studied. The tendency to form an amorphized structure is different for different alloys and depends on relative positions of the deformation temperature and starting point of the martensitic transformation Ms. Increasing of a pressure suppresses the tendency to form an amorphized structure as a consequence of the Ms lowering.

# Third International Symposium on Ultrafine Grained Materials: Posters

Sponsored by: Materials Processing & Manufacturing Division, MPMD-Shaping and Forming Committee
Program Organizers: Yuntian Ted Zhu, Los Alamos National Laboratory, Materials Science and Technology Division, Los
Alamos, NM 87545 USA; Terence G. Langdon, University of
Southern California, Departments of Aerospace & Mechanical
Engineering and Materials Engineering, Los Angeles, CA 90089-1453 USA; Terry C. Lowe, Metallicum, Santa Fe, NM 87501 USA;
S. Lee Semiatin, Air Force Research Laboratory, Materials & Manufacturing Directorate, Wright Patterson AFB, OH 45433 USA;
Dong H. Shin, Hanyang University, Department of Metallurgy and
Material Science, Ansan, Kyunggi-Do 425-791 Korea; Ruslan Z.
Valiev, Institute of Physics of Advanced Material, Ufa State Aviation Technology University, Ufa 450000 Russia

Mon PM/Tue/Wed	Room:	207A		
March 15-17, 2004	Location	n: Charlotte	Convention	Center

**Production of Fine-Grained Beryllium-6 wt% Copper for Fusion Ignition Capsules**: *David J. Alexander*<sup>1</sup>; Jason C. Cooley<sup>1</sup>; Dan J. Thoma<sup>2</sup>; Arthur Nobile<sup>3</sup>; <sup>1</sup>Los Alamos National Laboratory, MST-6 G770, Los Alamos, NM 87545 USA; <sup>2</sup>Los Alamos National Laboratory, ADWEM F654, Los Alamos, NM 87545 USA; <sup>3</sup>Los Alamos National Laboratory, MST-7, E549, Los Alamos, NM 87545 USA

Beryllium doped with 6 weight % copper is the material of choice for fabrication of target capsules for the National Ignition Facility because of its combination of attractive neutronic, physical, and mechanical properties. The target capsules are very small (2 mm in diameter) and thin-walled (150 microns) and must meet demanding dimensional specifications. The material must be fine-grained and of low inclusion content. Arc-melted Be-Cu is being produced to eliminate the oxide content that is inevitably present in conventional powder-metallurgy materials. Equal channel angular extrusion (ECAE) is being used to refine the as-cast grain structure. Be rods produced by the arc-melting process (5 mm in diameter by 30 mm in length) are enclosed in nickel cans with electron-beam welded plugs. The Be-in-Ni billets (9.5 mm in diameter by 45 mm in length) have been processed by ECAE at temperatures from 500 to 750°C. The resultant microstructures will be presented.

High Strain Rate Deformation Behavior of Ultra-Fine Grain Aluminum Produced by Equal Channel Angular Pressing: *Hiroyuki Miyamoto*<sup>1</sup>; <sup>1</sup>Doshisha University, Dept. of Mech. Engrg., 1-3 Miyakodani Tatara, Kyotanabe, Kyoto 610-0321 Japan

Deformation behavior of ultra-fine grained aluminum at high strain rates were investigated by impact tensile test, using Split Hopkinson Pressure Bar method. Ultra fine grained aluminum of commercial purity were produced by equal channel angular pressing by eight passes. Both the ultra-fine grained aluminum and polycrystalline aluminum of conventional grain size were deformed by the impact tensile tests and normal tensile test at the strai rate of 1200 1/s and 10-3 1-s, respectively under room temperature. It was found that ultra-fine grained aluminum show lower flow stress than that deformed at normal tensile stess while polycrystalline aluminum showed relatively similar stress in impact and tensile test. Microstructure after the tests were examined by transmission electron microscopy, and resuls were discussed in terms of dislocation dynamics.

**Computer Simulation of SPD Processes:** Alexander V. Spuskanyuk<sup>1</sup>; <sup>1</sup>Donetsk Physical & Technical Institute, 72 R. Luxemburg St., Donetsk 83114 Ukraine

New SPD processes Twist Extrusion and Equal Channel Multi-Angular Extrusion (ECMAE) have been studies by means of computer simulations. During twist extrusion a workpiece is extruded through the helical die with prismatic input and calibrating output channels localizing the twisting deformation in the beginning and in the end of helical die. ECMAE is performed by extruding a workpiece through constant cross-section channel with several changes of metal flowing direction. Computer simulation of the deformation and structure forming has been performed by combined use of mechanical FEM modeling for detailed study of the stressed-strained state evolution and original micromechanical multiscale model of polycrystalline aggregate to study the microstructure modification with emphasis on grain refinement. Correct correspondence of the simulation results with the experimental data for number of materials has allowed predicting of material structure and properties' evolution during processing, which made it possible to control and enhance these technologies.

Evolution of Grain Boundary Character Distribution in ECA-Pressed Pure Ti: Seng-Ho Yu<sup>1</sup>; *Sun-Keun Hwang*<sup>1</sup>; Dong-Hyuk Shin<sup>2</sup>; <sup>1</sup>Inha University, Sch. of Matls. Sci. & Engrg., #253, Yonghyun-Dong, Nam-Ku, Inchon 402-751 Korea; <sup>2</sup>Hanyang University, Dept. of Metall. & Matls. Sci., Kyunggi-Do, Ansan 425-791 Korea

Evolution of the grain shape, texture and grain boundary misorientation angle of commercially pure Ti during equal channel angular (ECA) pressing were studied with the use of microscopy, X-ray diffraction and electron back scattered diffraction. The grain size refinement was about a factor of 100 although the high angle boundaries were only realized with more than 4 passes using the route BC at various temperatures (250 to 550°C). Evolution of the texture during ECA pressing was derived from the complex combined activation of slip systems and twin systems, which was confirmed by texture prediction modeling based on visco-plastic self-consistent theory. Grain growth phenomena were studied with a Monte-Carlo computer simulation technique using a direct mapping concept. Overall the grain growth was characterized as a normal growth in the microstructure with stable random boundaries. The texture was found to be tenacious during subsequent heat treatment after ECA pressing.

Structural Changes of Severely Plastic Deformed Rail Steel: *Florian Wetscher*<sup>1</sup>; Richard Stock<sup>2</sup>; Baohui Tian<sup>1</sup>; Reinhard Pippan<sup>1</sup>; <sup>1</sup>Erich-Schmid Institute of Materials Science, Jahnstraße 12, Leoben 8700 Austria; <sup>2</sup>voestalpine Schienen GmbH, Tech./R&D, Kerpelystrasse 199, Leoben 8700 Austria

Severe Plastic Deformation (SPD) has been applied to ARMCOiron and the pearlitic rail steel S900A by means of High Pressure Torsion (HPT). In this study the evolution of the microstructure was investigated by different x-ray diffraction techniques and by transmission electron microscopy (TEM). The texture development in ARMCOiron and the rail steel as well as the obtained size of the structural elements will be compared. For the pearlitic steel the special features of microstructural evolution at larger strains, fragmentation of cementite lamellae, solution of carbon, etc. are described and discussed.

Processing of Aluminum Nickelides by Equal-Channel Angular Extrusion: Laszlo J. Kecskes<sup>1</sup>; Hyo Y. Kim<sup>1</sup>; Robert H. Woodman<sup>1</sup>; <sup>1</sup>US Army Research Laboratory, AMSRL-WM-MD, Deer Creek Loop, Aberdeen Proving Ground, MD 21005-5069 USA

Two series of nickel-coated aluminum (Al Ni) powder compositions were consolidated to full or near-full density by an equal channel engular extrusion technique. Mixtures of 78Al 22Ni at.% (63Al 37Ni wt.%) or 39Al 61Ni at.% (23Al 77Ni wt. %) were placed in squareshaped copper blocks, sealed, preheated to a range of temperatures from ambient to 700°C, and, once at a uniform temperature, dropped into a ECAE die and extruded. It was found that the preheating temperature affected the transformation of the initial Al Ni composition into aluminum nickelide (Al Ni) intermetallics. Scanning electron microscopy, energy dispersive x-ray spectroscopy, x-ray diffraction, and microhardness measurements were used to examine the nature of the resultant intermetallics. The onset and nature of the transformation from the precursors into the products were further studied by differential thermal analysis. These results and the role of ECAE on the transformation are discussed.

Generation of Sub-Micrometer Structures During Orthogonal Cutting of 1100Al: Mustafa Elmadagli<sup>1</sup>; Hai Ni<sup>1</sup>; Hai Ni<sup>1</sup>; Ahmet T. Alpas<sup>1</sup>; <sup>1</sup>University of Windsor, NSERC/GM of Canada Industrial Rsch. Chair, Mech., Auto. & Matls. Engrg., 401 Sunset Blvd., Windsor, Ontario N9B 3P4 Canada

Sub-micrometer structures developed in the material ahead of the tool tip in commercial purity 1100 Al samples (with an initial grain size of 4.6 mm and microhardness of 45 kg/mm2) that were subjected to an orthogonal cutting process were investigated using TEM. The microstructure of the primary deformation zone, where stains of the order of 1.5 were measured, was characterized by the formation of elongated dislocation cell structures of 370 nm in thickness, 725 nm in length that were composed of heavily tangled dislocation walls. Further grain refinement occurred in the chip as a result of dynamic

recrystallization and subdivision of the elongated cells into smaller equiaxed sub-micron size (300 nm diameter) grains. This was accompanied with a hardness increase to 80 kg/mm2. In this region strains were as high as 2.2. The strengthening arising from grain refinement is discussed using the Hall-Petch equation.

Microstructural Development in Interstitial Free Steel Processed by Equal Channel Angular Extrusion: Azdiar A. Gazder<sup>1</sup>; Elena V. Pereloma<sup>1</sup>; <sup>1</sup>Monash University, Sch. of Physics & Matls. Engrg., Bldg. 69, Monash Univ., Victoria 3800 Australia

Considerable grain refinement in bulk materials is achievable through the application of severe plastic deformation. In particular, equal channel angular extrusion could be utilized for this purpose. In current work, samples of interstitial free steel were pressed in air at room temperature. The tests were performed with the angle between channels of the die of 90 and 120° and up to 2 and 4 passes, respectively. The specimens were characterized using transmission electron microscopy and texture analysis. Effect of accumulated strain on the: (i) formation of systems of parallel microbands, delineated by planar boundaries, (ii) development of dislocation cells substructure, (iii) formation of shear bands and (iv) texture was evaluated.

**Response of Mechanical Properties Along the Workpiece Section to ECA-Pressing**: *Alexander I. Korshunov*<sup>1</sup>; <sup>1</sup>RFNC-VNIIEF, Tech. Div., Mira St., Bldg. 37, Sarov, Nizhny Novgorod Region 607190 Russia

Nonuniformity of mechanical properties along the workpiece section depending on the number of ECA-pressing operations was studied using annealed M1 Cu (min. Cu content 99.9%) as a sample material. The samples under examination had a square section with a side length of 8 mm and were cut out from an 8-mm thick sheet along the rolling direction. Microhardness distribution along the sample section was determined. Mechanical properties at drawing (conventional yield strength, ultimate strength, relative elongation and contraction) were determined at 9 points along the section using microsamples with a diameter of 1.5 mm cut out along the pressing direction. Strain diagrams were drawn. The investigations were carried out after 1, 2 and 4 pressing operations along the BC and C routes.

Structural Models of High-Energy Nanostructures in Metals and Intermetallic Materials Under Severe Plastic Deformation: Alexander Nikolaevich Tyumentsev<sup>1</sup>; Alexander Dmitrievich Korotaev<sup>2</sup>; 'Russian Academy of Science, Inst. of Strength Physics & Matls. Tech., Lab. of Struct. Transformations, 2/1, Academicheskii pr., Tomsk 634055 Russia; <sup>2</sup>Siberian Physicotechnical Institute, Tomsk 634050 Russia

Electron microscopy was used to investigate the features of the highly nonequilibrium structural states occurring in nanostructural metals and intermetallic compounds after severe plastic deformation caused by equichannel angular pressing, torsion in Bridgemen anvils, and cold rolling. A model has been proposed that treats nanostructural states as states with a high continual density of defects (dislocations and disclinations) in the bulk of submicrograins and a high density of partial disclinations) at their boundaries. Based on this model, methods for electron microscopic examination of local internal stress fields on the submicron scale have been developed. It has been shown that on the characteristic scale about 0.1 micrometer, these stresses reach values (~ E/30) close to the theoretical strength of the crystal and are responsible for the high stress gradients (moments), constituting the driving force of the collective rotational mode of deformation and recorientation of microvolumes.

Microstructure, Texture and Enhanced GB Energy in UFG Nickel: Alexandre P. Zhilyaev<sup>1</sup>; Jerzy A. Szpunar<sup>2</sup>; Maria Dolors Baró<sup>1</sup>; Terence G. Langdon<sup>3</sup>; <sup>1</sup>Universitat Autònoma de Barcelona, Dept. of Physics, Bellaterra, BCN 08193 Spain; <sup>2</sup>McGill University, Dept. of Metals & Matl. Engrg., 3610 Univ. St., Montreal H3A 2B2 Canada; <sup>3</sup>University of Southern California, Dept. Aeros. & Mech. Engrg., Los Angeles, CA 90089-1453 USA

Ultrafine-grained materials are expected to have higher strength and toughness comparing to their coarse-grained counterparts. Generally, grain refinement has been accomplished by using various thermomechanical processing treatments involving both heat treatments and mechanical working. But these procedures have the disadvantage that new and often complex procedures must be developed for each individual alloy. An alternative procedure is to use processes involving severe plastic deformation (SPD): equal channel angular pressing (ECAP) and high-pressure torsion (HPT). Thorough investigation of microstructure, texture and grain boundary statistics has been carried out in pure nickel samples fabricated by means of ECAP, HPT and their combination. It was accomplished that combination of ECAP and HPT leads to a deeper refinement of nickel samples possessing homogeneous and equiaxed microstructures. A difference between the released enthalpy in DSC experiments and the elastic energy evaluated by high-resolution x-ray diffractometry is attributed to the decrease in total surface energy during grain growth in ultrafine-grained nickel. The grain boundary (GB) surface energy of high angle boundaries was also evaluated.

**Destabilization of FCC Stable Materials at SPD Under High Pressure**: Boris M. Efros<sup>1</sup>; Yan Beygelzimer<sup>1</sup>; Anatoly Deryagin<sup>2</sup>; Natalia Efros<sup>1</sup>; Vitaliy Pilyugin<sup>2</sup>; *Dmitry Orlov*<sup>1</sup>; <sup>1</sup>University of the National Academy of Science, Donetsk Phys. & Tech. Inst., Physics of High Pressure & Advd. Tech. Dept., 72 R. Luxemburg St., Donetsk 83114 Ukraine; <sup>2</sup>Russian Academy of Science, Inst. of Metal Physics, Ekaterinburg 620219 Russia

It was shown that of a fine  $\alpha$ -phase was formed in the Hadfield steel a cold plastic deformation to  $\varepsilon = 50\%$ . Nuclei of the  $\alpha$ -phase of deformed samples reduced the decomposition start temperature of the austenite by 180C. Fine crystals of an  $\alpha$ -phase nearly 30 nm in size, whose concentration was as high as ~2.3%, were detected in a steel Fe79.55Mn17A13C0.45 after a SPD to  $\varepsilon = 92\%$ . A steel Fe61.2Cr18Mn20N0.7C0.1 contained fine crystals of a strain-induced  $\alpha$ -phase 20 nm in size after a low temperature plastic deformation. The  $\alpha$ -phase, which was formed under the given conditions, had an extremely low Curie temperature T<sub>c</sub> = 400C. When the steel was strongly deformed (e ~ 8) by SPD a strain-induced  $\alpha$ -phase have a normal Curie temperature T<sub>c</sub> = 600C. Thus, the obtained results indicate that SPD can result in a considerable destabilization of stable austenitic steels.

#### Fatigue Strength for Iron Based Nano-Composite: Chitoshi Masuda<sup>1</sup>; <sup>1</sup>Waseda University, Kagami-Memorial Lab. for Matls. Sci. & Tech., 2-8-26, Nishiwaseda, Sinjuku, Tokyo Japan

For electric refined iron having fine grain size the fatigue strength was about 300 MPa at the number cycles to failure of 107. This value is higher than that for a S25C carbon steels. It is suggested that the fatigue strength for iron and steels would be improved to be higher by the grain size or nano-structures. It has been reported that the iron having a nano-structures had a very high tensile strength up to about 1500 MPa, while the fatigue strength was not discussed yet. In this study, the fatigue strength and fatigue fracture mechanisms are discussed for iron having nano-structures. The iron powders of average size less than 45 mm were mixed by high energy ball mill and canning into the low carbon steel tube. The tube was welded for both sides and vacuumed at high temperature. After that the material was hot rolled and finally cold drawn in 5mm in diameter. The fatigue specimen was machined in order to remove the outer low carbon steel. The fatigue strength is about 500 MPa at the number cycles to failure of 107. The average fatigue strengths for S35C(12 Heats), S45C(11 Heats) and S55C(11 Heats) carbon steels quenched and tempered at 600°C are about 385, 437 and 463 MPa, respectively. The result obtained in this study is very higher than that for S35C, S45C and S55C carbon steels tempered at 600°C. Moreover, the fatigue strength for electric refined iron having the average grain size of 3mm was about 300 MPa at the number of cycles to failure reported. The fatigue strength for nanostructured iron was also 200 MPa higher than that for a iron having a fine grain size. Nano structured iron have a very fine grain size. It is more fine for nano-structured iron than electric refined iron cold drawn. The difference of fatigue strength beteen nano-structured iron and cold drawing electric refined iron would be caused by the decrease of the grain size and the dispersing the Fe2O3 nano-particles in iron matrix. Finally the fatigue strength and fatigue fracture mechanism for nano-structured composite will be compared with the material fabricated by powder iron, being the same as nano-composite, canning and drawing at room temperature.

#### **Developments in Equal Channel Angular Extrusion Technol**ogy: *David J. Alexander*<sup>1</sup>; <sup>1</sup>Los Alamos National Laboratory, MST-6 G770, Los Alamos, NM 87545 USA

Equal channel angular extrusion (ECAE) is the most developed method of severe deformation processing. Several extensions of the original ECAE technology have been developed at Los Alamos National Laboratory. These include: processing of long billets; processing of flat plate samples; continuous roll-fed ECAE; and dual-axis and triple-axis ECAE. These developments will be described and discussed.

#### Grain Refinement of Electron-Beam Melted Crystal Bar Zirconium by Equal Channel Angular Extrusion: David J. Alexander<sup>1</sup>; David A. Korzekwa<sup>1</sup>; <sup>1</sup>Los Alamos National Laboratory, MST-6 G770, Los Alamos, NM 87545 USA

Electron-beam melted crystal bar zirconium results in a very low oxygen content (approximately 100 ppm by weight), but a coarse grain structure (10s of mm) that must be refined. Cylindrical rods were sectioned by electrodischarge machining, and enclosed in seamless nickel tubing (1.2 mm wall thickness) by electron beam welding plugs in each end to make a final billet 9.5 mm in diameter by 60 mm in length. The billet was deformed by equal channel angular extrusion (ECAE) at room temperature in 120° tooling. After extrusion for 4 passes via route Bc the material was annealed in vacuum for 1 h at 550°C. Because of the low oxygen content, the Zr could be successfully deformed by ECAE to high strains at room temperature. The ascast grains were extensively subdivided by the processing. A fine uniform grain size of approximately 2 microns was achieved after the anneal.

Development of Crystallographic Texture During ECAPing of Beryllium: A Neutron Diffraction and Polycrystalline-Plasticity Modeling Study: Donald W. Brown<sup>1</sup>; David J. Alexander<sup>2</sup>; Irene J. Beyerlein<sup>3</sup>; Mark A.M. Bourke<sup>1</sup>; Carlos N. Tome<sup>1</sup>; Sven C. Vogel<sup>4</sup>; <sup>1</sup>Los Alamos National Laboratory, MST-8, MS-H805, Los Alamos, NM 87545 USA; <sup>2</sup>Los Alamos National Laboratory, MST-6, MS-G770, Los Alamos, NM 87545 USA; <sup>3</sup>Los Alamos National Laboratory, T-3, MS-B216, Los Alamos, NM 87545 USA; <sup>4</sup>Los Alamos National Laboratory, LANSCE-12, MS-H805, Los Alamos, NM 87545 USA

Beryllium samples were extruded from 1 to 4 passes through a 120° bend at 425°C following route Bc. In parallel, samples were also deformed under uniaxial compression at comparable strain rates and at 425°C. The crystallographic texture of each sample was determined using time-of-flight neutron diffraction techniques on the High Pressure Preferred Orientation (HIPPO) Diffractometer at LANSCE. A visco-plastic self-consistent (VPSC) model was developed to simulate the texture development during both deformation processes. Comparison of the model predictions of texture and flow strength to the simple uniaxial tests defined input parameters for the model, such as critical resolved shear stresses and hardening rates. These parameters were then used in an attempt to predict the more complicated deformation associated with ECAP'ing. A critical comparison of the observed and calculated texture development of the ECAP'ed samples will be given.

Mechanical Properties and Evolution of the Grain Structure of an Ultra-Fine Grained Cu-Al-O Alloy During Deformation: *Eduard V. Kozlov*<sup>1</sup>; Yurii F. Ivanov<sup>1</sup>; Anatolii N. Zhdanov<sup>2</sup>; Nina A. Koneva<sup>1</sup>; <sup>1</sup>Tomsk State University of Architecture and Building, Dept. of Physics, Solyanaya sq. 2, Tomsk 634003 Russia; <sup>2</sup>Altai State Technical University, Lenin Str., 46, Barnaul 656099 Russia

A dispersion strengthened Cu-Al-O alloy prepared by high-temperature extrusion was studied in this work. The samples with different average grain sizes in the range between 0.2 and 0.3 micron were studied. Deformation of the samples was performed in compression at room temperature. The structure of the alloys in the as-prepared state and after deformation was studied using TEM. A high yield stress and the stages III and V of work hardening were observed. Hall-Petch relationship was valid near the yield stress and at stress levels that correspond to developed plastic deformation. The analysis of the structure showed different behavior of grains with different sizes in a polycrystalline aggregate. During the deformation process, grain size distribution function, fraction of dislocation-free grains and their critical sizes are changing. The behavior of other parameters of the dislocation structure and the strengthening phases during deformation was also analyzed.

**Equal Channel Angular Pressing as an Efficient Technique for Grain Refiniment**: *Farid Z. Utyashev*<sup>1</sup>; Georgy I. Raab<sup>1</sup>; Ruslan Z. Valiev<sup>1</sup>; <sup>1</sup>Ufa State Aviation Technical University, Inst. of Physics of Advd. Matls., 12 K. Marx St., Ufa 450000 Russia

In the paper we compare various techniques for introducing large advanced strains leading to formation of fine grains and subgrains. Structural and mechanical analysis performed on the basis of experimental and theoretical data substantiates the need for formation of a homogeneous UFG structure refined down to the limit in materials of spatially non-monotone billet deformation in controlled thermomechanical conditions. Different examples of such deformation implementation are considered, including modified ECA pressing schemes, as well as microstructures and mechanical properties of a number of materials processed by severe plastic deformation, including hard-to-deform alloys.

**Processing Ultrafine Grained Composites of Elemental Titanium and Aluminum by Severe Plastic Deformation**: *Gajanan Chaudhari*<sup>1</sup>; Kazim Serin<sup>1</sup>; Viola L. Acoff<sup>1</sup>; <sup>1</sup>University of Alabama, Metallurgl. & Matls. Engrg., Box 870202, 126, 7th Ave., Tuscaloosa, AL USA

Ultrafine grained composite sheets of elemental titanium and aluminum foils were processed using the roll bonding process. These sheets were severely deformed by repeated cold rolling with interspersed folding of the sheets. The titanium layer was observed to neck and break down producing a finely dispersed intermixture of Ti-Al binary. The structural evolution of the resulting material was investigated using transmission electron microscopy (TEM). It revealed the formation of nano-scale grains in the composite. X-ray diffraction, differential scanning calorimetry (DSC) and scanning electron microscopy were also utilized to characterize the composites. Tensile testing, microhardness testing and nanoindentation were used to evaluate the mechanical properties of the resulting composite.

**Manufacturing of Long Specimens by ECAP**: *Gyorgy Krallics*<sup>1</sup>; Dmitry Malgin<sup>2</sup>; Georgy I. Raab<sup>3</sup>; Igor V. Alexandrov<sup>3</sup>; <sup>1</sup>Budapest University of Technology and Economics, Dept. of Matls. Sci. & Engrg., 7 Bertalan L., Budapest 1111 Hungary; <sup>2</sup>Drehsden Ltd., Budapest Hungary; <sup>3</sup>Ufa State Aviation Technical University, Inst. of Physics of Advd. Matls., 12 K. Marx St., Ufa, Bashkortostan 450000 Russia; <sup>3</sup>Ufa State Aviation Technical University, Inst. of Physics of Advd. Matls., 12 K. Marx St., Ufa, Bashkortostan 450000 Russia

ECAP is the most wide-spread technique for producing ultra-fine grained materials. Due to the cyclic nature of the process, it is difficult to produce specimens with a high length to diameter ratio. Ratios of 6-7 have been reported in the literature to date. Longer specimens, however, are useful since the homogenous part is larger and the relative size of end effects are smaller. Two methods were developed to obtain length to diameter ratios as high as 10. These methods allow using all routes (A, B, C) in the manufacturing process. This new technique was developed using the finite element computer simulation. The thermo-mechanical material tests before and after ECAP (1, 4 and 8 pass) are presented in this paper in order to show the influence of the process on mechanical properties of material (Al alloy 6082).

Use of Back Pressure During ECAP as a Means to Enhance the Deformability of Materials and Efficiently Refine the Structure: Georgy I. Raab<sup>1</sup>; Nickolay A. Krasilnikov<sup>2</sup>; Ruslan Z. Valiev<sup>1</sup>; <sup>1</sup>Ufa State Aviation Technical University, Inst. of Physics of Advd. Matls., 12 K. Marx st., Ufa 450000 Russia; <sup>2</sup>Ulyanovsk State University, 42 L. Tolstoy str., Ulyanovsk 432700 Russia

Equal channel angular pressing (ECAP) is an efficient technique for refinement of structure in bulk materials. However, fabrication by ECAP of samples out of low-ductile materials with a homogeneous ultrafine-grained structure without visible surface cracks and defects presents a problem. One of the techniques that enables to accomplish this task is use of back pressure in the process of ECAP allowing to control the stress strain in the strain center. By the example of copper (99.9%) and CP Ti it is shown that use of back pressure during ECAP leads to an increase in the number of passes before failure of the billet. Another advantage of ECAP with back pressure is formation of a more homogeneous structure with smaller grain size. The physical reasons and the role of back pressure for enhancement of strength and ductility in materials after ECAP are discussed in the present paper.

From Macro- to Meso-Level of Plastic Deformation During Equal-Channel-Angular Processing: Grigoreta Mihaela Stoica<sup>1</sup>; S. R. Agnew<sup>2</sup>; E. A. Payzant<sup>3</sup>; D. A. Carpenter<sup>4</sup>; P. K. Liaw<sup>1</sup>; <sup>1</sup>University of Tennessee, Matl. Sci. & Engrg., 323 Dougherty Bldg., Knoxville, TN 37996-2200 USA; <sup>2</sup>University of Virginia, Matls. Sci. & Engrg., Charlottesville, VA 22904 USA; <sup>3</sup>Oak Ridge National Laboratory, Metals & Ceram. Div., Oak Ridge, TN 37831 USA; <sup>4</sup>Y-12 National Security Complex, Oak Ridge, TN 37831 USA

Mg-alloy, ZK60, was subjected to Equal-Channel-Angular Processing (ECAP) using different strain paths: route A, B, and C. Optical microscopy, X-ray diffraction (XRD), and orientation-imaging microscopy (OIM) analyses are used for structural characterization at macro- and meso-levels of plastic deformation. The grain refinement, texture evolution, and elastic microstrain are determined, and correlated with the initiation of dynamic recrystallization during severe plastic deformation of ZK 60.

Influence of Experimental Parameters on the Plastic Flow Curve Obtained by Ball Indentation Testing: Gopinath R. Trichy<sup>1</sup>; Ronald O. Scattergood<sup>1</sup>; Kishore Ramaswamy<sup>1</sup>; Carl C. Koch<sup>1</sup>; K. L. Murty<sup>1</sup>; <sup>1</sup>North Carolina State University, Matls. Sci. & Engrg., Stinson Dr., Riddick Bldg., Raleigh, NC 27695-7907 USA

The techniques for material characterization need to be modified such that reliable data is obtained for the small samples typically produced for nanocrystalline materials. The ball indentation (BI) test is one such technique. BI tests were performed on steels, aluminum alloys and pure zinc (conventional and nanocrystalline) using a computer-controlled screw driven UTM. True stress and plastic strain were evaluated by changing the fixture compliance and indenter ball size. The plastic diameter of the impression was obtained by partial unloading, complete unloading, and optical measurement. BI tests were compared to conventional tensile tests and the influence of the experimental parameters on the flow curve is discussed. The theoretical background necessary for the BI methodology is also discussed.

An Evaluation of Cavity Development in the Tensile Testing of Ultrafine-Grained Iron Processed by ECAP: *Hsuankai Lin*<sup>1</sup>; Cheng Xu<sup>1</sup>; Bing Q. Han<sup>2</sup>; Enrique J. Lavernia<sup>2</sup>; Terence G. Langdon<sup>1</sup>; <sup>1</sup>University of Southern California, Aeros. & Mech. Engrg. & Matls. Sci., Los Angeles, CA 90089-1453 USA; <sup>2</sup>University of California, Chem. Engrg. & Matls. Sci., Davis, CA 95616-5294 USA

Iron of commercial purity was subjected to Equal-Channel Angular Pressing (ECAP) to reduce the grain size from an annealed value of ~200  $\mu$ m to a final value of ~0.2 - 0.4  $\mu$ m. Following ECAP, tensile samples were cut from the as-pressed billets with their tensile axes lying along the pressing direction. These samples were pulled to failure over a range of elevated temperatures using an initial strain rate of 1 x 10<sup>-3</sup> s<sup>-1</sup>. After fracture, samples were sectioned, polished and then examined carefully in an optical microscope equipped with a video camera and a facility for recording quantitative information on the size and shape of any internal cavities. Measurements were taken to record the average cavity area, the cavity shape in terms of the roundness coefficient and the orientation of the long axis of each cavity with respect to the tensile axis.

**Computer Simulation Analysis of Texture Formation Processes at ECAP**: *Igor V. Alexandrov*<sup>1</sup>; Andrey V. Shcherbakov<sup>1</sup>; Marina Zhilina<sup>1</sup>; Irene J. Beyerlein<sup>2</sup>; <sup>1</sup>Ufa State Aviation Technical University, Inst. of Physics of Advd. Matls., 12 K. Marx St., Ufa, Bashkortostan 450000 Russia; <sup>2</sup>Los Alamos National Laboratory, Theoretical Div., T-3, MS B216, Los Alamos, NM 87545 USA

Recent investigations have successfully demonstrated that the process of equal-channel angular pressing (ECAP) is accompanied by an intensive texture formation. However, the mechanisms of texture evolution are still not totally understood due to a complexity of the stress- strain state imposed on the sample by different routes of ECAP. In this work we represent the results of investigation of texture formation in pure copper using three types of polycrystalline models: the full constraints Taylor model, Sachs' model, and the visco-plastic selfconsistent model. Their predictive capability is compared for different ECAP routes and number of passes. The obtained simulation results are also compared with the available experimental measurements of texture in pure copper using X-ray diffraction. Conclusions about the influence of the mentioned simulation parameters on the character of the texture formation processes at ECAP are made.

**FEM Investigations of Equal-Channel Angular Pressing**: *Igor N. Budilov*<sup>1</sup>; Igor V. Alexandrov<sup>1</sup>; Yuriy V. Lukashchuk<sup>1</sup>; Irene J. Beyerlein<sup>2</sup>; Vladimir S. Zhernakov<sup>1</sup>; <sup>1</sup>Ufa State Aviation Technical University, 12 K. Marx St., Ufa, Bashkortostan 450000 Russia; <sup>2</sup>Los Alamos National Laboratory, Theoretical Div., T-3, MS B216, Los Alamos, NM 87545 USA

Realization of equal-channel angular pressing (ECAP) and as a result processing of bulk nanostructured billets possessing attractive exploitation properties represents a hard-to-perform task and is a many-factor experiment. In this connection application of computer simulation is very perspective. In the current report one may observe the results of the analysis of processes, which take place at ECAP of a copper billet applying the finite-elements method (FEM) by LS-DYNA and Superform codes. 3D analysis has revealed that in the area of contact interaction between the billet and the die-set a formation of areas with a considerable heterogeneity of plastic deformation fields takes place. There has been conducted an investigation of the influence of principal parameters of the technological process on the obtained results. There have been elaborated recommendations on the die-set construction's optimization for ECAP of copper billets with a square cross section.

Features of the Localization of Plastic Deformation of Ultrafine-Grained Copper: *Ivan Alexandrovich Ditenberg*<sup>1</sup>; Alexander Nikolaevich Tyumentsev<sup>2</sup>; <sup>1</sup>Siberian Physicotechnical Institute, Tomsk 634050 Russia; <sup>2</sup>Russian Academy of Science, Inst. of Strength Physics & Matls. Tech., Tomsk 634055 Russia

Electron microscopy was used to investigate the evolution of the microstructure of samples of ultrafine-grained (UFG) copper subjected to active tension at room temperature. It has been revealed that under these conditions, from the very beginning of the deformation process, a major mechanism for plastic flow is the formation of strain localization mesobands through quasi-periodic events of formation and relaxation of stress mesoconcentrators at the front of propagation of the mesobands. Mechanisms for the plastic relaxation of mesoconcentrators at the front of propagation of mesobands have been revealed and discussed, such as dynamic recrystallization, mechanical twinning, collective dislocation-disclination mechanisms for the deformation and

reorientation of the lattice in the zones where the local stresses of mesoconcentrators are maximum and inside deformation microtwins.

Microstructure Evolution and Mechanical Behavior of Bulk Copper Obtained by Consolidation of Micro and Nano Powders: Mohammed Haouaoui<sup>1</sup>; *Ibrahim Karaman*<sup>1</sup>; Hans J. Maier<sup>2</sup>; <sup>1</sup>Texas A&M University, Dept. of Mech. Engrg., MS 3123, College Sta., TX 77843 USA; <sup>2</sup>University of Paderborn, Lehrstuhl f. Werkstoffkunde, Paderborn 33095 Germany

Consolidation of micro and nano copper particles (-325 mesh, 130 nm, and 100 nm) was performed using room temperature equal channel angular extrusion (ECAE). The evolution of the microstructure and the mechanical behavior of the consolidates were investigated and related to the processing route. Possible deformation mechanisms are proposed and compared to those in ECAE processed bulk Cu. The effects of extrusion parameters for consolidation such as ECAE route, number of passes and extrusion rate are evaluated. Two extrusion passes were sufficient for obtaining full density. Combined high ultimate tensile stress (490 MPa) and ductility (~20% tensile fracture strain) with near elasto-plastic behavior was observed in consolidated -325 mesh Cu powder. On the other hand, early plastic instability took place leading to a continuous softening in flow stress of bulk ECAEd copper. Increase in both strength and ductility was evident with increasing number of passes in the bulk samples. Compressive strengths as high as 760 MPa were achieved in consolidated 130 nm copper powder. The average grain size of the consolidated 130 nm powder was about 90 nm. The simultaneous increase in strength and ductility in extruded bulk Cu observed in a microstructure with an average grain size of 300-500 nm appears to be inconsistent with grain boundary moderated deformation mechanisms as proposed before. Instead, the increase of ductility is attributed to dynamic recovery and local recrystallization forming bimodal microstructures. Near-perfect elastoplasticity was encountered in consolidated -325 mesh Cu powder. This effect is explained by a combined effect of strain hardening accommodated by large grains in the bimodal structure and softening caused by a recovery mechanism such as trapping of dislocations at grain boundaries. The present study shows that ECAE consolidation of nanoparticles opens a new possibility for the study of deformation mechanisms and mechanical behavior of bulk nanocrystalline materials as well as offering a new class of bulk materials for practical engineering applications. This work was supported by the National Science Foundation contract CMS 01-34554, Solid Mechanics and Materials Engineering Program, Directorate of Engineering, Arlington, Virginia and Deutsche Forschungsgemeinschaft.

Grain Refinement and Deformation Twinning in Severely Deformed AISI 316L Stainless Steel at High Temperatures (0.4 Tm - 0.65 Tm): G. Guven Yapici<sup>1</sup>; Yang Cao<sup>1</sup>; Ibrahim Karaman<sup>1</sup>; Zhiping Luo<sup>2</sup>; <sup>1</sup>Texas A&M University, Dept. of Mech. Engrg., MS 3123, College Sta., TX 77843 USA; <sup>2</sup>Texas A&M University, Microscopy & Imaging Ctr., College Sta., TX 77843 USA

The present work focuses on the grain refinement and deformation twinning of AISI 316L austenitic type stainless steel. Bulk stainless steel bars are processed using equal channel angular extrusion (ECAE) with a 90° tool angle. Microstructure and mechanical properties of successfully extruded billets are reported through light microscopy, electron microscopy, and mechanical experiments. X-ray analysis is conducted to report macro-texture evolution. Results are compared for different extrusion conditions including variations in temperature (450°C, 550°C, 600°C, 700°C and 800°C) and processing routes (one pass or two passes). Higher tensile and compressive strengths are obtained after ECAE compared to that of initial materials in relation with the grain refinement and deformation twinning. One pass extrusion at 700°C resulted in flow strength values more than 1000 MPa. Observed tension/compression asymmetry in the yield strength values and strain hardening was attributed to the deformation induced directional back stress, texture produced after ECAE and different deformation mechanisms under tension and compression. The goal is to produce desired end microstructures where deformation twinning is stabilized at high temperatures forming nanostructured AISI 316L stainless steel, leading to improved mechanical properties.

Peculiarities of the Reorientation of the Crystal Lattice During the Formation of Nanocrystals and Submicrocrystals of High-Nitrogen Austenitic Steel: *Igor Litovchenko*<sup>1</sup>; Alexander Nikolaevich Tyumentsev<sup>1</sup>; <sup>1</sup>Russian Academy of Science, Inst. of Strength Physics & Matls. Tech., Tomsk 634055 Russia

Transmission electron microscopy was used to study the evolution of the defect structure of a high-nitrogen austenitic steel in the process of its cold rolling. For profound strains of over 0.9 the crystal lattice of gamma-austenite is observed to disperse into nanocrystals with large-angle and small-angle disorientations. It has been revealed that the fragmentation of the crystal lattice into nanostructural states occurs with the participation of several mechanisms: the disclination mechanism for reorientation through collective rearrangements of substructures with a continual disclination density into nonequilibrium boundaries with high densities of grain-boundary disclinations; the prevailing mechanism for the formation of large-angle boundaries is mechanical twinning; a new mechanism for the deformation and reorientation of the lattice has been discovered which involves direct and reverse (over alternative systems) martensitic transformations in high local stress fields, leading to the formation of large-angle boundaries with reorientation vectors about 60°.

Microstructural Features and Mechanical Behavior of UFG Ti-6AI-4V Eli Alloy: Irina P. Semenova<sup>1</sup>; Yuntian Theodore Zhu<sup>2</sup>; Terry C. Lowe<sup>2</sup>; Georgy I. Raab<sup>1</sup>; Ruslan Z. Valiev<sup>1</sup>; <sup>1</sup>Ufa State Aviation Technical University, Inst. of Physics of Advd. Matls., 12 K. Marx St., Ufa, Bashkortostan 450000 Russia; <sup>2</sup>Los Alamos National Laboratory, Matls. Sci. & Tech. Div., MS G755, STC, Los Alamos, NM 87545 USA

This paper presents the research results of two-phase (a+b)Ti-6Al-4V Eli alloy, aimed at the formation of homogeneous ultra-fine grained (UFG) structure using severe plastic deformation (SPD) by means of ECAP and additional thermo-mechanical treatment. The mechanical behavior of the alloy during tensile tests at room teperature and their failure behavior were investigated. The study of structure formation and phase morphology features during deformation was carried out. It was found that SPD of Ti-6Al-4V Eli resulted in considerable enhancing of mechanical properties due to grain refinement and high internal stresses. For example, yield stress in processed samples increased by 30% in comparison with the initial state, preserving sufficient ductility. There were found some regularities in structure formation and properties of the alloy depending on the regimes of treatment. It was established that the combination of deformation and metastable phases' decomposition during SPD enabled to control microstructure and phase composition of the alloy and, correspondingly, its strength and ductility.

Structural Evolution by ECAP Processing of Copper and Tantalum: James M. O'Brien<sup>1</sup>; Joel W. House<sup>2</sup>; William F. Hosford<sup>4</sup>; Robert J. De Angelis<sup>3</sup>; <sup>1</sup>O'Brien and Associates, 406 S. Lane St., Blissfield, MI 49228 USA; <sup>2</sup>Air Force Reseach Laboratory, MNMW, 101 W. Eglin Blvd., Ste. 125, Eglin AFB, FL 32542-6810 USA; <sup>3</sup>University of Florida/ GERC, Shalimar, FL USA; <sup>4</sup>University of Michigan, Ann Arbor, MI 48109-4788 USA

Equal angular channel pressing (ECAP) provides practical advantages for material processing since the final geometry is unchanged from the initial geometry of the work piece. This attribute can be exploited in manufacturing environments where a) existing processing lines for specific part geometries are well established, or b) the part geometry dictates a specific processing route. If the in-service application of the part can utilize the unique properties attributable to ultra-fine grain structure than ECAP processing is a viable technology to be studied. In this investigation, tantalum and copper rods were processed by ECAP. A series of 2.5 inch diameter, 5 inch long cylinders of copper and tantalum were pushed through a 135° channel die. The cylinders were strained to a magnitude of 4 and 8 using Route B processing. Specimens of the materials were annealed after ECAP processing. The mechanical properties of the materials were characterized by hardness and tensile test measurements. The structural properties were characterized by grain size and grain orientation, via texture analysis. Results of the data analysis indicate the level of grain size reduction, uniformity and texture evolution that can be achieved by ECAP processing of copper and tantalum.

An Investigation on the Effect of Different Routes of Equal Channel Angular Pressing on Structure Evolution in a Commercial Low Carbon Steel: *Jingtao Wang*<sup>1</sup>; Junxia Huang<sup>2</sup>; ZhongZe Du<sup>2</sup>; Zheng Zhang<sup>2</sup>; Xicheng Zhao<sup>2</sup>; <sup>1</sup>Nanjing University of Science and Technology, Dept. of Matls. Sci. & Engrg., XiaoLingWei 200#, Nanjing 210094 China; <sup>2</sup>Xi'an University of Architecture and Technology, Sch. of Metallurgl. Engrg., Yanta Rd. No 13, Xi'an 710055 China

Structure evolution in a commercial low carbon steel (Fe-0.15%C-0.52%Mn) during equal channel angular pressing (ECAP) at room temperature was investigated comparatively via route C and Bc. Although in both cases the SAD pattern changes in a similar way, from a single crystal pattern with increasing azimuth spreading of the spots at low ECAP passes, to a discontinuous ring pattern with extensive azimuth spreading at high ECAP passes, indicating the formation of highly non-equilibrium structure with high grain boundary misorientations; with route C, nearly parallel bands of elongated substructures pertains in the ferrite microstructure after ECAP from 1 to 11 passes, with a slight decrease of the band width from 0.3-0.4 to 0.20.3 micrometers, while with route Bc, equiaxed grain structure with a grain size of about 0.25 micrometers forms at after 4 passes of ECAP. It is concluded in this investigation that ECAP route is critical to the formation of equiaxed grain structure in low carbon steel at room temperature.

Microstructure Evolution in a Lamellae Al-33%Cu Eutectic Alloy During Equal Channel Angular Pressing: *Jingtao Wang*<sup>1</sup>; Suk-Bong Kang<sup>2</sup>; Hyung-Wook Kim<sup>2</sup>; 'Nanjing University of Science and Technology, Dept. of Matls. Sci. & Engrg., XiaoLingWei 200#, Nanjing 210094 China; <sup>2</sup>Korea Institute of Machinery and Materials, Dept. of Matls. Engrg., Changwon 641-010 Korea

Strain driven transformation of lamellae structure in an eutectic Al-33%Cu alloy into a homogeneous equiaxed micro-duplex structure was investigated in equal channel angular pressing(ECAP) at 400°C via route Bc. Intensive strain during ECAP is accommodated by periodic bending, periodic shear banding, parallel shearing, and shear cutting of the lamellae in the eutectic. The transformation follows the stages of subdivision of the colonies into smaller lamellae blocks; the separation of these lamellae blocks into isolated islands, and finally the shrinkage to disappear of these islands, through the breaking down of the lamellae at near the lamellae block-equiaxed region boundaries. The kinetics of this strain driven microstructure transformation process, described by the dependence of relative lamellae area fraction on accumulated ECAP equivalent true strain, physiognomically resembles that of thermal activated transformation process.

Effect of Hard Cyclic Viscoplastic Deformation on Hardening/ Softening of SPD Copper: Lembit Kommel<sup>1</sup>; <sup>1</sup>Tallinn Technical University, Dept. of Matls. Engrg., Ehitajate tee 5, 19086, Tallinn Estonia

Detailed studies of ultrafine grained copper were performed on hard cyclic viscoplastic hardening/softening behavior. The hysteresis loops and axial stress amplitude analysis were made in the total deformation range 1%, 2% and 1+2+1% at 30 cycles accordingly. Special attention was paid to the role of structure condition depending on severe plastic deformation (SPD) passes number or grain sizes and heat treatment regimes of specimens. The results of this study show, that the ultrafine grained copper after SPD had a maximal axial stress, up to 435 MPa, the three times higher then annealed coarse grained copper after deformation hardening during viscoplastic deformation. In especially high cyclic hardening was measured of annealed at 400°C by low heating rate at 1°C/min of nanocrystalline copper but nanocrystalline copper, annealed at 200°C has minimal hardening/softening behavior and constant stress amplitudes during hard cyclic viscoplastic deformation. These behaviors are discussed in the terms of developing structures

An Examination of Cavity Development in an Aluminum-6061 Metal Matrix Composite Processed by Equal-Channel Angular Pressing: Megumi Kawasaki<sup>1</sup>; Yi Huang<sup>1</sup>; Cheng Xu<sup>1</sup>; Minoru Furukawa<sup>2</sup>; Zenji Horita<sup>3</sup>; Terence G. Langdon<sup>1</sup>; <sup>1</sup>University of Southern California, Aeros. & Mech. Engrg. & Matls. Sci., Los Angeles, CA 90089-1453 USA; <sup>2</sup>Fukuoka University of Education, Dept. of Tech., Munakata, Fukuoka 811-4192 Japan; <sup>3</sup>Kyushu University, Matls. Sci. & Engrg., Fac. of Engrg., Fukuoka 812-8581 Japan

An Al-6061 metal matrix composite, reinforced with 10 vol% of very fine Al2O3 particulates, was subjected to equal-channel angular pressing (ECAP). Inspection showed the grain size of the composite was reduced to the submicrometer level through processing by ECAP. The mechanical properties of the material were investigated using tensile testing at high temperatures over a range of strain rates. A detailed examination was conducted to evaluate the extent of cavitation in the samples pulled to failure and the results were recorded quantitatively using an appropriate analytical technique. This paper describes the development of cavities in the composite during tensile testing after ECAP and presents representative plots that summarize the cavity characteristics.

**On the Forces Generated During Friction Stir Processing of Aluminum 5052 Sheets**: Rajeswari R. Itharaju<sup>1</sup>; *Marwan K. Khraisheh*<sup>1</sup>; <sup>1</sup>University of Kentucky, Ctr. for Mfg., Mech. Engrg. Dept., 210 CRMS Bldg., Lexington, KY 40506-0108 USA

Friction Stir Processing (FSP) is a new advanced processing technique used to refine and homogenize the microstructure of alloy sheets. FSP has several advantages over traditional processing techniques including single step process, non-consumable and inexpensive tool, environmentally friendly, and easy to implement. Several studies have been conducted to optimize the process and relate various process parameters like rotational and translation speeds to the resulting microstructure. However, there is little data reported on the relation between forces generated during processing and the resulting microstructure. In this work, we discuss the relationship between the processing forces, the process parameters and the resulting microstructure of AA 5052. Sheets of 1/8 inch thickness were stir processed using a CNC HAAS vertical milling machine at different combinations of rotational and translational speeds. The forces were measured using a 3-component piezoelectric KISTLER dynamometer. The results indicate that the processing forces are sensitive to the process parameters and can be used to control and optimize the process.

On the Description of Intergranular Boundaries Misorientation During Severe Plastic Deformation: Nariman A. Enikeev<sup>1</sup>; Igor V. Alexandrov<sup>1</sup>; Ruslan Z. Valiev<sup>1</sup>; Tatiana S. Orlova<sup>2</sup>; Alexei E. Romanov<sup>2</sup>; <sup>1</sup>Ufa State Aviation Technical University, Inst. of Physics of Advd. Matls., ul. K.Marxa, 12, Ufa 450000 Russia; <sup>2</sup>Ioffe Physico-Technical Instutite, Polytechnicheskaya, 26, St. Petersburg 194021 Russia

There are numerous evidences that during severe plasctic deformation (SPD) mean misorientation evolution takes place and nanostructures with high angle grain bounaries are formed. In the given publication a theoretical description of transormation of low angle grain boundaries to high angle ones is discussed. A physical approach to this description connected with accumulating of sessile dislocations during deformation is considered. The interaction of interface boundaries with lattice dislocations is described and contribution of resulting defect structures to mean misorientation evolution is estimated. The obtained results are compared to experimental data available in literature.

**Evolution of the Structure of an Ultra-Fine Grained Cu During Plastic Deformation**: *Nina A. Koneva*<sup>1</sup>; Nataliya A. Popova<sup>1</sup>; Anatolii N. Zhdanov<sup>2</sup>; Lina N. Ignatenko<sup>1</sup>; Eduard V. Kozlov<sup>1</sup>; <sup>1</sup>Tomsk State University of Architecture and Building, Dept. of Physics, Solyanaya sq. 2, Tomsk 634003 Russia; <sup>2</sup>Altai State Technical University, Lenin Str., 46, Barnaul 656099 Russia

This paper is devoted to the study of plastic deformation and evolution of the structure of the ultra-fine grained Cu with the average grain size of 0.21 micron during compression at room temperature. The compression experiments revealed changes in the Cu substructure in the strain range between 0 and 90%. TEM of thin films and replicas was used to study the structure. The quantitative analysis of the substructure evolution during deformation was performed. The following parameters of the Cu structure were studied as a function of strain: grain size, density of boundaries of different types, scalar and excess dislocation densities, curvature-torsion of the crystal lattice, the amount of the dislocation slip within grains and grain boundary sliding. The chosen grain size ensured manifestation of the stages III and V of work hardening. The stage V was related to the oscillating behavior of most parameters of the dislocation structure with deformation.

Grain Refinement Mechanisms Operating During Severe Deformation of Aluminium Alloys Containing Second-Phase Particles: *Pete Apps*<sup>1</sup>; Philip B. Prangnell<sup>1</sup>; <sup>1</sup>UMIST, Manchester Matls. Sci. Ctr., Grosvenor St., Manchester M1 7HS UK

The effects of coarse second-phase particles (Al<sub>13</sub>Fe<sub>4</sub>), and fine coherent dispersoids (Al<sub>3</sub>Sc), on the evolution of ultra-fine grained structures have been examined in simple model aluminium alloys deformed by ECAE. The microstructural evolution has been studied using high-resolution EBSD and compared to previous work on single-phase alloys. It is shown that the presence of coarse particles dramatically increases the rate of grain refinement, and allows a uniform fine grain structure to be developed at a strain of ~5. In contrast, the presence of fine dispersoids appears to inhibit the formation of high-angle grain boundaries at low strain and, hence, retard the formation of a fine grain structure after severe deformation ( $\epsilon$ ~10). The microstructural mechanisms operating in each case are discussed.

Processing and FEM Simulation of a 5083 Aluminium Alloy at Room Temperature: Pedro A. Gonzalez Crespo<sup>1</sup>; Ignacio Puertas Arbizu<sup>1</sup>; Carmelo J. Luis Pérez<sup>1</sup>; <sup>1</sup>Public University of Navarre, Mech. & Matls. Engrg. Dept., Campus de Arrosadía s/n, Pamplona, Navarra 31006 Spain

The enhanced mechanical properties of crystalline materials is linked to very small grain sizes. ECAP is a technique for developing an ultrafine grained microstructure by introducing a severe plastic deformation in bulk materials by simple shear with no changes in their cross-section. The AA5083, an Al-Mg-Mn commercial alloy, is known for its superplastic behaviour. The room temperature mechanical properties of the extruded alloy were investigated through hardness measurements and tensile tests. Mechanical properties evolution during annealing is also considered. SEM-EBSD observations have been made in order to discuss the microstructural characteristics of the deformed alloy. Finite Element Modelling is used to predict the ECAE behaviour in different extrusions conditions and compared with experimental processes carried out in similar conditions.

Computer Simulation of Material Deformation Under Intense Plastic Strain During Equal-Channel Angular Pressing: Petr N. Nizovtsev<sup>1</sup>; <sup>1</sup>RFNC-VNIIEF, Teoretical Div., Mira St., Bldg. 37, Sarov, Nizhny Novgorod Region 607190 Russia

The analysis of behavior of material subjected to intense plastic strain (IPS) under the conditions of equal-channel angular pressing (ECAP) is an involved problem. When solving this problem, computer simulation of deformation processes at different scale levels plays an important role. At the macro-level, the material behavior can be described with a given scheme of deformation in accordance with its parameters. At the meso-level, which implies the study of grain and sub-grain structure and texture parameter evolution during the deformation, information about interrelation of the forming structure and properties of materials obtained can be acquired. The micro-level studies addressing elementary reactions of the atom-crystal defect interactions reveal the physical nature of the features of the processes that proceed. The paper presents the results of the first phase of the studies, i.e. macro-level material behavior simulation for one-pass ECAP with using a simple isotropic model of material (copper).

**Product Yield of ECAE Processed Material**: *Robert E. Barber*<sup>1</sup>; Tami Dudo<sup>1</sup>; Phillip B. Yasskin<sup>2</sup>; K. Ted Hartwig<sup>1</sup>; <sup>1</sup>Texas A&M University, Mech. Engrg., College Sta., TX 77843-3123 USA; <sup>2</sup>Texas A&M University, Math., College Sta., TX 77843-3368 USA

The growing study of ECAE has produced ever-increasing work on microstructural changes imparted to processed material. Little work, however, has been devoted to examining the resulting fully worked material volume in a given billet. In this paper, various processing schedules (routes) are studied, and the fully worked volume fraction and the billet region shapes reported. Each route is examined through at least eight passes, with billet aspect ratios ranging from 3:1 to 20:1. Volumes were calculated using Maple® math software and solid model techniques to verify the findings. This research will aid technology transfer to industry, since the useful volume fraction could greatly influence production efficiency and the final geometric shapes can influence the practicality of trimming operations, further reducing the useful material produced. The results to be reported are both surprising and interesting; route B ( $B_A$ ) for instance, was found to be far more efficient than route A.

Ultrafine Grained Steel After Heavy Warm Deformation of Ferritic - Pearlitic C-Mn Steels: Rongjie Song<sup>1</sup>; *Dirk Ponge*<sup>1</sup>; Radko Kaspar<sup>1</sup>; Dierk Raabe<sup>1</sup>; <sup>1</sup>Max-Planck-Institut für Eisenforschung, Max-Planck-Str. 1, 40237 Düsseldorf, Germany

In order to produce ultrafine ferrite in plain C-Mn steels with 0.15-0.3%C, the effect of heavy warm deformation with subsequent coiling on a ferritic-pearlitic structure was studied. It is shown that the resulting microstructure consists of ultrafine ferrite ( $\alpha$ ) grains (0.80-0.95 µm) and a homogeneously distributed cementite ( $\Theta$ ). Based on the results of Electron Back-Scattered Diffraction (EBSD), the fraction of highangle grain boundaries (> 15°) was in the range of 60% to 65%. Due to this refined microstructure, even these unalloyed steels exhibited excellent combinations of mechanical properties.

Microstructure and Mechanical Properties of Ultrafine Grained Low Carbon Steel Fabricated by Conventional Cold-Rolling and Annealing of Martensite: *Rintaro Ueji*<sup>1</sup>; Nobuhiro Tsuji<sup>1</sup>; Yoritoshi Minamino<sup>1</sup>; Yuichiro Koizumi<sup>1</sup>; <sup>1</sup>Osaka University, Dept. of Adaptive Machine Sys., 2-1, Yamadaoka, Suita, Osaka 565-0871 Japan

A new thermomechanical processing named the martensite process which can easily fabricate the ultrafine grained steels without severe plastic deformation was developed. In this process, martensite is used as the starting structure. The martensite starting structure was conventionally cold-rolled by various reductions and then annealed at various temperatures. The cold-rolled martensite mainly exhibited lamellar structure, which is typical in severely deformed materials. The area fraction of the lamellar structure increased and the mean spacing of the lamellar boundaries decreased with increasing the rolling reduction, accompanying significant strengthening. After subsequent annealing at warm temperatures, the lamellar structure turned to equiaxed ultrafine ferrite grains with carbides precipitated uniformly, and at higher temperatures conventional recrystallization occurred to form coarse grained structure. The recrystallization temperature became lower with increasing the rolling reduction. The specimen rolled to intermediate reduction (50%) performed the largest ductility keeping high strength around 900MPa after warm-temperature annealing.

The Effect of Rolling Strain on the Development of Ultrafine Grained Ti-Al-Nb Intermetallics: *Rengang Zhang*<sup>1</sup>; Viola L. Acoff<sup>1</sup>; Gajanan Chaudhari<sup>1</sup>; <sup>1</sup>University of Alabama, Dept. of Metallurgl. & Matls. Engrg., Box 870202, Tuscaloosa AL35487 USA

Ultrafine grained Ti-Al-Nb intermetallics were processed by cold rolling and reaction annealing of elemental Ti, Al and Nb foils to produce Ti-46Al-9Nb(at%) alloy. The microstructure and phase development during cold rolling and reaction annealing were characterized by XRD, SEM/EDS and TEM analysis. With increasing reduction in thickness, more Ti3Al and Nb3Al phases are expected to occur at the Ti/Al and Nb/Al interfaces. This study will characterize the effect of rolling strain on development of these phases. After two-stage reaction annealing, the microstructure is complex due to the presence of several phases. XRD pattern shows that mainly g-TiAl and a2-Ti3Al are present, but small amounts of a-Ti and AlNb3 can also be identified. The element Nb is mostly dissolved in the g phase where it replaces the Ti. The reactive phase formation sequence of the multilayer foils after annealing was studied for different reduction rates using DSC.

Novel Equal Channel Angular Extrusion Processing Schedules for Microstructural Refinement: Suveen N. Mathaudhu<sup>1</sup>; Jae-Taek Im<sup>1</sup>; Robert E. Barber<sup>1</sup>; K. Ted Hartwig<sup>1</sup>; <sup>1</sup>Texas A&M University, Mech. Engrg., Spence St., College Sta., TX 77842-3123 USA

Multipass equal channel angular extrusion (ECAE) has been utilized extensively for the purpose of grain refinement and for inducing or eliminating texture in a variety of materials. But reports have been conflicting and often contradictory as to what number of extrusions with which route produces the best results. In addition, the process yield (percentage of fully processed material) for these processing schedules has not been reported. In this paper, the recrystallized microstructures of a FCC material (Cu), a BCC material (Ta) and an intermetallic compound (Bi2Te3) processed by a novel processing schedule (route E) in 90° tooling are compared with the same materials processed using conventional ECAE processing routes. Grain size, microstructural uniformity and process yield are compared for each case. It is seen that route E effectively refines the microstructure of a variety of materials while retaining a higher level of process yield when compared to the conventional ECAE routes.

**Microstructure Refinement in Pure Metals by Machining**: *Travis* L. Brown<sup>1</sup>; Srinivasan Swaminathan<sup>1</sup>; Srinivasan Chandrasekar<sup>1</sup>; W. Dale Compton<sup>1</sup>; Kevin P. Trumble<sup>2</sup>; Alexander H. King<sup>2</sup>; <sup>1</sup>Purdue University, Sch. of Industrial Engrg., 315 N. Grant St., W. Lafayette, IN 47907-2023 USA; <sup>2</sup>Purdue University, Sch. of Matls. Engrg., 501 Northwestern Ave., W. Lafayette, IN 47907-2036 USA

A study has been made of microstructure and mechanical properties of machining chips created from commercially pure metals. Significant microstructure refinement has been observed, the resulting chip being composed entirely of ultrafine-grained structures. While the formation of these structures is a consequence of very large strain deformation imposed by the tool, characteristics of the microstructure are seen to be influenced by machining parameters, e.g. strain. Large plastic strains, typically between two and fifteen, are shown to be created in the chip in a single stage of deformation. The relationship between the strain, microstructure, and mechanical properties of the chip has been characterized. The results have provided unique insights into microstructure evolution and refinement during very large strain deformation. The viability of machining as a technique for studying the formation of ultrafine-grained pure metals, and extensions of the work to solid solutions and dispersion-strengthened metals will be discussed.

Enhanced Properties of Titanium and Titanium Alloys: Vladimir V. Latysh<sup>1</sup>; Ruslan Z. Valiev<sup>2</sup>; Terry C. Lowe<sup>3</sup>; Robert Asaro<sup>3</sup>; Yuntian Theodore Zhu<sup>4</sup>; <sup>1</sup>Scientific Engineering and Design Office "ISKRA", 81 Pushkin St., Ufa 450025 Russia; <sup>2</sup>Ufa State Aviation Technical University, Inst. of Physics of Advd. Matls., 12 K. Marx St., Ufa 450000 Russia; <sup>3</sup>Metallicum LLC, 1207 Callejon Arias, Santa Fe, NM 87501 USA; <sup>4</sup>Los Alamos National Laboratory, Matls. Sci. & Tech. Div., MS G755, STC, Los Alamos, NM 87545 USA

Severe plastic deformation (SPD) can modify the microstructures of metals to improve their mechanical properties. However, the variants of SPD methods that produce the best properties are best suited for the synthesis of small quantities and small volumes of metal. Recent work using a proprietary SPD process has demonstrated that exceptional properties can be achieved in billets of commercial purity (CP) titanium and Ti-6Al-4V ELI with diameters between 6.5 and 13 mm and lengths between 0.3 and 1 m. The increases in mechanical properties achieved in CP titanium over the as-received material include 102% increase in fatigue strength and 196% increase in yield strength. For Ti-6Al-4V ELI the increases are less, but still significant with 45% increase in fatigue strength and 66% increase in yield strength. These materials are promising for application in medical device, aerospace and automotive applications.

Nanostructures and Phase Transformations in Shape Memory TiNi-Based Alloys Subjected to Severe Plastic Deformation: Vladimir G. Pushin<sup>1</sup>; Ruslan Z. Valiev<sup>2</sup>; Dmitry V. Gunderov<sup>2</sup>; Nickolay I. Kourov<sup>1</sup>; Ludmila I. Yurchenko<sup>1</sup>; Terry C. Lowe<sup>3</sup>; Yuntian Theodore Zhu<sup>3</sup>; <sup>1</sup>Ural Division of Russian Academy of Sciences, Inst. of Metal Physics, 18 S. Kovalevskaya St., Ekaterinburg 620219 Russia; <sup>2</sup>Ufa State Aviation Technical University, Inst. of Physics of Advd. Matls., 12 K.Marx St., Ufa 450000 Russia; <sup>3</sup>Los Alamos National Laboratory, Matls. Sci. & Tech. Div., MS G755, STC, Los Alamos, NM 87545 USA

Using severe plastic deformation processing by HPT and ECAP we could produce nanostructured shape memory TiNi-based alloys with grain size near 100 mn and less. The paper presents the results of the first studies of phase and structure transformations in nanostructured SPD-processed TiNi-based alloys during cooling and heating using measurements of  $\rho(T)$  and  $\chi(T)$ , as well as the methods of TEM and X-ray diffraction. New mechanisms of thermoelastic martensitic transformations in the given alloys are revealed and their critical temperatures are determined. It is shown that use of SPD allows to vary essentially the temperatures and consecution of martensitic transformations in B2 TiNi-based alloys, their mechanical properties and shape memory effect. Above all, SPD ensures high reactive stress of SME which is necessary for application of high-strength nanostructured shape memory alloys for diminutive load-bearing units and elements.

Influence of High Pressure on 301 Stainless Steel Hardening Under Large Deformations in Diamond Anvil Apparatus: Victor Varyukhin<sup>1</sup>; Boris M. Efros<sup>1</sup>; Yan Beygelzimer<sup>1</sup>; Dmitry Orlov<sup>1</sup>; <sup>1</sup>National Academy of Science of Ukraine, Donetsk Phys. & Tech. Inst., 72 R. Luxemburg St., Donetsk 83114 Ukraine

The behaviour of metal gaskets between diamond anvils in a high pressure apparatus has been studied. Along with a basic function of pressure generation a gasket supports the anvils' working planes' peripheral area. The elastic-plastic deformation mechanics of a 301 stainless steel gasket was investigated while generating pressure up to 65 GPa on the gasket axis. It is showed deformation under high pressure leads to more larger hardening of the 301 stainless steel in comparison with the same deformation under normal conditions.

Influence of Outer Arc Angle on Mechanical Properties of Bulk Ultrafine Grained Pure Copper: Wei Wei<sup>1</sup>; Guang Chen<sup>1</sup>; *Jingtao Wang*<sup>1</sup>; <sup>1</sup>Nanjing University of Science and Technology, Matls. Sci. & Engrg., Xiao Lingwei Rd. 200, Nanjing, Jiangsu 210094 China

Equal channel angular pressing?iECAP?jis applied to 12mm?~12mm?~80mm billet of pure copper (99.98%) at room temperature. The effects of ECAP passes and the outer arc angle of the die on the hardness (HBS) and tensile properties of processed copper are studied. Optical microscopy is used to examine the shear deformation characteristics. The results of tensile test suggest that the outer arc angle close to 22??is in favor of improving the ductility of ECAPed specimens. Simultaneously the hardness value at =22??is higher than that of the other three outer arc angles beyond four passes. Two distinct stages representing different hardening characteristics were also observed at fourth pass.

**Grain Refinement at SPD: View of Metal Forming Engineer**: *Yan Beygelzimer*<sup>1</sup>; <sup>1</sup>National Academy of Sciences of Ukraine, Donetsk Phys. & Tech. Inst., High Pressure, Donetsk 83050 Ukraine

We offer and try to validate the following hypotheses. Every metal (under given thermo-speed conditions of deformation and a given value of hydrostatic pressure) possesses a certain stationary microstructure (SM), which is attained at sufficiently large quasi-monotonous deformations. SM is characterized by a certain size of fragments, and it guarantees for the metal its ideal plasticity under pressure in the sense that the deformation is fracture- and hardening- free. The SM of a given metal is formed faster by those processes that lead to a larger decrease of plasticity of this metal (under the same level of hydrostatic pressure in the center of deformation). In order to obtain UFG structures, it is necessary to carry out these processes under high hydrostatic pressure in the center of deformation. In this case, the relaxation of internal stress happens along the direction of crystalline refinement, not the direction of microvoid formation.

Equal Channel Angular Pressing as a Means of Improving the Hydrogen Absorption/Desorption Properties of Alloy ZK60: Vladimir Skripnyuk<sup>2</sup>; Eugen Rabkin<sup>2</sup>; Yuri Estrin<sup>1</sup>; *Rimma Lapovok*<sup>3</sup>; <sup>1</sup>Clausthal University of Technology, Matls. Engrg. & Tech., Agricolastrasse 6, Clausthal-Zellerfeld 38678 Germany; <sup>2</sup>Technion, Matls. Engrg., Haifa 32000 Israel; <sup>3</sup>Monash University, Sch. of Physics & Matls. Engrg., Clayton, Victoria 3800 Australia

Magnesium alloys are popular candidate materials for hydrogen storage in automotive applications. However, their hydrogen desorption kinetics are too slow for the purpose. An enhancement of the desoprtion rate is commonly achieved through microstructure refinement by means of high energy ball milling (HEBM). In the present work, an attempt was undertaken to reach the same goal by using equal channel angular pressing (ECAP). The object of the study was the commercial magnesium alloy ZK60 (Mg-4.95 wt.%Zn-0.71 wt. % Zr). ECAP was shown to have a significant accelerating effect on the hydrogen absorption/desorption kinetics, comparable with or even exceeding that of HEBM. An interesting feature associated with combined ECAP/HEBM processing is the disappearance of pressure hysteresis with regard to hydrogen absorption/desorption. This hydrogenation behavior is explained in terms of the microstructure of bulk samples and the morphology of dehydrogenated powders as observed by TEM and by high resolution scanning electron microscopy.

Effect of Microstructure on the Sliding Wear Performance of Ultrafine-Grained Aluminum Alloys by ARB: Yong-Suk Kim<sup>1</sup>; Jong Soo Ha<sup>1</sup>; Dong Hyuk Shin<sup>2</sup>; <sup>1</sup>Kookmin University, Advd. Matls. Engrg., 861-1 Chongnung-dong Songbuk-ku, Seoul 136-702 S. Korea; <sup>2</sup>Hanyang University, Dept. of Metall. & Matls. Sci., 1271 Sa 1-dong, Ansan, Kyunggi-Do 425-791 S. Korea

Dry sliding wear behavior of ultrafine-grained 5052 and 5083 Al alloys and commercial purity Al (1100) by an accumulative roll bonding (ARB) process was investigated. Pin-on-disk wear tests of the ultrafine-grained Al alloys were carried out under various applied load conditions using hardened bearing steel as a counterpart material. Wear resistance of the Al alloys was not increased by the grain refinement, though their strength (hardness) increased nearly two times after the ARB process. Wear rate of the ultrafine-grained Al alloys rather increased with the increase of the accumulative plastic strain (the number of ARB cycles). Worn surfaces and cross-sections of the worn specimens were examined with SEM and TEM to investigate the wear mechanism and to explain the rather unexpected wear behavior of the ultrafine-grained Al alloys. The high wear rate of the ultrafine-grained Al alloys was discussed with emphasis on the unstable and non-equilibrium microstructure of the Al alloys.

# TUESDAY

# 5th Global Innovations Symposium: Trends in LIGA, Miniaturization, and Nano-Scale Materials, Devices and Technologies: Small Volume Deformation

Sponsored by: Materials Processing & Manufacturing Division, MPMD-Powder Materials Committee, MPMD-Phase Transformations Committee-(Jt. ASM-MSCTS), MPMD-Computational Materials Science & Engineering-(Jt. ASM-MSCTS), MPMD/EPD-Process Modeling Analysis & Control Committee, MPMD-Surface Engineering Committee, MPMD-Shaping and Forming Committee, MPMD-Solidification Committee

*Program Organizers:* John E. Smugeresky, Sandia National Laboratories, Department 8724, Livermore, CA 94551-0969 USA; Steven H. Goods, Sandia National Laboratories, Livermore, CA 94551-0969 USA; Sean J. Hearne, Sandia National Laboratories, Albuquerque, NM 87185-1415 USA; Neville R. Moody, Sandia National Laboratories, Livermore, CA 94551-0969 USA

Tuesday AM	Room:	20	)2B		
March 16, 2004	Location	า:	Charlotte	Convention	Center

Session Chairs: Erica T. Lilleodden, Lawrence Berkeley National Laboratory, Matls. Sci. Div., Berkeley, CA 94720 USA; Sean J. Hearne, Sandia National Laboratories, Nanostruct. & Semiconductor Physics Dept., Albuquerque, NM 87185-1415 USA

## 8:30 AM Keynote

Some Challenges in Understanding Mechanical Properties at the Nanometer and Micrometer Length Scales: *William D. Nix*<sup>1</sup>; Feng Gang<sup>1</sup>; Julia R. Greer<sup>1</sup>; <sup>1</sup>Stanford University, Dept. of Matls. Sci. & Engrg., 416 Escondido Mall, Bldg. 550, Stanford, CA 94305-2205 USA

Nanomechanical devices are certain to play an important role in future technologies. Already sensors and actuators based on MEMS technologies are commonplace and new devices based on NEMS are just around the corner. These developments are part of a decades-long trend to build useful engineering devices and structures on a smaller and smaller scale. The creation of structures and devices calls for an understanding of the mechanical properties of materials at these small length scales. Size effects in plasticity are now well-known. Plastic deformation in small volumes requires higher stresses than are needed for plastic flow of bulk materials. The size dependence of the hardness of metals is described in terms of the geometrically necessary dislocations created in small indentations. This can be related to the continuum theory of strain gradient plasticity. It is equivalent to the effects of fine microstructures on strength, which can also be related to strain gradients. But such accounts break down when the size of the deformation volume begins to approach the spacing of individual dislocations. In this domain the nucleation of dislocations and plasticity under dislocation-starved conditions appears to be more important than strain gradients. In an effort to shed additional light on these topics, uniaxial compression experiments on tiny samples made by focused ion beam machining and integrated circuit fabrication methods are being conducted. These experiments involve by small deformation volumes and minimal strain gradients. They lead to some surprising results that are not yet understood.

#### 9:00 AM

Indentation Size Effects in Face-Centered Cubic Thin Films: From Micro to Nano: Z. Zong<sup>1</sup>; J. Lou<sup>1</sup>; Y. Huang<sup>2</sup>; Y. Huang<sup>1</sup>; D. Yang<sup>3</sup>; W. O. Soboyejo<sup>1</sup>; <sup>1</sup>Princeton University, PMI/MAE Dept., D404 E. Quad., Princeton, NJ 08544 USA; <sup>2</sup>University of Illinois, Dept. of Mech. & Industl. Engrg., 140 Mech. Engrg. Bldg., W. Green St., Urbana, IL 61801 USA; <sup>3</sup>Hysitron Inc., 5721 W. 73rd St., Minneapolis, MN 55439 USA

This paper presents the effects of a combined experimental and computational study of indentation size effects in metallic produced using LIGA and single crystal growth techniques. These include Ni, Au and Ag single crystals with 001, 110 and 111 orientations and LIGA Ni MEMS structures. Indentation size effects are studied in these systems using a combination of Vickers, Berkovitch and cube cornered indenters. Strong indentation size effects are reported for indents with sizes between the micron- and nano-scales. Sharper indenters are also shown to result in stronger size effects than blunter indenters. The measured trends in the indentation size effects are predicted using mechanismbased strain gradient plasticity theories. The limitations of strain gradient plasticity theory are also discussed before presenting some initial ideas for the modeling of indentation-induced plasticity at the nanoscale. The implications of the results are discussed for the modeling of contacts in micro- and nano-scale systems and devices.

#### 9:20 AM

The Effect of Length Scale on the Plastic Stability of Nanolayered Metals: Amit Misra<sup>1</sup>; *Richard G. Hoagland*<sup>1</sup>; Duncan L. Hammon<sup>1</sup>; Xinghang Zhang<sup>1</sup>; Eric Vanderson<sup>1</sup>; J. David Embury<sup>1</sup>; John P. Hirth<sup>1</sup>; <sup>1</sup>Los Alamos National Laboratory, Matls. Sci. & Tech. Div., MS G755, MST-8, Los Alamos, NM 87544 USA

Sputter deposited nanolayered metallic composites exhibit unusually high hardness when the bilayer periods approach nanometer dimensions. Self-supported Cu-Nb multilayered foils were room temperature rolled to study the deformation and fracture behavior at large plastic strains. At layer thickness of a few tens of nanometers, Cu-Nb multilayers exhibited extraordinary plastic stability undergoing uniform reduction in layer thickness to high levels of plastic strain. However, at layer thickness of a couple nanometers, fracture by shear localization was observed at rolling reductions of only a few percent. These observations are interpreted in terms of the effect of length scale on the dislocation mechanisms of deformation in nanolayered composites. The plastic stability of multilayers with alternating bilayer periods of tens of nanometers and few nanometers will also be discussed. This research is funded by DOE, Office of Science, Office of Basic Energy Sciences.

TUESDAY AM

# 9:40 AM

Mechanical Performance of ALD Films for Microdevice Coatings: *Neville R. Moody*<sup>1</sup>; Tom E. Buchheit<sup>2</sup>; Brad L. Boyce<sup>2</sup>; Tom M. Mayer<sup>2</sup>; Steve George<sup>3</sup>; <sup>1</sup>Sandia National Laboratories, Livermore, CA 94550 USA; <sup>2</sup>Sandia National Laboratories, Albuquerque, NM 87185 USA; <sup>3</sup>University of Colorado, Boulder, CO 80309 USA

Strength, friction, and wear are dominant factors in the performance and reliability of materials and devices fabricated using microsystem technologies. Applying coatings and films is one method to enhance device performance and reliability. This study characterizes films using Atomic Layer Deposition (ALD) as it is ideally suited for applying highly conformal, stress-free and well-adhered films necessary for coating microsystem devices. Results focus on the mechanical performance of tungsten and aluminum oxide ALD films. Nanoindentation and nanoscratch tests were used to assess properties and durability of both film systems. These tests showed that the properties varied with film thickness and composition. More importantly, they showed that the tungsten films exhibited pronounced susceptibility to delamination and spallation. These results will be discussed in terms of composition and structure of the ALD films and their impact on potential applications. This work supported by U.S. DOE Contract DE-AC04-94AL85000.

#### 10:00 AM Break

#### 10:20 AM

Using a Combined Modeling-Experiment Approach for Property Determination of Ultra-Thin ALD Films: John Michael Jungk<sup>1</sup>; Thomas E. Buchheit<sup>2</sup>; James A. Knapp<sup>3</sup>; Thomas M. Mayet<sup>4</sup>; Neville R. Moody<sup>5</sup>; Joel W. Hoehn<sup>6</sup>; William W. Gerberich<sup>1</sup>; <sup>1</sup>University of Minnesota, Chem. Engrg. & Matls. Sci., 421 Washington Ave., 151 Amundson Hall, Minneapolis, MN 55401 USA; <sup>2</sup>Sandia National Laboratories, Microsys. Matls., Trib. & Tech., PO Box 5800, MS 0889, Albuquerque, NM 87185 USA; <sup>3</sup>Sandia National Laboratories, Radiation-Solid Interactions, PO Box 5800, MS 1056, Albuquerque, NM 87185 USA; <sup>4</sup>Sandia National Laboratories, Thin Film, Vacuum & Pkgg., PO Box 5800, MS 0959, Albuquerque, NM 87185 USA; <sup>5</sup>Sandia National Laboratories, Microsys. & Matls. Mech., PO Box 969, MS 9404, Livermore, CA 94551 USA; <sup>6</sup>Seagate Technology LLC, 7801 Computer Ave., Minneapolis, MN 55435 USA

Thin-film coatings are often applied to microelectronic or MEMS devices to improve their corrosion resistance and tribological properties. One technique that is ideally suited for producing hard, ultra-thin, conformal coatings is atomic layer deposition (ALD). Through multiple half-reaction cycles, an ALD film may be grown to a specific thickness, usually between 2-50 nm. Typical ALD thicknesses are at the limit of accurate properties determination via nanoindentationbased techniques. This study investigated the mechanical characteristics of ALD films as a function of indentation depth and film thickness through nanoindentation-based methods coupled with ABAQUS finite element modeling to overcome the problem of characterizing these films. Details of this combined approach will be discussed. Hardness and modulus results were insensitive to film deposition at temperatures between 130C-200°C. These properties increase slightly as the deposition temperature was increased above 200°C. Detailed results from 5 and 20 nm alumina-ALD films will be presented. This work is supported by Seagate Technology LLC through a MINT grant and a part of it was performed at Sandia National Laboratories. Sandia is a multiprogram laboratory operated by Sandia Corporation, a Lockheed Martin Company, for the United States DOE under Contract DE-ACO4-94-AL85000.

#### 10:40 AM

Critical Thickness Theory and the Yield of Thin Beams: Andy Bushby<sup>1</sup>; *David Dunstan*<sup>1</sup>; <sup>1</sup>Queen Mary, University of London, Ctr. for Matls. Rsch., Mile End Rd., London E1 4NS UK

Although critical thickness theory was developed largely to understand the stability of strained epitaxial semiconductor layers, it is of much wider applicability to deformation in small volumes. It tells us that geometrically-necessary dislocations generated during yield should not lie within a certain depth h from a free surface. Implications for the observed yield point of a metal beam under a bending moment will be presented. In the size range below a few tens of microns thickness, the yield point is increased markedly. Experimental data on the bending of thin nickel beams will be reported and compared with the theory. Satisfactory agreement is obtained. We conclude that critical thickness theory may be sufficient to explain the observed size effects in the yield point, not only in beam-bending but in other geometries such as torsion and nano-indentation.

#### 11:00 AM

Adhesion of Hard Coatings on Electroplated Metals for Microelectronic Based Systems: *D. F. Bahr*<sup>1</sup>; M. J. Cordill<sup>1</sup>; N. R. Moody<sup>2</sup>; <sup>1</sup>Washington State University, Mech. & Matls. Engrg., PO Box 642920, Pullman, WA 99164-2920 USA; <sup>2</sup>Sandia National Laboratories, PO Box 969, MS 940, Livermore, CA 99550 USA

Thin film mechanical behavior and adhesion properties can be determined using nanoindentation. For electroplated films (such as those used in LIGA based technologies), tungsten films can provide wear resistance and can be used as a seed layer for electroplating. The hardness of an electroplated copper film will be related to the interfacial fracture toughness of the tungsten overlayer. The hardness of the overlayer, 50% changes in grain size to soften the film produce a more than doubling of the interfacial fracture energy. The copper surface after the removal of the buckled tungsten film shows a deformation induced plastic zone, and has been observed using both AFM and optical microscopy. The plastic zone is larger than the original buckle and exhibits a higher hardness than the bulk film when nanoindentation is carried out on the plastic zone.

#### 11:20 AM

The Nanoindentation Response of Ultrathin Dendrimer-Mediated Soft Metallic Films: *Xiao Li*<sup>1</sup>; Michael Curry<sup>1</sup>; Shane C. Street<sup>1</sup>; Mark L. Weaver<sup>1</sup>; <sup>1</sup>The University of Alabama, Ctr. for Matls. for Info. Tech., Box 35487-0209, Tuscaloosa, AL 35487-0209 USA

Nanoindentation tests were conducted on dendrimer-free and dendrimer-mediated Cu, Al and Ti films deposited on Si substrates to investigate the influence of dendrimer underlayers on their mechanical and tribological properties. Ultrathin (10 nm) metal films were deposited via direct current (DC) magnetron sputtering onto (100) oriented Si substrates. Half of the substrates were coated with a commercial polyamido-amine (PAMAM) dendrimer monolayer, which measured 4.6 nm in thickness. In the dendrimer-containing samples, microstructural analysis revealed the presence of a 2 nm thick mixed nanocomposite region that formed between the dendrimer and the metallic overlayer, presumably during deposition. The results from nanoindentation experiments were analyzed to produce conventional load-displacement (P-d) plots and P-d2 plots. Careful analysis revealed significant differences in the elastic and plastic responses of dendrimermediated specimens in comparison with dendrimer-free specimens, which could be correlated with the resultant hardness. The presence of a dendrimer interlayer was observed to reduce the amount of pileup around the indenter, as observed in AFM images. The composite hardness of samples was recalculated using the actual contact area, and the hardness of the samples with dendrimer was lower than that free of dendrimer at the low load range. The results for dendrimer-mediated and dendrimer free films are discussed relative to the indentation of bulk materials

# Advanced Materials for Energy Conversion II: Complex Hydrides I

Sponsored by: Light Metals Division, LMD-Reactive Metals Committee

*Program Organizers:* Dhanesh Chandra, University of Nevada, Metallurgical & Materials Engineering, Reno, NV 89557 USA; Renato G. Bautista, University of Nevada, Department of Chemical and Metal Engineering, Reno, NV 89557-0136 USA; Louis Schlapbach, EMPA Swiss Federal, Laboratory for Materials Testing and Research, Duebendorf CH-8600 Switzerland

 Tuesday AM
 Room: 203A

 March 16, 2004
 Location: Charlotte Convention Center

Session Chairs: Joseph R. Wermer, Los Alamos National Labortaory, Tritium Sci. & Engrg. Grp., Los Alamos, NM 87545 USA; Annik Percheron-Guegan, CRNS, Thais 94230 France; Jai-Young Lee, KAIST, Dept. of Matl. Sci. & Engrg., Dae-jeon 305-701 S. Korea

#### 8:30 AM Plenary

The State-of-the-Art of Alanates Development for Hydrogen Storage: Karl J. Gross<sup>1</sup>; <sup>1</sup>Hy-Energy Company, 33902 Juliet Cir., Fremont, CA 94555 USA

The discovery that hydrogen can be reversible absorbed and desorbed from sodium-aluminum-hydrides (the Alanates) has created an entirely new prospect for light-weight hydrogen storage<sup>1</sup>. These compounds release hydrogen through a series of decomposition / recombination reactions: NaAlH4 ? 1/3(?-Na3AlH6) + 2/3Al + H2 ? NaH + Al + 3/2H2 Initial work demonstrated that the addition of Ti-containing additives resulted in dramatically improved sorption rates and improved hydrogen storage properties. Since that time a increasing efforts have focused on the development of advanced additives, better synthesis methods, and especially on gaining a fundamental understanding of the role of titanium in the enhanced hydrogen-sorption mechanisms. Ultimately however, the practical hydrogen storage capacity of this system is limited to the 5.6 wt.% hydrogen content of the two-step reactions. This has been the driving force for new studies on the reversibility of other similar complex hydrides. The results of these studies along with their implications on the viability of these materials for on-board hydrogen storage will be presented. 1Bogdanovic and Schwickardi, J. Alloys and Compounds, Vol. 253 (1997) 1.

#### 9:00 AM Keynote

Metal-Hydrogen Complex Compounds as Hydrogen Storage Materials: Seijirau Suda<sup>1</sup>; <sup>1</sup>Kogakuin University, Dept. of Environml. & Chem. Engrg., 2665-1, Nakano-machi, Hachioji-shi, Tokyo 192-0015 Japan

The theorietical hydrogen storage capacity of numerous complex hydrides such as lithiumhydrides, alminohydrides, and borohydrides exceeds 10 mass% in general. Practically, Ti-doped LiAlH4 releases 5.2 mass% H2 at room temperature and T-doped NaAlH4 decomposes thermally up to 5 mass% H2 reversibly below 200°C, and alkaline solutions of NaBH4 releases 10.8 mass% H2 through catalytic hydrolysis at ambient temperature and pressure conditions. On the otherhand, conventional metal hydrides have been studied extensively over the past 30 years with the best available hydrogen content as a system of less than 2 wt% at reasonably lower temperture conditions. No futher increase of H-capacity can be expected to the series of conventional metal hydrides as hydrogen storage materials. With respect to high capacity hydrogen storage materials, the presentation will be focused on the recent status and future scopes of metal-hydrogen complex compounds and their reversible processes uder developing today. An important view scope on the exisiting state of hydrogen as diatomic (molecular), monatomic (protium), cationic (proton), and anionic (protide) will be discussed. As an illustration of the ionic bonding of hydrogen-rich anion of BH4- in sodium borohydride (NaBH4), an electrochemical application of protide (H-) will be introduced by DBFC (Direct Borohydride Fuel Cell).

#### 9:25 AM Keynote

**Electronic Structure of Hydrogen Storage Materials**: *Michèle Gupta*<sup>1</sup>; <sup>1</sup>Université Paris-Sud, EA3547, Bâtiment 415, Sci. des Matériaux, Orsay 91405 France

In this paper, we show that first principles electronic structure studies provide an understanding i) of the properties relevant to hydrogen storage applications such as the maximum hydrogen capacity, the preferred H sites occupancies, the stability of the materials. We discuss the relative contributions of elastic and electronic effects on the thermodynamic behaviour of the materials. ii) of the modification of the most fundamental properties of the matrix such as metalinsulator transitions, magnetism and superconductivity on hydrogen absorption. To illustrate these points, several examples of intermetallic compounds of AB, AB2 and AB5 type (where A and B are transition or rare earth elements), as well as mono and polysubstituted compounds will be discussed. Our results will be analysed in light of available experimental photoemission, structural and thermodynamic data.

#### 9:50 AM Keynote

Lithium-Based Aluminohydrides: From Basic Science to Future Energy Applications: Vitalij K. Pecharsky<sup>1</sup>; Viktor P. Balema<sup>1</sup>; Jerzy Wiench<sup>1</sup>; Marek Pruski<sup>1</sup>; <sup>1</sup>Iowa State University, Ames Lab. & Dept. of Matls. Sci. & Engrg., 242 Spedding, Ames, IA 5011-3020 USA

Hydrogen can be extracted from aluminohydrides in a number of different ways. The first group of methods involves controlled chemical decomposition with water or ammonia. The second technique - a thermochemical approach - is based on the thermal decomposition of sodium aluminohydride in the presence of transition metal catalysts. A third method involves the production of high purity hydrogen at ambient temperature during mechanical processing of lithium aluminohydride with inorganic transition metal catalysts. The mechanochemical approach combines the following attractive features: i) hydrogen is produced without heating; ii) the hydrogen gas is free of contaminants; iii) the input of mechanical energy can be easily managed, thus enabling easy control over the flow of hydrogen; iv) there is no fundamental barrier to the development of methods for dehydrogenated powder to be recharged with hydrogen, and v) mechanochemistry offers a unique pathway to direct synthesis of aluminohydrides from elements or from readily available precursors.

#### 10:15 AM Break

#### 10:30 AM Keynote

Hydrogen Storage Properties of Li-Based Complex Hydrides: Shin-ichi Orimo<sup>1</sup>; Yuko Nakamori<sup>1</sup>; <sup>1</sup>Tohoku University, Inst. for Matls. Rsch., 2-1-1, Katahira, Aoba-ku, Sendai, Miyagi 980-8577 Japan

Fundamental researches on complex hydrides are recently of great importance to develop applicable hydrogen storage materials with higher gravimetric hydrogen densities than those of conventional materials. First, we discuss the correlation between B-H atomistic vibrations in [BH4]-clusters and melting temperatures of MBH4 (M =Li, Na, and K), viewpoint from the charge densities at [BH4]-cluster sites from counter-cations. This investigation provides a way for destabilizing the Li-based complex hydrides. Next, as an example, the hydrogen desorption properties of LiNH2 and it partial substitution system are preliminary examined. We found that the starting and ending temperatures for the hydrogen desoprtion reaction are lowered about 50 K by the partial elemental substitution of Li by Mg, due probably to the increase of the charge densities at [NH2]-cluster site.

#### 10:55 AM Keynote

**Doped Sodium Aluminum Hydride: New Evidence for Bulk Dopant Substitution**: *Craig M. Jensen*<sup>1</sup>; Mark Conradi<sup>3</sup>; Tetsu Kiyobayashi<sup>2</sup>; Dalin Sun<sup>1</sup>; Walter Niemczura<sup>1</sup>; Steve Brady<sup>3</sup>; Keeley Murphy<sup>1</sup>; Sandra Eaton<sup>4</sup>; S. Sairaman Srinivasan<sup>1</sup>; Job Rijssenbeek<sup>5</sup>; Meredith Kuba<sup>1</sup>; <sup>1</sup>University of Hawaii, Dept. of Chmst., Honolulu, HI USA; <sup>2</sup>National Institute for Advanced Industrial Science and Technology, Osaka Japan; <sup>3</sup>Washington University, Dept. of Physics, St. Louis, MO USA; <sup>4</sup>University of Denver, Dept. of Chmst., Denver, CO USA; <sup>3</sup>GE Global Research Center, Niskayuna, NY USA

In 1997, Bogdanovic and Schwickardi reported that the elimination of hydrogen from solid NaAlH4 is markedly accelerated and rendered reversible under moderate conditions upon mixing the hydride with a few mole percent of selected transition metal complexes. This was a revolutionary finding in the area of metal hydrides as hydrogen cycling at moderate temperatures was unprecedented for saline hydrides. We subsequently discovered an improved method of doping of NaAlH4 that greatly promotes the kinetics of the reversible dehydrogenation of the hydride and stabilizes its hydrogen cycling capacity. It now appears that a variation of the doped hydride could possibly be developed as a viable means for the onboard storage of hydrogen. However, no dopant precursors have been found that give a greater kinetic enhancement than those cataloged in Bogdanovic's original 1995 patent. Similarly, only the sodium and mixed sodium, lithium salts of the alanates have been found undergo largely reversible dehydrogenation under moderate conditions upon doping. This lack of progress is surprising in view of the recent "gold rush" flurry of activity that has been direct towards the development of alanates as practical onboard hydrogen carriers. Clearly, these efforts have been handicapped by the dearth in the understanding of the nature and mechanism of action the dopants. We have therefore initiated efforts to elucidate the fundamental basis of the remarkable hydrogen storage properties of this material. In our early efforts, we obtained X-ray diffraction data that showed significant changes in the lattice parameters of the hydride occur upon doping. On the basis of these results, we proposed a model in which the dopants are substituted into the bulk hydride lattice. In order to verify this model, we have conducted solid state 1H and 2H nuclear magnetic resonance, electron paramagnetic resonance, and time-of-flight selective ion mass spectroscopic, as well as kinetic studies of the doped hydride. The results of these studies will be presented and discussed in terms of their relationship to our "substitutional" model of the doped hydride.

#### 11:20 AM

Studies of Ti Dopant in Single Crystal Sodium Aluminum Hydrides: Eric H. Majzoub<sup>1</sup>; David R. Tallant<sup>2</sup>; Vidvuds Ozolins<sup>3</sup>; <sup>1</sup>Sandia National Laboratories, Analytical Matls. Sci. Dept., MS 9403, Livermore, CA 94550 USA; <sup>2</sup>Sandia National Laboratories, Matls. Characterization Dept., MS 1411, Albequerque, NM 87123 USA; <sup>3</sup>University of California, Sch. of Engrg. & Applied Sci., Los Angeles, CA 90095-1595 USA

NaAlH4 is an alanate compound at the forefront of hydrogen storage technology, with a capacity ideally around 5.4 wt.% H2. The absorption and desorption rates for this material are known to be dramatically affected by the addition of a range of Ti-compounds such as TiCl3, TiH2, and nano-cluster Ti. The mechanism of enhanced kinetics in this system is still an open question, depending in part on the location of the Ti. Sample preparation techniques for pragmatic material often result in small coherence lengths making diffraction less effective as a tool due to large peak widths and the presence of multiple phases. In the present study, small single crystals of NaAlH4 were grown both in pure form and also in the presence of Ti. The crystals were then gently ground for powder diffraction and analyzed for lattice expansion and structure factor changes, which may provide information about the Ti location. In addition, results of Raman spectroscopy from the Ti-exposed and unexposed single crystals will be presented.

#### 11:40 AM

Kinetic Study and Determination of the Enthalpies of Activation of the Dehydrogenation of Titanium and Zirconium Doped NaAlH4 and Na3AlH6: *Tetsu Kiyobayashi*<sup>1</sup>; Sesha S. Srinivasan<sup>2</sup>; Dalin Sun<sup>2</sup>; Nobuhiro Kuriyama<sup>1</sup>; Craig M. Jensen<sup>2</sup>; <sup>1</sup>National Institute of Advanced Industrial Science and Technology, Special Div. for Green Life Tech., 1-8-31 Midorigaoka, Ikeda, Osaka 563-8577 Japan; <sup>2</sup>University of Hawaii, Dept. of Chmst., Honolulu, HI 96822 USA

The rates of the dehydrogenation of the sodium alanates, NaAlH4 and Na3AlH6 doped with 2mol% Ti or Zr have been measured over the temperature range 363-423K. NaAlH4 and Na3AlH6 undergo dehydrogenation at equal rates upon direct doping with titanium. However, Na3AlH6 arising from the dehydrogenation of Ti doped NaAlH4 undergoes dehydrogenation at much slower rates. Rate constants were determined from the slopes of the dehydrogenation profiles. The enthalpies of activation for the dehydrogenation reactions were determined to be 100 kJ/mol for both Ti doped NaAlH4 and Na3AlH6 and 135 kJ/mol for both Zr doped NaAlH4 and Na3AlH6. These results suggest that the dehydrogenation reaction pathways are highly sensitive to the nature and distribution of the dopant but not to differences in the Al-H bonding interactions in the complex anions. Furthermore, we conclude that the kinetics are probably influenced by processes such as nucleation and growth, and/or range atomic transport phenomenon.

# Advances in Superplasticity and Superplastic Forming: Advances in Superplastic AI-Mg Materials

Sponsored by: Materials Processing and Manufacturing Division, Structural Materials Division, MPMD-Shaping and Forming Committee, SMD-Mechanical Behavior of Materials-(Jt. ASM-MSCTS), SMD-Structural Materials Committee
Program Organizers: Eric M. Taleff, University of Texas, Mechanical Engineering Department, Austin, TX 78712-1063 USA; P. A. Friedman, Ford Motor Company, Dearborn, MI 48124 USA; Amit K. Ghosh, University of Michigan, Department of Materials Science and Engineering, Ann Arbor, MI 48109-2136 USA; P. E. Krajewski, General Motors R&D Center; Rajiv S. Mishra, University of Missouri, Metallurgical Engineering, Rolla, MO 65409-0340 USA; J. G. Schroth, General Motors, R&D Center, Materials and Processes Laboratory, Warren, MI 48090-9055 USA

Tuesday AM	Room:	201B
March 16, 2004	Location	Charlotte Convention Center

Session Chairs: Amit K. Ghosh, University of Michigan, Dept. of Matls. Sci. & Engrg., Ann Arbor, MI 48109-2136 USA; James G. Schroth, General Motors, R&D Ctr., Warren, MI 48090-9055 USA

#### 8:30 AM

Application of Superplastic Forming in the Transportation Industry: Anthony J. Barnes<sup>1</sup>; <sup>1</sup>Superform USA, Inc., 6825 Jurupa Ave., Riverside, CA 92504 USA

Planes, trains and automobiles and a whole lot more?.. Over the past 30 years Superplastic Aluminum Forming has emerged as a unique industry of highly specialized material, equipment and people. Almost from the outset it has found interest and application in the business of transportation, where the combined attributes of aluminum and superplastic forming have offered advantages over other materials and processes. This presentation reviews the state-of-the-art of superplastic aluminum alloys and forming technology and highlights the technoeconomic factors that impact the viability of current and future applications.

#### 8:55 AM

An Overview of Creep Deformation Behaviors in 5000-Series and Al-Mg Alloys: Eric M. Taleff<sup>1</sup>; <sup>1</sup>University of Texas, Dept. of Mech. Engrg., 1 Univ. Sta., C2200, Austin, TX 78712-0292 USA

The 5000-series Al alloys have wide practical utility because they exhibit a number of desirable properties and behaviors, including reasonable strength, good resistance to corrosion and stress-corrosion cracking, and weldability. Of more recent interest is the rather high ductilities which 5000-series alloys can achieve at elevated temperatures and low strain rates. Under such conditions, many 5000-series alloys can achieve enhanced ductilities of 100 to over 300% as a result of deformation by solute-drag creep. Because solute-drag creep does not require a fine grain size, enhanced ductilities are achieved from standard commercial grades without additional processing for grain refinement. Experiments using Al-Mg alloys with ternary additions reveal the relationship between deformation behaviors of the muchstudied Al-Mg binary alloys and their more complex commercial kin. Superplastic AA5083 alloys and their variants achieve superplasticity through significant grain refinement during sheet rolling and an increase in the content of intermetallic particles, which help retain a fine grain size by pinning grain boundaries. Despite the clearly demonstrated superplastic behavior of AA5083 materials, as temperature decreases and strain rate increases, they revert to the deformation behavior of less exotic 5000-series materials.

#### 9:15 AM

Texture Development and Dynamic Recrystallization in AA5083 During Superplastic Forming at Various Strain Rates: Paul E. Krajewski<sup>1</sup>; *Sumit Agarwal*<sup>2</sup>; Clyde L. Briant<sup>2</sup>; <sup>1</sup>General Motors, R&D Ctr., 30500 Mound Rd., MC 480-106-212, Warren, MI 48090 USA; <sup>2</sup>Brown University, Div. of Engrg, Box D, Providence, RI 02912 USA

Texture development in AA5083 during superplastic forming has been studied at strain rates varying from 0.0005/sec to 0.3/sec. As shown previously in the literature, a random texture is maintained at slower strain rates (grain boundary sliding), while at the higher strain rates, a fiber texture develops (dislocation creep). At the higher strain rates (>0.03/sec), dynamic recrystallization is observed in the necked region of the sample prior to failure. This results in a dramatic transition from very fine grains (~10 mm) to large grains (>100 mm) at a critical strain. At strains above this critical level the grain size decreases. The effect temperature, strain rate, and constituent particle distribution on the extent and character of the recrystallized region is described. The results are explained in terms of critical strain recrystallization phenomena.

#### 9:35 AM

**Bulge Testing of Superplastic 5083 Aluminum Sheet**: John R. Bradley<sup>1</sup>; <sup>1</sup>General Motors, R&D Ctr., Matls. & Proc. Lab., MC 480-106-212, Warren, MI 48090-9055 USA

High temperature pneumatic bulge testing has been established as an effective means of assessing the superplastic ductility of 5083 aluminum sheet for production applications. The constant-pressure bulge test provides a faster, simpler and less expensive method for screening the quality of incoming material than conventional tensile testing. A correlation was demonstrated between total superplastic tensile elongation and bulge test dome height for 5083 aluminum sheet based on an evaluation of more than twenty five candidate materials. The ability of the bulge test to discriminate among high and low quality production alloys was demonstrated. The test was also shown to be useful in the evaluation of experimental alloys. A tendency for materials from different suppliers to deform at significantly different strain rates under the same conditions of forming temperature and pressure was investigated.

#### 9:55 AM Break

#### 10:10 AM

**Deformation, Cavity Formation and Failure in Superplastic** AA5083: Keiichiro Oh-ishi<sup>1</sup>; John F. Boydon<sup>1</sup>; *Terry R. McNelley*<sup>1</sup>; <sup>1</sup>Naval Postgraduate School, Dept. of Mech. Engrg., 700 Dyer Rd., Monterey, CA 93943-5146 USA

The ductility of aluminum alloy AA5083 during superplastic forming is limited by cavity formation and linkage as well as by necking during elevated temperature deformation. Orientation Imaging Microscopy (OIM) methods have been used to assess the role of grain boundary disorientation in the processes of grain boundary sliding and separation that lead to the formation and growth of cavities. The contributions of dispersed intermetallic Al6Mn and Al3Fe particles have also been examined. Annealing of cold-rolled AA5083 at 450°C results in the formation of equiaxed grains 7 - 8 µm in size by particlestimulated nucleation of recrystallization as well as a near-random microtexture and random grain-to-grain disorientation distributions. Cavities form in conjunction with sliding and separation of boundaries having disorientations = 10° during deformation under grain boundary sliding controlled conditions. Cavity formation appears to begin at dispersed intermetallic particles although many smaller cavities in the cavity size distribution are not associated with particles. Data for cavity formation during biaxial tension and plane strain deformation conditions will be compared to data for cavity formation under uniaxial tension.

#### 10:35 AM

Superplastic Failure Mechanisms and Ductility of AA5083: Mary-Anne Kulas<sup>2</sup>; W. Paul Green<sup>1</sup>; Ellen C. Pettengill<sup>1</sup>; Paul E. Krajewski<sup>3</sup>; Eric M. Taleff<sup>1</sup>; <sup>1</sup>University of Texas, Mech. Engrg., 1 Univ. Sta., C2200, Austin, TX 78712-0292 USA; <sup>2</sup>University of Texas, Matls. Sci. & Engrg., 1 Univ. Sta., C2201, Austin, TX 78712-0292 USA; <sup>3</sup>General Motors Corp., R&D Ctr., 30500 Mound Rd., Warren, MI 48090-9056 USA

The aluminum alloy AA5083 is the most used aluminum material for superplastic forming operations. Advantages of AA5083, beyond its superplastic response, include moderate strength, good weldability, and corrosion resistance. Ductility of AA5083 during superplastic forming is limited by one of two failure mechanisms, necking and cavitation. Quantitative measurements of the contributions to failure from each mechanism are made using the newly developed Q parameter. This parameter provides insight into the deformation mechanisms active prior to failure in AA5083. AA5083 typically contains intermetallic particles of Al6Mn and Al3Fe, which can influence superplastic ductility. Particle size distributions are measured for several AA5083 materials and related to their ductilities and failure mechanisms.

#### 10:55 AM

Microstructural Characterization of SPF AA5083 Aluminum Sheet: Sooho Kim<sup>1</sup>; Michael P. Balogh<sup>2</sup>; Richard A. Waldo<sup>2</sup>; <sup>1</sup>General Motors, R&D Ctr., Matls. & Proc. Lab., MC 480-106-212, 30500 Mound Rd., Warren, MI 48090-9055 USA; <sup>2</sup>General Motors R&D Center, Chem. & Environml. Scis. Lab., MC 480-106-320, 30500 Mound Rd., Warren, MI 48090-9055 USA

Two superplastic forming (SPF) AA5083 aluminum sheets, exhibiting different elevated temperature elongations (335% and 254%), were selected for detailed microstructural characterization. Neither X- ray diffraction (XRD) nor metallography measurements could account for the differences in material behavior. Electron probe microanalysis (EPMA) and transmission electron microscopy (TEM) studies found differences in the composition and morphology of the constituent particles. The coarse constituent particles (>2 $\mu$ m) in the sample with the inferior elongation contain a lower concentration of silicon and are more angular with more internal cracks, which may create sources of cavitation during SPF. The fine dispersoid particles (<2 $\mu$ m) in the sample with the superior elongation are smaller, have a higher population density and are more uniformly distributed. These dispersoid particles are expected to effectively pin the grain-boundaries, thus limiting dynamic grain growth, producing better formability.

#### 11:15 AM

**Post-Form Properties of Superplastically Formed 5083 Aluminum Sheet**: John R. Bradley<sup>1</sup>; *John E. Carsley*<sup>1</sup>; <sup>1</sup>General Motors, R&D Ctr., Matls. & Proc. Lab., MC 480-106-212, Warren, MI 48090-9055 USA

The tensile and fatigue behavior of two 5083 aluminum alloys following various degrees of superplastic deformation have been examined in order to correlate post-formed mechanical properties with initial microstructure and cavitation. The unformed materials were characterized in terms of both constituent particle size distribution and recrystallized grain size. A reduction in mechanical properties of both alloys with increasing superplastic strain was quantified. An abrupt increase in cavitation observed in both alloys at true thickness strains greater than about -0.6 was consistent with the threshold strain for rapid cavitation reported earlier. Marked decreases in yield strength, ultimate tensile strength, uniform elongation, and fatigue performance were correlated with the extent of cavitation damage as a function of superplastic thinning. Poorer performance of one alloy compared to the other was shown to be the result of accelerated cavitation, which was attributed to a significantly larger recrystallized grain size (9.5 "m vs. 6.5 "m).

#### 11:35 AM

Rolling Process Optimization for Superplastic 5083 Aluminum Sheet: Ravi Verma<sup>1</sup>; <sup>1</sup>General Motors, R&D, Matls. & Proc. Lab., 30500 Mound Rd., Warren, MI 48090 USA

The effect of sheet rolling process on superplasticity of 5083 aluminum alloy sheet has been investigated. A synergistic effect between hot rolling and cold rolling processes has been observed which helps optimize an efficient sheet rolling practice. A "skewed" cold rolling process, in which successive reduction levels are tailored to maximize the alloy's hardening response to cold work, was developed. The "skewed" cold rolling process further helps improve superplastic response of rolled 5083 sheet. Superplastic tensile elongations greater than 400% have been obtained.

# Alumina and Bauxite: Bayer Plant Operations: White Side

Sponsored by: Light Metals Division, LMD-Aluminum Committee Program Organizers: Travis Galloway, Century Aluminum, Hawesville, KY 42348 USA; David Kirkpatrick, Kaiser Aluminum & Chemical Group, Gramercy, LA 70052-3370 USA; Alton T. Tabereaux, Alcoa Inc., Process Technology, Muscle Shoals, AL 35661 USA

Tuesday AM	Room: 2	18A
March 16, 2004	Location:	Charlotte Convention Center

Session Chair: Milind V. Chaubal, Sherwin Alumina Company, Corpus Christi, TX 78469 USA

#### 8:30 AM Cancelled

Effect of Total Soda on the Caustic Molar Ratio of the Agglomeration Zone in the Precipitation Circuit

#### 8:55 AM

Kinetics of Crystallization in Sodium Aluminate Liquors: Qun Zhao<sup>1</sup>; Yanli Xie<sup>1</sup>; Shiwen Bi<sup>1</sup>; Zijian Lu<sup>2</sup>; Yihong Yang<sup>1</sup>; Bo Li<sup>1</sup>; <sup>1</sup>Northeastern University, Sch. of Metall. & Matl., Shenyang, Liaoning 110004 China; <sup>2</sup>Henan Branch of CHALCO, Dept. of Tech., Changqian Rd., Shangjie Dist., Zhengzhou 450041 China

The kinetics of crystallization of alumina trihydroxide from sodium aluminate liquors under industrial conditions was studied in a laboratory batch isothermal precipitator. The kinetic equation was deduced from the mechanism of crystallization. The parameters were obtained by fitting experimental data to the equations. The kinetic equation of precipitation at low temperature is  $dC/dt=2.59[exp(-19.30\times10^3/RT)](C-C_8)^2$ , which is controlled by diffusion, while the equation at high temperature is  $dC/dt=1.117\times10^{-8}[exp(-73.44\times10^3/RT)](C-C_8)^2$ , which is controlled by interfacial reaction. Furthermore, the formula for calculating the optimum temperature was derived, and the values from the experiment were calculated. These are  $314.42^{\circ}K$  ( $41.27^{\circ}C$ ) for low temperature and  $346.24^{\circ}K$  ( $73.09^{\circ}C$ ) for high temperature, respectively.

#### 9:20 AM

The Application of Additives in the Precipitation of Bayer Sodium Aluminate Liquors: *Zijian Lu*<sup>1</sup>; Qun Zhao<sup>2</sup>; Yanli Xie<sup>3</sup>; Shiwen Bi<sup>3</sup>; Yihong Yang<sup>3</sup>; <sup>1</sup>Henan Branch of CHALCO, Changqian Rd., Shangjie Dist., Zhengzhou, Henan 450041 China; <sup>2</sup>Zhengzhou Light Metal Research Institute, No. 76 Jiyuan Rd., Shangjie Dist., Zhengzhou, Henan 450041 China; <sup>3</sup>Northeastern University, Nonferrous Metall., No. 11, Ln. 3, Wenhua Rd., Heping Dist., Shenyang, Liaoning 110004 China

Additives used in the precipitation of sodium aluminate liquors can not only increase precipitation ratio and achieve coarser product but are also simple to operate and easy to control. The use of additives in the precipitation of sodium aluminate liquors is introduced, and its mechanism is analyzed as well in this paper.

#### 9:45 AM Break

#### 9:55 AM

Attrition Behaviour of Laboratory Calcined Alumina from Various Hydrates and its Influence on SG Alumina Quality and Calcination Design: Hans W. Schmidt<sup>1</sup>; Alpaydin Saatci<sup>1</sup>; Werner Stockhausen<sup>1</sup>; *Michael Stroeder*<sup>1</sup>; Peter Sturm<sup>1</sup>; <sup>1</sup>Lurgi Metallurgie GmbH, Ludwig-Erhard-Strasse 21, D-61440 Oberursel Germany

Particle breakage and attrition in stationary calciners have been investigated since the introduction of this technology to the industry. Further to Outokumpu-Lurgi's experience of more than 40 calciners operating in the alumina industry with different hydrates new research work was undertaken to further improve the understanding of this important issue for smelter grade alumina quality. The attrition behaviour of various laboratory calcined aluminum hydrates was investigated in a special modified Forsythe-Hertwig apparatus at different temperatures. This modified test unit, which simulates certain sections of stationary calcination processes, is described. Various tests were carried out with different hydrates at a wide range of temperatures and other parameters. The fraction below 45 µm was analysed before and after the attrition tests. If the fraction difference is chosen as a measure for attrition, it can be shown that there is a clear relationship between attrition and mechanical impulse of the air jet in the orifice of the test unit. The temperature during the attrition test does not seem to have a significant influence on attrition. An approach to specify the hydrate quality regarding the attrition behaviour is discussed. Conclusions from the results for the design of large calciners are described.

#### 10:20 AM

A New Method for Smelting Grade Alumina (SGA) Characterization: Jean-Michel Lamérant<sup>1</sup>; Sonia Favet<sup>1</sup>; Valérie Martinent<sup>1</sup>; Laurent Ferres<sup>1</sup>; <sup>1</sup>Aluminium Pechiney, Direction de la Recherche et du Développement, BP. 54, Gardanne 13541 France

Pot operation efficiency in aluminium smelters is highly related to alumina quality. The properties currently measured (Specific Surface Area, Particle Size Distribution, Alpha Alumina content, Attrition Index, LOI, Chemical Analysis) are all relevant, but inadequate, to fully describe alumina behaviour in the pots, especially dissolution rate. The method under investigation analyses, by optical microscopy, SGA's diluted in a liquid having a Refractive Index of 1.73. The coloured pictures of samples reveal very significant differences between SGA's from different alumina refineries. As an example, it is possible to differentiate alumina from a fluid bed calciner and alumina from a rotary kiln, or to assess alpha alumina content and homogeneity of calcination. Quantification of differences is possible using Image Analysis software. Matching information from the new method with smelter data opens promising avenues. Potential for improved qualification of SGA's is under investigation.

#### 10:45 AM

New Approaches to Phase Analysis of Smelter Grade Aluminas: Toshifumi Ashida<sup>2</sup>; James B. Metson<sup>1</sup>; Margaret M. Hyland<sup>1</sup>; <sup>1</sup>University of Auckland, Light Metals Rsch. Ctr., PB 92019, Auckland New Zealand; <sup>2</sup>Kinki University, Dept. of Biotech. & Chmst., Sch. of Engrg. Japan

Specifications of smelter grade aluminas (SGA) represent a compromise between properties which are critical in performance and those which can be readily measured, but which provide only indirect

information on the quality and consistency of the alumina. For example, properties such as LOI (20-300°C) and LOI (300-1000), result from the relationship between the phase composition and the surface area required to meet the smelter specifications. Central to this is the problem that the phases which dominate SGA are largely poorly crystalline transition aluminas, and depend on calcining technology, but thus far a detailed phase analysis of SGA has proved intractable. Rietveld refinement of standard X-ray powder diffraction data and neutron diffraction studies have allowed us to explore a new model for the transition aluminas especially the gamma phase, optimized for SGA. In this model the structure of gamma alumina was assumed to consist of fcc lattice of oxygen, with 30% Al in the 4-fold site of a perfect spinel structure (filling 75% of the 4-fold sites), 45% Al in the 6-fold site of a perfect spinel structure (filling 56% of the 6-fold sites), 10% Al in a 4-fold interstitial site, 15% Al in 6-fold interstitial site, and 20% hydrogen substituted for Al. Thus the Al2O3 can be more accurately formulated as H2(Al3.0)[Al4.5]{Al1.0, Al1.5}O16.

#### 11:10 AM

Anti-Segregation of Alumina: Michael F. Barron<sup>1</sup>; Andreas Wolf; <sup>1</sup>Claudius Peters (Americas) Inc., 4141 Blue Lake Cir., Dallas, TX 75244 USA

In the process cycle prior to the actual production of an ingot of aluminium, that key ingredient goes through many transition points. Following its initial manufacture, alumina powder is conveyed, bucket elevated, blown, loaded, sucked or screwed out, re-conveyed, stored, retrieved, blown again and finally distributed over a bank of cells at the smelter. These many transition points usually involve at least two countries, a minimum of two ports (one loading the other for unloading) hundreds or thousands of meters of various types of conveyors and elevating devices and a couple or more of storage (silos). Each transition can have an effect; good or bad on the quality of the alumina delivered to the production cells. This paper covers how Claudius Peters Technologies GMBH has applied its extensive knowledge on silo storage and pneumatic conveying to ensure that aluminium producers in all five continents get a uniform, non-segregated alumina feed.

# Aluminum Can Recycling: Session I

Sponsored by: Extraction & Processing Division, Light Metals Division, LMD/EPD-Recycling Committee Program Organizers: Donald L. Stewart, Jr., Alcoa Inc., Alcoa Technical Center, Alcoa Center, PA 15069-0001 USA; W. Bryan Steverson, Alcoa Inc., Alcoa, TN 37701-3141 USA

Tuesday AM	Room: 2	17D
March 16, 2004	Location:	Charlotte Convention Center

Session Chairs: W. Bryan Steverson, Alcoa Inc., Alcoa, TN 37701-3141 USA; Donald L. Stewart, Jr., Alcoa Inc., Alcoa Tech. Ctr., Alcoa Ctr., PA 15069 USA

## 8:30 AM Introduction

#### 8:35 AM

Aluminum Can Recycling: That Was Then; This Is Now: Craig Covert<sup>1</sup>; <sup>1</sup>Alcoa Inc., Mkt. Dvlp. & Recycling, Alcoa Rigid Pkgg., 2300 N. Wright Rd., Alcoa, TN 37701 USA

Aluminum beverage can recycling began as a promotional vehicle to sell beer and soft drinks in aluminum cans to American consumers and has turned into a valuable source of metal to make more can sheet. Since its inception over 35 years ago, aluminum can recycling has captured the fancies of consumers across the U.S...and the world. Lately, there has been a decline in the aluminum beverage can recycling rate. What's in store for this American institution?

#### 9:00 AM

A Model for Thermal Decoating of Aluminium Scrap: Anne Kvithyld<sup>1</sup>; Jakub Kaczorowski<sup>2</sup>; Thorvald Abel Engh<sup>1</sup>; <sup>1</sup>Norwegian University of Science and Technology, Dept. of Matls. Tech., Trondheim N-7491 Norway; <sup>2</sup>Warsaw University of Technology, Fac. of Matls. Sci. & Engrg., Woloska 141, Warsaw, 02-507 Poland

A major problem in the recycling of aluminium is the presence of contaminants in the purchased scrap. This article attempts to give a fundamental description of thermal removal of lacquer in an industrial decoating unit. The material was aluminium sheet (420  $\mu$ m in thickness) coil-coated with 5 $\mu$ m thick polyester. The coating was decomposed, the evolved gases were measured, the residues left on the alu-

minium sheet were characterised and other microscopic investigations performed. The degradation was also monitored visually using a hot stage light microscope. Previous work has shown that the mass loss curves show three (or two) peaks in oxidizing (or inert) atmospheres. The microscopic examinations here support that each peak is associated with a stage in the degradation process. It is also revealed that the coating has "weak points". The investigations resulted to two slightly different models for the degradation of the coating.

## 9:25 AM

Mathematical Modelling for Recycling Furnaces Optimisation: Vincent Goutière<sup>1</sup>; Gaston Riverin<sup>1</sup>; Bruno Gariepy<sup>1</sup>; <sup>1</sup>Alcan International, ARDC- Ed 110 - 1955 Bd Mellon, Jonquiere G7S 4K8, Quebec Canada

Improvements achieved in the numerical modelling allowed obtaining new capacities in order to analyse the industrial remelt processes and find options aiming at decreasing the melting time or improving the thermal efficiency. Optimisation of the combustion furnaces becomes possible by changing the design, searching the best locations for the burners and their orientations, as well as choosing adequate types of burners. Following is presented the numerical methodology developed at Alcan International to improve the top charge furnaces. A two-step model is used: the first is dedicated to modelling the burner and its nearby region, and the second is to model the combustion chamber. After describing this model, different cases of improvements are shown.

#### 9:50 AM Break

#### 10:05 AM

The Impact of Hazardous Contaminants in Aluminum Used Beverage Containers During Processing: D. L. Stewart<sup>1</sup>; W. B. Steverson<sup>2</sup>; E. S. Martin<sup>3</sup>; <sup>1</sup>Alcoa Inc., 100 Technical Dr., Alcoa Ctr., PA 15069 USA; <sup>2</sup>Alcoa Inc., 2300 N. Wright Rd., N290, Alcoa, TN 37701-3141 USA; <sup>3</sup>Consultant, New Kensington, PA 15068 USA

Over 50 billion aluminum beverage cans (UBCs), approximately 700,000 metric tons, are recycled annually in the United States. The UBCs are collected at a large number of locations, where they are often baled or briquetted for convenient shipment to the ultimate processing location. These cans are recycled back into beverage can sheet and subsequent beverage containers in as little as 60 days. In a typical UBC recycling process, the baled material is subjected to sequential operations of shredding, magnetic material removal, delacquering to remove organic coatings, and melting. Potentially hazardous contaminants, such as aerosol cans containing flammable organics and live ammunition, have been found in the baled UBCs. The amount of energy, which will potentially be released by either of the hazardous contaminants during UBC processing, has been calculated and will be discussed, as well as steps to reduce the potential impact of the contaminants.

#### 10:30 AM

Some of the Factors Affecting Dross Formation in Aluminum 5182 RSI: *Qingyou Han*<sup>1</sup>; John Zeh<sup>2</sup>; Ray D. Peterson<sup>3</sup>; <sup>1</sup>Oak Ridge National Laboratory, Metals & Ceram. Div., One Bethel Valley Rd., PO Box 2008, Oak Ridge, TN 37831-6083 USA; <sup>2</sup>Logan Aluminum Inc., US Hwy. 431 N., PO Box 3000, Russellville, KY 42276 USA; <sup>3</sup>IMCO Recycling, Inc., 397 Black Hollow Rd., Rockwood, TN 37854 USA

Aluminum 5182 remelt secondary ingot (RSI) is prone to dross formation during the remelting processes. Recently we have found that dross formation in the center region of the RSI can be as high as 80% and is related to the cracking and porosity defect formation in that region. This article addresses dross formation in aluminum 5182 RSI under various processing conditions, such as the melting methods of the scrap materials, the composition of the alloy, the size of and the cooling rate in the RSI, and the casting temperature. Relationship between dross formation and the processing parameters are investigated and the mechanism of dross formation is discussed. It is suggested that the dross is formed during the solidification stage of the RSI processing. Dross formation increases with increasing magnesium concentration and decreasing cooling rate. Flux has little influence on dross formation.

# **Aluminum Reduction Technology: Pot Control**

Sponsored by: Light Metals Division, LMD-Aluminum Committee Program Organizers: Tom Alcorn, Noranda Aluminum Inc., New Madrid, MO 63869 USA; Jay Bruggeman, Alcoa Inc., Alcoa Center, PA 15069 USA; Alton T. Tabereaux, Alcoa Inc., Process Technology, Muscle Shoals, AL 35661 USA

Tuesday AM	Room: 2	13D
March 16, 2004	Location:	Charlotte Convention Center

Session Chair: Ric Love, Century Aluminum Corporation, Ravenswood, WV 26164-0098 USA

#### 8:30 AM

Metal Pad Temperatures in Aluminium Smelting Cells: Daniel Simon Whitfield<sup>1</sup>; Maria Skyllas-Kazacos<sup>1</sup>; Barry Welch<sup>1</sup>; Peter White<sup>2</sup>; <sup>1</sup>University of New South Wales, Ctr. for Electrochem. & Minerals Procg., Sydney, NSW 2052 Australia; <sup>2</sup>Heraeus Electro-Nite Intl. NV Belgium

Meaningful measurement of cell temperature is made difficult by a number of factors. Disturbances and errors are also introduced by the breaking and hole preparation for intermittent measurement, as well as errors associated with the depth of immersion. With the majority of the heat generated in a reduction cell originating in the electrolyte, with little heat generation in the metal pad, the thermal behaviour of the metal pad temperature is expected to be dependent on the electrolyte temperature. The large mass of liquid metal usually used in smelting cells gives a greater thermal inertia for the metal pad and it is partially isolated, or dampened, from the impact of frequent additions of cold alumina. Therefore it is expected that this will partially mitigate variation that occurs in the electrolyte when temperatures are measured in the metal pad. Investigation of the thermal behaviour of the metal pad and its relationship with the electrolyte indicated that the typical temperature difference between the two is 3-6C. The metal pad temperature also showed a dampened response to variation in the electrolyte temperature. Measurement of the metal pad temperature may potentially allow inferential measurement and monitoring of the cell thermal state.

#### 8:55 AM

#### Using Fume Duct Temperature for Minimizing Open Holes in Pot Cover: Neal R. Dando<sup>1</sup>; <sup>1</sup>Alcoa Technology, 100 Techl. Dr., Alcoa Ctr., PA 15069 USA

The presence of open holes in pot ore cover has been identified as a major source of elevated fluoride emissions at aluminum smelters. Several commercially available technologies exist for providing real time monitoring of vapor-phase fluoride, however capital cost and maintenance issues preclude their implementation on an every-pot basis. This presentation will discuss the efficacy of monitoring individual pot exhaust duct temperatures as a means of providing low-cost, real-time indicators of pot crust cover integrity. This methodology also allows for in-plant best-practice benchmarking and enabling systematic documentation of process-effect improvements in pot-tending practices.

#### 9:20 AM

Aspects of Alumina Control in Aluminium Reduction Cells: Daniel Simon Whitfield<sup>1</sup>; Maria Skyllas-Kazacos<sup>1</sup>; Barry Welch<sup>1</sup>; Fiona Stevens McFadden<sup>2</sup>; <sup>1</sup>University of New South Wales, Ctr. for Electrochem. & Minerals Procg., Sydney, NSW 2052 Australia; <sup>2</sup>Comalco Research and Technology, Thomastown, Victoria Australia

For all modern point fed aluminium-smelting cells, the alumina concentration is controlled within a band. This is achieved through inference indirectly by the general relationship between alumina concentration, inter-electrode distance and cell resistance. The standard strategy is to cycle the alumina feed rates, varying cell resistance and allowing inferential control of the alumina concentration. In this investigation, a magnetically compensated point fed cell, with four point feeders, was subjected to a typical feed cycle to test the response and quality of control. The variables measured in the response included the alumina concentration and its rate of change, temperature and pseudoresistance. As a result of this investigation, several phenomena were observed that concur with the hypothesis of an alumina layer at the bath-metal interface. Significant differences between the theoretical and measured pseudo-resistance were observed during the underfeed period, resulting in a flattening of the resistance curve. The net rate of alumina depletion was observed to correlate with temperature, possibly due to secondary feeding from a hypothesised alumina layer. It is also hypothesised that the pseudo-resistance may have an added temperature dependence due to the alumina layer.

## 9:45 AM

**Optimal Control System of Alumina Concentration in the Process of Aluminium Reduction when the Measuring Information is Incomplete:** *Robert G. Lokshin*<sup>1</sup>; *Mishel J. Fiterman*<sup>1</sup>; <sup>1</sup>JSC VAMI, Sredny Str. 86, Saint-Petersburg Russia

Secondary losses of aluminium during its electrolytic production depend on anode-cathode distance, temperature and alumina concentration in the bath. When the anode-cathode distance and temperature are preset the minimum of secondary losses correspond to the minimum voltage of the pot. Therefore, the task of alumina concentration control refers to the class of extreme control tasks and couldn't be solved in analytical form. To get a solution the special conversion of measuring equations is applied, which allowed the reduction of the task to the classical problem of the control having a full measuring information. Algorithms of optimal concentration estimation and optimal control of estimation obtained take care of this problem. Respective search system of alumina concentration control has an optimal combination of searching and controlling actions. The structure and computational algorithms of optimal control system are proposed and its numeral simulation under conditions of real perturbations is carried out. The comparison of optimal control system with standard industrial systems shows that in the industrial systems the correlation of searching and controlling actions is far from being optimally arranged.

#### 10:10 AM Break

#### 10:20 AM

Criterial Parameters in Evaluation of Cell's Potentialities for Computerized Control: Alexander I. Berezin<sup>1</sup>; *Peter V. Poliakov*<sup>2</sup>; Oleg O. Rodnov<sup>1</sup>; Pavel D. Stont<sup>3</sup>; Tatyana V. Piskajova<sup>1</sup>; <sup>1</sup>RUSAL Engineering & Techonology Center, Pogranichnikov st. 37, Krasnoyarsk 660111 Russia; <sup>2</sup>STC "Light Metals", Vavilova st. 60, Krasnoyarsk 660025 Russia; <sup>3</sup>Mayak PKF Ltd., Bograda st. 108, Krasnoyarsk 660021 Russia

In modern conditions to achieve high performance a cell has to operate at the limit of its functional potentials. The limit range of cell operation is determined by functional potentialities of its individual subsystems restricted by special process conditions. Criteria specifying performance of functions by major cell subsystems have been developed to evaluate cell conditions. The criteria employ controlled process parameters available in the plant process database. The criteria produced have been verified on a virtual model of a cell.

#### 10:45 AM

**Development of Aluminium Reduction Process Supervisory Control System**: *Vladimir Victorovich Yurkov*<sup>1</sup>; Victor Cristianovich Mann<sup>1</sup>; Konstantin Pheodorovich Nikandrov<sup>1</sup>; Oleg Alexandrovich Trebuh<sup>1</sup>; <sup>1</sup>Engineering-Technological Centre Ltd, RUSAL, Automation Div., 37, Pogranichnikov St., Krasnoyarsk 660111 Russia

Simple algorithms for cell control have significant limitations when process behaviours are highly variable. At this location, the source of these variations are changes in raw materials, seasonal ambient temperature differences and changes in electrical power input. An effective process control system must adequately compensate for these effects. At this plant, a Computerized Process Control System, which controls cell voltage, alumina feed and fluoride additions has been in full operation for some time and has operated as designed. Work has now commenced to integrate compensation for changes in thermal condition and bath composition and the interactions of these factors. This objective will be achieved by means of supervisory control of the alumina feeding algorithm and the normalized voltage set-point as well as through the aluminium fluoride daily dosing calculation. To this end an analytical dynamic model was developed, based on physicalchemical mechanisms and laws of mass and energy conservation. The core of this work is focused on alumina concentration forecasting by means of an alumina solution mathematical model, which is a part of the full reduction dynamics model. The dual-mode control system based on this model sends control actions to the middle-level system and, additionally, "learns" through adapting model coefficients. Alumina concentration forecasting and model calibration is performed in real time, by comparing the voltage of the real cell and that of the math model where this voltage is determined according to calculated alumina concentration.

# Automotive Alloys 2004: Session III

Sponsored by: Light Metals Division, LMD-Aluminum Committee Program Organizer: Subodh K. Das, Secat, Inc., Coldstream Research Campus, Lexington, KY 40511 USA

Tuesday AM	Room: 2	10A		
March 16, 2004	Location:	Charlotte	Convention	Center

Session Chair: Subodh K. Das, Secat Inc., Coldstream Rsch. Campus, Lexington, KY 40511 USA

#### 8:30 AM

**Development of Continuous Cast Aluminum Alloy Sheets for Automotive Applications**: *Zhong Li*<sup>1</sup>; Steve Kirkland<sup>2</sup>; Paul Platek<sup>2</sup>; <sup>1</sup>Commonwealth Aluminum, 1505 Bull Lea Rd., Lexington, KY 40511 USA; <sup>2</sup>Commonwealth Aluminum, 7319 Newport Rd., SE, Uhrichsville, OH 44683 USA

Commonwealth Aluminum has been developing continuous cast 5xxx series aluminum alloy sheet for automotive applications over the last several years. Continuous cast (CC) technology has the following advantages over conventional direct chill (DC) technology: (1) low capital investment; (2) high productivity; (3) low conversion cost and (4) short lead-time. The development work started by participating in the United States Automotive Materials Partnership (USAMP) CRADA. This research program ended in 1999 with auto parts (such as GM EV1 dash panel, Ford rear floor panel, etc) successfully stamped from CC sheet. Since then, Commonwealth Aluminum continued to carry on the development work with both domestic and foreign automobile manufacturers. The results showed that the continuous cast (twin belt casting technology) produced aluminum sheet can meet both the Aluminum Association and automobile manufacturer?s mechanical property specifications. In addition to the mechanical property requirements, CC 5754 alloy she et has met all the automotive requirements, such as, paint coating, spot welding, corrosion testing, phosphateability, adhesive compatibility, among others. So far, more than eighteen vehicle internal structural and heat shield parts have been successfully stamped from CC material manufactured by Commonwealth Aluminum. Additionally, some of these parts are now being commercially used by the automotive industry. Commonwealth Aluminum, Newport Rolling Mill, whose management systems are registered to OS9000: 1998 and ISO14001: 1996, has been approved as a raw material supplier for Ford Motor Company and General Motors Corporation. With the positive results of CC 5xxx aluminum alloy sheet, more automobile manufacturers are working with Commonwealth Aluminum in evaluating the benefits of using CC aluminum sheet in their automotive applications.

#### 9:00 AM

Friction Stir Welded Tailor Welded Blanks for Automotive Applications: *Glenn J. Grant*<sup>1</sup>; Richard W. Davies<sup>1</sup>; Douglas J. Waldron<sup>2</sup>; <sup>1</sup>Pacific Northwest National Laboratory, Energy Matls., 902 Battelle Blvd. K2-03, Richland, WA 99352 USA; <sup>2</sup>Advanced Joining Technologies, Inc., (A New Boeing Venture), 5222 Rancho Rd., Huntington Beach, CA 926417 USA

Tailor Welded Blanks (TWBs) are hybrid sheet products composed of either different materials or different thickness sheets that are joined together, then subjected to a forming or stamping operation to create a formed assembly. The strategy is employed generally to save weight and material costs in the formed assembly by placing higher strength or thicker sections only where needed. The forming or stamping process requires the joint to be severely deformed along with the parent sheets. Aluminum TWBs for automotive applications are particularly problematic because of the low formability of aluminum weld metal. This low formability is due to the fusion weld microstructure and the difficulty in making defect free aluminum fusion welds at the speeds appropriate for automotive applications. Friction Stir Joining is a process recently applied to Aluminum TWBs that has the potential to produce a higher quality weld at equivalent joining speeds to fusion welding. The current study presents data on the mechanical prop erties, formability, and FSJ weld process parameter development for Friction Stir Joined, Aluminum Tailor Welded Blanks. Data from microscopy, miniature tensile testing, and limited dome height formability tests will be presented on TWB joints in similar and dissimilar combinations of the following alloy types: 5182, 5052, and 6111.

#### 9:30 AM

Characterization of Springback Stresses in Deep Drawn Cups for Automotive Alloys: Thomas Gnäupel-Herold<sup>1</sup>; Timothy J. Foecke<sup>2</sup>; Henry J. Prask<sup>1</sup>; <sup>1</sup>National Institute of Standards and Technology, Matls. Sci. & Engrg. Lab., 100 Bureau Dr., Stop 8562, Gaithersburg, MD 20899 USA; <sup>2</sup>National Institute of Standards and Technology, Metall. Div., 100 Bureau Dr, Stop 8553, Gaithersburg, MD 20899-8553 USA

Springback is the elastic shape change of a sheet metal part after forming and removal from the die. The need for a more accurate prediction of elastic springback in sheet metal forming is accompanied by a need for a standardizable test for measuring and characterizing springback. A test that has received considerable attention consists of a ring sample taken from the sidewall of a flat bottom, deep drawn cup. We have performed high resolution through-thickness stress measurements in the intact and split ring for different materials, wall thicknesses, and axial and circumferential locations. The results provide a comprehensive picture of springback stresses in deep drawn cups.

#### 9:55 AM

In-Situ Synthesis of AlN Reinforced Magnesium Alloy Composites by Gas Bubbling Method: Sumit Ashok Tyagi<sup>1</sup>; Qingjun Zheng<sup>1</sup>; Ramana G. Reddy<sup>1</sup>; <sup>1</sup>University of Alabama, Dept. of Metallurgl. & Matl. Engrg., A129 Bevill Bldg., 126 7th Ave., Tuscaloosa, AL 35487 USA

Magnesium Metal Matrix Composites (Mg-MMCs) have been gaining attention in recent years as a challenging choice for automotive and aerospace applications. In-situ formation of AlN-reinforced Mg alloy composites by gas-bubbling method was investigated in this paper. Feasibility and conditions for formation of the composites were analyzed based on Gibb's energy minimization method. Quasi-regular solution model was used for the activities of Mg and Al to calculate the species distribution in the melts. The calculated results showed that formation of undesirable phase Mg3N2 in the Mg melts can be prevented if the partial pressure of precursor gas nitrogen is not above the critical value, above which Mg3N2 phase appears in the melt. The thermodynamic results show that sufficient volume% of AIN particles can be formed in the Mg alloy in the temperature range of 700-1000°C. Preliminary results showed that in-situ gas bubbling route for production of Mg-AlN composites is technically feasible. Experiments are und erway to confirm the thermodynamic predictions. The microstructure and phases of the composites formed in-situ are to be characterized using Scanning Electron Microscopy and X-Ray Diffraction.

#### 10:20 AM

Modelling the Interaction Between Recovery, Recrystallization and Precipitation During Annealing of Cold Rolled AA6111: Johnson Go<sup>1</sup>; Matthias Militzer<sup>1</sup>; Warren J. Poole<sup>1</sup>; Mary A. Wells<sup>1</sup>; <sup>1</sup>University of British Columbia, The Ctr. for Metallurgl. Process Engrg., Vancouver, BC V6T 1Z4 Canada

The recrystallization behaviour of commercial precipitation hardened alloys during annealing is complex as it may involve the simultaneous occurrence of recovery, recrystallization and precipitation. There are a number of possible interactions between precipitation and recrystallization. For example, the initial state of precipitation can affect the structure of the deformed state after cold rolling. In addition, it is well known that second phase particles may affect the kinetics of recrystallization significantly. In this study, a model framework is being developed to predict the recrystallization kinetics under the simultaneous occurrence of precipitation. Using the internal state variable approach an overall microstructure model is proposed where submodels for recovery, recrystallization and precipitation kinetics are coupled. Model predictions are validated with data obtained in isothermal annealing experiments which have been conducted on the cold rolled aluminum alloy AA6111 with systematically varied initial states of precipitation.

#### 10:45 AM

The Effect of Iron Content on the Mechanical Properties of Continuous Cast AA5754 Aluminum Alloy: Yansheng Liu<sup>1</sup>; David S. Wilkinson<sup>1</sup>; <sup>1</sup>McMaster University, Dept. of Matls. Sci. & Engrg., 1280 Main St. W., Hamilton, Ontario L8S 4L7 Canada

The influence of iron content on mechanical properties of Otemper continuous cast (CC) AA5754 aluminum alloy was investigated. The variations of grain size, particles and texture distribution were examined. R-value was measured and the relationship between Rvalue and texture is discussed by computer simulation based on the Continuum Mechanics of Textured Polycrystals(CMTP) model. The result indicates that iron content has significant impact on grain size evolution during annealing. It is concluded that mechanical properties and texture distributions are alternated in some extent by the variation of iron content. The result is important for optimizing the industrial processing of CC AA5754 aluminum alloy. Abnormal Grain Growth and Texture Evolution in AA5754 Strip Cast Aluminum Alloy: *Hamid N. Azari*<sup>1</sup>; David S. Wilkinson<sup>1</sup>; <sup>1</sup>McMaster University, Dept. of Matls. Sci. & Engrg., 1280 Main St. W., Hamilton, Ontario L8S 4L7 Canada

The effect of abnormal grain growth on the microstructural evolution and texture development in a twin-belt strip cast AA5754 aluminum alloy was investigated. The results indicate that when homogenized at 560°C for 6 hours the alloy becomes particularly prone to abnormal grain growth when subsequently cold rolled to 90% reduction and isothermally annealed at 450°C for duration higher than one minute. It is shown that prior to the onset of abnormal grain growth, the recrystallization texture is characterized by Cube ? {001}<100> - and Q ?  $\{013\} < 231 >$  components. As abnormal grain growth proceeds with annealing time, the Cube component is gradually reduced in intensity, while the Q intensifies. However, the most striking effect of the abnormal grain growth is the emergence of CH ? {001}<120> - and H ?  $\{001\} < 110 >$  - as the main texture components. The results are discussed in terms of particle-assisted nucleation, the possible effect of homogenization treatment on the size and volume fraction of second phase particles and the preferential growth of CH oriented grains into the neighboring orientations arising from their special orientation relationship.

#### 11:35 AM

The Influence of Severe Plastic Deformation on Mechanical Properties of AA6111 Sheet at Room Temperature: *Ki Ho Rhee*<sup>1</sup>; Rimma Lapovok<sup>1</sup>; Peter F. Thomson<sup>1</sup>; <sup>1</sup>Monash University, CRC for Cast Metals Mfg. (CAST), Sch. of Physics & Matls. Engrg., PO Box 69M, Victoria 3800 Australia

AA6111 has been chosen in many countries for automotive outer body panels, but low ductility remains a major obstacle to competition with steel. Equal channel angular extrusion (ECAE) was used as a tool to enhance the ductility and to produce fine-grained structures. Conventional grain sizes in the range of 9~50¥im were investigated to determine the effect of grain size on tensile properties of AA6111 sheet at room temperature. It has been found that grain refinement through ECAE followed by heat treatment leads to an increase in both strength and ductility. This increase of tensile properties was also significantly influenced by heat treatment temperature at the final stage of sheet process.

# Beyond Nickel-Base Superalloys: Precious Metal Alloys

Sponsored by: Structural Materials Division, SMD-Corrosion and Environmental Effects Committee-(Jt. ASM-MSCTS), SMD-High Temperature Alloys Committee, SMD-Mechanical Behavior of Materials-(Jt. ASM-MSCTS), SMD-Refractory Metals Committee *Program Organizers:* Joachim H. Schneibel, Oak Ridge National Laboratory, Oak Ridge, TN 37831-6115 USA; David A. Alven, Lockheed Martin - KAPL, Inc., Schenectady, NY 12301-1072 USA; David U. Furrer, Ladish Company, Cudahy, WI 53110 USA; Dallis A. Hardwick, Air Force Research Laboratory, AFTL/MLLM, Wright-Patterson AFB, OH 45433 USA; Martin Janousek, Plansee AG Technology Center, Reutte, Tyrol A-6600 France; Yoshinao Mishima, Tokyo Institute of Technology, Precision and Intelligence Laboratory, Yokohama, Kanagawa 226 Japan; John A. Shields, HC Stark, Cleveland, OH 44117 USA; Peter F. Tortorelli, Oak Ridge National Laboratory, Oak Ridge, TN 37831-6156 USA

Tuesday AM	Room: 211B	
March 16, 2004	Location: Charlotte Convention Center	

Session Chairs: Dallis Hardwick, Air Force Research Laboratory/ AFRL, Matls. & Mfg. Direct., Wright-Patterson AFB, OH 45433 USA; David R. Johnson, Purdue University, Sch. of Matl. Engrg., Lafayette, IN 47907-2044 USA

#### 8:30 AM Invited

Iridium-Base Alloys for High-Temperature Structural Applicatons: E. P. George<sup>1</sup>; C. G. McKamey<sup>1</sup>; C. T. Liu<sup>1</sup>; <sup>1</sup>Oak Ridge National Laboratory, Metals & Ceram. Div., Oak Ridge, TN 37831-6093 USA

Iridium is a platinum-group metal with the close-packed fcc crystal structure. Its high melting point (2443°C) and good oxidation/corrosion resistance make it an attractive candidate for high-temperature structural applications. A drawback of Ir-base alloys is low tensile duc-

tility when tested at conventional strain rates at ambient temperatures and at high strain rates at elevated temperatures. Another drawback is poor strength at high temperatures. Microalloying with ppm levels of Th and Ce has been shown to enhance grain-boundary cohesion and suppress brittle intergranular fracture in Ir alloys, whereas macroalloying with elements such as Hf and Zr increases high-temperature strength. In addition, harmful elements such as Si have also been identified that exacerbate brittle fracture in iridium. We will review the mechanisms of these effects and briefly discuss the successful use of iridium alloys aboard interplanetary spacecraft at temperatures to 1400°C. Research sponsored by the Office of Space and Defen se Power Systems and the Division of Materials Sciences and Engineering, Office of Basic Energy Sciences, U. S. Department of Energy, under Contract DE-AC05-000R22725 with UT-Battelle, LLC.

#### 9:00 AM Invited

Creep Properties of Ir-Base Refractory Superalloys: Yoko Yamabe-Mitarai<sup>1</sup>; Hiroshi Harada<sup>1</sup>; Yuefeng Gu<sup>1</sup>; Chen Huang<sup>1</sup>; <sup>1</sup>National Institute for Materials Science, High Temp. Matls. Grp., Sengen 1-2-1, Tsukuba, Ibaraki 305-0047 Japan

The Ir-based alloys with the fcc and L1<sub>2</sub> two-phase structure has been developed as next-generation high-temperature materials. We found that cuboidal L1<sub>2</sub> precipitates aligned along <100> directions in the Ir-Nb binary alloy similar to Ni-base superalloys. The creep properties of the Ir-Nb, Ir-Nb-Zr, Ir-Nb-Ni alloys were investigated at temperatures between 1773 and 2073 K under 137MPa. We found the addition of the third element was effective to improve the creep properties of the Ir-Nb alloy. For example, the minimum creep rate of Ir-Nb-Zr alloy at 2073 K was 10<sup>-6</sup> /s, two order lower than that of the Ir-Nb alloy. The effect of Ni or Zr will be discussed in terms of microstructure, lattice misfit, deformation structure, and grain boundary strength. Then the way for alloy design of high-temperature materials will be pointed out.

#### 9:30 AM

Experimental and Computational Investigations of the Al-Ni-Pt Ternary System: Sara Natalia Prins<sup>1</sup>; Zi-Kui Liu<sup>1</sup>; <sup>1</sup>Pennsylvania State University, Dept. of Matls. Sci. & Engrg., University Park, PA 16802 USA

A comprehensive understanding of the Al-Pt-Ni system is important from two perspectives. Firstly, the phases in the system form the basis of the phase equilibria and the phase transformation  $\beta$ -NiAl to  $\gamma^{-}$ Ni<sub>3</sub>Al in the environmentally protective aluminide coatings on Nibase superalloys (NBSA). Pt additions to the NBSA substrate before aluminising enhance the temperature and mechanical stability of the  $\beta$ -NiAl coatings significantly. Secondly, although Ni additions to Ptbased alloys lower the solvus temperature of the Pt<sub>3</sub>Al phase, these are beneficial to the mechanical properties and the unfavourable high density of Pt-based alloys. In the present work, the phase equilibria in the Al-Pt system, such as the structure and stability of the  $\beta$ -PtAl phase and the phase boundaries of the  $\gamma / (\gamma+\gamma') / \gamma'$  phases, are investigated as a base for the Al-Ni-Pt and other Pt-Al-X (X=Cr, Ti, Ta, Re) systems. The phase relations in the Al-Ni-Pt ternary system are also studied.

#### 9:45 AM

Partial Phase Relationships in Ir-Nb-Ni-Al and Ir-Nb-Pt-Al Quaternary Systems and Mechanical Properties of their Alloys: *Huang Chen*<sup>1</sup>; Yamabe-Mitarai Yoko<sup>1</sup>; Yu Xihong<sup>1</sup>; Nakazawa Shizuo<sup>1</sup>; Harada Hiroshi<sup>1</sup>; <sup>1</sup>National Institute for Materials Science (NIMS), High Temp. Matls. Grp., Refractory Superalloy Team, Sengen 1-2-1, Tsukuba, Ibaraki 305-0047 Japan

Two quaternary systems, Ir-Nb-Ni-Al, and Ir-Nb-Pt-Al were investigated successively to give assessments for ultra-high temperature applications. The phase relationships concentrated on fcc/L12 twophase region were primarily established and mechanical properties were studied. Ir-Nb-Ni-Al quaternary alloys around Ir-rich or Ni-rich sides showed coherent fcc/L12 two-phase structure, analogous to Nibase superalloys, however, most of the alloys presented three or four phases with two kinds of L12 phases. Although these alloys showed high compressive strain at high-temperature, they exhibited higher creep rate than Ir-base binary and ternary alloys. Another quaternary system Ir-Nb-Pt-Al showed promising results. Only fcc/L12 two-phase structure was found in all the alloys investigated with the compositions from Ir-rich to Pt-rich side, and the lattice misfit between fcc and L12 phases was small. The high-temperature strength at 1200 C of Ir-Nb-Pt-Al alloys was higher than that of Ir-Nb-Ni-Al alloys with the same Ir content (at.%). Moreover, Ir-Nb-Pt-Al alloys exhibited excellent creep-resistance.

#### 10:30 AM

**Dislocation Structure and Mechanical Behavior of Ir-Based**  $\gamma$ ' **Alloys:** Oleg Y. Kontsevoi<sup>1</sup>; Yuri N. Gornostyrev<sup>2</sup>; Andrey F. Maksyutov<sup>3</sup>; Arthur J. Freeman<sup>1</sup>; <sup>1</sup>Northwestern University, Physics & Astron., 2145 N. Sheridan Rd., Evanston, IL 60208 USA; <sup>2</sup>Institute of Metal Physics, Ekaterinburg 620219 Russia; <sup>3</sup>Russian Science Center "Kurchatov Institute", Moscow 123182 Russia

A new approach for the development of high-temperature  $\gamma/\gamma$ ' superalloys is based on using platinum group metals with higher melting temperatures and superior environmental properties. Indeed, refractory superalloys based on Ir are the strongest high-temperature materials developed to date. Unfortunately, there is no reliable information about dislocation properties and mechanisms driving the yield stress temperature dependence in Ir<sub>3</sub>X alloys. We analyzed the structure and mobility of dislocations in  $Ir_3X$  (X = Nb, Ti, Zr, Ta) within the modified Peierls-Nabarro model with first-principles generalized stacking fault energetics calculated using the highly-precise FLAPW method. SISF-bound superdislocations (Kear splitting scheme) are found to be strongly preferred energetically in Ir, Ta and Ir, Nb, whereas APB-bound superdislocations (Shockley splitting scheme) are predicted in Ir<sub>3</sub>Ti and Ir,Zr. Because APB-bound superdislocations are considered responsible for the yield stress anomaly, our results predict that a positive yield stress temperature dependence should be expected in Ir<sub>3</sub>Zr and Ir<sub>3</sub>Ti, and a negative behavior in Ir<sub>3</sub>Nb and Ir<sub>3</sub>Ta. We discuss the connection of the mechanical behavior of the  $Ir_3X$  alloys with the  $L1_2 \rightarrow D0_{19}$ structural instability. Supported by the AFOSR (grant No. F49620-01-0166).

#### 10:45 AM

**Tensile Properties of Pt-Based Superalloys**: Rainer Süss<sup>1</sup>; *Lesley Cornish*<sup>1</sup>; Lesley Heath Chown<sup>1</sup>; Lizelle Glaner<sup>1</sup>; <sup>1</sup>Mintek, Physl. Metall. Div., PB X3015, Randburg, Gauteng 2125 S. Africa

Since the Ni-based superalloys are reaching their temperature limit for operation in turbine engines, there is great interest in developing similar structured alloys based on a metal with higher melting point which can be used at temperatures of ~1300°C. Platinum has a higher melting point than nickel. Although Pt-based alloys are unlikely to replace all Ni-based superalloys on account of both higher price and density, Pt-based alloys with microstructures analogous to that of nickel based superalloys are being developed for possible use in the highest application temperature components. The optimum alloys, based around the composition Pt84:Al111:Ru2:Cr3, have good mechanical properties and high temperature oxidation resistance. Previous work on hardness measurements and creep were very promising. Tensile tests are now being undertaken for selected alloys. The results are being compared to the hardness measurements to ascertain whether a relationship exists between these two quantities, as in steels.

#### 11:00 AM

On the Development and Investigation of Quaternary Pt-Based Superalloys with Ni-Additions: Markus Wenderoth<sup>1</sup>; Lesley Cornish<sup>2</sup>; Rainer Süss<sup>2</sup>; Stefan Vorberg<sup>3</sup>; Bernd Fischer<sup>3</sup>; Uwe Glatzel<sup>1</sup>; Rainer Völkl<sup>1</sup>; <sup>1</sup>University Bayreuth, Metals & Alloys, Ludwig-Thoma-Str. 36b, Bayreuth 95440 Germany; <sup>2</sup>Council for Mineral Technology (MINTEK), Advd. Matls., 200 Hans Strijdom Dr., Randburg 2125 S. Africa; <sup>3</sup>University of Applied Sciences Jena, Carl Zeiss Promenade 2, Jena 07745 Germany

Platinum group metals are of increasing interest for very high temperature application. The objective of this work is to produce an alloy showing a microstructure similar to Ni-based superalloys, but with a base metal having a higher melting point than Ni. Having a fcc crystal structure with a L12 coherent embedded phase, it can be expected to have high strength and temperature resistance beyond Nibased superalloys. Our work concentrates on the development of a quaternary Pt-based superalloy. The elements Al, Cr and Ni were chosen as alloying components. In this stage we intend to vary the content of Ni between 0 and 10 at.%, the contents of the remaining components will be left in a fixed ratio. Additions of Ni may increase ductility and act also as solid solution strengthener. After arc-melting and heat treatment the alloys will be investigated, using SEM, calorimetric measurements and X-Ray diffraction.

#### 11:15 AM

Ruthenium Aluminides as Structural Materials and Coatings: Brian Tryon<sup>1</sup>; Fang Cao<sup>1</sup>; Tapash Nandy<sup>1</sup>; Qiang Feng<sup>1</sup>; *Tresa M. Pollock*<sup>1</sup>; <sup>1</sup>University of Michigan, Dept. of Matls. Sci. & Engrg., 2300 Hayward, Ann Arbor, MI 48109 USA

Systems based on RuAl are of potential interest for bulk structural applications as well as for bond coat interlayers in superalloy-TBC systems. The microstructure, mechanical properties and dislocation substructures observed in ternary and quaternary alloys based on this

system will be reviewed. Additions of Pt are of particular interest as Pt improves the oxidation characteristics of RuAl and changes the operative slip systems. To investigate the potential of this system to perform as a coating, a variety of interdiffusion studies have been conducted. A new ordered Ru-Al-Ta Heusler phase has been identified. Finally, microstructural evolution in Ru-containing coatings and the oxidation behavior of these coatings will be discussed.

#### 11:30 AM

**RuAl Eutectics**: *Todd Reynolds*<sup>1</sup>; David R. Johnson<sup>1</sup>; <sup>1</sup>Purdue University, Sch. of Matls. Engrg., 501 Northwestern Ave., W. Lafayette, IN 47907-2036 USA

Intermetallics are often considered candidate materials for high temperature structural applications due to the high melting temperature and good oxidation resistance of many compounds. One promising high temperature aluminide (Tmp>2000°C) is ruthenium aluminide due to that it may also have a good room temperature fracture toughness. To lower the cost of RuAl alloys, the ruthenium must be substituted with a less expensive element. With the greater ease in processing of the eutectic alloys, bulk sized samples of controlled microstructure can be produced for fracture toughness testing. Ru-Al-Mo alloys with compositions near the RuAl-Mo (B2-hcp) eutectic compositions have shown to have fracture toughness near  $37MPa\sqrt{m}$  and yield strength around 1100MPa. The oxidation resistance was low for the RuAl-Mo alloys, so the RuAl-Mo-Cr system was investigated. Mechanical property data from microhardness, compression, and four point bend tests will be reported for alloys of this system.

# 11:45 AM

**Microstructure and Mechanical Properties of Cr-Ru Alloys**: *Yuefeng Gu*<sup>1</sup>; Y. Ro<sup>1</sup>; T. Kobayashi<sup>1</sup>; H. Harada<sup>1</sup>; <sup>1</sup>National Institute for Materials Science, HTM21, Sengen 1-2-1, Tsukuba-shi, Ibaraki 305-0047 Japan

The metal chromium has been considered as a possible base for alloy systems since the last forties due to its higher melting points (1863°C), good oxidation resistance, low density and its high thermal conductivity. Major disadvantages that have held back its commercial exploitation are the high ductile-to-brittle transition temperature and further embrittlement resulting from nitrogen contamination during high-temperature air exposure. Since late of the last 1970s, chromium, as a practical alloy base, has remained virtually unstudied. Recently, a new look has been taken at chromium-base alloy systems. Analysis of rather scattered datum suggests that chromium-base alloys can be ductilized at ambient temperature and is quite capable of being strengthened to high levels at high temperature. New composition design and process would give high possibility to chromium-base alloys as structural materials in applications at temperatures up to 1300°C. This report will give our recent results on the microstructure and mechanical properties of Cr-Ru alloys.

# **Bulk Metallic Glasses: Fatigue and Fracture**

Sponsored by: Structural Materials Division, ASM International: Materials Science Critical Technology Sector, SMD-Mechanical Behavior of Materials-(Jt. ASM-MSCTS)

*Program Organizers:* Peter K. Liaw, University of Tennessee, Department of Materials Science and Engineering, Knoxville, TN 37996-2200 USA; Raymond A. Buchanan, University of Tennessee, Department of Materials Science and Engineering, Knoxville, TN 37996-2200 USA

Tuesday AM	Room: 2	209A
March 16, 2004	Location:	Charlotte Convention Center

Session Chairs: Reinhold H. Dauskardt, Stanford University, Matls. Sci. & Engrg., Stanford, CA 94305-2205 USA; Wole Soboyejo, Princeton University, Mech. & Aeros. Engrg., Princeton, NJ 08544 USA

#### 8:30 AM Invited

Fatigue Behavior of Zr-Based Bulk Metallic Glass: Reinhold H. Dauskardt<sup>1</sup>; Peter A. Hess<sup>1</sup>; Brian Menzel<sup>1</sup>; <sup>1</sup>Stanford University, Dept. of Matls. Sci. & Engrg., Stanford, CA 94305-2205 USA

The mechanisms of fatigue damage initiation and evolution in bulk metallic glasses (BMGs) are not well understood, limiting their use in safety-critical structural applications. We present recent studies of both the initiation of fatigue damage obtained from stress-life experiments on smooth specimens, and the growth of fatigue cracks measured under stable and transient cyclic loading conditions. The early stages of damage initiation and propagation resulting in the anomalously low reported fatigue endurance limits are discussed. In addition, both 'small' and 'long' fatigue crack growth rates were carefully characterized to elucidate the detailed mechanism of fatigue crack growth. High resolution characterization of fatigue specimen and fracture surfaces were used to provide the basis for micromechanical models of the resulting fatigue mechanism. Unlike the meniscus instability mechanism that has been used to explain fracture processes, a new mechanism involving out-of-plane shearing processes is used to rationalize the observed fatigue behavior.

#### 8:55 AM Invited

Nano Structured Bulk Glassy Alloys with High Fatigue Limit: *Yoshihiko Yokoyama*<sup>1</sup>; Peter K. Liaw<sup>2</sup>; Akihisa Inoue<sup>3</sup>; <sup>1</sup>Himeji Institute of Technology, Matls. Sci. & Chmst., Shosha 2167, Himeji, Hyogo 671-2201 Japan; <sup>2</sup>University of Tennessee, Matls. Sci. & Engrg., Rm. 427-B Dougherty Engrg. Bldg., Knoxville, TN 37996-2200 USA; <sup>3</sup>Tohoku University, Inst. for Matls. Rsch., Katahira 2-1-1, Aobaku, Sendai, Miyagi 980-8577 Japan

We examined S-N curves of Zr50Cu40A110, Zr50Cu30Ni10A110 and Zr50Cu37A110Pd3 bulk glassy alloys using a rotating-beam fatigue test to evaluate the effect of adding Ni and Pd elements on fatigue strength. As a result, we found that the fatigue limit was increased from 250 MPa to 500 MPa by adding 10 at% Ni instead of Cu to a Zr50Cu40A110 bulk glassy alloy. Furthermore, fatigue limit significantly increased over 1000 MPa by adding a 3 at% Pd instead of Cu to a Zr50Cu40A110 bulk glassy alloy. Zr50Cu37A110Pd3 bulk glassy alloy shows nano-crystallized network structure, which is considered as the origin of fatigue crack stopping.

#### 9:20 AM

Scattered Results and Premature Overload Fracture of Zirconium Based Bulk Metallic Glass Fatigue Specimens Tested in Vacuum: William Hutchison Peter<sup>1</sup>; Bing Yang<sup>1</sup>; Peter K. Liaw<sup>1</sup>; C. T. Liu<sup>2</sup>; Ray A. Buchanan<sup>1</sup>; Mark L. Morrison<sup>1</sup>; G. Y. Wang<sup>1</sup>; <sup>1</sup>University of Tennessee, Matls. Sci. & Engrg., 434 Dougherty Hall, Knoxville, TN 37996-2200 USA; <sup>2</sup>Oak Ridge National Laboratory, Metals & Ceram. Div., PO Box 2008, MS 6115, Oak Ridge, TN 37831-6115 USA

After a decade of fabricating "bulk metallic glasses" (BMGs), some fundamental concepts and observations regarding the fracture mechanisms of these glasses have been made. However, a full understanding of the degradation process of BMGs has not been realized. Early fatigue studies in air and vacuum of a Zr-Based BMG, Zr52.5Cu17.9Ni14.6Ti5Al10 (at %), revealed a high fatigue limit in air comparable to other high strength alloys. BMG samples tested in vacuum experienced similar results to those tested in air at high stress ranges, but vacuum results were scattered close to the air fatigue limit. This research will revisit this comparison while also making an effort to understand the location, time, and mechanism of crack initiation. In-situ thermography, optical microscopy, and acoustic emission will be used in an attempt to determine the relative life span of crack initiation to crack propagation, and to understand any correlation with the scattered vacuum data. This research effort was made possible by the funding of the National Science Foundation Integrative Graduate Education and Research Training (IGERT) Program on 'Materials Lifetime Science and Engineering' (DGE 9987548), with Drs. W. Jennings and L. Goldberg as contact monitors, and by the Division of Materials Science and Engineering, Department of Energy under contract DE-AC-00OR22725 with Oak Ridge National Laboratory (ORNL) operated by UT-Battelle, LLC.

#### 9:45 AM

Fatigue Behavior of Zr-Base Bulk Metallic Glasses: Gongyao Wang<sup>1</sup>; P. K. Liaw<sup>1</sup>; A. Peker<sup>2</sup>; Y. Yokoyama<sup>3</sup>; W. H. Peter<sup>1</sup>; B. Yang<sup>1</sup>; M. L. Benson<sup>1</sup>; W. Yuan<sup>1</sup>; L. Huang<sup>1</sup>; M. Freels<sup>1</sup>; R. A. Buchanan<sup>1</sup>; C. T. Liu<sup>4</sup>; C. R. Brooks<sup>1</sup>; <sup>1</sup>University of Tennessee, Dept. of Matls. Sci. & Engrg., 323 Dougherty Blvd., Knoxville, TN 37996 USA; <sup>2</sup>LiquidMetal Technologies Inc., Lake Forest, CA 92630 USA; <sup>3</sup>Himeji Institute of Technology, Matls. Sci. & Engrg., Shosha 2167, Himeji City Japan; <sup>4</sup>Oak Ridge National Laboratory, Metals & Ceram. Div., Oak Ridge, TN 37831 USA

High-cycle fatigue (HCF) experiments were conducted on zirconium (Zr)-based bulk metallic glasses (BMGs):  $Zr_{50}Al_{10}Cu_{40}$ ,  $Zr_{50}Al_{10}Cu_{30}Ni_{10}$ , and  $Zr_{41.2}Ti_{13.8}Ni_{10}Cu_{12.5}Be_{22.5}$ , in atomic percent. The HCF tests were performed using an electrohydraulic machine at a frequency of 10 Hz with a R ratio of 0.1 and under tension-tension loading. Note that  $R = \sigma_{min.} / \sigma_{max}$ , where  $\sigma_{min.}$  and  $\sigma_{max}$  are the applied minimum and maximum stresses, respectively. The test environments were air and vacuum. A high-speed and high-sensitivity thermographic infrared (IR) imaging system has been used for nondestructive evaluation of temperature evolution during fatigue testing of BMGs. Limited temperature evolution was observed during fatigue. However, a sparking phenomenon was observed at the final fracture moment of Zr<sub>50</sub>Al<sub>10</sub>Cu<sub>30</sub>Ni<sub>10</sub>. The effect of chemical composition on the fatigue behavior of the Zr-based BMGs was studied. The fatigue-endurance limit of Zr<sub>50</sub>Al<sub>10</sub>Cu<sub>30</sub>Ni<sub>10</sub> (865 MPa) is somewhat greater than that of  $Zr_{50}Al_{10}Cu_{40}$  (752 MPa) and  $Zr_{41,2}Ti_{13,8}Ni_{10}Cu_{12,5}Be_{22,5}$  (Batch 59: 703 MPa and Batch 94: 615 MPa) in air. The vein pattern and droplets with a melted appearance were observed in the apparent melting region. Fracture morphology indicates that fatigue cracks initiate from shear band or some defects. The fatigue lives in vacuum are generally comparable with those in air. The cracking shapes on the fatigue surfaces were analyzed and predicted. Fracture toughness was calculated from the measurement of the crack-propagation region of the fatigue-fractured surface. The present work is supported by the National Science Foundation (NSF), the Combined Research-Curriculum Development (CRCD) Program, under EEC-9527527 and EEC-0203415, the Integrative Graduate Education and Research Training (IGERT) Program, under DGE-9987548, and the International Materials Institutes (IMI) Program under DMR-0231320, with Ms. M. Poats, and Drs. P. W. Jennings, L. S. Goldberg, and C. Huber as contract monitors.

#### 10:10 AM Invited

Contact-Induced Deformation and Fracture/Fatigue Behavior in Bulk Metallic Glasses: C. Mercer<sup>1</sup>; R. Cirincione<sup>1</sup>; C. Fenton<sup>1</sup>; P. Anglin<sup>1</sup>; M. Huang<sup>1</sup>; W. O. Soboyejo<sup>1</sup>; <sup>1</sup>Princeton University, PMI/ Dept. of Mech. & Aeros., D404 E. Quad., Olden St., Princeton, NJ 08544 USA

This paper presents a combined experimental, analytical and computational study of contact-induced deformation in Zr-Be-based bulk metallic alloys. Contact-induced deformation is studied using Hertzian indentation techniques. The studies reveal the underlying surface and sub-surface shear bands, and the deformation patterns associated with Hertzian indentation. The deformation patterns are then correlated with stress components computed with finite element models. Subsequently, the fracture and toughening mechanisms are elucidated via resistance-curve experiments. The observed microcracks are shown to promote crack-tip shielding via microcrack shielding. The predicted shielding levels are consistent with the measured toughening levels. Finally, the paper examines the effects of stress ratio on the micromechanisms of fatigue crack growth. The crack growth rate data are shown to be consistent with a crack-tip opening displacement model. The implications of the results are then discussed for the design of amorphous bulk metallic alloys.

#### 10:35 AM Invited

**Deformation Behavior of Metallic Glasses and Metallic-Glass-Matrix Composites**: *Todd C. Hufnagel*<sup>1</sup>; <sup>1</sup>Johns Hopkins University, Matls. Sci. & Engrg., 102 Maryland Hall, 3400 N. Charles St., Baltimore, MD 21218-2681 USA

The disordered atomic-scale structure of amorphous alloys gives them mechanical behavior quite different from that of crystalline alloys. The most striking aspect of this behavior is the tendency for shear localization (at temperatures well below the glass transition) even at low strain rates. Although shear localization leads to fracture with relatively little macroscopic plastic deformation in single-phase metallic glasses, in two-phase materials a dramatic multiplication of shear bands can occur, making extensive macroscopic plastic deformation possible. In this talk, we will review the present understanding of fundamental aspects of plastic deformation of amorphous alloys, from both theoretical and experimental points of view. We will emphasize recent developments made possible by mechanical testing and structural characterization, including observations of dilatation associated with generation of excess free volume, and in situ x-ray diffraction observations of composite strain and microstructural evolution during deformation of metallic-glass matrix composites.

#### 11:00 AM Invited

**Deformation Mechanisms in Bulk Metallic Glass Matrix Composites**: *Ersan Ustundag*<sup>1</sup>; Bjoern Clausen<sup>2</sup>; Seung-Yub Lee<sup>1</sup>; Gregory S. Welsh<sup>1</sup>; <sup>1</sup>Caltech, Matls. Sci., MC 138-78, Pasadena, CA 91125 USA; <sup>2</sup>Los Alamos National Laboratory, Neutron Sci. Ctr., Los Alamos, NM 87545 USA

Bulk metallic glasses (BMGs) have attractive mechanical properties: yield strength > 2 GPa, fracture toughness > 20 MPa.m1/2 and elastic strain limit  $\sim 2\%$ . BMGs can also be processed into intricate shapes just like polymers. Unfortunately, monolithic BMGs fail catastrophically under unconstrained deformation by forming shear bands. To overcome this problem, BMG matrix composites with fiber and particulate reinforcements were proposed. We have recently investigated the deformation behavior of various BMG composites. We performed loading measurements during neutron or high-energy X-ray diffraction to determine the lattice strains in the crystalline reinforcements. We then combined the diffraction data with finite element and self-consistent modeling to determine the behavior of the matrix. We show that usually the reinforcements yield first, then start transferring load to the matrix. The results will be presented with an aim to identify the 'ideal' reinforcement and its morphology.

#### 11:25 AM

Deformation of In-Situ-Reinforced Bulk Metallic Glass Composites: Seung-Yub Lee<sup>1</sup>; Gregory S. Welsh<sup>1</sup>; Ersan Ustundag<sup>1</sup>; Bjoern Clausen<sup>2</sup>; Mark A.M. Bourke<sup>2</sup>; Jonathan D. Almer<sup>3</sup>; Ulrich Lienert<sup>3</sup>; Dean R. Haeffner<sup>3</sup>; <sup>1</sup>Caltech, Matls. Sci., MC 138-78, Pasadena, CA 91125 USA; <sup>2</sup>Los Alamos National Laboratory, Neutron Sci. Ctr., Los Alamos, NM 87545 USA; <sup>3</sup>Argonne National Laboratory, Advd. Photon Source, Argonne, IL 60439 USA

A promising bulk metallic glass (BMG) composite consists of crystalline dendrites that precipitate in situ during casting within an amorphous matrix. The reinforcements form an interpenetrating structure and enhance the ductility of the composite. To gain insight about the deformation mechanisms in these composites, a detailed neutron and high energy X-ray diffraction study was conducted. Specifically, the elastic deformation of the crystalline reinforcements was studied during mechanical loading of composites. In addition, self-consistent deformation models were employed to interpret the diffraction data and to deduce the evolution of load partitioning in the composites. The results suggest that the mechanical properties of the reinforcements, and hence the composite, are highly variable and quite sensitive to processing conditions.

# Carbon Technology: Green Anodes and Soderberg Paste

Sponsored by: Light Metals Division, LMD-Aluminum Committee Program Organizers: Markus Meier, R&D Carbon, Sierre CH 3960 Switzerland; Amir A. Mirchi, Alcan Inc., Arvida Research and Development Centre, Jonquiere, QC G7S 4K8 Canada; Alton T. Tabereaux, Alcoa Inc., Process Technology, Muscle Shoals, AL 35661 USA

Tuesday AM	Room: 2	13A
March 16, 2004	Location:	Charlotte Convention Center

Session Chair: Alberto Salvador Gomes, Albras Aluminio Brasileiro S.A., Carbon Plant, Barcarena, Para CEP 68.447-000 Brasil

#### 8:30 AM

Anode Paste Preparation by Means of a Continuously Operated Intensive Mixing Cascade at Aostar Qimingxin Aluminium China: Berthold Hohl<sup>1</sup>; André Pinoncely<sup>2</sup>; Jean Claude Thomas<sup>3</sup>; <sup>1</sup>Maschinenfabrik Gustav Eirich, Hardheim 74732 Germany; <sup>2</sup>Solios Carbone, Givors Cedex 69702 France; <sup>3</sup>Aluminium Pechiney, Centr' Alp, Voreppe Cedex 38341 France

In 2002, Aostar Qimingxin Aluminium announced the construction of a new anode plant at their 250 000 t/y greenfield smelter in the Sichuan Province in Central China. Solios Carbone were awarded a contract for the supply of a 35 t/h paste plant. For the design, new principles and ideas led to the so called Intensive Mixing Cascade (IMC) which was jointly developed by Eirich, Solios Carbone and Aluminium Pechiney. This new technology reduces significantly both the investment and operating cost of the paste plant and allows for the production of up to 50 t/h of anode paste in one single line. The Intensive Mixing Cascade combines a conventional preheating screw with a continuously operated intensive hot mixer, followed by a continuously operated intensive remixer-cooler. This paper recalls the development of the Intensive Mixing Cascade technology, and describes the main characteristics and the operating philosophy of that new plant.

#### 8:55 AM

**Fuzzy Control in Green Anode Plant Mixers**: Edson Silva Cruz<sup>1</sup>; <sup>1</sup>Albras - Alumínio Brasileiro SA, Rodovia PA 483 Km 21 Vila Murucupi, Barcarena, PA 68447000 Brazil

This paper presents the results obtained by using "Fuzzy Logic" to improve the control system of continuous green paste mixers at the ALBRAS anode plants. Fuzzy Logic is used to convert heuristic control rules stated by a human operator into an automatic control strategy. Through Fuzzy Logic the system is able to track the mixer current set point. A control strategy base was elaborated intuitively, observing how the operators commanded the mixer's damper. When the continuous mixer is being controlled adequately it produces a homogeneous green paste with the required qualities of mechanical rigidity, as well as a minimum standard deviation of the anode density. These paste characteristics depend directly on the damper control, and the previous system was unable to control this appropriately, causing variations in the mixture of the paste and consequently the amount of green scrap produced. Sometimes the operators needed to adjust the damper manually. The controller program was developed with ladder language and runs on programmable logical controller (PLC). The new system has been running since 2002 in the anode plants. The current used as the control varies around an established target. The results demonstrate the effectiveness and viability of the system that subsequently will be being implanted on other anode plant equipment.

#### 9:20 AM

Laboratory and Full Scale Experiments to Improve Quality of the VS Søderberg Secondary Anode: *Turid Vidvei*<sup>1</sup>; Roy Pedersen<sup>2</sup>; <sup>1</sup>Elkem Aluminium ANS Research, PO Box 8040 Vaagsbygd, N-4675 Kristiansand Norway; <sup>2</sup>Elkem Aluminium ANS Lista, PO Box 128, N-4551 Farsund Norway

The secondary anode made of baked stud hole paste under each vertical Søderberg cell stud should have high density, low electrical resistivity and make a low contact resistance both to the stud and the primary anode. A poor secondary anode can give anode problems as points or hanging ends and a high anodic voltage drop. The procedures for the stud changing and time between adding stud hole paste until the stud was reset were important for an optimized secondary anode quality. This was found through experiments at the laboratory and at full-scale experiments at Elkem Aluminium Mosjøen (EAM). To implement the results in the potroom a new system was developed to visualize the resetting time to the operators.

#### 9:45 AM

PAH Emissions from Soderberg Anodes with Standard and PAH-Reduced Binder Pitches: *Trygve Eidet*<sup>1</sup>; Alf-Yngve Guldhav<sup>2</sup>; Atle Olsvik<sup>3</sup>; Morten Sørlie<sup>1</sup>; <sup>1</sup>Elkem Aluminium ANS Research, PO Box 8040 Vagsbygd, N-4675 Kristiansand Norway; <sup>2</sup>Elkem Shared Services - Central Laboratory, PO Box 8040 Vagsbygd, N-4675 Kristiansand Norway; <sup>3</sup>Elkem Aluminium ANS Lista, PO Box 128, N-4551 Farsund Norway

Elkem Aluminium Lista has a point fed vertical spike Søderberg line where all anode tops are hooded and the pitch binder fumes are collected and cleaned in a dry scrubber. This set-up makes it possible to sample anode emissions from individual pots without any interference from neighboring anodes. In order to obtain nonbiased results on possible reductions in polyaromatic hydrocarbon (PAH) emissions using PAH-reduced binders, a number of hooded anode cells at the Lista smelter have been charged with a PAH-reduced paste over a period of several months. Sampling of pitch fumes has been performed during stable operating conditions (anode top normally at its warmest), after briquetting (anode top at its coldest) and during spike pulling (top punctured and high temperature pitch fumes and baking gases released). These results are compared to similar measurements on hooded anodes charged with a Søderberg paste containing a standard coal tar pitch (CTP) binder.

#### Cast Shop Technology: Casting

Sponsored by: Light Metals Division, LMD-Aluminum Committee Program Organizers: Corleen Chesonis, Alcoa Inc., Alcoa Technical Center, Alcoa Center, PA 15069 USA; Jean-Pierre Martin, Aluminum Technologies Centre, c/o Industrial Materials Institute, Boucherville, QC J4B 6Y4 Canada; Alton T. Tabereaux, Alcoa Inc., Process Technology, Muscle Shoals, AL 35661 USA

Tuesday AM	Room:	213B/C		
March 16, 2004	Location	: Charlotte	Convention	Center

Session Chairs: J. Les Kirby, Alcoa Inc., Alcoa Tech. Ctr., Alcoa Ctr., PA 15069 USA; J. Martin Ekenes, Hydro Aluminium AS, Otis Orchards, WA 99027-0603 USA

#### 8:30 AM

Surface Formation on VDC Casting: Ian Bainbridge<sup>1</sup>; John A. Taylor<sup>1</sup>; Arne K. Dahle<sup>1</sup>; <sup>1</sup>University of Queensland, Cooperative Rsch. Ctr. for Cast Metals Mfg. (CAST), Brisbane, Queensland 4072 Australia

A range of surface defects commonly formed on vertical direct chill (VDC) cast product have been examined by various metallographic techniques. Whilst the presently accepted model for the formation of cold folds on the cast surface can be reconciled to the details obtained from these examined samples, the explanations for the formation of other common surface defects could not. This paper describes current research efforts aimed at measuring the strength of molten aluminium alloy oxide surfaces under various conditions. This data is used as the basis for a hypothesis of the behaviour of the melt in the meniscus region in a VDC mould during casting. The results obtained from the malt strength tests and the metallographic examination of the cast samples are discussed and possible mechanisms for the formation of various surface defects are proposed.

#### 8:55 AM

Strontium Additions to Improve Ingot Surface Quality: David H. DeYoung<sup>1</sup>; Douglas A. Weirauch, Jr.<sup>1</sup>; <sup>1</sup>Alcoa Inc., Alcoa Tech. Ctr., 100 Tech. Dr., Alcoa Ctr., PA 15069 USA

The casting of rolling ingots is sometimes plagued by surface defects that can initiate cracking or hot tearing of the ingots. Vertical folds and oxide patches are examples of such surface defects. Because of the oxidation potential of high magnesium-containing 5xxx alloys, this alloy family is especially prone to surface defects. Recently it was found that small additions of strontium could markedly improve the surface of ingots and minimize cracking. This paper will review the development that is the subject of a recently issued U.S. patent.

#### 9:20 AM

Safety and Performance Issues of Conventional Sheet DC Moulds Under Pulsed Water Conditions: Yves Caron<sup>1</sup>; André Larouche<sup>1</sup>; Joseph Langlais<sup>1</sup>; *Denis Bernard*<sup>2</sup>; <sup>1</sup>Alcan International Ltd., Arvida R&D, 1955 Mellon Blvd., PO Box 1250, Jonquière, Québec G7S-4K8 Canada; <sup>2</sup>Alcan Primary Metal Group: Laterrière Works, PO Box 6301, Laterrière, Québec G7N-1A2 Canada

In DC casting of molten aluminium, the liquid aluminium is poured into an open mould. At first, a thin ingot shell is formed by the mould cooling, but as the ingot exits the mould this shell is severely quenched by the water jet coming from below the mould. The cooling of the ingot body is thus mainly achieved by heat transport through water evaporation that causes steam generation below the mould. During DC casting of sheet ingots using a slot-generated continuous water curtain, water can move upwards through the mould-ingot interface and onto the surface of the liquid pool forming the ingot head. This poses a serious safety hazard. The conditions under which this phenomenon occurs are not fully understood but it is clearly driven by the steam pressure build-up between the ingot and the water curtain. The use of conventional water hole moulds solved this problem mainly because the water outlet is discontinuous and allows the steam to escape and avoid any water vapour pressure build-up. However, it was found that certain conventional hole mould technology designs, under pulsed water start-up conditions, led to poor start-up performances on certain alloys. This paper presents the solutions that were applied to mould design in order to increase casting performance and recovery while maintaining the absence of water getting onto the ingot head.

#### 9:45 AM

Casting Metal Temperature Control by Launder Heating: Jan Migchielsen<sup>1</sup>; Jan D. de Groot<sup>1</sup>; <sup>1</sup>Thermcon Ovens B.V., Process Dept., PO Box 97, Geldermalsen 4190 CB The Netherlands

Launder preheating is an essential step in casting processes. Casting liquid aluminium through a launder that is not preheated is not feasible, even dangerous and would cause damage to the launder lining and contaminate metal with eroded material. For better process control launders, especially longer systems need to be equipped with permanently fitted and automated preheating systems. A casting launder can be provided with a continuous electrical heating system that offers full control to the metal temperature between the casting furnace and the casting machine. The paper makes a comparison between various methods of launder preheating and semi-continuous heating discussing the limitations and benefits of the methods and its implications for running cost and metal quality.

#### 10:10 AM Break

#### 10:45 AM

AutoPak - "Total Automation for D.C. Slab Casting": John V. Griffin<sup>1</sup>; <sup>1</sup>Pechiney Aluminum Engineering, Inc., 333 Ludlow St., Stamford, CT 06902 USA

Pechiney Aluminium Engineering has built on 20 years of continual improvements and advancements in automatic slab casting technology to develop the "AutoPak". Technology Concept: The Pechiney "AutoPak" technology is a complete automotive casting package consisting of "state-of-the-art" process equipment and a total integrated management and information system. The "AutoPak" process provides the cast house team with greater control over the operational casting station parameters; from the holding furnace(s) to the D.C. casting machine.

#### 11:10 AM

FATA Hunter Optiflow® Variable Tip Width Adjustment System for Aluminum Sheet Casting: *Dennis Smith*<sup>1</sup>; Özgül Keles<sup>2</sup>; Necmi Dogan<sup>2</sup>; <sup>1</sup>FATA Hunter, Inc., Tech. Dept., 1040 Iowa Ave., Riverside, CA 92507 USA; <sup>2</sup>Assan Aluminyum, Tuzla, Istanbul Turkey

FATA Hunter has recently developed and patented for the continuous twin roll casting lines an automated system which allows the end user to change the cast sheet width while casting in continuous operation. This system uses the new Optiflow boron nitride coated feed tip nozzle to ensure that the internal end dams glide with precise incremental movements. Typical cast house operations which would benefit the most from this system are continuous twin roll casting lines that frequently change the cast width for multiple end products. A program has been instituted to determine the effectiveness of this new design utilizing a range of the Fata Hunter twin roll casting lines from the old vintage casters to the new revolutionary SpeedCaster lines.

## 11:35 AM

**Crystallographic Texture Development of Twin-Roll Cast Aluminum Strips**: *Murat Dündar*<sup>1</sup>; Özgül Keles<sup>1</sup>; Bilal Kertý<sup>1</sup>; Necmi Dogan<sup>1</sup>; <sup>1</sup>Assan Aluminum, Tuzla, Istanbul Turkey

As compared to the traditional hot mill process, the relatively low capital cost of twin-roll casters, in combination with their lower energy and labor costs, have made twin-roll casting an increasingly popular method of producing a wide range of aluminum flat rolled products. In the highly competitive global market environment, the lower conversion cost advantages of twin-roll casting make it particularly attractive for the manufacturing of fin and foil products. Major challenge in this method is to reduce the casting gauge below 3 mm. Thin gauge casting provides significant improvement in the microstructure along with more isotropic mechanical properties in three different direction compared to the casting direction. Decrease in casting gauge is expected to result in higher load exerted on the cast sheet. This occurs in the "hot rolling" phase of the casting at the roll bite. Although there exists a limited plastic deformation, it would not be surprising to introduce a crystallographic texture to the sheet. Present study investigates the crystallographic texture development of as-cast aluminum strips, as the gauge is reduced from 5 to 1,80 mm. Pole figures are employed to characterize the dominant texture at different positions from the free surface of the strip. Casting width of the strips are 2200 mm for all the gauges. Macro and microstructural studies, along with the mechanical characterization, are also carried out on the samples. Texture analysis and mechanical characterization techniques are extended to 0,5 mm thick, "0" temper materials produced out of these strips.

# CFD Modeling and Simulation of Engineering Processes: MEMS/Microfluidics

Sponsored by: Materials Processing & Manufacturing Division, ASM/MSCTS-Materials & Processing, MPMD/EPD-Process Modeling Analysis & Control Committee, MPMD-Solidification Committee, MPMD-Computational Materials Science & Engineering-(Jt. ASM-MSCTS)

*Program Organizers:* Laurentiu Nastac, Concurrent Technologies Corporation, Pittsburgh, PA 15219-1819 USA; Shekhar Bhansali, University of South Florida, Electrical Engineering, Tampa, FL 33620 USA; Adrian Vasile Catalina, BAE Systems, SD46 NASA-MSFC, Huntsville, AL 35812 USA

Tuesday AM	Room: 206A
March 16, 2004	Location: Charlotte Convention Center

Session Chairs: Shekhar Bhansali, University of South Florida, Elect. Engrg., Tampa, FL 33620 USA; Mario Castro, Concurrent Technologies Corporation, Largo, FL 33773 USA

#### 8:30 AM Opening Remarks - Shekhar Bhansali

#### 8:35 AM Invited

**Design of an Asymmetric Waveform Spectrometer**: Mario H. Castro-Cedeno<sup>1</sup>; <sup>1</sup>Concurrent Technologies Corporation, 7995 114 Avenue, Largo, FL 33773 USA

The goal of this project was to model, design and prototype a MEMS chip that would be the drift channel in a high-field asymmetric waveform ion mobility spectrometer or FAIMS. FAIMS uses and asymmetric RF voltage signal to separate the various ions in a stream of incoming air. The separation occurs in the drift channel when the RF voltage signal is used to charge the top or bottom channel walls. The potential between the top and bottom attracts and can separate ions of different mobility. Ions that have higher mobility reach the top or bottom first and are neutralized. The remaining ions can be detected at the exit of the drift channel. Asymmetric square waveforms at very high frequencies have been found effective in causing separation of chemicals where only one kind of ion reaches the channel exit. This effort was successful in building a CFD model of the drift channel and in simulating the separation of chemicals with different ion mobility by using square asymmetric voltage waveforms. In addition, a MEMS drift channel chip was fabricated. The spectrometer can be used to detect trace amounts of chemical compounds in air at room conditions. Some examples are drugs, toxic chemicals and explosives.

#### 9:10 AM

**Design and Simulation of a Piezoresistive MEMS Pressure Sensor for Marine Applications**: *Shyam Aravamudhan*<sup>1</sup>; Shekhar Bhansali<sup>1</sup>; <sup>1</sup>University of South Florida, Dept. of Electl. Engrg., 4202 E. Fowler Ave., ENB 118, Tampa, FL 33620 USA

The physical and biological processes in the ocean are critically influenced by ocean parameters (pressure, salinity and temperature). There is a need to design inexpensive and reliable sensors to continuously measure large volumes of sea-space over long time spans. This paper reports the design and simulation results of a micromachined diaphragm-type piezoresistive pressure sensor with temperature compensation capable of operating over a dynamic range (0-1000 meters) with 0.1% or better resolution. The sensor functions when the resistivity of the sensing resistor changes as the diaphragm deflects due to applied pressure. We report the simulation results (output voltage and sensitivity analysis) using coupled MemPZR-MemMech module of the CoventorWare2003 tool to help in optimizing the design and performance of the wheatstone bridge arrangement in the diaphragm pressure sensor. The relationship between the sensing parameters including diaphragm thickness, length, doping concentration and depth is characterized to increase the sensitivity and linearity of response.

#### 9:40 AM

Influence of Materials and Processes on the Design of Micro Needles: Kiran Potluri<sup>1</sup>; Shekhar Bhansali<sup>1</sup>; <sup>1</sup>University of South Florida, Elect. Engrg., 4202 E. Fowler Ave., ENB 118, Tampa, FL 33620 USA

In this paper, we present the design and analysis of microneedles. We have designed and fabricated microneedles of different dimensions using various materials viz. SiO2, Oxide-Nitride-Oxide and Gold. The design, modeling and analysis was done using the Finite Element Analysis (FEA) software ANSYS<sup>TM</sup> 6.1. Angular strength analysis of the microneedles was done using angular loading in ANSYS<sup>TM</sup>, with the corresponding material property settings. Using the force-displacement settings, forces of varying magnitude in the range of 10 mN - 20 mN were applied on needles of different lengths (10 - 100µm) and side wall thicknesses (1µm and 1.5µm). Eigen Buckling analysis was performed to study the buckling characteristics of the microneedles. The buckling and force-displacement analyses show that O-N-O micro needles are more strong and robust compared to needles of other materials.

#### 10:10 AM Break

#### 10:40 AM

Transient Analysis of Microchannel Heat Transfer With Volumetric Heat Generation in the Substrate: Shantanu S. Shevade<sup>1</sup>; *Muhammad M. Rahman*<sup>1</sup>; <sup>1</sup>University of South Florida, Mech. Engrg., Coll. of Engrg., 4202 E. Fowler Ave., Tampa, FL 33620 USA

Liquid flow and heat transfer in microchannels are critical to the design and process control of various Micro-Electric-Mechanical-Systems (MEMS) and biomedical lab-on-a-chip devices. Experimental and theoretical studies in the literature have showed that a very high rate of heat and mass transfer in microchannels is the key to the extreme efficiencies in the technologies being developed. This paper presents a systematic analysis of fluid flow and heat transfer processes during the magnetic heating of the substrate material. Heat is generated in the substrate material when a magnetic field is imposed due to change in orientation of the molecules. As a result, the substrate temperature rises. The study considered microchannels with rectangular and square cross section with heat generation in the substrate due to imposed magnetic field. The results computed were for Gadolinium substrate and water as a working fluid. Gadolinium is the magnetic

material that exhibits high temperature rise during adiabatic magnetization around its transition temperature of 295 K. It has been experimentally observed that adiabatic temperature rise increases with magnetic field strength and can be as high 20 K when a magnetic field of 10 T is applied. The purpose of this study is to explore the transient heat transfer coefficient when the fluid is circulated through the substrate via microchannels. Equations governing the conservation of mass, momentum, and energy were solved in the fluid region. In the solid region, heat conduction was solved. In both fluid and solid regions, all material properties were assumed to vary with temperature. This is particularly important for the magnetic material where there is usually a large variation of properties near the transition temperature. From the simulation results, plots of heat transfer coefficient and Nusselt number were obtained over the length of the channel. A thorough investigation for velocity and temperature distributions was performed by varying channel aspect ratio, Reynolds number, and heat generation rate in the channel. It was found that the peripheral average heat transfer coefficient and Nusselt number is larger near the entrance and decreases downstream because of the development of the thermal boundary layer. With the increase in Reynolds number, the outlet temperature decreased and the average heat transfer coefficient increased.

# 11:10 AM

Improved MEMS Thermal Actuator Design by Modification of Hot-Arm Topology: Vandana Upadhyay<sup>1</sup>; Scott Samson<sup>2</sup>; Shekhar Bhansali<sup>1</sup>; <sup>1</sup>University of South Florida, Electl. Engrg., 4202 E. Fowler Ave., Tampa, FL 33613 USA; <sup>2</sup>University of South Florida, Coll. of Marine Sci., 140 7th Ave. S., St. Petersburg, FL 33701 USA

We present an improved design for a two-arm polysilicon thermal actuator. The classic thermal bimorph actuator design produces a localized hot spot at approximately the center of the thin actuator arm. This phenomenon limits the actuator efficiency, lifetime, and reliability. Since the deflection is based on thermal expansion of the material, advantage may be gained by making the temperature profile more uniform along the hot-arm length. In our design, the topology of the thin arm is modified by forming a nonlinear structure near the approximate location of the hot spot. Electromechanical simulations of this design show an increase in deflection and force, due to a flattening of the temperature profile along this hot arm. The solid model generation, finite element analysis and simulations are carried out using FEA software. Experimental devices are fabricated by using a polysilicon micromachining process. Finally, the simulation data is compared with the experimental results.

# Challenges in Advanced Thin Films: Microstructures, Interfaces, and Reactions: Modification, Characterization, and Modeling

Sponsored by: Electronic, Magnetic & Photonic Materials Division, EMPMD-Thin Films & Interfaces Committee *Program Organizers:* N. M. (Ravi) Ravindra, New Jersey Institute of Technology, Department of Physics, Newark, NJ 07102 USA; Seung H. Kang, Agere Systems, Device and Module R&D, Allentown, PA 18109 USA; Choong-Un Kim, University of Texas, Materials Science and Engineering, Arlington, TX 76019 USA; Jud Ready, Georgia Tech Research Institute - EOEML, Atlanta, GA 30332-0826 USA; Anis Zribi, General Electric, Global Research Center, Niskayuna, NY 12309 USA

Tuesday AM	Room: 2	18B	
March 16, 2004	Location:	Charlotte Convention Center	

Session Chairs: N. M. (Ravi) Ravindra, New Jersey Institute of Technology, Dept. of Physics, Newark, NJ 07102 USA; Jud Ready, Georgia Tech Research Institute, Atlanta, GA 30332-0826 USA; Anis Zribi, General Electric, Global Rsch. Ctr., Niskayuna, NY 12309 USA

#### 8:30 AM

A First-Principles Investigation of TiC and ZrC as Alternative Protective Coatings for Ferritic Steels: Ashok Arya<sup>1</sup>; Emily A. Carter<sup>2</sup>; <sup>1</sup>Bhabha Atomic Research Center, Matls. Sci. Div., Mumbai India; <sup>2</sup>University of California, Dept. of Chmst. & Biochmst., Los Angeles, CA USA

Given the wide use of steel in harsh operating environments, optimal protective coatings are desirable. The current chrome coating on ferritic steels contains inherent microcracks formed during the electrodeposition process, which causes material degradation. As a result, alternative coatings that can withstand high amplitude thermal and mechanical fluctuations and can protect steel against reactive/corrosive gas environments are of considerable interest. The mechanical and thermodynamic properties of TiC and ZrC are commensurate with steels as required for strong adhesion. Here we present a pseudopotentialbased density functional (DFT) investigation of TiC and ZrC coatings, wherein we predict the atomic structure, bonding, and the ideal work of adhesion of the interface between a TiC(ZrC)(100) coating and a bcc Fe(110) substrate.1 Characterization of the low-index TiC, ZrC, and Fe surfaces revealed that all surfaces retain near bulk termination, in agreement with experiment. The TiC(ZrC)(100)/Fe(110) interfaces exhibited a lattice mismatch which is less than 3%, leading to a smooth interface with only a small structural relaxation, except for the ultrathin 1 monolayer (ML) coating. We will present results of interface relaxation, interfacial bonding and adhesion strength of this interface. Further, the potential of TiC (ZrC) as an alternative protective coating material for steels will also be discussed. 1A. Arya and E.A. Carter, J. Chem. Phys., 118, (2003) 8982.

#### 8:45 AM Invited

Surface Modification of Metals and Alloys with Boron: *Roumiana* S. Petrova<sup>1</sup>; <sup>1</sup>New Jersey Institute of Technology, Dept. of Physics, Newark, NJ 07102 USA

Deterioration of metals and alloys in working conditions in most cases begins from their surface. Thermo-chemical treatment can be used to increase the operational life of parts subjected to wear, corrosion, and oxidation. This is a method by which nonmetals (C, N, B) or metals (Al, Cr, Zn) are penetrated by diffusion and subsequent chemical reaction into the surface. By thermo-chemical treatment, the surface layer changes its composition, structure, and properties. Thermochemical treatment is used to improve material surface properties of Ti, Mo, Nb, Ta, Zr, Co, Ni, Fe, and their alloys. Carburizing, nitriding, carbonitriding, chromizing, aluminizing are widely used methods in the industry. Boronizing is a method of surface diffusion treatment with Boron. It is a thermo-chemical surface hardening process that can be applied to variety of nonferrous, ferrous metals, alloys and cemented carbides. The process involves heating cleaned materials to high temperatures (800-1000°C), for a duration (2-8 h), in contact with a boroncontaining solid powder, paste, liquid, or gaseous medium. During boronizing, the diffusion and subsequent absorption of boron atoms into the ferrous alloy surface form boron compounds. The coating may consist of either a single phase boride (Fe2 B) or two phases boronized layer (Fe2 B+FeB) having a needle like structure, oriented perpendicular to the substrate grains. Boronized coating has a number of characteristic features compared with conventional casehardened layers. The extremely high hardness values of boronized layers produced on carbon steel (between 1450 and 2300 HV) illustrates that it exceeds the hardness of hardened tool steel, hard chrome electroplate, and is equivalent to that of tungsten carbide. Microstructure distribution, phase composition, interaction mechanisms with the substrate material, and effect on materials corrosion are experimentally studied and discussed.

#### 9:10 AM

Microstructure and Mechanical Properties of Ceramic/SAM Bilayer Coatings: Kaustubh Chitre<sup>1</sup>; Tolulope O. Salami<sup>2</sup>; Quan Yang<sup>1</sup>; Scott R. Oliver<sup>2</sup>; *Junghyun Cho*<sup>1</sup>; <sup>1</sup>State University of New York, Dept. of Mech. Engrg., Vestal Pkwy. E., PO Box 6000, Binghamton, NY 13902-6000 USA; <sup>2</sup>State University of New York, Dept. of Chmst., Vestal Pkwy. E., Binghamton, NY 13902-6000 USA

Thin ceramic coatings find their applications in various electronic devices, sensors and MEMS as a protection/barrier layer as well as a dielectric layer. The coatings, however, suffer from inherent brittleness and defects formed during processing. In an attempt to compensate for the weakness of the ceramic coating, we have developed a lowtemperature solution precursor process of creating strain-tolerant, protective bilayer coatings. The bilayer consists of an integrated ceramic-organic hybrid material. The top ceramic coating offers an inert, protective layer. At the same time, the underlying nanometer scale organic coating, fabricated by the self-assembly, provides compliance for the overlying hard coating upon mechanical and thermal stresses. In addition, this organic self-assembled monolayer (SAM) acts as a 'template' by forming a proper surface functionality for the subsequent growth of hard ceramic coatings. In this study, we will investigate the microstructure and mechanical properties of ZrO2/ SAM and YSZ/SAM bilayer coatings grown on Si. Molecular level understanding of the microstructure and micromechanics involved in the synthesis and processing of the coating is studied by a variety of characterization techniques, such as XRD, AFM, XPS, electron microscopes and nanoindentation.

#### 9:25 AM Invited

**Revealing Deformation Mechanisms Through In Situ Nanoindentation in a Transmission Electron Microscope**: Andrew M. Minor<sup>1</sup>; E. T. Lilleodden<sup>1</sup>; M. Jin<sup>2</sup>; E. A. Stach<sup>3</sup>; J. W. Morris<sup>3</sup>; W. A. Soer<sup>4</sup>; J. Th.M. De Hosson<sup>4</sup>; <sup>1</sup>Lawrence Berkeley National Laboratory, Matls. Sci. Div., 1 Cyclotron Rd., MS 66, Berkeley, CA 94720 USA; <sup>2</sup>University of California, Dept. of Matls. Sci. & Engrg., Berkeley, CA 94720 USA; <sup>3</sup>Lawrence Berkeley National Laboratory, Natl. Ctr. for Electron Microscopy, 1 Cyclotron Rd., Berkeley, CA USA; <sup>4</sup>University of Groningen, Netherlands Inst. for Metals Rsch., Dept. of Applied Physics, Groningen Netherlands

The deformation mechanisms of metals and ceramics have been investigated using the novel experimental technique of in situ nanoindentation in a transmission electron microscope. Al-Mg thin films were used to investigate the role of alloying constituents in the transmission of plasticity across grain boundaries. Al thin films with varying amounts of Mg were deposited onto silicon substrates, and the solutes at the grain boundaries will be shown to affect grain boundary mobility. Initial results suggest that in the Al-Mg alloys the solutes effectively pin the grain boundaries while in pure Al considerable grain boundary motion is observed. During in situ nanoindentation of single crystal silicon at room temperature, dislocation plasticity was observed in the absence of phase transformations. Typically, only phase transformation and fracture are though to be relevant deformation mechanisms during room temperature indentation of silicon. In our experiments, the dislocation activity and absence of phase transformations is explained by our sample geometry. Finite element analysis reveals an increase in the near-surface shear stress, relative to conventional sample geometries, which leads to preferential surface nucleation of dislocations.

#### 9:50 AM

Fracture, Adhesion, and Residual Stress in Piezoelectric Thin Films for MEMS: D. F. Bahr<sup>1</sup>; M. S. Kennedy<sup>1</sup>; M. C. Robinson<sup>1</sup>; K. E. Shafer<sup>1</sup>; C. D. Richards<sup>1</sup>; R. F. Richards<sup>1</sup>; <sup>1</sup>Washington State University, Mech. & Matls. Engrg., PO Box 642920, Pullman, WA 99164-2920 USA

Piezoelectric MEMS require a series of materials (metals, oxides, nitrides, and silicon) which have widely differing mechanical properties. This paper will demonstrate the effects of residual tensile stresses in lead zirconate titanate (PZT) on a platinized silicon substrate, and the subsequent control of the composite residual stress by the addition of thin metallic layers to provide a compressive stress to increase the mechanical compliance of micromachined membranes. Stresses between 200 and 400 MPa in 1000-2000 nm thick PZT films can be moderated by 100 nm thick metallic layers which have compressive stresses in the GPa range, producing a micromachined membrane with a 40% decrease in the compliance of the structure. The effects of thermal processing, control of plastic flow in the metallization layers, and the structure of the PZT film will be shown to impact the fracture and adhesion of these films with the application of mechanical strains over 0.1%.

#### 10:05 AM Break

#### 10:20 AM Invited

Interdiffusion Structures and Coefficients in Ternary Systems: Youngho Sohn<sup>1</sup>; <sup>1</sup>University of Central Florida, Advanced Matls. Procg. & Analysis Ctr., Dept. of Mech., Matls. & Aeros. Engrg., Orlando, FL 32816-2455 USA

An overview of interdiffusion phenomena in ternary systems is presented with an emphasis on the development of diffusion structure and determination of interdiffusion coefficients. Selected diffusion phenomena such as uphill diffusion, zero flux planes, demixing of phases, and development of various types of boundaries are highlighted using diffusion couples in several ternary systems. Methods available for the determination of ternary interdiffusion coefficients based on Onsager's formalism are reviewed and discussed in terms of applications and uncertainties. Development of a new analytical method to determine composition-dependent interdiffusion coefficients is presented. Utilization of advanced characterization tools for structural observations and determination of concentrations is also highlighted.

#### 10:45 AM

Interdiffusion in CdMnTe Thin Film Grown on CdTe Substrate: Sergej V. Kletsky<sup>1</sup>; Yung Soop Yoon<sup>2</sup>; <sup>1</sup>Institute of Semiconductor Physics, Dept. No. 38, Prospekt Nauki, 45, Kiev 03650 Ukraine; <sup>2</sup>Inha University, Rsch. Inst. of Semiconductor & Thin Film Tech., #253, Yonghyun-Dong, Nam-Ku, Inchon 402-751 Korea

Interdiffusion in II-VI solid solutions leads to the intensive degradation of initial abrupt profiles of concentration in semiconductor microstructures and, as result, to the changes in device characteristics. The main goal of this note is the quantitative description of intermixing in the system "substrate - growing layer" during epitaxial growth of CdMnTe/CdTe and approximate evaluation of the interdiffusion coefficient D. The model gives the possibility to calculate the concentration of metallic components diffused from the growing film into substrate and in the opposite direction and to determine D as a function of a total amount of diffused substances, time and rate of growth. Concrete calculations are made in particular cases when boundary concentration is constant, exponential function of time, sum of time deltafunctions (delta inclusions) and periodical time functions. The approach can be readily generalized for other pairs of components and other growth processes. Y.S. Yoon, S.V. Kletsky. Japan. J. Appl. Phys. v.42, No 4A, 2003, p.1709.

#### 11:00 AM

Numerical Simulation of Thermal Wave Propagation During Laser Processing of Thin Films: Xin Ai<sup>1</sup>; Ben Li<sup>1</sup>; <sup>1</sup>Washington State University, Sch. of Mech. & Matls. Engrg., Pullman, WA 99164 USA

A numerical model is developed to represent the thermal wave propagation during ultra-short pulsing laser processing of thin films. The model development is based on the solution of non-Fourier heat conduction problem with temperature and thermal flux delays using the discontinuous finite element method. The thermal wave phenomena are studied for both 1-D, 2-D and 3-D geometries. The temperature distributions in both Fourier and non-Fourier regions are discussed. Computed results for various conditions of relevance to laser annealing of thin films are discussed.

#### 11:15 AM Invited

Fluxon Pinning in the Nodeless Pairing State of Superconducting YBa2Cu3O7: Anthony T. Fiory<sup>1</sup>; Dale R. Harshman<sup>2</sup>; W. J. Kossler<sup>5</sup>; X. Wan<sup>5</sup>; A. J. Greer<sup>6</sup>; R. Noakes<sup>7</sup>; C. E. Stronach<sup>7</sup>; E. Koster<sup>8</sup>; A. Erb<sup>8</sup>; John D. Dow<sup>4</sup>; <sup>1</sup>New Jersey Institute of Technology, Dept. of Physics, Newark, NJ 07102 USA; <sup>2</sup>Physikon Research Corporation, PO Box 1014, Lynden, WA 98264 USA; <sup>4</sup>Arizona State University, Dept. of Physics, Tempe, AZ 85287 USA; <sup>5</sup>College of William and Mary, Dept. of Physics, Spokane, WA 99258 USA; <sup>6</sup>Gonzaga University, Dept. of Physics, Petersburg, VA 23806 USA; <sup>8</sup>University of British Columbia, Dept. of Physics, Vancouver, BC V6T-1Z1 Canada

The width of the local magnetic field distribution ("linewidth") produced by fluxon (or vortex) lattices in a high-purity YBa2Cu3O7 crystal in the superconducting mixed state was determined by the method of muon spin rotation (mSR) spectroscopy. Linewidth measurements in fluxon lattices convey information on the magnetic penetration depth, whose temperature dependence reveals the symmetry of the superconducting pairing state. Crystal lattice defects and thermal activation cause fluxon pinning, i.e., perturbations in the fluxon lattice formed by a superconductor in a magnetic field, and change the linewidth from its ideal value. The electronic anisotropy of YBa2Cu3O7 and fluxon pinning allow transverse disorder along the length of the fluxons, which tends to decrease the linewidth. Pinning also induces fluctuations in the distance between fluxons, which tend to increase the linewidth. By taking into account the expected fielddependent and temperature-activated fluxon disorder, the experimental results are shown to be consistent with a nodeless (s-wave) superconducting order parameter. The temperature dependence of the magnetic penetration depth is best described by a strong-coupling two-fluid model of s-wave superconductivity. It is shown that the data are statistically inconsistent with order parameters possessing nodes, such as those having dx2-y2 symmetry (d-wave).

#### 11:40 AM Invited

A Model on Thermoelectric Effect in Superconductivity: Eunjee Shin<sup>1</sup>; <sup>1</sup>Pennsylvania State University, Dept. of Math., University Park, State College, PA 16802 USA

In this talk we investigate a model for non-isothermal, non-equilibrium superconductivity exhibiting energy losses, and examine how these losses lead to the suppression of superconductivity. The principal unknown fields explored in the model are the complex valued Ginzburg-Landau order parameter, the magnetic vector potential, and the temperature (T). This model accounts for the interchange of thermal and electro-magnetic energies through Joule heating. We first establish a conservation of energy law implying that the total energy for an insulated superconducting body (thermal and electro-magnetic) is conserved. Through this, we prove global existence and uniqueness of classical solutions provided that the thermoelectric constant is sufficiently small. In particular, for the case where a classical Ohm's law is applied, we analyze the large time behavior of the solution and prove that the w-limit set as t ® ¥ consists of equilibrium solutions. We also prove that if the electro-magnetic energy of the supercondu ctor is sufficiently large at time zero, T will then rise beyond the critical temperature. In contrast to the earlier analytic work based only on an isothermal model, this work produces markedly different results as a consequence of considering non-isothermal electro-magnetic effects in superconductivity.

#### 12:00 PM

**Study of Electroimigration on Electronic Components**: *Xiaoxin Xiaa*<sup>1</sup>; John W. Denning<sup>1</sup>; Richard Griese<sup>1</sup>; <sup>1</sup>Northrop Grumman Space Technology, One Space Park, Redondo Beach, CA 90278 USA

Electromigration induced short circuit was observed on a single four pin DC connector during electrical testing. Optical and scanning electron microscope (SEM) analyses exhibited surface contamination and dendritic growth between the connector pin and ground, which led to the electrical shortage and component failure. The conductors were soldered using Pb88Sn10Agoz solder and no-clean flux. EDX analysis revealed that dendrites contained high Pb, 0 and C. It indicated that lead in the solder migrated and formed an electrical short from the connector pin to ground. The electromigration on the connector was probably related to the processing induced thermal stress. This stress can generate electrical potential and form electrical circuit, thus caused electromigration and mass transportation between the low and high stress concentration areas on the component. Temperature, stress distribution, chemical composition and microstructure of the electronic devices are main contributions to the electromigration. Moisture is known to be an accelerator. The mechanisms and effects of temperature, thermal stress and grain boundaries on electromigration are discussed in this paper.

# Computational Thermodynamics and Phase Transformations: Phase Field Modeling I

Sponsored by: ASM International: Materials Science Critical Technology Sector, Electronic, Magnetic & Photonic Materials Division, Materials Processing & Manufacturing Division, Structural Materials Division, MPMD-Computational Materials Science & Engineering-(Jt. ASM-MSCTS), EMPMD/SMD-Chemistry & Physics of Materials Committee

Program Organizer: Jeffrey J. Hoyt, Sandia National Laboratories, Materials & Process Modeling, Albuquerque, NM 87122 USA

Tuesday AM	Room:	202A		
March 16, 2004	Locatior	: Charlotte	Convention	Center

# Session Chair: TBA

# 8:30 AM Invited

Phase Field Modeling of Electrodeposition: Jonathan E. Guyer<sup>1</sup>; William J. Boettinger<sup>1</sup>; James A. Warren<sup>1</sup>; Geoffrey B. McFadden<sup>2</sup>; <sup>1</sup>NIST, Metall. Div., 100 Bureau Dr., Gaithersburg, MD 20899 USA; <sup>2</sup>NIST, Math. & Computational Scis. Div., 100 Bureau Dr., Gaithersburg, MD 20899 USA

We examine the kinetic behavior of a phase field model of the electrochemical interface in one dimension. We have previously shown that the equilibrium properties of this model (surface energy, surface charge, and differential capacitance) bear stronger resemblance to experimental measurements than to the predictions of existing sharpinterface models. For electrodeposition and electrodissolution conditionsm, using a single set of governing equations, we demonstrate ohmic conduction in the electrode and ionic conduction in the electrolyte. We find that, despite making simple, linear dynamic postulates, we obtain the nonlinear relationship between current and overpotential predicted by the classical "Butler-Volmer" equation and observed in electrochemical experiments. The charge distribution in the interfacial double layer is affected by the passage of current and, at sufficiently high currents, we find that the diffusion limited deposition of a more noble cation leads to alloy deposition with less noble species.

#### 9:00 AM Invited

Influence of Mobile Dislocations on Phase Separation in Binary Alloys: *Mikko Haataja*<sup>1</sup>; Francois Leonard<sup>2</sup>; <sup>1</sup>Princeton Materials Institute, Bowen Hall, 70 Prospect Ave., Princeton, NJ 08544 USA; <sup>2</sup>Sandia National Laboratories, Livermore, CA 94551 USA

In this talk we address the role of mobile dislocations on the phase separation process of a binary alloy by employing a phase-field model, which explicitly incorporates the coupled dynamics of the composition and dislocation fields. In our approach, the kinetics of the local composition and dislocation density are coupled through their elastic fields. We show both analytically and numerically that mobile dislocations modify the standard spinodal decomposition process, and lead to several regimes of growth. Depending on the dislocation mobility and observation time, the phase separation may be accelerated, decelerated or unaffected by mobile dislocations. At intermediate times, the dislocations segregate to interfaces, and their limited mobility creates a drag on the interfaces which decelerates the phase separation process. For any finite dislocation mobility, however, we show that the domain growth rate asymptotically becomes independent of the dislocation mobility, and is faster than the dislocation-free growth rate.

#### 9:30 AM

A Phase-Field Model for  $\theta$ ' Precipitation in Al-Cu Alloys: S. Y. Hu<sup>1</sup>; D. J. Seol<sup>1</sup>; C. Wolverton<sup>2</sup>; J. Murray<sup>3</sup>; H. Weiland<sup>3</sup>; Z. K. Liu<sup>1</sup>; L. Q. Chen<sup>1</sup>; <sup>1</sup>Pennsylvania State University, Dept. of Matls. Sci. & Engrg. & the Matls. Rsch. Inst., Univ. Park, 106 Steidle Bldg., State College, PA 16802 USA; <sup>2</sup>Ford Research Laboratory, MD3028/SRL, Dearborn, MI 48121-2053 USA; <sup>3</sup>Alcoa Technical Center, 100 Tech. Dr., Alcoa Ctr., PA 15069 USA

A phase-field model of  $\theta'$  (Al2Cu) precipitation is developed by linking it to thermodynamic and kinetic databases for Al-Cu alloys. To describe the  $\theta'$  precipitation, four field variables are employed, i.e. composition field describing Cu composition and three artificial fields describing three orientation variants of  $\theta'$  precipitates. The chemical free energies of matrix phase (solid solution) and  $\theta'$  phase from thermodynamic databases are directly used as the input to the phase-field model. The interface energy and interface mobility anisotropy as well as the elastic energy contribution are taken into account. We studied the growth of a single  $\theta'$  precipitate in one, two and three dimensions. It is shown that the both interface-controlled and diffusion-controlled transformations can be modeled. The effect of interface energy and interface mobility anisotropy and the elastic energy contribution on the morphology and growth rate of  $\theta'$  precipitates is studied using twoand three-dimensional simulations.

#### 9:50 AM

**Computational Simulation of θ' Precipitation During Stress Aging of Al-Cu Alloys:** D. J. Seol<sup>1</sup>; S. Y. Hu<sup>1</sup>; C. Wolverton<sup>2</sup>; J. Murray<sup>3</sup>; H. Weiland<sup>3</sup>; Z. K. Liu<sup>1</sup>; L.-Q. Chen<sup>1</sup>; <sup>1</sup>Pennsylvania State University, Matls. Sci. & Engrg., Univ. Park, PA 16802 USA; <sup>2</sup>Ford Research Laboratory, MD3028/SRL, Dearborn, MI 48121-2053 USA; <sup>3</sup>Alcoa Technical Center, 100 Tech. Dr., Alcoa Ctr., PA 15069 USA

Stress aging is a combined thermal treatment in which an elastic stress is applied during aging of materials. The directionality of the applied stress during the aging of age-hardenable Al-Cu alloys is known to be responsible for the oriented distribution of  $\theta'$  (Al<sub>2</sub>Cu) precipitates, which strongly affects their mechanical properties. In this study we use a phase-field model to describe  $\theta'$  precipitation under applied stress. The thermodynamic and kinetic parameters of the phase-field model have been obtained from databases for Al-Cu alloys with additional input from first-principles calculations. Four field variables are used, i.e. composition field, c(x,t), describing Cu composition and three artificial fields,  $\eta_i(x,t)$  (i=1,2,3), describing three orientation variants of  $\theta$ ' precipitates. We have simulated the effect of applied stress on the evolution of the  $\theta$  precipitates in the nucleation, growth, and coarsening stages, and analyzed the volume fraction and distribution of differently oriented  $\theta'$  precipitates with respect to the applied stress at various aging temperatures. The threshold value of the applied stress that must be exceeded for the oriented alignment of precipitates are determined.

#### 10:10 AM Break

#### 10:20 AM Invited

Stability of Layered Phases in Thin Films: Perry H. Leo<sup>1</sup>; <sup>1</sup>University of Minnesota, Aeros. Engrg., 107 Akerman Hall, 110 Union St. SE, Minneapolis, MN 55455 USA

The microstructural evolution of a layered, binary thin film is investigated by using a Cahn-Hilliard type equation. Evolution is triggered by elastic fields, which arise from composition dependence of the lattice parameter (compositional self-strain) and applied fields. Computations show that, depending on system parameters, the layered structure can persist through the evolution (one-dimensional evolution), or it can break down by a morphological instability at the interfaces between layers. We map the different behavior as a function of the elastic parameters of the system, and we discuss how an elastic substrate may be used to control the system's evolution.

#### 10:50 AM Invited

Cyclical Phase Transformations and Dynamic Equilibrium in Mechanical Alloying: *William C. Johnson*<sup>1</sup>; Jong K. Lee<sup>2</sup>; <sup>1</sup>Univer-

sity of Virginia, Dept. Matls. Sci. & Engrg., PO Box 400745, Charlottesville, VA 22904-4745 USA; <sup>2</sup>Michigan Technological University, Dept. Matls. Sci. & Engrg., Houghton, MI 49931 USA

A mixture of equilibrium and nonequilibrium phases are often synthesized during mechanical attrition (MA). In some cases, the phase fraction becomes constant after a certain time and a steady-state (dynamic equilibrium) is reached. In other systems, or for different milling power, cyclical transformations are observed in which the phase fractions continue to vary with time in a quasi-periodic manner. Using energy balance equations, we derive sets of coupled ordinary differential equations which describe the evolution of the system during MA. We obtain analytic approximations to the equations near steady-state conditions and show that the number of steady-state solutions and their stability can change with milling power (bifurcations). The analytic approximations are compared with numerical solutions illustrating the conditions for which cyclical phase transformation is realized. This work is supported by the Department of Energy.

#### 11:20 AM

Phase Transformations and Microstructure Evolutions Near Free Surfaces and in Thin Films: Phase Field Microelasticity Modeling: Yongmei M. Jin<sup>1</sup>; Yu U. Wang<sup>1</sup>; Armen G. Khachaturyan<sup>1</sup>; <sup>1</sup>Rutgers University, Ceram. & Matls. Engrg., 607 Taylor Rd., Piscataway, NJ 08854 USA

The elastic strain generated by the coherent phase transformations plays critical role in the microstructure evolutions. This elastic strain is significantly modified by the image forces near free surfaces and in thin films. Phase transformations and microstructure evolutions near free surfaces and in thin films are considered by using computer simulations to investigate the different behaviors from that in bulk crystals. The simulation model, which is based on the recent advances of the Phase Field Microelasticity approach, numerically solves the exact elasticity equation for a heterogeneous multi-phase multi-domain system with free surfaces. No ad hoc assumptions are made on the morphology of microstructures along the evolution path. Various examples are considered, including multi-variant martensitic transformations in FeNi and AuCd alloys. It is shown that the microstructures near free surfaces and in thin films are affected by the crystallography and epitaxy of the films. The effects of image forces are discussed.

#### 11:40 AM

Phase Field Microelasticity Modeling of Surface Roughening and Island Formation in Heteroepitaxial Films: Yu U. Wang<sup>1</sup>; Yongmei M. Jin<sup>1</sup>; Armen G. Khachaturyan<sup>1</sup>; <sup>1</sup>Rutgers University, Ceram. & Matls. Engrg., 607 Taylor Rd., Piscataway, NJ 08854 USA

The stress relaxations in heteroepitaxial films are investigated by using computer simulations. Two main mechanisms, surface roughening and dislocations, are considered. To address this problem, a Phase Field Microelasticity approach has been used to simulate the processes of surface roughening and dislocation dynamics in a deposited film driven by the relaxation of the epitaxial stress. The model is based on a numerical solution of the exact elasticity equation for a heteroepitaxial system with arbitrary surfaces. No ad hoc assumptions are made on the morphology of roughening along the evolution path that leads to the formation of multi-island configuration. The nonlinear diffusional evolution of the grooved film surface driven by the strain energy relaxation is investigated. The simulation shows that an initial small random roughening of a deposited flat film develops to form a quasiperiodical array of islands. The surface morphology simultaneously grows and coarsens. The fully coarsened morphology exhibits a dominant wavelength that is significantly greater than the one that follows from the linear analysis of initial instability. The equilibrium morphology corresponding to a periodic array of islands is reached through self-assembling independent of the initial fluctuations of the surface profile. Phase Field Microelasticity approach has been also used to study a motion of threading dislocation and operation of Frank-Read source in epitaxial films. The effect of image forces generated on the free surface on dislocation motions is consistently taken into account.

# Cost-Affordable Titanium Symposium Dedicated to Prof. Harvey Flower: Titanium Economics

Sponsored by: Structural Materials Division, SMD-Titanium Committee

*Program Organizers:* M. Ashraf Imam, Naval Research Laboratory, Washington, DC 20375-5343 USA; Derek J. Fray, University of Cambridge, Department of Materials Science and Metallurgy, Cambridge CB2 3Q2 UK; F. H. (Sam) Froes, University of Idaho, Institute of Materials and Advanced Processes, Moscow, ID 83844-3026 USA

Tuesday AMRoom: 206BMarch 16, 2004Location: Charlotte Convention Center

Session Chair: M. Ashraf Imam, Naval Research Laboratory, Washington, DC 20375-5343 USA

#### 8:30 AM

**Near Net Shape Production Of Titanium**: *J. C. Withers*<sup>1</sup>; R. Storm<sup>1</sup>; R. O. Loutfy<sup>1</sup>; <sup>1</sup>MER Corporation, Tucson, AZ 85706 USA

Near net shape fabrication using rapid prototyping, also called solid free form fabrication, has grown into a mature manufacturing process for a variety of materials including titanium. Titanium powder is fed into a molten pool that is manipulated by 3D computer-aided processing to build fully dense components in complex geometries including receding angles, passages and blind holes without the necessity of tooling or operator attendance. Energy sources to melt the feed powder or wire into the molten pool have included lasers of various types, electron beams and plasma processes. The plasma transferred arc achieves over 90% power efficiency and powder utilization in contrast to less than one-third for lasers and is not restricted by reflectivity problems associated with lasers. A plasma transferred arc solid free form fabrication system capable of producing components up to five meters has been used to near net shape produce titanium components in several alloy systems. The strength properties of the as produced titanium is typically 30% above wrought and heat treatments can further enhance strengths. A four component feed system permits producing select alloy compositions as well as functionally grading compositions. Examples include grading the titanium composition, as well as grading titanium to other alloy systems such as steels and aluminum. Composites are also produced by feeding particulate with the titanium, which has provided excellent wear resistance, as well as reduced coefficient of friction. Processing information, example components and properties will be discussed.

#### 9:00 AM

Development of Low Cost Titanium Alloy Sheets for Automotive Exhaust Applications: *Yoji Kosaka*<sup>1</sup>; Stephen P. Fox<sup>1</sup>; Kurt Faller<sup>2</sup>; Steven H. Reichman<sup>2</sup>; <sup>1</sup>TIMET, Henderson Tech. Lab., PO Box 2128, Henderson, NV 89009 USA; <sup>2</sup>TIMET, TIMET Auto., 900 Hemlock Rd., Morgantown, PA 19543 USA

The application of titanium sheets to the exhaust system of automobiles and motorcycles has been growing in recent years. A weight reduction of exhaust system is a primary purpose of the use of titanium. More than 40% of weight saving was realized using titanium to replace stainless steel. Although titanium is attractive to exhaust applications, oxidation resistance and softening of titanium at elevated temperature limit the use of titanium to parts exposed to relatively low temperatures. Low cost manufacturing is a key factor to reduce material cost to be accepted for automotive applications. Electron beam cold hearth melting has an important role to decrease an overall production cost. In the present work, alloy development was performed to achieve improved environmental and mechanical properties over CP titanium sheets. Properties of the sheets will be introduced and discussed.

# 9:30 AM

Low Cost Processes for Automotive Titanium Materials: *Yoji Kosaka*<sup>1</sup>; Kurt Faller<sup>2</sup>; Stephen P. Fox<sup>1</sup>; Steven H. Reichman<sup>2</sup>; Daniel J. Tilly<sup>3</sup>; <sup>1</sup>TIMET, Henderson Tech. Lab., PO Box 2128, Henderson, NV 89009 USA; <sup>2</sup>TIMET, TIMET Auto., 900 Hemlock Rd., Morgantown, PA 19543 USA; <sup>3</sup>TIMET, Vallejo Plant, 403 Ryder St., Vallejo, CA 94590 USA

Automotive application has been a prime target of emerging markets for titanium and its alloys for last two decades. Alloy development work was one of the major activities performed primarily by titanium manufacturers aiming the reduction of formulation cost with a maximized use of recycles or less expensive raw materials. TIMETAL LCB is one of good examples of alloys specifically designed for automotive applications. However, the reduction of the formulation cost alone will not be sufficient to reduce overall manufacturing cost of titanium parts for vehicles. In melting of titanium alloys, electron beam cold hearth melting is recognized as a versatile tool for the production of titanium and its alloys. A significant cost reduction is expected by combining effective operations with low cost alloys. This paper will introduce and discuss several examples that were aimed at automotive applications.

#### 10:00 AM

Torch Efficiency in Plasma Arc Cold Hearth Melting: Yuan Pang<sup>1</sup>; Chengming Wang<sup>2</sup>; Frank Spadafora<sup>3</sup>; Hao Dong<sup>1</sup>; Kuang-O (Oscar) Yu<sup>3</sup>; Daniel L. Winterscheidt<sup>4</sup>; <sup>1</sup>Concurrent Technologies Corporation, Product & Proc. Analysis, 425 Sixth Ave., Regional Enterprise Tower, 28th Floor, Pittsburgh, PA 15219-1819 USA; <sup>2</sup>The Procter & Gamble Company, Sharon Woods Tech. Ctr., 11450 Grooms Rd., SWTC Box C-21, GR-CNE72, Cincinnati, OH 45242 USA; <sup>3</sup>RMI Titanium Company, R&D, 1000 Warren Ave., Niles, OH 44446-0269 USA; <sup>4</sup>Concurrent Technologies Corporation, Mfg. Programs, 100 CTC Dr., Johnstown, PA 15904-1935 USA

During plasma arc cold hearth melting (PAM), multiple torches are used in the production of titanium ingots. Each torch generates a helium plasma jet, which transports heat to the titanium. If the amount of heat reaching the ingot is inadequate, a defect such as cold shuts can form on the surface that must be removed prior to forging. To cast PAM ingots of sufficient quality that no surface removal is necessary, an optimal combination of torch parameters must be considered for maximum thermal efficiency. This paper summarizes the experimental and computational results to illustrate the relationship between torch efficiency and parameters. Discussion is focused on experimentally measured power to the torch and numerically calculated energy to the metal using thermocouple data. The ratio of the prediction to the measurement yields estimated torch efficiency. How the present work will enhance a predictive model for ingot surface finish improvement is also addressed.

#### 10:30 AM

Blended Elemental Powder Metallurgy Approach to Produce Gamma Titanium Aluminide and Composite Ti-6Al-4V/TiAl/ Ti-6Al-4V Structures: V. S. Moxson<sup>1</sup>; V. A. Duz<sup>1</sup>; J. S. Montgomery<sup>2</sup>; F. H. (Sam) Froes<sup>3</sup>; F. Sun<sup>3</sup>; <sup>1</sup>ADMA Products, Inc., 8180 Boyle Pkwy., Twinsburg, OH 44087 USA; <sup>2</sup>Army Research Laboratory, Aberdeen Proving Ground, MA 21005-5066 USA; <sup>3</sup>University of Idaho, Inst. for Matls. & Adv. Proc. (IMAP), McClure Hall, Rm. 437, Moscow, ID 83844-3026 USA

Cost effective method of production of both chunky and flat components for potential military and terrestrial applications using a Blended Elemental (BE) powder metallurgy (P/M) approach will be discussed. This will include Gamma Titanium Aluminide and Ti-6Al-4V/TiAl/Ti-6Al-4V monolithic composites produced by innovative ADMATAL-23 processes. Detailed studies of the microstructures and interfaces developed in sintering and high temperature deformation will be presented.

# **Dislocations: Dislocation Structures and Patterning**

Sponsored by: ASM International: Materials Science Critical Technology Sector, Electronic, Magnetic & Photonic Materials Division, Materials Processing & Manufacturing Division, Structural Materials Division, EMPMD/SMD-Chemistry & Physics of Materials Committee, MPMD-Computational Materials Science & Engineering-(Jt. ASM-MSCTS)

*Program Organizers:* Elizabeth A. Holm, Sandia National Laboratories, Albuquerque, NM 87185-1411 USA; Richard A. LeSar, Los Alamos National Laboratory, Theoretical Division, Los Alamos, NM 87545 USA; Yunzhi Wang, The Ohio State University, Department of Materials Science and Engineering, Columbus, OH 43210 USA

Tuesday AM March 16, 2004 Room: 201A Location: Charlotte Convention Center

Session Chair: TBA

#### 8:30 AM Invited

**Dislocation-Based Multiscale Modeling of Plasticity**: *L. Kubin*<sup>1</sup>; B. Devincre<sup>1</sup>; T. Hoc<sup>2</sup>; <sup>1</sup>LEM, CNRS-ONERA, 29 Av. de la Division Leclerc, BP 72, 92322 Chatillon, Cedex France; <sup>2</sup>Ecole Centrale Paris, Lab. MSSMat, Grande Voie des Vignes, 92295 Chatenay-Malabry, Cedex France

By combining 3-D mesoscopic modeling, simulations and continuum modeling, it is now possible to construct multiscale models for crystal plasticity which have a predictive value in the absence of adjustable parameters. The application presented deals with fcc crystals, where the basic mechanisms governing plastic flow are dislocation interactions and cross-slip. These mechanisms are incorporated into a dislocation-based model for the evolution of the stored dislocation density in each slip system, in which the relevant material parameters are deduced from simulations at various scales. The three-stage stress strain curves of fcc single crystals in monotonic deformation are fully recovered by inserting this constitutive formulation into a Finite Element code for the polycrystal, which accounts for the lattice rotation during plastic deformation. It appears that, in some situations to be discussed, is it more important to properly account for elementary dislocation mechanisms than to attempt describing patterning phenomena.

#### 9:05 AM

Determination of Deformation Inhomogeneity in Polycrystalline Ni Under Uniaxial Tension With 3D X-Ray Microscope: Judy W. Pang<sup>1</sup>; Rozaliya Barabash<sup>1</sup>; Wenjun Liu<sup>1</sup>; Gene E. Ice<sup>1</sup>; <sup>1</sup>Oak Ridge National Laboratory, Metals & Ceram., PO Box 2008, MS 6118, Oak Ridge, TN 37831-6118 USA

Generation of deformation substructures has significant effects on materials development processes such as recrystallization. These substructures are caused by deformation inhomogeneities due to grain-tograin interactions. Measurement of misorientations introduced due to the formation of substructures is essential to understand deformation mechanisms. In this paper, evolution of lattice rotations within submicron volume elements of neighboring grains in a polycrystalline Ni samples was studied by 3D x-ray microscope as a function of plastic strain using polychromatic Laue technique. Each individual grain exhibits its own rotation pattern due to grain-to-grain interactions. Variation in rotation as a function of depth was also found for all the grains measured. The Laue patterns were analyzed using strain gradient plasticity theory to deduce the possible dislocation activities. Different slip systems were activated within the same grain as depth increases.

#### 9:25 AM

**Observations and Modeling of Dislocation Structures in a Crept High Volume Fraction Superalloy**: *Shuwei Ma*<sup>1</sup>; Bhaskar S. Majumdar<sup>1</sup>; <sup>1</sup>New Mexico Tech, Matls. & Metallurgl. Engrg. Dept., 801 Leroy Place, Socorro, NM 87801 USA

Creep experiments were performed on a polycrystalline superalloy, CM-247 LC, that contained a high volume fraction (~65%) of gamma-prime phase. TEM observations revealed that while the gammaprime phase remained largely undeformed, the narrow gamma channels were occupied by a network of dislocations. These are geometrically necessary dislocations that are accumulated in the narrow gamma channels to maintain strain compatability. We then used the concept of Ashby's plastic strain gradient to estimate the density of geometrically necessary dislocations, where the plastic strain gradient was calculated using a finite element method. The resultant elastic strains in the phases, for grains whose [001] direction lay along the tensile axis of the specimen, are compared with strain data obtained from neutron diffraction measurements through insitu creep tests at the Los Alamos Neutron Science Center. In addition, the observed dislocation densities are compared with theoretical predictions based on the concept of geometrically necessary dislocations. Together, these results are anticipated to provide additional quantitative insight on microstructural instability and rafting that accompany creep of superalloys at high temperatures.

#### 9:45 AM

Dislocation Structures and Their Relationship to {111} Microbands and Microtwins in Spherical and Plane Impact Deformed Nickel: Erika Vanessa Esquivel<sup>1</sup>; L. E. Murr<sup>1</sup>; <sup>1</sup>University of Texas, Metallurgl. & Matls. Engrg., 500 W. Univ. Ave., El Paso, TX 79968 USA

Microstructural studies involving transmission electron microscopy (TEM) have revealed that there is a transition of dislocation structures when the geometry of the impact changes from plane, as in plane-wave shock loading, to spherical, as in impact cratering. Planewave shock loaded nickel has revealed microtwins, 0.02 micrometers thick lying on {111} traces, above a critical shock twinning pressure of ~ 30 GPa while microbands, also lying on traces of {111} with an approximate 2° misorientation, have been observed below craters produced by spherical projectile impact at pressures well above the planewave shock critical twinning pressure. In contrast to microtwins the microbands are roughly 10 times thicker (~ 0.2 micrometers). Both types of impact have produced dislocation cells whose diameter increases with decreasing pressure, and the transition from the microband to microtwin formation is therefore believed to be strongly dependent on the shock wave geometry where a planar shock wave would promote microtwinning, while a spherical shock wave would facilitate cross-slip and allow microbanding. There is also a transition from microbands to dislocation cell structures in the spherical-shock impacted nickel and TEM observations have documented the details of the elongation of dislocation walls coincident with {111} to more randomly and equiaxed cell structures, and related dense dislocation wall structures.

## 10:05 AM Break

# 10:20 AM Invited

Atomistic Calculations of Shock Induced Phase Transformations and Microstructure Evolution: *M. I. Baskes*<sup>1</sup>; S. G. Srinivasan<sup>1</sup>; G. J. Wagner<sup>2</sup>; <sup>1</sup>Los Alamos National Laboratory, Los Alamos, NM USA; <sup>2</sup>Sandia National Laboratory, Albuquerque, NM 87185 USA

Shock waves in materials produce a number of interesting phenomena including microstructure evolution and phase transformations. Underlying these phenomena is the generation and motion of dislocations. This presentation will discuss recent calculations of these phenomena at the atomic level using an embedded atom method (EAM) potential. Since the phenomena of interest involve subtle energy differences in the phase transformations and generation of grain boundaries, a realistic many-body EAM potential that represents the properties of nickel, a typical fcc material is used. Using a standard flyerplate geometry of a single crystal, many calculations at different sample sizes and initial impact velocity were performed. In general the following observations about shock induced phase transformations at very high strain rates and stress may be made: (1) the fcc crystal transforms to a bcc-like crystal structure behind the shock wave; (2) after a period of time, the bcc structure transforms to domains of a highly faulted fcc structure; (3) the domains grow and form twin boundaries at the domain intersection; and (4) when the reflected shock wave traverses this material, the system mostly transforms back to polycrystalline fcc material containing a number of faults. These general observations appear to be insensitive to the in-plane sample periodicity, but the details, e.g., fault or twin spacing, appears to scale with this imposed periodicity. The role of dislocations in these processes will be discussed.

#### 10:55 AM

Characterization of Dislocation Structure Evolution in High Purity Aluminum During Small Strain Compression.: Pankaj B. Trivedi<sup>1</sup>; David P. Field<sup>1</sup>; <sup>1</sup>Washington State University, Sch. of Mech. & Matls. Engrg., PO Box 642920, Pullman, WA 99164-2920 USA

Dislocation structure evolution during small strain deformation (up to 20%) using channel die was studied in high purity aluminum. Samples from a coarse grained polycrystal and a single crystal were deformed to 15% and 20% strain and dislocation structure characterization was done using EBSD. Disorientation angle from an average orientation was studied for all the samples as a function of area and deformation. The distribution of disorientation angle as a function of area of the scanned region provides quantitative information about the average local variation of the crystal orientation and indirectly relates to dislocation cell structure. In an undeformed sample the distribution of disorientation angle remained same with increasing area. With increase in deformation in the case of single crystal the distribution of disorientation angle changed from mostly 2.1-2.20 at 0% deformation to 1.55-1.560 at 15% deformation and 2.05-2.20 after 20% deformation. In the case of single crystal after 15% deformation the di stribution of disorientation angle remained same with increasing area but after 20% deformation the distribution increased from predominantly 1.550 to 2.1-2.20. Dislocation cell size remained the same after 15% and 20% deformation for the single crystal whereas for the polycrystal there was a slight increase in cell size with increasing deformation. Grain orientation is shown to have an effect on the evolution of dislocation structure, and it appears that grains with lower Taylor factors form a well-organized cell structure.

#### 11:15 AM

**Dislocation Configurations and Long Range Internal Stresses:** *M. E. Kassner*<sup>1</sup>; M. A. Delos-Reyes<sup>1</sup>; L. E. Levine<sup>2</sup>; <sup>1</sup>Oregon State University, Mech. Engrg., Rogers Hall, Corvallis, OR 97331 USA; <sup>2</sup>NIST, Gaitherburg, MD 20899 USA

The concept of "long range internal stresses" (LRIS) is often utilized to explain various aspects of the mechanical behavior of materials, including cyclic deformation. These internal stresses are usually associated with the heterogeneous microstructure. Convergent beam electron diffraction (CBED) and dislocation dipole separation measurements have been performed that indicate an absence of measurable LRIS. "X-ray diffraction line profile analysis" (XRD, LPA), specifically, the interpretation of asymmetry in strain broadened Bragg diffraction peaks, has been extensively used to support LRIS. The asymmetry literature has been surveyed and re-analyzed in this work. It is found that there is more than one reasonable explanation for x-ray line asymmetry, and that LRIS is not required for asymmetry to be present. Computer modeling of x-ray diffraction from dislocated crystals is being performed using standard and novel approaches, and these will be discussed.

#### 11:35 AM

Static Recovery of Pure Copper at Low Homologous Temperature: *Chen-Ming Kuo*<sup>1</sup>; Chin-Sheng Lin<sup>2</sup>; <sup>1</sup>I-Shou University, Dept. of Mech. Engrg., 1, Sec. 1, Hsueh-Cheng Rd., Kaohsiung 84008 Taiwan; <sup>2</sup>I-Shou University, Dept. of Matls. Sci. & Engrg., 1, Sec. 1, Hsueh-Cheng Rd., Kaohsiung 84008 Taiwan

Static recovery experiments of pure copper near room temperature have been conducted via TEM, DSC, micro-hardness, and extensometer to explore the time and temperature dependent relationships. By using different applied strain rate, dislocation density is generated differently within specimens. Since strain hardening and dynamic recovery occur simultaneously during loading stage, for the lower applied strain rate specimens, dislocation density is less because it allows more time for dynamic recovery to occur. During static recovery experiments, the recovery phenomenon is more significantly as time and temperature increase, because dislocation annihilation occurs more considerably. Time dependent static recovery could be observed and measures by TEM, DSC, micro-hardness, and extensometer. On the other hand, extensometer measurement reveals temperature dependent static recovery. As temperature increases, static recovered strain is more appre ciably. Activation energy of static recovery of pure copper is 53.29 kJ/mole measured by extensometer.

# Electrochemical Measurements and Processing of Materials: Electrodeposition Processes

Sponsored by: Extraction & Processing Division, Materials Processing & Manufacturing Division, EPD-Aqueous Processing Committee, EPD-Process Fundamentals Committee, EPD-Pyrometallurgy Committee, ASM/MSCTS-Thermodynamics & Phase Equilibria Committee, EPD-Waste Treatment & Minimization Committee

*Program Organizers:* Uday B. Pal, Boston University, Department of Manufacturing Engineering, Brookline, MA 02446 USA; Akram M. Alfantazi, University of British Columbia, Department of Metel & Materials Engineering, Vancouver, BC V6T 1Z4 Canada; Adam C. Powell, Massachusetts Institute of Technology, Department of Materials Science and Engineering, Cambridge, MA 02139-4307 USA

Tuesday AM	Room:	212A
March 16, 2004	Locatior	: Charlotte Convention Center

Session Chairs: Uday B. Pal, Boston University, Dept. of Mfg. Engrg., Brookline, MA 02446 USA; Seshadri Seetharaman, Royal Institute of Technology, Matls. Sci. & Engrg., Stockholm 10044 Sweden

#### 8:30 AM Invited

Electrodeposition as a Means of Processing Semi-Conductor Industry Waste Streams Containing Copper: Ran Ding<sup>1</sup>; James William Evans<sup>1</sup>; Fiona M. Doyle<sup>1</sup>; <sup>1</sup>University of California, Dept. of Matls. Sci. & Engrg., Berkeley, CA 94720 USA

Copper is becoming the material of choice for metallization in the semi-conductor industry. When the copper is electrodeposited, deposited by electroless techniques or subjected to CMP then aqueous waste streams containing copper and other species are created. The paper results from an ongoing investigation aimed at removing copper and recovering the water by a combination of ion-exchange and electrodeposition. The focus of the paper is on copper electrodeposition and a companion paper in another session reports on ion-exchange. Studies at the rotating disc electrode have shown that additives commonly occurring in these streams (e.g. citric acid and glycine) can inhibit electrodeposition. Results from cells using porous or particulate electrode for copper removal are described.

#### 9:00 AM Invited

The Role of Surfactant Catalysts in Superfilling and Supersmoothing: *Daniel Josell*<sup>1</sup>; Thomas P. Moffat<sup>1</sup>; Daniel Wheeler<sup>1</sup>; <sup>1</sup>NIST, Metall. Div., 100 Bureau Dr., MS 8555, Gaithersburg, MD 20899 USA

I will discuss the role of surfactant catalysts in achieving superconformal, bottom-up filling of fine features during metal electrodeposition. I will discuss the particular cases of copper and silver superfill for fabrication of sub-100 nm metallizations, including the electrolyte-additive systems and how the impact of the catalyst is quantified through the Curvature Enhanced Accelerator Coverage (CEAC) mechanism; this mechanism accounts for local change of catalyst is adsorbed during metal deposition on nonplanar surfaces. I will also discuss the significance of these results for stabilization of surfaces against concentration gradient induced roughening, as expressed in the CEAC brightening mechanism.

#### 9:30 AM Invited

Electrolytic Preparation of Carbon Nanotubes in Molten Salts: Derek J. Fray<sup>1</sup>; Carsten Schwandt<sup>1</sup>; George Z. Chen<sup>1</sup>; <sup>1</sup>University of Cambridge, Matls. Sci. & Metall., Pembroke St., Cambridge CB2 3QZ UK

It has been found that by making graphite the cathode in a bath of molten salts and applying a potential such that the salt decomposes, it is possible to create carbon nanotubes and nanoparticles. The production of carbon nanotubes in molten NaCl and LiCl was investigated as a function of applied voltage, current density and time of electrolysis. It was concluded that the mechanism for the production of nanotubes was due to the intercalation of the discharged cation into the graphite structure and this was investigated electrochemically. By careful control of the conditions it was possible to maximise the production of nanotubes. If a salt with a lower decomposition potential that the alkali chloride, such as SnCl2, is introduced, the carbon nanotubes are full of tin. Possible applications for these materials are described.

## 10:00 AM Break

#### 10:30 AM

A Substructurally Composite Chromium Electrochemical Coating Formed on a Canned-Food Steel Sheet from a Low-Concentration Solution of Hexavalent Chromium-Based Compounds: *Oleg B. Girin*<sup>1</sup>; Igor D. Zakharov<sup>2</sup>; Volodymyr I. Ovcharenko<sup>1</sup>; <sup>1</sup>Ukrainian State University of Chemical Engineering, Dept. of Matls. Sci., Pr. Gagarina, 8, Dnipropetrovsk 49005 Ukraine; <sup>2</sup>Polimet Research and Technology Center, Lab. of Protective Coatings, Vul. Mandrykivska, 169, Dnipropetrovsk 49049 Ukraine

A composition of a low-concentration chrome-plating solution has been developed with the 100?20 g/l chromium anhydride content, and the process parameters have been tested for applying 0.01-0.03 mkm thick protective electrochemical coatings on canned-food steel sheet. The properties of the coatings have been studied taking into consideration their structure. There have been determined the optimum variants of applying on the steel sheet of composites comprised of chromium layers featuring different substructure anizotropy levels in the axial components of their texture that have improved protective properties. Based on the usage of the phenomenon of electrochemical deposition of metals via a supercooled metal liquid there has been developed a process of depositing on the canned-food steel sheet of a super-thin substructurally composite electrochemical chromium coating from a low-concentration solution based on hexavalent chromium compounds. This research project is financed by the Intergovernmental organization "Science & Technology Center in Ukraine", Project Agreement No.2520.

#### 11:00 AM

The Nucleation and Growth Mechanism in Tin Electrodeposition: Shixue Wen<sup>1</sup>; Sasha Omanovic<sup>2</sup>; Jerzy A. Szpunar<sup>1</sup>; <sup>1</sup>McGill University, Dept. of Mining, Metals & Matls. Engrg., 3610 Univ., Montreal, Quebec H3A 2B2 Canada; <sup>2</sup>McGill University, Dept. of Chem. Engrg., 3610 Univ., Montreal, Quebec H3A 2B2 Canada

Tin electrodeposition from sulfuric acid electrolytes was studied on a glassy carbon substrate by electrochemical techniques. The morphology of tin nuclei and crystallites was observed by scanning electron microscopy (SEM). The analysis of chronoamperomeric experiments reveals that at the nucleation and growth mechanism of tin is dependent on the applied cathodic potentials. At a cathodic potential of 495mV, 3D progressive nucleation mechanism occurs. As potentials become more negative, the nucleation mechanism changes to 3D instantaneous nucleation mechanism. At potentials between -575mV and -680mV, 3D instantaneous nucleation and growth mechanism takes place. As potentials become more negative than -680mV, due to hydrogen evolution, the mechanism lies in between 3D progressive and 3D instantaneous nucleation mechanism. The morphology of tin nuclei varies with applied potentials. At the potential of -510mV, tetragonal nuclei and crystallites are dominant. As the potentials become more negative, clusters of tin needles increase. At -700mV, all grains are tin needles.

# 11:30 AM

#### The Texture and Microstructure of Electrodeposited Tin Coatings: Shixue Wen<sup>1</sup>; Jerzy A. Szpunar<sup>1</sup>; <sup>1</sup>McGill University, Dept. of Mining, Metals & Matls. Engrg., Montreal, Quebec H3A 2B2 Canada

Due to its good corrosion resistance, non-toxicity and solderability, tin is widely used in food packaging and electronic industries. Tin elctrodeposition on copper substrates using stannous sulfate and sulfuric acid with organic additives was studied under different current densities and temperature. The macrotexture of the tin deposits was measured using an x-ray texture gonimeter. The orientation imaging microscopy (OIM) was used to measure the orientations of individual grains along with the microstructure. It was found that tin coating with a (001) fiber texture can be produced by electrodepositon. If the coating is thin, tin grains grow epitaxially on copper substrate that has a strong (001) [-100] texture and the coating has a (001) fibre texture. In a thick coating, the texture was changed to (110) fibre texture, which indicates that at a thick deposit, the texture becomes independent of substrate orientation. The grain size distribution and misorientation between grains were also measured. It is demonstrated that the OIM is an ideal and powerful tool to measure texture at different depth of the coating and to analyze texture nucleation and growth.

# **General Abstracts: Session IV**

Sponsored by: TMS

*Program Organizers:* Adrian C. Deneys, Praxair, Inc., Tarrytown, NY 10591-6717 USA; John J. Chen, University of Auckland, Department of Chemical & Materials Engineering, Auckland 00160 New Zealand; Eric M. Taleff, University of Texas, Mechanical Engineering Department, Austin, TX 78712-1063 USA

Tuesday AM	Room: 204
March 16, 2004	Location: Charlotte Convention Center

Session Chair: Ian Bainbridge, University of Queensland, CRC for Cast Metals Mfg., St. Lucia, QLD 4072 Australia

#### 8:30 AM

An Investigation of the Factors Affecting the Occurrence of the Grain Boundary Serration: Soo Woo Nam<sup>1</sup>; *Ki Jae Kim*<sup>1</sup>; <sup>1</sup>Korea Advanced Institute of Science and Technology, Matl. Sci. & Engrg., 373-1 Guseong-dong, Yuseong-gu, Daejeon 305-701 Korea

The purpose of this study is to investigate the role of factors affecting the occurrence of the grain boundary serration in an AISI 316 stainless steel. Among the factors affecting the grain boundary serration, the effects of the grain boundary characteristics have been investigated by using the EBSD(Electron BackScattered Diffraction) technique. And the effect of the chemical compositions on the grain boundary serration has also been investigated. And the relationship between grain boundary serration and heat treatment conditions has been investigated. It might be expected that in case of high temperature aging conditions, the grain boundary serration does not occur, since the grain growth is easily occurred so that the total energy of the system is reduced, on the other hands, in case of low temperature aging conditions, the grain boundary serration is occurred to reduce the total energy of the system, since the grain growth is not easily occurred.

#### 8:55 AM

Determination of Composition Dependent Ternary Interdiffusion Coefficients From a Single Diffusion Couple: *Abby Lee Elliott*<sup>1</sup>; Yongho Sohn<sup>1</sup>; <sup>1</sup>University of Central Florida, Advd. Matls. Procg. & Analysis Ctr., Box 162455, 4000 Central Florida Blvd., Orlando, FL 32816-2455 USA

A new method to extract composition dependent ternary interdiffusion coefficient from a single diffusion couple experiment is proposed. The calculations involve direct determination of interdiffusion fluxes from experimental concentration profiles and local integration and differentiation of Onsager's formalism. This new method was applied to concentration profiles obtained from selected diffusion couple experiments in the Cu-Ni-Al and Fe-Ni-Al systems. The calculated interdiffusion coefficients are consistent with those determined from Boltzmann-Matano analysis and alternate analyses based on the concept of average ternary interdiffusion coefficients and square-root diffusivity. The concentration and interdiffusion flux profiles calculated from the ternary interdiffusion coefficients are in good agreement with the experimental profiles including those exhibiting uphill diffusion and zero-flux planes.

# 9:20 AM

**Phase Transformation in a Nucleation and Growth Reaction: Application of Moments Methods**: *David T. Wu*<sup>1</sup>; Lin Zhuo<sup>1</sup>; <sup>1</sup>Yale University, Dept. of Mech. Engrg., PO Box 208284, New Haven, CT 06520-8284 USA

For a first-order phase transformation, the expression for the isothermal fraction transformed as a function of time is well known for site saturation and for constant nucleation and growth conditions. In realistic situations such as in casting, however, the temperature can depend both on time and position; hence the nucleation and growth rates will be more general functions. While the Johnson-Mehl-Avrami-Kolmogorov formalism gives an expression for fraction transformed when the nucleation and growth rates are arbitrary, its direct evaluation is rather inefficient. We show that using the method of moments and the quadrature method of moments, the fraction transformed can be evaluated very efficiently.

#### 9:45 AM Break

#### 9:55 AM

Microstructural Evolution of AA-6061 Subjected to Severe Plastic Deformation: *Yogesh Bhambri*<sup>1</sup>; Shravan K. Indrakanti<sup>1</sup>; Raghavan Srinivasan<sup>1</sup>; Prabir Chaudhury<sup>2</sup>; Qingyou Han<sup>3</sup>; <sup>1</sup>Wright State University, Dept. of Mech. & Matls. Engrg., 209 Russ Engrg. Ctr., 3640 Col. Glenn Hwy., Dayton, OH 45435 USA; <sup>2</sup>Intercontinental Manufacturing Company USA; <sup>3</sup>Oak Ridge National Laboratory, Metals & Ceram., Oak Ridge, TN USA

Grain size in metals can be substantially refined in bulk, to the submicrometer level, by imposing high strains through processes such as equal channel angular extrusion (ECAE). In this study, samples of annealed AA6061 with square cross-sections of 1/2-inch, 2-inch and 4inch were subjected to severe plastic deformation at room temperature by ECAE by multiple passes through dies with channel angles of 120°, 90° and 105°, respectively. The changes in microstructure including grain refinement for these samples were studied. Additionally in this alloy, fracture and redistribution of precipitates were studied for samples processed through 120° die. Initial results indicate the precipitates break during the deformation process and are more uniformly distributed. The deformed specimens were heated to study the stability of microstructure to retain the fine grain size up to the forging temperatures for this alloy. The results show that after a small increase in size, grains remain stable in 300-400°C temperature range.

#### 10:20 AM

Process Maps for Controlling Microstructure in Laser Deposited Ti-6Al-4V: Srikanth Bontha<sup>1</sup>; Nathan W. Klingbeil<sup>1</sup>; <sup>1</sup>Wright State University, Mech. & Matls. Engrg. Dept., 209 Russ Engrg. Ctr., 3640 Colonel Glenn Hwy., Dayton, OH 45435 USA

Laser deposition of titanium alloys is under consideration for aerospace applications, which require the consistent control of microstructure and resulting mechanical properties. The focus of this work is the development of process maps relating solidification cooling rate and thermal gradient (the key parameters controlling microstructure) to laser deposition process variables (e.g., laser power and velocity). General results are presented based on the Rosenthal solution for a moving point heat source traversing both thin-wall (2-D) and bulky (3-D) deposits, while the effects of finite geometry, temperaturedependent properties and latent heat of transformation are investigated through thermal finite element modeling. In addition, results are plotted on solidification maps for predicting grain morphology in laser deposited Ti-6Al-4V. The results of this work suggest that changes in process variables could result in a grading of the microstructure throughout the depth of the deposit, and that the size-scale of the laser deposition process is important.

#### 10:45 AM

Directional Recrystallization of Polycrystalline Nickel Cold-Rolled at 77K: *H. Chang*<sup>1</sup>; Ian Baker<sup>1</sup>; <sup>1</sup>Dartmouth College, Thayer Sch. of Engrg., Hanover, NH 03755 USA

Polycrystalline nickel sheets cold rolled to 90% thickness reduction after cooling in liquid nitrogen were statically annealed at 350C for 30 mins and then directionally annealed at 1000°C. A large temperature gradient of 1000° C/cm ahead of the hot zone was used during directional annealing and a wide range of hot zone velocities were examined. The as-rolled and directionally recrystallized microstructures were characterized using differentially scanning calorimetry, optical microscopy and electron back-scattered patterns from a scanning electron microscope. The results are contrasted with directional recrystallization of nickel rolled to 90% reduction at room temperature. Research supported by NSF grants DMI 9976509 and DMI 0217565.

#### 11:10 AM

Experimental Observation of the Type III Boundary in a Two-Phase Ternary Diffusion Couple: *Abby Lee Elliott*<sup>1</sup>; Yongho Sohn<sup>1</sup>; <sup>1</sup>University of Central Florida, Advd. Matls. Procg. & Analysis Ctr., Box 162455, 4000 Central Florida Blvd., Orlando, FL 32816-2455 USA

Morral has classified the Type 0, I, and II phase boundaries according to the number of phases that are added/subtracted upon crossing the phase boundary during the annealing of two-phase diffusion couple. This classification system is based on a binary system and has been annexed to include the Type III and IV phase boundaries that may occur in a ternary system due to the existence of a three phase region on a ternary isotherm. The movement of each phase boundary type is discussed in terms of degrees of freedom via Gibbs phase rule. Type I and Type II boundaries have been frequently observed experimentally. In this work, experimental observation of the Type III ternary boundary is presented for an Fe-Ni-Al isothermal diffusion couple. This observation establishes the existence of a ternary phase boundary joining a two-phase region with a single-phase region, each region sharing no common phase. The diffusion path for this couple exits out the vertex of the equilibrium tie triangle resulting in a boundary joining a two-phase region with a single phase region.

TUESDAY AM

# Hume Rothery Symposium: Structure and Diffusional Growth Mechanisms of Irrational Interphase Boundaries: Session III

Sponsored by: Electronic, Magnetic & Photonic Materials Division, Structural Materials Division, EMPMD/SMD-Alloy Phases Committee, MPMD-Phase Transformation Committee-(Jt. ASM-MSCTS)

*Program Organizer:* H. I. Aaronson, Carnegie Mellon University, Department of Materials Science and Engineering, Pittsburgh, PA 15213 USA

Tuesday AM	Room: 2	08A
March 16, 2004	Location:	Charlotte Convention Center

Session Chair: W. T. Reynolds, Virginia Tech, Matls. Sci. Engrg. Dept., Blacksburg, VA 24061 USA

#### 8:30 AM Invited

Atomistic Calculations of Incoherent Zr/ZrN Interfaces: Michael I. Baskes<sup>1</sup>; S. G. Srinivasan<sup>1</sup>; Sven P. Rudin<sup>2</sup>; <sup>1</sup>Los Alamos National Laboratory, Matls. Sci. & Tech. Div., MS G755, Los Alamos, NM 87545 USA; <sup>2</sup>Los Alamos National Laboratory, Theoretical Div., MS B221, Los Alamos, NM 87545 USA

The interfaces between Zr and ZrN (B1) have been studied at the atomistic level using the Modified Embedded Atom Method (MEAM) interaction model. Literature MEAM potentials have been used for Zr and N and the Zr/N potential was developed using both experimental data and generalized gradient approximation calculations. The interfaces studied have the orientation relationship  $[450]_{Zr}$  / / [-10-1]<sub>ZrN</sub> and  $(002)_{Zr}$  / / (-131)<sub>ZrN</sub> as seen in experiment. A major complication in the calculations is that the Zr (hcp) contains ~ 25 at% N and the ZrN (B1) is not stoichiometric, containing ~45 at% N. Atomistic models have been created at these compositions for various interface planes. The relaxed interface structure and energy have been calculated and are compared to what is observed in experiment. The calculations will be used to explain the distribution of interface planes seen in experiment. This work was supported by the Office of Basic Energy Sciences, U.S. DOE.

#### 9:10 AM Invited

**EAM Modelling of Edge-to-Edge Interfaces**: *W. T. Reynolds*<sup>1</sup>; Diana Farkas<sup>1</sup>; <sup>1</sup>Virginia Polytechnic Institute and State University, Matls. Sci. & Engrg. Dept., Holden Hall, MC 0237, Blacksburg, VA 24061 USA

The energies of high-index interphase boundaries are explored using molecular statics simulations with embedded atom potentials. We investigate planar boundaries between the alpha<sub>2</sub> and gamma phases in the Ti-Al system. The class of boundaries considered have a highindex boundary orientation, the orientation relationship between the alpha<sub>2</sub> and gamma phases also is high-index, and a set of planes from each phase meet edge-to-edge at the boundary plane. The boundaries are commensurate in one direction and coincide with a moire plane given by the so-called " $\Delta g$ " diffraction condition. The boundaries are not structurally singular, but they are energetically stable and do not appear to dissociate into other low energy configurations. Misfit compensating defects are not observed; misfit in directions other than the commensurate one appears to be distributed uniformly in the boundary. The relative boundary energy is evaluated as a function of the orientation relationship between the two phases.

#### 9:50 AM Invited

Edge Matching at Grain Boundaries and the Five Macroscopic Degrees of Freedom: Anthony D. Rollett<sup>1</sup>; <sup>1</sup>Carnegie Mellon University, Matls. Sci. & Engrg., 4315 Wean Hall, 5000 Forbes Ave., Pittsburgh, PA 15213 USA

The application of plane-edge-matching to grain boundaries is investigated. Phase transformations with heterophase interfaces exhibit edge matching only occur for certain specific orientation relationships. By contrast, there are many misorientations and boundary normals for which low index planes can satisfy edge matching criteria at homophase grain boundaries. Some simple mathematics that describes the situation for grain boundaries is described and its potential impact on grain boundary properties is explored.

#### 10:30 AM Break

#### 10:45 AM Invited

Observations of Interfaces Linking Proeutectoid Ferrite Allotriomorphs and Parent Austenite Crystals in an Fe-C-Mn-Si Alloy: Malcolm G. Hall<sup>1</sup>; Hui Guo<sup>2</sup>; Gary R. Purdy<sup>2</sup>; <sup>1</sup>University of Birmingham, Dept. of Metall. & Matls., Elms Rd., Edgbaston, Birmingham B15 2TT UK; <sup>2</sup>McMaster University, Dept. of Matls. Sci. & Engrg., 1280 Main St. W., Hamilton, Ontario L8S 4L7 Canada

An alloy of Fe-0.38%C-3.0%Mn-1.85%Si was first homogenized, quenched, austenitized at 950°C to yield a grain size of approximately 50 microns and isothermally transformed at 650°C, a temperature at which Mn partition is expected (and observed). The specimens were then held for 12 hours at 350°C to stabilize the austenite immediately adjacent to the grain boundary ferrite precipitates, and prepared as thin foils for electron microscopic observation. We report on four aspects of the transformation products: the precipitate morphology; the orientation relationships among the ferrite and austenite crystals; the distribution of manganese in the region of the ferrite-austenite interfaces; and structural aspects of the ferrite-austenite interfaces. In most cases, growth of ferrite was apparently confined to one side of the precipitate, the other side remaining relatively planar and coincident with the original austenite grain boundary position.

#### 11:25 AM Invited

Structure of Irrational Interphase Boundary Formed During Precipitation: Tadashi Furuhara<sup>1</sup>; Tadashi Maki<sup>1</sup>; <sup>1</sup>Kyoto University, Dept. of Matls. Sci. & Engrg., Yoshida-honmachi, Sakyo-ku, Kyoto, Kyoto 606-8501 Japan

Three kinds of irrational interphase boundaries formed in precipitation are discussed; (1) (partly) coherent boundary satisfying a rational (or near-rational) orientation relationship with an irrational macroscopic habit plane, (2) boundary with an irrational orientation relationship and habit plane and (3) incoherent boundary with a rational orientation relationship and habit plane with large difference in atomic density between precipitate and matrix phases. A geometrical model (near coincidence site model) can explain the crystallographic feature of those boundaries reasonably well. Some problems in the extension of modeling are also pointed out.

# Internal Stresses and Thermo-Mechanical Behavior in Multi-Component Materials Systems: Creep and Plasticity I

Sponsored by: Electronic, Magnetic & Photonic Materials Division, Structural Materials Division, EMPMD-Electronic Packaging and Interconnection Materials Committee, EMPMD-Thin Films & Interfaces Committee, SMD-Composite Materials Committee-Jt. ASM-MSCTS

*Program Organizers:* Indranath Dutta, Naval Postgraduate School, Department of Mechanical Engineering, Monterey, CA 93943 USA; Bhaskar S. Majumdar, New Mexico Tech, Department of Materials Science and Engineering, Socorro, NM 87801 USA; Mark A.M. Bourke, Los Alamos National Laboratory, Neutron Science Center, Los Alamos, NM 87545 USA; Darrel R. Frear, Motorola, Tempe, AZ 85284 USA; John E. Sanchez, Advanced Micro Devices, Sunnyvale, CA 94088 USA

Tuesday AM	Room: 2	209B
March 16, 2004	Location:	Charlotte Convention Center

Session Chairs: J. W. Morris, University of California, Berkeley, CA 94720 USA; J. C.M. Li, University of Rochester, Rochester, NY 14627 USA

#### 8:30 AM Keynote

Creep Resistance of the Directionally Solidified Ceramic Eutectic of Al2o3/C-Zro2 (Y2O3): Experiments and Models: A. S. Argon<sup>1</sup>; J. Yi<sup>1</sup>; <sup>1</sup>Massachusetts Institute of Technology, Cambridge, MA 02139 USA

The creep resistance of the directionally solidified (DS) ceramic eutectic of Al2O3/c-ZrO2 (Y2O3) was studied in the temperature range of 1200-1520°C both experimentally and by mechanistic dislocation models. The topologically continuous majority phase of Al2O3, has a nearly perfect growth texture in the [0001] direction and encapsulates the minority c-ZrO2 phase in a variety of morphologies. This encapsulated minority phase too has a <112> growth texture regardless of morphology. The two phases are separated by close to coherent and well structured interfaces. Upon growth, there are substantial levels of internal thermal misfit stresses present between the alumina and cubiczirconia phases in the GPa range. The creep of the eutectic in its growth direction exhibits an initial transient that is attributed to stress relaxation in the c-ZrO2 phase that also substantially eliminates the initial thermal misfit stresses. The steady state creep shows many of the same characteristics of creep in sapphire single crystals with c-axis orientation. The creep strain rate of the eutectic has stress exponents in the range of 4.5-5.0 and a temperature dependence suggesting a rate mechanism governed by oxygen ion diffusion in the Al2O3. Finite element analysis of stress distribution in the two phases under an applied tensile stress parallel to the axis, and a detailed dislocation model of the creep rate indicate that much of the nano-scale encapsulated c-ZrO2 must be too small to deform by dislocation creep so that the major contribution to the recorded creep strain is derived from the diffusion-controlled climb of pyramidal edge dislocations in the Al2O3 phase. The evidence suggests that these climbing dislocations must repeatedly circumvent the nano-scale cubic zirconia domains acting as dispersoids. This is equivalent to the presence of a sinusoidally varying set of internal stresses through which the climbing dislocations must negotiate, resulting in the stress exponents larger than 3. The creep model is in very good agreement with the experiments, and demonstrates that the DS eutectics have creep resistance superior to that of sapphire. Work supported by AFOSR under Grant F49620-99-1-0276.

#### 9:00 AM Invited

Development of Internal Stresses in Thermal Barrier Coatings as a Result of Bond Coat Plasticity and Phase Transformations: *Kevin J. Hemker*<sup>1</sup>; <sup>1</sup>Johns Hopkins University, Depts. of Mech. Engrg. & Matls. Sci. & Engrg., 3400 N. Charles St., Baltimore, MD 21218 USA

Thermal barrier coatings (TBCs) are widely used in commercial gas turbine engines to insulate the metallic components from the hot gas stream. TBCs are complex multilayered systems with a ceramic top coat, thermally grown oxide (TGO), intermetallic bond coat and superalloy substrate. The top coat is the insulator, the TGO slows oxidation, the bond coat provides a reservoir for the formation of the TGO and improved adherence and the substrate carries the loads. During thermal cycling, the interaction of these chemically and mechanically disparate layers results in the development of internal stresses, which lead to eventual spallation of the topcoat. Differences in thermal expansion, continued growth of the TGO, and deformation of the bond coat have been shown to result in interface rumpling. The elevated temperature bond coat properties have been measured with microsample tensile and creep testing. Moreover, observations of a martensitic transformation in the platinum modified nickel aluminide bond coat have been associated with inter-diffusion between the bond coat and the underlying superalloy substrate. TEM observations, differential thermal analysis and in situ X-ray diffraction experiments have been used to characterize the martensitic transformation, and results of FE simulations that incorporate these measurements point to the importance of this transformation in the generation of residual stresses in the TBC during thermal cycling.

#### 9:25 AM

Measurement and Modeling of Internal Stresses During Creep of a Polycrystalline Superalloy: S. Ma<sup>1</sup>; P. Rangaswamy<sup>2</sup>; Don W. Brown<sup>2</sup>; B. S. Majumdar<sup>1</sup>; <sup>1</sup>New Mexico Tech, Matls. Dept., Socorro, NM 87801 USA; <sup>2</sup>Los Alamos National Laboratory, Los Alamos, NM USA

The high temperature deformation and failure of superalloys containing a high volume fraction of gamma-prime phase are significantly influenced by the evolution of internal stresses in the gamma and gammaprime phases. During most of the creep life, deformation is confined to the very narrow gamma channels. We have conducted insitu creep experiments using a pulsed neutron source to monitor elastic micro-strain evolution in a high-volume fraction superalloy. FEM modeling showed that the redistribution of stress of the individual phases are only modest, in slight disagreement with previous work . Neutron diffraction data showed that in the tertiary stage there was a rapid build up of stresses in the gammaprime phase, but a substantial reduction in those of the gamma phase. We believe that the observed stress redistribution is caused by geometrically necessary dislocations, which induce stresses unaccounted for in FEM modeling. Results are complemented with TEM observations of interface dislocations.

#### 9:50 AM

In Situ Oxide Growth Strains in a FeCrAIY Alloy: Geoffrey A. Swift<sup>1</sup>; Ersan Ustundag<sup>1</sup>; Jonathan D. Almer<sup>2</sup>; David R. Clarke<sup>3</sup>; <sup>1</sup>California Institute of Technology, Dept. of Matls. Sci., Pasadena, CA 91125 USA; <sup>2</sup>Argonne National Laboratory, Advd. Photon Source, Argonne, IL 60439 USA; <sup>3</sup>University of California, Matls. Dept., Santa Barbara, CA 93106 USA

FeCrAlY alloys are known to form a uniform, adherent scale of ¥á-Al2O3 when oxidized and are good model systems for the investigation of residual stresses due to the formation of thermally grown oxide (TGO) layers in a typical thermal barrier coating (TBC) system. In this study, high energy synchrotron X-rays were used to monitor in situ the oxidation of a cylindrical FeCrAlY sample around 800-1200°C. Oxide growth strains at constant temperature were seen to be small suggesting dynamic stress relaxation via creep. Upon cooling to room temperature, however, large compressive stresses (several GPa) were generated in the oxide due to the thermal contraction mismatch between the oxide and the FeCrAlY substrate. Strain data obtained from XRD will be compared to luminescence measurements and predictions of several models.

# 10:15 AM Invited

**Constitutive Equations for High Temperature Deformation**: *J. W. Morris*<sup>1</sup>; H. G. Song<sup>1</sup>; W. H. Bang<sup>2</sup>; K. H. Oh<sup>1</sup>; <sup>1</sup>University of California, Dept. of Matls. Sci. & Engrg., Berkeley, CA 94720 USA; <sup>2</sup>Seoul National University, Dept. of Matls. Sci. & Engrg., Seoul Korea

It has long been recognized that steady-state creep rates in the multiphase materials used for solders and other purposes are well described by simple constitutive equations of the Dorn (power law) or, alternatively, Garafalo (hyperbolic sign) forms. Recent research has led to the useful result that these same equations often provide equally good predictions of shear strength and stress relaxation rates at elevated temperature. The present talk will discuss data taken from work by a number of investigators that documents the similarity of the stress-strain rate-temperature relations that pertain to steady state creep, shear strength and stress relaxation and will show specifically how the parameters that appear in the Dorn equation govern the rate and temperature dependence of the shear strength and the rate of stress relaxation.

#### 10:40 AM Invited

Stress Induced Phase Transformation in Uranium-Niobium Shape Memory Alloys: *Donald W. Brown*<sup>1</sup>; Mark A.M. Bourke<sup>1</sup>; Robert D. Field<sup>1</sup>; W. Larry Hults<sup>1</sup>; David F. Teter<sup>1</sup>; Daniel J. Thoma<sup>1</sup>; <sup>1</sup>Los Alamos National Laboratory, Matls. Sci. & Tech. Div., MS-H805, Bldg. 622, TA-53, Los Alamos, NM 87545 USA The shape memory effect (SME) has been reported in the uraniumniobium alloy system in the region of the phase diagram surrounding U6.5wt%Nb. In this regime, the material may have either an  $\alpha$ " monoclinic (U6Nb) or  $\gamma 0$  tetragonal structure (U7Nb) and is two phase near 6.5wt% niobium. In-situ neutron diffraction loading studies have revealed a stress induced phase transformation in U7wt%Nb from the  $\gamma 0$ to the  $\alpha$ " structure. The volume fraction of the  $\gamma 0$  phase decreased nearly linearly with plastic strain from 100% initially to ~25% after 3% plastic deformation and some reversion is observed on release. The initial stress state of the stress induced  $\alpha$ " grains will be discussed as well as the load sharing between the two phases.

#### 11:05 AM

Investigation of Silicon Nitride Creep Using Neutron Diffraction: Geoffrey A. Swift<sup>1</sup>; Ersan Ustundag<sup>1</sup>; Bjørn Clausen<sup>2</sup>; Mark A.M. Bourke<sup>2</sup>; <sup>1</sup>California Institute of Technology, Dept. of Matls. Sci., Pasadena, CA 91125 USA; <sup>2</sup>Los Alamos National Laboratory, Neutron Sci. Ctr., Los Alamos, NM 87545 USA

The deep penetration of neutrons in most materials allows in-situ studies in extreme environments. This advantage of neutron diffraction was utilized in the investigation of strain and texture evolution during high temperature deformation of in-situ reinforced Si3N4. Tension experiments were performed in the 1100°C-1400°C temperature regime using the new SMARTS diffractometer at Los Alamos Neutron Science Center. In particular, the hkl-dependent strains were measured and the results were compared to literature data. Evidence of grain boundary sliding was observed when diffraction data (i.e., elastic lattice strains) were compared to macroscopic strains collected by an extensometer.

# International Laterite Nickel Symposium - 2004: Pressure Acid Leaching

Sponsored by: Extraction & Processing Division, EPD-Aqueous Processing Committee, EPD-Copper, Nickel, Cobalt Committee, EPD-Process Fundamentals Committee, EPD-Process Mineralogy Committee, EPD-Pyrometallurgy Committee, EPD-Waste Treatment & Minimization Committee

Program Organizer: William P. Imrie, Bechtel Corporation, Mining and Metals, Englewood, CO 80111 USA

Tuesday AM	Room: 2	17B/C		
March 16, 2004	Location:	Charlotte	Convention	Center

Session Chairs: Roman M. Berezowsky, Dynatec Corporation, Metallurgical Technologies, Ft. Saskatchewan, Alberta T8L 4K7 Canada; Ian G. Skepper, BHP-Billiton, Ravensthorpe Nickel Project, Perth, WA 6850 Australia

#### 8:30 AM

**Co-Treatment of Limonitic Laterites and Sulfur-Bearing Materials as an Alternative to the HPAL Process**: *Cesar Joe Ferron*<sup>1</sup>; Larry Seeley<sup>1</sup>; Christopher A. Fleming<sup>1</sup>; <sup>1</sup>SGS Lakefield Research Limited, Metallurgl. Tech., 185 Concession St., PO Box 4300, Lakefield, Ontario K0L 2H0 Canada

High pressure acid leaching (HPAL) is used in four plants to treat limonitic laterites. Two major operating cost components are sulphuric acid and energy to heat the feed slurry. As an alternative to acid injection and steam heating, in-situ generation of sulphuric acid and heat from oxidation of sulfur-bearing materials blended with laterites, has been investigated at laboratory scale. Tested sulfur sources have included elemental sulfur, pyrrhotite, and nickel sulphide concentrates. At proper blend ratios, all sulfur sources generated sufficient acid to provide efficient dissolution of nickel and cobalt from both the host sulphide and the laterite. Significant improvement to the economics result from the use of sulfur sources containing valuable by-products, such as nickel/cobalt and/or precious metals (gold and PGMs). In the latter case, the HPAL must be operated under Platsol conditions (i.e. with the addition of 5-10 g/L of chloride) to ensure efficient recovery of the precious metals. Application examples for this concept are presented with discussion of its implication on autoclave design and downstream processes to recover values from leach solution.

#### 8:55 AM

Effect of Process Water on High Pressure Sulphuric Acid Leaching of Laterite Ores: *Debbie Marshall*<sup>1</sup>; Mohamed Buarzaiga<sup>1</sup>; <sup>1</sup>Noranda Inc./Falconbridge Ltd., Metallurgl. Tech. Grp., Falconbridge Tech. Ctr., Falconbridge, Ontario POM 1S0 Canada Process water is an important consideration in the development of a nickel lateritic project. Depending on the location of the ore body, sufficient fresh water may not be available and it may be necessary to use seawater (or saline groundwater) for ore preparation. This introduces various species, which have major effects on materials of construction and leaching chemistry. This paper summarizes batch testwork completed at the Falconbridge Technology Center. The leaching behavior of eleven different laterite ore samples was compared using seawater and fresh water. Each ore type was leached under identical conditions in both freshwater and seawater and the leaching chemistry was compared. The batch scale results were confirmed in a continuous pilot plant and leach kinetics for the two systems compared.

#### 9:20 AM

Effect of Eh in the High Pressure Acid Leaching of Nickel Laterite Ores: Julian Andrew Johnson<sup>1</sup>; Barry Ian Whittington<sup>1</sup>; Robbie Gordon McDonald<sup>1</sup>; David Michael Muir<sup>1</sup>; <sup>1</sup>AJ Parker CRC for Hydrometallurgy, CSIRO Minerals, PO Box 90, Bentley, WA 6892 Australia

The effect of changing redox potential on the high temperature sulfuric acid leaching of Western Australian dry-land nickel laterite ores has been investigated. In particular, the effect of added reductant (sulfur, sodium sulfite) or oxidant (potassium chromate) on Eh, leaching kinetics, metal extractions, acid utilisation and leach residues has been determined. Three separate ores - nontronitic ores from Murrin Murrin and Bulong, and limonitic ore from Cawse - were used in the study. Sulfur addition varied from 0 to 7.8 kg/t ore. The total acid loading was kept constant at 430 kg/t (Murrin Murrin ore) and 330 kg/ t (Cawse ore), whilst acid loading for Bulong ore was varied according to the presence of either reductant or oxidant. The extraction of both nickel and cobalt from limonite ore remained unaffected when small amounts of sulfur were added, but addition of even small amounts of reductant to nontronitic ore decreased both nickel and cobalt extraction. Increased manganese and iron dissolution were observed as the levels of reductant increased, accompanied by a decrease in chromium dissolution. As the iron dissolution increased, free acidity decreased, with a subsequent decrease in nickel extraction. In contrast, addition of oxidant lead to reduced iron and manganese dissolution and slower extraction of nickel and cobalt.

#### 9:45 AM

Solution Chemistry and Reactor Modeling of the PAL Process: Successes and Challenges: Vladimiros G. Papangelakis<sup>1</sup>; Haixia Liu<sup>1</sup>; Dmitri Rubisov<sup>1</sup>; <sup>1</sup>University of Toronto, Chem. Engrg. & Applied Chmst., 200 College St., Toronto, Ontario M5S 3E5 Canada

During the past five years, chemical modelling work at the University of Toronto has elucidated the role of soluble magnesium in the PAL process. It explained why feeds rich in magnesium, and other divalent metals, require more than the stoichiometric requirements for acid dissolution to ensure comparable Ni/Co leaching performance as with feeds low in magnesium and other divalents. This understanding has allowed the calculation of acid additions on a less empirical basis. Optimizing acid additions confers savings in neutralization costs, ensures high productivity and minimises unnecessary corrosion problems. Some theoretical concepts of chemical modelling of electrolyte systems at high temperature and software issues in support of this work are presented. Autoclave modelling based on better chemistry understanding and comparisons with pilot-plant data is also made. Finally, in spite of the above successes significant challenges lie ahead in theoretical data gaps and instrumentation, which are discussed.

#### 10:10 AM Break

#### 10:20 AM

Effect of Magnesium Content on Sulphuric Acid Consumption During High Pressure Acid Leaching of Laterite Ores: *Debbie* Marshall<sup>1</sup>; Mohamed Buarzaiga<sup>1</sup>; <sup>1</sup>Noranda Inc./Falconbridge Ltd., Metallurgl. Tech. Grp., Falconbridge Tech. Ctr., Falconbridge, Ontario POM 1S0 Canada

Nickel and cobalt in lateritic ores can be extracted by either a hydrometallurgical or a pyrometallurgical route. The high-iron limonitic fraction of a deposit is best processed hydrometallurgically while the magnesium-rich transitional and saprolitic fractions are more suited for pyrometallurgical processing. During hydrometallurgical processing, it may be attractive, for economic reasons, to blend the limonitic component with transitional and saprolitic ores, which contain higher nickel levels. However, blending increases the concentration of magnesium in the feed, leading to increased acid demands. The decision on how much ore to process then becomes an economic one. Ore samples with different magnesium contents were prepared for the leach test program by blending limonitic and transitional ores. The ore samples were slurried in seawater and tested in the Falconbridge Hydrometallurgical Pilot Plant. As expected, acid consumption increased with increasing magnesium content of the ore. For target extractions of 95% nickel and 92% cobalt, the required residual free acid concentration increased from 30 g/L at 1.7% magnesium to 50 g/L at 2.7% magnesium. When the magnesium content was raised to 3.8% and 4.6% in subsequent pilot plant testing, the final free acid requirements did not increase beyond what was observed at 2.7% magnesium. Thus, the cutoff ore composition to maximize nickel units and minimize acid requirements is between 1.7- 2.7% magnesium.

#### 10:45 AM

#### A Conceptual Design of PAL Using Tube-in-Tube Heat Exchangers: Don J. Donaldson<sup>1</sup>; <sup>1</sup>APTEC, 2314 Quail Point Cir., Medford, OR 97504 USA

The PAL process for recovering nickel from laterite ore requires large volumes of thick abrasive slurry to be raised to high temperature  $(255^{\circ}C +)$  and pressure (50 atm.+). Flow diagrams of the process typically result in facilities that have serious operating and reliability problems. Most of the problems can be attributed to using multiple pump stations to raise the slurry to autoclave pressure, large amounts of flash and live injection steam to heat the slurry to autoclave temperature, and several steps of flash cooling to lower the temperature and pressure of the abrasive autoclave slurry down to atmospheric conditions. It is proposed that operating and reliability problems of PAL facilities can be mitigated by using Tube-in-tube heat exchangers and "float type" positive displacement pumps. The subject paper describes an innovative application of such equipment in the facility design of the PAL process.

#### 11:10 AM

Improvements to the Acid Pressure Leaching of Nickel Laterite Ores: Walter Curlook<sup>1</sup>; <sup>1</sup>University of Toronto, Matls. Sci. & Engrg., 184 College St., Toronto, ON M5S 3E4 Canada

An improved process of hydrometallurgical treatment of laterite ores of the limonitic type for the recovery of nickel and cobalt using sulphuric acid has been developed and patented. The major improvement is brought about by recycling a significant portion of the "mother liquor" emanating from the pressure leaching reaction back to the feed preparation stage thereby substituting for all or at least a major proportion of the fresh water or de-ionized water that must be added. Concomitantly with the major savings in fresh water or de-ionized water requirements, a significant reduction in new sulphuric acid requirements is effected along with a corresponding saving in limestone and lime required for subsequent neutralizations.

#### 11:35 AM

#### **Cosimulation in Hydromet Process Design**: Lanre Oshinowo<sup>1</sup>; Ida Fok<sup>1</sup>; <sup>1</sup>Hatch Associates Ltd., 2800 Speakman Dr., Mississauga, Ontario L6X 4R8 Canada

Computational Fluid Dynamics (CFD) is used in complement with process modelling at HATCH to achieve a superior level of confidence in the process design of hydromet process plants. The use of these tools to evaluate designs through virtual prototyping reduces the risks associated with making design decisions. This paper highlights the development of a cosimulation strategy at Hatch for the seamless integration of process modeling software addressing different scales (process time and space): flowsheet level models and equipment level models. With cosimulation, the process design engineers can improve design accuracy, troubleshoot and optimize the performance, and influence decisions impacting equipment operation by representing specific unit operations in the flowsheet model software with detailed CFD models. Specifically, this paper will focus on the co-simulation of a Ni/Co high-pressure acid leach (HPAL) process including heaters/ heat exchangers and flash system, autoclave and quench/scrubber system. The knowledge developed can be transferable to other processes.

# Lead-Free Solders and Processing Issues Relevant to Microelectronic Packaging: Mechanical Properties and Fatique Behavior

*Sponsored by:* Electronic, Magnetic & Photonic Materials Division, EMPMD-Electronic Packaging and Interconnection Materials Committee

Program Organizers: Laura J. Turbini, University of Toronto, Center for Microelectronic Assembly & Packaging, Toronto, ON M5S 3E4 Canada; Srinivas Chada, Jabil Circuit, Inc., FAR Lab/ Advanced Manufacturing Technology, St. Petersburg, FL 33716 USA; Sung K. Kang, IBM, T. J. Watson Research Center, Yorktown Heights, NY 10598 USA; Kwang-Lung Lin, National Cheng Kung University, Department of Materials Science and Engineering, Tainan 70101 Taiwan; Michael R. Notis, Lehigh University, Department of Materials Science and Engineering, Bethlehem, PA 18015 USA; Jin Yu, Korea Advanced Institute of Science and Technology, Center for Electronic Packaging Materials, Department of Materials Science & Engineering, Daejeon 305-701 Korea

Tuesday AM	Room: 2	19B
March 16, 2004	Location:	Charlotte Convention Center

Session Chairs: James P. Lucas, Michigan State University, Dept. of Chem. Engrg. & Matls. Sci., E. Lansing, MI 48824-1226 USA; Kwang-Lung Lin, National Cheng Kung University, Dept. of Matls. Sci. & Engrg., Tainan 70101 Taiwan

#### 8:30 AM Invited

Roles of Service and Material Parameters on TMF of Sn-Based Solder Joints: H. Rhee<sup>1</sup>; J. G. Lee<sup>1</sup>; K. N. Subramanian<sup>1</sup>; <sup>1</sup>Michigan State University, Dept. of Chem. Engrg. & Matls. Sci., E. Lansing, MI 48824-1226 USA

Temperature extremes, differences in temperature, rates at which such temperature changes are imposed, and dwell times at the temperature extremes are service related parameters that can have significant effects on thermomechanical fatigue (TMF). Solder alloy, interfacial intermetallic layer and its thickness, and microstructural constituents within the solder joint, are material related parameters that contribute to TMF of a solder joint. This investigation examines the roles of these parameters and their relative importance on TMF by carrying out studies on Sn-based solder joints of realistic dimensions. Such studies include actual TMF cycling, and supporting studies under isothermal conditions. Work supported by the National Science Foundation under grant NSF DMR-0081796.

#### 8:55 AM

The Interfacial Adhesion Strength of the Sn-9Zn-xAg Lead-Free Solders Wetted on Cu Substrate After Thermal Shock Testing: *Tao-Chih Chang*<sup>1</sup>; <sup>1</sup>National Cheng Kung University, Dept. of Matls. Sci. & Engrg., 1 Ta-Hsueh Rd., Tainan 70101 Taiwan

In this study, the interfacial adhesion strength of the Sn-9Zn-xAg lead-free solders wetted on Cu substrate after thermal shock testing have been investigated by pull-off testing, scanning electron microscopy and energy dispersive spectrometry. The 63Sn-37Pb and Sn-3.5Ag solder alloys were tested for comparison. The Sn-3.5Ag solder alloy offers a more superior solder joint reliability than the others, the adhesion strength of the Sn-3.5Ag/Cu interface increases from 18.04  $\pm$ 1.03 to 21.75  $\pm$  1.25 MPa after 5 times thermal shock. But it decrease slightly from 21.75  $\pm$  1.25 to 18.47  $\pm$  0.98 MPa with increasing the thermal shock times from 5 to 10. After 15 thermal shock testing, it increases again to  $20.94 \pm 1.12$  MPa. The adhesion strength of the Sn-9Zn-xAg/Cu interface has a similar tendency to that of the Sn-3.5Ag/ Cu interface. A maximum value of  $14.60 \pm 0.82$  MPa is obtained for the Sn-9Zn-2.5Ag/Cu interface after 5 thermal shock testing. The 63Sn-37Pb solder alloy has a most inferior solder joint reliability in this test.

## 9:15 AM

Study of Pasty Zone and Latent Heat Release Mode for Sn-9ZnxAg Lead-Free Solder Alloys: *Ying-Ling Tsai*<sup>1</sup>; Weng-Sing Hwang<sup>1</sup>; 'National Cheng Kung University, Dept. of Matls. Sci. & Engrg., Tainan Taiwan

The pasty ranges and latent heat release modes of Sn-9Zn-xAg alloys, where x varies between 0.5 and 3.5, are measured in this study. The effects of alloy composition and cooling rate on the pasty range and latent heat release mode are also discussed. A Computer Aided-Cooling Curve Analysis (CA-CCA) technique is used to measure and

calculate the pasty ranges and latent heat release modes for Sn-9ZnxAg lead-free solder alloys. To comply with the requirements of CA-CCA, the experimental setup has to approach the heat transfer condition of a lumped system, where the alloy system is cooled down in a uniform fashion. Two thermocouples are inserted in a cylindrical crucible, where alloy is melted and subsequently cooled to solidify. The crucible is used with and without the wrappage of insulating material to obtain different cooling rates. The temperature readings show that the heat transfer condition in the experimental setup in this study indeed meets the requirement of a lumped system. The fraction of solid versus temperature relations; fs-T, for the various alloy compositions and cooling rates are then obtained from the temperature data analyzed by CA-CCA. The experimental results also shows that as silver content of the Sn-9Zn-xAg alloy increases, the pasty range also increases. As silver content is 0.5 wt%, silver has little effect on the microstructure, which is basically the Sn-9Zn eutectic phase. The fs-T relation is somewhat close to a vertical line. However, as silver content exceeds 1.5 wt%, the formation of intermetallic compound; AgZn3, becomes obvious. It causes the alloy composition to deviate from the eutectic composition and leans towards the tin side of the Sn-Zn phase diagram. This in turn causes the content of primary tin phase to increase and that of zinc-tin eutectic phase to decrease. It reflects on the fs-T relation by two distinct vertical lines. One corresponds to the primary tin phase and the other to the eutectic phase. As silver content increases, the effects of the intermetallic compound formation become even more obvious. Cooling rate shows no significant effect on either pasty range or fs-T relation. However, smaller cooling rate results in lower solidus temperature as well as liquidus temperature.

#### 9:35 AM

Effect of Cooling Rate on IMC and Mechanical Properties of Sn-Ag-Cu/Cu Pad: Sang Won Jeong<sup>1</sup>; Jong Hoon Kim<sup>1</sup>; *Hyuck Mo Lee*<sup>1</sup>; <sup>1</sup>KAIST, Dept. of Matls. Sci. & Engrg., 373-1 Kusung-dong, Yusung-gu, Taejon 305-701 Korea

Several solders of Sn-3.5Ag, Sn-3Ag-0.7Cu, Sn-3Ag-1.5Cu, Sn-3.9Ag-0.8Cu and Sn-6Ag-0.5Cu were cooled at different rates after reflow soldering on Cu pad above 250°C for 60s. Three different media of cooling were used to control cooling rates; water quenching, medium cooling on aluminum block and slow cooling in furnace. The resultant morphology of the interfacial intermetallic compound (IMC) of the samples was observed together with the lap shear strength of the joint measured. As content of Cu and Ag in solder alloys was increased, the thickness of the interfacial IMC increased and there was a change in phases of the IMC. With a slower cooling rate, the interfacial IMC became thicker and coarsened. At the same time, the lap shear joint showed lower shear strength and was fractured in a brittle mode between Cu6Sn5 and Cu3Sn phases. The microstructural observation agreed well with mechanical properties and a variation in the fracture mode.

#### 9:55 AM

Mechanical Properties of Near-Eutectic Sn-Ag-Cu Alloy Over a Wide Range of Temperatures and Strain Rates: *Tia-Marje K. Korhonen*<sup>1</sup>; Pekka Turpeinen<sup>1</sup>; Brian Bowman<sup>1</sup>; Larry P. Lehman<sup>2</sup>; George H. Thiel<sup>3</sup>; Raymond C. Parkes<sup>3</sup>; Matt A. Korhonen<sup>1</sup>; Donald W. Henderson<sup>3</sup>; Karl J. Puttlitz<sup>4</sup>; <sup>1</sup>Cornell University, Matls. Sci. & Engrg., 328T Bard Hall, Ithaca, NY 14853 USA; <sup>2</sup>Binghamton University, Binghamton, NY 13902 USA; <sup>3</sup>IBM Corporation, 1701 North St., Endicott, NY 13760 USA; <sup>4</sup>IBM Corporation, Hopewell Junction, NY 12533 USA

Creep tests, constant strain rates tests, and stress relaxation tests were used to measure the deformation properties of Sn-Ag-Cu alloy in temperatures ranging from -40 to 125°C. The three testing methods complement each other, because the creep and constant strain rate tests give the steady state properties, while stress relaxation tests reflect the properties at constant structure. Several different strain rates were used, down to 10E-9. The measurements were done with dob-bone specimens that have a cross section of 1mm, which corresponds to a typical solder joint diameter in ball grid arrays. Cooling rates of the samples were selected to be comparable to ones used in BGA manufacturing. It was shown that the mechanical properties are very different from slowly cooled bulk solders. The strain rate sensitivity of the fast cooled samples was very low. The effect of temperature was also small, the activation energy was about 0.4 eV. Optical microscopy, SEM and electron back-scatter diffraction were used to study the microstructures of the test samples. The slower cooled samples had large Ag3Sn platelets, but size of the platelets was significantly reduced with faster cooling rates. This was clearly reflected in the deformation behavior of the samples.

## 10:15 AM Break

#### 10:25 AM Invited

Influence of Interfacial Intermetallic Compounds on Mechanical Properties of Thin Pb-Free Solder Joints: J. G. Lee<sup>1</sup>; H. Rhee<sup>1</sup>; J. P. Lucas<sup>1</sup>; K. N. Subramanian<sup>1</sup>; T. R. Bieler<sup>1</sup>; <sup>1</sup>Michigan State University, Dept. of Chem. Engrg. & Matls. Sci., E. Lansing, MI 48824-1226 USA

Miniaturization of electronic packaging requires the same trends of the solder joints that electrically and mechanically connect components to particular substrates. As solder joints become thinner, concurrently, the extent of the substrate/solder interfacial intermetallic compound (IMC) layer increases in comparison to the overall solder volume of the joint. Moreover, as a result of isothermal or thermomechanical aging, the IMC layer can grow to such an extent that it may comprise 80-90% of the solder joint volume. Nanoindentation testing (NIT) will be used to investigate the mechanical properties of IMCs formed in thin (< 50 micron) solder joints. Various Sn-based eutectic and near-eutectic Pb-free solder alloys will be used. Creep studies will also be performed on as-reflow and aged solder joints to determine the influence of IMC layer thickness and evolving compositional change from predominately Cu<sub>6</sub>Sn<sub>5</sub> to Cu<sub>3</sub>Sn. This investigation reports on growth of the IMC layer in thin solder joints and the propensity of the IMC layer to affect subsequent mechanical properties.

## 10:50 AM

Advances in Producing Adaptive Lead-Free Solder Joints Via Shape-Memory Alloy Reinforcement of Solder Alloys: Deng Pan<sup>1</sup>; W. Scott Horton<sup>1</sup>; William Wright<sup>1</sup>; Zhixiang Wang<sup>2</sup>; B. S. Majumdar<sup>2</sup>; Indranath Dutta<sup>1</sup>; <sup>1</sup>Naval Postgraduate School, Mech. Engrg., 700 Dyer Rd., Monterey, CA 93943 USA; <sup>2</sup>New Mexico Tech, Matls. Sci. & Engrg., Socorro, NM 87801 USA

Microelectronic solder joints are typically exposed to aggressive thermo-mechanical cycling (TMC) conditions during service. During TMC, strain localization occurs near solder/bond pad interfaces, where large inelastic shear strains accumulate, eventually causing low-cycle fatigue failure of the joint. In this study, a new methodology to mitigate the effects of strain localization within the joint are discussed, wherein the solder alloy is reinforced with Ni-Ti based shape memory alloy (SMA) powders are used to reinforce a Sn-4.7%Ag-1%Cu solder. Details of processing and characterization of the solder composite will be discussed, particularly with respect to the particle size and distribution, and interfacial structure and chemistry. Ball-shaped solder joints between copper rods simulating flip chip (FC) or ball-grid array (BGA) joints were tested in shear under thermal mechanical cycling conditions. The behavior of the composite is compared with that of unreinforced solder and solder reinforced by copper particles to elucidate the impact of the shape-memory effect on the overall joint behavior. Experiments on model single-fiber NiTi-solder composites to provide insight into the mechanics of deformation of smart solders are also reported.

#### 11:10 AM

Comparison of 95.5Sn-3.8Ag-0.7Cu Solder Joint and Bulk Solder Properties: John H.L. Pang<sup>1</sup>; <sup>1</sup>Nanyang Technological University, Sch. of Mech. & Production Engrg., 50 Nanyang Ave. 639798 Singapore

Mechanical properties for lead-free 95.5Sn-3.8Ag-0.7Cu solder joint and bulk solder will be presented. A soldered lap shear joint specimen was used for characterizing the microstructure and mechanical properties of the solder joint. The specimens were soldered using 95.5Sn-3.8Ag-0.7Cu solder sphere with no-clean flux on FR-4 substrates by solder reflow process. Three solder reflow peak temperatures at 235°C, 240°C and 250°C were investigated. The average solder joint shear force were 4.1N, 4.8N and 5.0N respectively. Shear tests were carried out at three temperatures ( $25^{\circ}$ C,  $75^{\circ}$ C and  $125^{\circ}$ C) and at three constant strain rate ( $2.6 \times 10E-2$ ,  $2.6 \times 10E-3$  and  $2.6 \times 10E-4$ ) conditions. The stress strain properties in shear were converted to equivalent tensile stress strain values for comparison to tensile test results on 95.5Sn-3.8Ag-0.7Cu bulk solder. The apparent tensile modulus, yield stress and ultimate tensile stress will be presented as a function of temperature and strain rate.

#### 11:30 AM

Analysis of Deformation and Damage in Solder Joints During Lap Shear Tests: E. S. Ege<sup>1</sup>; X. Deng<sup>2</sup>; *Y.-L. Shen*<sup>1</sup>; N. Chawla<sup>2</sup>; <sup>1</sup>University of New Mexico, Mech. Engrg., MSC01 1150, Albuquerque, NM 87131 USA; <sup>2</sup>Arizona State University, Chem. & Matls. Engrg., Tempe, AZ 85287 USA

Thermomechanical testing of solder using the lap shear technique is commonly employed to quantify the shear stress-strain and fatigue behavior. In this study the effects of geometric and material parameters on the monotonic and cyclic mechanical response are evaluated in detail using numerical finite element analyses. Lap shear experimental results are compared with the modeling. The commonly observed cracking in solder near, but not at, the interface between solder and intermetallic can be explained by the development of plastic flow pattern during cyclic loading. It is also found that the conventional method for determining the nominal shear strain in solder is prone to large errors. The solder joint carries a smaller strain than that based on the far-field value, as confirmed by experiments. This is largely due to the delayed transmission of deformation from the substrate to the solder before solder fully yields plastically. Thicker, shorter, and stiffer substrates are shown to generate more accurate results. Other implications to practical characterizations and evaluations of solder properties are discussed.

# 11:50 AM

Segregation and Coarsening Effects on Mechanical Properties in Aged Tin-Silver-Copper Solder Joints: *Iver Eric Anderson*<sup>1</sup>; Joel L. Harringa<sup>2</sup>; Bruce A. Cook<sup>3</sup>; <sup>1</sup>Ames Laboratory (USDOE), Metal & Ceram. Scis. Prog., 222 Metals Dvlp. Bldg., Ames, IA 50011 USA; <sup>2</sup>Ames Lab (USDOE), Metal & Ceram. Scis. Prog., 252 Spedding Hall, Ames, IA 50011 USA; <sup>3</sup>Ames Lab (USDOE), Metal & Ceram. Scis. Prog., 47 Wilhelm Hall, Ames, IA 50011 USA

Since many new electronic assembly applications involve service at high temperature and stress levels a thorough investigation of promising Sn-Ag-Cu solder alloys is required to relate microstructural changes on high temperature aging to mechanical properties and fracture behavior. This effort has involved detailed characterization of solder joint microstructures, resistivity, and shear strength after isothermal aging at  $150^{\circ}$ C for time intervals out to 1,000 hrs. Elemental Cu substrates were joined with near eutectic Sn-Ag-Cu and Sn-Ag-Cu-X (X = Co, Fe) solder alloys for the study. Microanalytical electron probes were used to track phase coarsening and to determine the role of local segregation on embrittlement and partial debonding after extensive aging of joints, especially those lacking Co and Fe additions. Project funding received from Iowa State University Research Foundation with additional support from USDOE-BES through contract no.W-7405-Eng-82.

# Magnesium Technology 2004: Wrought Magnesium Alloys II/Corrosion and Coatings

Sponsored by: Light Metals Division, LMD-Magnesium Committee Program Organizer: Alan A. Luo, General Motors, Materials and Processes Laboratory, Warren, MI 48090-9055 USA

Tuesday AM	Room: 203B	
March 16, 2004	Location: Ch	arlotte Convention Center

Session Chairs: Xin Wu, Wayne State University, Detroit, MI 48202 USA; Eric Nyberg, Pacific Northwest National Laboratory, Richland, WA 99352 USA

# 8:30 AM

Infrared Processing of Magnesium Wrought Alloys: Joe A. Horton<sup>1</sup>; Sean R. Agnew<sup>2</sup>; Craig A. Blue<sup>3</sup>; <sup>1</sup>Oak Ridge National Laboratory, Metals & Ceram. Div., Bldg. 4500S, MS6115, PO Box 2008, Oak Ridge, TN 37831-6115 USA; <sup>2</sup>University of Virginia, Matls. Sci & Engrg., 116 Engineer's Way, Charlottesville, VA 22904-4745 USA; <sup>3</sup>Oak Ridge National Laboratory, Metals & Ceram. Div., Bldg. 4508, MS6083, PO Box 2008, Oak Ridge, TN 37831-6083 USA

It is of interest to produce magnesium wrought products more efficiently in order to make them more attractive for application. Previous studies have shown that heat treatments performed using radiant heating by plasma arc lamp can produce the same result in seconds as one hour anneals at 400C in a convection furnace. The influence of infrared radiant heating on the deformation processing of magnesium will be presented. Metallurgical structure and mechanical property measurements are used to compare with traditional processing. (Research sponsored by the U.S. Dept. of Energy, Assistant Secretary for Energy Efficiency and Renewable Energy, Office of Transportation Technology, Office of Heavy Vehicle Technology, at Oak Ridge National Laboratory, operated by UT-Battelle, LLC, under contract DE-AC04-000R22725.)

#### 8:50 AM

Superplasticity in Fine-Grained Mg-Zn-Y-(Zr) Alloy Sheets In-Situ Reinforced by Icosahedral Quasicrystalline Particles: D. H. Bae<sup>1</sup>; Y. Kim<sup>1</sup>; D. S. Kim<sup>1</sup>; I. J. Kim<sup>1</sup>; <sup>1</sup>Yonsei University, Dept. Metallurgl. Engrg., 134 Shinchondong Seodaemungu, Seoul 120-749 Korea

Superplastic deformation behavior of fine-grained Mg-rich Mg-Zn-Y-(Zr) alloy sheets, consisting of in-situ icosahedral quasicrystalline particles in the volume fraction up to 0.1, have been investigated in the temperature range of 300°C to 425°C (and constant strain-rate:  $5x10-4s-1 \sim 5x10-1s-1$ ). Fine-grained microstructure of the alloys in the range of 2 to 6 micrometer has been developed via particle-induced dynamic recrystallization processes by conventional thermomechanical processes. The alloys provide large elongation to failure up to 600%, increasing with increasing temperature and decreasing strain-rate. A sigmoidal relationship between log(stress) and log(strain-rate) is observed for each test condition. In the superplastic deformation regime, grain mantle creep is believed to be controlled by dislocation glide and climb processes by evaluation stress exponent (~ 2) and activation energy (~115kJ/mol) in the creep equation. Interestingly, although the alloys contain large number of particles, they do not provide cavitation significantly during superplastic deformation due to relatively low interfacial energy between the icosahedral quasicrystalline particle and the matrix.

#### 9:10 AM

**Development of Wrought Mg Alloys Via Strip Casting**: *Sung S. Park*<sup>1</sup>; Jung G. Lee<sup>1</sup>; Hak C. Lee<sup>1</sup>; Kwang S. Shin<sup>2</sup>; Nack J. Kim<sup>1</sup>; <sup>1</sup>POSTECH, Matls. Sci. & Engrg., San 31, Hyoja-dong, Nam-gu, Pohang, Kyungbuk Korea; <sup>2</sup>Seoul National University, Sch. of Matls. Sci. & Engrg., Seoul Korea

Mg alloys are the lightest commercial structural alloys and have the excellent specific strength and stiffness. They also have high damping capacity and good fatigue resistance. These characteristics of Mg alloys have made them quite attractive for automotive applications. However, the majority of Mg alloys currently in use are cast products and only a limited number of Mg alloys is available as wrought products. The development of wrought Mg alloys, particularly sheet alloys, would greatly expand the application areas of Mg alloys. Up to now, direct chill (DC) casting has been the most important casting technique for producing rolling slabs and extrusion billets of Mg alloys. It is believed that the strip casting process can be an alternative for the production of Mg alloys sheets. Strip casting process combines casting and hot rolling into a single step, having an advantage of one-step processing of flat rolled products. Besides being such a cost-effective process, strip casting also has beneficial effects on microstructure such as reducing segregation, improving inclusion size distribution and refining microstructural and textural homogeneity. The present research is aimed at studying the structure and properties of strip cast Mg alloys to establish the feasibility of strip casting for the production of wrought Mg alloys. Several alloy systems, including AZ and the experimental alloys, are strip cast and their structure-property relationships are established. Microstructure and mechanical properties of strip cast Mg alloys will be discussed with particular emphasis on the solidification behavior during strip casting. The effects of alloying additions and thermo-mechanical treatment will also be discussed.

**TUESDAY AM** 

## 9:30 AM

**Dynamic Mechanical Analysis of Pure Mg and Mg AZ31 Alloy:** *Abraham Munitz*<sup>1</sup>; David Dayan<sup>2</sup>; David Pitchure<sup>1</sup>; R. Ricker<sup>1</sup>; <sup>1</sup>National Institute of Standards and Technology-NIST, Metall. Div., Gaithersburg, MD 20899 USA; <sup>2</sup>NRCN, PO Box 9001, Beer-Sheva 841900 Israel

Dynamic mechanical analyses were performed on pure Mg and Mg AZ31 alloy to study the impact of thermo-mechanical state and grain structure on the complex modulus, creep, stress relaxation and springback. It was found that the storage and loss moduli of pure Mg depend on grain size and grain morphology. Large grain size has storage modulus of about 42 GPa and the grain boundary loss modulus peak is at about 210°C. Decreasing the grain size decreased the storage modulus to 40 GPa and moved the grain boundary peak to about 235°C. It was found that the activation energy for grain relaxation is 1.386 eV, which is very close to the activation energy of the self-diffusion of Mg (1.408 eV). The storage and loss moduli of AZ31 depend on grain size and on solute distribution of Al and Zn in the grains. Cold work, which was achieved via rolling or biaxial strain at temperatures up to 350°C, decreases the storage modulus to about 34.5 GPa while the loss modulus remains almost the same (between 180 and 200°C). On the other hand solute distribution has an impact on the internal friction (loss modulus) while the storage modulus remains almost unaffected.

#### 9:50 AM Break

#### 10:20 AM

**Corrosion Protection of a Die Cast Magnesium Automotive Door**: *G. T. Bretz*<sup>1</sup>; K. A. Lazarz<sup>1</sup>; D. J. Hill<sup>1</sup>; P. J. Blanchard<sup>1</sup>; <sup>1</sup>Ford Research & Advanced Engineering Staff, Dearborn, MI USA

It is well known that magnesium alloys, in close proximity to other alloys, are susceptible to galvanic corrosion. Combined with this fact, in automotive applications, it is rare that magnesium will be present in the absence of other alloys such as steel or aluminum. Therefore, in wet applications where the galvanic cell is completed by the formation of an electrolyte, it is necessary to isolate the magnesium in order to prevent accelerated corrosion. There are numerous commercial pretreatments available for magnesium, however this paper will focus on conversion coatings in conjunction with a spray powder coat. By means of example, results for a hem flange joint on an AM50 die cast magnesium door structure will be presented. The outer door skin is an aluminum alloy hemmed around a cast magnesium flange. An adhesive is used between the inner and outer to help with stiffness and NVH (Noise Vibration and Harshness). Results from bonded coupon tests that have been exposed to accelerated corrosion cycles are presented. A second phase of this work considered a surrogate hem flange coupon, which was similarly exposed to the same accelerated corrosion cycle. Results from both of these tests are presented within this paper along with a discussion as to their suitability for use within automotive applications

# 10:40 AM

Chemical Conversion Coating on AZ91D and its Corrosion Resistance: *En-Hou Han*<sup>1</sup>; Wanqiu Zhou<sup>1</sup>; Dayong Shan<sup>1</sup>; Wei Ke<sup>1</sup>; <sup>1</sup>Chinese Academy of Sciences, Inst. of Metal Rsch., 72 Wenhua Rd., Shenyang, Liaoning 110016 China

The chromium-free conversion coating could be obtained when AZ91D magnesium alloy was immersed in a solution containing a manganese salt, phosphate and an inhibitor. Corrosion resistance of the chemical conversion coating was evaluated by anodizing polarization curve and salt immersion. The passivation region is quite large for more than 200mv. XRD analysis showed that the conversion coating was mainly composed of Mn3(PO4)2 with amorphous structure. The morphology of the coating in different time is observed by SEM. The corrosion rate is lower than that of Dow 7 conversion coating and Shadan conversion coating, and the conversion coating with manganese oxide and MgF from KMnO4 and HF, although there exist microcracks on surface.

#### 11:00 AM

Pretreatment Schemes for Magnesium/E-Coat Automotive Applications: *William C. Gorman*<sup>1</sup>; <sup>1</sup>Technology Applications Group, Inc., 4957 10th Ave. S., Grand Forks, ND 58201 USA

The use of magnesium in exterior applications in the automotive industry is rapidly increasing and with this trend comes the need for a robust corrosion protection scheme. A properly designed protection scheme must allow for the convenient installation of the magnesium component without compromising the coating, thereby minimizing the risk of galvanic corrosion, and provide a high level of corrosion resistance throughout the lifetime of the part. This paper will look at the cyclic corrosion rate and galvanic corrosion of popular magnesium pretreatments coupled with E-coat as well as an anodized coating/E-coat system. The pretreatments to be investigated are iron phosphate, NH35 and Alodine® along with the anodized coating, Tagnite. These pretreatment schemes will be applied to popular magnesium die cast alloys followed by E-coat paint for this evaluation.

## 11:20 AM

The Application of Power Ultrasound to the Preparation of Anodizing Coatings Formed on Magnesium Alloys: Xingwu Guo<sup>1</sup>; Wen Jiang Ding<sup>1</sup>; Chen Lu<sup>1</sup>; ChunQuan Zhai<sup>1</sup>; <sup>1</sup>Shanghai Jiao Tong University, Matl. Sci. & Engrg., Huashan Rd. 1954, Shanghai 200030 China

This paper reports the application of power ultrasound to the anodizing of magnesium alloys. The influence of power ultrasound at a constant frequency of 25kHz on the structure and composition of anodizing coatings formed on magnesium alloy AZ31 was investigated. Results clearly show that ultrasound enhances the growth rate of anodic coatings and plays a very important role in the formation of coating structure and the distribution of coating composition. The anodic coatings consist of only one layer if the ultrasound field was not applied in the solution used in this paper. However, the anodic coatings will consist of two layers when the ultrasound field was applied and the acoustic power value increases to 400W. The inner layer is compact and enriched in aluminum and fluorine. In contrast, the contents of aluminum and fluorine in the external layer are very low and its thickness is non-uniform.

## 11:40 AM

Corrosion Performance Evaluation of Magnesium Alloys by Electrochemical Polarization Technique: B. Rajagopalan<sup>1</sup>; P. S. Mohanty<sup>1</sup>; P. K. Mallick<sup>1</sup>; R. C. McCune<sup>2</sup>; M. S. Rickkets<sup>2</sup>; <sup>1</sup>University of Michigan, 4901 Evergreen Rd., Dearborn, MI 48128 USA; <sup>2</sup>Ford Motor Company, Scientific Rsch. Lab., 2101 Village Rd., Dearborn, MI 48121 USA

The repeatability of electrochemical polarization tests for magnesium alloys in aqueous solutions has been investigated in this study. The investigation includes pure Mg and two magnesium alloys (AM60 and AZ91D), various pH's (both buffered and unbuffered) and chloride concentrations. In unbuffered solutions AM60 showed extreme scatter in corrosion rate relative to AZ91D, especially at pH 4 and pH 10. In general, as the salt concentration increased the relative corrosion rate of AM60 with respect to AZ91D dropped, though at all times it was greater than AZ91D. At pH 4, the greatest spread in corrosion rates of AM60 was observed at all chloride concentrations. In buffered solutions the extreme scatter found in the case of unbuffered solutions was absent, thus suggesting that use of buffered solutions offered a more reproducible analysis by reducing the local pH change that occurs near the working electrode during polarization. In a buffered solution of pH 6 and 0.1% NaCl concentration, pure Mg, AM60 and AZ91D showed the greatest spread in relative corrosion rates, suggesting this regime to be optimal for further evaluations.

# Materials by Design: Atoms to Applications: Computational and Experimental Strategies

*Sponsored by:* Electronic, Magnetic & Photonic Materials Division, EMPMD/SMD-Chemistry & Physics of Materials Committee

*Program Organizers:* Krishna Rajan, Rensselaer Polytechnic Institute, Department of Materials Science and Engineering, Troy, NY 12180-3590 USA; Krishnan K. Sankaran, The Boeing Company, Phantom Works, St. Louis, MO 63166-0516 USA

Tuesday AM	Room: 2	10B	
March 16, 2004	Location:	Charlotte	Convention Center

*Session Chairs:* Surendra Saxena, Florida International University, Miami, FL 33199 USA; Craig S. Hartley, Air Force Office of Scientific Research, Arlington, VA USA

#### 8:30 AM

Inverse Problems and Optimization in Solidification Using Electric, Magnetic and Thermal Fields: George S. Dulikravich<sup>1</sup>; <sup>1</sup>Florida International University, Mech. & Matls. Engrg., 10555 W. Flagler St., Miami, FL 33714 USA

When growing a large single crystal from a melt, such as a semiconductor crystal, it is desirable to achieve a distribution of the dopant in the solid crystal that is as uniform as possible. This is easier to realize under pure heat conduction with no convection]. Since semiconductor melts are highly electrically conducting, it should be possible to use magnetic and electric fields to suppress the buoyancy induced flows. This presentation outlines numerical simulations that can be used to gether with optimization to determine the distributions of the magnets and electrodes that will control the convective flow throughout the melt. The computational results suggests the possibility of developing smart manufacturing protocols for creating objects that will have functionally graded physical properties.

## 9:00 AM

Inverse Methods for Construction of Microstructures for Simulation and Modeling of Nanoscale Crystalline Materials: Mo  $Li^1$ ; 'Georgia Institute of Technology, Sch. of Matls. Sci. & Engrg., Atlanta, GA 30332 USA

Similar to polycrystalline materials, nanocrystalline materials are characterized by the same microstructure attributes such as grain size, grain boundaries, and various crystallographic and atomic structures. Extracting those detailed microstructure properties experimentally proves to be a difficult endeavor because of the small characteristic scales of the material. Very often it is the mean values of grain size, limited number of characterization of grain boundaries and crystallographic properties are available. As a consequence, computer modeling and simulation of nanocrystalline materials in the past resort to various ad hoc approaches. In this talk, I shall present several approaches we developed that are intended to represent microstructures, which can be justified physically. Among these methods are (1) Inverse Monte Carlo method, (2) kinetic grain growth methods, and (3) geometric models which are both computationally efficient and accurate in generating microstructures. Topological and atomic structural properties of the microstructures from these different methods will be compared and analyzed. Examples of atomistic and continuum modeling of mechanical and magnetic properties using these microstructures will also be presented.

# 9:30 AM

Informatics and Combinatorial Based Strategies for Materials Design and Selection: K. Rajan<sup>1</sup>; <sup>1</sup>Rensselaer Polytechnic Institute, 110 Matls. Rsch. Ctr., 110 8th St., Troy, NY 12180 USA

In this presentation we discuss a materials by design methodology which use a combination of data mining and computational materials science tools with combinatorial methods in experimental techniques. The impetus for this approach is that usually only incremental progress is made in specific technological areas of interest. On the other hand we need to have a means of exploring vast combinations of structureproperty relationships. If new significant advances in materials science are to be made, we need to have search tools that can accelerate the discovery process. Data mining is envisaged as a tool to exploit the masses of available data to accelerate the discovery of these relationships and possible new associations. We provide examples of how we are integrating the informatics tools with high throughput materials synthesis and characterization of multicomponent alloys to aid in the rapid selection and design of materials.

#### 10:00 AM Break

## 10:15 AM

High Throughput Ab-Initio Computing: Phase Stability Prediction: Stefano Curtarolo<sup>1</sup>; Dane Morgan<sup>1</sup>; Gerbrand Ceder<sup>1</sup>; <sup>1</sup>Massachusetts Institute of Technology, Dept. Matls. Sci. & Engrg., Rm. 13-4069, 77 Mass. Ave., Cambridge, MA 02139 USA

High throughput ab-initio computational materials science is a new and powerful tool to describe and analyze similarities between different systems. We have used such an approach to calculate the stable crystal structures in nearly 80 systems, thereby creating a library of ~15,000 ab-initio structural energies. From this library it is possible to extract rules that generalize well known phenomenological approaches such as the one by Miedema or Pettifor. In our case, these rules are formulated as mathematical correlations between structural energies so that they can be used to make predictions in completely new systems. In this work we describe the method we have implemented, and list the results of new crystal structure predictions. This large study also benchmarks the accuracy of LDA ultra-soft pseudopotentials approaches.

#### 10:45 AM

**Computer Aided Engineering and Design**: *Farrokh Mistree*<sup>1</sup>; David L. McDowell<sup>1</sup>; <sup>1</sup>Georgia Institute of Technology, Mech. Engrg., Atlanta, GA 30332-0405 USA

Abstract not available.

# 11:15 AM

## Combinatorial Exploration of Magnetic Materials Using Thinfilm Techniques: Ichiro Takeuchi<sup>1</sup>; <sup>1</sup>University of Maryland, MD USA

We have developed a methodology for performing combinatorial investigation of a variety of magnetic materials. Combinatorial pulsed laser deposition systems and an ultra high vacuum magnetron cosputtering system are used to investigate metal oxide systems and metallic systems, respectively. Thin-film combinatorial libraries and composition spreads of different designs are utilized to effectively map large compositional landscapes on individual chips. High-throughput characterization of magnetic properties is performed using room temperature scanning SQUID microscopes. Systems studied to date include ferromagnetic shape memory alloys, exchanged coupled magnetic bilayers and artificial magnetoelectric materials. Scanning x-ray diffractometry is used to map the phase distribution of entire combinatorial samples in order to rapidly establish composition-structureproperty relationships across compositional phase diagrams.

# Materials Processing Fundamentals: Liquid Metal Processing

Sponsored by: Extraction & Processing Division, Materials Processing & Manufacturing Division, EPD-Process Fundamentals Committee, MPMD/EPD-Process Modeling Analysis & Control Committee

*Program Organizers:* Adam C. Powell, Massachusetts Institute of Technology, Department of Materials Science and Engineering, Cambridge, MA 02139-4307 USA; Princewill N. Anyalebechi, Grand Valley State University, L. V. Eberhard Center, Grand Rapids, MI 49504-6495 USA

Tuesday AM	Room: 2	12B		
March 16, 2004	Location:	Charlotte	Convention	Center

Session Chair: TBA

## 8:30 AM Invited

**Control of Convection in Containerless Processing**: *Robert W. Hyers*<sup>1</sup>; Douglas M. Matson<sup>2</sup>; Kenneth F. Kelton<sup>3</sup>; Jan R. Rogers<sup>4</sup>; <sup>1</sup>University of Massachusetts, Dept. of Mech. & Industrial Engrg., 160 Governors Dr., Amherst, MA 01003 USA; <sup>2</sup>Tufts University, Dept. of Mech. Engrg., Medford, MA 02155 USA; <sup>3</sup>Washington University, Dept. of Physics, St. Louis, MO 63130 USA; <sup>4</sup>NASA Marshall Space Flight Center, MC SD46, Hunstville, AL 35812 USA

Many different containerless processing techniques are employed in materials research, with the common goals of eliminating chemical reactions with the crucible and reducing heterogeneous nucleation sites. Each containerless method has different driving forces for flow in a liquid sample, and each has different relations between the flow variables and the process parameters. Often more than one technique is required to achieve the objectives of an experimental program. For example, one project requires solidification experiments over a range of almost two orders of magnitude in flow velocity, in both laminar and turbulent flow, while another requires a particular combination of shear rate and cooling rate, leading to a different processing strategy. The results of a modeling effort to determine the best combination of methods to meet the requirements of these two different experimental programs are presented.

# 9:00 AM

The Influence of Internal and External Convection in the Transformation Behavior of Fe-Cr-Ni Alloys: *Rakesh Venkatesh*<sup>1</sup>; Robert W. Hyers<sup>2</sup>; Douglas M. Matson<sup>1</sup>; <sup>1</sup>Tufts University, Mech. Engrg., 200 College Ave., 025 Anderson, Medford, MA 02155 USA; <sup>2</sup>University of Massachusetts, Dept. of Mech. & Industrial Engrg., 160 Governors Dr., Engrg. Lab Bldg., Amherst, MA 01003 USA

A difference in the transformation delay times was observed between electromagnetic levitation (EML) and electrostatic levitation (ESL) experiments on steel alloys. This deviation is due to the difference in convection. Using high speed imaging, we can observe the frequency of nucleation as a function of declination angle measured from the equatorial plane and we can observe the delay between nucleation events. These measurements show no preference for location in ESL testing. For EML tests, primary recalescence preferentially occurs on the top hemisphere where cooling gas impinges on the surface. Delay times did not vary significantly between top and bottom hemispheres and thus external convection does not explain the deviation observed. For EML tests, the frequency of secondary nucleation appears to disfavor positions along the equator and both poles, where internal flows are minimized, indicating that internal convection is responsible for the observed deviation.

# 9:20 AM

**Experimental Measurement of Melt Flow With and Without an Applied Magnetic Field**: X. Bing<sup>1</sup>; *Ben Li*<sup>1</sup>; <sup>1</sup>Washington State University, Sch. of Mech. & Matls. Engrg., Pullman, WA 99164 USA

This paper discusses the measurement of melt flows induced by thermal gradients with and without an applied magnetic field. An experimental system has been setup when low meting point melt flow is driven by buoyancy forces. The melt velocity is measured by a hot wire probe. The measurements are conducted with and without an externally applied magnetic field. The measured data are compared with numerical predictions and a reasonably good comparison is obtained. Study on the Motion States of Impurity Particles in Static Magnetic Field: L. Zhang<sup>1</sup>; G. C. Yao<sup>1</sup>; W. L. Jiao<sup>1</sup>; <sup>1</sup>Northeastern University, Sch. of Matl. & Metall., Liaoning, Shenyang 110004 China

The physical property differences between impurity particles and mother metal including conductivity and magnetic suscepbility were used for electromagnetic separation, which would bring different motion rules in magnetic field to make the mother metal more purified. The motion states of impurity particles (metallic particles magnetized) imposed by magnetic force in static magnetic field were studied mainly. After analyzing of force imposed and theoretic calculation, the final motion velocities of impurity particles imposed by magnetic force were confirmed. The separating efficiencies of impurity particles were made out adopting the models of piston and trajectory according to the different fluxion states of molten metal, respectively. From the results, it was found that the influence factors of separating efficiency were different obviously when the melt was in the different fluxion states. This conclusion was applicable to weak magnetism melt, especially to molten aluminum.

10:00 AM Break

## 10:20 AM Invited

Metallurgical Processes and Non-Equilibrium Thermodynamics: *Ji He Wei*<sup>1</sup>; <sup>1</sup>Shanghai University, Coll. of Matls. Sci. & Engrg., Dept. of Metallic Matls., Rm. 301, No. 1, 669 Long, Ping Xing Guan Rd., Shanghai City China

Taking the vacuum circulation (RH) refining of clean steel (ultralowcarbon and ultralow-sulphur steel) as an example, the non-linear and non-equilibrium features of metallurgical processes have been illustrated. The similarities and differences between metallurgical reaction eingineering and non-equilibrium thermodynamics have been analyzed. The necessity and feasibility investigating and dealing with practical metallurgical processes from the viewpoints, fundamentals and methods of non-equilibrium thermodynamics with metallurgical reaction engineering have been discussed. It is pointed out that non-equilibrium thermodynamics should and can play its role in the metallurgical area.

# 10:40 AM

The Dissolved Element and Nucleant Influence on the Aluminum Alloys Grain Refining Degree: *Petru Moldovan*<sup>1</sup>; Gabriela Popescu<sup>1</sup>; Mihai Butu<sup>1</sup>; Ioana Apostolescu<sup>1</sup>; <sup>1</sup>Polytechnic University Bucharest, Matls. Sci. & Engrg., Spaiul Independentei 313, Sect. 6, Bucharest 77206 Romania

The aim of this paper is to study the titanium and boron, introduced in the melt as AITi10 and AITiB master alloy, influence on the grain refining of AIMgSi alloy. The laboratory research underlined the role of free Ti and borides on the cast alloys grain dimensions. Microstructure analyzes realized by optical (Buehler OMNIMET EXPRESS) and electronic (SEM with EDAX) microscopy highlighted the titanium and boride role during the nucleation and grain growth processes in cast bars. The paradigms of dissolved elements and nucleant were verified during the grain refining process of deformable alloys.

#### 11:00 AM

# **Precipitation of Inclusions in Iron Melts Treated with Ti and Mn**: *Sukru Talas*<sup>1</sup>; Ayhan Erol<sup>1</sup>; <sup>1</sup>A. Kocatepe University, Techl. Educ. Faculty, A.N.S. Campus, B Block, Afyon, Afyon 03200 Turkey

Precipitation of inclusions in steelmaking process is of prime importance since it affects the mechanical properties during its service life. The nucleation and formation of inclusions especially in weld metals occurs as a result of complex reactions and sequence of nucleation is not well understood when it forms in non-equilibrium conditions. In this work, the sequence of inclusion formation in melts produced using copper chilled substrate has been documented and the effect of each inclusion forming alloying elements on the solidification behavior is also presented.

# 11:20 AM

A Method to Study the Effect of Alloying Elements at Low O Levels: *Ayhan Erol*<sup>1</sup>; Sukru Talas<sup>1</sup>; <sup>1</sup>A. Kocatepe University, Tech. Educ. Fac., A.N.S. Campus, B Block, Afyon 03200 Turkey

A method developed to study the effect of each alloying elements at very low level of O is to be presented. With this method, laboratory size melts can be obtained with very low O contents as low as 58 ppm without the addition of Al or Si deoxidizing elements. Method involves the use of high purity powders and a sequence of various processing routes ensuring low O content and free of impurities. This method was used to study the effect of C, Mn, and Ti on the morphology of iron and similar microstructures of steels can also be obtained.

#### 11:40 AM

Effects of Impurities in Aluminum Alloys Processing: Shengjun Zhang<sup>1</sup>; <sup>1</sup>Pennsylvania State University, Dept. Matl. Sci. & Tech., 107 Steidle Bldg., State College, PA 16801 USA

Calcium, lithium and sodium are impurity elements in aluminumbased alloys. They increase the hydrogen solubility in the melt and promote the formation of porosity in aluminum castings. During fabrication of aluminum alloys, these three elements cause the hot-shortness and embrittlement owing to cracking. In the present work, the thermodynamic description of the Al-Ca-Li-Na quaternary system is studied using the Calphad modeling approach to understand the effects of Ca, Li and Na on phase stability of aluminum alloys. Combining proper models and thermodynamic databases, the surface tension and viscosity of Al-base alloys are calculated. This work is beneficial to better understand and resolve some industry problems, such as viscosity decreasing and blistering during Al-alloy processing.

# Nanostructured Magnetic Materials: Magnetic Tunnel Junctions and Semiconductor Spintronics

Sponsored by: Electronic, Magnetic & Photonic Materials Division, EMPMD-Superconducting and Magnetic Materials Committee, EMPMD-Nanomaterials Committee Program Organizers: Ashutosh Tiwari, North Carolina State University, Department of Materials Science & Engineering, Raleigh, NC 27695-7916 USA; Rasmi R. Das, University of Wisconsin, Applied Superconductivity Center, Materials Science and Engineering Department, Madison, WI 53706-1609 USA; Ramamoorthy Ramesh, University of Maryland, Department of Materials and Nuclear Engineering, College Park, MD 20742 USA

Tuesday AM	Room: 215
March 16, 2004	Location: Charlotte Convention Center

Session Chair: TBA

#### 8:30 AM Invited

**Tunnel Junction Spin Injectors for Semiconductor Spintronics**: *Stuart Parkin*<sup>1</sup>; <sup>1</sup>IBM Almaden Research Center, K11-D2, 650 Harry Rd., K11-D1, San Jose, CA 95120-6099 USA

Using a combination of spin-dependent tunneling in magnetic tunneling junctions (MTJ) and spin filtering effects in ultra-thin ferromagnetic layers we have created a source of highly spin polarized electrical current, a magnetic tunneling transistor. This three-terminal hot-electron device marries a magnetic tunneling junction with a GaAs or Si semiconducting collector.1 For GaAs based devices thirty-fold collector current changes are observed in small magnetic fields consistent with about 95% spin-polarized current. Using a quantum-well light emitting diode as a detector we have demonstrated that the collector current injected into GaAs is more than 10% spin-polarized.<sup>2</sup> Recent results showing evidence for much higher spin polarized currents using tunnel junction injectors will also be discussed. 1"Nonmonotonic bias voltage dependence of magnetocurrent in GaAs-based magnetic tunnel transistors", S. van Dijken, X. Jiang and S.S.P. Parkin, Phys. Rev. Lett. 90, 197203 (2003). 2"Optical detection of hot electron spin injection into GaAs from a Magnetic Tunnel Transistor Source"?, X. Jiang, R. Wang, S. van Dijken, R. Shelby, R. Macfarlane, G. Solomon, J. Harris and S.S.P. Parkin, Phys. Rev. Lett. 90, 256603 (2003).

# 9:00 AM Invited

Recent Development in Magnetic Tunnel Junctions: John Q. Xiao<sup>1</sup>; Xiaohai Xiang<sup>1</sup>; Tao Zhu<sup>2</sup>; F. Shen<sup>3</sup>; Z. Zhang<sup>3</sup>; <sup>1</sup>University of Delaware, Dept. of Physics & Astron., Newark, DE 19716 USA; <sup>2</sup>Chinese Academy of Science, Inst. of Physics, State Key Lab. for Magnetism, Beijing 100080 China; <sup>3</sup>Chinese Academy of Science, Institute of Physics, Beijing Lab. of Electron Microscopy, Beijing 100080 China

Recent developments in magnetic tunnel junctions (MTJs) will be discussed. First, we will present results of possibly using electron holography technique to directly probe the energy profile of tunnel barrier. Barriers with different oxidation conditions (over, optimum, and overoxidized) have been investigated. One important finding is that there is always slight oxidation of the top electrode. Second, we will discuss an alternative barrier material which leads to the observation of an inversed tunneling magnetoresistance (TMR) at a high bias. A model is proposed to explain the behavior. The finding leads to the possibilities of achieving better signals at high bias in real applications. Finally, we will discuss the TMR dependence on both magnetic and nonmagnetic electrode thicknesses. The results indicate the existence of bulk-like contribution to TMR.

# 9:30 AM Invited

Spin Dependent Transport in Magnetic Oxide Junctions: Yuri Suzuki1; 1University of California, Dept. of Matls. Sci. & Engrg., 380 Hearst Memorial Mining Bldg., MC 1760, Berkeley, CA 94720-1760 USA

Highly spin polarized ferromagnetic materials have been the focus of recent fundamental and technological studies. In particular, half metallic materials with nominally 100% spin polarization at the Fermi level are of interest. The degree and sign of spin polarization of the carriers in these materials have been probed in a variety of spin polarized tunnel junctions. The spin polarization of the material is positive if the majority spin at the Fermi level is parallel to the bulk magnetization and negative if the minority spin at the Fermi level is parallel to the bulk magnetization. Negative spin polarization, however, has rarely been observed. Magnetite (Fe<sub>3</sub>O<sub>4</sub>) is unique in that it is predicted not only to have negative spin polarization but also to be a half-metallic ferromagnet. We have fabricated epitaxial oxide trilayer junctions composed of Fe<sub>3</sub>O<sub>4</sub> and doped manganite (La<sub>0.7</sub>Sr<sub>0.3</sub>MnO<sub>3</sub>). The junctions exhibit inverse magnetoresistance as large as -25% in fields of 4kOe. The inverse magnetoresistance confirms the theoretically predicted negative spin polarization of Fe<sub>3</sub>O<sub>4</sub>. Transport through the barrier can be understood in terms of hopping transport through localized states that preserves electron spin information. The junction magnetoresistance versus temperature curve exhibits a peak around 60K that is explained in terms of the paramagnetic to ferrimagnetic transition of the CoCr<sub>2</sub>O<sub>4</sub> barrier. In collaboration with Guohan Hu and Rajesh Chopdekar.

# 10:00 AM Invited

Computational Design of New Spintronic Materials: Nicola Spaldin1; 1University of California, Matls. Dept., Santa Barbara, CA 93106 USA

Spin-polarized electronics is a rapidly expanding research area, both because of the fascinating fundamental physics observed in new spintronic materials, and because of their potentially far-reaching technological applications. In this talk we illustrate the utility of theoretical and computational methods in the design and optimization of three new spintronic systems. First we explore the influence of the interface on the spin transport in cobalt-contacted carbon nanotube transistors. Second we investigate the effects of doping and clustering on the magnetic properties of diluted magnetic semiconductors. And third we describe the successful prediction and subsequent synthesis of a new "multiferroic" material (which is simultaneously ferromagnetic and ferroelectric). Finally we mention some recent advances in computational methods that have allowed us both to understand the novel phenomena observed in spintronic materials, and to design improved materials for specific technological applications.

# 10:30 AM Invited

High-Temperature Ferromagnetism in Co-Doped Semiconductors: Samuel E. Lofland1; 1Rowan University, Ctr. for Matls. Rsch. & Educ., 201 Mullica Hill Rd., Glassboro, NJ 08028-1701 USA

We have completed a thorough study of Co-doped anatase TiO<sub>2</sub> and TiNF in thin-film and bulk forms by a variety of techniques, including magnetization, Hall effect, transmission electron microscopy, electron energy loss spectroscopy. While bulk material and highly substituted thin films (> 5% Co substitution) are either nonmagnetic or show signs of clustering of elemental Co, thin films with smaller Co doping are semiconducting with a Curie temperature of about 600 K. We discuss these results and our work on Co-doped SnO<sub>2</sub>, which we have recently shown to be a ferromagnetic semiconductor but is optically transparent and has an anomalously large Co moment (~ 8 mB). This work was supported in part by NSF MRSEC Grant DMR 00-80008 and the New Jersey Commission on Higher Education.

# 11:00 AM

Rectifying Electrical Characteristics of ZnO/LSMO Heterostructure: A. Tiwari<sup>1</sup>; C. Jin<sup>1</sup>; J. Narayan<sup>1</sup>; <sup>1</sup>North Carolina State University, Matls. Sci. & Engrg., Raleigh, NC 27695 USA

We have fabricated a p-n junction, consisting of hole-doped (ptype) manganite and electron-doped (n-type) ZnO layers grown on sapphire substrate. These junctions exhibit good electrical rectifying behavior over the temperature range 20-300K. Electrical characteristics of La<sub>0.7</sub>Sr<sub>0.3</sub>MnO<sub>3</sub> (LSMO) film in this heterostructure is found to be strongly modified by the built-in electric field of the junction. It has been shown that by applying the external bias voltage, the thickness of the depletion layer and hence the electrical and magnetic characteristics of LSMO film can be modified.

## 11:20 AM

Structural and Magnetic Properties of Fe Doped Zn1-xMgxO Thin Films: Rasmi R. Das1; Pijush Bhattacharya1; Gyana R. Pattanaik2; Jose Nieves<sup>1</sup>; Yuri I. Yuzyuk<sup>1</sup>; Ram S. Katiyar<sup>1</sup>; <sup>1</sup>University of Wisconsin, Applied Superconductivity Ctr., Matls. Sci. & Engrg. Dept., 2163 ECB, 1550 Engrg. Dr., Madison, WI 53706-1609 USA; <sup>2</sup>Indian Institute of Technology, Dept. of Physics, Hauz Khas, New Delhi 110016 India

ZnO is a versatile wide band gap material for optoelectronic devices due to its higher excitonic energy (~60 meV). The band gap of ZnO is often enhanced with increase in Mg concentrations within the solid solubility limit. Recently, there is an increasing interest to use ZnO host with doped 3d transition elements or cations having magnetic moment in order to manipulate the spin that will be useful for spintronic applications. We have prepared high quality ZnO and (ZnMg)O alloy with different concentrations of Fe using pulsed-laser deposition technique on sapphire substrates. It was observed that Fe starts segregating after certain concentrations (> 10%) in ZnO as observed from the x-ray diffraction and Raman scattering. Micro Raman spectra of ceramics as well as thin films showed disorder induced Raman bands besides standard wurtzite ZnO modes. Optical absorption data showed an additional absorption band towards lower bandgap energy (3 eV) with the increase in Fe content and was believed to be due to the secondary phase. The influence of Fe on magnetic properties of ZnO was studied using a vibration sample magnetometer. The remanence and coercievity of the ZnO films was found to be maximum for the sample with 10% Fe contents. The detailed results of structural and magnetic properties will be correlated with intrinsic properties of the doped cations.

# **Nanostructured Materials for Biomedical** Applications: Session III

Sponsored by: Electronic, Magnetic & Photonic Materials Division, EMPMD-Thin Films & Interfaces Committee Program Organizers: Roger J. Narayan, Georgia Tech, School of Materials Science and Engineering, Atlanta, GA 30332-0245 USA; J Michael Rigsbee, North Carolina State University, Department of Materials Science and Engineering, Raleigh, NC 27695-7907 USA; Xinghang Zhang, Los Alamos National Laboratory, Los Alamos, NM 87545 USA

Tuesday AM	Room
March 16, 2004	Locat

n: 219A tion: Charlotte Convention Center

Session Chairs: Jackie Y. Ying, Institute of Bioengineering and Nanotechnology, Singapore 117586 Singapore; Andres J. Garcia, Georgia Institute of Technology, Sch. of Mech. Engrg., Atlanta, GA 30332 USA; Yadong Wang, Georgia Institute of Technology, Coulter Dept. of Biomed. Engrg., Atlanta, GA 30332-0535 USA

# 8:30 AM Invited

Growth, Structure and Mechanical Properties of Abalone Shell: Marc Andre Meyers1; Albert Lin1; 1University of California, Dept. of Mech. & Aeros. Engrg., MC 0411, La Jolla 92093-0411 USA

The self-assembly of aragonitic calcium carbonate found in the shell of abalone (Haliotis) is studied through examination of laboratory-grown flat pearl samples and slices of the nacreous shell. The growth occurs by the successive nucleation of crystals and their arrest by means of a protein-mediated mechanism, forming terraced cones. The protein layer is virtually absent where plates on a same plane abut(along lateral surfaces of tiles). A mechanism is proposed through c-axis aragonite growth arrest by the deposition of a protein layer of approximately 10-30 nm, periodically activated. This determines the thickness of the aragonite platelets, which are remarkably constant (0.5 µm). This platelet size was found to be independent of shell size. The overall growth process is expressed in terms of parameters incorporating the anisotropy of growth velocity in aragonite (Vc, the velocity along c axis, and Vab, the velocity in basal plane). Naturallydeveloped abalone exhibits mesolayers ~0.3 mm apart; these mesolayers result from seasonal interruptions in feeding patterns, creating thicker (~10-20 µm) layers of protein. These mesolayers play a critical role in the mechanical properties, and are powerful crack deflectors. The mechanisms of deformation are discussed and a novel mode of compressive failure is described. The role of the organic intertile layer is modeled.

# 9:00 AM Invited

3-D Nanoparticle Structures with Self-Replicating Shapes and Synthetically-Tailored Compositions: Ken H. Sandhage1; Christopher S. Gaddis<sup>1</sup>; Matthew B. Dickerson<sup>1</sup>; Samuel Shian<sup>1</sup>; Rajesh R. Naik<sup>2</sup>; Morley O. Stone<sup>2</sup>; Mark M. Hildebrand<sup>3</sup>; Brian P. Palenik<sup>3</sup>; <sup>1</sup>Georgia Institute of Technology, Sch. of Matls. Sci. & Engrg., 771 Ferst Dr., Atlanta, GA 30332-0245 USA; <sup>2</sup>Air Force Research Laboratory, MLPJ Hardened Matls. Branch, Biotech. Grp., Wright-Patterson AFB, Dayton, OH 45433-7702 USA; <sup>3</sup>University of California, Scripps Oceanographic Inst., Marine Bio. Rsch. Div., 9500 Gilman Dr., La Jolla, CA 92093-0202 USA

Widespread use of nanostructured materials in biomedical and other applications has been hampered by conflicting requirements for precise control over fine features and for mass production. Nature provides numerous examples of mineralized (bioclastic) structures with precise 3-D shapes that are mass-produced under ambient conditions. Particularly striking examples are the microshells of diatoms (singlecelled algae). Each of the 105 diatom species assembles a uniquelyshaped 3-D microshell of silica nanoparticles. Sustained diatom reproduction can vield enormous numbers of identical microshells. A revolutionary processing paradigm that utilizes such precise (geneticallycontrolled) and massively-parallel biological replication to generate nanoparticle structures with tailored shapes and chemistries will be presented: the BaSIC (Bioclastic and Shape-preserving Inorganic Conversion) process. The BaSIC process has been used to convert bioclastic or biosculpted structures into MgO, CaO, TiO<sub>2</sub>, ZrO<sub>2</sub>, SiC, and polymeric materials for biomedical or other applications. Various biogenic preforms and conversion methods will be discussed.

# 9:30 AM Invited

Designing Biomimetic Nano-Structured Scaffolds for Tissue Engineering: Peter X. Ma<sup>1</sup>; <sup>1</sup>University of Michigan, Dept. of Biologic & Matls. Scis., 1011 N. Univ. Ave., 2211 Dental Sch., Ann Arbor, MI 48109-1078 USA

Our group focuses on biomimetic design and fabrication of polymer scaffolds for tissue engineering. The scaffolds mimic certain advantageous aspects of natural extracellular matrix, and impart certain controllable structural features and properties from the synthetic materials design. These scaffolds serve as 3D templates to guide tissue regeneration, and eventually degrade and resorb, leaving nothing foreign in the body. To mimic bone matrix, biodegradable polymer/nanobioceramic composite scaffolds have been developed. To mimic the nano fibrous architecture and to overcome the concerns of immunorejection and disease transmission associated with collagen from a natural source, synthetic nano fibrous scaffolds have been developed in our laboratory. To optimize scaffolding function, a variety of macropore networks have been designed in the nanofibrous material. These novel nano-structured scaffolds selectively adsorb certain proteins, and enhance cell adhesion and function. Our experimental data demonstrate that the biomimetic design of nano-structured scaffolds is a powerful approach in tissue engineering.

#### 10:00 AM Invited

**Bio-Inspired Nanostructured Materials**: Jun Liu<sup>1</sup>; <sup>1</sup>Sandia National Laboratories, Chem. Synthesis & Nanomatls., PO Box 5800, MS 1411, Albuquerque, NM 87185 USA

The formation and functions of biomaterials and organisms are fundamentally different from those of synthetic materials and devices. Synthetic materials tend to have static structures that are not compatible with biomaterials, and are not capable of adapting to the functional needs of changing environments. In contrast, living systems have hierarchical structural ordering on multiple length scales, and are capable of responding to internal and external stimuli to heal and reconfigure in a dynamic fashion. In this talk, we will first discuss strategies to develop self-assembled nanostructures based on lessons from biomineralization. By controlling the surface chemistry and the crystallization behavior, we are able to produce complex two dimensional and three dimensional microstructures showing remarkable resemblance to those observed in biominerals. These novel materials showed great potential for enhancing the activities of biomaterials (proteins) and demonstrated the possibility for ultrasensitive sensing. We are also investigating strategies to use active proteins such as motor proteins and microtubules to assemble dynamic materials. This strategy is used by biomaterials to form complex shells of diatoms and responsive pigment arrays in chameleons and other organisms to change their color. We hope our approach will lead to new concepts and new materials for controlled release, tissue engineering and healing.

## 10:30 AM Invited

Proteomic Understanding of Novel Cellular Factors for Controlling Growth of Nanocrystals: Xian Chen<sup>1</sup>; <sup>1</sup>Los Alamos National Laboratory, Biosci. Div., M888, Los Alamos, NM 87545 USA

Certain microorganisms such as Candida glabrata and Schizosaccharomyces pombe in nature are able to mediate the deposition of metal nanocrystals in vivo with high accuracy and efficiency. It is of tremendous interest to understand the cellular machinery of these microorganisms at molecular level by which nanocrystalline particles are synthesized as well as the regulatory mechanism(s) by which their sizes and morphologies are strictly controlled. We have used the state-of-the-art mass spectrometry-based technology to analyze the composition and spatial organization of cellular machinery of certain microorganisms that are able to produce nanocrystals. We have systematically identified the celluar factors involved in the biologically mediated synthesis of CdS nanocrystals. For example, yeast cells were cultured in exposure to different Cd(II) concentrations, and subjected to MS-based proteome analysis at certain intervals of time. We have established an in vitro system in which formation of nanocrystals is mediated by the identified proteins.

#### 11:00 AM Invited

Molecular Biomimetics Approach to Engineered Polypeptides for Nanobiotechnology: *Mehmet Sarikaya*<sup>1</sup>; <sup>1</sup>University of Washington, Matls. Sci. & Engrg., Roberts Hall, Box 352120, Seattle, WA 98195 USA

Structures and, therefore, functions of all biological hard and soft tissues in organisms are controlled by proteins based on their unique and specific interactions with other macromolecules (lipids, DNA, polysaccharides, and other proteins) and inorganics. Taking lessons from biology and using the tools of molecular biology, polypeptides can be genetically engineered to bind specifically to selected inorganics for use in nano- and biotechnology, a new field we call molecular biomimetics. Using bacterial cell surface and phage coat and coat proteins, we combinatorially select short (7-14 amino acid) polypeptide sequences with affinity to bind to (noble) metals and semiconducting oxides (Cu-, Zn-, Cd-, Al-, etc.). These genetically engineered polypeptides for inorganics (GEPIs) can be used as molecular erector sets for assembly of functional nanostructures. Based on the three fundamental principles of molecular recognition, self-assembly and DNA manipulation, I will demonstrate successful uses of GEPI in nanotechnology (molecular electronics) and nanobiotechnology (biosensors) applications.

# 11:30 AM Invited

Synthetic Biology and Nanobiotechnology: *Glen A. Evans*<sup>1</sup>; <sup>1</sup>Egea Biosciences, Inc., 6759 Mesa Ridge Rd., Ste. 100, San Diego, CA 92069 USA

The information accumulated by genome sequencing projects provides raw materials for the creation new generations of industrial proteins, protein drugs, biomaterials and ultimately nanomachines and synthetic life. Synthetic Biology is a new way of developing proteins and protein devices through large scale DNA synthesis where DNA is "programmed" to produce novel substances and regulatory mechanisms. One aspect of synthetic biology is protein design where realm of possible protein sequences, and variations around naturally occurring protein sequences, defines an astronomically large sequence space that must be evaluated in developing new protein structures. A second challenge is the development and construction of synthetic pathways and genetic systems, designed to recapitulate the systems biology inherent in living organisms. Egea Biosciences is utilizing automated large scale DNA synthesis to develop new protein drugs and genetic pathways by producing libraries of protein variants and systematic screening them for enhanced properties. This approach provides basic information representing "rules" or design specifications for protein engineering and allows development of a common language for rational protein design.

# Phase Stability, Phase Transformation, and Reactive Phase Formation in Electronic Materials III: Session III

Sponsored by: Electronic, Magnetic & Photonic Materials Division, Structural Materials Division, EMPMD/SMD-Alloy Phases Committee

*Program Organizers:* C. Robert Kao, National Central University, Department of Chemical and Materials Engineering, Chungli City 32054 Taiwan; Sinn-Wen Chen, National Tsing-Hua University, Department of Chemical Engineering, Hsinchu 300 Taiwan; Hyuck Mo Lee, Korea Advanced Institute of Science & Technology, Department of Materials Science & Engineering, Taejon 305-701 Korea; Suzanne E. Mohney, Pennsylvania State University, Department of Materials Science & Engineering, University Park, PA 16802 USA; Michael R. Notis, Lehigh University, Department of Materials Science and Engineering, Bethlehem, PA 18015 USA; Douglas J. Swenson, Michigan Technological University, Department of Materials Science & Engineering, Houghton, MI 49931 USA

Tuesday AMRoom: 214March 16, 2004Location: Charlotte Convention Center

Session Chairs: H. M. Lee, Korea Advanced Institute of Science and Technology, Dept. of Matls. Sci. & Engrg., Taejon 305-701 Korea; K. N. Subramanian, Michigan State University, Dept. of Chem. Engrg. & Matls. Sci., E. Lansing, MI 48824-1226 USA

# 8:30 AM Invited

Multiphase Field Simulations of the Evolution of Intermetallic Layer During Soldering Reactions: *Joo-Youl Huh*<sup>1</sup>; Kyung-Kuk Hong<sup>1</sup>; <sup>1</sup>Korea University, Div. of Matls. Sci. & Engrg., 5-1, Anam-Dong, Sungbuk-Ku, Seoul 136-701 Korea

Intermetallic compounds form at the interface between a liquid solder and a metallic substrate during soldering reaction and are indicative of joint adhesion. As the dimension of the solder joint continues to decrease in electronic packaging technology, the morphology and thickness of the intermetallic layer formed during soldering reaction become ever important for the mechanical properties of solder joints and thus for the integrity of electronic packaging. In this study, twodimensional simulations of the microstructural evolution of intermetallic (Cu6Sn5) layer during soldering reactions between liquid Sn-Cu solder and Cu substrate were carried out using a multiphase field method. The intermetallic layer consists of grains which coarsen simultaneously as the intermetallic layer grows. The simulation results will be presented with the emphasis on the effects of intermetallic grain boundary diffusion on the morphology and growth kinetics of the intermetallic layer, and will be discussed in comparison with experimental observations

# 8:50 AM Invited

Solder Reaction of Bare Cu and Kirkendall Void Formation During Solid State Ageing: *Kejun Zeng*<sup>1</sup>; Roger Stierman<sup>1</sup>; <sup>1</sup>Texas Instruments Inc., Semiconductor Pkgg. Dvlp., 13536 N. Central Expressway, MS 940, Dallas, TX 75265 USA

Reaction of bare Cu with lightly-alloyed SnPb solders and Pb-free SnAgCu has been studied. After reflow, samples were annealed at different temperatures up to 80 days, then cross sectioned for microanalysis. Focused ion beam was used to polish the cross sections after mechanical grinding to reveal the Kirkendall voids. While the number and size of Kirkendall voids after reflow are so small that they can be ignored from the reliability perspective, the voiding of interface after high temperature thermal ageing is so extensive that its impact on solder joint reliability should not be ignored in extreme temperature applications or tests. Although the IMC layers were flattening and growing during ageing, this effect on joint reliability is expected to be much less than that of the interfacial voids. Thermodynamically calculated phase diagrams of the SnPbCu and SnAgCu systems are used to rationalize the formation of IMCs. The growth of IMC layers and formation of voids are also discussed.

# 9:10 AM Invited

Microstructual Features Contributing to Enhanced Behavior of Sn-Ag Based Solder Joints: J. G. Lee<sup>1</sup>; K. N. Subramanian<sup>1</sup>; <sup>1</sup>Michigan State University, Dept. of Chem. Engrg. & Matls. Sci., E. Lansing, MI 48824-1226 USA This study investigated the role of microstructure of solder joints made with eutectic Sn-Ag solder and Sn-Ag solder with Cu and/or Ni additions on the creep and thermomechanical fatigue (TMF) properties. Quaternary alloys containing small amounts of Cu and Ni exhibited better creep resistance at higher temperatures, and also better TMF resistance with longer dwell times at high temperature extreme, than eutectic Sn-Ag, and Sn-Ag-Cu ternary alloy solder joints. Microstructural studies of the quaternary solder alloys revealed the presence of ternary Cu-Ni-Sn intermetallic compound (IMC) at Sn grain boundaries. These precipitates can retard grain boundary sliding that can occur during TMF with longer dwell times at high temperature extreme, and high temperature creep. Acknowledgement: Work supported by the National Science Foundation under grant NSF DMR-0081796.

# 9:30 AM

The Influence of Dissolved Element on the Nanoindentation Characteristics of Cu6Sn5 and Ni3Sn4 Intermetallic Compound in the Solder Bump: *Guh Yaw Jang*<sup>1</sup>; Jenq Gong Duh<sup>1</sup>; Jyh Wei Lee<sup>2</sup>; <sup>1</sup>National Tsing Hua University, Dept. of Matls. Sci. & Engrg., 101, Kuang Fu Rd., Sec. 2, Hsinchu 300 Taiwan; <sup>2</sup>Tung Nan Institute of Technology, Mech. Engrg., No. 152, Sec. 3, PeiShen Rd., ShenKeng, Taipei 222 Taiwan

The interfacial reactions between solders and under bump metallization (UBM) are the focused issue in flip chip technology. Two kinds of intermetallic compound (IMC), i.e. (Cu, Ni)6Sn5 and (Ni, Cu)3Sn4, formed between Sn-37Pb solder and Ni/Cu UBM. In this study, nanoindentation technique was employed to investigate the nanohardness and elastic modulus of (Cu, Ni)6Sn5 and (Ni, Cu)3Sn4 IMCs. Alloys of Cu-5wt%Ni and Ni-5w%Cu were immersed in the molten Sn at 240°C for 0.5, 1, 4, 9 hours. (Cu1-x, Nix)6Sn5 and (Ni1y, Cuy)3Sn4 IMCs were revealed. The concentration variation in the IMC was carefully measured with the aid of an electron probe microanalyzer. As compared with the property of (Cu, Ni)6Sn5 with Cu6Sn5, the hardness and elastic modulus of (Cu, Ni)6Sn5 IMC was enhanced by the dissolved Ni. In contrast, the dissolved Cu slightly decreased the hardness and elastic modulus of (Ni, Cu)3Sn4 IMC. In addition, the strain rate sensitivity of (Cu, Ni)6Sn5 and (Ni, Cu)3Sn4 IMCs was also evaluated.

# 9:45 AM

Nanoindentation of Intermetallics Formed in Pb-Free Solder Joints: Experiments and Simulation: X. Deng<sup>1</sup>; M. C. Koopman<sup>2</sup>; N. Chawla<sup>1</sup>; K. K. Chawla<sup>2</sup>; <sup>1</sup>Arizona State University, Dept. of Chem. & Matls. Engrg., Tempe, AZ 85287 USA; <sup>2</sup>University of Alabama, Dept. of Matls. Sci. & Engrg., Birmingham, AL 35294 USA

A knowledge of the elastic properties of Cu and Ag-based intermetallics, formed during reflow of Sn-rich solder joints on Cu, is extremely important in understanding and predicting the mechanical behavior of the joint. Bulk testing of these intermetallics is problematic because of the difficulty in achieving fully-dense materials, and because the microstructure in bulk form is often quite different from that observed in the joint. In this study, we have used nanoindentation to probe the mechanical properties of intermetallics in the joint in situ. The Continuous Stiffness Measurement (CSM) method was used during indentation to obtain the instantaneous Young's modulus as a function of depth. The Young's moduli of Cu6Sn5, Cu3Sn, Ag3Sn, Sn-Ag solder, pure Sn, and Cu, were measured by nanoindentation. After indentation, the surface characteristics of each phase were examined using atomic force microscopy (AFM). Significant pile-up due to dislocations was observed in Sn, Sn-Ag solder, and Cu. Finite element analysis was conducted to investigate and predict the deformation behavior during indentation and correlated very well with the experimental results.

#### 10:00 AM

Electromigration Characteristics of SnPb and SnAgCu Thin Stripe Lines: *Min-Seung Yoon*<sup>1</sup>; Shin-Bok Lee<sup>1</sup>; Young-Chang Joo<sup>1</sup>; 'Seoul National University, Sch. of Matls. Sci. & Engrg., 30-503, Seoul 151-742 S. Korea

Rapidly decreasing size of electronic packages has brought about drastic increase in the current density through the flip chip bumps, and this caused a failure due to electromigration at the bumps. We have investigated the electromigration characteristics of eutectic SnPb and SnAgCu. Thin stripe-type test structures were fabricated and tested at 80-120°C with the current densities of 4-8\*10<sup>4</sup> A/cm<sup>2</sup>. Scanning electron microscope and energy-dispersive X-ray spectroscopy were used to investigate the damaged morphology and the compositional changes. Hillocks were formed near the anode of the stripe pattern, and voids were observed at the cathode of the line. In eutectic SnPb, the content of Pb increased monotonically with the distance from the cathode to

the anode, and the activation energy for electromigration was 0.77eV. Accumulation of Ag atoms at the anode of line was observed in SnAgCu. The electromigration parameters and effects of compositional change on electromigration in solders are discussed.

# 10:15 AM Break

#### 10:30 AM Invited

Impact Reliability of Solder Joint: Masayoshi Date1; Tatsuya Shoji2; Masaru Fujiyoshi2; Koji Sato3; King-Ning Tu1; 1University of California, Dept. of Matls. Sci. & Engrg., 405 Hilgard Ave., Los Angeles, CA 90095-1595 USA; <sup>2</sup>Hitachi Metals, Ltd., Metallurgl. Rsch. Lab., Yasugi, Shimane 692-8601 Japan; 3Hitachi Metals, Ltd., Yasugi Works, Yasugi, Shimane 692-8601 Japan

When a portable electronic device drops to the ground, it may fail due to solder joint fracture. Owing to reliability concern of consumer electronic products, the measurement of impact toughness of solder joints is required. We conducted the measurement by using a small size Charpy test. Four kinds of solder balls (eutectic Sn-Pb, near-eutectic Sn-Ag-Cu, eutectic Sn-Zn and Sn-Zn-Bi) bonded to either Cu or Au/ Ni(P) pad were tested with and without aging. Among them, the Sn-Zn-Bi on the Au/Ni(P) showed the best impact toughness. Interestingly, the Sn-Zn-Bi on the Cu showed a significant loss of the toughness with aging. We also compared the impact test to the conventional shear test. They are similar in shear deformation except that the shear rate of the former is three orders higher than the latter. The results of these tests were different. The impact test revealed more failure due to interfacial fracture.

#### 10:55 AM Invited

Phase Stability and Interfacial Reaction in Palladium/Solder Diffusion Couples: Gautam Ghosh1; 1Northwestern University, Dept. of Matls. Sci. & Engrg., 2225 N. Campus Dr., Evanston, IL 60208-3108 USA

Palladium and palladium-containing alloys are commonly used as metallizations in electronic packaging. Due to high thermodynamic driving forces and also due to kinetic reasons, Pd reacts fairly rapidly with Sn-base solders. This is of particular interest due to use of Pb-free solders which are very Sn-rich. We have carried out a systematic study of interfacial reaction between Pd and solders (both Pb-Sn and Pbfree). The results show that the interfacial microstructure is time dependent. These results will be discussed in terms of phase stability of the Pd-Sn system, and also diffusion paths in Pd-Sn-X systems.

#### 11:15 AM Invited

Self-Assembled Metallic Nanodots: L. J. Chen1; 1National Tsing Hua University, Matls. Sci. & Engrg., 101, Sect. 2, Kung-Fu Rd., Hisnchu Taiwan

The fabrication of self-assembled metallic nanodots is of both fundamental interest and technological importance. Highly regular selfassembled 2-D and 3-D Au and Ag nanodots were formed using twophase reaction with a phase transfer catalyst. Honeycomb structure of metal nanoparticles on silicon was drop-cast from the metal nanoparticle solution under appropriate conditions. Hexagonal networks with discrete metal particles were generated in samples annealed in N2 ambient. NiSi, TiSi2 and CoSi2 nanodots were formed on Si0.7Ge0.3 on (001)Si with a sacrificial amorphous Si (a-Si) interlayer. The formation of the one-dimensional ordered structure is attributed to the nucleation of NiSi, TiSi2 and CoSi2 nanodots on the surface undulations induced by step bunching on the surface of SiGe film owing to the miscut of the wafers from normal to the (001)Si direction. The two-dimensional, pseudo-hexagonal structure was achieved under the influence of repulsive stress between nanodots.

#### 11:35 AM

Electromigration-Induced Cu Dissolution Rate in Sn(Cu) Flip-Chip Solder Joints: Ling Ke1; C. Y. Liu1; 1National Central University, Dept. of Chem. & Matls. Engrg., No. 300 Jung-Da Rd., Jung-Li City Taiwan

Electromigration-induced Cu dissolution has been observed by Kao. Yet, it is of important to know the rate of Cu dissolution due to the current stressing. In this study, flip-chip solder joint of Cu/Sn/Cu structure were stressed by a current density of 105 A/cm2 at three elevated temperature, which are 150°C, 180°C, 200°C. We found that the consumption of Cu foil at the current-entering interface was faster than that at the current-existing interface. By estimating the amount of Cu consumption at the current-entering interface, the Cu dissolution rates due to the current stressing were determined. Also, the activation energy of EM-induced Cu dissolution will be estimated and reported in this talk. In this talk, we will also present the effect of Cu additive on the EM-induced Cu dissolution rate. Two Sn(Cu) alloys will be studies, which are Sn0.7Cu, and Sn3.0Cu.

#### 11:50 AM

Electromigration in Flip Chip Solder Bump of 97Pb-3Sn/37Pb-63Sn Combination Structure: Jae Woong Nah1; Jong Hoon Kim1; Kyung Wook Paik1; Hyuck Mo Lee1; 1KAIST, Dept. of Matls. Sci. & Engrg., Kusung-Dong 373-1, Yusong-Gu, Taejon 305-701 Korea

Electromigration damage in the flip chip solder bump of 97wt%Pb-3wt%Sn/37wt%Pb-63wt%Sn combination structure was studied after current stressing up to 20 hr. The UBM for 97wt%Pb-3wt%Sn solder on the chip side was TiW/Cu/electroplated Cu while the bond-pad for 37wt%Pb-63wt%Sn solder on the PCB side was electroless Ni/Au. We observed in the thermo-electromigration test that failure occurred at the top of the bump with a downward electrical current flow while there was no failure in the opposite current polarity. The Pb atoms were found to move in the same direction as with the electron current flow. Therefore, in the case of downward electron flow, the composition of the upper solder bump changed from 97wt%Pb-3wt%Sn to 83wt%Pb-17wt%Sn and it enabled the Cu6Sn5 phase to precipitate at on chip side. Due to precipitation and growth of the Cu6Sn5 IMC, the Cu UBM was quickly consumed and the subsequent void formation induced failure.

#### 12:05 PM

Effects of Ni and Cu Additive on Electromigration in Sn Solder Lines: S. C. Hsu1; H. T. Chiew1; C. C. Lu1; C. Y. Liu1; Fay Hua2; <sup>1</sup>National Central University, Dept. of Chem. & Matls. Engrg., No. 300 Jung-Da Rd., Jung-Li City Taiwan; <sup>2</sup>Intel Corporation, Matls. Tech. Operation, Santa Clara, CA 95054 USA

The Cu and Ni alloying effects on Electromigration (EM) in Sn solder lines have been studied under different ambient temperatures. Small Cu additive was found to enhance EM rate. However, we found that the Ni additives retarded EM rate. The possible mechanism will be proposed during this talk and the important effective charge number of Sn(Cu) and Sn(Ni) alloys will be estimated and reported. Under elevated ambient temperature, a faster EM rate was observed. Hillock and void formation are very different from that in the room temperature. Also, the Cu and Ni additives have distinct effects on the interfacial compound morphologies under EM tests.

# Phase Transformations and Deformation in Magnesium Alloys: Solidification and Precipitation

Sponsored by: Materials Processing and Manufacturing Division, MPMD-Phase Transformations Committee-(Jt. ASM-MSCTS) Program Organizer: Jian-Feng Nie, Monash University, School of Physics and Materials Engineering, Victoria 3800 Australia

Tuesday AM	Room: 205
March 16, 2004	Location: Charlotte Convention Center

Session Chairs: Jian-Feng Nie, Monash University, Sch. of Physics & Matls. Engrg., Victoria 3800 Australia; Gordon W. Lorimer, University of Manchester/UMIST, Manchester Matls. Sci. Ctr., Manchester M1 7HS UK

## 8:30 AM Invited

Mechanisms of Grain Refinement of Magnesium Alloys: David H. StJohn1; Ma Qian1; 1University of Queensland, CAST CRC, Div. of Matls. Engrg., St Lucia, Brisbane, Queensland 4072 Australia

Unlike most other alloy systems a fine grain size is required for good creep resistance for most magnesium alloys so that a thin intermetallic phase forms along the boundaries preventing grain boundary sliding. For magnesium alloys that do not contain aluminium, zirconium is the best grain refiner. To minimise cost and thus the amount of zirconium added it is important to understand the mechanism by which zirconium refines these alloys. The mechanism revealed by recent work and the resultant improved refiner addition that was developed is described. In contrast, magnesium alloys that contain aluminium do not have a reliable and easy to use grain refiner addition. This paper describes the range of grain refining technologies that have been developed. These are considered in the light of the current theory of grain refinement. Directions for research are suggested that could lead to a commercially viable refiner for magnesium-aluminium based alloys.

#### 9:05 AM Invited

Simulations of Continuous and Discontinuous Precipitations in Mg-Al Alloys: Zi-Kui Liu1; Jingzhi Zhu1; Long-Qing Chen1; 1Pennsylvania State University, Matls. Sci. & Engrg., 209 Steidle, Univ. Park, PA 16802 USA

In Mg-Al alloys, when an  $\alpha$ -Mg phase homogenized at high temperatures is quenched to low temperatures, the Mg<sub>17</sub>Al<sub>12</sub> intermetallic phase precipitates from the  $\alpha$ -Mg matrix. Experimental observations reported in the literature showed that continuous precipitation, i.e. the direct precipitation of Mg<sub>17</sub>Al<sub>12</sub> particles from the matrix, is favored at high and low temperatures, while discontinuous precipitation, i.e. the cellular type of cooperative growth of  $\alpha$ -Mg and Mg<sub>17</sub>Al<sub>12</sub> into the  $\alpha$ -Mg matrix, dominates at intermediate temperatures. In the present work, the thermodynamic and atomic mobility databases of the Mg-Al system are integrated into the phase-field simulation to understand the transition between the continuous and discontinuous precipitations.

# 9:40 AM Invited

Precipitation in Magnesium Rare Earth Alloys: G. W. Lorimer<sup>1</sup>; <sup>1</sup>University of Manchester/UMIST, Manchester Matls. Sci. Ctr., Grosvenor St., Manchester M1 7HS UK

The precipitation sequence in binary magnesium alloys with rare earth metals of the cerium subgroup, including Mg-Nd and Mg-La, is: Mg(ssss) -> GP zones ->  $\beta$ " (DO19)' ->  $\beta$ ' ->  $\beta$ . The crystal structures of the  $\beta$ ' and  $\beta$  phases are system specific. In the binary magnesium alloys with rare earth metals of the yttrium group (except Yb) the precipitation sequence has been reported as: Mg(ssss) ->  $\beta$ " ->  $\beta$ . No GP zones have been observed and there is still considerable debate concerning the crystal structure of the phases in different alloy systems. In alloys such as WE43 and WE54, that contain rare earth metals of both the cerium and yttrium groups, the precipitation sequence can involve several intermediate precipitates: Mg(ssss) -> plates ->  $\beta$ ' (BCO) ->  $\beta_1$ (FCC) ->  $\beta$ (FCC). Extremely complicated precipitation security precipitates.

# 10:15 AM Break

# 10:30 AM Invited

Characterisation of Precipitate Phases in Mg-Zn-Al Casting Alloys: Jian-Feng Nie<sup>1</sup>; Xiao-Ling Xiao<sup>1</sup>; Laure Bourgeois<sup>1</sup>; <sup>1</sup>Monash University, Sch. of Physics & Matls. Engrg., Victoria 3800 Australia

It has recently been demonstrated that Mg-Zn-Al casting alloys are age-hardenable and exhibit creep resistance superior to that of binary Mg-Al alloys. Despite the engineering importance of this group of alloys, there is currently a lack of understanding of the structure, orientation, morphology, composition, and distribution of strengthening precipitate phases in these Mg-Zn-Al alloys and the factors that control the age hardening and creep behaviours of these alloys. The present work involves detailed characterisation using transmission electron microscopy of precipitate microstructures in Mg-8wt%Zn-(4-8)wt%Al casting alloys. It will be shown that the microstructure of peak-aged samples of the Mg-Zn-Al alloys contains predominantly a fine-scale distribution of precipitates of a ternary phase that appears to have a quasicrystalline structure. The creep resistance of these alloys will also be briefly discussed in the context of the microstructural observations.

# 11:05 AM Invited

Interfacial Structure and Orientation Relationship Between Mg<sub>17</sub>Al<sub>12</sub> and Matrix: *Wenzheng Zhang*<sup>1</sup>; Min Zhang<sup>1</sup>; Fei Ye<sup>1</sup>; <sup>1</sup>Tsinghua University, Matls. Sci. & Engrg., Beijing 100084 China

A small angular deviation from the Burgers orientation relationship (OR) between  $Mg_{17}Al_{12}$  and matrix was found and confirmed repeatedly in previous investigations. The deviation angle was first explained with a  $\Delta g$  parallelism criterion, a method originally used for calculating the primary O-lines. However, the criterion of the primary O-line structure in a habit plane is only valid for small misfit systems. For large misfit systems, such as  $Mg_{17}Al_{12}/Mg$ , the relationship between the interfacial structure and  $\Delta g$  parallelism criterion is different. This paper presents a comparison of simulated interfacial structures between  $Mg_{17}Al_{12}$  and matrix for the Burgers OR and for the OR that obeys a  $\Delta g$  parallelism rule. The result shows that a small rotation from the Burgers OR (~0.5°) can lead to singular interfacial structures in both habit plane and major side facet, so that the lattice point matching is optimized.

#### 11:40 AM Invited

Novel Structure in Rapidly Solidified Mg-Zn-RE Alloys: Yoshihito Kawamura<sup>1</sup>; Eiji Abe<sup>2</sup>; <sup>1</sup>Kumamoto University, Matls. Sci. & Engrg., 2-39-1 Kuro-kami, Kumamoto 860-8555 Japan; <sup>2</sup>National Institute for Materials Science, 1-2-1 Sen-gen, Tsukuba 305-0047 Japan

High strength Mg-Zn-Y alloys have been developed by rapidly solidified powder metallurgy (RS P/M) processing. RS P/M  $Mg_{97}Zn_1Y_2$  alloy exhibits high tensile yield strength of 610 MPa and elongation of 5%. We employ a unique atomic-resolution high-angle annular dark-field scanning transmission electron microscopy to investigate the

microstructure of recently developed nanocrystalline Mg alloys with small additions of Zn and rare earth metals. A novel long-period ordered structure was observed in the RS P/M  $Mg_{97}Zn_1Y_2$  alloy, which had a unit cell composed of six close-packed planes of the magnesium crystal, with a stacking sequence of ABCBCB' where A and B' layers are significantly enriched in Zn and Y. This result demonstrate that the additional elements of a few atomic percent to Mg can lead to formation of a long-period, chemically-ordered as well as stacking-ordered structure. Results of other RS Mg-Zn-RE alloys will also be presented.

# Processing, Microstructure and Properties of Powder-Based Materials: Session II

Sponsored by: Materials Processing and Manufacturing Division, MPMD-Powder Materials Committee

*Program Organizers:* K. B. Morsi, San Diego State University, Department of Mechanical Engineering, San Diego, CA 92182 USA; James C. Foley, Los Alamos National Laboratory, Los Alamos, NM 87545 USA; Karl P. Staudhammer, Los Alamos National Laboratory, Nuclear Materials Technology Division, Los Alamos, NM 87545 USA

Tuesday AM	Room:	208B
March 16, 2004	Locatior	n: Charlotte Convention Center

Session Chair: Karl P. Staudhammer, Los Alamos National Laboratory, Nucl. Matls. Tech. Div., Los Alamos, NM 87545 USA

# 8:30 AM Invited

**Powder Processing of Metallic Hot Gas Filters**: *Iver E. Anderson*<sup>1</sup>; Robert L. Terpstra<sup>1</sup>; Brian Gleeson<sup>1</sup>; <sup>1</sup>Ames Laboratory, Metal & Ceram. Scis., 222 Metals Dvlp., Ames, IA 50011 USA

Successful development of metallic filters with high temperature oxidation/corrosion resistance and high mechanical reliability for flyash capture is a key to enabling advanced coal combustion and power generation technologies. A beneficial metallic filter structure, composed of a thin wall (0.5mm) tube with uniform porosity (about 30 to 40%), is being developed using spherical powder processing and partial sintering, combined with porous sheet rolling and resistance welding. Modified superalloys, e.g., Ni-16Cr-9.0Al-3Fe (wt.%), are being tested in porous and bulk samples for oxide scale stability in simulated oxidizing/sulfidizing atmospheres found in combustion systems at temperatures up to 850°C. Analysis of "hanging o-ring" samples from coalfired combustion exposure testing enabled study of combined corrosion effects from particulate deposits and hot exhaust gases. Additional studies have explored the correlation between sintered microstructure, tensile strength, and permeability of porous sheet samples. Support is gratefully acknowledged from DOE-FE (ARTD) through Ames Lab contract No. W-7405-Eng-82.

## 8:50 AM

Processing, Microstructure and Uses of Borated Aluminum Metal Matrix Composites: Monte D. Hart<sup>1</sup>; Ann M. Hagni<sup>1</sup>; <sup>1</sup>EaglePicher Technologies, LLC, Boron Dept., PO Box 798, 798 Hwy. 69A, Quapaw, OK 74363 USA

Borated aluminum has been utilized in the nuclear industry for twenty years providing criticality control in spent fuel storage systems. The matrix is a precipitation hardened 6000 series aluminum alloy where strength is required and 1100 alloy for non-structural use. The process involves the reaction of a proprietary salt with molten aluminum forming secondary boride phases (either AlB2 or TiB2). The proprietary salt contains boron enriched in the B-10 isotope (> 95 wt%) for enhanced thermal neutron absorption. The borides range in size from 1-5  $\mu$ m for TiB2 and 5-10  $\mu$ m for AlB2. Semi-continuous direct chill casting is used to produce ingots for subsequent extrusion or rolling. Neutron transmittance measurement and real-time neutron radiographic inspection techniques are used to determine the concentration and dispersion of 10B. A process for the manufacture of a MMC by co-injection of B4C powder with atomized Al is currently being evaluated.

#### 9:10 AM

A Model to Predict the Damping Characteristics of Piezoelectric-Reinforced Metal Matrix Composites: A. Goff<sup>1</sup>; A. O. Aning<sup>1</sup>; S. L. Kampe<sup>1</sup>; <sup>1</sup>Virginia Tech, Matls. Sci. & Engrg., 213 Holden Hall, Blacksburg, VA 24061 USA

A numerical model based on the Eshelby equivalent inclusion method has been developed as a means to gauge the energy absorption (damping) capability of piezoelectric-reinforced metal matrix composites. The model computes the joule heating generated within a variety of metallic matrices as a consequence of the mechanical excitation of various randomly dispersed piezoelectric reinforcement formulations. The model predicts that enhanced damping performance by such a mechanism would, in general, be realized for highly conductive metallic matrices containing reinforcements with high piezoelectric capability.

# 9:30 AM

Synthesis of In Situ Piezoelectric-Reinforced Metal Matrix Composites: J. S. Franklin<sup>1</sup>; A. O. Aning<sup>1</sup>; S. L. Kampe<sup>1</sup>; <sup>1</sup>Virginia Tech, Matls. Sci. & Engrg., 213 Holden Hall, Blacksburg, VA 24061 USA

A series of in situ metal matrix composites containing dispersed piezoelectric-capable ceramic reinforcements have been synthesized using mechanical alloying or reaction synthesis techniques. Specifically, copper matrices containing 20, 30, and/or 40 volume percent of BaTiO3, PbTiO3, or ZnO have been produced and microstructurally characterized using metallographic and x-ray diffraction techniques. The results indicate that the successful in situ synthesis of a complex piezoelectric ceramic composition within a metal matrix relies on process approach, percentage of reinforcement within the formulation, and formulation chemistry.

#### 9:50 AM

# Centrifugal Infiltration of Particulate Metal Matrix Composites: Jessada Wannasin<sup>1</sup>; Merton C. Flemings<sup>1</sup>; <sup>1</sup>Massachusetts Institute of Technology, Dept. of Matls. Sci. & Engrg., 77 Mass. Ave., Rm. 8-402, Cambridge, MA 02139 USA

A novel high pressure liquid infiltration process utilizing centrifugal force is described. The high pressure obtained in this process can be used to fabricate metal matrix composites containing high volume fractions of very fine reinforcements. This paper will discuss the design and development of the process. Experimental results are presented of infiltration of Sn-Pb alloy into performs of different particle types ranging in size from 25 to 0.3 microns, and of resulting micro-structures.

## 10:10 AM Break

#### 10:20 AM

Synthesis of Ni-CaO Material from Selective Reduction of Oxide Precursors: *Benjamin C. Church*<sup>1</sup>; Thomas H. Sanders<sup>1</sup>; Robert F. Speyer<sup>1</sup>; <sup>1</sup>Georgia Institute of Technology, Matls. Sci. & Engrg., 771 Ferst Dr., Atlanta, GA 30332-0245 USA

Oxide dispersion strengthened (ODS) alloys are known for having excellent mechanical properties at elevated temperatures. Traditionally, nickel base ODS alloys have been made via mechanical alloying of metal powders. An alternative processing technique of selective reduction is used to create a dispersion of CaO in a nickel matrix. This technique is well suited for the production of Ni-ODS metal honeycomb structures made by the extrusion and subsequent reduction of metal oxide pastes. A series of Ni-CaO materials have been produced from solid solution oxide powder precursors. The reduction and sintering of the materials have been studied using x-ray diffraction and dilatometry. The structure has been observed using a combination of optical, scanning electron, and transmission electron microscopy. Processing-structure relationships are determined and issues relating to the fabrication of more complex Ni-ODS alloys (ex. Ni-Fe-Cr-CaO) using this technique are discussed.

#### 10:40 AM

Influence of Composition on Fracture Mechanism in Al-Al4C3 Materials: Michal Besterci<sup>1</sup>; Jozef Ivan<sup>2</sup>; Oksana Velgosova<sup>3</sup>; <sup>1</sup>Slovac Academy of Science, Inst. of Matls. Rsch., Watsonova 47, Kosice 04353 Slovakia; <sup>2</sup>Slovak Academy of Sciences, Inst. of Matls. & Machine Mech., Raèianska 75, Bratislava 838 12 Slovakia; <sup>3</sup>Technical University, Faculty of Metall., Dept. of Non-Ferrous Matls. & Waste Treatment, Letna 9/A, Kosice 04200 Slovakia

Method of "in-situ tensile test in SEM" is suitable for investigation of fracture mechanism because it enables to document deformation processes, by which the initiation and development of plastic deformation and fracture can be reliably described. The aim of the present study is to evaluate the influence of volume fraction of Al4C3 particles (8 and 12 vol.%) on the fracture mechanism. Detailed study of the deformation changes showed that the crack initiation is caused by decohesion, and occasionally also by rupture of the large particles. Decohesion is a result of different physical properties of different phases of the system. The Al matrix has significantly higher thermal expansion coefficient and lower elastic modulus than both Al4C3 and Al2O3 particles. Based on the microstructure changes observed in the process of deformation, the following model of fracture mechanism has been proposed.

# 11:00 AM

Mixed Rare Earth Iron Boride Powders for Bonded Isotropic Permanent Magnets: Nick Buelow<sup>1</sup>; Iver E. Anderson<sup>2</sup>; William McCallum<sup>2</sup>; Matthew J. Kramer<sup>2</sup>; Kevin Dennis<sup>2</sup>; Wei Tang<sup>2</sup>; <sup>1</sup>Iowa State University, Matls. Sci. & Engrg., 221 Metals Dvlp., Ames, IA 50011 USA; <sup>2</sup>Ames Laboratory, Metals & Ceram. Sci., Ames, IA 50011 USA

Bonded isotropic permanent magnets (BPMs) formed by injection or compression molding offer good corrosion resistance and net shape manufacturing. Substituting Y and Dy for Nd in  $Nd_2Fe_{14}B$  results in a mixed rare earth iron boride (MRE-Fe-B) for use in BPMs. MRE-Fe-B exhibits stabilization of the remanence and coercivity loss up to the Curie temperature. Extrinsically, maximum energy product (BH<sub>max</sub>) is improved by increasing the fill factor (f) of BPMs due to the reduction in BH<sub>max</sub> proportional to f<sup>2</sup>. Spherical powders, which exhibit high fill factors, made by gas atomization are being explored. Gas atomization offers rapid solidification effects that promote glass formation or uniform fine microsegregation to the particulate. Microstructures of MRE-Fe-B powders directly affect the magnetic properties of the BPMs. A review of recent activities in this area will be presented. Support from USDOE-EE is acknowledged through contract no. W-7405-Eng-82.

# 11:20 AM

Preparation of Pyroelectric Material by Spark Plasma Sintering: Kazuyuki Kakegawa<sup>1</sup>; Shinnosuke Yoshida<sup>1</sup>; Naofumi Uekawa<sup>1</sup>; <sup>1</sup>Chiba University, Fac. of Engrg., 1-33 Yayoi-cho, Inage-ku, Chibashi, Chiba 263-8522 Japan

Pyroelectric material, Pb{Zr,Ti,(Zn<sub>1/3</sub>Nb<sub>2/3</sub>)}O<sub>3</sub>, was prepared using spark plasma sintering technique (SPS). This material has a transition point between ferroelectric-ferroelectric phases, and exhibits a peak of Pyroelectric constant. The peak is too sharp, so that this cannot be used as an infrared sensor for the normal wide temperature region. A pyroelectric material that exhibits high pyroelectric coefficient over a wide temperature region was successfully prepared by a combination of different compositions and partial diffusion technique. Initially, starting material that has a desired compositional distribution was prepared. This was sintered by SPS technique SPS technique produced a sintered material without changing the compositional distribution.

# R.J. Arsenault Symposium on Materials Testing and Evaluation: Session III

Sponsored by: Structural Materials Division, SMD-Mechanical Behavior of Materials-(Jt. ASM-MSCTS), SMD-Nuclear Materials Committee-(Jt. ASM-MSCTS)

*Program Organizers:* Raj Vaidyanathan, University of Central Florida, AMPAC MMAE, Orlando, FL 32816-2455 USA; Peter K. Liaw, University of Tennessee, Department of Materials Science and Engineering, Knoxville, TN 37996-2200 USA; K. Linga Murty, North Carolina State University, Raleigh, NC 27695-7909 USA

Tuesday AM	Room: 2	11A
March 16, 2004	Location:	Charlotte Convention Center

Session Chairs: Raj Vaidyanathan, University of Central Florida, AMPAC/MMAE, Orlando, FL 32816-2455 USA; Hahn Choo, University of Tennessee, Matls. Sci. & Engrg., Knoxville, TN 37996-2200 USA

#### 8:30 AM Invited

Insights on Polycrystalline Deformation from Neutron Diffraction and In Situ Deformation: Mark A.M. Bourke<sup>1</sup>; D. W. Brown<sup>1</sup>; B. Clausen<sup>1</sup>; S. C. Vogel<sup>1</sup>; T. Sisneros<sup>1</sup>; <sup>1</sup>Los Alamos National Laboratory, MS H805, Los Alamos, NM 87545 USA

By making neutron diffraction measurements during deformation of a polycrystalline material unique physical insights can be achieved that complement other techniques. The inherently bulk sampling of a neutron measurement ensures a representative average response, whereas the diffraction physics probes deformation at the microstructural level. The SMARTS spectrometer at Los Alamos is instrumented with a 230 kN tension or compression loading capability with simultaneous temperature control from +1800 K to 77 K. Over the last two years it has been used to study a broad range of metals, ceramics and in a few cases bulk metallic glasses. Areas of study have included; composite codeformation, twinning, stress induced phase transformations, creep, and validation of polycrystalline plasticity models. This talk will illustrate, by example, the range of insights that can be achieved by making in situ neutron diffraction measurements.

# 9:00 AM Invited

Neutron Diffraction Study of Residual Stresses in Fe-Mn-Si Based Shape Memory Alloys With and Without VN Precipitates: Edward C. Oliver<sup>1</sup>; Tsutomu Mori<sup>2</sup>; Mark R. Daymond<sup>1</sup>; Philip J. Withers<sup>2</sup>; <sup>1</sup>Rutherford Appleton Laboratory, ISIS Facility, Chilton, Didcot, Oxon OX11 0QX UK; <sup>2</sup>Manchester Materials Science Centre, Grosvenor St., Manchester M1 7HS UK

The role of residual stresses in the reported improvement of shape memory behaviour in Fe-Mn-Si based alloys due to the addition of carbide or nitride precipitates has been investigated using neutron diffraction. This method provides information on the evolution of lattice strains, volume fractions and preferred orientation in both the parent and product phases. Diffraction spectra were recorded in situ during tensile loading and subsequent shape recovery heat treatment of two alloys: one a standard composition alloy, the other containing 0.2% VN precipitates. Texture changes demonstrate the preferential transformation of parent grains having <110> parallel to the tensile axis. This is close to that grain orientation having the greatest Schmid factor for the transformation shear. The precipitate-containing alloy in the virgin state exhibits as good a shape recovery as that of the standard alloy after training treatment. We associate this with back stresses caused by the presence of the non-transforming precipitates.

# 9:30 AM

#### Lattice Strain Evolution During Creep Deformation of an Austenitic Stainless Steel: *Hahn Choo*<sup>1</sup>; Wanchuck Woo<sup>1</sup>; <sup>1</sup>University of Tennessee, Matls. Sci. & Engrg., 434 Dougherty Hall, Knoxville, TN 37996-2200 USA

Intergranular strain evolution was studied during high-temperature creep deformation of an austenitic 316L stainless steel using in-situ time-resolved neutron diffraction. In this study, changes in the elastic/ plastic anisotropy were investigated as a function of time to understand the effects of accumulation of creep-induced plastic strains on the hkl-specific lattice strain evolution. A series of tensile-creep measurements were carried out between 723 and 823K under stresses corresponding to the elastic regime, power-law creep regime, and plastic regime. The relationship between the creep-induced lattice strain behavior and plastic anisotropy obtained from a tension test is discussed. In particular, the crystallographic anisotropy (e.g., behavior of plastically-deforming and load-bearing orientations) and geometrical anisotropy (i.e., axial and transverse behavior) are discussed as well as the signs and magnitudes of the lattice strains accumulated with time during the creep deformation. These observations provide a fundamental understanding of creep-induced elastic-lattice strain evolution in a single-phase, polycrystalline fcc alloy.

#### 9:50 AM

A Neutron Diffraction Investigation of Linear Superelasticity in NiTi: C. R. Rathod<sup>1</sup>; B. Clausen<sup>2</sup>; M. A.M. Bourke<sup>2</sup>; Raj Vaidyanathan<sup>1</sup>; <sup>1</sup>University of Central Florida, AMPAC/MMAE, Engr-I Rm. 381, 4000 Central Florida Blvd., Orlando, FL 32816-2455 USA; <sup>2</sup>Los Alamos National Laboratory, Los Alamos, NM 87545 USA

The superelastic effect in NiTi occurs due to a reversible stressinduced phase transformation from a cubic austenite phase to a monoclinic martensite phase. There is usually a hysteresis associated with the forward and reverse transformations which translates to a hysteresis in the stress-strain curve during loading and unloading. This hysteresis is reduced in cold-worked NiTi and the macroscopic stressstrain response is more linear, a phenomenon called linear superelasticity. Here we report on in situ neutron diffraction measurements during loading and unloading in plastically deformed (up to 11%) NiTi. The experiments relate the macroscopic stress-strain behavior (from an extensometer) with the texture, phase volume fraction and strain evolution (from neutron diffraction spectra) in linear superelastic NiTi. This work is supported by NASA and NSF (CAREER DMR-0239512).

# 10:10 AM Break

#### 10:30 AM

Nuclear Spin Relaxation for In-Situ Characterization of Dynamical Behavior of Line and Point Defects During Deformation of Materials: K. Linga Murty<sup>1</sup>; Otmar Kanert<sup>2</sup>; <sup>1</sup>North Carolina State University, Coll. of Engrg., Burlington Engrg. Labs., Box 7909, Raleigh, NC 27695-7909 USA; <sup>2</sup>Universitat Dortmund, 44221 Dortmund Germany

Nuclear spin relaxation rates (NSR) were determined using NMR pulse techniques to characterize the dynamical behavior of vacancies (atomic motion/diffusion) and dislocations (jump distances) during deformation of pure and doped alkali halide single crystals (NaCl and NaF) and thin (25 mm thick) pure (99.999%) Al foils. Spin-lattice relaxation times in rotating frame (T1r) enabled an evaluation of the

dislocation jump distances in NaCl during constant strain-rate deformation and creep at temperatures below about 500K, while atomic motion dominated at higher temperatures. Effects of impurities are considered by examining NaCl single crystals doped with Ca++ and K+. The mean jump distance of the mobile dislocations, evaluated from the NSR without deformation and during creep, decreased (from around 200b) with time/strain reaching a constant value (around 20b) during the steady-state creep regime. These jump distances are orders of magnitude smaller than the subgrain size and dislocation-dislocation spacing while are in good agreement with the climb distances predicted by Weertman's pill-box model (60b) and Arsenault's computer simulations involving climb of dislocations in the subgrain boundaries (10b-30b). At higher temperatures, the relaxation was seen to be due to point defect diffusion that was enhanced by excess vacancies produced during deformation. CUT-sequence pulse technique allowed an evaluation of the strain-induced vacancy concentration as a function of strain-rate, strain and temperature in NaCl, NaF and Al. Experimental results correlated with models based on vacancy production through mechanical work (versus thermal jogs) while in-situ annealing of excess vacancies becomes important at higher temperatures. The investigations clearly reveal the utility of NMR in non-evasively characterizing the dynamical behavior of defects in materials during deformation.

# 10:50 AM

In Situ Neutron Diffraction Studies on the Fatigue of Haynes 230® Nickel Based Superalloy: *Tarik A. Saleh*<sup>1</sup>; Michael L. Benson<sup>1</sup>; Hahn Choo<sup>1</sup>; Peter K. Liaw<sup>1</sup>; Raymond A. Buchanan<sup>1</sup>; Mark A.M. Bourke<sup>2</sup>; Bjorn Clausen<sup>2</sup>; Donald W. Brown<sup>2</sup>; Thomas Sisneros<sup>2</sup>; Dwaine L. Klarstrom<sup>3</sup>; <sup>1</sup>University of Tennessee, Dept. of Matls. Sci., 434 Dougherty, Knoxville, TN 37996-2200 USA; <sup>2</sup>Los Alamos National Laboratory, Manuel Lujan Jr. Neutron Scattering Ctr., Los Alamos, NM 87545 USA; <sup>3</sup>Haynes International, Inc., Kokomo, IN 46904-9013 USA

Haynes 230, a single phase FCC, Ni based superalloy, shows anomalous fatigue behavior: the fatigue life is shorter at high strains at 816°C than at 927°C. Previous work with neutron diffraction in fatigue has shown the development and disappearance of residual strains as fatigue progresses. To explore this effect in Haynes 230 we have performed neutron diffraction at the Spectrometer for Materials Research at Temperature and Stress (SMARTS) facility at the Los Alamos Neutron Science Center (LANSCE). Specimens of Haynes 230 alloy were subjected to hold time, an R ratio of 0.1, a  $\sigma_{max} = 1.75 * \sigma_{yield}$ , at 3 separate temperatures: 23°C, 816°C and 923°C. The sample was held for 15 minutes at the  $\sigma_{max}$  of each cycle, during which a diffraction pattern was taken. The hkl and lattice strains were monitored in both the transverse and loading direction for each cycle for approximately 100 cycles. The evolution of residual elastic strains in the polycrystal-line matrix is discussed in the context of constitutive behavior and fatigue lifetime.

#### 11:10 AM

Texture and Strain Measurements During Tensile-Compressive Loading of Shape-Memory NiTi: A. L. Little<sup>1</sup>; C. R. Rathod<sup>1</sup>; D. W. Brown<sup>2</sup>; M. A.M. Bourke<sup>2</sup>; Raj Vaidyanathan<sup>1</sup>; <sup>1</sup>University of Central Florida, AMPAC/MMAE, Engr-I Rm. 381, 4000 Central Florida Blvd., Orlando, FL 32816-2455 USA; <sup>2</sup>Los Alamos National Laboratory, Los Alamos, NM 87545 USA

Shape-Memory NiTi differs in its mechanical response under tension and compression. Neutron diffraction measurements during loading offer a way to obtain in situ texture and strain measurements from bulk, polycrystalline samples. Here we report on in situ neutron diffraction measurements during tensile and compressive loading of polycrystalline shape-memory martensitic NiTi with no starting texture. The diffraction spectra are analyzed to follow the texture and strain evolution due to twinning and elastic deformation in martensitic NiTi. Both single peak fits and Rietveld refinement of diffraction spectra are used to link the macromechanical and micromechanical behaviors in tension and compression and examine reasons for the differences. This work is supported by NASA and NSF (CAREER DMR-0239512).

# 11:30 AM

Non-Destructive Evaluation of Micro-Strains in High-Cycle Fatigue by Neutron Time-of-Flight Diffraction: Alexandru Dan Stoica<sup>1</sup>; Xun-Li Wang<sup>1</sup>; Derek J. Horton<sup>2</sup>; Yan Dong Wang<sup>1</sup>; Hongbo Tian<sup>2</sup>; Peter K. Liaw<sup>2</sup>; James W. Richardson<sup>3</sup>; Even Maxey<sup>3</sup>; <sup>1</sup>Oak Ridge National Laboratory, Spallation Neutron Source, 701 Scarboro Rd., Oak Ridge, TN 37830 USA; <sup>2</sup>University of Tennessee, Dept. of Matls. Sci. & Engrg., Rm. 427-B Dougherty Engrg. Bldg., Knoxville, TN 37996-2200 USA; <sup>3</sup>Argonne National Laboratory, Intense Pulsed Neutron Source, Argonne, IL 60439 USA Neutron time-of-flight diffraction was used to study 316 stainless steel under high-cyclic fatigue. The experimental data show that in early stage of fatigue testing, the grain-orientation-dependent intergranular strain oscillates between two extreme states with identical symmetry but a sign reversal, as the cyclic deformation includes successive loadings in tension and compression. In late stage, the intergranular strain vanishes for tests ending in tension and remains the same for tests ending in compression. The different behaviours in tension and compression are related to the crack initiation and growth characteristics of fatigue tests. As the diffraction contrast is sensible to the dislocations type and distribution, the elastic intra-granular strain developed around immobile dislocations (mainly of edge type) can be evaluated, as well as the energy stored into the distorted lattice. The intra-granular strain evolution is a fingerprint of the material hardening process and can be related with the successive stages of deformation.

# Solidification of Aluminum Alloys: Microstructural Evolution I

Sponsored by: Materials Processing & Manufacturing Division, MPMD-Solidification Committee

*Program Organizers:* Men Glenn Chu, Alcoa Inc., Alcoa Technical Center, Alcoa Center, PA 15069 USA; Douglas A. Granger, GRAS, Inc., Murrysville, PA 15668-1332 USA; Qingyou Han, Oak Ridge National Laboratory, Oak Ridge, TN 37831-6083 USA

Tuesday AM	Room:	207B/C		
March 16, 2004	Location	Charlotte	Convention	Center

Session Chairs: Men G. Chu, Alcoa Inc., Alcoa Technical Center, Alcoa Ctr., PA 15069 USA; Qingyou Han, Oak Ridge National Laboratory, Metals & Ceram. Div., Oak Ridge, TN 37831-6083 USA

# 8:30 AM Opening Remarks

# 8:35 AM Keynote

Phase Formation and Solidification Path Analysis of Multicomponent Aluminum Alloys: *Austin Chang*<sup>1</sup>; Fanyou Xie<sup>2</sup>; Xinyan Yan<sup>3</sup>; Shuanglin Chen<sup>2</sup>; <sup>1</sup>University of Wisconsin, Dept. of Matls. Sci. & Engrg., 1509 Univ. Ave., Madison, WI 53706 USA; <sup>2</sup>CompuTherm, LLC, Madison, WI USA; <sup>3</sup>Alcoa Technical Center, PMD, 100 Tech. Dr., Alcoa Ctr., PA 15069 USA

A metallurgist can, in many cases, forecast the phase formation sequence or solidification path of a ternary alloy when its liquidus projection is known. However, the task becomes more challenging for a higher order system even when the liquidus projection is available. In actuality, these projections are rarely available for these systems. However, recent advancement achieved in phase diagram calculations resolves this dilemma. In the presentation we will show that the predicted solidification paths of multicomponent aluminum alloys using a simple Scheil model coupled with phase diagram calculation are in reasonable agreement with experiments. An example will be also presented to demonstrate its utility in welding research and practice. On the other hand, the calculated microsegregations within the dendrites using the Scheil model is not satisfactory. However, when coarsening, back diffusion and undercooling are incorporated with the basic Scheil model, the calculated microsegregations are in accord with results obtained from directional solidification.

# 9:05 AM

Conduction and Radiation Parameters for Analytical Models of Differential Scanning Calorimetry Instruments: Adrian S. Sabau<sup>1</sup>; Wallace D. Porter<sup>2</sup>; Jay I. Frankel<sup>3</sup>; <sup>1</sup>Oak Ridge National Laboratory, Metals & Ceram. Div., Bldg. 4508, MS 6083, Oak Ridge, TN 37831-6083 USA; <sup>2</sup>Oak Ridge National Laboratory, High Temp. Matls. Lab., Bldg. 4515, MS 6064, Oak Ridge, TN 37831 USA; <sup>3</sup>University of Tennessee, Mech. & Aero. Engrg. & Engrg. Sci. Dept., 402 Dougherty Hall, Knoxville, TN 37996-2210 USA

The Differential Scanning Calorimetry (DSC) measurements are routinely used to determine enthalpies of phase change, phase transition temperatures, and heat capacities. DSC data has also been used to estimate the fractional latent heat release during phase changes. To date, DSC measurements are plagued by temperature lags due to the use of thermocouples that are placed at different location than that of the sample. In this study, the temperature lags, which are inherent to the measurement process, are estimated through a computational analysis of the raw DSC data. An analytical model is presented that accounts for different heat transfer mechanisms among instrument components. Through a direct analysis of an experimental data set, it is shown that the proposed analytical model can accurately describe the experimental data. The direct analysis presented is to be complemented by inverse process analysis in order to determine more accurate values for the model parameters.

#### 9:25 AM Keynote

Nucleation and Growth Temperature and the Formation of Microstructure in Steady State Solidification of Aluminum-Based Alloys: *Howard Jones*<sup>1</sup>; <sup>1</sup>University of Sheffield, Dept. of Engrg. Matls., Sir Robert Hadfield Bldg., Mappin St., Sheffield S1 3JD UK

Recent work (primarily by the author and his collaborators) on measurement of formation temperature of constituents of Al-based alloys under Bridgman solidification conditions is reviewed. Together with associated microstructural observations, the results indicate control by heterogeneous nucleation in the case of polygonal primary silicon in Al-18.3wt % Si alloy, while competitive growth is controlling in the case of aluminide dendrites in Al-Fe, Al-Ni and Al-Ce or La alloys, for which measured tip undercoolings are in good agreement with values calculated from dendrite growth models. Extrapolation to zero growth velocity of measured growth temperatures of eutectics in such systems agree closely with reliable values by other methods and values of kinetic constants A and BEU for dendrites and eutectic derived from measured velocities for extinction of the dendritic constituent are shown to be in accord with direct measurements. The sometimes dramatic effects of ternary alloy or trace additions remain to be fully explored.

## 9:55 AM

**Modelling of Microstructural Evolution in Bridgman Specimens**: *T. E. Quested*<sup>1</sup>; A. L. Greer<sup>1</sup>; <sup>1</sup>University of Cambridge, Dept. of Matls. Sci. & Metall., Pembroke St., Cambridge CB2 3QZ UK

A Bridgman furnace is used to investigate fundamental issues associated with solidification during DC casting (e.g. primary microstructure and secondary-phase selection). Thin, cylindrical specimens held in alumina sheaths are directionally solidified by their controlled removal from the furnace into a quenching water bath. Modelling and experiment has been carried out to determine the microstructural evolution of Al-Mg alloys inoculated with TiB2 within the Bridgman furnace. Two approaches to modelling were used: (a) cellular-automaton finite-element (CAFE) software Calcosoft2D® to create graphic representations of the predicted primary microstructures; (b) simulations which calculate the evolution of volume fraction of solid given laws governing dendritic growth rates and grain initiation events; grain initiation is assumed to be determined by the free-growth criterion, rather than by nucleation itself. This allows prediction of grain size and the steady-state conditions for the columnar-to-equiaxed transition.

# 10:15 AM Break

#### 10:35 AM

Directional Solidification of Type AA3003 Alloys with Additions of Zn and Si: Majed Jaradeh<sup>1</sup>; *Torbjörn Carlberg*<sup>1</sup>; <sup>1</sup>Mid Sweden University, Engrg., Physics & Math., Holmgatan 10, Sundsvall 85170 Sweden

To improve alloys of the AA3003 type for heat exchanger applications it is important to increase the basic knowledge of structure formation during solidification. A technique, to study the effect of different alloy additions and solidification parameters on the structure formation, is Bridgman directional solidification with quenching. In the first phase of this work parameters, such as growth rate and temperature gradient, have been adjusted to simulate the solidification in DC cast ingots, and a comparison has been made between Bridgman grown and DC cast structures. Modifications of the alloy by Zn additions improve the strength of the matrix of the material through solid solution hardening. At a level of 5% the hardness is improved by about 50%, but the solidification structure becomes less promising. The DAS and the secondary phases become coarse, and the solidification range increases significantly as the Zn content increases from 2.5 to 5%.

#### 10:55 AM

Characterization by the p\* Method of Eutectic Aggregates Spatial Distribution in As-Cast 3xxx and 5xxx Aluminum Alloys Cast in Wedge Molds and Comparison with SDAS Measurements: *Philippe P. Jarry*<sup>1</sup>; <sup>1</sup>Pechiney CRV, BP27, Voreppe F-38341 France

In order to quantitatively compare the microsegregation patterns of as cast aluminum alloys, and in the future, to objectively compare computed microstructures with real ones, a quantitative metallography index named p\* for as cast microstructures based on an image analysis algorithm has been developed within Pechiney and shared among the participants of the European project VIRCAST. The present paper presents the results of a benchmark study done by all participants within the project on the use of the p\* measurement, on two families of alloys (3xxx and 5xxx) cast in Corus laboratories in a wedge shaped mold in order to scan various solidification rates. It is shown that the p\* algorithm provides a quantitative and reliable assessment of the average size of particle free zones in as cast microstructures as long as proper parameters are used in terms of sampling vs resolution compromise. The p\* values have been shown to correlate with the main alloy and solidification parameters (cooling rate, grain refinement, eutectic fraction) inasmuch as these parameters exert interactive influences on the morphological or topological patterns of the solidification structure.

# 11:15 AM

Solidification of Aluminum Alloy A356 Under Ultrasonic Vibration: X. Jian<sup>1</sup>; Q. Han<sup>2</sup>; H. Xu<sup>1</sup>; T. T. Meek<sup>1</sup>; S. Viswanathan<sup>3</sup>; <sup>1</sup>University of Tennessee, Matl. Sci. & Engrg., 434 Dougherty Bldg., Knoxville, TN 37996 USA; <sup>2</sup>Oak Ridge National Laboratory, Metals & Ceram. Div., Bethel Valley Rd., PO Box 2008, Oak Ridge, TN 37831-6083 USA; <sup>3</sup>Sandia National Laboratories, Albuquerque, NM 87185-1134 USA

Ultrasonic vibration has been shown to be an effective way of obtaining globular grains, but its influence on the nucleation and growth grains is unclear. In the present study, thermodynamic simulations were carried out to determine the temperature versus solid fraction curve of AA 3004 alloy. The alloy was then treated at various temperatures using ultrasonic vibrations. Color metallography was employed to reveal grain size of the specimens. Initial results indicate that it's difficult to obtain globular grains if the specimens are treated at temperatures in the mushy zone. This means that dendrite fragmentation may play a less important role in producing globular grains. Applying ultrasonic vibrations to the alloy close to its liquidus temperatures resulted in fine globular grains if the treated specimens were cooled quickly. The experimental results suggest that nucleation plays a key role in the formation of globular grains when the specimens are under ultrasonic vibrations.

#### 11:35 AM

Formation of Iron-Rich Intermetallic Phases During Solidification of Aluminum Casting Alloys: Liming Lu<sup>1</sup>; Arne K. Dahle<sup>1</sup>; Mal J. Couper<sup>2</sup>; <sup>1</sup>The University of Queensland, CRC for Cast Metals Mfg. (CAST), Div. of Matls., Sch. of Engrg., Brisbane, Queensland 4072 Australia; <sup>2</sup>Comalco Research and Technical Support, 15 Edgars Rd., Thomastown, Vic 3074 Australia

Iron is the most common and detrimental impurity in aluminum casting alloys and has long been associated with impaired properties and often an increase in casting defects. While the negative effects of iron are clear, the mechanism involved is not fully understood. It has generally been associated with the formation of iron-rich intermetallic phases. However, the conditions that control the formation of these phases are not well understood. Many factors, including solute elements, melt treatment, iron level and cooling rate, could play a role. In the present study, the interactions between iron and other common alloying elements in aluminum casting alloys were investigated. The iron-rich intermetallic phases were characterized using the electron probe microanalysis technique (EPMA) and compared with the results predicted from Thermocalc. The implications of these iron-effects on eutectic solidification and casting defect formation are also outlined.

# Solidification Processes and Microstructures: A Symposium in Honor of Prof. W. Kurz: Microstructures

Sponsored by: Materials Processing & Manufacturing Division, MPMD-Solidification Committee

*Program Organizers:* Michel Rappaz, Ecole Polytechnique Fédérale de Lausanne, MXG, Lausanne Switzerland; Christoph Beckermann, University of Iowa, Department of Mechanical Engineering, Iowa City, IA 52242 USA; R. K. Trivedi, Iowa State University, Ames, IA 50011 USA

Tuesday AM	Room: 207D
March 16, 2004	Location: Charlotte Convention Center

Session Chair: Rohit Trivedi, Iowa State University, Ames, IA 50011 USA

# 8:30 AM Invited

Dendritic Scaling Laws: Application to Microstructure Prediction: Martin E. Glicksman<sup>1</sup>; <sup>1</sup>Rensselaer Polytechnic Institute, Matls. Sci. & Engrg., 110 8th St., CII-9111, Troy, NY 12180-3590 USA

Understanding the kinetics of dendritic growth is essential for controlling solidification processes and microstructures, and for improving modeling at small scales. The Isothermal Dendritic Growth Experiments (IDGE) is a series of microgravity experiments designed to study dendrites in ultra-pure materials. Data resulting from these spaceflight experiments reveal fundamental aspects of the solidification process: 1) thermal transport occurring at mesoscopic scales, 2) microstructural scaling laws, 3) dynamic shapes of dendrites, and 4) the possible presence of eigenfrequencies during growth. It was found that once convection phenomena in the melt are suppressed adequately, diffusion-limited models become reliable. Scaling laws connecting microstructure length scales and growth rates were found to be robust and independent of convection in the melt, permitting applications of the theories to many metallic systems, including alloys. The author and Professor Kurz have collaborated on these topics, and it is with considerable pleasure to recount this activity in his honor.

#### 9:00 AM Invited

Selection of Eutectic Carbides in Multi-Component High Speed Steel Type Cast Irons: Takateru Umeda<sup>1</sup>; Toshimitsu Okane<sup>2</sup>; <sup>1</sup>Chulalongkorn University, Fac. of Engrg., Dept. of Metallurgl. Engrg., Phayathai Rd., Phathumwan, Bangkok 10330 Thailand; <sup>2</sup>National Institute of Advanced Industrial Science and Technology, Digital Mfg. Rsch. Ctr., 1-2-1 Namiki, Tsukuba-shi, Ibaraki 305-8564 Japan

High speed steel type cast iron to maintain high fracture toughness and wearing resistance is necessary to control eutectic carbides,  $M_3C$ ,  $M_7C_3$ ,  $M_6S$ ,  $M_2C$  and MC. To predict carbide formation under certain solidification conditions of multi-component cast iron, interface temperature analysis and quantitative maximum temperature criterion are needed. Interface undercooling, DT, for eutectic growth was given as a function of growth rate, V; DT=kV1/2. Interface temperature of each eutectic carbide formed in Fe-M-C (M; Cr, V, Mo) systems;  $g + M_3C$  and  $g + M_7C_3$  eutectics in the Fe-C-C system, g + VC eutectics in Fe-V-C system and  $g + M_6C$  and  $g + M_2C$  eutectics in Fe-Mo-C system, was measured during unidirectional solidification process. The k values of eutectic carbides were then estimated. Relationships between k, carbide spacing and growth rate were discussed. Application of k values obtained in ternary systems to more multi-component systems was also discussed.

# 9:30 AM

Extending the Lipton-Kurz-Trivedi Dendrite Growth Model into the Two-Phase Regime: *Douglas M. Matson*<sup>1</sup>; Joan E. Kertz Yurko<sup>2</sup>; Robert W. Hyers<sup>3</sup>; <sup>1</sup>Tufts University, Mech. Engrg., 200 College Ave., 025 Anderson, Medford, MA 02155 USA; <sup>2</sup>Massachusetts Institute of Technology, Dept. of Matls. Sci. & Engrg., 77 Mass Ave., Cambridge, MA 02139 USA; <sup>3</sup>University of Massachusetts, Dept. of Mech. & Industrial Engrg., 160 Governors Dr., Engrg. Lab Bldg., Amherst, MA 01003 USA

The rapid solidification transformation behavior of Fe-Cr-Ni steel alloys was examined using electromagnetic levitation and high-speed imaging. A revision of the Lipton-Kurz-Trivedi growth model is proposed to explain the observed acceleration of growth rates for the stable austenite phase following primary solidification of metastable ferrite. This model is based on an effective mushy zone heat capacity where an additional heat rejection mechanism exists involving isothermal melting of the pre-existing metastable solid to promote enhanced dendritic growth.

# 9:45 AM

The Effect of Dimensionality on Microstructures in Directionally Solidified SCN-Salol Alloys: Shan Liu<sup>1</sup>; Myung-Jin Suk<sup>1</sup>; Rohit K. Trivedi<sup>1</sup>; <sup>1</sup>Iowa State University, Ames Lab.-USDOE, Ames, IA 50011 USA

Directional solidification has been conducted in SCN-Salol system with an emphasis on morphological evolution and pattern formation under different geometrical conditions. There are two sample configurations used in this study: traditional thin sandwiched glass cell and capillary tube. For thin sample cells, five different thicknesses were used: 12, 25, 50, 100 and 200  $\mu$ m. While keeping alloy composition, temperature gradient and growth velocity the same, we found that the growth morphology is significantly dependent on the sample thickness. For example, in a 12  $\mu$ m thick sample, cells cannot form even at a velocity <1.0  $\mu$ m/s; while for a sample larger than 100  $\mu$ m, smooth cells have been observed across solid/liquid interface. For capillary samples, three diameters-45, 75 and 100  $\mu$ m-have been employed and the cellular patterns in these capillaries will be presented to disclose the scaling relationship among the different length scales describing cellular growth morphology.

Characteristic Substructure in Directionally Solidified Dilute Al-Cu Alloys: Osvaldo Fornaro<sup>1</sup>; Hugo A. Palacio<sup>2</sup>; Heraldo Biloni<sup>3</sup>; <sup>1</sup>University Nacional del Centro de la Provincia de Buenos Aires, IFIMAT-Fac. Cs. Exactas & CONICET, Pinto 399, Tandil B7000GHG Argentina; <sup>2</sup>University Nacional del Centro de la Provincia de Buenos Aires, IFIMAT-Fac. Cs. Exactas & CICPBA, Pinto 399, Tandil B7000GHG Argentina; <sup>3</sup>CICPBA

Al-0.2 wt.% Cu alloy samples were directionally solidified under similar thermal gradient conditions. As the growth velocity was increased, the transition among successive stages from planar, nodes, bidimensional, regular and irregular cells, was characterized through careful metallographic analysis of the microsegregation. During the different transitions, a nodal precipitation mechanism seems to be responsible for the evolution of the substructure, where the eutectic precipitation at the nodes plays a fundamental role in the fixation of the substructure. During planar to bands transition, the nodes slow down the interface in certain critical points of it, and the primary spacing can be well defined. This phenomenon seems to be similar during the transition of all the substructure stages under study. The primary spacing fits the order of magnitude of maximum rate wavelength predicted by Morphological stability theory. In several cases, a second order microsegregation pattern at cellular wall level has been observed, that seems to be due to small variation in the microsegregation during the lateral growth of the cells in an enriched intercellular liquid. The secondary microsegregation pattern detected has a rugosity close to the minimum unstable wavelength.

10:15 AM Break

#### 10:45 AM

Effect of Lead and Antimony on the Grain Structure of Directionally Solidified Zn-Al Alloys: *M. Rappaz*<sup>1</sup>; A. S. Quiroga<sup>1</sup>; A. Sémoroz<sup>2</sup>; <sup>1</sup>EPFL, Inst. of Matls., Computational Matls. Lab., MXG, Lausanne CH-1015 Switzerland; <sup>2</sup>Alstom (Switzerland) Ltd., TGTT-D, Pav. 4, Baden CH-5400 Switzerland

Zinc alloys with 0.2% Al are widely used to protect steel sheets against corrosion. The thin coatings (typically 20-30 µm), deposited by hot dipping, exhibit fine grains (typically 1 mm in diameter), but with small additions of lead or antimony, the grains become much larger (typically 1 cm). In order to investigate this phenomenon, bulk specimens have been solidified in a standard Bridgman (SB) furnace and in a water-cooled directional solidification (DS) experiment. In this last device, a pre-coated steel sheet was immersed in the melt parallel to the solidification direction in order to induce a competition between regular columnar grains and grains nucleated on the substrate and growing in a transverse direction. In the SB specimens, it was found that the structure changed from columnar to equiaxed when the Al content was increased from 0.2 wt% to 3 wt%. However, with 0.11 wt% Pb addition, the Zn - 3 wt%Al exhibited again a fully columnar structure. In Zn-0.2%Al DS alloys, the structure was columnar almost up to the top of the specimen, but transverse grains could form at the surface of the sheet. Their extension was analyzed using a model similar to that of Hunt for the columnar-to-equiaxed transition. With small additions of Sb, these transverse grains totally disappeared. From microstructure observations and EBSD analyses, it is concluded from both experiments that Pb and Sb most likely poison the nucleation sites.

# 11:00 AM

Peritectic Reaction in Fe-Co Alloys: Neill John McDonald<sup>1</sup>; Sridhar Seetharaman<sup>1</sup>; <sup>1</sup>Carnegie Mellon University, Matls. Sci. & Engrg., 5000 Forbes Ave., Pittsburgh, PA 15213 USA

Recent work by Professor Kurz along with Dr. Sumida studied the directional solidification of Fe-Co peritectic alloys in order to reevaluate the Fe-rich part of the phase diagram. Comparing the results of Thermocalc modeling to those of Harris and Hume-Rothery Kurz and Sumida found that there was a significant difference and a new phase diagram, based on experiments completed with a Bridgmann apparatus, was suggested. Using the Confocal Scanning Laser Microscope (CSLM) at Carnegie Mellon University, an investigation of the solidus and liquidus temperatures for hypo- and hyperperitectic Fe-Co samples was performed and the results compared with those of Kurz and Sumida. Also, the rate of austenite formation and growth along the delta-ferrite/liquid boundary was measured and compared to available plate-growth models and past CSLM observations for Fe-Ni. Finally, wavelength dispersive spectroscopy was used to measure the cobalt concentration through the various phases present.

#### 11:15 AM

On Crystallographic Effects in Thin and Bulk Lamellar Eutectic Growth: Gabriel Paul Faivre<sup>1</sup>; <sup>1</sup>CNRS, GPS (Groupe de Physique des Solides, GPS - Campus Boucicaut -140 Rue de Lourmel -F-75015, Paris 75015 France

We study the effects of a weak surface tension anisotropy on lamellar eutectic microstructures. We report in situ observations made in 10µm and 300-µm thick, single-grain samples of the transparent alloy CBr<sub>4</sub>-C<sub>2</sub>Cl<sub>6</sub>, and calculations performed in a planar-front approximation. We find that a stationary lamellar pattern actually travels laterally at a definite rate v<sub>d</sub>, which is of the order of  $10^{-2}xV$  (V: solidification rate), depends on the orientation of the two solid phases, and thus changes from a eutectic grain to another. Therefore, lamella terminations, lamella creations and other dynamical defects occur repetitively along eutectic grain boundaries, preventing the pattern from reaching a stationary state in multigrain samples. This may explain the permanent dispersion of the lamellar spacing observed in long-lasting solidification runs, and the fact that lamellar mismatches ("faults") are observed in transverse cross-sections along subgrain boundaries.

## 11:30 AM

**Mechanisms of Morphological Selection in Al-Si Eeutectics**: *Ralph E. Napolitano*<sup>1</sup>; Luke G. England<sup>1</sup>; Choonho Jung<sup>1</sup>; Halim Meco<sup>1</sup>; 'Iowa State University, Dept. of Matls. Sci. & Engrg., 204A Wilhelm Hall, Ames, IA 50011 USA

Morphological transitions in Al-Si eutectic solidification are investigated experimentally at both high and low growth rates. Si growth morphology, branching mechanisms, and the selection of overall eutectic structure are examined at directional solidification rates ranging from 5x10-7 to 2x10-3 m/s. Time evolution of Si particle morphology, interface structure, phase distribution, and crystallographic orientation are measured. Mechanisms of spacing adjustment and crystallographic competition are examined, and the role of interfacial properties is discussed.

#### 11:45 AM

**3D** Observation of Eutectic Structure of Al<sub>2</sub>O<sub>3</sub>-YAG System: *Hideyuki Yasuda*<sup>1</sup>; Itsuo Ohnaka<sup>1</sup>; Akira Sugiyama<sup>1</sup>; Yoshiki Mizutani<sup>1</sup>; Yishiharu Waku<sup>2</sup>; Akira Tsuchiyama<sup>3</sup>; Tsukasa Nakano<sup>4</sup>; Kentaro Uesugi<sup>5</sup>; <sup>1</sup>Osaka University, Dept. of Adaptive Machine Sys., Yamadaoka 2-1, Suita, Osaka 5650871 Japan; <sup>2</sup>UBE Industries, Ube Rsch. Lab., Ube, Yamaguchi 7558633 Japan; <sup>3</sup>Osaka University, Dept. of Earth & Space Sci., Toyonaka, Osaka 560-0043 Japan; <sup>4</sup>National Institute of Advanced Industrial Science and Technology, Geological Survey of Japan, Tsukuba, Ibaragi 3058567 Japan; <sup>3</sup>Japan Synchrotron Radiation Research Institute, Mikazuki, Hyogo 6795198 Japan

The unidirectionally solidified Al<sub>2</sub>O<sub>3</sub>-YAG(Y<sub>3</sub>Al<sub>5</sub>O<sub>12</sub>) eutectic composites have excellent mechanical properties at high temperatures and their mechanical properties are closely related to the characteristic eutectic structure. 3D observation will be useful to understand the structure development, since unidirectionally solidified specimens remain time-evolution of the eutectic structures in the growth direction. This paper presents 3D observation of eutectic structures of Al<sub>2</sub>O<sub>3</sub>-YAG oxide system and metallic systems (Sn-Pb and Sn-Bi alloys). The micro X-ray computer tomography using monochromatized X-ray of a synchrotron radiation source and a high-resolution detector (0.5mm/ pixel) was performed for 3D observation. In the Al<sub>2</sub>O<sub>3</sub>-YAG composite, both phases were continuous and the sequential branching of Al<sub>2</sub>O<sub>3</sub> and YAG in the growth direction resulted in the characteristic eutectic structure in which the constituent phases were entangled each other. The branching sequence was significantly different from the metallic alloys exhibiting the regular and the irregular eutectic structure.

## 12:00 PM

Lamellar/Rod Transition in Al-Cu Alloys: Shan Liu<sup>1</sup>; Jehyun Lee<sup>2</sup>; Rohit K. Trivedi<sup>1</sup>; <sup>1</sup>Iowa State University, Ames Lab.-USDOE, Ames, IA 50011 USA; <sup>2</sup>Changwon National University, Dept. of Metall., Changwon S. Korea

It is generally accepted that binary eutectic either takes lamellar or rod-like form and the transition between them depends on the volume fraction of the minor constituent in the eutectic structure. Through detailed experimental studies in Al-Cu system, we have examined the regimes of the stability of these two morphologies and characterized the dynamics of the transition. We found that the transition is not sharp and the two morphologies can co-exist over a range of volume fraction of the minor phase. Experiments in hyper-eutectic alloys showed that the inter-dendritic or inter-cellular eutectic would always be lamellar. However with the disappearance of the primary phase, the eutectic first becomes rod-like; and then rod and lamellar eutectic coexist over the cross-section of the sample with the rod eutectic region located in the center of the sample. A modified criterion for the regimes of their stability is developed. Phase Selection in Unidirectional Growth of Sn-Ag3Sn Eutectic Alloy: *Hisao Esaka*<sup>1</sup>; Kei Shinozuka<sup>1</sup>; Manabu Tamura<sup>1</sup>; <sup>1</sup>National Defense Academy, Matls. Sci. & Engrg., 1-10-20 Hashirimizu, Yokosuka 239-8686 Japan

The Sn-Ag3Sn eutectic alloy is one of the candidates for lead-free solders. The solidified structure of this eutectic system is complex. To understand the coupled zone of this alloy, the unidirectional solidification experiments have been carried out. At lower growth velocity, eutectic interface appears. On the other hand, Sn-dendrite appears as a primary phase at higher growth velocity. The distance between the dendrite tip and following eutectic interface (L) are measured with varying the growth velocity (V). L increases rapidly near the transition velocity from eutectic of Sn-dendrite interface with increasing V. L remains constant at higher growth velocity, which indicates that the temperature difference between Sn-dendrite tip and eutectic interface is almost constant, even though the both interface temperatures are the function of V.

## 12:30 PM

Formation and Effects of Al2Si2Ce-Type Phase in Hypereutectic Al-Si Alloy Castings Containing Additions of Phosphide Inoculant and Rare Earths: *Howard Jones*<sup>1</sup>; <sup>1</sup>University of Sheffield, Dept. of Engrg. Matls., Sir Robert Hadfield Bldg., Mappin St., Sheffield S1 3JD UK

The effect of 2, 4 and 7wt% cerium mischmetal (RE) additions on constitution and microstructure of Al-20wt%Si-100 ppm P sand shell mould castings is reported. Increasing amounts of primary Al<sub>2</sub>Si<sub>2</sub>Ce phase are produced together with the primary silicon with the number of primary silicon particles per unit area of section showing a maximum at 2wt%RE while size distribution of the longest silicon particle dimension showed a peak at a value which decreased with increasing RE addition. The XRD data from the Al<sub>2</sub>Si<sub>2</sub>Ce phase is consistent with the P m1 space group of La<sub>2</sub>0<sub>3</sub> and lattice parameters a = 421.5 pm and c = 689.7 pm with the cerium in one of the oxygen positions in the La<sub>2</sub>0<sub>3</sub> unit cell. Positioning of RE atoms on silicon attachment sites provides one possible explanation for the growth restricting effects on primary silicon of RE additions.

# Surfaces and Interfaces in Nanostructured Materials: General Phenomena & Processes

Sponsored by: Materials Processing and Manufacturing Division, MPMD-Surface Engineering Committee

*Program Organizers:* Sharmila M. Mukhopadhyay, Wright State University, Department of Mechanical and Materials Engineering, Dayton, OH 45435 USA; Arvind Agarwal, Florida International University, Department of Mechanical and Materials Engineering, Miami, FL 33174 USA; Narendra B. Dahotre, University of Tennessee, Department of Materials Science & Engineering, Knoxville, TN 37932 USA; Sudipta Seal, University of Central Florida, Advanced Materials Processing and Analysis Center and Mechanical, Materials and Aerospace Engineering, Oviedo, FL 32765-7962 USA

Tuesday AM	Room:	217A
March 16, 2004	Location	: Charlotte Convention Center

Session Chair: Sharmila M. Mukhopadhyay, Wright State University, Dept. of Mech. & Matls. Engrg., Dayton, OH 45435 USA

# 8:30 AM Invited

**Commercialization Programs in Nanostructured Materials**: *T. James Rudd*<sup>1</sup>; <sup>1</sup>Industrial Innovation, National Science Foundation

The Small Business Innovation Research (SBIR) and Small Business Technology Transfer (STTR) Programs of the National Science Foundation (NSF) provide grants to small companies who are pursuing commercialization of new products based on nanostructured materials. This paper will describe NSF's strategy for nanotechnology development through the SBIR/STTR program. Examples of nanostructured materials will be given that are being commercialized by the small business community and will demonstrate how features of the surfaces and interfaces are being engineered to provide uniquely differentiated products for advanced nanocomposites in chemical, structural, electronic, and biotechnology products.

#### 8:55 AM

Nanoscale Morphology Control Using Ion Beams: Michael J. Aziz<sup>1</sup>; <sup>1</sup>Harvard University, Div. of Engrg. & Appl. Scis., 29 Oxford St., Cambridge, MA 02138 USA

Low energy ion irradiation of a solid surface can be used to control surface morphology on length scales from 1 micron to 1 nanometer. Focused or unfocused ion irradiation induces a spontaneous self-organization of the surface into nanometer-sized ripples. Dots, or holes; it also induces diameter increases and decreases in a pre-existing nanopore by a tradeoff between sputter removal of material and stimulated surface mass transport. Here we report experiments that illuminate the kinetics of evolution of the surface morphological instability; the influence of initial and boundary conditions on guiding the self-organization; and the kinetics governing the fabrication of nanopores for single-molecule detectors.

#### 9:15 AM

Impurity Effects on the Fracture of Nanocrystalline Fe Using Atomistic Simulations: *Diana Farkas*<sup>1</sup>; Brian Hyde<sup>1</sup>; Antoine Latapie<sup>1</sup>; <sup>1</sup>Virginia Polytechnic Institute and State University, Matls. Sci. & Engrg., 201-A Holden Hall, Blacksburg, VA 24061 USA

Crack propagation studies in nanocrystalline alpha-iron samples with grain sizes ranging from 6 to 12 nm are reported at temperatures ranging from 100K to 600K using atomistic simulations and empirical many body potentials. The mechanisms of plastic deformation energy release are studied in detail. Intergranular fracture is shown to proceed by the coalescence of nano-voids formed at the grain boundaries ahead of the crack. The simulations also show that at an atomistic scale the fracture resistance and plastic deformation energy release mechanisms increase with increasing temperature. The influence of carbon impurities present on the grain boundaries is studied and our results show that the presence of C impurities increases fracture resistance.

# 9:35 AM

Transformation Behavior in Nanoscale Powders of Binary Aluminum Alloys: Jixiong Han<sup>1</sup>; Martin J. Pluth<sup>1</sup>; Kazuo Furuya<sup>2</sup>; Jai A. Sekhar<sup>1</sup>; Vijay K. Vasudevan<sup>1</sup>; <sup>1</sup>University of Cincinnati, Chem. & Matls. Engrg., Cincinnati, OH 45221-0012 USA; <sup>2</sup>National Institute of Materials Science, Nanomatls. Lab., Sakura 3-13, Tsukuba 305-0003 Japan

Nanoparticles of Al-Cu and Al-Zn were synthesized by plasma ablation of precursor ingots and the structure of these particles as well structural changes in these on aging at temperatures between 65-190°C for times to 100h studied by electron diffraction, nanoprobe energy dispersive x-ray spectroscopy and HRTEM. The particles were supersaturated fcc state in both cases, but displayed a variation in the individual particle composition when compared with the precursor bulk alloys. A 3-5 nm thick oxide layer was present around all the particles. On aging the Al-Cu nanoparticles, a precipitation sequence consisting of nearly pure Cu precipitates to  $\theta$ ' to the equilibrium  $\theta$  was observed, with all three forming only along the outer oxide-particle interior interface. The structure of  $\theta$ ' and its interface with the Al matrix was characterized in detail. In the Al-Zn alloy, a spinodal structure was noted in the as-synthesized nanoparticles, which coarsened on aging into a fine scale structure composed of f.c.c twin-related platelets within which were contained platelets with a hcp structure. This morphology led to relatively complicated diffraction effects, which were analyzed in detail. Nearly-pure Zn precipitates, with an hcp structure, also formed along the oxide-particle interface and consumed the spinodal structure with time. Details of the precipitation sequence, nature and structure of second phase precipitates and interphase interfaces and formation mechanisms will be reported. Finally, if time permits results on the precipitation behavior in ultrafine (5-25 nm) Al-Cu nanoparticles will also be presented. Support for this research from AFOSR under grant no. F49620-01-1-0127, Dr. Craig S. Hartley, Program Monitor, is deeply appreciated.

# 9:55 AM

In-Situ TEM Observation of Crystalline-to-Liquid Phase Change in Nanometer-Sized Alloy Particles: Jung-Goo Lee<sup>1</sup>; Hirotaro Mori<sup>1</sup>; <sup>1</sup>Osaka University, Rsch. Ctr. for Ultra High Voltage Electron Microscopy, Yamadaoka 2-1, Suita, Osaka 565-0871 Japan

Alloy phase formation in nanometer-sized particles has been studied using particles in the Sn-Bi system at elevated temperatures. In the tin-rich side, with increasing bismuth concentration, an approximately 8-nm-sized particle of the terminal tin solid solution directly changed into a liquid phase, without taking a stage of solid-liquid coexistence. In the bismuth-rich side, an approximately 8-nm-sized particle of the terminal bismuth solid solution changed first to a particle with a crystal/liquid two-phase microstructure and eventually to a liquid phase, with increasing tin concentration. An approximately 5-nm-sized particle of the terminal bismuth solid solution, however, directly changed into a liquid phase with increasing tin concentration. From these results, it is expected that the contribution of solid/liquid interface to the total Gibbs free energy is so large with decreasing system size that the behavior of crystalline-to-liquid phase change in nanometer-sized alloy particles is significantly different from that of the corresponding bulk materials.

# 10:15 AM Invited

## Superconducting and Mechanical Aspects of Nanocrystalline Systems: Chandra Shekhar Pande<sup>1</sup>; Robert A. Masumura<sup>1</sup>; <sup>1</sup>Naval Research Laboratory, Code 6325, Washington, DC USA

Critical current (Jc ) of superconductors and mechanical strength of normal materials depend sensitively on grain size, leading to a potentially high Jc in fine grained superconductors and the mechanical softening (Inverse Hall Petch) in normal nanocrystalline systems. This paper will discuss the physical mechanisms leading to these results and present analytical expressions describing these properties.

## 10:40 AM

Critical Factors That Determine FCC to BCC Phase Transformation in Sputter Deposited Austenitic Stainless Steel Films: *Xinghang Zhang*<sup>1</sup>; Amit Misra<sup>1</sup>; Haiyan Wang<sup>1</sup>; C. J. Wetteland<sup>1</sup>; Roland K. Schulze<sup>1</sup>; John D. Embury<sup>1</sup>; R. G. Hoagland<sup>1</sup>; M. Nastasi<sup>1</sup>; <sup>1</sup>Los Alamos National Laboratory, Matls. Sci. & Tech. Div., MS G755, Los Alamos, NM 87545 USA

Bulk austenitic stainless steels (such as 304 SS and 316 SS) have face centered cubic (fcc) structure. However, sputter deposited films synthesized using 304 austenitic stainless steel targets usually exhibit body centered cubic (bcc) structure, while 330 SS films showed fcc structure. The effect of processing parameters on the phase stability of 304 and 330 SS thin films are studied. 304 SS thin films with inplane, biaxial residual stresses in the range of  $\sim 1$  GPa (tensile) to  $\sim 300$ MPa (compressive) exhibited only bcc structure. The retention of bcc 304 SS after high temperature annealing followed by slow furnace cooling is consistent with a depletion of Ni in the as-sputtered 304 SS films. Rutherford backscattering spectroscopy and Auger depth profiling also indicated slight decrease in the Ni content below the ~8% needed to stabilize fcc structure at room temperature. The concentration of Ni, substrate temperature and energy of deposited atoms are considered crucial factors in determining the phase transformations in sputter deposited austenitic SS films.

#### 11:00 AM

Surface Damage Mechanisms in Clay-Filled Polymer Nanocomposites: Aravind Dasari<sup>1</sup>; Pankaj Nerikar<sup>1</sup>; Santosh D. Wanjale<sup>2</sup>; Jyoti P. Jog<sup>2</sup>; Devesh K. Misra<sup>1</sup>; <sup>1</sup>University of Louisiana, Dept. of Chem. Engrg., PO Box 44130, Lafayette, LA 70504-4130 USA; <sup>2</sup>National Chemical Laboratory, Pashan, Pune, Maharashtra 411008 India

Resistance to surface damage introduced by scratching or mechanical deformation process is important to many engineering applications. The paper describes micromechanisms of surface deformation and subsequent propagation into the bulk in clay-filled polymer nanocomposites. The potential of atomic force microscopy is combined with high resolution scanning electron microscopy to examine micro- and nanoscale deformation processes.

# Symposium on Microstructural Stability in Honor of Prof. Roger D. Doherty: Microstructural Stability: Plastic Deformation

Sponsored by: Aluminum Association, Materials Processing and Manufacturing Division, Structural Materials Division, MPMD-Solidification Committee, SMD-Physical Metallurgy Committee *Program Organizer:* Anthony D. Rollett, Carnegie Mellon University, Department of Materials Science & Engineering, Pittsburgh, PA 15213-3918 USA

Tuesday AM	Room: 2	16A		
March 16, 2004	Location:	Charlotte	Convention	Center

Session Chair: Roger D. Doherty, Drexel University, Matls. Engrg. Dept., Philadelphia, PA 19104 USA

#### 8:30 AM

Deformation and Annealing Structures in Cold-Rolled Aluminium (AA1200): Niels Hansen<sup>1</sup>; Xiaoxu Huang<sup>1</sup>; Grethe Winther<sup>1</sup>; Qingfeng Xing<sup>1</sup>; <sup>1</sup>Risø National Laboratory, Matls. Rsch. Dept., Ctr. for Fundamental Rsch., Metal Structures in 4-D, Roskilde DK-4000 Denmark

TEM investigations of metals deformed to low and medium strains have shown a correlation between the crystallographic orientation and the deformation microstructure, which is characterized by a number of structural parameters, e.g., morphology, spacing between and misorientation angle across dislocation boundaries and high angle grain boundaries. To examine if such a correlation also exists after deformation to large strains, aluminium of commercial purity (AA1200) was cold rolled to a strain of 2 and characterized by TEM and Kikuchi pattern analysis. The examination of longitudinal sections showed elongated volumes on a relatively large scale belonging to different texture components and within each of these a fine lamellar structure composed of extended boundaries and short interconnecting boundaries. The deformation was followed by annealing at 200 and 220°C for 2 hours, which gave rise to a structural coarsening and a change in morphology from a lamellar structure towards a more equiaxed microstructure. The observations were discussed, especially the correlations between crystallographic orientation and microstructural parameters both in the deformed state and after annealing.

#### 9:00 AM

**Orientation Changes of Individual Bulk Grains During Deformation**: *Grethe Winther*<sup>1</sup>; Lawrence Margulies<sup>1</sup>; Henning Friis Poulsen<sup>1</sup>; 'Risoe National Laboratory, Matls. Rsch. Dept., Ctr. for Fundamental Rsch., Metal Structures in 4-D, DK-4000 Roskilde Denmark

Modelling deformation textures has mainly been based on experimental bulk textures. An essential question is the relative effects of the initial orientation of a grain and its local environment, i.e. grain interaction. To effectively address this question, data on individual grains is needed. Studies of surface grains provide such data but surface conditions may deviate strongly from bulk. To mimic bulk conditions, split samples have been used. Recently, three dimensional X-ray diffraction has proven capable of measuring the behaviour of individual grains in the bulk of AA 1050 during tension has been investigated. The grain size was 75 micrometer and the elongation 6%. The data are analysed for the relative effects of initial grain orientation and grain interaction. Comparison with the Taylor model is made, revealing that it works well in some cases but not in others.

# 9:25 AM

Definition Elaboration for Recrystallization Either Dynamic or Static: Hugh J. McQueen<sup>1</sup>; <sup>1</sup>Concordia University, Mech. Engrg., 1455 Maisonneuve Blvd. W, Montreal, Quebec H3G 1M 8 Canada

Currently there are controversial descriptions of hot strain induced microstruc-tures in aluminum or ferrite: either as dynamic recovery (DRV) or as continuous dynamic recrystallization (DRX). For steady state creep, DRV adequately explains the substructure remaining constant in character and axial ratio in elongating grains; however in warm working, some random subboundary segments (other than transition boundaries between deformation bands) attain misorientations above 8°. While DRV theory predicts these would be subject to rearrangement, continuous DRX theory claims they constitute recrystallzation. The controversy would end if the definition of recrystallized grains required the formation of regions surrounded by relaxed high angle boundaries that (i)are not responsive to stress and (ii)can migrate without dislocation participation. With this definitional requirement, polygonized misoriented regions in warm working, like layer bands after heavy cold rolling, are not recrystallized until annealed.

#### 9:50 AM

Twinning and Stages of Deformation in Low Stacking Fault Energy Austenitic Steel Single Crystals: *Ibrahim Karaman*<sup>1</sup>; Huseyin Schitoglu<sup>2</sup>; Hans J. Maier<sup>3</sup>; Yuriy I. Chumlyakov<sup>4</sup>; <sup>1</sup>Texas A&M University, Dept. of Mech. Engrg., MS 3123, College Sta., TX 77843 USA; <sup>2</sup>University of Illinois, Dept. of Mech. & Industrial Engrg., 1206 W. Green St., Urbana, IL 61801 USA; <sup>3</sup>University of Paderborn, Lehrstuhl f. Werkstoffkunde, Paderborn 33095 Germany; <sup>4</sup>Siberian Physical-Technical Institute, Revolution Sq. 1, Tomsk 634050 Russia

The works of Prof. Roger D. Doherty on fcc materials have helped understanding of the mechanisms of the work-hardening stages in these materials. The present authors have been often inspired by his works on their study on the deformation of low stacking fault energy austenitic steels, in particular on the stainless steel and Hadfield manganese steel single crystals. In the present talk, our recent findings on these materials will be summarized in regards to the competition between slip and twinning, texture evolution, interstitial atom content and precipitation. Twinning was observed as a primary deformation mechanism at the onset of deformation in certain orientations. The volume fraction of twinning was increased with increasing carbon concentration but first decreased and then increased by increasing nitrogen concentration. Incoherent precipitates did not suppress twinning but increased the flow stress level. In the orientations where twinning theoretically is impossible, extrinsic stacking faults and very thin twins were observed. In the conditions in which twinning is the case, an upward stress-strain response was evident. The single crystal data has provided insight into the operating microstructural mechanisms and the orientation relationships, and the micromechanisms behind the aforementioned observations are explained. We have used the data obtained on polycrystals for the mesoscopic and macroscopic model development and for verification purposes. The vehicle for the quantitative bridge between single and polycrystal results is crystallographic texture measurements. Major thrust of the modeling studies have been the treatment of the competing effects of several deformation mechanisms (cell structure, twinning, coherent and incoherent precipitates). These effects are being incorporated into single crystal hardening laws with a sound mechanism-based internal state variable theory and validated through the stress-strain response, and microstructural and texture evolution of several single crystal orientations. The part of the research conducted at Texas A&M University was supported by the National Science Foundation contract CMS 01-34554, Solid Mechanics and Materials Engineering Program, Directorate of Engineering, Arlington, Virginia. The part of the work conducted at The University of Illinois was supported by the National Science Foundation contract CMS 99-00090, Mechanics of Materials Program, Directorate of Engineering, Arlington, Virginia.

#### 10:10 AM

The Effect of Twinning on the Work Hardening Behavior of Hafnium: *E. K. Cerreta*<sup>1</sup>; C. A. Yablinsky<sup>2</sup>; G. T. Gray<sup>1</sup>; <sup>1</sup>Los Alamos National Laboratory, MST-8, MS G755, Los Alamos, NM 87545 USA; <sup>2</sup>Carnegie Mellon University, Matls. Sci. Dept., 5000 Forbes Ave., Pittsburgh, PA 15213 USA

In many HCP metals, both twinning and slip are known to be important modes of deformation. However, the interaction of the two mechanisms and their effect on work hardening is not well understood. In hafnium, twinning and work hardening rates increase with increasing strain, increasing strain rate, and decreasing temperature. At low strains and strain rates and at higher temperatures, slip dominates deformation and rates of work hardening are relatively lower. To characterize the interaction of slip and twinning, Hf specimens were prestrained quasi-statically in compression at 77K, creating specimens that were heavily twinned. These specimens were subsequently reloaded at room temperature. Twinning within the microstructures was characterized optically and using transmission electron microscopy. The interaction of slip with the twins was investigated as a function of prestrain and correlated with the observed rates of work hardening.

# 10:30 AM

**Evaluation of Path Dependency in Shock Wave Damage Through Electron Backscatter Diffraction**: *Benjamin L. Henrie*<sup>1</sup>; Thomas A. Mason<sup>1</sup>; George (Rusty) T. Gray<sup>1</sup>; David B. Holtkamp<sup>2</sup>; <sup>1</sup>Los Alamos National Laboratory, MST-8, PO Box 1663, MS G755, Los Alamos, NM 87545 USA; <sup>2</sup>Los Alamos National Laboratory, P-22, PO Box 1663, MS D410, Los Alamos 87545 USA

A number of plate impact experiments using an 80-mm launcher and direct high explosive (HE) experiments were performed to study dynamic damage in high-purity copper and tantalum. Real time free surface velocity (VISAR) measurements were captured and specimens were recovered for subsequent postmortem characterization using optical metallography and electron backscatter diffraction (EBSD). Analysis of the intensity and quality of the EBSD patterns yields greater insight into the characterization of strain localization. This analysis will be used to compare the damage arising in samples shocked with square and Taylor waves.

#### 10:50 AM

Effect of Deformation Twinning on the Strain Hardening of hcp Titanium: A. A. Salem<sup>1</sup>; S. R. Kalidindi<sup>2</sup>; R. D. Doherty<sup>2</sup>; S. L. Semiatin<sup>3</sup>; <sup>1</sup>Universal Technology Corporation, 1270 N. Fairfield Rd., Dayton, OH 45432 USA; <sup>2</sup>Drexel University, Matls. Engrg. Dept., Philadelphia, PA 19104 USA; <sup>3</sup>Air Force Research Laboratory, Matls. & Mfg. Direct., AFRL/MLLM, Wright-Patterson AFB, OH 45433 USA

The stress-strain behavior of two grades of textured alpha-titanium was established using quasi-static simple compression tests at ambienttemperature. Compression samples cut from the specimen reference directions (RD, TD, and ND) were used to evaluate the effect of crystallographic texture on the stress-strain response. Plots of the strain-hardening rate versus stress revealed three distinct stages for the material that had the basal pole close to the compression axis or perpendicular to it. The sudden increase in the strain-hardening rate was correlated to the onset deformation twinning. Microhardness measurements revealed that the deformation twins were harder (immediately after being formed) than the matrix. This observation supported the Basinski model for the hardening associated with twinning. As a result, deformation twinning leads to two competing effect on the overall strain hardening response: (1) strain hardening via the Hall-Petch and Basinski hardening mechanisms and (2) texture softening due to reorientation of the twinned areas.

# 11:10 AM

The Effect of Surface Shear From Rolling on Surface Texture, Recrystallization, and Functional Properties in Pure Cu and Pure Nb: Hairong Jiang<sup>1</sup>; Alireza Fallahi<sup>1</sup>; *Thomas R. Bieler<sup>1</sup>*; Chris C. Compton<sup>2</sup>; Terry L. Grimm<sup>2</sup>; <sup>1</sup>Michigan State University, Dept. Chem. Engrg. Matl. Sci., 2527 Engrg. Bldg., E. Lansing, MI 48824 USA; <sup>2</sup>Michigan State University, Natl. Superconducting Cyclotron Lab., E. Lansing, MI 48824 USA

Pure Cu and pure Nb are used to make RF (radio frequency) cavities used in particle accelerators. The performance of RF cavities is degraded by electron emission, which is strongly dependent on crystal orientation and surface roughness. Analyses of texture gradients from the surface to the interior in rolled and recrystallized pure Nb shows strong <111> // ND (normal direction) fiber texture in the center, similar to IF (interstitial free) steels, but the surface has a high population of grains with <100> // ND, unlike IF steels. The work function for electron emission of <100> grains is much smaller than for <111> grains, making <100> grains undesirable for Nb RF cavities. Using tapered specimens of pure Nb and pure Cu, the effect of the amount of reduction and the rolling path are examined to determine how they affect recrystallization textures on the surface as compared to the interior. The recrystallization phenomena and mechanisms of surface grains are discussed and compared to existing studies in other FCC and BCC metals.

# 11:35 AM

The Relationship Between the Shearable/Non-Shearable Transition and the Mechanical Response of 6000 Series Alloys: Warren J. Poole<sup>1</sup>; John David Embury<sup>2</sup>; David J. Lloyd<sup>3</sup>; <sup>1</sup>University of British Columbia, Dept. of Metals & Matls. Engrg., 309-6350 Stores Rd., Vancouver, BC V6T 1Z4 Canada; <sup>2</sup>McMaster University, Dept. of Matls. Sci. & Engrg., 1280 Main St. W., Hamilton, ON L8S 4L7 Canada; <sup>3</sup>Alcan International, Kingston R&D Ctr., 945 Princess St., Kingston, ON Canada

Currently, there is a particular interest in the application of 6000 series alloys in the automotive sector. This has led to the desire for the development of process models to predict mechanical properties for a variety of multi-step ageing treatments. This work focuses on the dependence of the yield strength, work hardening rate and strain rate sensitivity on the precipitate size, volume fraction and the size distribution. A yield strength model has been developed which explicitly includes the effect of the precipitate size distribution which was quantified by detailed transmission electron microscope (TEM) studies. The work hardening behaviour have been understood in the Kocks-Mecking framework after suitable modifications to include an appropriate flow stress superposition law and a geometric dislocation storage term when precipitates are non-shearable. It was observed that there were significant changes in the material behaviour at the shearable/ non-shearable transition, i.e. after the transition, slip lines cannot be observed on the surface and there is a characteristic increase in the rate of dynamic recovery. Detailed TEM and high resolution TEM studies were conducted to examine the details dislocation/precipitate interactions for the cases of shearable and non-shearable precipitates. It was found that the work hardening behaviour, slip line and TEM observations are consistent.

# 12:00 PM

Deformation Twinning in FCC and HCP Metals: New Insights from Collaborations with Roger Doherty: Surya R. Kalidindi<sup>1</sup>; <sup>1</sup>Drexel University, Matls. Sci. & Engrg., Philadelphia, PA 19104 USA

Deformation twinning has been known to play a significant role in the mechanical response of hcp metals (e.g. Ti alloys) and low stacking fault energy fcc metals (e.g. Brass). This has been a major area of research collaboration between the author and Professor Roger D. Doherty for the last ten years. This collaboration has provided tremendous new insight into the physics of how deformation twins influence the mechanical behavior of these metals. Although there are major differences in the driving factors for the formation of deformation twins in these two distinctly different classes of materials, the consequence on the mechanical behavior shows remarkable similarity in several aspects. The main results of this collaborative effort will be

# The Didier de Fontaine Symposium on the Thermodynamics of Alloys: First Principle Calculations and Cluster Expansion Techniques

Sponsored by: Materials Processing and Manufacturing Division, MPMD-Computational Materials Science & Engineering-(Jt. ASM-MSCTS)

*Program Organizers:* Diana Farkas, Virginia Polytechnic Institute and State University, Department of Materials Science and Engineering, Blacksburg, VA 24061 USA; Mark D. Asta, Northwestern University, Department of Materials Science and Engineering, Evanston, IL 60208-3108 USA; Gerbrand Ceder, Massachusetts Institute of Technology, Department of Materials Science and Engineering, Cambridge, MA 02139 USA; Christopher Mark Wolverton, Ford Motor Company, Scientific Research Laboratory, Dearborn, MI 48121-2053 USA

Tuesday AM	Room:	216	В		
March 16, 2004	Location	n: C	harlotte	Convention	Center

Session Chair: TBA

# 8:30 AM Invited

Electronic Structure, Stability, and Order in V-X (X=Ru,Rh,Pd) Alloys: Patrice E.A. Turchi<sup>1</sup>; Vaclav Drchal<sup>2</sup>; Josef Kudrnovsky<sup>2</sup>; Richard M. Waterstrat<sup>3</sup>; <sup>1</sup>Lawrence Livermore National Laboratory, PO Box 808 (L-353), Livermore, CA 94551 USA; <sup>2</sup>Academy of Sciences of the Czech Republic, Inst. of Physics, Na Slovance 2, Prague 8, CZ 182-21 Czech Republic; <sup>3</sup>National Institute of Science and Technology, Matls. Sci. & Engrg. Lab., 100 Bureau Dr., Gaithersburg, MD 20899-8551 USA

Using a first-principles methodology, electronic structure, ordering trends and stability properties of V-X alloys, where X=Ru, Rh, and Pd, are presented. The methodology is based on the Generalized Perturbation Method (GPM) applied to the fully relativistic Tight-Binding Linear Muffin-Tin Orbital (TB-LMTO) description of the electronic structure of the chemically random configuration of the alloy within the Coherent Potential Approximation (CPA). Density of states at the Fermi energy and g of specific heat measurements are compared as functions of composition for the three alloys. Finally ordering trends and stability properties are rationalized as functions of simple electronic parameters. Work performed under the auspices of the U. S. Department of Energy by the University of California Lawrence Livermore National Laboratory under Contract W-7405-ENG-48. This work has benefited from the experimental results of the late R. Kuentzler.

# 9:00 AM

# Prediction of Complex Binary Ground State Structures in bcc-Based Refractory Alloys: Volker Blum<sup>1</sup>; Alex Zunger<sup>1</sup>; <sup>1</sup>National Renewable Energy Laboratory, 1617 Cole Blvd., Golden, CO 80401 USA

The stability of bcc-based binary ground state configurations is often discussed in terms of simple interatomic interactions, which stabilize simple usual-suspect structures. Using realistic interactions from the LDA-based mixed-basis cluster expansion method, we find unexpectedly complex ground states in the bcc-based refractory alloy systems Ta-Mo and Nb-W. In Ta-Mo (Ref. 1), a quasi-continuous series of Mo-rich (100) superlattices (including C11b and B2) coexists with Ta-rich large-cell ground states (13 and 16 atoms per unit cell). Surprisingly, the ground states of Nb-W are quite different from Ta-Mo, with (111) superlattices as the dominant motif. We then predict order-disorder transition temperatures and the mixing enthalpy and short-range order of the solid solution phase at \$T>0\$ for both systems from canonical Monte Carlo simulations. <sup>1</sup>Volker Blum and Alex Zunger, "Are binary bcc ground states more complex than we knew: The case of bcc Mo-Ta", submitted to Phys. Rev. B (2003).

# 9:20 AM

First-Principles Thermodynamic Calculations of Phase Equilibria of Fe-Based Alloy Systems: *Ying Chen*<sup>1</sup>; Shuichi Iwata<sup>1</sup>; Tetsuo Mohri<sup>2</sup>; <sup>1</sup>University of Tokyo, Dept. of Quantum Engrg. & Sys. Sci., Hongo 7-3-1, Bunkyo-ku, Tokyo 113-8655 Japan; <sup>2</sup>Hokkaido University, Grad. Sch. of Engrg., Div. of Matls. Sci. & Engrg., Kita-13 Nishi-8, Kita-ku, Sapporo, Hokkaido 060-8628 Japan By combining FLAPW total energy calculations with the Cluster Variation Method via Cluster Expansion Method, first-principles investigation of phase equilibria on three kinds of Fe-based alloy systems has been attempted. The particular emphasis is placed on the L10disorder phase equilibria. With the effective cluster interaction energies extracted based on the total energies of stable ordered phases, the transition temperature is well reproduced with high accuracy for each system. Two major modifications are attempted. The first one is the incorporation of lattice vibration effects through quasi harmonic approximation, and the resultant transition temperature is further improved. The second modification is to introduce the information of hypothetical ordered phases to include long distant or larger cluster interactions. For this, additional total energy calculations are performed for L11 and D022 ordered phases. The resultant phase equilibria is critically examined.

#### 9:40 AM

Phase Stability of Al-Ti-Zn System: Integration of Ab Initio Results and Computational Thermodynamics: Gautam Ghosh<sup>1</sup>; Zhe Liu<sup>1</sup>; Axel van de Walle<sup>1</sup>; Mark D. Asta<sup>1</sup>; <sup>1</sup>Northwestern University, Dept. of Matls. Sci. & Engrg., 2225 N. Campus Dr., Evanston, IL 60208-3108 USA

As a part of our research effort to design precipitation stregthened Al-base alloys, we present two major results concerning the phase stability modeling of the Al-Ti-Zn system. First, the results of ab initio phase stability of the Ti-Zn system where a part of the phase diagram is known but there is no measured thermodynamic data. Second, ab initio results of vibrational entropy contributions to the phase stability of selected intermetallic compounds. To facilitate calculation of binary and ternary phase diagrams, ab initio results are successfully integrated within computational thermodynamics formalism. We also present the application of phase stability modeling and computational thermodynamics to design new Al-base alloys.

# 10:00 AM Invited

Structure, Dynamics and Thermodynamics of Metal Surfaces from First-Principles: *Nicola Marzari*<sup>1</sup>; <sup>1</sup>Massachusetts Institute of Technology, Dept. of Matls. Sci. & Engrg., 77 Mass. Ave., Cambridge, MA 02139 USA

The thermodynamical stability of metal surfaces has been investigated using ab-initio molecular dynamics and linear-response techniques. Several systems exhibited unexpected characteristics, and were strongly influenced by temperature and crystallographic orientation. The reasons for this variety lie in the subtle balance between energetic and entropic effects, and in the wide range of environments that surface atoms experience. First-principles calculations provide an unbiased description of such bonding, while the small barriers involved allow for affordable thermalization timescales. (a) Clean Al(110) is shown to be strongly anharmonic, where the first interlayer distance contracts with increasing temperature. The atoms in the second layer show large mean square displacements that are preliminary to the ejection of adatoms onto the surface. (b) The diffusion of adatoms on Al(100) becomes increasingly complex with temperature, switching from direct exchanges to long, concerted exchanges, and leading to a reversible, local melting around the adsorption sites. (c) Al(111) and Ag(111) surfaces have small barriers between stable and metastable stackings, allowing the vibrational entropy to become the driving force tuning the stability of small islands.

# 10:30 AM Break

# 10:40 AM Invited

Large Scale Simulations of the Relaxor Ferroelectric Pb(Sc<sub>1/</sub> <sub>2</sub>Nb<sub>1/2</sub>)O<sub>3</sub>: *Benjamin P. Burton*<sup>1</sup>; Umesh Waghmare<sup>2</sup>; Eric Cockayne<sup>1</sup>; <sup>1</sup>National Institute for Science and Technology, Ceram., 1 Bureau Dr., A226/223, Gaithersburg, MD 20899 USA; <sup>2</sup>J. Nehru Center for Advanced Scientific Research, Bangalore 560 064 India

Experiments indicate that both chemical order-disorder and Pbvacancies strongly affect the dielectric properties of relaxor ferroelectrics such as  $Pb(Sc_{1/2}Nb_{1/2})O_3$  (PSN) and  $Pb(Mg_{1/3}Nb_{2/3})O_3$  (PMN). Of particular interest are microstructures with 4-10 nm short-range ordered (SRO) domains in a disordered matrix. We use a first-principles based effective Hamiltonian to investigate the effects of ordered microdomains on temperature-dependent properties of PSN. Our model is based on Pb-centered polar variables and includes the local random fields at Pb-sites which are caused by: 1) B-site chemical disorder; 2) Randomly placed Pb-O vacancy pairs. We create supercells (40x40x40primitive cells) that contain a variety of ordered and partially ordered states: Fully ordered; Random; ~4 nm ordered PSN domains in a disordered matrix; a short-range ordered state and some long-range ordered states with various degrees of disorder, that were calculated from firstprinciples via the cluster expansion approach. The Calculated Thermodynamic Properties of Al, Ni, NiAl, and Ni3Al: Yi Wang<sup>1</sup>; Zikui Liu<sup>1</sup>; Longqing Chen<sup>1</sup>; <sup>1</sup>Pennsyvania State University, Matls. Sci. & Engrg., 106 Steidle Bldg., State College, PA 16802-5006 USA

The thermodynamic properties of Al, Ni, NiAl, and Ni3Al have been studied through the first-principles approach. The 0-K total energies are calculated using the ab initio plane wave pseudopotential method within the generalized gradient approximation. The contribution to the free-energy from the lattice is calculated using the phonon densities of state derived by means of the ab inito linear-response theory. The thermal electronic contribution to the free-energy is calculated from the one-dimensional numerical integration over the electronic density-of-state. With the deduced Helmholtz free energy thereafter, the thermal expansion and enthalpy as a function of temperature between 0 K and melting temperatures are calculated and compared with the experimental data.

# 11:30 AM

First Principles Calculation of Diffusion in Binary Alloys: Anton Van der Ven<sup>1</sup>; Gerbrand Ceder<sup>1</sup>; <sup>1</sup>Massachusetts Institute of Technology, Dept. of Matls. Sci. & Engrg., Rm. 13-4053, 77 Mass. Ave., Cambridge, MA 02139 USA

Diffusion in multicomponent solids plays an important role in battery and fuel cell applications as well as during the synthesis of a material as this is often accompanied by phase transformations involving atomic redistribution. We have extended the mathematical tools of alloy theory (theory of first principles phase-diagram calculations) for the study of diffusion in solids with configurational disorder. We have applied this formalism to study diffusion in Al-Li alloys as a function of alloy composition and temperature from first principles. We predict that the vacancy concentration in this alloy has a strong dependence on the short-range order among lithium and aluminum atoms with the vacancy prefering aluminum over lithium in its first nearest neighbor shell. Furthermore, the vacancy concentration is predicted to depend strongly on alloy composition within the ordered Al3Li L12 phase. While the vacancy prefers aluminum rich environments, first principles calculations of activation barriers predict that Li has a lower activation barrier than Al for exchange with a neighboring vacant site. With the cluster expansion formalism combined with kinetic Monte Carlo simulations, we have calculated the alloy diffusion coefficients using Green-Kubo relations. These can be used in phase-field models to predict the kinetics of precipitation transformations in this alloy.

#### 11:50 AM

**Hydrogen in Aluminum:** *Chris Wolverton*<sup>1</sup>; Mark D. Asta<sup>2</sup>; Vidvuds Ozolins<sup>3</sup>; <sup>1</sup>Ford Motor Company, MD 3083/SRL, PO Box 2053, Dearborn, MI 48121 USA; <sup>2</sup>Northwestern University, Dept. of Matls. Sci., Evanston, IL 60208 USA; <sup>3</sup>University of California, Dept. of Matls. Sci. & Engrg., Los Angeles, CA 90095-1595 USA

Despite decades of study, several key aspects of the Al-H system remain the subject of considerable debate. We perform a thorough study of this system using first-principles density functional calculations. We show that generalized gradient calculations provide an accurate picture of energetics, phase stability and structure, diffusion, and defect binding in the Al-H system. A series of calculations for hydrides in the M-H systems (M = Al, Ba, Ca, K, Mg, La, Li, Na, Ni, Pd, Sc, Sr, Ti, V, and Y) also shows that the GGA calculations are a quantitatively accurate predictor of hydride formation energies. For Al-H, we find: 1) Atomic relaxation and anharmonic vibrational effects play important roles in the interstitial site preference. 2) The calculated heat of solution and hydride energetics are both consistent with experimental measurements. 3) Interstitial H interacts strongly with Al vacancies, with vacancies strongly influencing the migration energy of H diffusion.

# Third International Symposium on Ultrafine Grained Materials: UFG Material Fundamentals

Sponsored by: Materials Processing & Manufacturing Division, MPMD-Shaping and Forming Committee
Program Organizers: Yuntian Ted Zhu, Los Alamos National Laboratory, Materials Science and Technology Division, Los Alamos, NM 87545 USA; Terence G. Langdon, University of Southern California, Departments of Aerospace & Mechanical Engineering and Materials Engineering, Los Angeles, CA 90089-1453 USA; Terry C. Lowe, Metallicum, Santa Fe, NM 87501 USA; S. Lee Semiatin, Air Force Research Laboratory, Materials & Manufacturing Directorate, Wright Patterson AFB, OH 45433 USA; Dong H. Shin, Hanyang University, Department of Metallurgy and Material Science, Ansan, Kyunggi-Do 425-791 Korea; Ruslan Z.
Valiev, Institute of Physics of Advanced Material, Ufa State Aviation Technology University, Ufa 450000 Russia

Tuesday AM	Room: 207A	
March 16, 2004	Location: Cha	rlotte Convention Center

Session Chairs: Yuntian T. Zhu, Los Alamos National Laboratory, Matls. Sci. Tech. Div., Los Alamos, NM 87545 USA; Dieter Wolf, Argonne National Laboratory, Matls. Sci. Div., Argonne, IL 60516 USA; Minoru Umemoto, Toyohashi University of Technology, Toyohashi, Aichi 441-8580 Japan

# 8:30 AM Invited

Deformation Mechanisms in Nanocrystalline Materials by Molecular Dynamics Simulation: *Dieter Wolf*); <sup>1</sup>Argonne National Laboratory, Matls. Sci. Div., 9700 S. Cass Ave., Bldg. 212, Argonne, IL 60516 USA

We describe large-scale molecular-dynamics simulations of nanocrystalline-Al and Pd model microstructures to demonstrate how and why the conventional dislocation-slip mechanism shuts down with decreasing grain size, in favor of a grain-boundary based deformation mechanism. Our simulations of textured and fully three-dimensional Al polycrystals reveal that, instead of from the usual Frank-Read sources, dislocations nucleate from the grain boundaries and grain junctions. As the grain size decreases, the magnitude of the stress-dependent splitting distance of these dissociated dislocations eventually becomes comparable to the grain size, preventing their complete nucleation and hence contributing ever less to the total strain. Our simulations also reveal that, in the absence of grain growth and any dislocation activity, nanocrystalline fcc metals deform via a mechanism involving an intricate interplay between grain-boundary sliding and grainboundary diffusion.

#### 8:50 AM Invited

What Simulations Suggest on Deformation Mechanism in nc-Metals: *Helena Van Swygenhoven*<sup>1</sup>; P. M. Derlet<sup>1</sup>; A. Hasnaoui<sup>1</sup>; <sup>1</sup>Paul Scherrer Institute, NUM-ASQ, CH-5232, Villigen Switzerland

Large-scale molecular dynamics simulations of fully 3Dnanocrystalline (nc) Ni samples provide intriguing insights into the effects of grain size and grain boundary (GB) structure on nc structural and mechanical properties. The simulations suggest a deformation mechanism intrinsic to the nanosized GB network where the GB structure plays a central role consisting of an interplay between (1) GB sliding accommodated by GB and Triple Junction migration and (2) dislocation emission and absorption in GBs, both of which are at the origin of the formation of local shear planes that facilitates plastic deformation explaining the dimple-like features seen on experimental fracture surfaces. The proposed mechanisms are interpreted in terms of recent experimental results such as work hardening, activation volume and in-situ rms strain measurements in the Swiss Light Source.

# 9:10 AM Invited

Mechanical Behavior of Nanostructured Metals: New Mechanisms and Applications: Evan Ma<sup>1</sup>; <sup>1</sup>Johns Hopkins University, Matls. Sci. & Engrg., 3400 N. Charles, Baltimore, MD 21218 USA

The mechanical properties of nanostructured materials are of considerable interest at present. New phenomena and opportunities are expected to emerge when the grain sizes of the metals are brought down to the ultrafine-grained or nanocrystalline regime. For example, at the high stresses needed for the nanostructured metals to plastically deform, the formation of stacking faults and deformation twins can become prevalent, as the role of the partial dislocations becomes important.<sup>1</sup> Also, with nanoscale grains, one has now extra room to manipulate the grain structure in favor of high strength, ductility, or a combination of both.<sup>2</sup> The altered mechanical responses, in terms of the strain rate/temperature dependences and the tendency for shear localization<sup>3,4</sup> for example, may be desirable in certain applications. Examples will be presented in this talk to discuss the various aspects outlined in the preceding paragraph. <sup>1</sup>M.W. Chen et al., Science 300 (2003) 1275. <sup>2</sup>Y.M. Wang et al., Nature 419 (2002) 912. <sup>3</sup>D. Jia et al., Acta mater. 51 (2003) 3495. <sup>4</sup>Q.M. Wei et al., unpublished data.

# 9:30 AM Invited

# Compact and Dissociated Dislocations in Al: Implications for Deformation in fcc Metals: S. G. Srinivasan<sup>1</sup>; M. I. Baskes<sup>1</sup>; X. Z. Liao<sup>1</sup>; R. J. McCabe<sup>1</sup>; Y. H. Zhao<sup>1</sup>; Y. T. Zhu<sup>1</sup>; <sup>1</sup>Los Alamos National Laboratory, Matls. Sci. & Tech., Los Alamos, NM 87545 USA

Recently, our high-resolution electron-microscopy studies revealed the existence of both compact and dissociated dislocations in ultrafine-grained aluminum. We examine the consequences of this dual core state using atomistic simulations, employing two state of the art embedded atom method Al potentials. The calculated minimum stress (Sp) required moving an edge dislocation is approximately 20 times smaller for dissociated than for equivalent compact dislocations. The well-accepted generalized stacking fault energy paradigm, however, predicts similar Sp values for both configurations. Additionally, Frank's rule and Schmid law are also disobeyed. We examine the implications of these results in addressing the long-standing problem of the magnitude of Sp in face-centered-cubic metals.

# 9:50 AM Invited

Stacking Fault and Twinning in Ultrafine-Grained Al: Xiaozhou Liao<sup>1</sup>; Yonghao Zhao<sup>1</sup>; Srivilliputhur G. Srinivasan<sup>1</sup>; Fei Zhou<sup>2</sup>; Enrique J. Lavernia<sup>2</sup>; Michael I. Baskes<sup>1</sup>; Yuntian T. Zhu<sup>1</sup>; <sup>1</sup>Los Alamos National Laboratory, Matl. Sci. & Tech. Div., MS G755, Los Alamos, NM 87545 USA; <sup>2</sup>University of California, Dept. Chem. Engrg. & Matl. Sci., Davis, CA 95616 USA

Ultrafine-grained (UFG) materials with grain sizes ranging from 10-1000 nm are believed to deform by different mechanisms from their coarse-grained counterparts. Here we report the experimental observations of stacking faults (SF) ribbons and deformation twinning in UFG Al processed by severe plastic deformation. The SF ribbons are 1.4-8.6 nm in width, which is 3-17 times the width of SFs in coarse-grained Al. The deformation twinning was formed by new mechanisms different from conventional pole mechanism. Partial dislocations emitted from grain boundaries played a critical role in the formation of SFs and twinning. These results are surprising because 1) partial dislocation emission from grain boundaries has never been experimentally observed and 2) deformation twinning have never been reported in Al due to its high SF energy. These observations directly validate some recent molecular dynamics simulations and provide further insights on deformation mechanisms in UFG materials.

#### 10:10 AM

Formation Mechanisms of Colossal Stacking Fault in Ultrafine-Grained Al: Yuntian T. Zhu<sup>1</sup>; Xiaozhou Liao<sup>1</sup>; Yonghao Zhao<sup>1</sup>; Srivilliputhur G. Srinivasan<sup>1</sup>; Michael I. Baskes<sup>1</sup>; <sup>1</sup>Los Alamos National Laboratory, Matl. Sci. & Tech. Div., MS G755, Los Alamos, NM 87545 USA

Colossal stacking fault ribbons have been observed in UFG Al processed by severe plastic deformation (SPD). The stacking fault ribbons are 1.4-8.6 nm in width, which is 3-17 times the width of stacking faults in coarse-grained Al. This observation are really surprising considering the high stacking fault energy. Our analytical modelling indicates that these colossal stacking faults were formed due to the size effect in ultrafine-grained Al and the high density of stacking faults and full dislocations. They present a new critical piece to the puzzle of deformation mechanisms in ultrafine-grained materials and provide a good explanation for the good ductility in ultrafine-grained materials.

#### 10:25 AM

**3D** Atom Probe Investigation of a Pearlitic Steel Deformed by High Pressure and Torsion: Xavier Sauvage<sup>1</sup>; Ruslan Z. Valiev<sup>2</sup>; <sup>1</sup>Université de Rouen, Groupe de Physique des Matériaux, CNRS - UMR 6634, Ave. de l'université, BP 12, Saint-Etienne du Rouvray 76801 France; <sup>2</sup>Ufa State Aviation Technical University, Inst. of Physics of Advd. Matls., 12, K. Marx St., Ufa 450000 Russia

The nanostructure and the phase composition of a pearlitic steel deformed by high pressure and torsion (HPT) were investigated by field ion microscopy (FIM) and 3D atom probe (3D-AP). In spite of the extremely high level of plastic deformation, the original lamellar structure of pearlite remains in the deformed material. The interlamellar spacing is however strongly reduced and 3D reconstructions at the atomic scale show that cementie (Fe3C) lamellae are dissolved. The lamellar nanostructure is made of ferrite lamellae almost carbon free and of carbon rich region (former Fe3C) with a carbon amount in a range of 4 to 14 at%. These data are compared with previous investigations of the same pearlitic steel processed by cold drawing.

# 10:40 AM Break

## 10:50 AM Invited

**Plasticity of Ultrafine Grained Materials**: *Horst W. Hahn*<sup>1</sup>; 'TU Darmstadt, Inst. of Matls. Sci., Petersenstr. 23, Darmstadt, Hesse 64287 Germany

From the beginning of research on nanocrystalline metals and ceramics the mechanical properties and in particular the plasticity of this novel class of materials have attracted much attention. This is due to the fact, that the strong grain size dependence of mechanical properties can lead to plastic behavior in brittle materials. There are many reports on mechanical properties of nanocrystalline metals, ceramics and composites. Some surprising results, i.e. the inverse Hall-Petch relationship observed in nanocrystalline metals and alloys, have led to the development of new theoretical models of the deformation processes of materials with nanometer sized grains. In addition, computer simulations have been employed substantially in the last few years to analyze the atomistic processes during deformation. In the talk the experimental results, the phenomenological models and the results of computer simulations will be presented and compared critically.

#### 11:10 AM Invited

**X-Ray Analysis of SPD Metals**: *Igor V. Alexandrov*<sup>1</sup>; Ascar R. Kilmametov<sup>1</sup>; <sup>1</sup>Ufa State Aviation Technical University, Inst. of Physics of Advd. Matls., 12 K. Marx St., Ufa, Bashkortostan 450000 Russia

The results of recent experimental x-ray investigations of bulk ultrafine-grained (UFG) metals, processed with the help of various severe plastic deformation (SPD) techniques are summarized in the given report. At the same time a special attention is paid to the analysis of the processes of preferred orientations as a result of SPD. Metals having different types of the crystal lattice, different SPD schemes (high pressure torsion and equal-channel angular pressing), routes and accumulation strain degrees are considered. The results of low-temperature investigations of metals having different structure, formed at different SPD stages are represented. Regularities in the formation of enhanced atomic displacements depending on the structure state of SPD metals have been established and analyzed.

#### 11:30 AM Invited

Grain Boundary Structure of Nanocrystalline Cu Processed by Cryomilling: J. Y. Huang<sup>1</sup>; X. Z. Liao<sup>2</sup>; Y. T. Zhu<sup>2</sup>; F. Zhou<sup>3</sup>; E. J. Lavernia<sup>3</sup>; <sup>1</sup>Boston College, Dept. Physics, Chestnut Hill, MA 02467 USA; <sup>2</sup>Los Alamos National Laboratory, Matls. Sci. & Tech, Los Alamos, NM 87545 USA; <sup>3</sup>University of California, Dept. Chem. Engrg. & Matl. Sci., Davis, CA 95616 USA

The microstructures of cryogenically ball-milled Cu was investigated by high-resolution electron microscopy. It was found that the grain-size reduction is a dislocation-controlled continuous process, consists of the formation of small-angle grain boundaries, a gradual increase of misorientations as a result of accumulation of more dislocations, and finally, the formation of large-angle grain boundaries (GBs). The grain boundaries were generally curved, wavy or faceted, and heavily strained, which are typical characteristics of nanostructured materials. In addition, extrinsic dislocations were found in many GBs, indicating that most are in a high-energy, non-equilibrium configuration, which is consistent with observations in equal-channel angular pressing processed Cu, Ni, and Al-Mg, repetitive corrugation and straightening processed Cu and room-temperature ball-milled Cu. These results support a still-disputed concept that GBs in nanostructured metals processed by severe plastic deformation are mostly in non-equilibrium states.

## 11:50 AM Invited

Grain Boundary Diffusion and Plasticity of Polycrystalline and Nanostructured Metals and Alloys: Yuri Romanovich Kolobov<sup>1</sup>; <sup>1</sup>SB Russian Academy of Science, Inst. of Strength Physics & Matls. Sci., Lab. Phys. Matls. Sci., Akademicheskii 2/1, Tomsk 634021 Russia

The regular features of grain boundary diffusion in polycrystalline and nanostructured metals and alloys produced by electrodeposition and severe plastic deformation, as well as in the corresponding coarsegrain counterparts are considered. It has been found that the grainboundary diffusivities obtained for nanocrystalline and nanostructured metals far exceeds (by one to four orders) those of the coarse-grain counterparts. The probable physical causes for the above distinguishing features manifested by the diffusion in nanostructured materials are addressed. An investigation was performed for a range of polycrystalline, fine-grained and nanostructured metals, which allowed to reveal a hither to unknown creep activation effect, i.e. initiation of grain boundary sliding by diffusion impurity fluxes from the environment. Using the Mo(Ni) and Fe(Ni) systems by way of an example, it was shown that the action of grain boundary sliding by diffusant fluxes from an external source might cause superplastic state to be realized in the material.

## 12:10 PM

Work Hardening Behaviour of Fine Grained Materials: *Chad* S. Sinclair<sup>1</sup>; Warren J. Poole<sup>1</sup>; Yves Brechet<sup>2</sup>; <sup>1</sup>University of British Columbia, Metals & Matls. Engrg., 309-6350 Stores Rd., Vancouver, BC V6T 1Z4 Canada; <sup>2</sup>Institut National Polytechnique de Grenoble, LTPCM, 1130 rue de la Piscine, Domaine Universitaire, BP 75, Grenoble France

The plastic deformation of fine grained copper and an Al-3.5Mg alloys has been characterized by tensile tests over the temperature range from 77 K to ambient temperature. The temperature dependence of the yield stress and the work hardening behaviour has been examined with particular attention to the influence of grain size. Work hardening behaviour has been characterized by plots of the work hardening rate vs flow stress and energy storage rate vs. flow stress. The results of these experiments are critically evaluated against the classic Kocks-Mecking formulation.

## 12:25 PM

HRTEM and EFTEM Investigation of the Eutectoid Steel After Severe Plastic Deformation: Yulia Ivanisenko<sup>1</sup>; Ian MacLaren<sup>2</sup>; Harald Rösner<sup>1</sup>; Ruslan Z. Valiev<sup>3</sup>; Hans-Jörg Fecht<sup>1</sup>; <sup>1</sup>Forschungszentrum Karlsruhe, INT, PO Box 3640, Karlsruhe D-76021 Germany; <sup>2</sup>Darmstadt University of Technology, Inst. for Matls. Sci., Darmstadt 64287 Germany; <sup>3</sup>Ufa State Aviation Technical University, Inst. of Phys. of Advd. Matls., Ufa 450000 Russia

The nanocrystalline structure of a eutectoid steel after severe plastic deformation by High Pressure Torsion (HPT) was studied by means of High Resolution TEM (HRTEM) and Energy Filtered TEM (EFTEM). In an as-processed specimen nano-sized areas of modulated fringe contrast were revealed. It was shown, that in most cases the observed fringes can be explained as Moiré patterns resulting from the overlapping of two lattices: normal iron and a highly distorted lattice with a structure similar to BCC iron. It seemed most likely that these distorted regions were transitional carbon-containing phases. Distortions due to dislocation networks were shown to be unlikely in this case. EFTEM investigation revealed a fairly uniform distribution of carbon in the HPT steel that corresponds well with our previous results about total cementite dissolution as a result of HPT, although some small carbon enrichments were seen, which correspond to the distorted phases observed by HRTEM.

# 5th Global Innovations Symposium: Trends in LIGA, Miniaturization, and Nano-Scale Materials, Devices and Technologies: Properties and Characterization of Materials for Microsystem/LIGA Applications

Sponsored by: Materials Processing & Manufacturing Division, MPMD-Powder Materials Committee, MPMD-Phase Transformations Committee-(Jt. ASM-MSCTS), MPMD-Computational Materials Science & Engineering-(Jt. ASM-MSCTS), MPMD/EPD-Process Modeling Analysis & Control Committee, MPMD-Surface Engineering Committee, MPMD-Shaping and Forming Committee, MPMD-Solidification Committee

*Program Organizers:* John E. Smugeresky, Sandia National Laboratories, Department 8724, Livermore, CA 94551-0969 USA; Steven H. Goods, Sandia National Laboratories, Livermore, CA 94551-0969 USA; Sean J. Hearne, Sandia National Laboratories, Albuquerque, NM 87185-1415 USA; Neville R. Moody, Sandia National Laboratories, Livermore, CA 94551-0969 USA

 Tuesday PM
 Room: 202B

 March 16, 2004
 Location: Charlotte Convention Center

Session Chairs: James P. Lucas, Michigan State University, Chem. Engrg. & Matls. Sci., E. Lansing, MI 48824-1226 USA; John Jungk, University of Minnesota, Chem. Engrg. & Matls. Sci., Minneapolis, MN 55401 USA

## 2:00 PM

New Nanoindentation and Scanning Probe Tools and Techniques: Warren C. Oliver<sup>1</sup>; <sup>1</sup>MTS Nano Instruments Innovation Center, 1001 Larson Dr., Oak Ridge, TN 37931 USA

Recent developments in the tools and techniques associated with Nanoindentation and probe scanning techniques will be presented. New calibration techniques provide simpler verification of system performance and accuracy. Quantitative sample scanning equipment and techniques provide the user with new tools for the mechanical characterization of miniature structures (MEMS) and allow for new types of mechanical properties testing of films. Indentation, uniaxial and biaxial tensile testing of thin films will be described.

#### 2:20 PM

Fatigue of LIGA Ni MEMS Structures: J. Lou<sup>1</sup>; S. Allameh<sup>1</sup>; R. Rabeeh<sup>1</sup>; B. L. Boyce<sup>2</sup>; T. E. Buchheit<sup>1</sup>; W. O. Soboyejo<sup>1</sup>; <sup>1</sup>Princeton University, PMI/MAE Dept., D404 Engr. Quad., Olden St., Princeton, NJ 08544 USA; <sup>2</sup>Sandia National Laboratories, PO Box 5800, Albuquerque, NM 87185-5800 USA

This paper presents the results of recent studies of fatigue in LIGA Ni MEMS structures. Following a brief review of microstructures and micro-textures, the micromechanisms of fatigue are elucidated for cyclic deformation under uniaxial tension and bending conditions. Stress-life and strain-life are also presented, along with Coffin-Manson approaches to the modeling of low- and high-cycle fatigue. Finally, the results from recent fatigue crack growth experiments are described before discussing the implications of the current work for the design and assessment of reliable LIGA Ni MEMS devices.

#### 2:40 PM

High Temperature Tensile and Creep Properties of LIGA Materials: *Thomas E. Buchheit*<sup>1</sup>; Steven H. Goods<sup>2</sup>; Brad L. Boyce<sup>1</sup>; Joseph R. Michael<sup>3</sup>; James J. Kelly<sup>4</sup>; <sup>1</sup>Sandia National Laboratories, Dept. 1851, MS 0889, PO Box 5800, Albuquerque, NM 87185 USA; <sup>2</sup>Sandia National Laboratories, Dept. 8725, MS 9404, PO Box 969, Livermore, CA 94551 USA; <sup>3</sup>Sandia National Laboratories, Dept. 1822, MS 0886, PO Box 5800, Albuquerque, NM 87185 USA; <sup>4</sup>Sandia National Laboratories, Dept. 8729, MS 9401, PO Box 969, Livermore, CA 94551 USA

Specific applications utilizing the LIGA (Lithography, Electroforming, Molding) technology require materials with reasonable strength and creep resistance up to ~600°C. The primary processing method utilized within the LIGA technology is electrodeposition, thus pure metals with a successful electroplating history, such as Ni and Cu, remain the favored LIGA structural materials. However, pure metals anneal soften readily and have poor strength and creep resistance at even modest elevated temperatures. To meet specified properties criteria necessary for high temperature applications, new material systems must be developed within the electroplating constraints imposed by LIGA technology. This presentation focuses on high temperature and creep testing results from one promising LIGA alloy, pulse plated Ni- (0.5-1.0at%) Mn. LIGA Ni-Mn results will be compared baseline pure LIGA Ni results and results from a previously reported study on LIGA fabricated oxide dispersion strengthened nickel (ODS-Ni). When appropriate, commensurate microstructure analysis was performed. Results indicate that improved elevated temperature strength and creep resistance can be realized through appropriate choice of the electrodeposited material. Sandia is a multiprogram laboratory operated by Sandia Corporation, a Lockheed Martin company, for the United States Department of Energy under Contract DE-AC04-94AL85000.

#### 3:00 PM

Characterization of Twinning in Electrodeposited Ni-Mn for Microsystems Applications: Gene A. Lucadamo<sup>1</sup>; Nancy Y.C. Yang<sup>1</sup>; James J. Kelly<sup>2</sup>; Alec Talin<sup>3</sup>; Douglas L. Medlin<sup>4</sup>; <sup>1</sup>Sandia National Laboratories, Analytical Matls. Sci., MS 9161, PO Box 969, Livermore, CA 94551-0969 USA; <sup>2</sup>Sandia National Laboratories, Microsys. Procg., MS 9410, PO Box 969, Livermore, CA 94551-0969 USA; <sup>3</sup>Sandia National Laboratories, Nanolithography, MS 9409, PO Box 969, Livermore, CA 94551-0969 USA; <sup>4</sup>Sandia National Laboratories, Thin Film & Interface Sci., MS 9161, PO Box 969, Livermore, CA 94551-0969 USA

Twinning is ubiquitous in electrodeposited metals. We have investigated twinning in Ni-Mn alloys developed for use in the LIGA process. In this material, twins are present at high densities with widths on the order of nanometers. The presence of many twin boundaries combined with an overall refinement in grain size enhances the mechanical strength in the alloy electrodeposits. Transmission electron microscopy (TEM) was used to characterize twinning in as-plated microstructures. In general, the orientation of the twin planes with respect to the plating direction depends directly on the crystallographic texture. For instance, in {110} textured deposits twinning can occur on {111} planes perpendicular and oblique to the substrate. However, planview TEM images of Ni-Mn show that twins are formed primarily on those planes parallel to the plating direction. Consequently, repeated twinning on equivalent planes results in multiply-twinned particles and grains enclosed by twin boundaries. Measurements of twin density in Ni-sulfamate with and without Mn indicate that while the addition of <1 wt.% Mn clearly refines the microstructure, it also dramatically increases the incidence of twin formation. Another consequence of this high twinning density is the formation of a large number of junctions where the twin boundaries intersect. Our measurements show that the junction density is comparable to the density of dislocations in a cold-worked metal. The strain fields associated with these junctions can interact with dislocations and act as pinning sites. A comparison shows that the twin microstructure in direct and pulsedcurrent deposits are qualitatively similar. Sandia is a multiprogram laboratory operated by Sandia Corporation, a Lockheed Martin Company, for the United States Department of Energy's National Nuclear Security Administration under contract DE-AC04-94AL85000.

#### 3:20 PM Break

# 3:40 PM

Nanostructured Metals for Enhanced Performance of LIGA Components: Mohammadreza Baghbanan<sup>1</sup>; Uwe Erb<sup>1</sup>; Gino Palumbo<sup>2</sup>; <sup>1</sup>University of Toronto, Matls. Sci. & Engrg., Rm. 140, 184 College St., Toronto, Ontario M5S 3E4 Canada; <sup>2</sup>Integran Technologies Inc., #1 Meridian Rd., Toronto, Ontario M9W 4Z6 Canada

This paper addresses the issues of performance variability and reliability concerns frequently encountered with metallic microsystem components produced by electrodeposition methods such as LIGA. Experimental results will be presented which demonstrate that microsystem components produced by conventional electrodeposition approaches show relatively low overall hardness and considerable variations in Young's modulus and hardness throughout the cross section of the components. These undesirable properties are traced back to i) the microstructure of the deposits which is characterized by grain size gradients resulting from the fine grained to columnar structure transition and ii) the relatively large grain size in comparison to the overall component size. In past efforts both post deposition recrystallization annealing and texture control during the electroplating process have been used to alleviate these concerns, with some limited success. In this paper we present a new approach which essentially involves the modification of the electrodeposition process to produce fully dense nanostructured deposits throughout the entire cross section of the component without transition from fine to large grained columnar structure. Results will be presented for such components which show i) uniform hardness and Young's modulus in cross section and ii) significant enhancements in hardness and other important performance indicators such as specific strength, elastic energy storage capacity and wear resistance.

Combining On-Chip Testing and Electron Microscopy to Obtain a Mechanistic Understanding of Fatigue and Wear in Microelectromechanical Systems: Daan Hein Alsem<sup>1</sup>; Eric A. Stach<sup>2</sup>; Christopher L. Muhlstein<sup>3</sup>; Michael T. Dugger<sup>4</sup>; Robert O. Ritchie<sup>1</sup>; <sup>1</sup>University of California, Dept. of Matls. Sci. & Engrg., 1 Cyclotron Rd., MS 72/150, Berkeley, CA 94720 USA; <sup>2</sup>Lawrence Berkeley National Laboratory, Natl. Ctr. for Electron Microscopy, 1 Cyclotron Rd., MS 72/150, Berkeley, CA 94703 USA; <sup>3</sup>Pennsylvania State University, Dept. of Matls. Sci. & Engrg., 310 Steidle Bldg., Univ. Park, PA 16802 USA; <sup>4</sup>Sandia National Laboratory, Matls. & Process Scis. Ctr., PO Box 5800, Albuquerque, NM 87185-0889 USA

Wear and fatigue are important factors in determining the reliability of microelectromechanical systems (MEMS). While the reliability of MEMS has received extensive attention, the physical mechanisms responsible for these failure modes have yet to be conclusively determined. In our work, we use a combination of on-chip testing methodologies and electron microscopy observations to investigate these mechanisms. Our previous studies have shown that fatigue in polysilicon thin films is a result of a "reaction-layer" process, whereby high stresses induce a room-temperature mechanical thickening of the native oxide, which subsequently undergoes environmentally-assisted cracking. In this presentation, we discuss how the initial native oxide thickness affects the fatigue life and report on new in vacuo observations, which exploit a phase-lock loop control system to drive the test system at resonance. This allows us to characterize both the changes in fatigue behavior and development of reaction layers in a relatively oxygenfree environment. Additionally, we have used polysilicon MEMS sidewall friction test specimens to study active mechanisms in sliding wear, including the role of the surface roughness and the presence of lubricants (such as an oxide layer or a thin film of water). In particular, we have performed in vacuo and in-situ experiments in the scanning electron microscope, with the objective of determining the mechanisms causing both wear development and debris.

# 4:20 PM

Fabrication and Testing of Ultra Small-Scale Samples: S. J. Polasik<sup>1</sup>; H. L. Fraser<sup>1</sup>; M. J. Mills<sup>1</sup>; M. D. Uchic<sup>2</sup>; D. M. Dimiduk<sup>2</sup>; <sup>1</sup>Ohio State University, Matls. Sci. & Engrg. Dept., Columbus, OH 43210 USA; <sup>2</sup>Air Force Research Laboratory, Matls. & Mfg. Direct., Wright-Patterson AFB, OH 4533-7817 USA

In this talk we describe an ultra small-scale mechanical testing methodology capable of investigating the mechanical behavior of small volumes of material with dimensions of tens of micrometers. This method alleviates the need to fabricate macroscopic specimens that may differ in chemistry, microstructure, scale, and impurity content from the manufactured component. Dual Beam Focused Ion Beam (DB-FIB) microscopes provide the capability to site specifically machine micron-scale three dimensional structures that function as test specimens. DB-FIB machined cylindrical compression specimens, with diameters ranging from 5µm to 40µm, are tested in uniaxial compression at room temperature using a nanoindenter equipped with a flatended tip. Presently, single crystal Ti-6Al is under investigation as a model for the a-phase of commercial Ti alloys. The comparison of this data with the bulk sample response will be discussed. Additionally, this talk will also discuss the development of a tensile testing methodology capable of characterizing samples at this size scale.

#### 4:40 PM

Mechanical Property Measurements of Pure Ni, Ni<sub>3</sub>Al, and Ni-Base Superalloys at the Micron-Size Scale: *Michael D. Uchic*<sup>1</sup>; Dennis M. Dimiduk<sup>1</sup>; Michael J. Seekely<sup>1</sup>; Jeff N. Florando<sup>2</sup>; William D. Nix<sup>3</sup>; <sup>1</sup>Air Force Research Laboratory, Matls. & Mfg. Direct., AFRL/ MLLMD, 2230 Tenth St., WPAFB, OH 45433-7817 USA; <sup>2</sup>Lawrence Livermore National Laboratory, Livermore, CA USA; <sup>3</sup>Stanford University, Dept. of Matls. Sci. & Engrg., Stanford, CA 94305-2205 USA

In order to measure the critical resolved shear stress from individual grains of a fully-processed polycrystalline engineering alloy, we have developed a test methodology to extract mechanical test samples from the bulk that have micron-size dimensions. The test methodology consists of using both a Focused Ion Beam microscope to fabricate compression specimens from the bulk, and a nanoindenter fitted with a flat tip to perform uniaxial compression tests. Using this methodology, we have performed microsample compression experiments on three different metallic bulk single crystals-pure Ni, Ni<sub>3</sub>(Al, Ta), and a Ni-base superalloy (gas turbine blade alloy composition)-and a polycrystalline Ni-base superalloy (gas turbine disk alloy composition). The fabrication of microsamples from bulk single crystals has allowed us to compare the effect of microsample specimen size on the resultant mechanical properties, and we have tested samples ranging in size from tens of microns to sub-micron in diameter in order to find the

size limit where the microsamples deviate from bulk behavior. Of note, we have measured a significant size effect for Ni<sub>3</sub>Al (where the yield strength increases dramatically with decreasing sample size), whereas more subtle size effects are observed for the pure Ni and Nibase superalloy. We also show measurements of the single crystal mechanical properties for specimens isolated within single grains of a polycrystalline superalloy using this test methodology.

# Advanced Materials for Energy Conversion II: Complex Hydrides II

Sponsored by: Light Metals Division, LMD-Reactive Metals Committee

*Program Organizers:* Dhanesh Chandra, University of Nevada, Metallurgical & Materials Engineering, Reno, NV 89557 USA; Renato G. Bautista, University of Nevada, Department of Chemical and Metal Engineering, Reno, NV 89557-0136 USA; Louis Schlapbach, EMPA Swiss Federal, Laboratory for Materials Testing and Research, Duebendorf CH-8600 Switzerland

Tuesday PM	Room: 2	03A		
March 16, 2004	Location:	Charlotte	Convention	Center

*Session Chairs:* Klaus Yvon, Université de Genève, Lab. de Cristallographie, Geneva Switzerland; Reiner Kirchheim, Universitaet Goettingen, Inst. fuer Materialphysik, Goettingen D-37077 Germany; Hiroyuki T. Takeshita, Kansai University, Fac. of Engrg., Suita, Osaka 564-8680 Japan

# 2:00 PM Keynote

Complex Metal Hydrides for Hydrogen Storage: What Are Their Limits of Performance?: Klaus Yvon<sup>1</sup>; <sup>1</sup>Université de Genève, Lab. de Cristallographie, Geneva Switzerland

In principle, solid-state metal hydrides provide the safest and most energy efficient means of storing reversibly hydrogen at ambient conditions. However, in spite of considerable R&D efforts the materials presently available do not meet performance targets for a great variety of applications, both stationary and mobile, such as fuel cells. Critical issues are weight efficiency, reversibility, kinetics and cost. Some thousand binary, ternary and quaternary metal hydrides are known and more are about to be discovered. Those considered to have greatest potential at present are the so-called "complex" metal hydrides that derive their name from the presence of discrete metal-hydrogen complexes in their structures (for reviews see refs.1 and 2). The complexes are centred by either p-elements such as B and Al or d-elements such as Mn, Fe, Co, Ni, Cu and Zn. In this contribution an attempt is made to evaluate the potential of complex metal hydrides to meet performance targets such as those recently reformulated for the transportation sector by various national research funding agencies. At first sight p-metal hydrides appear to be favoured over d-metal hydrides because of weight and cost considerations. However, the situation is far from being clear-cut. While the performance limits with respect to weight, reversibility and cost are relatively well known for p-elements such limits are less apparent for d-elements. The hydrogen-to-metal ratio, for example is limited to H/M~3 for current p-metal hydrides while it may exceed H/M=4 for d-metal hydrides. Thus the door for new discoveries among d-metal hydrides remains wide open. Finally, it is argued that performance targets for hydrogen storage should not be based exclusively on present-day technology, consumer habit and profit seeking. Additional aspects such as sustainability, energy saving and environment must be taken into account in order to avoid over-ambitious performance targets, unrealistic expectations and undesirable side effects such as blocking of promising research fields that are wrongly considered unapt to meet preset performance targets. 1K. Yvon : Solid state transition metal complexes, in Encycl. Inorg. Chem. (Ed. R.B. King) 3, 1401 John Wiley (1994); see also Chimia 52, 613. (1998). 2G. Sandrock and B. Bogdanovic, MRS bulletin.

#### 2:25 PM Invited

Electrochemical Insertion of Lithium into Si-C Composite Prepared by Mechanical Ball Milling: *Jai-Young Lee*<sup>1</sup>; Ki-Tae Kim<sup>1</sup>; Yong-Ju Lee<sup>1</sup>; Yong-Mook Kang<sup>1</sup>; You-Min Kim<sup>2</sup>; Seo-Jae Lee<sup>2</sup>; Ki-Young Lee<sup>2</sup>; <sup>1</sup>KAIST, Dept. of Matl. Sci. & Engrg., 373-1, Kuseongdong, Yuseong-gu, Dae-jeon 305-701 Korea; <sup>2</sup>Battery Research Institute, LG Chem. Ltd. Rsch. Park, 104-1, Yuseong-gu, Daejeon 305-380 Korea

In recent years, graphite materials have been an anode in lithium secondary battery. In spite of their successful commercialization, however, various new anode materials have been investigated to overcome

the limited theoretical capacity of graphite (372 mAh/g). Intermetallic compounds such as Sn, Sb, and Si have been extensively investigated because of high capacity. Among them, tin or silicon based intermetallic compounds appear to be promising anode materials. However, large irreversible capacity at the first charge-discharge cycle and poor cyclability are still serious problems. These problems are caused by a large volume change of particles or grains during Li insertion and extraction. Therefore, modified micro or nano structure which can accommodate the volume expansion is required for practical use. In this study, we report the electrochemical properties of Si-C composite prepared by mechanical ball milling. Micro or nano structure of Si-C composite can be controlled by mechanical ball milling because it can apply high energy to material. Further, lithium insertion/extraction behavior into/from Si-C composite was investigated. Si-C composite showed 3 distinct peaks at the first cycle in CV measurement. The two peaks at about 1.7 V and 0.7 V correspond to the electrolyte decomposition and SEI formation respectively. After 2nd cycle, 1.7 V peak and  $0.7\ V$  peak were hardly observable. Constant current (0.2 C rate) was performed between 1.5 and 0.005 V (versus Li/Li+) at 1st cycle, and between 1.5 and 0.01 V (versus Li/Li+) from 2nd cycle. The discharge capacity of 1st cycle was about 1020 mAh/g, and after 2nd cycle it was deceased to about 680 mAh/g. Coulombic efficiency was higher than 98.7% after 3rd cycle. It is conformed by XRD data that Li was intercalated to the C first, and then reacted with Si during Li insertion at 1st cycle. Further, Li was deintercalated from C first, and then extracted from Si during Li extraction at 1st cycle. It is expected that strong bonding, observed by XPS and FTIR should increase the contact between Si and C. We think that Si-C electrical connection will be maintained because of their strong bonding. From the charge/discharge capacity analysis, it was conformed that Si and C were partially participated in the reaction. After 50th cycle, capacity was maintained about 678 mAh/g, which is remarkable result. We can summarize the reasons for good cyclability of Si-C composite. First reason is the partial participation of Si and C in the reaction with Li. Second reason is the strong bonding between Si and C, which will maintain the electrical contact. And the final reason is the stored stress in carbon layer due to the earlier reaction with Li than that of Si. The Si-C composite prepared by high energy ball milling can be suggested as a new anode active material with high capacity and good cyclability for Li ion batteries.

# 2:50 PM Invited

## Structural and Thermodynamic Aspects of Alanates for Hydrogen Storage: Karl J. Gross<sup>1</sup>; <sup>1</sup>Hy-Energy LLC, 33902 Juliet Cir., Fremont, CA 94555 USA

The discovery that hydrogen can be reversible absorbed and desorbed from NaAlH4 by doping with Ti and other transition metals has created an entirely new prospect for lightweight hydrogen storage<sup>1</sup>. NaAlH4 releases hydrogen through the following set of decomposition reactions. NaAlH4 -> 1/3(Na3AlH6) + 2/3Al + H2 -> NaH + Al + 3/2H2 An overview is presented of recent advances in the development of new and improved alanates for hydrogen storage applications and in the fundamental understanding of how Ti-doping enhances hydrogen absorption. New methods of preparing and doping the alanates, absorption/desorption performance, safety aspects, cycle-life studies, and results on other complex hydrides will be discussed. <sup>1</sup>Bogdanovic and Schwickardi, J. Alloys and Compounds Vol. 253,1 (1997).

# 3:15 PM Break

3:30 PM Cancelled

# Hydrogen Storage in Graphitic Nanofibres

# 3:55 PM

Alkaline-Earth Metals and Alloys for Energy Storage: *Hiroyuki T. Takeshita*<sup>1</sup>; <sup>1</sup>Kansai University, Fac. of Engrg., Dept. of Matls. Sci. & Engrg., 3-3-35, Yamate-chou, Suita, Osaka 564-8680 Japan

Alkaline Earth Metals and Alloys are one of the promising candidates for hydrogen storage system of hydrogen energy system. Mg and  $Mg_2Ni$ -based alloys are attractive as hydrogen fuel storage tank of fuel cell electric vehicles because of their high gravimetric hydrogen storage capacities, while some Ca-Mg-Ni based alloys such as  $(Ca,Mg)Ni_3$ , which have been recently developed, exhibit reversible hydrogenation/ dehydrogenation properties at ambient temperatures and pressures, accompanied by very flat plateau, and are expected to be applied to hydrogen stations as inexpensive hydrogen absorbers. In this talk, some recent topics will be introduced on Mg and Mg\_2Ni based alloys,  $(Ca,Mg)Ni_2$  and  $(Ca,Mg)Ni_3$  alloys and metastable MgNi and CaNi based hydrides which can be obtained by mechanical alloying.

# 4:15 PM Canceled

# A Mechanism for Sodium Alanate Decomposition

#### 4:35 PM

Outgassing in the LiD/LiOH System: Long N. Dinh<sup>1</sup>; William McLean<sup>1</sup>; Marcus A. Schildbach<sup>1</sup>; James D. LeMay<sup>1</sup>; Wigbert J. Siekhaus<sup>1</sup>; Mehdi Balooch<sup>1</sup>; <sup>1</sup>Lawrence Livermore National Laboratory, Chmst. & Matls. Sci., 7000 East Ave., PO Box 808, L-356, Livermore, CA 94551 USA

Temperature programmed decomposition and complimentary microscopy from the surface inward. The energy barriers measured for the decomposition of surface and near-surface lithium hydroxide are noticeably smaller than the values associated with bulk counterpart. The conversion of Li2O grains back to lithium hydroxide during moisture exposure was also found to proceed from the surface inw/spectroscopy techniques were performed on micrometer-grain lithium hydroxide. The results reveal that lithium hydroxide grains are thermally decomposed into Li2O, releasing H2O, following a three dimensional phase boundary movementard such that surface states are filled before bulk states. In a different set of experiments, nanometer composite grains composed of LiD inner cores and LiOH outer layers were observed to form on top of pressed polycrystalline LiD upon moisture exposure. A diffusion coefficient on the order of 10-23 m2/sec was measured for the diffusion controlled reaction of LiOH with LiD in the nanopowder at room temperature in a dry environment. The measured kinetics in this work were used to construct the evolution steps in the LiD/LiOH composite system in a dry environment.

# Advances in Superplasticity and Superplastic Forming: Advances in Superplastic Forming of Light Alloys

Sponsored by: Materials Processing and Manufacturing Division,
Structural Materials Division, MPMD-Shaping and Forming
Committee, SMD-Mechanical Behavior of Materials-(Jt. ASM-MSCTS),
SMD-Structural Materials Committee
Program Organizers: Eric M. Taleff, University of Texas,
Mechanical Engineering Department, Austin, TX 78712-1063 USA;
P. A. Friedman, Ford Motor Company, Dearborn, MI 48124 USA;
Amit K. Ghosh, University of Michigan, Department of Materials
Science and Engineering, Ann Arbor, MI 48109-2136 USA; P. E.
Krajewski, General Motors R&D Center; Rajiv S. Mishra, University of Missouri, Metallurgical Engineering, Rolla, MO 65409-0340
USA; J. G. Schroth, General Motors, R&D Center, Materials and Processes Laboratory, Warren, MI 48090-9055 USA

Tuesday PMRoom: 201BMarch 16, 2004Location: Charlotte Convention Center

Session Chairs: Peter A. Friedman, Ford Motor Company, Dearborn, MI 48121 USA; Eric M. Taleff, University of Texas, Dept. of Mech. Engrg., Austin, TX 78712-0292 USA

# 2:00 PM

Research Opportunities for Automotive SPF Alloys: Paul E. Krajewski<sup>1</sup>; <sup>1</sup>General Motors, R&D Ctr., 30500 Mound Rd., MC 480-106-212, Warren, MI 48090 USA

General Motor's extensive experience with superplastic forming has resulted in a unique opportunity to produce, characterize, and understand superplastic materials capable of high volume automotive production. This work has included investigations into the effects of composition, second phase particles, and thermomechanical processing on elevated temperature behavior as well as understanding deformation mechanisms, elevated temperature fracture, and surface phenomena. The goal of this paper is to identify opportunities for research to improve the performance of superplastic materials, which could ultimately result in wider use of superplastic forming in the automobile industry.

## 2:25 PM

Particle Interface Damage Effect on Cavitaion Control in Superplastic Aluminum Sheet: *Amit K. Ghosh*<sup>1</sup>; Ruth Cleveland<sup>1</sup>; <sup>1</sup>University of Michigan, Matls. Sci. & Engrg., 2300 Hayward St., Ann Arbor, MI 49109-2136 USA

Recent studies have confirmed that cavitation in commercial alloys used in superplastic forming application start primarily at the interface of hard second phase particles and inclusions. Analysis of preexisting damage on particle surface has demonstrated that the nuclei for cavities typically undergo plasticity growth to become eventually visible under the optical microscope. In this work, we obtained evidence that damage is produced at particle-matrix interface during cold rolling of the alloy, which is generally not fully recovered during annealing or recrystallization practice. In this regard, prior sintering models appear to be inconsistent with the times required for void closure. However, the application of high hydrostatic pressure at elevated temperature has been found to improve the integrity of the particle-matrix interface, and significantly reduce the cavitation tendencies of these alloys. The experimental results will be viewed in relation to theoretical considerations and discussed in this paper.

### 2:45 PM

Superplasticity in a 15% Vol. Al2O3 Particulate-Reinforced 6061Al Alloy Composite: Lihong Han<sup>1</sup>; Henry Hu<sup>1</sup>; Derek Northwood<sup>1</sup>; <sup>1</sup>University of Windsor, Dept. of Mech., Auto. & Matl. Engrg., Windsor, Ontario N9B 3P4 Canada

The superplastic characteristics of a 15% vol.% Al2O3 particulatereinforced 6061Al alloy composite have been studied. The composite was fabricated by Powder Metallurgy techniques and hot-extruded with two different extrusion ratios. The grain size after extrusion is approximately 3 im and is stable at high temperatures. The composite exhibits superplasticity (with an elongation to failure of 200%) at lower strain rates (approximately 10-4). The superplastic properties of the composite, including elongation, strain rate sensitivity, and activation energy, were characterized. Differential Thermal Analysis (DTA) was used to ascertain the possibility of any partial melting in the vicinity of the optimum superplastic temperature. Scanning Electron Microscopy (SEM) was used to observe the distribution of reinforcement in matrix and the failure characteristics of the surface of the specimen, and Transmission Electronic Microscopy (TEM) was used to characterize for the interfacial behaviors (grain-grain and grainreinforcement) and the configuration of dislocations in the matrix.

#### 3:05 PM

Analysis of Superplastic Deformation of Al-Al4C3 Composites: *Michal Besterci*<sup>1</sup>; Oksana Velgosova<sup>2</sup>; <sup>1</sup>Slovac Academy of Science, Inst. of Matls. Rsch., Watsonova 47, Kosice 04353 Slovakia; <sup>2</sup>Technical University, Fac. of Metall., Dept. of Non-Ferrous Matls. & Waste Treatment, Letna 9/A, Kosice 04200 Slovakia

Mechanical alloying technique, such as dry, high energy ball milling process, is suitable for producing composite metal powders with a fine controlled microstructure. This method is crucial for obtaining a homogeneous distribution of nano-sized dispersoids in a more ductile matrix (e.g. aluminium- or copper based alloys). Dispersoids can be formed in a solid state reaction of materials that react with the matrix during milling or during subsequent heat treatment. Superplastic deformation is a combination of parallel processes such a slip on grain boundaries, dislocation creep, and recrystalisation. The aim of this work is to investigate deformation process in the AI-AI4C3 systems with different second phase particle content under different temperatures and strain rates, and analyse the corresponding deformation process.

# 3:25 PM Break

# 3:45 PM

Achieving Superplasticity in Light Alloys Through the Application of Severe Plastic Deformation: Cheng Xu<sup>1</sup>; Minoru Furukawa<sup>2</sup>; Zenji Horita<sup>3</sup>; *Terence G. Langdon*<sup>1</sup>; <sup>1</sup>University of Southern California, Aeros. & Mechl. Engrg. & Matls. Sci., Los Angeles, CA 90089-1453 USA; <sup>2</sup>Fukuoka University of Education, Dept. of Tech., Munakata, Fukuoka 811-4192 Japan; <sup>3</sup>Kyushu University, Matls. Sci. & Engrg., Faculty of Engrg., Fukuoka 812-8581 Japan

The light alloys, such as aluminum and magnesium, have considerable potential for use in the automotive industry. However, the superplastic forming of conventional alloys, where the grain sizes are often ~5  $\mu$ m or larger, tends to occur at strain rates which are generally too slow for use in the processing of high volumes of components. This limitation may be removed, and the superplastic forming operation achieved at a faster rate, by reducing the grain size of the alloy to the submicrometer or even the nanometer level. This paper describes the process of achieving grain refinement and superplastic properties in representative Al and Mg alloys using a procedure in which the alloys are subjected to severe plastic deformation. The results show that this processing technique is capable of producing excellent superplastic properties in alloys that are nominally not superplastic.

#### 4:10 PM

High Strain Rate Superplasticity in Friction Stir Processed Aluminum Alloys: *Rajiv S. Mishra*<sup>1</sup>; Zong Yi Ma<sup>1</sup>; Indrajit Charit<sup>1</sup>; <sup>1</sup>University of Missouri, Dept. of Metallurgl. Engrg., 1870 Miner Cir., Rolla, MO 65409 USA

Friction stir processed aluminum alloys exhibit enhanced superplasticity. In addition, friction stir processing can enable several new concepts, such as, selective superplasticity, thick plate superplasticity and superplasticity of contoured plates. A brief review of the state-ofthe-art will be presented. The constitutive relation for friction stir processed aluminum alloys show an enhancement of more than 20 times. Friction stir processing is an enabling concept that can extend the use of superplastic forming for new applications. The support of the National Science Foundation through grants DMI-0085044 and DMI-0323725 is gratefully acknowledged.

#### 4:30 PM

High Strain Rate Superplasticity in a Commercial Al-Mg-Li-Sc-Zr Alloy Subjected to Hot Intense Plastic Straining: Fanil Musin<sup>1</sup>; Rustam O. Kaibyshev<sup>1</sup>; Ksenia Saytaeva<sup>1</sup>; <sup>1</sup>Institute for Metals Superplasticity Problems, Khalturina 39, Ufa 450001 Russia

The superplastic properties of an Al-4.1%Mg-2.0%Li-0.16%Sc-0.07%Zr alloy subjected to intense plastic straining by equal-channel angular extrusion (ECAE) at 400°C was studied in the temperature interval 250-500°C at strain rates ranging from  $1.4\times10^{-5}$  to  $1.4 \text{ s}^{-1}$ . The grain size after ECAE was about 3 µm and the fraction of high angle boundaries was about 90%. The highest elongation to failure of about 3000% appeared at a temperature of 450°C and initial strain rate of  $1.4\times10^{-2} \text{ s}^{-1}$  with the strain rate sensitivity coefficient of about 0.65. It was shown that the ECAE processed alloy exhibits high strain rate superplasticity properties in the temperature range 350-500°C with ductility higher than 1000%. Microstructural evolution and cavitation during high strain rate deformation were examined in detail.

# Alumina and Bauxite: Technology and Future Trends

Sponsored by: Light Metals Division, LMD-Aluminum Committee Program Organizers: Travis Galloway, Century Aluminum, Hawesville, KY 42348 USA; David Kirkpatrick, Kaiser Aluminum & Chemical Group, Gramercy, LA 70052-3370 USA; Alton T. Tabereaux, Alcoa Inc., Process Technology, Muscle Shoals, AL 35661 USA

Tuesday PM	Room:	218A
March 16, 2004	Location	: Charlotte Convention Center

Session Chair: Lester A.D. Chin, McDonough, GA 30252-3917 USA

#### 2:00 PM

Solubility of Calcium in Bayer Liquor: Marie Raty<sup>1</sup>; Kenneth T. Stanton<sup>1</sup>; B. K. Hodnett<sup>1</sup>; M. Loan<sup>1</sup>; <sup>1</sup>University of Limerick, Matl. Sci. & Tech. Dept., Plassey Technological Park, Limerick Ireland

There is empirical evidence which suggests that calcium inhibits precipitation of gibbsite (AI2O3.3H20) in the Bayer process. This phenomenon may be used in the mud circuit as a means of preventing loss of product or scale reduction. Here, we present a comprehensive study of calcium solubility in water, caustic soda, synthetic Bayer liquor and also in a liquor obtained from an alumina refinery. Experiments were based on Ca added as CaCO3 and solubility was determined in each case as a function of time and temperature. In addition, solubilities in NaOH and Bayer liquors were determined as a function of causticity and concentration of aluminate respectively. Surprisingly, results show little difference in Ca solubility in water as a function of temperature. Solubility increases with caustic concentration up to 1 M NaOH and decreases thereafter. Also, greater concentration of aluminate in synthetic liquors decrease the solubility.

# 2:25 PM

**Organic Control Technologies in Bayer Process**: *Gervais Soucy*<sup>1</sup>; Jacques E. Larocque<sup>2</sup>; Guy Forté<sup>3</sup>; <sup>1</sup>Université de Sherbrooke, Chem. Engrg. Dept., 2500 Blvd. Université, Sherbrooke, Québec J1K 2R1 Canada; <sup>2</sup>Consultant, Asbestos, Québec J1T 1W6 Canada; <sup>3</sup>Alcan International Ltd., Arvida R&D Ctr., 1955 Blvd. Mellon, CP 1250, Jonquière, Québec G7S 4K8 Canada

Many Bayer plant problems originate from organics contamination of the Bayer liquor. Organics can decrease liquor productivity either by increasing alumina solubility or by covering active sites on alumina hydrate seeds. Organics also induce coloration of the liquor, cause excessive foaming, and increase liquor viscosity, density and boiling point. All these examples have deleterious effects on the Bayer process. This paper describes a full survey of patent literature including more than 60 patents filed between 1953 and 2001. Most patents in use today were issued in the early 80's. Apart from sodium oxalate control, very few patents are still in use with the sole objective of controlling organic carbon species in Bayer liquor. The most likely **TUESDAY PM** 

explanation is the poor economic viability of organics control in general. Most of the recent patents combine several different methods to reach the objective of organics control. A new innovative technology will be presented. It involves treatment of Bayer spent liquor by direct contact with thermal submerged plasma. The multi-forms of energy provided by the plasma are efficiently used. Preliminary results will be given.

## 2:50 PM

## Alumina Refinery Brownfield Expansion - Hindalco Experience: *R. P. Shah*<sup>1</sup>; Sheo Nandan Gararia<sup>1</sup>; R. J. Singh<sup>1</sup>; <sup>1</sup>Hindalco Industries Ltd., PO Renukoot 231 217, Sonbhadra, UP India

Recently Hindalco Alumina Refinery has created a landmark by enhancing its production capacity by 210,000 TPY with benchmark capital cost of US \$271 per annual tonne through radical modernization and up-gradation schemes. The innovative approach involves Introduction of Sweetening Process, Modernization of Digestion Units and Up-gradation of Precipitation Circuit. The addition of sweetening slurry to digestion units substantially increased 'equilibrium alumina to caustic ratio'. The Free Caustic Threat was adequately addressed by converting the units to single stream flows incorporating innovative Mixing Tube concept. The schemes achieved an increase in caustic concentration by 30-35 gpl and A/C ratio by about 60 units. To minimize capital expenditure, maximum use of existing equipment was ensured. The state-of-the-art Alusuisse Precipitation Technology was successfully incorporated to increase liquor productivity from 58 to 77.3 gpl. The entire project, in addition to increasing production and productivity, has started yielding reduction of operating cost by 10-12%.

#### 3:15 PM

The Third Generation of Autoclave Feed Pumps: Berry van den Broek<sup>1</sup>; <sup>1</sup>Weir Netherlands b.v., Business Dvlp., PO Box, Venlo 5900 AE The Netherlands

Piston Diaphragm Pumps have been in use for the feed of autoclaves since the mid 1980's. Heat Barrier Pumps have been designed to effectively handle abrasive and hot slurries. The first generation of these pumps was developed for the refractory gold ore autoclaves in Nevada/USA. The second generation of Heat Barrier Pumps was supplied in the mid 1990's and handles slurry temperatures of up to 200°C and capacities of approximately 400 m<sup>3</sup>/h at the lateritic nickel processing plants in Western Australia. This paper describes the optimisations and enhancements of the Third Generation of Heat Barrier Pumps. These pumps will be supplied to the Rio Tuba Laterite Nickel Processing Plant in the Philippines. These enhancements allow reduction in investment as well as operating cost, whilst improving the reliability of the equipment. In alumina refineries, Heat Barrier Pumps can be an attractive proposition for the feed of high pressure digesters with hot bauxite slurries.

# 3:40 PM Break

#### 3:50 PM

The Trends of China Alumina Production with Combined Process: *Qingjie Zhao*<sup>1</sup>; Qiyuan Chen<sup>2</sup>; Qiaofang Yang<sup>3</sup>; <sup>1</sup>Central South University and Zhengzhou Research Institute of Aluminum Corporation, China, Ltd. China; <sup>2</sup>Central South University China; <sup>3</sup>Zhengzhou Research Institute of Aluminum Corporation, China, Ltd. China

Most of Chinese bauxite is diasporic bauxite, which has the characteristics of high alumina, high silicon and low iron. Furthermore, the impurity minerals of this bauxite are complex, so most of Chinese alumina is produced by the combined process or the sintering process with high energy consumption. To save energy and reduce costs, it is suggested that the present combined process be reconstructed with a parallel-combined process. Then the bauxite with Al2O3/SiO2 (A/S) weight ratio higher than 10 is dealt with by the Bayer process and the bauxite with A/S 5-8 by the sintering process. The concentration of green liquor in the sintering system is almost the same as that in the Bayer process, and the productivity of both present Bayer and sintering parts can be improved. An economic analysis shows that economic benefit can obviously be obtained. Therefore, the parallel-combined process is a suitable new way for reconstruction of present Chinese alumina production.

### 4:15 PM

A Study of the New Technology Combined with Bayer Process in Manufacture of Calcium Aluminate Cements: Jinyong Zhu<sup>1</sup>; <sup>1</sup>Aluminum Corporation of China, Ltd., Zhengzhou Rsch. Inst., Shangjie Dist., Zhengzhou City, Henan 450041 China

A new technology combined with the Bayer process in manufacture of calcium aluminate cements (CAC) is proposed. Al2O3 in the Bayer spent liquor is precipitated by adding lime, and the washed sediment (calcium aluminate hydrate) has a major phase of 3CaO·Al2O3·6H2O with very fine particle size and large specific surface, which becomes 12CaO·7 Al2O3 and CaO when dehydrated by heating. The sediments mixed with certain amounts of alumina and/or aluminum trihydrate can be sintered into CAC containing 70 to 80% Al2O3 content. The major phases of the CAC are CaO·Al2O3 and CaO·2Al2O3, and the impurities of Fe2O3 and Na2O in the CAC are low. The spent liquor with very low Al2O3 concentration returns to the Bayer digestion step, after concentration by evaporation, with a 95% increase in digestion capability.

# 4:40 PM

**Tube Digesters: Protection of Heating Surfaces and Scale Removal:** A. G. Suss<sup>1</sup>; I. V. Paromova<sup>1</sup>; T. N. Gabrielyan<sup>1</sup>; S. S. Snurnitsyna<sup>1</sup>; A. V. Panov<sup>1</sup>; I. V. Lukyanov; <sup>1</sup>Russian National Aluminium & Magnesium Institute (VAMI), Dept. of Alumina Tech., 86, Sredny pr, St. Petersburg 199106 Russian Federation

Tube digesters have recently found wide application for alumina extraction from bauxite in the Bayer process. In spite of many advantages in construction and operation, tube digesting has the problem of incrustation scales formation on heating surfaces that affects hydraulic resistance of the tube digester and impairs heat transfer, thus sharply decreasing productivity. There are several ways of protecting heating surfaces and removing scale- including use of magnetic and electric fields, ultrasound, thermal treatment, mechanical cleaning, and mainly hydro-monitoring (high pressure water "jetting") and chemical cleaning, used before hydro-monitoring to soften and loosen scale. In VAMI we have performed a number of tests for selection of the most efficient mixtures of acids and inhibitors for chemical cleaning of heating surfaces. It was shown that sulfuric acid (used at present at many alumina plants) has low effectiveness since the majority of high-temperature scales contain calcium oxide. As a result of the investigations, an effective technique of chemical cleaning of tube digester heating surfaces was developed allowing neutralization and disposal of the spent solutions.

# 5:05 PM

Alumina Surface Material with High Thermal Stability: Wangxing Li<sup>1</sup>; Donghong Li<sup>1</sup>; *Qingwei Wang*<sup>1</sup>; <sup>1</sup>Zhengzhou Research Institute of Light Metals, Special Alumina Dept., No. 82 Jiyuan Rd., Shangjie, Zhengzhou 450041 China

A new preparation method of high-purity and superfine alumina is introduced in this paper. By molecule- structure-designing, the organic space resistance factors are imported in the aluminate molecular structure and forming organic envelope around aluminum ions. After thermal decomposition, high-purity (4N) alumina surface material which original particle sizes 20-30nm and apparent particle sizes less than 80nm was obtained. By leading mould-guiding and thermal stability agents into aluminate molecular structure, ultimately the high-purity and active alumina with high thermal stability was attained. Which specific surface area more than 148m2/g, and original particle sizes is 0.1-0.2µm. The size and morphology of the apparent particle can be controlled. This alumina product is very suitable for application in automotive exhaust catalysts and luminescent and opitcal coating materials.

# Aluminum Reduction Technology: Modeling -Industry Trends

Sponsored by: Light Metals Division, LMD-Aluminum Committee Program Organizers: Tom Alcorn, Noranda Aluminum Inc., New Madrid, MO 63869 USA; Jay Bruggeman, Alcoa Inc., Alcoa Center, PA 15069 USA; Alton T. Tabereaux, Alcoa Inc., Process Technology, Muscle Shoals, AL 35661 USA

Tuesday PM	Room: 2	13D
March 16, 2004	Location:	Charlotte Convention Center

Session Chair: Mike Barber, Arvida Research and Development Centre, Jonquiere, Quebec G7S 4K8 Canada

#### 2:00 PM

Using System Dynamic Modelling for Scenario Simulations in Electrolysis Plants: *Ole-Jacob Siljan*<sup>1</sup>; <sup>1</sup>Norsk Hydro ASA, Matls. Dvlp., Rsch. Ctr. HPI, Hydro Porsgrunn, N3907 Porsgrunn 3907 Norway

This paper presents the development of a scenario simulation model in Hydro Aluminium based on system dynamics. The purpose of the model was to perform high-level analysis to support discussions on a common "best practice" operational philosophy in the new Hydro Aluminium. The model is based on technical, organisational and financial relationships, and the simulations are performed through defined scenarios and what/if analysis. The model has proved to be a useful tool, and the simulation results give firm indications on consequences of technological and organisational changes. Simulating effects of changes more reliable and construction improved mental models, allows the model to be used to carve out strategies for reducing the impact of changes on operating results, through pointing out preventive actions prior to and during the changes.

#### 2:25 PM

Lowering Energy Intensity and Emissions in the Aluminum Industry with Government/Industry Partnerships: *Thomas P. Robinson*<sup>1</sup>; William T. Choate<sup>2</sup>; <sup>1</sup>US Department of Energy, Energy Efficiency & Renewable Energy, Industrial Tech. Prog. EE-2F, 1000 Independance Ave., SW, Washington, DC 20585-0121 USA; <sup>2</sup>BCS, Inc., 5550 Sterrett Pl. #306, Columbia, MD 21044 USA

The US Department of Energy, Energy Efficiency and Renewable Energy (EERE) Office's Industrial Technologies Program (ITP) seeks to lower the energy intensity of the U.S. aluminum industry through a coordinated program of research and development, validation, and dissemination of energy efficiency technologies and operating practices. Science fundamentals show a direct correlation between energy efficiency improvements and CO2 emission reductions. ITP's Aluminum Industries of the Future (IOF) has partnered with more than 70 firms in over 35 R&D projects. These projects have focused on wetted cathodes, inert anodes, magnetohydrodynamic stability, process control systems, dross reduction and many other topics. This paper presents an overview of ITP's Aluminum IOF partnerships and their impact on energy intensity and emissions. It covers the technical progress, expected benefits, demonstration status and market projections for the portfolio's projects, emphasizing the energy savings and environmental impact reductions. The authors also describe new opportunities for R&D projects, BestPractice programs and other EERE R&D for lowering energy intensity and emissions.

# 2:50 PM

Inert Anodes: An Update: *Rudolf P. Pawlek*<sup>1</sup>; <sup>1</sup>Technical Info Services & Consulting, Le Forum des Alpes, Ave. du Rothorn 14, CH - 3960 Sierre Switzerland

To reduce the emission of greenhouse gases the primary aluminium industry is under increasing pressure to replace carbon anodes with inert anodes. During the last few years much effort has gone into developing inert anodes for the aluminium industry. Besides further developments of Alcoa's cermet anodes, interest also focussed on Moltech's metal anodes. Alcoa fine-tuned its recipes for the manufacture of inert anodes and for their introduction into conventional aluminium reduction cells. On the other hand Moltech reported about special efforts to prevent dissolution of metal anodes into the bath and, reported about tests in a 20 kA pilot cell, as well as about wear rates of only 3.5 mm per year from 1000 A cell tests. Other research teams have performed laboratory tests with inert anodes with other compositions than the Alcoa cermets and metal oxides. Laboratory scale tests determined dissolution rates of oxides into the electrolyte, how these contaminate the aluminium, and their dissolution mechanisms.

### 3:15 PM

Aluminum Versus Steel: Production Trends - Past, Present and Future: Torstein Arnfinn Utigard<sup>1</sup>; <sup>1</sup>University of Toronto, Matls. Sci. & Engrg., 184 College St., Toronto, Ontario M5S 3E4 Canada

The evolution of production technologies of aluminum and steel are compared both for primary as well as secondary metals production. Steel got a head start on aluminum since it was easier and cheaper to produce on a large scale. Over the last 100 years, steel production technologies have changed frequently while for aluminum the basic technology has prevailed with gradual and continuous improvements. For steel there has already been a dramatic shift from primary to secondary scrap production. This has lead to a significant drop in primary steelmaking with no new integrated plant built in North-America for 40 years. Secondary aluminum production is also increasing, but since there still is good growth and since the "inventory" of old aluminum scrap is limited, the primary aluminum industry has until very recently, been shielded from these structural changes. The differences in cost and energy requirements between primary and secondary processing, are much greater for aluminum than for steel, suggesting that future changes for aluminum may be equally significant.

#### 3:40 PM Break

# 3:50 PM

Analytical System of Long-Term Forecasting of Base Metals World Prices: Boris Arlyuk<sup>1</sup>; <sup>1</sup>Alumconsult Ltd., 2, Shkiperski protok, St. Petersburg 199106 Russia

The complex system has been developed for long-term assessment of world prices and sale volume of base metals or commodities when using the analytical model of the market and market supply forecasts as well as economy development in the Western countries characterized by the industrial production indices. As example of developed approach is used the market of primary aluminium. The model has been developed for forecasting of the degree of capacities utilization rate of smelters depending on the aluminium price level in the world. The model contains a statistic part corresponding to the capacities distribution by the production cost, and a dynamic part determining the deviation from the static depending on the price variation dynamics. The developed complex model has been identified by the actual data of conservation and reactivation of aluminium production in the Western countries within the period from 1985 to 2002 and it is characterized by the average error of assessment of the part of idled capacities of 2.4%, this value variation being 3.3%. The error of longterm forecasting of average annual prices is 7% of the average price value, provided at the forecasting of new capacities commissioning and industrial production indices are correct. Similar models can be used for the world market and long term price forecast of base metals and commodities.

# 4:15 PM

The Development of 65kA Three-Layer Electrolysis Cell for Refining of Aluminum: Huimin Lu<sup>1</sup>; Ruixin Ma<sup>1</sup>; Zongren Liu<sup>2</sup>; Bin Wu<sup>2</sup>; Yingqian Zhang<sup>2</sup>; <sup>1</sup>University of Science and Technology, Metall. Engrg. Sch., Light Metal Rsch. Inst., 30 Xueyuan Rd., Beijing, Beijing 100083 China; <sup>2</sup>Xinjiang Join-world Co., Ltd., 18 Kashidong Rd., Wulumuqi, Xinjiang 830013 China

Xinjiang Join-world Co., Ltd. is the largest refined aluminum producer in China. It had 64 32kA three-layer electrolysis cells for refining of aluminum with the Gadeau process electrolyte system and capacity of 5,000t/y before October 2002. To reach the target capacity of 20,000t/y, it was proposed to build 65kA three-layer electrolysis cells with the SAIA process electrolyte system. A pilot plant of 64 65kA three-layer electrolysis cells (XJ-65) was commissioned in October 2002. Advanced design and new materials were applied for the cell shell and lining to get better stability of magnetic hydrodynamics and heat balance. The two process electrolyte systems were tested in four 65kA three-layer electrolysis cells. At last, the Gadeau process electrolyte system with solid refined aluminum cathode was selected for the pilot plant. With eight months test production, the cathodic current efficiency is up to 99%, DC power consumption 15000kWh/t aluminum.

# Automotive Alloys 2004: Session IV

Sponsored by: Light Metals Division, LMD-Aluminum Committee Program Organizer: Subodh K. Das, Secat, Inc., Coldstream Research Campus, Lexington, KY 40511 USA

Tuesday PM	Room: 210A
March 16, 2004	Location: Charlotte Convention Center

Session Chair: Subodh K. Das, Secat Inc., Coldstream Rsch. Campus, Lexington, KY 40511 USA

#### 2:00 PM

Comparison of the Auto Aluminum Sheets Blanked with Laser and Traditional Mechanical Processes: *Frank Feng*<sup>1</sup>; <sup>1</sup>Alcan International Ltd., Kingston R&D Ctr.

1 mm thick 6111 aluminum sheets cut with three different processes were compared in this study. They are high-speed laser cutting, traditional punch shearing and mill machining. The stretch ability of these cut edges was evaluated based on the hoop strain limits of the specimens with 2" diameter holes on a 4" diameter dome tester. It was found that the stretch ability of the laser cut edges, even though not as good as milling machined, are superior to the punch sheared edges. The cut edges were also characterized with a 3D WYKO non-contact profilometer, optical and scanning electron microscopy and microhardness survey.

# 2:30 PM

Dynamic Side Impact Simulation of Aluminum Road Wheels Incorporating Material Property Variations: Robert Shang<sup>1</sup>; Naiyi Li<sup>2</sup>; William Altenhof<sup>1</sup>; Henry Hu<sup>1</sup>; <sup>1</sup>University of Windsor, Dept. of Mech., Autom. & Matls. Engrg., 401 Sunset Ave., Windsor, Ontario N9B 3P4 Canada; <sup>2</sup>Ford Motor Company, Ford Rsch. Lab., 2101 Village Rd., Dearborn, MI 48124 USA

The performance of road wheel impact resistance is a major concern related to new designs of automotive road wheels and their optimization. In this study, nonlinear dynamic finite element analysis has been employed to numerically investigate side impact of an aluminum road wheel. Based upon the experimental side impact testing device and method described in SAE J175, a numerical model incorporating the aluminum road wheel and a steel loading striker was developed using the parametric mesh generating software TrueGrid. The road wheel was mounted at an incline of 13° to the horizontal and the loading block was prescribed an initial velocity to simulate a 230mm vertical drop. Different simulated impacts at radial locations on the wheel spoke and in between spokes were conducted to investigate the structural performance of the road wheel. The material structural inhomogenity was taken into consideration by assigning different material properties (including yield stress, ultimate tensile strength, and material elongation) to specific sections of the road wheel, which were evaluated by conducting standardized tensile tests on specimens extracted from various regions of the road wheel. Consideration of material variation throughout the road wheel within the numerical model better represents its actual mechanical behavior.

# 3:00 PM

**Optical Technique to Measure Distortion on Heat Treated Parts In Situ**: *Federico Mariano Sciammarella*<sup>1</sup>; Phillip Nash<sup>1</sup>; Calvin Tszeng<sup>1</sup>; <sup>1</sup>Illinois Institute of Technology, Thermal Procg. Tech. Ctr., 10 W. 32nd St., Chicago, IL 60616 USA

The automotive industry continually seeks to improve and extend the use of aluminum. The heat treatments of these parts are very vital in providing the properties needed for their particular applications. Moreover understanding the effects of heat treatments that may cause distortion to a part is critical. Most of the work carried out in this field is a pre and post measurement after part has experienced its treatment. In this study, we carry out in-situ measurements of the distortions that a heat-treated part undergoes when subjected to temperatures near melting followed by a slow cooling. In order to confirm the experimental measurements HOTPOINT a modeling package was used to simulate the experiment and compare results. This study will provide much needed insight to the complex occurrences that aluminum parts undergo during heat treatment.

#### 3:30 PM

Surface Modification of Titanium by Adding SiC, WC and BN2 to the Surface of Ti 6-4 Alloy: *Glen A. Stone*<sup>1</sup>; William J. Arbegast<sup>1</sup>; Glenn J. Grant<sup>2</sup>; Stanley M. Howard<sup>1</sup>; <sup>1</sup>South Dakota School of Mines and Technology, Matls. & Metall. Engrg., 501 E. St. Joseph St., Rapid City, SD 57701-3995 USA; <sup>2</sup>Pacific Northwest National Laboratory, Matls. Procg. & Performance/Energy Matls., 902 Battelle Blvd. K2-03, Richland, WA 99356 USA

The Advanced Materials Processing Center (AMP) at the South Dakota School of Mines and Technology in conjunction with the Pacific Northwest National Lab is developing methods to stir micron size particles into the surface of titanium and other metals to create surface regions enriched in ceramic particulate for enhancement of wear, hardness, or thermal barrier properties. Hard particle reinforcement of the surface of titanium may have numerous industrial applications in rotating or reciprocating assemblies, engines, or other situations where bulk strength, light weight, and surface wear resistance is needed over conventional monlithic materials. Studies of tool geometry, Friction Stir Processing (FSP) parameters as a function of carbide and nitride particle distribution are presented. Tool materials currently being explored are Tungsten-Rhenium and Ferro-TiC HT-6A.

# 4:00 PM

Method for Testing Tension/Compression of Sheet Alloys: R. K. Boger<sup>1</sup>; R. H. Wagoner<sup>1</sup>; M. G. Lee<sup>2</sup>; K. Chung<sup>2</sup>; <sup>1</sup>Ohio State University, Dept. of Matls. Sci. & Engrg., 477 Watts Hall, 2041 College Rd., Columbus, OH 43210 USA; <sup>2</sup>Seoul National University, Sch. of Matls. Sci. & Engrg., 56-1 Shinlim-dong, Kwanak-gu, Seoul 151-742 Korea

The mechanical behavior of sheet alloys under reversed loading and other non-proportional paths is important for simulating forming and springback behavior. A new method for obtaining large-strain compression/tension has been developed and optimized for use with a standard tensile testing machine. Compressive strains greater than 15% have been obtained and have revealed new behavior. Interpretation of the test requires simple analysis to compensate for frictional and off-axis loading effects. The development, optimization, and capabilities of the new method will be presented, along with preliminary results of its application to the Bauschinger effect, to room-temperature creep, and to anelasticity.

#### 4:30 PM

The Effects of Mg and Mn Precipitation on Serrated Yielding and on Texture Evolution During Cold Rolling and Subsequent Annealing: *Wei Wen*<sup>1</sup>; James G. Morris<sup>1</sup>; <sup>1</sup>University of Kentucky, Chem. & Matls. Engrg., 177 F. Paul Anderson Hall, Secat Inc., 1505 Bull Lea Rd., Lexington, KY 40506 USA

Continuous Cast (CC) AA5182 aluminum alloy was subjected to a high temperature heat-treatment of 482°C for 48hr and a low temperature heat-treatment of 182°C for 100hr. In the first case, fine MnAl<sub>6</sub> dispersoids were precipitated out of solid solution while in the latter case, large and dense Mg<sub>2</sub>Al<sub>3</sub> particles were formed mainly along the grain boundaries. Tensile results show that the intensity of serrated yielding was greatly reduced for the material with the low temperature heat-treatment (182°C) while that with the high temperature treatment the serrated yielding was significantly increased. This is understandable, since it is well known that Mg atoms in solid solution interact with mobile dislocations and cause serrated yielding. The more Mg atoms in solid solution, the more intense is the serrated yielding. On the other hand, Mn atoms, due to their much slower diffusion rate and a higher binding energy with vacancies, do not interact significantly with mobile dislocations and at the same time block the path for the diffusion of Mg atoms. To investigate the effects of Mg and Mn precipitation on the texture evolution during cold rolling and subsequent annealing, the hotband was first annealed at 399°C for 4hr to obtain a completely recrystallized condition before the aforementioned high- and low-temperature heat-treatments. After the heattreatments, the materials were cold rolled from 0% to 90% reduction in thickness to investigate the texture evolution during cold rolling. For the material cold rolled to 70% reduction, further salt bath annealing was carried out to investigate the texture evolution during annealing. During cold rolling, the material with Mg precipitation (182°C treatment) has a lower rate of "disappearance" of the Cube+r-Cube component, a higher rate of "disappearance" of the random component and a higher rate of "formation" of the  $\beta$  fiber component than the material heat-treated at 482°C. During subsequent annealing, due to the large Mg<sub>2</sub>Al<sub>3</sub> particles formed during low temperature annealing, new grains are nucleated and grow much faster. On the other hand, the fine MnAl<sub>6</sub> dispersoids formed during high temperature heat-treatment have a retarding effect on recrystallization.

## 5:00 PM

Fabrication of P/M Processed Super High Strength Aluminum Alloy: Kozo Osamura<sup>1</sup>; Hiroki Adachi<sup>1</sup>; Jun Kusui<sup>2</sup>; Ken Kikuchi<sup>2</sup>; <sup>1</sup>Kyoto University, Dept. MSE, Sakyo-ku, Yoshida-honmachi, Kyoto 606-8501 Japan; <sup>2</sup>Toyo Aluminium, R&D Lab., Shiga 529-16 Japan

Recently our group developed extremely high strength AlZnMgCu alloys (MesoaliteTM) by means of powder metallurgy. The air-atomized powder was canned into the aluminum container and then pressed under hydrostatic pressure of 392 MPa. After degassing, the compact piece was hot-extruded at 773K. The extrusion ratio was selected as 10 or 20. Several kinds of alloys including alloy elements of Zn, Mg, Cu, Mn and Ag were investigated. The present technique can provide a large scale product, for instance, the rod with dimension of 60 mm dia and 1000 mm length. As a standard procedure of heat treatment, the solution treatment was carried out at 763 K for 7.2ks and followed by water quenching. The standard condition of aging treatment as T6 was 393 K and 86.4 ks. A selected alloy (MESO20) with composition of Al-9.5%Zn- 3.0%Mg- 1.5%Cu- 4.0%Mn- 0.04%Ag in mass% recorded tensile strength of 910 MPa and compressive strength of 1032MPa. The present super-high strength aluminum alloys could be achieved by the combination of several strengthening mechanisms; (1) fibre reinforcening, (2) fine grain strengthening and (3) precipitation hardening. Especially nano-scale coherent particles are very effective to achieve the high strength materials.

# Beyond Nickel-Base Superalloys: Molybdenum Silicides II

Sponsored by: Structural Materials Division, SMD-Corrosion and Environmental Effects Committee-(Jt. ASM-MSCTS), SMD-High Temperature Alloys Committee, SMD-Mechanical Behavior of Materials-(Jt. ASM-MSCTS), SMD-Refractory Metals Committee *Program Organizers:* Joachim H. Schneibel, Oak Ridge National Laboratory, Oak Ridge, TN 37831-6115 USA; David A. Alven, Lockheed Martin - KAPL, Inc., Schenectady, NY 12301-1072 USA; David U. Furrer, Ladish Company, Cudahy, WI 53110 USA; Dallis A. Hardwick, Air Force Research Laboratory, AFTL/MLLM, Wright-Patterson AFB, OH 45433 USA; Martin Janousek, Plansee AG Technology Center, Reutte, Tyrol A-6600 France; Yoshinao Mishima, Tokyo Institute of Technology, Precision and Intelligence Laboratory, Yokohama, Kanagawa 226 Japan; John A. Shields, HC Stark, Cleveland, OH 44117 USA; Peter F. Tortorelli, Oak Ridge National Laboratory, Oak Ridge, TN 37831-6156 USA

Tuesday PM	Room: 2	11B		
March 16, 2004	Location:	Charlotte	Convention	Center

Session Chairs: S. G. Fishman, US Navy, Office of Naval Rsch., Arlington, VA 22217 USA; Martin Janousek, Plansee AG, Tech. Ctr., A-6600 Reutte/Tyrol Austria

# 2:00 PM Invited

Characterization of a Primary Deformed Moss-Mo5SiB2-Mo3Si Composite Material: Pascal Jéhanno<sup>1</sup>; Dirk Handtrack<sup>2</sup>; Martin Heilmaier<sup>3</sup>; Heinrich Kestler<sup>1</sup>; Andreas Venskutonis<sup>1</sup>; Michael Schaper<sup>2</sup>; <sup>1</sup>Plansee AG, Tech. Ctr., Reutte in Tirol 6600 Austria; <sup>2</sup>Technische Universität Dresden, Inst. für Werkstoffwissenschaft, Helmholtzstraße 7, Berndt-Bau, Dresden 01069 Germany; <sup>3</sup>Otto von Guericke Universität Magdeburg, Inst. für Werkstofftechnik und Werkstoffprüfung, Ernst Schiebold Gebäude, Große Steinermetischstraße, Magdeburg 39016 Germany

A ternary Molybdenum-Silicon-Boron alloy with the compositon Mo - 8,9 % Si - 7,7 % B (at.%) was manufactured using an industrial powder metallurgical processing route, comprising gas atomization and hot isostatic pressing. Subsequently, the material was primary deformed via high temperature extrusion in order to obtain a microstructure consisting of a molybdenum solid solution matrix surrounding intermetallic particles. The microstructure was characterized by SEM, EDX and X-ray diffraction including Rietveld analysis. Mechanical properties were investigated using tensile tests at temperatures ranging from 1000°F (538°C) to 2000°F (1093°C). The primary deformation of the material resulted in a revolutionary incease of the strength in comparison with as-HIPed prematerial, reaching values equivalent to TZM. Additionally, the ductile to brittle transition temperature decreased by 200°C and the strain to failure increase to 25-30% at tempertures as low as 2000°F (1093°C).

## 2:30 PM

Effect of Al Addition on Ultra-High Temperature Performance of Mo/Mo<sub>5</sub>SiB<sub>2</sub> In-Situ Composites: *Kyosuke Yoshimi*<sup>1</sup>; Akira Yamauchi<sup>1</sup>; Masafumi Tsunekane<sup>2</sup>; Shuji Hanada<sup>1</sup>; <sup>1</sup>Tohoku University, Inst. for Matls. Rsch., 2-1-1 Katahira, Aoba-ku, Sendai, Miyagi 980-8577 Japan; <sup>2</sup>Tohoku University, Dept. of Matls. Procg., 2-1-1 Katahira, Aoba-ku, Sendai, Miyagi 980-8577 Japan

Mo/Mo<sub>5</sub>SiB<sub>2</sub> in-situ composites are one of promising candidates for ultra-high temperature structural applications. In this work, the effect of Al addition on the ultra-high temperature performance of Mo/  $Mo_5SiB_2$  in-situ composites is investigated.  $(Mo-8.7Si-17.4B)_{1-x}Al_x$  (x = 0, 1, 3 and 5%) alloys were prepared by arc-melting, and homogenized at 2073 K for 24 h in an Ar gas atmosphere. In binary Mo-8.7Si-17.4B, fine two-phase microstructure is developed by the heat treatment, suggesting eutectic or eutectoid reaction occurs at this composition. It is identified by XRD that the matrix is Mo<sub>5</sub>SiB<sub>2</sub> and fine precipitates are Mo solid solution. The binary Mo/Mo<sub>s</sub>SiB<sub>2</sub> in-situ composite exhibits excellent high temperature strength, for instance about 1 GPa even at 1773 K. The melting point, microstructure, and high temperature oxidation resistance and strength are varied with Al concentration. Therefore, it is found that the Al addition affects the ultra-high temperature performance of the Mo/Mo<sub>5</sub>SiB<sub>2</sub> in-situ composites.

# 2:45 PM

Mechanical Properties of the T<sub>2</sub> Phase in the Mo-Si-B System and Related Mo Based Alloys: *Kazuhiro Ito*<sup>1</sup>; Taisuke Hayashi<sup>1</sup>; Masakuni Fujikura<sup>2</sup>; Masaharu Yamaguchi<sup>1</sup>; <sup>1</sup>Kyoto University, Matls. Sci. & Engrg., Sakyo-ku, Kyoto 606-8501 Japan; <sup>2</sup>Japan Ultra-high Temperature Materials Research Center Ltd., Tajimi, Gifu 507-0801 Japan

Plastic deformation was observed only for [021] and [443] oriented single crystals of the T<sub>2</sub> phase with the D8<sub>1</sub> structure in the Mo-Si-B system at 1773 K at a strain rate of 1x10-<sup>5</sup> s<sup>-1</sup>. Slip on [001](010) was observed in the [021] oriented crystals, but other slip systems were not observed. While, [0001], [13<sup>-4</sup>0], [22<sup>-4</sup>9] oriented single crystals of the Mo<sub>3</sub>Si<sub>3</sub>C with the D8<sub>8</sub> structure can be plastically deformed at temperatures higher than 1573 K. Slip occurs on {0001}<11<sup>-20></sup> and an unidentified non-basal system. This is similar case of Mo<sub>3</sub>Si<sub>3</sub> with the D8<sub>m</sub> structure. The creep strength at elevated temperature of single crystalline and polycrystalline Mo<sub>3</sub>SiB<sub>2</sub> is superior to those of MoSi<sub>2</sub>, Mo<sub>3</sub>Si<sub>3</sub> and Si<sub>3</sub>N<sub>4</sub> based structural ceramics. The directionally solidified T<sub>2</sub>/Mo<sub>ss</sub> eutectic alloy has the room temperature fracture toughness of about 11 MPa $\sqrt{m}$ . It is substantially improved from that of the monolithic T<sub>2</sub>.

# 3:00 PM

The Fracture Toughness and Toughening Mechanisms of Wrought LCAC, TZM, and ODS Molybdenum Plate Stock: Brian V. Cockeram<sup>1</sup>; <sup>1</sup>Bechtel Bettis Laboratory, PO Box 79, W. Mifflin, PA 15122-0079 USA

The high-temperature strength and creep resistance of Low Carbon Arc Cast (LCAC)pure molybdenum, Oxide Dispersion Strengthened (ODS) molybdenum, and TZM molybdenum make these alloys of interest for various high-temperature structural applications. However, these same alloys have been poorly characterized as to fracture toughness (Kic) and transition temperatures from brittle to ductile behavior. This work reports Kic testing performed in accordance with ASTM E399 methods over a temperature range of -150C to 1000C using LCAC, ODS, and TZM molybdenum plate stock. The use of bend specimens and compact tension specimens of varying sizes showed that the results obtained with sub-sized bend and disc-CT specimens were comparable to values obtained with conventional specimens. Based on the fracture toughness data and failure mode, the transition temperature to brittle behavior was defined to occur in a range of toughness values between 26 to 34 MPa m^1/2. The ductile to brittle transition temperature (DBTT) for ODS m olybdenum was below roomtemperature for both the transverse and longitudinal orientations. The DBTT for LCAC and TZM molybdenum in the longitudinal direction was between 100C and 150C, while the transition temperature for the transverse orientation was 150C to 200C. It has been postulated that the refined microstructure of ODS molybdenum produces the significantly lower DBTT. Thin sheet toughening is shown to be the dominant toughening mechanism for all molybdenum alloys.

# 3:15 PM

Role of Microstructure in Creating High Toughness Mo-Si-B Alloys: Jamie J. Kruzic<sup>1</sup>; Joachim H. Schneibel<sup>2</sup>; *Robert O. Ritchie*<sup>1</sup>; <sup>1</sup>Lawrence Berkeley National Laboratory, Matls. Scis. Div., 1 Cyclotron Rd., Bldg. 62R0100-8255, Berkeley, CA 94720-8139 USA; <sup>2</sup>Oak Ridge National Laboratory, Metals & Ceram. Div., PO Box 2008, Oak Ridge, TN 37831-6115 USA

Mo-Si-B based alloys containing α-Mo, Mo<sub>3</sub>Si, and Mo<sub>5</sub>SiB<sub>2</sub> (T2) phases have been targeted for high temperature turbine engine applications. However, to achieve adequate resistance to oxidation, creep, fracture and fatigue, microstructural optimization is necessary. To further this goal, an understanding of how microstructural features affect the fracture and fatigue properties at ambient to high temperature is presented. Specifically, the fracture toughness and fatigue-crack growth resistance have been investigated from 25°-1300°C for several Mo-Si-B alloys with both  $\alpha$ -Mo and intermetallic matrix microstructures. These alloys were produced by both ingot and powder metallurgy processing routes with compositions nominally as Mo (bal.), 12-20 at.% Si, 8-10at.% B. The role of microstructural variables including volume fraction of α-Mo, its ductility, and the morphology and coarseness of the microstructure are considered in terms of how each variable affects the observed toughening mechanisms. Such mechanisms have been identified as crack trapping, crack bridging, and microcrack toughening. Work supported by the Department of Energy, through the Office of Science (Basic Energy Sciences) under Contract No. DE-AC03-76SF00098 (for JJK and ROR), and the Office of Fossil Energy (Advanced Research Materials) under Contract No. DE-AC05-000R22725 (for JHS).

# 3:30 PM Break

# 4:00 PM

Fracture Toughness and Hardness of Multiphase Mo-Si-B Alloys: Zeynep Kasapoglu<sup>1</sup>; David R. Johnson<sup>1</sup>; Mysore A. Dayananda<sup>1</sup>; <sup>1</sup>Purdue University, Sch. of Matls. Engrg., 501 Northwestern Ave., W. Lafayette, IN 47907-2044 USA

In this study multiphase Mo-Mo<sub>5</sub>SiB<sub>2</sub>(T2)-Mo<sub>3</sub>Si alloys with different compositions were examined for microstructure and fracture toughness. The alloys were prepared by using the arc zone-melting technique. For the reduction of grain boundary embrittlement, 0.8%Yttrium was added to selected compositions. In addition, for alloys with near-eutectic compositions Mo was substituted with Nb to explore equilibrium among the Mo, T2 and Mo<sub>5</sub>Si<sub>3</sub> phases. The alloys were characterized by SEM, optical microscopy and XRD techniques. Fourpoint bending tests and Vickers hardness tests were performed with alloy specimens to determine their fracture toughness and hardness.

# 4:15 PM

**Cyclic Deformation of Mo-Si-B Alloys**: Amruthavalli P. Alur<sup>1</sup>; Ping Wang<sup>1</sup>; *Sharvan Kumar*<sup>1</sup>; <sup>1</sup>Brown University, Div. of Engrg., 182 Hope St., Box D, Providence, RI 02912 USA

The cyclic deformation behavior of two Mo-Si-B alloys (Mo-2Si-1B and Mo-3Si-1B) in the isothermally forged condition has been characterized in terms of their room-temperature S-N response and crack growth behavior using precracked compact tension specimens. Crack growth studies were conducted in air in the temperature range 20°C-600°C and compared to TZM subjected to similar loading history. Additionally, fatigue crack growth experiments were also performed in vacuum at 600°C to delineate the effects of environment on fatigue crack growth resistance. The interaction of the advancing crack tip with the microstructure on the specimen surface was examined to obtain an appreciation of the role of the matrix and intermetallic phases in contributing to fatigue resistance. Fracture surfaces were characterized in all instances to help understand the measured properties.

#### 4:30 PM

High-Temperature Compression Response of TZM and Mo-Si-B Alloys: Amruthavalli P. Alur<sup>1</sup>; Ping Wang<sup>1</sup>; Molly Curran<sup>1</sup>; Sharvan Kumar<sup>1</sup>; <sup>1</sup>Brown University, Div. of Engrg., 182 Hope St., Box D, Providence, RI 02912 USA

The 1000°C-1400°C compression response of a powder-metallurgy processed TZM alloy (MT 104) and two Mo-Si-B alloys (a twophase alloy, Mo-2Si-1B and a three-phase alloy, Mo-3Si-1B) was evaluated. At 1000°C, the flow stress at 4% strain of TZM varies between 300 MPa and 250 MPa for nominal strain rates ranging from 10-4s-1 to 10-6s-1 respectively. In contrast, for a two-phase Mo-Si-B alloy, the corresponding flow stress values are ~1150 MPa and ~800 MPa; however, when the strain rate is decreased to 10-7s-1, the flow stress for the two-phase Mo-Si-B alloy drops to ~400 MPa. At 1400°C and a strain rate of 10-4s-1, a flow stress of ~250 MPa is obtained for the MoSiB alloy. The initial and deformed microstructures were examined in a transmission electron microscope and microstructural observations will be discussed in the context of measured properties.

#### 4:45 PM

**Optimization of Mo-Si-B Intermetallics**: Joachim H. Schneibel<sup>1</sup>; Robert R. Ritchie<sup>2</sup>; Jamie J. Kruzic<sup>2</sup>; Peter F. Tortorelli<sup>1</sup>; <sup>1</sup>Oak Ridge National Laboratory, Metals & Ceram., PO Box 2008, Oak Ridge, TN 37831 USA; <sup>2</sup>Lawrence Berkeley National Laboratory and University of California, Matls. Scis. Div. & Dept. of Matls. Sci. & Engrg., Berkeley, CA 94720 USA

Mo-Si-B intermetallics based on the phases Mo3Si, Mo5SiB2, and Mo solid solution offer promise as ultra-high temperature structural materials. By varying the composition, microstructural scale, and microstructural topology, the oxidation resistance, creep resistance, or fracture toughness properties of these alloys can be improved. Experiments illustrating the ways in which the various properties can be enhanced will be described. Work on improving the fracture toughness of Mo-Si-B alloys by additions of Zr and the ductility of the Mo solid solution phase by adding MgAl2O4 spinel particles is in progress. This work was sponsored by the Office of Fossil Energy, Advanced Research Materials (ARM) Program, and the Division of Materials Sciences and Engineering, U.S. Department of Energy, under contract DE-AC05-000R22725 with Oak Ridge National Laboratory managed by UT-Battelle, LLC.

# Bulk Metallic Glasses: Theoretical Modeling and Shear Bands

Sponsored by: Structural Materials Division, ASM International: Materials Science Critical Technology Sector, SMD-Mechanical Behavior of Materials-(Jt. ASM-MSCTS)

*Program Organizers:* Peter K. Liaw, University of Tennessee, Department of Materials Science and Engineering, Knoxville, TN 37996-2200 USA; Raymond A. Buchanan, University of Tennessee, Department of Materials Science and Engineering, Knoxville, TN 37996-2200 USA

Tuesday PM	Room: 209A
March 16, 2004	Location: Charlotte Convention Center

Session Chairs: James R. Morris, Ames Laboratory, Physics, Ames, IA 50011-3020 USA; Katharine H. Flores, Ohio State University, Matls. Sci. & Engrg., Columbus, OH 43210-1178 USA

#### 2:00 PM Invited

Shear Banding in the Self-Consistent Dynamic Free Volume Model: Sven Bossuyt<sup>1</sup>; A. Lindsay Greer<sup>1</sup>; William L. Johnson<sup>2</sup>; <sup>1</sup>University of Cambridge, Dept. of Matls. Sci. & Metall., Pembroke St., Cambridge CB2 3QZ UK; <sup>2</sup>California Institute of Technology, Engrg. & Appl. Sci., MC 138-78, Pasadena, CA 91125 USA

Recently, a self-consistent free volume model was proposed to analyze the Newtonian and non-Newtonian uniform flow data for bulk glass forming liquids such as those of the Zr-Ti-Cu-Ni-Be Vitreloy family. The model is based on the traditional free volume model of the glass transition, the Vogel-Fulcher-Tamman equation, and a simple treatment of free volume production and annihilation during flow. In this paper, we consider the implications of this model regarding flow localization into shear bands, by applying linear stability analysis and numerical finite element methods within the self-consistent dynamic free volume framework.

# 2:25 PM Invited

Mechanisms of Deformation-Assisted Decomposition in a Metallic Glass: *Michael Atzmon*<sup>1</sup>; Wenhui Jiang<sup>1</sup>; <sup>1</sup>University of Michigan, NERS/MSE, Cooley Bldg./N. Campus, Ann Arbor, MI 48109-2104 USA

Nanocrystallites have been observed to form at shear bands resulting from deformation in several metallic glass alloy types. Although there is a driving force for crystallization below the melting point, the kinetics are typically too sluggish at room temperature. There is both fundamental and practical interest in the effect of plastic deformation on the stability of a metallic glass. We have used transmission electron microscopy (TEM) to study the nanocrystallization mechanisms in amorphous  $Al_{90}Fe_5Gd_5$  deformed by bending and nanoindentation. In bent samples, nanocrystallites are observed in the predominantly compressive region only. Using high-resolution TEM and image filtering, we observe nanovoids within the shear bands in the predominantly tensile region only. During nanoindentation, the nucleation rate is sensitive to the applied loading rate. The results are consistent with free-volume annihilation kinetics of order higher than one. Ruling out a temperature effect, we interpret the results in terms of diffusion enhancement by free-volume production. This work was funded by the US National Science Foundation, Grant DMR-9902435.

# 2:50 PM Invited

**Deformation Induced Structural Changes in Bulk Metallic Glasses:** *Katharine M. Flores*<sup>1</sup>; <sup>1</sup>Ohio State University, Dept. of Matls. Sci. & Engrg., 2041 College Rd., Columbus, OH 43210-1178 USA

The magnitude and distribution of free volume is thought to play a central role in shear band formation and the resulting flow behavior in metallic glasses. To elucidate the influence of free volume, structural changes after plastic deformation and thermal relaxation have been investigated. Positron annihilation spectroscopy studies on a Zr-Ti-Cu-Ni-Be alloy suggest that most of the free volume is associated with the larger solvent atoms (Zr and Ti) and that plastic deformation results in a net free volume increase and redistribution. Similar investigations of Cu-based alloys have been undertaken and will be discussed. Shear band formation in the vicinity of a sharp crack tip has also been investigated. Previous investigations of crack tip deformation under tensile loading reveal significant increases in fracture toughness to more than 80 MPa√m, 4-5 times the inherent toughness of the alloy, due to the formation of a large damage zone. Controlling the formation of such a damage zone is integral to the optimization of bulk metallic glass composites.

Fundamental Mechanisms of Deformation in Simulations of Metallic Glass Nanoindentation: S. B. Biner<sup>1</sup>; J. R. Morris<sup>1</sup>; <sup>1</sup>Iowa State University, Ames Lab., Metal & Ceram. Scis., Ames, IA 50011 USA

The localized plastic deformation behavior of amorphous solids were examined by molecular dynamic simulations of nanoindentation. The model system was two-dimensional and composed of a binary alloy with a two-body Lennard-Jones potential. It will be shown that the mechanism of shear localization and the formation of shear bands is a dynamic process balancing transient events of dilatation and contraction in regions involving a limited number of atoms. These shear localization regions were characterized in terms of the initial stress state, stiffness and free volume. A connection is also established with the serrated plastic flow that is seen during the nanoindendation experiments on metallic glasses. This work was performed for the United States Department of Energy by Iowa State University under contract W-7405-Eng-82. This research was supported by the Director of Energy Research, Office of Basic Sciences.

## 3:40 PM

Modeling the Propagation of Shear Bands in Bulk Metallic Glasses: Brian J. Edwards<sup>1</sup>; Kathleen Feigl<sup>2</sup>; Peter K. Liaw<sup>3</sup>; <sup>1</sup>University of Tennessee, Chem. Engrg., 419 Dougherty Hall, Knoxville, TN 37996-2200 USA; <sup>2</sup>Michigan Technological University, Applied Math., 311 Fisher Hall, Houghton, MI 49931 USA; <sup>3</sup>University of Tennessee, Matls. Sci. & Engrg., Knoxville, TN 37996-2200 USA

Recent observations have indicated that shear bands originate and propagate in bulk metallic glasses (BMGs) under tensile loading once plastic deformation has begun. These shear bands propagate and dissipate on the order of milliseconds, as witnessed with high-speed and high-sensitivity infrared thermography. In this presentation, we present results of a study aimed at understanding the onset, propagation, and eventual dissipation of these shear bands under tensile loading in BMGs. Initial results are discussed, based on the application of a non-equilibrium thermodynamics approach to this problem, which results in a system of equations that couples the applied stress distribution within the sample with temperature and an additional vector field associated with the free volume in BMGs. This set of equations describes the shear-band formation, propagation, and dissipation within the BMGs, and gives hints concerning the origination of shear bands, their speeds of propagation, and the magnitude of any permanent plastic deformation that occurs across them.

## 4:05 PM

Interaction of Shear Bands with Inclusions in Metallic Glasses: Alan C. Lund<sup>1</sup>; Christopher A. Schuh<sup>1</sup>; <sup>1</sup>Massachusetts Institute of Technology, Matls. Sci. & Engrg., 77 Mass. Ave., Cambridge, MA 02139 USA

Shear bands represent the only mechanism for plastic accommodation in metallic glasses at low temperature, so the physics of shear strain development are therefore central to the international effort in metallic glass development. Recent works have shown that shear bands interact with inclusions at both the nano- and macro-scales, and load sharing with such inclusions may be a viable means of increasing glass ductility. Here we explore the development of shear strain in simulated metallic glasses with and without nano-scale crystalline inclusions. In particular, we examine the effect of these particles on the strength of the glass as well as the tendency for shear localization. Preliminary results are presented for inclusions of different sizes, and compared with existing experimental literature.

#### 4:30 PM

Shear Band Formation and Ductility of Metallic Glasses: Alla V. Sergueeva<sup>1</sup>; Nathan A. Mara<sup>1</sup>; Amiya K. Mukherjee<sup>1</sup>; <sup>1</sup>University of California, Chem. Engrg. & Matls. Sci. Dept., 1220 Bainer Hall, Davis, CA 95616 USA

Variations in microstructure and chemical compositions of the metallic glasses found in the literature, as well as an overall lack of experimental data on inhomogeneous behavior of metallic glass makes the formulation of a conclusion on the shear band/fracture behavior effects on mechanical properties of metallic glasses difficult. Investigating the effect of strain localization alone on inhomogeneous flow seems to be a first step in approaching this problem. Mechanical behavior of metallic glasses at room temperature and various strain rates in tension and compression was investigated. Formation of multiple shear bands was observed at high strain rates. An increase in strain rate leads to enhance ductility in tension, whereas, the ductility of the material in compression decreases with increasing strain rate. Differences in deformation processes in tension and compression were compared. This work is supported by ONR Grant N00014-03-1-0149.

#### 4:55 PM

In-Situ Observations of the Evolution of Plasticity in Metallic Glasses: A. Bastawros<sup>2</sup>; A. Antoniou<sup>2</sup>; C. C.H. Lo<sup>1</sup>; *S. B. Biner*<sup>1</sup>; <sup>1</sup>Iowa State University, Ames Lab., Metal & Ceram. Scis., Ames, IA 50011 USA; <sup>2</sup>Iowa State University, Dept. of Aeros. Engrg. & Engrg. Mech., Ames, IA 50011 USA

The on set and evolution of plastic deformation under a cylindrical indentor in a metallic glass (Zr41.2-Ti13.8-Cu12.5-Ni10-Be22.5, atomic %) on a micro scale was continuously monitored by using a microscopic digital image correlation system. The plastic zone beneath the indentor is comprised of near orthogonal sets of shear band traces. They almost follow the  $\alpha$  and  $\beta$  characteristic lines of the Prandtl slip line field for a cylindrical indentor. and the whole field evolves essentially in a self-similar way. By matching the experimentally observed load-displacement curves with finite element predictions, a general constitutive behavior that describes the shear band evolution was developed. Also, detailed examinations of shear bands by atomic force microscopy and transmission electron microscopy will be presented. This work partially funded by USDOE to Iowa State University under contract W-7405-Eng-82. This research was also partially supported by the Director of Energy Research, Office of Basic Sciences.

# Carbon Technology: Anode Baking

Sponsored by: Light Metals Division, LMD-Aluminum Committee Program Organizers: Markus Meier, R&D Carbon, Sierre CH 3960 Switzerland; Amir A. Mirchi, Alcan Inc., Arvida Research and Development Centre, Jonquiere, QC G7S 4K8 Canada; Alton T. Tabereaux, Alcoa Inc., Process Technology, Muscle Shoals, AL 35661 USA

Tuesday PM	Room: 213A
March 16, 2004	Location: Charlotte Convention Center

Session Chair: Masood T. Al Ali, Dubal Aluminum Company Ltd., Dubai United Arab Emirates

#### 2:00 PM

**Performance Enhancement of Anode Baking Furnaces at Hindalco's Aluminium Smelter**: S. C. Tandon<sup>1</sup>; <sup>1</sup>Hindalco Industries Ltd., Renukoot, Sonebhadra, UP India

Hindalco is India's largest integrated aluminium complex and one of the lowest cost producers in the world with primary aluminium smelting capacity of 342 KT/Y, besides having its own captive power plant, alumina refinery and down stream fabrication facilities. With increased aluminium smelting capacity, enhancement of anode baking capacity became necessary. A performance enhancement plan of anode baking furnaces was undertaken to optimize fuel oil consumption, increase production capacity, reduce fire cycle time, improve baked anode quality and enhance refractory life. Based on Hindalco's long experience in bake furnace operation, a strategic plan was worked out for regulating the heat distribution in furnaces through introduction of microprocessor based firing and draft control system. There is substantial gain in anode baking capacity and quality besides reduction in fuel oil consumption. This paper describes the technology and strategy and presents the improvement in plant performance based on actual plant data.

# 2:25 PM

**Expansion of an Albras Bake Furnace in Continuous Operation**: Alexandre Manuel Aquino<sup>1</sup>; Ronaldo Raposo Moura<sup>2</sup>; Jorge Magalhães Mello<sup>1</sup>; <sup>1</sup>ALBRAS Albras Aluminio Brasileiro SA, Carbon Process Engrg., Rodovia Pa 483, Km21, Vila Murucupi, Barcarena, Para 68447-000 Brazil

In order to support the growing anode demand it was needed to increase the total anode baking capacity by around 10%. As the increase of anode demand took place before we were able to increase our anode baking capacity, was needed to reduce the anode baking cycle to build-up sufficient anode inventory to permit us to stop a furnace. This article shows how the expansion work of an Open Ring Baking Furnace with 36 sections was done to add 18 more sections without shut down it - increasing the anode production capacity by 2160 blocks per month. In this article are explained aspects about logistic of the physical construction, as well as planning and operational aspects that made it possible the continuous operation of the furnace during the construction work. Then, the production gains obtained with this procedure were evaluated and showed that the anode quality was not affected.

A Simplified Baking Furnace Model for Improving Flue Wall Design: John A. Johnson<sup>1</sup>; Alexander V. Rozin<sup>2</sup>; Alexander P. Skibin<sup>3</sup>; <sup>1</sup>RUSAL Engineering & Technical Center, Head, Anode Tech. & Carbon Matls., Pogranichnikov St. 37, Krasnoyarsk, Krasnoyarsk Krai 660111 Russia; <sup>2</sup>Lomonosov Moscow State University, Inst. of Mech., 1 Michurinsky Pr., Moscow 119899 Russia; <sup>3</sup>Lomonosov Moscow State University, 1 Michurinsky Pr., Moscow 119899 Russia

A simplified mathematical model for solving the conjugate heat transfer problem in the anode baking furnace is developed. The air motion in the flue induced by the exhaust draft is described by the system of differential equations for the viscous compressible multicomponent gas taking into account heat and mass transfer. The flow is turbulent and the k- $\epsilon$  model is used. Turbulencecontrolled eddy breakup model governs the combustion. The diffuse method is used for calculating the radiation flux. It is shown that the problem can be simplified if we treat the processes in the flue as stationary and solve the transient thermal conductivity equation only in the pit. The fields of pressure, velocity, temperature and concentrations are obtained in the flue and time dependent temperature distributions for each of the baking anodes evaluated.

# 3:15 PM

TUESDAY PM

## A Unique Refractory Solution for Anode Baking Furnace Flues: James R. Uhrig<sup>1</sup>; <sup>1</sup>RESCO Products Inc., Penn Ctr. W. Two, Ste. 430, Pittsburgh, PA 15276 USA

Large quantities of refractories continue to be used for initial construction and replacement of flue walls in anode baking furnaces operated by primary aluminum producers. Refractory industry consolidation has led to a reduction in the number of acceptable product offerings available for this critical application, a continuing increase in costs, and concerns about on-going product availability. Failure mechanisms of flue walls are well known. Stresses caused by thermal expansion, reactions from intrusion of aluminum and sodium fluorides that cause varying chemical and physical alteration across the width of the wall, along with thermal cycling, are generally manifested by subsidence, cracking, and bowing. In addition, graphite rich deposits on the pit side of the walls can lead to high maintenance costs for cleaning or premature replacement due to reduced pit capacity, and less efficient thermal transfer. Although there has been a gradual and almost universal upgrading in refractory selection for flue walls to fired brick of about 50% alumina content, flue failures ultimately occur for the same reasons cited above. Considerable past experience showed that extruded shapes of about 42% alumina content based on a unique domestic pyrophyllite/andalusite raw material, characterized by low impurity oxide content, provided excellent service in this application. In addition to improved resistance to chemical and physical destructive mechanisms, pit side build-up was dramatically reduced. Since thicker shapes can be made, flue construction is faster, reducing labor costs. This non-traditional approach for flue wall construction has the potential to be a superior and cost effective alternative to current refractory practice. This paper discusses the properties and unique features, benefits and performance characteristics of this product.

# Cast Shop Technology: Metal Treatment

Sponsored by: Light Metals Division, LMD-Aluminum Committee Program Organizers: Corleen Chesonis, Alcoa Inc., Alcoa Technical Center, Alcoa Center, PA 15069 USA; Jean-Pierre Martin, Aluminum Technologies Centre, c/o Industrial Materials Institute, Boucherville, QC J4B 6Y4 Canada; Alton T. Tabereaux, Alcoa Inc., Process Technology, Muscle Shoals, AL 35661 USA

Tuesday PM	Room: 2	13B/C		
March 16, 2004	Location:	Charlotte	Convention	Center

Session Chairs: Pierre Le Brun, Pechiney, Ctr. de Recherches de Voreppe, Voreppe, Cedex 38341 France; Lawrence D. Ray, Alcoa Inc., Global Pkgg. & Consumer Grp., Richmond, VA 23237 USA

# 2:00 PM

Investigation of Ultrasonic Degassing in Molten Aluminum A356 Alloy: *Hanbing Xu*<sup>1</sup>; Xiaogang Jian<sup>1</sup>; Thomas T. Meek<sup>1</sup>; Qingyou Han<sup>2</sup>; <sup>1</sup>University of Tennessee, Dept. of Matls. Sci. & Engrg., 434 Dougherty Hall, Knoxville, TN 37996 USA; <sup>2</sup>Oak Ridge National Laboratory, Metals & Ceram. Div., PO Box 2008, MS6083, Oak Ridge, TN 37831-6083 USA

This article addresses ultrasonic degassing in aluminum A356 alloy. An experimental setup has been built for the degassing of aluminum using ultrasonic vibration at a frequency of 20 kHz and vibration intensities up to 1500 W. Ultrasonic degassing has been tested in a small volume of aluminum melt at various processing temperatures and durations. The efficiency of degassing is evaluated by density measurement of the reduced pressure samples. Initial experimental results indicate that a steady-state hydrogen concentration can be obtained within a few minutes of ultrasonic vibration, regardless of the initial hydrogen concentration in the melt. The dynamics of hydrogen evolution as a function of processing time, melt temperature, and initial hydrogen concentration have been investigated. The mechanism of ultrasonic degassing is discussed. It is suggested that ultrasonic vibration can be used to reduce porosity formation in aluminum alloys.

#### 2:25 PM

**Evaluation of Relative Efficiency of Various Degassing Lances for Molten Aluminum Treatment Applications**: *Q. T. Fang*<sup>1</sup>; Marshall A. Klingensmith<sup>1</sup>; Ronald E. Boylstein<sup>1</sup>; Larry Podey<sup>2</sup>; <sup>1</sup>Alcoa Inc., Alcoa Tech. Ctr., 100 Tech. Dr., Alcoa Ctr., PA 15069 USA; <sup>2</sup>Alcoa Kentucky Casting Center, 1660 State Rte. 271N, Hawesville, KY 42348 USA

A water model was used to compare the relative efficiency of three selected types of degassing lances for molten aluminum treatment applications using the oxygen decay method. The selected lances were then tested in molten aluminum in a continuous operation with metal flow rates in the range of 400 to 1200 lbs per hour. Satisfactory results were obtained in terms of maintaining metal vacuum density consistently above 2.60 for 8 to 10 weeks. It was found that with the selected lance replacing a previous rotary degassing unit, the dross generated inside the hot zone in the adjacent holding furnace was decreased by an average of 69%, due to significantly less churning of metal. In addition, the argon consumption was reduced by 50~60%. The implementation of the lance degassing unit in place of the previous rotary degassing unit in a production line has resulted in a cost savings of 85% per unit, or \$9,200 per unit per year, due to less capital, less maintenance, reduced argon consumption, and reduced metal loss associated with dross formation.

# 2:50 PM

Study of Molten Aluminium Cleaning Process Using Physical Modelling and CFD: Jin Long Song<sup>1</sup>; *Mark R. Jolly*<sup>1</sup>; Waldemar Bujalski<sup>2</sup>; Alvin W. Nienow<sup>2</sup>; Fabio Chiti<sup>3</sup>; <sup>1</sup>University of Birmingham, IRC in Sch. of Engrg., Birmingham, W. Midlands B15 2TT UK; <sup>2</sup>University of Birmingham, Dept. of Chem. Engrg., Birmingham, W. Midlands B15 2TT UK; <sup>3</sup>Dipartimento di Ingegneria Chimica, Via Diotisalvi 2, Pisa 56126 Italy

With the increasing demand for high quality aluminium alloys, there is a growing need for improved cleanliness of molten aluminium. Generally alkalis, non-metallic inclusions and dissolved hydrogen have to be reduced to a minimum before casting. Traditionally a chlorine/inert gas mixture was injected into the liquid aluminium. In recent years the fluxing process has been modified through the introduction of impellers and injection of particulate salts. In this paper, through laboratory physical modelling and CFD simulation, both lance bubbling and mechanical agitation processes have been investigated to study the underlying science. Particle image velocimetry (PIV) was used to obtain instantaneous liquid velocities. Mixing times have been calculated using CFD models and compared with decolourization experiments. It was found that, at the same mean specific energy dissipation rate, mechanical agitation with an impeller will lead to much more efficient and controlled fluxing than the lance bubbling process.

#### 3:15 PM

The Pick-Up of Micro Bubbles During LiMCA II Measurements Post an Inline Gas Fluxing Unit: Arild Hakonsen<sup>1</sup>; Geir Maland<sup>1</sup>; Terje Haugen<sup>1</sup>; Erling Myrbostad<sup>1</sup>; Ann Oygard<sup>2</sup>; <sup>1</sup>Hydro Aluminium, Hycast a.s., PO Box 225, Sunndalsora 6601 Norway; <sup>2</sup>Hydro Aluminium, R&D Matl. Tech., PO Box 219, Sunndalsøra 6601 Norway

The most common and reliable method of documenting the removal efficiency of a particle filter is to use the LiMCA apparatus. This method measures the electrical resistance through a 300im opening of an insulating aluminosilicate probe as melt is sucked into the probe. As particles are passing the orifice the resistance is continuously changing. The resistance verus time information is used to calculate the number and size of particle. All gas fluxing units produces various amounts of micro bubbles which stays in the melt for a long time. These small bubbles are to some extent measured as particles in the LiMCA measurements. This work has focused on determine the pick-up of micro bubbles in the LiMCA apparatus after the I-60 SIR melt refining unit. After this unit an probe with an extension tube were used to minimize the micro bubble pick-up. Only micro bubbles smaller than diameter 40-50im were found to be picked up in the LiMCA measurements. The measurements in the 15-20im range were largely influenced by the micro bubbles. Finally the removal efficiency of the SIR unit was calculated accounting for the micro bubble pick-up. The removal efficiency was estimated to be 50% for particles of diameter 20im, 98% for particles of diameter 40im and close to 100% for particles with diameter larger than 50 im.

## 3:40 PM Break

#### 4:15 PM

Laboratory and Full Scale Measurements of Bubble Behavior in Gas Fluxing Units: Autumn Fjeld<sup>1</sup>; James W. Evans<sup>1</sup>; D. Corleen Chesonis<sup>2</sup>; <sup>1</sup>University of California, Matls. Sci. & Engrg., Berkeley, CA 94720 USA; <sup>2</sup>Alcoa Inc., Alcoa Tech. Ctr., 100 Tech. Dr., Alcoa Ctr., PA 15069 USA

The performance of gas-fluxing units, as reflected in removal of impurities and throughput of metal, is dependent on the behavior of the bubbles formed as gas is injected into the aluminum. For example, unless the bubbles are dispersed throughout the volume of the metal, a fraction of the capacity of the unit may be wasted. The surface area of the bubbles, and therefore the bubble size, can influence the rate at which impurities are removed. Circulation of the metal, which in some units is promoted by the rising gas bubbles, plays a role in homogenizing the melt. A potential problem arising from bubble behavior is the disturbance of the metal surface as the bubbles burst, causing splashing and ejection of droplets at high gas flow rates. This paper describes measurements at Berkeley and Alcoa Technical Center on bubbles and bubble phenomena in molten aluminum. A "capacitance probe" has been used to measure the frequency of occurrence of bubbles in both laboratory and full-scale melts to determine the distribution of bubbles and what factors affect that distribution. Results of the calculation of bubble-driven flow using the computational fluid-dynamics software FLUENT® are given. In another aspect of the investigation, a highspeed digital camera has been used to study the bubble breaking phenomena at the surface of a low melting point alloy to discover how splashing and droplet formation might be controlled.

## 4:40 PM

## Ceramic Rotary Degassers - Designing for Optimum Material Performance: David P. Bacchi<sup>1</sup>; Ted L. Collins<sup>1</sup>; *Michael J. Hanagan*<sup>1</sup>; <sup>1</sup>Blasch Precision Ceramics, 580 Broadway, Albany, NY 12204 USA

The use of ceramic as a replacement for traditional graphite material used for rotary degassers has the potential for overall economic savings. In order to maximize the performance of the ceramic material some rotor design modifications are generally needed. A traditional graphite rotor design and several rotors re-designed to optimize the material properties of the ceramic were compared. Thermomechanical evaluations of the various rotor designs were conducted using finite element analysis. The degassing efficiency for each design was measured using a flowing water test trough to simulate an inline degassing system.

#### 5:05 PM

A 2D Lattice-Boltzmann Model of Aluminium Depth Filtration: *Carlos Rivière*<sup>2</sup>; Hervé Duval<sup>1</sup>; Jean-Bernard Guillot<sup>1</sup>; <sup>1</sup>Ecole Centrale Paris, L.E.M., Grande Voie des Vignes, Châtenay-Malabry F-92295 France; <sup>2</sup>Pechiney, Ctr. de Recherches de Voreppe, 725, rue Aristide Bergès, BP 27, Voreppe F-38341 France

A two-dimensional mathematical model of the initial stage of depth filtration has been developed. This model describes the fluid flow and the inclusion transport and capture in a two-dimensional representative section of the filter. A typical simulation can be sketched as follows: in a first step, the flow field is computed in the whole complex void space of the two-dimensional filter using the lattice-Boltzmann method. Indeed, this method is particularly suitable to investigate fluid flow at low values of the Reynolds number and in complex geometry. In a second step, the trajectory analysis is derived by applying Newton's second law to suspended inclusions in the flowing fluid. This approach is applied to the liquid aluminium filtration within a ceramic foam filter. The effects of the interception number, the gravitational number and the adhesive-surface forces on the filter coefficient are studied.

# CFD Modeling and Simulation of Engineering Processes: Advanced Casting and Solidification Processes II

Sponsored by: Materials Processing & Manufacturing Division, ASM/MSCTS-Materials & Processing, MPMD/EPD-Process Modeling Analysis & Control Committee, MPMD-Solidification Committee, MPMD-Computational Materials Science & Engineering-(Jt. ASM-MSCTS)

*Program Organizers:* Laurentiu Nastac, Concurrent Technologies Corporation, Pittsburgh, PA 15219-1819 USA; Shekhar Bhansali, University of South Florida, Electrical Engineering, Tampa, FL 33620 USA; Adrian Vasile Catalina, BAE Systems, SD46 NASA-MSFC, Huntsville, AL 35812 USA

Tuesday PM	Room: 2	06A
March 16, 2004	Location:	Charlotte Convention Center

Session Chairs: Adrian V. Catalina, BAE Systems, Huntsville, AL 35812 USA; Dilip K. Banerjee, National Institute of Standards and Technology, Advd. Tech. Prog., Gaithersburg, MD 20899-4730 USA; Robert F. Dax, Concurrent Technologies Corporation, Pittsburgh, PA 15219 USA

# 2:00 PM Opening Remarks - Adrian Catalina

# 2:05 PM

Numerical Simulation of Solidification and Microstructure Evolution of Single Crystal Investment Castings: Zuojian Liang<sup>1</sup>; Qingyan Xu<sup>1</sup>; Jiarong Li<sup>2</sup>; Hailong Yuan<sup>2</sup>; Shizhong Liu<sup>2</sup>; Baicheng Liu<sup>1</sup>; 'Tsinghua University, Dept. of Mech. Engrg., Qinghua Garden, Beijing 100084 China; <sup>2</sup>Beijing Institute of Aeronautical Materials, Lab. of Advd. High Temp. Structural Matls., Beijing 100095 China

The solidification process of single crystal investment castings causes a number of problems that have to be solved such as casting defects and complexity of production process. In the paper, a mathematical model for the three dimensional simulation of solidification of single crystal growth of investment castings was developed based on the crystal growth mechanism and the basic transfer equations such as heat, mass and momentum transfer equations. Many factors including constitutional undercooling, curvature undercooling and anistropy, which had vital influences on the microstructure evolution, were considered in the model. Temperature, velocity and solute distributions, dendritic morphologies, crystal orientations and stray crystal of single crystal superalloy investment castings were invetigated at different withdrawal rates. The study indicates three dimensional solidification simulation is a powerful tool for understanding the formation of grain defects in the single crystal investment castings.

#### 2:40 PM Cancelled

**3D** Modeling of Porosity Formation in Aluminum Alloys: A Comparison Between Two Numerical Models and With Experimental Results for an A356 Alloy Plate Casting

#### 3:10 PM

Solidification of Aluminum Alloys on Uneven Surfaces: Deep Samanta<sup>1</sup>; Nicholas Zabaras<sup>1</sup>; <sup>1</sup>Cornell University, Sibley Sch. of Mech. & Aeros. Engrg., Matls. Process Design & Control Lab., 188 Frank H. T. Rhodes Hall, Ithaca, NY 14853-3801 USA

Solidification of aluminum on uneven surfaces modeled in the form of sinusoidal curves is simulated. Wavelength and amplitude effects of these sinusoidal surfaces on heat transfer, fluid flow and solid-liquid front morphology in the early stages of solidification will be reported. Interfacial heat transfer between the solid shell and mold will be modeled in terms of empirical correlations to highlight the variable nature of heat flux on the boundary. The same analysis will be extended to aluminum alloys. A recently developed stabilized finite element formulation for simulating flow in binary alloy solidification and porous media will be used to simulate the macrosegregation and growth of the solid shell. Sensitivity analysis to demonstrate the importance of wavelengths on the heat transfer, fluid flow and front morphology will be discussed. The analysis will then be expanded to include meniscus formation and their role in surface segregation.

3:40 PM Break

# 4:00 PM Cancelled

Simulation and Real-Time X-Ray Observation of Foam Pattern Permeability Effects on the Lost Foam Casting Process

#### 4:30 PM

Validation and Improvement of Computer Modeling of Lost Foam Casting Process Via Real Time X-Ray Technology: Wanliang Sun<sup>1</sup>; Preston Scarber<sup>1</sup>; Harry E. Littleton<sup>1</sup>; <sup>1</sup>University of Alabama, Matls. Sci. & Engrg., 917 Bldg., 1530 3rd. Ave. S., Birmingham, AL 35294 USA

Lost Foam Casting (LFC) process is relatively immature when comparing other casting processes. To make the process more robust, computer modeling is needed in lead time and casting defects deduction. In this study, metal filling of lost foam aluminum castings was visualized using the state-of-art real time X-Ray technology. Meanwhile, the metal filling of the lost foam casting was simulated using a commercial software package. The result of the computer simulation was validated with the results of the real time X-Ray visualization. Some of the computer simulation agreed well with the results from the real time X-Ray visualization, but some did not. Based on other studies using real time X-Ray technology, new input variables, such as foam density field and gas permeability field were developed for the computer modeling. With the new variables, the modeling of the lost foam casting process becomes more realistic.

# 5:00 PM

TUESDAY PM

Mathematical Modeling of a Liquid Metal Feeding System for Single Belt Casters: Roberto Parreiras Tavares<sup>1</sup>; Frederico da Costa Fernandes<sup>1</sup>; Guilherme Antonio Defendi<sup>1</sup>; Júlio César Sousa Pena<sup>1</sup>; Vangleik Ferreira da Cruz<sup>1</sup>; <sup>1</sup>Federal University of Minas Gerais, Metallurgl. & Matls. Engrg., Rua Espírito Santo, 35-Sala 229, Metalurgia - Centro, Belo Horizonte, Minas Gerais 30160-030 Brazil

Near-net-shape casting is an important area of research in the iron and steel industry today. Among the "Near-Net-Shape" casting processes, the single-belt caster seems to be the most promising, since it is the only one that can achieve levels of productivity similar to those obtained with conventional continuous casting machines. One of the most important aspects in the single-belt casting is the feeding system used to deliver liquid metal over the belt. This system determines the velocity distribution and the levels of turbulence of the liquid metal and affects the quality of the strips. In the present work, a metal delivery system having a simple geometry was proposed. Using the CFD codes CFX4.4 and CFX 5.5, a mathematical model to simulate three-dimensional turbulent fluid flow and heat transfer in that system has been developed. This model was used to analyze different configurations of the metal delivery system and the free surface shape of the fluid was also determined. A physical model of the feeding system was built and used to validate the predictions of the mathematical model. The fluid flow calculations have been validated by dye injection experiments and laser doppler anemometry. Measurements of the free surface levels have also been performed. These experiments provided supporting evidence for the predictions of the mathematical model.

# Challenges in Advanced Thin Films: Microstructures, Interfaces, and Reactions: Design, Process, and Property Control of Functional and Structural Thin-Films

Sponsored by: Electronic, Magnetic & Photonic Materials Division, EMPMD-Thin Films & Interfaces Committee *Program Organizers:* N. M. (Ravi) Ravindra, New Jersey Institute of Technology, Department of Physics, Newark, NJ 07102 USA; Seung H. Kang, Agere Systems, Device and Module R&D, Allentown, PA 18109 USA; Choong-Un Kim, University of Texas, Materials Science and Engineering, Arlington, TX 76019 USA; Jud Ready, Georgia Tech Research Institute - EOEML, Atlanta, GA 30332-0826 USA; Anis Zribi, General Electric Global Research Center, Niskayuna, NY 12309 USA

Tuesday PM	Room: 2	18B
March 16, 2004	Location:	Charlotte Convention Center

Session Chairs: Choong-Un Kim, University of Texas, Matls. Sci. & Engrg., Arlington, TX 76019 USA; Jud Ready, Georgia Tech Research Institute, Atlanta, GA 30332-0826 USA; David P. Field, Washington State University, Sch. of Mech. & Matls. Engrg., Pullman, WA 99164-2920 USA

## 2:00 PM Invited

Dielectric Films for Silicon Solar Cell Applications: Bhushan Sopori<sup>1</sup>; <sup>1</sup>National Renewable Energy Laboratory, 1617 Cole Blvd., Golden, CO 80401 USA

Silicon solar cells use thin films of a variety of dielectrics, primarily for the purposes of enhancing antireflection (AR) or reflection characteristics of various interfaces and for surface passivation. Typically, different materials are required to meet different demands of optical and electronic properties. For example, although SiO2 layers can give excellent surface passivation, they are not well suited for AR purposes because of a low refractive index. Typical AR coating materials for solar cells consist of TiO2 and SiN, which have a refractive index of > 2. However, to minimize the cost of solar cell fabrication, it is desirable to use only one coating that can accomplish both electronic and optical demands. Recently, it was determined that hydrogenated SiN (SiN:H) can satisfy these needs, and now this material has become a very popular dielectric. The advantages of SiN:H are that: (i) it has a dielectric constant that matches well for AR effects, and (ii) it has capability to accumulate a positive charge at the interface to give a high degree of surface passivation. Recently, additional advantages of SiN:H have been discovered. It has been determined that a silk-screened metal pattern on a thin layer of SiN:H can be directly fired through it to yield excellent ohmic contacts to solar cells. Use of a nitride, deposited by plasma-enhanced chemical vapor deposition, offers yet other advantage by creating a source of H, which can diffuse into Si to passivate impurities and defects. This mechanism can improve the performance of a low-cost solar cell by about 4 absolute percentage points to about 16%. However, as the number of functions that a dielectric has to perform increases, the complexity of understanding and controlling various functions become more crucial. This paper will review various properties of dielectric films needed for solar cell applications, discuss processing requirements, and discuss methods of optimizing cell performance.

## 2:25 PM Invited

**Progress in Crystalline Multijunction and Thin-Film Photo**voltaics: *Donna Cowell Senft*<sup>1</sup>; <sup>1</sup>Air Force Research Laboratory, Space Vehicles Direct. USA

Photovoltaics are important for power generation in terrestrial applications such as remote power and renewable energy but are the primary source of electrical power for space systems. Development of solar cells for space, where priorities are high conversion efficiency and resistance to degradation from ionizing radiation, is driving research into crystalline III-V multijunction solar cells and lower efficiency but flexible, lightweight polycrystalline or amorphous thin-film solar cells. Crystalline triple junction III-V solar cells have reached conversion efficiencies of 30% at Air Mass Zero (AMO), but identifying and growing additional junction materials with the appropriate bandgap and lattice constant are creating challenges to higher efficiency cells. New lattice mismatch techniques and new classes of nitride materials hold promise for increasing the efficiency of these cells. Thin-film solar cells, on the other hand, generally have efficiencies of <15%, but provide the benefits of greater radiation resistance,

lower cost, flexibility, and lower mass. Development work in thin-film solar cells centers on increasing efficiency in polycrystalline materials such as Cu(In,Ga)Se2 or CdTe and amorphous silicon.

#### 2:50 PM

A Novel Process for the Synthesis of Multinary Thin Films: *Billy J. Stanbery*<sup>1</sup>; <sup>1</sup>HelioVolt Corporation, Ste. 100F, 1101 S. Capital of Texas Hwy., Austin, TX 78746 USA

A novel method is described for the rapid reactive formation of (I-III)-VI thin films suitable for applications as photovoltaic absorbers. This technique circumvents the limitations of prior approaches by a combination of (1) reduced thermal budget and volatile reactant loss, (2) facilitating optimal precursor deposition while avoiding deleterious pre-reactions, (3) direct control of pressure during synthesis, and (4) application of an electrostatic field during synthesis to athermally modify ionic transport. This is a two-stage process, wherein reaction precursors are first separately deposited onto two surfaces, one the film substrate, and the other a reusable tool that has been coated with a dielectric release layer. In the second stage, the tool and substrate are brought together and pressure applied, in this case by electrostatic compression resulting from an electrical bias between the two, and heated in a rapid thermal processor. Application of the method to CIGS photovoltaic devices will be described.

# 3:05 PM Invited

**Ion Beam Mixing of Silicon-Germanium for Solar Cell Applications**: *Sufian Abedrabbo*<sup>1</sup>; D. Arafah<sup>1</sup>; Anthony Fiory<sup>2</sup>; Bhushan Sopori<sup>3</sup>; N. M. Ravindra<sup>2</sup>; <sup>1</sup>University of Jordan, Dept. of Physics, Amman 11942 Jordan; <sup>2</sup>New Jersey Institute of Technology, Dept. of Physics, Newark, NJ 07102 USA; <sup>3</sup>National Renewable Energy Laboratory, Golden, CO 80401 USA

A brief overview of silicon-germanium alloys for solar cell and light emitting diode applications is presented here. The overview considers factors such as methods of formation, and device performance. In particular, results of preliminary experiments of ion-beam mixing of silicon germanium multi-layers deposited by physical vapor deposition and subsequently ion-implanted with varying doses of argon are described.

# 3:30 PM

Magnetic and Transport Properties of Magnetic Semiconductors CdCr2Se4 Thin Films Diluted by In: L. J. Maksymowicz<sup>1</sup>; M. Lubecka<sup>1</sup>; B. T. Cieciwa<sup>1</sup>; Z. St. Sobkow<sup>1</sup>; R. Szymczak<sup>2</sup>; M. Sikora<sup>3</sup>; Cz. Kapusta<sup>3</sup>; <sup>1</sup>AGH University of Science and Technology, Dept. of Elect., Al. Mickiewicza 30, Krakow 30-059 Poland; <sup>2</sup>Polish Academy of Sciences, Inst. of Physics, Al. Lotnikow 32/46, Warszawa 02-668 Poland; <sup>3</sup>AGH University of Science and Technology, Dept. of Solid State Physics, Fac. of Physics & Nucl. Techniques, Al. Mickiewicza 30, Krakow 30-059 Poland

The spinel structure for compound A[B2]X4 was realized by thin films of magnetic semiconductor (Cd1-yIny)[Cr2-2xIn2x]Se4. The increase in the lattice parameter with increasing dilution level was detected. The field-cooled and zero field-cooled DC magnetization measurements, carried out with a SQUID magnetometer, show that magnetic ordering changes with increasing In concentration. For CdCr2Se4 the magnetic state with reentrant transition is obtained, while we have the SG state when x=0 and y>0 or y=0 and x>0. The randomly canted state was found for x>0 and y>0. Changes of the local atomic environments around Cr and Se ions were observed by EXAFS with the increase of dilution level. Spectral voltage responsivity of the films was found using a lock-in technique. It was found that the voltage sensitivity of the investigated films is altered with the amount of indium and temperature. The maximum of voltage sensitivity is shifted toward the infrared region with reduced dilution level. The largest voltage sensitivity was obtained for the lightly diluted samples, below Curie temp

# 3:45 PM Break

#### 4:00 PM

**Dynamic Nonlinear Response of Semiconducting Oxides to the Ambient Atmosphere**: *T. Pisarkiewicz*<sup>1</sup>; W. Maziarz<sup>1</sup>; <sup>1</sup>AGH University of Science and Technology, Dept. of Elect., Al. Mickiewicza 30, Krakow 30-059 Poland

LTCC and micromachined structures were developed as substrates for deposited metal oxide SnO2, In2O3 or ZnO semiconductors interacting with ambient reducing or oxidizing atmospheres. The dynamic response of a single sensor with modulated temperature, where pulse or sinusoidal voltage is applied to the sensor heater, was analysed. The time dependent interaction of semiconductor surface with the ambient gas is related to both the kinetics of gas molecules at the surface (adsorption, desorption, diffusion and oxidation) and the chemical structure and concentration of the gas species. The authors performed a series of experiments by varying the temperature and modulation frequency range for selected sensitive oxides and gas species. The oxidation process caused by ionosorbed oxygen was particularly investigated during interaction of semiconductor surface with ambient air of varying humidity.

# 4:15 PM

**Novel PLD- VO<sub>2</sub> Thin Film for Ultrafast Applications**: *Huimin Liu*<sup>1</sup>; Omar Vasquez<sup>1</sup>; Victor R. Santiago<sup>1</sup>; Luz Diaz<sup>1</sup>; Felix E. Fernandez<sup>1</sup>; <sup>1</sup>UPRM, Physics, PO BOX 5023, Mayaguez, PR 00681-5023 USA

VO<sub>2</sub> thin films deposited on fused quartz substrate were successfully fabricated by pulsed laser deposition (PLD) technique using excimer laser and metallic vanadium target for ablation. Microscopic examination and X-ray diffraction scans of all samples show a very broad diffraction peak under  $2\theta = 25^\circ$ , corresponding to amorphous material. The film shows fast, passive thermochromic effect of insulatorto-metal or semiconductor-to-metal phase transition (PT) with a characteristic hysterisis at the temperature near 68°C. Thermochromic effect was measured as resistivity or optical transmission and reflectance versus temperature. Ultrafast PT from monoclinic semiconductor phase to a metallic tetragonal rutile structure could also be induced optically by laser excitation. Nd:YAG pulsed laser operating at 532 nm with pulse duration of 30 psec was used to drive the PT. Degeneratefour-wave-mixing technique was used to detect the ultrafast PT. In this paper we report correlation between the ultrafast PT and the dynamical process of the excited states. It is also the first time, to our knowledge, to report the extremely large polarizability and the potential photonic applications.

# 4:30 PM

Pulsed Laser Deposited Coatings for Hydrogen and Hydrogen Isotope Permeation Resistance: *Thad Matthew Adams*<sup>1</sup>; James Fitz-Gerald<sup>2</sup>; <sup>1</sup>Savannah River Technology Center, Bldg. 773-41A/151, Aiken, SC 29808 USA; <sup>2</sup>University of Virginia, Matls. Sci. & Engrg., 116 Engineer's Way, Charlottesville, VA 22904 USA

To date several coating materials and materials systems have been investigate to reduce the permeation of hydrogen and hydrogen isotopes through common structural materials such as stainless steels. These materials include oxide ceramics, thermally grown oxides, metals, intermetallics, and amorphous systems. Permeation response for these coatings system has also been shown to be highly dependent on application techniques-thermal spray, CVD, EBPVD. The current research is focused on three coatings systems applied using pulsed laser deposition on 304L stainless steel substrates. The stainless steel substrates have been coated with aluminum oxide, chromium oxide, titanium carbide and an Al-Ni-Gd amorphous alloy using PLD. Characterization of the coating-substrate system adhesion has been performed using scratch adhesion testing and microindentation. Coating stability and environmental susceptibility has also been evaluated for two conditions-air at 350°C and Ar-H2 at 350°C for up to 100 hours. Lastly, thermal cycling and hydrogen charging-5,000-10,000psi-testing has been performed to evaluate overall coating performance.

#### 4:45 PM

Microstructural Characterizations of (11-20)a-Plane ZnO Thin Films Grown on (1-102)r-Plane Sapphire: Jin-Serk Hong<sup>1</sup>; Won-Yong Kim<sup>2</sup>; *Sung-Hwan Lim*<sup>1</sup>; <sup>1</sup>Kangwon National University, Dept. of Advd. Matls. Sci. & Engrg., Chunchon 200-701 Korea; <sup>2</sup>Korea Institute of Industrial Technology, Advd. Matls. R&D Div., Inchon 404-254 Korea

There has been considerable interest in the development of ZnO films for optoelectronic devices.1 Nakamura et al. succeeded in the growth of ZnO films on (1-102) r-plane sapphire via ECR-assisted MBE. However, a critical problem is a high concentration of various defects in the growth of ZnO films. These defects can act as traps and recombination centers. Thus, understanding of the characteristics of structural defects was a major emphasis of the present ZnO research. In this presentation we describe the structural characteristics of nonpolar (11-20) a-plane ZnO films grown on r-plane sapphire. The structural analyses were carried out using electron diffraction, weak beam microscopy, and HREM. The in-plane orientation of the ZnO with respect to the sapphire was confirmed to be [0001]ZnO||[0-111]sapphire and (11-20)ZnO||(01-12)sapphire. Threading dislocations and stacking faults, observed in plan-view and cross-sectional TEM images, dominated the a-ZnO microstructure with densities of about 10 11 cm-2 and 10 6 cm-1, respectively. 1S.-H. Lim and D. Shindo, Phys. Rev. Lett. 86. 3795 (2001).

#### 5:00 PM Invited

SAM-Ceramic Protective Bilayers for MEMS Device Packaging: Tolulope O. Salami<sup>1</sup>; Sergei Zarembo<sup>1</sup>; Quan Yang<sup>2</sup>; Kaustubh Chitre<sup>2</sup>; Junghyun Cho<sup>2</sup>; *Scott R.J. Oliver*<sup>1</sup>; <sup>1</sup>SUNY, Dept. of Chmst., Vestal Pkwy. E., Binghamton, NY 13902 USA; <sup>2</sup>SUNY, Dept. of Mech. Engrg., Vestal Pkwy. E., Binghamton, NY 13902 USA

Structures and devices in microelectromechanical systems (MEMS) require hermetic packaging for protection, reliability and proper function. The recent reduction in the size of MEMS structures creates several problems, such as an increase in resistive forces, leading to increased friction/stiction and wear. We are developing a protective bilayer thin film coating to solve these problems. The bilayer is an inorganic-organic hybrid material, consisting of a hard inorganic ceramic coating (ZrO2, YSZ) and a compliant underlying organic buffer layer. Nanoscale ultrathin organic coatings, fabricated by self-assembly, are used as a 'template' for the subsequent growth of the hard ceramic coating. We chemically tune the organic terminal groups, as well as vary ceramic synthetic conditions, in order to promote growth of the top inorganic layer. Molecular level understanding of the microstructure and micromechanics involved in the synthetic process are studied by a variety of characterization techniques, such as electron microscopy, XRD, AFM and nanoindentation. Our presentation will overview some of our results.

## 5:15 PM

Study on Deposition Procession, Structure and Properties of Super Hard Protective TiB<sub>2</sub> Coatings by Cathode Arc Ion Reactive Method: Jiansheng Zhao<sup>1</sup>; Kwang-Leng Choy<sup>2</sup>; <sup>1</sup>Huazhong University of Science and Technology, Dept. of Matls., Wuhan, Hubei 430074 China; <sup>2</sup>Nottingham University, Dept. of Matls., Nottingham UK

Using pure metal titanium as a target, diborane as the reactive gas, the super hard protective  $TiB_2$  coatings were deposited by cathode arc ion reactive platting method. The structures and properties of the deposited coatings were analyzed by means of XPS, XRD and scratch test. The results show that the coatings have very high hardness of above HV30Gpa. The structures of the coatings related to the deposition procession. While the flow rate of diborane changed from 20 sccm to 160 sccm, the structures of the coatings changed from Ti + TiB ?"TiB+ TiB<sub>2</sub>?"TiB<sub>2</sub>. The pure TiB<sub>2</sub> coatings could be obtained in the flow rate of diborane 160sccm. The adhesion stresses between the coatings and the substrates decreased from 913MPa to 770.7MPa along with the increasing of flow rate of diborane. The possible reason of this decreasing was related to the residual stresses existing in the coatings.

# Computational Thermodynamics and Phase Transformations: Phase Field Modeling II

Sponsored by: ASM International: Materials Science Critical Technology Sector, Electronic, Magnetic & Photonic Materials Division, Materials Processing & Manufacturing Division, Structural Materials Division, MPMD-Computational Materials Science & Engineering-(Jt. ASM-MSCTS), EMPMD/SMD-Chemistry & Physics of Materials Committee

Program Organizer: Jeffrey J. Hoyt, Sandia National Laboratories, Materials & Process Modeling, Albuquerque, NM 87122 USA

Tuesday PM	Room:	202A		
March 16, 2004	Location	: Charlotte	Convention	Center

Session Chair: TBA

#### 2:00 PM Invited

**Phase Field Simulations of Coarsening in Three-Dimensional Topologically Complex Structures:** I. Savin<sup>1</sup>; R. Mendoza<sup>1</sup>; P. W. *Voorhees*<sup>1</sup>; <sup>1</sup>Northwestern University, Matls. Sci. & Engrg., 2225 N. Campus Dr., Cook Hall, Evanston, IL 60208 USA

The coarsening process in systems consisting of spherical particles in a matrix has been studied extensively. In contrast, coarsening in systems that possess both positive and negative curvatures have received less study. We employ three-dimensional phase field calculations to follow the evolution of such a topologically complex dendritic solid-liquid mixture during coarsening. We use the phase field method to determine the instantaneous interfacial velocities for a given experimental microstructure. Using this information we compute the average time rate of change of a given pair of principle interfacial curvatures. We show that this information can be used to predict qualitatively the evolution of the interface with a given pair of principle curvatures, and to understand the mechanisms responsible for coarsening in these topologically complex systems. A comparison between the predictions of the calculations and experiments will be given.

#### 2:30 PM Invited

Modeling Solidification, Elasticity and Structural Stability Using Phase Field Crystals: Ken R. Elder<sup>1</sup>; <sup>1</sup>Oakland University, Physics, Rochester, MI 48309-4401 USA

Elastic and plastic deformations often play a significant role in determining the microstructures that emerge during non-equilibrium processing. The microstructures produced in these phenomena are important since they can significantly alter the structural properties of the material. In this talk I would like to discuss a phase field technique that can predict both the creation and structural properties of non-equilibrium microstructures. The technique will be applied to a number of phenomena including, liquid phase epitaxial growth, spinodal decomposition, eutectic solidification and dendritic growth.

#### 3:00 PM

Phase-Field Modeling of Solidification Under Stress: Julia Slutsker<sup>1</sup>; Geoffrey B. McFadden<sup>2</sup>; Alexander L. Roytburd<sup>3</sup>; William J. Boettinger<sup>1</sup>; James A. Warren<sup>1</sup>; <sup>1</sup>NIST, MSEL, 100 Bureau Dr., Gaithersburg, MD 20899 USA; <sup>2</sup>NIST, Math & Computer Sci., 100 Bureau Dr., Gaithersburg, MD 20899 USA; <sup>3</sup>University of Maryland, Matls. Sci. & Engrg., College Park, MD 20742 USA

The phase field model of the non-isothermal solidification taking into account the stress field is developed. This model has been applied to the kinetics of melting and solidification in confined sphere. The complete numerical solutions taking into account the time-space evolution of temperature, order parameter and stress field has been obtained. It has been shown that at some boundary and initial conditions the evolution results in steady states corresponding time-independent distribution of order parameter and uniform temperature. The value of interface energy has been estimated by comparing the phase fraction in the steady states with the equilibrium following from the sharpinterface model. It has been shown that at small radiuses of sphere the equilibrium two-phase states significantly shifted and their unstability appears due to effect of interface energy. This effect is particularly significant if the radius of sphere on the nano-scale level is considered.

#### 3:20 PM Cancelled

A Phase-Field Approach to the Nanocrystallization of Metallic Glasses

## 3:40 PM Break

## 3:50 PM Invited

Modeling Thermodynamics and Microstructure Evolution of Ni-Base Superalloys: J. Zhu<sup>1</sup>; S. Zhou<sup>1</sup>; Yi Wang<sup>1</sup>; T. Wang<sup>1</sup>; Z. K. Liu<sup>1</sup>; C. Woodward<sup>2</sup>; R. A. MacKay<sup>3</sup>; A. J. Ardell<sup>4</sup>; *Long-Qing Chen*<sup>1</sup>; <sup>1</sup>Pennsylvania State University, Matls. Sci. & Engrg., Univ. Park, PA 16802 USA; <sup>2</sup>UES Inc., Dayton, OH USA; <sup>3</sup>NASA Glenn Research Center; <sup>4</sup>University of California, Matls. Sci. & Engrg., Los Angeles, CA USA

Ni-based superalloys consist of ordered intermetallic gamma-prime precipitates embedded in a disordered face-centered cubic (fcc) gamma matrix. The control of the gamma+gamma-prime two-phase microstructure and its high-temperature stability is the key to the success for the design of superalloys with desired high temperature properties. This presentation will discuss our recent work to integrate various computational tools ranging from first-principles calculations, thermodynamic and materials property database development, to microstructure prediction using the phase-field approach. The initial effort is on the Ni-Al-Mo-Ta quaternary system and its binary and ternary subsystems. It will be demonstrated that it is possible to predict quantitatively, both in time and spatial scales, the microstructure evolution in Ni-base superalloys through first-principles assisted database development and phase-field simulations. The focus will be on the validation of the computational results by comparing with analytical theories for simple model systems and with existing experimental measurements in Ni-base alloys. The work is supported by NASA.

#### 4:20 PM Invited

Quantitative Phase Field Modeling of Interdiffusion Microstructures in Multi-Phase and Multi-Component Alloys: Kaisheng Wu<sup>1</sup>; John E. Morral<sup>1</sup>; Yunzhi Wang<sup>1</sup>; <sup>1</sup>Ohio State University, Matls. Sci. & Engrg., 2041 College Rd., Columbus, OH 43210 USA

Most earlier simulation work on diffusion couples containing dispersed phases was limited to one-dimensional (1D) models. The models assumed that all diffusion occurs in the matrix phase and that precipitates are point sources or sinks of solute. Microstructural evolution in the interdiffusion zone and its effect on diffusion kinetics were ignored. There has been an increasing interest recently in apply-

TUESDAY PM

TUESDAY PM

ing the phase field method to study explicitly microstructural evolution in the interdiffusion zone and its effect on diffusion path. So far the work has been limited to prototype model systems without material-specific inputs. In this presentation we will discuss quantitative phase field modeling of interdiffusion microstructures by linking directly the free energies and mobility data to available databases developed by the CALPHAD method. Its applications are demonstrated for microstructural evolution in single-phase/two-phase and two-phase/ two-phase diffusion couples of Ni-Al-Cr alloys. The simulated microst ructural features and kinetics of boundary migration agree well with experimental observations at the same length and time scales. The diffusion paths calculated from the phase field simulations are compared with analytical predictions and 1D diffusion calculations. The work is supported by the National Science Foundation.

## 4:50 PM

Phase Decomposition in Polymeric Membrane Formation by Immersion Precipitation: *Bo Zhou*<sup>1</sup>; Adam C. Powell<sup>1</sup>; <sup>1</sup>Massachusetts Institute of Technology, Dept. of Matls. Sci. & Engrg., 77 Mass. Ave., 4-117, Cambridge, MA 02139 USA; <sup>1</sup>Massachusetts Institute of Technology, Dept. of Matls. Sci. & Engrg., 77 Mass. Ave., 4-043, Cambridge, MA 02139 USA

Abstract Most commercial microporous membranes, which enjoy widespread use in filtration and purification, are made by the immersion precipitation process. This process begins with liquid-liquid demixing of a non-solvent/solvent/polymer ternary system into polymer-rich and polymer-lean phases; this demixing step determines much of the final morphology. In this work, a ternary Cahn-Hilliard formulation incorporating a Flory-Huggins homogeneous free energy function and coupled with variable-viscosity interface-driven fluid flow is used to simulate phase separation during liquid-liquid demixing. Simulations begin with uniform initial condition with a small random fluctuation to simulate spinodal decomposition, and also with a two-layer polymer-solvent/nonsolvent initial condition to simulate actual membrane fabrication conditions. 2-D and 3-D simulation results are presented which demonstrate the effects of K\_{ij}(gradient penalty coefficients) and compostion change in the coagulation bath and polymer solution on phase separation behavior.

#### 5:10 PM

**On Some Computational Issues of Allen-Cahn Equation in the Phase Field Modeling**: Qiang Du<sup>1</sup>; *Wenxiang Zhu*<sup>1</sup>; <sup>1</sup>Pennsylvania State University, Math., 307 McAllister Bldg., Univ. Park, PA 16802 USA

In this paper, first we study the exponential time differencing (ETD) schemes and demonstrate the effectiveness of the ETD type schemes through the numerical solution of Allen-Cahn equation in phase field modeling and through the comparisons with other existing methods. Secondly, we demonstrate benchmarking test results on the comparisons of the numerical solutions of the Allen-Cahn equation by finite difference method and spectral method as the interfacial width  $\varepsilon$  goes to 0.

# Cost-Affordable Titanium Symposium Dedicated to Prof. Harvey Flower: Creative Processing

Sponsored by: Structural Materials Division, SMD-Titanium Committee

*Program Organizers:* M. Ashraf Imam, Naval Research Laboratory, Washington, DC 20375-5000 USA; Derek J. Fray, University of Cambridge, Department of Materials Science and Metallurgy, Cambridge CB2 3Q2 UK; F. H. (Sam) Froes, University of Idaho, Institute of Materials and Advanced Processes, Moscow, ID 83844-3026 USA

Tuesday PM	Room:	206B		
March 16, 2004	Location	: Charlotte (	Convention	Center

Session Chair: David Rugg, Rolls Royce, Derby DE248BJ UK

## 2:00 PM

Electrochemical Deoxidation Mechanisms of Titanium Oxides in Molten Calcium Chloride: Kevin Frederick Dring<sup>1</sup>; Martin Jackson<sup>1</sup>; Richard J. Dashwood<sup>1</sup>; Harvey M. Flower<sup>1</sup>; Douglas Inman<sup>1</sup>; <sup>1</sup>Imperial College London, Matls., Royal Sch. of Mines, Prince Consort Rd., London SW7 2AZ England

Titanium oxides were successfully deoxygenated to below 1500ppm oxygen levels by electrochemical reduction in molten calcium chloride via the Fray-Farthing-Chen (FFC) process. Electrolysis was performed below the standard decomposition potential of CaCl<sub>2</sub> at 950°C and using an yttria stabilised zirconia counter electrode. Oxide preforms of near-bulk density were prepared by sintering precursor powders, under vacuum as necessary. Material was characterised pre- and post-reduction by scanning electron microscopy, x-ray energy dispersive spectrometry, and secondary ion mass spectrometry. Cyclic voltammetry and chronopotentiometry studies were conducted at various stages of reduction to ascertain the characteristics of the oxygen ionisation reaction at the cathode-electrolyte interface.

#### 2:30 PM

Properties of Cost-Affordable High-Performance Titanium Alloy Series "Super-TIX™": Akira Kawakami<sup>1</sup>; Hideki Fujii<sup>2</sup>; Kazuhiro Takahashi<sup>3</sup>; Yoshito Yamashita<sup>1</sup>; Takeshi Hirata<sup>1</sup>; Takashi Oda<sup>1</sup>; 'Nippon Steel Corporation, Titanium Div., Otemachi 2-6-3, Chiyoda, Tokyo 100-8071 Japan; <sup>2</sup>Nippon Steel Corporation, Steel Rsch. Labs., Shintomi 20-1, Futtsu, Chiba Japan; <sup>3</sup>Nippon Steel Corporation, Hikari Rsch. Lab., Shimata 3434, Hikari, Yamaguchi Japan

Super-TIX<sup>™</sup> series were originally developed in order to enlarge titanium use in new application fields, such as automotives, sports and utility goods, etc by featuring their cost-affordability and high-performance. Although they contain only inexpensive alloying elements, Fe, O, N and Al, they possess unique properties such as a wide range of tensile strength from 700 to 1100MPa, good ductility, excellent hot & cold workability and high-fatigue properties, depending on compositions. Ti-5%Al-1%Fe (Super-TiX51AF) and Ti-1%Fe-0.35%O-0.01%N (Super-TiX800) are defined as the core alloys. The former shows mechanical properties similar to that of Ti-6Al-4V with hot workability higher than that of Ti-6Al-4V. The latter has tensile strength between that of Ti-3Al-2.5V and Ti-6Al-4V with hot workability as high as that of CP. Alloy design concept and performances of the alloys are introduced. Moreover, some attentions to be paid when the alloys are actually used are also discussed.

## 3:00 PM

Affordable Ti-6Al-4V Castings: Kevin L. Klug<sup>1</sup>; Mehmet N. Gungor<sup>1</sup>; Ibrahim Ucok<sup>1</sup>; Christopher Hatch<sup>2</sup>; Robert Spencer<sup>3</sup>; Ronald Lomas<sup>4</sup>; <sup>1</sup>Concurrent Technologies Corporation, MTF, 100 CTC Dr., Johnstown, PA 15904 USA; <sup>2</sup>United States Marine Corps, PEO-Ground Combat & Support Systems, SFAE-GCSS-JLW, Bldg. 151, Picatinny Arsenal, NJ 07806 USA; <sup>3</sup>PCC Structurals, Inc., 4600 S.E. Harney Dr., Portland, OR 97206 USA; <sup>4</sup>BAE Systems - RO Defence, HIP - Bldg. B40, Barrow-in-Furness, Cumbria LA14 1AF UK

To extend the application of structural titanium alloy components beyond aerospace systems, the affordability of such parts must be addressed through reduced raw material, manufacturing and inspection costs. One example of a titanium-intensive land-based system is the XM777 Lightweight Howitzer (LWH), which is being developed to meet the U.S. Marines' and U.S. Army's increased operational thresholds for mobility, survivability and deployability. In an on-going Navy MANTECH program, investment casting was selected over machining and welding titanium plate to reduce part count and associated manufacturing expense for several LWH components. A study was also undertaken to reduce raw material costs through the utilization of scrap titanium that conforms to chemical constraints that are broader than aerospace standards. The microstructures and mechanical properties of experimental investment cast Ti-6Al-4V alloy sample plates were evaluated and compared to investment cast aerospace grade Ti-6Al-4V. Test results for the investigated materials will be presented and compared. This work was conducted by the National Center for Excellence in Metalworking Technology, operated by Concurrent Technologies Corporation under contract No. N00014-00-C-0544 to the U.S. Navy as part of the U.S. Navy Manufacturing Technology Program.

#### 3:30 PM

Development of a New Process for Producing Low Cost TiAl and Ti3Al/TiAl Powders: *Deliang Zhang*<sup>1</sup>; Gorgees Adam<sup>1</sup>; Jing Liang<sup>1</sup>; Guangsi Guo<sup>1</sup>; <sup>1</sup>University of Waikato, Dept. of Matl. & Proc. Engrg., Private Bag 3105, Hamilton 2001 New Zealand

With the increasing potential of using gamma titanium aluminides in mass production of automotive parts and aerospace components and structures, TiAl based powders will likely become a valuable commodity. The cost of the TiAl based powders produced by the traditional method of alloying Ti and Al and then atomising the melt still proves to be too expensive to be used in large scale. Being able to produce high quality TiAl based powders at a significantly lower cost is essential for the use of TiAl based materials for mass production of components and sheets. At Waikato University, we have developed a new process which can be used to produce TiAl based powders with a strong potential of lowering the cost of this type of powders. The process uses TiO<sub>2</sub> and other oxides and Al metal powders as raw materials, and it combines solid state reactions between TiO2 and Al, sintering, mechanical milling, and other physical and chemical processes. Through reaction between TiO<sub>2</sub> and Al, mechanical milling and a physical process, a Ti(Al,O)/Al<sub>2</sub>O<sub>3</sub> or Ti<sub>3</sub>Al/Al<sub>2</sub>O<sub>3</sub> based powder with a low volume fraction of Al<sub>2</sub>O<sub>3</sub> can be produced and then this powder can be used as a raw material to produce TiAl based powders using a chemical process. This paper will use production of TiAl and Ti<sub>3</sub>Al/TiAl alloy powders as an example to introduce the scientific principles underlying the process, and discuss the implications of the research results.

## 4:00 PM

Cold Formability Response to Solution Treatment Temperature of Low Cost Beta Ti Alloys for Welfare Goods: Masahiko Ikeda<sup>1</sup>; Shinya Komatsu<sup>1</sup>; Mitsuhide Ueda<sup>2</sup>; Akihiro Suzuki<sup>3</sup>; <sup>1</sup>Kansai University, Matls. Sci. & Engrg., 3-3-35, Yamate-cho, Suita, Osaka 564-8680 Japan; <sup>2</sup>Kansai University, Suita, Osaka 564-8680 Japan; <sup>3</sup>Daido Steel Co., LTD

Ti-4.3Fe-7.1Cr and 3.0Al alloys were developed as low cost beta Ti alloys for welfare goods. These alloys have good tensile properties in solution treated state, and compares well to the developed beta Ti alloys. In general beta Ti alloys have better cold formability than those of alpha and alpha+beta Ti alloys. It is important to investigate cold formability of these alloys for welfare goods, e.g. wheel chair. In this study, cold formability of these alloys was evaluated by cold compression test. In solution treated condition below the beta transus temperature, partially re-crystallized structure was observed, whereas only re-crystallized structure was observed in specimens solution-treated at or above the beta transus temperature. In these alloys quenched from a temperature above the beta transus temperature, true strain exceeded value of one. Details of results will be presented.

## 4:30 PM

The Way to Reduce the Cost of Titanium Alloys: Y. Q. Zhao<sup>1</sup>; H. Chang<sup>1</sup>; Y. L. Li<sup>1</sup>; <sup>1</sup>Northwest Institute for Nonferrous Metal Research, PO Box 51, Xi'an, Shaanxi 710016 China

Titanium alloys possess excellent properties and have been widely put into practical applications. However, their high cost limits their extensive applications in civil field. There are several ways to reduce Ti cost. This paper mainly discusses three ways. One is low cost Ti alloys developed with cheap alloying element, such as Fe. Using this way, Ti12LC and Ti8LC low cost alloy were developed by using cheap Fe-Mo master alloy. These two alloys have good mechanical properties. The second way is to use large deformation to process Ti12LC and Ti8LC alloys and P/M method to produce typical parts from Ti12LC alloy. The third way is semi-solid deformation.

## **Dislocations: Novel Experimental Methods**

Sponsored by: ASM International: Materials Science Critical Technology Sector, Electronic, Magnetic & Photonic Materials Division, Materials Processing & Manufacturing Division, Structural Materials Division, EMPMD/SMD-Chemistry & Physics of Materials Committee, MPMD-Computational Materials Science & Engineering-(Jt. ASM-MSCTS)

*Program Organizers:* Elizabeth A. Holm, Sandia National Laboratories, Albuquerque, NM 87185-1411 USA; Richard A. LeSar, Los Alamos National Laboratory, Theoretical Division, Los Alamos, NM 87545 USA; Yunzhi Wang, The Ohio State University, Department of Materials Science and Engineering, Columbus, OH 43210 USA

Tuesday PM	Room: 2	01A
March 16, 2004	Location:	Charlotte Convention Center

Session Chair: TBA

## 2:00 PM Invited

Internal Structure of Geometrically Necessary Dislocation Boundaries in fcc Metals: *Rodney J. McCabe*<sup>1</sup>; S. G. Srinivasan<sup>2</sup>; Amit Misra<sup>2</sup>; Michael I. Baskes<sup>2</sup>; Terence E. Mitchell<sup>2</sup>; <sup>1</sup>Los Alamos National Laboratory, MST/MST-6, MS G770, Los Alamos, NM 87545 USA; <sup>2</sup>Los Alamos National Laboratory, MST/MST-8, MS G755, Los Alamos, NM 87545 USA

Experiments and modeling were used to study the structure within geometrically necessary dislocation boundaries (GNB) in fcc metals. Using weak beam and stereo transmission electron microscopy, a crystallographic GNB in rolled copper was found to be composed primarily of dislocations from the three highest stressed slip systems. The boundary also contained a large number of dislocation nodes and Lomer locks. The general boundary minimum energy solution to Frank's formula does not agree well with the experimentally observed configuration. Alternate forms of Frank's formula were considered, some resulting in much better agreement. Dislocation simulations were used to provide insight into the formation of the observed structure.

#### 2:35 PM

**Dislocations and the Distortion of Materials**: Craig S. Hartley<sup>1</sup>; <sup>1</sup>AFOSR, Direct. of Aeros. & Matls. Scis., 4015 Wilson Blvd., Rm. 713, Arlington, VA 22203 USA

The scale of experimental measurements of the distortion of a material subjected the changes in its thermo-mechanical environment has dramatically decreased in recent years. It is now possible to measure the distortion of grids or other surface features over distances corresponding to several thousand atoms. Parallel advances in techniques for measuring the distortion of crystal lattices by diffraction techniques employing synchrotron x-radiation, electron backscattered diffraction (EBSD) and neutron scattering provide an unparalleled opportunity for verifying the validity of relationships between lattice distortion, total shape distortion and dislocation distortion. This paper reviews these relationships in an effort to clarify the physical nature of quantities measured by the two types of techniques and to describe experiments that would assist in revealing the role of dislocations in deformation at the nano- and micro-scale.

#### 2:55 PM

Characterization of the Dislocation Density Tensor With White Beam Diffraction: *Rozaliya Barabash*<sup>1</sup>; Gene E. Ice<sup>1</sup>; Judy W. Pang<sup>1</sup>; Wenjun Liu<sup>1</sup>; <sup>1</sup>Oak Ridge National Laboratory, Metals & Ceram., MS 6118, One Bethel Valley Rd., Oak Ridge, TN 37831 USA

The white beam intensity distribution is sensitive to the organization of the dislocations, which occurs at several structural levels. Near a Bragg reflection the intensity distribution in reciprocal space exhibits characteristic features due to dislocations. At the lowest level individual dislocations can exist within a crystal. At a higher structural level dislocations can organize into strongly correlated arrangements including walls and sub-boundaries. The distribution of scattered intensity in reciprocal space is sensitive to these dislocation ensembles. After some kinds of plastic deformation unpaired dislocations of one sign n+ (geometrically necessary dislocations) as well as geometrically necessary boundaries may be formed in the crystal. These cause not only random deformation, but also strongly correlated local rotations within the crystal, grain, or subgrain. Such correlated deformation changes the conditions for x-ray (or neutron) scattering in the transverse plane of each reflection. In the framework of strain gradient plasticity we describe the plastic deformation by a dislocation density tensor ?Ñij and strain gradient tensor of the third rank. A primary set of geometrically necessary dislocations or dislocation walls and subboundaries results in elongated streaks in the Laue image. The direction of the streak depends on the mutual orientation of all activated dislocation slip systems and on the components of dislocation density tensor. Laue images collected using synchrotron x-ray microbeams can reveal nano/meso-scale distribution of the primary paired and unpaired dislocations and dislocation walls. White beam diffraction analysis of several examples of deformation inhomogeneities in poly- and single crystals are discussed.

## 3:15 PM

Dislocation Density Measurements in CP Titanium Using Electron Channeling Contrast Imaging: Martin A. Crimp<sup>1</sup>; John T. Hile<sup>1</sup>; Thomas R. Bieler<sup>1</sup>; Michael G. Glavicic<sup>2</sup>; <sup>1</sup>Michigan State University, Dept. Chem. Engrg. & Matls. Sci., E. Lansing, MI 48824-1226 USA; <sup>2</sup>UES Inc., (AFRL/MLLM), 4401 Dayton-Xenia Rd., Dayton, OH 45432-1894 USA

Dislocation densities have been measured in warm rolled commercially pure Ti using electron channeling contrast imaging (ECCI) and compared to values determined from x-ray line broadening analysis. Samples were rolled to reductions of 1.08%, 2.16%, 5.17% and 15.05% at 366 K. The samples were mechanically prepared and electropolished to remove surface contamination and superficial damage. ECCI, a scanning electron microscopy technique that allows imaging of near surface dislocations in bulk samples, was carried out on the polished samples. Dislocation densities were determined by measuring the number of dislocation/surface intersections per unit area. Electron backscattered diffraction (EBSD) patterns were used to determine the orientation of individual grains, facilitating identification of the active slip planes through trace analysis. Comparison of the results from ECCI and x-ray line broadening studies demonstrates the two techniques are effective at measuring dislocation densities at significantly different plastic strain levels. This work has been supported by Air Force Research Laboratory, Materials and Manufacturing Directorate, and the Air Force Office of Scientific Research, Grant # F49620-01-1-0116.

# Electrochemical Measurements and Processing of Materials: Electrochemical Refining

Sponsored by: Extraction & Processing Division, Materials Processing & Manufacturing Division, EPD-Aqueous Processing Committee, EPD-Process Fundamentals Committee, EPD-Pyrometallurgy Committee, ASM/MSCTS-Thermodynamics & Phase Equilibria Committee, EPD-Waste Treatment & Minimization Committee

*Program Organizers:* Uday B. Pal, Boston University, Department of Manufacturing Engineering, Brookline, MA 02446 USA; Akram M. Alfantazi, University of British Columbia, Department of Metel & Materials Engineering, Vancouver, BC V6T 1Z4 Canada; Adam C. Powell, Massachusetts Institute of Technology, Department of Materials Science and Engineering, Cambridge, MA 02139-4307 USA

Tuesday PM Room: 212A March 16, 2004 Location: Charlotte Convention Center

*Session Chairs:* Donald R. Sadoway, Massachusetts Institute of Technology, Matls. Sci. & Engrg., Cambridge, MA 02139-4307 USA; Ramana G. Reddy, University of Alabama, Metallurgl. & Matls. Engrg., Tuscaloosa, AL 35487-0202 USA

## 2:30 PM Invited

Electrochemical Measurement of Dissolved Gases in Molten Metals: *Jeffrey W. Fergus*<sup>1</sup>; <sup>1</sup>Auburn University, Matls. Rsch. & Educ. Ctr., 201 Ross Hall, Auburn, AL 36849 USA

Gases dissolved in molten metals during processing can lead to defects, such as porosity and inclusions, and thus must be carefully controlled. Optimization of processes for such control requires online measurement of dissolved gas content. Solid-electrolyte-based electrochemical sensors are well-suited for such measurements and have been used for many years to measure the oxygen content in molten iron and steel. Other electrochemical sensors, such as those for measuring the amount of hydrogen in molten aluminum, are less fully developed, but offer potential improvements in process control. The high temperatures and low oxygen partial pressures present in molten or ionic defects, which creates challenges in sensor development. In this paper, this and other issues in the development of sensors for measuring oxygen and hydrogen in molten metals will be discussed.

## 3:00 PM Invited

The Refining Effect of Cold Plasma on Liquid Metal: Weizhong Ding<sup>1</sup>; Xionggang Lu<sup>1</sup>; <sup>1</sup>Shanghai University, Sch. of Matls. Sci. & Engrg., No. 149, Yanchang Rd., Shanghai 200072 China

An interesting phenomenon has been observed in this investigation: the refining effect of cold plasma on liquid metal. The impurity elements in metal may be removed by distillation and gas evolution process. The purification of metal can be enhanced if ionic gas exists in a reaction chamber of the process. In the above case nitrogen, sulfur and phosphorus as impurities in liquid metal are converted into volatile compounds and distilled off. This refining process could not be done under normal atmosphere. The refining effect of cold plasma has made it possible to develop a new technology, which can be used to produce very clean metal. According to the experimental result, the refining mechanism of the cold plasma has been discussed.

## 3:30 PM

Recycling of Al-Metal Matrix Composites in Ionic Liquids Via Low Temperature Electrolysis: Venkat Kamavaram<sup>1</sup>; Ramana G. Reddy<sup>2</sup>; <sup>1</sup>University of Alabama, Metallurgl. & Matls. Engrg., A129 Bevill Bldg., PO Box 870202, Tuscaloosa, AL 35487 USA; <sup>2</sup>University of Alabama, Dept. of Metallurgl. & Matls. Engrg. & Ctr. for Green Mfg., A129 Bevill Bldg., PO Box 870202, Tuscaloosa, AL 35487 USA

Recycling of aluminum metal matrix composites via electrolysis in ionic liquids at low temperatures was investigated. The electrolytic melt comprised of 1-butyl-3-methylimidazolium chloride (BMIC) and anhydrous AlCl<sub>3</sub>. Impure aluminum composite (Duralcan MMC Al-380, 20 vol% SiC) was electrochemically dissolved at the anode and pure aluminum (99.9%) was deposited on a copper cathode. The de-

posits were characterized by scanning electron microscope, X-ray diffraction, and mass spectrometer. The recycling process yielded current densities in the range of 200-500 A/m<sup>2</sup>, and average current efficiency of about 90% in all the cases. The results indicated that impurities such as Si, Cu, Ni, Fe, Mg, Mn, and SiC particles were removed as anode residue. Energy consumption of about 3.0 kWh/kg-Al was obtained at a cell voltage of 1.0V and cell temperature of 105°C. Low energy consumption and no emission of pollutants are the two main advantages of this process compared to present industrial processes.

## 4:00 PM Break

#### 4:30 PM

Deoxidation of Molten Steel with Application of Electrochemical Technique: *Hyun-Woo Koo*<sup>1</sup>; Hae-Geon Lee<sup>1</sup>; <sup>1</sup>Pohang University of Science and Technology (POSTECH), Dept. of Matls. Sci. & Engrg., San31, Hyoja-Dong, Namgu, Pohang, Kyungbuk 790-784 S. Korea

Deoxidation of molten steel was studied by employing an electrochemical cell principle using a solid oxide electrolyte. This technique enabled to deoxidize liquid steels without leaving deoxidation products in the steel. A number of different combinations and arrangements of solid electrolytes and deoxidizers were designed and tested. Among various solid electrolytes Y2O3-stabilized ZrO2 (YSZ) and Gd2O3-doped CeO<sub>2</sub> (GDC) were found to exhibit a good oxygen ion conduction. Various deoxidants including C(s)/CO mixture, metallic Ti, and Al were examined and compared of their efficiency in reacting with oxygen ion transported though an electrolyte. In order to improve electronic as well as ionic conductivity of the electrolytes, several different materials were mixed to or coated on the electrolytes. All experimental works were carried out at 1873K under an inert atmosphere by flowing purified argon gas. It was found that the rate of deoxidati on was dependent to a large extent on the electronic and ionic conductivities of the electrolyte. The rate of deoxidation was also dependent on the deoxidant used. Solid deoxidants such as Al and Ti performed poorly in taking oxygen due to chemical interaction with the electrolyte material and also due to the formation of oxidation product layer between the electrolyte and deoxidant. The deoxidant of C/CO mixture, although its equilibrium oxygen potential was much higher than that of either Al or Ti, exhibited much faster deoxidation. Based on the present study, the possibility of industrial application of this technique for production of ultra-clean steels was discussed.

TUESDAY PM

#### 5:00 PM

A New Unpolluted Deoxidation Way: *Xionggang Lu*<sup>1</sup>; Guozhi Zhou<sup>1</sup>; Weizhong Ding<sup>1</sup>; <sup>1</sup>Shanghai University, Sch. of Matls. Sci. & Engrg., No. 149, Yanchang Rd., Shanghai 200072 China

Using a deoxidizer placed into a magnesia-stabilized zirconia (MSZ) tube and an electronic conductor sealed the open of the MSZ tube, the deoxidization units are prepared. According to the principle of the short-circuited deoxidization of solid electrolyte cell, oxygen atoms in the melt obtain electrons and transform into oxygen ions at the melt/ electrolyte interface, oxygen ions diffused through the electrolyte to the electrolyte/deoxidizer interface react with the deoxidizer and produce deoxidization product. The electrons produced transfer through the electronic conductor to the melt/electrolyte interface and neutralize the positive charges accumulated, the electronic field stopping the diffusion of oxygen ions is destroyed. So the deoxidization process will go on until the deoxidization equilibrium. Deoxidization product remained inside deoxidization unit is removed together, so this deoxidized way will not pollute the melt and is a novel method which is experimentally verified to be effective. The rate and limit of deoxidization are got, and a model is established and simplified.

## 5:30 PM

Measurement of Conductivity and Electronic Conduction of Cryolite Alumina Melts: Ye Ya Ping<sup>1</sup>; Zheng Yunyou<sup>1</sup>; Li Fushen<sup>2</sup>; Li Lifen<sup>2</sup>; Zhou Guozhi<sup>2</sup>; <sup>1</sup>University of Science & Technology, Applied Sci. Sch., Beijing 100083 China; <sup>2</sup>University of Science & Technology, Lab. on Solid Electrolytes & Metallurgl. Testing Techniques, Beijing 100083 China

The conductivity of molten Na3AIF6 with Al2O3 was measured using AC impedance spectrum. The dependence of the conductivity of cryolite alumina upon temperature and concentration of alumina in the molten were studied. According to these data, a rule of conductivity vs. composition and temperature for molten cryolite could be found under 1010?•. The electronic conductivity measurements were also performed using the Wagner measurement technique under inverse polarization conditions.

325

## **General Abstracts: Session V**

Sponsored by: TMS

*Program Organizers:* Adrian C. Deneys, Praxair, Inc., Tarrytown, NY 10591-6717 USA; John J. Chen, University of Auckland, Department of Chemical & Materials Engineering, Auckland 00160 New Zealand; Eric M. Taleff, University of Texas, Mechanical Engineering Department, Austin, TX 78712-1063 USA

Tuesday PM	Room: 204
March 16, 2004	Location: Charlotte Convention Center

Session Chair: Anis Zribi, General Electric, Global Rsch. Ctr., Niskayuna, NY 12309 USA

## 2:00 PM

Characteristics of Ti5Si3 Dispersed Titanium Alloy Prepared by Powder Metallurgy: *Toshiyuki Nishio*<sup>1</sup>; Keizo Kobayashi<sup>1</sup>; Akihiro Matsumoto<sup>1</sup>; Kimihiro Ozaki<sup>1</sup>; <sup>1</sup>Aist chubu, Aichi, Nagoya 463-8560 Japan

Titanium silicide Ti5Si3 is expected as a high temperature structural material for aerospace use because of its own low density and a high melting temperature. Therefore, Ti5Si3 is potentially a one of effective dispersoid in titanium matrix to improve mechanical properties. Ti-Ti5Si3 composite has been prepared by powder metallurgy and also the properties of the composite has been investigated. Elemental titanium(30mm), silicon(20mm) and a fine silicon (<1mm) powders were used in this work. The fine silicon powder was mechanically ground for 45ks. Ti5Si3 was synthesized in a vacuum furnace. When using a fine silicon powder, Ti5Si3 was successfully synthesized at a relatively lower temperature. The synthesized Ti5Si3 was milled into fine powder by ball milling. The powder mixture of the composition of Ti-10mass%Ti5Si3 was consolidated by pulsed current sintering equipment. Microstructural observation of the composite revealed Ti5Si3 particles were homogeneously dispersed in the titanium matrix without pores.

#### 2:25 PM

Microstructure Effects of Shear Localization Evaluated With Electron Backscatter Diffraction: *Benjamin L. Henrie*<sup>1</sup>; Qing Xue<sup>1</sup>; George (Rusty) T. Gray<sup>1</sup>; <sup>1</sup>Los Alamos National Laboratory, PO Box 1663, MS G755, Los Alamos, NM 87545 USA

Adiabatic shear localization was studied in 316L stainless steel and tantalum. A force shear technique was utilized under high-strain-rate loading using a compression split-Hopkinson pressure bar and hat-shaped specimens. Electron backscatter diffraction (EBSD) was used to understand how the microstructure changed as a function of position relative to the shear band. Using EBSD, spatially coordinated crystallographic information was achieved immediately adjacent to the shear band. For the 316L stainless steel significant grain deformation occurred within a few grains of the shear band. In the tantalum case no shear band formed and some grains experienced ~250% strain while only experiencing a 10 degree grain misorientation.

#### 2:50 PM Cancelled

Castability and Microstructure Characterization of Reduced and Lead Free Brasses for Sanitary Applications

#### 3:15 PM

Microstructure and Mechanical Properties of a Dispersion Strengthened Al-Nano Al<sub>2</sub>O<sub>3</sub> Composite: Jixiong Han<sup>1</sup>; Yong-Ching Chen<sup>2</sup>; Vijay K. Vasudevan<sup>1</sup>; <sup>1</sup>University of Cincinnati, Chem. & Matls. Engrg., Cincinnati, OH 45221-0012 USA; <sup>2</sup>Cummins Inc., Metallurgl. Engrg., MC 50183, Columbus, IN 47201 USA

The microstructure, thermal stability and mechanical properties of a novel aluminum matrix composite reinforced with a high volume fraction nanoscale Al2O3 particles was studied. This material was produced by a casting route by Chesapeake Composites. The as-received dispersion strengthed composite (DSC) material was observed to possess an unusual microstructure composed of clusters of nanoscale (30-100 nm diameter) Al<sub>2</sub>O<sub>3</sub> particles surrounded by the Al matrix. Annealing at high temperatures lead to coalescence of these particles to larger size entities, giving rise to an interesting Al-Al<sub>2</sub>O<sub>3</sub> composite that is otherwise thermally stable and retains impressively high hardness (~170HV). The tensile strength of the DSC material decreased nearly linearly from ~40 ksi at room temperature to ~20 ksi at 400°C, the latter value being impressively high for an Al alloy. The fracture morphology correspondingly changed from brittle to ductile/dimpled rupture with presence of microvoids containing oxide particles in their interior. Thermal soaking at high temperatures for times to 500h led

to no degradation of the tensile properties. Although the macroscopic ductility remained low over the entire temperature range in both the unsoaked and soaked materials, there was substantial evidence for high localized plasticity as manifested by stretching, tearing and void formation in the Al matrix around the oxide particles. These results will be presented and discussed.

## 3:40 PM Break

#### 3:50 PM

Study of Solid Solution Strengthening by Ternary Elements Additions on Mo<sub>3</sub>Si Matrix: *I. Rosales*<sup>1</sup>; H. Martinez<sup>2</sup>; <sup>1</sup>Centro de Investigación en Ingeniería y Ciencias Aplicadas-FCQ e Ing. UAEM., Av Univ. 1001 Col. Chamilpa, Cuernavaca, Mor. 62210 Mexico; <sup>2</sup>Centro de Ciencias Físicas, UNAM, Av Univ. s/n Col. Chamilpa, Cuernavaca, Mor. 62210 Mexico

Ternary element addition on a  $Mo_3Si$  matrix resulted in mechanical variation properties. Solid solution additions in the alloys, were evaluated by Microhardness test, Lattice parameter measurements by Xray diffraction method and Youg's Modulus determination by indentation technique. Microhardness test shown in the case of the alloys with Cr no disparity for the different concentrations is observed. However samples with V and Nb addition shown a remarkable variation on the properties for the different Nb concentrations High temperature compression test at 1300 and 1400°C at 10<sup>-5</sup> s<sup>-1</sup> shown a strong temperature and composition dependence, the calculated stress exponent from compressive analysis resulted to be n= 6.

#### 4:15 PM

Syntheses and Studies on BST: MgTiO3 Ceramic Composites and Sputtered Thin Films: Tai-Nan Lin<sup>1</sup>; Jinn P. Chu<sup>1</sup>; Sea-Fue Wang<sup>2</sup>; J. Michael Rigsbee<sup>3</sup>; Wen-Rong Wu<sup>2</sup>; C. C. Lin<sup>1</sup>; C. H. Lin<sup>1</sup>; <sup>1</sup>National Taiwan Ocean University, Inst. of Matls. Engrg., No. 2, Pei-Ning Rd., Keelung 202 Taiwan; <sup>2</sup>National Taipei University of Technology, Dept. of Matls. & Mineral Resources, 1, Sec. 3, Chung-Hsiao E. Rd., Taipei 106 Taiwan; <sup>3</sup>North Carolina State University, Dept. of Matls. Sci. & Engrg., 229 Riddick Engrg. Labs, Box 7907, Raleigh, NC 27695 USA

The (Ba,Sr)TiO<sub>3</sub> (BST) system is well known for its high response of the dielectric constant to an applied electric field. However, the large dielectric constants found in this system limit its usefulness at microwave frequencies. Some research groups have used composite structures to dilute the dielectric constant and to minimize the dielectric loss of BST for microwave applications. (1-x) BST(Ba<sub>0.3</sub>Sr<sub>0.7</sub>TiO<sub>3</sub>) : x MT(MgTiO<sub>3</sub>) [BSMT(x)] composites were fabricated by conventional solid state reaction process. Thin films were thus prepared from the corresponding targets, i.e., pure BST, BSMT(0.05), BSMT(0.1), BSMT(0.2), BSMT(0.4), BSMT(0.6), BSMT(0.8) and pure MT (x is mole fraction). The decrease in the dielectric constants of BSMT(x) composites with increasing x is observed. The microwave quality factor Q and Q x f values exhibit a decreasing trend at x < 0.6. At x = 0.1, the dielectric constant is 154 and the Q x f value is 1883 GHz. As for the composite thin films, the dielectric constants also exhibit a decreasing trend between 0< x <0.2.

#### 4:40 PM

Manufacture and Performance of Bi-Layer Tetrahedral Truss Core Sandwich Panels: Gregory William Kooistra<sup>1</sup>; Haydn N.G. Wadley<sup>1</sup>; <sup>1</sup>University of Virginia, Matls. Sci. & Engrg. Dept., 116 Engineer's Way, Charlottesville, VA 22904 USA

Sandwich panels with cores made of period cellular metals are produced by a variety of techniques. This presentation gives a method for the manufacture bi-layer tetrahedral truss cores from a single sheet of patterned and stamped 6061 aluminum alloy. The cores are joined to facesheets of the same alloy via the brazing process creating an open architecture sandwich panel suitable for multifunctional applications. The performance of these panels is compared with honeycomb, truss, textile, and foam structures. Analytical models are developed to describe the relative mechanical properties of the core material. Experimental results demonstrate a strong performance dependent relationship to the condition of the parent alloy in both the elastic and plastic deformation regimes.

## 5:05 PM

Instrumentation for Determining the Local Damping Capacity in Honeycomb Sandwich Composites: John D. Lincoln<sup>1</sup>; L. E. Rieger<sup>1</sup>; J. C. Earthman<sup>1</sup>; <sup>1</sup>University of California, Matls. Sci. & Engrg., Engrg. Tower 644F, Henry Samueli Sch. of Engrg., Irvine, CA 92697 USA

A mechanical tapping probe originally designed for determining the damping capacity of dental implants has been adapted to assess the local damping capacity of honeycomb sandwich composites without inflicting damage on the structure. The new instrumentation is light, portable, and inexpensive when compared with other testing techniques. Furthermore, it allows quick access to areas not easily accessible by ultra-sonic methods. The damping capacity of honeycomb sandwich composite structures is of interest to engineers as it reflects the ability of a material to absorb and isolate vibration, both acoustic and mechanical. Honeycomb sandwich structures with various damping treatments were constructed and accurately evaluated with the instrumentation.

# Hume Rothery Symposium: Structure and Diffusional Growth Mechanisms of Irrational Interphase Boundaries: Session IV

Sponsored by: Electronic, Magnetic & Photonic Materials Division, Structural Materials Division, EMPMD/SMD-Alloy Phases Committee, MPMD-Phase Transformation Committee-(Jt. ASM-MSCTS) Program Organizer: H. I. Aaronson, Carnegie Mellon University, Department of Materials Science and Engineering, Pittsburgh, PA 15213 USA

Tuesday PM	Room:	20	8A		
March 16, 2004	Locatior	n:	Charlotte	Convention	Center

Session Chair: T. Furuhara, Kyoto University, Dept. of Matls. Sci. & Engrg., Kyoto 606-8501 Japan

#### 2:00 PM Invited

Interfacial Structure of Cementite Dendrites Formed at Austenite Grain Boundaries: Milo V. Kral<sup>1</sup>; George Spanos<sup>2</sup>; <sup>1</sup>University of Canterbury, Mech. Engrg., PO Box 4800, Christchurch New Zealand; <sup>2</sup>US Naval Research Laboratory, Phys. Metall. Brch., 4555 Overlook Ave., SW, Washington DC 20375 USA

A Fe-13Mn-1.3%C alloy has been studied extensively using threedimensional analysis techniques and electron diffraction techniques. The 3D work showed that grain boundary cementite assumes a dendritic or fern-like morphology with dendrite arms growing along the grain boundary plane. Electron backscatter diffraction pattern analysis showed that many of these precipitates obtain a (near) rational orientation relationship with one of the adjacent austenite grains and an irrational orientation with the other austenite grain. The interfacial structure of cementite:austenite interfaces on both sides of cementite grain boundary precipitates will be studied using high-resolution transmission electron microscopy.

## 2:40 PM Invited

Interphase Boundaries in the Massive Transformation: Vijay K. Vasudevan<sup>1</sup>; James E. Wittig<sup>2</sup>; <sup>1</sup>University of Cincinnati, Chem. & Matls. Engrg., Cincinnati, OH 45221-0012 USA; <sup>2</sup>Vanderbilt University, Elect. Engrg. & Compu. Sci., Nashville, TN 37235-1683 USA

The massive-matrix interphase interfaces associated with the  $\alpha$  to  $\gamma_M$  massive transformation in Ti-(46-48)Al alloys were studied. The transformation was arrested at an early stage utilizing either special heat treatments or by rapid solidification. Orientation relations between the  $\gamma_M$  and parent  $\alpha$  (retained  $\alpha_2$ ) phases were determined using EBSD in an SEM and by electron diffraction, and the interphase interfaces and defect structures in the  $\gamma_{M}$  phase characterized by two-beam bright-field/weak-beam dark-field TEM and HRTEM. The results reveal that the  $\gamma_M$  forms at grain boundaries generally with a low-index orientation relation and coherent interface with one parent grain, but grows into the adjacent grain with a high-index/irrational orientation relation. In the case of  $\gamma_{M}$  formed at grain edges and corners, no lowindex orientation relations were found with any of the surrounding parent grains. The growth interphase boundaries between the two phases are generally free of misfit dislocations or other defects and consist of curved parts as well as planar facets whose macroscopic habit planes are of generally high-index/irrational orientation and deviate substantially from the close-packed planes. On an atomic scale the growth interphase boundaries are sometimes found to be faceted along {111} planes, as well as along other planes, with closely spaced steps, but are concluded to be incoherent with respect to the parent grain into which growth occurs. The results obtained will be compared with those in other alloy systems and their implications on the nucleation and growth mechanisms associated with the massive transformation will be discussed.

## 3:20 PM Invited

Structure of Irrational Interfaces Operative During the Pearlite Reaction: Gary J. Shiflet<sup>1</sup>; <sup>1</sup>University of Virginia, Matls. Sci. & Engrg., PO Box 400745, 116 Engineers Way, Charlottesville, VA 22904-4745 USA

This presentation will examine the microstructural consequences associated with crystallographic constraints associated with irrational interphase boundaries at the pearlite growth front. A generalization of the calculations by Lee and Aaronson concerning grain boundary precipitate embryo equilibrium morphologies to interphase boundaries will be developed. These results will then be applied to Fe-C-V pearlite growing with concomitant interphase boundary precipitation of VC. A critical and quantitative comparison between growth interphase boundaries that are irrational, but have a deference to crystallographic constraints, and disordered growth fronts that do not will be made. Support by the National Science Foundation, DMR is acknowledged.

## 4:00 PM Break

## 4:15 PM Invited

Structure of Irrational Interphases Operative During the Cellular Transformation: *Gary J. Shiflet*<sup>1</sup>; Max W.H. Braun<sup>2</sup>; Jan H. van der Merwe<sup>3</sup>; <sup>1</sup>University of Virginia, Matls. Sci. & Engrg., PO Box 400745, 116 Engrs. Way, Charlottesville, VA 22904-4745 USA; <sup>2</sup>University of Pretoria, Dept. of Physics, Pretoria S. Africa; <sup>3</sup>University of South Africa, Dept. of Physics, Pretoria S. Africa

The cellular, or discontinuous precipitation, reaction occurs widely in alloys. Although it is often modeled possessing a disordered growth front, extensive experimental work in binary Cu-Ti alloys has shown that even though the individual lamellae interphase boundary growth fronts are indeed irrational, deference to crystallography still occurs, which includes periodic misfit compensating defects. This paper will provide a theoretical framework illustrating the energetics associated with irrational orientation relationships that still have energies lowered by matching at the advancing phase boundary. The Embedded Atom Method (EAM), coupled with van der Merwe's mathematical approach, is applied to examine specific irrational interphase boundary structures and energies for this system. Support by the National Science Foundation, DMR is acknowledged.

# Internal Stresses and Thermo-Mechanical Behavior in Multi-Component Materials Systems: Creep and Plasticity II

Sponsored by: Electronic, Magnetic & Photonic Materials Division, Structural Materials Division, EMPMD-Electronic Packaging and Interconnection Materials Committee, EMPMD-Thin Films & Interfaces Committee, SMD-Composite Materials Committee-Jt. ASM-MSCTS

*Program Organizers:* Indranath Dutta, Naval Postgraduate School, Department of Mechanical Engineering, Monterey, CA 93943 USA; Bhaskar S. Majumdar, New Mexico Tech, Department of Materials Science and Engineering, Socorro, NM 87801 USA; Mark A.M. Bourke, Los Alamos National Laboratory, Neutron Science Center, Los Alamos, NM 87545 USA; Darrel R. Frear, Motorola, Tempe, AZ 85284 USA; John E. Sanchez, Advanced Micro Devices, Sunnyvale, CA 94088 USA

Tuesday PM	Room: 209B
March 16, 2004	Location: Charlotte Convention Center

Session Chairs: David C. Dunand, Northwestern University, Evanston, IL 60208 USA; Bhaskar S. Majumdar, New Mexico Tech, Socorro, NM 87801 USA

## 2:00 PM Invited

Internal Stress in Plasticity and Microplasticity: James C.M. Li<sup>1</sup>; <sup>1</sup>University of Rochester, Dept. of Mech. Engrg., Matls. Sci. Prog., Rochester, NY 14627 USA

While the yield stress is the minimum stress to start plastic deformation, internal stress is that to sustain plastic deformation. After yielding, the applied stress needed to continue deformation may be lower than the yield stress so the internal stress must be measured during deformation such as by stress relaxation. Obviously the internal stress relates to the microstructure developed during deformation and hence it can be altered by further deformation, reverse deformation, deformation in another direction as well as by annealing. The role of internal stress played in work hardening, latent hardening, ductility and fracture is reviewed. Internal stress development in micro and nanoindentation will be reported also. Work supported by the N.Y. State Infotonics Center of Excellence and by NSF through DMR9623808 monitored by Dr. Bruce MacDonald.

# 2:25 PM Invited

Internal Stresses and Constitutive Behavior of Ferroelectrics: Ersan Ustundag<sup>1</sup>; Robert Rogan<sup>1</sup>; S. Maziar Motahari<sup>1</sup>; Bjørn Clausen<sup>2</sup>; Chad Landis<sup>3</sup>; <sup>1</sup>California Institute of Technology, Dept. of Matls. Sci., Pasadena, CA 91125 USA; <sup>2</sup>Los Alamos National Laboratory, Neutron Sci. Ctr., Los Alamos, NM 87545 USA; <sup>3</sup>Rice University, Dept. of Mech. Engrg. & Matls. Sci., Houston, TX 77251 USA

Ferroelectric materials exhibit a unique response to electromechanical loading and can be used as both sensors and actuators. This presentation will first review recent studies that employed diffraction to investigate strain and texture evolution in various ferroelectrics under electromechanical loading. In addition, our recent work on the multiscale internal stress characterization of Pb(Zr,Ti)O3 and BaTiO3 materials will be discussed. Then a new self-consistent micromechanics model will be presented. This model considers different domain variants and attempts to estimate strain and texture (or domain switching) evolution during the loading of ferroelectrics. Finally, the diffraction data will be compared to the predictions of this model.

#### 2:50 PM Invited

In Situ Study of Cyclic Mechanical and Thermal Loading in a Two Phase System Using Diffraction: Mark R. Daymond<sup>1</sup>; <sup>1</sup>Rutherford Appleton Laboratory, ISIS Fac., Chilton, Didcot, Oxfordshire OX11 0QX UK

Neutron and synchrotron x-ray diffraction allow the monitoring of the bulk internal stress state of polycrystalline materials during in situ loading. In multi-phase materials the stress partitioning between the two phases can be monitored. In both multi-phase and single phase materials the redistribution of load between differently oriented grain families within the polycrystal material can be monitored. By comparing diffraction results with predictions from micromechanical models (both finite element and self-consistent) we can obtain an insight into the deformation mechanisms occurring in the material. Recent studies of cyclic mechanical and thermo-mechanical loading of two phase systems will be described, in particular Al/SiC and two phase steels. As well as illustrating the interplay between continuum and grain level assumptions, these results bring an insight into slip system cross hardening and Bauschinger effects.

#### 3:15 PM Invited

A Methodology for Determining Internal Stresses in Multi-Component Materials: *Bjorn Clausen*<sup>1</sup>; Mark A.M. Bourke<sup>2</sup>; Donald W. Brown<sup>2</sup>; Ersan Ustundag<sup>3</sup>; <sup>1</sup>Los Alamos National Laboratory, LANSCE-12, PO Box 1663, MS H805, Los Alamos, NM 87545 USA; <sup>2</sup>Los ALamos National Laboratory, MST-8, PO Box 1663, MS H805, Los Alamos, NM 87545 USA; <sup>3</sup>California Institute of Technology, Matls. Sci. Dept., Keck Lab., MC 138-78, 1200 E. Calif. Blvd., Pasadena, CA 91125 USA

In most cases, determining the constitutive behavior of a composite is not as simple as using the rule of mixtures, especially for the inelastic properties such as phase yield stress and hardening. Furthermore, the processing conditions will most likely alter the properties of the constituents compared to their monolithic properties due to changes in the microstructure and introduction of thermal residual stresses. A methodology for determining the internal stresses in multiphase materials based on neutron diffraction measurements and finite element modeling (FEM) will be presented. The diffraction technique is inherently phase specific, and it yields information about internal elastic lattice strains in bulk crystalline materials. The combination of the experimental results and FEM enables us to indirectly determine the in-situ properties of the constituent phases. As an example, the constitutive performance of fiber reinforced composites will be presented for tungsten fiber composites with either Kanthal or bulk metallic glass matrix.

#### 3:40 PM Invited

Internal-Stress Plasticity in Iron Wires by Rapid Thermal Cycling Through the Allotropic Transformation: John Marvin<sup>1</sup>; David C. Dunand<sup>1</sup>; <sup>1</sup>Northwestern University, Matls. Sci., 2220 Campus Dr., 2043 Cook Hall, Evanston, IL 60208 USA

Iron and eutectoid steel wires, ca. 0.5 mm in diameter, were rapidly cycled through the alpha-gamma phase transformation range by direct current Joule heating while being subjected to a tensile stress. The wires deform plastically after each crossing of the phase transformation, as reported in the literature for bulk iron and steel samples subjected to slow thermal cycling. The mechanism responsible for this phenomenon is called internal-stress plasticity, and relies on the biasing by the external stress of the internal mismatch stresses due to the co-existence of both alpha and gamma phases with different density. The present experiments demonstrate that internal-stress plasticity can be achieved under very rapid cycling (2.5-second cycles, or 0.4 Hz),

which is two order of magnitude faster that has been achieved so far with bulk samples (4-minute cycles or 0.004 Hz).

## 4:05 PM Invited

The Relationship Between Microstructure and Ductility in Cast Aluminum: *Stephen J. Harris*<sup>1</sup>; James Boileau<sup>1</sup>; Wen Yang<sup>1</sup>; Bhaskar S. Majumdar<sup>2</sup>; Somnath Ghosh<sup>3</sup>; <sup>1</sup>Ford Research and Advanced Engineering, Dept. of Matls. Sci., Dearborn, MI 48121 USA; <sup>1</sup>Ford Research and Advanced Engineering, PES Dept., MD #3083, SRL Bldg., 2101 Village Rd., Dearborn, MI 48121 USA; <sup>2</sup>New Mexico Institute of Technology, NM USA; <sup>3</sup>Ohio State University, Mech. Engrg., OH USA

The increased use of cast aluminum for automotive applications highlights the need to develop a better database of mechanical and physical properties for cast Al alloys. In general, improvements in all mechanical properties are often desired. However, in practice, the difficulty in increasing both strength and ductility simultaneously can lead to undesirable tradeoffs. Because of this, a study was undertaken to correlate microstructure with ductility and strength in cast 319 and 356 Al alloys. 3-point bending tests were performed on a set of specimens with similar strengths but different ductilities and on a set of specimens with similar ductilities but different strengths. The tests were done in-situ in an SEM. The resulting images were analyzed to yield local displacement and strain fields. Complementary micro-Raman experiments were carried out under an optical microscope and yielded direct measurements of strain in selected Si particles. The results will be discussed in terms of the particular microstructural features (e.g., Si particles, intermetallics) that are responsible for ductile fracture in these alloys and how their actions are controlled by local stresses and strains.

#### 4:30 PM

**Constitutive Behavior of Pb(Zr,Ti)O3 Ferroelectrics**: *Robert Rogan*<sup>1</sup>; Ersan Ustundag<sup>1</sup>; S. Maziar Motahari<sup>1</sup>; Bjørn Clausen<sup>2</sup>; Ulrich Lienert<sup>3</sup>; Mark R. Daymond<sup>4</sup>; <sup>1</sup>California Institute of Technology, Dept. of Matls. Sci., Pasadena, CA 91125 USA; <sup>2</sup>Los Alamos National Laboratory, Neutron Sci. Ctr., Los Alamos, NM 87545 USA; <sup>3</sup>Argonne National Laboratory, Advd. Photon Source, Argonne, IL 60439 USA; <sup>4</sup>Rutherford-Appleton Laboratory, ISIS Neutron Scattering Facility, Chilton, Didcot OX11 0QX

Electromechanical loading was applied to monitor strain and texture (domain switching) evolution in various Pb(Zr,Ti)O3 or PZT ceramics using neutron and high energy X-ray diffraction. In-situ uniaxial compression experiments were performed on various PZTs using neutron diffraction to determine their ferroelastic behavior. PZTs near the edge of the morphotropic phase boundary as well as single phase (tetragonal and rhombohedral) specimens were investigated. Analysis of the diffraction patterns allowed for observation of the onset and culmination of domain switching through modeling of the sample texture using the March-Dollase model. In a separate experiment, high energy XRD with an area detector provided information about the ferroelectric response of a La-doped PZT to cyclic electrical loading. Diffraction data suggested a high degree of anisotropy and a complicated internal stress state in all specimens. The data were also compared to the predictions of a new self-consistent model to describe the constitutive behavior of PZTs.

# International Laterite Nickel Symposium - 2004: Process Development for Prospective Projects

Sponsored by: Extraction & Processing Division, EPD-Aqueous Processing Committee, EPD-Copper, Nickel, Cobalt Committee, EPD-Process Fundamentals Committee, EPD-Process Mineralogy Committee, EPD-Pyrometallurgy Committee, EPD-Waste Treatment & Minimization Committee *Program Organizer:* William P. Imrie, Bechtel Corporation,

Mining and Metals, Englewood, CO 80111 USA

Tuesday PM	Room: 217B/C
March 16, 2004	Location: Charlotte Convention Center

*Session Chairs:* Peter G. Mason, Principle Consultant, Hydrometallurgy, Falconbridge, Queensland Australia; Larry Seeley, President & CEO, SGS Lakefield Research Limited, Lakefield, Ontario KOL 2H0 Canada

## 2:30 PM

**Development of Process Design in Coral Bay Nickel Project**: *Naoyuki Tsuchida*<sup>1</sup>; <sup>1</sup>Sumitomo Metal Mining Co., Ltd., Non-Ferrous Metals Div. Coral Bay Project Dept., 11-3, Shinbashi 5-Chome, Minatoku, Tokyo 105-8716 Japan

Sumitomo Metal Mining Co. Ltd. (SMMC) is currently developing the flowsheet to treat stockpiled limonite, a type of laterite ore, at Rio Tuba on southern Palawan Island, Philippines. The new plant will be commissioned at the end of 2004. Rio Tuba Nickel Mining Corporation (RTNMC) has been mining saprolite since 1977, and the limonite ore located above the saprolite ore body has been stockpiled separately according to nickel and magnesium content. Ore from these stockpiles will be blended and used for the operation. The annual production of nickel will be 10,000 metric tons for the next twenty years. The proposed process consists of ore preparation, high pressure acid leach (HPAL), counter-current decantation wash, impurity removal and sulfide precipitation. Precipitated mixed sulfide will be processed to electrolytic nickel by the Matte Chlorine Leach Electrowinning (MCLE) process at Niihama, Japan. SMMC has established new technologies during the process development, such as zinc removal and sulfide precipitation. Applying this technology, preferential removal of zinc can be achieved by hydrogen sulfide gas with negligible loss of nickel. Precipitation of nickel by hydrogen sulfide gas is carried out at low temperature. Slow kinetics is selected for control of the particle size of the precipitated mixed sulfide

## 2:55 PM

A Complete Approach to Complex Flowsheet Development-Niquel do Vermelho (CVRD) Case Study: *Michael Adams*<sup>1</sup>; Dwight van der Meulen<sup>1</sup>; John Ernest Angove<sup>1</sup>; <sup>1</sup>SGS, Lakefield Oretest Pty Ltd, 431 Victoria Rd., Malaga, Perth, Western Australia 6090 Australia

A comprehensive pre-feasibility study has been conducted on CVRD's Niquel do Vermelho nickel laterite deposit. Five integrated flowsheet options were developed, via batch and pilot campaigns at Lakefield Oretest over an intensive five-month period, from ore receival to final reporting. Key objectives included demonstrating the technical viability of the beneficiation of several ore types, processing through integrated PAL/MHP and PAL/MSP circuits and treatment of barren liquors to meet stringent environmental requirements. Refining of the MHP was by ammonia re-leach and solvent extraction to produce LME-grade nickel cathodes, NiCO3, NiO and CoS. LME grade nickel and cobalt was also produced by oxidation of the MSP and hydrogen reduction on the leachate. The database and acquisition system, along with web-based reporting, enabled rapid turnaround on both daily and comprehensive run reports, with speedy and confident setpoint decisions on complex flowsheets. The high value of such data is thus given due recognition and will play a pivotal role in the successful progression of laterite projects through to sustainable commercial viability.

#### 3:20 PM

**Development of a Fluid-Bed Pyrohydrolysis Process for Inco's Goro Nickel Project**: *Ahmed Vahed*<sup>1</sup>; Fred Colton<sup>1</sup>; Jean-Paul Duterque<sup>2</sup>; Wilhelm Karner<sup>3</sup>; Frank Baerhold<sup>3</sup>; <sup>1</sup>Inco Technical Services Limited, 2060 Flavelle Blvd., Sheridan Park, Mississauga, Ontario L5K 1Z9 Canada; <sup>2</sup>Goro Nickel S.A., Imm. Le Kariba, 7 Bis, Rue Suffren, B.P. 218-98845, Noumea New Caledonia; <sup>3</sup>Ruthner Surface Technologies, Eibesbrunnergasse 20, Vienna A-1121 Austria

The Goro Nickel Project is situated in the Southern Province of New Caledonia. Inco Limited and Goro Nickel S.A. have developed a process that features the use of pyrohydrolysis to produce nickel oxide. The process treats a blend of laterites by Pressure Acid Leaching followed by solvent extraction of nickel and cobalt using Cyanex 301®. Purified nickel chloride solution is converted to high purity NiO product and 6M hydrochloric acid, which is recycled back to the SX circuit. In co-operation with Andritz AG, spray roaster and fluidbed pyrohydrolysis technologies were examined for this purpose. Tests were conducted at the Andritz AG pilot plant in Vienna, Austria, and at Goro in larger scale installations. The latter served to establish process engineering design parameters for scale-up. Several process variables were investigated in both technologies and the off-gas characteristics were established. Fluid-bed pyrohydrolysis was selected for the Goro commercial plant, primarily because it produced a granular nickel oxide. The main focus of this paper is to outline the results obtained in a 0.8 m diameter fluid-bed pyrohydrolysis circuit.

#### 3:45 PM Break

#### 3:55 PM

Piloting of the Beneficiation and EPAL® Circuits for Ravensthorpe Nickel Operations: *Mike Adams*<sup>1</sup>; Dwight van der Meulen<sup>1</sup>; Chad Czerny<sup>1</sup>; Peter Adamini<sup>1</sup>; John Turner<sup>1</sup>; Sunil Jayasekera<sup>1</sup>; Jason Amaranti<sup>1</sup>; John Mosher<sup>2</sup>; Mike Miller<sup>3</sup>; David White<sup>3</sup>; Geoff Miller<sup>3</sup>; <sup>1</sup>SGS Lakefield Oretest, 431 Victoria Rd., Malaga, Western Australia 6090 Australia; <sup>2</sup>AR McPherson Consultants Ltd; <sup>3</sup>Ravensthorpe Nickel Operations

Comprehensive pilot testwork has been conducted on BHP Billiton's Ravensthorpe nickel laterite deposit over a fifteen-month period at Lakefield Oretest. Some 228 tonnes of ore were processed in a beneficiation pilot-plant comprising scrubbing, attrition scrubbing, screening and thickening over sixteen pilot runs with an average mass closure of 99.2%. This produced a suitable feed for hydrometallurgical piloting over seven runs covering 1,680 hours of operation. The integrated EPAL® (enhanced pressure acid leach) circuit comprised a limonite pressure acid leach front end discharging into a saprolite atmospheric leach circuit and subsequently to induced jarosite precipitation. counter-current decantation, iron removal, mixed hydroxide precipitation, and manganese removal. The pilot plant met its key objectives in demonstrating the flowsheet's technical viability, and generating raw data inputs for the project feasibility study. Rapid, intensive data capture, collation and reporting helped solve key flowsheet issues. The pilot plant also demonstrated its value as a risk management tool in the resolution of numerous engineering, metallurgical and materials selection issues at a manageable scale. A disciplined approach to experimental planning, operation and management was a significant contributor to the overall success of the campaign.

#### 4:20 PM

Niquel do Vermelho Project-Prefeasibility Study: Vanessa de Macedo Torres<sup>1</sup>; Marcelo Lopes Costa<sup>1</sup>; Omar Antunes Carmo<sup>1</sup>; Ruy Lacourt Rodrigues<sup>1</sup>; Salomao Solino Evelin<sup>1</sup>; <sup>1</sup>Companhia Vale do Rio Doce, Base Metals Projects Dept., BR 262-Km 296, Santa Luzia, MG 33030-970 Brazil

Cia. Vale do Rio Doce is currently developing Niguel do Vermelho Project. The laterite deposit is located at Carajas Mineral Province at less than 15 km from Sossego Copper Project, scheduled for start-up on 2004. The available infrastructure, includes paved roads, large capacity railroad and port complex owned by CVRD, power supply and good quality water. The project was evaluated in the past for ferronickel production. In the late 1990s, CVRD switched its attention to investigating the usage of pressure acid leaching. The combination of good metallurgical behaviour for pressure acid leach (PAL) process route with reasonable mineable grades, and existing infrastructure justified the start of engineering studies in 2002. The project approach at the engineering phase is based on the dual objective of minimizing risks while maximizing project profitability and value. CVRD is currently completing the Niquel do Vermelho prefeasibility study. This paper outlines the main outcomes of the study and future perspectives for the project.

TUESDAY PM

#### 4:45 PM

The Jaguar Nickel Inc. Sechol Laterite Project Atmospheric Chloride Leach Process: G. B. Harris<sup>1</sup>; T. J. Magee<sup>1</sup>; V. I. Lakshmanan<sup>2</sup>; R. Sridhar<sup>2</sup>; <sup>1</sup>Jaguar Nickel Inc., 55 Univ. Ave., Ste. 910, Toronto, ON M5J 2H7 Canada; <sup>2</sup>Process Research ORTECH Inc., 2395 Speakman Dr., Mississauga, ON L5K 1B3 Canada

Jaguar Nickel Inc. is developing the Sechol Nickel-Cobalt Laterite Project in Guatemala, Central America. Recognizing the potential advantages offered by chloride brine chemistry, Jaguar, at the facilities of Process Research ORTECH Inc, Mississauga, has developed an Atmospheric Chloride Leaching Process using a mixed chloride lixiviant to recover the nickel and cobalt, whilst leaving the majority of the iron and magnesium in the leach residue. Subsequent solution purification and mixed nickel/cobalt hydroxide product recovery is by standard precipitation methods, using recycled caustic magnesia, with a final stage of pyrohydrolysis of a portion of the concentrated magnesium chloride brine for recycling both the caustic magnesia and chloride lixiviant. The flowsheet that has been developed also offers opportunities for by-product recovery and efficient, environmentally clean process effluent management. The paper discusses some of the early leaching results in the context of strong chloride brine chemistry, with emphasis on how the controlling of water activity, hydrogen ion activity and chloride concentration permits the selective leaching of nickel and cobalt from an iron-magnesium matrix.

# International Laterite Nickel Symposium - 2004: Roasting and Smelting

Sponsored by: Extraction & Processing Division, EPD-Aqueous Processing Committee, EPD-Copper, Nickel, Cobalt Committee, EPD-Process Fundamentals Committee, EPD-Process Mineralogy Committee, EPD-Pyrometallurgy Committee, EPD-Waste Treatment & Minimization Committee Program Organizer: William P. Imrie, Bechtel Corporation,

Mining and Metals, Englewood, CO 80111 USA

Tuesday PMRoom: 217DMarch 16, 2004Location: Charlotte Convention Center

Session Chairs: John G. Schofield, Pyrometallurgical Consultant, Nanoose Bay, BC V9P 9G5 Canada; Egil J.M. Jahnsen, Pyrometallurgical Consultant, Hagan, 4480 Kvinesdal Norway

## 2:30 PM

Contribution to the Recycling of Rotary Kiln Dust in Nickeliferous Laterite Reduction: Reduction Behavior of the Dust: *Elias Rigopoulos*<sup>1</sup>; Ismene-Polyxeni Kostika<sup>2</sup>; Emmanuel N. Zevgolis<sup>2</sup>; Iliana Halikia<sup>2</sup>; <sup>1</sup>Silver and Baryte Ores Mining Co. S.A, Milos Island, Milos Greece; <sup>2</sup>National Technical University of Athens (NTUA), Sch. of Mining & Metallurgl. Engrg., Zografou Campus, 5780, Athens Greece

In the present study the reductive behavior of dust from the rotary kilns (R/K) in ferronickel production from nickeliferous Greek laterites is investigated. The study concerns dust of various origins (washing towers, electrostatic filters, polycyclones) and pellets made from the dust. Reducibility was studied in the temperature range of 700°C to 850°C in a laboratory tube furnace. Experimental results showed that reduction degree increases with temperature up to about 800°C. The rate of reduction is great during the first minutes, giving a reduction degree R% equal to about 25%, in only a few minutes. After this, the rate is decreasing until it diminishes to zero after about 10-20 minutes of reaction. Maximum reduction degrees at various temperatures are higher for the dust samples than those of the respective pellet samples.

## 2:50 PM

**Calcination and Reduction of Laterite Nickel Ores**: *Andreas Orth*<sup>1</sup>; Bernd Kerstiens<sup>1</sup>; <sup>1</sup>Outokumpu Lurgi Metallurgie GmbH, Ferrous Tech., Ludwig-Erhard-Str. 21, Oberursel 61440 Germany

Outokumpu Lurgi Metallurgie has developed a process for the calcination and reduction of laterite nickel ores where the reduction of iron and nickel to the wuestite/metallic states respectively, is performed in a fluidized bed reactor using reduction gas generated very cost effectively from natural gas in an auto thermal catalytic reactor. As an option coal can be used as reductant as well as additional fuel. The process of reduction and calcination is very energy-optimized. It uses the off gas from the fluidized bed reduction reactor, which still contains sufficient energy to dry and calcine the nickel ore fines, in a primary stage circulating fluidized bed (CFB) reactor. The product shows high metallization of nickel and reduced iron oxides to the wuestite state. This results in considerable energy savings in smelting to ferronickel from the pre-reduced product. Alternatively the product can be leached to produce nickel. Laboratory tests showed a very high recovery of nickel and cobalt.

## 3:10 PM

Liquidus Temperatures of Ferro-Nickel Smelting Slags: Shengqi Chen<sup>1</sup>; Lourens Erasmus<sup>2</sup>; Steve C.C. Barnett<sup>3</sup>; Evgueni Jak<sup>1</sup>; *Peter Charles Hayes*<sup>1</sup>; <sup>1</sup>University of Queensland, Pyrometall. Rsch. Ctr., Frank White Bldg., Brisbane, Qld 4072 Australia; <sup>2</sup>Samancor Chromium, Simmons St., Johannesburg S. Africa; <sup>3</sup>BHPBilliton, Stainless Steel Matls., Neathouse Place, London SW1V 1BH England

The reduction smelting of nickel laterites produces slag, consisting principally of the chemical components MgO, "FeO", SiO<sub>2</sub>, and Al<sub>2</sub>O<sub>3</sub>, and ferro-nickel alloy. Despite the fact that the phase equilibria for the ternary MgO-"FeO"-SiO<sub>2</sub> up to 1500°C is well established limited experimental data are available in the MgO-"FeO"-SiO<sub>2</sub>-Al<sub>2</sub>O<sub>3</sub> system, which is relevant to commercial operation of the process. A methodology has been developed for the experimental investigation of the liquidus temperatures for the multi-component system MgO-"FeO" - SiO<sub>2</sub>-Al<sub>2</sub>O<sub>3</sub>-Cr<sub>2</sub>O<sub>3</sub> in equilibrium with metallic iron. Experiments have been carried out using high temperature equilibration, quenching, followed by electron probe X-ray microanalysis (EPMA). Liquidus temperatures have been determined in the silica primary phase field in the composition ranges directly relevant to the Cerro Matoso S.A. ferro-

nickel smelting slag. Liquidus isotherms have been determined for temperatures between 1450 to 1600°C. The study enables the liquidus to be described for a range of MgO/FeO ratios. It was found that liquidus temperatures in the silica primary phase field decrease significantly with the addition of  $Al_2O_3$ .

#### 3:30 PM

Dust Issues from Rotary Devices: Causes and Cures: Ronald K. Riddle<sup>1</sup>; <sup>1</sup>FFE Minerals, Pyro Tech. Grp., 3235 Schoenersville Rd., Bethlehem, PA 18016-0810 USA

The processing of lateritic ores in rotary drying and preheating/ pre-reduction systems has historically been plagued by problems associated with significant dust generation. These problems include handling issues, kiln capacity limitations, negative impacts on furnace stability, a reduction in nickel recovery and higher operating costs. The dust is formed in the rotary devices during heating and tumbling due to the following three mechanisms: (1) mechanical decrepitation during rapid vaporization of internal free and bound water, and the (3) loss of free moisture which functions as a binder. This paper investigates the causes of dust formation, provides methods to reduce dust carryover from the rotary devices, describes systems for the handling and transportation of dust, and finally offers methods to recover the dust in the existing pyrometallurgical process.

## 3:50 PM Break

## 4:00 PM

Nickel Ore Treatment in Rotary Kilns and Cyclone Reactors: Norbert Patzelt<sup>1</sup>; Thomas Schmitz<sup>1</sup>; Guido Grund<sup>1</sup>; <sup>1</sup>Polysius AG, Dept. Minerals, Graf-Galen-Strasse 17, Beckum D-59269 Germany

The demand for nickel is growing and will continue to do so for the foreseeable future. This will make the construction of new leaching and smelting plants necessary. This paper described a number of possible alternative processes. The first projects with new technology are currently undergoing trials and feasibility studies. Experience from other industrial sectors and from existing plants is being incorporated into these investigations. The question is, to what extent the old nickel producing concepts will continue to be applied in the future

## 4:20 PM

Developments in Integrated Furnace Controls to Enhance Furnace Operation and Crucible Integrity in Shielded-Arc Laterite Smelting: *Frank Allan Stober*<sup>1</sup>; Terry Gerritsen<sup>1</sup>; Jakob Janzen<sup>1</sup>; Andre Kepes<sup>1</sup>; <sup>1</sup>Hatch, Tech., 2800 Speakman Dr., Sheridan Sci. & Tech. Park, Mississauga, Ontario L5K 2R7 Canada

The paper describes the development of components in an Integrated Furnace Control system for shielded-arc smelting focusing on operation and crucible integrity enhancement. The paper reviews the mechanisms of power, feed and energy input and losses into the shieldedarc smelting process and describes the furnace control system module development and integration to tailor the process. The ultimate success of a furnace control system application is transfer of knowledge, training, and operational support during furnace start-up and ramp-up phases and model for how this has been achieved is discussed. The control modules of a shielded-arc laterite smelting furnace are described in detail including measured results and screen captures from application in laterite smelting furnaces. This paper focuses on developments in Integrated Furnace Controls tailored to shielded-arc laterite smelting but development of common furnace control modules for improved crucible and tapping operation integrity applied to other furnace processes including immersed-arc smelting are covered.

#### 4:40 PM

**Furnace Technology for Ferro-Nickel Production – An Update:** *N. Voermann*<sup>1</sup>; T. Gerritsen<sup>1</sup>; I. Candy<sup>1</sup>; F. Stober<sup>1</sup>; A. Matyas<sup>1</sup>; <sup>1</sup>HATCH, 2800 Speakman Dr., Mississauga, Ontario L5K 2R7 Canada

This paper describes developments in ferro-nickel furnace technology, specifically improvements to cooling methods, furnace controls, and high voltage furnace operating regime. The evolution of these technologies is briefly presented, as context for describing the current state of the art that has enabled ferro-nickel furnace operation at over 75 MW and specific energy consumption of less that 400 kWh/t dry ore. Examples from existing operations are used to illustrate present best practices, and potential future trends are discussed. The paper begins with an overview of the fundamental aspects of pyrometallurgical treatment of lateritic ores that drive ferro-nickel furnace design. Furnace wall cooling methods are related to the requirements resulting from specific furnace process conditions, including slag and metal compositions, as well as arc and bath power. The benefits of high productivity and low specific energy consumption resulting from high voltage (shielded-arc) operating practice are discussed, along with the furnace controls and electrical power train that enable such operation even with captive power generation. This paper is an update to that which the authors prepared for the Infacon X ferro-alloys conference.

## 5:00 PM

**SPLC - A Power Supply for Smelting Furnaces**: *Terry Gerritsen*<sup>1</sup>; Tom Ma<sup>1</sup>; Mohammed Sedighy<sup>1</sup>; Jakob Janzen<sup>1</sup>; Frank A. Stober<sup>1</sup>; Nils Voermann<sup>1</sup>; <sup>1</sup>Hatch Associates, 2800 Speakman Dr., Mississauga, Ontario L5K 2R7 Canada

Electrode control systems regulate power by physically positioning electrodes. Due to the size and weight of the electrodes, this is a slow process where power fluctuations of less than a few seconds are not fully corrected. Nickel laterite AC furnaces operating in high voltage, shielded arc mode typically incur frequent power variations of approximately +/- 20% around the power set point. To provide enhanced power control, Hatch has recently supplied, at commercial scale, a thyristor-switched reactance system called an SPLC. The SPLC incorporates predictive control software to operate furnaces at the maximum transformer rating by reducing the large power swings experienced without the SPLC. The resulting higher average power enables higher production, without increasing transformer or power plant capacity. A 60 MW production version of the SPLC has been commissioned on Falconbridge Dominicana's laterite nickel furnace, yielding excellent results with a 3 to 1 reduction in power fluctuations.

# Lead-Free Solders and Processing Issues Relevant to Microelectronic Packaging: Electromigration and Creep in Leadfree Solders

*Sponsored by:* Electronic, Magnetic & Photonic Materials Division, EMPMD-Electronic Packaging and Interconnection Materials Committee

Program Organizers: Laura J. Turbini, University of Toronto, Center for Microelectronic Assembly & Packaging, Toronto, ON M5S 3E4 Canada; Srinivas Chada, Jabil Circuit, Inc., FAR Lab/ Advanced Manufacturing Technology, St. Petersburg, FL 33716 USA; Sung K. Kang, IBM, T. J. Watson Research Center, Yorktown Heights, NY 10598 USA; Kwang-Lung Lin, National Cheng Kung University, Department of Materials Science and Engineering, Tainan 70101 Taiwan; Michael R. Notis, Lehigh University, Department of Materials Science and Engineering, Bethlehem, PA 18015 USA; Jin Yu, Korea Advanced Institute of Science and Technology, Center for Electronic Packaging Materials, Department of Materials Science & Engineering, Daejeon 305-701 Korea

Tuesday PM	Room: 27	19B
March 16, 2004	Location:	Charlotte Convention Center

*Session Chairs:* Jin Yu, Korea Advanced Institute of Science and Technology, Ctr. for Elect. Pkgg. Matls., Dept. of Matls. Sci. & Engrg., Daejeon 305-701 Korea; Paul T. Vianco, Sandia National Laboratories, MS0889, Albuquerque, NM 87185-0889 USA

#### 2:00 PM

**Creep of Pb-Free Solder Joints at Small Length Scales**: *Matthew Kerr*<sup>1</sup>; Nik Chawla<sup>1</sup>; Fay Hua<sup>2</sup>; <sup>1</sup>Arizona State University, Dept. of Chem. & Matls. Engrg., PO Box 876006, Tempe, AZ 85287-6006 USA; <sup>2</sup>Intel Corporation, Santa Clara, CA USA

The differences in the thermal expansion coefficient between components in an electronic package generate shear stresses in the solder. In particular, the behavior of the solder under creep conditions is quite important because of the long-term nature of the applied stress. The microstructure of bulk solder may be quite different from that of the solder sphere, because of differences in cooling rate that arise from the differences in surface-to-volume ratio. Thus, the correlation of bulk creep data to the creep behavior at smaller length scales may be misleading. In this talk, we report on the creep behavior of individual solder spheres. Sn-3.5wt% Ag solder spheres, 1 mm in diameter, were reflowed onto copper substrates to form lap shear specimens and creep tests were preformed. The specimens were tested over a temperatures range between 25 to 130°C. Microstructure of the joints upon reflow and the evolution of damage during creep were characterized. The stress exponents and activation energies for creep were determined, and these will be described in terms of the underlying mechanisms for creep deformation in these materials.

## 2:20 PM

Role of Grain Boundary Sliding in Creep of Pb-Free Solders: Felipe A. Ochoa<sup>1</sup>; Rajen Sidhu<sup>1</sup>; Xin Deng<sup>1</sup>; *Nikhilesh Chawla*<sup>1</sup>; <sup>1</sup>Arizona State University, Dept. of Chem. & Matls. Engrg., PO Box 876006, Tempe, AZ 85287-6006 USA

While the creep behavior of Pb-free solders has been studied extensively, there appears to be a lack of consensus on the underlying creep deformation mechanisms. Two major creep mechanisms have been proposed in the literature: (a) Thermally-induced climb of dislocations over fine intermetallic particles (such as Ag<sub>3</sub>Sn) and (b) grain boundary sliding (GBS). In this talk, we report on a systematic study on the role of GBS in creep of bulk Sn-3.5 wt% Ag solder alloys at 60°C and 120°C. The solder microstructure was varied by cooling at two different rates: 24°C/s (finer microstructure) and 0.08°C/s (coarser microstructure). Fiducial lines were inscribed on the solder surface and creep tests were interrupted to quantify the evolution of microstructure and strain due to GBS. The microstructure evolution due to creep deformation was characterized using atomic force microscopy (AFM) and scanning electron microscopy (SEM). Measurements of the transverse offset in the fiducial marks twere carried out and the strain due to GBS was quantified. It will be shown that, in general, the strain due to GBS is quite inhomogeneous and is a small fraction of the total creep strain (in the primary and steady-state creep regimes), although the contribution of GBS varies with temperature and microstructure.

## 2:40 PM Invited

The Compression Creep Behavior of Sn-Ag-0.6Cu Solder: *Paul T. Vianco*<sup>1</sup>; Jerome A. Rejent<sup>1</sup>; J. Mark Grazier<sup>1</sup>; <sup>1</sup>Sandia National Laboratories, PO Box 5800, MS0889, Albuquerque, NM 87185-0889 USA

Unified creep-plasticity models, which predict the reliability of Pbfree solder interconnections, incorporate time independent (stressstrain) and time dependent (creep) deformation in the constitutive equation. The creep behavior of the 95.5Sn-3.9Ag-0.6Cu (wt.%) solder was studied with the constant load compression technique. Samples were evaluated in the as-fabricated condition and following aging treatments for 24 hours at 125C or 150C. Test temperatures ranged from -25C to 160C and true stresses of 2 to 40 MPa. The steady-state strain rate kinetics were temperature dependent, indicating a fast diffusion process at T<75C and bulk diffusion process at T>75C. The stress magnitude caused only a subtle power law breakdown effect. The aging treatments impacted creep behavior, albeit, there was no noticeable change to solder microstructure. Sandia is a multi-program laboratory operated by Sandia Corporation, a Lockheed Martin Company, for the United States Department of Energy under Contract DE-AC04-94AL85000.

## 3:05 PM

Accelerated Thermal Fatigue of Lead-Free Solder Joints as a Function of Reflow Cooling Rate: Yan Qi<sup>1</sup>; Mike Agia<sup>2</sup>; Hamid Raza Ghorbani<sup>1</sup>; Polina Snugovsky<sup>3</sup>; Jan K. Spelt<sup>1</sup>; <sup>1</sup>University of Toronto, Mech. & Industrial Engrg., 5 King's College Rd., Toronto, ON M5S 3G8 Canada; <sup>2</sup>Digital Security Controls Ltd., 3301 Langstaff Rd., Concord, ON L4K 4L2 Canada; <sup>3</sup>Celestica, 20/429, 844 Kon Mills Rd., Toronto, ON M3C 1V7 Canada

The introduction of lead-free solders has focused the need to better understand their thermomechanical behavior. In this paper we examine lead-free solder joints reliability as a function of reflow cooling rate. The test vehicle was a Leadless Chip Resistor assembly, manufactured using both traditional SnPb and lead-free (Sn3.8Ag0.7Cu) solders. The lead-free LCR test vehicles were assembled using three different cooling rates. They were then exposed to an accelerated thermal cycling (ATC). The test results indicated that lead-free solder joints have better creep-fatigue performance compared with the SnPb solder joints while the lead-free LCR built with medium cooling rate showed the longest fatigue life. The number of cycles to failure was significantly correlated to the void defect rate and interface microstructures. Failure analyses were done using cross-sectioning methods and SEM.

## 3:25 PM

The Creep Properties of Sn Joints: *Ho Geon Song*<sup>1</sup>; John William Morris<sup>1</sup>; Fay Hua<sup>2</sup>; <sup>1</sup>University of California, Matls. Sci., One Cyclotron Rd., Bldg. 66R0200-8254, Berkeley, CA 94720 USA; <sup>2</sup>Intel Corp., Matls. Tech. Operation, 3065 Bowers Ave., Santa Clara, CA 95054 USA

Creep tests on solder joints of Sn-rich, Pb-free solders show anomalies in creep behavior at temperatures near room temperature. The anomalies include a strong temperature dependence of both the stress exponent and the apparent activation energy. The anomalies appear to have their source in the behavior of the Sn constituent itself. The microstructures of these solders are, primarily, Sn, and test joints of pure Sn show the same anomalies. The present paper discusses this anomalous behavior in terms of the creep behavior of pure Sn and the microstructures of the solder joints.

## 3:45 PM Break

## 3:55 PM Invited

The Effect of IMC Morphology on Cu Diffusion in Sn-Ag and Sn-Pb Solder Bump on Ni/Cu UBM: Chien Sheng Huang<sup>1</sup>; Guh Yaw Jang<sup>1</sup>; Jenq Gong Duh<sup>1</sup>; <sup>1</sup>National Tsing Hua University, Dept. of Matls. Sci. & Engrg., 101, Sect. 2 Kuang Fu Rd., Hsinchu 300 Taiwan

The eutectic Sn-Ag solder alloy is one of strong candidates to replace the conventional Sn-Pb solder. In this study, diffusion behaviors of Cu in eutectic Sn-Ag and Sn-Pb solder with Ni/Cu under bump metallization (UBM) were investigated with a joint assembly of solder/Ni/Cu/Ti/Si3N4/Si multiplayer structure. The atomic flux of Cu diffused through Ni was evaluated by detailed quantitative analysis in an electron probe microanalyzer. The atomic flux of Cu diffusion in the Sn-Pb system was rather larger than that in the Sn-Ag system. With regard to the amounts of Cu diffusion, they increased dramatically during reflow in the Sn-Pb system. However, they remained identical in the Sn-Ag case. The distinct diffusion behaviors between these two systems could be related to the microstructure evolution and grain size of intermetallic compound (IMC). The role played by the IMC in the Cu diffusion from the UBM toward the solder bump was probed and discussed.

#### 4:20 PM

Ultra Fast Cu Dissolution Induced by Electric Current in Flip Chip Solder Joints: C. M. Tsai<sup>1</sup>; Y. H. Lin<sup>1</sup>; Y. C. Hu<sup>1</sup>; Y. L. Lin<sup>1</sup>; C. Robert Kao<sup>1</sup>; <sup>1</sup>National Central University, Dept. of Chem. & Matls. Engrg., Chungli City 320 Taiwan

The effect of electric current on the failure mechanism of flip chip solder joints was studied. The solder used was Pb-Sn eutectic, and the joints had a diameter of 100 micron. The soldering pad on the chipside had a Cu metallurgy, and that on the board-side had an Au/Ni/Cu metallurgy. The flip chip packages were placed in an oven set at 100°C, with 2x10<sup>4</sup> A/cm<sup>2</sup> electric current passing through some of the joints in the packages. The rest of the solder joints, which were in the same package but without current passing through, were used as control. A new failure mode induced by the electric current was found. The joints failed by very extensive Cu dissolution on the chip-side. Not only part of the Cu soldering pad was dissolved, but also part of the internal Cu conducting trace within the chip. The dissolved region was back-filled with solder. Large amount of Cu<sub>6</sub>Sn<sub>5</sub> intermetallic was present inside the solder joint. The source of Cu in Cu<sub>6</sub>Sn<sub>5</sub> was from the dissolved Cu pad and trace. The site of failure was at the conducting trace that had been back-filled with solder, where a much greater current density was present due to a smaller cross-section.

## 4:40 PM

Behavior of Eutectic Sn-Zn, Sn-Ag and Sn-Pb Solders Under High Current Stressing Conditions: Jenn-Ming Song<sup>1</sup>; Dong-Yuan Tsai<sup>1</sup>; Truan-Sheng Lui<sup>1</sup>; Li-Hui Chen<sup>1</sup>; <sup>1</sup>National Cheng Kung University, Dept. of Matls. Sci. & Engrg., Tainan 701 Taiwan

Due to the trend of miniaturization and subsequent high interconnect density, solder joints may suffer a high density current. This study aims to explore the behavior of some two-phase eutectic solder alloys, Sn-Pb, Sn-Zn and Sn-Ag, under high current-stressing. Results show that when the current is raised constantly, there exists a critical current for the solder strip to break off. It can be also found that the critical current varies directly with the electrical conductivity. Sn-Zn with the lowest electrical resistance possesses a higher critical current to failure than Sn-Ag, and also higher than Sn-Pb. This is closely related to the microstructural characteristics.

## 5:00 PM

Electromigration Studies on Lead-Free Sn(Cu) and Sn(Ni) Solder Stripes: C. C. Wei<sup>1</sup>; C. Y. Liu<sup>1</sup>; <sup>1</sup>National Central University, Chem. Engrg. & Matls. Engrg., No. 300 Jung-Da Rd., Chung-Li Taiwan

Blech structure of Sn-based alloys stripes were fabricated by lithography method on Si substrate. The thickness of solder stripes were about 2 micrometers and the lengths of Sn alloys stripes are ranging from 50  $\mu$ m to 1 cm. Under the EM (Electromigration) tests with 104 A/cm2 current stressing, the voiding area and hillocks were observed at the cathode and anode side, respectively. Since EM rate could be determined by the depletion area at the cathode side, the important Cu and Ni alloying effects on EM rate were observed. Besides, our preliminary results imply that the length of solder stripe show no significant influence on the EM rate. The possible mechanism of alloying and length effects will be proposed and discussed in this talk. Also, we will report the effect of current gradient by using the so-called hang-over structure at the cathode side.

## 5:20 PM

**Electromigration on Electronic Components**: (Susan) Xiaoxin Xiao<sup>1</sup>; John W. Denning<sup>1</sup>; Richard Griese<sup>1</sup>; <sup>1</sup>Northrop Grumman Space Technology, Elect. Production Tech. Ctr., One Space Park, M573, R6/ 1587, Redondo Beach, CA 90287 USA

Electromigration induced short circuit was observed on a single four pin DC connector during electrical testing. Optical and scanning electron microscope (SEM) analyses exhibited surface contamination and dendritic growth between the connector pin and ground, which led to the electrical shortage and component failure. The conductors were soldered using Pb88Sn10Ag02 solder and no-clean flux. EDX analysis revealed that dendrites contained high Pb, O and C. It indicated that lead in the solder migrated and formed an electrical short from the connector pin to ground. The electromigration on the connector was probably related to the processing induced thermal stress. This stress can generate electrical potential and form electrical circuit, thus caused electromigration and mass transportation between the low and high stress concentration areas on the component. Temperature, stress distribution, chemical composition and microstructure of the electronic devices are main contributions to the electromigration. Moisture is known to be an accelerator. The mechanisms and effects of temperature, thermal stress and grain boundaries on electromigration are discussed in this paper.

#### 5:40 PM

Electromigration in SnAg3.8Cu0.7 Lead-Free Solder Thin Film Lines: *Ying Chao Hsu*<sup>1</sup>; Chih Chen<sup>1</sup>; <sup>1</sup>National Chao Tung University, Dept. of Matls. Sci. & Engrg., 1001 Ta Hsueh Rd., Hin Chu 300 Taiwan

A novel method for preparing thin film solder lines has been developed. Electromigration of lead-free SnAg3.8Cu0.7 solder thin film lines was studied under high current densities and various temperature. To measure the activation energy for electromigration, samples has been stressed at 50°C, 100°C, and 150°C. Electromigration rate is obtained by measuring the void volume near the cathode end. Effective charge numbers, Z\*, is also measured from the depletion near the cathode. By applying various current density from 1 x 104 A/cm2 to 1 x 105 A/cm2, threshold current density has been obtained.

# Magnesium Technology 2004: Primary Processing and Environmental Issues

Sponsored by: Light Metals Division, LMD-Magnesium Committee Program Organizer: Alan A. Luo, General Motors, Materials and Processes Laboratory, Warren, MI 48090-9055 USA

Tuesday PM	Room: 203B
March 16, 2004	Location: Charlotte Convention Center

Session Chairs: Howard Kaplan, US Magnesium LLC, Salt Lake City, UT 84116 USA; Ramaswami Neelameggham, US Magnesium LLC, Salt Lake City, UT 84116 USA

## 2:00 PM

A New Technique of Magnesium Electrolysis With Bischofite From Qinghai Salt Lakes in China: Huimin Lu<sup>1</sup>; Lanlan Yu<sup>1</sup>; Ruixin Ma<sup>1</sup>; Yitian Liang<sup>2</sup>; Bei Liang<sup>2</sup>; Youkun Yang<sup>2</sup>; <sup>1</sup>University of Science and Technology, Metall. Engrg. Sch., Light Metal Inst., 30 Xueyuan Rd., Beijing 100083 China; <sup>2</sup>Qinghai University, Non-Ferrous Metal Metallurgl. Rsch. Inst., 97 Ningzhang Rd., Xining, Qinghai 810016 China

Qinghai salt lakes in China have plenty of magnesium and potassium resources. Every year, Potassium fertilizer is produced with the by-product of bischofite. At present, bischofite cannot be used and is discarded. This cause not only the waste of resources, but also the formation of magnesium harm to the ecological environment. Therefore, comprehensive utilization of bischofite is emergent. This paper presents a combined process of comprehensive using bischofite: preparation of magnesia with ammonia and direct electrolysis of magnesia with the RECl3-MgCl2 system as support electrolyte. This process produces magnesium with the by-product of magnesia with 99.5% of purity, the current efficiency is 90%, the energy consumption is 11.5kWh/kg Mg and carbon dioxide is discharged on carbon anode. This new technique has low energy consumption, high current efficiency and less pollution for the environment. Experimental Observations on the Use of a Hydrogen Anode in the Production of Electrolytic Magnesium: Gus Van Weert<sup>1</sup>; Mazi Rejaee<sup>2</sup>; <sup>1</sup>ORETOME Limited, Caledon, ON Canada; <sup>2</sup>CELLMAG Inc., Montreal, QC Canada

Most electrolytic magnesium metal production utilizes a magnesium oxide feed material. One process route requires hydrochloric acid for feed dissolution, which in turn requires cleaning, drying, compression and combustion of the chlorine gas produced in the electrowinning process. An alternative route utilizes the chlorine in the anhydrous reduction of MgO to MgCl2. Either operation constitutes a significant part of the capital investment and operating cost of an electrolytic magnesium facility. This work explores the concept of producing hydrogen chloride gas on the anode in molten salt electrowinning of magnesium metal, which in addition to offering capital savings can also lower the cell voltage by one (1) Volt compared to chlorine gas evolution. The experimental cell used in the testwork is described and results are presented.

#### 2:40 PM

Production of Dense Rod from Magnesium Swarf for Re-Melting: Rimma Lapovok<sup>1</sup>; P. F. Thomson<sup>1</sup>; <sup>1</sup>Monash University, CAST CRC, SPME, Clayton, Vic, 3800, Melbourne Australia

This work was aimed on investigation of swarf compaction technique leading to increase recovery rate of Mg in re-melting due to eliminating melting loses at the surfaces and decrease hazards of transportation of swarf. The new method to enhances compaction to the density of bulk magnesium is developed, namely Equal Channel Angular Extrusion (ECAE) with back-pressure. It was found that ECAE promotes compaction very effectively. Parameters affecting the compaction process were investigated. This technique still has a disadvantage of high surface to volume ratio leading to melt losses, high oxide content and hazards during transportation. The role of grease and other contaminants, lubricants, oxide films and the need to remove them, were also considered. It was shown by re-melting experiments that recovery of magnesium increased significantly to 77% for swarf uncleaned from machining oil and to 92-96% for a cleaned swarf. The comparison with conventional technology of briquetting of swarf has been done. The briquetting technique allows to produce batches with density of 1.4-1.5 g/cm3 and has shown the recovery rate of 46 and 68% for cleaned and uncleaned swarf respectively.

#### 3:00 PM

Study of Electrolyte Impurities Effect on the Magnesium Oxides Speciation Techniques: Sina Kashani-Nejad<sup>1</sup>; Ka Wing Ng<sup>1</sup>; Ralph Harris<sup>1</sup>; <sup>1</sup>McGill University, Mining, Metals & Matls. Engrg., 3610 Univ. St., Wong Bldg., Montreal, Quebec H3A 2B2 Canada

Oxide containing compounds in the electrolytic magnesium production processes can be present either in the form of MgO or as "hydroxychlorides". The physical and chemical properties of MgO as an insoluble specie in the electrolyte are different from those of the soluble hydroxychlorides such that they have differing effects on the magnesium production process. As a result, oxide speciation techniques have been developed for process control and optimization. Industrial electrolytes also contain minor element impurities in the form of oxides, chlorides and fluorides as well as metallic particles. These impurities can interfere with the speciation measurements. In this work, different electrolyte impurities and their effect on currently available speciation techniques were studied. Also the distribution of the impurities based on their solubility in the electrolyte, is presented.

#### 3:20 PM

Qualitative Characterization of MgOHCl/MgO Mixture with Infrared Spectroscopy (IR): Sina Kashani-Nejad<sup>1</sup>; Ka Wing Ng<sup>1</sup>; Ralph Harris<sup>1</sup>; <sup>1</sup>McGill University, Mining, Metals & Matl. Engrg., 3610 Univ. St., Wong Bldg., Montreal, Quebec H2W 1S7 Canada

Oxide species are detrimental to the electrolytic magnesium production processes and severely lower the efficiency of electrolytic cells. These oxides are either in the form of MgO or Hydroxychlorides. As the result, it is possible to use infrared spectrometry for the characterization of hydroxyl ion bounded to the magnesium chloride in an isolated mixture of magnesium oxides. This paper describes an analytical procedure for the IR spectrometry of magnesium oxides. It was found essential to eliminate water interference by using methanol leaching prior to the IR analysis. It was also found that MgOHCl characteristic absorption peak is located at 3550 cm-1 and change in the composition and crystal structure of the hydroxychlorides shifts the characteristic hydroxyl absorption peak from 3550 cm-1 to 3720 cm-1.

## 3:40 PM Break

## 3:50 PM

The Environmental Impact of New Magnesium Alloys on the Transportation Industry: *Eli Aghion*<sup>1</sup>; Boris Bronfin<sup>1</sup>; Zeev Rubinovich<sup>1</sup>; <sup>1</sup>Dead Sea Magnesium Ltd., Rsch., POB 1195, Beer-Sheva 84111 Israel

The increased environmental demand from the transportation industry to reduce CO2 emissions by 30% till 2010 generated various actions aiming at addressing this demand. One of the most important solutions is weight reduction, which can be implemented by using light structural materials and Mg alloys particular. Currently the properties of the existing Mg alloys are limited. Many applications that require an adequate combination of cost competitiveness and properties such as increased creep, ductility and corrosion resistance are difficult to address. The present paper aims at evaluating the transportation's industry requirements in terms of combined properties and processing technologies. The major focus will be directed to new Mg alloys and the prospects that they may introduce. This will be related to casting and wrought magnesium alloys for practical applications such as engine blocks, gearbox housings, oil pumps, instrumental panels, thin wall body parts, seat frames and road wheels. Special attention will be given to the affordability of new alloys in terms cost of raw material and process technologies. The paper will also try to indentify the main stream of alloys development programs and their compatibility with the 21st century transportation requirements. This will relate to particular examples such as presented by electric cars and secondary structures and systems in aerospace applications.

## 4:10 PM Cancelled

Protective System for Magnesium Melt

#### 4:30 PM

A Comparison of the Greenhouse Impact of Magnesium Produced by Pidgeon and Electrolytic Processes: Subramania Ramakrishnan<sup>1</sup>; Paul Koltun<sup>1</sup>; <sup>1</sup>CSIRO, Mfg. & Infrastruct. Tech., Locked Bag No. 9, Preston, Vic 3072 Australia

The growing use of lightweight magnesium components in automobiles to reduce greenhouse emission requires a clear understanding of the life cycle greenhouse impact of producing magnesium. There are two practical methods for producing magnesium: (i) electrolysis of magnesium chloride; and (ii) reduction of magnesium oxide with ferrosilicon by a thermal process, known as the Pidgeon process. The Pidgeon process is used mainly in China, which now supplies approximately 40% of the world demand for magnesium. This paper compares the results of the life cycle greenhouse impact of the magnesium or magnesium alloy ingots produced by these two methods, by using realistic life cycle inventory data for the two routes. The paper considers the following two cradle-to-gate product systems: (i) Magnesite entering the system is processed using the Australian Magnesium process to deliver magnesium alloy ingots; and (ii) Dolomite ore is cacined and reduced in China using the Pidgeon process to produce metal ingots. The cradle-to-gate impacts of the ingots produced by the two product systems are estimated in terms of kg of carbon dioxide equivalent (kg CO2-e) for a product functional unit of 1 kg of magnesium alloy ingot. The study shows that the cradle-to-gate GHG impact of Chinese magnesium ingots is ~ 42 kg CO2-e/kg Mg ingot. This value is based on the current usage of sulphur powder for blanketing molten magnesium while casting. The GHG emission of the ingots produced by the Australian Magnesium process is approximately 24 kg CO2-e/kg of Mg ingot. The Australian Magnesium process is assumed to use HFC-134a as the cover gas, and electricity is generated using Australian black coal. The sensitivity of the results to the cover gas used for melt protection, and to the geographical location of alloying plants are discussed in the paper.

#### 4:50 PM

Collaborative Study of Protective Cover Gas Reaction Products: Scott Charles Bartos<sup>1</sup>; <sup>1</sup>U.S. Environmental Protection Agency, Climate Protection Partnerships Div., 1200 Penn. Ave. NW 6202J, Washington, DC 20460 USA

Historically, the magnesium industry has primarily used sulfur hexafluoride (SF6) as a cover gas to inhibit surface oxidation, which can result in fires if not controlled. Modern science has determined SF6 to be an extremely potent and long-lived greenhouse gas. The magnesium industry, working in cooperation with national governments, is making great strides towards implementing more environmentally friendly cover gases. Some of the cover gases identified are strong greenhouse gases themselves or the gas may generate potent global warming byproducts (e.g., PFCs) in a magnesium furnace environment. This measurement study builds upon EPA's previous investigation of SF6 cover gas reactions with molten magnesium to deter-

# Materials by Design: Atoms to Applications: Designing Nanostructures

Sponsored by: Electronic, Magnetic & Photonic Materials Division, EMPMD/SMD-Chemistry & Physics of Materials Committee

*Program Organizers:* Krishna Rajan, Rensselaer Polytechnic Institute, Department of Materials Science and Engineering, Troy, NY 12180-3590 USA; Krishnan K. Sankaran, The Boeing Company, Phantom Works, St. Louis, MO 63166-0516 USA

Tuesday PM	Room:	210B		
March 16, 2004	Location	: Charlo	tte Convention Cente	er

Session Chair: B. B. Rath, Naval Research Laboratory, Washington, DC USA

## 2:00 PM

Films, Lines and Dots: Dimensional Effects on the Strength of Nanoscale Structures: Krystyn J. Van Vliet<sup>1</sup>; Yoonjoon Choi<sup>1</sup>; Ju Li<sup>2</sup>; Subra Suresh<sup>1</sup>; <sup>1</sup>Massachusetts Institute of Technology, Matls. Sci. & Engrg., 77 Mass. Ave., Rm. 8-309, Cambridge, MA 02139 USA; <sup>2</sup>Ohio State University, Matls. Sci. & Engrg., Columbus, OH 12345 USA Whon the physical and microstructured dimension of alextrnin(

When the physical and microstructural dimensions of electronic/ photonic structures are reduced to the nanometer scale, feature dimensions approach those typical of atomistic deformation processes. Thus, there is considerable interest in whether and how the mechanical integrity of critical components will be affected in this length scale regime. Here, we employ systematic experiments and computations to investigate the effects of dimensional constraint on the elastic and yielding characteristics of metallic thin films, lines and dots. We find that the resistance to plastic deformation is a strong function of dimensional constraint in nanoscale structures, and that these effects are modeled most accurately by atomistic simulations. From this synthesis of experiments and computations in a model system, we develop criteria to predict the mechanical behavior of nanoscale structures in current applications.

#### 2:30 PM

Novel Nanostructured Materials by Design: Jagdish Narayan<sup>1</sup>; <sup>1</sup>North Carolina State University, Matls. Sci. & Engrg., Raleigh, NC 27695 USA

We have developed a novel method based upon pulsed laser deposition to produce nanocrystalline metal, semiconductor and magnetic material thin films and composites. The size of nanocrystals was controlled by interfacial energy, number of monolayers and substrate temperature. By incorporating a few monolayers of W during PLD, the grain size of copper nanocrystals was reduced from 160nm (Cu on Si (100)) to 4nm for a multilayer (Cu/W/Cu/W/Si (100)) thin film. The hardness increased with decreasing grain size up to a certain value (7nm in the case of copper) and then decreased below this value. While the former is consistent with Hall-Petch model, the latter involves a new model based upon grain boundary shear and deformation. We have used the same PLD approach to the form nanocrystalline metal (Ni, Co, Fe embedded in -Al2O3 and MgO) and semiconductor (Si, Ge, ZnO, GaN embedded in AlN and -Al2O3) thin films. These nanocrystalline composites exhibit novel magnetic properties and novel optoelectronic properties with quantum confinement of electrons, holes and excitons in semiconductors. We review advanced PLD processing, detailed characterization, structure property correlations and potential applications of these materials.

## 3:00 PM

Nanostructured Magnetic Materials: Mutsuhiro Shima<sup>1</sup>; <sup>1</sup>Rensselaer Polytechnic Institute, Dept. of Matls. Sci. & Engrg., Troy, NY 12180 USA

Finely structured magnetic materials attract a great deal of interest driven by emerging needs for nanotechnology applications.<sup>1</sup> Recently extensive efforts have been made to gain comprehensive and systematic understanding of synthesis-structure-property correlation in this class of materials, so that they can be predictably tailored as functional materials for specific applications. Knowledge available in the field until now clearly indicates that nanomagnets are useful for a range of applications including data storage and sensor devices as well as biomedical applications. Nanosized magnetic objects often exhibit a drastic change in the magnetic properties, depending on the fabrication process and geometric factors such as size, shapes<sup>2</sup> and interfaces<sup>3</sup> of the magnetic objects, where the thermal instability of magnetization becomes more significant.<sup>4</sup> In the finite size regime materials can exhibit multiple phases depending on the size. For instance, it is well known that iron exists in different allotropic forms, where at ambient conditions the most stable phase is ferromagnetic body-centered cubic a-Fe and the face centered cubic g-Fe is thermodynamically unstable and not ferromagnetic. We have found that iron catalyst nanoparticles trapped in carbon nanotubes form are indeed ferromagnetic g-Fe at room temperature. The unusual magnetic moment observed for g-Fe nanoparticles is explained by a lattice expansion due to insertion of carbon atoms into the interstitial sites. We have also recently demonsrated that magnetic nanoparticles can be grown onto sequenced peptide molecular nanotubes. Such a nano-scale magnetic structure can provide an excellent building block that permits engineering to design novel device architectures for future technological applications. In this paper our recent works on magnetic nanoparticles assembly with nanotubes will be presented. 1S. D. Bader, Surf. Sci. 500, 172 (2002). <sup>2</sup>M. Shima, M. Hwang and C. A. Ross, J. Appl. Phys. 93, 3440 (2003). <sup>3</sup>R. M. Bhatkal and K. Rajan, J. Electronic Mater. 23, 907 (1994). <sup>4</sup>X. Batlle and A. Labarta, J. Phys. D 35, R15 (2002).

3:30 PM Break

## 3:45 PM

Chemical Design of Inorganic Nanowires and Nanowire-Networks: *M. K. Sunkara*<sup>1</sup>; <sup>1</sup>University of Louisville, Dept. of Chem. Engrg., Louisville, KY 40292 USA

Inorganic nanowires and nanotubes, if available in large quantities, could enable bottom-up assembly of next generation devices, sensors, thin films, composites and systems. In addition, the availability of several types of materials in nanowire format will speed up our studies on the physical and chemical behavior of low-dimensional solids. The progress in the synthesis of nanowires has been rapid but requires further innovation to be useful. In this regard, our group has focused on developing new concepts for bulk synthesis of nanowires for a variety of systems, i.e., metals, elemental semiconductors, oxides and nitrides. For example, we illustrated that multiple nucleation and growth of one-dimensional structures could occur out of immiscible molten metals. In addition to bulk synthesis of nanowires, we illustrated the formation of nanowire networks (nanowebs) by coalescence of nanowires during growth parallel to substrate. We acknowledge National Science Foundation and US AFOSR for financial support.

## 4:15 PM

**First Principles Study of Spin Assisted Transport in Nanoscale Systems:** *Saroj Nayak*<sup>1</sup>; <sup>1</sup>Renneselaer Polytechnic Institute, Dept. of Physics, Troy, NY 12180-3590 USA

Electron transport through a single molecule attached to electrodes forms the core of molecular electronics. The coupling between a molecule and magnetic electrodes gives rise to new transport phenomena, such as spin-polarized electron transport. The use of an externally applied local magnetic field to obtain the anti-parallel spin alignment between two contacts separated by molecules of sub-nanometer length has been a daunting task and has hindered experimental investigation of spin transport behavior at the molecular level. Here, using parameter free first-principles density functional theory and the Landauer-Büttiker formalism, we study the spin-polarized transport in atomic and molecular wires. Quantum conductance calculations reveal that for the parallel alignment (ON) of spins at the opposite ends of the molecular wire, the conductance is significantly higher than that in the anti-parallel alignment (OFF). We also find, for the first time, that the ground state of such a system has the anti-parallel alignment suggesting that experiments could be performed in such a structure (with magnetic cluster contacts) where an external magnetic field would be needed only for the ferromagnetic alignment to turn from the OFF state to the ON state. This information will be critical to our understanding of the basic phenomena underlying the application of molecular systems to spintronics.

#### 4:45 PM Invited

Modeling of Composites with Self-Assembling Micro- and Nanostructures: Alexander L. Roytburd<sup>1</sup>; Julia Slutsker<sup>2</sup>; Andrei Artemev<sup>3</sup>; <sup>1</sup>University of Maryland, Matls. Sci. & Engrg., College Park, MD 20742 USA; <sup>2</sup>National Institute of Standards and Technology, MSEL, Gaithersburg, MD 20899 USA; <sup>3</sup>Carleton University, Mech. & Aeros. Engrg., Ottawa, ON Canada

The theory and phase-field modeling of formation and deformation of adaptive nano-composites containing polydomain martensitic layers are developed. It has been shown that superplastic and superelastic deformation of heterophase and polydomain martensite structures are reversible in the composites to the contrary to bulk shape memory materials. The stress-strain constitutive equations are obtained for an adaptive composite. By the engineering of constraint controlled polydomain structures can be designed and characteristics of the superelastic and superplastic deformation can be optimized. This work is supported by AFOSR.

# Materials Processing Fundamentals: Smelting and Refining

Sponsored by: Extraction & Processing Division, Materials Processing & Manufacturing Division, EPD-Process Fundamentals Committee, MPMD/EPD-Process Modeling Analysis & Control Committee

*Program Organizers:* Adam C. Powell, Massachusetts Institute of Technology, Department of Materials Science and Engineering, Cambridge, MA 02139-4307 USA; Princewill N. Anyalebechi, Grand Valley State University, L. V. Eberhard Center, Grand Rapids, MI 49504-6495 USA

Tuesday PM	Room: 2	212B	
March 16, 2004	Location:	Charlotte Convention Cente	r

Session Chair: TBA

## 2:30 PM

Method for Computation and Investigation of Thermal Performance of Flash Smelting Processes: V. M. Paretsky<sup>1</sup>; <sup>1</sup>State Research Center of Russian Federation, State Rsch. Inst. of Nonferrous Metals, 13, Acad. Korolyov St., 129515 Moscow Russia

A method has been developed for definition of mathematical threedimensional zonal models of heat exchange in autogenous smelting furnaces oxygen-flame furnace (KFP). The paper presents the results of studies into the thermal performance of an operating KFP-1 furnace at the Almalyk copper smelter in case of smelting of standardgrade concentrate and demonstrates the feasibility of the smelting process with burners located in the furnace roof without any furnace design modification. A full-scale KFP furnace with vertical arrangement of the flame has lining temperature lower by 110-175C as compared with a similar furnace with horizontal burners and a similar cooling system; the offgas temperature at the furnace outlet decreases also by 52C, while the temperatures of matte and slag at the furnace outlet virtually do not change. An analysis of the thermal efficiency of two design modifications of a planned KFP-2 furnace has been made for the second stage of the Almalyk copper smelter extension. Optimal cooling conditions for the furnace lining have been determined depending on the length of sulfide flame, feed charge supply rate and the heat generation by the feed charge.

#### 2:55 PM

**Distribution of Metals Between Highly Basic Slag and Nickel Matte in CaO-FeOx-FeS-Ni3S2 System**: V. M. Paretsky<sup>1</sup>; A. V. Tarasov<sup>1</sup>; S. D. Klushin<sup>1</sup>; <sup>1</sup>State Research Center of Russian Federation, State Rsch. Inst. of Nonferrous Metals, 13, Acad. Korolyov St., 129515 Moscow Russia

The experimental results demonstrated that, in the process of contacting of matte and ferrite-calcium slag, redistribution of nickel, cobalt, sulfur and iron between the phases took place and, at the same time, the number of phases changed. In tests with feed mattes containing from 15.0% to 57.9% Ni, the concentrations of non-ferrous metals in the bottom phase (sulfide-metal alloy) increased, while the iron and sulfur concentrations decreased. This fact was also confirmed by changes in the ferrite-calcium slag composition, i.e., increasing concentrations of sulfur and ferrous iron (along with a simultaneous decrease in the content of ferric iron). When converter matte (75.4% Ni) was used as feed sulfide material, then iron was transferred from slag to matte, probably. The new equilibrium state reached by the matte-slag system was to a substantial degree dependent on the oxidizing ability of the initial slag, i.e., the ratio of ferric to ferrous iron ions and the iron content in relation to the matte. The data obtained indicates that nickel losses can be reduced in the process of upgrading of matte with respect to non-ferrous metals by decreasing the degree of sulfidization (by increasing the metallization) of matte and by increasing the concentrations of calcium and aluminum oxides in the slag.

#### 3:20 PM

**Distribution of Metals Between Combined Slag and Nickel Converter Matte in CaO - FeOx - SiO2 - Ni3S2 System**: A. V. *Tarasov*<sup>1</sup>; S. D. Klushin<sup>1</sup>; V. M. Paretsky<sup>1</sup>; <sup>1</sup>State Research Center of Russian Federation, State Rsch. Inst. of Nonferrous Metals, 13, Acad. Korolyov St., 129515 Moscow Russia

When studying the compositions of the mattes produced and equilibrium slags it was found that in case of contacting of molten converter matte with iron-containing slag saturated with Fe2+ a new equilibrium state was established and the concentrations of nickel and sulfur in the sulfide melt decreased, while that in the slag increased. In slags in equilibrium with mattes containing 67.1-71.3% Ni and 0.08-0.15% Ñî the concentrations of nickel and cobalt were from 1.7% to 2.8% and from 0.03% to 0.06%, respectively. A change in the basicity (CaO / SiO2) of the slag had an effect on the concentrations of nonferrous metals in matte and slag, as well as on the distribution coefficients of /la/ / (la) and sulfur. High nickel and cobalt distribution coefficients were obtained when using slags containing over 16% CaO. Factors have been identified which permit control of the metals distribution (Ni and Co) between matte and slag in the FeOx - CaO - SiO2 -Ni3S2 system. By changing the degree of matte sulfidization and the basicity of slag, it is possible to transfer the bulk of cobalt into slag, minimizing thereby the loss of nickel.

## 3:45 PM

**Behavior of Zinc in Oxide-Sulfide Melts**: *A. V. Tarasov*<sup>1</sup>; <sup>1</sup>State Research Center of Russian Federation, State Rsch. Inst. of Nonferrous Metals, 13, Acad. Korolyov St., 129515 Moscow Russia

Studies into the effect of temperature (1200-1300C), oxygen content of the gaseous phase (50% to 70% by vol.) and the composition of the sulfide melt of Cu - Fe - Zn - S system (40% to 60% Cu and 3% to 8% Zn by weight) on the degree of transfer of zinc to oxide melt under conditions of complete desulfurization have been carried out using methods of integrated thermal analysis and chemical analysis of smelting products. It has been found that depending on the smelting conditions the degree of zinc transfer into oxide melt varies from 61% to 100%. Investigations of zinc sulfide behavior under a layer of slag containing magnetite have shown that zinc sulfide dissolved in the slag is oxidized by magnetite to form zinc oxide and sulfur dioxide. Zinc oxide is reduced by ferrous iron contained in the slag resulting in zinc vapor formation. The constant of zinc evaporation rate from the melt is virtually dependent on the smelting temperature. The experimental results obtained in the process of investigations have been used for selection of process conditions for pilot-scale tests of smelting of copper-zinc sulfide concentrates in molten bath.

## 4:10 PM Break

#### 4:20 PM

NiModel - A Thermodynamic Model and Computer Program of Nickel Smelting and Converting Processes: Pengfu Tan<sup>1</sup>; <sup>1</sup>Portovesme Nonferrous Metallurgy Company, S. P. n. 2 - Carbonia/ Portoscuso - km. 16.5, Portoscuso, CA I-09010 Italy

NiModel, a thermodynamic model, database and computer program, has been developed to predict the distribution behavior of Ni, Cu, Co, Fe, S, O, As, Sb and Bi, and heat balance in the nickel pyrometallurgical processes such as Outokumpu flash smelting, Outokumpu direct high-grade matte smelting, INCO flash smelting, and Peirce-Smith converting processes. In this model, as much as 16 elements (Ni, Cu, Co, Fe, As, Sb, Bi, S, O, Al, Ca, Mg, Si, N, C and H) are considered. The model predictions were compared with the known industrial data from Kalgoorlie Nickel Smelter in Australia, Outokumpu Harjavalta Nickel Smelter in Finland and INCO Metals Company in Canada, and an excellent agreement was obtained. In this paper, the applications of NiModel in the nickel pyro-metallurgical industries have been presented. NiModel has been used by Jinchuan Group Limited in China plant.

## 4:45 PM

**CuModel - A Thermodynamic Model of Copper Smelting and Converting Processes and its Applications in the Industry**: *Pengfu Tan*<sup>1</sup>; <sup>1</sup>Portovesme Nonferrous Metallurgical Company, S. P. n. 2 -Carbonia/Portoscuso - km. 16,5, Portoscuso, CA I-09010 Italy

A thermodynamic model, database and software, CuModel, has been developed to simulate the element distribution behaviors, and heat balance in copper smelting process, matte converting process and copper continuous smelting process. In this model, 21 elements (Cu, S, Fe, Ni, Co, Sn, As, Sb, Bi, Pb, Zn, Au, Ag, O, N, C, H, Ca, Mg, Al and Si) are considered. It can be predicted for any set of controllable process parameters such as feed composition, smelting temperature, degree of oxygen enrichment and volume of oxygen enriched air. This model accounts for physical entrainment in the melts. The predictions by the present computer model are compared with the known commercial data from several companies, good agreements are obtained. The model has been used to optimize the actual industrial operating condi-

tions of flash furnace at Guixi Smelter in China and PASAR in Philippines, and Noranda furnace at Daiye Smelter in China.

### 5:10 PM

Comparison of Two Control Strategies of the Vanadium Roast Process: Bernhard Voglauer<sup>1</sup>; Wolfgang Geyrhofer<sup>1</sup>; Hanns Peter Jörgl<sup>1</sup>; <sup>1</sup>Vienna University of Technology, Inst. for Machine & Proc. Automation, Gusshausstraße 27-29, E 328, Vienna 1040 Austria

A well known routine for the production of vanadium is alkaline roasting of steel slag in a multiple hearth furnace or rotary kiln. Previous work concerning this process was carried out by the authors and contains the design of a dynamic model capable of calculating mass flow, temperature and concentrations of major components in a multiple hearth furnace, an empirically obtained model of the chemical reaction kinetics and a controller design mainly based on operational knowledge of an industry scale plant. The current work compares the performance of a model based control system to the previously published knowledge based control system. The knowledge based control system represents a robust system due to the implementation of expert knowledge gained in many years of manual control. The comparison shall show expected advances of process efficiency by the use of advanced control strategies.

# Nanostructured Magnetic Materials: Self Assembly and Patterned Nanostructures

Sponsored by: Electronic, Magnetic & Photonic Materials Division, EMPMD-Superconducting and Magnetic Materials Committee, EMPMD-Nanomaterials Committee *Program Organizers:* Ashutosh Tiwari, North Carolina State University, Department of Materials Science & Engineering, Raleigh, NC 27695-7916 USA; Rasmi R. Das, University of Wisconsin, Applied Superconductivity Center, Materials Science and Engineering Department, Madison, WI 53706-1609 USA; Ramamoorthy Ramesh, University of Maryland, Department of Materials and Nuclear Engineering, College Park, MD 20742 USA

Tuesday PMRoom: 215March 16, 2004Location: Charlotte Convention Center

Session Chair: TBA

## 2:00 PM Invited

Novel Nanostructured Magnetic Materials: J. Narayan<sup>1</sup>; A. Tiwari<sup>1</sup>; H. Zhou<sup>1</sup>; <sup>1</sup>North Carolina State University, Dept. of Matls. Sci. & Engrg., Raleigh, NC 27695-7916 USA

We synthesized novel nanostructured materials using a self-assembly processing in a controlled way. The orientation and size of nanoparticles were controlled by providing a template for epitaxial growth and controlling the flux of depositing species. The structures were characterized with a resolution of 0.16 nm using STEM-Z contrast imaging for atomic structure, chemical composition and bonding characteristics. The primary goal was to establish correlation of these parameters with magnetic properties. Modeling of magnetic properties was found to be consistent with experimental observations. Role of the strain in the fabrication of novel magnetic structures will be discussed.

## 2:30 PM Invited

**2D and 3D Arrays of Magnetic Nanoparticles**: Sara Majetich<sup>1</sup>; <sup>1</sup>Carnegie Mellon University, Physics Dept., 5000 Forbes Ave., Pittsburgh, PA 15213-3890 USA

Self-assembled arrays of monodisperse Fe nanoparticles are ideal for studying magnetic interaction effects. Here the arrays are formed from surfactant-coated monodisperse iron nanoparticles. These particles are up to 9 nm in diameter and have specific magnetizations over 170 emu/g. The strength and nature of the magnetic coupling can be adjusted by varying the particle size and interparticle spacing, and by altering the self-assembly conditions to form monolayers, multilayers, or three-dimensional nanoparticle crystals. As the particle interactions are increased, the zero field cooled (ZFC) magnetization curve broadens, indicating a range of magnetic environments. The coercivity and remanence increase somewhat, and magnetic relaxation is slower. The existence of magnetic domains is suggested by small angle neutron scattering. 3D nanoparticle crystals have large structural coherence lengths in all directions. Their ZFC magnetization curve is nearly flat, and they have faster magnetic relaxation than the 2D arrays.

#### 3:00 PM Invited

Self-Assembled Epitaxial Magnetic Nanostructures Via MBE Growth: Dongqi Li<sup>1</sup>; <sup>1</sup>Argonne National Laboratory, Matls. Sci. Div., Bldg. 223, Argonne, IL 60439 USA

We have fabricated self-assembled magnetic nanostructures with molecular beam epitaxy (MBE) on single-crystal substrates. For example, epitaxial Co dots, antidots, and dot-chains, each dot ~100nm wide and several nm thick, were grown on flat and patterned Ru(0001) as driven by strain and diffusion during epitaxial growth. Fe nanowires (1 atomic layer thick, several nm wide) were grown along the step edges of vicinal Pd(110) via step-flow growth mode. The high degree of crystalline ordering of these structures allows us to observe intrinsic new magnetic properties due to confinement, which are understood with micromagnetic modeling and in terms of low dimensional physics in general, such as 2D-to-1D finite size scaling and 1D Ising chains. Work supported by the US DOE BES-Materials Sciences under contract # W-31-109-ENG-38.

## 3:30 PM Invited

Synthesis and Characterization of Self-Assembled Magnetic Nanoparticles: D. Kumar<sup>1</sup>; <sup>1</sup>North Carolina A&T State University, Dept. of Mech. & Chem. Engrg., Greensboro, NC 27411 USA

A novel thin film processing method is reported based on pulsed laser deposition to process nanocrystalline materials with accurate size and interface control with improved magnetic properties. Using this method, single domain nanocrystalline Fe and Ni particles in the 5-10 nm size range embedded in amorphous alumina as well as in crystalline TiN have been produced. By controlling the size distribution in confined layers, it was possible to tune the magnetic properties from superparamagnetic to ferromagnetic behavior. Magnetic hysteresis characteristics below the blocking temperature are consistent with single-domain behavior. The paper also presents our results from investigations in which scanning transmission electron microscopy with atomic number contrast (STEM-Z) and electron energy loss spectroscopy (EELS) were used to understand the atomic structure of Ni nanoparticles and interface between the nanoparticles and the surrounding matrices. It was interesting to learn from EELS measurements at interfaces of individual grains that Ni in alumina matrix does not from an ionic bond indicating the absence of metal-oxygen bond at the interface. The absence of metal-oxygen bond, in turn, suggests the absence of any dead layer on Ni nanoparticles even in an oxide matrix.

## 4:00 PM Invited

Magnetic Nanostructures from Diblock Copolymer Templates: Mark T. Tuominen<sup>1</sup>; <sup>1</sup>University of Massachusetts, Physics Dept., 411 Hasbrouck Lab, Amherst, MA 01003 USA

Many future applications of magnetic technology require nanoscale magnetic elements configured into system architectures that provide useful functionalities. This talk will focus on highly dense arrays of magnetic and superconducting nanoscale elements made by new integrated nanofabrication techniques that utilize the guided microphase separation of diblock copolymers together with electrochemical deposition. First the magnetization properties of cobalt and permalloy nanowire arrays will be discussed as a model patterned magnetic system. We analyze the behavior these arrays with regards to magnetocrystalline anisotropy, shape anisotropy, and magnetostatic interactions. Secondly research will be presented on integrated magnetotransport nanowire devices in lateral and vertical transport geometries. Fabrication is achieved by combining nanoporous polymer templates with electron beam lithography. Measurements include spin-dependent electron transport GMR and AMR behavior, and Andreev-coupled superconducting behavior in nanoscale device geometries. This work is supported by NSF grants DMI-0103024, DMR-0071756, and MRSEC.

#### 4:30 PM Invited

Metastable Cation Distribution in Nano-Size Mn-Zn Ferrites: Naresh C. Mishra<sup>1</sup>; Chandana Rath<sup>1</sup>; S. Anand<sup>2</sup>; R. P. Das<sup>2</sup>; C. Upadhaya<sup>3</sup>; H. C. Verma<sup>3</sup>; <sup>1</sup>Utkal University, Physics Dept., Bhubaneswar, Orissa India; <sup>2</sup>Regional Research Laboratory, Bhubaneswar, Orissa India; <sup>3</sup>Indian Institute of Technology, Physics Dept., Kanpur, UP 208016 India

 $Mn_{1,x}Zn_xFe_2O_4$  (x = 0 to 1) nanosize particles prepared through hydrothermal route has been studied by X-ray diffraction, magnetization measurements, Mossbauer spectroscopy, transmission electron microscopy and differential scanning calorimetry. The particle size was found to decrease from 13 to 4 nanometers with increasing Zn concentration from 0 to 1. The chemical composition is thus shown to influence the physical size of the nanoparticles. The as prepared samples are largely ferrimagnetic with ferri- to paramagnetic transition temperature increasing from 175C to 500C with decreasing Zn content. These Curie temperatures were much higher than the corresponding bulk values. At compositions within x = 0.35 and 0.5, the temperature dependence of the magnetization exhibits a cusp like behavior below the Curie temperature. The cusps irreversibly disappear on annealing at 550C, which indicate a redistribution of cations from a metastable state to a stabler state. The cationic redistribution occurs between the two chemically inequivalent sites in the cubic lattice of the ferrite. In contrast to general expectations, annealing of the nanoparticles is shown to convert the ferrimagnetic particles to superparamagnetic ones. Such a conversion is shown to be a consequence of the cation redistribution also.

## 5:00 PM

Self Assembled Magnetic Nanomaterials: Mircea Chipara<sup>1</sup>; Jagannathan Sankar<sup>2</sup>; Septimiu Balascuta<sup>1</sup>; <sup>1</sup>Indiana University, Cyclotron Facility, 2401 Milo B Sampson Ln., Bloomington, IN 47403 USA; <sup>2</sup>North Carolina A&T State University, Dept. of Mech. Engrg., Greensboro, NC 27411 USA

Barium ferrite (BaFe) magnetic nanoparticles have been obtained by energetic mechanical milling. The average size of magnetic nanoparticles was estimated from the line width of Wide Angle X Ray Scattering spectra. The nanoparticles have been introduced into dilute solutions of polystyrene-polyisoprene-polystyrene copolymer (SIS) and sonicated for 50 hours at room temperature. Thin films of BaFe-SIS have been obtained by spin coating the solution onto Si substrates. The solvent has been removed by heating the samples in vacuum at 50C for 24 hours. The magnetic features of the films were investigated by SQUID, in the temperature range 4 K to 300 K, and by ferromagnetic resonance spectroscopy (X Band). The angular dependence of ferromagnetic spectra is consistent with an anisotropic distribution of magnetic nanoparticles. Atomic Force Microscopy investigations revealed that the introduction of a small amount of magnetic nanoparticles into SIS is not disturbing its self-assembled structure.

# Nanostructured Materials for Biomedical Applications: Session IV

Sponsored by: Electronic, Magnetic & Photonic Materials Division, EMPMD-Thin Films & Interfaces Committee *Program Organizers:* Roger J. Narayan, Georgia Tech, School of Materials Science and Engineering, Atlanta, GA 30332-0245 USA; J. Michael Rigsbee, North Carolina State University, Department of Materials Science and Engineering, Raleigh, NC 27695-7907 USA; Xinghang Zhang, Los Alamos National Laboratory, Los Alamos, NM 87545 USA

Tuesday PM	Room: 2	219A
March 16, 2004	Location:	Charlotte Convention Center

Session Chairs: Mehmet Sarikaya, University of Washington, Matls. Scis. & Engrg., Seattle, WA 98195 USA; Kenneth H. Sandhage, Georgia Institute of Technology, Sch. of Matls. Scis. & Engrg., Atlanta, GA 30332-0245 USA

## 2:00 PM Invited

Orthopaedic Implants and Biomaterials - Clinical Problems and the Development of Current Implants: William G. Ward<sup>1</sup>; <sup>1</sup>Wake Forest University School of Medicine, Med. Ctr. Blvd., Winston-Salem, NC 27157 USA

Orthopaedic uses of metals and biomaterials have expanded greatly over the past few decades, especially in the internal fixation of fractures and in joint replacement. The materials utilized for internal fixation of fractures have evolved from stainless steel implants into the super alloys of titanium and other materials. The greatest developments however, have been in the materials used for total joint replacements (arthroplasty). The problems of frictional wear and the biologic response to the wear-generated debris have led to an evolution of bearing surface materials. Chrome cobalt bearing surfaces articulating with ultra high molecular weight polyethylene have been utilized for approximately forty years. However, late loosening of such implants due to wear debris-induced osteolysis has led to the development of newer articulations, including metal on metal, ceramic on metal, ceramic on polyethylene and ceramic on ceramic. These developments and the associated products will be demonstrated, along with clinical examples.

#### 2:45 PM Invited

Nanostructured Ti-Base Alloys for Biomedical Applications: Guo He<sup>1</sup>; Satoshi Emura<sup>1</sup>; Masuo Hagiwara<sup>1</sup>; <sup>1</sup>National Institute for Materials Science, Light Matls. Grp., 1-2-1 Sengen, Tsukuba, Ibaraki 305-0047 Japan

Ti-base alloys for biomedical applications have received much attention due to their excellent biocompatibility, low density, excellent corrosion resistance and good balance of mechanical properties. However, some problems are difficult to solve. For example, the Young's modulus of the available biomedicine-used Ti-base alloys is too high compared to that of bone. This is harmful for bone healing and remodeling. When attempts were made to reduce the Young's modulus, the strength was also severe degraded. Recently, we found that the nanostructured Ti-base alloys exhibit very low elastic modulus and very high strength. This just meets the demands of the biomaterials. By delicate composition design we can directly obtain bulk nanostructured Ti-base alloys. Using in situ composite techniques, we can overcome the shortcomings of low ductility of the nanostructured metallic materials and achieve the high performance of the Ti-base alloys for the biomedical applications.

## 3:30 PM Invited

Nanostructured Titanium Oxide Based Surface for Enhanced Bone Growth: Sungho Jin<sup>1</sup>; Brian Oh<sup>1</sup>; <sup>1</sup>University of California, Dept. of Mech. & Aeros. Engrg., 9500 Gilman Dr., La Jolla, CA 92093-0411 USA

Titanium and its alloys are widely utilized in orthopedic and dental implants by virtue of their load-bearing capability, light weight and bio-compatibility. As Ti can not directly bond to bone, the addition of bio-active surface coatings are desirable. The anatase phase of titanium oxide is known to promote the formation of hydroxyapatite and bone growth. We have studied the dependence of anatase vs rutile phase formation on microstructural and processing parameters in titanium oxide coating, and evaluated the effect of nano- vs micro-scale dimensional and morphological control on hydroxyapatite and bone growth. Various processing techniques including anodic oxidation have been employed to produce a variety of shapes and sizes of nano features, and their behavior and properties have been compared.

## 4:15 PM Invited

Plasma-Sprayed ZrO2 Bond Coat as an Intermediate Layer for Porcelain Veneered on Commercially Pure Titanium: *Tsung-Nan Lo*<sup>1</sup>; Truan-Sheng Lui<sup>1</sup>; Tai-Nan Lin<sup>2</sup>; <sup>1</sup>National Cheng Kung University, Dept. Matls. Sci. & Engrg., No. 1, Univ. Rd., Tainan 701 Taiwan; <sup>2</sup>National Taiwan Ocean University, Inst. of Matls. Engrg., No. 2, Pei-Ning Rd., Keelung 202 Taiwan

This investigation was to study the strength of the ZrO<sub>2</sub> bond coat introduced as an intermediate layer between porcelain and titanium. Four-point bending test was used to measure the bond strength of single-layer porcelain coating and two-layer porcelain/ZrO<sub>2</sub> coating on titanium. Experimental results indicate that an improved bond strength of porcelain/ZrO<sub>2</sub> composite coating on titanium was found. The bond strength increases from 23.0+-2.1 Mpa of porcelain coating to 35.8+-5.7 Mpa of porcelain/ZrO<sub>2</sub> composite coating. The fracture regions between the ceramic coatings and titanium were analyzed by using scanning electron microscopy (SEM) and thin-film X-ray diffraction techniques. Elemental diffusion was found at porcelain/ZrO<sub>2</sub> interface. It promotes the chemical bonding between porcelain/ZrO2 interface to strengthen the bonding of porcelain veneered on titanium. The surface roughness of the plasma-sprayed ZrO<sub>2</sub> coating were investigated by surfcoder. It also indicated that the ZrO<sub>2</sub> bond coat provided rougher surface morphology to aid in the bonding for porcelain veneered on titanium.

# Phase Stability, Phase Transformation, and Reactive Phase Formation in Electronic Materials III: Session IV

Sponsored by: Electronic, Magnetic & Photonic Materials Division, Structural Materials Division, EMPMD/SMD-Alloy Phases Committee

*Program Organizers:* C. Robert Kao, National Central University, Department of Chemical and Materials Engineering, Chungli City 32054 Taiwan; Sinn-Wen Chen, National Tsing-Hua University, Department of Chemical Engineering, Hsinchu 300 Taiwan; Hyuck Mo Lee, Korea Advanced Institute of Science & Technology, Department of Materials Science & Engineering, Taejon 305-701 Korea; Suzanne E. Mohney, Pennsylvania State University, Department of Materials Science & Engineering, University Park, PA 16802 USA; Michael R. Notis, Lehigh University, Department of Materials Science and Engineering, Bethlehem, PA 18015 USA; Douglas J. Swenson, Michigan Technological University, Department of Materials Science & Engineering, Houghton, MI 49931 USA

Tuesday PMRoom: 214March 16, 2004Location: Charlotte Convention Center

*Session Chairs:* John H.L. Pang, Nanyang Technological University, Sch. of Mech. & Production Engrg., Singapore 639798 Singapore; Paul T. Vianco, Sandia National Laboratories, Albuquerque, NM 87185-0889 USA

## 2:00 PM Invited

Interfacial Reactions Between Sn-Ag-0.6Cu Solder and Silver (Ag) Substrates: *Paul T. Vianco*<sup>1</sup>; Joseph J. Martin<sup>1</sup>; Robert D. Wright<sup>2</sup>; <sup>1</sup>Sandia National Laboratories, PO Box 5800, MS0889, Albuquerque, NM 87185-0889 USA; <sup>2</sup>Sandia National Laboratories, PO Box 5800, MS 0886, Albuquerque, NM 87185-0886 USA

Silver (Ag) is an important surface finish in electronic packaging, more so with the advent of immersion Ag coatings for the conductive features on printed circuit boards. A study was performed which examined the physical metallurgy and rate kinetics of reactions between the 95.5Sn-3.9Ag-0.6Cu (wt.%) solder and Ag. The first task examined the consumption rate and intermetallic compound layer growth between molten Sn-Ag-0.6Cu solder and Ag under temperatures of 240 to 350C and time periods of 5 to 240 s. The second task investigated the solid-state intermetallic compound layer development between the Pb-free solder and Ag under aging temperatures of 55 to 205C and time periods of 1 to 400 days. Concurrent experiments were performed with 63Sn-37Pb solder to provide baseline data. Sandia is a multiprogram laboratory operated by Sandia Corporation, a Lockheed Martin Company, for the United States Department of Energy under Contract DE-AC04-94AL85000.

## 2:20 PM Invited

IMC Formation on BGA Package with Sn-Ag-Cu and Sn-Ag-Cu-Ni-Ge Solder Balls: *Kwang-Lung Lin*<sup>1</sup>; Po-Cheng Shih<sup>1</sup>; <sup>1</sup>National Cheng Kung University, Matls. Sci. & Engrg., 1 Ta-Hsuey Rd., Tainan, Taiwan 701 China

The BGA substrate with Cu/Ni-P/Au metallization was attached with solder balls. The compositions of the solder ball are Sn-3.2Ag-0.5Cu and Sn-3.0Ag-0.5Cu-0.07Ni-0.01Ge. The package was subjected to thermal aging at 240°C from 100 to 1000 hours for investigating the IMC formation behavior. Cross section of IMC layer as well as top view, revealed by etching off the uncreated solder, was inspected and analyzed with SEM and EDX. The IMC mainly consists of two types of morphology, hexagonal and whisker. The hexagonal crystal was identified to be (Cu, Ni)6Sn5 and the whisker crystal is (Ni, Cu)3Sn4. The dissolution of Ni in the Cu6Sn5 compound results in a synergistic effect on enhancing the growth of the compound, while similar effect was not observed for the dissolved Cu in Ni3Sn4 compound. This phenomenon was explained through the vacant energy band of the 3dorbital of Ni. Ag3Sn compound was also detected in the solder region near the interfacial IMC. The Ag3Sn compound was not in direct contact with BGA substrate.

## 2:40 PM Invited

Differences in Formation and Growth of Interface Between Sn-Ag and Sn-Ag-Cu Lead-Free Solder with Ni-P/Au Plating: *Chi-Won Hwang*<sup>1</sup>; Katsuaki Suganuma<sup>1</sup>; Masayuki Kiso<sup>2</sup>; Shigeo Hashimoto<sup>2</sup>; <sup>1</sup>ISIR, Osaka University, Mihogaoka 8-1, Ibaraki, Osaka 567-0047 Japan; <sup>2</sup>C. Uyemura & Co., Ltd., Deguchi 1-5-1, Hirakata, Osaka 573-0065 Japan

The formation and growth mechanism of the interfaces of Sn-Ag(-Cu) lead-free solder with Au/Ni-6wt%P plating were studied. During the soldering at 230°C, Au dissolved into molten solder, and double reaction layers of  $Ni_3Sn_4/Ni_3SnP$  formed between Sn-3.5Ag solder and Ni-6P. P content increases in the surface region of the Ni-6P layer due to the depletion of Ni diffused into molten solder, resulting in the formation of Ni\_3P+Ni layer. For Sn-3.5Ag-0.7Cu solder, an (Ni,Cu)\_3Sn\_2 single layer, containing Cu of about 50 at%, formed as a reaction layer. With increasing of reaction time, both interface of Sn-Ag and Sn-Ag-Cu reaction systems repeatedly undergo thickening and thinning in their thickness, while the mechanisms are different. This fluctuation of the reaction layer thickness affects joint strength, which also exhibits repeated strengthening and degrading.

## 3:00 PM

Interfacial Reactions and Shear Strengths Between Sn-Ag Based Pb-Free Solder Balls and Au/EN/Cu Metallization: Sang-Won Kim<sup>1</sup>; Jeong-Won Yoon<sup>1</sup>; Seung-Boo Jung<sup>1</sup>; <sup>1</sup>Sungkyunkwan University, Dept. of Advd. Matls. Engrg., 300 Chunchun-dong, Changangu, Suwon, Kyounggi-do 440-746 Korea

Several Sn-Ag system Pb-free solders have been identified to replace Sn-Pb eutectic solder in reflow process applications. Also, electroless Ni-P (EN) has been adopted and used as a diffusion barrier in the under-bump metallurgy (UBM) for flip-chip application. In this study, the alloy compositions of solder balls included Sn-3.5Ag, Sn-3.5Ag-0.75Cu, and Sn-3Ag-6Bi-2In. And, the solder ball pads were a copper substrate with an Au/electroless Ni-P surface finish. The formation and growth of the intermetallic phases at the solder joints were investigated. Also, ball shear strength was measured to investigate the effect of the microstructures and interfacial reactions on the reliability of solder bumps.

## 3:15 PM

Multi-Component Base Metal Dissolution and Inter-Metallic Compound Formation in Porous Noble Metal Thick Films: Kenneth L. Erickson<sup>2</sup>; Polly L. Hopkins<sup>2</sup>; Paul T. Vianco<sup>1</sup>; Joseph J. Martin<sup>1</sup>; Gary A. Zender<sup>3</sup>; <sup>1</sup>Sandia National Laboratories, PO Box 5800, MS0889, Albuquerque, NM 87185-0889 USA; <sup>2</sup>Sandia National Laboratories, PO Box 5800, MS 0834, Albuquerque, NM 87185-0834 USA; <sup>3</sup>Sandia National Laboratories, PO Box 5800, MS0886, Albuquerque, NM 87185-0886 USA

Previous studies showed that preferential dissolution of base metal constituents influenced short-term, base metal erosion and long-term inter-metallic compound (IMC) growth. Experiments with 76Au-21Pt-3Pd (wt%) alloy sheet and molten 63Sn-37Pb (wt.) solder indicated that preferential Au dissolution produced Pt-rich IMC layers that caused induction periods during subsequent IMC growth. Induction periods were a significant concern in previous work to develop models for IMC growth in 76Au-21Pt-3Pd porous thick films contacted with 63Sn-37Pb solder. Results are described which come from recent experiments which examined dissolution and simultaneous IMC growth in 76Au-21Pt-3Pd porous thick films contacted with 63Sn-37Pb solder. The analysis uses a previously reported model for multi-component dissolution and IMC growth based upon diffusion coefficients derived from Sn-Pb couples with 76Au-21Pt-3Pd alloy sheet. Sandia is a multiprogram laboratory operated by Sandia Corporation, a Lockheed Martin Company, for the United States Department of Energy under Contract DE-AC04-94AL85000.

## 3:30 PM

The Effect of Gold Thickness on Solder/UBM Interfacial Reaction in Flip Chip Package: Y. L. Lin<sup>1</sup>; C. M. Tsai<sup>1</sup>; Y. C. Hu<sup>1</sup>; Y. H. Lin<sup>1</sup>; C. Robert Kao<sup>1</sup>; <sup>1</sup>National Central University, Dept. of Chem. & Matls. Engrg., Chungli City 320 Taiwan

Flip-chip technology provides a solution for smaller, thinner, and more powerful IC package. As the package size continues to shrink, the bump size becomes smaller as well. Consequently, the effect of gold thickness of Ni/Au surface finish will become more important. In this research, the effect of gold thickness of Ni/Au surface finish during long-term thermal aging in flip chip package was studied. The solder used was eutectic lead-tin. The under bump metallization (UBM) on the chip side was Cu/Ni(V)/Al, and the surface finish on the substrate side was Ni/Au. Two different gold thickness, 0.045 im and 0.85im, were used. After thermal aging, the results showed that thick gold caused the formation of  $(Au_xNi_{1-x})Sn_4$  compounds at the interface, and had a higher Ni consumption rate.

## 3:45 PM Break

## 4:00 PM Invited

Intermetallic Growth Studies on Sn-Ag-Cu Lead-Free Solder Joints: John H.L. Pang<sup>1</sup>; X. Q. Shi<sup>2</sup>; W. Zhou<sup>1</sup>; S. L. Ngoh<sup>1</sup>; <sup>1</sup>Nanyang Technological University, Sch. of Mech. & Production Engrg., 50 Nanyang Ave., Singapore 639798 Singapore; <sup>2</sup>Singapore Institute of Manufacturing Technology, Joining Tech. Grp., 71 Nanyang Dr., Singapore 638075 Singapore

Intermetallic growth studies on 95.8Sn-3.5Ag-0.7Cu lead-free solder joint subjected to iso-thermal aging exposure will be presented. The motivation for this study is to characterize the solid-state diffusion mechanism for intermetallic growth behavior with respect to isothermal aging test parameters of temperature and time. Solder joint reliability qualification process often employ accelerated temperature cycling tests where the temperature profile effects of cycle time, ramp rate and dwell time are important parameters. Intermetallic growth studies on 95.5Sn-3.8Ag-0.7Cu lead-free solder joint subjected to thermal cycling (TC) aging and thermal shock (TS) aging will be reported. Iso-thermal aging studies on intermetallic growth behavior for lap shear soldered specimens were investigated. The lap shear specimens were soldered using 95.8Sn-3.5Ag-0.7Cu solder paste on copper specimen parts coated with Ni and Au surface finish at the wetted area. Isothermal aging tests for three aging temperatures (125°C, 150°C, and 175°C) and four aging time exposures (24, 72, 144 and 336 hours) were conducted. Digital imaging techniques were employed in the measurement of the average intermetallic growth thickness. Details of the intermetallic growth behavior will be discussed with respect to the aging test parameters and curve-fitted to solid-state diffusion mechanisms. Intermetallic growth studies on 95.5Sn-3.8Ag-0.7Cu solder joint specimens subject to temperature cycling aging were investigated. The specimen consist of a 0.5mm solder sphere (of 95.5Sn-3.8Ag-0.7Cu composition) soldered between two FR-4 substrates at the copper pad terminals. The copper pads were coated with Ni and Au surface finish. The thermal cycling (TC) aging test, cycles between -40°C to 125°C, with a cycle time of 56 minutes and a dwell time of 15 minutes at the upper and lower temperature limits. The thermal shock (TS) aging test, alternates between -55°C to 125°C, with a cycle time of 17 minutes, and a dwell time of 5 minutes at each temperature limit. Similar intermetallic growth measurement technique was employed as in iso-thermal aging experiments. Comparison between intermetallic growth behavior for TC and TS exposure for 0, 500, 1000 and 2000 cycles of aging exposure will be reported. A framework for correlating intermetallic growth behavior subjected to TC, TS and Iso-thermal aging conditions will be proposed.

## 4:20 PM Invited

Mechanism of Interfacial Reaction for SnPb Solder Bump with Ni/Cu UBM in Flip Chip Technology: Chien Sheng Huang<sup>1</sup>; Jenq Gong Duh<sup>1</sup>; <sup>1</sup>National Tsing Hua University, Dept. of Matls. Sci. & Engrg., 101, Sect. 2 Kuang Fu Rd., Hsinchu 300 Taiwan

Ni-based under bump metallization has been widely used in flip chip technology due to the slow reaction rate with Sn. In this study, solder joints after reflow were employed to investigate the mechanism of interfacial reaction between Ni/Cu UBM and eutectic Sn-Pb solder. After deliberately quantitative analysis with an electron probe microanalyzer, the effect of Cu content in solder near the interface of solder/IMC on interfacial reaction could be probed. After the first cycle of reflow, only one layered (Ni1-x, Cux)3Sn4 with homogeneous composition was found between the solder bump and UBM. However, after multiple reflows, another type of intermetallic compound (Cu1y, Niy)6Sn5 formed between solder and (Ni1-x, Cux)3Sn4. It was observed that the concentration of Cu in solder near solder/IMC interface increased to a specific value. When (Cu1-y, Niy)6Sn5 IMC formed, the Cu contents in (Ni1-x, Cux)3Sn4 were not uniform anymore. The values of x varied from 0.09 to 0.35. With the aid of microstructure evolution, quantitative analysis, and related phase equilibrium data of Sn-Ni-Cu, the reaction mechanism of interfacial phase transformation between Sn-Pb solder and Ni/Cu UBM could be revealed.

#### 4:40 PM Invited

Control of Interface Reaction Mechanism Between Cu and Sn-Based Solder Alloys: *Choong-Un Kim*<sup>1</sup>; Jaeyong Park<sup>1</sup>; Rajendra Kobade<sup>1</sup>; Viswanadham Puligandla<sup>2</sup>; Ted Carper<sup>2</sup>; <sup>1</sup>University of Texas, Matls. Sci. & Engrg., Arlington, TX 76019 USA; <sup>2</sup>Nokia Mobile Phones, Inc., Rsch. & Tech. Access, 6000 Connection Dr., Irving, TX 75039 USA

Interface reaction between Cu and molten solder is one of the most extensively studied subjects in metallurgy. It is the key reaction for solder joint formation yet is a reliability concern because, if excessive, it can weaken the mechanical properties of the joint. While several theories on the interface reaction mechanism exist, they provide only limited understanding. Recently, we found that the interface reaction mechanism can be altered by the addition of minor additives to solder alloys. These additives are elements having a strong affinity to Cu, such as Au and Ni, and induce the formation of ternary Cu-Sn intermetallic phases. The interplay between 1) the migration of these elements in molten solder and 2) the change in the thermodynamic potential for reaction results in a change in the reaction mechanism and produces a unique interface microstructure consisting of an intermetallic phase and Sn islands. While the composite microstructure is proven to be effective in enhancing solder reliability, the study of its formation provides new insights into the reaction mechanism between Cu and solder alloys. This paper presents a self-consistent reaction mechanism explaining the formation of intermetallic phases and their subsequent morphology and property changes.

#### 5:00 PM

Interfacial Metallurgical Reaction Kinetics During Lead-Free Soldering: *Jin Liang*<sup>1</sup>; Nader Dariavach<sup>1</sup>; Paul Callahan<sup>1</sup>; Stuart Downes<sup>1</sup>; <sup>1</sup>EMC, 176 South St., Hopkinton, MA 01748 USA

Intermetallic growth and substrate dissolution take place rather rapidly during a normal soldering operation. Since lead-free soldering requires substantially higher temperatures (around 250°C), the rates for intermetallic growth and substrate dissolution are expected to increase significantly compared to the current Sn-Pb eutectic soldering. This study attempts to investigate and to model the intermetallic growth kinetics for three lead-free solders (SnAg eutectic, SnCu eutectic and SnAgCu eutectic) with copper substrates, and other metal finishes, such as Ni/Au, OSP, and Pd. A thorough understanding of leadfree solder/substrate interfacial metallurgical reactions would lead to optimum lead-free soldering processes and optimum lead-free coating thickness for component and PCB terminal finishes, as well as USM for flip-chip and BGAs.

## 5:15 PM

Effects of Pd Addition on Au Stud Bumps/Al Pads Interfacial Reactions and Bond Reliability: *Hyoung-Joon Kim*<sup>1</sup>; Jong-Soo Cho<sup>2</sup>; Yong-Jin Park<sup>2</sup>; Jin Lee<sup>2</sup>; Kyung-Wook Paik<sup>1</sup>; <sup>1</sup>Korea Advanced Institute of Science and Technology (KAIST), Matls. Sci. & Engrg., Rm. 2423, Appl. Engrg. Bldg., 373-1, Guseong-Dong, Yuseong-Gu, Daejeon 305-701 Korea; <sup>2</sup>MK Electron Co., Ltd., R&D Ctr., 316-2, Kumeu-ri, Pogok-myun, Yongin, Kyunggi-do 449-812 Korea

Pd has been used as one of the important alloying elements in Au bonding wire manufacturing processes. Therefore, in this study, Aulwt%Pd wire was used to make Au stud bumps on Al pads. To investigate the effects of Pd on Au/Al interfacial reactions, thermal aging was performed at 150, 175, and 200°C for 0 to 1200 hours, respectively. Cross-sectional SEM, EDS, and EPMA were performed to identify the IMC (Intermetallic Compound) phase and Pd behavior at Au/Al bonding interface. According to the experimental results, the dominant IMC was Au5Al2 and Pd-rich layers were formed in front of the Au-Al IMC. Furthermore, TEM study has been performed as a supplement. Finally, ball shear tests were performed to know the effects of Pd-rich layers on bond reliability. Therefore, after ball shear tests, fractured pads and balls were investigated with SEM and EDS, and failure analysis was executed.

# Phase Transformations and Deformation in Magnesium Alloys: Plastic Deformation and Texture

Sponsored by: Materials Processing and Manufacturing Division, MPMD-Phase Transformations Committee-(Jt. ASM-MSCTS) *Program Organizer:* Jian-Feng Nie, Monash University, School of Physics and Materials Engineering, Victoria 3800 Australia

Tuesday PM	Room:	205		
March 16, 2004	Location	: Charlotte	Convention	Center

*Session Chairs:* David Embury, McMaster University, Dept. of Matls. Sci. & Engrg., Hamilton, Ontario L8S 4M1 Canada; Sean R. Agnew, University of Virginia, Dept. of Matls. Sci. & Engrg., Charlottesville, VA 22904-4745 USA

#### 2:00 PM Invited

The Effect of Texture on the Deformation Mechanisms of AZ31B: Sean R. Agnew<sup>1</sup>; *Carlos N. Tome*<sup>2</sup>; Donald W. Brown<sup>2</sup>; <sup>1</sup>University of Virginia, Matls. Sci. & Engrg., 116 Engineer's Way, Charlottesville, VA 22904-4745 USA; <sup>2</sup>Los Alamos National Laboratory, MST-8, Los Alamos, NM USA

In-situ neutron diffraction measurements of internal stress and texture development have been employed to elucidate the roles of various deformation mechanisms with magnesium alloy AZ31B. Three different wrought forms of the alloy have been studied due to the striking differences in crystallographic texture and mechanical behavior. 1) Hot-rolled plate with a basal fiber texture oriented parallel to the plate normal direction, 2) Extruded bar with basal poles oriented perpendicular to the extrusion axis, and 3) Equal Channel Angular (ECA) processed bar with a strong basal fiber inclined 45° from the bar axis. Each sample was tested in tension and compression along the prior working directions. Rolled and extruded samples exhibited strong tension/compression asymmetry associated with twinning, while the ECA processed sample did not. A viscoplastic self-consistent polycrystal model elucidated the aspects of the twinning mechanism, while an elastoplastic self-consistent model provided insights regarding slip-dominated deformation and corresponding internal stress development.

## 2:35 PM Invited

Plastic Anisotropy and its Effects on Mechanical Parameters in Mg Alloys at RT: Junichi Koike<sup>1</sup>; <sup>1</sup>Tohoku University, Dept. of Matls. Sci., 02 Aoba, Aramaki, Aoba-ku, Sendai, Miyagi 980-8579 Japan

Mg alloys exhibit substantial plastic anisotropy at ambient temperature. The plastic anisotropy complicates the interpretation of various mechanical parameters, such as, elastic modulus, yield stress, rvalue, homogeneous strain, and fracture. Physical basis of plastic anisotropy and its effects on the mechanical parameters can be delineated based on dominant deformation mechanisms under given conditions. The present paper deals with various possibilities of deformation mechanisms, including dislocation glide on basal and nonbasal planes, twinning, and grain-boundary sliding. The necessary conditions to activate each mechanism are discussed in relation to grain size and crystallographic texture. The effects of each mechanism on the mechanical parameters are also discussed with an aim to help improve shape forming capabilities of Mg alloy sheets.

#### 3:10 PM Invited

Grain Size of Wrought Magnesium: Manipulation and Mechanical Effects: Matthew R. Barnett<sup>1</sup>; <sup>1</sup>Deakin University, Sch. of Engrg., Pigdons Rd., Geelong, VIC 3217 Australia

Controlling the grain size is one of the key tools used in engineering mechanical properties. The present paper reviews the main approaches used to achieve this in the manufacture of wrought magnesium. It also briefly examines the current knowledge of the influence of the grain size on mechanical response. Results of a series of deformation experiments are examined to reveal the influence of processing conditions on the grain size. The mechanisms considered include continuous dynamic recrystallization, discontinuous dynamic recrystallization, static recrystallization and meta-dynamic recrystallization. The influence of grain size on the mechanisms activated in subsequent deformation treatments is also reported. It is shown that the grain size exerts a significant influence on the activation of twinning. A subset of the possible grain sizes and stresses is defined within which {10-12} twinning will not occur, irrespective of the crystallographic texture. The results of both of these avenues of investigation, i.e. the control of grain size and the effects of grain size on mechanical behaviour, are summarized in a single deformation map in strain rategrain size space.

#### 3:45 PM Break

#### 4:00 PM Invited

Processing of Magnesium Alloys Using Severe Plastic Deformation: Zenji Horita<sup>1</sup>; Yuichi Miyahara<sup>1</sup>; Terence G. Langdon<sup>2</sup>; <sup>1</sup>Kyushu University, Matls. Sci. & Engrg., Fac. of Engrg., Fukuoka 812-8581 Japan; <sup>2</sup>University of Southern California, Aeros. & Mech. Engrg. & Matls. Sci., Los Angeles, CA 90089-1453 USA

Magnesium alloys are potentially attractive for use in structural applications because of their low density and good machinability. Nevertheless, their use tends to be restricted because of the inherent difficulties in forming structural components. It appears in principle that it may be possible to overcome this difficulty by refining the grain size to the submicrometer level through the application of severe plastic deformation. This paper describes recent attempts to achieve a superplastic forming capability in Mg-based alloys through the use of a two-step process, termed EX-ECAP, in which the Mg alloys are initially extruded and then processed using equal-channel angular pressing. It is demonstrated that this two-step procedure leads to excellent superplastic properties with elongations to failure up to >500%.

#### 4:35 PM Invited

**Deformation and Plasticity of Magnesium Alloys - Materials Design by Understanding from Ab Initio Calculation**: *Kenji Higashi*<sup>1</sup>; <sup>1</sup>Osaka Prefecture University, Dept. of Metall. & Matls. Sci., 1-1 Gakuen-cho, Sakai, Osaka 599-8531 Japan

Recently magnesium alloys have been expected to be one of the most promising structural materials. However, it is a large problem that magnesium alloys have low plastic formability at room temperature and less resistance to creep at elevated temperatures. Investigations to develop correct ideas for understanding the deformation mechanism are very much in order. In the present paper, two problems in the deformation mechanism are discussed using ab initio calculation that gives a reliable and accurate description of structural properties and of the distribution of electrons that accompanies the atomic bond for the magnesium-based materials. First, the effect of the substitutional-alloying-elements on the generalized stacking fault (GSF) energy is investigated for the inclusive understanding of the dominant diffusioncreep process at elevated temperatures. It is precisely determined that both Y and Ca among the elements investigated in the present paper are the promising elements to improve the resistance to creep controlled by dislocation-climb in the Mg-based alloys. Second, the misfit strain for some substitutional-alloying-elements, which is obtained from the distortion of atomic positions by ab initio calculation, is calculated as a first step of searching most effective solute element for the solid-solution strengthening in Mg-based substitutional solid solution. Additionally, based on the results of ab initio calculation, materials design for the optimum chemical compositions will be applied to developing new Mg-based alloys exhibiting high strength with reasonable high ductility.

## Processing, Microstructure and Properties of Powder-Based Materials: Session III

Sponsored by: Materials Processing and Manufacturing Division, MPMD-Powder Materials Committee

*Program Organizers:* K. B. Morsi, San Diego State University, Department of Mechanical Engineering, San Diego, CA 92182 USA; James C. Foley, Los Alamos National Laboratory, Los Alamos, NM 87545 USA; Karl P. Staudhammer, Los Alamos National Laboratory, Nuclear Materials Technology Division, Los Alamos, NM 87545 USA

Tuesday PM	Room: 2	08B		
March 16, 2004	Location:	Charlotte	Convention	Center

Session Chair: James C. Foley, Los Alamos National Laboratory, Matls. Tech., Los Alamos, NM 87545 USA

#### 2:00 PM Invited

**Processing of High-Porosity NiTi by Powder Densification and Subsequent Gas Bubble Expansion**: Scott M. Oppenheimer<sup>1</sup>; *David C. Dunand*<sup>1</sup>; <sup>1</sup>Northwestern University, Dept. of Matls. Sci. & Engrg., Evanston, IL 60201 USA

Powders of nickel-rich NiTi (Ni-49 wt.%Ti, with superelastic composition) were densified by hot-isostatic pressing in the presence of argon, resulting in a continuous NiTi preform containing a large number of isolated, pressurized argon bubbles with volume fraction below ca. 1%. Annealing this preform above 1000°C resulted in the expansion of these gas-filled bubbles due creep of the surrounding NiTi matrix. The resulting NiTi "foams" exhibit porosity in excess of 30 vol. % with pore size above 100 micrometers. Foaming kinetics, maximum porosity and pore connectivity to the surface are explored as a function of annealing temperature and initial argon pressure.

#### 2:20 PM

Stress Relaxation of Powder Metallurgy Disk Superalloys: Timothy P. Gabb<sup>1</sup>; Jack Telesman<sup>1</sup>; Peter T. Kantzos<sup>2</sup>; Peter J. Bonacuse<sup>3</sup>; Robert L. Barrie<sup>3</sup>; Paul Prevey<sup>4</sup>; <sup>1</sup>NASA Glenn Research Center, 21000 Brookpark Rd., Cleveland, OH 44135 USA; <sup>2</sup>Ohio Aerospace Institute, 22800 Cedar Point Rd., Cleveland, OH 44142 USA; <sup>3</sup>Army Research Laboratories, 21000 Brookpark Rd., Cleveland, OH 44135 USA; <sup>4</sup>Lambda Research, 5521 Fair Ln., Cincinnati, OH 45227 USA

Modern powder metallurgy (PM) processed disk superalloys have improved mechanical properties and temperature capabilities over previous cast and wrought disk alloys, due to improved microstructural uniformity and higher refractory element contents. However, these PM improvements have been accompanied by increased sensitivities to notches and defects at disk surfaces. These surface sensitivities can be addressed by applying beneficial compressive residual stresses at disk surfaces. The compressive residual stresses are produced with surface enhancement processes such as shot peening which plastically deform the near-surface material, usually performed after final disk machining. Such compressive residual stresses act to preclude or delay surface cracking during service due to loading, defects, handling or foreign object damage, and environmental attack. An issue of general concern is the potential relaxation of beneficial compressive surface residual stresses as engine temperatures increase. The objective of this study was to assess the relaxation of stresses at increasing temperatures in several PM disk superalloys. The effects of temperature, time, and plasticity were examined, and potential approaches to minimize stress relaxation will be discussed.

## 2:40 PM

**Consolidation of Powders by Severe Plastic Deformation**: *K. Ted Hartwig*<sup>1</sup>; *Ibrahim Karaman*<sup>1</sup>; Suveen N. Mathaudhu<sup>1</sup>; Jae-Taek Im<sup>1</sup>; <sup>1</sup>Texas A&M University, Mech. Engrg., 319 Engrg. Phys. Bldg., College Sta., TX 77843-3123 USA

Advances in the production of nanostructured powders over the past decade have given materials engineers new opportunities for the creation of high strength bulk materials. Mechanical alloying, gas atomization, electro-explosion and other novel synthesis methods coupled with better alloy composition selections have enabled the production of a wide variety of metastable extremely fine structured powders. Bulk material with extraordinary properties should result if such powders can be consolidated without significant changes to the microstructure. In the work reported here, one method of severe plastic deformation (equal channel angular extrusion - ECAE) is evaluated for effective consolidation of several different nanostructured materials including copper, Ti, stainless steel and Bi2Te3 alloy. The effects of particle size, starting microstructure, and several extrusion conditions are investigated by metallographic examination and mechanical testing. The results show that ECAE possesses interesting benefits for consolidation of particulate and is a viable method for fabrication of bulk nanostructured materials.

#### 3:00 PM

Fabrication of Bulk Nanocrystalline Metals by the Consolidation of Nanoparticles Using Equal Channel Angular Extrusion: *Ibrahim Karaman*<sup>1</sup>; Mohammed Haouaoui<sup>1</sup>; G. Guven Yapici<sup>1</sup>; Hans J. Maier<sup>2</sup>; <sup>1</sup>Texas A&M University, Dept. of Mech. Engrg., MS 3123, College Sta., TX 77843 USA; <sup>2</sup>University of Paderborn, Lehrstuhl für Werkstoffkunde, Paderborn 33095 Germany

Materials with ultrafine grains and nanostructures (< 100 nm) have attracted considerable interest because of their unique properties as compared with conventional materials. Although this class of materials seems to offer new opportunities for small scale applications, utilizing them in large scale structural applications is still a challenge due to the difficulty of fabricating nanocrystalline materials in bulk. The present work is focussed on fabrication of near full density bulk nanocrystalline copper and stainless steel from powder precursors using equal channel angular extrusion (ECAE). The initial powder sizes were 50 nm, 150 nm and 45 micron for copper and 100 nm for stainless steel. Different processing routes were selected for comparison purposes and to determine the best processing route for specific end microstructures. The microstructure is characterized for different ECAE routes and number of passes. The stress-strain responses are determined by tension and compression tests at room temperature. The effect of initial powder size and resulting consolidate grain size on the mechanical properties are discussed in view of the Hall-Petch relationship. In this talk, some of these experimental observations will be presented in comparison with microcrystalline consolidates and with severely deformed pure copper and stainless steel. This study helps to clarify the relationship between different ECAE processing parameters, mechanical properties and the microstructure of nanocrystalline metals with low and medium stacking fault energies. This work was supported by the National Science Foundation contract CMS 01-34554, Solid Mechanics and Materials Engineering Program, Directorate of Engineering, Arlington, Virginia and Deutsche Forschungsgemeinschaft.

## 3:20 PM

**Corrosion Resistance of Laser Deposited 316L Stainless Steels:** *Eswar R. Yarrapareddy*<sup>1</sup>; Alan J. Anderson<sup>1</sup>; James W. Sears<sup>1</sup>; <sup>1</sup>South Dakota School of Mines & Technology, Advd. Matls. Procg. Ctr., 501 E. St. Joseph St., Rapid City, SD 57701 USA

Laser Powder Deposition (LPD) involves injecting particles (metallic and/or ceramic) into a molten pool produced by a focused laser beam. A computer-controlled robot controls the position of the molten pool. The process allows for sequential layering to produce solid free form shapes directly from a CAD/CAM interface. The Process parameters were implemented to control the molten pool size by modulating laser power and process speed. In the current study, the corrosion behavior of laser deposited 316L stainless steels were investigated in 3.5% NaCl solution at 23°C by cyclic potentiodynamic polarization method. From this, the corrosion potential, pitting potential, protection potential and current density were calculated and polarization curves were generated. The susceptibility of intergranualar corrosion (IGC) was studied by hot boiling sulphuric sensitization test. The pit morphology after polarization test was also examined by optical microscopy.

## 3:40 PM Break

#### 3:50 PM

High Density Infrared Processing of ã-TiAl Sheet: John D.K. Rivard<sup>1</sup>; <sup>1</sup>Oak Ridge National Laboratory, Metals & Ceram., 1 Bethel Valley Rd., MS 6083, Oak Ridge, TN 37831 USA

Gamma titanium aluminide (g-TiAl) alloys are of interest for engineering solutions in the aerospace and the automotive industry because of a unique combination of low density, oxidation resistance, burn resistance and high temperature strength. Current productions methods limit the implementation of ã- TiAl in regular use due to high cost and long cycle times of production. A difficulty is that engineers have a talent for making existing technology work by trading off other parameters at a reduced cost. But, a recently developed method for the fabrication of sheet materials has made the regular use of ã-TiAl one step closer to reality. This novel method utilizes high-density infrared (HDI) radiant heating from a plasma arc lamp to rapidly heat and liquid phase sinter powder metal precursors. In this study, ã-TiAl sheet was produced from tape cast Ti-48Al-2Cr-2Nb. Predictive finite volume modeling was used to determine appropriate processing parameters. A complete database of the appropriate thermophysical properties was also compiled. Thin gage ã-TiAl sheet was produced in panels measuring up to 10cm x 10cm. Resultant microstructures will be presented as well as mechanical properties. Comparisons of conventional and HDI processed a-TiAl will be presented.

#### 4:10 PM

The Influence of Heterogeneous Microstructure on Fatigue Crack Growth in Powder Metallurgy Steels: George B. Piotrowski<sup>1</sup>; Xin Deng<sup>1</sup>; Nikhilesh Chawla<sup>1</sup>; <sup>1</sup>Arizona State University, Dept. Chem. & Matls. Engrg., PO Box 876006, Tempe, AZ 85287-6006 USA

Powder metallurgy steels processed by pressing and sintering generally exhibit a highly heterogeneous microstructure. In Ni-containing steels, it is not uncommon for Ni-rich retained austenite, pearlite, and bainite to all be present in the microstructure (in addition to porosity). Thus, fatigue crack growth is directly dependent on the local character of the microstructure. In this study, we have correlated the local microstructure with fatigue crack growth in a Fe-2Ni-0.85Mo-0.6C steel at three different densities: 7.0, 7.4, 7.6 g/cm3. The microstructure at each density was characterized by optical microscopy, scanning electron microscopy, and indentation to identify the phases present and quantify the fractions of each phase. The microstructure consisted of Ni-rich austenite regions, pearlite, and bainite. Fatigue crack growth tests were conducted at several R-ratios, ranging from -1 to 0.8. Increasing density and decreasing R-ratio resulted in an increase in  $\Delta K_{th}$ . The interaction between fatigue cracks and the local microstructure was conducted by in situ crack growth measurements through a traveling microscope. The crack growth resistance of each of the phases was quantified and will be discussed in terms of strategies for developing sintered steels with enhanced fatigue crack growth resistance.

## 4:30 PM

Aluminium and Aluminium Alloy Powders for P/M Applications: Ray Cook<sup>1</sup>; Henry S. Meeks<sup>2</sup>; Isaac T.H. Chang<sup>3</sup>; Lucian C. Falticeanu<sup>3</sup>; <sup>1</sup>The Aluminium Powder Company Ltd., Forge Ln., Minworth, Sutton Coldfield, W. Midlands B76 1AH UK; <sup>2</sup>Ceracon Inc., 5150 Fair Oaks Blvd. #101-330, Carmichael, CA 95608 USA; <sup>3</sup>University of Birmingham, Sch. of Metall. & Matls., Edgbaston, Birmingham B15 2TT UK

Aluminium is becoming of more interest in various P/M industries due to the possibilities of lightweighting components. There are many processes for manufacturing from powder feedstocks that are either in production, becoming commercialised or still undergoing development. The nature of these processes and the required properties of the end products mean that powders of different particle size, shape, composition and microstructure must be produced. The requirements of various processes requiring aluminium and aluminium alloy powders for metal matrix composites, laser sintering, powder forging and metal injection moulding are discussed in relation to powder particle size and structure. The key requirement of the powder manufacturer is to supply cost effective materials for these different processes. This may require compromises to be made by the supplier and consumer while the techniques evolve from development to large scale production.

## 4:50 PM

Processing and Properties of Porous Structures Made from Filamentary Nickel Powders: David S. Wilkinson<sup>1</sup>; Valery Chani<sup>1</sup>; Alex Zaitsev<sup>2</sup>; <sup>1</sup>McMaster University, Matl. Sci. & Engrg., 1280 Main St. W., Hamilton, ON L8S 4L7 Canada; <sup>2</sup>INCO Technical Services, Sheridan Park, Mississauga, ON L5K 1Z9 Canada

INCO Ltd. manufactures a range of filamentary nickel powders that have high aspect ratios and irregular shapes. Such powders pack rather poorly making them ideal for the manufacture of low density structures (typical porosity levels are about 15 vol%). We have recently shown that the application of colloidal processing methodologies can be used to significantly increase the strength of such materials without increasing relative density. In the application of these materials in batteries adhesion to a rigid substrate is also important. We will discuss how this can be achieved through careful control of additives and the sintering process.

# R.J. Arsenault Symposium on Materials Testing and Evaluation: Session IV

Sponsored by: Structural Materials Division, SMD-Mechanical Behavior of Materials-(Jt. ASM-MSCTS), SMD-Nuclear Materials Committee-(Jt. ASM-MSCTS)

*Program Organizers:* Raj Vaidyanathan, University of Central Florida, AMPAC MMAE, Orlando, FL 32816-2455 USA; Peter K. Liaw, University of Tennessee, Department of Materials Science and Engineering, Knoxville, TN 37996-2200 USA; K. Linga Murty, North Carolina State University, Raleigh, NC 27695-7909 USA

Tuesday PM	Room: 211A	
March 16, 2004	Location: Charlotte Convention Cente	r

Session Chairs: Raj Vaidyanathan, University of Central Florida, AMPAC/MMAE, Orlando, FL 32816-2455 USA; Nik Chawla, Arizona State University, Dept. of Chem. & Matls. Engrg., Tempe, AZ 6006 USA

## 2:00 PM Invited

Adhesion Test Using Cylindrical Indenters: James C.M. Li<sup>1</sup>; <sup>1</sup>University of Rochester, Dept. of Mech. Engrg., Rochester, NY 14627 USA

The JKR (K. L. Johnson, K. Kendall and A. D. Roberts, Proc. Roy. Soc. London, A324, 301-313, 1971) theory of adhesion test between two spheres or a sphere and a plate has a hysteresis problem between the experimental loading curve and that of unloading. Most likely it is due to the change of interfacial energy with time or load or both. Such hysteresis prevents accurate calculation of adhesion energy at the time of pull-off from the JKR theory. A cylindrical indenter with a flat end avoids such problem and provides a more precise way of measuring adhesion energy at the instant of separation. This technique on thin films coated over a rigid substrate as well as the effect of moisture which may cause the formation of a thin layer of water between contact surfaces are reported. Work supported by N.Y. State Infotonics Center of Excellence and by NSF through DMR9623808 monitored by Dr. Bruce MacDonald.

#### 2:30 PM

**Evaluation of Ambient and Elevated Temperature Mechanical Behavior of Silicon Microdevices**: *Brad L. Boyce*<sup>1</sup>; Justin J. Van Den Avyle<sup>1</sup>; Thomas E. Buchheit<sup>1</sup>; <sup>1</sup>Sandia National Laboratories, Matls. & Proc. Scis. Ctr., PO Box 5800, MS 0889, Albuquerque, NM 87185-0889 USA

The emergence of microelectromechanical systems (MEMS) has required the concurrent development of techniques to determine their mechanical reliability. Testing at the relevant size scale is paramount due to the potential size-scale effects. Specifically, in brittle materials such as polycrystalline silicon, failure is thought to be size dependent due to the statistical sampling of flaws: smaller gage volumes have a lower likelihood of containing a large flaw. However, at the microsystem scale, non-standardized test techniques have led to ambiguous interpretations of size effects. In the current study, refined test methodology capable of testing at temperatures up to 800°C is coupled with self-aligning 2 micron wide micro-tensile specimens that span over two orders of magnitude in sampling volume. The results clearly show the size-dependence of strength on sampling volume, and are consistent with Weibull strength distributions. Discussion will focus on the implications with respect to the underlying material flaw distribution and reliable design. Sandia is a multiprogram laboratory operated by

Sandia Corporation, A Lockheed Martin Company, for the United States Department of Energy's National Nuclear Security Administration under contract DE-AC04-94AL85000.

#### 2:50 PM

Micromechanical Testing at Small Length Scales: Nik Chawla<sup>1</sup>; <sup>1</sup>Arizona State University, Dept. of Chem. & Matls. Engrg., Ira A. Fulton Sch. of Engrg., PO Box 876006, Tempe, AZ 85287 USA

With increasing interest in materials at nanometer and micrometer length scales, new innovative techniques are required to conduct mechanical testing. In this talk, we report on a micromechanical testing system with ultra-low force and high resolution capability for materials at small volumes. Mechanical testing of three types of materials will be cited as examples: (a) creep of Pb-free solder microspheres, (b) tensile and fatigue testing of high performance ceramic fibers, and (c) tensile testing of Al/SiC multilayered nanolaminates. The advantages and challenges associated with micromechanical testing at small length scales will be discussed.

## 3:10 PM

Measures of Plasticity in Single Crystals from Surface Deformation and Lattice Rotation Measurements Around Indents: *Pedro D. Peraltal*; Robert Dickerson<sup>2</sup>; Majid Al Maharbi<sup>3</sup>; Mehdi Hakik<sup>1</sup>; <sup>1</sup>Arizona State University, Dept. of Mech. & Aeros. Engrg., Engrg. Ctr., G Wing, Rm. 346, Tempe, AZ 85287-6106 USA; <sup>2</sup>Los Alamos National Laboratory, Matls. Sci. & Tech. Div., MST-8, MS G755, Los Alamos, NM 87545 USA; <sup>3</sup>Arizona State University, Sci. & Engrg. of Matls. Prog., Tempe, AZ 85287 USA

Vickers and Spherical indents on several monocrystalline substrates have been characterized using optical, electron and scanning probe microscopy as well as profilometry. Orientation Imaging Microscopy was used to map changes on the local crystallographic orientation of the surface surrounding one indent on copper to obtain maps of the lattice rotation due to plastic deformation. The results indicate that sink-in and pile-up behavior depend strongly on the in-plane crystallographic orientation of the diagonals of the indent and is related to local multiplicity of slip. Regions with multiple slip show larger lattice rotations and sink-in, whereas regions with lower slip density had lower lattice rotations and show pile-ups. Strains surrounding the indents were obtained from OIM data using kinematical relations for single crystal plasticity. An average strain of 29% next to a Vickers indent was deduced from the analysis, which agrees quite well with the characteristic strain reported for Vickers indents.

## 3:30 PM Break

#### 3:50 PM

An Instrumented Indentation Study of Deformation in Shape-Memory NiTi: S. Rajagopalan<sup>1</sup>; Raj Vaidyanathan<sup>1</sup>; <sup>1</sup>University of Central Florida, AMPAC/MMAE, Eng-I Rm. 381, 4000 Central Florida Blvd., Orlando, FL 32816-2455 USA

Shape-memory alloys (SMAs) are of theoretical and commercial interest for the deformation phenomena they exhibit - twinning and stress-induced/temperature-induced phase transformation. Here we report on the use of instrumented indentation to capture the formation of stress-induced martensite and twinning from load-depth indentation responses in NiTi and assess the effect of geometrical and microstructural length scales on deformation behavior. Load-depth curves from indentation of SMAs usually call for specific thermomechanical properties and a variety of compositions and thermomechanical treatments can thus be empirically attempted in centimeter scaled buttons and indented prior to large scale production, resulting is substantial cost savings. This work is supported by NASA and NSF (CAREER DMR-0239512).

### 4:10 PM

Miniaturized Impression Creep of Sn-3.5Ag Microelectronic Solder Balls and Associated Mechanics-Related Effects: Deng Pan<sup>1</sup>; Robert A. Marks<sup>1</sup>; Indranath Dutta<sup>1</sup>; <sup>1</sup>Naval Postgraduate School, Mech. Engrg., 700 Dyer Rd., Monterey, CA 93943 USA

Impression creep, in which a flat-ended cylindrical indenter is used to load a small area of the specimen surface under a constant compressive stress, has been used to study the creep behavior of a wide range of materials. One of the attractive features of the impression creep test is its ability to test specimens of very small material volumes and miniaturized components with minimal sample preparation. In this paper, we report the development of an apparatus and approach for impression creep testing of microelectronic solder balls of 0.75mm diameter attached to a ball grid array (BGA) substrate, using a 0.1-mm diameter indenter. This approach enables direct on-substrate or onchip testing of solder balls. Details of apparatus design, experimental methodology, and experimental creep results based on lead-free solders (Sn-Ag and Sn-Ag-Cu) will be presented. A mechanics-induced complication of impression creep, particularly under conditions of slow deformation, which can potentially cause anomalous interpretation of the resultant creep data, is also discussed. A methodological remedy of this problem is proposed, and validated via experiments.

### 4:30 PM

A Technique for Measuring Compressive Properties of Single Microballoons: *Kipp B. Carlisle*<sup>1</sup>; Mark C. Koopman<sup>1</sup>; Krishan K. Chawla<sup>1</sup>; Gary M. Gladysz<sup>2</sup>; <sup>1</sup>University of Alabama, 1150 10th Ave. S., BEC 254, Birmingham, AL 35294 USA; <sup>2</sup>Los Alamos National Laboratory, Engrg. Scis. & Applications Div., Weapon Matls. & Mfg., MS C930, Los Alamos, NM 87545 USA

A technique has been developed to obtain mechanical properties of individual hollow microspheres, or microballoons. This technique utilizes a nanoindentation instrument equipped with a cylindrical sapphire tip, thereby replicating a conventional mechanical compression test on a nanometer scale. The procedure has thus been termed nanocompression, since the extreme sensitivity of the nanoindentation instrument provided a load resolution of 50 nN and a displacement resolution better than 0.02 nm. The load-displacement curves resulting from this test provided mechanical properties including maximum load and strain to failure. Materials tested included polymer, glass, and carbon microspheres, with the primary focus being carbon microballoons. Characterization of the microballoons, in terms of wall thickness and diameter, was undertaken through quantitative microscopy in an effort to correlate morphology to mechanical properties. A trend has been observed between strain to failure and carbon microballoon diameter. This work was supported by DOE/LANL subcontract 44277-SOL-02 4X, LA-UR-03-5700.

#### 4:50 PM

**High Temperature Tensile and Creep of 7034 Aluminum Alloy:** *K. Xu*<sup>1</sup>; R. F. Alessi<sup>1</sup>; D. S. Kmiotek<sup>1</sup>; R. Zawierucha<sup>1</sup>; <sup>1</sup>Praxair, Inc., 175 E. Park Dr., Tonawanda, NY 14051 USA

Conventional 7xxx aluminum alloys have excellent mechanical properties at room temperature. However, their strength degrades rapidly at elevated temperatures due to the coarsening of the precipitates. Spray forming is a relatively new technology in material fabrication which produces near net shape preforms by rapid solidification of atomized droplets in a single step. In this investigation, the tensile and creep properties of spray formed 7034 aluminum alloy (Al-Zn-Mg-Cu-Zr) were studied in the temperature range of 90 to 150C. It was found that the new alloy not only had a superior strength at room temperature, its creep resistance was also greatly improved compared with 7075-T6. The high strength of the alloy was achieved by the high Zn content, which resulted in a high percentage of precipitates. The enhancement in creep resistance was attributed to the addition of Zr which formed finely dispersed stable intermetallic compound Al3Zr. The spray forming process made it possible to produce the high Zn aluminum alloy without macro segregation and cracking.

# Solidification of Aluminum Alloys: Microstructural Evolution II

Sponsored by: Materials Processing & Manufacturing Division, MPMD-Solidification Committee

*Program Organizers:* Men Glenn Chu, Alcoa Inc., Alcoa Technical Center, Alcoa Center, PA 15069 USA; Douglas A. Granger, GRAS, Inc., Murrysville, PA 15668-1332 USA; Qingyou Han, Oak Ridge National Laboratory, Oak Ridge, TN 37831-6083 USA

Tuesday PM	Room: 2	207B/C
March 16, 2004	Location:	Charlotte Convention Center

Session Chairs: Douglas A. Granger, GRAS Inc., Murrysville, PA 15668-1332 USA; David E.J. Talbot, Consultant, Ruislip HA 47TG, Middlesex UK

## 2:00 PM

**Recent Progress in Understanding Eutectic Solidification in Aluminum-Silicon Foundry Alloys:** Arne K. Dahle<sup>1</sup>; Stuart D. McDonald<sup>2</sup>; Kazuhiro Nogita<sup>2</sup>; Liming Lu<sup>1</sup>; <sup>1</sup>University of Queensland, CRC for Cast Metals Mfg., Div of Matls. Engrg., Brisbane, Qld 4072 Australia; <sup>2</sup>University of Queensland, Div. of Matls. Engrg., Brisbane, Qld 4072 Australia

It is now well established that three different eutectic solidification mechanisms may occur in Al-Si foundry alloys. The operation of each mechanism can be controlled by altering chemical composition and casting conditions. Recent research has focussed on the understanding of the mechanisms determining the eutectic solidification mode by investigating the growth mechanisms in ultra-high purity and commercial purity alloys, the effect of a wide range of different potential modifier elements and investigating the eutectic nucleation mode. It is concluded that nucleation of eutectic grains is prolific in unmodified commercial purity alloys. In contrast, high-purity alloys have relatively few nuclei and only a few grains nucleate. Nuclei can also be removed, or rendered inactive, by the addition of modifying elements to commercial purity alloys. Nucleation frequency has an effect on the morphology, as does also some modifier elements. The practical implications of the eutectic nucleation and growth modes are discussed.

## 2:20 PM

The Role of Iron in the Nucleation of Eutectic Silicon in Aluminum-Silicon Hypoeutectic Alloys: *Sumanth Shankar*<sup>1</sup>; Yancy W. Riddle<sup>1</sup>; Makhlouf M. Makhlouf<sup>1</sup>; <sup>1</sup>Worcester Polytechnic Institute (WPI), Advd. Casting Rsch. Ctr., Metal Procg. Inst. (MPI), Dept. of Mech. Engrg., 100 Inst. Rd., Worcester, MA 01609 USA

Understanding the mechanism of evolution and modification of the eutectic phases in the hypoeutectic Al-Si alloys greatly enhances our understanding and predictive capabilities of casting properties such as feedability, porosity distributions, heat treatment responses, etc. For the past eighty years there has been various contradicting hypotheses proposed to understand the evolution and modification of the eutectic phases in hypoeutectic Al-Si alloy. One of the main reasons for the lack in understanding is due to the lack of technology to critically analyze the microstructures and support a working mechanism. Novel emerging technologies such as Focused Ion Beam (FIB) milling, advanced Transmission Electron Microscopy (TEM) and Electron Back Scatter Diffraction patterns (EBSD) aided an in-depth understanding of the evolution of the eutectic phases in Al-Si cast alloys. A theory has being proposed in this paper to explain the nucleation of the eutectic phases: Si and Al during solidification. It was observed that iron is a critical impurity in Aluminum-Silicon alloys that affects the nucleation of the eutectic phases in the alloy. Results show that the eutectic Si nucleates on a (Al,Si,Fe) phase in the solute field ahead of the primary aluminum dendrites and the eutectic aluminum grains nucleate on the eutectic Si. Another theory is also presented in this paper to explain the modification of the eutectic phases in the alloy. A working mechanism has been proposed wherein the drastic change in the fluid properties of the interdendritic eutectic liquid upon adding modifiers such as Sr, Na, etc. plays a critical role in modification of the eutectic phases. The change in wetting characteristics of the eutectic liquid delays the nucleation event of the eutectic silicon phase and results in considerable undercooling of the melt at the eutectic transformation temperature. Addition of modifiers to the alloy melt results in refinement of the silicon morphology from flaky to fibrous structure and in refinement of the eutectic aluminum grains by at least an order of magnitude.

TUESDAY PM

#### 2:40 PM

Effects of Simultaneous Na and Sr Additions in a Eutectic Al-Si Casting Alloy: Hamish R. McIntyre<sup>1</sup>; *Milo V. Kral*<sup>1</sup>; Jason Looij<sup>2</sup>; <sup>1</sup>University of Canterbury, Mech. Engrg., PO Box 4800, Christchurch New Zealand; <sup>2</sup>CWF Hamilton, PO Box 709, Christchurch New Zealand

The eutectic modification of Al-Si casting alloys through additions of modifying elements has been studied extensively in previous work. Sodium has a rapid modification effect with short duration while strontium is associated with a slower acting but longer lasting effect. It is also known that simultaneous additions of Na and Sr can be beneficial but this phenomenon is not particularly well-documented or understood. The purpose of this work was to characterise the effects of combined Na and Sr additions to a commercial eutectic Al-Si alloy in comparison with the separate additions of Na and Sr. The influence of modification on the morphology and size of iron-rich intermetallics was also of interest. Eutectic and intermetallic particle morphology, tensile strength and compositional data were obtained from samples taken at intervals during extended melt holding periods. A predictive model for the diminishing effect of modifiers over time is proposed.

## 3:00 PM

High-Rate Growth Transitions in Al-Si Eutectic: Luke G. England<sup>1</sup>; Ralph E. Napolitano<sup>1</sup>; <sup>1</sup>Iowa State University, MSE, 104 Wilhelm Hall, Ames, IA 50011 USA

The high-rate growth-mode transition (i.e. quench modification) observed in the eutectic solidification of Al-Si alloys was studied using directional solidification over a wide range of growth velocities. Measurements of interface undercooling, phase spacing, particle morphology, and crystallographic orientation were performed to understand the role of interfacial properties and crystallographic anisotropy on mechanisms of spacing adjustment, texturing, and morphological selection through the quench modification transition.

#### 3:20 PM Break

## 3:40 PM Keynote

Grain Refinement of Aluminum Alloys: A. Lindsay Greer<sup>1</sup>; <sup>1</sup>University of Cambridge, Matls. Sci. & Metall., Pembroke St., Cambridge CB2 3QZ UK

This review describes recent studies of the mechanisms by which inoculation refines the as-cast grain structure of aluminum alloys. The emphasis is on where fundamental understanding can improve industrial practice with existing refiners and also can assist the development of new refiners. The problems of relating fundamental studies to industrial practice are also addressed. The nucleation of new grains is difficult to analyze because many parameters are not known with precision; nevertheless in favorable cases grain size can be predicted quantitatively as a function of alloy composition and processing conditions. Topics to be covered include: nucleation mechanisms, growth restriction by solute, fade of refiner performance, the various mechanisms of poisoning and ways to avoid it, design of refiners, comparison of different refiners from both main types Al-Ti-B and Al-Ti-C, prediction of grain size, and prediction of the columnar-to-equiaxed transition.

## 4:10 PM

Factors Affecting the Development of a Fine Grained Solidification Microstructure in Aluminum Alloys: *Mark Easton*<sup>1</sup>; David StJohn<sup>2</sup>; <sup>1</sup>Monash University, CRC for Cast Metals Mfg. (CAST), Sch. of Physics & Matls. Engrg., PO Box 69, Melbourne, Victoria Australia; <sup>2</sup>University of Queensland, CRC for Cast Metals Mfg. (CAST), Div. of Matls., Brisbane, Queensland Australia

In addition to the need for potent heterogeneous particles to activate nucleation, the alloy content, described by the growth restriction factor, and the solidification conditions, in particular the cooling rate and the amount of undercooling produced when pouring metal into a chill mold, also affect the final grain size achieved. This paper overviews recent work that investigates these factors for the addition of Al-Ti-B type grain refiners in a variety of wrought aluminum alloys. It was found that relatively simple relationships can be developed between the potency and number of nucleant particles and the cooling rate, that allow the determination of the most effective means of achieving a particular grain size. The influence of using thermal undercooling to generate wall crystals and its effect on the grain size is also discussed. The findings are then applied to the problem of achieving lowest cost grain refiner additions in VDC casting.

#### 4:30 PM

An Investigative Study of Si Poisoning in Al-Si Alloys Using the Metallic Glass Technique: *Brian John McKay*<sup>1</sup>; P. Schumacher<sup>1</sup>; <sup>1</sup>University of Leoben, Inst. of Gießereikunde, Franz-Josef Str. 18, Leoben A-8700 Austria

An Al80Cu10Ni8Si2 (at. %) alloy was selected for a metallic glass study. Melt-spinning the alloy and a Al-5Ti-1B grain refiner rod resulted in heterogeneous boride particles being embedded within a glass matrix. The degree of nucleation and crystallization of the glass on borides within the matrix was controlled by the quench rate. Results indicate that Al nucleates on the borides with the close packed planes and directions being parallel: {111}Al//{001}TiB2, <110>Al// <100>TiB2. However, with a high Ti content (0.09 at. %) and with long holding times (30 minutes) a silicide phase was found nucleating on the borides: the borides displaying no evidence of nucleating Al. This silicide phase observed was not present under the previous conditions. It is proposed that the silicides consume heterogeneous nucleation sites thus preventing a-Al from nucleating. This mechanism is suggested to be the one that is commonly referred to in the literature as 'Si poisoning'. Other intermetallics were also found to nucleate on the borides.

#### 4:50 PM

Columnar-to-Equiaxed Transition Studies in Al-2wt%Cu, Al-4wt%Cu, Al-10wt%Cu, Al-20wt%Cu and Al-33.2wt%Cu Alloys: Alicia Esther Ares<sup>2</sup>; Rubens Caram<sup>3</sup>; *Carlos Enrique Schvezov*<sup>1</sup>; <sup>1</sup>University of Misiones, 1552 Azara St., Posadas-Misiones 3300 Argentina; <sup>2</sup>CONICET, 1552 Azara St., Posadas-Misiones Argentina; <sup>3</sup>State University of Campinas, CP 6122, Campinas-Sao Paulo CP 6122 Brazil

The columnar to equiaxed transition (CET) was studied in Al-2wt%Cu, Al-4wt%Cu, Al-10wt%Cu, Al-20wt%Cu and Al-33.2wt%Cu alloys, which were solidified directionally from a chill face. The main parameters analyzed include the temperature gradients, solidification velocities of the liquidus and solidus fronts, and grain size. The transition does not occur in an abrupt form in the samples and is present when the gradient in the liquid ahead of the columnar dendrites reaches critical and minimum values, being negative in most of cases. In addition, there is an increase in the velocity of the liquidus front faster than the solidus front, which increases the size of the mushy zone. The size of the equiaxed grains increase with distance from the transition, an observation that was independent of alloy composition. The results are compared with those obtained by other authors.

# Solidification Processes and Microstructures: A Symposium in Honor of Prof. W. Kurz: Rapid Solidification

Sponsored by: Materials Processing & Manufacturing Division, MPMD-Solidification Committee

*Program Organizers:* Michel Rappaz, Ecole Polytechnique Fédérale de Lausanne, MXG, Lausanne Switzerland; Christoph Beckermann, University of Iowa, Department of Mechanical Engineering, Iowa City, IA 52242 USA; R. K. Trivedi, Iowa State University, Ames, IA 50011 USA

Tuesday PM	Room: 2	207D
March 16, 2004	Location:	Charlotte Convention Center

Session Chair: W. J. Boettinger, National Institute for Standards and Technology, Gaithersburg, MD 20879 USA

#### 2:00 PM Invited

Rapid Dendrite Growth in Undercooled Melts: Experiments and Modeling: Dieter M. Herlach<sup>1</sup>; <sup>1</sup>German Aerospace Center, Inst. of Space Simulation, Linder Hoehe, Cologne, NRW D-51170 Germany

Essential progress of modeling of rapid dendrite growth in undercooled melts was achieved by the "classic" work of Wilfried Kurz et al. [1]. At the same time new experimental techniques were developed to measure rapid dendrite growth velocities as a function of undercooling in metallic melts. In the present work, non-equilibrium phenomena are reviewed occurring during rapid growth of dendrites in undercooled melts. Experimental results and their analysis within dendrite growth models are presented for the solidification of segregation-free microstructures and disordered superlattice structures of intermetallics. It will be shown that the short range order in the undercooled melt and its similarity/dissimilarity to the short range order of the solidifying phase has an essential impact on the atomic attachment kinetics and thus the kinetic interface undercooling of the solidification front. J. Lipton, W. Kurz, and R. Trivedi, Acta Metall. 35 (1987) 957-964.

## 2:30 PM Invited

Tests of Theories for Nonplanar Growth During Rapid Alloy Solidification: *Michael J. Aziz*<sup>1</sup>; <sup>1</sup>Harvard University, Div. of Engrg. Appl. Scis., 29 Oxford St., Cambridge, MA 02138 USA

During rapid solidification, kinetically suppressed solute partitioning at the crystal/melt interface, as well as kinetic interfacial undercooling, become important. Both of these effects are expected to have significant stabilizing influences on a planar interface during rapid solidification. We will present experimental tests of models for the transition from planar to cellular growth, and for the velocity-undercooling function of the dendrite tip, in the velocity regime where nonequilibrium interface kinetics are important.

#### 3:00 PM Invited

**Phase Selection Transitions During Undercooled Melt Solidification**: John H. Perepezko<sup>1</sup>; <sup>1</sup>University of Wisconsin, Dept. Matls. Sci. & Engrg., 1509 Univ. Ave., Madison, WI 53706 USA

Alloy phase selection is often controlled by nucleation during solidification of undercooled melts. The structure options are defined by thermodynamics, but the selection process is determined by a nucleation kinetics competition. During product phase transitions that develop with changing undercooling level or alloy composition, competitive nucleation can yield mixed phase microstructures as shown for rapid solidification of eutectics and glass forming alloys. Alternatively, at increasing rates, an initial solidification reaction can be superseded by a new nucleation controlled phase selection transition due to growth kinetic limitations that can develop during resolidification following surface melting or due to modification of heterogeneous nucleants. The complete analysis of solidification microstructure evolution during phase selection transitions also requires the consideration of solid-state reactions. The support of ARO (DAAD 19-01-1-0486) and NASA (NAG8-1672) are gratefully acknowledged.

## 3:30 PM Break

## 4:00 PM Invited

**Rapid Solidification Microstructures**: *Rohit K. Trivedi*<sup>1</sup>; <sup>1</sup>Iowa State University, Matls. Sci. & Engrg., 100 Wilhelm Hall, Ames, IA 50011 USA

During the past 20 years, significant theoretical and experimental contributions have been made by Wilfried Kurz that have advanced our understanding of microstructure evolution under rapid solidification conditions. These contributions are presented with specific emphasis on the application of the models to the data obtained by laser processing and by the solidification of fine droplets. Key concepts in the microstructure evolution under rapid solidifications that still remain to be addressed quantitatively will be discussed.

#### 4:30 PM

**Diffuse Solid-Liquid Interfaces and Solute Trapping**: *Reza Abbaschian*<sup>1</sup>; Wilfried Kurz<sup>2</sup>; <sup>1</sup>University of Florida, Matls. Sci. & Engrg., PO Box 116400, Gainesville, FL 32611 USA; <sup>2</sup>EPFL, Metallurgie Physics, MXG-Ecublens, CH 1015 Lausanne Switzerland

A phenomenological model is presented for partitioning of solute atoms across solid-liquid interface during solidification. The model treats the interface as being "diffuse", for which the transition from one phase to another takes place gradually when time-averaged over the entire layer of atoms parallel to the interface. For such an interface, the chemical potential of species also changes continuously from those in the liquid side of the interface to those in the solid. Moreover, the solute redistribution coefficient during solidification will depend on the diffuseness of the interface, which in turn is related to the interfacial peclet number. The latter is related to the interface velocity, its thickness and the overall migration rate on the solute trapping will be discussed and compared to other solute trapping models.

#### 4:45 PM

**Glass Forming Ability and Type of Eutectic-Coupled Zone**: Yong Zhang<sup>1</sup>; Hao Tan<sup>1</sup>; Dong Ma<sup>1</sup>; *Yi Li*<sup>1</sup>; <sup>1</sup>National University of Singapore, Dept. of Matls. Sci., Lower Kent Ridge Rd., Singapore 119260 Singapore

As the critical cooling rate for metallic glass formation has been reduced dramatically over the last ten years, e.g. 0.1 K/s for Pd based alloys, the microstructure control, particularly the primary dendrite plus amorphous matrix becomes possible by conventional solidification processing techniques, e.g. copper mould casting and directional solidification technique. Many crystalline reinforced metallic glass matrix in-situ composites by have been reported with improved mechanical properties. We report our experimental results on the formation of crystalline phase reinforced amorphous matrix in-situ composite and the microstructral changes in several novel bulk glass forming alloys, processed by Bridgman technique. The emphasis will be on the dendritic spacing, and volume fraction of the crystalline phases and their effect on the mechanical properties of these composites in Pd, La and Zr based amorphous forming alloys. We will also attempt to correlate glass forming ability and the microstructure changes with the types of the eutectic-coupled zone of these alloys.

#### 5:00 PM

**Optimum Stability in Rapidly Solidified Nickel-Based Alloys:** *Paul R. Algoso*<sup>1</sup>; William H. Hofmeister<sup>1</sup>; Robert J. Bayuzick<sup>1</sup>; <sup>1</sup>Vanderbilt University, Chem. Engrg., VU Sta. B 351604, Nashville, TN 37235-1604 USA

Solidification velocities of various nickel-based alloys were measured as a function of undercooling. A leveling in the solidification velocity (or 'plateau') was observed at intermediate undercoolings due to the presence of solute. This result does not agree with the IMS model (Ivantsov solution with marginal stability arguments), which relates dendrite growth velocity to total undercooling. The IMS model does not predict a velocity plateau at intermediate undercoolings for alloys with a sufficiently high equilibrium partition coefficient,  $k_{\rm E}{>}0.1$ , although a plateau exists for a wide range of alloys regardless of the value of  $k_{\rm E}$ . The disagreement between the IMS model and experiment is due to the restriction of the marginal stability parameter to a constant,  $\sigma^*=0.025$ . Another interfacial stability model, the optimum stability conjecture (OSC), allows for  $\sigma^*$  to vary as a function of Peclet number,  $\sigma^*=\sigma^*(\rm Pe)$ . The OSC exhibits excellent agreement with experimental results.

## 5:15 PM

Nonequilibrium Phase Selection During Weld Solidification of Fe-C-Mn-Al Steels: Sudarsanam Suresh Babu<sup>1</sup>; John M. Vitek<sup>1</sup>; John W. Elmer<sup>2</sup>; Stan A. David<sup>1</sup>; <sup>1</sup>Oak Ridge National Laboratory, M&C Div., 1 Bethel Valley Rd., Bldg. 4508; MS 6096, Oak Ridge, TN 37831-6096 USA; <sup>2</sup>Lawrence Livermore National Laboratory, Livermore, CA USA

The phase selection phenomena as a function of composition and interface growth velocity were investigated in Fe-0.2C-0.5Mn-Al (wt.%) self-shielded flux cored arc weld metal deposits. Two aluminum concentrations (1.8 and 3.7 wt.%) were investigated to observe different  $\delta$ -ferrite stabilizing effects on the microstructure. Under normal weld cooling conditions, the primary solidification in these steels occurs by  $\delta$ -ferrite formation, however, solidification morphology changes at high cooling rates. The changes in weld cooling rates were produced by changes in the arc welding conditions, and it was shown that, above a critical interface velocity, a shift was induced in the primary solidification mode to nonequilibrium austenite. Moreover, the change in primary solidification mode occurred irrespective of aluminum concentration. The above phase selection phenomenon was tracked insitu using a time-resolved X-ray diffraction technique employing Synchrotron radiation. Using the theoretical treatment of dendritic solidification and phase selection maps advanced by Kurz and his co-workers, the microstructure evolution at high weld solidification rates was evaluated. The dendrite growth theories for multicomponent solidification suggest that phase selection in this alloy system may be closely related to high carbon concentrations in these steels that cannot be trapped in the  $\delta$ -ferrite phase at high solid-liquid interface velocities. This in-turn leads to enrichment of carbon in the liquid phase and the subsequent change in primary solidification mode from primary δferrite to nonequilibrium austenite. Research sponsored by the U.S. Department of Energy, Division of Materials Sciences and Engineering under contract Number DE-AC05-00OR22725 with UT-Battelle, LLC. A portion of this work was performed under the auspices of the U. S. Department of Energy, Lawrence Livermore National Laboratory, under Contract No. W-7405-ENG-48.

#### 5:30 PM

Femtosecond Laser Micromachining of Superalloy Single Crystals: *Q. Feng*<sup>1</sup>; Y. N. Picard<sup>1</sup>; H. Liu<sup>2</sup>; S. M. Yalisove<sup>1</sup>; G. Mourou<sup>2</sup>; T. M. Pollock<sup>1</sup>; <sup>1</sup>University of Michigan, Dept. of Matls. Sci. & Engrg., 2300 Hayward St., Ann Arbor, MI 48109 USA; <sup>2</sup>University of Michigan, Ctr. for Ultrafast Optical Sci., 2200 Bonisteel Blvd., Ann Arbor, MI 48109 USA

Femtosecond laser micromachining with ultrafast laser pulses is attractive for a range of applications in manufacturing and life sciences, where minimal collateral damage, a limited heat affected zone and high precision processing are required. One potential application is the drilling of cooling holes in aircraft engine components, such as turbine blades and vanes. Femtosecond laser micromachining of Nibased superalloy single crystals and thermal barrier coated (TBC) superalloys have been carried out on a laser system using a series of 780nm wavelength, 150fs pulse-length laser shots. Microstructural analyses of regions machined with multiple pulses revealed no indication of negative effects such as microcracking and remelting layers in the vicinity of the laser-machined holes. Further, the studies were conducted using transmission electron microscopy (TEM). The damaged region near 5 µm diameter laser-machined holes drilled in prethinned TEM foils was less than 2  $\mu$ m and 0.5  $\mu$ m with the laser power intensity at 10 times ablation threshold and near the threshold, respectively. A high density of dislocations and dislocation networks were found inside the channels of the  $\gamma$  matrix within 4  $\mu$ m from the edge of holes. The deformation substructures of the samples will be compared to those observed in high temperature creep and high strain rate deformation.

## 5:45 PM

Microstructure Selection During Rapid Solidification of Al-Si Powder: Amber L. Genau<sup>1</sup>; Iver E. Anderson<sup>2</sup>; Rohit Trivedi<sup>2</sup>; <sup>1</sup>Iowa State University, 223 Metals Dvlp., Ames, IA 50011 USA; <sup>2</sup>Ames Laboratory, Ames, IA 50011 USA

Gas atomization techniques provide access to regions of extreme undercooling in metal alloys. The rapid solidification which occurs at such extremes often produces unique and desirable microstructures, while also presenting an opportunity to study the fundamental processes of nucleation and growth. Aluminum-silicon was chosen as a model for simple eutectic systems displaying a faceted/unfaceted interface. Fine droplets of Si-15Al and Si-18Al (wt. %) were produced using high-pressure gas (He) atomization. Quantitative measurements of eutectic spacing were made using SEM and TEM images of crosssectioned particles. The spacings were compared to those predicted by theoretical solidification models and a maximum undercooling was estimated for the particles. A variation in the selection of nucleation sites as a function of particle size was also observed. These results are analyzed to predict microstructure selection as a function of both

# Surfaces and Interfaces in Nanostructured Materials: Grain & Phase Boundaries

Sponsored by: Materials Processing and Manufacturing Division, MPMD-Surface Engineering Committee

*Program Organizers:* Sharmila M. Mukhopadhyay, Wright State University, Department of Mechanical and Materials Engineering, Dayton, OH 45435 USA; Arvind Agarwal, Florida International University, Department of Mechanical and Materials Engineering, Miami, FL 33174 USA; Narendra B. Dahotre, University of Tennessee, Department of Materials Science & Engineering, Knoxville, TN 37932 USA; Sudipta Seal, University of Central Florida, Advanced Materials Processing and Analysis Center and Mechanical, Materials and Aerospace Engineering, Oviedo, FL 32765-7962 USA

Tuesday PM	Room:	217A		
March 16, 2004	Location	: Charlotte	Convention	Center

*Session Chairs:* Sharmila M. Mukhopadhyay, Wright Sate University, Dept. of Mech. & Matls. Engrg., Dayton, OH 45435 USA; Sudipta Seal, University of Central Florida, Advd. Matls. Procg. & Analysis Ctr., Oviedo, FL 32765-7962 USA

## 2:00 PM Invited

Nanoanalysis of Advanced Materials: *Manfred Rühle*<sup>1</sup>; <sup>1</sup>MPI für Metallforschung, Heisenbergstr. 3, Stuttgart 70569 Germany

Advanced materials are mostly designed so that they possess specific properties for specific applications. Quite often it is also important that the overall dimensions of a component made out of advanced materials is small since for many applications, e. g. in telecommunication systems and microelectronics, only restricted space is available. In addition, often nanomaterials are also used as advanced materials. For nanomaterials at least one dimension of the component is in the nanometer scale. By advanced TEM techniques the structure and composition of specific areas of nanomaterials can be analyzed to the atomic level. The most interesting areas are concentrated around crystal lattice defects, such as interfaces, dislocations, etc. In the presentation recent results, opportunities and limitations of advanced TEM techniques will be described.

#### 2:25 PM Invited

Dislocations, Dislocation Boundaries and High Angle Boundaries in Nanocrystalline Copper Deformed by Sliding: Darcy A. Hughes<sup>1</sup>; Niels Hansen<sup>2</sup>; <sup>1</sup>Sandia National Laboratories, PO Box 969, MS 9405, Livermore, CA 94551-0969 USA; <sup>2</sup>Riso National Laboratory, Ctr. for Fundamental Rsch., Metal Structures in Four Dimensions, PO Box 49, Roskilde Denmark

Quantitative measurement and analysis of structural parameters have shown that the microstructural evolution follows a universal path of grain subdivision down to the nanoscale. This behavior has allowed an analysis of the formation and evolution of graded nanoscale structures produced by sliding. Transmission electron microscopy studies and scaling analyses of such these structures show the dominating role of dislocations in the development of deformation microstructures at multiple length scales. The crucial role of dislocations has been documented by high resolution electron microscope (HREM) analysis which has revealed the presence of a large number of glide dislocations in layers between boundaries with indivdiual spacing a fine as 5 nm. HREM has also been used to survey the structure of dislocation and high angle boundaries including grain orientation, boundary misorientation angle and boundary width. This work was supported by the Office of Basic Energy Sciences, the U.S. D.O. E. under contract no. DE-AC04-94AL85000.

#### 2:50 PM

Atomistic Modeling of Point Defects and Diffusion in Grain Boundaries: Akira Suzuki<sup>1</sup>; Yuri Mishin<sup>1</sup>; <sup>1</sup>George Mason University, Sch. of Computational Scis., 4400 Univ. Dr., MS 5C3, Fairfax, VA 22030-4444 USA

A variety of atomistic simulation techniques have been applied to study point defects and diffusion in metallic grain boundaries and the impact of grain-boundary kinetics on the materials behavior. The simulations have been performed for Al, Cu, and the Cu-Ag system. Atomic interactions are modeled by embedded-atom potentials fit to both experimental and first-principles data. Atomic mechanisms of vacancy and interstitial formation and migration in a large set of grain boundaries have been studied by molecular dynamics and other methods. New structural forms of point defects have been found, such as unstable vacancies and delocalized vacancies and interstitials. Besides the standard vacancy mechanism, grain boundary diffusion is often mediated by collective processes involving 2-4 atoms. The diffusion coefficients in grain boundaries calculated by molecular dynamics and kinetic Monte Carlo simulations compare well with experimental data. Possible mechanisms of defect formation and migration in non-equilibrium grain boundaries are discussed.

## 3:10 PM Break

#### 3:30 PM

Differences in Lattice Constant Between the <100> and <111> Oriented Grains in Nanocrystalline Ni and Ni-20 % Fe Electrodeposits: Dong Nyung Lee<sup>1</sup>; <sup>1</sup>Seoul National University, Rsch. Inst. of Advd. Matls., Seoul 151-742 Korea

Park et al. (2002)measured the deposition and annealing textures of nanocrystalline 30 mm thick Ni and 20 mm thick Ni-20 % Fe electrodeposits obtained from Watts-type solutions (nickel chloride, iron sulfate, boric acid, saccharine and other additives) using an x-ray diffraction method. They found that the deposition texture of major <100> + minor <111> changed to the texture characterized by major <100> + minor <100> after annealing. They also found that the lattice constants of the <100> oriented grains in the as-deposited state are larger than those of the <111> oriented grains, which were measured by a Synchrotron x-ray diffraction of 8C1 POSCO beam line. In this paper, a model has been advanced to explain the unusual results of lattice constants and the texture transition after annealing has been discussed based on differences in grain boundary energy and mobility between the <100> and <111> oriented grains.

#### 3:50 PM Invited

Lattice Microstrain and Grain Boundary Structure in a Nanocrystalline Al Alloy Prepared Via Mechanical Alloying: Alexandre L. Vasiliev<sup>1</sup>; Angel L. Ortiz<sup>2</sup>; Leon L. Shaw<sup>1</sup>; <sup>1</sup>University of Connecticut, Metall. & Matls. Engrg., Storrs, CT 06269 USA; <sup>2</sup>Universidad de Extremadura, Depto. de Electrónica e Ingeniería Electromecánica, Badajoz 06071 Spain

Lattice microstrains in a nanocrystalline Al93Fe3Cr2Ti2 alloy prepared via mechanical alloying (MA) starting from elemental powders have been investigated through the X-ray diffraction (XRD) Rietveld method coupled with the line-broadening analysis. The microstrains so-determined are related to the structure in the interiors and at the grain boundaries of the nanograins determined via transmission electron microscopy (TEM) and high-resolution electron microscopy (HREM). Although the nanograins are produced via severe plastic deformation, the interiors of the nanograins are free of dislocations. The high lattice microstrains produced in these nanograins are attributed to lattice bending induced by the stresses imposed by the nonequilibrium grain boundaries. Annealing at intermediate temperatures results in more stable grain boundary structure and thus lower lattice microstrains.

## 4:15 PM

Interface-Controlled Nanocrystal Phase Transformations: Gerhard Wilde<sup>1</sup>; Peter Bunzel<sup>1</sup>; Harald Roesner<sup>1</sup>; Ruslan Z. Valiev<sup>2</sup>; Jörg Weissmueller<sup>1</sup>; <sup>1</sup>Forschungszentrum Karlsruhe, Inst. of Nanotech., PO Box 3640, Karlsruhe 76021 Germany; <sup>2</sup>Ufa State Aviation University, Inst. of Physics of Advd. Matls., Ufa 450 000 Russia

The impact of interface properties and - more specifically - of the morphology of the interface of matrix-encased metallic nanoparticles on macroscopic properties such as the melting behavior has been investigated experimentally by a combination of microscopic, microanalytical and calorimetric measurement methods. In order to elucidate the interface contribution clearly, material of identical chemical composition has been synthesized by mechanical attrition or, alternatively, by rapid melt quenching. Additionally, thermal annealing and high-pressure torsion straining have been applied to modify the interface morphology for the differently pre-treated material in order to investigate the reversibility of the relation between interface morphology and macroscopic materials properties. As one result, the measurements clearly indicate that the shift of the melting temperature at small system size is thermodynamic in nature, as opposed to explanations based on nucleation kinetics. In addition, internal interfaces become important if multiphase alloy nanoparticles are concerned. Here, first results on the constitutive behavior of nanoscaled binary alloy systems will be discussed. This work is supported by the DFG under contract no. WI 1899/2-2.

## 4:35 PM

Grain Boundary Dissociation in Nanocrystalline Gold: *Dou*glas L. Medlin<sup>1</sup>; G. A. Lucadamo<sup>1</sup>; D. Cohen<sup>1</sup>; S. M. Foiles<sup>2</sup>; 'Sandia National Laboratories, Thin Film & Interface Sci. Dept., MS 9161, 7011 East Ave., Livermore, CA 94551 USA; 'Sandia National Laboratories, Matls. & Proc. Modlg. Dept., MS 1411, Albuquerque, NM 87185 USA

A common structural relaxation at grain boundaries in low stacking-fault-energy metals is the dissociation of the interface into dense arrays of stacking faults. This phenomenon is of particular importance in nanocrystalline materials because it increases the volume fraction of material associated with interfacial sites and because the constraints of geometric compatibility in such small-grained systems can locally promote the dissociation. Here, using HRTEM observations and atomistic simulations, we consider the structure of dissociated boundaries in nanocrystalline, [110]-textured Au films. We discuss how the specific interfacial stacking in dissociated layers is connected to the intergranular misorientation via the geometric properties of Shockley partial dislocations. To illustrate, we examine the specific orientations that lead to 9R and HCP stacking. This work is supported by the U.S. Department of Energy under contract No. DE-AC04-94AL85000 by the Office of Basic Energy Science, Division of Materials Science.

# Symposium on Microstructural Stability in Honor of Prof. Roger D. Doherty: Microstructural Stability: Precipitation and Other Topics

Sponsored by: Aluminum Association, Materials Processing and Manufacturing Division, Structural Materials Division, MPMD-Solidification Committee, SMD-Physical Metallurgy Committee *Program Organizer:* Anthony D. Rollett, Carnegie Mellon University, Department of Materials Science & Engineering, Pittsburgh, PA 15213-3918 USA

Tuesday PM	Room:	216A	
March 16, 2004	Location	: Charlotte Conve	ntion Center

Session Chair: A. K. Vasudevan, Office of Naval Research, Arlington, VA USA

## 2:00 PM

Modeling the Dispersoid Effect on Recrystallization in Hot Deformed Aluminum Alloys: Jaakko P. Suni<sup>1</sup>; <sup>1</sup>Alcoa, Inc., Alcoa Techl. Ctr., 100 Techl. Dr., Alcoa Ctr., PA 15069 USA

A model framework, involving evolutionary size distributions of subgrains and recrystallized grains is described, including the effect of fine particle drag. The model is applied to a well characterized data set, consisting of different dispersion levels for commercially hot rolled aluminum alloy 3004. In this case, the normal Zener drag term is inadequate, in that substantially more drag is required to fit recrystallization kinetic data than is provided by the standard equation. Similarly, fitting recovery data using an evolved mean subgrain size also requires greater dispersoid drag than is normally obtained. By simply increasing the Zener drag by a factor 3-4, improvement can be obtained in the fit to this particular kinetic data. However, the effect of dispersion on recrystallized grain size is not well fit in this case. These results, in addition to other work in the literature, suggest that the drag provided by dispersoids on recovery, recrystallization and even normal grain growth is not well understood. Specifically, it appears that different mathematical treatment may be required for the drag situation pertaining to differences in grain size, misorientation and stored energy. An attempt is made to illustrate these requirements, within the context of an evolutionary model comprising recovery, recrystallization and normal grain growth.

### 2:40 PM

High Temperature Control of Recrystallization in Wrought Al Alloys Using Sc and Zr: Yancy W. Riddle<sup>1</sup>; <sup>1</sup>Worcester Polytechnic Institute, MPI/Advd. Casting Rsch. Ctr., 100 Inst. Rd., Worcester, MA 01609-2280 USA

Addition of dispersoid-forming elements to aluminum alloys has long been recognized as a route leading to successful retention of strain-hardened microstructure and restricted grain growth. Potency of resultant dispersoids depends largely on volume fraction, spatial dispersion, and coarsening rate. In practice it is also important to understand the effect of the dispersoid-forming elements on processing and, of course, economics. To date addition of Zr, which can form metastable Al3Zr with L12 structure, has proven itself as one of the most effective dispersoids currently in use. Recent research established Sc addition and its Al3Sc dispersoid, also with L12 structure, as a powerful recrystallization inhibitor. However both Zr and Sc also have undesirable characteristics. The current research seeks to enhance effectiveness of dispersoids by leveraging the benefits from combined addition of both Zr and Sc. Ironically one way this benefit is realized is by demoting detrimental properties associated with Zr and/or Sc in Al using synergistic effects. Alloys with significantly higher recrystallization resistance in both temperature and time have been created using this alloy development approach. This paper will discuss how increased recrystallization resistance and restricted grain growth resulting from the Al3(Sc,Zr) dispersoids is more effective then either Al3Zr or Al3Sc dispersoids acting alone. Discussion will include effects in basic alloy systems of Al-(Zr)-(Sc) as well as practical implications in many of the wrought alloy systems.

## 3:20 PM

Influence of Predeformation on Precipitation Kinetics and Ageing Behavior of the AA6022 Alloy: Reza Shahbazian Yassar<sup>1</sup>; David Paul Field<sup>1</sup>; <sup>1</sup>Washington State University, Sch. of Mech. & Matls. Engrg., Spokane St., Pullman, WA 99163-2920 USA

During the industrial hot deformation of heat treatable aluminum alloys, both precipitation reactions and development of dislocation structure occur simultaneously. These processes are coupled which makes it difficult to define a physically based model for the microstructure evolution. The aim of this paper is to investigate the effect of dislocation structure on precipitate morphology and mechanical properties of an Al-Mg-Si alloy (AA6022) by using DSC, TEM and hardness measurements. Selected samples were subjected to different level of deformation before ageing treatment. The evolution of precipitates morphology and ageing characteristics of the predeformed samples in comparison to undeformed samples has been investigated. It is found that pre-deformation has a significant effect on precipitation sequences and volume fraction of precipitates. Also in the case of predeformed samples, a decrease in peak hardness has been seen.

## 3:50 PM

Improvements in Modeling Quench Sensitivity of Aluminum Alloys Via C-Curves and Their Application to 2090-T8 Plate: *Murat Tiryakioglu*<sup>1</sup>; James T. Staley<sup>2</sup>; Ralph T. Shuey<sup>3</sup>; <sup>1</sup>Robert Morris University, Dept. of Engrg., John Jay Engrg. Lab., Moon Twp., PA 15108 USA; <sup>2</sup>Retired, Durham, NC USA; <sup>3</sup>Alcoa, Inc., Alloy Tech., Alcoa Ctr., PA 15069 USA

We discuss the recent progress we have made in modeling quench sensitivity of heat-treatable aluminum alloys by using C-curves. Instead of allowing all the coefficients in the critical time, Ct, equation, we propose the use of independent thermodynamic data for two of the constants. In addition, we introduce a physically-based ómin equation to represent the growth limit. Following this new approach, we reanalyze the data for 2090-T8 plate, used by Staley, Doherty and Jaworski in their 1993 publication. We highlight the additional insight about the physical metallurgy of the alloy gained by the improved model. We also discuss extrapolations into modeling fracture toughness by C-curves.

#### 4:20 PM

Orientation Imaging Microscopy of Deformation in Extruded Al3Mg and 6063 Aluminum Alloys: *Raja K. Mishra*<sup>1</sup>; Anil K. Sachdev<sup>1</sup>; Clyde L. Briant<sup>2</sup>; <sup>1</sup>General Motors, R&D Ctr., MC 480-106-212, 30500 Mound Rd., Warren, MI 48090 USA; <sup>2</sup>Brown University, Div. of Engrg., Providence, RI 02912 USA

In this paper we use orientation imaging to examine the differences in deformation in 6063 and Al3Mg aluminum alloys. We show that in the 6063 material the deformation proceeds by dislocation rearrangement into subgrains and ultimately to localization in planar arrays. These arrays are precursors to shear band formation and failure. In the Al3Mg alloy, deformation leads to grain break up, grain rotation and grain elongation that, in combination, alter the microtexture and texture and determines the failure mechanism. These results compare well with previous TEM studies while providing important insight into deformation mechanisms and initiation of instability. We demonstrate that much of the information obtained by TEM can be deduced from these OIM studies that examine a much larger volume of material.

#### 4:50 PM

Microstructure Design Employing 2-Point Correlation Functions: Brent Larsen Adams<sup>1</sup>; <sup>1</sup>Brigham Young University, Mech. Engrg., 435 CTB, Provo, UT 84602 USA

Continua with microstructure can be described by (spatial) correlation functions of the local state variables (order parameters). Advances in a spectral representation of the 2-point correlation functions are described, including application to the problem of microstructure design. A conservation relationship is obtained as a necessary condition on the physical realizability of 2-point correlations in representative volumes of finite size. The implications of the conservation relationship are explored in terms of solutions for optimal elastic/ plastic properties obtained by sequential quadratic programming.

# 5:20 PM

#### Environmental Effects on the Resistance of Long Fatigue Cracks: A. K. Vasudevan<sup>1</sup>; K. Sadananda<sup>2</sup>; <sup>1</sup>Office of Naval Research, Arlington, VA USA; <sup>2</sup>Naval Research Labs., Washington, DC USA

Environment affects the kinetics of fatigue crack growth through the time and stress dependent processes. This is reflected in the reduction the Kmax component of the cycle compared to the DK. It is observed that the environmental effects on crack resistance falls broadly into four types of behavior, kinetics of each depending on the combination of time and stress. These four types of mechanisms seem to be common to most commercial materials. Examples of experimental results from Al- alloys and AERMET-100 steels will be presented to show these four processes on a DK-Kmax fatigue map. Such a map provides a tool to the basic understanding of the overall fatigue behavior of the alloys.

# The Didier de Fontaine Symposium on the Thermodynamics of Alloys: Interatomic Potentials and Cluster Expansion Techniques

Sponsored by: Materials Processing and Manufacturing Division, MPMD-Computational Materials Science & Engineering-(Jt. ASM-MSCTS)

*Program Organizers:* Diana Farkas, Virginia Polytechnic Institute and State University, Department of Materials Science and Engineering, Blacksburg, VA 24061 USA; Mark D. Asta, Northwestern University, Department of Materials Science and Engineering, Evanston, IL 60208-3108 USA; Gerbrand Ceder, Massachusetts Institute of Technology, Department of Materials Science and Engineering, Cambridge, MA 02139 USA; Christopher Mark Wolverton, Ford Motor Company, Scientific Research Laboratory, Dearborn, MI 48121-2053 USA

Tuesday PMRoom: 216BMarch 16, 2004Location: Charlotte Convention Center

Session Chair: TBA

#### 2:00 PM

Interatomic Bond-Order Potentials and Cluster Expansions: David G. Pettifor<sup>1</sup>; <sup>1</sup>University of Oxford, Dept. of Matls., Parks Rd., Oxford OX1 3PH UK

This talk will outline recent developments in the application of interatomic bond-order potentials (BOPS) to modelling the growth of semiconductor films and the defect properties of bcc transition metals and high temperature intermetallics. The link between BOPs and the cluster expansions at the heart of Didier de Fontaine's research will be explored.

## 2:30 PM

Atomistic Modeling of Extended Crystal Defects in Alloys: Vaclav Vitek<sup>1</sup>; <sup>1</sup>University of Pennsylvania, Dept. of Matls. Sci. & Engrg., 3231 Walnut St., Philadelphia, PA 19104 USA

Extended crystal defects, in particular grain boundaries and dislocations, govern mechanical properties of crystalline materials. This is particularly pronounced in alloys, where segregation to grain boundaries controls their propensity to fracture while dislocation glide often differs significantly from that in elemental solids even if their crystal structure is the same or very similar. This is the reason why atomistic modeling of extended defects has always been striving to tackle alloys although the majority of such calculations were invariably done for elemental solids as the first step. In this paper we shall reflect on the development of the atomistic modeling in metallic alloys in the last twenty years. In the first place we shall discuss the impact of the advancement of central-force many-body potentials, i. e. EAM and Finnis-Sinclair potentials, on such studies. As a specific example we present investigation of bismuth segregation to grain boundaries in copper and studies of segregation to grain boundaries in Ni3Al. The next important step in the development of the methods of description of interatomic forces is a more appropriate incorporation of the electronic structure effects, i. e. the chemistry of alloys. Obviously, this is

done most completely in DFT based calculations. However, those are rarely feasible for extended defects and the best alternative is at present methods based on the tight-binding approach. Specifically, bond-order potentials (BOPs) that are an order N method usable in real space. As examples we shall present recently developed BOPs for Ti-Al alloys, their application in studies of dislocations in TiAl with the L10 structure, as well as the development of BOPs for molybdenum silicides. In this context we shall discuss how essential is inclusion of directional bonds into the modeling of defects in alloys with mixed metallic and covalent bonding.

## 3:00 PM

Thermodynamics Emerging from Embedded Atom Models of Alloys: *Alfredo Caro*<sup>1</sup>; Patrice E.A. Turchi<sup>1</sup>; Edmundo Lopasso<sup>2</sup>; Magdalena Caro<sup>2</sup>; <sup>1</sup>Lawrence Livermore National Laboratory, Chmst. & Matls. Sci. Direct., PO Box 808 - L-371, Livermore, CA 94551 USA; <sup>2</sup>Centro Atomico Bariloche, Bariloche 8400 Argentina

Most of the large body of research using empirical potentials for MD simulations addresses properties of pure elements. Alloys have been difficult to model with the present degree of complexity of the potentials used. Basic thermodynamic properties, as the equilibrium crystal structure, are absent form the formalism and can only be incorporated in an indirect way. In most cases the thermodynamics that emerges from these empirical models is unknown. Here we present recent results on the computational calculation of the exact phase diagram of several binary alloys as described by widely used EAM potentials. These results clearly show the power and limitations of empirical potentials, as well as the need of more involved descriptions of cohesion in transition metals. We also discuss the possibility of using this information to help develop new potentials with known thermodynamic properties. Some applications to ultra fast solidification occurring in radiation-damaged materials are also presented.

#### 3:20 PM

Configurational Thermodynamics of the Sigma Phase in the Ru-W System: Chris C. Fischer<sup>1</sup>; Gerbrand Ceder<sup>1</sup>; Eric Wu<sup>1</sup>; <sup>1</sup>Massachusetts Institute of Technology, Dept. of Matls. Sci. & Engrg., 77 Mass. Ave., Rm. 13-4061, Cambridge, MA 02139 USA

Using a cluster expansion parameterization of configurational energetics obtained from ab initio calculations, thermodynamic stability in the Ru-W system is investigated. Finite temperature equilibration is performed with the Monte Carlo method. The Ru-W system, a phase separating system, displays finite temperature stability of the sigma phase. The sigma structure, a topologically close packed structure with space group P4sub2/mnm, presents a challenge with regard to the structure inversion method due to a large unit cell and/or lack of symmetry. While the structure of the sigma phase contains a large number of symmetrically distinct clusters, giving rise to challenges in the implementation of the cluster expansion, configurational energetics are likely dominated by short range interactions due to the topologically close packed character of the structure. Sources of error in the structure inversion method are discussed in the context of crossvalidation score, and effective cluster interaction variance. An algorithm for interaction selection is presented whose purpose is to minimize cross-validation, as implemented in the Alloy Theoretic Automated Toolkit, while maximizing robustness of fit.

#### 3:40 PM Break

#### 3:50 PM

Cluster Expansion Techniques to Describe Size Calibration of Nanostructures: *Hugues C. Dreysse*<sup>1</sup>; Vasyl Tokar<sup>2</sup>; <sup>1</sup>IPCMS, GEMME, 23 rue du Loess, Strasbourg 67034 France; <sup>2</sup>National Academy of Sciences, Inst. of Magnetism, 36-b Vernadsky str., Kiev-142 03142 Ukraine

In heteroepitaxy, a lattice size mismatch betweeen substrate and adlayer is common In this contribution, we propose an atomistic model for the growth of submonolayer. By assuming a coherent deposition, the systems is projected on a lattice gas model in a way similar to cluster expansion in the theory of alloy.<sup>1</sup> The 1D case has been solved exactly.<sup>2</sup> It is possible to show, that if the nearest-neighbors interaction is attractive and if the lattice size mismatch is large enough, at low temperature the atoms self assemble into size calibrated clusters. Moreover under certain conditions, the clusters display self-organisation. It is even possible to have self-assembly at finite temperature which vanishes at T =0K. <sup>1</sup>V. Tokar et H. Dreyssé, Comp. Mat. Sci.24 (2002) 72. <sup>2</sup>V. Tokar et H. Dreyssé, Phys. Rev. E (2003) under press.

**Origin of the Complex Wetting Behavior in Co-Pt Alloys**: *Yann M. Le Bouar*<sup>1</sup>; Annick Loiseau<sup>1</sup>; Alphonse Finel<sup>1</sup>; <sup>1</sup>CNRS-ONERA, LEM, 29, av de la Division Leclerc, BP 72, Chatillon 92322 France

In the Co-Pt system, a simple cooling experiment can drive a sample ordered in the tetragonal  $L1_0$  structure (CuAu type) close to the two-phase region involving  $L1_0$  and the cubic  $L1_2$  (Cu<sub>3</sub>Au type) structure. Using transmission electron microscopy observations, we show that interfaces in the  $L1_0$  structure are decorated: orientational domain walls are wetted by a single layer of  $L1_2$  structure whereas three macroscopic layers ( $L1_2/L1_0/L1_2$ ) appear at the antiphase boundaries. We then analyse this complex behavior in the framework of the Ising model with interactions limited to first and second nearest neighbors. The finite temperature properties of the various  $L1_0/L1_0$  interfaces are computed with a Low Temperature Expansion and Cluster Variation Method simulations in the inhomogeneous Tetrahedron-Octahedron approximation. The results are in full agreement with our experimental observations concerning the wetting of interfaces.

## 4:40 PM

## Cluster Expansion-Based Precipitate Modeling for Magnesium Alloys: Gus Hart<sup>1</sup>; <sup>1</sup>Northern Arizona University, Physics & Astron., PO Box 6010, Flagstaff, AZ 86011-6010 USA

We have generalized the reciprocal-space formulation of the cluster expansion approach to treat the long range strain effects in alloys of any crystal structure (not just cubic alloys as has been done previously). We use this improved approach to study precipitate formation (precipitate size vs. shape vs. temperature) in several common magnesium-based alloys.

## 5:00 PM

Cluster Expansion of bcc Al-Cu: The Role of Mechanical Instabilities: *Chao Jiang*<sup>1</sup>; Christopher Wolverton<sup>2</sup>; Zi-Kui Liu<sup>1</sup>; Long-Qing Chen<sup>1</sup>; <sup>1</sup>Pennsylvania State University, Matls. Sci. & Engrg., Univ. Park, PA 16802 USA; <sup>2</sup>Ford Research Laboratory, MD3028/ SRL, Dearborn, MI 48121 USA

First-Principles total energy calculations have shown that the bcc structure of both Al and Cu are mechanically unstable with respect to tetragonal deformations. Consequently, many bcc-based superstructures actually become fcc after full relaxation. This poses a serious problem for the cluster expansion of the Al-Cu bcc structure, which is stable in the Al-Cu system at high temperatures. In the present work, the total energies of all bcc-based superstructures are calculated by relaxing only the volume and cell-internal degrees of freedom. In this way, all structures still remain bcc. Using the obtained cluster expansions, Monte-Carlo simulations are performed to obtain the enthalpy of mixing of the bcc solution at various compositions and temperatures. The results are compared with direct calculations using Special Quasirandom Structures (SQS). The presence of SRO and the role of vibrational entropy is discussed.

# Third International Symposium on Ultrafine Grained Materials: Microstructure and Properties

Sponsored by: Materials Processing & Manufacturing Division, MPMD-Shaping and Forming Committee
Program Organizers: Yuntian Ted Zhu, Los Alamos National Laboratory, Materials Science and Technology Division, Los
Alamos, NM 87545 USA; Terence G. Langdon, University of
Southern California, Departments of Aerospace & Mechanical
Engineering and Materials Engineering, Los Angeles, CA 90089-1453 USA; Terry C. Lowe, Metallicum, Santa Fe, NM 87501 USA;
S. Lee Semiatin, Air Force Research Laboratory, Materials & Manufacturing Directorate, Wright Patterson AFB, OH 45433 USA;
Dong H. Shin, Hanyang University, Department of Metallurgy and
Material Science, Ansan, Kyunggi-Do 425-791 Korea; Ruslan Z.
Valiev, Institute of Physics of Advanced Material, Ufa State Aviation
Technology University, Ufa 450000 Russia

Tuesday PM	Room: 207A
March 16, 2004	Location: Charlotte Convention Center

Session Chairs: S. Lee Semiatin, Air Force Research Laboratory, Matls. & Mfg. Direct., Wright Patterson AFB, OH 45433 USA; Zhe Jin, Alcoa Technical Center, Alcoa Ctr., PA 15069 USA; Terry R. McNelley, Naval Postgraduate School, Dept. Mech. Engrg., Monterey, CA 93943-5146 USA

## 2:00 PM Invited

Structural and Mechanical Fatigue Properties of Nanostructured Cu Subjected to Severe Plastic Deformation: Kai Zhang<sup>1</sup>; Julia R. Weertman<sup>1</sup>; <sup>1</sup>Northwestern University, Matls. Sci. & Engrg., 2220 N. Campus Dr., Evanston, IL 60208 USA

Comparatively little is known and reported about the fatigue properties of nanocrystalline materials, in particular, effect of cyclic deformation on their internal microstructure. In the present work, an initial set of fatigue testing has been carried out on nanocrystalline Cu subjected to cryogenic cold-rolling and further thermal treatment. The primary goal is to study cyclic deformation and fatigue lifetimes in comparison with time-independent uniaxial tensile experiments. Results regarding microstructural stability and deformation mechanism during cycling are reported. This research was supported under US DoE grant DE-FG02-02ER46002.

## 2:20 PM

New Observations of High Strength and Ductility in SPD-Produced Nanostructured Materials: Ruslan Z. Valiev<sup>1</sup>; <sup>1</sup>Ufa State Aviation Technical University, Inst. of Physics of Advd. Matls., 12 K. Marx St., Ufa 450000 Russia

Bulk nanostructured metals with a mean grain size of about 50 -100 nm very often demonstrate high hardness but poor ductility. However, recent works demonstrate that very high strength and quite high ductility can be observed in nanostructured metals produced by severe plastic deformation (SPD). In this paper we show that the combination of high strength and ductility is originated not only from the presence of fine grains, but a structure of grain boundaries and internal stresses, as well as disperse precipitations of second phases. The origin of this phenomenon is considered and discussed in this work based on analysis of performed mechanical tests and thorough microstructural studies. High strength and ductility are of great engineering importance, in particular for attaining high fatigue properties and fracture toughness.

#### 2:35 PM

The Microstructure-Mechanical Properties Relationship of Ultrafine Grained Structural Materials Processed by Equal Channel Angular Pressing: *Dong Hyuk Shin*<sup>1</sup>; Byung Du Ahn<sup>1</sup>; Hyun Soo Cho<sup>1</sup>; Kyung Tae Park<sup>2</sup>; <sup>1</sup>Hanyang University, Dept. of Metall. & Matls. Sci., Ansan, Kyunggi-Do 425-791 Korea; <sup>2</sup>Hanbat National University, Div. of Advd. Matls. Sci. & Engrg., Taejon 305-719 Korea

During the past decade, the characterization of bulk ultrafine grained (UFG) structural materials processed by equal channel angular pressing (ECAP) has been one of the hottest subjects in the materials research field. However, UFG materials fabricated by ECAP exhibit both superior and inferior mechanical properties, as the prominent structural materials, compared to coarse grained ones. For instance, the superior mechanical properties are ultrahigh strength and exceptional high temperature ductility (i.e. superplasticity) and the inferior mechanical properties are a degraded strain hardening capability and low room

temperature ductility. In this study, the microstructure-mechanical properties relationship of UFG structural materials fabricated by ECAP will be reviewed in order to provide insight broadening their future applicability. In addition, recent effort overcoming their mechanical inferiorities will be addressed by referring various sources.

### 2:50 PM

TEM Observation of Strain Rate Dependent Dynamic Recrystallization of Ferrite in Low Carbon Steel: Seung Chan Hong<sup>1</sup>; Seung Ki Seo<sup>1</sup>; Chong Seung Yoon<sup>1</sup>; Kyung Jong Lee<sup>1</sup>; Dong Hyuk Shin<sup>1</sup>; Kyung Sub Lee<sup>1</sup>; <sup>1</sup>Hanyang University, Matls. Sci. & Engrg., 17 Haeng dang dong, Seong dong gu, Seoul 133-791 Korea

The dynamic recrystallization (DRX) of ferrite was investigated under different strain rates and initial grain sizes in low carbon steel. Hot compression tests were carried out at 735C ( $\alpha$ +  $\gamma$  region) by Gleeble 1500. The dislocation movement during the DRX was observed using a heating strain holder in TEM. The DRX of ferrite occurred by two different mechanisms depending on the strain rate. Below the strain rate of 0.1/s (Z= 3.29E13/s, Q: 280 kJ/mol), dynamic discontinuous recrystallization occurred via bulging of grain boundaries resulting in dislocation-free grains with a size of 5 um. As the strain rate increased to 5/s (Z=1.64E15/s), dynamic continuous recrystallization took place by clustering of dense dislocation walls which led to the progressive increase of the misorientation angles between sub-grains. As a result of the dynamic continuous recrystallization, much smaller ferrite grains with a size of 1 um were obtained.

## 3:05 PM

**Reciprocating Sliding Wear of Ultra-Fine Grained Ti-6Al-4V**: Eliana K.Y. Fu<sup>1</sup>; H. Chandana Bellam<sup>2</sup>; *H. J. Rack*<sup>2</sup>; Vladimir Stolyarov<sup>3</sup>; Ruslan Z. Valiev<sup>3</sup>; <sup>1</sup>Allvac, 2020 Ashcraft Ave., Monroe, NC 28110 USA; <sup>2</sup>Clemson University, Sch. of Matls. Sci. & Engrg., Clemson, SC 29634 USA; <sup>3</sup>Ufa State Aviation Technical University, Inst. of Physics of Advd. Matls., 12 K. Marx St., Ufa 450000 Russia

The reciprocating dry sliding wear performance of ultra-fine grained (UFG) Ti-6Al-4V (Ti-64) and annealed medical grade Ti-6Al-4V ELI against hardened steel have been investigated. Equal channel angular extrusion (ECAE) of Ti-64 to a true strain of 6.5 resulted in primary • grain refinement and increased microstructure homogeneity. This microstructure enhancement was found to result at a contact stress of 5 MPa, in a reduction of the dynamic friction coefficient. However little difference between the steady-state dry reciprocating sliding wear rate of UFG Ti-64 and medical grade Ti-64 was observed under high stress steady-state conditions. Indeed at low apparent stresses, 1.5 MPa, the dry reciprocating-sliding wear resistance of UFG Ti-64 was lower than annealed Ti-64. This difference in wear performance is consistent with the expected evolution of the surface and sub-surface microstructure in these two materials with increasing reciprocating sliding distance.

## 3:20 PM

The Effect of Mn on Microstructure and Mechanical Properties After Heavy Warm Deformation of C-Mn Steel: *Rongjie Songl*; Radko Kaspar<sup>1</sup>; Dirk Ponge<sup>1</sup>; Dierk Raabe<sup>1</sup>; <sup>1</sup>Max Planck Institute for Iron Research, Microstruct. Physics & Metal Forming, Max-Planck-St. 1, Duesseldorf, Nordrhein-Westfalen D-40237 Germany

The effect of Mn on the ferrite grain refinement has been investigated in plain 0.2%C-Mn steels after heavy warm deformation processed by plane strain compression. The final microstructure consists of spheroidized cementite within ultrafine grained ferrite matrix. It was observed that an increase in the Mn content from 0.7mass.% to 1.5 mass.% leads to a drop in the average ferrite grain size and to a change in grain shape from an elongated to a more equiaxed morphology. The fraction of high-angle grain boundaries changed from 55% to 74%. The ultimate tensile strength increased from 590MPa to 680MPa, while the total elongation of 18% was the same for both materials. EDS analysis revealed an enrichment of Mn in the fine cementite particles.

#### 3:35 PM

Microstructure of Austenitic and Ferritic Steels Produced by Severe Plastic Deformation and Subsequent Annealing: Andreas Vorhauer<sup>1</sup>; Reinhard Pippan<sup>1</sup>; Siegfried Kleber<sup>2</sup>; <sup>1</sup>Austrian Academy of Sciences, Erich Schmid Inst. of Matls. Sci., Jahnstrasse 12, Leoben A-8700 Austria; <sup>2</sup>Böhler Edelstahl GmbH & Co KG, Kapfenberg A-8605 Austria

In this paper an austenitic and a ferritic steel are subjected to SPD at room temperature ( $\sim$ 0.16Tm) followed by subsequent annealing. The aim of this materials processing is the refinement of the initially coarse microstructure. The microstructural change during SPD as a function of applied plastic strain (maximum 32) is analyzed for both steels by Back Scattered Electrons micrographs captured in a SEM.

The same microstructural analysis is performed for samples, which are annealed at different annealing parameters. A correlation between microstructure and mechanical properties at different states of materials processing is realized by subsize tensile tests. Additionally the microtexture of selected samples is measured by the automated Electron Back Scattering Diffraction method within a SEM. The size of the structural elements in the SPD state is clearly below 100nm. Appropriate thermal treatments transform these metastable deformation microstructures into more stable grained microstructures with grain sizes smaller than 500nm.

#### 3:50 PM Break

## 4:00 PM Invited

**Characterization of Nanocrystalline Materials by X-Ray Peak Profile Analysis:** *Tamás Ungár*<sup>1</sup>; <sup>1</sup>Eötvös University Budapest, Dept. of Gen. Physics, H-1518, POB 32, Budapest Hungary

During the past couple of years several research groups have spent extended efforts to improve the method of X-ray diffraction peak profile analysis (XDPPA) in order to characterize the microstructure of crystalline materials in terms of size and size-distribution and strain. As a result, a variety of different procedures are now available which enable this. The prerequisite for all different approaches is to start with best quality experimental data. These are either provided by high resolution synchrotron experiments, or by special high resolution laboratory diffractometers, possibly equipped by incident beam monochromators, or by well aligned Bregg-Brentano diffractometers using long enough counting periods. Model based evaluation approaches provide crystallite size distribution in terms of log-normal or gamma distributions and strain in terms of dislocations, stacking- or twin faults and in special cases disclinations. If large enough number of peaks are available, strain anisotropy enables the determination of slip systems or Burgers vector populations. In textured samples the dislocation structure in the individual texture components can also be evaluated.

#### 4:20 PM Invited

**Deformation and Recrystallization Textures of Shear Deformed 1050 Aluminum Alloy**: *Dong Nyung Lee*<sup>1</sup>; 'Seoul National University, Rsch. Inst. of Advd. Matls., Seoul 151-742 Korea

A study has been made of the deformation and recrystallization textures of aluminum alloy sheets deformed by ECAP. The ECAP was performed under varied shear deformation histories. The deformation textures of the sheets showed an inhomogeneous distribution through the thickness, even though they were mainly the shear deformation textures which can be approximated by the ND //{111} and {001}<110> components. The recrystallization textures of sheets ranged from weakened deformation textures to the cube texture depending on the density of cube component in the deformation texture. The deformation and recrystallization textures were discussed based on a texture simulation and the strain energy release maximization model, respectively.

#### 4:40 PM

Structure and Property Evolutions of ECAP Processed 7075 Al Alloy During Annealing: Yonghao Zhao<sup>1</sup>; Xiaozhou Liao<sup>1</sup>; Zhe Jin<sup>2</sup>; Ruslan Z. Valiev<sup>3</sup>; Yuntian T. Zhu<sup>1</sup>; <sup>1</sup>Los Alamos National Laboratory, Matl. Sci. & Tech. Div., MS G755, Los Alamos, NM 87545 USA; <sup>2</sup>Alcoa Technical Center, Alcoa Ctr., PA 15069 USA; <sup>3</sup>Ufa State Aviation Technical University, Inst. of Phys. of Advd. Matls., 12 K. Marx St., 450000 Ufa Russia

Microstructure and microhardness evolutions of ECAP-processed and coarse grained (CG) 7075 Al alloy during differential scanning calorimeter (DSC) annealing were investigated by x-ray diffraction (XRD), transmission electron microscopy (TEM) and microhardness measurements. Upon annealing, the microhardness of the ECAP processed sample decreases gradually, while there exists a hardening peak for the CG sample. XRD and TEM show that the hardening peak of the CG sample is mainly caused by the second phase precipitation hardening. For the ECAP processed sample, upon annealing the microstrain (dislocation density) decreases and the crystallites grow, which decrease the overall hardness in spite of precipitation strengthening. DSC analysis indicates that the ECAP process does not change the sequence of phase precipitation. It only changes the aging kinetics.

#### 4:55 PM

Microstructure and Mechanical Properties of Severely Deformed Ti-6Al-4V and Ti-6Al-4V+10%TiC Metal Matrix Composite: Guney Guven Yapici<sup>1</sup>; Ibrahim Karaman<sup>1</sup>; Zhiping Luo<sup>2</sup>; <sup>1</sup>Texas A&M University, Dept. of Mech. Engrg., MS 3123, College Sta., TX 77843 USA; <sup>2</sup>Texas A&M University, Microscopy & Imaging Ctr., College Sta., TX 77843 USA

The present work focuses on the severe plastic deformation of Ti-6Al-4V and Ti-6Al-4V reinforced with 10% TiC metal matrix composites using equal channel angular extrusion (ECAE). The initial materials that were manufactured by hot isostatic pressing of the alloy powders were canned in stainless steel and extruded non-isothermally through two channels of equal cross section intersecting at an angle of 90°. Microstructure and mechanical properties of successfully extruded billets were reported using light microscopy, transmission electron microscopy (TEM), tension and compression experiments and hardness measurements. The effects of extrusion conditions (temperature and processing route) on the microstructure and mechanical properties are investigated. ECAE shear deformation causes refinement in  $\alpha$  plates, elimination of prior ß boundaries without forming bimodal microstructures and thus possibly without alloy partitioning effect. Decreasing extrusion temperature and increasing number of passes decreases  $\alpha$ plate size and grain size, leading to significant increase in tensile and compressive flow stresses at room temperature. Tension/compression asymmetry in flow strengths and strain hardening coefficients is because of the activation of different deformation systems along tension and compression axis of the test samples.

## 5:10 PM

Synthesis of Ultrafine-Grained Alloys by Repeated Cold-Rolling: Guru Prasad Dinda<sup>1</sup>; Harald Roesner<sup>1</sup>; *Gerhard Wilde*<sup>1</sup>; <sup>1</sup>Forschungszentrum Karlsruhe, Inst. of Nanotech., PO Box 3640, Karlsruhe 76021 Germany

Repeated cold-rolling with intermediate folding represents a technique to obtain severe plastic deformation that avoids excessive heating at the internal interfaces and that proceeds without the simultaneous action of a high pressure in the range of several GPa. Aside from the opportunity to obtain amorphous bulk samples, the processing pathway also allows for synthesizing dense, bulk nanocrystalline materials. In the present work, massive Ni<sub>50</sub>Ti<sub>50</sub> samples with average grain sizes below 10 nm have been synthesized at ambient temperature using two different processing pathways that start from individual elemental sheets and, alternatively, from a pre-alloyed NiTi intermetallic compound. The development of the microstructure in dependence of deformation was investigated by X-ray diffraction and scanning and transmission electron microscopy. As one result, a cyclic cross-over between grain-size refinement and coarsening as a function of continuous strain energy input has been observed for Ni-Ti. The development of the nanoscale microstructure during intense deformation- including the early and the late stages of deformation-induced nanocrystal formation - is analyzed in terms of the major thermodynamic and mechanical properties that govern grain refinement and intermixing. This work is supported by the DFG under contract no. WI 1899/1-2.

## 5:25 PM

Microstructure Evolution to Nanometer Scale of 1200 and 3103 Aluminum Alloys Processed Via Equal Channel Angular Pressing: Marcello Cabibbo<sup>1</sup>; Enrico Evangelista<sup>1</sup>; Erik Nes<sup>2</sup>; <sup>1</sup>Polytechnic University of Marche, Dept. of Mech., Via Brecce Bianche, Ancona I-60131 Italy; <sup>2</sup>NTNU, Inst. of Matls. Tech., Alfred Guess GIT7, Trondheim VEI-2B Norway

The deformation processes occurring in two aluminum alloys (1200 and 3103) after Equal Channel Angular Pressing (ECAP) have been studied by means of TEM and EBSP techniques. Grains and subgrains spacing and misorientation evolution upon increasing ECAP passes were studied by EBSP on a FEGSEM, whilst the ultrafine and low-misorientation subgrain structure was studied by TEM. A nano-structure was achieved after 6 ECAP passes for both the materials and the High Angle Grain Boundary misorientation constantly increased reaching a 58% fraction among the total amount of boundaries. The mean subgrain misorientation was of 4-5° and the mechanism of transformation from Low-Angle Boundary subgrain to High-Angle Boundary grain, i.e. those higher than 15°, was documented via TEM inspections. Finally, the grain refining results attained through ECA pressing were compared to the published results in the Cold-Rolling of the same 1000 and 3000 aluminum alloy series.

## 5:40 PM

Structure of Martensite Transformed from Severely Deformed Austenite in Fe-28.5at.%Ni Alloy: *Hiromoto Kitahara*<sup>1</sup>; Takashi Kimura<sup>1</sup>; Nobuhiro Tsuji<sup>1</sup>; Yuichiro Koizumi<sup>1</sup>; Yoritoshi Minamino<sup>1</sup>; <sup>1</sup>Osaka University, Dept. of Adaptive Machine Sys., 2-1, Yamadaoka, Suita, Osaka 565-0871 Japan

Grain refinement of bulk materials by the SPD process followed by martensite transformation was investigated. Fe-28.5at.%Ni alloy sheets were severally deformed in austenite structure by the ARB process, and then cooled down to 77 K to cause martensite transformation. The

ARB processed sheets deformed to 4.0 of total equivalent strain were filled with the ultra-fine lamellar boundary structure having about 200 nm of average lamellar spacing. Martensite transformation starting temperature decreased with increasing the total equivalent strain. Martensite having characteristic morphologies appeared from the ultrafine lamellar austenite in the sheet ARB processed by 5 cycles, although martensite transformed from conventionally recrystallized specimens with several tens micrometers of grain sizes showed typical plate (lenticular) morphology. It was concluded that the grain refinement by martensite transformation from ultrafine grained austenite is possible but low-angle boundaries in the austenite are not effective for refinement by martensite transformation.

# WEDNESDAY

# 5th Global Innovations Symposium: Trends in LIGA, Miniaturization, and Nano-Scale Materials, Devices and Technologies: Properties, Processes, and Modeling

Sponsored by: Materials Processing & Manufacturing Division, MPMD-Powder Materials Committee, MPMD-Phase Transformations Committee-(Jt. ASM-MSCTS), MPMD-Computational Materials Science & Engineering-(Jt. ASM-MSCTS), MPMD/EPD-Process Modeling Analysis & Control Committee, MPMD-Surface Engineering Committee, MPMD-Shaping and Forming Committee, MPMD-Solidification Committee

Program Organizers: John E. Smugeresky, Sandia National Laboratories, Department 8724, Livermore, CA 94551-0969 USA; Steven H. Goods, Sandia National Laboratories, Livermore, CA 94551-0969 USA; Sean J. Hearne, Sandia National Laboratories, Albuquerque, NM 87185-1415 USA; Neville R. Moody, Sandia National Laboratories, Livermore, CA 94551-0969 USA

Wednesday AM	Room:	20	)2B		
March 17, 2004	Location	n:	Charlotte	Convention	Center

Session Chairs: Andy Minor, Lawrence Berkeley National Laboratory, Matls. Sci. Div., Berkeley, CA 94720 USA; Tom Buchheit, Sandia National Laboratories, Albuquerque, NM 87185 USA

#### 8:30 AM

Integrating Scientific Disciplines for Future Nanotechnologies: *John Charles Barbour*<sup>1</sup>; <sup>1</sup>Sandia National Laboratories, Nanostruct. & Semiconductor Physics, MS 1415, Org 1112, Albuquerque, NM 87185-1415 USA

Future technologies will rely on a complex integration of materials and functionalities that bridge several length scales to connect nanometer-scale architectures to the real world of man. The Center for Integrated Nanotechnologies (CINT), which is operated jointly by Sandia National Laboratories and Alamos National Laboratory, has a unique technical vision focused on integrating scientific disciplines and expertise across multiple length scales, and can therefore address the nanoscience challenges of coupling the nano- and micro-length scales. The core disciplines within CINT include: Nanomechanics, Nano-biomicro Interface, Nanoelectronics/photonics, Complex Functional Materials, and Simulation and Modeling. This talk will present examples from these disciplines where the performance of existing microsystems has been improved by adding nanoscience, and where work is proceeding to understand fundamental mechanisms which govern properties of future nanosystems. This work is supported by the DOE Office of Basic Energy Sciences. Sandia is multiprogram laboratory operated by Sandia Corporation under contract DE-AC04-94AL85000.

#### 9:00 AM

Mechanical Characterization of Nanoscale Gold Beam Structures Using AFM and Nanoindentation Techniques: Xiaodong Li<sup>1</sup>; Patrick Nardi<sup>1</sup>; Chang-Wook Baek<sup>2</sup>; Jong-Man Kim<sup>2</sup>; Yong-Kweon Kim<sup>2</sup>; <sup>1</sup>University of South Carolina, Dept. of Mech. Engrg., 300 Main St., Columbia, SC 29208 USA; <sup>2</sup>Seoul National University, Sch. of Elect. Engrg. & Compu. Sci., San 56-1, Shillim-Dong, Kwanak-ku, Seoul 151-742 S. Korea

In the design of micro/nanoelectromechanical systems (MEMS/ NEMS) devices, mechanical properties of the MEMS/NEMS building structures are essential because most material properties are known to be size-dependent. Mechanical characterization of nanoscale gold beams with widths ranging from 200 to 500 nm has been carried out. Hardness and elastic modulus of the unreleased beams were measured using a nanoindenter. Bending tests were performed on the released cantilever and fix-fix beams using a nanoindnter in conjunction with an atomic force microscope (AFM). Residual stress in the beams was measured. Effect of residual stress on the mechanical properties is discussed. Deformation behavior of the beams was studied using a scanning electron microscope and finite element analysis.

#### 9:20 AM

Mechanical Behavior and Oxidation of Pt-Ir Alloy Thin Films: Richard R. Chromik<sup>1</sup>; Thirumalesh Bannuru<sup>1</sup>; Walter L. Brown<sup>1</sup>; Richard P. Vinci<sup>1</sup>; <sup>1</sup>Lehigh University, Dept. of Matls. Sci. & Engrg., 5 E. Packer Ave., Bethlehem, PA 18015 USA

MEMS applications often require novel electrode materials with both robust electrical and mechanical properties. Stress relaxation and morphological stability present problems, especially at high temperatures. Alloying is sometimes used to address these issues, but its effectiveness in thin films may be reduced from that of bulk alloying. The mechanical behavior of oxidized and unoxidized Pt-Ir thin films have been studied, where oxide dispersion strengthening and solid solution strengthening are expected respectively. Alloy films were fabricated by sputter co-deposition with compositions ranging from 0 to 25at% Ir, as measured by x-ray photoelectron spectroscopy (XPS). Mechanical properties of the films were measured by nanoindentation and wafer curvature. For unoxidized specimens, solid solution strengtheing was observed, where films with higher Ir content exhibited higher hardness. Oxidation studies were carried out to form Ir oxide particles and examine the dispersion strengthening mechanisms as well.

## 9:40 AM

Deformation Mechanisms in Nanostructured Aluminum Alloys Processed by Cryomilling Techniques: Bing Q. Han<sup>1</sup>; Enrique J. Lavernia<sup>1</sup>; <sup>1</sup>University of California, Chem. Engrg. & Matls. Sci., Davis, CA 95616 USA

Cryomilling process is proven to be an effective approach to process bulk nanostructured aluminum alloys. In the present study, microstructural characteristics and deformation behavior of bulk nanostructured aluminum alloys processed via consolidation of cryomilled powders were reviewed. The microstructure of supersaturated solid solution with equiaxed grains from 50 nm to 300 nm was observed in several as-extruded cryomilled Al alloys. Tensile behavior was characterized by high strength and low strain hardening. The high strength at room temperature was primarily attributed to three types of strengthening: grain size effect, solid solution hardening and Orowan strengthening. Cryomilled Al-Mg alloys with bimodal microstructure show both high strength and improved ductility.

#### 10:00 AM Break

#### 10:20 AM

Tension/Compression Asymmetry, Anisotropy and Size Effects in the Plastic Deformation of Ti-6242 Single Colonies: Dave M. Norfleet<sup>1</sup>; Michael J. Mills<sup>1</sup>; Michael D. Uchic<sup>2</sup>; Mike F. Savage<sup>3</sup>; Joe Tatalovich<sup>1</sup>; <sup>1</sup>Ohio State University, Matls. Sci. & Engrg., 477 Watts Hall, 2041 College Rd., Columbus, OH 43210 USA; <sup>2</sup>Air Force Research Laboritory, Matls. & Mfg. Direct., Wright Patterson AFB, Dayton, OH 45433 USA; <sup>3</sup>Pratt & Whitney, E. Hartford, CT 06108 USA

The constant strain rate deformation behavior of individual ??? colonies of the titanium aeroengine alloy Ti-6Al-2Sn-4Zr-2Mo-0.1Si (composition in wt.%) has been studied through an ultra small-scale compression technique. Using a FEI Dual Beam Focused Ion Beam, cylindrical compression samples were micromachined into the gripends of sub-millimeter-scale samples that previously had been tested in tension. Thus, one goal of the work is determine if a pronounced tension/compression asymmetry exists for these single colony crystals, while performing the test on the same samples and using the same deformation axis. Six single colony crystal orientations are being explored, associated with single slip in the HCP alpha phase along the three distinct a-type slip systems on both basal and prism planes. The compression samples, having diameters ranging from 10 to 35 microns, were mechanically tested using an MTS Nano Indenter XP fitted with a flat tip to apply uniaxial compression at a constant strain rate. The effect of sample size on the flow properties will be discussed. The resulting data will be correlated with tensile results, and TEM studies will be presented.

### 10:40 AM Cancelled

Average Stresses in Simulated Thin Films

#### 11:00 AM

Molecular Dynamics Simulation of Dislocation Formation During Vapor Deposition of Multilayers: Xiaowang Zhou<sup>1</sup>; Haydn N.G. Wadley<sup>1</sup>; <sup>1</sup>University of Virginia, Dept. of Matls. Sci. & Engrg., Charlottesville, VA 22903 USA

Molecular dynamics has been used to study dislocation formation during NiFe/Au/NiFe/Au and CoFe/NiFe/CoFe/Cu multilayer deposition. A direct nucleation of misfit dislocations on (111) interfaces was observed in the NiFe/Au/NiFe/Au system. Both dislocation configuration and density were in good agreement with HRTEM experiments. A misfit energy increasing dislocation structure was found in the simulated CoFe/NiFe/CoFe/Cu multilayers. It formed by atomic assembly mechanisms. During deposition on the (111) surface of an f.c.c. lattice, adatoms may either occupy f.c.c. sites or h.c.p. sites. This results in partial dislocations at the f.c.c and h.c.p. domain boundaries. These boundaries tend to have missing atoms, and therefore, a later deposited layer tends to have less planes compared to a previously deposited layer. This effect is negligible for large lattice mismatch systems such as NiFe/Au, but is relatively significant for small lattice mismatch systems such as CoFe/NiFe. Growth conditions affecting dislocations are discussed.

## 11:20 AM

Molecular Dynamics Simulations of Single Asperity Contacts: Monotonic and Cyclic Loading: *Pil-Ryung Cha*<sup>1</sup>; David J. Srolovitz<sup>1</sup>; <sup>1</sup>Princeton University, Dept. of Mech. & Aeros. Engrg., Princeton Matls. Inst., 70 Prospect Ave., Princeton, NJ 08544 USA

Many state-of-the-art micro-electronic-photonic and MEMS devices are based upon micro/nano-scale contacts. Descriptions of such contacts must account for elastic/plastic deformation, adhesion and contact shape evolution. Plastic deformation is fundamentally different on the nanoscale. We present a molecular dynamics study of single asperity contacts in EAM Au as a function of contact loading and unloading at different frequencies. We monitor the full force-displacement curve, the evolution of the atomic structure/asperity morphology, dislocation nucleation and motion. Plastic deformation causes the disappearance of individual atomic layers with concomitant abrupt jumps in the applied force-displacement curve. Dislocations nucleated upon loading tended to be partials. Stacking fault pyramids are created and then annihilated causing abrupt jumps in force-displacement curves. Upon unloading, dislocations run out of the asperities, leaving dislocation-free structures. The tensile stresses generated during pull-of f produce twin-like structures. The nature of the deformation produced in cyclic loading was extremely sensitive to the deformation rate.

# Advanced Materials for Energy Conversion II: Metal Hydrides III

Sponsored by: Light Metals Division, LMD-Reactive Metals Committee

*Program Organizers:* Dhanesh Chandra, University of Nevada, Metallurgical & Materials Engineering, Reno, NV 89557 USA; Renato G. Bautista, University of Nevada, Metallurgical and Materials Engineering, Reno, NV 89557-0136 USA; Louis Schlapbach, EMPA Swiss Federal, Laboratory for Materials Testing and Research, Duebendorf CH-8600 Switzerland

Wednesday AM	Room:	203A		
March 17, 2004	Location	n: Charlotte	Convention	Center

Session Chairs: Ricardo B. Schwarz, Los Alamos National Laboratory, MS G755, Los Alamos, NM 87545 USA; Etsuo Akiba, National Institute of Advanced Studies, Energy Elect. Inst., Tsukuba, Ibaraki 305-8565 Japan; R. Tom Walters, Westinghouse Savannah River Co. LLC, Strategic Matls. Tech. Dept., Aiken, SC 29808 USA

## 8:30 AM Plenary

The Role of Defects on the Hydrogen Storage Capacity of Metals: *Reiner Kirchheim*<sup>1</sup>; Astrid Pundt<sup>1</sup>; Christian Kluthe<sup>1</sup>; Mohamed Suleiman<sup>1</sup>; <sup>1</sup>Universitaet Goettingen, Inst. fuer Materialphysik, Tammannstrasse 1, Goettingen D-37077 Germany

Hydrogen storage alloys used today are multicomponent and structurally disordered containing large fractions of dislocations and grain boundaries. The current status of modelling pressure composition isotherms and H-diffusivity for these hydrogen-metal systems will be reviewed. Recent experimental results on the interaction between hydrogen on the one hand and subsurface sites, dislocations, grain boundaries and phase boundaries on the other hand are presented for model systems. These model systems are small Pd-clusters, nanocrystalline, deformed, and internally oxidized Pd and metallic multylayers. Corresponding experimental results are obtained by small angle neutron scattering, Synchrotron X-ray diffraction and by tomographic atom probe analysis.

## 9:00 AM Keynote

**Hysteresis in the Reversible Storage of Hydrogen in Metals**: *R. B. Schwarz*<sup>1</sup>; A. Khachaturyan<sup>2</sup>; <sup>1</sup>Los Alamos National Laboratory,

MST-8, MS G755, Los Alamos, NM 87545 USA; <sup>2</sup>Rutgers University, Ceram. & Matls. Engrg., 607 Taylor Rd., Piscataway, NJ 08854 USA

In many metal-hydrogen systems, the plateau pressure during hydrogenation is higher than that during hydrogen removal, in what is known as hysteresis. Since the plateau pressure reflects equality between hydrogen chemical potentials in the transforming phases, and classical thermodynamics cannot explain lack of ergodicity, early models attributed the hysteresis to the irreversible generation of lattice defects. The recent model of Schwarz and Khachaturyan [PRL 74(1995)2523] attributes the hysteresis to the effect of the coherency strains between the solid-solution and hydride phases. We summarize this model and present evidence supporting it. In particular, we show that hysteresis is also observed between the pressure necessary to form Pd-hydride precipitates in a Pd single crystal and the pressure required to form Pd-crystal precipitates in a Pd-hydride single crystal. Therefore, the generation of dislocations, which cannot be avoided during the transformation due to the large mismatch strain, is not the cause for the hysteresis.

## 9:25 AM Invited

**Diffraction Studies of Alanates**: *Hendrik W. Brinks*<sup>1</sup>; Bjørn C. Hauback<sup>1</sup>; Didier Blanchard<sup>1</sup>; Craig M. Jensen<sup>2</sup>; <sup>1</sup>Institute for Energy Technology, Physics Dept., PO Box 40, Kjeller NO-2027 Norway; <sup>2</sup>University of Hawaii, Dept. Chmst., 2545 The Mall, Honolulu, HI 96822 USA

Alanates, metal hydrides based on the AlH<sub>4</sub> · unit, is one of the most promising groups of metal hydrides for reversible hydrogen storage at moderate temperatures. Their storage capacity is very large, e.g. NaAlH<sub>4</sub> and LiAlH<sub>4</sub> can release 5.6 and 7.9 wt%, respectively, below 200°C. The pioneering work of Bogdanovic et al. in 1997 revealed that Ti additives increased the desorption kinetics of NaAlH4 and made rehydrogenation possible. In order to get a better understanding of the reactions, detailed studies of the structure is essential. In particular, it is important to understand the nature of the additive in order to improve the kinetics. Our structural studies of NaAlD<sub>4</sub>, with different additives will be presented. Crystal structures of LiAlD<sub>4</sub>, NaAlD<sub>4</sub>, Li<sub>3</sub>AlD<sub>6</sub> and KAlD<sub>4</sub> will be presented, as well as in-situ diffraction results of the decomposition. LiAlD<sub>4</sub> has been shown to decompose completely to LiD, Al and D<sub>2</sub> at 127°C, releasing 7.9 wt% H<sub>2</sub>. Addition of VCl<sub>3</sub> by ball milling increases the reaction rate.

## 9:50 AM Invited

Advances in Hydrogen Storage: Arnulf J. Maeland<sup>1</sup>; Bjorn C. Hauback<sup>1</sup>; <sup>1</sup>Institute for Energy Technology, Dept. of Physics, PO Box 40, Kjeller 2027 Norway

The advancement of hydrogen and fuel cell technologies in transportation as well as stationary and portable applications depend very much on efficient and safe storage of hydrogen. Storage technologies, gaseous and liquid hydrogen storage and chemical storage, will be reviewed and discussed. Particular emphasis will be placed on hydrogen storage in the form of metal hydrides.

## 10:15 AM Break

#### 10:30 AM Invited

The Use of Hydrogen Driven Metallurgical Reactions (HDMR) to Produce Reactive, Nano-Scale and Nano-Composite Materials: J. J. Reilly<sup>1</sup>; J. R. Johnson<sup>1</sup>; J. Wegryzn<sup>1</sup>; <sup>1</sup>Brookhaven National Laboratory, Dept. of Energy Sci. & Tech., Upton, NY 11733 USA

The direct reaction of hydrogen with a metal to form a metal hydride phase results in a large volume change which can result in pulverization of the material. This hydrogen decrepitation (HD) process was exploited some years ago to produce rare earth alloy powders. More recently the HDDR (hydriding, dehydriding, disproportionation, recombination) process was introduced which exploits thermodynamic instability of many alloys at high temperatures in the presence of H2 gas and was used to produce improved magnetic alloys. We have extended this process to produce nanocomposite materials by introducing a reducible metal oxide which greatly increases the number of possible reactions. Such solid state reactions fall into a wide class which may be designated as hydrogen driven metallurgical reactions (HDMR). We will discuss the versatility of this process to produce many types of nanocomposite (or nano-scale) materials, particularly those of interest for use as Li anodes in batteries and for improved hydrogen storage compounds.

## 10:55 AM

Palladium Composite Membranes for Hydrogen Separation: Stephen N. Paglieri<sup>1</sup>; Stephen A. Birdsell<sup>1</sup>; Ronny C. Snow<sup>1</sup>; Vincent B. Hesch<sup>1</sup>; Frank M. Smith<sup>1</sup>; <sup>1</sup>Los Alamos National Laboratory, PO Box 1663, MS-C348, Los Alamos, NM 87545 USA A palladium membrane reactor can be used to efficiently generate hydrogen from hydrocarbons. Two types of palladium composite membranes were investigated for hydrogen separation. A palladium alloy membrane was prepared by electroless plating a thin (~20 micron) layer of palladium and then copper onto a commercially available porous (nominal 0.2 micron pores) alpha-alumina substrate. The resulting multilayer metal film was annealed at 360°C for several days to promote metallic interdiffusion and alloy formation. During the heat treatment, a maximum hydrogen flux of 0.15 mol (STP)/m<sup>2</sup>·s was observed at 360°C and a pressure drop across the membrane of 100 psi. The hydrogen/argon ideal separation factor was 68 at these conditions, however, the separation factor decreased upon thermal cycling. The other type of membrane fabricated was a palladium coated vanadium-copper alloy foil. New methods are being developed for sealing the thin (40 micron) foil into modules for testing.

#### 11:15 AM

Hydrogen Storage Properties of Li Related and C Related Materials: *Takayuki Ichikawa*<sup>1</sup>; Hironobu Fujii<sup>1</sup>; <sup>1</sup>Hiroshima University, Natural Sci. Ctr. for Basic R&D, 1-7-1 Kagamiyama, Higashi-Hiroshima, Hiroshima 739-8521 Japan

We are investigating hydrogenating/dehydrogenating properties about the 1:1 mixture of lithium amide and lithium hydride containing a small amount of TiCl3 (1mol %) as a candidate of hydrogen storage materials. The product desorbs a large amount of hydrogen (~5.5 wt.%) in the temperature range from 150 to 250°C under the heating rate condition of 5°C/min and also shows an excellent cycle retention with an effective hydrogen capacity of more than 5 wt.% until at least 3 cycles. In addition, we are also studying the hydrogen desorption properties about hydrogenating graphite made by ball milling under hydrogen atmosphere. The results indicate that a small amount of iron contamination during milling plays a quite important role as a catalyst for hydrogen desorption in the TDS profile is due to existence of high dispersing iron on graphite.

# Advanced Materials for Energy Conversion II: Thermodynamics, Superconductors & Batteries

Sponsored by: Light Metals Division, LMD-Reactive Metals Committee

*Program Organizers:* Dhanesh Chandra, University of Nevada, Metallurgical & Materials Engineering, Reno, NV 89557 USA; Renato G. Bautista, University of Nevada, Metallurgical and Materials Engineering, Reno, NV 89557-0136 USA; Louis Schlapbach, EMPA Swiss Federal, Laboratory for Materials Testing and Research, Duebendorf CH-8600 Switzerland

Wednesday AM	Room:	204
March 17, 2004	Locatior	: Charlotte Convention Center

*Session Chairs:* Ramana G. Reddy, University of Alabama, Dept. of Metallurgl. & Matls. Engrg., Tuscaloosa, AL 35487-0202 USA; Brent Fultz, California Institute of Technology, Matls. Sci., Pasadena, CA 91125 USA; Olivia A. Graeve, University of Nevada, Metallurgl. & Matls. Engrg., Reno, NV 89557-0136 USA

#### 8:30 AM Invited

**Origin of Entropy of Intercalation of Li into Li\_yCoO\_2**: Brent Fultz<sup>1</sup>; Yvan Reynier<sup>2</sup>; Tabitha Swan-Wood<sup>1</sup>; Jason Graetz<sup>1</sup>; Peter Rez<sup>3</sup>; Rachid Yazami<sup>2</sup>; <sup>1</sup>California Institute of Technology, Matls. Sci., Mail 138-78, Pasadena, CA 91125 USA; <sup>2</sup>California Institute of Technology/CNRS-LEPMI, Matls. Sci., Mail 138-78, Pasadena, CA 91125 USA; <sup>3</sup>Arizona State University, Dept. of Physics & Astron., Tempe, AZ 85257-1504 USA

We studied the thermodynamics of lithium insertion into LiCoO\_2, the cathode material of commercial rechargeable Li batteries. The entropy of lithium intercalation, dS, and enthalpy of intercalation, dH, were determined from measurements of the open circuit voltage of electrochemical half-cells at different temperatures. The present work addresses the entropy. A large change of 2 k\_B/atom was observed for the difference in entropy of intercalation of lithium into Li\_0.6CoO\_2 and Li\_1CoO\_2. The three sources of entropy of lithium concentration in Li\_yCoO\_2 are: 1) configurational entropy, 2) electronic entropy, and 3) vibrational entropy. The first two contributions were obtained by calculation, using combinatoric estimates for 1, and electronic structure calculations with the VASP package for 2. Configurational entropy, and surprisingly, electronic entropy, account for most of the entropy difference measured by electrochemical methods. The third contribution, vibrational entropy, was measured by inelastic neutron scattering, and found to be small.

#### 8:55 AM Keynote

Recent Developments in Materials and Design Concepts for Bipolar Plates in Fuel Cells: Ramana G. Reddy<sup>1</sup>; <sup>1</sup>University of Alabama, Dept. of Metallurgl. & Matls. Engrg., PO Box 870202, Tuscaloosa, AL 35487-0202 USA

The fuel cell technology is predestined to provide a major breakthrough in the way we power our very existence on the planet, powering virtually everything from cars to mobiles. The widespread commercialization of the technology has still not been made possible due to high costs associated with the fuel cell components. One such component in the fuel cell stack is the bipolar/end plate. This presentation reviews some of the recent developments in the materials, design, and concepts for bipolar/end plates in the polymer electrolyte membrane fuel cell stack from the author's experience at The University of Alabama. Experimental results for use of Fe-, Cu-based alloys for bipolar/end plate as an alternative to the expensive conventionally used graphite material are presented. The developments of the models for optimizing the design parameters in the gas flow-field of these plates are discussed. Based on these simulations results, some of the new concepts for these plates were urbanized. These include: use of met al foam in the gas flow-field and corrugated thin sheet bipolar/end plate. Experimental results with these new concepts are presented and will be compared with the model predicted results. Applications of these new concepts in the development of commercial fuel cell stacks are discussed.

#### 9:20 AM Keynote

Vibrational Energy Scavenging Via Thin Flim Piezoelectric Ceramics: *Elizabeth Kathryn Reilly*<sup>1</sup>; Eric Carleton<sup>1</sup>; Paul Kenneth Wright<sup>1</sup>; <sup>1</sup>University of California, Mechl. Engrg., 2111 Etchverry Hall, Berkeley, CA 94720 USA

This work focuses on constructing a vibrational energy scavenging device with a specific application to MEMS wireless sensor networks. The device utilizes vibrations produced by HVAC ducts, traffic in a room, and even wind hitting a window. The advantages of using thin film (~1 micron) PZT (Pb1.15(Zr0.47, Ti0.53)O3) over a larger scale bimorph will be addressed. The thin films are grown using pulsed laser deposition (PLD) to deposit the film epitaxially on MgO. The PZT is then removed from the MgO using excimer laser liftoff and attached to a metallic shim, thus creating a usable bimorph. Discussion of the constituent equations will reflect that of system with an external force applied perpendicular to the beam at its tip. Characterization and material analysis will illustrate the effectiveness of this technique in creating an energy scavenging device.

#### 9:45 AM

In-Situ Production of Nano-Structured Ceramics by Spray Solution Technique: Konstantin Krasimirov Konstantinov<sup>1</sup>; Zheng Wei Zhao<sup>1</sup>; Ling Yuan<sup>1</sup>; Hua Kun Liu<sup>1</sup>; Shi Xue Dou<sup>1</sup>; <sup>1</sup>University of Wollongong, ISEM, Northfields Ave., Wollongong, NSW 2522 Australia

Various nano-structured ceramic materials e.g. LiCo1-xNixO2, CoO, Co3O4 and SnO2 have been prepared in-situ by a spray pyrolysis method. The effect of the temperature and sintering time on nanocrystallinity, phase composition, and different physical and electrochemical parameters have been studied in detail. Different methods including X-ray diffraction, gas sorption analysis (for estimation of BET surface area), ICP-OES analysis, TEM and SEM techniques, combined with EDX analysis and standard battery testing methods have been used to characterized the powders obtained. We have demonstrated that the method used is very flexible and universal, and it permits good control of the crystal size and phase product, allowing in-situ production of simple or complex ceramics possessing specific surface areas that are generally larger than for the corresponding materials obtained via conventional technology. The obtained materials have promising potential applications not only as anode or cathode battery materials, but also as catalysts or capacitors.

# 10:05 AM Break

10:20 AM Invited Secondary Lithium Ion Polymer Microbatteries: Daniel A. Steingart<sup>1</sup>; James W. Evans<sup>1</sup>; Paul K. Wright<sup>1</sup>; <sup>1</sup>University of California, Dept. of Matls. Sci. & Engrg., 2117 Etcheverry Hall, Berkeley, CA 94720 USA

The next generation of wireless sensor networks requires the energy production and storage mechanism to be integrated on chip. We are designing a micro-scale lithium secondary battery to be deposited on the backside of a millimeter scale wireless sensor. The battery will continuously be charged by energy scavenging devices such as MEMS piezo-benders or heat pumps. The battery novelty comes from designing the cell around the duty cycle for a given application. The material novelty in the system lies in adaptation of Dunn's  $V_2O_5$  aerogel cathode and Kostecki's pyrolyzed carbon anode for micro scale implementation. We will fabricate the entire cell on campus: the cathode from sol gel processing, the anode from standard micro fabrication photolithography, and combining them in a SiN2 or similar enclosure. Theoretical performance from proposed geometries will be discussed, as well as characterization and optimization of the half-cell reactions.

## 10:45 AM Invited

Processing and Properties of Nickel Foams for Battery Electrodes: David S. Wilkinson<sup>1</sup>; Vladimir Paserin<sup>2</sup>; <sup>1</sup>McMaster University, Dept. of Matl. Sci. & Engrg., 1280 Main St. W., Hamilton, ON L8S 4L7 Canada; <sup>2</sup>INCO Technical Services, Sheridan Park, Mississauga, ON L5K 1Z9 Canada

Ni-metal hydride foams generally utilize nickel foams as the electrode phase. Amongst several methods for the manufacture of these chemical vapour deposition onto a polymer foam substrate is one of the most attractive. In this paper we will present several issues related to the processing of these foams and their properties in the as-deposited condition. We will show what factors control the high strength and consequent brittleness of the as-deposited foams. We will also present data on the optimum sintering conditions for these materials.

## 11:10 AM

Surface Modification of Spinel Li1+xMn2O4 Cathode Material in Li-Ion Battery by Li2O-2B2O3 Glass: Hong Wei Chan<sup>1</sup>; Shyang Roeng Sheen<sup>2</sup>; Jenq Gong Duh<sup>1</sup>; <sup>1</sup>National Tsing Hua University, Dept. of Matls. Sci. & Engrg., 101, Sect. 2 Kuang Fu Rd., Hsinchu 300 Taiwan; <sup>2</sup>Coremax Taiwan Corporation, R&D, 11 Wen Hwa Rd., Hsinchu Hsien 303 Taiwan

Lithium borate glass, Li2O-2B2O3, coated on the surface of the lithium manganese oxide cathode material in Li-ion batteries have been synthesized to achieve electrochemical cyclability and structural stability in this study. The heat treatment temperature was evaluated according to TG/DTA analysis. The Li1+xMn2O4 powder derived from co-precipitation method was calcined under various weight percent of Li2O-B2O3 glass to form fine powder of single spinel phase with different particle size, size distribution and morphology. The pure spinel Li1+xMn2O4 coated with LBO glass were successfully obtained by well-mixed solid-state method. The structure was confirmed by XRD along with the composition measured by EPMA and ICP-AES. The lattice parameter decreased with the content of the LBO wt's. From FESEM image and Laser Scattering measurements, the average particle size was in the range of 2-8?Ým. The electrochemical behavior of LiMn2O4 powder was examined by using two-electrode test cells consisted of a cathode, metal lic lithium anode, and an electrolyte of 1M LiPF6 in a 1:1 (volume ratio) mixture of EC/DMC. Cyclic charge/ discharge testing of the coin cells, fabricated by both Li1+xMn2O4 and LBO-coated Li1+xMn2O4 cathode material provided high discharge capacity. Furthermore, the LBO-coated Li1+xMn2O4 powder showed better cyclability than un-coated Li1+xMn2O4 after 16 cycles test. The introduction of LBO-coated Li1+xMn2O4 revealed high capacity and apparently decreased the decay rate after cyclic test.

#### 11:30 AM

Synthesis and Electrochemical Characterization of Cobalt -Manganese Oxide: Nagireddy Ravinder Reddy<sup>1</sup>; Ramana G. Reddy<sup>1</sup>; <sup>1</sup>University of Alabama, Dept. of Metallurgl. & Matls. Engrg., A-129 Bevill Bldg., 126 Seventh Ave., PO Box 870202, Tuscaloosa, AL 35487-0202 USA

Cobalt - MnO2 was prepared using sol-gel method in ambigel form. Prepared material was studied as electrode material for electrochemical capacitors (EC's). Co - MnO2 was characterized using various techniques like XRD, SEM, TGA and BET. Co-MnO2 was electrochemically characterized using cyclic voltammetric technique. Cyclic Voltametry (CV) experiments were carried out using three electrode system. Saturated calomel electrode, platinum mesh and Co-MnO2 rolled in between titanium meshes were used as reference electrode, counter electrode and working electrode respectively. Non-capacitative behavior was observed in the first cycle and progressive charge enhancement was observed up to 100 cycles. Co-MnO2 electrode showed maximum capacitance of 105 F/g at a scan rate of 5 mV/s in 1M NaCl electrolyte. Capacitance fading was not observed up to 800 cycles. The results were compared with the capacitative behaviour of pure MnO2.

# Advances in Superplasticity and Superplastic Forming: Advanced Superplastic Materials and the Science of Superplasticity

Sponsored by: Materials Processing and Manufacturing Division, Structural Materials Division, MPMD-Shaping and Forming Committee, SMD-Mechanical Behavior of Materials-(Jt. ASM-MSCTS), SMD-Structural Materials Committee
Program Organizers: Eric M. Taleff, University of Texas, Mechanical Engineering Department, Austin, TX 78712-1063 USA;
P. A. Friedman, Ford Motor Company, Dearborn, MI 48124 USA; Amit K. Ghosh, University of Michigan, Department of Materials
Science and Engineering, Ann Arbor, MI 48109-2136 USA; P. E.
Krajewski, General Motors R&D Center; Rajiv S. Mishra, University of Missouri, Metallurgical Engineering, Rolla, MO 65409-0340
USA; J. G. Schroth, General Motors, R&D Center, Materials and Processes Laboratory, Warren, MI 48090-9055 USA

Wednesday AM	Room:	20	)1B		
March 17, 2004	Location	1:	Charlotte	Convention	Center

Session Chairs: Rajiv S. Mishra, University of Missouri, Metallurgl. Engrg., Rolla, MO 65409-0340 USA; Amit K. Ghosh, University of Michigan, Dept. of Matls. Sci. & Engrg., Ann Arbor, MI 48109-2136 USA

## 8:30 AM

**Cooperative Processes in Large Plastic and Superplastic Deformation**: *Michael Zelin*<sup>1</sup>; Amiya Mukherjee<sup>2</sup>; <sup>1</sup>The Goodyear Tire & Rubber Company, Akron, OH 44309 USA; <sup>2</sup>University of California, Chem. Engrg. & Matls. Sci., One Shields Ave., Davis, CA 95616 USA

Despite drastic differences in occurrence and mechanisms of normal plastic deformation (ND) and superplastic deformation (SPD), there is close similarity between the two with regard to mechanical aspects of deformed system-reaction to the applied force, non-uniformity of plastic flow, and its dislocation nature. In both ND and SPD, deformation is initiated at surfaces of maximum shear stress causing a long range correlation in grains deformation, i.e. its cooperative manner. This paper focuses on cooperative character of ND and SPD revealed at different microstructural levels. Results of targeted observations of deformation occurring in a drawn eutectoid steel wire and superplastic lead-tin eutectic are presented and discussed invoking different approaches. Observed macroscopic pattern of localized deformation surfaces can be explained from the point of view of solid mechanics. Sequential progress of deformation at localized deformation surfaces can be modeled in terms of cellular dislocations. Microscopic aspects of progress of ND and SPD can be rationalized in terms of lattice and grain boundary dislocations, respectively. Work supported in part by NSF/DMR grant 9903321/0240144.

## 8:55 AM

Influence of Grain Boundary Structure and Composition on Superplastic Deformation: John S. Vetrano<sup>1</sup>; C. H. Henager<sup>1</sup>; R. J. Kurtz<sup>1</sup>; R. G. Hoagland<sup>1</sup>; V. Guertsman<sup>2</sup>; <sup>1</sup>Pacific Northwest National Laboratory, MSIN P8-16, PO Box 999, Richland, WA 99352 USA; <sup>2</sup>CANMET/MTL, 568 Booth St., Ottawa, ON K1A 0G1 Canada

Grain boundary sliding (GBS) plays a large role in superplastic deformation and dictates not only the deformation characteristics but also the final failure. As part of a program to better elucidate the nature of GBS we have studied the interplay between the sliding of grains and their structure and composition in model Al-Mg alloys. Tools such as high-resolution analytical transmission electron microscopy and molecular dynamic computer simulations were utilized to investigate the influence of Mg and Sn on grain boundary structure, and examining how those different structures affect the ability of the boundary to slide. This paper will examine these effects from the atomistic level (grain boundary dislocations, microsegregation) to the micro- and macro-scale (precipitates and cavitation). Work supported by the Materials Science Division, Office of Basic Energy Sciences, U.S. Department of Energy under contract DE-AC06-76RLO-1830.

## 9:20 AM

Superplasticity in Zr-Based Bulk Metallic Glasses: A Critical Overview: Martin Heilmaier<sup>1</sup>; <sup>1</sup>Otto-von-Guericke-University Magdeburg, Inst. of Matls. Engrg. & Testing, PO Box 4120, Magdeburg D-39016 Germany

With the recent advent of multi-component bulk glassy alloys exhibiting wide supercooled liquid region, amorphous metals have matured from a lab curiosity to potential structural materials with unique mechanical and physical properties. However, applications are often limited by the uncertainty about the appropriate processing window. The compressive deformation behavior of Zr-based BMG matrices with and without second phase precipitates in a wide temperature and strain rate range within the supercooled liquid region is reviewed<sup>1</sup> and compared with tensile data on bulk samples and thin ribbons<sup>2.3</sup>. Truly Newtonian viscous flow with m = 1 and homogeneous deformation at constant viscosity is observed for strain rates as high as  $10^{-2}$  s<sup>-1</sup>. Application of Spaepens free volume theory clearly indicates that superplastic deformation in BMGs is controlled by atomic diffusion, or more specific by the competing effects of free volume generation and annihilation. <sup>1</sup>A. Reger-Leonhard et al., Scripta Mater. 43 (2000), 459. <sup>3</sup>J.P. Chu et al., Scripta Mater. 49 (2003), 435. <sup>3</sup>Y. Kawamura et al., Scripta Mater. 37 (1997), 431.

#### 9:45 AM

**Transformation Superplasticity of Titanium by Reversible Hydrogen Cycling:** Heeman Choe<sup>1</sup>; *David C. Dunand*<sup>1</sup>; <sup>1</sup>Northwestern University, Dept. of Matls. Sci. Engrg., Evanston, IL 60208 USA

Commercially-pure titanium was reversibly alloyed and dealloyed with hydrogen at 860°C, thus repeatedly triggering the transformation between hydrogen-free  $\alpha$ -Ti and hydrogen-alloyed  $\beta$ -Ti. Under an externally applied tensile stress, the internal mismatch stresses produced by the  $\alpha$ - $\beta$  transformation are biased, resulting in a strain increment accumulated after each chemical cycle in the direction of the applied stress. These strain increments are linearly proportional to the applied stress at small stress levels ( $\sigma < \cong 2$  MPa), as previously reported for transformation superplasticity achieved by thermal cycling of hydrogen-free  $\alpha$ -Ti. The present study investigates systematically the effect hydrogen partial pressure, cycle time, and external stress upon the value of the superplastic strain increments, as well as the concurrent contribution of creep as a deformation mechanism.

#### 10:10 AM Break

## 10:30 AM

Research and Development Towards Grain-Boundary-Plasticity from Superplasticity: *Kenji Higashi*<sup>1</sup>; <sup>1</sup>Osaka Prefecture University, Dept. of Metall. & Matls. Sci., 1-1, Gakuen-cho, Sakai, Osaka 599-8531 Japan

Superplasticity is generally associated with fine grains, grain boundary sliding, accommodation, high tensile ductility and high strain-ratesensitivity at elevated temperatures. The attention is paid to the highstrain-rate superplasticity and/or low-temperature superplasticity of the fine-grained materials in order to shed light on the mechanism of superplastic flow. The recently reported results after the project entitled "Towards Innovation in Superplasticity (1997~1999)" will be summarized with focusing to (a) novel processing procedures to achieve ultra-fine structures, (b) pertinent deformation models and (c) new phenomena of low-temperature superplasticity and nanocrystalline superplasticity. The new research area of grain boundary plasticity, furthermore, will be discussed.

#### 10:55 AM

Deformation of Superplastic Al2O3/Y-TZP Particulate and Particulate Laminate Composites: Jue Wang<sup>2</sup>; Desiderio Kovar<sup>1</sup>; Eric M. Taleff<sup>1</sup>; <sup>1</sup>University of Texas, Dept. of Mech. Engrg., 1 Univ. Sta., C2200, Austin, TX 78712-0292 USA; <sup>2</sup>University of Texas, Matls. Sci. & Engrg. Prog., 1 Univ. Sta., C2200, Austin, TX 78712-0292 USA Particulate composites of Al<sub>2</sub>O<sub>3</sub> and Y-TZP were some of the ear-

liest and are still among the most successful superplastic ceramic composites. Superplastic Y-TZP is required in Al<sub>2</sub>O<sub>3</sub>/Y-TZP particulate composites to retain fine grain sizes in the Al<sub>2</sub>O<sub>3</sub> phase, which normally coarsens at elevated temperatures. However, the high cost of Y-TZP relative to Al<sub>2</sub>O<sub>3</sub> provides incentive to understand the effect volume fraction has on deformation behavior of this composite system in order to engineer composites which minimize the expensive Y-TZP phase while achieving desired behaviors. To this end, a number of particulate and particulate laminate Al2O3/Y-TZP composites have been investigated over a range of compositions. These composites were mechanically tested over a range of strain rates and a limited range of temperatures near 1350°C. Particulate laminate composites were tested in both the isostress and isostrain orientations. A constrained isostrain model is found to best describe, among current models, the behaviors of both particulate composites and particulate laminate composites tested in either the isostress or isostrain orientations. The similarity in behaviors between particulate laminates in the isostress and isostrain orientations is attributed to layer constraint, which enables the strongest layer to dominate deformation behavior.

#### 11:15 AM

**Texture and Microstructure of Superplastic 7475 Aluminum:** *Alexandre J. Blander*<sup>1</sup>; Jerzy A. Szpunar<sup>1</sup>; <sup>1</sup>McGill University, Matls. Engrg., 3610 Univ. St., Montreal, Quebec H3A 2B2 Canada

Orientation imaging microscopy (OIM) and x-ray diffraction were used to determine the effect of the superplastic response with respect to texture, grain boundary character distribution (GBCD) and microstructure in a 7475 statically recrystallized aluminum alloy. Results indicate the initial normal behavior of a microstructure deforming mainly by accommodated grain boundary sliding which induces rapid texture and grain boundary randomization. At latter stages of deformation, the accommodation mechanism is disrupted at a threshold strain, where the deformation mechanism is altered and dislocations are observed be concentrated at triple junctions. After this threshold strain is reached, crystallographic slip is observed as well as unaccommodated grain boundary sliding which ultimately leads to cavitation and fracture. Cavitation occurs at grain boundaries and triple junction where dislocations are concentrated, and is a result of difference in deformation behavior of adjacent grains having different Taylor factors. The kernel average misorientation function of OIM was used to indicate the level of strain within the grains and how the accommodation mechanism, or lack of it, affects the internal grain strain.

#### 11:35 AM

Studies of Void Growth and Interaction in a Eutectic Sn-Pb Alloy: *Matthew Mulholland*<sup>1</sup>; Victor Caraveo<sup>1</sup>; Tariq Khraishi<sup>1</sup>; Yu-Lin Shen<sup>1</sup>; Mark Horstemeyer<sup>2</sup>; <sup>1</sup>University of New Mexico, Mech. Engrg. Dept., MSC01-1150, Albuquerque, NM 87131 USA; <sup>2</sup>Mississippi State University, Mech. Engrg. Dept., 206 Carpenter Bldg., PO Box ME, Mississippi State, MS 39762 USA

In this work, an extensive set of parametric experimental studies have been performed on the plastic deformation of voids and their interaction in a superplastic solder alloy (eutectic Sn-Pb). To begin with, the strain-rate sensitivity, i.e. the m-curve, of the alloy has been fully characterized. The effect of the number of voids and their initial size on the rate of void growth has been investigated. Finite-element computations have also been performed to shed some light on the micromechanics of void deformation. Explanation of the ensuing ductility is attempted based on the m-curve.

# Aluminum Reduction Technology: Emerging Technologies

Sponsored by: Light Metals Division, LMD-Aluminum Committee Program Organizers: Tom Alcorn, Noranda Aluminum Inc., New Madrid, MO 63869 USA; Jay Bruggeman, Alcoa Inc., Alcoa Center, PA 15069 USA; Alton T. Tabereaux, Alcoa Inc., Process Technology, Muscle Shoals, AL 35661 USA

Wednesday AM	Room:	21	3D		
March 17, 2004	Location	1:	Charlotte	Convention	Center

Session Chair: Halvor Kvande, Hydo Aluminium, Metal Prod. Div., Oslo N-0240 Norway

#### 8:30 AM

Integrated Multiphysics & Computational Fluid Dynamics Modeling of a Carbothermic Aluminium Reactor: Dimitrios I. Gerogiorgis<sup>1</sup>; B. Erik Ydstie<sup>1</sup>; <sup>1</sup>Carnegie Mellon University, Dept. of Chem. Engrg., Doherty Hall DH 3112, 5000 Forbes Ave., Pittsburgh, PA 15213 USA

The present simulation study elaborates on a FE CFD model (Gerogiorgis et al., 2003) developed for the core stage of a carbothermic reduction reactor (Johansen and Aune, 2002), which is aimed at the industrial implementation of carbothermic aluminium production. Carbothermic reduction is an alternative to the conventional Hall-Héroult electrolysis process and is characterized by cost and environmental advantages and by its challenging complexity. The quadruple PDE problem (electric charge, heat, momentum and molar species balances) for the slag flow in the core reactor stage is solved using a commercial solver (FEMLAB® v. 2.3), to obtain potential, temperature, velocity and species concentration distributions in a 2D domain representing the complete core second stage of a proposed carbothermic reactor design. The interaction among Joule heating, endothermic reaction, natural Boussinesq convection and turbulent flow phenomena is of paramount importance for understanding the performance of the core stage; conducting CFD simulations in order to advance with the latter goal is very important, since reliable high-temperature measurements are remarkably costly and laborious. The main objective of this CFD study is to extract reactor design guidelines and conclusions about the reactive slag flow, under the instantaneous thermodynamic equilibrium assumption. Explicitly addressing the effect of design parameters on state variable distributions is vital: the sensitivity analyses conducted with respect to crucial process design variables reveal the controllability margin of the ARP reactor, exposing nontrivial heating optimization problems.

## 8:55 AM

Alumina Solubility Study in Ionic Liquids with PF<sub>6</sub> Anion: Mingming Zhang<sup>1</sup>; Ramana G. Reddy<sup>2</sup>; <sup>1</sup>University of Alabama, Dept. of Metallurgl. & Matls. Engrg., 254 Bevill Bldg., 126 Seventh Ave., Tuscaloosa, AL 35487 USA; <sup>2</sup>University of Alabama, ACIPCO, Ctr. for Green Mfg., Dept. of Metallurgl. & Matls. Engrg., PO Box 870202, A-129 Bevill Bldg., 126 Seventh Ave., Tuscaloosa, AL 35487-0202 USA

Traditional cryolite electrolysis process in the production of aluminum has severe environmental problems and are extremely energy intensive. High temperature electrolysis(900-1000°C) inevitably has high production costs and pollutants emission. While using ionic liquids as electrolyte near room temperature can easily avoid these problems. In this paper, the solubility of alumina in several kinds of ionic liquids with PF<sub>6</sub> anion was studied. Two different methods(emf, mechanic stirring) were used to determine the solubility. The solubility of alumina in ionic liquids was found to be relatively low as comparing to that in molten cryolite. The measured solubility also depended on method used to determine the dissolved alumina. From 100°C or higher temperature to their decomposition points,  $C_6$ mimPF<sub>6</sub> and  $C_8$ mimPF<sub>6</sub> exhibited measurable ability to dissolve alumina, which reach about 1 wt% and 0.5 wt% respectively at 200°C. Possible methods were also given in order to enhance the solubility of alumina in ionic liquids.

## 9:20 AM

New Opportunities for Aluminum Electrolysis with Metal Anodes in a Low Temperature Electrolyte System: *Jianhong Yang*<sup>1</sup>; John N. Hryn<sup>1</sup>; Greg K. Krumdick<sup>1</sup>; Joseph A. Pomykala<sup>1</sup>; Boyd R. Davis<sup>2</sup>; Alain Roy<sup>2</sup>; <sup>1</sup>Argonne National Laboratory, 9700 S. Cass Ave., Argonne, IL 60439 USA; <sup>2</sup>Kingston Process Metallurgy, Inc., Kingston, Ontario Canada

A new electrolyte system for low-temperature aluminum electrolysis was investigated. Analysis indicated that the solubility of alumina was about 4 wt% at 700°C. Baseline electrolysis tests at 700°C (graphite materials as both anode and cathode) showed the process works well with automatic alumina feeding. Metal anodes have been tested at 700°C in 10A, 20A and 100A cells for up to 100 hours at an anode current density of 0.5 A/cm2. With TiB2-C composite as the cathode, the current efficiency was around 85% based on recovered aluminum. Aluminum product purity was typically better than 99.5 wt%, with the major impurity being copper, typically less than 0.2 wt%. The promising results suggest that aluminum electrolysis with inert metal anodes in the new low temperature electrolyte system can be realized. This work is supported by the U.S. Department of Energy, Assistant Secretary for Energy Efficiency and Renewable Energy under contract W-31-109-Eng-38.

#### 9:45 AM

Laboratory Test and Industrial Application of a Ambient Temperature Cured TiB2 Cathode Coating for Aluminum Electrolysis: Qingyu Li<sup>1</sup>; *Jie Li*<sup>2</sup>; *Yonggang Liu*<sup>3</sup>; Yanqing Lai<sup>2</sup>; Jianhong Yang<sup>2</sup>; Yexiang Liu<sup>2</sup>; <sup>1</sup>Guangxi Normal University, Chmst. Dept., Gueilin, Guangxi 5410043 China; <sup>2</sup>Central South University, Sch. of Metallurgl. Sci. & Engrg., Changsha, Hunan 410083 China; <sup>3</sup>Aluminum Corporation of China Limited Guangxi Branch, Pingguo, Guangxi 531400 China

A concept of ambient temperature curable TiB2 cathode coating is put forward for aluminum electrolysis, and the ambient temperature curable TiB2 cathode coating has been prepared successfully. Differing from previous TiB2 cathode coating solidified approximately at 200?•, the ambient temperature curable TiB2 cathode coating can be solidified at room temperature, so the heating equipment is not necessary, which simplifies the preparation process and facilitates the industrial application of TiB2 cathode coating. Laboratory test results show that the properties of the cathode coating are excellent, the electrical resistivity is 23.8?Ê?¶.m, the compressive strength is 33.6MPa, and sodium expansion of cathode in aluminium electrolysis is reduced about 50%. Results from commercial prebaked anode aluminium electrolysis cells show that the coated cells have much better current distribution, lower cathode voltage drop, higher current efficiency, and less sodium related damage compared to the contrastive cells.

#### 10:10 AM Break

#### 10:20 AM

Iron-Nickel Alloy Slow-Consumable Anode for Aluminum Electrolysis: *Zhongning Shi*<sup>1</sup>; Junli Xu<sup>1</sup>; Zhuxian Qiu<sup>1</sup>; <sup>1</sup>Northeastern University, Light Metals Metall. Inst., Sch. of Matls. & Metall., PO Box 117#, Shenyang, Liaoning 110004 China

An alloy Fe-43Ni (wt.%) made by powder metallurgy as an anode for aluminum electrolysis is described in the present paper. Electrolysis by the anode was conducted for ten hours at 850°C in molten salts which consisted of NaF-43.7%AlF3-8%NaCl-5%CaF2-4%Al2O3 by mass. The anodic current density was set at 0.75A/cm2. Electrolysis was conducted smoothly with a fluctuation of cell voltage within 3.8-4.1V. The results by Electron Probe Micro-analyzer and X-ray Diffraction show that the generation film on the anodic substrate consisted of iron oxide major phase and nickel oxide, nickel ferrite minor phase. The alloy anode shows good performance in terms of antioxidation and resistant corrosion. Average annual wear rate is 20.77 millimeter, and purity of primary aluminum is 97-98%.

#### 10:45 AM

An Improved Pyroconductivity Test of Spinel-Containing Cermet Inert Anodes in Aluminum Electrolysis: *Yanqing Lai*<sup>1</sup>; *Jie Li*<sup>1</sup>; Zhongliang Tian<sup>1</sup>; Gang Zhang<sup>1</sup>; Qingwei Qin<sup>1</sup>; Qingyu Li<sup>1</sup>; Yexiang Liu<sup>1</sup>; 'Central South University, Sch. of Metallurgl. Sci. & Engrg., Changsha, Hunan 410083 China

An improved pyroconductivity test device, consisting of a specially constructed closed furnace and a potentiostat, was constructed based on the conventional direct current four-point technique. Symmetrical current distribution in the specimen was obtained by keeping a fixed pressure and good contact between the specimen and clamps at any temperature. The potentiostat was used to supply direct current and continuously monitor the current intensity and voltage between two probes, which can be adjusted outside the heating furnace to maintain good contact with the specimen. Test results of copper and graphite specimens show that the reliability and reproducibility were excellent. The electrical conductivity as a function of temperature for various spinel-containing cermet inert anodes was investigated spanning the Hall cell operating temperature. The factors influencing the electrical behavior were studied, which included the particle size of raw materials, manufacture process, phase composition and morphology et al.

# **Beyond Nickel-Base Superalloys: Niobium Silicides**

Sponsored by: Structural Materials Division, SMD-Corrosion and Environmental Effects Committee (Jt. ASM-MSCTS), SMD-High Temperature Alloys Committee, SMD-Mechanical Behavior of Materials-(Jt. ASM-MSCTS), SMD-Refractory Metals Committee *Program Organizers:* Joachim H. Schneibel, Oak Ridge National Laboratory, Oak Ridge, TN 37831-6115 USA; David A. Alven, Lockheed Martin - KAPL, Inc., Schenectady, NY 12301-1072 USA; David U. Furrer, Ladish Company, Cudahy, WI 53110 USA; Dallis A. Hardwick, Air Force Research Laboratory, AFTL/MLLM, Wright-Patterson AFB, OH 45433 USA; Martin Janousek, Plansee AG Technology Center, Reutte, Tyrol A-6600 France; Yoshinao Mishima, Tokyo Institute of Technology, Precision and Intelligence Laboratory, Yokohama, Kanagawa 226 Japan; John A. Shields, HC Stark, Cleveland, OH 44117 USA; Peter F. Tortorelli, Oak Ridge National Laboratory, Oak Ridge, TN 37831-6156 USA

Wednesday AM	Room: 211B
March 17, 2004	Location: Charlotte Convention Center

Session Chairs: Kazuhiro Ito, Kyoto University, Matls. Sci. & Engrg., Kyoto 606-8501 Japan; Hongbin Bei, University of Tennessee, Dept. of Matls. Sci. & Engrg., Knoxville, TN 37996 USA

## 8:30 AM Invited

A Comparative Overview of Mo- and Nb-Base Metal/Silicide Systems for High Temperature Structural Applications: Madan G. Mendiratta<sup>1</sup>; Sarath K. Menon<sup>1</sup>; Triplicane A. Parthasarathy<sup>1</sup>; Dennis M. Dimiduk<sup>2</sup>; Dallis A. Hardwick<sup>2</sup>; Patrick L. Martin<sup>2</sup>; <sup>1</sup>UES Inc., Matls. & Processes Div., 4401 Dayton-Xenia Rd., Dayton, OH 45432-1894 USA; <sup>2</sup>AFRL/MLLMD, Metals, Ceram. & NDE Div., 2230 Tenth St., Wright-Patterson AFB, OH 45433-7817 USA

Research and development efforts are presently underway to explore alloys within Mo-Si-B and Nb-Ti-Cr-Si-Hf-Al-Sn systems with a goal to significantly exceed the temperature capability of the current

Ni-base superalloy for jet engines. Both these alloys systems consist of a refractory metal phase for fracture resistance and silicides and other intermetallic phases for high temperature oxidation and creep resistance. This presentation is a comparative overview of the progress made on the systems through continuing research at AFRL/UES and other organizations. Physical properties (density, melting point, thermal conductivity, and thermal expansion coefficients) will be discussed in the context of design. Presentation will also include compositions, processing, microstructural evaluation, oxidation behavior and mechanical properties. Cyclic oxidation experiments have been carried out from 600-1350°C and tensile, compressive, fatigue, toughness and creep properties have been determined from RT-1400°C. T he oxidation mechanisms as well as fracture and damage mechanisms will be compared for the two alloy systems. Results of on-going research as well as venues for further critical work will be presented. Worked performed on AFRL/MLLM Contract #F33615-01-C-5214.

#### 9:00 AM

Phase Stability and Conceptual Microstructures for the Design of Nb-Base Superalloys: *Gautam Ghosh*<sup>1</sup>; Axel van de Walle<sup>1</sup>; Mark D. Asta<sup>1</sup>; Greg B. Olson<sup>1</sup>; <sup>1</sup>Northwestern University, Dept. of Matls. Sci. & Engrg., 2225 N. Campus Dr., Evanston, IL 60208-3108 USA

As a part multi-institutional and multi-disciplinary research under AFOSR-MEANS program, we present phase stability modeling and conceptual microstructures for the design Nb-base superalloys, with emphasis on conceptual design principles and tools employed. In the absence of sufficient experimental information, successful integration of ab initio phase stability data with CALPHAD fomalism constitutes one of the key components of this research. To demonstrate the efficacy of this approach, we present the results phase stability modeling of Nb-Al-Pd-Hf system. To design microstructures analogous to Ni-Base superalloys, bcc-based ordered aluminides (B2 and Heusler) are chosen as strengthening phases for Nb-base alloys. Prototype ternary and quarternary alloys heat treated at 1000 and 1200C over extended time show the evidence for high microstructural stability.

#### 9:15 AM

Microstructure Evaluation of LENS<sup>™</sup> Deposited Nb-Ti-Cr-Si Alloys: Ryan Richard Dehoff<sup>1</sup>; Peter C. Collins<sup>1</sup>; Hamish L. Fraser<sup>1</sup>; Michael J. Mills<sup>1</sup>; <sup>1</sup>Ohio State University, Matls. Sci. & Engrg. Dept., 2041 College Rd., Columbus, OH 43210 USA

Nb-Si "in-situ" metal ceramic composites consist of Nb<sub>3</sub>Si and Nb<sub>5</sub>Si<sub>3</sub> intermetallic phases in a body centered cubic Nb solid solution, and show promising potential for elevated temperature structural applications. The drawback to the binary Nb-Si system is oxidation and high metal loss rate at elevated temperatures however, the addition of Cr and Ti have been shown to increase the oxidation resistance at high temperatures. In this study, the LENS™ (Laser Engineered Net Shaping) process is being implemented to construct the Nb-Ti-Cr-Si alloy system from elemental powder blends due to availability of material and low relative cost. Advantages of the LENSTM process include the ability to produce near net shaped components with graded compositions as well as a more uniform microstructure resulting from the negative enthalpy of mixing associated with the silicide phases. The optimum LENSTM processing parameters were determined to produce a graded composition with a Nb:Ti ratio at 2:1, a Cr composition of 10 at %, and a range of Si contents from 5 to 15 at.%. The various microstructures were examined using SEM and TEM techniques. Hardness measurements and microtensile testing are being performed to evaluate the mechanical behavior of these alloys.

#### 9:30 AM

### Microstructural Properties of Nb-Si-B Alloys: Stefan Drawin<sup>1</sup>; Pierre Petit<sup>1</sup>; <sup>1</sup>ONERA, DMMP, BP72, Châtillon 92322 France

Refractory metal silicide based alloys are currently studied as candidate materials for future high performance turbine engines submitted to high airfoil temperatures (up to 1300°C). Addition of boron may improve their oxidation resistance, which remains a crucial issue for these materials. This has been applied to both the Mo-Si system and, more recently, to the Nb-Si system. Alloys with compositions in the Nb-rich corner of the Nb-Si-B system have been prepared by multiple cold crucible arc-melting and homogenised at high temperature. The microstructural properties of theses alloys have been investigated using scanning electron microscopy, electron probe micro-analysis and X-ray diffraction and will be presented. Rietveld analysis has been used to investigate the structure of each phase.

#### 9:45 AM

Phase Relation and Mechanical Property of Nb-Si Based Refractory Intermetallic Alloys with Ternary Elements: *Won-Yong Kim*<sup>1</sup>; In-Dong Yeo<sup>1</sup>; Sung-Hwan Lim<sup>2</sup>; <sup>1</sup>Korea Institute of Industrial Technology, Advd. Matls. R&D Div., 472 Kajwa-dong, Suh-ku, Inchon 404-254 Korea; <sup>2</sup>Kangwon National University, Dept. of Advd. Matls. Sci. & Engrg., Chunchon, Kangwon 200-701 Korea

Ternary phase diagrams, microstructure and mechanical properties of Nb-Si based refractory intermetallic alloys containing ternary alloying element were investigated. Molybdenum and Vanadium were chosen as ternary alloying elements because of their high melting point and smaller atomic size than Nb in order to expect a high temperature strength and room temperature fracture toughness. It was found that both ternary alloying elements have a significant effect to modify the microstructure from dispersed structure to maze-like structure in Nb solid solution/Nb<sub>3</sub>Si<sub>3</sub> intermetallic composites. 0.2% offset yield strength at room temperature increased with increasing content of ternary elements in Nb solid solution and volume fraction of Nb<sub>5</sub>Si<sub>3</sub> for both ternary alloy systems. At 1773 K, Mo addition has a positive role to increase yield strength, on the contrary V addition has a role to decrease yield strength. Fracture toughness of ternary alloys was superior to the binary alloys.

#### 10:00 AM Break

### 10:30 AM

**Oxidation Resistance and Mechanical Properties of a Powder Metallurgical (PM) Nb-Silicide Alloy**: *P. Jéhanno*<sup>1</sup>; M. Boening<sup>1</sup>; A. Venskutonis<sup>1</sup>; B. Bewlay<sup>2</sup>; M. R. Jackson<sup>2</sup>; <sup>1</sup>Plansee AG, Tech. Ctr., Reutte in Tirol 6600 Austria; <sup>2</sup>General Electric, Global Research, Schenectady, NY USA

A niobium-silicide alloy with additions of Ti, Hf, Cr and Al was manufactured using a powder metallurgical processing route comprising melting and atomization of a pre-sintered ingot. After compaction of the powder via HIP, the material was extruded using a reduction in area of 6:1. The microstructural characterization of both HIPed and extruded materials occurred via SEM, EDS and XRD analysis. The microstructure consisted of a Nb solid solution surrounding intermetallic particles with Nb5Si3- and Nb3Si-type structure. Tensile tests were performed at temperatures ranging from 800°C to 1300°C. A strength level equivalent or in some cases superior to directionally solidified alloys was observed. Furthermore, the excellent oxidation resistance of the base material was confirmed by isothermal heat treatments in air at temperatures ranging from 800 to 1200°C. The microstructures and mechanical properties will be compared with those of cast alloys.

#### 10:45 AM

Atomic Diffusion and Phase Equilibria at the Interfaces of CoAl/ Ir Multi-Layer on Co<sub>3</sub>AlC- and Nb<sub>5</sub>Si<sub>3</sub>-Base Alloys: Yoshisato Kimura<sup>1</sup>; Sachiyori Shiina<sup>2</sup>; Tatsuya Shimizu<sup>2</sup>; Yoshinao Mishima<sup>1</sup>; <sup>1</sup>Tokyo Institute of Technology, Matls. Sci. & Engrg., 4259 Nagatsuta, Midori-ku, Yokohama, Kanagawa 226-8502 Japan; <sup>2</sup>Tokyo Institute of Technology, Matls. Sci. & Engrg., 4259 Nagatsuta, Midori-ku, Yokohama, Kanagawa 226-8502 Japan

Protection against severe oxidation damages is an inevitable issue of heat resistant alloys and it becomes much more important at significantly high temperatures beyond 1273 K. Multi-layered functional coating is one of attractive solutions without sacrificing mechanical properties. Phase equilibria information plays a quite important role in designing heat resistant alloys since atomic diffusion is extremely active at such high temperatures. In the present work, we selected B2-CoAl as Al-reservoir for Al2O3 formation and Ir solid-solution as diffusion barrier especially against Al inward-diffusion. Base materials are E21- Co3AlC based and Nb5Si3 based heat resistant alloys. Atomic diffusion and phase equilibria have been investigated in detail using several diffusion couples. To evaluate the potential of Ir as diffusion barrier, temperature dependence of the diffusion coefficient of Al in Ir solidsolution (Ir-8at%Al) has been quantitatively determined, for instance 8.9x10-19 m<sup>2</sup>/s at 1573 K, using Boltzmann-Matano model with electron probe micro-analysis.

## 11:00 AM

**Processing, Microstructure and Mechanical Properties of (Nb)**/ **Nb<sub>5</sub>Si<sub>3</sub> Two-Phase Alloys**: *Yoshinao Mishima*<sup>1</sup>; Yoshisato Kimura<sup>1</sup>; Nobuaki Sekido<sup>2</sup>; Hiroaki Yamaoka<sup>1</sup>; <sup>1</sup>Tokyo Institute of Technology, Dept. of Matls. Sci. & Engrg., 4259 Nagatsuta, Midoriku, Yokohama, Kanagawa 226-8502 Japan; <sup>2</sup>University of Wisconsin, Dept. of Matls. Sci. & Engrg., 1509 Univ. Ave., Madison, WI 53706 USA

It has been shown that a fine lamellar structure composed of Nb solid solution, (Nb), and Nb<sub>5</sub>Si<sub>3</sub> is formed through eutectoid decomposition in the Nb-Si binary system and its ternary derivatives. Alloys with such microstructure would exhibit a high strength at over 1400 K yet showing room temperature toughness of over 20MPa  $m^{1/2}$  if a proper lamellar spacing is chosen In the present work, effects of processing on the microstructure evolution and mechanical properties are investigated on the Nb-18at%Si alloys prepared by hot pressing

and spark plasma sintering(SPS). The powders used in the present work are of pure Nb and Nb<sub>5</sub>Si<sub>3</sub> in order for the fabrication to become possible at temperatures higher than the melting point of Si and to reduce the formation of SiO<sub>2</sub>. The results show that the SPS yields more uniform two-phase microstructure but the alloys fabricated by hot pressing tends to provide higher elevated temperature strength.

## 11:15 AM

Effect of Ternary Elements on the Eutectoid Decomposition Behavior of Nb<sub>3</sub>Si into (Nb)/Nb<sub>5</sub>Si, in the Nb-Si-X Alloys: *Seiji Miura*<sup>1</sup>; Miki Aoki<sup>1</sup>; Yasuhiko Saeki<sup>1</sup>; Kenji Ohkubo<sup>1</sup>; Yoshinao Mishima<sup>2</sup>; Tetsuo Mohri<sup>1</sup>; <sup>1</sup>Hokkaido University, Div. of Matls. Sci. & Engrg, Kita-13, Nishi-8, Kita-ku, Sapporo, Hokkaido 060-8628 Japan; <sup>2</sup>Tokyo Institute of Technology, Dept. of Matls. Sci. & Engrg., 4259 Nagatsuta, Midori-ku, Yokohama, Kanagawa 226-8502 Japan

Alloys based on Nb-aluminides and silicides have been shown to exhibit superior high temperature strength than the commercial nickel base superalloys, however lack of room temperature ductility and high temperature oxidation resistance is the major drawback for further development. In order to improve the toughness of these alloys, microstructure control is a key method by which ductile phase toughening could effectively play a role in the alloys based on brittle intermetallic compounds. In the present work, effect of various ternary additions on the microstructure evolution of (Nb)/Nb<sub>5</sub>Si<sub>3</sub> lamellar structure is investigated in the Nb-Si-X alloys. It has been shown that the kinetics of the eutectoid decomposition of high temperature Nb<sub>3</sub>Si into (Nb) and Nb<sub>5</sub>Si<sub>3</sub> was sluggish in the binary Nb-Si system and that it is enhanced by Ti additions. The TTT diagrams for the decomposition experimentally determined and the microstructure of the products formed under various conditions is observed in the ternary system with an element such as Zr. Then the role of the ternary element on the decomposition kinetics is discussed.

#### 11:30 AM

Study of the Effects of Ti, Mo and B Additions on the Microstructure of Nb-Silicide Based In Situ Composites: Jie Geng<sup>1</sup>; Panayiotis Tsakiropoulos<sup>1</sup>; Guosheng Shao<sup>1</sup>; <sup>1</sup>University of Surrey, Sch. of Engrg., Mech. & Aeros. Engrg., Metall. Rsch. Grp., Guildford, Surrey GU2 7XH England

The effects of Ti, Mo and B additions on phase selection and microstructure development in as cast and heat-treated Nb-Si-Cr-Al in situ composites have been studied. In the alloys the Cr + Al and Si contents and the Si/(Cr+Al) ratio have been selected for optimum oxidation resistance and creep behaviour. The alloys were prepared using clean melting and casting in water-cooled copper crucibles/moulds. Molybdenum offers solid solution strengthening and Ti and B play important roles in phase selection and microstructure control in both the as cast and the heat treated alloys. In our study particular attention has been paid on the dependence of phase selection on cooling rate in ingots and on phase equilibria involving the Nbss, the MxSiy (M=Mo, Nb, Ti), T2 and Laves phases. The results of microstructural characterization will be presented and discussed.

## Bulk Metallic Glasses: Bio, Corrosion, and Fracture Behavior

Sponsored by: Structural Materials Division, ASM International: Materials Science Critical Technology Sector, SMD-Mechanical Behavior of Materials-(Jt. ASM-MSCTS)

*Program Organizers:* Peter K. Liaw, University of Tennessee, Department of Materials Science and Engineering, Knoxville, TN 37996-2200 USA; Raymond A. Buchanan, University of Tennessee, Department of Materials Science and Engineering, Knoxville, TN 37996-2200 USA

Wednesday AM	Room: 2	09A		
March 17, 2004	Location:	Charlotte	Convention	Center

Session Chairs: Joe A. Horton, Oak Ridge National Laboratory, Metals & Ceram. Div., Oak Ridge, TN 37830 USA; John J. Lewandowski, Case Western Reserve University, Matls. Sci. & Engrg., Cleveland, OH 44106 USA

### 8:30 AM Invited

**Biomedical Applications of Bulk Metallic Glasses**: *Joe A. Horton*<sup>1</sup>; Doug E. Parsell<sup>2</sup>; Mark L. Morrison<sup>3</sup>; Don M. Nicholson<sup>1</sup>; <sup>1</sup>Oak Ridge National Laboratory, Metals & Ceram. Div., Bldg. 4500S-MS6115, PO Box 2008, Oak Ridge, TN 37830 USA; <sup>2</sup>University of Mississippi, Dept. of Biomatls., Med. Ctr., Jackson, MS 39216 USA; <sup>3</sup>University of Tennessee, Dept. of Matls. Sci. & Engrg., Knoxville, TN 37966-2200 USA

Bulk metallic glasses (BMG) have a number of unique mechanical properties including a high elastic limit, low modulus, high tensile strength and reasonable hardness and toughness that make them attractive for some biomedical applications. For future implant materials, magnetic properties are also critical due to possible need for subsequent MRIs. Even with 14.6% Ni, MRI images of our reference material are excellent. First applications of BMG materials in the biomedical arena may be as tools used in interventional MRI procedures where imaging characteristics of the tools are critical. Preliminary biocompatability, corrosion, and fatigue results will be presented. This research was sponsored by the ORNL seed money program and by the Division of Materials Sciences and Engineering, Office of Basic Energy Sciences, U.S. Department of Energy under Contract DE-AC05-000R22725 with ORNL operated by UT-Battelle, LLC.

#### 8:55 AM Cancelled

Zirconium-Based Bulk Metallic Glasses for Biomedical Applications

#### 9:20 AM

Comparisons of Aqueous Corrosion Behaviors of Zr-Based Bulk Metallic Glasses and Nanocomposites: *Brandice Green*<sup>1</sup>; William Peter<sup>1</sup>; Raymond Buchanan<sup>1</sup>; Yoshihiko Yokoyama<sup>2</sup>; Peter Liaw<sup>1</sup>; Mark Morrison<sup>1</sup>; <sup>1</sup>University of Tennessee, Matls. Sci. & Engrg., 434 Dougherty Engrg. Bldg., Knoxville, TN 37996-2200 USA; <sup>2</sup>Himeji Institute of Technology, Matls. Sci. & Engrg., Shosha 2167, Himeji City Japan

To date, the research on the corrosion properties of Zr-based bulk metallic glass (BMG) nanocomposites has been limited. Most reported research on corrosion properties has been on fully amorphous Zrbased BMGs and has focused on one chemical composition. Furthermore, few studies have investigated the possible similarities and contrasts among nano-structured BMGs and completely amorphous BMGs. In the present work, the aqueous electrochemical corrosion behaviors of  $Zr_{50}Cu_{40}Al_{10}$ ,  $Zr_{50}Cu_{30}Al_{10}Ni_{10}$ , and nano-structured  $Zr_{50}Cu_{37}Al_{10}Pd_3$  were studied. Cyclic-anodic-polarization, immersion, and dynamic-anodicpolarization experiments were conducted on each composition in a 0.6 M NaCl electrolyte (simulated seawater) at room temperature. The cyclic-anodic-polarization results showed that Zr<sub>50</sub>Cu<sub>30</sub>Ni<sub>10</sub>Al<sub>10</sub> exhibited passive behavior at the open-circuit corrosion potential with a low corrosion rate. However, Zr<sub>50</sub>Cu<sub>30</sub>Ni<sub>10</sub>Al<sub>10</sub> was found to be susceptible to pitting corrosion at elevated potentials. On the other hand, Zr<sub>50</sub>Cu<sub>40</sub>Al<sub>10</sub> was found to be highly susceptible to pitting corrosion, with pit initiation occurring at, or slightly above, the corrosion potential and accelerating at higher potentials. To confirm the polarization results, BMG samples were immersed in the 0.6 M NaCl electrolyte and observed to determine incubation-time periods for pit initiation. Pit initiation did not occur over a 3-hour time period for Zr<sub>50</sub>Cu<sub>30</sub>Ni<sub>10</sub>Al<sub>10</sub>. However, pit initiation occurred within 15 minutes for  $Zr_{50}Cu_{40}Al_{10}$ . Preliminary observations indicated that the nano-structured Zr<sub>50</sub>Cu<sub>37</sub>Al<sub>10</sub>Pd<sub>3</sub> will have significantly different corrosion properties than the amorphous BMG compositions. This research effort was made possible by the funding of the National Science Foundation Integrative Graduate Education and Research Training (IGERT) Program on "Materials Lifetime Science and Engineering" (DGE-9987548), with Drs. W. Jennings and L. Goldberg as contract monitors and by Tennessee Advanced Materials Laboratory (TAML).

#### 9:45 AM

Electrochemical Studies of a Zr41.2 Ti13.8 Ni10 Cu12.5 Be22.5 Bulk Amorphous Alloy in Physiologically-Relevant Environments: Mark L. Morrison<sup>1</sup>; Raymond A. Buchanan<sup>1</sup>; Atakan Peker<sup>2</sup>; William H. Peter<sup>1</sup>; Joe A. Horton<sup>3</sup>; Peter K. Liaw<sup>1</sup>; <sup>1</sup>University of Tennessee, Dept. of Matls. Sci. & Engrg., 434 Dougherty, Knoxville, TN 37996-2200 USA; <sup>2</sup>Liquidmetals Technologies, 25800 Commercentre Dr., Ste. 100, Lake Forest, CA 92630 USA; <sup>3</sup>Oak Ridge National Laboratory, Metals & Ceram. Div., PO Box 2008, MS6115, Oak Ridge, TN 37831-6115 USA

Cyclic-anodic-polarization tests were conducted on a Zr-based bulk amorphous alloy with a chemical composition of  $Zr_{41,2}Ti_{13,8}Ni_{10}Cu_{12,5}Be_{22}$  $_5$  (at.%). Samples were compared in two different electrolytes. A series of tests were conducted in an aerated 0.6 M NaCl electrolyte at room temperature and in a phosphate-buffered saline (PBS) electrolyte with a physiologically-relevant dissolved oxygen content at 37°C. For both electrolytes, the alloy demonstrated passive behavior up to the mean pitting potentials. The mean corrosion penetration rates were low but a susceptibility to localized pitting corrosion was observed in both electrolytes. Furthermore, the differences between the protection potentials and the open-circuit corrosion potentials in each electrolyte were relatively low. Thus, the material may undergo pitting corrosion at surface flaws or after incubation time periods, depending upon the local and bulk environments.

## 10:10 AM

H Charging of a Zr-Based Bulk Metallic Glass: Ping Wang<sup>1</sup>; Sharvan Kumar<sup>1</sup>; <sup>1</sup>Brown University, Div. of Engrg., 182 Hope St., Box D, Providence, RI 02912 USA

The potential to use a Zr-based bulk metallic glass as a hydrogen storage medium is explored. Hydrogen was cathodically charged into the glass using an electrochemical cell with acid and base media, and to a lesser extent by gas charging at temperature and pressure. Charging parameters were systematically varied including current density, solution concentration and solution temperature; the effects of pre-anneal and intermediate anneal on charging kinetics were also examined. A significant amount of hydrogen can be introduced in the glass before it exhibits cracks (the maximum in this study being H/M = 1.46). In all cases, the material remains amorphous. Attempts to extract the hydrogen from the glass were however fulle; the residual hydrogen interferes with the devitrification process and also affects the glass transition temperature. These results will be discussed and the potential for bulk metallic glasses to store and release hydrogen will be examined.

#### 10:35 AM Invited

## Effects of Changes in Loading Mode on Bulk Metallic Glasses and Bulk Metallic Glass Composites: *Alex K. Thurston*<sup>1</sup>; John J. Lewandowski<sup>1</sup>; <sup>1</sup>Case Western Reserve University, Matls. Sci. & Engrg., 10900 Euclid Ave., White Bldg., Cleveland, OH 44106 USA

Bulk Metallic Glass composites are of interest because of the unique properties of the amorphous structure, while utilizing some additional deformation capabilities provided by the composite additions. Tests are being conducted on the Bulk Metallic Glass as well as the composites in both notched bending and in fatigue precracked conditions. The effects of changes in the test temperature on mechanical properties and fractography will be presented. In addition, the effects of changes in loading mode on the fracture behavior are being determined.

#### 11:00 AM Cancelled

#### Glass Formation Ability and Mechanical Properties of Cu-Zr-Ti-Sn Bulk Metallic Glasses

#### 11:25 AM

Internal Strain Measurements in Bulk Metallic Glasses (BMG) and BMG Composites Using Pair Distribution Function (PDF) Analysis: Bjorn Clausen<sup>1</sup>; Thomas E. Proffen<sup>1</sup>; Seung-Yub Lee<sup>2</sup>; Ersan Ustundag<sup>2</sup>; <sup>1</sup>Los Alamos National Laboratory, LANSCE-12, PO Box 1663, MS H805, Los Alamos, NM 87545 USA; <sup>2</sup>California Institute of Technology, Matls. Sci. Dept., Keck Laboratory, M/C 138-78, 1200 E. California Blvd., Pasadena, CA 91125 USA

The development of bulk metallic glass (BMG) matrix composites is driven by the need to improve the ductility and failure behavior over the monolithic BMG. Similar developments have taken place for metal and ceramic matrix composites (MMCs and CMCs). Neutron powder diffraction have been used extensively in this research to in-situ determine the load sharing between the phases in MMC and CMC composites with crystalline phases. However, the powder diffraction technique is not capable of yielding information about the BMGs due to their amorphous structure. In the present work we have used pair distribution function (PDF) analysis - also called the "total scattering technique" - to obtain information about the changes in inter atomic distances in the BMG as a function of applied load. In-situ neutron PDF measurements were made during compression tests of Vitreloy 106 ( $Zr_{57}Nb_{5}Al_{10}Cu_{15.4}Ni_{12.6}$ ) monolith and composite samples using the SMARTS and NPDF instruments at LANSCE.

## Carbon Technology: Anode Quality and Performance

Sponsored by: Light Metals Division, LMD-Aluminum Committee Program Organizers: Markus Meier, R&D Carbon, Sierre CH 3960 Switzerland; Amir A. Mirchi, Alcan Inc., Arvida Research and Development Centre, Jonquiere, QC G7S 4K8 Canada; Alton T. Tabereaux, Alcoa Inc., Process Technology, Muscle Shoals, AL 35661 USA

Wednesday AM	Room: 213A
March 17, 2004	Location: Charlotte Convention Center

Session Chair: Jim Kissane, Mozal Aluminium Smelter, Maputo Mozambique

#### 8:30 AM

**Optimization of Rodding Room Operation to Enhance Productivity:** *Masood Talib Al Ali*<sup>1</sup>; Raja Javed Akhtar<sup>1</sup>; Saleh Ahmad Rabba<sup>1</sup>; <sup>1</sup>Dubal Aluminium Company Limited, PO Box 3627, Dubai United Arab Emirate

In 1989 DUBAL retrofitted its Rodding Room to support production of over 536,000 tonnes of aluminium per year. The retrofitted plant was designed to produce 750 anodes in two-shifts operation of 8 hours each. The third shift was dedicated entirely to carryout maintenance activities and a built in spare capacity for the security of the plant operation. During 2001/2002 a decision was made to increase DUBAL metal out put to 710,000 tonnes per annum under a project code named "Kestrel". Therefore, Anode Plant Management was given another challenging target of completing the current requirement of 750 anodes in 12 hours shift operation. Achieving this target was essential to maintain the status quo in the Roddng Operation. This paper describes step-by-step approach to identify bottlenecks, finetuning of plant and process followed by tests and trails along with other improvement to confirm the practicality of the proposal. The confidence achieved during the trials lead to a decision to carryout permanent modification as identified during the trials to enhance Rodding Room Operation to produce 920 anodes in two shifts of 8 hours each to support post Kestrel metal prduction without significant increase in its resources.

### 8:55 AM

Going Beyond SPC - Why We Need Statistical Thinking in Operations Such as Carbon Plants: *Keith Sinclair*<sup>1</sup>; Barry Alexander Sadler<sup>2</sup>; 'Sinclair Associates Inc., 2006 Northwood Dr., Maryville, TN 37803 USA; <sup>2</sup>Net Carbon Consulting Pty Ltd., Unit 1, 21 Luck St., Eltham, Victoria 3095 Australia

Statistical thinking is based on the principles that all work occurs in interconnected processes, variation exists in all processes, and reducing this variation is the key to process improvement. The effective use of statistical methods such as Statistical Process Control requires that an implementation framework be established through statistical thinking. Several examples relevant to Carbon Plant operations are provided where the failure to apply statistical thinking to process monitoring and improvement has resulted in waste and lost opportunities. Some appropriate actions for Managers in applying statistical thinking are then outlined.

#### 9:20 AM

Survey on Worldwide Prebaked Anode Quality: Raymond C. Perruchoud<sup>1</sup>; Markus W. Meier<sup>1</sup>; Werner K. Fischer<sup>1</sup>; <sup>1</sup>R&D Carbon Ltd., PO Box 362, Sierre 3960 Switzerland

Anode quality data of 60 prebaked carbon plants were reviewed. The ranges and mode values of the means and of the variability of anode properties were determined and discussed. Some examples of distribution of properties are examined. Causes of inferior or excellent anode quality figures were considered and their effects on the anode behavior and on pot performance are addressed. Interrelationships of thermal shock relevant properties are reported. The bench mark anode quality that can be achieved in a modern plant using typical raw materials is also given.

#### 9:45 AM

Outlook of the Anode Requirement for the World Aluminium Industry in 2015: Werner K. Fischer<sup>1</sup>; *Ulrich Mannweiler*<sup>2</sup>; Age J. de Vries<sup>3</sup>; <sup>1</sup>R&D Carbon Ltd., PO Box 362, Sierre 3960 Switzerland; <sup>2</sup>Mannweiler Consulting, Hadlaubstrasse 71, Zurich 8006 Switzerland; <sup>3</sup>Research and Development Services W.L.L., Manama Bahrain Aluminium is a metal with unbroken growth - with 25 Mio. tons produced in 2002 and a growth rate between 2 to 3%, an additional smelter capacity of more than 500'000 tpa is required each year. A shift of classical production locations can be observed from Europe and USA to new locations with sea port access and low energy cost. A shift can also be observed from many small to few large producers with increased current intensities. Soederberg cells are replaced by prebaked anode technology in particular for brownfield expansions. Accordingly an adapted trend for the anode production sites can be observed. Thereby main focus is given to optimize the specific production cost. This document gives an assumption about the worldwide anode requirement up to 2015 by taking into consideration today's situation and the changing needs.

## Cast Shop Technology: Alloying and Furnace Processing

Sponsored by: Light Metals Division, LMD-Aluminum Committee Program Organizers: Corleen Chesonis, Alcoa Inc., Alcoa Technical Center, Alcoa Center, PA 15069 USA; Jean-Pierre Martin, Aluminum Technologies Centre, c/o Industrial Materials Institute, Boucherville, QC J4B 6Y4 Canada; Alton T. Tabereaux, Alcoa Inc., Process Technology, Muscle Shoals, AL 35661 USA

Wednesday AM	Room: 2	13B/C
March 17, 2004	Location:	Charlotte Convention Center

Session Chairs: Denis Bernard, Alcan Primary Metal Group, Laterriere Works, Laterriere, QC G7N 1A2 Canada; David H. DeYoung, Alcoa Inc., Alcoa Tech. Ctr., Alcoa Ctr., PA 15069 USA

## 8:30 AM

A Method for Prediction of Compacting Behaviour and Mechanical Resistance of Mn Compacts for Aluminium Alloying: Ricardo Fernández-Serrano<sup>2</sup>; Gaspar González-Doncel<sup>2</sup>; Raquel Antolín<sup>1</sup>; Tomás Posada<sup>1</sup>; Gregorio Borge<sup>1</sup>; <sup>1</sup>Bostlan SA, Techl., Polig Ind Trobika, Mungia 48100 Spain; <sup>2</sup>Centro Nacional de Investigaciones Metalúrgicas (CENIM-CSIC), Phys. Metall., Gregorio del Amo, 8, Madrid 28040 Spain

Mn is usually added to aluminium furnaces using compacted mixtures of Mn and Al powders. Many Al producers are highly concerned with breakage of the compacts during transportation and handling, since Mn fine powders release due to compacts weakness can lead to low recoveries and safety concerns during alloying. Mechanical resistance of compacted powders depend on different factors, such as shape and size of the compact, kind of pressing machine, applied pressure, and quality of the raw materials. This work presents an experimental, systematic, and reproducible method for establishing a useful mechanical resistance concept for Mn-Al compacts. Different Mn-Al minitablets have been studied using this method, and an empirical model for predicting the mechanical behaviour of Mn compacts has been developed. The method allows to predict the mechanical resistance of Mn80, Mn85, Mn90, and Mn95 compact powders considering characteristics of the raw materials and the pressing process.

## 8:55 AM

Aluminum Weighing Measurement in Tilting Furnaces: Daniel Audet<sup>1</sup>; Luc Parent<sup>2</sup>; Marlene Deveaux<sup>2</sup>; John Courtenay<sup>3</sup>; <sup>1</sup>Universite du Quebec a Chicoutimi, 555 boul. de l'Universite, Chicoutimi, Quebec G7H 2B1 Canada; <sup>2</sup>BDHTech, 200 Clement-Gilbert, Chicoutimi, Quebec G7H 5B1 Canada; <sup>3</sup>MQP LTD, 6 Hallcroft, Knowle Soli Hull B93 9EW GB UK

The best way to prepare aluminum alloys is to know the heel weight at the end of the previous cast and the weight of pure aluminum added. Many systems have been tried to measure the aluminum weight in tilting furnaces, including load cells, lasers and radars. None of these systems are satisfactory. A measuring system based on the pressure in the piston used to tilt the furnace has been developed. It is easily retrofitted to the existing furnaces and measure weight with an accuracy of  $\pm$  200 kg. The system can be used to monitor the weight either it is a heel or a completely full furnace. It can also measure weight in real time during the transfer from the holding furnace. Results of the system in plant operation will be presented.

## 9:20 AM

Combined Metal Skimming and Melt Treatment System for Metal Transport Crucibles: Jon Hjaltalin Magnusson<sup>1</sup>; <sup>1</sup>ALTECH JHM hf, Lynghals 10, Reykjavik IS 110 Iceland

In metal transported in large crucibles from potrooms to casthouse are impurities and on the metal surface is bath remains and dross. Aluminium smelters therefore install an automatic melt treatment and skimming system for cleaning the metal in these crucibles. The main aim is to improve metal quality (ISO 9001) and improve the skimming efficiency and at the same time the health, safety and environmental conditions for the employees (ISO 14001) by avoiding manual skimming. For melt treatment AlF3 flux is recommended. Controlled by a PLC program, the flux will be injected into the melt and distributed by the double rotor of the Melt Treatment System. Before ending the treatment cycle the introduced treatment gas will support the purification of the melt by floating inclusions (e.g. aluminium carbides) to the surface and removing hydrogen for degassing. Before the melt purification cycle a Skimming System will remove dross and bath remains from the metal surface in the crucible and after the melt treatment it will repeat the surface cleaning before the metal is transported to the holding furnaces in the casthouse. The effective removal of the bath material, dross and impurities from the surface of the metal in the transport crucibles, ensures the cleanliness of the metal.

## 9:45 AM

In-Furnace Refining Using Pyrotek's HD-2000 and FIF-50 Rotary Injector Systems: *Robert A. Frank*<sup>1</sup>; Peter J. Flisakowski<sup>1</sup>; <sup>1</sup>Pyrotek, Inc., SNIF Systems, 100 Clearbrook Rd., Ste. 325, Elmsford, NY 10523-1116 USA

Demand for high quality aluminum, environmental restrictions, and economic pressures create the need for improvements in the melt treatment process. Pyrotek's HD-2000 is designed to replace conventional furnace treatments, such as steel flux wands, graphite flux tubes, and porous plugs. In addition, the combination of the HD-2000 with Pyrotek's FIF-50 can be used for injecting solid fluxes and refining agents. This paper describes the improvements in hydrogen, alkali metal, and inclusion removal of the HD-2000 system versus previous processing at a specific plant. Improvements in emissions, dross formation, production rate, and downstream metal quality are also documented.

## 10:10 AM Break

## 10:45 AM

Improved Molten Metal Quality at the Outlet of the Furnace Through the IRMA Treatment: *Pierre Le Brun*<sup>1</sup>; Alain Mathis<sup>1</sup>; <sup>1</sup>Pechiney, Ctr. de Recherches de Voreppe, 725, rue Aristide Berges, BP 27, Voreppe Cedex 38341 France

In the '80, Pechiney developed a furnace treatment technology aiming at a significant quality increase. The technology is based on rotary gas treatment of the molten metal. Since its first implementation, this technology has widely developed inside Pechiney casthouses. The paper reviews the basics of the technology. The improvements of the molten metal quality that can be obtained through this technology are presented in detail: hydrogen, inclusion, and alkaline or alkalineearth elements removal. Environmental and economic issues are also discussed.

## 11:10 AM

Mathematical Modeling of Aluminum Refining by Rotary Injection: *Pierre Proulx*<sup>1</sup>; Fouzi Kerdouss<sup>1</sup>; Jean-François Bilodeau<sup>2</sup>; Sébastien Vaudreuil<sup>2</sup>; <sup>1</sup>Université de Sherbrooke, Chem. Engrg., 2500 Blvd. Université, Sherbrooke, Québec J1K 2R1 Canada; <sup>2</sup>Alcan International Ltd., Arvida R&D Ctr., PO Box 1250, 1955 Blvd. Mellon, Jonquière, Québec G7S 4K8 Canada

The successful implementation of rotary injection technologies for molten metal treatment depends on the understanding and control of the complex fluid dynamics involved. Computational fluid dynamics offer a powerful tool in order to understand and optimize the rotary flux injection process in holding furnaces (RFI). In the proposed work, the impeller is explicitly described in three dimensions using a Multiple Reference Frames model. Dispersed gas bubbles and molten salt droplets dynamics in the turbulent molten metal are modeled using an Eulerian-Eulerian approach with a dispersed k-epsilon turbulent model. Bubble and droplet size distribution dynamics account for coalescence and break-up mechanisms. The alkali removal reaction is assumed to be controlled by mass transfer. The reaction rate is then determined by the interfacial area calculated from the bubble and droplet dynamics. The modeling results are compared with experimental data for fluid dynamics and chemical reaction.

## 11:35 AM

A Kinetic Study on the Magnesium Removal from Molten Aluminum Using SF<sub>6</sub> Gaseous Mixtures: *Alfredo Flores*<sup>1</sup>; David Villegas<sup>1</sup>; Marco Antonio González<sup>1</sup>; Jose Escobedo; <sup>1</sup>CINVESTAV-IPN, Unidad Saltillo, PO Box 663, 25000 Saltillo, Coahuila México Magnesium removal from molten aluminum scrap has been currently performed at cast shop level in industrial facilities. However, chlorine is still in use in many foundries, with the ecological and technical problems concerning its usage. Instead of using chlorine, gaseous mixtures containing small amounts of SF<sub>6</sub>, O<sub>2</sub>, in argon are proposed, as strong oxidizing conditions for selective magnesium removal are attained. In this paper, a kinetic study is presented, using pneumatic injection through porous lances. The magnesium removal rates were measured as a function of temperature, gas flow rate, composition of the gaseous mixtures, and design of the injection lance. High removal efficiencies, in the order of 97%, were obtained for a combination of operating conditions. Analysis of solidified samples, slags and fumes produced permitted to determine the chemical reactions taking place. Finally, low losses of molten metal were obtained, in the order of 10% in weight.

## CFD Modeling and Simulation of Engineering Processes: Process Modeling I

Sponsored by: Materials Processing & Manufacturing Division, ASM/MSCTS-Materials & Processing, MPMD/EPD-Process Modeling Analysis & Control Committee, MPMD-Solidification Committee, MPMD-Computational Materials Science & Engineering-(Jt. ASM-MSCTS)

*Program Organizers:* Laurentiu Nastac, Concurrent Technologies Corporation, Pittsburgh, PA 15219-1819 USA; Shekhar Bhansali, University of South Florida, Electrical Engineering, Tampa, FL 33620 USA; Adrian Vasile Catalina, BAE Systems, SD46 NASA-MSFC, Huntsville, AL 35812 USA

Wednesday AM	Room: 206A
March 17, 2004	Location: Charlotte Convention Center

Session Chairs: Adrian S. Sabau, Oak Ridge National Laboratory, Metals & Ceram. Div., Oak Ridge, TN 37836-6083 USA; Kanchan Kelkar, Innovative Research, Plymouth, MN 55447 USA

## 8:30 AM Opening Remarks - Adrian Sabau

#### 8:35 AM

Computational Fluid Dynamics: A Tool for the Materials Technology: *Aniruddha Mukhopadhyay*<sup>1</sup>; <sup>1</sup>Fluent Inc., Matls. Procg., 10 Cavendish Ct., Lebanon, NH 03766 USA

Starting with Chorin (1959) and Harlow (1965), over the past several decades Computational Fluid Dynamics (CFD) has come up as a matured analysis tool for conducting virtual experiments with significant time and cost savings. It complements and reduces physical testing. CFD has penetrated diverse materials industry much the same way as Computer-Aided-Design (CAD) did more than a decade ago. As the toolkits for background mathematical algorithms improved, reliability, consistency, and user-friendliness aspects improved significantly too. Recent trends have contributed to the rapid growth and widespread adoption of CFD. In this presentation, brief historical perspective of CFD applications in several materials processing industry will be presented using a few case studies. Emphasis will be on metals, glass and polymer applications.

## 9:10 AM

A Study of the Weld Pool Dimensions and Temperature Profiles Generated for GTA Welds of Gamma Titanium Aluminide (TiAl): Kirtikumar B. Bisen<sup>1</sup>; *Viola L. Acoff*<sup>1</sup>; Mario Arenas<sup>1</sup>; Nagy El-Kaddah<sup>1</sup>; <sup>1</sup>University of Alabama, Dept. of Metallurgl. & Matls. Engrg., 126 7th Ave., Tuscaloosa, AL 35401 USA

Stiff competition in industries requiring high strength, lightweight materials has forced manufacturers to seek ways to implement materials with more attractive properties. Gamma titanium aluminides are a class of materials that maintain their strength at high temperatures and are light in weight which make them attractive for automobile and aerospace applications. In both of these industries, fusion welding is used extensively to join the various components. Several results have been published on the structural characterization of gas tungsten arc welding (GTA) of gamma titanium aluminide however, only a few of these studies concentrate on the physics of arc welding. This study investigates the physics of arc welding as a function of welding parameters for GTA welding of gamma titanium aluminides. Experiment results were used to provide a comprehensive validation of the model. The experimental observations were in close agreement with the model predictions.

#### 9:35 AM

Analysis of Heating Pattern With the Kind of Steel in Induction Heating Furnace: K. H. Cho<sup>1</sup>; Young-jin Jung<sup>2</sup>; <sup>1</sup>RIST, Energy Team, #32, Hyoja-Dong, Namku, Pohang, Kyung-buk 790-600 Korea; <sup>2</sup>Pusan National University, Mech. Engrg., 30, JangJunDong, KumJungKu, Pusan 609-735 Korea

Induction heating is a very common process for melting metals and alloys. If an alternating magnetic field is applied to the workpiece, it penetrates the surface of it and delivers heat within the material, heating it more rapidly and evenly than any other diffusion-dependent processes. However, some operating control condition with the variation of operating condition and the kind of steel is necessary to increase the quality and the productivity. A precise knowledge about the electromagnetic field, the eddy currents and the temperature distribution is necessary to optimize continuous induction heating process. Studies were conducted on the numerical model to predict the temperature of workpiece effectively and correctly. The validity of numerical model is proved by the comparison of calculated and measured temperature distributions through the workpiece. In the future, this could be extended to include more complex model and melting of any material including alloy and heat treating processes.

#### 10:00 AM

Numerical Simulation of Vacuum Dezincing of Lead Alloy: George Stefanov Djambazov<sup>1</sup>; Chris Bailey<sup>1</sup>; Mayur K. Patel<sup>1</sup>; Jennifer Shrimpton<sup>1</sup>; <sup>1</sup>University of Greenwich, Computing & Math. Scis., Old Royal Naval College, Park Row, Greenwich, London, England SE10 9LS UK

Removing zinc by distillation can leave the lead bullion virtually free of zinc and also produces pure zinc crystals. Batch distillation is considered in a hemispherical kettle with water-cooled lid, under high vacuum (50 Pa or less). Sufficient zinc concentration at the evaporating surface is achieved by means of a mechanical stirrer. The numerical model is based on the multiphysics simulation package PHYSICA. The fluid flow module of the code is used to simulate the action of the stirring impeller and to determine the temperature and concentration fields throughout the liquid volume including the evaporating surface. The rate of zinc evaporation and condensation is then modelled using Langmuir's equations. Diffusion of the zinc vapour through the residual air in the vacuum gap is also taken into account. Computed results show that the mixing is sufficient and the rate-limiting step of the process is the surface evaporation driven by the difference of the equilibrium vapour pressure and the actual partial pressure of zinc vapour. However, at higher zinc concentrations, the heat transfer through the growing zinc crystal crust towards the cold steel lid may become the limiting factor because the crystallization front may reach the melting point. The computational model can be very useful in optimising the process within its safe limits.

#### 10:25 AM Break

10:45 AM

The Application of CFD to the Design of Electric Furnaces: Lowy Gunnewiek<sup>1</sup>; *Lanre Oshinowo*<sup>1</sup>; Tom Plikas<sup>1</sup>; Ross Haywood<sup>2</sup>; <sup>1</sup>Hatch Associates Ltd., 2800 Speakman Dr., Mississauga, Ontario L5K 2R7 Canada; <sup>2</sup>Hatch, 152 Wharf St., Brisbane, Queensland 4000 Australia

Electric furnace smelting is one of the principal unit operations for ferroalloy production, and increased process intensity, improved availability, minimal maintenance and a longer campaign life are common objectives for electric furnace operation in order to obtain favourable economics of production. Furnace designers have continued to develop innovative solutions that have allowed these objectives to be realised, e.g., furnace cooling systems, and numerical modelling plays a key role in the design process. Enhanced understanding of the energy transfer process in the furnace and the ability to develop, evaluate and optimise components of the crucible design to match process requirements are the key motivators for modelling. This paper provides an overview of recent applications of numerical modelling to the design of electric furnaces. Several examples are presented, including furnace bath modelling, crucible cooling system design, taphole design, baking of Soderberg electrodes, off-gas systems, and fume control and building ventilation.

#### 11:10 AM

Simulation of Combustion and Metal Heating in a Mobile Heat Treatment Furnace: *Yongxiang Yang*<sup>1</sup>; Reinier A. de Jong<sup>1</sup>; Markus A. Reuter<sup>1</sup>; <sup>1</sup>Delft University of Technology, Applied Earth Scis., Mijnbouwstraat 120, Delft 2628 RX The Netherlands

In this paper, a mobile heat treatment furnace from Akkermans Gloeitechniek, a Dutch company, was simulated with Computational Fluid Dynamics (CFD). The furnace is cylindrical and has four oil burners, and large metal products such as dredging pumps and fans can be flexibly heat treated to obtain required microstructure and mechanical properties through stress relief, annealing, hardening and tempering. The furnaces are exposed to the open air, and thus the heat loss becomes significant and varies from day to day and from season to season. Since the temperature of the metal products to be heat treated can only be measured on the surface, the temperature evolution inside the metal could not be tracked in practice. CFD simulation provides a useful tool to predict the temperature evolution within the metal pieces and within the combustion space of the furnace. Energy distribution and heat loss can be subsequently estimated. An overall energy balance through temperature measurement indicted relatively low energy efficiency. Especially during the soaking period, the high energy supplied is barely used to compensate the heat loss of the furnace to maintain a constant temperature of the metal piece. The current CFD modelling aims to give advice on how to modify the design and optimize the operation to reach higher energy efficiency and low heat loss. The CFD model consists of turbulent combustion model, radiative model in participating media, and conjugate heat transfer between the combustion space and solid metal. Temperature measurement was carried out to provide thermal boundary conditions and overall energy balance of the operation. After the model validation with temperature measurement within the combustion space and metal surfaces, furnace optimization will be conducted.

## Computational Thermodynamics and Phase Transformations: Phase Equilibria and Thermodynamic Assessments

Sponsored by: ASM International: Materials Science Critical Technology Sector, Electronic, Magnetic & Photonic Materials Division, Materials Processing & Manufacturing Division, Structural Materials Division, MPMD-Computational Materials Science & Engineering-(Jt. ASM-MSCTS), EMPMD/SMD-Chemistry & Physics of Materials Committee

Program Organizer: Jeffrey J. Hoyt, Sandia National Laboratories, Materials & Process Modeling, Albuquerque, NM 87122 USA

Wednesday AM	Room: 20	02A
March 17, 2004	Location:	Charlotte Convention Center

Session Chair: TBA

## 8:30 AM

On the Ab Initio and CALPAHD Approaches to Lattice Stability: Zi-Kui Liu<sup>1</sup>; Yi Wang<sup>1</sup>; Lonq-Qing Chen<sup>1</sup>; <sup>1</sup>Pennsylvania State University, Matls. Sci. & Engrg., Univ. Park, PA 16802 USA

The bct, bcc, and fcc structures of a pure element can be related through a continuous crystal axis expansion and contraction of the same crystal lattice. In the present work, ab initio calculations are carried out for various pure elements and binary systems with either fcc or bcc as their stable structures. The total energies are plotted as a function of the c/a ratio. It is observed that if the total energy of the fcc structure for a pure element is a minimum, then that of the bcc structure is a maximum, and vice versa. The relative magnitude of the total energies of the fcc and bcc structures in binary systems changes with composition. These results are discussed in connection with the lattice stability used in the CALPHAD community.

#### 8:50 AM

Thermodynamic Modelling of Multicomponent Systems - Design of Critical Experiments: Karin Frisk<sup>1</sup>; <sup>1</sup>Swedish Institute for Metals Research, Drottning Kristinas väg 48, SE\_11428 Stockholm Sweden

Thermodynamic modelling is a powerful tool in alloy development, and the CALPHAD (CALculation of PHAse Diagrams) method is today widely spread. The method involves coupling of the phase diagram and thermochemistry of all the possible stable or metastable phases in a system. The CALPHAD method has proved to be successful when applied to complex materials with many components and phases, where limited experimental information is available and experimental determinations are time consuming. However, when extending to composition or temperature ranges that have not previously been studied, validation by experiments is needed. A few examples of experimental validation of thermodynamic databases for multicomponent alloys performed for steel and cemented carbides are given. The choice of experiments and the interpretation of the results are discussed. The discrepancies between calculations and experiments that were found could be explained by inconsistencies in binary and ternary systems due to lack of experimental information, or a need for better descriptions of metastable phases. It was found that the accuracy of the calculations was improved by performing new analysis of metastable phases. To increase the ranges where reliable extrapolations can be made, critical experiments were designed to determine interactions in ternary systems. The methods to select critical experiments, and the resulting improvement of the thermodynamic description is discussed.

### 9:10 AM

Thermodynamic Assessment of the Ag-Cu-Ti System: Raymundo Arroyave<sup>1</sup>; <sup>1</sup>Massachusetts Institute of Technology, Matls. Sci. & Engrg., 77 Mass. Ave., Rm. 4-047, Cambridge, MA 02139 USA

A thermodynamic description for the Ag-Ti binary system was developed using all the existing experimental phase diagram data available and the resulting parameters were discussed in light of very recent thermochemical measurements of Ag-Ti melts. Using the description of the Ag-Ti binary and with the accepted descriptions for the Ag-Cu and Cu-Ti sub-systems, the Ag-Cu-Ti ternary system is critically assessed and a thermodynamic model is developed so the available experimental data are represented as accurately as possible. The phases CuTi2 and AgTi2 are modeled using a single two-sublattice model, (Ag,Cu)1(Ti)2, assuming that these phases form a continuous solid solution. The CuTi and AgTi phases are also modeled using a single sublattice model, (Ag,Cu,Ti)1(Ag,Cu,Ti)1, and their penetration into the ternary compositional triangle is correctly predicted. Ternary interactions for the liquid phase were incorporated. Experimental and calculated results are compared and the reliability of the model is confirmed.

#### 9:30 AM

Phase Equilibria and Thermodynamic Modeling of Al-Based Metallic Glasses: *Michael C. Gao*<sup>1</sup>; Necip Unlu<sup>1</sup>; Gary J. Shiflet<sup>1</sup>; <sup>1</sup>University of Virginia, Matls. Sci. & Engrg., 116 Engineer's Way, PO Box 400745, Charlottesville, VA 22904-4745 USA

Thermodynamic and phase equilibria studies were performed for two aluminum-based glass-forming systems, namely, Al-Co-Ce and Al-Ni-Nd over a compositional range of 60-100 at% Al. First the glass formation range was determined using melt-spinning techniques and its crystallization behavior was studied using XRD, DSC and TEM. Then a number of alloys in each system were chosen for solid-state phase equilibria study using XRD, SEM and TEM, while DTA was used to characterize the solidus and liquidus temperatures. Using these results combined with other published data, these systems were thermodynamically optimized in their Al-rich corners using the CALPHAD approach. The relationship among thermodynamics, glass forming ability and crystallization behavior will be discussed.

#### 9:50 AM Break

#### 10:00 AM

The Calculated Energetics of Ni-Mo and Ni-Ta Alloy: Yi Wang<sup>1</sup>; Shihuai Zhou<sup>1</sup>; Zikui Liu<sup>1</sup>; Longqing Chen<sup>1</sup>; <sup>1</sup>Pennsylvania State University, Matls. Sci. & Engrg., 106 Steidle Bldg., State College, PA 16802-5006 USA

The energetics of the binary compounds, Ni8Mo, Ni4Mo, Ni3Mo, Ni2Mo, delta-Ni24[Ni4xMo4(5-x)]Mo12 (x = 0 - 5), Ni8Ta, Ni3Ta, Ni2Ta, Ni6Ta7, and NiTa2, are studied using the first-principles calculations. It is shown that delta-Ni24(Ni4Mo16)Mo12, has the lowest energy of formation among the range of x examined. The calculated formation energies demonstrates that the delta-NiMo phase is meta-stable at 0 K and that Ni8Mo and Ni2Mo are stable at 0 K whereas the experimental high temperature phase diagram shows no Ni8Mo and Ni2Mo. For the Ni-Ta system, our results show that Ni8Ta, Ni2Ta, and NiTa2 are stable at 0 K while Ni6Ta7 is not. Experimentally, there are three types of Ni3Ta, i.e. Ni3Ta(2)S, Ni3Ta(3)S, and Ni3Ta(12)S, existed with Ni3Ta(12)S being the most stable one at temperature above 1128 K. However, our calculation shows that Ni3Ta(3)S is the most stable one at 0 K with Ni3Ta(2)S is the next and then Ni3Ta(12)S.

## 10:20 AM

First-Principles Calculations and Modeling on Lattice Parameters of the Ni-Al-Mo-Ta System: *Tao Wang*<sup>1</sup>; Yi Wang<sup>1</sup>; Long-Qing Chen<sup>1</sup>; Zi-Kui Liu<sup>1</sup>; <sup>1</sup>Pennsylvania State University, Dept. of Matls. Sci. & Engrg., Univ. Park, PA 16802 USA

The lattice parameter is an important material property. In the present work, the temperature and composition dependences of lattice parameters of the gamma and gamma prime phases in the Ni-Al-Mo-Ta system are modeled phenomenologically using the CALPHAD approach. In this approach, phases are described by sublattice models. To model the composition dependence, the lattice parameters of all endmembers in the sublattice models are needed, and some of these endmembers are not stable. First-principles calculations are thus carried out to compute the lattice parameters of those end-members using the full-potential linearized augmented plane wave (FP-LAPW) method implemented in the WIEN2k package. Lattice parameters in the Ni-Al-Mo-Ta are thus calculated and compared with available experimental data.

#### 10:40 AM

Investigation of Enthalpy of Formation for All the Possible Binary Laves Phases of Group IIA: Yu Zhong<sup>1</sup>; Jorge O. Sofo<sup>2</sup>; Zi-Kui Liu<sup>3</sup>; <sup>1</sup>Pennsylvania State University, Matls. Sci. & Engrg., 107 Steidle Bldg., Univ. Park, PA 16802 USA; <sup>2</sup>Pennsylvania State University, Matls. Simulation Ctr., Univ. Park, PA 16802 USA; <sup>3</sup>Pennsylvania State University, Matls. Sci. & Engrg., 209 Steidle Bldg., Univ. Park, PA 16802 USA

First-principles calculations are performed for all combinations of elements in Group IIA (Be, Mg, Ca, Sr, Ba, Ra) for the possible binary A2B laves phases in C14, C15 and C36 structures. According to the work of Zhu et al.,<sup>1</sup> the atomic ratio of the two elements is the most important factor in determining the stability of the laves phases. A lave phase can be considered to have two sublattices with preferable occupancies of individual atoms. In the current thermodynamic modeling, they are modeled with a two-sublattice model, i.e. (A,B)2(A,B). This model has 4 end-members: A2B, A2A, B2B, B2A. Their enthalpies of formation are calculated to examine its relationship with the stability and solubility range of laves phases. <sup>1</sup>J. H. Zhu, C. T. Liu, L. M. Pike and P. K. Liaw, "Enthalpies of formation of binary Laves phases" Intermetallics, 10 (2002) 579-595.

#### 11:00 AM

Evaluation of the Thermodynamic Properties of the Ni-Mo-Ta System Incorporating First-Principles Calculations: Shihuai Zhou<sup>1</sup>; Yi Wang<sup>1</sup>; Tao Wang<sup>1</sup>; JingZhi Zhu<sup>1</sup>; Rebecca A. MacKay<sup>2</sup>; Long-Qing Chen<sup>1</sup>; Zi-Kui Liu<sup>1</sup>; <sup>1</sup>Pennsylvania State University, Dept. of Matls. Sci. & Engrg., 107 Steidle Bldg., State College, PA 16802 USA; <sup>2</sup>NASA Glenn Research Center, Matls. Div., 21000 Brookpark Rd., Cleveland, OH 44135 USA

The phase equilibria and thermodynamic properties of the ternary Ni-Mo-Ta system were analyzed. The enthalpies of formation of the stable or metastable d-NiMo, Ni2Mo, Ni3Mo, Ni4Mo, Ni8Mo, NiTa2, NiTa, Ni2Ta, Ni3Ta and Ni8Ta phases were calculated by the firstprinciples method using Vienna Ab-initio Simulation Package (VASP) at 0 K. The results indicate that the compounds, Ni2Mo, Ni3Mo with the Cu3Ti structure, Ni4Mo, Ni8Mo, NiTa2, Ni2Ta, Ni3Ta with the Al3Ti structure and Ni8Ta are stable phases at 0K, while the compounds, d-NiMo, Ni3Mo with the Al3Ti structure, NiTa, Ni3Ta with the Cu3Ti and Pt3Ta structures are metastable phase at 0K. In the thermodynamic description, the stable Ni3Mo and metastable Ni3Ta phases with the Cu3Ti structure were treated as same phase, while the metastable Ni3Mo and stable Ni3Ta phases with the Al3Ti structure were described as same phase. The non-stoichiometric stable Ni3Ta phase at high temperature with the Pt3Ta structure and Ni3Mo phase with the Cu3Ti structure were described with a two sublattice model. With the first-principles and experimental phase equilibrium data, the Gibbs energy function of individual phase was determined. The calculated results of the ternary Ni-Mo-Ta system were compared with the first-principles data and the experimental data in the literature.

#### 11:20 AM

First-Principles Study of the Order-Disorder Transition of the Al4Cu9(Gamma) Phase: Chao Jiang<sup>1</sup>; Long-Qing Chen<sup>1</sup>; Zi-Kui Liu<sup>1</sup>; <sup>1</sup>Pennsylvania State University, Matls. Sci. & Engrg., Univ. Park, PA 16802 USA

Based on recent experimental observations, the gamma phase in Al-Cu system undergoes a D83->D82 order-disorder transition, which is of second-order type instead of the previously believed first-order. In the present work, this transition was investigated using the first-principles/CALPHAD hybrid computational approach. The gamma phase was modeled using a (Al,Cu)3(Al,Cu)3(Al,Cu)1(Al,Cu)1(Cu)5 five-sublattice model. The formation enthalpies of all the end-members were obtained from first-principles total energy calculations. All structures are fully relaxed with respect to cell-internal and -external degrees of freedom. The entropies of formation of the end-members and the interaction parameters within each sublattice were adjusted to fit the order-disorder transition temperature and the phase diagram. The model calculations are compared with experimental observations.

## Cost-Affordable Titanium Symposium Dedicated to Prof. Harvey Flower: Creative Fabrication

Sponsored by: Structural Materials Division, SMD-Titanium Committee

*Program Organizers:* M. Ashraf Imam, Naval Research Laboratory, Washington, DC 20375-5000 USA; Derek J. Fray, University of Cambridge, Department of Materials Science and Metallurgy, Cambridge CB2 3Q2 UK; F. H. (Sam) Froes, University of Idaho, Institute of Materials and Advanced Processes, Moscow, ID 83844-3026 USA

Wednesday AM	Room: 20	06B		
March 17, 2004	Location:	Charlotte	Convention	Center

Session Chair: Vladimir Moxson, ADMA Products Inc., Twinsburg, OH 44087 USA

#### 8:30 AM

Commercialization of the Armstrong Process for Producing Titanium Alloy Powder: Richard P. Anderson<sup>1</sup>; William Ernst<sup>1</sup>; Lance Jacobsen<sup>1</sup>; Dariusz Kogut<sup>1</sup>; <sup>1</sup>ITP, 20634 W. Gaskin Dr., Lockport, IL 60441 USA

The Armstrong Process produces high purity titanium and titanium alloy powders by injecting a jet of vaporized TiCl4 (or mixed metal chlorides for alloys) into a stream of flowing sodium. The powder characteristics (size distribution, morphology, flow and packing characteristics) may be tailored for various applications by varying the system operating parameters. Development of the Armstrong process has gone through the traditional pre-commercialization stages. A pilot plant became operational in early '03. The small size and benign operating conditions (low temperature and pressure) in the reactor, combined with the continuous nature of the overall process, allows for production of high purity powder at a fraction of the current production cost of titanium powder and ingot. The overall economics of the process will be discussed and compared with other production technologies. Powder samples and parts made from the powder will be available for inspection.

#### 9:00 AM

The Utilization of Recycled Titanium Ores and Innovative Plasma Arc Technology for the Production of Low Cost Titanium Metal Powders: Lowell V. Sieck<sup>1</sup>; Mark S. Shuey<sup>1</sup>; Daniel I. Kaplan<sup>1</sup>; <sup>1</sup>Industrial Technologies of New York, LLC, Yonges Island, SC 29449 USA

Titanium metal alloys remain the metals of choice for advance materials use in the aerospace, automotive, and medical implant industries. As is widely recognized, the use of titanium metal alloys in these industries is presently limited by the availability of low cost titanium metal alloy powders and available fabrication processes. While recent advances in fabrication processes, including use of titanium powder alloys for improved near-net shapes and laser and electron beam methods for joining, have improved opportunities for use of titanium alloys; the availability of low cost, high quality, titanium metal alloy powders has not significantly improved. However, recent advances that have been made in a combination of technologies involving: 1) recovering titanium ore from industrial waste streams, 2) smelting low cost, recycled, titanium ore directly into titanium metal stock using innovative plasma arc technology, and 3) an innovative design for gas atomization of titanium metal stock may result in significant reductions in the cost of high quality titanium powders. These innovations could allow the development and marketing of low cost titanium metal powders that can augment the use of titanium powders in many existing industries as well as contribute to the development of new commercial applications for titanium metals.

#### 9:30 AM

Powder Metallurgy Ti-6Al-4V Components Produced from Low Cost Blended Elemental Powders by Hot Pressing: V. A. Duz<sup>1</sup>; V. S. Moxson<sup>1</sup>; F. H. (Sam) Froes<sup>2</sup>; F. Sun<sup>2</sup>; J. S. Montgomery<sup>3</sup>; <sup>1</sup>ADMA Products, Inc., 8180 Boyle Pkwy., Twinsburg, OH 44087 USA; <sup>2</sup>University of Idaho, Inst. for Matls. & Adv. Proc. (IMAP), McClure Hall, Rm. 437, Moscow, ID 83844-3026 USA; <sup>3</sup>Army Research Laboratory, Aberdeen Proving Ground, MA 21005-5066 USA

Cost effective method for manufacturing Ti-6Al-4V chunky components from Blended Elemental (BE) powder using a hot pressing consolidation technique will be discussed. Large size preforms with various sintered densities have been used for hot consolidation to near net densities (over 99% of theoretical). Various microstructures developed in sintering and high temperature deformation will be presented.

## 10:00 AM

Effect of Oxygen Content on Properties of Cast Ti-6Al-4V Alloy: Mustafa Guclu<sup>1</sup>; Ibrahim Ucok<sup>1</sup>; Joseph R. Pickens<sup>1</sup>; <sup>1</sup>Concurrent Technologies Corporation, 100 CTC Dr., Johnstown, PA 15904 USA

An objective of the Combat Vehicle Research (CVR) Program at Concurrent Technologies Corporation is to effect greater use of lowcost titanium alloys such as Ti-6-4 in combat vehicle and other defense applications. It is clear from various defense programs that in the near term, use of high-oxygen (up to 0.25 wt%) titanium alloys such as those made by single-melt processing, is leading the way in reducing costs and expanding the use of titanium alloys in defense applications. Ti-6-4 components, including the gun pod and elevation arms for the Mobile Gun System, were fabricated with different oxygen levels, by investment casting and the rammed graphite casting processes. The effect of oxygen content on mechanical properties was examined. Tensile properties were determined, as required by typical casting specifications, and found to exceed the minimum requirements for all oxygen levels investigated. Extensive mechanical testing and evaluation will be needed to further expand application areas of lowcost titanium castings.

## 10:30 AM

**Cost Effective Powder Metallurgy Approach to Produce Titanium Alloy Plates:** *V. S. Moxson*<sup>1</sup>; V. A. Duz<sup>1</sup>; J. S. Montgomery<sup>2</sup>; F. H. (Sam) Froes<sup>3</sup>; <sup>1</sup>ADMA Products, Inc., 8180 Boyle Pkwy., Twinsburg, OH 44087 USA; <sup>2</sup>Army Research Laboratory, Aberdeen Proving Ground, MA 21005-5066 USA; <sup>3</sup>University of Idaho, Inst. for Matls. & Adv. Proc. (IMAP), McClure Hall, Rm. 437, Moscow, ID 83844-3026 USA

Cost effective method for manufacturing Ti-6Al-4V plates using a Blended Elemental (BE) powder metallurgy (P/M) approach will be discussed. 48" wide plates with various thickness produced by this method has been metallographic evaluated at various stages of production. Detailed studies of the microstructures developed in sintering and high temperature rolling will be presented.

## 11:00 AM

**Titanium Eddy Current Measurement**: John Paul Wallace<sup>1</sup>; Robert M. Siegfried<sup>2</sup>; Jerome Dunn<sup>3</sup>; <sup>1</sup>Casting Analysis Corp., 8379 Ursa Ln., Weyers Cave, VA 24486 USA; <sup>2</sup>Adelphi University, Dept. Math. & Comp. Sci., South Ave., Garden City, NY 11530 USA; <sup>3</sup>Casting Analysis Corp, 48 Montague Rd., Sunderland, MA 01375 USA

In process eddy current measurements for oxygen variation, weld detection and defect detection are compromised by two physical properties of alpha-titanium. These are the hexagonal crystal symmetry which complicates the conductivity measurement and the BCC-HCP phase transition alters texture and microstructure of the metal upon cooling from solidification. Multifrequency application of inverse analysis using probes allows the removal of geometric effects of shape and liftoff. What remains is the analysis of the normal sources of conductivity variations such as impurity alloying, cold work, recovery and recrystallization structures. Modifying sensors to detect the symmetry contributions of a textured structure and extending the inverse analysis to probe depth variations of the local electrical conductivity tensor allows a separation of texture verses alloying contributions to the conductivity. In the simplest measurement application where one wants to separate oxygen alloying effects by measuring the bulk electrical conductivity, a local understanding of the microstructure is required in order to separate the contributions of the oxygen from the microstructure. Base line data will be presented from high purity single crystals through cold worked structures showing the range of responses of the key effects influencing conductivity variation. Then the procedure of automating this analysis in real time will presented for application to in process monitoring and inspection.

## 11:30 AM

**Titanium in the Family Automobile: The Cost Challenge:** F. H. (Sam) Froes<sup>1</sup>; H. Friedrich<sup>2</sup>; J. Kiese<sup>3</sup>; D. Bergoint<sup>4</sup>; <sup>1</sup>University of Idaho, Inst. for Matls. & Advd. Processes, McClure Bldg., Rm. 437, Moscow, ID 83844-3026 USA; <sup>2</sup>Volkswagen AG, Letter Box 1777, Wolfsburg D-38436 Germany; <sup>3</sup>Volkswagen AG, Wolfsburg D-38436 Germany; <sup>4</sup>Bergoint Engineering GmbH, Akazienweg 11, Alsbach 64665 Germany

With advances in extraction/fabrication techniques and ever increasing gasoline prices the advantage of using lightweight materials such as titanium in automobiles continues to increase. The major drawback - high cost - is omnipresent. However innovative extraction and fabrication approaches are leading to a deceased cost. The present status and future potential for titanium use in the family automobile will be presented.

## **Dislocations: Plasticity, Voids, and Fracture**

Sponsored by: ASM International: Materials Science Critical Technology Sector, Electronic, Magnetic & Photonic Materials Division, Materials Processing & Manufacturing Division, Structural Materials Division, EMPMD/SMD-Chemistry & Physics of Materials Committee, MPMD-Computational Materials Science & Engineering-(Jt. ASM-MSCTS)

*Program Organizers:* Elizabeth A. Holm, Sandia National Laboratories, Albuquerque, NM 87185-1411 USA; Richard A. LeSar, Los Alamos National Laboratory, Theoretical Division, Los Alamos, NM 87545 USA; Yunzhi Wang, The Ohio State University, Department of Materials Science and Engineering, Columbus, OH 43210 USA

Wednesday AM	Room: 201A	
March 17, 2004	Location: Charlotte Convention Center	er

Session Chair: TBA

## 8:30 AM Invited

A Multi-Phase Field Theory of Dislocation Dynamics: M. P. Ariza<sup>1</sup>; A. M. Cuitino<sup>2</sup>; M. Koslowski<sup>3</sup>; *M. Ortiz*<sup>1</sup>; <sup>1</sup>California Institute of Technology, Div. of Engrg. & Applied Sci., Pasadena, CA 91125 USA; <sup>2</sup>Rutgers University, Mech. & Aeros. Engrg. Bldg., Rm. D158, Piscataway, NJ 08854 USA; <sup>3</sup>Los Alamos National Laboratory, Theoretical Div., MS B268, Los Alamos, NM 87545 USA

A multi-phase field theory of dislocation dynamics and strain Hardening in ductile single crystals is developed. The theory accounts for: an arbitrary number and arrangement of dislocation lines over multiple slip systems; the long-range elastic interactions between dislocation lines; the core structure of the dislocations; the interaction between the dislocations and an applied stress field; and the (possibly irreversible) interactions with short-range obstacles and other dislocations, resulting in hardening. A chief advantage of the present theory is that it is analytically tractable with the aid of standard tools of analysis such as the discrete Fourier transform and Gamma-convergence. The multi-phase field representation enables complex geometrical and topological transitions in the dislocation ensemble, including dislocation loop nucleation, bow-out, pinching, and the formation of Orowan loops. The theory predicts a range of behaviors which are in qualitative agreement with observation, including: hardening and dislocation multiplication in single slip under monotonic loading; the Bauschinger effect under reverse loading; the fading memory effect, whereby reverse yielding gradually eliminates the influence of previous loading; the evolution of the dislocation density under cycling loading, leading to characteristic 'butterfly' curves; the formation of dislocation networks and cellular structures; and others.

## 9:05 AM

The Effects of Grain Size and Dislocation Source Density on the Strengthening Behavior of Polycrystals a Two Dimensional Discrete Dislocation Simulation: S. B. Biner<sup>1</sup>; J. R. Morris<sup>1</sup>; <sup>1</sup>Iowa State University, Ames Lab., Metal & Ceram. Scis., Ames, IA 50011 USA

The evolution of the flow stress for grain sizes ranging from about 11 to 0.5  $\mu$ m under shear deformation was examined. The grain boundaries were assumed to be both the only sources for dislocation nucleation and also the only obstacles to the dislocation motion. The simulations were carried out for two sets of system sizes and grain morphologies. For the grain size ranges considered, an inverse relationship between the grain size and 0.2% offset flow stress in the form of Hall-Petch relationship [d]-<sup>1/2</sup> was observed, although there is some uncertainty in the exponent. The evolution of flow stress follows a narrow band when expressed as a function of dislocation density divided by the dislocation source density and hence suggests a scaling with the grain size as seen in our earlier study. This work was performed for the USDOE by Iowa State University under contract W-7405-Eng-82. This research was supported by the Director of Energy Research, Office of Basic Sciences.

## 9:25 AM

Relationships of Fracture Toughness and Dislocation Mobility in Intermetallics: *Kwai S. Chan*<sup>1</sup>; <sup>1</sup>Southwest Research Institute, 6220 Culebra Rd., San Antonio, TX 78238 USA

An analytical method has been developed and utilized to compute the Peierls-Nabarro (P-N) barrier energy for relevant slip systems in several intermetallics. The P-N barrier energy and generalized fault energy are combined and used as a measure of dislocation mobility. Furthermore, a fracture model has been developed to describe the process of thermally activated dislocations moving away from the crack tip and to predict the corresponding fracture resistance. The correlation indicates that fracture toughness increases with decreasing values of the P-N barrier energy and the generalized stacking fault energy, in accordance with the fracture model formulated based on thermally activated slip. The use of the fracture model for predicting the effects of slip behavior, temperature, and alloy additions on fracture resistance is demonstrated for selected intermetallics including NiAl, TiAl, Laves phase, and Nb-based silicides. Work supported by AFOSR through Contract No. F4962001-C-0016, Dr. Craig S. Hartley, Program Manager.

## 9:45 AM

**Dislocation Analysis of Fatigue Crack Growth**: *Kuntimaddi* Sadananda<sup>1</sup>; <sup>1</sup>Naval Research Laboratory, Matls. Sci. & Tech. Div., Code 6323, Washington, DC 22152 USA

Fatigue crack growth behavior is analyzed using discrete dislocations. Equilibrium configuration of both crack-dislocations and crystal-lattice dislocations are determined by minimizing the total elastic energy of the system. The effect of plastic zone on the crack tip stress intensity factor is calculated using Lin-Thomson equations. Crack is then extended elastically, while the plastic zone moves behind the crack tip forming crack wake plasticity. The effect on the crack tip stress intensity factor is determined to evaluate the role of crack tip plasticity on crack growth rate. The role of internal stresses, effects of overloads and underloads are estimated.

#### 10:05 AM

Laser Shock Compression of Copper Monocrystals: Mechanisms for Dislocation and Void Generation: Matthew S. Schneider<sup>1</sup>; Bimal Kad<sup>1</sup>; Fabienne Gregori<sup>2</sup>; Daniel H. Kalantar<sup>3</sup>; Bruce A. Remington<sup>3</sup>; Marc A. Meyers<sup>1</sup>; Vlado A. Lubarda<sup>1</sup>; <sup>1</sup>University of California, Matls. Sci. & Engrg., MC 0418, La Jolla, CA 92093 USA; <sup>2</sup>University of Paris 13 France; <sup>3</sup>Lawrence Livermore National Laboratory, Livermore, CA 94450 USA

Copper and copper aluminum with two orientations ([001] and [134]) were subjected to high intensity laser (energy levels of 40-300 J; energy densities of 15-70 MJ/m2 and durations below 10 ns). The defects created are characterized by transmission electron microscopy. An orientation-dependent threshold stress for twinning is observed. The results are rationalized in terms of a criterion in which slip and twinning are considered as competing mechanisms. A constitutive description is applied to the two orientations, incorporating both slip and twinning. The predictions are in agreement with experiments. The threshold stress for twinning in the [001] orientation is 20-40 GPa, whereas the one for the [134] orientation is 40-60 GPa. The threshold stress is calculated, considering the effect of shock heating. The constitutive description provides a rationale for the experimental results; the calculated thresholds are 18 GPa for [001] and 25 GPa for [134]. A mechanism for void generation and growth based on the emission of geometrically necessary dislocations is proposed and analytically formulated.

## Electrochemical Measurements and Processing of Materials: Electrochemical Metal Production

Sponsored by: Extraction & Processing Division, Materials Processing & Manufacturing Division, EPD-Aqueous Processing Committee, EPD-Process Fundamentals Committee, EPD-Pyrometallurgy Committee, ASM/MSCTS-Thermodynamics & Phase Equilibria Committee, EPD-Waste Treatment & Minimization Committee

*Program Organizers:* Uday B. Pal, Boston University, Department of Manufacturing Engineering, Brookline, MA 02446 USA; Akram M. Alfantazi, University of British Columbia, Department of Metel & Materials Engineering, Vancouver, BC V6T 1Z4 Canada; Adam C. Powell, Massachusetts Institute of Technology, Department of Materials Science and Engineering, Cambridge, MA 02139-4307 USA

Wednesday AM	Room: 212A
March 17, 2004	Location: Charlotte Convention Center

Session Chairs: Adam C. Powell, Massachusetts Institute of Technology, Matls. Sci. & Engrg., Cambridge, MA 02139-4307 USA; James W. Evans, University of California, Matls. Sci. & Mineral Engrg., Berkeley, CA 94720 USA

8:30 AM Invited

Zirconia-Based Inert Anodes for Green Synthesis of Metals and Alloys: Uday B. Pal<sup>1</sup>; Ajay Krishnan<sup>1</sup>; Christopher Manning<sup>1</sup>; Sourav Sen'; <sup>1</sup>Boston University, Mfg. Engrg., 15 St. Mary's St., Boston, MA 02215 USA

The research work demonstrates the technical viability of employing zirconia-based inert anodes for environmentally sound and costeffective production of metals such as magnesium, tantalum, aluminum, etc., directly from their oxides. The inert anode consists of the oxygen-ion-conducting stabilized zirconia membrane in intimate contact on one side with a catalytically active electronic phase. The opposite (other) side of the zirconia membrane is placed in contact with an ionically conducting solvent phase. A cathode is placed in the solvent and an appropriate electric potential is applied between the electrodes to synthesize the metals from their oxides. The full-benefit of the process can be realized if it is conducted at temperatures between 1100-1400°C. At these temperatures the ohmic resistance drop across the stabilized zirconia membrane are low and therefore high current densities on the order of 1 A/cm2 or greater can be obtained. In addition, the process efficiency can be further increased by directly reforming hydrocarbon fuel over the anode. This paper reports the recent progress of a continuing laboratory-scale investigation involving different types of zirconia-based inert anodes employed at temperatures between 1100-1400°C. The topics covered include: stability of the zirconia membrane in the selected molten solvent (flux), volatility of the flux, potentiodynamic sweeps, electrolysis experiments, and analysis of the metals produced.

#### 9:00 AM Invited

Towards Carbon-Free Metals Production by Molten Oxide Electrolysis: Donald R. Sadoway<sup>1</sup>; <sup>1</sup>Massachusetts Institute of Technology, Dept. of Matls. Sci. & Engrg., 77 Mass. Ave., Rm. 8-203, Cambridge, MA 02139-4307 USA

Molten oxide electrolysis (MOE) is an extreme form of molten salt electrolysis, a technology that has been producing tonnage metal for over 100 years: aluminum, magnesium, lithium, sodium, and the rare-earth metals are all produced in this manner. MOE is distinguished by the avoidance of halide electrolytes and carbon anodes which enables the production of oxygen gas instead of halogens or  $CO_2$ . Accurate knowledge of the electrical properties of candidate electrolytes is needed for the design of industrial electrolytic cells because joule heating establishes the thermal balance. In the absence of a fully satisfactory technique for making high-accuracy measurements, the coaxial cylinders technique was invented. The variation of electrical conductivity and transference number with temperature and composition has been measured for melts in the FeO - MgO - CaO - SiO<sub>2</sub> system. Electrolysis at 1450°C produced iron at the cathode and oxygen gas at the anode.

## 9:30 AM Invited

Production of Titanium Powder Through an Electronically Mediated Reaction: *Toru H. Okabe*<sup>1</sup>; Takahito Kakihira<sup>2</sup>; Takashi Abiko<sup>2</sup>; <sup>1</sup>University of Tokyo, Inst. of Industrial Sci., 4-6-1 Komaba, Meguro-ku, Tokyo 153-8505 Japan; <sup>2</sup>University of Tokyo, Grad. Sch. of Engrg., 4-6-1 Komaba, Meguro-ku, Tokyo 153-8505 Japan

In the recent years, a new titanium reduction process directly from titanium oxide (TiO2) by the electrochemical reduction of TiO2 in molten calcium chloride (CaCl2) was investigated as an alternative process of the Kroll process [Chen et al.: Nature, 407 (2000) 361], and there is a large variety of titanium reduction processes currently under investigation [Ono & Suzuki: Journal of Metals, 54 Feb., (2002) 59]. In this study we explored the production of titanium powder by an electronically mediated reaction (EMR) [Okabe & Sadoway: J. Materials Research, 13 (1998) 3372]. Feed material, TiO2, and reductant calcium alloy containing nickel, etc. were charged into electronically isolated locations in a CaCl2 molten salt at 1173 K. The flow of current through an external path between the feed and reductant locations, and electrochemical potentials of the feed electrode were monitored during the reduction experiment [Okabe et al.: J. Alloys and Compounds, 288(1999) 200]. After the experiment, pure titanium powder with low nickel content was obtained although liquid Ca-Ni alloy was used as the reductant. This clearly demonstrates that titanium metal powder can be produced by electrochemical reactions, without direct physical contact between the feed (TiO2) and reductant (calcium alloy). In some experiments, pure titanium in sponge form with 99.5 mass% purity (3500mass ppmO) was obtained. The method has the potential for preventing accumulation of impurities into titanium deposits because impurities in the molten salt can be trapped by the reductant alloy placed in the different location from the titanium reduction site. Energy efficiency of the reduction process can also be improved when combined with conventional molten salt electrolysis (MSE) of CaCl2 for reductant production. For producing calcium alloy reductant, MSE of CaCl2-CaO molten salt is investigated. Difference and features of various reduction processes are discussed.

### 10:00 AM Break

#### 10:30 AM

A Phase-Field Model of the Cathode Interface in Transport-Limited Metal Reduction and Refining Processes: Wanida Pongsaksawad<sup>1</sup>; Adam C. Powell<sup>1</sup>; <sup>1</sup>Massachusetts Institute of Technology, Matls. Sci. & Engrg., 77 Mass. Ave., Rm. 4-043, Cambridge, MA 02139 USA

In the transport-limited electrochemical reactions coupled with fluid flow such as metal reduction and refining processes, the cathode exhibits a Mullins-Sekerka instability, resulting in the growth of dendrite of solid metal into the electrolyte. To simulate the cathode interface dynamics, a two-dimension model is developed using the Cahn-Hillard phase field method. In this work, the system of interest includes a solid cathode in molten salt electrolyte. A detailed multicomponent two-phase flux-metal model is presented, which describes vorticity flow in the electrolyte and multicomponent diffusion driven by the chemical and electrical potentials at the diffuse interface. As a result of these simulations, the effect of shear flow rate on the growth of dendrites under the electrochemical reactions can be studied.

## 11:00 AM

Reaction Mechanism of Electrochemical Reduction of Titanium Dioxide: Wang Shulan<sup>1</sup>; Li Yingjun<sup>1</sup>; <sup>1</sup>Northeastern University, Dept. of Chmst., No. 3-11, Wenhua Rd., Heping Dist., Shenyang, Liaoning 110004 China

The electrochemical reduction mechanism of TiO2 in molten CaCl2 was studied systematically by using cyclic voltammetry, chronoamperometry and A.C impedance techniques in temperature range from 1073K to 1133K. The reaction mechanism of electrochemical reduction of TiO2 was found to be the two-step reactions: TiO2 is reduced to the intermediate production TiO, and then reduced to pure Ti.

## Failure of Structural Materials: Fundamentals

Sponsored by: Structural Materials Division, SMD-Structural Materials Committee

*Program Organizers:* Michael E. Stevenson, Metals and Materials Engineering, Suwanee, GA 30024 USA; Mark L. Weaver, University of Alabama, Metallurgical and Materials Engineering, Tuscaloosa, AL 35487-0202 USA

Wednesday AM	Room: 211A
March 17, 2004	Location: Charlotte Convention Center

Session Chair: Mark L. Weaver, University of Alabama, Metallurgl. & Matls. Engrg., Tuscaloosa, AL 35487-0202 USA

## 8:30 AM Keynote

Failure of Structural Materials: Michael E. Stevenson<sup>1</sup>; <sup>1</sup>Metals & Materials Engineers, 1039 Industrial Ct., Suwanee, GA 30093 USA

Failures of engineered structures and components pose substantial threats in terms of economic cost, and often, public safety. The analysis of such failures, therefore, takes on an important role in safegaurding against said losses. This paper will discuss the analysis of structural failures from the perspective of metallurgical/mechanical analysts. Topics such as investigation methodology, emerging analytical tools, and computational modeling will be discussed.

#### 9:00 AM

**Fracture Mechanics Applications in Aircraft Structural Failure Analysis**: *Jeffrey L. McDougall*<sup>1</sup>; <sup>1</sup>Metals & Materials Engineers, 1039 Industrial Court, Suwanee, GA 30024 USA

Cracked aluminum alloy structural components observed during routine post-flight inspection of corporate-type aircraft were subjected to a full-scale failure investigation. The failures were fatigue related. Inadequate mechanical properties were also involved. Through the use of fatigue striation spacing and fracture mechanics, it was able to be determined if operative stress levels in combination with other factors such as residual stresses and recent material changes contributed to the failures.

## 9:20 AM Invited

Material Degradation and Structural Collapse from the Fire Investigator's Perspective: Eric Stauffer<sup>1</sup>; <sup>1</sup>ATS, Fire Investigation Unit, 1190 Atlanta Industrial Dr., Marietta, GA 30066 USA

The purpose of fire investigation is to determine the origin and the cause of a fire. The first step in doing so is recognizing, observing, and analyzing burn patterns. The second step is identifying and evaluating fuel availability, ignition source, and the interaction between them. While the examination of artifacts for failure analysis is beyond the competence of the fire investigator and is not pertinent in most fire scenes, observations of material degradations and structural collapses are essential to proper investigation. The goal of this presentation is to introduce the patterns and characteristics of a fire scene that interest fire investigators and to interpret these from a fire investigator's perspective. These include burn patterns, depth of char, melted metals, such as steel, copper, and aluminum, and displacement of walls and floors, etc. Scientifically incorrect concepts such as glass crazing and concrete spalling will be presented and demystified.

#### 9:40 AM

Characterization of Ship Hull Steel Plates After Explosive Loading and Conventional Mechanical Testing: Christian Klinger<sup>1</sup>; Joachim Kinder<sup>1</sup>; Dietmar Klingbeil<sup>1</sup>; Werner Österle<sup>1</sup>; *Pedro Dolabella Portella*<sup>1</sup>; <sup>1</sup>Federal Institute for Materials Research and Testing (BAM), Matls. Engrg., Unter den Eichen 87, Berlin D-12205 Germany

The capsizing of the MV Estonia in the Baltic Sea in September 1994 lead to the loss of 852 lives. The ship wreck lies on the ground at a depth of about 70 meters in an international area. An intergovernmental commission concluded that the accident was caused by the loss of the bow visor due to the failure of its hinges and locks. However, independent groups sustain that the loss of the bow visor was primarily due to explosions on board of the Estonia. Some of these groups organized an expedition in August 2000, allowing divers to cut two pieces out of the forward bulk head of the Estonia. These pieces were located at the border of holes in the hull, whose aspect could be compatible with an explosion. In order to confirm the hypothesis of an explosion, steel plates of the same quality used in the building of the ship were submitted to different mechanical tests in a very broad interval of strain rates. Further specimens of the steel plates were submitted to explosions using different types of explosives as employed either for civil or military applications. The microstructure of the steel plates deformed either in mechanical tests or in explosions was characterized using light and electron microscopy. The only microstructural feature which could be unambiguously traced back to an explosive loading was the presence of deformation twins across the whole thickness of the plates in the vicinity of the fracture surface. Since deformation twins are not present in the specimens recovered from the Estonia, it was concluded that no explosion occurred in the vicinity of these specimens.

## 10:00 AM

Microstructural Characteristics of Shear Localization in a Cold Rolled 316L Stainless Steel: *Qing Xue*<sup>1</sup>; George T. Gray<sup>1</sup>; Shuh Rong Chen<sup>1</sup>; <sup>1</sup>Los Alamos National Laboratory, Matls. Sci. & Tech., MST-8, G755, Los Alamos, NM 87545 USA

The microstructural characteristics of adiabatic shear localization in a cold-rolled 316L stainless steel (316L SS) was studied. A forced shear technique on a split-Hopkinson pressure bar was utilized to generate localized deformation on "hat-shaped" specimens. The prestraining effect of the cold rolling was examined by using transmission electron microscopy. Comparison of the initial microstructure between the as-received and the cold-rolled 316L SS characterized the defect effects on the formation of shear localization. The as-received steel was seen to possess a low density of defects while the cold rolled steel included a high density of slip bands, microbands and deformation twins. The existence of profuse defects and their substructure in the cold-rolled steel led to a higher susceptibility to shear localization. The microstructure near and inside the shear bands was carefully investigated. Fine subgrains with an average size of 100 nm were found inside shear bands.

## 10:20 AM Break

#### 10:35 AM

Microstructural Influences on the Failure of Large Gray Iron Castings: *Jeffrey L. McDougall*<sup>1</sup>; <sup>1</sup>Metals & Materials Engineers, 1039 Industrial Ct., Suwanee, GA 30024 USA

Hydrostatic pressure testing of two large gray iron castings resulted in brittle overload failures. Thorough failure investigations revealed casting defects associated with both origins. Both incidences were related to the mold. The first incident involved a defect that resulted in a stress concentration that reduced the normally large critical flaw size to the microstructural level. Material selection was also a concern of the manufacturer. Through the use of fracture mechanics, the viability of faribeating from gray iron was also determined. A microstructural gradient was observed at the fracture origin of another casting. Inadequate mold desgin resulted in rapid cooling at a thin-walled region of the casting. The development of the microstructural gradient was investigated.

### 10:55 AM

Failure Analysis of a Steel Gear: *Itamar Ferreira*<sup>1</sup>; Ângela Cristina Mazzei<sup>1</sup>; Ruís Camargo Tokimatsu<sup>2</sup>; <sup>1</sup>UNICAMP, Fac. of Mech. Engrg., Matls. Engrg., PB 6122, Campinas, São Paulo 13083-970 Brazil; <sup>2</sup>UNESP, Fac. of Engrg., Mech. Engrg., Av. Brasil Centro, 56, Ilha Solteira, São Paulo 15385-000 Brazil

The hydrogen embrittlement is a very common problem. In spite of a large number of researches that has been made, some steel components still failure by this phenomenon. The gear steels are usually very susceptible to hydrogen embrittlement. The hydrogen contamination of the steel can occur in the initial steps of the steel fabrication process or in the heat treatment or carburizing process of the gear. The objective of this paper is the identification of the cause of a cylindrical gear failure (875 mm of external diameter and 241 mm of width) made of a forged 17CrNiMo6 steel, that was designed for using in an Alcohol Plant, in São Paulo state, Brazil. The gear failure was observed during the start up of the gearbox. The gearbox assemblage was finished in March 2002 and the failure of the gear was detected in April 2002, six weeks after assembling. The gear was assembled on the shaft by interference fit. Chemical analysis, metallography, hardness and fracture toughness tests have been conducted. A visual inspection indicated that the gear fractured from the keyway. It was observed that the chemical composition is in accordance with the steel specification. The microstructures at the core (bainite) and at the carburizing case (tempered martensite) are also as expected from the gear fabrication process. The Rockwell Hardness results, 30 to 35 HRC at the core and near the keyway, 40 to 42 HRC some millimeters from the carburizing case, and 52 HRC at the carburizing case, are also as expected. The median value of fracture toughness is 71.2 MPm1/2, in terms of KQ, and 0.045 mm, in terms of CTODc, obtained from three-point bend tests, by using specimens of 10 mm thick machined from the steel near the keyway, indicate that the gear steel is not embrittled. Quasicleavage has been identified as the predominant micromechanism of fracture on the fracture surface of the gear, intergranular fracture in same regions on the carburizing case, and micro voids coalescence near the carburizing case and a decreasing quantity of micro voids when going to the core of the gear. Considering that (a) the gear fracture was of the delayed type, in presence of normal stress due to the assembling the gear on the shaft by using interference fit; (b) the chemical composition, the microstructure, and hardness of the steel are in accordance with the specifications and as expected from the fabrication process; (c) the fracture toughness levels of the steel near the keyway are reasonable; (d) the predominant fracture micromechanism is quasicleavage: (e) the stress levels from the inference fit are as expected; it is possible to conclude that the failure of the gear was due to hydrogen embrittlement.

#### 11:15 AM

WEDNESDAY AM

Study on the Cold Formability of Drawn Non-Heat Treated Steels: K. S. Park<sup>1</sup>; D. L. Lee<sup>2</sup>; C. S. Lee<sup>1</sup>; <sup>1</sup>Postech, Matls. Sci. & Engrg., San 31, Hyoja-dong, Nam-gu, Pohang, Kyungbuk 790-784 Korea; <sup>2</sup>POSCO, Tech. Rsch. Labs., 1, Koedong-dong, Nam-gu, Pohang, Kyungbuk 790-600 Korea

Non-heat treated steels are attractive in the steel-wire industry since the spheroidization and quenching-tempering treatment are not involved during the processing. Therefore, it is important to investigate optimum materials showing a good combination of strength and formability after the drawing process. In this study, three different steels such as dual phase steels, low-Si steel, and ultra low carbon bainitic steel were used to study their mechanical properties and the cold formability. The cold formability was investigated by estimating the deformation resistance and the forming limit. The deformation resistance was estimated by calculating the deformation energy and the forming limit was evaluated by measuring the critical strain revealing crack initiation at the notch tip of the specimens. The results showed that deformation resistance was the lowest in the low-Si steel, and the forming limit strains of ultra low carbon bainitic steel, low-Si were higher than that of commercial SWECH45F steel.

## **General Abstracts: Session VI**

Sponsored by: TMS

*Program Organizers:* Adrian C. Deneys, Praxair, Inc., Tarrytown, NY 10591-6717 USA; John J. Chen, University of Auckland, Department of Chemical & Materials Engineering, Auckland 00160 New Zealand; Eric M. Taleff, University of Texas, Mechanical Engineering Department, Austin, TX 78712-1063 USA

Wednesday AM	Room: 208B
March 17, 2004	Location: Charlotte Convention Center

Session Chair: Thomas Battle, DuPont Titanium Technologies, Wilmington, DE 19880 USA

#### 8:30 AM

The Effects of Hysteresis on Solder Wetting: *F. Michael Hosking*<sup>1</sup>; Frederick G. Yost<sup>2</sup>; Cynthia L. Schwartz<sup>3</sup>; <sup>1</sup>Sandia National Laboratories, PO Box 5800, MS 0889, Albuquerque, NM 87185-0889 USA; <sup>2</sup>Trapezium Technology, 2549 Elfego Rd. NW, Albuquerque, NM 87107 USA; <sup>3</sup>MO-SCI Corporation, 4000 Enterprise Dr., Rolla, MO 65401 USA

The phenomenon of solder hysteresis is investigated. During typical solder wetting, the advancing and receding contact angle and associated wetting force, which corresponds to the solder meniscus weight, can exhibit a wide range of measured values. Wilhelmy plate wetting experiments were conducted to determine the effects of temperature, cycling rate, dwell time and immersion depth on hysteresis. The test materials were 60Sn-40Pb (wt. %) solder and oxygen free high conductivity (OFHC) copper. Solder hysteresis was confirmed with no evidence of a constant equilibrium wetting force at the advancing and receding steady-state conditions. It is concluded that wetting forces and dynamic contact angles are dependent upon dynamic test conditions rather than inherent solder and substrate properties. Hysteresis also appears to decrease with increasing test cycle, strongly suggesting that solder/substrate and substrate/flux reactions, which take place early in the wetting process, play a key role in determining the extent of hysteresis.

#### 8:55 AM

**Dissolution of Copper Oxide in Molten Fluxes**: *Peng Fan*<sup>1</sup>; W. D. Cho<sup>1</sup>; <sup>1</sup>University of Utah, Dept. of Metallurgl. Engrg., Salt Lake City, UT 84112 USA

The dissolution rate and the solubility of solid copper oxides (CuO and Cu2O) in various molten fluxes based on CaO-Al2O3 have been studied at high temperatures. The effects of temperature and flux composition on the dissolution rate and the solubility have been determined for the two copper oxides. Based on the physical and chemical properties of the molten fluxes and the interaction between solid copper oxides and the molten fluxes, the mechanism of the dissolution is discussed.

## 9:20 AM

The Precipitate Selectivity of Perovskite in FCSTMA Slag: Liaosha Li<sup>1</sup>; Dong Yuanchi<sup>1</sup>; Sui Zhitong<sup>2</sup>; <sup>1</sup>Anhui University of Technology, Key Lab. of Metallurgl. Engrg. & Resources Recycling, Hudong Rd., Maanshan, Anhui Province 243002 China; <sup>2</sup>Northeastern University, Sch. of Matl. & Metall., HePing Div., ShenYang, Liaoning Province 110006 China

The slag studied is a deoxidization system of FeOx-CaO-SiO2-TiOy-MgO-Al2O3. The behavior of TiO2 selectively enriched in Perovskite was investigated and discussed at given conditions as following: Oxidization of molten slag could change multivalent Ti-bearing oxides into TiO2 and increase the activity of TiO2 within slag, which made TiO2 combine with CaO in slag to form Perovskite. The oxidation not only changed compositions and structures of slag phases but also promoted majority of TiO2 migrating into Perovskite. The increment of Perovskite precipitated by oxidization could go up to  $30\% \sim 40\%$  of the precipitation in its original slag. Besides, raising the slag basicity could increase the activity of CaO in slag that facilitated the selective precipitation of Perovskite as well. If slag basicity was adjusted up to 1.3, about 80% amount of TiO2 in slag could be collected in Perovskite.

#### 9:45 AM

Adsorption Study on Rejected Muds of Bayers Process Using Different Flocculants: Benjamin Toppo<sup>1</sup>; Balakrushna Padhi<sup>1</sup>; S. P. Mahapatra<sup>1</sup>; <sup>1</sup>National Aluminium Company Limited, Damanjodi, Orissa 763008 India

High molecular weight water soluble polymers (flocculants) are commonly added to mineral slurries formed during hydro-mineralogical processing to improve solid-liquid separation. Choice of flocculants for gravity settling devices such as thickeners has historically based on settling tests performed in the laboratory. A mechanistic information about settling of resudial muds (hematite, alumino-goethite) of bayers process for extraction of alumina by alkali digestion of bauxite has been emphasized in the present study. In addition to monitoring the adsorption of polyacrylate in situ as a function of time, ionic strength and temperature has provided information related to adsorption (surface area) and absorption study. A FTIR and XRD technique has shown to be applicable to investigating the adsorption of flocs using synthetic and natural flocculating agents which can provide the adsorption segments onto mud (hematite, alumino-goethite) and (loop & tails) of the polymer at different caustic concentration and slurry concentration in bayer's process.

#### 10:10 AM Break

### 10:20 AM

Reduction of Zinc-Containing Metallurgical Residues in a Fluidized Bed Reactor: S. M. Taghavi<sup>1</sup>; M. Halali<sup>1</sup>; <sup>1</sup>Sharif University of Technology, Matl. Sci. & Engrg. Dept., Tehran Iran

In this report, the possibility of recovering zinc oxide from zinc oxide containing wastes has been studied. The ore was reduced in a fluidized bed furnace using a CO/CO2 mixture as reducing agent. It has been shown that with increasing in temperature and time of reaction, recovery percent will increase, also when depth of bed increases, recovery percent will decrease. The best result was shown that zinc oxide content in product was more than %93.5.

#### 10:45 AM

**Removal of Toxic Ions from Dilute Waste Streams by Novel Electrodeposition Techniques**: *Michael L. Free*<sup>1</sup>, <sup>1</sup>University of Utah, Metallurgl. Engrg., 135 S. 1460 E., Rm. 416, Salt Lake City, UT 84109 USA

Removal of toxic ions from dilute waste streams by novel electrodeposition techniques will be discussed. The effects of electrode types, potentials, and electrodeposition parameters will be presented.

#### 11:10 AM

New Generation Special Cements and the Using Theirs in Industry: *N. Ilyoukha*<sup>1</sup>; V. Timofeeva<sup>1</sup>; <sup>1</sup>Academic Ceramic Center, 8 Frunze Str., 61002, Kharkov Ukraine

New cements produced by the solid state sintering, contents compounds having double oxides was used as the raw stuff. Its are efficient bonds for castables, rammed mixes, covering and guniting. Refractory composite materials based on them are meant to protect units from influence of temperature more than 18000 C and aggressive media and used for manufacturing lining in petrochemistry reactors, energy headtreatment and high-temperature gas-dynamic channels (more 20000 C), in refractory lining of quarts glass tanks, for production crucibles used in the melting of pure metals, including alloys on rare-earth elements, high-temperature oxides, in burial of wastes nuclear reactors. Composites from oxides zirconium, hafnium are intended for use as solid electrolytes in the high temperatures electrolyzes, fuel elements, gas analyzers sensors and oxidability steel sensors, oxygen pumps as well as for the service at the temperatures up to 23000 C as construction products (pipes, sheaths, crucibles). The using of composites based on special cements ensures to increase in the heating units up to more 23000 C, to production of monocrystal high purity degree at the expense of theirs contamination exclusions by the harmful admixtures. The production of special cements and composites based on them can be organized at a joint venture.

## High Risk Technologies in Metallurgy with Commercial Potential: Session I

Sponsored by: TMS, PGA-Public and Governmental Affairs Committee

*Program Organizers:* Jean-Louis Staudenmann, NIST, Advanced Technology Program, Division 473, Gaithersburg, MD 20899-4730 USA; Diran Apelian, Worcester Polytechnic Institute, Metal Processing Institute, Worcester, MA 01609-2280 USA

Wednesday AM	Room: 210A
March 17, 2004	Location: Charlotte Convention Center

Session Chairs: Jean-Louis Staudenmann, NIST, Advd. Tech. Prog., Gaithersburg, MD 20899-4730 USA; Diran Apelian, Worcester Polytechnic Institute, Metal Procg. Inst., Worcester, MA 01609-2280 USA

#### 8:30 AM Introductory Remarks

#### 8:40 AM

Accelerated Materials Development by Computational Design: Greg B. Olson<sup>1</sup>; <sup>1</sup>Northwestern University/QuesTek Innovations LLC, 225 Sheridan Rd., Evanston, IL 60208 USA

Responding to the excessive time and cost of traditional empirical materials development, a multi-institutional multidisciplinary research initiative over the past two decades has delivered a revolutionary Materials by Design(TM) technology based in computational systems design. First demonstrated in nanodispersion-strengthened high-performance steels, the technology is now being applied to Ni-base, Nbbase and Al-base superalloys, advanced shape-memory alloys and bulk metallic glasses. In a collaboration with the Center for Heat Treating Excellence (CHTE) at WPI, mechanistic simulations accelerate the process optimization of a new class of High-Temperature Carburizing steels for advanced gear and bearing applications. Under the DARPA-AIM initiative, simulation and probabilistic modelling are integrated with efficient experimentation to accelerate the full development and qualification cycle. An early demonstration of the AIM methodology is underway in the ESTCP certification testing of the computationallydesigned QuesTek Ferrium S53(TM) stainless landing gear steel.

#### 9:05 AM

High Viscosity Liquid and Semi-Solid Metal Casting: Processes and Products: Merton C. Flemings<sup>1</sup>; *William L. Johnson*<sup>2</sup>; <sup>1</sup>Massachusetts Institute of Technology, Dept. of Matls. Sci. & Engrg., 77 Mass. Ave., Rm. 4-415, Cambridge, MA 02139 USA; <sup>2</sup>California Institute of Technology, Dept. of Matls. Sci., 1200 E. Calif. Blvd., MC 138-78, 339 Keck Lab., Pasadena, CA 91125 USA

Semi-solid forming has now taken its place among advanced industrial processing methods. It is becoming a process of choice for cast aluminum automotive parts requiring high strength and integrity. The main benefits of semi-solid forming being exploited today arise from the high viscosity of the semi-solid metal and from its reduced solidification shrinkage. In spite of the fact that the process in now over thirty years old, we continue to learn much about the fundamentals of formation of the desired metallurgical structure, the rheological properties of this structure, and about new economic ways of practicing the technology. Another, much newer, casting process that also benefits from high viscosity and low solidification shrinkage is that of forming bulk metallic glasses. These glasses have properties that make them attractive for a number of applications ranging from cell phone cases to sports applications. Our understanding of the rheological behavior of these materials is now developing quickly, as are concepts for new forming processes that will take advantage of the unique rheology.

## 9:30 AM

The Rapid Plasma Quench Production of Ultrafine Metal and Ceramic Powders: *Alan Donaldson*<sup>1</sup>; Ronald Cordes<sup>1</sup>; <sup>1</sup>Idaho Titanium Technologies, Idaho Falls, ID USA

The plasma quench process uses plasma to heat reactants to a temperature where desired reactions take place, then expanding the product gases through a Delaval supersonic expansion nozzle into a cold gas to prevent back reactions. Cooling rates are in excess of a billion Kelvins per second. We have produced high yields of titanium, magnesium, and aluminum by this process, in several reactor configurations. The initial product is always a submicron powder that has condensed from the rapidly cooling gas, but we are developing methods for increasing the particle size into the low micron range by recycling the gas-entrained powder back through the condensation zone. An inline classifier removes particles when they reach the desired size. Supersonic gas exiting the nozzle drives the recirculation and rapidly and efficiently mixes the product gas with the cold quench gas by the eductor effect. We are currently working on problems associated with scaling up.

#### 9:55 AM

## The Development of the Isothermal Melting Process for Aluminum - A High Risk/High Value Technology: C. Edward Eckert<sup>1</sup>; <sup>1</sup>Apogee Technology, Inc., 1600 Hulton Rd., Verona, PA 15147 USA

The thermal efficiency of conventional fuel fired reverberatory melting furnaces used in the aluminum industry ranges from 15 to 45%. Melt loss averages 5 to 8%. The industry wide implementation of a melting process capable of a gross thermal efficiency of 70% and 3% melt loss would result in a U.S. energy savings of 46 trillion BTU/ year, if such a process were available. This paper describes a joint program between Apogee Technology, the U.S. Department of Energy, and Commonwealth Aluminum to develop a melting process that is capable of eclipsing the performance of 70% efficiency/3% melt loss. The key technology enabler for the process is a high heat flux direct immersion resistance heater. Such heaters do not commercially exist and therefore had to be developed under this program. The development of the heater is described in this paper, along with methods of risk management. Novel methods for heat production thorough electrical energy conversion, internal heater heat transfer, and overall protection of the system from molten aluminum had to be developed. Such a heater was developed with versions currently in b - site evaluation and, is discussed at length, in this paper.

#### 10:20 AM Break

#### 10:30 AM

UltraCem<sup>TM</sup>: A Coating With High Wear Resistance and With a Low Coefficient of Friction: *E. McComas*<sup>1</sup>; Richard H. Bourret<sup>1</sup>; T. Dyer<sup>1</sup>; <sup>1</sup>Universal Chemical Technologies, Inc., 7825 SW Ellipse Way, Stuart, FL 34997 USA

UltraCem<sup>™</sup> is a multifunctional tribological coating comprised of approximately 95% nickel and 6% boron that creates a hard, wear resistant surface with a low coefficient of friction, while achieving a metallurgical bond to ferrous alloys and a greater than 10,000 PSI bond on non-ferrous alloys. The topographic surface of UltraCem<sup>™</sup> is nodular, resulting in the reduction of surface contact with mating surfaces and excellent locations for entrapment of lubrication. UltraCem<sup>™</sup> is uniform as deposited, eliminating the requirement for secondary machining. Thickness can range from 2-500 microns and is deposited by autocatalytic reduction. UltraCem<sup>™</sup> does not induce hydrogen embrittlement. As deposited, UltraCem<sup>™</sup> is not completely amorphous and is in a transitional state between an amorphous mixture of nickel-boron and very fine crystalline nickel. As plated, the hardness is approximately equal to that of hard chrome or approximately 1000 KpH. After heat-treatment at between 400°F and 725°F, the coating crystallizes and clusters of nickel boride form to further increase hardness to approximately 1,400 KpH. The coating is unique in that it works extremely well against itself to reduce friction and eliminate the requirement for wet lubrication and mating surfaces. The result is a single coating with a high hardness, low friction, uniform deposit, achieving a metallurgical bond to ferrous substrates and a superior mechanical bond to even titanium without the induction of hydrogen embrittlement. The technology of UltraCem<sup>™</sup> will be presented, its development will be reviewed, and the commercial impact it is making in both defense and commercial sectors will be discussed.

#### 10:55 AM

Issues in the Commercialization of the Laser Engineered Net Shaping (LENS®) Process: *William Hofmeister*<sup>1</sup>; Michelle Griffith<sup>2</sup>; <sup>1</sup>Vanderbilt University, Chem. Engrg., Olin Hall Room 107, 24th & Garland Ave., Nashville, TN 37212 USA; <sup>2</sup>Sandia National Laboratory USA

The promise of "on-demand" part fabrication from computeraided design (CAD) to direct metal deposition led Sandia National Laboratories to form a Cooperative Research and Development Activity (CRADA) to support the LENS® process. Twelve industrial partners joined the CRADA team with interests spanning from injection mold to aerospace parts fabrication. Over the four years, the group covered a wide range of issues; including development of process parameters, mechanical testing of LENS® deposited parts, refinement of tool path generation codes, sensors for process control, process modeling, machine development, cost analysis, and various intellectual property issues. Despite this large body of development work, the full commercial potential of the LENS® process has not been realized. We will outline the CRADA path to the development of the LENS® process and discuss the issues involved in acceptance of the process by the fabrication community.

## 11:20 AM

High Speed Identification and Sorting of Nonferrous Metal Scrap: David B. Spencer<sup>1</sup>; <sup>1</sup>Spectramet, LLC, 7 Alfred Cir., Bedford, MA 01730 USA

Each year, U.S. industry discards tens of billions of pounds of nonferrous metals as waste because it is either impractical or uneconomical to recover this material using current technology. In addition, billions of pounds of nonferrous metals are shipped overseas to China and elsewhere, for separation into higher value scrap grades using low cost labor for visual identification and hand sortation. Methods of scrap metal sortation using spark testing, chemical analysis, and optical emission or spectrographic analyzers are typically slow and cumbersome. Heavy media techniques are rapid, but can only sort by density. Color sortation techniques are effective for grouping alloys but cannot effectively sort by alloy type. An opportunity exists to recover low-grade nonferrous scrap by sorting them into various alloys with high accuracy by applying spectrographic analysis techniques. A new company dedicated to commercializing this technology, named Spectramet® LLC, is in the midst of developing a platform of new, high-speed identification and sorting technologies using optoelectronic methods. The Spectramet Technology can sort a wide range of metals and alloys both quickly and accurately. This paper will describe the progress of work funded by the National Science Foundation and the NIST Advanced Technology Program aimed at high-speed identification and sorting of mixed nonferrous metal scrap.

#### 11:45 AM

Fluidized Beds - The Quantum Leap in Thermal Processing: James Van Wert<sup>1</sup>; <sup>1</sup>Amcast Industrial Corporation, Dayton, OH 45459 USA

As companies move to implement lean manufacturing concepts to achieve the ultimate goal of "one piece flow", the first step in achieving the goal is to map the "value stream". A value stream is all the actions or process steps, both value added and non-value added, currently required to produce the product. In the foundry industry and in many other metal-processing industries, one of the main process steps in the value stream is the thermal treatment process, commonly called "heat treatment". As the industrial engineers working on the future state value stream map soon find out, what they have discovered is not only the most significant bottleneck, but also a plant monument. Many of the thermal treatment practices and equipment were developed decades ago and have seen little improvement until now. This paper will attempt to describe the next generation in thermal processing equipment, to achieve a reduction in solution heat treatment and artificial aging times by as much as 125%. The primary aluminum alloy families currently being studied are the Aluminum-Silicon-Magnesium alloys and the Aluminum-Silicon-Copper-Magnesium alloys. These alloys have demonstrated significant microstructural changes along with dramatic cycle time reductions.

## Hume Rothery Symposium: Structure and Diffusional Growth Mechanisms of Irrational Interphase Boundaries: Session V

Sponsored by: Electronic, Magnetic & Photonic Materials Division, Structural Materials Division, EMPMD/SMD-Alloy Phases Committee, MPMD-Phase Transformation Committee-(Jt. ASM-MSCTS)

*Program Organizer:* H. I. Aaronson, Carnegie Mellon University, Department of Materials Science and Engineering, Pittsburgh, PA 15213 USA

Wednesday AM	Room:	208A		
March 17, 2004	Location	n: Charlotte	Convention	Center

Session Chair: W.-Z. Zhang, Tsinghua University, Beijing 100084 China

## 8:30 AM Invited

Edge-to-Edge Matching in Thin Films: Christophe Detavernier<sup>1</sup>; Christian Lavoie<sup>1</sup>; Ahmet Ozcan<sup>2</sup>; <sup>1</sup>IBM T.J. Watson Research, 1101 Kitchawan Rd., Rte. 134, PO Box 218, Yorktown Heights, NY 10598 USA; <sup>2</sup>Boston University, Dept. of Physics, 590 Commonwealth Ave., Boston, MA 02215 USA We demonstrate the presence of a new type of texture in thin films of cubic CoSi<sub>2</sub>, tetragonal  $\alpha$ -FeSi<sub>2</sub> and orthorhombic NiSi formed on Si(100) substrates. Pole figures for these films consist of complex patterns of narrow lines. For NiSi, the patterns are created by grains for which the NiSi(202) or (211) planes are parallel to Si(110)-type planes in the substrate. Because of the constraint that a set of planes in the film is preferentially parallel to a set of planes in the substrate, the texture manifests itself as an off-normal fiber texture, with the fiber axis perpendicular to Si(110)-type planes (i.e. at 45° and 90° from the surface normal). Since the spacing between NiSi(202) or (211) planes is nearly identical to the spacing of 0.1920nm between Si(220) planes, an alignment of these planes will result in an interface that is periodic along one direction in the plane of the interface.

#### 9:10 AM Invited

The Orientation Relationships and Interfacial Structure of S Phase Precipitates in Al-Cu-Mg Alloys: *Barry Muddle*<sup>1</sup>; Jian-Feng Nie<sup>1</sup>; Graham Winkelman<sup>1</sup>; <sup>1</sup>Monash University, Sch. of Physics & Matls. Engrg., Victoria 3800 Australia

One of the major precipitate phases in Al-Cu-Mg alloys is S phase that has an orthorhombic structure. It is a common view that this S phase forms in the form of lath, with its habit plane and long axis parallel to {210} and <001>, respectively, of the matrix phase. It was reported recently that this S phase also form in other orientation relationships. However, the interfacial structure of the S phase in these newly observed orientation relationships and its role in the growth are yet to be established. This paper reports results of detailed characterisation of the orientation and interfacial structure of S phase precipitates using high-resolution transmission electron microscopy and electron microdiffraction. The existence of a discrete set of orientation relationships between S and  $\alpha$ -Al matrix will be demonstrated, each related by a small angular rotation about a common axis parallel to the long axis of the laths. The correlation between interfacial structure and orientation of precipitates, and the applicability of a Moire plane approach to the morphology of the S phase will be described and discussed.

#### 9:50 AM Invited

Atomic Structure of Incoherent Interfaces in Zr-N Alloys: Peng Li<sup>2</sup>; James M. Howe<sup>1</sup>; William T. Reynolds<sup>3</sup>; <sup>1</sup>University of Virginia, Dept. of Matls. Sci. & Engrg., Charlottesville, VA 22904-4745 USA; <sup>2</sup>Arizona State University, Ctr. for Solid State Sci., Tempe, AZ 85287-1704 USA; <sup>3</sup>Virginia Polytechnic Institute, Dept. of Matls. Sci. & Engrg., Blacksburg, VA 24060 USA

The atomic structures of incoherent interfaces in metal alloys are not well understood. In this investigation, conventional and highresolution transmission electron microscopy (TEM), crystallographic analyses and near-coincident-site (NCS) atom modeling were used to investigate the atomic structures of planar {111} and {110} ZrN interfaces between the Zr and ZrN phases in a Zr-34at.%N alloy. In all cases, the Zr and ZrN phases have high-index orientation relationships and display poor atomic matching in the high-resolution TEM images and NCS atom analyses, indicating that the interfaces are atomically incoherent. The {111} ZrN interfaces are faceted over hundreds of nanometers and contain atomic steps, suggesting that such features cannot be used to define partial coherency at interfaces. The {110} ZrN interface is rougher than the {111} ZrN interfaces, indicating that there may be both atomically faceted and rough incoherent interfaces. This research was supported by NSF under Grant DMR-9908855.

#### 10:30 AM Break

## 10:45 AM Invited

**On Relationships between Coherency, Structure and Energetics of Irrational Interphase Boundaries**: *Thaddeus (Ted) B. Massalski*<sup>1</sup>; William A. Soffa<sup>2</sup>; David E. Laughlin<sup>1</sup>; <sup>1</sup>Carnegie Mellon University, Matls. Sci. & Engrg., 5000 Forbes Ave., Pittsburgh, PA 15213 USA; <sup>2</sup>University of Pittsburgh, Matls. Sci. & Engrg., Benedum 842, Pittsburgh, PA 15260 USA

In this paper we will put the above topic in perspective, first by reviewing the classical definition(s) of coherency and then by reviewing the reasons for the perceived need to extend this concept to include one dimensional commensuration. We shall consider critically both past and current ideas in this area (including the present symposium). The experimental observations will be reviewed and discussed, as will be the work which is theoretical and/or simulated. The importance of energetics will be explored for both the nucleation and the growth processes of irrational boundaries.

## Internal Stresses and Thermo-Mechanical Behavior in Multi-Component Materials Systems: Anisotropy and Residual Stresses

*Sponsored by:* Electronic, Magnetic & Photonic Materials Division, Structural Materials Division, EMPMD-Electronic Packaging and Interconnection Materials Committee, EMPMD-Thin Films & Interfaces Committee, SMD-Composite Materials Committee-Jt. ASM-MSCTS

*Program Organizers:* Indranath Dutta, Naval Postgraduate School, Department of Mechanical Engineering, Monterey, CA 93943 USA; Bhaskar S. Majumdar, New Mexico Tech, Department of Materials Science and Engineering, Socorro, NM 87801 USA; Mark A.M. Bourke, Los Alamos National Laboratory, Neutron Science Center, Los Alamos, NM 87545 USA; Darrel R. Frear, Motorola, Tempe, AZ 85284 USA; John E. Sanchez, Advanced Micro Devices, Sunnyvale, CA 94088 USA

Wednesday AM	Room:	209B		
March 17, 2004	Location	h: Charlotte	Convention	Center

Session Chairs: John J. Lewandowski, Case Western Reserve University, Cleveland, OH 44106 USA; Mark A.M. Bourke, Los Alamos National Laboratory, Neutron Sci. Ctr., Los Alamos, NM 87545 USA

#### 8:30 AM Invited

In-Situ Deformation and Fracture Response in Ti-Al Based Alloys: *Bimal Kad*<sup>1</sup>; Bjorn Clausen<sup>2</sup>; Mark A.M. Bourke<sup>2</sup>; <sup>1</sup>University of California, Structural Engrg., 409 Univ. Ctr., La Jolla, CA 92093-0085 USA; <sup>2</sup>Los Alamos National Laboratory, LANSCE-12, Los Alamos, NM 84505 USA

TiAl-based low-symmetry alloys with single or two-phase microstructures are probed via neutrons during in-situ compression loading at ambient temperatures. Strain measurements are recorded for the predominant  $\gamma$ -TiAl phase and the minority  $\alpha_2$  phase both parallel and perpendicular to the loading axis, in the loaded and unloaded states, in the elastic and plastic regimes. Single phase  $\alpha_2$ -Ti<sub>2</sub>Al and  $\gamma$ -TiAl behavior is extracted using sample compositions to the left and right respectively of the  $\alpha_2 + \gamma$  phase field. The composite response is probed using a variety of alloy compositions and processing conditions within the  $\alpha_2 + \gamma$  phase field. The deformation anisotropy of the constituent phases, particularly in the <a> and <c> directions, following load excursions into the plastic regime is elucidated. This anisotropy is correlated with the underlying crystallographic deformation systems (slip and/or twinning) in the constituent phases. Such anisotropic response is modified in the two-phase alloys with subtle evidence of the particular contribution of the  $\alpha_2$ -phase in improving the bulk response in commercially viable alloys.

## 8:55 AM

**Co-Deformation and Residual Stress Accumulation in Alpha-Beta Brass**: *Kelly T. Conlon*<sup>1</sup>; David Dye<sup>2</sup>; <sup>1</sup>National Research Council of Canada, Chalk River Labs., Sta. 18, Chalk River, Ontario K0J 1J0 Canada; <sup>2</sup>Imperial College London, Dept. of Matls., S. Kensington Campus SW7 2AZ UK

We have investigated the accumulation of microstrains during the deformation of alpha-beta Cu-Zn alloys using in-situ neutron diffraction. Dual phase Cu-Zn alloys were fabricated by melting and casting elemental Cu and Zn granules of nominal 99.9% purity. Subsequent hot extusion of the ingots results in a modest rod-like texture in both phases, with alpha (111) and beta (110) fibres aligned along the extrusion axis of the rod. In-situ neutron diffraction experiments were carried out on specimens machined from the rods using a tesile testing rig mounted on a neutron diffractometer. The sign and magnitude of the residual strains in the minority beta phase following the application of tensile plastic strains demonstrate an unusual grain orientation dependence. Beta phase grains with a (002) orientation aligned along the tensile axis accumulate enormous residual tensile elastic strains of 1% following a deformation of 10%. On the other hand, the sign and magnitude of the strains in beta grains with a (220) orientation are modest and compressive, indicating the onset of yield and subsequent co-deformation with the alpha matrix. These unusual results will be discussed in light of older results obtained by Izumi and co-workers on dual phase alpha-beta bi-crystals.

#### 9:20 AM Invited

Residual Stress Analysis in Graphite/Pmr-15 Composites Using X-Ray Diffraction: B. Benedikt<sup>1</sup>; M. Lewis<sup>1</sup>; P. Rangaswamy<sup>1</sup>; M. Kumosa<sup>2</sup>; P. Predecki<sup>2</sup>; M. Gentz<sup>2</sup>; <sup>1</sup>Los Alamos National Laboratory, Engrg. Scis. & Applications Div., Los Alamos, NM 87545 USA; <sup>2</sup>University of Denver, Div. for Advd. Matls. & Struct., Dept. of Engrg., Denver, CO 80208 USA

This work addresses the problem of determining thermally induced residual stresses in graphite/PMR-15 composites from embedding aluminum inclusions between the first and second plies of 6-ply unidirectional and 4-ply woven laminates. The stresses in the inclusions were measured using X-ray diffraction (XRD) from the (422) aluminum diffracting planes. These stresses were than used to calculate the average thermal residual stresses in the composites using the visco-elastic Eshelby method. Furthermore a comparison were made between the measured stresses from Xrd experiments and calculated stresses from the Eshelby method with predictions obtained from the visco-elastic CLPT (inter-laminar model) and the Eshelby method (intra-laminar model). The accuracy of these results was further validated using a four-point bend test for the same material using different bending moments. The talk will highlight the merits of the proposed methodology of using metallic filler particles as sensors to measure internal and applied stresses in polymeric composite systems. The application of this methodology towards investigating the effect of matrix degradation on thermally induced residual stresses by aging in air and nitrogen for 1064 hours and 1170 hour, respectively, at 315°C will also be presented.

#### 9:45 AM Invited

A Study of Residual Stresses and Mechanical Properties of Thermal Spray Coating Systems: *Thomas Gnäupel-Herold*<sup>1</sup>; Frank S. Biancaniello<sup>2</sup>; Henry J. Prask<sup>1</sup>; <sup>1</sup>National Institute of Standards and Technology, Matls. Sci. & Engrg. Lab., 100 Bureau Dr., Stop 8562, Bldg. 235, Rm. B105, Gaithersburg, MD 20899 USA; <sup>2</sup>National Institute of Standards and Technology, Metall. Div., 100 Bureau Dr., Stop 8556, Gaithersburg, MD 20899-8556 USA

The thermal spray process produces a deposit characterized by residual stress (RS) and a microstructure with high defect density. The first is caused by the differences of temperatures and coefficients of thermal expansion (CTE) between deposit and substrate. The imperfect microstructure is caused by the deposition of individual droplets which creates incomplete contact between splats as well as porosity and inclusions. For several coating systems we have conducted an investigation of residual stresses, elastic constants, defect structure and adhesive properties. We found that for medium to high porosities the RS are controlled by the drop in the effective coating elastic modulus. For low defect densities the coating properties approach the bulk values, and both the CTEs and the deposition temperature determine the RS. The elastic modulus depends on the defect density which is controlled by, among other parameters, the particle/droplet size.

#### 10:10 AM Invited

#### Effects of Residual Stresses on Fatigue of Composite Systems: John J. Lewandowski<sup>1</sup>; H. Hassan<sup>1</sup>; C. Liu<sup>1</sup>; <sup>1</sup>Case Western Reserve University, Dept. of Matls. Sci. & Engrg., Cleveland, OH 44106 USA

Discontinuously reinforced aluminum based composites have been prepared to contain different levels of residual stress. The levels of residual stress were characterized by X-ray diffraction as well as via measurement of the Bauschinger effect in materials heat treated to different conditions. The low cycle fatigue behaivor was characterized in these cases. In addition, the effects of residual stresses on fatigue crack growth in laminated aluminum composites were also evaluated after heat treatment as well as after different thermal exposures.

#### 10:35 AM

In-Situ Neutron Diffraction Studies of Directionally Solidified NiAl-Mo Fibrous Composites During Tensile Loading: *H. Bei*<sup>1</sup>; E. P. George<sup>2</sup>; Hahn Choo<sup>1</sup>; Donald W. Brown<sup>3</sup>; G. M. Pharr<sup>1</sup>; <sup>1</sup>University of Tennessee, Matls. Sci. & Engrg., Knoxville, TN 37996 USA; <sup>2</sup>Oak Ridge National Laboratory, Metals & Ceram. Div., Oak Ridge, TN 37831 USA; <sup>3</sup>Los Alamos National Laboratory, Lujan Ctr., Los Alamos, NM 87545 USA

NiAl-Mo pseudo-binary eutectic alloys were directionally solidified in a high temperature optical floating zone furnace to produce wellaligned fibrous composites in which NiAl is the continuous matrix phase and Mo the discontinuous rod-like phase. Specimens machined parallel to the long axes of the fibers were loaded in tension at temperatures in the range 700-1000°C and stresses of 300-500 MPa while in-situ neutron diffraction experiments were performed to investigate the detailed deformation mechanisms in the composite. In particular, changes in load partitioning in the two phases were studied in various stress and temperature regimes where the matrix and fiber are elastic/ elastic, plastic/elastic, and plastic/plastic. In addition, attempts were made to estimate dislocation densities in each phase by observing line broadening.

#### 11:00 AM

Thermal Residual Stress Characterization in TiC-Ni3Al Intermetallic Matrix Composties Via In-Situ Neutron Diffraction: James J. Wall<sup>1</sup>; Hahn Choo<sup>2</sup>; James W. Richardson<sup>3</sup>; Terry N. Teigs<sup>4</sup>; Peter K. Liaw<sup>2</sup>; <sup>1</sup>University of Missouri, Dept. of Mech. & Aeros. Engrg., Columbia, MO 65211 USA; <sup>2</sup>University of Tennessee, Matls. Sci. & Engrg. Dept., Knoxville, TN 37996 USA; <sup>3</sup>Argonne National Laboratory, Intense Pulsed Neutron Source, Argonne, IL 60439 USA; <sup>4</sup>Oak Ridge National Laboratory, Metals & Ceram. Div., Oak Ridge, TN 37831 USA

TiC-Ni3Al composites were produced by reactive vacuum sintering of TiC/Ni/NiAl compacts, followed by low-pressure hot-isostatic pressing. Upon cooling from the processing temperature, thermal residual stress (TRS) was developed in the composite due to the thermal expansion coefficient mismatch of the two constituents. The residual stress was measured using in-situ neutron diffraction over a temperature range of approximately 50-1250K. A 3-dimensional elasto-viscoplastic (EVP) finite-element model (FEM) was used to predict the TRS evolution. The measured TRS behavior deviated from that predicted by the EVP model. The Ni3Al matrix demonstrated a high resistance to both creep relaxation and low-temperature plasticity under the temperature regime studied. Possible reasons for the unanticipated TRS evolution are discussed. This work is supported by the NSF International Materials Institutes (IMI) Program DMR-02331320.

#### 11:25 AM

**Multiscale Internal Stress Investigation of BaTiO3**: Robert Rogan<sup>1</sup>; Ersan Ustundag<sup>1</sup>; Nobumichi Tamura<sup>2</sup>; Lawrence Margulies<sup>3</sup>; Henning Poulsen<sup>3</sup>; Ulrich Lienert<sup>4</sup>; Mark R. Daymond<sup>5</sup>; <sup>1</sup>California Institute of Technology, Dept. of Matls. Sci., Pasadena, CA 91125 USA; <sup>2</sup>Lawrence Berkeley National Laboratory, Advd. Light Source, Berkeley, CA 94720 USA; <sup>3</sup>Risø National Laboratory, Matls. Rsch. Dept., Roskilde Denmark; <sup>4</sup>Argonne National Laboratory, Advd. Photon Source, Argonne, IL 60439 USA; <sup>5</sup>Rutherford-Appleton Laboratory, ISIS Neutron Scattering Facility, Chilton, Didcot OX11 0QX UK

For the first time, internal and residual stresses in BaTiO3 were investigated at multiple length scales using X-ray microdiffraction. Tetragonal BaTiO3 single and polycrystals and thin films were scanned with X-ray beams ranging in size from 1 mm to 200 mm. Laue patterns were collected from regions around cracks and highly stressed areas. These patterns yielded information about orientation relationships caused by domain boundaries as well as the three-dimensional strain tensor associated with each feature. In one particular study, the evolution of elastic strain and texture (domain switching) in a single embedded grain of a polycrystalline BaTiO3 under electrical loading was investigated. The results suggest the presence of significant internal stress/strain fields and complicated domain formations inside BaTiO3.

## International Laterite Nickel Symposium - 2004: Process and Operational Lessons Learned - Part I

Sponsored by: Extraction & Processing Division, EPD-Aqueous Processing Committee, EPD-Copper, Nickel, Cobalt Committee, EPD-Process Fundamentals Committee, EPD-Process Mineralogy Committee, EPD-Pyrometallurgy Committee, EPD-Waste Treatment & Minimization Committee Program Organizer: William P. Imrie, Bechtel Corporation,

Mining and Metals, Englewood, CO 80111 USA

Wednesday AM	Room: 2	17B/C
March 17, 2004	Location:	Charlotte Convention Center

Session Chairs: Ian G. Skepper, BHP-Billiton, Ravensthorpe Nickel Project, Perth, WA 6850 Australia; John G. Reid, Director, Reid Resource Consulting Pty. Ltd., Indooroopilly, Brisbane 4068 Australia

#### 8:30 AM

Sixty Years of Caron: Current Assessment: Faustino G. Prado<sup>1</sup>; Faustino L. Prado<sup>1</sup>; <sup>1</sup>Prado Technology Corporation, Mining & Minerals, PO Box 274206, Tampa, FL 33688 USA

For more than a century, the AAC (ammonia/ammonium carbonate) process has been applied to the recovery of various metals. A variation of it, the Caron Process was first used in the early 1940's in Cuba for the extraction and recovery of nickel from laterites. The original Nicaro plant has been in continuous operation since then. Years later the Caron process was used again in Australia at the Greenvale (Yabulu) Nickel/Cobalt plant, commissioned in 1974. Other projects (Sered, Niquelandia, Nonoc, Punta Gorda, Albania) as well as several studies have been carried out. The Caron Process is alive and still promising. Members of our organization have been working with AAC and the Caron Process since 1952. This paper will review current approaches and potential improvements (enhancement of recoveries of Ni and Co, reduced energy consumption and maintenance simplification).

#### 9:00 AM

Yabulu 25 Years On: John G. Reid<sup>1</sup>; John E. Fittock<sup>2</sup>; <sup>1</sup>Reid Resource Consulting Pty Ltd., 1 Carnoustie Ct., Indooroopilly, Brisbane, Qld 4068 Australia; <sup>2</sup>BHP Billiton, QNI Pty Ltd., PMB 5, Mail Ctr., Townsville, Qld 4818 Australia

When the paper "Operations at the Greenvale Nickel Project Mine and Refinery" was delivered at the 1st Laterite Symposium in 1979, the Yabulu plant had been operating for only 4 years. The design was based on the Caron plant at Nicaro, Cuba, built in 1944, also by Freeport. Yabulu had 10 Herreshoff ore roasters and production in 1978 was 18,680 tonne of nickel in impure oxide sinter and 763 tonne cobalt in an impure mixed sulphide. In the past 25 years two more roasters have been added, but ore processing rate increased only marginally, to 2.4M t/y, to allow a lower feed rate per roaster, with associated higher recovery. Imported ore has replaced the closed Greenvale mine. Nickel production in the past 25 years has risen by 67% and cobalt by 146% and the products have changed completely. The plant changes that have contributed to the increased recovery, production and product value are discussed.

## 9:30 AM

The Evolution of the Greek Ferronickel Production Process: Emmanuel N. Zevgolis<sup>1</sup>; <sup>1</sup>National Technical University of Athens, Sch. of Mining & Metallurgl. Engrg., 9 Heroon Polytechniou Str., Athens, Zografou 15780 Greece

After the Krupp-Renn process was shown to be unsuitable for treatment of the Greek nickeliferous laterites, the LM process was developed. It involved roasting reduction up to metallic iron in a Rotary Kiln (R/K) and smelting in an Electric Furnace (E/F). Ferronickel (with 15% Ni) produced in the E/F, was upgraded to 90-95% Ni in an O2 converter. Raw Ni was then electrolyzed to pure Ni. The LM process was not applied for very long however, due to various problems. So, the Larco process was developed, i.e., pre-reduction in R/Ks, smelting of the calcine in E/Fs for ferronickel production (15% Ni) and enrichment to 20% Ni, in an O2 converter. Until now, many technological improvements have been invented and applied or adjusted to the process, which have made it a fully reliable and competitive one. Some of the improvements were the invention and application of a new granulation process for liquid ferronickel, the modification of the existing R/Ks, E/Fs and converters and the design of new ones, and others that are described in the paper.

## 10:00 AM Break

#### 10:10 AM

The Optimisation and Control of Process Chemistry at Bulong Nickel Operations: John Frederick O'Callaghan<sup>1</sup>; <sup>1</sup>BHP Billiton, Ravensthorpe Nickel Ops., Mt Newman House, Level 12, 200 St. Georges Tce, Perth, Western Australia 6000 Australia

Bulong remains the only hydrometallurgical process plant in the world that recovers nickel and cobalt directly from high pressure acid leach (HPAL) laterite leach liquors without need for precipitation of an intermediate product (e.g. sulphide, hydroxide or carbonate). Direct solvent extraction (DSX) of both nickel and cobalt in combination with electrowinning of nickel has been operation at Bulong since early 1999. Focus in the first years has been on ramp-up and resolution of commissioning problems. More recently the focus has been on debottlenecking and process optimisation. A number of significant process problems have been resolved, the most difficult being the formation of gypsum in the nickel solvent extraction circuit. Sound control of process chemistry is essential to ensure the production of high quality nickel and cobalt products at the lowest possible cost. This paper describes the numerous changes and enhancements to the process chemistry and plant equipment at Bulong and discusses the importance of ore leach chemistry on downstream impurity metal removal. Potential additional enhancements to further reduce unit costs are also presented.

#### 10:40 AM

**Two Steps Forward and One Step Back: A Case in Arrested Development in Laterite Processing**: *Larry M. Southwick*<sup>1</sup>; Stanley Duda<sup>2</sup>; <sup>1</sup>L.M. Southwick & Associates, 992 Marion Ave., Ste. 306, Cincinnati, OH 45229 USA; <sup>2</sup>Consulting Engineer, PO Box 1014, La Canada, CA 91011 USA

Considerable process and equipment development and analysis were conducted during design of Freeport Sulfur's laterite nickel facilities in the late 1950' s. These covered ore concentration at Moa Bay, Cuba, and concentrate refining at Port Nickel, Louisiana. Both facilities utilized acid pressure leaching and product refining steps that were similar to those later used elsewhere in the laterite processing industry. Unfortunately, developments in Cuba removed the Moa Bay facilities from Freeport control. This deprived the project of a start-up that would have allowed thorough resolution of difficulties and a quicker attainment of production capacity. This meant lost opportunity to positively prove and complete the technology when optimum resources and staff were available. This paper reviews the original rationale of how design was developed via laboratory, bench scale and pilot studies by Freeport Sulfur. Some later operating problems will also be discussed. This case is unusual, but the lessons learned may be instructive in the application of difficult and complicated technologies, as well as the need to understand and retain access to the original development and design activities.

#### 11:10 AM

Reduction in Energy Costs in Cuban Caron Process Plants: Raul Rodriguez Gan<sup>1</sup>; <sup>1</sup>Principle Specialist for Nickel, Ministry of Basic Industries Cuba

Since the 1973 energy crisis, high fuel oil costs have been eroding the economy of the Nicaro and Punta Gorda Plants that employ the Caron Process for laterites processing. Since 1995, cuban crude oil production has growth dramatically, with progressive utilization in power generation and nickel production plants. It is explained how Punta Gorda and Nicaro have been able to burn high density cuban crude oil with high sulphur content, to replace the expensive Bunker C fuel oil that previously was purchased at low preferential price from USSR and achieving a profitable operation. Problems that arouse due to the high sulphur content of the cuban crude oil, have demanded extensive investigations in the process chemistry and novelty solutions, with corresponding changes in process conditions. Innovative options are shown that will allow further cost reductions in the future.

## Lead-Free Solders and Processing Issues Relevant to Microelectronic Packaging: Interfacial Interactions, Intermetallics and Substrates

*Sponsored by:* Electronic, Magnetic & Photonic Materials Division, EMPMD-Electronic Packaging and Interconnection Materials Committee

Program Organizers: Laura J. Turbini, University of Toronto, Center for Microelectronic Assembly & Packaging, Toronto, ON MSS 3E4 Canada; Srinivas Chada, Jabil Circuit, Inc., FAR Lab/ Advanced Manufacturing Technology, St. Petersburg, FL 33716 USA; Sung K. Kang, IBM, T. J. Watson Research Center, Yorktown Heights, NY 10598 USA; Kwang-Lung Lin, National Cheng Kung University, Department of Materials Science and Engineering, Tainan 70101 Taiwan; Michael R. Notis, Lehigh University, Department of Materials Science and Engineering, Bethlehem, PA 18015 USA; Jin Yu, Korea Advanced Institute of Science and Technology, Center for Electronic Packaging Materials, Department of Materials Science & Engineering, Daejeon 305-701 Korea

Wednesday AM	Room: 2	19B		
March 17, 2004	Location:	Charlotte	Convention	Center

*Session Chairs:* C. Robert Kao, National Central University, Dept. of Chem. & Matls. Engrg., Chungli City 320 Taiwan; K. N. Subramanian, Michigan State University, Dept. of Chem. Engrg. & Matls. Sci., E. Lansing, MI 48824-1226 USA

#### 8:30 AM Invited

Morphology and Kinetics of Interfacial Reaction Between SnAg3.5 Solder and Electroless Ni-P Metallization: Zhong Chen<sup>1</sup>; Min He<sup>1</sup>; Guojun Qi<sup>2</sup>; <sup>1</sup>Nanyang Technological University, Sch. of Matls. Engrg., Nanyang Ave., Singapore 639798 Singapore; <sup>2</sup>Singapore Institute of Manufacturing Technology, Surface Engrg., 71 Nanyang Dr., Singapore 638075 Singapore

This work summarizes the interfacial reaction between lead-free solder SnAg3.5 and electrolessly plated Ni-P metallization in terms of morphology of the intermetallic compound (IMC) and its growth kinetics. Comparison with pure Ni as metallization is made whenever

possible so that the role of P in electroless nickel can be clarified. Three major aspects will be highlighted in this paper: 1. The effect of post-reflow cooling rate: It is found that the cooling rate significantly affects the morphology of IMC. For the first time we report the formation of a secondary phase nucleating on Ni3Sn4 IMC surface when the cooling rate exceeds certain limit. 2. Liquid-solid reactions: The formation and growth of Ni-Sn IMC are examined at different reflow parameters. IMC spallation and Kirkendall voids have been observed and discussed. 3. Solid-state reactions: The growth kinetics at different annealing temperatures has been studied. Kirkendall voids are found at the interface between Ni3P layer and Ni-P metallization after prolonged thermal aging.

## 8:55 AM

Effect of Cu Concentration on the Solid-State Reactions Between SnAgCu and Ni: W. C. Luo<sup>1</sup>; J. Y. Tsai<sup>1</sup>; C. W. Chang<sup>1</sup>; Y. C. Shieh<sup>1</sup>; C. Robert Kao<sup>1</sup>; <sup>1</sup>National Central University, Dept. of Chem. & Matls. Engrg., Chungli City 320 Taiwan

The SnAgCu solder is considered a very promising lead-free replacement for the Sn-37Pb solder. For industrial uses, a 0.2% uncertainty in composition is generally accepted. However, our recent study revealed that, during soldering, the Cu concentration had a very strong effect on the reactions between SnAgCu solders and Ni. When the Cu concentration was low (x=0.3 and lower), the reaction product was (Ni<sub>1-x</sub>Cu<sub>x</sub>)<sub>3</sub>Sn<sub>4</sub> at the interface of a solder joint. At high Cu concentrations (x=0.6 and higher), the reaction product was (Cu<sub>1-y</sub>Ni<sub>y</sub>)<sub>6</sub>Sn<sub>5</sub>. When the Cu concentration was in-between (x=0.4 and 0.5), both (Ni<sub>1</sub>- $_{x}Cu_{x})_{3}Sn_{4}and (Cu_{1,y}Ni_{y})_{6}Sn_{5}$ , formed. In other words, during soldering, the Cu concentration must be strictly controlled in order to obtain consistent results. In this study, we would like to extend our earlier study to investigate whether this strong concentration dependency also occurs during the solid-state aging of the solder joints. We aged solder joints at the solid-state at several different temperatures for time as long as 4000 hours. The solder compositions studied include SnAg0.2Cu, SnAg0.3Cu, SnAg-0.4Cu, SnAg-0.5Cu, SnAg-0.6Cu, SnAg-0.7Cu, and SnAg-1.0Cu. Analysis techniques used include optical microscope, SEM, EPMA, and XRD.

### 9:15 AM

Interfacial Reaction Study of Solder Joint with Sn-Ag-Cu Solder Ball and Various Solder Pastes in Lead Free WLCSP: *Huann-Wu Chiang*<sup>1</sup>; Morris Chen<sup>1</sup>; *Jeffrey C.B. Lee*<sup>2</sup>; Johnson Liu<sup>2</sup>; Simon Li<sup>2</sup>; <sup>1</sup>I-SHOU University, Matls. Sci. & Engrg., #1, Sec. 1, Hsueh-Cheng Rd., Ta-Hsu Hsiang, Kaohsiung County, Taiwan 84008 Taiwan; <sup>2</sup>Advanced Semiconductor Engineering, Inc., Engrg. Ctr., 26, Chin 3rd Rd., Nantze Export Procg. Zone, Kaohsiung 811 Taiwan

The interfacial reactions of solder joint between Sn-Ag-Cu solder ball and various solder pastes such as, Sn-3.0Ag-0.5Cu, 63Sn-37Pb and Sn-8Zn-Al, will be investigated in wafer level CSP package. After appropriate SMT reflow process on PCB with Cu <sup>-</sup>COSP and Cu-NiAu surface finish, samples will be subject to TCT (-40~125jæ) 1000 cycle and HTS (150jæ) 1000hrs reliability test. Sequentially, the cross-section analysis is also scrutinized by SEM/EDX to observe metallurgical evolution in the interface and solder bulk itself. The relationship among morphology, shear strength, and solder paste composition will be explored in the study. A mature Sn-37Pb solder ball wafer level CSP will be used for comparison as well.

#### 9:35 AM

An Investigation of Intermetallic Phase Morphology in Lead-Free Solders: Mohammad Faizan<sup>1</sup>; Robert A. McCoy<sup>2</sup>; <sup>1</sup>Youngstown State University, Civil Engrg. Dept., Youngstown, OH 44555 USA; <sup>2</sup>Youngstown State University, Mech. Engrg. Dept., Youngstown, OH 44555 USA

During soldering of a copper substrate using Sn-rich, lead-free solders, a Sn-Cu interaction takes place at the copper/solder interface. Copper is dissolved into the molten solder and subsequently intermetallic compounds (IMC's) are formed at the interface. Understanding of the growth rate and morphology of IMC's at the copper/solder interface is critical in achieving reliable soldered joints. This paper presents an analysis of an experimental investigation of soldering of a copper substrate using two solder compositions: pure Sn and Sn-3.5% Ag. Experimental results indicated that the solder composition, the temperature of the molten solder, and the dwell time (time the molten solder remains in contact with the substrate) controlled the growth of the IMC's. The IMC's grew in a scalloped shape for both solders but the IMC's for the Sn-Ag solder were detected as more irregular with needle-like scallops.

#### 9:55 AM

The Effect of Isothermal Aging on the Thickness of Intermetallic Compound Layer Growth Between Low Melting Point Solder and Ni Plated Cu Substrate: *Dae-Gon Kim*<sup>1</sup>; Seung-Boo Jung<sup>1</sup>; Chang-Youl Lee<sup>1</sup>; <sup>1</sup>Sungkyunkwan University, Dept. of Advd. Matls. Engrg., 300 chunchun-dong, jangan-gu, Suwon, Gyeonggi-do 440-746 Korea

The growth kinetics of intermetallic compound layer formed between low melting point solder (pure In, In-48Sn solder) and Ni/Cu substrate by solid state isothermal aging were examined for 0 to 100 days. A guantitative analysis of the intermetallic compound layer thickness as a function of time and temperature was performed. Experimental results showed that the intermetallic compounds, such as In27Ni10 and In11Sn23Ni16 were observed for different solders, respectively. The layer growth of intermetallic compound in the couple of low melting point solders/electrolytic Ni system satisfied the parabolic law at given temperature range. As a whole, because the values of time exponent(n) have approximately 0.5, the layer growth of the intermetallic compound was mainly controlled by diffusion mechanism over the temperature range studied. The apparent activation energies for intermetallic compound growth were 60.03 kJ/mol for In27Ni10 and 72.83 kJ/mol for In11Sn23Ni16, respectively.

#### 10:15 AM Break

#### 10:25 AM Invited

Interfacial Reaction of Lead-Free Sn-3.8Ag-0.7Cu, Sn-0.7Cu, and Sn-1.7Cu Solders with Pt: Tae hyun Kim<sup>1</sup>; Young Ho Kim<sup>1</sup>; <sup>1</sup>Hanyang University, Matls. Engrg., Haengdang-dong, seongdong-gu, Seoul 133-791 S. Korea

The interfacial reaction and the intermetallic formation in the interface betweem Sn solder containing small amount of Cu with Pt were investigated. Sn-0.7wt%Cu and Sn-1.7wt%Cu solders were reacted with Pt by dipping the Pt/Ti/Si specimens into the molten solder at 260°. Sn-3.8wt%Ag-0.7wt%Cu solder was reacted with Pt by reflowing the solder paste on the Pt/Ti/Si substrae at 250°. The intermetallic formation was characterized by using scanning electron microscopy, energy dispersive x-ray spectroscopy, x-ray diffractometry, and transmission electron microscopy. Pt-Sn intermetallic formed in the solder/Pt interface and Cu6Sn5 type interfacial intermetallic was not observed in all specimens. A parabolic relationship exist, between the thickness of the Pt-Sn intermetallic layer with reaction time, which indicates the intermetallic formation in the solder/Pt interface is diffusion-control.

## 10:50 AM

Intermetallic Compounds and Adhesion Strength Between the Sn-9Zn-1.5Ag-0.5Bi Lead-Free Solder and Unfluxed Cu Substrate: *Tzih-Yao Liu'*; Moo-Chin Wang<sup>2</sup>; Min-Hsiung Hon<sup>1</sup>; <sup>1</sup>National Cheng Kung University, Dept. of Matls. Sci. & Engrg., 1 Ta-Hsueh Rd., Tainan 70101 Taiwan; <sup>2</sup>National Kaohsiung University of Applied Science, Dept. of Mech. Engrg., 415 Chien-Kung Rd., Kaohsiung 80872 Taiwan

The intermetallic compounds (IMCs) formed at the interface between the Sn-9Zn-1.5Ag-0.5Bi lead-free solder alloy and unfluxed Cu substrate have been investigated by X-ray diffraction (XRD), optical microscopy (OM), scanning electron microscopy (SEM), transmission electron microscopy (TEM) and energy dispersive spectrometry (EDS). The melting point and melting range of the Sn-9Zn-1.5Ag-0.5Bi solder alloy are determined as 196°C and 10°C, respectively, by differential scanning carolimeter (DSC). The Cu6Sn5 and Cu5Zn8 IMCs were identified at the Sn-9Zn-1.5Ag-0.5Bi/unfluxed Cu interface as wetted at 250°C for 10 s. The interfacial adhesion strength increases from 7.36  $\pm$  0.72 to 10.85  $\pm$  0.56MPa with increasing the soldering time from 10 to 30 s.

#### 11:10 AM

Coupling Effect on Interfacial Reactions of Flip Chip Solder Joints with Ti/Cr-Cu/Cu Under Bump Metallization and Ni-P/ Cu/Au Pad Metallization During Reflow in Microelectronic Packaging: *Tung Liang Shao*<sup>1</sup>; Yuan Ming Huang<sup>1</sup>; Te Sheng Chen<sup>1</sup>; Chih Chen<sup>1</sup>; <sup>1</sup>National Chiao Tung University, Dept. of Matls. Sci. & Engrg., Jsin Shu 300 Taiwan

The soldering technology is still important and widely applied in the advanced flip chip product. The purpose of this study was to identify and prove the existence of coupling effect on interfacial reactions between flip chip solder bumps and the under bump metallization (UBM) systems. Eutectic Sn/Pb solders were applied for the samples. Three types of sample (including the dumped die, the bumped substrate and the flip chip package) were examined. The binary Cu-Sn compounds and the Ni-Sn compounds were formed for the bumped die and the bumped substrate after the first reflow. The tenary Ni-Cu-Sn compounds were formed for the flip chip package during the second reflow. By comparing the composition of intermetallic compounds (IMC) for these three types of sample, the coupling effect on interfacial reactions of solders and the flip chip systems was proved. Not only Ni and Cu coupling were observed, but also Au coupling effect was found, which Au-Sn IMC was found on the surface of Ni-Cu-Sn IMC on the chip side.

## 11:30 AM

Inhibiting Growth of Ni3P Crystalline Layer in Ni(P) Substrate by Reacting with Cu-Doped SnAg Solders: S. J. Wang<sup>1</sup>; H. R. Kao<sup>1</sup>; C. Y. Liu<sup>1</sup>; <sup>1</sup>National Central University, Dept. of Chem. Engrg. & Matls. Engrg., No. 300 Jung-Da Rd., Chung-Li Taiwan

Interfacial reactions between Sn(Cu) alloys and Ni(P) substrates have been studied. Comparing to Sn/Ni(P), the formation of Ni3P layers in Sn(Cu)/Ni(P) reaction couples were very limited. The sluggish growth of Ni3P layer attributed to a layer of Cu-Sn compound layer formed on the Ni(P) substrate, which effectively isolated the Ni(P) substrate from reacting with solder. The eventual formation of Ni3P compound layer depended on the Ni diffusion in the Cu-Sn compound. Also, we found that the higher Cu-content Sn(Cu) alloys had less Ni3P formation. In this talk, we will present the kinetics of the interfacial reactions between Sn(Cu) alloys and Ni(P) substrates under solid-state aging and liquid-state reflowing. The correlation between the mechanical strength of solder joints and the interfacial reactions will be also reported.

### 11:50 AM

Effects of Substrate Metallization and Pad Structure on the UBM Degradation of Flip Chip Packages Under Thermal Aging: Jenq-Dah Wu<sup>1</sup>; <sup>1</sup>Advanced Semiconductor Engineering, RD Lab, 26, Chin 3rd Rd. Nantze Export Processing Zone, Kaohsiung 811 Taiwan

Thermal aging of flip chip packages is performed to investigate reliability issues associated with structural evolution of UBM and solder interconnects. UBM employed is a thin film Al/Ni(V)/Cu metal stack; while bump material is eutectic Sn/Pb solder. Structural integrity of UBM/bump system is characterized by die pull/shear tests of FCBGAS without underfill. Fracture strength degradation and transition of failure patterns from ductile solder cleavage to brittle UBM fracture at Ni(V) layer provides evidence of UBM degradation under prolonged thermal aging. Two substrate surface finishes are considered in this paper, i.e. electroless Ni/immersion Au and OSP. It is observed that solder bumps of FCBGAs with OSP substrates remain intact after 3,000 hrs of HTST, while UBM failure is found for FCBGAs with Ni/Au substrates. This implies that Ni/Au substrate metallization plays critical role on the interfacial reactions of Al/Ni(V)/Cu UBM and solder bumps.

## Magnesium Technology 2004: Casting Processes and Properties

Sponsored by: Light Metals Division, LMD-Magnesium Committee Program Organizer: Alan A. Luo, General Motors, Materials and Processes Laboratory, Warren, MI 48090-9055 USA

Wednesday AM	Room: 203B
March 17, 2004	Location: Charlotte Convention Center

Session Chairs: Darryl Albright, Hydro Magnesium, Livonia, MI 48152 USA; Eli Aghion, Dead Sea Magnesium, Beer-Sheva 84111 Israel

#### 8:30 AM

Effect of Inhibitor Gas on Mould - Magnesium Reactions in Investment Casting: Zhan Zhang<sup>1</sup>; Guy Morin<sup>2</sup>; <sup>1</sup>Intermag-Modelex Inc., Saint-Nicolas, PQ Canada; <sup>2</sup>Centre Intégré de Fonderie et de Métallurgie, Trois-Rivières, PQ Canada

In order to assess the behaviour of mould-magnesium reaction, the ceramic shell moulds with different binder and refractory particles were prepared for pouring AZ91 magnesium alloy. To restrict mould-magnesium reactions, inhibitor gas was guided into shell moulds for removal of oxygen in shell moulds and formation of barrage between mould and magnesium. The results of experiments show that a mixture of CO2 and proper concentration of SF6 used as inhibitor gas can effectively limit mould-magnesium reactions even if the temperature of ceramic shell moulds is higher than 450°C. A surface analysis with AES (auger electron spectroscopy) and ESCA (electron spectroscopy for chemical analysis) has been performed on the surface of magne-

sium parts cast under the inhibitor gas. It was discovered that a special layer appeared on the surface, in which the elements such as magnesium, oxygen, fluorine, aluminium, carbon, silicon, etc. were detected. The thickness of fluorine-containing layer varies with the variation of the concentration of fluorine in the gas mixture. The models of mouldmagnesium reactions and their preventions are described in this paper.

## 8:50 AM

The Role of Microstructure and Porosity in Ductility of Die Cast AM50 and AM60 Magnesium Alloys: *Gurjeev Chadha*<sup>1</sup>; John E. Allison<sup>2</sup>; J. Wayne Jones<sup>1</sup>; <sup>1</sup>University of Michigan, Matls. Sci. & Engrg., Ann Arbor, MI 48105 USA; <sup>2</sup>Ford Motor Company, Matls. Sci. Dept., Dearborn, MI 48124 USA

The deformation and fracture behavior of die-cast AM50 and AM60 magnesium alloys have been examined to determine the processes leading to fracture in bending and tension and to elucidate the influences of microstructure and porosity on ductility. Damage accumulation in terms of crack initiation, growth, linking and eventual failure was quantified as a function of strain for as-cast plates with section thicknesses of 2, 6 and 10mm. Microstructure and porosity distribution are dependent on section thickness, with bands of high porosity resulting from the nature of die filling. In both tensile and three-point bend studies, damage accumulation, and subsequent ductility at fracture, are strongly influenced by the heterogeneity in porosity distribution, with early crack formation occurring in regions of highest porosity. The role of microstructure on the growth of cracks from porosity during straining has been examined in situ by scanning electron microscopy and the critical strains to fracture have been studied by a surface strain mapping technique to determine the nature of strain localization around pores in these alloys. Using this information, a model is constructed that relates the observed ductility of these alloys with critical microstructural features.

## 9:10 AM

First Magnesium V-Process Casting: Sayavur I. Bakhtiyarov<sup>1</sup>; Ruel A. Overfelt<sup>1</sup>; <sup>1</sup>Auburn University, Mech. Engrg., 202 Ross Hall, Auburn, AL 36849-5341 USA

The Solidification Design Center (Auburn University, AL, a NASA Research Partnership Center) and Jones Engineering, Inc. (Lawrenceville, GA) conducted the first successful magnesium V-process (vacuum sealed molding process) casting. Since the invention of the V-process casting technique in Japan in 1971, it has been believed that the unique casting process is suitable for any metal (gray, ductile, malleable iron, various grades of steel or aluminum and copper base alloys) except magnesium. Currently die casting is the primary technique for production of magnesium parts for high volume automotive applications. However, the need for magnesium structural components spurs the need for alternative processes. Application of this vacuum-sealed manufacturing process for magnesium casting directly addresses the high priority needs identified in the Metalcasting Industry Technology Roadmap and the primary mission of the AFS Magnesium Division - the development of alternative casting processes for magnesium. An exploration of the possibility of combining the benefits of V-process casting with the advantages of magnesium was really challenging mainly due to low thermal heat content and high chemical reactivity of magnesium. In this paper we present casting procedures of the first magnesium V-process casting. The major mechanical properties and metallography of the casting are studies and compared to those obtained for magnesium sand casting.

## 9:30 AM

Evaluation Between Mechanical Properties and Die Casting Process Control by Toguchi Method for Magnesium Alloy AM60B: *Chi Ming Hung*<sup>1</sup>; Mao Sheng Chang<sup>1</sup>; <sup>1</sup>Metal Industries Research & Development Center, Casting Tech. Sect., 1001 Kaonan Hwy., Kaohsiung, Taiwan 811 Taiwan

On demanding of environmental protection, light metals are used more and more in automobiles in recent years. It is a good choice to apply more magnesium castings to an automobile to reduce its weight so that the emission amount of CO2 will decrease. When it comes to automobile parts, the mechanical properties are very important. However, the mechanical properties of die casting are significantly influenced by the process parameters. The study is to examine the effects of cold chamber die casting process parameters on mechanical properties of AM60B magnesium alloy. We choose four process parametersdie temperature, second phase speed, pressure and cooling time- as the control factors, and use Toguchi method to analyze which of them has important influence on mechanical properties of AM60B.

#### 10:20 AM

Characterization of Mg Alloy Solidification and As-Cast Microstructures: Y. W. Riddle<sup>1</sup>; M. M. Makhlouf<sup>1</sup>; <sup>1</sup>Worcester Polytechnic Institute, Advd. Casting Rsch. Ctr., Worcester, MA USA

In previous research presented at TMS 2003 we established a nonequilibrium thermal analysis method and apparatus for the study of Mg alloy solidification. In the present research a specialized dendrite coherency cell has been developed and used to enhance understanding of solid network formation during Mg alloy solidification. Combining thermal analysis and dendrite coherency measurements from the liquid-to-solid state, and microscopy on the as-cast microstructure provides a thorough description of salient solidification features and forms a basis for understanding liquid-to-solid processing behavior in Mg alloys. Alloys from all families of Mg cast alloys including several of the newly developed alloys have been studied using thermal analysis, dendrite coherency, and microscopy with the results presented here. The aim of this project is to form a coherent and complete encyclopedia of solidification features and pursuant as-cast microstructures from the full range of Mg casting alloys as a practical tool for foundry metallurgists and future researchers interested in alloy development. When practical, comparison of conventionally cast and high-pressure die cast microstructures is included.

#### 10:40 AM

Industrial Sludge Investigations in AZ91D, AM60B and AM50A Die-Casting Operations: Chris Patrick Corby<sup>1</sup>; Ma Qian<sup>1</sup>; Nigel Jeffery Ricketts<sup>2</sup>; Rob Bailey<sup>3</sup>; <sup>1</sup>University of Queensland, CRC for Cast Metals Mfg. (CAST), Div. of Matls., Sch. of Engrg., Brisbane, QLD 4072 Australia; <sup>2</sup>CSIRO, Mfg. & Infrastructure Tech., 2643 Moggill Rd., Pinjarra Hills, Brisbane, QLD 4069 Australia; <sup>3</sup>Australian Magnesium Corporation, Covington, KY USA

Excess sludge generation is a costly problem facing the magnesium casting industry. With a view to address this economic concern, an investigation into the constituents of several sludge samples found in AM50A, AM60B and AZ91D die-casting operations was conducted. Chemical analysis from the literature suggests that the major proportion of sludge is entrapped Mg metal and oxide. Electron microscopy was used to confirm that the major chemical species in industrial die casting sludge samples were magnesium oxide, Mn-Al-Fe intermetallic particles and a high proportion of entrained metal. The iron content of the intermetallic phases present in the sludge was found to be very low, suggesting that the intermetallic particles in the sludge are mainly Mn-Al phases. Process parameters are discussed with a view to minimising sludge formation in magnesium die casting furnaces.

## 11:00 AM

Filling Characteristic of AZ91D Magnesium Alloys During EPC: *Shae K. Kim*<sup>1</sup>; Gue-Serb Cho<sup>1</sup>; Kyong-Whoan Lee<sup>1</sup>; Hyung-Ho Jo<sup>1</sup>; <sup>1</sup>Korea Institute of Industrial Technology, Advd. Matl. R&D Ctr., 472 KaJwa-Dong, Seo-Ku, Incheon 404-254 Korea

Magnesium alloys are gaining increased importance for automotive applications due to their low density and high strength-to-weight ratio. Diecasting is currently used for magnesium components for the excellent castability of magnesium alloys allowing very thin and complicated sections to be cast. With increasing the number of potential applicastions, however, other forming processes, especially, other casting processes should be considered and developed. The aim of this study is to develop a complete EPC (Expendable Pattern Casting) for magnesium alloys. The special attention will be given to metal-mold reaction and fluidity of AZ91D magnesium alloys during the process.

#### 11:20 AM

Numerical Understanding of Forced Convection in Melt of Squeeze Casting Magnesium Alloy: *Alfred Yu*<sup>1</sup>; Naiyi Li<sup>2</sup>; Henry Hu<sup>1</sup>; <sup>1</sup>University of Windsor, Mech., Auto. & Matls. Engrg., 401 Sunset Ave., Windsor, Ontario N9B 3P4 Canada; <sup>2</sup>Ford Motor Company, Mfg. Sys. Dept., Ford Rsch. Lab., Dearborn, MI 48121 USA

As a continuous effort on fundamental study of squeeze casting of magnesium alloys, a 3-D mathematical model has been developed to simulate the melt flow, heat transfer and solidification phenomena. In this paper, the developed model simulates the events of metal flow with various initial filling velocities during squeeze casting of magnesium alloys. The influence of forced convection resulting from initial filling velocities on heat transfer between the melt and the mold is examined. The temperature distribution in the squeeze casting during and after filling is also predicted. The significance of taking forced convection into consideration for precision of computing solidification patterns following the filling stage is discussed and highlighted.

## Materials by Design: Atoms to Applications: Design for Mechanical Functionality I

Sponsored by: Electronic, Magnetic & Photonic Materials Division, EMPMD/SMD-Chemistry & Physics of Materials Committee

*Program Organizers:* Krishna Rajan, Rensselaer Polytechnic Institute, Department of Materials Science and Engineering, Troy, NY 12180-3590 USA; Krishnan K. Sankaran, The Boeing Company, Phantom Works, St. Louis, MO 63166-0516 USA

Wednesday AM	Room: 210B
March 17, 2004	Location: Charlotte Convention Center

Session Chair: Krishnan K. Sankaran, The Boeing Company, Phantom Works, St. Louis, MO 63166-0516 USA

#### 8:30 AM Invited

The Design and Development of an Age Hardenable Aluminum Alloy for Moderate Temperature Application: E. A. Starke, Jr.<sup>1</sup>; B. M. Gable<sup>1</sup>; G. J. Shiflet<sup>1</sup>; A. W. Zhu<sup>1</sup>; <sup>1</sup>University of Virginia, Dept. of Matls. Sci. & Engrg., Charlottesville, VA 22904-4745 USA

This presentation will describe both the alloy design methodology and our most recent experimental results directed towards the development of an age hardenable wrought aluminum alloy for moderate temperature applications. The design process involves extensive empirical research, theoretical simulation and modeling, first principle atomistic calculations, calculated phase diagrams and quantitative analytical techniques. Our research focuses on the Al-Cu-Mg-(Ag) system and we have used the CALPHAD (CALculation of PHAse Diagrams) method to determine the phase field that gives the most promise for having q' and W precipitates, without the interference of the S phase. First principle total energy calculations using VASP (Vienna Ab initio Simulation Program) were conducted to evaluate the proposed crystal structures and to determine interfacial energies and elastic constants of the strengthening phases. The elastic strain energy associated with the formation of plate-like elemental clusters in the aluminum matrix was determined. These clusters may function as either precursors or non-precursors for the desired precipitates. Combined with the strain energy considerations, thermodynamic analysis of short-range order was employed to identify useful trace elements and deleterious impurities for the formation of the desired precipitates having a fine and uniform distribution. Due to the competitive nature of precipitation in this alloy system the relative volume fractions of precipitates on {111} and {100} habit plans can be modified by thermal-mechanical treatments. Our modeling and predictions are being verified by experimental measurements. The ultimate objective of this program is to streamline alloy design and, therefore, to aid in early insertion of new high performance materials into aerospace systems. Sponsored by the Air Force Office of Scientific Research under Grant S49620-01-1-0090.

#### 9:00 AM

Atomistic Design of Ductile Transition-Metal Solid Solution Alloys: Kwai S. Chan<sup>1</sup>; <sup>1</sup>Southwest Research Institute, 6220 Culebra Rd., San Antonio, TX 78238 USA

A computational approach is applied to design ductile bcc transition-metal solid solution alloys on the basis of a recent discovery that the d + s electrons affect the Peierls-Nabarro (P-N) barrier energy and dislocation mobility. For designing compositions of ductile alloys, the number of d + s electrons per atom in the solid solution alloy are tailored to achieve three objectives: (1) increasing the dislocation line energy, (2) decreasing the shear modulus in the slip direction, and (3) reducing the P-N barrier energy. Applications of this atomistic method to designing ductile bcc Ti-, Nb-, and Mo-base solid solution alloys are illustrated and compared against experimental data. The results indicates that design of ductile transition-metal solid solution alloys can be achieved solely by manipulating the number of d + s electrons to increase dislocation mobility via a reduction of the P-N barrier energy. Furthermore, the atomistic approach provides insights on the roles of electronic bonding in solid solution toughening and embrittlement in transition metals. Material parameters and electronic bonding that affect brittle-to-ductile fracture transition in transition metals are identified and discussed in conjunction with experimental observations. Work supported by AFOSR through contracts F4962001-C-0016 and F49620-01-1-0547, Dr. Craig S. Hartley, Program Manager.

Atomic Level Modeling for the Computer Design of Naval Steels: Michael J. Mehl<sup>1</sup>; Dimitrios A. Papaconstantopoulos<sup>1</sup>; Yuri Mishin<sup>2</sup>; <sup>1</sup>Naval Research Laboratory, Ctr. for Computational Matls. Sci., Code 6390, Washington, DC 20375-5000 USA; <sup>2</sup>George Mason University, Sch. of Computational Scis., Fairfax, VA 22030 USA

Computer modeling on the electronic and atomic levels offers a way of reducing the costs and accelerating the development cycle of Naval steels. This paper reports on our recent efforts in that direction. First-principles (LAPW/GGA) calculations have been performed for many ordered fcc and bcc-based compounds of the Fe-Ni system. The results of these calculations are used to construct tight-binding and angular-dependent atomistic potentials for the Fe-Ni system. The potentials are applied to calculate the structures, energies and equilibrium segregation at several grain boundaries in fcc Fe-Ni alloys (austenite). Mechanical properties of the grain boundaries are evaluated by modeling the process of decohesion. The observed relations between the grain boundary energies, cohesive strength, temperature and the alloy composition provide useful input for mesoscopic continuum simulations of plastic deformation and fracture of Naval steels. The ongoing efforts to extend this work to multicomponent steel alloys are discussed.

#### 10:00 AM Break

#### 10:15 AM

Micro- and Nano-Contacts: Multi-Scale Models and Experiments: W. O. Soboyejo<sup>1</sup>; Z. Zong<sup>1</sup>; J. Lou<sup>1</sup>; A. Widjaja<sup>2</sup>; E. Van der Giesen<sup>2</sup>; E. Bittencourt<sup>3</sup>; A. Needleman<sup>4</sup>; <sup>1</sup>Princeton University, MAE Dept./PMI, Olden St., Princeton, NJ 08544 USA; <sup>2</sup>University of Gronigen, Dept. of Appl. Physics, Gronigen The Netherlands; <sup>3</sup>University of Sao Paulo, Sao Paulo Brazil; <sup>4</sup>Brown University, Div. of Engrg., Providence, RI 02912 USA

This paper presents a multi-scale framework for the modeling of micro- and nano-contacts that are relevant to micro-electro-mechanical systems (MEMS) and microelectronic devices. The framework includes the use of discrete dislocations models for the modeling of contact-induced plasticity in the nano-scale regime. However, in the sub-micron and micron-scale regimes, local and non-local strain gradient plasticity models are used to model the deformation induced by sharp and blunt contacts. Predictions of indentation size effects and material pile-up are compared with experimental measurements obtained from Berkovitch, cube-cornered and Vickers indenters. The implications of the results are then discussed for contact-induced deformation in MEMS switches and magnetic storage devices.

## 10:45 AM

Micromechanics Study of Gamma-TiAl Material: Sheng Chang<sup>1</sup>; Dan Hong<sup>1</sup>; Fu-Pen Chiang<sup>1</sup>; <sup>1</sup>State University of New York, Dept. of Mechl. Engrg., Stony Brook, NY 11794-2300 USA

The knowledge of the micromechanical properties of gamma Titanium Aluminide is essential to the design of high performance gas turbine engines or low emission-high efficiency internal combustion engines. A novel experimental micromechanics technique SIEM (Speckle Interferometry with Electron Microscopy) was employed to examine the inter-lamellar deformation and the deformation within the lamellar colony of gamma Titanium Aluminide. SIEM is a micromechanics measurement technique that has a spatial resolution approaching to a few nanometers. It is able to perform the full field displacement mapping over a region of only several microns in diameter. A dog-bone specimen was tested under uniaxial tension and intercolony shear was found in the displacement contours. Another fatiguecracked specimen was tested under 3-point bending load at 1000x magnification. The deformation fields around the crack tip were obtained. It shows that the crack propagation path tends to align with the crystal orientation.

#### 11:15 AM

Atomistic Modeling of High-Temperature Structural Aliminides: Y. Mishin<sup>1</sup>; <sup>1</sup>George Mason University, Sch. of Computational Scis., 4400 Univ. Dr., MSN 5C3, Fairfax, VA 22030-4444 USA

Overview of our recent work on the atomistic modeling of ordered intermetallic compounds of the Ni-Al and Ti-Al systems. Atomic interactions in these systems are modeled by semi-empirical potentials fit to both experimental and first-principles data. The methodology includes a large variety of techniques ranging from harmonic lattice dynamics to molecular dynamics and Monte Carlo simulations. The properties studied include lattice characteristics (elastic constants, phonons, thermal expansion), point-defect properties, atomic diffusion, generalized stacking faults, dislocations, surfaces, grain boundaries, interphase boundaries, phase diagrams and so on. It is discussed how the output of such calculations can be used for the computer design of advanced intermetallics.

## Materials Education to Revitalize the Workforce: Session I

Sponsored by: TMS, Public & Governmental Affairs Committee, TMS-Education Committee

*Program Organizers:* Reza Abbaschian, University of Florida, College of Engineering, Gainesville, FL 32611-6400 USA; Iver E. Anderson, Iowa State University, Ames Laboratory, Ames, IA 50011-3020 USA

Wednesday AM	Room:	217D		
March 17, 2004	Location	: Charlotte	Convention	Center

Session Chair: TBA

#### 8:30 AM Keynote

Training for a High Tech Society: Larry Keen<sup>1</sup>; <sup>1</sup>North Carolina Community College System, Economic & Workforce Dvlp., 5001 Mail Service Ctr., Raleigh, NC 27699-5001 USA

The dynamic nature of the world's economies require organizations, states and nations to provide training and educational services that result in rapid adaptation to changes organizationally and technologically by an adaptable workforce in high-tech societies. The educational enterprises' conceptualization by which the opportunities available in promising disciplines are organized, promoted and delivered may rest with greater inter-institution collaboration that could lead to the enhancement of a high-tech workforce in a high-tech society. Potential solutions to inform and train for a high-tech society may be an answer to consider and may result in seamless training and educational systems to meet the need.

#### 9:00 AM

Making Science Exciting for the Future Workforce: *Robert A. Childs*<sup>1</sup>; <sup>1</sup>Massachusetts Institute of Technology, Plasma Sci. & Fusion Ctr., 190 Albany St., NW21-109, Cambridge, MA 02139 USA

One of the perceived notions that trouble us today is that working in a science related field is somehow less glamorous and less financially rewarding than say a career as a doctor, lawyer or sports hero. We have to show the youth of today that there can be excitement and comfortable earnings in a career in science that is more personally rewarding than the image they have today. Moderate strides have been made in the last couple of decades to correct this notion but more needs to be done. This talk will show samples of work being done by scientific societies, universities and local school systems in the K-12 range that have been successful. We need to continue making the jobs available but we also need to raise the level of excitement in those future workers if we are going to fill those jobs from within.

#### 9:30 AM

Career Resource Center for MSE: Gerald L. Liedl<sup>1</sup>; <sup>1</sup>Purdue University, Sch. of Matls. Engrg., W. Lafayette, IN 47907 USA

In response to a NAS study that indicated initial career decisions are made in the absence of realistic information about life in science and engineering professions, the Alfred P. Sloan Foundation funded a group of professional societies to generate information for their fields in the early 1990's. TMS in collaboration with other materials-oriented societies generated the Career Resource Center for MSE. Components of the Center included surveys to provide statistical information about professionals in the field, development of a career guidance booklet, a web site, and a career CD ROM. The evolution and utilization of the components of the Center will be discussed as well as the impact of the integrated Sloan Career Cornerstone web site on distribution of information about MSE.

#### 10:00 AM Break

#### 10:20 AM

**MSE Teach: An Undergraduate Recruitment Tool**: *Paul H. Holloway*<sup>1</sup>; Elliot Douglas<sup>1</sup>; <sup>1</sup>University of Florida, Dept. of Matls. Sci. & Engrg., Gainesville, FL 32611-6400 USA

A number of techniques are necessary to successfully recruit undergraduates to MSE, including university information directed towards the potential student. However, the student is in daily contact with her/his high school or community college teachers, and this provides another avenue for supplying information about a career in materials. Since 1995, we have organized a workshop on materials science and engineering for 6th-12th grade and community college science teachers. Using a combination of tutorial lectures, typical applications, hands-on demonstrations, and laboratories conducted by graduate students and faculty, we have introduced these teachers to the fundamental and exciting topics in MSE. The teachers in turn have developed lesson plans and passed this excitement to their students, resulting in applications from 10835 undergraduates designating MSE as their degree choice. Details of the MSE Teach program will be discussed and illustrated.

#### 10:50 AM

Materials Engineering Technology: The Role of Community Colleges in Preparing the Technical Workforce of the 21st Century: John McKay<sup>1</sup>; Michael Kenney<sup>2</sup>; Pat Pohar<sup>1</sup>; John Pridgeon<sup>3</sup>; <sup>1</sup>South Piedmont Community College, Monroe, NC USA; <sup>2</sup>ASM International, Matls. Park, OH USA; <sup>3</sup>Allvac (retired), Monroe, NC USA

US companies involved in manufacturing are experiencing both a shortage of qualified workers and a need to retrain existing personnel on new technologies. Both of these situations can easily be addressed through two-year college educational programs. Advantages of the Community College include proximity to the workplace, knowledge and understanding of the needs of adult learners, and strong community ties. This presentation will present a case study of the efforts of South Piedmont Community College in collaboration with a local employer, Allvac, and ASM International. Lessons learned, both positive and negative, of a unique degreeprogram will be highlighted.

## Materials Processing Fundamentals: Aqueous Processing

Sponsored by: Extraction & Processing Division, Materials Processing & Manufacturing Division, EPD-Process Fundamentals Committee, MPMD/EPD-Process Modeling Analysis & Control Committee

*Program Organizers:* Adam C. Powell, Massachusetts Institute of Technology, Department of Materials Science and Engineering, Cambridge, MA 02139-4307 USA; Princewill N. Anyalebechi, Grand Valley State University, L. V. Eberhard Center, Grand Rapids, MI 49504-6495 USA

Wednesday AM Room: 212B March 17, 2004 Location: Charlotte Convention Center

Session Chair: TBA

### 8:30 AM

Study on the Thermodynamic Equilibrium of the Ni(II)-Ammonia-Carbonate Aqueous System and its Application to the Precipitation of Basic Nickel Carbonate Particles: Guo Xueyi<sup>1</sup>; Huang Kai<sup>1</sup>; Zhang Duomo<sup>1</sup>; <sup>1</sup>Central South University, Sch. of Metallurgl. Sci. & Engrg., Yuelu Dist., Changsha, Hunan 410083 China

Based on the principles of simultaneous equilibrium and mass equilibrium, the thermodynamic equilibrium equations of Ni(II)-ammoniacarbonate aqueous system at ambient temperature were deduced theoretically and the thermodynamic diagrams of lg[Ni2+] versus pH at different solution compositions were drawn. It was founded by experiments that the obtained theoretical diagrams were useful to explain the formation mechanism of precipitation particles with different microscopic shapes. When pH of the solution below 7.0, the loose flocculation particles were produced due to fast coagulation which was the dominant growth mechanism on this condition, while pH above 7.0, because of the coordination of nickel ion with ammonia, the precipitation proceeded slowly accompanying with the release of Ni2+ from the complexes, which easily results in the formation of the dense spherical particles.

#### 9:00 AM

Application of Chemical Pattern Recognition to the Preparation of Monodispersed NiO Precursor Particles by Homogeneous Precipitation: *Huang Kai*<sup>1</sup>; *Guo Xueyi*<sup>1</sup>; Zhang Duomo<sup>1</sup>; <sup>1</sup>Central South University, Sch. of Metallurgl. Sci. & Engrg., Yuelu Dist., Changsha, Hunan 410083 China

Mono-dispersed NiO precursor particles were prepared by homogeneous precipitation in the presence of urea. Optimal discrimination plan method, one of the chemical pattern recognition techniques, was applied to analyzing the experimental data and the calculating results were visualized in the mapping figures, in which the different class of samples were divided distinctly and the corresponding semi-experienced mathematic model was deduced. The model can be well used to predict the relationships of the characteristics of the precipitated particles with operational parameters. It proved experimentally that the model fit well with the experimental results and it was quite effective to guide the process design.

#### 9:20 AM

Study on the Thermodynamic Equilibrium of the Ni(II)-Ammonia-Oxalate Aqueous System and its Application to the Precipitation of Fine Nickel Oxalate Particles: *Huang Kai*<sup>1</sup>; *Guo Xueyi*<sup>1</sup>; *Zhang Duomo*<sup>1</sup>; <sup>1</sup>Central South University, Sch. of Metallurgl. Sci. & Engrg., Yuelu Dist., Changsha, Hunan 410083 China

Based on the principles of simultaneous equilibrium and mass equilibrium, a series of thermodynamic equilibrium equations of the complex system of Ni(II)-ammonia-oxalate aqueous system at ambient temperature were deduced theoretically and the relationship of lg[Ni(II)] versus pH at different solution compositions was established quantitatively. From the thermodynamic diagrams, it was indicated that when pH less than 8.0, free Ni(II) was the dominant metal ion in the solution; while pH higher than 8.0, most of the nickel ions coordinate with the ammonia as the complex in the solution. The experimental results show that when pH in solution less than 8.0, the nickel oxalate particles in cubic morphology precipitated; while pH higher than 8.0, the needle-like nickel oxalate was obtained. Comparing the thermodynamic diagram with the experimental data, it was founded that the different existing forms of nickel ion led to the formation of the above-obtained two kinds of particles.

#### 9:40 AM Break

#### 10:10 AM

Viscosity and Drift Flux Analysis: *Ramiro Escudero*<sup>1</sup>; Francisco J. Tavera<sup>1</sup>; <sup>1</sup>Universidad Michoacana de San Nicolás de Hidalgo, Inst. de Investigaciones Metalúrgicas, Santiago Tapia 403, C.P. 58000, Morelia, Mich. México

Column flotation are enjoying renewed interest due to new applications such as de-inking of recycled paper, industrial effluents treatment, and de-oiling of water. According to reported results, the efficiency of a given dispersion process depends on the characteristics of the dispersed phase. In order to predict an appropriate gas holdup, bubble surface area flux, and bubble size for a given duty, a mathematical model known as Drift Flux Analysis is currently applied. Drift Flux Analysis assumes a constant dynamic viscosity of the continuous phase (1 grame/centimetre-second) not matter the changes as result of the pulp consistency or solids content. This paper shows the relevance of considering the real value of the dynamic viscosity in terms of the characteristics of a gas dispersion. Viscosity of water was varied by using a polymer and the bubble size, bubble surface area, and gas holdup were calculated through the Drift Flux Model.

#### 10:40 AM

Phase Transformation Relationships in the CaSO4-H2SO4-H2O System: Yuanbing Ling<sup>1</sup>; George P. Demopoulos<sup>1</sup>; <sup>1</sup>McGill University, Dept. of Mining & Metallurgl. Engrg., 3610 Univ. St., Montreal, Quebec H3A 2B2 Canada; <sup>1</sup>McGill University, Metals & Matls. Engrg., 3610 Univ. St., Montreal, Quebec H3A2B2 Canada

As part of a boarder research topic, seeking the development of a cost-effective technology for direct production of a high value building/dental material, alpha-calcium sulfate hemihydrate, from sulfuric acid at atmospheric as opposed to elevated pressure conditions, some fundamental work has been done. This includes experimental monitoring of phase transformation reactions and thermodynamic analysis of the relationships among the various phases, namely, calcium sulfate dihydrate, hemihydrate and anhydrite in aqueous sulfuric acid solution at temperatures ranging from 20°C to boiling point. Account of these fundamental studies is presented in this paper.

#### 11:00 AM

Leaching of Cu-Co Oxidized Ore and Concentrate as Alternative to Conventional Sulphidization: Eduardo Patino<sup>1</sup>; <sup>1</sup>University Arturo Prat, Engrg. Dept., Av Arturo Prat 2120, Iquique, 57 Chile

The Luiswishi deposit belongs to the copper-cobalt oxides deposit of the Southern Group of the Katangian Copper Belt and is operated by a joint venture between EGMF (Enterprise Générales Malta Forrest) and Geacamines (Générale des Carrières et des Mines). The coopercobal ore is beneficiated by the sulphidization process at the NCK (New concentrator of Kipushi) at Kipushi. Sulphidization followed by flotation with sulphydryl collectors is a common practice for the treatment of oxidized base metals ores. However, this process is very complex and its application at the industrial scale is quite sensitive. In central Africa it is also a cost intensive treatment as the sulphidizing agent has to be imported. A new laboratory research program was carry out to find an alternative route of treatment using hydrometallurgical approach. Ore is composed by malachite, chrysocol, tenorite, and heterogenite with grades of 1.98% and 1.51% in copper and cobalt, respectively. The study was focussed in leaching techniques using sulphuric acid and ferrous iron as reductant to extract copper and cobalt, respectively. Two methods were compared: agglomerate-curate-leach of ore and ore Geocoat-ed with conventional concentrate. Results obtained reach copper and cobalt extractions up 80%.

## Metals for the Future: Structural Materials

Sponsored by: TMS

*Program Organizers:* Manfred Wuttig, University of Maryland, Department of Materials & Nuclear Engineering, College Park, MD 20742-2115 USA; Sreeramamurthy Ankem, University of Maryland, Department of Material & Nuclear Engineering, College Park, MD 20742-2115 USA

Wednesday AM	Room: 2	15
March 17, 2004	Location:	Charlotte Convention Center

Session Chair: K. L. Murty, North Carolina State University, Raleigh, NC 27695-7909 USA

#### 8:30 AM Opening Remarks by Dr. Haworth

### 8:40 AM Invited

Research on Structural Materials: Quo Vadis?: Ronald Gibala<sup>1</sup>; <sup>1</sup>University of Michigan, Dept. of Matls. Sci. & Engrg., 2300 Hayward, 2026 H.H. Dow Bldg., Ann Arbor, MI 48109-2136 USA

In spite of irregularly appearing discussions and opinions to the contrary, the future of applications of and research on structural materials, especially metals, appears to be substantial. Examination of data from several industrial sectors for applications and from funding agencies for applied and fundamental research demonstrates that, at worst, a few specific areas of research on metallic materials have declined and a few others may have stabilized. In general, however, the application of new techniques - experimental, theoretical, computational - offers many innovative opportunities for research on all types of structural materials. This talk will amplify on these points, offer several examples of current and exciting research on structural materials (at least to the author), and suggest areas of future research opportunities.

#### 9:10 AM Invited

Recent Developments on the Low Temperature Creep Deformation Behavior of Titanium Alloys: Sreeramamurthy Ankem<sup>1</sup>; <sup>1</sup>University of Maryland, Matls. Sci. & Engrg., Stadium Dr., Bldg. 090, College Park, MD 20742-2115 USA

Recent investigations revealed that alpha beta and beta titanium alloys could creep at low temperatures, such as room temperature. The factors that effect creep deformation include stress level, grain size, morphology of phases, and stability of phases. In this presentation, these developments will be reviewed and the future challenges that must be addressed in this area will be outlined. This work is being supported by the National Science Foundation under grant number DMR-0102320.

## 9:40 AM Invited

Morphological Control and Applications of Nanoporous Gold: Jonah D. Erlebacher<sup>1</sup>; <sup>1</sup>Johns Hopkins University, Matls. Sci. & Engrg., 102 Maryland Hall, 3400 N. Charles St., Baltimore, MD 21218 USA

The morphological evolution and applications of nanoporous gold (NPG) will be reviewed. NPG is a material with nanometer-scale porosity formed by selective dissolution of silver from silver/gold alloys. NPG has a huge surface area to volume ratio, and is chemically modifiable so as to change both its morphology and also the chemical reactivity of its surface. We will specifically address methods to create NPG with a hierarchy of pore sizes (i.e., large channels with porous sidewalls), methods to coat the surface of NPG with catalytically active nanoparticles, and applications for surface modified-NPG as fuel cell electrodes and sensor components.

## 10:10 AM Break

#### 10:25 AM Invited

Nanostructured Intermetallic Alloys - Annealing Behavior, Microstructural Control and Influence of Scale in Reversibly Ordering Systems: Jorg M.K. Wiezorek<sup>1</sup>; <sup>1</sup>University of Pittsburgh, Matls. Sci. & Engrg., 848 Benedum Hall, Pittsburgh, PA 15261 USA

The annealing behavior of intermetallics after cold-deformation represents an underdeveloped field of physical metallurgy. This research uses combinations of measurements by DSC, magnetometry and mechanical testing together with microstructural observations by SEM, TEM and XRD to study the annealing behavior of deformed binary intermetallics that undergo the ordering transformation in the solid state (reversibly ordering systems). The L1o- and L12-ordering Fe-Pd alloys used here are excellent model systems for many other intermetallics and offer attractive properties for permanent magnet applications. Furthermore, utilizing severe plastic deformation (SPD) processing bulk nanostructured Fe-Pd alloys will be fabricated, thereby enabling the systematic investigation of microstructural scale effects. The main goals of this effort are to: a) Develop physical mechanism based descriptions of the annealing behavior; b) Fabricate nanostructured bulk Fe-Pd alloys; c) Control alloy microstructures across the length scales; d) Determine processing-microstructure-property relationships for the Fe-Pd intermetallics. Thus, knowledge pertaining to this important area of physical metallurgy will be advanced.

10:55 AM Panel Discussion with R. Gibala, H. Fraser, S. Ankem and K. L. Murty

## Multiphase Phenomena in Materials Processing: Session I

Sponsored by: Extraction & Processing Division, Light Metals Division, Materials Processing and Manufacturing Division, EPD-Process Fundamentals Committee, MPMD/EPD-Process Modeling Analysis & Control Committee, MPMD-Solidification Committee Program Organizers: Ben Q. Li, Washington State University, School of Mechanical and Materials Engineering, Pullman, WA 99164-2920 USA; Stavros A. Argyropoulos, University of Toronto, Department of Materials Science and Engineering, Toronto, Ontario M5S 3E4 Canada; Christoph Beckermann, University of Iowa Department of Mechanical Engineering, Iowa City, IA 52242 USA; Bob Dax, Concurrent Technologies Corporation, Pittsburgh, PA 15219 USA; Hani Henein, University of Alberta, Edmonton, AB T6G 2G6 Canada; Adrian S. Sabau, Oak Ridge National Laboratory, MS-602, Oak Ridge, TN 37831-6083 USA; Brian G. Thomas, University of Illinois, Department of Mechanical and Industrial Engineering, Urbana, IL 61801 USA; Srinath Viswanathan, Sandia National Laboratories, Albuquerque, NM 87185-1134 USA

Wednesday AM	Room:	218B
March 17, 2004	Location	Charlotte Convention Center

Session Chairs: Ben Q. Li, Washington State University, Sch. of Mech. & Matls. Engrg., Pullman, WA 99164-2920 USA; Stavros A. Argyropoulos, University of Toronto, Dept. of Matls. Sci. & Engrg., Toronto, Ontario M5S 3E4 Canada

## 8:30 AM Invited

Application of an Online Iterative ECT Image Reconstruction Method in Multiphase Flow Measurement: Shi Liu<sup>1</sup>; Fan Jiang<sup>1</sup>; Haigang Wang<sup>1</sup>; <sup>1</sup>Chinese Academy of Sciences, Inst. of Engrg. Thermophysics, Beijing 100080 China

Electrical capacitance tomography (ECT) has been applied in imaging multiphase distributions since the 90's of the last century. The most widely used simplistic image reconstruction method, namely linear-back-projection (LBP), is fast (e.g 140 frames per second) but often produce unsatisfactory results. Therefore, enhanced image reconstruction methods, such as iterative methods, are required to improve the quality of the images. While iterative image reconstruction algorithms may produce improved tomographic images, they are timeconsuming and can be used off-line only, which is not a favourable feature for monitoring rapidly changing industrial processes. This paper describes the development of a new image reconstruction algorithm and its applications in gas-solid two phase flows. For the new algorithm, firstly a coefficient matrix is generated through an off-line iteration sequence. The matrix is then used for on-line image reconstruction, in the same way as a sensitivity map is used in the popular LBP algo rithm. This new algorithm can produce similar quality images to the Landweber iteration algorithm with a constant sensitivity map, but at the same speed as the LBP. An optimal step length has been incorporated into the new algorithm for improved convergence. The new algorithm was evaluated by both simulation and experiment. The new scheme has been applied to the online measurement of solids distribution in square circulating fluidized beds (CFBs), in gas-solids wavy flow in pipes, and in a cyclone gas-solids separator. From the measurement of solids distribution in CFBs in different flow regimes, the solids concentration profile, temporal variation of average solids concentration and frequency spectra are obtained. The results reveal noticeable solids fraction in the central region of the CFBs, which agrees with the nature of bubbling or turbulent fluidization in the bottom zone but could not be reconstructed by LBP. Meanwhile, closely distributed multiple voids (gas bubbles) are distinguished that is not pos sible for LBP. Solids concentrations in the conical part of a cyclone separator are also measured. The cross-correlation technique was combined with the solids concentration measurements to obtain the flow rate through the dip-leg of the cyclone. The same technique applied in a dense phase pneumatic transport pipe provides the solids concentration, and the flow rate of a wavy gas-solids flow. The capability of the online iterative ECT method in providing much improved instantaneous spatial and temporal information on two-phase flow is unique, and can be of great value in the study of multiphase processes. Also, the obtained data are valuable references for further studies.

#### 8:55 AM

Study on the Air Flow and Heat Transfer in Gravel Embankments in the Permafrost Areas Between Qinghai and Tibet: *Jiang Fan*<sup>1</sup>; <sup>1</sup>Chinese Academy of Sciences, Inst. of Engrg. Thermophysics, PO Box 2706, Beijing 100080 China

Winter-time natural convection in open-graded gravel embankments has been suggested as a technique which can be used to provide passive cooling and thereby avoid thaw-settlement of roadways located in permafrost areas. Heat transfer in open-graded gravel embankment is studied using numerical simulation, based on unsteady two-dimensional momentum and energy equations. Two different models, one being porous media model, the other gravels model in which the embankment is composed of stones and air, have been adopted to investigate the temperature and velocity fields in embankment. Simulation results show that in summer, a gentle clockwise rotation of the pore air extending throughout most of the embankment. The pore-air motion is very weak which results in relatively straight horizontal isotherm lines. And heat transfer is mainly maintained through conduction. Whereas in winter, pore-air velocities are higher and multiple vortexes are formed in the embankment. Natural convection then becomes the dominant influence on the isotherm shapes within the embankment. As a result of low ambient temperatures acting on the embankment surface during winter months, an unstable air density gradient develops within the embankment. This convection increases the heat flux out of the embankment. Therefore, the winter-time convection can lower the temperature of the foundation soil beneath the open-graded embankment. In addition, stones within the embankment with different dimensions have been analyzed and compared using the gravel model. It shows that in winter, Ö200mm stones lead to stronger vortexes in the embankment compared with that of Ö60mm stones. Consequently, the zone of low-temperature beneath the embankment is broadened.

#### 9:15 AM

A Two-Phase Flow Model for Particle-Gas Flows and Comparison with Experimental Measurements: W. Song<sup>1</sup>; Ben Li<sup>1</sup>; <sup>1</sup>Washington State University, Sch. of Mech. & Matls. Engrg., Pullman, WA 99164 USA

Many materials processing systems involve the gas-particle two phase flow phenomena. In this presentation, a two-phase flow model is developed for spouting gas-particle reactors used for chemical vapor deposition processes. A physical model is also developed and the results are compared with the numerical model predictions. The predictions of various gas-particle flow models such as gas-kinetic models, granular flow models and two phase Eulerian models are presented and their advantages and limitations in the gas-particle flow modeling are discussed in light of the comparison with the measurements taken on the physical model.

## 9:35 AM

**Optimization of Flow Modifiers in McGill Heat Pipes**: *Pietro Navarra*<sup>1</sup>; Hujun Zhao<sup>1</sup>; Frank Mucciardi<sup>1</sup>; <sup>1</sup>McGill University, Dept. of Mining, Metals & Matls. Engrg., 3610 Univ., Montreal, Quebec H3A 2B2 Canada

A heat pipe is a two-phase heat exchanger with a very high effective thermal conductivity. Such devices were developed extensively in the 1960's and have become standard heat extraction devices in many fields. The metallurgical industry has traditionally been beyond the operational range of these devices as the heat fluxes encountered are often above the critical heat flux, causing film boiling within conventional heat pipes. Recent research at McGill University has led to a new type of heat pipe capable of overcoming the film boiling limitation encountered at high heat fluxes. Several industrial-scale tests have proven the commercial viability of the new McGill Heat Pipe in applications such as oxygen lance injection, furnace equipment cooling and permanent mould casting. A heat pipe consists of three main components: a condenser and an evaporator section, and a working fluid contained within. Condenser design is somewhat trivial, whereas the evaporator section encompasses the key behind McGill Heat Pipes. The evaporator section contains a flow modifier which generates a centrifugal force that suppresses the formation of a vapour film at the wall/fluid interface during operation. Thus the "swirler" flow modifier is the key to extending the operational range of heat pipes in terms of maximum heat flux capability. This paper summarizes a study to model fluid flow within the evaporator section of McGill Heat Pipes and optimize the flow modifier design parameters to attain the maximum critical heat flux.

#### 9:55 AM Break

#### 10:10 AM

An Integrated Model for Microwave Heating of Ceramics and Dielectric Materials: Y. Huo<sup>1</sup>; Ben Q. Li<sup>1</sup>; Ravindra Akarapu<sup>1</sup>; J. Tang<sup>1</sup>; <sup>1</sup>Washington State University, Sch. of Mech. & Matls. Engrg., Pullman, WA 99164 USA

An integrated model is developed to represent the three-dimensional electromagnetic wave propagation and thermal phenomena during microwave heating of ceramics and dielectric/biological materials. The model development is based on the edge finite element formulation for electromagnetic fields and the node finite element formulation for thermal phenomena. Results are presented for both simple systems and complex real processes used for ceramic processing and biomaterials processing.

#### 10:30 AM

Undercooling and Demixing of Cu-Co Melts in the TEMPUS Facility During Parabolic Flight: *M. Kolbe*<sup>1</sup>; S. Reutzel<sup>2</sup>; A. Patti<sup>3</sup>; I. Egry<sup>1</sup>; L. Ratke<sup>1</sup>; D. M. Herlach<sup>1</sup>; <sup>1</sup>Institute of Space Simulation, German Aeros. Ctr., DLR, D-51170 Köln Germany; <sup>2</sup>Ruhr-University Bochum, Inst. of Experimental Physics IV, D-44780 Bochum Germany; <sup>3</sup>Royal Melbourne Institute of Technology, Melbourne Australia

Cu-Co has a metastable miscibility gap in the region of the undercooled melt. Undercooling of the melt below the binodal leads to separation of the melt into a Co-rich L1-phase and a Cu-rich L2phase. Experimentally, undercooling into the metastable miscibility gap can be realised by means of electromagnetic levitation (EML), processing in drop tube (DT) and by melt flux embedding. As undercooling is large in these experiments, the velocity of the solidification front is high and the microstructure is frozen in instantaneously. Samples have been undercooled and solidified in the TEMPUS-facility (containerless electromagnetic processing under weightlessness) during parabolic flight under reduced gravity conditions. Microstructures of solidified samples have been analysed and compared to those processed under terrestrial conditions. The influence of convection on phase growth is much less in the TEMPUS-facility than in terrestrial processing: The microstructure shows spherical droplets of the minority phase, statistically dispersed in the majority phase.

#### 10:50 AM

Effects of Magnetic Field and Internal Radiation on Flow and Solidification of Oxide Melts: Yan Shu<sup>1</sup>; Ben Q. Li<sup>1</sup>; Kelvin Lynn<sup>1</sup>; <sup>1</sup>Washington State University, Sch. of Mech. & Matls. Engrg., Pullman, WA 99164 USA

This paper discusses the effects of magnetic field and internal radiation on the melt flow and solidification morphology during solidification processing of oxide crystals for optoelectronic and remote sensing applications. The numerical solution of the integral differential equation characterizing the internal radiation and the magnetohydrodynamic equations describing the magnetic and transport phenomena is obtained by applying the combined discontinuous and continuous finite element method. The results show that both internal radiation and an externally applied magnetic field can have important effects on the melt flow and solidification behavior during the melt processing of oxide materials.

### 11:10 AM

Influence of an External Electric Field Applied During the Solution Heat Treatment of the Al-Mg-Si Alloy AA 6022: Kang Jung<sup>1</sup>; Hans Conrad<sup>1</sup>; <sup>1</sup>North Carolina State University, Matls. Sci. & Engrg. Dept., Raleigh, NC 27695-7907 USA

The effects of an external dc electric field E = 5 kV/cm applied during solution heat treatment (SHT) of AA 6022 on the resistivity r and hardness H following quenching were determined. Both r and H increased with E. The results are analyzed in terms of the influence of the field on the enthalpy deltaHs and entropy deltaSs of solution and the constants relating r and H to the concentration of Mg2Si in solution. Peculiarities of Phase Creating in the Ag-Fe-Graphite Compositions During Processing by Electric Current: O. I. Raychenko<sup>1</sup>; V. P. Popov<sup>1</sup>; O. V. Derev<sup>2</sup>yanko<sup>1</sup>; <sup>1</sup>IPMS, NAS of Ukraine

Two series of experiments with powder mixtures Ag-graphite and Ag-Fe-graphite were performed. Equipment for experiment was installation for electrodischarge sintering ERAN 2/1. The processing was carried out in moulds of the dense graphite and of the alloy on Ni-Cr basis. The objects of processing were 1)graphite powder cladded by Ag, and 2)cladded graphite powder-Fe. During processing the metal components in compositions were solid or melted. Behavior of melted metal happens under electromagnetic forces. Addition of Fe results in hardening.

## Nanostructured Materials for Biomedical Applications: Session V

Sponsored by: Electronic, Magnetic & Photonic Materials Division, EMPMD-Thin Films & Interfaces Committee Program Organizers: Roger J. Narayan, Georgia Tech, School of Materials Science and Engineering, Atlanta, GA 30332-0245 USA; J. Michael Rigsbee, North Carolina State University, Department of Materials Science and Engineering, Raleigh, NC 27695-7907 USA; Xinghang Zhang, Los Alamos National Laboratory, Los Alamos, NM 87545 USA

Wednesday AM	Room: 219A
March 17, 2004	Location: Charlotte Convention Center

*Session Chairs:* Xinghang Zhang, Los Alamos National Laboratory, Los Alamos, NM 87545 USA; Marc Meyers, University of California, Mech. & Aeros. Engrg., La Jolla, CA 92093-0411 USA

## 8:30 AM Invited

Nanostructured Calcium Phosphates: Opportunities and Challenges for Biomedical Applications: *Prashant Nagesh Kumta*<sup>1</sup>; Charles Sfeir<sup>2</sup>; Daiwon Choi<sup>1</sup>; Sarah Petricca<sup>1</sup>; <sup>1</sup>Carnegie Mellon University, Matls. Sci. & Engrg., 4309 Wean Hall, 5000 Forbes Ave., Pittsburgh, PA 15213 USA; <sup>2</sup>University of Pittsburgh, Dept. of Oral Medicine & Pathology, 574 Salk Hall, 3501 Terrace St., Pittsburgh, PA 15261-1964 USA

Nanotechnology is a revolutionary area that has impacted several areas of materials science. Since the discovery of apatite and their close structural similarity to natural bone, calcium phosphates (CaP) have become synonymous to natural bone. Hydroxyapatite (HA) is the most well-known CaP studied for biomedical applications. Engineering bone at a defective site is largely dependent on the material displaying favorable characteristics promoting growth of healthy osseous tissue. The higher reactivity of nano-sized materials has led to significant activity in the synthesis and design of nanostructured materials. Our research has focused in the development of novel chemical and mechanochemical strategies for synthesizing stoichiometric, nanostructured HA for a number of bone tissue engineering applications ranging from scaffolds to potential bone sensor as well as novel carriers of plasmid DNA for gene delivery. Results of these studies and the potential biomedical benefits and challenges of nanostructured HA will be presented.

## 9:15 AM Invited

A Novel Technique for Processing Functionally Graded HA Coatings: Afsaneh Rabiei<sup>1</sup>; <sup>1</sup>North Carolina State University, Mech. & Aeros. Engrg. & Biomed. Engrg. Depts., 2417 Broughton Hall, Campus Box 7910, Raleigh, NC 27695-7910 USA

A new generation of calcium phosphate coatings for dental implants, in which film crystallinity and structure is optimized, for enhanced bioactivity, osseointegration, and adhesion for promotion of the coating lifetime has been developed. The osseointegration provides mechanical stability to an implant in situ, minimizes motioninduced damage to surrounding tissues, and is imperative for the clinical success of bone implants. In this manner, the health relatedness of this project is to increase bonding between an implant and juxtaposed bone so that a patient who has received joint or dental replacement surgery may quickly return to a normal active lifestyle. Furthermore, the present study aimed to increase the service-life of an orthopedic material by creating materials that form a strong, long lasting, bond with juxtaposed bone. A functionally graded Hydroxyapatite coating with graded Crystallinity and grain size has been produced using Ion Beam Assisted Deposition with insitu heat treatment method. HA coating shows larger grain size and Crystallinity at the interface of the coating with the substrate. The Crystallinity and the grain size decreases towards the surface of the coating. Both early and long-term bone responses have been assessed in small rat models, both prior to and after prosthesis loading. The desire to introduce this innovative technology to the field of dental implantology is based on two primary advantages of the process over existing technology used to apply HA coatings to implants. First, the chemical composition, Crystallinity and grain size of the applied coating can be precisely controlled over a wide range of values, without the need for post deposition annealing. Second, the HA coatings can be deposited as thin films from 1 to 5µm thick, much thinner than coatings applied using plasma spray technology. Thinner coatings can provide a higher interfacial strength and better fracture resistance than thicker plasma spray coatings. Additionally, this processing technique is causing less residual stresses at the interface of the coating and the substrate that will lead to a better adhesion bonding.

## 10:00 AM Cancelled

Synthesis of Hydroxyapatite/Gelatin Nanocomposites for Orthopedic Applications and Their Properties

#### 10:45 AM Invited

Effects of Diamond Like Carbon Coating and Surface Treatment on Bioactivity of Ti-6%Al-4%V: Janet Hamipikian<sup>1</sup>; S. N. Dunham<sup>1</sup>; J. L. McKillip<sup>1</sup>; B. F. Bell<sup>1</sup>; D. Scholvin<sup>1</sup>; J. Hampikian<sup>1</sup>; Roger J. Narayan<sup>1</sup>; <sup>1</sup>Georgia Institute of Technology, Sch. of Matls. Sci. & Engrg., Atlanta, GA 30332-0245 USA

In recent years there has been a growing need for biomedical implants with excellent surface properties. Titanium alloys have been of particular interest due to their high strength, wear resistance, and biocompatibility. Several surface treatments of Ti-6%Al-4%V alloy are presented in this work. These coatings have been characterized using SEM, XRD, Raman spectroscopy, and simulated body fluid studies.

## 11:30 AM Plenary

Nanostructured Materials for Orthopaedic/Dental Applications: Rena Bizios<sup>1</sup>; R. W. Siegel<sup>2</sup>; P. M. Ajayan<sup>2</sup>; L. S. Schadler<sup>2</sup>; <sup>1</sup>Rensselaer Polytechnic Institute, Dept. of Biomed. Engrg., 110 8th St., Troy, NY 12180-3590 USA; <sup>2</sup>Rensselaer Polytechnic Institute, Depts. of Matls. Sci. & Engrg., & Rensselaer Nanotech. Ctr., Troy, NY 12180-3590 USA

New tissue formation in vitro and in vivo can be enhanced by biomaterials designed with properties similar to those of physiological bone, which is characterized by ceramic grains in the nanometer range connected by polymer. It is now possible to design and formulate nanostructured ceramic/polymer composites, which exhibit improved cytocompatibility and mechanical behavior that simulate those properties of natural bone. Nanoceramics (specifically, alumina, titania, and hydroxylapatite), composites of these nanoceramics with polymers (specifically, poly(L-lactic) acid and poly(methylmethacrylate)), as well as composites of poly(L-lactic) acid and carbon nanotubes were evaluated using cellular in vitro models. The results provide evidence that, compared to pure ceramics, nanoceramic composites exhibit improved mechanical properties and that carbon-nanotube containing composites can be successfully used to expose osteoblasts (the boneforming cells) to electrical stimulation. The most significant result, however, was that all of the nanostructured materials tested promote osteoblast functions pertinent to new bone formation. Thus, nanostructured materials can promote osseointegration, a critical requirement for the clinical success of orthopaedic/dental implants in vivo. This research exemplifies alternative strategies and novel approaches that, although extremely promising, remain as yet unexplored for bone regeneration purposes and in tissue engineering applications. This work was supported by Philip Morris USA and the Nanoscale Science and Engineering Initiative of the National Science Foundation under NSF Award No. DMR-D117792.

## Phase Stability, Phase Transformation, and Reactive Phase Formation in Electronic Materials III: Session V

Sponsored by: Electronic, Magnetic & Photonic Materials Division, Structural Materials Division, EMPMD/SMD-Alloy Phases Committee

Program Organizers: C. Robert Kao, National Central University, Department of Chemical and Materials Engineering, Chungli City 32054 Taiwan; Sinn-Wen Chen, National Tsing-Hua University, Department of Chemical Engineering, Hsinchu 300 Taiwan; Hyuck Mo Lee, Korea Advanced Institute of Science & Technology, Department of Materials Science & Engineering, Taejon 305-701 Korea; Suzanne E. Mohney, Pennsylvania State University, Department of Materials Science & Engineering, University Park, PA 16802 USA; Michael R. Notis, Lehigh University, Department of Materials Science and Engineering, Bethlehem, PA 18015 USA; Douglas J. Swenson, Michigan Technological University, Department of Materials Science & Engineering, Houghton, MI 49931 USA

Wednesday AM	Room: 2	214		
March 17, 2004	Location:	Charlotte	Convention	Center

Session Chairs: Sinn-Wen Chen, National Tsing-Hua University, Dept. of Chem. Engrg., Hsin-chu 300 Taiwan; Eric J. Cotts, Binghamton University, Dept. of Physics & Matls. Sci., Binghamton, NY 13902 USA

#### 8:30 AM Invited

**Evolution of the Microstructure of Pb Free Solder Joints**: *Eric J. Cotts*<sup>1</sup>; Lawrence P. Lehman<sup>1</sup>; Lubov Zavalij<sup>1</sup>; Robert Kinyanjui<sup>1</sup>; <sup>1</sup>Binghamton University, Physics & Matls. Sci., Sci. 2, Vestal Pkwy. E., PO Box 6000, Binghamton, NY 13902 USA

A study of how the adoption of Pb-free solders affects manufacturing processes for electronics packages is in progress. Focus is on issues affecting the mechanical properties of solder joints, to facilitate the development of reliability models. The composition and microstructure of solder joints are characterized as a function of solder joint metallurgy and heat treatment, including reflow schedule and subsequent annealing treatments. Solder joints are constructed in ball-onsubstrate geometries, annealed either in a calorimeter or by standard reflow techniques. The evolution of the microstructure of solder joints is determined by optical microscopy and scanning electron microscopy. We characterize grain and precipitate sizes and orientations as a function of cooling rate and composition. Our goal is to characterize the effect of thermal anneals and associated microstructures on joint reliabilities. Support from the National Science Foundation, DM0218129 is gratefully acknowledged.

#### 8:50 AM Invited

Effects of Phosphorus Content on the Phase Transformation and Stress Evolution During the Reaction Between Electroless Ni(P) and Sn Film: J. Y. Song<sup>1</sup>; Y. C. Sohn<sup>1</sup>; Jin Yu<sup>1</sup>; <sup>1</sup>KAIST, Ctr. for Elect. Pkgg. Matls., MS&E, 373-1 Guseong-dong, Yuseong-gu, Daejeon 305-701 Korea

Electroless Ni(P) has been widely used as under bump metallization (UBM) for low cost flip chip technology because of its merits such as maskless process and slow reaction rate, etc. In this study, the reactions between electroless Ni(P) and Sn film were investigated by varying phosphorous content (low, medium and high) in the Ni(P) film. The phase transformation of the Ni(P) film during the reactions was examined by thermal analysis using differential scanning calorimetry. Also, the intrinsic stress evolutions, which accompanied the amorphous-crystalline phase transformation and the intermetallic compound (IMC) formation between Ni(P) and Sn, were investigated by conducting the isochronic and isothermal heat treatment and measuring the curvature change of the Si substrate. Results indicate that: 1) solder reaction facilitated phase transformation of Ni(P) into Ni3P and Ni by reducing the transformation temperature and released heat, 2) isochronic thermal cycling tests showed that formation of Ni3Sn4 and Ni3P out of Ni(P) and Sn films produced tensile stresses for the high P content films, but compressive stresses for the low P content films, 3) stress evolution caused by IMC formation was larger than that produced by Ni(P) crystallization, 4) thick and dense Ni3Sn4 compound with strong (111) texture formed on nanocrystalline Ni(low P) compared to that formed on amorphous Ni(high P).

#### 9:10 AM Invited

The Effects of Bath Composition on the Morphologies of Electroless Nickel UBM on Al I/O Pad: Jae-Ho Lee<sup>1</sup>; Jinsoo Bae<sup>1</sup>; Ingun Lee<sup>2</sup>; Tak Kang<sup>2</sup>; Namseog Kim<sup>3</sup>; Seyong Oh<sup>3</sup>; <sup>1</sup>Hong-Ik University, Dept. of Met. Engrg. & Matl. Sci.; <sup>2</sup>Seoul National University, Div. of Matls. Sci.; <sup>3</sup>Samsung Electronics Co., Div. of Pkg. Dlvp.

For the flip chip packaging, the interests on UBM have been increased. Even though lead free solder bumps were obtained successfully, the failure in flip chip could be occurred on the interface of pad and bump if the interphacial regions were not well prepared. The adhesion of nickel on aluminum pad is very important in reliability of bump. The electroless nickel plating on zincated aluminum pad was investigated. The nickel deposition rate with bath composition and operating conditions were measured. The surface morphlogies of electroless plated nickel were influenced by the nature of zinc on aluminum. The deposition potential with time was also observed.

#### 9:30 AM

Phase Equilibria of the Ag-Sn-Cu-Ni Quaternary System at the Sn-Rich Corner: Sinn-wen Chen<sup>1</sup>; Cheng-An Chang<sup>1</sup>; <sup>1</sup>National Tsing-Hua University, Chem. Engrg. Dept., #101, Sec. 2, Kuang-Fu Rd., Hsin-Chu, Taiwan 300 Taiwan

Knowledge of phase equilibria of the Sn-Ag-Cu-Ni quaternary system at the Sn-rich corner is important for the understanding of the interfacial reactions at the Sn-Ag-Cu/Ni contacts which are frequently encountered in the recent microelectronic products. Various Sn-Ag-Cu-Ni alloys were prepared and equilibrated at 250°C. The alloys were then quenched and analyzed. The existed phases were determined both by metallography and compositional analysis. No quaternary phases were found. The phase equilibrium relationship was proposed from the experimental results and the 250°C isothermal sections of the three constituent ternary phases, Sn-Ag-Cu, Sn-Ag-Ni, and Sn-Cu-Ni. Since there are no ternary phases in all these three systems, all the compounds are in fact binary compounds with various solubilities of the other two elements.

#### 9:45 AM

Phase Stability of Sn-Cu Intermetallic Compounds Upon Current Stressing: Ching Jung Yang<sup>1</sup>; Ying Chao Hsu<sup>1</sup>; Chia Hui Lin<sup>1</sup>; Chih Chen<sup>1</sup>; <sup>1</sup>National Chiao Tung University, Dept. of Matls. Sci. & Engrg., 1001 Ta Hsueh Rd., Hsinchu Taiwan

The evolution of Sn-Cu intermetallic compound (IMC) within the eutectic SnPb solder was studied under the current density of  $1.0 - 10^{4}$  A/cm<sup>2</sup> in the temperature range from room temperature to 100°. The measurement of growth rate and grain size change of IMC indicated the dependence on temperature effect, current density, and electric polarity. The contribution of electromigration to the microstructure change of IMC is emphasized in our study.

#### 10:00 AM

Effect of Intermetallic Compound Formation on Electrical Properties of Cu/Sn Interfaces During Thermal Treatment: Chien-Neng Liao<sup>1</sup>; Chung-Ting Wei<sup>1</sup>; <sup>1</sup>National Tsing Hua University, Matls. Sci. & Engrg., 101, Kuang Fu Rd., Sec. 2, Hsinchu 300 Taiwan

The influence of intermetallic compound (IMC) formation on electrical properties of Cu/Sn interfaces is investigated using an in-situ electrical probing method. A Cu/Sn bilayer thin film was deposited on thermally oxidized silicon wafers using a sputtering and thermal evaporation method, respectively. The resistance of the bimetallic films was measured while heating the specimen at a fixed ramping rate from 25°C to 225°C. It is found that the resistance change of the specimen depends on the formation of Cu6Sn5 and Cu3Sn phases during thermal treatment. The activation energy of Cu-Sn IMC formation is found to be 1.1 eV. The micro-structural and compositional evolution of the Cu/Sn thin film couple was studied by Rutherford Backscattering Spectrometry, x-ray diffraction, scanning electron microscopy, secondary ion mass spectrometer, respectively. In addition, a lithographicallypatterned structure is also fabricated to investigate the reactions of solder/UBM thin films during electrical stressing.

## 10:15 AM Break

#### 10:30 AM Invited

Interaction of Ag-In-Sn Solders with Pd Contacts: A Phase Diagram Approach: *Herbert Ipser*<sup>1</sup>; Jan Vrestal<sup>2</sup>; Ales Kroupa<sup>3</sup>; <sup>1</sup>University of Vienna, Inst. f. Anorganische Chemie, Waehringerstr. 42, Wien A-1090 Austria; <sup>2</sup>Masaryk University, Fac. of Scis. - Dept. of Theorical & Phys. Chmst., Kotlárská 2, Brno CZ-61137 Czech Republic; <sup>3</sup>Czech Academy of Sciences, Inst. of Physics of Matls., Zizkova 2, Brno CZ-61662 Czech Republic

The use of lead-containing solders will be ruled out within the European Union by July 1, 2006. Currently, Sn-Ag and Sn-Ag-Cu are

the leading candidates as lead-free solder materials, however, it will be of interest to search for alternative materials. One possible solution at least for special applications - could be Sn-Ag-In alloys where the melting temperature can be tailored over a considerable range by varying the composition. In order to understand the interaction of such Sn-Ag-In solders with contacts containing Pd, the quaternary phase diagram Ag-In-Pd-Sn should be well known, at least in the part rich in In and Sn. As a first step toward this goal, the ternary systems In-Pd-Sn and Ag-In-Pd were investigated by means of X-ray diffraction (XRD), electron probe microanalysis (EPMA), and differential thermal analysis (DTA). The corresponding experimental results, together with all available thermodynamic information from literature, were used as input data for CALPHAD-type optimizations.

### 10:50 AM Invited

Formation and Characterization of SnBi and Bi Coated Solder Alloy: Jae-sik Lee<sup>1</sup>; Woong-ho Bang<sup>2</sup>; *Jae-Pil Jung*<sup>1</sup>; Kyu-hwan Oh<sup>2</sup>; Norman Zhou<sup>3</sup>; <sup>1</sup>University of Seoul, Matls. Sci. & Engrg., Seoul Korea; <sup>2</sup>Seoul National University, Matls. Sci. & Engrg., Seoul Korea; <sup>3</sup>University of Waterloo, Mech. Engrg., Waterloo, Ontario Canada

Electroplating method was used to form SnBi and Bi coated solder alloy. To produce a uniformed SiBi alloy, applied current density, bath temperature and stirring rate were carefully controlled. The compositions of plated SiBi layer was investigated by EPMA. Soldered Samples were tested to evaluate Microstructures and characteristics of intermetallic compounds. Test temperatures were 200C, 220C, and 250C. Further investigation by EPMA area mapping to study Bi distribution on the intermetallic compounds and inner solder, which affects mechanical and thermal property of Solder, was performed after soldered at 220C. According to SEM observation, coated solder at 2 and 4A/ dm2 showed intermetallic compounds developed well on the interface of Cu plate at 200C, due to abundant Bi amount in the plated solder where forming transient liquid phase bonding. Bi was not observed on the intermetallic compounds and inner solder, and it implies that the solder was homogenized after soldering.

#### 11:10 AM

A Study of Eutectic Sn-Pb Solder Wetting Behavior on Cu Strips Under Thermal Stressing: Chien-Neng Liao<sup>1</sup>; Wen-Tai Chen<sup>1</sup>; <sup>1</sup>National Tsing Hua University, Matls. Sci. & Engrg., 101, Kuang Fu Rd., Sec. 2, Hsinchu 300, Taiwan China

The wetting reaction between the eutectic Sn-Pb solder and copper metallization has been an important topic owing to academic and industrial research interests. In this study we will investigate the wetting behavior of eutectic Sn-Pb solder on a patterned Cu strip that is subjected to a thermal gradient. The non-uniform temperature distribution on the Cu strip is generated by applying an electric current through a fractional segment of the Cu strip. The preliminary results show that the capillary flow direction and moving distance of the eutectic solder depend on the geometry of the Cu strip and can be modulated by the electric current applied. The details of the testing structure and experimental results will be presented in this paper. The "thermo-migration" phenomenon of solder on Cu metallization will also be discussed.

## Phase Transformations and Deformation in Magnesium Alloys: Creep Deformation

Sponsored by: Materials Processing and Manufacturing Division, MPMD-Phase Transformations Committee-(Jt. ASM-MSCTS) Program Organizer: Jian-Feng Nie, Monash University, School of Physics and Materials Engineering, Victoria 3800 Australia

Wednesday AM	Room: 2	205
March 17, 2004	Location:	Charlotte Convention Center

Session Chairs: Barry Mordike, Technical University of Clausthal, Inst. of Matls. Engrg. & Tech. Germany; Wolfgang Blum, Universität Erlangen-Nürnberg, Inst. f. Werkstoffwissenschaften, Erlangen 91058 Germany

## 8:30 AM Invited

Creep Deformation Mechanisms in High Pressure Die Cast Magnesium Alloys: *Wolfgang Blum*<sup>1</sup>; Yujiao Li<sup>1</sup>; Xiaohui Zeng<sup>1</sup>; Berthold von Grossmann<sup>2</sup>; Christoph Haberling<sup>2</sup>; H.-G. Haldenwanger<sup>2</sup>; <sup>1</sup>University Erlangen-Nurnberg, Inst. f. Werkstoffwissenschaften, Martensstr. 5, Erlangen 91058 Germany; <sup>2</sup>Audi AG, Abt. I/EG-34, Ingolstadt 85045 Germany Creep is described as an integral part of plasticity in terms of stressstrain rate-strain relations. Creep tests yield information on yield stress, work hardening, maximum deformation resistance (minimum creep rate) and work softening. Testing in compression avoids influences by fracture. Data on the new creep resistant alloy AJ52 (5Al, 2Sr) in the temperature range between 100 and 200°C are presented. Comparison with AZ91 and AS21 demonstrates that AJ52 has the highest creep resistance among the three. Electron microscopy shows that the microstructures of die cast Mg-Al-alloys consist of fine grains with a mantle containing large intermetallic precipitates. Dislocation structure evolution is different in both regions with stronger tendency to subgrain formation in the mantle. The difference in creep resistance are discussed in terms of differences in strength and stability of the intermetallic phases.

#### 9:05 AM Invited

The Role of Precipitates for the Creep Behavior of Magnesium Die-Cast Alloys: Oliver Kraft<sup>1</sup>; Michael Vogel<sup>2</sup>; Eduard Arzt<sup>3</sup>; <sup>1</sup>Forschungszentrum Karlsruhe, Inst. fuer Materialforschung II, Postfach 3640, Karlsruhe 76021 Germany; <sup>2</sup>SiCrystal AG, Paul-Gossen-Str. 100, Erlangen 91052 Germany; <sup>3</sup>Max-Planck-Institut fuer Metallfoschung, Heisenbergstr. 3, Stuttgart 70569 Germany

Microstructure and creep behavior of ZA85 and two alloy modifications with 0.3 and 0.9 wt.% Ca (ZACa8503 and ZACa8509) were investigated in die-cast and annealed conditions. In general, it was found that the addition of Ca leads to a more creep resistant material. High temperature dislocation creep controls the deformation at low stresses as well as high stresses in all conditions. Further, the creep behavior is dominated by the formation and coarsening of  $\tau$ -phase precipitates near grain boundaries. It will be shown that the creep behavior of all alloys and conditions can be described phenomenologically by a threshold concept for creep deformation. It is argued that the addition of Ca increases the threshold leading to the increased creep resistance. However, for long-term applications at elevated temperatures, our experiments highlight the role of microstructural stability for the creep deformation of Mg die-cast alloys as the precipitates will coarsen and the threshold is no longer effective.

## 9:40 AM Invited

On the Creep Resistance of Magnesium Die Casting Alloys: *Qingyou Han*<sup>1</sup>; Bimal K. Kad<sup>2</sup>; Srinath Viswanathan<sup>3</sup>; <sup>1</sup>Oak Ridge National Laboratory, Metals & Ceram. Div., One Bethel Valley Rd., PO Box 2008, Oak Ridge, TN 37831-6083 USA; <sup>2</sup>University of California, Dept. of Structural Engrg., 409 Univ. Ctr., La Jolla, CA 92093-0085 USA; <sup>3</sup>Sandia National Laboratories, MS 1134, Org. 1835, PO Box 5800, Albuquerque, NM 87185-1134 USA

The microstructure of die cast magnesium alloys is highly nonuniform, which leads to a non-uniform distribution of the solidus/ homologous temperature in the  $\alpha(Mg)$  phase and a non-uniform distribution of stress in the specimen during creep testing. As a result, the creep deformation in the specimen is also non-uniform. More creep deformation occurs in the  $\alpha(Mg)$  phase in and adjacent to the eutectic regions than that in the primary  $\alpha(Mg)$  dendrites. This article addresses the effect of the non-uniformity in the microstructure on the creep resistance of die cast magnesium alloys. Computational thermodynamic simulations were carried out to determine solute segregation, solidus temperature, and the corresponding homologous temperature distribution in the  $\alpha(Mg)$  phase. Transmission electron microscopy (TEM) studies provided evidence of non-uniform creep deformation in the creep tested specimens. The results suggest that the creep resistance of magnesium alloys is determined by the weakest phase in the alloy, viz., the  $\alpha(Mg)$  phase in and adjacent to the eutectic regions. Factors that increase the homologous temperature or reinforce the eutectic  $\alpha(Mg)$  phase increase the creep resistance of the magnesium alloys.

## 10:15 AM Break

## 10:30 AM Invited

Mechanisms of Creep Deformation in Mg-Sc Based Alloys: *Barry Mordike*<sup>1</sup>; I. Stulíková<sup>2</sup>; B. Smola<sup>2</sup>; <sup>1</sup>Technical University, Clausthal, Inst. of Matls. Engrg. & Tech. Germany; <sup>2</sup>Charles University, Faculty of Math. & Physics Czech Republic

Binary Mg-Sc alloys exhibit only poor age hardening due to the low diffusivity of Sc in Mg and consequently are less resistant to creep than the WE alloys. A small addition of Manganese (< 1.5 wt. %) improves the creep behaviour significantly. The minimum creep rates are up to two orders of magnitude lower than those of commercially available WE alloys at temperatures over 300°C. This is due to the finely dispersed Mn<sub>2</sub>Sc phase in the form of discs on the basal plane, which are very effective obstacles in restricting creep. At these temperatures, this implies restricting cross slip of basal dislocations and non

basal slip. The addition of Ce improves the creep resistance even further due to the effect of a grain boundary eutectic. The effect of the  $Mn_2Sc$  discs is observed also in alloys with a low content of Sc (~ 1 wt. %) and the addition of a rare earth element (Gd, Y, Ce ~ 4 wt. %). Very thin hexagonal plates containing the rare earth and Mn and also parallel to the basal plane of the Mg matrix strengthen the effect of  $Mn_2Sc$ precipitates at elevated temperatures (~ 250°C). A triangular arrangement of prismatic plates of metastable or stable phases of Mg-rare earth systems controls effectively the movement of basal dislocations during creep of these alloys at elevated or high temperatures. The combined control of basal slip, cross slip of basal dislocations and of non basal slip in these alloys ensures the minimum creep rates of one order of magnitude lower than those in WE alloys both at elevated and high temperatures.

## 11:05 AM Cancelled

Recent Studies of Diffusional Creep in Magnesium Alloys and Other Materials

#### 11:40 AM Invited

Creep Behavior and Deformation Substructure of Mg-Y and Mg-Y-Zn Alloys: Mayumi Suzuki<sup>1</sup>; Tsuyoshi Kimura<sup>2</sup>; Noritsugu Nakamura<sup>1</sup>; Jun-ichi Koike<sup>1</sup>; Kouichi Maruyama<sup>1</sup>; <sup>1</sup>Tohoku University, Grad. Sch. of Environmental Studies, Ecomatl. Design & Proc. Engrg. Course, 02 Aobayama, Aoba-Ku, Sendai, Miyagi 980-8579 Japan; <sup>2</sup>Tohoku University, Grad. Sch. of Engrg., Matls. Sci., 02 Aobayama, Aoba-Ku, Sendai, Miyagi 980-8579 Japan

Compressive creep behavior of Mg-Y and Mg-Y-Zn alloys was investigated at 550K to 650K. Deformation substructures have been observed by using TEM. Creep strength of Mg-Y alloys is significantly higher than other Mg based alloys. Furthermore, Creep rate of Mg-Y alloys decreased to 1/10 by the addition of zinc.High activation energy for creep was observed in Mg-Y and Mg-Y-Zn alloys even in dilute solid solution range. In microstructural observation, the activation of non-basal slip of a-dislocations was observed in Mg-Y alloys. In Mg-Y-Zn alloys, a high density of planar fault was observed on (0001) matrix planes, which suppress the non-basal slip of a-dislocations. Furthermore, many extended a-dislocations on basal planes were observed due to the decrease of the stacking fault energy. The simultaneous addition of yttrium and zinc can reduce the content of expensive yttrium without losing creep strength.

## Roytburd Symposium on Polydomain Structures: Elastic Domains in Structural Materials

Sponsored by: TMS, MPMD-Phase Transformations Committee-(Jt. ASM-MSCTS)

*Program Organizers:* Julia Slutsker, National Institute of Standards and Technology, CTCMS, Gaithersburg, MD 20899 USA; Greg B. Olson, Northwestern University, Department of Materials Science and Engineering, Evanston, IL 60208 USA

Wednesday AM	Room: 21	16A
March 17, 2004	Location:	Charlotte Convention Center

Session Chairs: Greg B. Olson, Northwestern University, Dept. of Matls. Sci. & Engrg., Evanston, IL 60208 USA; Julia Slutsker, National Institute of Standards and Technology, CTCMS, Gaithersburg, MD 20899 USA

#### 8:30 AM Invited

From "Old" Martensite to Engineering of Polydomain Nanostructures: Alexander L. Roytburd<sup>1</sup>; <sup>1</sup>University of Maryland, Matls. & Nucl. Engrg., College Park, MD 20742 USA

The talk focuses on developing a new approach for materials engineering: using mescoscopic design of composites with transformable components to control self-assembling micro- and nano-structures arising during structure phase transformations. Such self-assembling polydomain structures are natural products of phase transformations in solids. The trend to minimize the energy of long-range elastic interactions leads to the formation of self-organized arrangements of domains of different phases or differently oriented domains of the same phases (twins). Transformations in bulk materials usually result in the formation of complex irregular polydomain structures that are difficult to control. In contrast, it is possible to obtain a completely controlled structure in a single crystalline film through constraint. The constraint can be imposed by embedding transformable materials in a composite architecture. Thus, the combination of engineered mesostructures and self-organized micro- and nano- polydomain structures presents broad opportunities to design new materials with wellcontrolled structures.

## 9:05 AM Invited

Combining Thermodynamics, Elasticity, Interfaces and Kinetics for Interpreting the Evolution of Microstructures and the Materials Properties Which Result: John W. Cahn<sup>1</sup>; <sup>1</sup>NIST, MESL, Gaithersburg, MD 20899-8555 USA

For the inquisitive and thoughtful materials theorist we honor today, microstructures and their evolution have displayed an amazingly rich variety of interesting phenomena. Phase diagrams provide only a partial explanation of what is seen. The free energies that form the basis of the phase diagrams greatly extend the predictive power of thermodynamics, especially if these energies are augmented with those due to the induced stresses and interfaces that form en route. Concepts of local and coherent equilibrium, polydomain and other energy-minimizing structures all have developed from careful observation and thought. The introduction of kinetics consistent with this richly augmented thermodynamics has provided an expanding basis for understanding and predicting microstructural processes and new properties in materials as diverse as steels, magnetic alloys, ferro-electrics, and thin films. The progress over the last 40 years has been astonishing, but much remains to be done.

## 9:40 AM Invited

Self-Assembling of Structural Domains in Phase Transformations: Armen G. Khachaturyan<sup>1</sup>; Yongmei M. Jin<sup>1</sup>; Yu U. Wang<sup>1</sup>; Dwight Viehland<sup>2</sup>; Jie-Fang Li<sup>2</sup>; <sup>1</sup>Rutgers University, Ceram. & Matls. Engrg., 607 Taylor Rd., Piscataway, NJ 08854 USA; <sup>2</sup>Virginia Polytechnic Institute and State University, Matls. Sci. & Engrg., 201 Holden Hall (0237), Blacksburg, VA 24061 USA

Given the similarity of stress-induced interaction with dipole-dipole interaction, the coherent phase transformations producing crystallographically equivalent orientation variants form domain structure similar to those of ferromagnetic and ferroelectrics. 3D simulations using Phase Field Microelasticity were performed for the domain structures formed in single-crystals, polycrystals, and thin films. Since the domain size is proportional to the square root of the domain wall energy, a drastic reduction of this energy results in domain miniaturization to nano- or subnano-scale and formation of a mixed adaptive state that usual diffraction methods see as a homogeneous phase with a microdomain-averaged lattice. This phase has special property - the high adaptivity provided by a high mobility of the low energy domain walls and the multivariant character of the polydomain structure. If the transformation is ferroelectric, it is an adaptive ferroelectric. Evidence of a ferroelectric adaptive phase in PMN-PT near the morphotropic boundary will be presented.

## 10:15 AM Break

### 10:30 AM Invited

**Coherent Phase Equilibria in Ag-Au-Cu Nanoparticles**: *Will-iam C. Johnson*<sup>1</sup>; James M. Howe<sup>1</sup>; Jooyoul Huh<sup>2</sup>; <sup>1</sup>University of Virginia, Dept. of Matls. Sci. & Engrg., PO Box 400745, Charlottesville, VA 22904-4745 USA; <sup>2</sup>Korea University, Dept. of Matls. Sci. & Engrg., 5-1, Anam-Dong, Seoul, Sungbuk-Ku 136-701 Korea

Professor Roytburd has made many contributions to our understanding of solid-state phase transformations. Of particular interest to us is his clarification of the interplay between compositional strain, misfit strain, and imposed geometrical constraints on the characteristics of phase equilibria in coherent systems. Here, we extend his work to consider the effect of particle size on coherent phase equilibria in small (10-50 nm diameter) Au-Cu-Ag nanoparticles. Transmission electron microscopy observations showing the presence of an L1\_2 ordered phase in the nanoparticles at temperatures more than 250K above the bulk ordering temperature are investigated by considering the influence of surface stress on phase equilibria. This work is supported by the U.S. National Science Foundation.

#### 11:05 AM Invited

Engineering of Elastic Domain Structures in Constrained Layers: Julia Slutsker<sup>2</sup>; Andrei Artemev<sup>1</sup>; Alexander L. Roytburd<sup>3</sup>; <sup>1</sup>Carleton University, Mech. & Aeros. Engrg., 1125 Colonel By Dr., Ottawa, ON K1S 5B6 Canada; <sup>2</sup>NIST, Gaithersburg, MD 20899 USA; <sup>3</sup>University of Maryland, Matls. Sci. & Engrg., College Park, MD 20742 USA

The formation and evolution of polydomain microstructure under external stress in the constrained layer are investigated by phase-field simulation. The reversible superelastic deformation of two-phase austenite/martensite mixture has been modeled as well as superplastic deformation of martensite polydomain structure.

## Solidification of Aluminum Alloys: Solidification Cracking/Mechanical Properties

Sponsored by: Materials Processing & Manufacturing Division, MPMD-Solidification Committee

*Program Organizers:* Men Glenn Chu, Alcoa Inc., Alcoa Technical Center, Alcoa Center, PA 15069 USA; Douglas A. Granger, GRAS, Inc., Murrysville, PA 15668-1332 USA; Qingyou Han, Oak Ridge National Laboratory, Oak Ridge, TN 37831-6083 USA

Wednesday AM	Room: 2	07B/C		
March 17, 2004	Location:	Charlotte	Convention	Center

Session Chairs: David R. Poirier, University of Arizona, Matls. Sci. & Engrg., Tucson, AZ 85721 USA; Men G. Chu, Alcoa Inc., Alcoa Technical Center, Alcoa Ctr., PA 10569 USA

## 8:30 AM Keynote

How Does Coalescence of Dendrite Arms or Grains Influence Hot Tearing?: *M. Rappaz*<sup>1</sup>; V. Mathier<sup>1</sup>; P.-D. Grasso<sup>1</sup>; J.-M. Drezet<sup>1</sup>; A. Jacot<sup>1</sup>; <sup>1</sup>EPFL, Inst. of Matls., Computational Matls. Lab., MXG, Lausanne CH-1015 Switzerland

Hot tearing, a severe defect occurring during solidification, is the conjunction of tensile stresses that are transmitted to the mushy zone by the coherent solid underneath and of an insufficient liquid feeding to compensate for the volumetric change. In most recent hot tearing criteria, one of the critical issues is the definition of a coherency point which, in low-concentration alloys, corresponds to the bridging or coalescence of the primary phase. A coalescence model has been developed recently using the concept of the disruptive pressure in thin liquid films.1 It has been shown that large-misorientation grain boundaries, which are characterized by an interfacial energy,  $\gamma_{sh}$ , larger than twice the solid-liquid interfacial energy,  $\gamma_{sl}$ , solidify at an undercooling  $\Delta T_b$  =  $(\gamma_{gb} - 2\gamma_{sl})/(\Delta s_f \delta)$ , where  $\Delta s_f$  is the entropy of fusion and  $\delta$  the thickness of the diffuse interface. When  $\gamma_{gb} < 2\gamma_{sl}$  (e.g., weak-misoriented grain boundaries), dendrite arms coalesce as soon as they impinge on each other. Using such concepts and a back-diffusion model, the percolation of equiaxed, randomly oriented grains has been studied in 2D: it is shown that the grain structure gradually evolves from isolated grains separated by a continuous interdendritic liquid film, to a fully coherent solid with a few remaining wet boundaries. The implication of such findings for the hot cracking tendency of aluminum alloys will be discussed. <sup>1</sup>M. Rappaz, A. Jacot and W. J. Boettinger, Last stage solidification of alloys: a theoretical study of dendrite arm and grain coalescence. Met. Mater. Trans. 34A (2003) 467-79.

## 9:00 AM

A New Two-Phase Thermo-Mechanical Model and its Application to the Study of Hot Tearing Formation During the Start-Up Phase of DC Cast Ingots: M. M'Hamdi<sup>1</sup>; H. G. Fjær<sup>2</sup>; A. Mo<sup>1</sup>; D. Mortensen<sup>2</sup>; S. Benum<sup>3</sup>; <sup>1</sup>SINTEF Materials Technology, PB 124 Blindern, N-0314 Oslo Norway; <sup>2</sup>Institute for Energy Technology, PB 40, N-2007 Kjeller, Oslo Norway; <sup>3</sup>Hydro Aluminium, N-6600 Sunndalsøra Norway

The purpose of this work is to present a new 2D two-phase simulator, TearSim, for the prediction of hot tearing formation in DC casting of aluminum ingots. In this model, the main mechanisms for the formation of hot tears during solidification, namely too severe thermally-induced deformations, and the lack of liquid feeding to compensate for solidification shrinkage and viscoplastic volumetric dilatation, are addressed simultaneously. In the modelling, the liquid flow, the stresses and the strains in the two-phase mushy zone are calculated using an advanced model for the viscoplastic deformation of the semisolid material. In the present article, the modeling equations are solved numerically for the direct-chill casting of axi-symmetric aluminum extrusion ingot. In order to study the effect of the casting speed on the formation of center hot-cracks, new hot tearing criteria based on the mechanical quantities resulting from the simulations are compared to experimental results from casting trials with varying the casting speed ramping during the casting process.

## 9:20 AM

The Influence of Hydrogen on the Hot Tearing Susceptibility of Aluminium-Silicon Alloys: *Russell S. Barnett*<sup>1</sup>; John A. Taylor<sup>1</sup>; David H. StJohn<sup>1</sup>; <sup>1</sup>University of Queensland, FAST Casting Ctr. of Excellence, Brisbane, Queensland 4072 Australia

An automotive company has recently adopted procedures to control the melt hydrogen content of their cast aluminium air-intake manifolds. This arose because the hydrogen content showed a strong correlation with the incidents of hot tearing. Although the literature typically reports a negative impact of hydrogen on hot tearing it was clearly observed that higher hydrogen levels decreased hot tearing susceptibility in the manifold. Based on these in-house observations a series of experiments have been conducted using the common ring test mould. The impact of hydrogen content on hot tearing with varying solute (silicon) content and eutectic modification was closely examined using a hot tearing severity index that was established from ring crack dimensions. Results from the hydrogen trials showed the typical lambda curve for hot tearing versus solute content that has been well documented. The relationship between gas content and hot tearing is analysed with a view to establishing new insight into the mechanistic processes of hot tear formation.

## 9:40 AM

An Experimental Method for Determining Mechanical Properties of Non-Equilibrium Mushy Zone: *Qingyou Han*<sup>1</sup>; Mohamed I. Hassan<sup>2</sup>; Srinath Viswanathan<sup>3</sup>; Subodh K. Das<sup>4</sup>; <sup>1</sup>Oak Ridge National Laboratory, Metals & Ceram. Div., One Bethel Valley Rd., Oak Ridge, TN 37831-6083 USA; <sup>2</sup>University of Kentucky, Dept. of Mech. Engrg., 151 RGAN Bldg., Lexington, KY 40506-0108 USA; <sup>3</sup>Sandia National Laboratories, PO Box 5800, Albuquerque, NM 87185-1134 USA; <sup>4</sup>Secat Inc., 1505 Bull Lea Rd., Lexington, KY 40511 USA

The mushy zone of an alloy during solidification is non-equilibrium and the mechanical properties of this non-equilibrium mushy zone, especially at small liquid fractions, are closely related to the formation of hot tearing during solidification of castings. Experimentally it is very difficult to measure the mechanical properties of the non-equilibrium mushy zone with a small liquid fraction because the liquid fraction decreases rapidly due to back diffusion in the solid. This paper describes a new experimental method for determining the mechanical properties of the non-equilibrium mushy zone. Back diffusion in the solid of the mushy zone is considered in order to prevent liquid from disappearing. Specimens were taken from castings so that their grain sizes are same to the relevant casting. Initial experimental results indicate that the method can be used to capture the brittleness of an alloy at temperatures close to the non-equilibrium solidus temperature of the alloy.

#### 10:00 AM Break

## 10:20 AM Keynote

**Constitutive Behaviour and Hot Tearing During Aluminum DC Casting**: *Laurens Katgerman*<sup>1</sup>; Willem-Maarten Van Haaften<sup>2</sup>; Pim Kool<sup>1</sup>; <sup>1</sup>Delft University of Technology, Matls., Rotterdamseweg 137, Delft 2628AL The Netherlands; <sup>2</sup>Corus RD&T, IJmuiden The Netherlands

The constitutive behaviour of two non-heat treatable industrial aluminum alloys (AA3104 and AA5182) is investigated. This is done by testing the as-cast material in tension at low strain rates and from room temperature to semi-solid temperatures, similar to the conditions during DC casting. The parameters of two constitutive equations, the extended Ludwik equation and a combination of the Sellars-Tegart equation with a hardening law, were determined. To evaluate the quantified constitutive equations, tensile tests were performed simulating the deformation and cooling history experienced by the material during casting. In the semi-solid state the behavior is dominated by the solid network but the geometry of the liquid determines how much of the solid network contributes to the strength. A simple modification of a standard creep law, which takes into account the geometry of the liquid film, provides a continuous description of the constitutive behaviour of these alloys from the creep regime into the semi-solid state. It is concluded that the constitutive behaviour of the alloys in as-cast condition is well described by both the extended Ludwik equation and an adapted form of the Sellars-Tegart equation. Although the extended Ludwik equation describes the data better, the adapted form of the Sellars-Tegart equation is easier to implement in DC casting models, because the temperature appears explicitly in this equation. In order to study the hot tearing mechanism, tensile tests are carried out in semi-solid state and at low strain rates and crack propagation is studied in-situ by SEM. Microstructural investigations of these cracks indicates that they initiate at any weak spot such as a pore or partially liquid grain boundary and occur by a combination of fluid film separation and rupture of solid bridges. This leads to brittle behaviour on the large scale although local deformation can be very ductile. Similarities between hot tears in the industrial ingot and cracked specimens indicate that important aspects of hot tearing during casting can be simulated by tensile experiments at semi-solid temperatures.

**Tensile Properties of As-Cast AA5182 Aluminum Alloy Close to the Solidus Temperature**: *L. J. Colley*<sup>1</sup>; M. A. Wells<sup>1</sup>; D. M. Maijer<sup>1</sup>; S. Cockcroft<sup>1</sup>; <sup>1</sup>University of British Columbia, Dept. of Metals & Matls. Engrg., 309-6350 Stores Rd., Vancouver, BC V6T 1Z4 Canada

In order to address the demand for accurate mechanical property data in the partially solidified state, an experimental apparatus has been developed to perform tensile measurements of aluminum alloys at temperatures close to the solidus temperature. Measurements of the tensile properties of an industrially DC cast AA5182 aluminum alloy have been carried out between  $500^{\circ}$ C and  $580^{\circ}$ C, under strain rate conditions of ~10-4s<sup>-1</sup> to ~10-2s<sup>-1</sup>. The fracture surfaces and microstructures of the tested specimens have been examined using optical microscopy, SEM and EDX analysis to develop a relationship between tensile properties, fracture behaviour and changes in microstructure. Literature values of the solidification characteristics of AA5182 have also been used to relate the properties and microstructure with fraction liquid.

#### 11:10 AM

Effects of 1-4% Copper Additions on Semi-Solid Aluminum Alloy 357: Jon T. Carter<sup>1</sup>; Vjekoslav Franetovic<sup>1</sup>; <sup>1</sup>General Motors, R&D Ctr., Matls. & Processes Lab., MC 480-106-212, 30500 Mound Rd., Warren, MI 48090-9055 USA

The effects of copper additions on aluminum alloy 357 were studied in the course of alloy development for semi-solid forming. Copper additions of 1-4% were found to (a) increase the overall hardness and greatly increase the microhardness of the regions between the primary alpha grains, (b) inhibit spheroidization of alpha dendrites during the heat treatment in which the interdendritic constituents are melted, and (c) slightly refine the dendritic grains and promote a divorced form of the eutectic constituent in the as-cast microstructure. Data are presented in the forms of hardness plots, micrographs, solidification cooling curves, and heating curves.

#### 11:30 AM

**Rheocasting of Aluminum Alloys**: *Sungbae Park*<sup>1</sup>; Ian C. Stone<sup>1</sup>; Brian Cantor<sup>2</sup>; <sup>1</sup>University of Oxford, Dept. of Matls., Parks Rd., Oxford OX1 3PH UK; <sup>2</sup>University of York, York UK

Many processes have been developed for semi-solid casting. Recently, UBE Industries has introduced a new semi-solid casting process which comprises the preparation of the semi-solid slurry directly from the melt in-line with the casting machine. In the UBE rheocasting process semi-solid slurries with globular microstructures are formed using continuous controlled cooling, and in this study, the resulting semi-solid microstructures have been characterised quantitatively as a function of different slurry making conditions. In order to determine the deformability of the semi-solid slurries, thermomechanical analysis (TMA) has been carried out. This paper describes the optimum slurry making conditions in the UBE rheocasting process.

## Solidification Processes and Microstructures: A Symposium in Honor of Prof. W. Kurz: Phase Field

Sponsored by: Materials Processing & Manufacturing Division, MPMD-Solidification Committee

*Program Organizers:* Michel Rappaz, Ecole Polytechnique Fédérale de Lausanne, MXG, Lausanne Switzerland; Christoph Beckermann, University of Iowa, Department of Mechanical Engineering, Iowa City, IA 52242 USA; R. K. Trivedi, Iowa State University, Ames, IA 50011 USA

Wednesday AM	Room: 20	07D
March 17, 2004	Location:	Charlotte Convention Center

Session Chair: Andreas Ludwig, University of Leoben, Dept. of Metall., Leoben 8700 Austria

## 8:30 AM Invited

**Fractal Solidification Patterns**: *Heiner Mueller-Krumbhaar*<sup>1</sup>; <sup>1</sup>Forschungszentrum Juelich, Inst. Festkoerperforschung, D-52425 Juelich Germany

Fractal structures are frequently observed in solidification processes. A short overview is given starting with dendrites and seaweed structures<sup>1</sup> and covering also our recent results on elastic effects in segregation and in fractal layer growth on substrates.<sup>2</sup> <sup>1</sup>E.Brener, H. Mueller-Krumbhaar, D. Temkin, T. Abel, Morphology Diagram of Possible Structures in Diffusional Growth Physica A 249, 73 (1998); H. Mueller-Krumbhaar, T. Abel, E. Brener, M. Hartmann, N. Eissfeldt, D. Temkin; Growth-Morphologies in Solidification and Hydrodynamics; JSME International Journal B 45, 1, 2002. <sup>2</sup>H. Mueller-Krumbhaar, F. Gutheim, R. Spatschek, E. Brener; Elastic effects on growth processes, Appl. Surface Science, 7160, 1 (2001); F. Gutheim, H. Muller-Krumbhaar, E. Brener, V. Kagan; Thermal Roughening of a Solid-On-Solid Model with Elastic Interactions, Phys. Rev. B 67, 195404 (2003).

#### 9:00 AM Invited

**Phase Field Simulation of Directional Solidification**: Jonathan A. Dantzig<sup>1</sup>; Bari Athreya<sup>1</sup>; <sup>1</sup>University of Illinois, Dept. of Mech. & Industrial Engrg., MC-244, 1206 W. Green St., Urbana, IL 61801 USA

Prof. Kurz has made numerous important contributions to the understanding of microstructure development. Much of this work has been done by studying transparent binary alloys in directional solidification, where the temperature gradient and growth velocity are independently controlled, and the ensuing microstructure is examined. The sample is confined between microscope slides to make observation easier. In this work, we examine the directional solidification process in binary alloys. In particular, we examine the role of the confinement of the diffusion fields by the microscope slides on the development of microstructure. We demonstrate that 3-D effects are important, and compare our results to those found in experiments, and in simulations performed using 2-D approximations.

#### 9:30 AM Invited

**Globular-Dendritic Transition in Equiaxed Alloy Solidification**: Hermann-Josef Diepers<sup>1</sup>; *Alain S. Karma*<sup>1</sup>; <sup>1</sup>Northeastern University, Dept. of Physics, Boston, MA 02139 USA

Depending on the growth conditions, equiaxed grains can develop dendritically or form a globular morphology that is often associated with a high density of nucleants. Despite the widespread observation of both dendritic and globular grains, the transition between these two morphologies remains poorly understood. Existing equiaxed growth models assume lvantsov-like dendrite tip kinetics that is only valid for well-developed dendritic grains, and Zener's classical theory of growth transients only describes the initial development of spherical nuclei. We have carried out a phase-field study of the unsteady growth regime in between these two extremes that provides new insight into the globular-dendritic transition. The results reveal the existence of robust scaling laws that relate quantitatively the critical total grain size for this transition with the cooling rate and alloy parameters. These laws are interpreted with the help of simple analytical models.

## 10:00 AM Break

#### 10:30 AM

**Examination of Binary Alloy Dendrite Tip Operating State with a Phase-Field Model:** Juan Ramirez<sup>1</sup>; *Christoph Beckermann*<sup>1</sup>; <sup>1</sup>University of Iowa, Dept. Mech. & Industrial Engrg., 2412 SC, Iowa City, IA 52242 USA

The description of free dendritic growth into an undercooled binary alloy melt is most commonly performed with the Lipton, Glicksman and Kurz (LGK) model. Taking into account heat and solute diffusion, this model describes the variation of the steady-state dendrite tip velocity and radius with solute concentration. The LGK model assumes the existence of a selection parameter that remains constant and independent of undercooling and initial melt concentration. The LGK model is re-examined using a recently developed phase-field model. This thermosolutal phase-field model allows for the simulation of dendritic growth without interface kinetics and is used to examine the variation of the dendrite tip operating state with initial melt solute concentration. As predicted by the LGK theory, a maximum in the steady-state tip velocity is observed for small but finite melt concentrations, but other results indicate that additional study is needed.

#### 10:45 AM

**Microstructure Evolution in the Presence of Foreign Particles**: James A. Warren<sup>1</sup>; Laszlo Granasy<sup>2</sup>; <sup>1</sup>NIST, CTCMS, 100 Bureau Dr., Stop 8554, Gaithersburg, MD 20899-8554 USA; <sup>2</sup>RISSPO, PO Box 49, H-1525, Budapest Hungary

The evolution of microstructure during solidification is the focus of much of Wilfried Kurz's research. While great progress has been made in the theory of perfect single crystals of either a single component or a binary alloy, Nature has not obliged us with circumstances where such systems are easily realized. A major focus of our research has been the extension of phase field models of solidification to include polycrystalline materials. In this talk we will assess the range of applicability of this model, in particular examining the role that foreign particles can play during dendritic growth, as well as the occurrence of spherulitic growth during solidification of both metals and polymers. Three-Dimensional Phase-Field Simulations of Directional Solidification: Marcus Dejmek<sup>1</sup>; Roger Folch<sup>1</sup>; Andrea Parisi<sup>1</sup>; *Mathis Plapp*<sup>1</sup>; <sup>1</sup>CNRS/Ecole Polytechnique, Lab. PMC, Rte. de Saclay, Palaiseau 91120 France

The phase-field method has become in recent years the method of choice for simulating microstructural pattern formation during solidification. One of its main advantages is that time-dependent threedimensional simulations become feasible. This makes it possible to address long-standing questions of pattern stability. Here, we investigate the stability of hexagonal cells and eutectic lamellae. For cells, it is shown that the geometry of the relevant instability modes is detemined by the symmetry of the steady-state pattern, and that the stability limits strongly depend on the strength of crystalline anisotropy, as was previously found in two dimensions. For eutectics, preliminary investigations of lamella breakup instabilities are presented that are carried out with a newly developed phase-field model of twophase solidification.

## 11:15 AM

**Experimental Observation and Phase-Field Modeling of Interface Morphological Transition in Solidification**: *Taiming Guo*<sup>1</sup>; Haijun Xu<sup>2</sup>; Thein Kyu<sup>2</sup>; G-X. Wang<sup>1</sup>; <sup>1</sup>University of Akron, Dept. of Mech. Engrg., Akron, OH 44325-3903 USA; <sup>2</sup>University of Akron, Dept. of Polymer Engrg., Akron, OH 44325-0301 USA

Depending on the relative extent of the anisotropy of the interface energy, a growing solidification interface may develop with various distinguished patterns, such as normal dendrites, degenerate dendrite, and seaweed. This presentation will present experimental observations of the dynamic variation of various interface morphologies in a horizontal unidirectional solidification system using succinonitrile. Under certain circumstances, non-dendritic interface morphologies have been observed. It is found that formation of any specific morphology depends on the interface growth velocity and the temperature gradient. Dynamic transition from one pattern to another has also been observed and documented. The formation and transition of these non-dendiritc patterns are then simulated by using a 2-D phase-field model coupled with heat conduction equation in which the anisotropy of the interface energy can be artificially set and adjusted. Both unidirectional and unconstrained crystal growth process have been simulated using the model. It is found that the interface morphology could transit from seaweed to dendritic pattern because of the variation of parameters K and e of heat conduction equation, where K is proportional to the latent heat released at the interfacial front and inversely proportional to the supercooling, and e is related to the thermal diffusivity. These numerical results confirm qualitatively the experimental observations. Quantitative comparisons between the numerical and experimental results are also attempted and will be presented.

## 11:30 AM

Phase Field Modeling of Step Flow With Dendritic Pattern: Seong Gyoon Kim<sup>1</sup>; Won Tae Kim<sup>2</sup>; <sup>1</sup>Kunsan National University, Dept. of Matls. Sci. & Engrg., Kunsan 573-360 Korea; <sup>2</sup>Chongju University, Appl. Sci. Div., 36 Naedok Dong, Chongju 360-764 Korea

Macrosteps with dendritic pattern have been observed on the vicinal (0001) surface of sapphire during evaporation in vacuum at temperatures between 1923K and 2223K. To clarify the pattern formation mechanism of the steps, we perform the linear stability analysis, as well as phase-field computations, based on the classical Burton-Cabrera-Frank model. With increasing annealing temperature evaporation rate and dendritic growth rate increased. The growth rate dependence of the dendritic tip radius was different from the well known scaling law (R<sup>2</sup>V with R: tip radius, V: growth rate) observed in solidification process. Tip radius was not strongly dependent of the growth rate. This could be explained by the co-existence of adatom evaporation and adatom diffusion within the diffusional field on upper terrace, which is in contrast with the solute diffusion only in liquid phase during solidification. A 2-D phase-field modeling including the multiple step interaction via diffusional field and the decomposition of accelerating steps near the step source could reproduce all the characteristics of the patterns with temperature.

## 11:45 AM

Phase Field Modeling of Dendritic Growth With Facets in an Undercooled: Seong Gyoon Kim<sup>1</sup>; Won Tae Kim<sup>2</sup>; Toshio Suzuki<sup>3</sup>; <sup>1</sup>Kunsan National University, Dept. Matls. Sci. & Engrg., Kunsan 573-360 Korea; <sup>2</sup>Chongju University, Appl. Sci. Div., 36 Naedok Dong, Chongju 360-764 Korea; <sup>3</sup>University of Tokyo, Dept. of Metall. Sys. Engrg. for Matls., Tokyo 113-8656 Japan

We extend our new phase field model of alloy solidification, characterized by localization of solute redistribution into a narrow region to minimize anomalous interface effects in the thin interface model, to model the solidification of faceted materials. This approach consists of finding missing orientations in an equilibrium shape, regularization of anisotropy based on the method proposed by Eggleston et al [Physica D, 150(2001),91]. The phase field equation was solved on 2D geometry at the vanishing interface kinetics condition with various anisotropies between  $0 < \delta < 0.3$ . When  $\delta < 1/15$ , a normal dendrite without cusps appeared as expected and dendrite with cusps appeared at  $\delta > 1/15$ . As the anisotropy  $\delta$  increases from 0 to 1/15, steady state tip radius decreased while tip growth rate increased. A transition in tip growth rate appeared when normal dendrite changes to dendrite with cusps. With further increase in anisotropy  $\delta$  above 1/15, steady state growth rate increased and reached a saturation value. Scaling laws between tip radius and tip growth rate will be discussed.

### 12:00 PM

A 2-Dimensional Model Coupled to a Thermodynamic Database for the Prediction of Solidification Microstructures in Multi-Component Alloys: *Alain Jacot*<sup>1</sup>; Qiang Du<sup>1</sup>; <sup>1</sup>Ecole Polytechnique Fédérale de Lausanne, Matls. Inst., Computational Matls. Lab, Lausanne 1015 Switzerland

A two-dimensional model based on the pseudo-front tracking method was presented recently as an interesting approach to predict the formation of globulo-dendritic grains during solidification in multi-component systems.1 This method permits to calculate the evolution of solid/liquid interfaces which are governed by solute diffusion and anisotropic surface tension. It is based on a finite volume method for the resolution of the diffusion equations and a geometrical approach for the calculation of the interface curvature. The present contribution deals with a recent extension of the pseudo-front tracking method to the formation of secondary phases. The secondary phase model is based on a mixture approach and the assumption that the interdendritic regions are composed of liquid and secondary particles locally in thermodynamic equilibrium. The model accounts for back-diffusion in the primary phase, which continuously modifies the composition of the interdendritic regions. The phase diagram software Thermo-Calc is used to obtain the equilibrium concentrations to be prescribed as boundary conditions at the primary phase/liquid interface and, during the second stage of solidification, to calculate the composition of the mixture in the interdendritic region. The model is applied to the description of microstructure formation in commercial aluminum alloys solidified under different cooling conditions. Comparisons between experimental and calculated microstructures will be shown. 1A. Jacot and M. Rappaz, Acta Materialia 50, (2002), pp. 1909-1926.

#### 12:15 PM

A Cellular Automaton for Growth of Solutal Dendrites: Factors Influencing Artificial Anisotropy in Growth Kinetics: *Srinivasan Raghavan*<sup>1</sup>; Matthew John M. Krane<sup>1</sup>; David R. Johnson<sup>1</sup>; <sup>1</sup>Purdue University, Sch. of Matls. Engrg., 501 Northwestern Ave., W. Lafavette, IN 47907-2036 USA

Cellular automaton is used to simulate the dendritic growth controlled by solutal effects. The model does not explicitly track the interface velocity by the flux equations; the interface motion results from the combined effect of maintaining equilibrium composition, solute rejection and the diffusion of solute at the interface. The grid of the cells introduces artificial anisotropy in the growth of dendrites, favoring growth at angles 0° or 45° from the vertical on a square grid. We propose a solution to reduce the anisotropy by suitable choice of growth rules and by identifying the appropriate dependence of cell size and time step on material properties and process parameters. The cell size is limited by the diffusion length and the imposed velocity. Finally, the simulated results are compared with analytical and experimental results for the tip radius, undercooling and primary dendritic arm spacing and fraction primary solid to test the validity of the model.

## Surfaces and Interfaces in Nanostructured Materials: Synthesis & Processing

Sponsored by: Materials Processing and Manufacturing Division, MPMD-Surface Engineering Committee

*Program Organizers:* Sharmila M. Mukhopadhyay, Wright State University, Department of Mechanical and Materials Engineering, Dayton, OH 45435 USA; Arvind Agarwal, Florida International University, Department of Mechanical and Materials Engineering, Miami, FL 33174 USA; Narendra B. Dahotre, University of Tennessee, Department of Materials Science & Engineering, Knoxville, TN 37932 USA; Sudipta Seal, University of Central Florida, Advanced Materials Processing and Analysis Center and Mechanical, Materials and Aerospace Engineering, Oviedo, FL 32765-7962 USA

Wednesday AM	Room: 2	17A
March 17, 2004	Location:	Charlotte Convention Center

Session Chair: Arvind Agarwal, Florida International University, Dept. of Mech. & Matls. Engrg., Miami, FL 33174 USA

#### 8:30 AM Invited

The Formation of Nanoparticles in Sapphire and Silica by Ion Implantation: Janet M. Hampikian<sup>1</sup>; <sup>1</sup>Georgia Institute of Technology, Sch. of Matls. Sci. & Engrg., 771 Ferst Dr., NW, Atlanta, GA 30332-0245 USA

The formation of nano-composites comprising metal clusters (5 to 20 nm in diameter) embedded in dielectric hosts via ion implantation is presented. Two basic approaches yield embedded nanoparticles: first, the implantation of noble metal ions, and second, the implantation of highly reactive metal ions that reduce the substrate cations to form metal atoms. An example of the former approach is the formation of gold clusters via gold ion implantation of sapphire. The latter approach relies on the reduction of the substrate. An example of this is the formation of aluminum clusters in sapphire via yttrium ion implantation. The thermodynamics and kinetics of the latter approach are presented, including the effects of ion energy, ion fluence and implantation temperature. The metal particles so formed are amorphous and do not contribute to electron diffraction. Therefore, energy filtered transmission electron microscopy is used as a characterization tool in conjunction with TEM, PEELS and EDS. Optical absorption measurements of the modified surfaces are also presented.

#### 8:55 AM

Synthesis and Processing of Nanocrystalline Magnetic Materials: Jeffrey E. Shield<sup>1</sup>; <sup>1</sup>University of Nebraska, Mech. Engrg., N104 WSEC, Lincoln, NE 68588-0656 USA

Interfacial interactions in magnetic materials lead to many interesting effects, among them exchange-spring behavior. The exchangespring interaction involves spins coupling across interfaces, resulting in remanence enhancement and improved energy densities. In order to exploit the interfacial effects in magnetic materials for applications, it is necessary to develop techniques and alloys that result in nanoscale structures, with grain sizes less than 40 nm. In addition, combinations of hard and soft magnetic phases are desirable for optimum magnetic properties. In this talk, various processing routes to a nanoscale structure will be discussed. These include atom-up approaches such as cluster deposition, and more tradition bulk routes such as melt spinning. In the cluster deposition approach, gas phase condensation results in the formation of 8 nm Fe clusters, which have been imbedded in a hard magnetic matrix. In melt-spinning, efforts have concentrated on understanding the nanostructural development and in controlling the grain size and distribution through alloying additions in both the Nd-Fe-B and Sm-Co systems. This talk will summarize efforts in these areas

## 9:15 AM

Surface Nanocrystalline Metallic Materials Fabricated by Surface Severe Plastic Deformation: *Nobuhiro Tsuji*<sup>1</sup>; Masahide Sato<sup>1</sup>; Yoritoshi Minamino<sup>1</sup>; Yuichiro Koizumi<sup>1</sup>; <sup>1</sup>Osaka University, Dept. of Adaptive Machine Sys., 2-1 Yamadaoka, Suita, Osaka 565-0871 Japan

Severe plastic deformation (SPD) above 4 of equivalent strain can produce ultrafine grained (UFG) metallic materials whose mean grain sizes are around 100 nm. In order to fabricate bulk UFG materials, however, special equipment and/or techniques as well as huge amount of plastic working energy are necessary. Meanwhile, the present authors have succeeded in fabricating surface nanocrystalline materials in bulky shape, where only subsurface layers have nanocrystalline structures, by a surface-SPD process using simple wire-brushing. Nanocrystals with mean diameters below 100 nm formed at surface layers of various kinds of Al alloys, Cu alloys and steels after the surface-SPD processing at ambient temperature. In case of commercial purity aluminum, the depth of the nanocrystalline layer was about 15 micro-meters. Interesting properties of the surface nanocrystalline materials will be also introduced. For example, the surface nanocrystalline aluminum performed significantly higher proof stress than the coarse grained material without nanocrystalline surface.

#### 9:35 AM Cancelled

Development of Nanocrystalline Light Metals Via Mechanochemical Processing

#### 9:55 AM Invited

Processing Bulk Structures from Nanopowders of Aluminum: Jixiong Han<sup>1</sup>; Martin J. Pluth<sup>1</sup>; Jai A. Sekhar<sup>1</sup>; Vijay K. Vasudevan<sup>1</sup>; <sup>1</sup>University of Cincinnati, Chem. & Matls. Engrg., Cincinnati, OH 45221-0012 USA

A study was made of the compaction, sintering behavior and workability of nanoscale aluminum powders into bulk structures. The nanoparticles of pure Al ranged in diameter from ~30 to 150 nm and contained a 2-5 nm outer oxide layer. The powders were cold-compacted in air, then sintered between 500 and 650°C for various times. Both hot and cold rolling of the pressed pellets was also utilized to assess workability and hardness after processing. Density was measured, and thin foils were prepared for TEM. Observations revealed that the oxide scale remained intact on sintering at 500°C, but showed evidence of breakage at higher temperatures, although in both cases a very interesting Al matrix-Al oxide nanocomposite resulted. TEM observations revealed that both constituents retained nanoscale dimensions, though there was evidence of growth of the Al grains compared with the initial particles. High densification, coupled with high hardness could be achieved. In addition, the sintered materials could be cold-rolled a s high as 60% reduction in thickness with additional densification and hardness increase. High-resolution SEM observations revealed nanoscale cracks in the rolled materials. These various results will be presented and discussed. In addition, attempts were made to produce extrusions from the nanopowders. The results of the microstructure, thermal stability and mechanical properties of these materials will also be presented. Support for this research from AFOSR under grant no. F49620-01-1-0127, Dr. Craig S. Hartley, Program Monitor, is deeply appreciated.

### 10:20 AM

Modern Lithographic Techniques for the Fabrication of Patterned Self-Assembled Monolayers on Metallic Surfaces: *Francesco Stellacci*<sup>1</sup>; <sup>1</sup>Massachusetts Institute of Technology, Dept. of Matls. Sci. & Engrg., 77 Mass. Ave., Rm. 13-5049, Cambridge, MA 02139 USA

One of the main challenge in nanotechnology is to generated surfaces with controlled morphology properties. Here we present two techniques based on scanning probe microscopes that allow for the patterning of functionalized molecules on metallic surfaces. The first technique is Dip Pen Nanolithography (DPN) that allows for the controlled deposition of molecules on surfaces. Patterns can be written with 20 nm resolution. We show that, in DPN, by varying the writing speed and the relative humidity it is possible to control the morphology of the written self-assembled monolayers (SAMs) for both hydrophobic and hydrophilic thiolated molecules on a gold surface. We have used this properties to control the self-assembly of nanoparticles on this surface or to generate efficient etching masks. The second technique is replacement lithography (RL) that allows for RL to pattern supramolecular fluorescent nanowires.

#### 10:40 AM

**Plasma Engineered Nanostructured Spherical Powders**: *Tapas Laha*<sup>1</sup>; Brandon Potens<sup>2</sup>; Arvind Agarwal<sup>3</sup>; Sudipta Seal<sup>4</sup>; <sup>1</sup>Florida International University, Mech. & Matls. Engrg., 10555 W. Flagler St., CEAS 3362, Miami, FL 33174 USA; <sup>2</sup>Florida International University, Mech. & Matls. Engrg., 10555 W. Flagler St., Miami, FL 33174 USA; <sup>3</sup>Florida International University, 10555 W. Flagler St., GEAS 3464, Miami, FL 33174 USA; <sup>4</sup>University of Central Florida, Mech. Matls. & Aeros. Engrg., Engrg. Bldg. 1, Rm. 381, PO Box 162455, Orlando, FL 32816 USA

Nano-structured spherical powders of Al and Al2O3 were synthesized by plasma spraying irregular shaped micron sized powders. The sprayed powders were collected under extreme cooling condition of liquid nitrogen to ensure the retention of nanograins in the powders. Both the as-received powders and the plasma-engineered powders were observed in Scanning Electron Microscope to study the change in chemical composition, morphology and size of the powders due to plasma processing. X-Ray Diffraction investigations were made to carry out the phase study and grain size measurement. The formation of nanograins in plasma-engineered powders was examined by performing Transmission Electron Microscopy.

### 11:00 AM Invited

**Directed Assembly of Mesoarchitectures and Networks from 0-D and 1-D Nanounits**: *G. Ramanath*<sup>1</sup>; <sup>1</sup>Rensselaer Polytechnic Institute, Dept. of Matls. Sci. & Engrg., Troy, NY 12180 USA

There is widespread interest in harnessing nanotubes and nanowires for applications such as device interconnection, switching, field emission, sensing, molecular sieving, and structural reinforcements for nanocomposites. In order to realize these exciting possibilities, it is essential to controllably create mesoscale architectures and networks from nanoscale units, placed in desired locations and orientations, by scaleable approaches. This talk will describe two powerful bottom-up strategies to assemble: a) mesonetworks of metallic nanowires from nanoparticles, and b) multidirectional mesoarchitectures of carbon nanotubes (CNTs). The first example will illustrate a room-temperature templateless wet-chemical method for producing metal nanowires from nanoparticles using biphasic liquid mixtures. Nanoparticles are forced to impinge and coalesce at high mobility liquid-liquid interfaces leading to the formation of polycrystalline nanowires. The role of surface processes and liquid-interface chemistries in the mo rphological evolution of the nanowires will be described based on electron microscopy, diffraction, and electron and optical spectroscopy measurements. The second example will describe a hybrid processing approach that combines substrate-selective CVD and lithographic chiseling of substrates to controllably place and grow CNTs at premeditated nucleation sites and orientations. The CNTs selectively grow on silica surfaces in exclusion to silicon, in an orientation parallel to the surface normal. By shaping the silica templates by lithography, we obtain a variety of 2D and 3D mesoscale relief, porous, architectures with complex shapes, configurations, and lengths. Salient features of the growth mechanism will be discussed. If time permits, a newly discovered strategy to site-selectively anchor nanoclusters to CNTs will also be presented.

## 11:25 AM

Hydrogen Storage Properties of Multiwall Carbon Nanotubes Grown in Oxygen Added PECVD: Jai-Young Lee<sup>1</sup>; Hyun-Seok Kim<sup>1</sup>; Ho Lee<sup>1</sup>; Jin-Ho Kim<sup>1</sup>; <sup>1</sup>Korea Advanced Institute of Science and Technology, Dept. of Matls. Sci. & Engrg., 373-1, Guseong-dong, Yuseong-gu, Daejon 305-701 Korea

Hydrogen storage properties of the two kinds of multiwall carbon nanotubes (MWNTs) synthesized by microwave PECVD were evaluated. The first sample grown in CH4/H2 reaction gas was curly shaped nanotubes with blocked nanoholes and closed caps and the next sample grown in CH4/H2/O2 reaction gas had less defective structure with connected holes and open caps. The hydrogen storage properties of the carbon nanotubes with these closed and open structures were compared by thermal desorption technique. Though the MWNTs with blocked and closed structure had two different desorption ranges such as 290-330 and about 420 K and evolved about 0.64 and 0.03 wt% of hydrogen respectively, the MWNTs with open MWNTs evolved about 1.94 wt% of hydrogen at ambient temperature. And the hydrogen desorption activation energy was calculated. The obtained hydrogen desorption activation energy of MWNTs with closed and open structure at ambient temperature was -18.5 kJ/mol H2 and -16.5 kJ/mol H2, respectively. The activation energy of high temperature hydrogen desorption in MWNTs with closed structure was -124.4 kJ/mol H2. The hydrogen desorbed between 290 and 330 K was the hydrogen physi-sorbed in nano-hole and the hydrogen desorbed at about 420 K was that chemi-sorbed in defects of nanotubes

## The Didier de Fontaine Symposium on the Thermodynamics of Alloys: Joint Session with Computational Thermodynamics and Phase Transformations I

Sponsored by: Materials Processing and Manufacturing Division, MPMD-Computational Materials Science & Engineering-(Jt. ASM-MSCTS)

*Program Organizers:* Diana Farkas, Virginia Polytechnic Institute and State University, Department of Materials Science and Engineering, Blacksburg, VA 24061 USA; Mark D. Asta, Northwestern University, Department of Materials Science and Engineering, Evanston, IL 60208-3108 USA; Gerbrand Ceder, Massachusetts Institute of Technology, Department of Materials Science and Engineering, Cambridge, MA 02139 USA; Christopher Mark Wolverton, Ford Motor Company, Scientific Research Laboratory, Dearborn, MI 48121-2053 USA

Wednesday AM	Room: 2	16B	
March 17, 2004	Location:	Charlotte Convention	Center

Session Chair: TBA

## 8:30 AM Invited

The Ground State of Binary Compounds from First Principles: Alex Zunger<sup>1</sup>; <sup>1</sup>NREL, Basic Sci., 1617 Cole Blvd., Golden, CO 80401 USA

Finding the ground state structures of compounds has become a cornerstone problem in inorganic structural chemistry, metallurgy, and solid state physics. I will briefly review the way this problem was first approached in the early classical literature, and then describe the "modern", Mixed-Basis-Cluster-Expansion approach to it. In this approach, first-principles total energy methods of just a handful of compounds are maped into a generalized Ising-like expansion that accounts for atomic relaxation, long-range strain effects, and generic bonding effects. Human intervention is minimal, and no adjustable parameters exist. Didier's seminal contributions to this approach will be discussed.

## 9:00 AM Invited

Multi-Scale Thermodynamics Calculations from the First-Principles: *Tetsuo Mohri*<sup>1</sup>; Ying Chen<sup>2</sup>; Munekazu Ohno<sup>1</sup>; <sup>1</sup>Hokkaido University, Grad. Sch. of Engrg., Div. of Matls. Sci. & Engrg., Kita-13 Nishi-8, Kita-ku, Sapporo 060-8628 Japan; <sup>2</sup>University of Tokyo, Dept. of Quantum Engrg. & Sys. Sci., Hongo 7-3-1, Bunkyo-ku, Tokyo 113-8655 Japan

Based on FLAPW total energy calculations combined with Cluster Expansion Method and Cluster Variation Method, extensive studies on phase equilibria for Fe-Ni, Fe-Pd and Fe-Pt systems have been attempted. The transition temperatures of L10-disorder were well reproduced with high accuracy. In order to extend the present studies to predict microstructural evolution process, Phase Field Method has been employed. The preliminary calculations have been successfuly performed to reproduce the essential feature of three kinds of multiscale phenomena; 1. Atomistic ordering process, 2. Nucleation of Anti Phase Domain and its wetting process and 3. Growth and coalescence process of APD. In order to evaluate gradient energy coefficient term without resorting to empirical means, the possibility of first-principles calcualtion has been explored.

## 9:30 AM Invited

Kinetic Pathways for Solid State Transformations: Georges Martin<sup>1</sup>; <sup>1</sup>CEA, Cabinet du Haut Commissaire, 33 rue de la Fédération, Paris 75015 France

Provided that the enthalpy  $H({r})$  of a set of atoms is known as a function of the position  ${r}$  of all the atoms, and that the enthalpy hyper-surface  $H({r})$  exhibits well defined minima separated by barriers of some kT, the classical transition state theory permits to compute the transition probability per unit time, Wij, between two configurations, i and j of the set of atoms. Once the set of the Wij's is known for all possible configurations, Kinetic Monte Carlo techniques generate realistic kinetic pathways for solid state coherent unmixing and/or ordering. Based mainly on broken bounds models for  $H({r})$ , but also on cluster expansions, the activity in this field is flourishing. I'll focus on what has been understood recently on the effect of the diffusion mechanism on kinetic pathways, a question of importance for practical metallurgy: - vacancy diffusion mechanism, with conserved and non-conserved vacancies; - monomer versus n-mer solute mobil-

ity; - competition between thermally activated atomic jumps and ballistic jumps in the case of "driven alloys". The link with mean field approximations and phase field models will be briefly discussed at the end.

## 10:00 AM Break

#### 10:10 AM Invited

**Phase Field Method: Microstructure Evolutions and Plasticity:** *Alphonse Finel*<sup>1</sup>; Yann M. Le Bouar<sup>1</sup>; Quentin Bronchart<sup>1</sup>; <sup>1</sup>ONERA, LEM (CNRS-ONERA), BP 72, Chatillon 92322 France

The Phase Field Method is extensively used to study the dynamics of microstructures inherited from phase transformations and it has recently been extended to the dynamics of dislocations, and thus to the domain of plastic deformation. We will present recent advances in these two fields. In particular, we will address the problem of fluctuations and time scale for microstructural evolution, as well as the problem of the short range elastic interactions between dislocations.

### 10:40 AM Invited

Site Preference in Frank-Kasper Intermetallic Compounds: Marcel H.F. Sluiter<sup>1</sup>; Alain Pasturel<sup>2</sup>; Yoshiyuki Kawazoe<sup>1</sup>; <sup>1</sup>Tohoku University, Inst. for Matls. Rsch., 2-1-1 Katahira, Aoba-ku, Sendaishi, Miyagi-ken 980-8577 Japan; <sup>2</sup>CNRS, Laboratoire de Physique et Modelisation des Milieux Condenses, Maison des magistees BP 166, Grenoble-Cedex 09 38042 France

Site occupation in a variety of Frank-Kasper type intermetallic phases has been predicted using density functional electronic structure methods. For the rather limited number of cases where experimental verification is possible, generally good agreement is found. As a number of systems have been examined, the validity of simple rules of thumb can be examined. The applicability of rules based on atomic size and coordination number, on nearest neighbor like and unlike pair counts, and on approximate local point symmetry and valence electron per atom ratios have been evaluated. As a result an amalgam of rules of thumb can be put forward which generally explains the findings obtained so far. Such general rules are expected to be of utility in the thermodynamic modeling for phase diagram calculations.

#### 11:10 AM

Formation Process of Anti-Phase Boundaries in Al5Ti3 Type Superstructure Studied by Monte Carlo Simulation: Satoshi Hata<sup>1</sup>; Takayoshi Nakano<sup>2</sup>; Kiyoshi Higuchi<sup>1</sup>; Yousuke Nagasawa<sup>2</sup>; Masaru Itakura<sup>1</sup>; Noriyuki Kuwano<sup>3</sup>; Yoshitsugu Tomokiyo<sup>1</sup>; Yukichi Umakoshi<sup>2</sup>; <sup>1</sup>Kyushu University, Dept. of Appl. Sci. for Elect. & Matls., 6-1 Kasugakouen, Kasuga, Fukuoka 816-8580 Japan; <sup>2</sup>Osaka University, Dept. of Matls. Sci. & Engrg. & Handai Frontier Rsch. Ctr., Grad. Sch. of Engrg., 2-1 Yamadaoka, Suita, Osaka 565-0871 Japan; <sup>3</sup>Kyushu University, Advd. Sci. & Tech. Ctr. for Coop. Rsch., 6-1 Kasugakouen, Kasuga, Fukuoka 816-8580 Japan

Al-rich TiAl forms metastable  $Al_5Ti_3$  superstructure in the  $L1_0$  matrix. It is expected that  $Al_5Ti_3$  can introduce many types of anti-phase boundaries (APBs) because of its large unit cell. However, most of the APBs observed experimentally are of A-type that is composed of structural units of  $Al_5Ti_3$ . The formation process of APBs in  $Al_5Ti_3$  was analysed by Monte Carlo simulation in a two-dimensional Ising lattice. For reproducing the  $Al_5Ti_3$  type ordering in the (002) disordered matrix, effective pairwise interactions reported by Kulkarni were modified. In the early stage of ordering, segments of A-type APBs appear with a higher frequency than those formed by random-nucleation and subsequent bounding of  $Al_5Ti_3$  microdomains. The A-type APBs grow with  $Al_5Ti_3$  domains and sweep out the other types of APBs. Such a formation process is due to quite low energy of A-type APB that creates wrong atomic bonds only at large coordination distances.

## The Role of Grain Boundaries in Material Design: Grain Boundary Character

Sponsored by: Materials Processing and Manufacturing Division, ASM/MSCTS-Texture & Anisotropy Committee, MPMD-Computational Materials Science & Engineering-(Jt. ASM-MSCTS) *Program Organizers:* Brent L. Adams, Brigham Young University, Department of Mechanical Engineering, Provo, UT 84602-0001 USA; Thomas R. Bieler, Michigan State University, Department of Chemical Engineering and Materials Science, East Lansing, MI 48824-1226 USA

Wednesday AM	Room: 218A
March 17, 2004	Location: Charlotte Convention Center

Session Chairs: Brent L. Adams, Brigham Young University, Dept. of Mech. Engrg., Provo, UT 84602-0001 USA; Gregory Rohrer, Carnegie Mellon University, Dept. of Matls. Sci. & Engrg., Pittsburgh, PA 15123-3890 USA

### 8:30 AM Opening Comments

#### 8:35 AM Invited

A New Approach to Grain Boundary Engineering in the 21st Century: Tadao Watanabe<sup>1</sup>; <sup>1</sup>Tohoku University, Nanomech., Aramaki-Aza-Aoba 01, Aoba-Ku, Sendai, Miyagi 980-8579 Japan

Grain boundaries can play crucial roles in designing high performance advanced structural and functional materials. They have a large variety of structure-dependent properties and geometrical configurations. A new principle of materials design and development, called Grain Boundary Design/Control or Engineering has been established based on systematic studies of the relationship between grain boundary structure and properties, and the control of grain boundary microstructures. It is strongly required that a large variety and a wide flexibility of grain boundaries should be effectively utilized in future materials design and development. The development of useful processing techniques for grain boundary engineering has been attempted in order to confer desirable property and high performance to a polycrystalline material in the last decade. This paper will present a prospect of grain boundary engineering in the 21st century, referring to a new approach to grain boundary engineering including nanocrystalline materials and the rejuvenation of damaged materials.

### 9:00 AM Invited

**Evolution of Higher Order Correlations in Microstructures During Annealing**: *Mukul Kumar*<sup>1</sup>; <sup>1</sup>Lawrence Livermore National Laboratory, 7000 East Ave., L-356, Livermore, CA 94550 USA

Sequential thermomechanical processing consisting of several cycles of moderate strain and high temperature annealing has been shown to systematically modify the topology of the microstructure. The optimization treatments performed on FCC metals and alloys with low stacking fault energies have resulted in microstructures with high fractions of S3n variants and other special boundaries. Concurrently, there are dramatic changes in the triple junction distributions owing to the higher order correlations imposed by crystallography. However, a fundamental question regarding the stability of such microstructures during high temperature excursions under service conditions is still open for debate. EBSD orientation mapping and transmission electron microscopy observations of the deformed and annealed states will be presented. These will be correlated with the changes in the microstructural topology such as the network of random grain boundaries. This work was performed under the auspices of the U.S. Department of Energy by University of California, Lawrence Livermore National Laboratory under contract No. W-7405-Eng-48.

#### 9:25 AM Invited

Non-Destructive Characterization of Grain Boundaries in 3D: Dorte Juul Jensen<sup>1</sup>; Xiaowei Fu<sup>1</sup>; Soren Schmidt<sup>1</sup>; <sup>1</sup>Riso National Laboratory, Ctr. for Fundamental Rsch., Metal Structures in 4-D, Roskilde DK 4000 Denmark

A grain boundary is classified by the crystallographic misorientation across it (3 parameters) and by the grain boundary plane (2 parameters). Additional four parameters describe the precise atomic arrangement at the boundary. Experimentally it is straightforward to determine the misorientation, e.g. by EBSP, and these 3 parameters may be sufficient to understand given materials properties. However in other cases also the grain boundary planes have to be determined. In the present presentation, it is described how all 5 grain boundary parameters can be determined fast and non-destructively for large bulk specimens by 3 Dimensional X-Ray Diffraction Microscopy. Results for Al samples are presented. The precision in the determination is explained and options for improvements are discussed.

#### 9:50 AM Invited

**Grain Boundary Plane Textures in Polycrystals**: *Gregory S. Rohrer*<sup>1</sup>; David M. Saylor<sup>2</sup>; <sup>1</sup>Carnegie Mellon University, Matls. Sci. & Engrg., 5000 Forbes Ave., Pittsburgh, PA 15213-3890 USA; <sup>2</sup>National Institute of Standards and Technology, Matls. Sci. & Engrg. Lab., Gaithersburg, MD 20899 USA

To distinguish one type of grain boundary from another, the values of five independent parameters must be specified. Three parameters describe the lattice misorientation and two parameters describe the normal to the grain boundary plane. Our recent observations of five parameter grain boundary distributions in microstructures that result from extensive grain growth have led to the following conclusions. First, there is significant texture in the space of grain boundary plane orientations, even when there is no significant misorientation texture. Second, low energy interfaces are observed more frequently than higher energy interfaces. Furthermore, for high angle grain boundaries, the anisotropy associated with the grain boundary plane orientation is greater than that associated with the misorientation. The relative amounts of grain boundary anisotropy in several materials (magnesia, strontium titanate, titania, spinel, and aluminum) will be compared and the origin of the texture will be discussed.

## 10:15 AM Break

#### 10:30 AM

## Design of the Grain Boundary Character Distribution in Polycrystals: Brent Larsen Adams<sup>1</sup>; <sup>1</sup>Brigham Young University, Mech. Engrg., 435 CTB, Provo, UT 84602-4201 USA

Material properties that depend upon the grain boundary character distribution (GBCD) is the focus of this presentation. Methodology for incorporating the GBCD in the Fourier framework for microstructure design is described. A failure criterion is postulated that requires the fraction of susceptible grain boundaries to exceed the percolation threshold. This criterion is extended to the statistical ensemble, and its dependence upon critical crack length is examined. The relationship with other aspects of microstructure design is also described.

## 10:55 AM Invited

Length Scales in Grain Boundary Manifolds: Elizabeth A. Holm<sup>1</sup>; Erin McGarrity<sup>2</sup>; Jan H. Meinke<sup>2</sup>; Phillip M. Duxbury<sup>2</sup>; <sup>1</sup>Sandia National Laboratories, Dept. 1834, PO Box 5800, MS 1411, Albuquerque, NM 87185 USA; <sup>2</sup>Michigan State University, Dept. of Physics & Astron., Lansing, MI 48824-1116 USA

Although the tools of microstructural analysis - microscopy, image acquisition, computers, and computational science - have advanced, the measures of microstructure remain the traditional planar parameters of quantitative stereology, developed early in this century. While two-dimensional (2D) parameters like grain size, phase fraction, and particle aspect ratio are undeniably important, many properties are controlled by the characteristics of the three-dimensional (3D) grain boundary manifold. For example, the distribution of weak grain boundaries controls the location and roughness of the preferred fracture plane. Likewise, the connectivity of twin-type boundaries governs the corrosion resistance of grain boundary engineered materials. In this paper, we examine critical length scales in grain boundary manifolds, and we derive their relationships to interface properties such as energy, roughness, and connectivity. These new, experimentally accessible length scales provide a more precise tool for microstructural quantification as well as new insight into microstructure/property relationships.

## 11:20 AM

The Role of Grain Size and Grain Boundary Character on the Creep Behavior of INCONEL Alloy 718: C. J. Boehlert<sup>1</sup>; D. Dickmann<sup>1</sup>; S. Civelekoglu<sup>1</sup>; R. C. Gundakaram<sup>1</sup>; N. Eisinger<sup>2</sup>; <sup>1</sup>Alfred University, Sch. of Ceram. Engrg. & Matls. Sci., 2 Pine St., Alfred, NY 14802 USA; <sup>2</sup>Special Metals Corporation, Huntington, WV USA

Grain boundary engineering of metals and alloys is typically accomplished through changing the grain boundary character distribution (GBCD) by thermomechanical processing techniques. The resulting GBCD can have a significant impact on mechanical behavior especially for properties which are significantly influenced by intergranular deformation, such as creep. The GBCD of INCONEL alloy 718 has been evaluated and the results indicate that the grain boundary character is significantly dependent on processing and subsequent heat treatment, where grain size plays an important role. The grain size and GBCD also have a significant impact on the creep behavior, especially within the creep regimes associated with diffusion and grain boundary sliding. This research was supported by the NSF grant DMR-0134789.

## Third International Symposium on Ultrafine Grained Materials: Mechanical Properties

Sponsored by: Materials Processing & Manufacturing Division, MPMD-Shaping and Forming Committee
Program Organizers: Yuntian Ted Zhu, Los Alamos National Laboratory, Materials Science and Technology Division, Los Alamos, NM 87545 USA; Terence G. Langdon, University of Southern California, Departments of Aerospace & Mechanical Engineering and Materials Engineering, Los Angeles, CA 90089-1453 USA; Terry C. Lowe, Metallicum, Santa Fe, NM 87501 USA; S. Lee Semiatin, Air Force Research Laboratory, Materials & Manufacturing Directorate, Wright Patterson AFB, OH 45433 USA; Dong H. Shin, Hanyang University, Department of Metallurgy and Material Science, Ansan, Kyunggi-Do 425-791 Korea; Ruslan Z.
Valiev, Institute of Physics of Advanced Material, Ufa State Aviation Technology University, Ufa 450000 Russia

Wednesday AM	Room: 20	07A	
March 17, 2004	Location:	Charlotte Convention Center	

Session Chairs: Michael J. Zehetbauer, University of Vienna, Inst. Matls. Physics, Wien 1090 Austria; Alexei Yu Vinogradov, Osaka City University, Dept. Intelligent Matls. Engrg., Osaka 855-8585 Japan; Carl C. Koch, North Carolina State University, Matls. Sci. & Engrg., Raleigh, NC 27695 USA

## 8:30 AM Invited

Effect of Processing Techniques on the Mechanical Properties of Nanocrystalline/Ultrafine Grained Metals: Carl C. Koch<sup>1</sup>; Khaled M.S. Youssef<sup>1</sup>; <sup>1</sup>North Carolina State University, Matls. Sci. & Engrg., 233 Riddick Bldg., 2401 Stinson Dr., Raleigh, NC 27695 USA

Elemental metals with nanoscale and/or ultrafine grain sizes have been prepared by ball milling and compaction of powders and by cold rolling of bulk sheets at liquid nitrogen temperature followed by controlled annealing treatments. The metals studied include an fcc structure metal, Cu, and bcc metals Ta and Fe. The structures/microstructures are characterized by XRD and TEM. Of major importance is the grain size distribution which is obtained using dark field TEM. The mechanical behavior of these materials is probed by microhardness, miniaturized disk bend tests (MDBT), automated ball indentation tests (ABI), and shear punch tests. The results of these experiments are compared with recent work in our laboratory on Zn and research reported in the literature, which suggests that a combination of nanoscale and submicron (or even micron) size grains provides the optimum values of strength and ductility.

## 8:50 AM Invited

**Tough Ultrafine-Grained Metals at Cryogenic Temperatures:** *Yinmin Wang*<sup>1</sup>; En (Evan) Ma<sup>1</sup>; Rulsan Z. Valiev<sup>2</sup>; Yuntian T. Zhu<sup>3</sup>; <sup>1</sup>Johns Hopkins University, Matls. Sci. & Engrg., Baltimore, MD 21218 USA; <sup>2</sup>Ufa State Aviation Technical University, Inst. of Physics of Advd. Matls., Ufa 450000 Russia; <sup>3</sup>Los Alamos National Laboratory, Matls. Sci. & Tech., Los Alamos, NM 87545 USA

Ultrafine-grained metals are a new class of materials that in general own a good combination of strength and ductility at room temperature. However, the tensile stress-strain curves of these materials show a small uniform tensile elongation that limits their practical utility. In this talk, our recent experimental findings regarding the tensile properties of ultrafine-grained metals at cryogenic temperatures will be presented. The data of ultrafine-grained copper (fcc, grain size in the range of 190-300 nm), titanium (hcp, 260 nm), and iron (bcc, 200 nm) indicate that a much higher yield strength and a larger uniform tensile elongation are obtained at low temperatures. The mechanisms leading to the coexistence of the high strength and ductility at cryogenic temperatures are discussed. In particular, different from conventional metals, ultrafine-grained fcc metals (Cu and Ni) exhibit obvious temperature dependence of the yield strength, and ultrafine-grained bcc metals (e.g., Fe) show pronounced ductility at 77 K.

## 9:10 AM Invited

Deformation Behaviors of Ultrafine-Grained Al Alloys Processed by Cryomilling Techniques: F. A. Mohamed<sup>1</sup>; B. Q. Han<sup>2</sup>; E. J. Lavernia<sup>2</sup>; <sup>1</sup>University of California, Chem. Engrg. Matls. Sci., Irvine, CA 92697 USA; <sup>2</sup>University of California, Chem. Engrg. Matls. Sci., Davis, CA 95616 USA Most recently, ultrafine-grained and nanostructured aluminum alloys with grain sizes ranging from 100 nm to 500 nm have been successfully manufactured by consolidation of cryomilled aluminum powders. In the present study, uni-axial deformation behavior was used to investigate deformation mechanisms. Microstructure characteristics and X-ray diffraction patterns were also used in the present study. Characteristics of high strength and low work hardening were observed in deformation of cryomilled nanostructured aluminum alloys. The relationship among processing, microstructural characterization and mechanical deformation mechanisms was discussed.

#### 9:30 AM

#### **Cold-Deformed Cu-Ag Composite with Ultra-Fine Microstructures**: *Ke Han*<sup>1</sup>; <sup>1</sup>National High Magnetic Field Laboratory, 1800 E. Paul Dirac Dr., Tallahassee, FL 32309 USA

Co-deformation of in-situ Cu-Ag and Cu-Nb composites produces high-strength-high-conductivity materials. The composites have various applications such as winding high field magnets. The Ag and Nb were chosen to add into Cu because they have different lattice parameter from Cu and have almost no solubility in Cu at room temperature so that additions of Ag or Nb introduce limited decreasing of the conductivity. Co-deformation provides the composites with a strength level as high as 1000MPa. This strength level is significantly higher than that predicted by a law-of-mixture and it is about 1/25 of the theoretical strength of Cu (25000MPa). Moreover, the stress-strain curves indicate internal stresses developed in the materials. This paper reports an investigation of the strengthening mechanisms and internal stresses in Cu-Ag and Cu-Nb composites.

#### 9:45 AM

Compression Tests to Approximate the ECAP Deformation and Further Post-Processing of NanoSPD CP-Ti: Leonhard Zeipper<sup>1</sup>; Gerald Gemeinböck<sup>1</sup>; Michael Zehetbauer<sup>2</sup>; Georg Korb<sup>1</sup>; <sup>1</sup>ARC Seibersdorf Research GmbH, Matls. & Production Engrg., A-2444 Seibersdorf Austria; <sup>2</sup>University of Vienna, Inst. of Matls. Physics, Boltzmanngasse 5, A-1090 Vienna Austria

Ultrafine-grained and nanostructured CP-Ti exhibits extraordinary mechanical properties. A tremendous increase in strength and parallel in ductility can be achieved by an increasing number of Equal Channel Angular passes. The in situ stress-strain behaviour on the post-deformation by compression is studied using the Mecking-plot to illustrate different hardening stages. Different crack types nucleate during compression of different SPD pre-strained samples at room temperature and are discussed. Within the equal forming limit, the ECAP process is approximated by uniaxial compression tests at elevated temperatures. Furthermore the tensile behavour is reported and compared with the compressive counterpart. Links to technological post-deformation procedures like rolling and forging are given. Finally, the changing of deformation paths is seen to be a feature for further increasing the nanoSPD materials' properties.

#### 10:00 AM

Effect of Grain Size from Millimeter to Nanometers on the Flow Stress of Low Stacking Fault Energy FCC Metals: Kang Jung<sup>1</sup>; *Hans Conrad*<sup>1</sup>; <sup>1</sup>North Carolina State University, Matls. Sci. & Engrg. Dept., Raleigh, NC 27695-7907 USA

The effect of grain size d on the flow stress of Cu, Ag, Au and Pd consists of three regimes: Regime I ( $d > -10^{-6}$ m), Regime II ( $d = -10^{-8} - 10^{-6}$ m) and Regime III ( $d < -10^{-8}$ m). Grain size hardening occurs in Regimes I and II and grain size softening in Regime III. Dislocation cells occur in Regime I, but are essentially ascent in Regime II. Regime III is characterized by the absence of intergranular dislocations. The rate-controlling mechanism(s) operative in each regime are discussed.

#### 10:15 AM

# Fatigue Crack Growth in Ultrafine Grained Al-7.5Mg: Peter S. Pao<sup>1</sup>; Harry N. Jones<sup>1</sup>; Jerry C.R. Feng<sup>1</sup>; <sup>1</sup>Naval Research Laboratory, Code 6323, 4555 Overlook Ave. SW, Washington, DC 20375 USA

The fatigue crack growth rates of ultrafine grained (g.s. ~ 0.25  $\mu$ m) Al-7.5Mg produced by SPD techniques were investigated and were compared to those of powder-metallurgy (P/M) Al-7Mg (g.s. ~ 2  $\mu$ m) and ingot-metallurgy (I/M) Al-7Mg (g.s. ~ 100  $\mu$ m). Ultrafine grained Al-7.5Mg was obtained by extruding nanocrystalline particulates, which were prepared by mechanically ball milling spray atomized Al-7.5Mg powders in liquid nitrogen. Fatigue crack growth rates of ultrafine grained Al-7.5Mg are significantly higher than those of P/M Al-7Mg. The fatigue crack growth threshold is the lowest in the ultrafine grained Al-7.5Mg, follows by P/M Al-7Mg, and is the highest in I/M Al-7Mg. The higher fatigue crack growth rates and lower thresholds in ultrafine

grained Al-7.5Mg may be attributed to the much smoother fracture surface morphology and lower roughness induced crack closure.

## 10:30 AM Break

#### 10:40 AM Invited

**Deformation Behavior of Ultrafine-Grained Iron Processed by Equal-Channel-Angular Pressing**: *E. J. Lavernia*<sup>1</sup>; B. Q. Han<sup>1</sup>; F. A. Mohamed<sup>2</sup>; <sup>1</sup>University of California, Chem. Engrg. & Matls. Sci., Davis, CA 95616 USA; <sup>2</sup>University of California, Chem. Engrg. & Matls. Sci., Irvine, CA 92697 USA

In the present study, the microstructural evolution during pressing and the deformation behavior of ultrafine-grained pure Fe processed via equal-channel angular pressing (ECAP) was investigated by means of transmission electron microscopy, tensile and compressive tests. Intensive dislocation-cell blocks as well as ultrafine grains were observed after severe plastic deformation. Because of the presence of ultrafine-grained microstructure and non-equilibrium grain boundaries, the materials display a distinct mechanical behavior from their counterpart unprocessed materials. Several mechanical issues including high strength, necking deformation and low ductility were discussed.

### 11:00 AM Invited

Plastic Flow and Mechanical Behavior of Some Mg- and Al-Alloys Deformed by Equal-Channel-Angular Pressing: Peter K. Liaw<sup>1</sup>; Grigoreta Mihaela Stoica<sup>1</sup>; L. J. Chen<sup>2</sup>; E. A. Payzant<sup>3</sup>; S. R. Agnew<sup>4</sup>; C. Xu<sup>5</sup>; T. G. Langdon<sup>5</sup>; D. E. Fielden<sup>1</sup>; <sup>1</sup>University of Tennessee, Matl. Sci. & Engrg., 323 Dougherty Bldg., Knoxville, TN 37996-2200 USA; <sup>2</sup>Shenyang University of Technology, Shenyang 110023 China; <sup>3</sup>Oak Ridge National Laboratory, Metals & Ceram. Div., Oak Ridge, TN 37831 USA; <sup>4</sup>University of Virginia, Matl. Sci. Engrg., Charlottesville, VA 22904 USA; <sup>5</sup>University of Southern California, Dept. Aeros. & Mech. Engrg. & Matl. Sci., Los Angeles, CA 90089 USA

Equal-Channel-Angular Pressing (ECAP) is an efficient method of severe plastic deformation for use with metals and composites to produce novel mechanical properties. ECAP is examined as a deformation mode derived from orthogonal cutting. Some practical approaches to evaluate the induced strain during ECAP, including strain inhomogeneity, are discussed. The deformation characteristics of the magnesium alloy, ZK60, aluminum alloy, 6061Al, and aluminum composite, 6061Al/Al2O3, are reviewed. The results of grain refinement, as well as its influence on the material behavior under tensile and cyclic loading, are presented. After processing by ECAP, ZK 60 has a ductility that increases by 2-3 times, and the 6061Al/Al2O3 composite exhibits higher strength and lower ductility by comparison with the unpressed materials.

#### 11:20 AM

Fatigue Properties of Ultra-Fine Grain Materials Fabricated by Severe Plastic Deformation - The Effect of Strain Path: Alexei Yu. Vinogradov<sup>1</sup>; <sup>1</sup>Osaka City University, Dept. of Intelligent Matls. Engrg., Sumiyoshi-ku, Sugimoto 3-3-138, Osaka 855-8585 Japan

The experimental results concerning the fatigue behavior of ultrafine grain materials fabricated by severe plastic deformation (SPD) are reviewed. The possibility to significantly enhance the fatigue performance of meals and alloys after grain reduction down to nano-scopic scale is demonstrated. A special attention is paid to the influence of strain path and the amount of strain imposed during manufacturing on fatigue life and to the role of alloying and precipitation hardening in fatigue of SPD metals. The key importance of grain boundaries in fatigue damage of SPD metals is argued. The main reason limiting the fatigue life under constant stress or strain cyclic loading is supposed to be related to structural instability resulting from severe plastic deformation. Possibilities to enhance the fatigue performance of SPD materials are explored via structural stabilization through post-processing heat treatment, alloying and precipitation hardening.

#### 11:35 AM

Mechanical Behaviour of IF Steel Processed by Equal Channel Angular Pressing: Joke De Messemaeker<sup>1</sup>; Bert Verlinden<sup>1</sup>; Jan Van Humbeek<sup>1</sup>; <sup>1</sup>K.U. Leuven, Dept. of Metall. & Matls. Engrg., Kasteelpark Arenberg 44, Heverlee 3001 Belgium

The evolution of the yield stress and hardening rate measured in a compression test of IF steel processed by equal channel angular pressing (ECAP) at 200°C via route  $B_A$ , is followed up to a von Mises equivalent strain of 9. At the highest strain the dependence of the mechanical behaviour on strain path is established by comparison of the 4 classical routes A, C,  $B_A$  and  $B_C$ . The evolution and strain path dependence are linked to TEM observations of the microstructure, and the compression test data is compared with hardness measurements made on the plane of TEM observation. After annealing at 500°C for

3h the recovered microstructure, showing slight grain growth, was quantitatively analysed by EBSD. The change in yield stress and hardening rate with respect to the as-deformed samples is discussed.

#### 11:50 AM Invited

Mechanical Properties of SPD Metals and Their Physical Backgrounds: Michael Josef Zehetbauer<sup>1</sup>; <sup>1</sup>University of Vienna, Inst. of Matls. Physics, Boltzmanngasse 5, Wien 1090 Austria

This contribution reviews the exceptional mechanical properties of SPD metals (strength, ductility, and fracture toughness) and discusses the physical processes behind. Most investigations have been done on strength, showing that the hydrostatic pressure of the SPD method governs the scale of grain structure and thus the resulting strength. Since the same is true for the deformation temperature, a model has been successfully suggested by the author which correlates the resulting grain size with the extent of dislocation annihilation. As for the ductility of SPD materials, hitherto only qualitative ideas exist which either consider the number of high angle boundaries, or the high density of deformation induced vacancies both increasing the probability for grain boundary sliding. For the fracture toughness, an ultrafine grained structure should be beneficial, too, because of an increase of total fracture energy, but this has not always been confirmed by experiment.

## 12:10 PM

Mechanical Property Characterization Using Shear - Punch Tests: Ramesh Kumar Guduru<sup>1</sup>; Ronald Otto Scattergood<sup>1</sup>; <sup>1</sup>North Carolina State University, Matls. Sci. & Engrg., PO Box 7907, Raleigh, NC 27695-7907 USA

The evaluation of mechanical properties from small specimens is critical when the availability of material is limited. Shear punch testing is one such miniaturized specimen test technique from which one can obtain mechanical properties like yield strength, ultimate strength and strain hardening exponents. A shear punch testing procedure was standardized in our laboratory and the mechanical properties for different materials; mild steel, pure Al, pure Zn, austenitic stainless steel, Al 6061 alloy and martensitic stainless steel were evaluated. A linear correlation for the yield and ultimate strength was established between data obtained from shear punch and uni-axial tensile tests. The dependency of the shear strength (yield and ultimate) was studied as a function of the sample thickness and die clearance for medium and high strength materials. The effect of die/punch clearance for a given thickness was also investigated. Results will be compared for conventional and nanocrystalline materials.

## 12:25 PM

Effect of Grain Size on Fatigue Properties for Electric Refined Iron: *Chitoshi Masuda*<sup>1</sup>; <sup>1</sup>Waseda University, Kagami-Memorial Lab. for Matls. Sci. & Tech., 2-8-26, Nishiwaseda, Sinjuku, Tokyo Japan

The fatigue strength, fatigue crack propagation properties, fatigue fracture mechanisms have been studied for many metallic materials. Especially for steels many effects have been discussed. Recently the steels having fine grain size near 1 mm have been developed and their tensile strengths have increased with decreasing the grain size. The tensile strengths have been linearly related with the inverse square root of grain sizes, that is, the Hall-Petch relationship for welded steels up to about the tensile strength of 800MPa. The fatigue strengths and fatigue fracture mechanism for welded steels having fine grain size have not so cleared. In this study, the fatigue strength and fatigue fracture mechanisms are fundamentally discussed with the cast steel using electric refined iron. The ingot was forged and rolled at a medium temperature. Finally the iron was drawn into 4mm in diameter at room temperature. The average grain size was about 3 mm. The fatigue test was performed by rotating bending machine at room temperature at the stress ratio of -1. Fatigue strength for electric refined cast iron was about 300 MPa at the number of cycles to failure of 107. For S25C carbon steel normalized and S35C carbon steels(12Heats) quenched and tempered at 600°C(11 Heats), the average fatigue strengths were about 243 and 385 MPa, respectively. The electric refined iron has medium fatigue strength between S25C and S35C carbon steels. The reason of increase of the fatigue strength for electric refined iron would be caused by the decrease of the grain size of material. The fatigue crack initiation mechanism for fine grain size steels have not yet been discussed. The fatigue crack initiates on the specimen surface by slip mechanism and propagates into the outermost one grain by mode II, III or their combined mode(Stage I type crack). After pass through the outermost grain the crack direction change into the normal direction of stress axis(Stage II type crack). If the grain size is fine, the Stage I type crack propagation mechanism initiated from the specimen surface is the same as for slip mechanism proposed by Laird, the Stage I type crack is quickly change its direction and the fatigue

strength would not be expected high. But the fatigue strength for electric refined iron having fine grain size is very high. Therefore the another fatigue crack initiation mechanism would be operated.

# 5th Global Innovations Symposium: Trends in LIGA, Miniaturization, and Nano-Scale Materials, Devices and Technologies: Manufacturing and Evaluation of Lavered Nano-Scale Materials

Sponsored by: Materials Processing & Manufacturing Division, MPMD-Powder Materials Committee, MPMD-Phase Transformations Committee-(Jt. ASM-MSCTS), MPMD-Computational Materials Science & Engineering-(Jt. ASM-MSCTS), MPMD/EPD-Process Modeling Analysis & Control Committee, MPMD-Surface Engineering Committee, MPMD-Shaping and Forming Committee, MPMD-Solidification Committee

*Program Organizers:* John E. Smugeresky, Sandia National Laboratories, Department 8724, Livermore, CA 94551-0969 USA; Steven H. Goods, Sandia National Laboratories, Livermore, CA 94551-0969 USA; Sean J. Hearne, Sandia National Laboratories, Albuquerque, NM 87185-1415 USA; Neville R. Moody, Sandia National Laboratories, Livermore, CA 94551-0969 USA

Wednesday PM	Room:	2	02B		
March 17, 2004	Location	1:	Charlotte	Convention	Cente

Session Chairs: Dave F. Bahr, Washington State University, Mech. & Matls. Engrg., Pullman, WA 99164-2920 USA; Steven H. Goods, Sandia National Laboratories, Dept. 8725, Livermore, CA 94551-0969 USA; Richard G. Hoagland, Los Alamos National Laboratory, Matls. Sci. & Tech. Div., Los Alamos, NM 87545 USA

#### 2:00 PM

Nanoimprint Technology: A Low Cost, Mass Manufacture of Nanostructures: *Khershed P. Cooper*<sup>1</sup>; <sup>1</sup>Naval Research Laboratory/ Office of Naval Research, Matls. Sci. & Tech. Div., Code 6325, 4555 Overlook Ave. SW, Washington, DC 20375-5320 USA

Nanomanufacturing seeks to exploit new opportunities from the manipulation of physical, mechanical, chemical and biological processes at the nanoscale in order to produce new materials with unique properties and new devices with unique functionalities. One nanomanufacturing technology that is receiving attention is nanoimprinting. It involves using a rigid or flexible mold to imprint nano-scale forms into resist-coated materials. After reactive ion etching and lift-off, nanostructures are produced in silicon and other materials. The technique is now capable of producing simple structures, such as gratings and gates. Nanoimprinting is being promoted as a means to break the barrier that "traditional" lithography will face as the demand increases for smaller (<100nm) feature and device sizes. A variant is laser-assisted direct imprinting. It consists of directly imprinting nanostructures in rapidly-melted surfaces. This paper will review the requirements for nanomanufacturing, the current status of nanoimprinting, and materials-related issues facing techniques such as direct imprinting.

## 2:20 PM

Advances in Assembling Microsystems with Adhesives: John A. Emerson<sup>1</sup>; Neville R. Moody<sup>2</sup>; Rachel K. Guinta<sup>1</sup>; <sup>1</sup>Sandia National Laboratories, MS 0958, Albuquerque, NM 87185-0958 USA; <sup>2</sup>Sandia National Laboratories, MS 0969, Livermore, CA 94551-0969 USA

As electronic and optical microsystems reach the micro- and nanoscales, efficient assembly and packaging requires the use of adhesive bonds. A primary issue is that as bondline thickness decreases, knowledge of the stability and dewetting dynamics of thin adhesive films is important for obtaining robust, void-free adhesive bonds. While researchers have studied dewetting dynamics of thin films of model, non-polar polymers, little experimental work has been done regarding dewetting dynamics of thin adhesive films, which exhibit more complex short-range interactions. Also, the adhesion of such submicron thick bond lines is found to depend strongly on the strength of the interfacial bonding, which in turn, depends on the interfacial chemistry. In this presentation we will report on tests to date showing that the interfacial fracture toughness of thin epoxy films attached to aluminum substrates decreases with film thickness, reaching a lower limiting value of 1.5 Jm-2.

#### 2:40 PM

White Beam Diffraction Analysis of Plastic Deformation in 2D Systems: *Rosa I. Barabash*<sup>1</sup>; Gene E. Ice<sup>1</sup>; Nobumichi Tamura<sup>2</sup>; Bryan C. Valek<sup>3</sup>; John C. Bravman<sup>3</sup>; Ralph Spolenak<sup>4</sup>; Jim Patel<sup>2</sup>; <sup>1</sup>Oak Ridge National Laboratory, Metals & Ceram., MS-6118, One Bethel Valley Rd., Oak Ridge, TN 37831-6118 USA; <sup>2</sup>Berkeley National Laboratory, Advd. Light Source, Cyclotron Rd., Berkeley, CA 94720 USA; <sup>3</sup>Stanford University, Matls. Sci. & Engrg., Stanford, CA 94305 USA; <sup>4</sup>Max Planck Institut fur Metallforschung, Heisenbergstrasse 3, Stuttgart D-7056 Germany

White beam X-ray microdiffraction is particularly well suited to the study of salient features of mechanical behavior when the characteristic size associated with microstructure and/or deformation approaches the nano-scale. The mechanical properties and deformation mechanisms of materials at very small length scales gain additional features comparing with bulk deformation microstructures. Surfaces and interfaces create additional constraints and change the conditions for dislocation formation and movement in 2D systems. A statistical description of diffraction from dislocations in 2D systems is presented. White beam diffraction analysis of several distinct examples of dislocation structures in 2D systems is discussed.

#### 3:00 PM

Stress Evolution During Electrodeposition of Ni Thin Films: Sean J. Hearne<sup>1</sup>; Steve C. Seel<sup>1</sup>; Jerrold A. Floro<sup>1</sup>; Chris Dyck<sup>1</sup>; Wenjun Fan<sup>2</sup>; S. R.J. Brueck<sup>2</sup>; <sup>1</sup>Sandia National Laboratories, Nanostruct. & Semiconductor Physics Dept., PO Box 5800 MS 1415, Albuquerque, NM 87185-1415 USA; <sup>2</sup>University of New Mexico, Albuquerque, NM 87106 USA

The majority of thin films used in industrial applications grow via an islanding (Volmer-Weber) mode, where discrete islands grow until they coalesce into a continuous film. It is commonly accepted that a tensile stress is induced when these islands coalesce. However, prior to this work there had been no systematic demonstration of the functional stress generation behavior associated solely with the coalescence process. To address this Ni films were electroplated onto patterned substrates to obtain a direct comparison of the experimentallymeasured tensile stress due to island coalescence with theoretical predictions. This allowed for the systematic variation of island size and geometry while avoiding stochastic island coalescence that have plagued previous measurements obtained over the last 30 years. In the presentation, we will compare our experimentally measured results with those predicted by a Hertzian contact model recently proposed by Freund and Chason1, and with finite element models. This work was partially supported by the DOE Office of Basic Energy Sciences and by the ARO/MURI in Deep Subwavelength Optical Nanolithography. Sandia is a multiprogram laboratory of the United States Department of Energy operated by Sandia Corporation, a Lockheed Martin Company, under contract DE-AC04-94AL85000. 1 - L.B. Freund, E. Chason, JAP 89, 4866 (2001).

#### 3:20 PM

Low Stress, High Reflectivity Thin Films for MEMS Mirrors: David P. Adams<sup>1</sup>; <sup>1</sup>Sandia National Laboratories, Thin Film, Vacuum & Pkgg. Dept., PO Box 5800, Albuquerque, NM 87185 USA

The need for optical MEMs devices that handle powers approaching 1 Watt has motivated this research of high-reflectivity, low-stress thin films and their performance. While methods are established for depositing highly reflective multilayers for different wavelengths of interest, it remains challenging to apply similar films to MEMs devices that are  $\sim 2$  microns thick and hundreds of microns in width. Towards this end, we discuss the properties of low residual stress layers that have been developed for MEMs applications. Films discussed in this talk include Au with various adhesion promotion layers, Si/SiN Bragg reflectors and additional high damage threshold materials. We discuss several issues including: the mechanical properties of sputter deposited layers, stress changes that occur over months and the relationship(s) to processing, application to MEMs devices and performance during laser irradiation. In conclusion, we demonstrate the ability to maintain lambda/40 flatness (lambda= 1319nm) for mirrors as large as 500 microns.

## 3:40 PM Break

#### 4:00 PM

Deformation Recovery Processes of Nano Indents Made in Erbium Hydride Thin Films: James P. Lucas<sup>1</sup>; Neville R. Moody<sup>2</sup>; <sup>1</sup>Michigan State University, Chem. Engrg. & Matl. Sci., 3526 Engrg. Bldg, E. Lansing, MI 48824-1226 USA; <sup>2</sup>Sandia National Laboratories, Livermore, CA 94551 USA

Deformation recovery of small indents in thin erbium hydride (ErH) films made using the nano indenter was investigated by scanning probe microscopy (SPM). The thickness of the ErH films on sapphire was nominally 1200 angstroms. The degree of recovery was determined by measuring the depth change of the indent impression with time and temperature subsequent to initial indentation of the film. By relating the rate of deformation recovery via the change in surface curvature of the bottom of the indent along with the Gibbs-Thompson relation-

ship, surface diffusivity has been assessed in soft viscoelastic materials. A similar approach is taken in assessing deformation recovery processes in hard ErH films and will be presented.

## 4:20 PM

Improved Hydrogen Sensing Characteristics of Nanocrystalline Doped Tin Oxide Sensor at Lower Temperature: Satyajit Shukla<sup>1</sup>; Sudipta Seal<sup>1</sup>; Lawrence Ludwig<sup>2</sup>; Clyde Parish<sup>2</sup>; <sup>1</sup>University of Central Florida, Mech. Matls. Aeros. Engrg. (MMAE) & Advd. Matls. Procg. & Analysis Ctr. (AMPAC), Engrg. # 381, 4000 Central Florida Blvd., Orlando, FL 32816 USA; <sup>2</sup>National Aeronautics and Space Administration, John F. Kennedy Space Ctr., Kennedy Space Ctr., FL 32899 USA

Nanocrystalline tin oxide semiconductor thin film is coated on Pyrex glass (silica) substrate using the sol-gel dip-coating technique. The thin film is characterized using different analytical techniques such as scanning electron microscopy (SEM), x-ray photoelectron spectroscopy (XPS), atomic force microscopy (AFM), and high-resolution transmission electron microscopy (HRTEM). The HRTEM sample preparation is done using focused ion-beam (FIB) milling technique. Under given processing conditions, tin oxide thin film having thickness 100-150 nm and nanocrystallite size 6-8 nm is obtained. The nanocrystalline tin oxide thin film sensor is doped with 6.5 and 13 mol % indium oxide to enhance hydrogen sensitivity at lower operating temperatures. The effect of calcination and operating temperatures, chamber pressure, electrode design, and the exposure to ultraviolet radiation on hydrogen gas sensitivity, the response and the recovery time, is systematically investigated. Models have been developed to explain low temperature hydrogen gas sensitivity of doped nanocrystalline tin oxide sensor.

#### 4:40 PM

Nanoscale Mechanical Characterization of Silver Nanowires and Cu2O Nanocubes: *Xiaodong Li*<sup>1</sup>; Hongsheng Gao<sup>1</sup>; Catherine J. Murphy<sup>2</sup>; Linfeng Gou<sup>2</sup>; K. K. Caswell<sup>2</sup>; <sup>1</sup>University of South Carolina, Dept. of Mech. Engrg., 300 Main St., Columbia, SC 29208 USA; <sup>2</sup>University of South Carolina, Dept. of Chem. & Biochmst., 631 Sumter St., Columbia, SC 29208 USA

The hardness and elastic modulus of silver nanowires and Cu2O nanocubes was measured using a nanoindenter in conjunction with an atomic force microscope (AFM). The indentation hardness and elastic modulus values were compared with the bulk materials. Nanoscaole deformation behavior was studied by in situ AFM imaging of the indents. An array of nanoscale indents was successfully made on the silver wires and Cu2O cubes by directly indenting them. The shape and size of the indents are controllable. The nanoindentation approach permits the direct machining of a single silver nanowire and a Cu2O nanocube without complications of conventional lithography.

## 5:00 PM

Carbon Nanotubes and Other Fullerene-Related Nanocrystals in the Environment: A TEM Study: L. E. Murr<sup>1</sup>; J. J. Bang<sup>1</sup>; E. V. Esquivel<sup>1</sup>; <sup>1</sup>University of Texas, Metallurgl. & Matls. Engrg., 500 W. Univ. Ave., El Paso, TX 79968-0520 USA

We have discovered that carbon nanotubes and other fullerenerelated nanocrystals are pervasive in the atmosphere - both indoor and outdoor. In fact, these carbon nanostructures have been observed even in a 10,000 year-old ice core sample, which is an indication that they have existed naturally in antiquity. Controlled experiments with methane flames (methane burning with air) has allowed a great variety of carbon nanocrystals and tubes to be examined by collecting complex aggregates on transmission electron microscope (TEM) grids coated with a thin formvar/carbon support substrate films in a specially designed thermal precipitator. These studies serve as a frame of reference for the examination of hundreds of other nanoparticulate examples collected randomly in the environment and observed in the TEM. Carbon/graphitic nanotubes and nanocrystals are observed in graphite brake-lining debris and air sampling near interstate highways; and may account in part for an estimated 10 million tons of brakelining debris created in the U.S. alone over the past decade. The health implications, especially those related to respiratory illnesses are of course currently unknown, but a whole new global perspective on atmospheric nanoparticles is becoming apparent in light of these TEM observations over the past 2 years.

# Advanced Materials for Energy Conversion II: Metal Hydrides IV - Dynamics of Metal Hydrides, and Tritium Gettering

Sponsored by: Light Metals Division, LMD-Reactive Metals Committee

*Program Organizers:* Dhanesh Chandra, University of Nevada, Metallurgical & Materials Engineering, Reno, NV 89557 USA; Renato G. Bautista, University of Nevada, Metallurgical and Materials Engineering, Reno, NV 89557-0136 USA; Louis Schlapbach, EMPA Swiss Federal, Laboratory for Materials Testing and Research, Duebendorf CH-8600 Switzerland

 Wednesday PM
 Room:
 203A

 March 17, 2004
 Location:
 Charlotte Convention Center

Session Chairs: G. Louis Powell, BWXT Y-12, Y-12 National Security Complex, Oak Ridge, TN 37831-8096 USA; Arndt Remhof, Ruhr Universität Bochum, D-44780 Bochum, Germany; Jeff LaCombe, University of Nevada, Metallurgl. & Matls. Engrg., Reno, NV 89557 USA

## 2:00 PM Keynote

Visualization of the Refraction-Like Behavior of Diffusion Fronts in Solid State Diffusion: Arndt Remhof<sup>1</sup>; <sup>1</sup>Ruhr Universität Bochum, D-44780 Bochum Germany

The large mobility of hydrogen in metals make metal hydrides ideal systems for investigations of diffusion fronts and waves in solids. The diffusion coefficient, which determines the velocity of the diffusing hydrogen ions, can be varied over a wide dynamical range. In order to study the analogies (or dissimilarities) between hydrogen diffusion waves and photon diffusion in turbid media, heterostructures with locally varying diffusion constants have to be realized. With planar structures such as interfaces or "prisms" one can investigate the behaviour of hydrogen diffusion fronts when they encounter these structures. The applicability of Snell's law to this diffusive system will be discussed. The distribution of hydrogen is visualized by means of an Y switchable mirror layer. Our measurements are in good agreement with numerical simulations.

## 2:30 PM Plenary

Separation of Small Amounts of Tritium from Nitrogen and Argon Gas Streams: Joseph Raymond Wermer<sup>1</sup>; David W. Howard<sup>2</sup>; <sup>1</sup>Los Alamos National Laboratory, Tritium Sci. & Engrg. Grp., MS C348, PO Box 1663, Los Alamos, NM 87545 USA; <sup>2</sup>Westinghouse Savannah River Company, Hydrogen Tech. Sect., Bldg. 735-11A, Savannah River Site, Aiken, SC 29808 USA

Traditional methods of removing small quantities of tritium from nitrogen or argon streams have involved oxidizing the hydrogen isotopes to form water, absorption of the tritiated water on a solid absorbent (typically molecular sieve), and disposal of the absorbent as solid radioactive waste. The handling concerns with tritiated water (HTO) as well as the cost of recycle or disposal has prompted new technology development. Recent advances in tritium processing technology has focused on methods of removing very small amounts of tritium from nitrogen or argon gas streams which 1) have high efficiency, 2) do not produce oxides of hydrogen, and 3) can be easily regenerated. Both palladium diffusers and metal getter technologies, or a combination of both, have been employed to solve this problem. In the metal getter area, a large effort has been underway for some time to find suitable materials that are compatible with the carrier gas streams.

## 3:00 PM Keynote

Relations Between Characteristics of Oxidation Overlayers and Hydride Development on Polycrystalline Uranium Surfaces: *M. Brill*<sup>1</sup>; J. Bloch<sup>1</sup>; Y. Ben-Eliyahu<sup>1</sup>; D. Hamawi<sup>1</sup>; T. Livneh<sup>1</sup>; M. H. Mintz<sup>2</sup>; <sup>1</sup>Nuclear Research Center Negev, PO Box 9001, Beer Sheva 84190 Israel; <sup>2</sup>Ben Gurion University of the Negev, Dept. of Nucl. Engrg., PO Box 653, Beer Sheva 84105 Isreal

The initial stages of hydrides development on hydride-forming metal surfaces are significantly affected by the chemical-structural properties of the oxidation overlayers that usually coat those surfaces. In the present study, controlled oxidation procedures were utilized to grow such thin (100-200Å) overlayers on polycrystalline uranium. The hydrides precipitation and growth kinetics were continuously monitored on these samples utilizing Hot-Stage-Microscopy (HSM). Correlations between certain properties of oxide layers and the hydride development kinetics were evaluated. It turned out that hightemperature, low pressure oxidation processes, yield significantly more protective layers than ambient oxidation. Utilizing X-Ray Diffraction (XRD) and Raman spectroscopy it is concluded that such high temperature oxidation produces surface dioxide that is less defected than native oxide formed on uranium under ambient conditions. For a given high temperature oxidation procedure, the protective ability of the oxide depends on the oxygen exposure time, passing through a maximum. The occurrence of such a maximum is accounted for by the texture-thickness varieties of the layers.

## 3:25 PM Keynote

Effects of Surface Conditions and Thermomechanical Processing on Uranium Hydride Kinetics: *David F. Teter*<sup>1</sup>; Robert J. Hanrahan<sup>1</sup>; <sup>1</sup>Los Alamos National Laboratories, MST6, Bikini Atoll Rd., MS G770, Los Alamos, NM 87545 USA

The nucleation kinetics of uranium hydride depend strongly on the surface condition of the metal. In most bulk hydriding kinetics measurements, the surface is either pre-hydrided or activated to remove the nucleation barrier so that repeatable reaction kinetics are measured. In the present study, the effect of the surface condition of the metal on the hydriding kinetics was examined. Oxidized uranium rods with varying thicknesses were exposed to hydrogen to study the nucleation of hydride pits. The time to nucleation was found to increase with increasing oxide thickness. Also the nucleation time was dramatically reduced when the sample was vacuum outgassed even though the oxide thickness was unchanged. These observations are consistent with diffusion of hydrogen through the oxide layer being the ratelimiting step for hydride nucleation. Results of the effects of flow stress on the hydriding kinetics of uranium wires will also be presented.

## 3:50 PM Break

#### 4:05 PM Plenary

Reaction of Oxygen With Uranium Hydride: George L. Powell<sup>1</sup>; <sup>1</sup>BWXT-Y12, LLC, Tech. Dvlp., PO Box 2009, Bear Creek Rd., Oak Ridge, TN 37831-8096 USA

Kinetics of the  $O_2$  with  $UH_3$  sponsored by DOE's National Spent Nuclear Fuels Program through INEEL was measured to deduce a defendable model for this reaction. The sample was located in an infrared gas cell with a mass spectrometer. The U was reacted isobarically with  $H_2$  to yield  $UH_3$  that was further characterized by surface sorption and desorption of  $H_2$ . Subsequent experiments used  $O_2$  expansion to effect the reaction. The production and sorption of  $H_2$  on the  $UH_3$  yielded the reaction kinetics at low  $O_2$  pressures and balanced the chemical equation for the reaction. Infrared gas analysis excluded  $H_2O$  as a reaction product. Light emission synchronized with the  $O_2$  gas transfer and subsequent mass spectrometric analyses showed the quenching of the reaction by  $H_2$ . \*Managed by BWXT Y-12, LLC for the U.S. Department of energy under contract DE-AC05-00OR22800.

#### 4:35 PM Invited

Thermal Desorption Measurements of Hydrogen on Uranium Metal Surfaces: *Quirinus G. Grindstaff*<sup>1</sup>; <sup>1</sup>BWXT-Y12, LLC, Tech. Dvlp., PO Box 2009, Bear Creek Rd., Oak Ridge, TN 37831-8096 USA

Environmental corrosion of uranium metal produces an oxide film in which the oxygen/water/hydrogen "equilibrium" within the film regulates its growth. At high temperatures, this reaction produces hydrogen that absorbs into the bulk metal affecting subsequent mechanical properties (ductility) upon cooling. At low temperatures and in closed systems, this residual hydrogen in the oxide film may result in the formation of uranium hydride pits, which subsequently may lead to external hydrogen embrittlement, or fires upon exposure to air. Thermal desorption experiments using mass spectroscopy to monitor the rate that hydrogen desorbs from uranium coupons during heating in vacuum is being pursued as a method of determining the nature and distribution of hydrogen in and on uranium. In particular, the thermal desorption rates are being used to discriminate between hydrogen distributed within the metal, hydrogen as uranium hydride on the metal surface, and as other hydrogen species in the uranium oxide film. \*Managed by BWXT Y-12, LLC for the U.S. Department of energy under contract DE-AC05-00OR22800.

#### 5:00 PM Invited

## Reaction of Hydrogen With an Organic Hydrogen Getter: George L. Powell<sup>1</sup>; <sup>1</sup>BWXT-Y12, LLC, Tech. Dvlp., PO Box 2009, Bear Creek Rd., Oak Ridge, TN 37831-8096 USA

DEB (1,4 bis (phenyl ethynyl) benzene typically mixed with 25 wt.% C-1 wt.% Pd) are made into organic hydrogen getters in porous pellet form by Honeywell Federal Manufacturing and Technologies Kansas City Plant. The hydrogen gettering reactions are very effective, and irreversible since the hydrogen gas is converted into an or-

ganic hydrocarbon. A simple two-volume system was used to incrementally titrate DEB pellets resulted in a series of pressure drop curves, from which the reaction rate was determined as a function of H2 pressure, DEB reaction extent, and temperature. Experimental methods are described for obtaining the measurements along with data analysis for reducing the pressure decay curves to a four-dimensional reaction rate model. \*Managed by BWXT Y-12, LLC for the U.S. Department of energy under contract DE-AC05-00OR22800.

# Advanced Materials for Energy Conversion II: Magnetic Materials & Hydrogen Permeation

Sponsored by: Light Metals Division, LMD-Reactive Metals Committee

*Program Organizers:* Dhanesh Chandra, University of Nevada, Metallurgical & Materials Engineering, Reno, NV 89557 USA; Renato G. Bautista, University of Nevada, Metallurgical and Materials Engineering, Reno, NV 89557-0136 USA; Louis Schlapbach, EMPA Swiss Federal, Laboratory for Materials Testing and Research, Duebendorf CH-8600 Switzerland

Wednesday PM	Room: 2	04
March 17, 2004	Location:	Charlotte Convention Center

Session Chairs: Jay Keller, Sandia National Laboratory, Livermore, CA 94550 USA; Shin-ichi Orimo, Tohoku University, Inst. for Matls. Rsch, Sendai, Miyagi 980-8577 Japan; Renato G. Bautista, University of Nevada, Metallurgl. & Matls. Engrg., Reno, NV 89557-0136 USA

#### 2:00 PM Keynote

Control of Magnetocaloric Effects by Hydrogen Absorption into La(FexSi1-x)13 Magnetic Refrigerants: *Kazuaki Fukamichi*<sup>1</sup>; Asaya Fujita<sup>1</sup>; <sup>1</sup>Tohoku University, Dept. of Matls. Sci., Grad. Sch. of Engrg., Aoba-yama 02, Sendai, Miyagi 980-8579 Japan

Instead of conventional gas refrigerations, we are yearning for the development of new-type high performance refrigerants because of energy efficiency and environmental safety. Recently, we have developed promising magnetic refrigerant compounds  $La(Fe_xSi_{1-x})_{13}$  $(0.86 \le ?? \le 0.90)$  which show the first-order of the itinerant-electron metamagnetic transition from the paramagnetic state to the ferromagnetic state in applied magnetic fields. These compounds exhibit large values of the isothermal magnetic entropy change  $\Delta S_m$  and the adiabatic temperature change  $\Delta T_{ad}$  in the vicinity of the Curie temperature  $T_c \sim 190K$ . Controlling  $T_c$  of  $La(Fe_xSi_{1-x})_{13}H_y$  by absorbing hydrogen, we can control easily T<sub>c</sub> and also the working temperature covering room temperature. Furthermore, thermal conductivity and diffusivity of the present compounds are excellent, comparable tho se of Gd metal reported as one of the candidates for magnetic refrigerants. Finally, it should be emphasized that the elements of the present compounds are very cheap economically and also completely harmless for human life.

#### 2:30 PM Keynote

Advances in Magnetic Cooling: Karl A. Gschneidner<sup>1</sup>; Vitalij K. Pecharsky<sup>1</sup>; <sup>1</sup>Iowa State University, Ames Lab., Ames, IA 50011-3020 USA

Magnetic refrigeration can be cost effective and save considerable energy (20 to 30%) over conventional gas compression technology. It is also an environmentally friendly technology, eliminating ozone depleting chemicals (CFCs), green house gases, (HCFCs and HFCs) and hazardous chemicals (NH<sub>3</sub>). In 1997 Astronautics Corp. of America and Ames Laboratory demonstrated that magnetic refrigeration is a viable technology for near room temperature applications, such as large scale building air conditioning, refrigeration/freezer food processing plants and supermarket chillers. Since then seven other magnetic refrigerators have been reported to be operational - a second Astronautics Corp. of America refrigerator, three by the Japanese, and one each in Canada, China and France. Most of the recent devices use permanent magnets as the magnetic field source, and thus are aimed at the consumer markets for household refrigerator/freezers and air conditioners, and automotive climate control. The future prospects of magnetic cooling are quite favorable.

#### 2:55 PM

Rare-Earth Free Magnetostrictive Fe-Ga-X Alloys for Actuators and Sensors: Pinai Mungsantisuk<sup>1</sup>; Robert P. Corson<sup>1</sup>; *Sivaraman Guruswamy*<sup>1</sup>; <sup>1</sup>University of Utah, Metallurgl. Engrg., 135 S. 1460 E., Rm. 412, Salt Lake City, UT 84112-0114 USA In our earlier work, we have shown that rare-earth free bcc Fe-Ga based alloys have an excellent combination of large low-field room temperature magnetostriction, good mechanical properties, and low hysteresis. These alloys are very attractive in numerous energy conversion device applications such as acoustic sensors and generators, linear motors and actuators. This paper examines the influence of partially substituting Ga in FeGa alloys with Al, Si, Ge, and Sn on the magnetostrictive behavior of FeGa based alloys. Magnetic, magnetostrictive, and elastic properties of the various ternary alloys are presented. It is shown that substitution of Ga with Al can be made in FeGa alloys in certain composition ranges without a reduction in magnetostriction, and the addition of Si, Ge, and Sn results in a decrease of magnetostriction. The FeGaAl ternary alloy maintains all the attractive features in the binary FeGa alloys. Work supported by NSF Grant #0241603.

### 3:20 PM Break

## 3:40 PM Invited

Hydrogen Permeation of Ternary Ti-Ni-Nb Alloys: Kiyoshi Aoki<sup>1</sup>; Kazuhiro Ishikawa<sup>1</sup>; Kunihiko Hashi<sup>1</sup>; Takeshi Matsuda<sup>1</sup>; <sup>1</sup>Kitami Institute of Technology, Matls. Sci., Koen-chyo, Kitami, Hokkaido 090-8507 Japan

Hydrogen permeation characteristics of ternary Ni-Ti-Nb alloys were investigated in the pressure range of 0.2-0.97 MPa on the upstream side and the temperature range of 523-673 K. Hydrogen permeability of the B2-NiTi phase is 10-10 [mol H2 m-2 s-1 Pa-0.5] figures and that of the Ni30Ti31Nb39 alloy is1.93x10-8 [mol H2 m-2 s-1 Pa-0.5] at 673 K. The Ni30Ti31Nb39 alloy consists of the primary phase, bcc-NbTi, and the eutectic NiTi-NbTi alloys. The NiTi phase plays a major role in prevention of hydrogen brittleness for the NbTi phase, and the NbTi phase contributes mainly to the hydrogen permeation of this alloy.

#### 4:05 PM

Hydrogen Permeation in Nickel Based Alloys: Joshua H. Lamb<sup>1</sup>; Venugopal Arjunan<sup>1</sup>; Dhanesh Chandra<sup>1</sup>; <sup>1</sup>University of Nevada, Metall. & Matls. Sci., 1664 N. Virginia St., MS 388, Reno, NV 89557-0136 USA

The hydrogen permeation properties of the nikel based alloy C-22 were examined. The alloy C-22 has been chosen to play a critical role in the storage of high level nuclear waste at the Yucca Mountain High Level Waste Repository. The expected humid enviornment within the waste repository has the potential for creating a cathodic charge on the surface of materials to be used in the facility. The presence of a cathodic charge stimulates the ionization of hydrogen, which will then diffuse into the material. The level of suceptibility of C-22 to this phenomenon is determined using an electrochemical method. The level of suceptibility of C-22 to both hydrogen diffusion and hydrogen induced cracking is found.

#### 4:25 PM

The Influence of Group IVA Elements on the Magnetostriction of Fe: *Robert P. Corson*<sup>1</sup>; Pinai Mungsantisuk<sup>1</sup>; Sivaraman Guruswamy<sup>1</sup>; <sup>1</sup>University of Utah, Metallurgl. Engrg., 135 S. 1460 E., Rm. 412, Salt Lake City, UT 84112-0114 USA

This paper examines the changes in magnetostriction of Fe when Group IVA elements (Si, Ge, and Sn) are added to Fe in the concentration range of 2 to 15%. Each of these elements has a filled or empty dshell, and have similar ground state valence electron configuration (s2p2). However, the atomic size increases as one moves down the column. The alloys were prepared by directional solidification to obtain (100) texture. Magnetostrictive, x-ray and elastic properties of the alloys were measured. Correlations between changes in magnetostriction, magnetic properties, elastic properties, and lattice parameter are performed. The results are contrasted with earlier work on Ga and Al additions that result in large increases in the magnetostriction of iron. This research effort seeks to understand how the alloying additions modify the magnetostriction in Fe and develop the ability to engineer alloys for various actuation and sensing applications.

## 4:50 PM

Influence of Ordering on the Magnetostriction of Fe-(27.5- y) at.% Ga- y at.% Al Alloys: *Rebecca Charlotte Chandler*<sup>1</sup>; Sivaraman Guruswamy<sup>1</sup>; <sup>1</sup>University of Utah, Metallurgl. Engrg., 135 S. 1460 E., Rm. 412, Salt Lake City, UT 84112-0114 USA

Fe-27.5 at. % Ga alloys can be heat treated to obtain ordered phases based on a DO3(ordered bcc), D019 (ordered hexagonal), and L12 (ordered fcc) structures. This work examines the heat treatment conditions required to obtain these different phases and how the substitution of Ga with Al influences these ordering reactions. An evaluation of how the different ordering treatments influence the magnetostriction in polycrystalline Fe-27.5 at.%Ga, Fe-13.75 at.% Ga-13.75 at.% Al, and Fe-20.625 at.% Ga -6.875 at.% Al alloys is made. The samples were annealed first in the disordered bcc (A2) phase region to obtain a disordered bcc solid solution, followed by ordering-heat treatment in the appropriate temperature region of stability of each of the ordered phases. X-ray diffraction was used to characterize the phases after heat treatments. Magnetostriction measurements were made at different prestress levels. Magnetic properties were measured using a VSM. Work supported by NSF-DMR Grant # 0241603.

# Advances in Superplasticity and Superplastic Forming: Modeling of Superplastic Forming Processes and Materials

Sponsored by: Materials Processing and Manufacturing Division,
Structural Materials Division, MPMD-Shaping and Forming
Committee, SMD-Mechanical Behavior of Materials-(Jt. ASM-MSCTS),
SMD-Structural Materials Committee
Program Organizers: Eric M. Taleff, University of Texas,
Mechanical Engineering Department, Austin, TX 78712-1063 USA;
P. A. Friedman, Ford Motor Company, Dearborn, MI 48124 USA;
Amit K. Ghosh, University of Michigan, Department of Materials
Science and Engineering, Ann Arbor, MI 48109-2136 USA; P. E.
Krajewski, General Motors R&D Center; Rajiv S. Mishra, University
of Missouri, Metallurgical Engineering, Rolla, MO 65409-0340
USA; J. G. Schroth, General Motors, R&D Center, Materials and
Processes Laboratory, Warren, MI 48090-9055 USA

Wednesday PM	Room: 2	01B
March 17, 2004	Location:	Charlotte Convention Center

Session Chairs: James G. Schroth, General Motors, R&D Ctr., Matls. & Processes Lab., Warren, MI 48090-9055 USA; Peter A. Friedman, Ford Motor Company, Dearborn, MI 48124 USA

## 2:00 PM

Influence of Friction and Die Geometry on Simulation of Superplastic Forming of Al-Mg Alloys: *N. R. Harrison*<sup>1</sup>; S. G. Luckey<sup>2</sup>; P. A. Friedman<sup>2</sup>; Z. C. Xia<sup>2</sup>; <sup>1</sup>University of Michigan, Dept. of Mech. Engrg., 2350 Hayward St., Ann Arbor, MI 48109 USA; <sup>2</sup>Ford Motor Company, Scientific Rsch. Lab., 2101 Village Rd., MD 3135/SRL, Dearborn, MI 48124 USA

The ability to form complex shapes from aluminum sheet makes superplastic forming an attractive option in the automotive industry. Al-Mg alloys such as AA5083 show moderate superplastic characteristics while also having adequate post-formed properties. However, the additional cost associated with processing these materials to be suitable for superplastic forming has prevented their widespread use. Recent work has shown that it may be possible to superplastically form conventionally-processed Al-Mg alloys, such as AA5182, for relatively simple parts where high strains are not required. However, the lower strain-rate sensitivity associated with these conventionally-processed, lower-cost alloys can result in premature thinning and failure in forming operations. This paper compares the influence of friction and die geometry on the forming simulation of both alloys using the Abaqus standard finite element software. The 2-dimensional simulation of a long rectangular box where plane strain is assumed was performed using solid elements. The motivation for this work lies in the understanding of the thinning behavior of materials with different strainrate sensitivities (m-value) through observation of depth of draw, forming time and pressure cycle.

## 2:20 PM

Development of MARC for Analysis of Quick Plastic Forming Processes: Krishna Murali<sup>2</sup>; *G. Paul Montgomery*<sup>1</sup>; James G. Schroth<sup>3</sup>; <sup>1</sup>General Motors, R&D Ctr., MC 480-106-359, 30500 Mound Rd., Warren, MI 49090-9055 USA; <sup>2</sup>General Motors, Warren, MI 48090-9055 USA; <sup>3</sup>General Motors, R&D, MC 490-106-212, 30500 Mound Rd., Warren, MI 48090-9055 USA

MARC, an implicit finite element code developed by MARC Analysis Research Corporation and later acquired by MacNeal-Schwendler Corporation, has been used to simulate the Quick Plastic Forming (QPF) process. For accurate simulations, GM developed pressure control algorithms to maintain the desired strain rate, a job-termination criterion to stop a simulation at the correct stage, and constitutive equations to describe material behavior accurately. These tools have been used successfully in plane-strain, generalized-plane-strain, and 3D MARC analyses of QPF panels. The first application of 3D MARC analysis was to the GM EV1 wheelhouse. Simulation was performed while the production tool was being machined. Changes recommended by the analysis were implemented in the tool and parts were successfully manufactured. Good correlation was obtained between predicted and measured thickness in the panels.

#### 2:40 PM

# Effect of the Constitutive Equation on MARC Analysis of Quick Plastic Forming: *G. Paul Montgomery*<sup>1</sup>; 'General Motors, R&D Ctr., MC 480-106-359, 30500 Mound Rd., Warren, MI 48090-9055 USA

A constitutive equation that explicitly includes the dependence of stress on both strain and strain rate has been developed for aluminum alloy AA5083 by fitting tensile-test data. This paper uses the MARC finite element code to compare the results of Quick-Plastic-Forming (QPF) simulations that use this new equation with results of previous simulations which used constitutive equations that depend only on strain rate. Test cases include plane strain analysis of a section through the G90 side-frame outer (original design) and 3D analyses of a rectangular butter tray and the EV1 wheelhouse. This paper also investigates the effect of allowing a higher maximum pressure during the forming process.

#### 3:00 PM Break

## 3:20 PM

## Mechanical Behavior and Modeling of AA5083 at 450C: Paul E. Krajewski<sup>1</sup>; G. Paul Montgomery<sup>1</sup>; <sup>1</sup>General Motors, R&D Ctr., 30500 Mound Rd., MC 480-106-212, Warren, MI 48090 USA

The mechanical behavior of AA5083 at 450°C, which was determined from tensile tests, was characterized for strain rates ranging from 0.0005/s to 0.3/s. As strain rate increased, a transition occurred from classic power-law-type hardening to transient behavior where a pronounced yield point was followed by strain softening. The powerlaw-type hardening regime was accurately modeled using a physicsbased model that contained quasi-static, thermally activated, and viscous drag components. The complete stress-strain curve as a function of strain rate was modeled using a three-part phenomenological equation that incorporated hardening, transient, and damage components.

## 3:40 PM

#### **Forming Limit Diagram of a Superplastic Formable AA5083 Aluminum Alloy**: *Mihai Vulcan*<sup>1</sup>; Klaus Siegert<sup>1</sup>; <sup>1</sup>University of Stuttgart, Inst. for Metal Forming Tech., Holzgartenstrasse 17, Stuttgart 70174 Germany

The theoretical and experimental work on superplastic materials at the Institute for Metal Forming Technology (IFU) of the University of Stuttgart, Germany is focused on aluminum alloys. Two analytical models have been used for bulging superplastic materials using circular and elliptical draw rings. The experiments have been carried out with an in-house built equipment in order to verify the theoretical models and to determine the forming limit diagram for a superplastic aluminum alloy AA5083 at a specific forming temperature and strain rate. The pressure-time paths determined from the analytical models were also verified by FEM process simulations. Finally, further FEM simulations have been done in order to determine the pressure-time path for the superplastic forming process of an automotive body part. The part, a license pocket plate of the rear deck lid, has been superplastically formed using the matrice forming technique.

#### 4:00 PM

Integrated Approach for Optimization of Superplastic Forming: Pushkarraj V. Deshmukh<sup>1</sup>; Naveen V. Thuramalla<sup>1</sup>; Fadi K. Abu-Farha<sup>1</sup>; Marwan K. Khraisheh<sup>1</sup>; <sup>1</sup>University of Kentucky, Ctr. for Mfg., Mech. Engrg. Dept., 210 CRMS Bldg., Lexington, KY 40506-0108 USA

In this work, the Superplastic Forming Process (SPF) is optimized using microstructure-based constitutive models of deformation and failure. Superplastic deformation is modeled within the continuum theory of viscoplasticity with an anisotropic yield function and a microstructure-based overstress function. A multi-scale stability criterion taking into account both geometrical (macroscopic) and microstructural features, including grain growth and cavitation, is presented. These models are incorporated into a FE code and are used to generate optimum forming pressure profiles. It is shown that the FE results on forming time and thinning using the optimum pressure profile are better than those obtained using other forming conditions.

#### 4:20 PM

Aspects of Element Formulation and Strain Rate Control in Numerical Modeling of Superplastic Forming: S. G. Luckey<sup>1</sup>; P. A. Friedman<sup>1</sup>; Z. C. Xia<sup>1</sup>; <sup>1</sup>Ford Motor Company, Scientific Rsch. Lab., 2101 Village Rd., MD 3135/SRL, Dearborn, MI 48124 USA

The ability to accurately and cost effectively simulate superplastic forming (SPF) processes is an essential step to achieving widespread use of this technology in the automotive industry. Practical and fundamental understanding of the capabilities and limitations of different finite element formulations in SPF is paramount to establishing simulation tools that are critical to die design and process development. In this paper, the results of a study comparing different element formulations in simulating superplastic forming with the ABAQUS finite element software are discussed. Simulations were performed with solid, shell and membrane elements to predict forming characteristics and pressure-time curves. Simulation of the 2-dimensional forming process with layered solid elements of a long rectangular cavity accurately predicted strain localization in the vicinity of the die entry radii. However, this thinning phenomenon was not captured in simulations with shell or membrane elements. Furthermore, FEA predictions of SPF pressure-time curves have been found to be greatly affected by the element type and the type of strain rate control methods instituted in the simulation. Two methods of strain rate control were applied in this study: an algorithm based on limiting the rate of deformation in the element with the largest strain rate and a second algorithm which limits the rate of deformation based on an average of the fastest straining elements. The resulting pressure-time curves for each of these formulations were compared with respect to each type of element. Application of the averaging scheme in controlling strain rate was found to reduce the differences between the predicted pressuretime curves for the different types of elements.

#### Aluminum Reduction Technology: Environmental

Sponsored by: Light Metals Division, LMD-Aluminum Committee Program Organizers: Tom Alcorn, Noranda Aluminum Inc., New Madrid, MO 63869 USA; Jay Bruggeman, Alcoa Inc., Alcoa Center, PA 15069 USA; Alton T. Tabereaux, Alcoa Inc., Process Technology, Muscle Shoals, AL 35661 USA

Wednesday PM	Room: 213D
March 17, 2004	Location: Charlotte Convention Center

Session Chair: Ken Martchek, Alcoa Inc., Wexford, PA 15090 USA

#### 2:00 PM

Ventilation Rates of Smelter Buildings in Northern Climates: Edgar Dernedde<sup>1</sup>; <sup>1</sup>Kroll International, 1820 Rue Nancy, Brossard, Quebec J4Y 2M5 Canada

Modern smelter buildings are ventilated by natural ventilation, which makes good use of the large heat loss from aluminum reduction cells. Ventilation rates are usually high during the summer period. During winter, however, the ventilation rate is reduced in smelters located in northern climates, in order to maintain adequate working conditions inside the cell room. During the cooler seasons sidewall, basement and roof openings of a smelter building may be closed partially, which effectively reduces the ventilation rate. Airflows through cell rooms with 180 kA S/S prebake cells were estimated theoretically for ventilation conditions during all seasons of the year. The results were compared with measurements taken on scale models of a smelter building. The agreement was satisfactory.

## 2:25 PM

Improvement of Pot Gas Collecting Efficiency by Implementation of Impulse Duct System: *Michael Sahling*<sup>1</sup>; Elmar Sturm<sup>1</sup>; Geir Wedde<sup>2</sup>; <sup>1</sup>Hamburger Aluminium-Werk GmbH, Potrms., Dradenauer Hauptdeich 15, Hamburg 21111 Germany; <sup>2</sup>Alstom Power, Environment, Ole Deviks vei 10, Oslo 0666 Norway

At existing dry scrubbers the drop of differential pressure is given by design of bag filters and the pot ducting at a given gas volume. To meet new regulations for HF-emissions at increased production referring to pot gas capture efficiency the total gas volume of a plant has to be increased which result in higher duct losses. At the HAW smelter in Germany the new impulse duct principle has been installed in the ducting from the pots to the dry scrubber. The gas volume was increased by 20% by adding more filter and fan capacity. The additional pot duct losses could be fully compensated for by the impulse duct system and reveals as a good additional cost effective solution for retrofitting of dry scrubbers.

#### 2:50 PM

**Experiences With High Performance Dry and Wet Scrubbing Systems for Potlines**: *Geir Wedde*<sup>1</sup>; Astrid Holmsen<sup>1</sup>; Terje Opsahl<sup>1</sup>; <sup>1</sup>Alstom Power Norway AS, Ole Deviks Vei 10, Oslo Norway For recent smelter potline expansions in Norway, the ABART system for dry scrubbing of fluorides with downstream seawater scrubbers for SO2 removal, have been installed. This has been successfully implemented with low power consumption and extremely low emissions of both fluorides and SO2 as a result. This paper reviews recent experiences and performances with the ABART dry scrubbing technology as well as the seawater desulphurisation process.

## 3:15 PM

Alumina Structural Hydroxyl as a Continuous Source of HF: Margaret M. Hyland<sup>1</sup>; Barry J. Welch<sup>2</sup>; Edwin Patterson<sup>1</sup>; Toshifumi Ashida<sup>3</sup>; James B. Metson<sup>2</sup>; <sup>1</sup>University of Auckland, Chem. & Matls. Engrg., PB 92019, Auckland New Zealand; <sup>2</sup>University of Auckland, Light Metals Rsch. Ctr., PB 92019, Auckland New Zealand; <sup>3</sup>Kinki University, Dept. of Biotech. & Chmst., Sch. of Engrg. Japan

The link between moisture on alumina and HF generation in aluminium reduction cells has been long established. The assumption has usually been that the 'culprit' is the loosely bound adsorbed water, generating HF via bath hydrolysis as this surface water is flashed off during alumina feeding. Structural water, or more correctly, structural hydroxyl, also makes a significant contribution to HF generation. Laboratory experiments show that hydroxyl can dissolve in molten cryolitic electrolytes and gives rise to electrochemically generated HF. The electrochemically generated HF could be readily distinguished from HF generated via thermal hydrolysis. Experiments with aluminas of varying combinations of high and low surface adsorbed moisture and structural hydroxyl (as measured by their LOI (20-300) and LOI (300-1000), respectively) confirmed the importance of electrochemically generated HF from structural hydroxyl. While some of the structural hydroxide reacts rapidly at the time of feeding, it also contributes to the steady state HF emission. From plant studies it was estimated that up to 8 kg F/tonne Al was generated from structural hydroxyl, for aluminas containing 0.4 wt % LOI (300-1000) and assuming 3wt% alumina in the bath. Structural hydroxyl is found in transition alumina phases in smelter grade aluminas. Their presence ensures that even conservative smelter specifications of surface areas of 60-80 m2/g can be met. Paradoxically, this surface area is specified to ensure that the HF adsorption capacity of the alumina is sufficient for scrubber requirements, but for reasons of both surface and structural water incorporation, having a high surface area also means that the alumina will generate more HF. This reopens the debate on the merits of high surface area aluminas.

## 3:40 PM Break

## 3:50 PM

International Aluminium Institute Anode Effect Survey Results: Willy Bjerke<sup>1</sup>; Robert Chase<sup>1</sup>; Reginald Gibson<sup>1</sup>; Jerry Marks<sup>1</sup>; <sup>1</sup>International Aluminium Institute, New Zealand House, Haymarket, London SW1 Y 4TE UK

The International Aluminium Institute (IAI) conducts annual surveys of member companies on anode effect performance data. The anode effect data allows calculation of specific emissions of PFCs and also allows survey participants to benchmark anode effect performance with others operating with similar technology. IAI member companies now account for over seventy-five% of world primary aluminum production. The survey data collected include average anode effect frequency, average anode effect duration and anode effect overvoltage. The data show that in the twelve years covering the period 1990 to 2001 IAI members reduced CO2 equivalent emissions from 4.0 to 1.2 metric tons of carbon dioxide equivalents per metric ton of primary aluminium for the two combined PFCs, a reduction of 70%. This substantial reduction in specific emissions for a greenhouse gas have been reduced even as total production has increased.

## 4:15 PM

**PFC Emission Measurements at DUBAL Potlines**: *Ahmed Karim Gupta*<sup>1</sup>; Vijayakumar C. Pillai<sup>1</sup>; Jerry Marks<sup>2</sup>; <sup>1</sup>Dubai Aluminium Company Ltd., Environml. Control, Smelter Ops., Jebel Ali, PO Box 3627, Dubai United Arab Emirates; <sup>2</sup>J Marks & Associates, 312 NE Brockton Dr., Lee Summit, MO 64064 USA

Measurements of the perfluorocarbon compounds (PFC) tetrafluoromethane (CF4) and hexafluoroethane (C2F6) were carried out for Dubal's D18 (180kA bar broken CWPB) and CD20 (210kA PFPB) cell technologies using FTIR Spectrometry, according to the US EPA Draft Protocol for PFC Measurements from Primary Aluminium Production. CF4 was measured by collecting time average samples from the exhaust duct at the entrance to the dry scrubber. The ratio of C2F6 to CF4 was measured by extractive FTIR in a continuous and real time manner. The measurement results were compared with anode effect (AE) data to derive the Intergovernmental Panel on

Climate Change (IPCC) Tier 3b coefficients. The coefficients are used in the IPCC Tier 3 method that is recommended for the most accurate inventory of PFCs from primary aluminium production. Dubal's ability to collect process data for both AE voltage and time on AE allowed the determination of both the Slope and Overvoltage equation coefficients. This paper presents the results of the PFC measurements and the calculated IPCC Tier 3b coefficients. The paper also compares the efficacy of the Slope method and the Overvoltage method for estimating PFC emissions. Finally results of measurements of PFC emissions from new cells following bath-up are presented. The results confirm the evolution of PFC during early high voltage cell operation and provide insight into the time and voltage dynamics of these emissions during new cell start up.

## 4:40 PM

In-Plant Performance Comparison of Fourier Transform and Photoacoustic Infra-Red PFC Monitors: Neal R. Dando<sup>1</sup>; Weizong Xu<sup>1</sup>; Luis Espinoza-Nava<sup>1</sup>; <sup>1</sup>Alcoa Technology, 100 Techl. Dr., Alcoa Ctr., PA 15069 USA

Several different infra-red (IR)-based technologies have been proposed for monitoring perfluorocarbon (PFC) emissions at aluminum smelters. Unfortunately comparative in-plant performance data is virtually non-existant for these technologies. This paper presents the results of several in-plant comparative performance evaluations of Fourier transform (FT) and photoacoustic (PA)-IR based PFC monitors and discusses the relative merits of each technology for executing capable in-plant PFC montoring campaigns.

# Aluminum Reduction Technology: Materials and Fundamentals

Sponsored by: Light Metals Division, LMD-Aluminum Committee Program Organizers: Tom Alcorn, Noranda Aluminum Inc., New Madrid, MO 63869 USA; Jay Bruggeman, Alcoa Inc., Alcoa Center, PA 15069 USA; Alton T. Tabereaux, Alcoa Inc., Process Technology, Muscle Shoals, AL 35661 USA

Wednesday PM	Room: 2	13A
March 17, 2004	Location:	Charlotte Convention Center

Session Chair: John J.J. Chen, The University of Auckland, Chem. & Matls. Engrg., Auckland New Zealand

## 2:00 PM

**20 Years of Bath Recycling Using Autogenous Mills**: Andre Pinoncely<sup>1</sup>; <sup>1</sup>Solios Carbone, 32 Rue Fleury Neuvesel, Givors 69702 France

In 1984, Aluminium Becancour Inc. awarded FCB, the former company name of Solios, a contract for the supply of the first fully airswept autogenous grinding system dedicated to the cryolitic bath processing. Today 16 industrial references are in operation worldwide, and the 20th anniversary give us the opportunity to draw up the successive developments brought to the original design in order to comply with the ever-demanding requirements of bath processing: separate storage of bath qualities, full ingots feeding, and semi-hot bath processing. This paper will also focus on the latest very hot bath pre-cooling system and its contribution to reduce the smelter HF emissions.

## 2:25 PM

Impregnation of Cathode Blocks With Boron Oxide: Rudolf Keller<sup>1</sup>; Brian J. Barca<sup>1</sup>; David G. Gatty<sup>1</sup>; <sup>1</sup>EMEC Consultants, 4221 Roundtop Rd., Export, PA 15632 USA

It was shown that boron oxide in cathode blocks suppresses cyanide formation and promotes wetting of the surface by aluminum if the metal contains some titanium. EMEC Consultants developed a method to impregnate cathode blocks with boron oxide. In a custom-built autoclave, half-length blocks were exposed to a melt of boron oxide and some borax. Pressures of 160 psi were typically maintained at temperatures of about 800°C. Amorphous cathode blocks gained about 12 wt% in the average, graphitized blocks around 14 wt% with a minimum of 10 wt% being a targeted value. Some impregnated blocks were made available for exposure in commercial cells for 6 months, and a pot at Century Aluminum of West Virginia was fully equipped.

## 2:50 PM

Plant Experience With an Experimental Titanium Diboride Cell: Marilou McClung<sup>1</sup>; John Browning<sup>1</sup>; Scott Carte<sup>2</sup>; Craig Lightle<sup>1</sup>; Richard O. Love<sup>1</sup>; Ron Zerkle<sup>3</sup>; <sup>1</sup>Century Aluminum of West Virginia, Tech., PO Box 98, Ravenswood, WV 26164 USA; <sup>2</sup>Century Aluminum of West Virginia, Potrm. Production, PO Box 98, Ravenswood, WV 26164 USA; <sup>3</sup>Century Aluminum of West Virginia, Pot Repair, PO Box 98, Ravenswood, WV 26164 USA

Century Aluminum of West Virginia, partnered with EMEC Consultants, SGL Carbon, Century Aluminum of Kentucky, and Golden Northwest Aluminum with support from the Department of Energy on a project to create a lower resistance at the carbon cathode-metal interface in the aluminum reduction cell. The approach was to provide a replenishing source of boron within the cathode to react with a titanium laced meal pad to generate a titanium diboride layer at the cathode. The target result is a surface layer of TiB2 that should create a reduction in energy consumption, an increase in production and potentially an increase in pot life. This project has had three phases. Phase two, completed in 2002, involved replacing three standard blocks with three blocks impregnated with boron oxide. In the third phase a full cell of impregnated blocks was installed. This paper documents the methods and results of the second phase of this test and nine months operational information on the phase three full pot and control pot.

### 3:15 PM

#### Experiences with Olivine-Based Refractories in Potlinings of Aluminium Electrolysis Cells: Ole-Jacob Siljan<sup>1</sup>; <sup>1</sup>Norsk Hydro ASA, Rsch. Ctr. HPI, N3907 Porsgrunn Norway

Olivine-based refractory materials have been tried for an extensive period of time as lining materials in aluminium reduction cells. Olivine provides a cost efficient and thermally stable lining for aluminium reduction cells. The lower chemical stability of pure olivine towards cryolitic melts can be overcome by adding smaller amounts of aluminosilicate minerals to the refractory product. The performed trials with this modified olivine-based brick material (ALUBRICK 2092) clearly indicate that operating results of cells lined with olivine-based bricks are at least comparable to the results of standard lined cells with fireclay materials. The data presented in the paper show that the chemical resistivity of ALUBRICK 2092 is at least as good as for standard fireclay bricks. Likewise, the data also indicate that the deterioration and the subsequent alteration of thermal properties of ALUBRICK 2092 results in potentially smaller changes to the cell heat balance than the corresponding deterioration of fireclay materials.

#### 3:40 PM Break

#### 3:50 PM

Wear of Silicon Nitride Bonded SiC Bricks in Aluminium Electrolysis Cells: *Flemming Bay Andersen*<sup>1</sup>; Guido Dorsam<sup>1</sup>; <sup>1</sup>Corus Research, Development & Technology, Ceram. Rsch. Ctr., PO Box 10000, IJmuiden 1970 CA The Netherlands

Samples from a sidewall of an aluminium electrolysis cell were submitted for study of the wear mechanism of the SiC-brick. Samples were studied using a combination of chemical analysis, microscopy, SEM-EDS and XRD. Unused bricks from 2 suppliers were used as reference material. The unused bricks are very similar to each other. Differences are found in the grain size of the SiC and in the binder (b-Si3N4 contents varies between bricks). All bricks have a coarse matrix and higher porosity in the core. The wear mechanism of the bricks seems a combination of attack by Na, HF, oxidation and moisture in the different zones. Below bath level first oxidation and then Na play a major role but bricks are here the least attacked. At bath level attack is severe but observations were complicated through a repair of what cause secondary reactions to occur. Above bath level the bricks disintegrate but reaction products are almost absent. Here we hypothesize that HF-vapor transformed the reaction products into volatile fluor ides and other gasses. This study shows that the corrosion tests currently used for Si3N4 bonded SiC-bricks, does not simulate the wear mechanism described in this report. In order to evaluate the performance of these bricks it is important to develop a new corrosion test. A proposal for such a new test is presented.

#### 4:15 PM

**Corrosion Tests and Electrical Resistance Measurement of SiC-Si3N4 Refractory Materials**: *Bingliang Gao*<sup>1</sup>; Zhaowen Wang<sup>1</sup>; Zhuxian Qiu<sup>1</sup>; <sup>1</sup>Northeastern University, Sch. of Matls. & Metall., Mail Box 117, Shenyang, Liaoning 110004 China

Silicon nitride bonded silicon carbide materials have excellent properties, such as resistance to molten aluminum and cryolite and air oxidation in aluminum electrolysis cells, so they are used in some Chinese industrial cells as sidewall materials. In this paper, we tested SiC-Si3N4 materials made in China, in molten cryolite, liquid aluminum and high temperature air by various devices. In order to simulate the extremely corrosive conditions when no side-ledge is present in industrial aluminum cells, co-corrosion tests were carried out. The electrical resistance of SiC-Si3N4 materials attacked by aluminum electrolyte for 48 hours was measured from room temperature up to 950°. It is demonstrated that SiC refractory materials used for cell lining have better properties than carbon lining material.

## Beyond Nickel-Base Superalloys: Other Systems and Physical Properties of Silicides

Sponsored by: Structural Materials Division, SMD-Corrosion and Environmental Effects Committee-(Jt. ASM-MSCTS), SMD-High Temperature Alloys Committee, SMD-Mechanical Behavior of Materials-(Jt. ASM-MSCTS), SMD-Refractory Metals Committee *Program Organizers:* Joachim H. Schneibel, Oak Ridge National Laboratory, Oak Ridge, TN 37831-6115 USA; David A. Alven, Lockheed Martin - KAPL, Inc., Schenectady, NY 12301-1072 USA; David U. Furrer, Ladish Company, Cudahy, WI 53110 USA; Dallis A. Hardwick, Air Force Research Laboratory, AFTL/MLLM, Wright-Patterson AFB, OH 45433 USA; Martin Janousek, Plansee AG Technology Center, Reutte, Tyrol A-6600 France; Yoshinao Mishima, Tokyo Institute of Technology, Precision and Intelligence Laboratory, Yokohama, Kanagawa 226 Japan; John A. Shields, HC Stark, Cleveland, OH 44117 USA; Peter F. Tortorelli, Oak Ridge National Laboratory, Oak Ridge, TN 37831-6156 USA

Wednesday PM	Room: 211B
March 17, 2004	Location: Charlotte Convention Center

Session Chairs: Ridwan Sakidja, University of Wisconsin, Dept. of Matls. Sci. & Engrg., Madison, WI 53706 USA; Joachim H. Schneibel, Oak Ridge National Laboratory, Metals & Ceram. Div., Oak Ridge, TN 37831-6115 USA

#### 2:00 PM

Role of Different Alloying Elements in Modifying the Microstructures of Nb-Si-Ti-Al-Cr-X Alloys for High Temperature Aeroengine Applications: Raghvendra Tewari<sup>1</sup>; Hyojin Song<sup>1</sup>; Amit Chatterjee<sup>2</sup>; Vijay K. Vasudevan<sup>1</sup>; <sup>1</sup>University of Cincinnati, Dept. of Chem. & Matls. Engrg., Cincinnati, OH 45221-0012 USA; <sup>2</sup>Rolls-Royce Corporation, 2001 S. Tibbs Ave., Indianapolis, IN 46241 USA

Niobium silicides have drawn a considerable interest for possible applications at high temperatures. The binary niobium silicides, however, exhibit low room temperature ductility and poor oxidation at elevated temperatures. A multi element approach is being adopted to improve these properties. The present paper reports role of different alloying elements in the development of the microstructures under -as cast, -heat treated and -hot deformed conditions in the Nb-Si-Ti-Cr-Al-X alloys. The morphological distribution, structure and chemical composition of various phases under different treatments have been studied in detail. Our investigations have revealed a strong solute partitioning tendency of various elements, dissolution and re-precipitation of the phases during various heat treatments. The role of different alloying elements has been examined in influencing the properties of the alloys. These results reveal that additional strengthening of the matrix phase can be achieved through the precipitation of the different phases. In addition, materials have been thermomechanically processed and microstructural changes have been investigated.

#### 2:15 PM

Structure and Thermal Expansion of Mo5Si3 and (Mo1.xVx)5Si3 Compounds: Claudia J. Rawn<sup>1</sup>; Joachim H. Schneibel<sup>1</sup>; Thomas R. Watkins<sup>1</sup>; <sup>1</sup>Oak Ridge National Laboratory, Metals & Ceram. Div., 1 Bethel Valley Rd., PO Box 2008, MS 6064, Oak Ridge, TN 37831-6064 USA

Tetragonal Mo5Si3 exhibits a coefficient of thermal expansion (CTE) in the c-direction that is more than twice as large as that in the a-direction. This high thermal expansion anisotropy causes microcracking and is therefore detrimental for components made from Mo5Si3. To decrease this pronounced thermal expansion anisotropy other elements such as Nb, Cr, V, and Ti have been introduced. High temperature x-ray powder diffraction has been used to study the changes in the CTE(c)/CTE(a) ratio. With the addition of V into the structure the anisotropy ratio reduces rapidly for small concentrations and levels out at approximately 1.25 for higher concentrations. With high quality diffraction data Rietveld refinements can give information on the site occupancies of the various elements in the structure. This type of information is used to explain how the thermal expansion anisotropy correlates with the atomic structure. Research sponsored by the Division of Materials Sciences, Office of Basic Energy Sciences; the Division of Materials Sciences and Engineering and by the Assistant Secretary for Energy Efficiency and Renewable Energy, Office of

FreedomCAR and Vehicle Technologies, as part of the High Temperature Materials Laboratory User Program. ORNL is operated by UT-Battelle, LLC, for the U.S. DOE under contract DE-AC05-000R22725.

#### 2:30 PM

**Processing, Microstructures and Mechanical Properties of Directionally Solidified V-V<sub>3</sub>Si In Situ Composites**: *H. Bei*<sup>1</sup>; E. P. George<sup>2</sup>; G. M. Pharr<sup>1</sup>; <sup>1</sup>University of Tennessee, Dept. of Matls. Sci. & Engrg., 434 Doughtery Engrg., Knoxville, TN 37996 USA; <sup>2</sup>Oak Ridge National Laboratory, Metals & Ceram. Div., Oak Ridge, TN 37831 USA

The intermetallic V<sub>3</sub>Si has low density, high melting point and high strength at elevated temperatures. However, it suffers from intrinsic brittleness and low fracture toughness at ambient temperature. In this study, V-V<sub>3</sub>Si eutectic alloys were directionally solidified to produce ductile phase toughened composites in a high temperature optical floating zone furnace. Depending on the solidification conditions several microstructures were observed, such as well-aligned lamellar, fibrous and cellular. The interphase spacings increase with decreasing solidification rates in agreement with the Jackson-Hunt theory. The mechanical properties of the individual phases were investigated by nanoindentation. It is found that the elastic modulus and nanoindentation hardness of V<sub>3</sub>Si are 214 and 13.8 GPa, respectively, and those of the V solid solution 185 and 3.4 GPa, respectively. The high temperature strength was also examined by tensile testing at elevated temperature. Prelimary results show that the ductile to brittle transition temperature is about 800°C for this composite, and its strength is significantly higher than those of conventional V solid solution alloys.

## 2:45 PM

Effects of Thermomechanical Processing on Texture Formation in Rolled Molybdenum Sheets: *Werner Skrotzki*<sup>1</sup>; Ingwar Hünsche<sup>1</sup>; Carl-Georg Oertel<sup>1</sup>; Wolfram Knabl<sup>2</sup>; <sup>1</sup>Technische Universität Dresden, Inst. für Strukturphysik, Dresden 01062 Germany; <sup>2</sup>Plansee AG, Technologiezentrum, Reutte 6600 Austria

The deformation of polycrystalline materials strongly depends on microstructure and texture. While grain size and Taylor factor determine the strength of the material grain shape and texture may lead to anisotropic flow. To improve the formability of molybdenum sheets the mechanisms of microstructure and texture formation during hot rolling and annealing have been investigated. The texture measurements were done by X-ray and electron backscatter diffraction. The microstructure was observed by orientation imaging microscopy and orientation contrast. The structural parameters of deformed and recrystallized molybdenum sheets were characterized in detail with respect to reduction in thickness, through-thickness texture gradient, annealing temperature and annealing time, i.e. recrystallization kinetics. The results may be used to optimize the deep-drawing properties of molybdenum sheets.

#### 3:00 PM

Microstructure and Oxidation Studies in the Cr-Si-Al System: Zhicong Yuan<sup>1</sup>; *Panayiotis Tsakiropoulos*<sup>1</sup>; Guosheng Shao<sup>1</sup>; John Watts<sup>1</sup>; <sup>1</sup>University of Surrey, Sch. of Engrg., Mech. & Aeros. Engrg., Metall. Rsch. Grp., Guildford, Surrey GU2 7XH England

The Cr-Si-Al system has been chosen to study phase equilibria and microstructure development and oxidation behaviour in intermetallic based alloys, owing to the importance of this system in the development of new materials to replace the Ni base superalloys that are used currently in gas turbine engines. The alloys were prepared using clean melting and casting in water-cooled copper crucibles/moulds and were studied in the as cast and heat-treated conditions. In our study particular attention has been paid to the solidification microstructures and on phase equilibria involving the Cr-Si silicides and Cr-Al intermetallics and on the role of Al additions in controlling phase selection and oxidation behaviour. Selected alloys have also been evaluated for their oxidation behaviour using isothermal oxidation tests that cover the whole range from pest, to intermediate to high temperature oxidation. The results of microstructural characterization will be presented and discussed.

## 3:15 PM

Defect Structure and Low-Temperature Mechanical Properties of Cr<sub>2</sub>Zr -Cr<sub>2</sub> Nb Pseudo-Binary Laves Phase Alloys: *Takayuki Takasugi*<sup>1</sup>; Yoshiyasu Nakagawa<sup>1</sup>; Yasuyuki Kaneno<sup>1</sup>; Hirofumi Inoue<sup>1</sup>; <sup>1</sup>Osaka Prefecture University, Dept. of Metall. & Matls. Sci., 1-1 Gakuen-cho, Sakai, Osaka 599-8531 Japan

The effect of composition on the  $Cr_2Zr$  - $Cr_2Nb$  pseudo-binary alloys which are composed of single Laves phase and the duplex microstructure with Cr solid solution was investigated, focusing upon the defect structure and low-temperature mechanical properties. The de-

fect structures were analyzed using XRD and density measurement while the low-temperature mechanical properties were evaluated based on Vickers hardness and the fracture toughness. The C15 phase field is continuous between  $Cr_2Zr$  - $Cr_2Nb$ , with a maximum phase field width of about 15at.% solubility. The defect mechanism is governed by antisite constitutional defects for alloys along the pseudo-binary line, but by the mixture of vacancy and anti-site defects for alloys along the constant Zr/Nb plethal section. The relationships between the defect structure and low-temperature mechanical response are discussed, in correlation with the retained high-temperature Laves phase and atomic size of constituent elements.

## 3:30 PM

**Development of Chromium-Tungsten Alloys**: *Omer N. Dogan*<sup>1</sup>; Jeffrey A. Hawk<sup>1</sup>; <sup>1</sup>US Department of Energy, Albany Rsch. Ctr., 1450 Queen Ave., SW, Albany, OR 97321 USA

Cr alloys containing 0-30 weight % W were investigated for their high temperature strength and oxidation resistance. These experimental alloys are intended for use in elevated temperature applications. Alloys were melted in a water-cooled, copper-hearth arc furnace. Microstructure of the alloys was studied using X-ray diffraction, scanning electron microscopy, and light microscopy. Meyer and Vickers hardness tests were utilized for measuring room temperature strength. A hot hardness tester with a spherical ruby indenter was used to study the strength of these materials between 800°C and 1200°C. A parabolic relationship was observed between load and indent size at all temperatures. On the other hand, decrease in hardness of the alloys with temperature was linear up to 1200°C.

## 3:45 PM

**Electrical and Thermal Transport Properties of Single Crystalline Mo<sub>5</sub>X<sub>3</sub> (X=Si, B, C):** *Taisuke Hayashi***<sup>1</sup>; Kazuhiro Ito<sup>1</sup>; HIroyuki Nakamura<sup>1</sup>; Masaharu Yamaguchi<sup>1</sup>; <sup>1</sup>Kyoto University, Matls. Sci. & Engrg., Sakyo-ku, Kyoto 606-8501 Japan** 

 $Mo_5X_3$  (X=Si, B, C) intermetallic compounds such as  $Mo_5SiB_2$  (D8<sub>1</sub>),  $Mo_5Si_3$  (D8<sub>m</sub>) and  $Mo_5Si_3C$  (D8<sub>8</sub>) have a great potential for ultra-high temperature applications, such as an oxidation protective coating and a heating element. We measured the thermal conductivity and electrical resistivity of the  $Mo_5X_3$  single crystals. The thermal and electrical conductivity at room temperature for  $Mo_5SiB_2$  are about 30 W/mK and  $2.5x10^6 \ \Omega^{-1} \ m^{-1}$ . They are higher than those of  $Mo_5Si_3$  and  $Mo_5Si_3C$ single crystals, but are much smaller than those of  $MoSi_2$  and Mo. The resistivity of  $Mo_5SiB_2$ ,  $Mo_5Si_3$  and  $Mo_5Si_3C$  single crystals exhibited a negative curvature  $(d^2\rho(T)/dT^2<0)$ , with a tendency towards saturation. In the  $Mo_5Si_3C$  with large  $\rho_0$  due to impurity carbon atoms, resistivity saturation is pronounced. In contrast, a much higher temperature is required to reach saturation in the  $Mo_5SiB_2$ .

## 4:00 PM

Microstructure Evolution of E2<sub>1</sub>-(Co, Ni)<sub>2R</sub>AIC Based Heat Resistant Alloys: *Shinya Teramoto*<sup>1</sup>; <sup>1</sup>Tokyo Institute of Technology, Matls. Sci. & Engrg., 4259 Nagatsuta, Midori-ku, Yokohama, Kanagawaken 226-8502 Japan

We are designing new class of (Co, Ni)-base heat resistant alloys strengthened by E2<sub>1</sub>-(Co, Ni)<sub>3</sub>AlC. The E2<sub>1</sub> type ordered crystal structure is almost the same as that of the L1<sub>2</sub> type excluding that a carbon atom occupies the octahedral interstice at the body-center. It's reported E2<sub>1</sub>-(Co, Ni)<sub>3</sub>AlC forms continuous solid solution between E2<sub>1</sub>-Co<sub>3</sub>AlC in the Co-Al-C system and L1<sub>2</sub>-Ni<sub>3</sub>Al in the Ni-Al system. The addition of Ir or/and Pt is thought to effectively improve the elevated temperature strength to go beyond Ni and Co-base superalloys. Objective of the present work is to conquest proper microstructures by controlling alloy composition, alloy process and heat treatment. They include not only the cuboidal E2<sub>1</sub> precipitates in the  $\alpha$ -(Co, Ni) matrix, but also discontinuous precipitation of E2<sub>1</sub>/ $\alpha$  and directional solidification of the eutectic E2<sub>1</sub>///000 1/, and so forth. We have also investigated phase stability of E2<sub>1</sub> phase from the viewpoint of magnetic proper ties.

## 4:15 PM Concluding Remarks Joachim H. Schneibel

# Bulk Metallic Glasses: Phase Transformation and Alloy Design

Sponsored by: Structural Materials Division, ASM International: Materials Science Critical Technology Sector, SMD-Mechanical Behavior of Materials-(Jt. ASM-MSCTS)

*Program Organizers:* Peter K. Liaw, University of Tennessee, Department of Materials Science and Engineering, Knoxville, TN 37996-2200 USA; Raymond A. Buchanan, University of Tennessee, Department of Materials Science and Engineering, Knoxville, TN 37996-2200 USA

Wednesday PM	Room:	209A	
March 17, 2004	Location	: Charlotte Co	nvention Center

Session Chairs: Michael K. Miller, Oak Ridge National Laboratory, Metals & Ceram. Div., Oak Ridge, TN 37831-6136 USA; Todd C. Hufnagel, Johns Hopkins University, Matls. Sci. & Engrg., Baltimore, MD 21218-2681 USA

# 2:00 PM Invited

Apt Characterization of the Decomposition of Bulk Metallic Glasses: Michael K. Miller<sup>1</sup>; <sup>1</sup>Oak Ridge National Laboratory, Metals & Ceram. Div., PO Box 2008, Oak Ridge, TN 37831-6136 USA

The early stages of decomposition and phase separation of bulk metallic glasses may be quantified by atom probe tomography to provide information on their stability. Atom probe tomography has been applied to several bulk metallic glasses to reveal changes in the atomic arrangement of atoms in the as-cast state and after annealing in the vicinity of the glass transition temperature. The composition and morphology of coexisting phases may be characterized from the earliest stages of decomposition to the final crystalline microstructure. Research at the SHaRE User Center was sponsored by the Division of Materials Sciences and Engineering, U. S. Department of Energy, under Contract DE-AC05-000R22725 with UT-Battelle, LLC.

## 2:25 PM Invited

In-Situ Scattering Studies of Phase Transformation Behaviors in Bulk Metallic Glass: Xun-Li Wang<sup>1</sup>; C. T. Liu<sup>2</sup>; J. K. Zhao<sup>1</sup>; Weihua Wang<sup>3</sup>; <sup>1</sup>Oak Ridge National Laboratory, Spallation Neutron Source, 701 Scarboro Rd., Oak Ridge, TN 37831 USA; <sup>2</sup>Oak Ridge National Laboratory, Metals & Ceram. Div., Oak Ridge, TN 37831 USA; <sup>3</sup>Chinese Academy of Sciences, Inst. of Physics, Beijing 100080 China

Phase transformation is a promising way for making nanostructured materials in large quantities. Phase transformations involving nanostructured materials usually occur under conditions far from equilibrium. Although thermodynamics ultimately determines the equilibrium phase for a given set of conditions, the answers as to whether and how the nanostructured phase is produced from the meta-stable precursor depend on the kinetic processes. Here, we describe some recent in-situ synchrotron scattering experiments aiming to understand the kinetics of phase transformation in bulk metallic glass. For Zr52.5Cu17.9Ni14.6Al10Ti5, simultaneous measurements of diffraction and small angle scattering data provided first direct demonstration of a phase separation prior to the amorphous-to-crystalline phase transformation. Our data support the view that crystalline nucleation is achieved via phase separation through a mechanism of short-range diffusion of small atoms (e.g., Ni) whereas the growth is determined by long-range d iffusion. For Nd60Al10Fe20Co10, a magnetic bulk amorphous alloy, we have identified two distinctively different decomposition processes from scaling of the in-situ small angle scattering data. A correlation is established between the decomposition kinetics and the magnetic properties of the alloy. Research supported by Division of Materials Sciences and Engineering, Office of Basic Energy Sciences, U.S. Department of Energy under Contract DE-AC05-00OR22725 with UT-Battelle.

2:50 PM Cancelled

Exploration of Bulk Metallic Glasses Based on Ti-Ni-Si

#### 3:15 PM

**Development Strategy for Bulk Aluminum Glass**: *Wynn Steven Sanders*<sup>1</sup>; <sup>1</sup>Air Force Research Laboratory, AFRL/MLLMD, 2230 Tenth St., Bldg. 655, Rm. 025, Wright-Patterson AFB, OH 45324 USA

This paper presents a strategy for the development of bulk aluminum metallic glass. Recent research has led to new insights into the criteria for bulk metallic glass formation. First, bulk metallic glasses obey a unique topological relationship as shown in atomic size distribution plots. Additionally, there are preferred radius ratios that are beneficial to efficient atomic packing. Finally, appropriate alloying element selection can depress the liquidus relative to the glass transition temperature. These revised criteria are being used to guide efforts to develop new bulk metallic glasses based on aluminum. Composition space of known ternary marginal glass formers is being systematically explored via the addition of quaternary and higher order alloying elements based upon topological and chemical considerations. This approach has resulted in an increase in the glass forming ability of marginal aluminum glasses. The specific approach applied in this exploration study will be described and results will be presented.

#### 3:40 PM

Effect of Oxygen Impurities on Al-, Cu-, and Ti-Based Metallic Glass: *Wynn Steven Sanders*<sup>1</sup>; 'Air Force Research Laboratory, AFRL/ MLLMD, 2230 Tenth St., Wright-Patterson AFB, OH 45324 USA

Oxygen contamination has been shown to dramatically reduce the glass forming ability of alloys. Although the effect of oxygen impurities have been extensively studied in the Zr-based bulk metallic glass forming systems, little work has been done on marginal glasses. The magnitude of this effect becomes important as new glass-forming systems are investigated and produced. This effect is even more critical for glasses that require high cooling rates; oxygen impurities can prevent glass formation entirely. The levels of oxygen impurity levels have been varied in aluminum-, copper-, and titanium-based marginal glass formers and its effect has been characterized by differential scanning calorimetry and x-ray diffraction. Initial results indicate that these alloys exhibit varying amounts of sensitivity to oxygen. Results from this analysis will be presented.

## 4:05 PM

Compaction of Amorphous Aluminum Alloy Powder by Direct Extrusion and Equal Channel Angular Extrusion: O. N. Senkov<sup>1</sup>; S. V. Senkova<sup>1</sup>; D. B. Miracle<sup>2</sup>; <sup>1</sup>UES, Inc., Matls. & Processes Div., 4401 Dayton-Xenia Rd., Dayton, OH 45432 USA; <sup>2</sup>Air Force Research Laboratory, Matls. & Mfg. Direct., AFRL/MLLM, Wright-Patterson AFB, OH 45433 USA

Al<sub>89</sub>Gd<sub>7</sub>Ni<sub>3</sub>Fe<sub>1</sub> alloy powder produced by gas atomization was consolidated using equal channel angular extrusion (ECAE) and direct extrusion. The powder particle size was below 40 µm (-325 mesh grade) and the powder was ~80% amorphous. Compaction was conducted in the temperature range of 200°C to 500°C. Densities above 98% of the theoretical density were achieved after compaction at temperatures below 250°C and 100% density was achieved above 420°C. In the temperature range of 250°C to 420°C very poor consolidation of the powder occurred due to formation of brittle intermetallic phases. Non-homogeneous deformation of the powder was detected during consolidation at low temperatures and the consolidated material had an amorphous structure with precipitations of crystalline phases. After compaction at 450°C and 500°C, the material was fully dense and had a nanocrystalline structure. Features of interactions of the powder particles with amorphous and crystalline phases during consolidation are outlined.

#### 4:30 PM

Topological Criteria for Amorphization Based on Thermodynamic Approach: Oleg N. Senkov<sup>1</sup>; Daniel B. Miracle<sup>2</sup>; <sup>1</sup>UES, Inc., Matls. & Processes Div., 4401 Dayton-Xenia Rd., Dayton, OH 45432 USA; <sup>2</sup>Air Force Research Laboratory, Matls. & Mfg. Direct., AFRL/ MLLM, Wright-Patterson AFB, OH 45433 USA

A thermodynamic model for amorphization is proposed that allows analysis of the effect of composition, atomic radii, and elastic constants of constitutive elements on amorphization. The model is based on comparison of the Gibbs free energy and entropy of a non-equilibrium crystalline solid solution and the undercooled liquid. According to this model, the amorphous state is thermodynamically stable (relative to the crystalline solid solution) only for certain alloy compositions. The larger is the atom size of the solvent element, the better is the condition for amorphization. To achieve global instability of the crystal lattice, the atomic radius ratio R of solute and solvent elements should fall in a particular range of R. This range becomes wider when the size of the solvent element increases. The glass transition temperature increases with the atom size of the solvent element and it has a maximum at a certain concentration of the solute.

#### 4:55 PM

Study of Glass Forming Ability and its Correlation with Eutectic Alloys: *Yi Li*<sup>1</sup>; <sup>1</sup>National University of Singapore, Dept. of Matls. Sci., Lower Kent Ridge Rd., Singapore 119260 Singapore

Many bulk metallic glasses have been found in many alloy systems over the last ten years. Despite the fact that many parameters have been used to find the best glass forming alloys and some of them are very successful, the way to find the alloy composition with the optimum glass forming ability within one alloy system is still not clear. We have analyzed the glass forming ability around eutectic composition in terms of the competitive growth/formation of primary dendrites, eutectic and glass. It is concluded that the glass forming ability of a eutectic alloy system depends on the type of the eutectics, i.e. symmetric or asymmetric eutectic coupled zone. For the alloy systems with symmetric eutectic coupled zone, the best glass forming alloys should be at or very close to the eutectic composition. For the alloy system depended zone, the best glass forming alloys should be at off-eutectic compled zone, the best glass forming alloys should be at off-eutectic compositions, probably towards the side of the faceted phase with a high entropy in the phase diagram. We will show our latest results on the glass formation in Zr, Pd, La and Ni based alloy discovered using the above analysis method.

# **Cast Shop Technology: Grain Refining**

Sponsored by: Light Metals Division, LMD-Aluminum Committee Program Organizers: Corleen Chesonis, Alcoa Inc., Alcoa Technical Center, Alcoa Center, PA 15069 USA; Jean-Pierre Martin, Aluminum Technologies Centre, c/o Industrial Materials Institute, Boucherville, QC J4B 6Y4 Canada; Alton T. Tabereaux, Alcoa Inc., Process Technology, Muscle Shoals, AL 35661 USA

Wednesday PM	Room:	213B/C
March 17, 2004	Location	: Charlotte Convention Center

*Session Chairs:* David H. StJohn, CAST Cooperative Research Center, University of Queensland, Brisbane, Queensland 4068 Australia; A. Lindsay Greer, University of Cambridge, Dept. of Matls. Sci. & Metall., Cambridge CB2 3QZ UK

## NOTE: Session begins at 2:25 PM

#### 2:25 PM

Investigation of Grain Refinement Fading in Hypoeutectic Aluminium-Silicon Alloys: *Tomasz Stuczynski*<sup>1</sup>; Zbigniew Zamkotowicz<sup>1</sup>; Boguslaw Augustyn<sup>1</sup>; Marzena Lech-Grega<sup>1</sup>; Wladyslaw Wezyk<sup>1</sup>; <sup>1</sup>The Institute on Non-Ferrous Metals, Light Metals Div., Pilsudskiego 19, Skawina 32-050 Poland

The results of the investigations concerning the grain refinement process in hypoeutectic silumins (using master alloys AlTi5B1, AlTi1.7B1.4 and AlTiC as grain refiners) will be presented. Using master alloys AlTi1.7B1.4 and AlTi5B1 as grain refiners, the fading of grain refinement effect was observed. Carried out examinations indicated the effect of the grain refinement fading is caused by sedimentation of boron compounds clusters in molten silumins and this process depends, among others, on the quantity of the free titanium in tested alloys.

#### 2:50 PM

Synthesis of Al-Ti-B Master Alloys by Different Techniques Using Ti and B Bearing Salts: M. A. Shaheen<sup>2</sup>; Ibrahim Hamed Aly<sup>3</sup>; Aly Bastaweesy<sup>3</sup>; *Abdel-Nasser M. Omran*<sup>1</sup>; <sup>1</sup>Aluminium Company of Egypt, R&D, Nag-Hammady Egypt; <sup>2</sup>Suez Canal University, Metallurgl. Dept., Fac. of Engrg., Suez Egypt; <sup>3</sup>Minia University, Chem. Engrg. Dept., Fac. of Engrg., El-Minia Egypt

An Al-Ti-B alloys containing up to 10% titanium and 5% boron has been obtained by reacting of B and Ti bearing salts with aluminium. The parameters affecting the reaction process were studied. The experiments were carried out in two techniques: first by using mixture of KBF<sub>4</sub> and K<sub>2</sub>TiF<sub>6</sub> and second by using mixture of KBF<sub>4</sub>, K<sub>2</sub>TiF<sub>6</sub> and granular aluminium. The results obtained were indicated that, the first technique is the best one. The efficiency of the Ti, B recovery up to 99% and 94% respectively. Microstructure examination, X-ray diffraction tests were carried out on the produced alloys.

## 3:15 PM

**Grain Refiner Fade in Aluminium Alloys**: *Paul L. Schaffer*<sup>1</sup>; Jacob W. Zindel<sup>2</sup>; Arne K. Dahle<sup>1</sup>; <sup>1</sup>University of Queensland, Div. of Matls., Frank White Bldg. (Bldg. 43), Cooper Rd., St. Lucia, Queensland 4072 Australia; <sup>2</sup>Ford Motor Company, MD 3182 SRL, PO Box 2053, Dearborn, MI 48121 USA

Grain refinement is usually an integral part of melt treatment undertaken in order to consistently produce castings with premium mechanical properties. However, the successful grain refinement of foundry alloys compared to wrought alloys has proven difficult due to a higher alloy content and long holding times encountered in the foundry. Often a melt is held for long periods and the grain refinement efficiency decreases, or fades, with time. Depending on the severity of fade, significant variations in the grain size can occur, which in turn can affect the mechanical properties, porosity distribution and consistency of the casting. Settling of the grain refining particles is believed to make a significant contribution to the mechanism of fade. However, the rate of fade is much faster than predicted by Stokes law and this suggests that other factors such as particle agglomeration, formation of oxide layers and melt turbulence also contribute to the loss of grain refinement during casting. Dedicated laboratory t rials have been conducted to determine the contributions of the separate mechanisms to the overall fade observed.

#### 3:40 PM Break

## 4:15 PM

Reducing the Cost of Grain Refiner Additions to DC Casting: Mark A. Easton<sup>1</sup>; David H. StJohn<sup>2</sup>; Elizabeth Sweet<sup>3</sup>; <sup>1</sup>Monash University, CRC for Cast Metals Mfg. (CAST), Sch. of Physics & Matls. Engrg., PO Box 69, Melbourne, Victoria 3800 Australia; <sup>2</sup>University of Queensland, CRC for Cast Metals Mfg. (CAST), Div. of Matls. Engrg., Brisbane, Queensland 4068 Australia; <sup>3</sup>Comalco Research and Technical Support, Thomastown, Victoria Australia

This paper describes implementation of technology developed at the CAST CRC for reducing the cost of grain refiners added in VDC casting of billet. Experimental work showed that cost savings could be made in some alloys by reducing the amount of boron-containing rod grain refiner addition, and compensating for this by the addition of titanium to the alloy to increase the value of the growth restriction factor. A grain refiner calculator has been developed so that the lowest cost addition can be determined for a particular alloy while still achieving the desired fine grain microstructure. Recently the results from this calculator have been applied at Comalco casthouses without an increase in hot cracking rates. The methodology of implementation and the potential benefits of this technology are described.

#### 4:40 PM

**Opticast: A Method for Optimized Aluminum Grain Refinement**: Lennart Backerud<sup>1</sup>; Holm Boettcher<sup>2</sup>; John Courtenay<sup>3</sup>; *Rein Vainik*<sup>1</sup>; <sup>1</sup>Opticast AB, Junkergatan 13, SE-12653, Hagersten, Stockholm Sweden; <sup>2</sup>AMAG, PO Box 32, A-5282 Ranshofen Austria; <sup>3</sup>MQP Limited, 6 Hallcroft Way, Knowle, Solihull B93 9EW UK

By measuring the grain size in samples taken from the casting furnace, the necessary amount of grain refiner can be calculated for each single cast. The Opticast method involves rapid sample preparation and grain size analysis, which allows the method to be used on-line in all cast houses. The grain sizes measured are compared against calibration curves and the optimum amount of addition is calculated. The method can also be used for production of ingots in any specified grain size range, within narrow limits. In practical application in two cast houses, cost savings of up to 90% have been accomplished for certain alloys, while the mean savings for the whole production is at least 50%. Due to decreased grain refiner additions considerable quality improvement has also been achieved.

## 5:05 PM

Production of Al-B Master Alloys from Boron-Bearing Salts Using Different Techniques: Ibrahim Hamed Aly<sup>3</sup>; A. Bastaweesy<sup>3</sup>; M. A. Shaheen<sup>2</sup>; *Abdel-Nasser M. Omran*<sup>1</sup>; <sup>1</sup>Aluminium Company of Egypt, R&D, Nag-Hammady Egypt; <sup>2</sup>Suez Canal University, Metallurgl. Dept, Fac. of Engrg., Suez Egypt; <sup>3</sup>Minia University, Chem. Engrg. Dept., Fac. of Engrg., El-Minia Egypt

An Al-B alloys containing about 5% boron has been obtained by reacting of potassium fluoroborate (KBF<sub>4</sub>) with aluminium. The parameters affecting the reaction process such as: temperature, time, mixing speed, potassium fluoroborate to aluminium weight ratio and particle size were studied. The experiments were carried out in three techniques: first by using KBF<sub>4</sub> only, second adding mixture of KBF<sub>4</sub> and granular aluminium and third using mechanical alloying. The results indicated that, the second technique is considered to be the best one. Microstructure examinations and X-ray diffraction tests were carried out on the produced alloys.

# CFD Modeling and Simulation of Engineering Processes: Process Modeling II

Sponsored by: Materials Processing & Manufacturing Division, ASM/MSCTS-Materials & Processing, MPMD/EPD-Process Modeling Analysis & Control Committee, MPMD-Solidification Committee, MPMD-Computational Materials Science & Engineering-(Jt. ASM-MSCTS)

*Program Organizers:* Laurentiu Nastac, Concurrent Technologies Corporation, Pittsburgh, PA 15219-1819 USA; Shekhar Bhansali, University of South Florida, Electrical Engineering, Tampa, FL 33620 USA; Adrian Vasile Catalina, BAE Systems, SD46 NASA-MSFC, Huntsville, AL 35812 USA

Wednesday PM	Room:	206A		
March 17, 2004	Location	: Charlotte	Convention	Center

*Session Chairs:* Aniruddha Mukhopadhyay, Fluent Inc., Lebanon, NH 03766 USA; Michel Bellet, Ecole des Mines de Paris, Paris France; Alain Jardy, Ecole des Mines de Nancy, Nancy France

# 2:00 PM Opening Remarks - Aniruddha Mukhopadhyay

#### 2:05 PM Invited

Simulation of Bubble Formation Based on the Lattice Boltzmann Method: Johannes Steiner<sup>1</sup>; Christian Redl<sup>1</sup>; Wilhelm Brandstaetter<sup>1</sup>; Alois Triessnig<sup>2</sup>; <sup>1</sup>Mining University Leoben, Christian-Doppler-Lab. for Applied Computational Thermofluiddynamics, Franz-Josef-Strasse 18, Leoben 8700 Austria; <sup>2</sup>RHI AG, Rsch., Magnesitstrasse 2, Leoben 8700 Austria

The results of numerical simulations of bubble detachment from an orifice in a horizontal plate submerged in liquid are presented. The simulations are performed with a two-dimensional Lattice Boltzmann (LB) scheme. In previous works the same problem has been investigated by two-phase simulations in which surface tension effects were considered by an interaction potential formulation between the phases. In contrast, in the present work a volume of fluid (VOF) model consisting of a carrier fluid and a passively advected scalar function for the calculation of gravitational and surface tension forces, respectively, is used. The aim of this study is to verify the theoretical and experimental predictions of the dependencies of the departure diameter on gravitational forces, surface forces and wettability effects. Nonlinear fits to the simulation data yield functional dependencies which are in good agreement with the predictions.

## 2:40 PM

**Computer Simulation on Flow Phenomena in Pot of Continuous Galvanizing Line**: *Bo-Young Hur*<sup>1</sup>; *Xiangying Zhu*<sup>1</sup>; Arai Hiroshi<sup>1</sup>; <sup>1</sup>Gyeongsang National University, Dept. of Metallurgl. & Matls. Engrg., Kajoadong 900#, Chinju 660-701 S. Korea

Dross flow behavior and aluminum mixing process are important phenomena in continuous hot dip galvanizing process, which influences the quality of coating layer and then influences the anti-corrosive performance. In this paper, these two phenomena have been investigated using computer simulation technique that is based on finite element method. In order to avoid the adhesion of dross, baffle is generally used to prevent the bottom dross re-flotation. A comparison study of dross flow behavior was performed between baffled case and unbaffled case using computer simulation. Aluminum mixing route was mainly followed the top surface, and accumulation of Al concentration occurred near the corner between strip and free top surface. This route would be reasonable if the affection of the streak line of zinc flow and the lower density of the zinc solution due to containing high level Al were considered.

## 3:05 PM

**CFD Modeling of Sintering Phenomena During Iron Ore Sintering**: *Pengfu Tan*<sup>1</sup>; Dieter Neuschutz<sup>2</sup>; <sup>1</sup>Portovesme Nonferrous Metallurgical Company, S. P. n. 2 - Carbonia/Portoscuso - km. 16,5, Portoscuso, CA I-09010 Italy; <sup>2</sup>Lehrstuhl fur Werkstoffchemie, Rheinisch-Westfalische Technische Hochschule Aachen, D-52056 Aachen Germany

A CFD model of nickel flash furnace has been developed. Some results are presented in this work.

#### 3:30 PM

**Modeling Dissolution in Aluminum Alloys**: *Tracie Zoeller*<sup>1</sup>; T. H. Sanders<sup>2</sup>; G. Paul Neitzel<sup>1</sup>; <sup>1</sup>Georgia Institute of Technology, Sch. of

Mech. Engrg., Atlanta, GA 30332-0405 USA; <sup>2</sup>Georgia Institute of Technology, Matls. Sci. & Engrg., Atlanta, GA 30332-0245 USA

The dissolution of particles in a matrix is an important process that occurs during heat treatment of many materials. The effect of the heat treatment, or homogenization step, on spherical precipitates in an aluminum matrix was considered in this study. Upon solidification, an aluminum alloy microstructure is highly segregated. The microstructure consists of cored dendrites with various soluble and insoluble phases present in the dendritic regions. Subsequent heat treatments are performed to homogenize the microstructure. The microstructure evolution after each processing step is dependent upon the previous microstructures. The variation in local chemical composition may promote or hinder precipitation of new phases. A large volume fraction of coarse insoluble phases can lead to the occurrence of recrystallized grains via particle stimulated nucleation, while inhomogeneous solute distribution can lead to the precipitation of an uneven distribution of dispersoid phases. Understanding the dissolution of these secondary phases is important in predicting microstructural evolution in the alloy. A simple model will be presented to describe this moving boundary problem. Local equilibrium conditions are assumed at the precipitate-matrix interface. Composition profiles and dissolution times will be compared to experimental data and other models found in the literature.

### 3:55 PM Break

#### 4:15 PM

**Computational Model to Predict the Degradation of Particulate Material During Pneumatic Conveying**: *Mayur K. Patel*<sup>1</sup>; P. Chapelle<sup>1</sup>; N. Christakis<sup>1</sup>; M. Cross<sup>1</sup>; <sup>1</sup>University of Greenwich, Sch. of Computing & Math. Scis., Old Royal Naval College, 30 Park Row, Greenwich SE10 9LS London

Pneumatic conveying of granular materials is relied upon in many industrial situations, because of its simplicity/flexibility. However, attrition/degradation of particulate material conveyed is commonly observed, in dilute phase flow, which affects "product-quality" and causes difficulties in subsequent materials handling operations. It is well-known that degradation during dilute phase pneumatic conveying results mainly from high-velocity impacts of the particles with pipe-walls at bends. Available computational models concentrate on the detailed description of the flow of the solids/gas phases and ignore the damage imparted to the particle. The objective of the paper is to report the development of a Computational framework to describe/model flow of the gas-solids mixture and to predict particle degradation during dilute phase pneumatic conveying. The key feature of the model is the prediction of particle breakage, due to particle-wall impacts. Calculations of propensity of degradation are based on the use of parametrised impact data obtained via laboratory scale degradation tests. Results of the approach are presented and compared against experimental data.

## 4:40 PM

Numerical Study of Fluid Flow in an Agitated Quench Tank: Mohammed Maniruzzaman<sup>1</sup>; Mike Stratton<sup>1</sup>; Richard Sisson<sup>1</sup>; <sup>1</sup>Worcester Polytechnic Institute, Ctr. for Heat Treating Excellence, Mech. Engrg. Dept., 100 Inst. Rd., Worcester, MA 01609 USA

Distortion and cracking of a metallic part quenched in a liquid quenchant can be reduced greatly by improving quench uniformity. Agitation of the quenchant is one of the important factors for quench uniformity. Agitation greatly enhances heat extraction rate from the quenched part surface. The flow in a quench tank can be optimized using computational fluid dynamics (CFD) as a tool for quench tank/ agitation system design. In this study, numerical experiments are performed to predict the optimum impeller and tank design for uniform agitation in a quenched tank. Experiments are performed to validate the predictions.

# Computational Thermodynamics and Phase Transformations: Thermodynamics and Phase Transformations

Sponsored by: ASM International: Materials Science Critical Technology Sector, Electronic, Magnetic & Photonic Materials Division, Materials Processing & Manufacturing Division, Structural Materials Division, MPMD-Computational Materials Science & Engineering-(Jt. ASM-MSCTS), EMPMD/SMD-Chemistry & Physics of Materials Committee

Program Organizer: Jeffrey J. Hoyt, Sandia National Laboratories, Materials & Process Modeling, Albuquerque, NM 87122 USA

 Wednesday PM
 Room: 202A

 March 17, 2004
 Location: Charlotte Convention Center

Session Chair: TBA

#### 2:00 PM

Alloy Thermodynamics by the Screened Generalized Perturbation Method: A. V. Ruban<sup>1</sup>; S. I. Simak<sup>2</sup>; S. Shalcross<sup>2</sup>; H. L. Skriver<sup>1</sup>; <sup>1</sup>Technical University of Denmark., Physics Dept., Bldg. 307, Lyngby 2800 Denmark; <sup>2</sup>Uppsala University, Physics Dept., Uppsala SE-75121 Sweden

The screened generalized perturbation method (SGPM) is an ab initio technique for calculating Ising-type interactions in alloys. Although it is based on a number of approximations (the coherent potential approximation is one of the most serious), it appears to yield a quantitatively accurate description of the configurational alloy energetics in many different type of alloys. Besides, in contrast to the widely used structure inversion method it is extremely efficient and provides a transparent physical picture of the "chemical" ordering. We demonstrate this point by applying the SGPM to calculations of the ordering energies, short-range parameters, order-disorder transition temperatures, and alloy configurations on the surfaces in CuZn, CuAu and PtCo systems.

#### 2:20 PM

Prediction and Measurement of the Phonon Entropy of Alloying in Dilute Substitutional Alloys: *Olivier Delaire*<sup>1</sup>; Tabitha Swan-Wood<sup>1</sup>; Brent Fultz<sup>1</sup>; <sup>1</sup>CALTECH, Matls. Sci., Keck MC 138-78, Pasadena, CA 91125 USA

In this study, we investigate the entropic effects associated with changes in the vibrational modes of crystals sustained upon dilute substitutional alloying. Using inelastic neutron scattering techniques, we have measured the change in the phonon entropy of vanadium associated with the alloying of a few percent impurities of Ni, Pd, Pt or Co. The phonon entropy change upon alloying in vanadium was shown to be large and negative. In the case of 6-7% Pt and Co impurities, it is equal in magnitude to the configurational entropy gain of the alloy. We also present experimental results on Mo-7%Co alloys. Using a computational model based on the classical Born-von Karman approach, we extracted interatomic force-constants from our experimental data, from which phonon dispersion curves and density of states (DOS) could be calculated. In an effort to trace the microscopic origin of the effect observed, we also performed ab-initio calculations of the lattice-dynamics of these alloys. We calculated phonon dispersions and DOS curves with pseudo-potential based plane-wave density functional theory techniques, using a supercell approach to model the random substitutional alloys. We present a comparison of our ab-initio dynamics predictions with the results of our experimental measurement.

#### 2:40 PM

Evolution of Precipitates in Systems With Heterogeneous Nucleation Sites: Ernst Kozeschnik<sup>1</sup>; Franz Dieter Fischer<sup>2</sup>; Jiri Svoboda<sup>3</sup>; <sup>1</sup>Graz University of Technology, Inst. for Matls. Sci., Welding & Forming, Kopernikusgasse 24, Graz 8010 Austria; <sup>2</sup>University of Mining, Inst. of Mech., Franz-Josef Straße 18, Leoben 8700 Austria; <sup>3</sup>Academy of Science of the Czech Republic, Inst. of Physics of Matls., Zizkova 22, Brno 61662 Czech Republic

In many metallic systems, precipitates can nucleate on various heterogeneous nucleation sites, such as dislocations, grain-boundaries or sub-grain boundaries. For instance, in typical martensitic-ferritic CrMo-steels, M23C6 precipitates are formed on austenite grain boundaries during cooling from the liquid state. Later, after martensite transformation and during heat treatment, precipitates of the same type also nucleate on the sub-boundaries of the martensite lath-structure. The precipitates on the prior austenite grain boundary (PAGB) are usually larger than the precipitates formed later inside the transformed austenite grain. If the evolution of these two populations of precipitate is modelled under the assumption of a random distribution, the larger particles on the PAGD will coarsen on the expense of the particles on the sub-grain boundaries, and the latter population will dissolve completely in relatively short time. In reality, the two populations evolve in a more or less independent way with a weak interaction between the system of particles on the PAGB and the martensite substructure. A model taking these aspects into account has been developed and it will be discussed in detail together with some typical applications.

#### 3:00 PM

Analytical Sharp-Interface Model for Massive Transformations in Substitutional Alloys: *Jiri Svoboda*<sup>1</sup>; Franz Dieter Fischer<sup>2</sup>; Ernst Gamsjäger<sup>2</sup>; <sup>1</sup>Institute of Physics of Materials, Zizkova 22, Brno 61662 Czech Republic; <sup>2</sup>Montanuniversität Leoben, Inst. of Mech., Franz-Josef-Strasse 18, Leoben 8700 Austria

In the initial period of the massive transformation thin concentration spikes are formed in front of the moving interface. After a transition the interface moves together with spikes in a stationary manner (with a constant velocity) as long as all parent phase is transformed. Very recently a new sharp-interface finite-interface-mobility model for diffusional phase transformations in substitutional alloys was developed by means of application of Onsager's thermodynamic extremal principle. Under the assumption of the constraint diffusional fluxes of substitutional components the model predicts the jumps across the migrating interface of all chemical potentials to be the same. These jump conditions together with the conservation laws at the migrating interface represent the proper number of contact conditions for the coupling of the interface migration and bulk diffusion in adjacent grains. Based on Fick laws the steady state concentration profiles were calculated analytically. The steady state solutions predic t no concentration profiles in the product phase and exponential spikes in the parent phase. The jumps of the concentrations (height of the spikes) as well as the driving force acting at the interface are calculated from the jump conditions for chemical potentials across the interface. The kinetics of the massive transformation is determined by the interface driving force and by the interface mobility. It can be shown that the dissipation due to diffusion in the spikes corresponds to the difference of the total driving force and the driving force acting on the interface. The analytical model predicts, that the massive transformation is controlled exclusively by the interface migration characterized by the interface mobility. Furthermore, the model shows that the half-thickness of spikes is proportional to the tracer diffusion coefficient of the component and inverse proportional to the interface velocity. The analytical model is used for simulations of the massive transformation kinetics and spike properties in Fe-Cr-Ni system. The results are compared with the new sharp-interface finite-interface-mobility model. The agreement is very good.

### 3:20 PM

Modeling the Kinetics of Bainite Formation in Low-Carbon TRIP Steels: *Fateh Fazeli*<sup>1</sup>; Matthias Militzer<sup>1</sup>; <sup>1</sup>University of British Columbia, The Ctr. for Metallurgl. Process Engrg., 309-6350 Stores Rd., Vancouver, BC V6T 1Z4 Canada

Isothermal bainitic ferrite formation in the temperature range of 350 to 450°C for a model 0.18C-1.55Mn-1.7Si TRIP steels is investigated in terms of transformation kinetics and bainite morphology. Both single-phase austenite and austenite embedded in the ferrite matrix have been adopted as initial parent phase to study the role of nucleation condition and austenite grain size on the reaction kinetics. In addition, austenite-to-bainite transformation studies are extended to an Fe-0.6C-1.5Mn-1.5Si alloy with a nominal carbon content similar to that expected in the remaining austenite of a low-carbon TRIP steel at the start of the bainite formation. The experimental transformation results provide an appropriate database to examine the predictive capabilities of the existing modeling approaches for the bainite reaction, i.e. Johnson-Mehl-Avrami-Kolmogorov, diffusion and displacive methodologies. Employing these modeling philosophies to analyze the measured kinetics, a thorough comparison of the different models is provided and potential limitations of the existing models are delineated. The challenges will be discussed to replicate the bainite formation kinetics in TRIP steels from a fundamental point of view for a wide range of investigated temperatures where different bainite morphologies have been detected.

## 3:50 PM

Modeling Martensitic Phase Transformations in the Presence of Plasticity: *Dnyanesh Nitin Pawaskar*<sup>1</sup>; <sup>1</sup>California Institute of Technology, Engrg. & Applied Sci., 1200 E. Calif. Blvd., MC 104-44, Pasadena, CA 91125 USA

An approach to producing hard, but tough, steel is through the judicious use of retained austenite. The optimization of properties in this approach requires an understanding of the amount of retained austenite, the amount of plastic deformation and the martensitic morphology. We describe a model that studies the martensitic phase transformation in the presence of plasticity. The model is implemented using the finite elements and captures the microstructure evolution and plasticity. Our results reveal the complex interaction between the driving force for transformation, the morphology and the plasticity.

#### 4:10 PM

**ITR:** Computational Tools for Multicomponent Materials Design: *Zi-Kui Liu*<sup>1</sup>; Lonq-Qing Chen<sup>1</sup>; Qiang Du<sup>2</sup>; Padma Raghavan<sup>3</sup>; Jorge Sofo<sup>4</sup>; Stephen A. Langer<sup>5</sup>; Christopher C. Wolverton<sup>6</sup>; <sup>1</sup>Pennsylvania State University, Dept. of Matls. Sci. & Engrg., Steidle Bldg., Univ. Park, PA 16802 USA; <sup>2</sup>Pennsylvania State University, Dept. of Math., Univ. Park, PA 16802 USA; <sup>3</sup>Pennsylvania State University, Dept. of Computer Sci. & Engrg., Univ. Park, PA 16802 USA; <sup>3</sup>Pennsylvania State University, Dept. of Physics, Univ. Park, PA 16802 USA; <sup>4</sup>Pennsylvania State University, Dept. of Physics, Univ. Park, PA 16802 USA; <sup>5</sup>National Institute of Standards and Technology, Math. & Computational Scis. Div., 100 Bureau Dr., Stop 8910, MD 20899 Gaithersburg; <sup>6</sup>Ford Motor Company, Ford Rsch. Lab., MD3028/SRL, Dearborn, MI 48121-2053 USA

The medium size Information Technology Research (ITR) project funded by the National Science Foundation (NSF) in 2002 for five years will be presented. This collaborative research project involves two materials scientists (Zi-Kui Liu, Long-Qing Chen), a computer scientist (Padma Raghavan), a mathematician (Qiang Du), and three physicists (Stephen Langer, Christopher Wolverton, Jorge Sofo) from academia, industry and national laboratory. It is a synergistic effort that leverages the overlapping and complimentary expertise of the researchers in the areas of scalable parallel scientific computing, firstprinciples and atomistic calculations, computational thermodynamics, mesoscale microstructure evolution, and macroscopic mechanical property modeling. The research progress up to date will be reported in this presentation.

### 4:30 PM

Automating Multicomponent Materials Design: Padma Raghavan<sup>1</sup>; Keita Teranishi<sup>1</sup>; Zi-Kui Liu<sup>2</sup>; <sup>1</sup>Pennsylvania State University, Computer Sci. & Engrg., 308 Pond Lab., Univ. Park, PA 16802-6106 USA; <sup>2</sup>Pennsylvania State University, Matls. Sci. & Engrg., 0209 Steidle Bldg., Univ. Park, PA 16802 USA

We will report on the design of our client-server software architecture for determining the macroscopic properties of Al-Cu-Si-Mg systems. The server couples the following four main steps asynchronously through the use of intermediate databases: (1) computing abinitio results, (2) CALPHAD data optimization to determine thermodynamic properties, (3) phase-field simulation to generate microstructures, and, (4) finite-element analysis using OOF to determine macrostructural properties. Our server is "grid-enabled" using Globus and can deploy compute-intensive simulations for any step on multiprocessors and networks of workstations; additionally, it can access and update intermediate databases which could also be distributed over a wide area network. To answer design questions posed by web-enabled clients, the server will instantiate specific simulations using a rule-based system. The latter allows the server to meaningfully explore the design space to determine feasible compositions of the four main steps and precomputed results in intermediate databases.

#### 4:50 PM

**Computational Design of an Experiment on Super-Rapid Resolidification of Bi Via Shock Wave Release**: *Jeff D. Colvin*<sup>1</sup>; Alan Jankowski<sup>1</sup>; Wayne King<sup>1</sup>; Mukul Kumar<sup>1</sup>; Bryan Reed<sup>1</sup>; Babak Sadigh<sup>1</sup>; <sup>1</sup>Lawrence Livermore National Laboratory, Matls. Sci. & Tech. Div., PO Box 808, L-356, Livermore, CA 94550 USA

When a material transforms from one solid state to another through a melt-refreeze transition after undergoing shock compression, it is not known whether the material recrystallizes back into the initial microstructure. There are no data at all on recrystallized microstructures at very high cooling rates (> 1e+7 K/s). We are doing experiments using Bi, a metal that has an anomalous melt curve, meaning that it can resolidify at lower density than the liquid density. This implies that shock-melted liquid Bi will immediately resolidify upon release of the pressure, with an effective cooling rate up to 1e+10 K/ s. We present details of the computational design of a laser-driven experiment to shock-melt Bi on the Hugoniot after preheating the sample to 400 K and driving a pressure pulse of 20-30 kbar into it using the technique of tamped ablation (Colvin et al., Phys.Plasmas 10/7, July 2003).

## Cost-Affordable Titanium Symposium Dedicated to Prof. Harvey Flower: Low Cost Titanium

Sponsored by: Structural Materials Division, SMD-Titanium Committee

*Program Organizers:* M. Ashraf Imam, Naval Research Laboratory, Washington, DC 20375-5000 USA; Derek J. Fray, University of Cambridge, Department of Materials Science and Metallurgy, Cambridge CB2 3Q2 UK; F. H. (Sam) Froes, University of Idaho, Institute of Materials and Advanced Processes, Moscow, ID 83844-3026 USA

Wednesday PM	Room: 2	06B		
March 17, 2004	Location:	Charlotte	Convention	Center

Session Chair: James Sears, South Dakota School of Mines, Advd. Matls. Procg. Ctr., Rapid City, SD 57701 USA

#### 2:00 PM

Chemical Reactions of Ti<sub>3</sub>Al(O), Al<sub>3</sub>Ti(O), and Al<sub>2</sub>O<sub>3</sub> with NaOH in Aqueous Solution: *G. Adam*<sup>1</sup>; D. L. Zhang<sup>1</sup>; B. K. Nicholson<sup>2</sup>; <sup>1</sup>University of Waikato, Dept. of Matl. & Proc. Engrg., PB 3105, Hamilton New Zealand; <sup>2</sup>University of Waikato, Dept. of Chmst., PB 3105, Hamilton New Zealand

This study deals with the chemical reaction between Ti<sub>3</sub>Al(O), Al<sub>3</sub>Ti(O), and Al<sub>2</sub>O<sub>3</sub> phases in the Ti<sub>3</sub>Al(O)/Al<sub>2</sub>O<sub>3</sub>, or Al<sub>3</sub>Ti(O)/Ti<sub>3</sub>Al(O)/Al<sub>2</sub>O<sub>3</sub> powders produced by high energy mechanical milling of Al, and TiO<sub>2</sub> followed by heat-treatment. Separating the Al<sub>2</sub>O<sub>3</sub> phase out of the systems to give material with titanium-rich phases was the main goal behind this study. The reactions of Ti<sub>3</sub>Al(O)/Al<sub>2</sub>O<sub>3</sub>, or Al<sub>3</sub>Ti(O)/Ti<sub>3</sub>Al(O)/Ti<sub>3</sub>Al(O)/Al<sub>2</sub>O<sub>3</sub> wit aqueous solutions of NaOH were performed at elevated temperature to chemically leach the Al<sub>2</sub>O<sub>3</sub>. The reaction proceed faster than the reaction between Al<sub>3</sub>Ti(O) in Al<sub>3</sub>Ti(O)/Ti<sub>3</sub>Al(O)/Al<sub>2</sub>O<sub>3</sub> at the same condition. Under the same reaction conditions, the reaction between Ti<sub>3</sub>Al(O) and H<sub>2</sub>O results in formation of TiO<sub>1.04</sub>.

#### 2:30 PM

Influences of Alloy Chemistry and Microstructure on the Machinability of Titanium Alloys: *Yoji Kosaka*<sup>1</sup>; Stephen P. Fox<sup>1</sup>; <sup>1</sup>TIMET, Henderson Tech. Lab., PO Box 2128, Henderson, NV 89009 USA

In many applications, machining is a major contributor to the cost of parts. Titanium alloys are recognized to be difficult to machine materials due primarily to their low thermal conductivity, high chemical reactivity and low modulus of elasticity compared with steels. There have been a number of studies regarding the conditions and the characteristics in the machining of Ti-6Al-4V, which is the most widely used alpha/beta titanium alloy in aerospace and non-aerospace applications. It is generally understood that the strength is one of the factors that determines the machinability of titanium alloys. Microstructure is believed to influence the machinability of titanium alloys, although few studies have been reported on this subject. In the present work drill machinability was studied on various alpha/beta titanium alloys. The effects of alloying elements and the microstructure on the tool life of drills will be discussed.

#### 3:00 PM Cancelled

# Characterisation of Ex-Situ Ti-TiB2 MMC Parts Produced by Mechanical Milling

#### 3:30 PM

Analysis-Based Design of Experiments for Improving Ingot Surface Finish During Plasma Arc Cold Hearth Melting: Yuan Pang<sup>1</sup>; Chengming Wang<sup>2</sup>; Frank Spadafora<sup>3</sup>; Kuang-O (Oscar) Yu<sup>3</sup>; Hao Dong<sup>1</sup>; Daniel L. Winterscheidt<sup>4</sup>; <sup>1</sup>Concurrent Technologies Corporation, Product & Proc. Analysis, 425 Sixth Ave., Regional Enterprise Tower, 28th Floor, Pittsburgh, PA 15219-1819 USA; <sup>2</sup>The Procter & Gamble Company, Sharon Woods Tech. Ctr., 11450 Grooms Rd., SWTC Box C-21, GR-CNE72, Cincinnati, OH 45242 USA; <sup>3</sup>RMI Titanium Company, R&D, 1000 Warren Ave., Niles, OH 44446-0269 USA; 4Concurrent Technologies Corporation, Mfg. Programs, 100 CTC Dr., Johnstown, PA 15904-1935 USA

During casting of titanium ingots using plasma arc cold hearth melting (PAM), cold shuts can form on the surface. Cold shuts must be removed by machining to avoid cracks developing in billet conversion. Subsequent vacuum arc remelting is currently required to eliminate this defect. The present work uses analysis tools to guide the design of experiments for achieving single-melt casting. Computational results for casting of subscale ingots are presented to show the effects of process parameters on metal temperatures. The surface conditions of three ingots are compared to demonstrate the importance of heat distribution and the model capability. The best combination of torch parameters suggested by the analysis has resulted in the most improved surface finish, which is of sufficient quality that no machining is necessary. How this methodology can be scaled up to achieve balanced heating between the ingot center and edge in large-diameter ingots is also addressed.

## 4:00 PM

Thermodynamic Modeling of Ti-Al-V Alloys: Vasisht Venkatesh<sup>1</sup>; Fan Zhang<sup>2</sup>; <sup>1</sup>TIMET Corp, HTL, PO Box 2128, Henderson, NV 89009 USA; <sup>2</sup>CompuTherm, LLC, 437 S. Yellowstone Dr., Ste. 217, Madison, WI 53719 USA

Implementation of computational modeling tools to improve titanium processing, via extrinsic (e.g., temperature, pass reduction, etc.) and intrinsic (e.g., grain size, chemistry, etc.) parameter optimization, has resulted in significant cost savings through the elimination of shop/laboratory trials and tests. PANDAT, a thermodynamic modeling software developed by CompuTherm, LLC, is being utilized to design new alloys and control heat treatment processes based on alloy chemistry. A special thermodynamic database for titanium alloys was developed for the determination of beta transus, phase proportions, partitioning coefficients and phase boundaries. Model predictions of beta transus, phase fractions and element partitioning are compared to experimental results for a range of Ti-Al-V-Fe-O-C chemistries. In addition, the effect of these alloying elements on beta transus will also be discussed.

## 4:30 PM

A New Source of Affordable Titanium Alloy Powder: A. B. Godfrey<sup>1</sup>; S. R. Thompson<sup>1</sup>; C. M. Ward-Close<sup>1</sup>; <sup>1</sup>QinetiQ Ltd., Cody Tech. Park, Ively Rd., Farnborough, Hampshire UK

This paper will announce the establishment of a new process for the production of titanium alloy powder based on Electrolytic De-Oxidation (the FFC Cambridge Process). Details of the different titanium powder products will be given and scale-up of production with a new purpose built facility in the UK at QinetiQ, Farnborough will be described. The current state of titanium powder metallurgy technology will be reviewed and the potential of new high-quality titanium alloy powder to reduce the cost of finished components will be discussed.

#### 5:00 PM

Improving Grindability and Wear Resistance of Titanium Alloys: *Toru Okabe*<sup>1</sup>; Masafumi Kikuchi<sup>1</sup>; Chikahiro Ohkubo<sup>1</sup>; Marie Koike<sup>1</sup>; Osamu Okuno<sup>1</sup>; Yutaka Oda<sup>1</sup>; <sup>1</sup>Baylor College of Dentistry, Dept. of Biomatls. Sci., 3302 Gaston Ave., Dallas, TX 75246 USA

Titanium is becoming an important material in dentistry, but not all of the properties of pure titanium lend themselves to dental applications. To optimize the properties of titanium for use in dentistry, alloying is necessary. This presentation will describe work on characterizing some titanium alloys for grindability, wear, and corrosion resistance, which are all important properties for dentistry. The metals tested included CP Ti, Ti-6Al-4V, Ti-15Mo-2.8Nb-0.25Si, Ti-13Zr-13Nb, Ti-15V-3Cr-3Sn-3Al, and experimental binary Ti-Cu alloys. Improvements in grindability and wear seemed to occur with the presence of the eutectoid in the alloy. The alloys tested had excellent corrosion characteristics in the oxidation potential range of the human mouth.

## **Dislocations: Dislocations in Complex Materials**

Sponsored by: ASM International: Materials Science Critical Technology Sector, Electronic, Magnetic & Photonic Materials Division, Materials Processing & Manufacturing Division, Structural Materials Division, EMPMD/SMD-Chemistry & Physics of Materials Committee, MPMD-Computational Materials Science & Engineering-(Jt. ASM-MSCTS) *Program Organizers:* Elizabeth A. Holm, Sandia National Laboratories, Albuquerque, NM 87185-1411 USA; Richard A. LeSar, Los Alamos National Laboratory, Theoretical Division, Los Alamos, NM 87545 USA; Yunzhi Wang, The Ohio State University, Department of Materials Science and Engineering, Columbus, OH

Wednesday PM Room: 201A March 17, 2004 Location: Charlotte Convention Center

Session Chair: TBA

43210 USA

#### 2:00 PM Invited

Connection Between Dislocation Fine Structure and the Creep Properties of Metallic Alloys: *Michael J. Mills*<sup>1</sup>; <sup>1</sup>The Ohio State University, Dept. of Matls. Sci. & Engrg., Columbus, OH 43210 USA

The importance of dislocation fine structure (core structure, dissociation, etc.) in determining the yield behavior of BCC metals, and some intermetallic compounds such as Ni3Al, has been well established. By comparison, the crucial role that dislocation fine structure plays in determining the creep performance of materials has received relatively little attention. This presentation will highlight the recent development of dislocation models of creep deformation in several important alloy systems. These models have originated from a detailed knowledge of dislocation core structure and morphology based on extensive weak beam and high resolution TEM investigation. Two classes of behavior will be discussed. For cases in which dislocation cores are compact, as in a-Ti solid solution alloys and ordered g-TiAl, the appearance of jogged-screw dislocations is a ubiquitous microstructural feature following creep deformation. On the basis of these observations, the classic jogged-screw dislocation model for creep has been modified. This modified model appears to provide an excellent, quantitative prediction of the creep properties in these alloy systems, and provides important insight into important alloy-development issues such as the source of solute strengthening and finite-size effects. As a second example, the shearing of g' precipitates during high-temperature, low-stress creep of Ni-based superalloys will be discussed. A novel mechanism for this shearing process via the movement of dissociated a<100> dislocations has been identified. These dislocations move via a coupled-climb and glide process. Under the assumption that a<100> dislocation motion in the g' precipitates is the rate-limiting recovery process, a creep rate equation has been developed which provides promising agreement with measurements. The important role that computational modeling can play in further developing these ideas will also be highlighted.

## 2:35 PM Cancelled

# Computer Simulation of Dislocation Dynamics in a Solid Solution

#### 2:55 PM

**Strengthening of Nb3Sn Composite**: *Jingping Chen*<sup>1</sup>; Ke Han<sup>1</sup>; Peter Kalu<sup>1</sup>; <sup>1</sup>National High Magnet Field Laboratory, 1800 E. Paul Dirac Dr., Tallahassee, FL 32310 USA

Fabrication of Nb3Sn type superconductor composites requires a final heat treatment at about 700°C to form an A15 phase embedded in an annealed Cu-Sn solid solution matrix. The high temperature annealing diminishes many strengthening mechanisms which relate to strain hardening by accumulation of dislocations and decreasing the size of the dislocation cells, and the A15-Nb3Sn is a brittle hard phase which renders further deformation strengthening of Cu-Sn difficult. The most feasible approaches for strengthening the composite are either solid solution or dispersion strengthening. This paper assesses and compares the efficiency of the solid solution and dispersion strengthening in superconductor composite by consideration of both the fabrication procedures and interaction between dislocation and particles. The size of the strengthening particles, which range from the solute of single atom to the second phase is used to link the solid solution and dispersion strengthening and to optimize the design of the superconductor composites.

A Peierls Model of the Critical Stress to Transmit a Screw Dislocation from a Disordered to an Ordered Phase: Yao Shen<sup>1</sup>; Peter M. Anderson<sup>1</sup>; <sup>1</sup>Ohio State University, Matls. Sci. & Engrg. Dept., 477 Watts Hall, 2041 College Rd., Columbus, OH 43210 USA

This presentation will describe the features and predictions of a 2D Peierls model of screw dislocation transmission from a disordered to an ordered phase. The incoming and outgoing slip planes, and also the interface, are described by a local shear stress-shear displacement relation that is derived from the gamma surface for that region. Consequently, the configuration of the dislocation core changes during the transmission process, including potential core spreading into the interface. An idealized geometry is considered in which the incoming and outgoing slip planes are oriented perpendicular to a coherent interface, so that no residual dislocation content remains in the interface following transmission. The effect of unstable stacking fault energies associated with the slip planes and interface, the mismatch in elastic moduli, and the antiphase boundary energy of the ordered phase are varied to understand their effect on the critical stress for dislocation transmission.

#### 3:35 PM Break

#### 3:50 PM Invited

Apt Characterization of Solute Segregation to Individual Dislocations: Michael K. Miller<sup>1</sup>; <sup>1</sup>Oak Ridge National Laboratory, Metals & Ceram. Div., PO Box 2008, Bldg. 4500S, MS 6136, Oak Ridge, TN 37831-6136 USA

The solute segregation to individual dislocations may be quantified by atom probe tomography. Dislocations may be observed in the field ion images by a change of the normal concentric atom terraces to spirals. Dislocations are detected in atom maps by enhanced levels of solute along linear features. The magnitude of the solute segregation may be quantified with the use of the maximum segregation envelope method. Examples will be presented of solute segregation to dislocations in nickel aluminides, neutron irradiated pressure vessel steels and a mechanically alloyed, oxide dispersion strengthened (MA/ODS) ferritic alloy. Research at the SHaRE User Center was sponsored by the Division of Materials Sciences and Engineering, U. S. Department of Energy, under Contract DE-AC05-00OR22725 with UT-Battelle, LLC and by the Office of Nuclear Regulatory Research, U. S. Nuclear Regulatory Commission under inter-agency agreement DOE 1886-N695-3W with the U. S. Department of Energy.

### 4:25 PM

Phase-Field Simulation of Spinodal Decomposition in a Constrained Film With Mobile Interfacial Dislocations: Shen-Yang Hu<sup>1</sup>; Long-Qing Chen<sup>1</sup>; <sup>1</sup>Pennsylvania State University, Dept. of Matls. Sci. & Engrg., Univ. Park, PA 16802 USA

Spinodal decomposition in binary alloy thin films with an arbitrary distribution of mobile interfacial dislocations, and subject to elastically substrate constraint is studied. Composition evolution and dislocation motion are described by Cahn-Hilliard and Ginzburg-Landau equations, respectively. Elastic solutions, derived for elastically anisotropic thin films with stress free surface and substrate constraint, are employed. Temporal evolution of Cahn-Hilliard equation under thin film boundary conditions (the fluxes normal to the surface and the interface are zero) is solved by a semi-implicit Fourier-spectral method. The effect of the mobility of dislocations, the types and distributions of dislocations on spinodal decomposition process and microstructures are studied.

#### 4:45 PM

Towards a Full Analytic Treatment of the Hall-Petch Behavior in Multilayers: Putting the Pieces Together: Lawrence H. Friedman<sup>1</sup>; <sup>1</sup>Pennsylvania State University, Dept. of Engrg. Sci. & Mech., 212 Earth & Engrg. Sci. Bldg., Univ. Park, PA 16802 USA

Elastically inhomogeneous multilayer films are exploited for use as hard coatings. These films exhibit a strong dependence between the compositional wavelength and hardness. The hardness also depends on the granular texture within a layer. According to the model of A. Misra and H. Kung (Adv.Eng.Mat.3(4),2001,p217), the yielding mechanism of dislocation transmission across grains competes with the mechanism for dislocation transmission across layer interfaces. Here, both mechanisms of transmission are discussed in light of a semi-analytic model that is qualitatively and quantitatively distinct from the classical Hall-Petch Relation, but still rooted in dislocation pile-up theory. A full analytic treatment of the Hall-Petch-like size-effect in multilayers must account for anomalous stress-concentration at the layer interfaces, dislocation source characteristics, and a variable dislocation pinning stress. From scaling arguments, the criteria for such an equation are described, and an approximate analytic formula is suggested that meets these criteria.

### 5:05 PM

Formation of Misfit Dislocations in Nano-Scale Ni-Cu Bilayer Films: David Mitlin<sup>1</sup>; Amit Misra<sup>1</sup>; Michael Nastasi<sup>1</sup>; Velimir Radmilovic<sup>2</sup>; Richard Hoagland<sup>1</sup>; David J. Embury<sup>3</sup>; J. P. Hirth<sup>1</sup>; Terence E. Mitchell<sup>1</sup>; <sup>1</sup>Los Alamos National Laboratory, MST-8, MS G755, Los Alamos, NM 87545 USA; <sup>2</sup>Lawrence Berkeley National Laboratory, Natl. Ctr. for Electron Microscopy, 1 Cyclotron Rd., Berkeley, CA 94720 USA; <sup>3</sup>McMaster University, Dept. of Matls. Sci., Hamilton, Ontario L8S 4H3 Canada

We investigated the mechanism of interface dislocation formation in a 5.0 nm Ni film epitaxially deposited on 100 nm of (001) Cu. Threading dislocations that pre-exist in the Cu substrate extend into the coherent Ni overlayer during growth and propagate in the [110] and directions along the interface. These dislocations are perfect glide dislocations with mixed character and lying on the {111} Ni planes, and were by far the most numerous in the microstructure. Lomer edge dislocations lying on the (001) Ni-Cu interface were also detected, constituting approximately 5% of the total interface dislocations having the same Burgers vector were commonly observed at the interface. This dislocation configuration, along with several others that were observed, is explained in terms of the ability of favorably oriented dislocations to cross-slip.

# Educational Issues in Transport Phenomena in Materials Processing: Presentations and Panel Discussion

Sponsored by: Materials Processing & Manufacturing Division, TMS-Education Committee

*Program Organizers:* Matthew John M. Krane, Purdue University, Department of Materials Engineering, West Lafayette, IN 47907 USA; Adam C. Powell, Massachusetts Institute of Technology, Department of Materials Science and Engineering, Cambridge, MA 02139-4307 USA

Wednesday PM	Room: 209B
March 17, 2004	Location: Charlotte Convention Center

Session Chairs: Adam C. Powell, Massachusetts Institute of Technology, Matls. Sci. & Engrg., Cambridge, MA 02139-4307 USA; Matthew John M. Krane, Purdue University, Matls. Sci. & Engrg., W. Lafayette, IN 47907-2044 USA

#### 2:00 PM Invited

Transport Education in the Materials Curriculum: Innovative Approaches, Exercises, and New Challenges: Adam Clayton Powell<sup>1</sup>; <sup>1</sup>Massachusetts Institute of Technology, Dept. of Matls. Sci. & Engrg., 77 Mass. Ave., Rm. 4-117, Cambridge, MA 02139-4307 USA

This talk will address three areas in teaching transport phenomena in the materials science and engineering curriculum as it is practiced currently and envisioned to change in the future at MIT. The first covers innovative approaches to teaching individual concepts and structuring a transport course to meet the needs of upper-level undergraduates in an existing curriculum. The second introduces a new internet resource with exercises which may be used for homework assignments or supplementary reading examples in this subject. The third discusses changes in course design to support new curriculum needs in materials processing, from computational modeling to micro- and macroeconomic implications.

#### 2:30 PM

A Software Tool for Teaching Transport Phenomena: J. Bernardo Hernández-Morales<sup>1</sup>; Rafael Fernández-Flores<sup>2</sup>; J. Sergio Téllez-Martínez<sup>1</sup>; <sup>1</sup>Universidad Nacional Autónoma de México, Depto. de Ingeniería Metalúrgica, Facultad de Química, Edificio "D", Cd. Universitaria, México, D.F. 04510 Mexico; <sup>2</sup>Universidad Nacional Autónoma de México, Inst. de Matemáticas, Circuito Institutos s/n, Cd. Universitaria, México, D.F. 04510 Mexico

Students taking courses on transport phenomena usually solve a large number of problems but do not have the opportunity to explore each problem in detail, mainly due to time constraints. But solving a problem just to get a single answer does not give the students a feel for the impact of the difeerent variables on the final result. To help alleviate this problem we have designed a user-friendly software tool that allows the student to solve traditional problems but also to change any given variable or even to work with a range of values for the relevant variables and plot the results. The software was built using VisualBasic 6 but may be distributed as an stand-alone application. An important feature of the software is its capability to handle different units for a given problem. However, the answer is always given in the SI system. The software deals with fluid flow, heat transfer and mass transfer problems.

#### 2:50 PM

Introduction to Mathematical Modelling Through a Laboratory Exercise: J. Bernardo Hernandez-Morales<sup>1</sup>; J. Sergio Téllez-Martínez<sup>1</sup>; <sup>1</sup>Universidad Nacional Autónoma de México, Depto. de Ingeniería Metalúrgica, Fac. de Química, Edif. "D", Cd. Universitaria, México, D.F. 04510 Mexico

Transport phenomena are the basis of mathematical modelling of materials processing. However, there is usually little effort spent to make students aware of this fact in courses on transport phenomena. Through a laboratory exercise, the concepts of empirical and fundaments mathematical models are introduced stressing the shortcomings of the former one; it also serves as an introduction to the fundamental concepts of heat transfer. In this lab the newtonian cooling of a carbon steel bar is studied both experimentally and theoretically. Starting the heat transfer course with this exercise offers the students a problem that is easier to grasp than the traditional approach found in textbooks.

#### 3:10 PM

Lecture Modules in Materials Science: An NSF Educational Activity at Rensselaer Polytechnic Institute: Afina Lupulescu<sup>1</sup>; Martin E. Glicksman<sup>1</sup>; <sup>1</sup>Rensselaer Polytechnic Institute, Dept. of Matls. Sci. & Engrg., 110 8th St., Troy, NY 12180 USA

Diffusion in solids, kinetics, solidification and crystal growth are broadly applicable subfields of materials. A 3-year NSF grant proposes developing electronic modules to parallel and amplify texts and notes already established for these quantitative courses at Rensselaer. The modules, designed for ease of adoption by others, consist of standalone PowerPoint files that succinctly present the content of each lecture topic, adding commentary, animation, and emphases that extend the limits of notes and texts. Given the prior success encountered with our modules for diffusion in solids, we extended the approach to include Kinetics, Solidification and Crystal Growth. Topical contents are selected on the basis of the books and course notes already in use to teach these courses. In addition, areas of conceptual, or mathematical difficulty encountered by our students and known to us will be explicated, and appropriate comments and examples added to alert students and instructors adopting our modules.

#### 3:40 PM

Teaching and Learning Transport Phenomena and Analytical Methods in Materials Engineering to Graduate Students: Makhlouf M. Makhlouf<sup>1</sup>; *Richard D. Sisson*<sup>1</sup>; <sup>1</sup>Worcester Polytechnic Institute, Matls. Sci. & Engrg., 100 Inst. Rd., Worcester, MA 01609 USA

For more than 20 years, we have been teaching a one semester introductory graduate course in analytical methods for materials engineering to M.S. and Ph.D. students in Materials Science and Engineering. Chemical and mechanical engineering graduate students also take this course as an elective. The learning objectives for this course are: 1. Understand and be able to apply the fundamentals of heat transfer and solid state diffusion to materials processing and engineering problems. 2. Understand and be able to apply the fundamentals of mathematical modeling to analytical and numerical solutions to the heat equation and other problems. This course follows selected topics from the Bird, Stewart and Lightfoot approach to transport phenomena via the Geiger and Poirier text Transport Phenomena in Metallurgy. The materials processes used to illustrate the fundamentals and meet the learning objectives include: heat treating, carburization/decarburization of steel, quenching and cooling, phase transformations and hydrogen permeation and diffusion. In addition, examples from ceramics and coatings have frequently been included. In this presentation, we will discuss the various strategies that have been used to aid the student learning including laboratory experiments coupled with model simulations.

## 4:10 PM Break

## 4:30 PM Panel Discussion

This discussion will develop the themes introduced by the presentations, with a focus on changes in the way this topic will be taught in Materials Science and Engineering Departments in the future.

## Electrochemical Measurements and Processing of Materials: Electrochemical Sensors and Measurements

Sponsored by: Extraction & Processing Division, Materials Processing & Manufacturing Division, EPD-Aqueous Processing Committee, EPD-Process Fundamentals Committee, EPD-Pyrometallurgy Committee, ASM/MSCTS-Thermodynamics & Phase Equilibria Committee, EPD-Waste Treatment & Minimization Committee

*Program Organizers:* Uday B. Pal, Boston University, Department of Manufacturing Engineering, Brookline, MA 02446 USA; Akram M. Alfantazi, University of British Columbia, Department of Metel & Materials Engineering, Vancouver, BC V6T 1Z4 Canada; Adam C. Powell, Massachusetts Institute of Technology, Department of Materials Science and Engineering, Cambridge, MA 02139-4307 USA

Wednesday PM	Room:	212A
March 17, 2004	Location	: Charlotte Convention Center

*Session Chairs:* Daniel Josell, National Institute of Standards and Technology, Metall., Gaithersburg, MD 20899 USA; Xionggang Lu, Shanghai University, Sch. of Matls. Sci. & Engrg., Shanghai 200072 China

## 2:00 PM Invited

Interdiffusivity Measurements in Oxide Systems by Solid State Galvanic Cell Method: Seshadri Seetharaman<sup>1</sup>; Du Sichen<sup>1</sup>; Anders Jakobsson<sup>1</sup>; <sup>1</sup>KTH, Matls. Sci. & Engrg., Stockholm 10044 Sweden

A galvanic cell method incorporating  $ZrO_2$ -CaO solid electrolyte was successfully developed in the present laboratory. This technique has the advantage of monitoring of interdiffusion in oxide systems continuously. A typical cell in case of the study of the interdiffusivities in the system MO-NO can be written as (-) Pt, M (s), MO-NO (s) ||  $ZrO_2$ -CaO || MO (s), M (s), Pt (+) where the oxide in the left-hand electrode is initially a mechanical mixture of the two oxides. As the interdiffusion proceeded, the EMF followed a typical S-type diffusion curve, starting from zero tending towards thermodynamic equilibrium. The results were treated by a model based on Dunwald-Wagner relationship in order to evaluate the diffusivities. The method was applied to NiO-MgO solid solutions as well as interdiffusion between NiO and CoO-doped MgO. The results compare well with the results of diffusion couple experiments as well as dynamic high temperature X-ray studies.

## 2:30 PM Invited

Development of Electrochemical Sensors and Their Application for Characterizing the Metal/Electrolyte System During Localized Corrosion: Howard W. Pickering<sup>1</sup>; Konrad G. Weil<sup>1</sup>; Ryan C. Wolfe<sup>2</sup>; Barbara A. Shaw<sup>2</sup>; <sup>1</sup>Pennsylvania State University, Matls. Sci. & Engrg., 326 Steidle Bldg., Univ. Park, PA 16802 USA; <sup>2</sup>Pennsylvania State University, Engrg. Sci. & Mech., 212 Earth & Engrg. Scis., Univ. Park, PA 16802 USA

Electrochemical microprobes for in-situ monitoring of the electrochemical conditions inside recesses are needed to better understand how localized corrosion and other charge transfer processes occur in confined spaces. The electrode potential distribution can be routinely measured in cavities of  $> 100 \ \mu m$  opening dimension, but the ability to measure the concentrations of chemical species and their change with time in the presence of potential gradients is only recently becoming possible. Microprobes for pH and chloride ion will be described and results with these sensors will be presented and discussed for creviced iron samples in aqueous electrolytes. Available results reveal that these species change in concentration and distribution with time both during the induction period before crevice corrosion starts and during propagation of crevice corrosion. Preliminary data show that ionic concentrations peak at locations of highest metal dissolution rate on the crevice wall.

#### 3:00 PM

Electrochemical Atomic Force Microscopic Studies on the Localized Corrosion in Sputtered Chromium Nitride Thin Film: *Jyh-Wei Lee*<sup>1</sup>; Peng-Tzu Chen<sup>2</sup>; Hung-Kai Chen<sup>2</sup>; Jenq Gong Duh<sup>2</sup>; <sup>1</sup>Tung Nan Institute of Technology, Dept. Mech. Engrg., #152, Sec. 3, Pei-Shen Rd., Shen-Ken, Taipei County 222 Taiwan; <sup>2</sup>National Tsing Hua University, Dept. Matls. Sci. & Engrg., #101, Sec. 2, Kuang-Fu Rd., Hsin Chu 300 Taiwan Electrochemical atomic force microscopy (ECAFM) has become a useful tool to study the surface properties and reactions of corrosion down to atomic scale. With the aid of electrochemical control, detailed surface morphology changes can be in-situ observed. In this study, the sodium chloride aqueous solution was employed to be the corrosive media to investigate the corrosion behavior of a sputtered chromium nitride thin film on stainless steel substrate. In-situ timelapse sequences of images were obtained and the real-time polarization curves were recorded using the ECAFM. Localized pittings were observed on the thin film surface. Traditional electrochemical tests were used as a comparison. Scanning electron microscopy and electron probe micro analyzer were also conducted to explore the chemical composition changes around corrosion pits. The correlation between surface defects and corrosion pits of the chromium nitride film were discussed.

#### 3:30 PM Break

## 4:00 PM

Non-Destructive Microstructural Evaluation of Thermal Barrier Coatings by Electrochemical Impedance Spectroscopy: Srinivas Vishweswaraiah<sup>1</sup>; *Balaji Jayaraj*<sup>1</sup>; Tianbao Du<sup>1</sup>; Vimal Desai<sup>1</sup>; Yong-ho Sohn<sup>1</sup>; <sup>1</sup>University of Central Florida, Advd. Matl. Procg. & Analysis Ctr., PO Box 162455, 4000 Central Florida Blvd., Orlando, FL 32826 USA

Electrochemical impedance spectroscopy (EIS) is being developed as a non-destructive evaluation (NDE) technique of thermal barrier coatings (TBCs) for quality control and life-remain assessment. The durability and reliability of TBCs play an important role in the service reliability and durability of hot-section components in advanced turbine engines. In this investigation, EIS was employed to non-destructively examine TBCs, as a function of microstructure, chemistry and thermal exposure during isothermal and cyclic oxidation in air at 1121°C. TBCs examined in this study include electron beam physical vapor deposited (EB-PVD), air-plasma sprayed (APS) ZrO2-7wt.%Y2O3 (YSZ) and APS CaTiO3 (CTO) on NiCoCrAlY or (Ni,Pt) Al bondcoat. Impedance response of the specimens at room temperature was recorded at corrosion potential for TBCs using an electrolyte solution, and analyzed with an equivalent AC circuit based on the multi-layered micro-constituents of the TBCs. Specimens were then characterized by optical and e lectron microscopy. Relative changes in values of resistance and capacitance for constituent components in TBCs were correlated to the variation in the microstructure, chemistry and the degradation induced by thermal cycling.

## 4:30 PM

#### Response of Poly (3-Hexylthiophene) Thin Film Chemiresistor Sensor to Hydrazine Vapor: Hong Yang<sup>1</sup>; Bryan A. Chin<sup>1</sup>; <sup>1</sup>Auburn University, Matls. Engrg., 201 Ross Hall, Auburn, AL 36849 USA

Hydrazine is a widely used missile propellant that is highly toxic to humans even in low exposures. Therefore, on-line monitoring to rapidly identify an accidental release of hydrazine is required to protect personnel from dangerous exposures. In this research, a low cost, passive, and highly sensitive chemiresistor sensor for hydrazine vapor detection has been developed. The sensor is fabricated using standard microelectronic manufacturing techniques and is integrated with a hydrazine sensitive conducting polymer thin film. As the sensor is exposed to hydrazine vapor, a permanent reduction in the conductivity of the polymer film occurs. Preliminary results have shown the sensor has a rapid response time of less than a few seconds and a detection range from a few ppb to hundreds of ppm hydrazine. Experiments have been conducted to investigate the effects of temperature on the response of sensor. Possible theoretical models that describe the observed behavior are discussed and compared with the experimental results

#### Failure of Structural Materials: Fatigue

Sponsored by: Structural Materials Division, SMD-Structural Materials Committee

*Program Organizers:* Michael E. Stevenson, Metals and Materials Engineering, Suwanee, GA 30024 USA; Mark L. Weaver, University of Alabama, Metallurgical and Materials Engineering, Tuscaloosa, AL 35487-0202 USA

Wednesday PM	Room: 211A
March 17, 2004	Location: Charlotte Convention Center

Session Chairs: Mark L. Weaver, University of Alabama, Metallurgl. & Matls. Engrg., Tuscaloosa, AL 35487-0202 USA; Michael E. Stevenson, Metals & Materials Engineers, Suwanee, GA 30093 USA

#### 2:00 PM

Fatigue Issues in Structural Aircraft Components: James F. Lane<sup>1</sup>; <sup>1</sup>Applied Technical Services, Inc., Matls. Testing, 1190 Atlanta Industrial Dr., Marietta, GA 30066 USA

Fatigue is the most prominent failure mechanism associated with fixed-wing aircraft. Structural components are specifically at risk on aircraft, since their inability to perform adequately may result in catastrophic failure. Identification of the fracture mechanism and the cause are imperative for the mitigation of these failures. This presentation will identify some structural components that have experienced fatigue failures and identify the cause for the initiation of fatigue cracks.

## 2:30 PM

Crystallographic Facet Determination from Fatigue Fracture Surfaces: Yun Jo Ro<sup>1</sup>; Sean R. Agnew<sup>1</sup>; Richard P. Gangloff<sup>1</sup>; <sup>1</sup>University of Virginia, Matls. Sci. & Engrg., 116 Engineer's Way, Charlottesville, VA 22904-4745 USA

Fatigue crack growth in aerospace aluminum alloys is accelerated within a moist environment, as compared to vacuum. SEM fractography is employed to determine qualitative fatigue damage mechanisms for alloy C47A (Al-2.7Cu-1.7Li-0.7Zn-0.6Mn-0.3Mg) tested in vacuum, wet air and 3%NaCl. All samples exhibit a faceted appearance in a low stress intensity range (< 4MPaiîm). Quantitative crystallographic facet orientations are determined by combining traditional stereology with Electron Back Scattered Diffraction (EBSD). In vacuum, the fracture surface is transgranular, strongly tortuous and faceted in the entire stress intensity range. Quantitative analysis reveals that 86% of facets orientations are within 10"- of {111} in vacuum, suggesting a mechanism associated with intense slip localization due to with precipitate shearing. Cracking in the moist environments is transgranular and nearly mode I throughout the whole stress intensity range. Facet orientations cover the entire irreducible triangle between {001} and {011} with an absence of facets near {111}.

## 2:50 PM

Ultrasonic Effects on Fatigue Behavior of Small Cracks in Age-Hardened Al Alloys: *Qiang Chen*<sup>1</sup>; Norio Kawagoishi<sup>1</sup>; Qingyuan Wang<sup>2</sup>; Xishu Wang<sup>3</sup>; <sup>1</sup>Kagoshima University, Mech. Engrg. Dept., 1-21-40 Korimoto, Kagoshima, Kagoshima 890-0065 Japan; <sup>2</sup>Sichuan University, Dept. of Civil Engrg. & Mech., Chengdu, Sichuan 610065 China; <sup>3</sup>Tsinghua University, Dept. of Engrg. Mech., Beijing 100084 China

Fatigue strengths of two age-hardened Al alloys, 6061-T6 and 7075-T6, were investigated in the super high cycle region by using ultrasonic techniques. The main concern of the present study focused on the initiation and propagation of small cracks in the age-hardened Al Alloys subjected to ultrasonic fatigue at a frequency of ~19.5 kHz. The results were compared with those obtained under conventional rotating bending fatigue at a frequency of ~55 Hz in order to assess the influence of loading frequency on the fatigue properties of the Al alloys.

## 3:10 PM

Effect of Grain Boundaries on the Growth Behavior of Short Fatigue Cracks in a 2xxx Al-Alloy: *Jinxia Li*<sup>1</sup>; Tongguang Zhai<sup>1</sup>; Matthew Garratt<sup>2</sup>; Gary Bray<sup>2</sup>; <sup>1</sup>University of Kentucky, Chem. & Matls. Engrg, 177 Anderson Hall, Lexington, KY 40506 USA; <sup>2</sup>Alcoa Technical Center, 100 Tech. Dr., Alcoa Ctr., PA 15069 USA

A study on the fatigue properties and fracture characteristic of a high strength 2xxx Al alloy has been done. Specimens were cyclically deformed over a range of stress amplitudes with a self-aligning four point bending rig. It was found that short cracks propagated in a crystallographic mode and were deflected at each grain boundary they interacted with. Periodical steps were found which ran all the way across each grain and varied from one grain to another in terms of the density on the fracture surface. The fracture stepping by the crack front at a grain boundary could be directly correlated with the twist angle of the crack face deflection across the grain boundary. The twist angle of the crack plane deflection across the grain boundary was the key factor that controlled the crack growth through the boundary. Denser fracture steps across one grain boundary indicated a larger twist angle of crack deflection at the grain boundary and gave rise to a lower crack growth rate. The work provided further evidence that supported the previously reported model that a grain boundary with a large twist component caused retardation of a short crack crossing the boundary in planar slip alloys.

## 3:30 PM

Fracture Mechanism of Al Alloys Under Ultrasonic Fatigue: *Qiang Chen*<sup>1</sup>; Norio Kawagoishi<sup>1</sup>; Qingyuan Wang<sup>2</sup>; <sup>1</sup>Kagoshima University, Mech. Engrg. Dept., 1-21-40 Korimoto, Kagoshima 890-0065 Japan; <sup>2</sup>Sichuan University, Dept. of Civil. Engrg. & Mech., Chengdu, Sichuan 610065 China

Ultrasonic fatigue tests were conducted for two age-hardened Al alloys, 6061-T6 and 7075-T6. The fracture surfaces of fatigued Al alloys were analyzed in detail under a scanining electron microscope and compared with those failed under conventional rotating bending fatigue. The objective of the present study is aimed at investigating the fracture mechanism that are involved in the ultrasonic fatigue of the age-hardened Al Alloys for better understanding the influence of loading frequency on the fatigue properties of the Al alloys. Special attentions were given to the formation and distribution of fatigue voids under ultrasonic loading as well as the effect of fatigue voids on the fatigue life.

## 3:50 PM Break

## 4:05 PM

Advanced Experimental and Modelling Assessment of Roughness-Induced Crack Closure Behaviour in Damage Tolerance Aluminium Alloys: Kern Hauw Khor<sup>1</sup>; Nicolas Kamp<sup>1</sup>; Harvinder Singh Ubhi<sup>2</sup>; Hiroyuki Toda<sup>4</sup>; Jean-Yves Buffiére<sup>3</sup>; Wolfgang Ludwig<sup>3</sup>; Ian Sinclair<sup>1</sup>; <sup>1</sup>University of Southampton, Engrg. Matls. Rsch. Grp., Sch. of Engrg. Scis., Highfield, Southampton, Hampshire SO17 1BJ UK; <sup>2</sup>QinetiQ Ltd., Cody Tech. Park, Ively Rd., Farnborough, Hampshire GU14 0LX UK; <sup>3</sup>GEMPPM INSA Lyon, 20 Ave. Albert Einstein, Lyon, Villeurbane Cedex 69621 France; <sup>4</sup>Toyohashi University of Technology, Dept. of Production Systems Engrg., Toyohashi, AICHI 441-8580 Japan

Fatigue crack closure, especially roughness-induced crack closure (RICC), has been recognized as a significant extrinsic factor in determining fatigue crack growth rates via the shielding of external cyclic loads to the crack-tip region. In this work, several 2024-type aluminium alloys, with different dispersoid contents and degrees of recrystallisation have been studied for their RICC micro-mechanistic influences on fatigue crack growth behaviour. Detailed assessment of texture variant distributions, grain boundary separations and threedimensional crack surface topography was carried out using electron backscattering diffraction (EBSD) and surface profilometry. A novel analytical RICC model has been developed to predict crack closure levels, which is found to be comparable to the current experimental results. High resolution X-Ray microtomography was used in conjunction with a gallium grain boundary wetting technique to visualise and analyse the correlation between three-dimensional structure of the grains and fatigue crack behaviour.

## 4:25 PM

Effects of Local Grain Orientation on Fatigue Crack Nucleation and Growth in Multicrystalline FCC Metallic Materials: *Pedro D. Peralta*<sup>1</sup>; Krishnakumar Komandur<sup>1</sup>; Robert Dickerson<sup>2</sup>; <sup>1</sup>Arizona State University, Dept. of Mech. & Aeros. Engrg., Engrg. Ctr., G Wing, Rm. 346, Tempe, AZ 85287-6106 USA; <sup>2</sup>Los Alamos National Laboratory, Matls. Sci. & Tech., MST-8, MS G755, Los Alamos, NM 87545 USA

The effect of local crystallography was studied in multicrystalline Compact-Tension specimens of pure nickel and a cast Ni-based superalloy. Samples were characterized using Orientation Imaging Microscopy to obtain the crystallographic orientations of the grains ahead of a notch. A fatigue crack growth test was then performed to characterize the crack nucleation sites and initial path in relation to the grain orientations. Results showed that crack could either grow with small deviations through all the grains ahead of it or experience large deflections from model. This behavior is correlated to the crystallographic characteristics of the local crack environment and the stress state obtained using finite elements. Intergranular cracks were found to prefer high angle boundaries, whereas transgranular cracks had a tendency to nucleate and grow following slip lines of systems with high Schmid factors. In addition, crack path tortuosity was more pronounced in grains with loading axes close to <111>.

## 4:45 PM

**Fractography of Two Solute-Strengthened Superalloys Haynes 230 and Hastelloy X High-Temperature Fatigue Failed in Air**: Y. L. Lu<sup>1</sup>; P. K. Liaw<sup>1</sup>; G. Y. Wang<sup>1</sup>; L. J. Chen<sup>1</sup>; M. L. Benson<sup>1</sup>; S. A. Thompson<sup>2</sup>; J. W. Blust<sup>2</sup>; P. F. Browning<sup>2</sup>; A. K. Bhattacharya<sup>2</sup>; J. M. Aurrecoechea<sup>2</sup>; D. L. Klarstrom<sup>3</sup>; <sup>1</sup>University of Tennessee, Dept. of Matls. Sci. & Engrg., Knoxville, TN 37996-2200 USA; <sup>2</sup>Solar Turbines, Inc., 2200 Pacific Hwy., PO Box 85376, MZ R-1, San Diego, CA 92186-5376 USA; <sup>3</sup>Haynes International, Inc., 1020 W. Park Ave., PO Box 9013, Kokomo, IN 46904-9013 USA

Low-cycle-fatigue and fatigue-crack-growth tests with different hold times were conducted on Haynesâ 230 and Hastelloyâ X at 816 and 927°C in air. The fractography was investigated. The fracture surfaces, especially at 927°C, were covered with oxides, which made the identification of the fracture mechanism difficult. Different cleaning techniques were tried to remove the oxides on the fracture surfaces. The cleaning results of different techniques were compared. The fracture mechanism was found to change from a transgranular mode to an intergranular one as the hold time or temperature increases. This work is supported by the Solar Turbines Inc., Haynes International, Inc., the Center for Materials Processing, the University of Tennessee, and the U. S. Department of Energy's Advanced Turbine System Program. We also acknowledge the financial support of the National Science Foundation, the Combined Research-Curriculum Development Program, under EEC-9527527 and EEC-0203415, and the Integrative Education and Research Training (IGERT) Program under DGE-9987548, and the International Materials Institutes (IMI) Program, under DMR-0231320, to the University of Tennessee, Knoxville, with Dr. D. Durham, Ms. M. Poats, Dr. W. Jennings, Dr. L. Goldberg, and Dr. C. Huber as contract monitors, respectively.

## 5:05 PM

Quantitative Analysis on Low Cycle Fatigue Damage: A Microstructural Model for the Prediction of Fatigue Life: *Hyun Jin Kim*<sup>1</sup>; Joon Sik Park<sup>1</sup>; Chong Soo Lee<sup>1</sup>; <sup>1</sup>Postech, Matl. Sci. & Engrg., San 31, Hyojadong, Nam-gu, Pohang, Kyungbuk 790-784 Korea

The present investigation is aimed to develop a model predicting the low cycle fatigue life of a material in relation to its microstructural variables. Since the grain size is important in determining the number and the size of persistent slip bands, which are considered as the major crack initiation sites, the low cycle fatigue life is expected to vary depending on the grain size. To achieve this goal, the concept of damage accumulation by multiple surface cracks has been adopted. Statistical analyses were carried out to investigate the relationship between the density of surface cracks and the low cycle fatigue damage. Also, one-dimensional percolation solution was used to describe the interactions between multiple surface cracks. To verify the suggested model, low cycle fatigue tests were conducted for the steels with the various grain sizes. The results showed good agreements between the experimental data and the predicted curve.

# **General Abstracts: Session VII**

Sponsored by: TMS

*Program Organizers:* Adrian C. Deneys, Praxair, Inc., Tarrytown, NY 10591-6717 USA; John J. Chen, University of Auckland, Department of Chemical & Materials Engineering, Auckland 00160 New Zealand; Eric M. Taleff, University of Texas, Mechanical Engineering Department, Austin, TX 78712-1063 USA

Wednesday PM	Room: 208B
March 17, 2004	Location: Charlotte Convention Center

Session Chair: Arne Dahle, University of Queensland, Div. of Matls. Engrg., Brisbane, QLD 4072 Australia

## 2:00 PM

**Control of Grain Size and Age Hardening in AA2618 Forgings Processed by Rapid Infrared Radiant Heating**: *Hui Lu*<sup>1</sup>; Puja B. Kadolkar<sup>2</sup>; Teiichi Ando<sup>1</sup>; Craig A. Blue<sup>2</sup>; Rob Mayer<sup>3</sup>; <sup>1</sup>Northeastern University, Mech., Industrial & Mfg. Engrg., 360 Huntington Ave., 334 Snell Engrg. Ctr., Boston, MA 02115 USA; <sup>2</sup>Oak Ridge National Laboratory, Metals & Ceram. Div., 1 Bethel Valley Rd., Oak Ridge, TN 37831 USA; <sup>3</sup>The Queen City Forging Company, 235-B Tennyson St., Cincinnati, OH 45226 USA Effects of rapid infrared (RI) radiant processing on the microstructure and mechanical properties of AA2618 aluminum forgings were investigated. Extruded bars were forged after RI-preheating to  $425^{\circ}$ C and solutionized at  $530^{\circ}$ C also in a RI furnace for different soaking times. Rapid preheating prior to forging produced uniform grain sizes (27-32 µm) in solutionized specimens while conventional furnace preheating produced coarser grain sizes (~40 µm) in the same 2618 alloy. Use of RI preheating for forging and subsequent solution heat treatment produced sufficient age hardening in 2618 forgings, which was verified by hardness and tensile tests. RI processing potentially leads to energy-efficient, low cost commercial production.

#### 2:25 PM

# Magnetostriction of Nanocrystalline Fe2Tb Alloy: *Pekka Reino Ruuskanen*<sup>1</sup>; <sup>1</sup>Technical Research Centre of Finland, Processes, PO Box 1607, FIN-33101, Tampere Finland

High magnetostrictive nanocrystalline Fe2Tb was prepared with a solid state mechanical alloying method. As starting materials elemental Fe and Tb were used. As-alloyed powder consists of amorphous and nanocrystalline phases. As-alloyed powder was cold compacted followed by annealing at 500°C. This temperature is 30°C above the crystallisation temperature of the as-alloyed powder. After annealing the microstructure of the material consists of a single phase nanocrystalline Fe2Tb the crystal size being 7-8 nm. The magnetostriction of the nanocrystalline material was measured with and without a biasing magnetic field. Using a biasing magnetic field a maximum magnetostriction 1 (Dl/1) = 1580\*10-6 was measured. This value was measured without a prestress. The stress sensitivity of the magnetostriction of the nanocrystalline material was found to be small.

#### 2:50 PM

A Model for Delayed Hydride Cracking in Zirconium Alloys: Young S. Kim<sup>1</sup>; Yeo B. Yoon<sup>1</sup>; Sung S. Kim<sup>1</sup>; Yong M. Cheong<sup>1</sup>; In S. Kim<sup>2</sup>; <sup>1</sup>Korea Atomic Energy Research Institute, Zirconium Team, PO Box 105, Yuseong, Daejeon 305-353 Korea; <sup>2</sup>Korea Advanced Institute of Science and Technology, Nucl. Engrg. Dept., Kuseong-dong, Daejeon 305-701 Korea

The objective of this study is to identify factors governing the crack growth velocity and threshold stress intensity factor during delayed hydride cracking (DHC) of zirconium alloys and to propose a DHC model that can satisfactorily explain all the unresolved issues related to DHC. To this end, DHC tests have been conducted at temperatures ranging from 100 to 300°C on Zr-2.5Nb alloys with different yield strengths and hydrogen concentrations of 12 to 100 ppm. With increased supersaturated hydrogen concentration, DHC velocity (DHCV) of the Zr-2.5Nb alloys has been increased to a constant and its threshold stress intensity factor, KIH has also been decreased. Thus, DHCV and K<sub>IH</sub> can be nicely described as a function of the supersaturated hydrogen concentration over the terminal solid solubility for dissolution (TSSD) independent of temperatures. Another factor to control DHCV is the yield strength of the Zr-2.5Nb pressure tube: faster DHCV for the Zr-2.5Nb tubes with a higher yield strength. Consequently, we conclude that delayed hydride cracking of Zr-2.5Nb pressure tubes is governed by their yield strength and a difference in the hydrogen concentration in solution between the crack tip and the bulk regions. Based on these findings, we suggest a new DHC model: a driving force for DHC is a concentration difference of hydrogen between the bulk region and the crack tip incurred by the nucleation of reoriented hydrides only at the crack tip subjected to applied tensile stress while its velocity is governed by a hydrogen concentration gradient determined by a stress gradient formed ahead of the crack tip. This DHC model has been validated through a supplementary experiment demonstrating that little supersaturated hydrogen concentration in the bulk region of zirconium alloys suppresses DHC and by correlating the yield strength effect and the striation spacings.

## 3:15 PM

#### A Hot Fracture Criterion for Processing of High-Mg 5xxx Aluminum Alloys: *Paul T. Wang*<sup>1</sup>; <sup>1</sup>Alcoa Inc., Proc. Tech., 100 Tech. Dr., Alcoa Ctr., PA 15069 USA

An investigation of hot fracture behavior of high Magnesium 5xxx aluminum alloys is pursued under both tensile and shear tests at various temperature and strain rate conditions. The test results are used for the purpose of constructing a hot fracture limit diagram. The diagram is composed of hot ductility as a function of strain rate, temperature, and hydrostatic stress, and represents two fracture modes - ductile and hot short. To further confirm these two fracture modes, fracture surfaces were analyzed by optical metallography and FEG-SEM. This leads to the development of a multiple-mode fracture criteria suitable for use in thermomechanical processing of aluminum. Hot rolling of multiple pass situations in the frame of Arbitrary Lagrangian-Eulerian encompassed the fracture criterion are simulated and compared with lab rolling experimental results.

## 3:40 PM Break

#### 3:50 PM

Ageing Hardening and Softening Behavior of the Mg-RE Alloys: Y. B. Xu<sup>1</sup>; J. H. Zhang<sup>1</sup>; <sup>1</sup>Shenyang National Laboratory for Materials Science, Inst. of Metal Rsch., Chinese Acad. of Scis., Shenyang 110016 China

Ageing hardening and softening behavior of the Mg-RE alloys has been investigated by TEM. The results show that the first hardeningpeak occurs at 475K for about 2 hours, and then the hardness of the alloy decreases sharply. The second hardening-peak appears during the following ageing. After ageing at 523K for 600 hours, the alloy starts to be softening. Investigations by TEM reveal that the first hardening-peak is due to the occurrence of the dispersed precipitates with the sizes of 5nm in diameter, and the sharp fall of the hardness results from the dissolution of the MgY phases. â-precipitation leads to the second hardening of the alloys, and the alloy softening again is proposed to attribute to the growth of the â-precipitates.

### 4:15 PM Cancelled

#### The Way to Reduce the Cost of Titanium Alloys

#### 4:40 PM

Microstructure and Creep Behavior of a Cast Mg-RE Alloy: Guiying Sha<sup>1</sup>; Yongbo Xu<sup>1</sup>; Enhou Han<sup>1</sup>; <sup>1</sup>Shenyang National Laboratory for Materials Science, Inst. of Metal Rsch., Chinese Acad. of Scis., Shenyang 110016 China

The compress creep tests of a cast Mg-RE alloy were carried out at constant stress on Mayes fatigue machine in air-creep behavior of the alloy has been investigated at different temperatures. Observations by SEM and TEM show that the creep resistance of the alloy is relatively high at 473K under stress  $\leq$  100MPa and the steady creep rate is lower than s-1. The eutecticBphase comprised Ce, La, Nd etc elements and dynamic precipitation during creep is proposed to be the principal strengthening mechanism of the alloy - whereas the main reason for the decrease of the creep resistance is attributed to be twins shear deformation and cracking of the eutecticBphases.

## 5:05 PM

Magnesium Semi-Fabricated Products at Industrial Scale: Juan Gomez-Cordobes<sup>1</sup>; <sup>1</sup>Rauch Melting Technique, Innovation, Fichtenweg 3, Gmunden, Upper Austria 4810 Austria

In the year 2001, the European production of aluminium semifabricated products (rolled, extruded and forged products) did triplicate the shipments from aluminium casting processes in any of its forms. Due to quality, price and availability issues, the market structure in the magnesium world is drastically different, and while casting shipments world wide surpassed 130.000 tons in 2002, wrought alloys applications are still almost non existent. Based on the learnings gathered in two parallel projects in operation since 2002, the following paper provides an insight into the manufacture of magnesium semi-fabricated products at industrial scale. The study concentrates on the production of the material needed for the subsequent forming processes. It is in this area where a newly developed liquid metal handling and feeding concept has allowed for the production at industrial scale of high quality bars, billets and thin sheet to be subsequently utilised in forging, extrusion and rolling processes.

# General Abstracts: Session VIII

Sponsored by: TMS

*Program Organizers:* Adrian C. Deneys, Praxair, Inc., Tarrytown, NY 10591-6717 USA; John J. Chen, University of Auckland, Department of Chemical & Materials Engineering, Auckland 00160 New Zealand; Eric M. Taleff, University of Texas, Mechanical Engineering Department, Austin, TX 78712-1063 USA

Wednesday PM	Room: 207D
March 17, 2004	Location: Charlotte Convention Center

Session Chair: Margaret Hyland, University of Auckland, Dept. of Chem. & Matls. Engrg., Auckland New Zealand

### 2:00 PM

Morphology of Resultant Surfaces from Electro Discharge Machining and Electro Discharge Sawing: V. Narsimha Rao<sup>1</sup>; N. N. Ramesh<sup>2</sup>; P. Laxminarayana<sup>3</sup>; <sup>1</sup>CITD, Balanagar, Hyderabad 500 037 India; <sup>2</sup>Osmania University, Mech. Engrg. Dept., Hyderabad 500 007 India; <sup>3</sup>Osmania University, Mech. Engrg. Dept., College of Tech., Hyderabad 500 007 India

Electrical discharge machining (EDM) employs high frequency sparks for machining difficult to machine metals. Its slow erosion rates renders it unsuitable for large and faster cuts like sawing. A modified process called Electro discharge sawing (EDS) has been developed which is a hybrid process. In place of dielectric an electrolyte, Sodium silicate plus water, is used to promote arcing in place of sparking, to produce a passivating film on work surface to prevent short circuits and to quench the eroded debris and carry them off the inter electrode gap. The electrode is a steel belt continuously moving through ceramic guides. The erosion rates are extremely high. Morphological studies of erosded surfaces under scanning electron microscope for mechanism of erosion indicate the EDM surfaces to be matty with overlapping spark craters whereas EDS surfaces shows pitting erosion from arcing and short circuiting pulses.

## 2:25 PM

Microstructure-Property Studies of Sputter Deposited Cu(1x)Ta(x) Thin Films: Shannon Marie Jackson<sup>1</sup>; J. Michael Rigsbee<sup>1</sup>; <sup>1</sup>North Carolina State University, Dept. of Matls. Sci. & Engrg., 229 Riddick, Campus Box 7907, Raleigh, NC 27695-7907 USA

A series of  $Cu_{1,x}Ta_x$  (x = 0.05 to 0.5) thin films have been produced by DC magnetron sputter deposition using co-deposition (alloy) and sequential (layered) deposition modes at room and elevated temperatures. The nanoscale microstructures of these non-equilibrium "alloy" films have been investigated chemically and structurally using x-ray diffraction, scanning electron microscopy and high resolution, z-contrast transmission electron microscopy. The effects of Ta composition, deposition temperature and deposition mode on microstructure will be discussed, along with nanoindentation studies of selected samples.

## 2:50 PM

Effect of Material Characteristics on the Surface Texture From Burnishing Processes: Voleti Sri Ram Murti<sup>1</sup>; K. Sudhakar<sup>1</sup>; M. Rama Linga Reddy<sup>1</sup>; Syed Abraruddin Hasan<sup>1</sup>; <sup>1</sup>Osmania University, Mech. Engrg. Dept., Hyderabad, Andhra Pradesh 500 007 India

The present paper seeks to study the significant influence of Material Characteristics on the final texture of burnishing surfaces generated by Cold working of roughness peaks by hard pressed ball or roller. The analytical approach includes not only the conventional roughness indices but also their spatial and shape characteristics. The stratification of the surface texture was analyzed through its structure function. Plastic flow from cold working of roughness peaks resulting in their flattening appears to be the dominant mechanism in ductile materials. However rupture of the peaks cannot be ruled out which is the dominant mechanism for brittle materials. In Powder Metallurgy materials the closure of voids results in lower plastic flow. The stratification is prominently illustrated and analyzed through the structure function which proves to have highest sensitivity to identify stratification characteristics.

## 3:15 PM

High Temperature Performance of Novel Ti-Al-Oxide Composite Coatings Produced by Plasma Spraying: *Jing Liang*<sup>1</sup>; Byung-Young Choi<sup>2</sup>; Kai Zhang<sup>1</sup>; Deliang Zhang<sup>3</sup>; Wei Gao<sup>1</sup>; <sup>1</sup>The University of Auckland, Dept. of Chem. & Matls. Engrg., PB 92019, 20 Symonds St., Auckland New Zealand; <sup>2</sup>Chonbuk National University, Korea, Sch. of Advd. Matls. Engrg., Rsch. Ctr. of Industrial Tech., Chonju 561-756, Chonbuk Korea; <sup>3</sup>University of Waikato, Dept. of Matls. & Procg. Engrg., Hamilton New Zealand

TiAl/Al2O3 composite powder was produced by mechanical alloying, sintering and grounding. Thermal plasma spraying was used to coat this powder onto Ti-6Al-4V alloy samples. The high temperature oxidation and hot corrosion behaviour of the coatings was studied in dry air and Na2SO4 + NaCl vapour, respectively. The results showed that Ti-Al-oxide coatings have a much improved oxidation and hot corrosion resistance compared to the substrate Ti-6Al-4V alloy. The oxide formed on the surface of the coatings after high temperature exposure is composed of a mixture of a large portion of Al2O3 and a small portion of TiO2. The oxide scales have excellent adhesion to the coatings, showing superior scale spallation resistance. The mechanisms with which the coatings improved the oxidation resistance were studied based on microstructural analysis. It is believed this development can provide a new generation of coatings to the Ti based alloys which will be able to raise the application temperature of Ti alloys from 650°C to 800-900°C.

## 3:40 PM Break

## 3:50 PM

**Construction and Applications of Wear Maps for Ferrous Thermal Spray Coatings**: *Afsaneh Edrisy*<sup>1</sup>; Tom Perry<sup>2</sup>; Yang-Tse Cheng<sup>2</sup>; Ahmet T. Alpas<sup>1</sup>; <sup>1</sup>University of Windsor, Mech., Auto. & Matls. Engrg., 401 Sunset Ave., Windsor, Ontario N9B 3P4 Canada; <sup>2</sup>General Motors, R&D Ctr., Matls. & Proc. Lab, MC 480-106-224, 30500 Mound Rd., Warren, MI 48090-9055 USA

Ferrous coatings with nominal 1020 composition were produced using two types of thermal spray deposition processes namely PTWA, and HVOF on aluminum alloy substrates in order to assess their wear resistances. Micomechanisms that control wear resistances of the coatings included deformation of the steel splat tips and their fracture that resulted in high wear rates at high loads, and the formation of oxide layers on the contact surfaces. The formation and spallation of friction-induced oxides controlled wear rates at high sliding velocities. The composition and thickness of the oxides that formed on the surfaces depended on the production methods. The results were summarized in the form of Wear Mechanism Maps using normal load vs. sliding speed axes on which the dominant wear mechanisms in each wear regime were marked. The wear maps help illustrate the effects of composition and structure on wear behavior of thermal sprayed coatings for automotive engine applications.

## 4:15 PM

A Comparison of Surfactant Aggregation Transition Concentration Determined Using Electrochemical Quartz Crystal Microbalance Tests, Surface Tension Measurements, Corrosion Inhibition Tests, and Theoretical Methods: Dong Youp Ryu<sup>1</sup>; Michael L. Free<sup>1</sup>; <sup>1</sup>University of Utah, Dept. of Metallurgl. Engrg., 135 S. 1460 E., Rm. 412, Salt Lake City, UT 84112 USA

The surfactant aggregation transition concentration (atc) is the concentration associated with the transition from surfactant monomers to micelles in solutions. The atc is also related to the transition from monolayer to multilayer coverage of surfactant molecules at interfaces. Usually these values are similar although they are usually not identical due to surface energy issues associated with interfacial adsorption. These values can be determined by various methods such as Electrochemical Quartz Crystal Microbalance (EQCM), surface tension, and corrosion inhibition tests as well as theoretical methods. This paper discusses various approaches for determining the atc values as well as the factors that affect atc values.

# 4:40 PM

Microstructural Refinement of Fe-40a%Al Alloy by Thermomechanical Processing: Tomasz Sleboda<sup>3</sup>; Norman S. Stoloff<sup>1</sup>; Jason Kane<sup>1</sup>; Roger N. Wright<sup>1</sup>; David J. Duquette<sup>1</sup>; Seetharama C. Deevi<sup>2</sup>; <sup>1</sup>Rensselaer Polytechnic Institute, Matls. Sci. & Engrg., 110 8th St., Troy, NY 12180 USA; <sup>2</sup>Philip Morris USA, Richmond, VA 23234 USA; <sup>3</sup>Rensselaer Polytechnic Institute, Matls. Sci. & Engrg., Troy, NY 12180 USA (on leave from the AGH University of Science and Technology, Metall. & Matls. Sci. Dept., Al. Mickiewicza 30, 30-059 Krakow, Poland)

This research is focused on thermomechanical grain refinement of a Fe-40at.%Al alloy. Hot isostatic pressing of as-received and ball milled powder at relatively low pressures resulted in fully densified products. Ball milling caused significant powder particle size reduction, resulting in a finer structure after HIPing. Fully densified, as-received as well as ball milled, FeAl powders were tested in compression on a Gleeble thermomechanical simulator in the temperature range 700°C to 1100°C. Flow stress curves and microstructural changes were investigated after Gleeble tests. Room temperature compression tests revealed that grain refinement strongly influenced the mechanical properties of the investigated material. A separate part of this investigation involved a study of the evolution of recovery, recrystallization and grain growth in cold-rolled Fe-40Al sheet. Anneals were carried out over a temperature range of 100-1200°C for various selected times. Structural changes were characterized by o ptical microscopy and changes in mechanical properties were characterized by microhardness testing. Research supported by Philip Morris USA.

# High Risk Technologies in Metallurgy with Commercial Potential: Session II

Sponsored by: TMS, PGA-Public and Governmental Affairs Committee

*Program Organizers:* Jean-Louis Staudenmann, NIST, Advanced Technology Program, Division 473, Gaithersburg, MD 20899-4730 USA; Diran Apelian, Worcester Polytechnic Institute, Metal Processing Institute, Worcester, MA 01609-2280 USA

Wednesday PMRoom: 210AMarch 17, 2004Location: Charlotte Convention Center

Session Chairs: Diran Apelian, Worcester Polytechnic Institute, Metal Procg. Inst., Worcester, MA 01609-2280 USA; Jean-Louis Staudenmann, NIST, Advd. Tech. Prog., Gaithersburg, MD 20899-4730 USA

## 2:00 PM

Nucleated Casting for the Production of Large Superalloy Ingots: *William T. Carter*<sup>1</sup>; Robin M. Forbes Jones<sup>2</sup>; <sup>1</sup>General Electric Global Research Center, Ceram. & Metall. Tech., One Rsch. Cir., Bldg. K1, Rm. 279MB, Niskayuna, NY 12309 USA; <sup>2</sup>Allvac, An Allegheny Tech. Co., Monroe, NC USA

To reduce the cost of electricity generated by land based gas turbines, designers and manufacturers of turbines strive to improve the design of future machines by increasing the thermodynamic efficiency, electrical output and reliability. Doing so requires higher firing temperatures and larger turbines. This, in turn, increases the temperatures and stresses on critical components such as the turbine wheel. To accommodate these increased temperatures and stresses, turbine wheel designers have changed the materials of construction from iron based alloys to increasingly more complicated nickel based superalloys. For example in a recent design change, one manufacturer changed from Alloy 706 to Alloy 718, and for future turbines, is projecting further increases in turbine wheel size. The current manufacturing process for making superalloy wheels results in only one wheel from each cast ingot. It is unlikely that the projected future increases in turbine wheel size can be accommodated using the standard triple melt ingot casting technique, which is limited by metallurgical requirements to maintain properties and minimize segregation. New casting technology will be required. A review of several promising alternative technologies resulted in the a selection of Nucleated Casting as the one that offered the most promise for making the larger ingots. Nucleated Casting separates the melting process from the solidification process, providing additional degrees of freedom in process control. However, several new technologies must be developed, making it a high technical risk solution with a long time before commercialization. A long-term technology development strategy was identified in which a research partnership between a turbine manufacturer and a ingot supplier, reinforced by a US Government program, was an essential ingredient. To increase the chances of successful completion within the four-year timeframe, a detailed list of the technical risks was identified and the project was structured to mitigate each of the risks. The development plan entails concurrent subscale process development along with development of validated process models. A successful program will allow the use of validated models to extrapolate findings to a commercial scale suitable for use in the next generations of gas turbines.

#### 2:25 PM

### Application of Composite Materials and Design for Advanced Wind Turbine Rotor: Steven R. Kopf<sup>1</sup>; <sup>1</sup>AdvanTek International, LLC, 7 Creek Pkwy., Ste. 770, Boothwyn, PA 19061 USA

Instantaneous Power Control<sup>TM</sup> (IPC<sup>TM</sup>) is a new and revolutionary concept in rotor design and power control for utility scale wind turbines that offers the potential of increasing the rotor diameter by 30% without an equivalent increase in the capital cost of the system. IPC<sup>TM</sup> integrates an active control system, featuring sensors, high bandwidth actuators, and a computer controller, into wind blade design, and is expected to bring down wind energy cost by capturing more power at lower wind speeds without overloading the gearbox and generators during high winds. However, in order to successfully demonstrate this advanced rotor so that it can be commercialized, several high-risk technological hurdles must be overcome. One of these risks is the optimal application of advanced composite materials to the IPC<sup>TM</sup> rotor and control system. The IPC<sup>TM</sup> blades are much longer and more slender than a state-of-the-art blade system. As a result, the blade root bending moment and fatigue loads are much higher. Material selection and design methodology are critical to insuring that the blade meets commercial cost targets. Another identified risk area is fact that the power performance of the IPC<sup>TM</sup> blades is extremely sensitive to both manufacturing tolerances and structural deflections during turbine operations. Small variations in certain critical blade geometries can negate the advantage gained by the increase in rotor diameter. The paper will present an overview of the methodology that is being used to overcome these high-risk technological hurdles to allow the successful demonstration and subsequent commercialization of the IPC<sup>TM</sup> rotor and control technology.

#### 2:50 PM

## Heat Treating Aluminum Alloys Utilizing Fluidized Bed Quenching: Jay Keist<sup>1</sup>; Chuck Bergman<sup>1</sup>; <sup>1</sup>Technomics, LLC, 17200 Medina Rd., Plymouth, MI 55447 USA

To achieve optimum mechanical properties after heat treating, rapid quenching is critical to obtain a supersaturated solution. To obtain rapid quenching, manufacturers often employ water as a quenchant. The drawback of water is that a vapor barrier initially forms during the quenching which leads to variations in quenching rates from one section to another within the part. The large variations in quenching rates often manifests as unacceptable part warpage and high residual stresses. An attractive alternative is quenching in a fluidized bed. A vapor barrier is not formed during fluidized bed quenching thus drastically reducing residual stresses and warpage. We analyzed the quenching curves and resulting mechanical properties for various castings of aluminum alloys 319, 354, and 356. Water and fluidized bed quenching was compared at various temperatures. Smaller parts (less than 10 lbs) exhibited similar mechanical properties between water quenched and fluidized bed quenched samples. Despite the significantly longer quenching times, larger parts quenched in fluidized beds exhibited only a small decrease in mechanical properties as compared to water quenched samples. Furthermore, quenching in fluidized sand at relatively high temperatures (300 to 400°F) still yielded acceptable properties. The ability to quench at aging temperatures may lead simplified heat treating processes by quenching in the aging bed directly after solution.

#### 3:15 PM Break

#### 3:30 PM

Triboelectric Purification, Rapid Optical Analyses and Metallurgical Characterization of Powdered Metals: John M. Stencel<sup>1</sup>; Tapiwa Z. Gurupira<sup>1</sup>; Charles L. Jones<sup>1</sup>; Lou Lherbier<sup>2</sup>; David Novotnak<sup>2</sup>; Gregory Del Corso<sup>2</sup>; <sup>1</sup>Tribo Flow Separations, 1525 Bull Lea Rd., Ste. 10, Lexington, KY USA; <sup>2</sup>Tribo Flow Separations, 600 Mayer St., Bridgeville, PA USA

The economic manufacturing of high alloy metal powders into full dense parts has been impaired for years by variations in powder cleanliness. Ceramic inclusions inherent in most gas-atomized, induction melted powders can seriously affect the quality of some consolidated parts. Current remedies include screening the powder to finer mesh cuts to eliminate large inclusions and/or conducting extensive testing of the consolidated material to ensure quality requirements prior to customer shipment. Besides being time consuming, metallurgical techniques like tensile, Charpy impact, ultrasonic, water elutriation, metallographic and EDM tests that are used to evaluate quality only examine a small faction of the material actually produced. The development of triboelectric purification (TEPTM) is a promising manufacturing process that can remove significant amounts of ceramic impurities from metal powders. Its application could increase usable atomized yields by 10-20%, while at the same time reduce quality losses. TEPTM also eliminates the uncertainty associated with evaluating a small sample of material by various test procedures since all of the powder from an atomized lot is purified by the process. To prove the efficacy of TEP<sup>™</sup> in a timely manner, material subjected to purification can be characterized by using a newly developed, automated optical microscopic analysis (OMA<sup>TM</sup>) technique that obviates the need for using the costly and time-consuming metallurgical tests. Because statistically significant OMA<sup>™</sup> data are attainable within a 24 hour time period, a rapid assessment of atomized powder purity is possible. Results obtained on high-speed steel and prosthetic implant alloy, gas atomized powders using TEPTM processing and OMATM analyses will be described.

#### 3:55 PM

Measurements, Standards, and Data: Overcoming Technical Barriers to the Reductions of the Time-to-Market Cycle for Advanced Metals: *Clare M. Allocca*<sup>1</sup>; <sup>1</sup>National Institute of Standards and Technology, Matls. Sci. & Engrg. Lab., 100 Bureau Dr., Stop 8500, Bldg. 223/B316, Gathersburg, MD 20899-8500 USA

Current business realities present continuing challenges for the commercial application of advanced metals. Customers demand the development and adaptation of materials more rapidly and efficiently than ever before. The simultaneous need for the reduction of the time-tomarket cycle and final cost drives the need for new approaches to materials development. These drivers have placed renewed emphasis on the role of measurement science and computational modeling as enablers of advanced metals development. This presentation will describe some of the ways in which the NIST Materials Science and Engineering Laboratory has responded to these needs: Standard tests, metrology and models that can enable the accurate determination of sheet metal mechanical response, which in turn reduce the die tryout time for die sets for automotive bodies; Measurements, models, data, and standards needed by the microelectronics industry to evaluate the national standard Pb-free alloy and processes needed to use the alloy in circuit board assembly; Combinatorial methods for the acceleration of materials discovery and the reduction of development time of engineered materials; GMR; Superalloys. These and other activities will be discussed. Methods for interactions with NIST will also be addressed NIST Combinatorial Methods Center, and facilities such as the NIST Center for Neutron Research.

# Hume Rothery Symposium: Structure and Diffusional Growth Mechanisms of Irrational Interphase Boundaries: Session VI

Sponsored by: Electronic, Magnetic & Photonic Materials Division, Structural Materials Division, EMPMD/SMD-Alloy Phases Committee, MPMD-Phase Transformation Committee-(Jt. ASM-MSCTS)

*Program Organizer:* H. I. Aaronson, Carnegie Mellon University, Department of Materials Science and Engineering, Pittsburgh, PA 15213 USA

Wednesday PM	Room:	208A
March 17, 2004	Location	: Charlotte Convention Center

Session Chair: B. C. Muddle, Monash University, Sch. of Physics & Matls. Engrg., Victoria 3800 Australia

2:00 PM General Discussion

# International Laterite Nickel Symposium - 2004: Process and Operational Lessons Learned - Part II

Sponsored by: Extraction & Processing Division, EPD-Aqueous Processing Committee, EPD-Copper, Nickel, Cobalt Committee, EPD-Process Fundamentals Committee, EPD-Process Mineralogy Committee, EPD-Pyrometallurgy Committee, EPD-Waste Treatment & Minimization Committee *Program Organizer:* William P. Imrie, Bechtel Corporation,

Mining and Metals, Englewood, CO 80111 USA

Wednesday PM	Room: 2	17B/C		
March 17, 2004	Location:	Charlotte	Convention	Center

Session Chairs: John G. Schofield, Pyrometallurgical Consultant, Nanoose Bay, BC V9P 9G5 Canada; Steve C.C. Barnett, V-P HSEQC Stainless Steel Materials, BHP-Billiton, London SW1V 1BH UK

## 2:00 PM

The Steps Required to Meet Production Targets at PT INCO: A New Innovative Business Strategy: Chris Doyle<sup>1</sup>; Management & Staff<sup>1</sup>; Management & Staff<sup>2</sup>; <sup>1</sup>PT INCO, Sorowako, Sulawesi Selatan 91984 Indonesia; <sup>2</sup>Inco Technical Services Ltd., 2060 Flavelle Blvd., Sheridan Park, Mississauga, Ontario L5K 1Z9 Canada

From 1997-2000, PT INCO undertook the Fourth Line Expansion Project (FLEX) to increase annual production rates from 90-100 to 150 Mlbs Ni/year. In 2003, PT INCO nickel production underwent a major sustainable step jump that finally exceeded the targeted rate. This paper presents the changes that led to this achievement. The focus of mining changed. Improving Ni grade was important but only if electric furnace feed met target chemistry so that on-specification slag could be produced. The intensity of diamond core drilling for exploration was dramatically upgraded, mine planning strategy was totally re-vamped and an ore chemistry quality assurance team was formed. In the processing plant, measurement systems were upgraded for better control. Teamwork between sections vastly improved. The final step jump in production occurred when the fifth hydro-electric power generator was added to the furnace grid to allow the powerstarved furnaces to cruise in operation at 70+ MW.

## 2:30 PM

Falcondo's Revisited: Edwin de Jesús Deveaux<sup>1</sup>; Francisco Geraldo Longo<sup>1</sup>; <sup>1</sup>Falconbridge Dominicana, Mining & Dvlp., Box 1343, Santo Domingo Dominican Republic

After 32 years of operations beneficiating lateritic nickel ore in a fully integrated pyrometallurgical complex, Falconbridge Dominicana (FALCONDO), situated at Bonao and La Vega Provinces, Dominican Republic, has become profitable with one of the lowest nickel grade content processing plants in the world, and literally without any by-product (granulated slag, will be utilized in the future as a post-processing subproduct). To December 2002, mineral reserves were 64.1 million tonnes containing laterite grading as low as 1.15 % Ni when full dilution is applied. At a cut-off grade of 1.20% Ni, the reserves will provide 15-20 years of production. The mineralized thickness over the seven active deposits averages 6 m. Development of very selective and unique mining practices, together with improvements in the process plant, are key to achieving the production goal (30 kt Ni/yr) and to meet the quality standards for the ferronickel produced.

## 3:00 PM

Falconbridge Dominicana Reduction Shaft Furnace Advanced Control Development: Lionel Ryan<sup>1</sup>; J. Frias<sup>2</sup>; P. Rodriguez<sup>2</sup>; A. Morrow<sup>3</sup>; M. Boland<sup>3</sup>; David Sandoz<sup>4</sup>; <sup>1</sup>Noranda Inc./Falconbridge Ltd., Metallurgl. Tech. Grp., Falconbridge Tech. Ctr., Falconbridge, Ontario POM 1SO Canada; <sup>2</sup>Noranda Inc./Falconbridge Ltd., Falconbridge Dominicana C. Por A., PO Box 1343, Santo Domingo Dominican Republic; <sup>3</sup>Invensys (Foxboro), 33 Commercial St. C42-2E, Foxboro, MA 02035 USA; <sup>4</sup>Perceptive Engineering, Brindley House, 4 Bridgewater Ct., Barsbank Ln., Lymm WA13 0ER Cheshire

In 1996, the Dominican Republic operation of Falconbridge (Falcondo) developed a 5-year Process Control Plan in conjunction with the corporate Process Control group located in Sudbury, Ontario, Canada. This plan was further refined into an analysis of the areas of the highest potential economic return for the company with the reduction shaft furnace operation being the most promising. Historically, the reduction plant has been the bottleneck of ferronickel production. Since 1996 there has been a history of control development with the shaft furnaces, with a current status of 11 of the 12 furnaces running advanced model-based multi-variable predictive control. The combination of Advanced Process Control (APC), improved control system performance, and improved process information management has resulted in an increased throughput of 6% per shaft furnace and a reduction in operating costs of 4.5 US cents/lb of Ni. This paper reviews some of the major milestones that have been achieved in this development.

## 3:30 PM Break

#### 3:50 PM

A Historical Overview of the Cerro Matoso Operation 1980 to 2003: Julian Robert Kift<sup>1</sup>; <sup>1</sup>Cerro Matoso S. A., Tecnología, Calle 114 No. 9-01. Torre A, Piso 5. Oficina 509, Bogotá, DC Colombia

The Cerro Matoso S.A. mine and smelter, in the Cordoba lowlands of northwestern Colombia, consist of a dedicated laterite nickel mine, ore blending, drying and an RKEF process to produce high-quality ferronickel. At a project investment of \$400M, first production of ferronickel was in September 1982, and in its inaugural year CMSA produced 6,150 tons of contained Ni from a mined ore grade of 3.2% Ni. Initial operational difficulties resulted in a number of furnace runouts, which impacted ramp up to design ore throughput of 128 dry t/h. Since then CMSA has steadily incorporated process improvements and initiatives to take the single line operation to an ore throughput of 175 dry t/h. A second 175 dry t/h line was added in 2001 (investment of US\$ 300M) to consolidate CMSA as one of the world's lowest cost Ni producers with an installed annual production capacity of over 50,000 tons Ni. The most recent addition is commissioning of Phase 1 of an ore-upgrading project to counteract the effect of declining ore grades.

## 4:20 PM

Recent Improvement of Reduction Rotary Kilns at Hyuga Smelting Co., Ltd.: K. Moriyama<sup>1</sup>; M. Yamagiwa<sup>1</sup>; A. Kaikake<sup>1</sup>; *H. Takano<sup>1</sup>*; <sup>1</sup>Hyuga Smelting Co., Ltd., Production Sect., Funaba-cho 5, Hyuga City, Miyazaki Pref 883-8585 Japan

Operation improvement efforts at Hyuga Smelting Co., Ltd. have focused on calcining capacity in the reduction rotary kilns ("the kilns"), whose limited feed rate capacity had capped production at around 18,000t-Ni/Y since 1995. To improve the kilns' feed rate capacity of

80 wet t/hr, attempts were made to increase the gas flow in the kilns by increasing the capacity of the off-gas fans. However, as the increased gas flow resulted in only limited improvement of the kilns' feed rate, a scoop feeder was installed on each kiln to add coal to the middle of each kiln's interior to gain a higher efficiency of thermal supply and conversion. With these gas flow and coal charge addition operations, the kilns' feed rate capacity increased up to 120 wet t/hr, with burner fuel efficiency increasing by approx.10% (approx. 5% in total with the additional coal included). As a result, production was raised to a level of 22,000t-Ni/Y.

# Lead-Free Solders and Processing Issues Relevant to Microelectronic Packaging: Microstructural Characterization and Evolution

Sponsored by: Electronic, Magnetic & Photonic Materials Division, EMPMD-Electronic Packaging and Interconnection Materials Committee

Program Organizers: Laura J. Turbini, University of Toronto, Center for Microelectronic Assembly & Packaging, Toronto, ON M5S 3E4 Canada; Srinivas Chada, Jabil Circuit, Inc., FAR Lab/ Advanced Manufacturing Technology, St. Petersburg, FL 33716 USA; Sung K. Kang, IBM, T. J. Watson Research Center, Yorktown Heights, NY 10598 USA; Kwang-Lung Lin, National Cheng Kung University, Department of Materials Science and Engineering, Tainan 70101 Taiwan; Michael R. Notis, Lehigh University, Department of Materials Science and Engineering, Bethlehem, PA 18015 USA; Jin Yu, Korea Advanced Institute of Science and Technology, Center for Electronic Packaging Materials, Department of Materials Science & Engineering, Daejeon 305-701 Korea

Wednesday PM	Room: 27	19B		
March 17, 2004	Location:	Charlotte	Convention	Center

Session Chairs: Michael R. Notis, Lehigh University, Dept. of Matls. Sci. & Engrg., Bethlehem, PA 18015 USA; Eric J. Cotts, Binghamton University, Physics & Matls. Sci., Binghamton, NY 13902-6000 USA

#### 2:00 PM Invited

The Microstructure of Pb Free Solder Joints: Eric J. Cotts1; Lawrence P. Lehman<sup>1</sup>; Lubov Zavalij<sup>1</sup>; Robert Kinyanjui<sup>1</sup>; <sup>1</sup>Binghamton University, Physics & Matls. Sci., Sci. 2, Vestal Pkwy. E., PO Box 6000, Binghamton, NY 13902-6000 USA

The microstructural evolution of the widely used lead free solder, Sn95.5Ag3.5Cu1.0 and a variety of close compositions, Sn100-yxAgxCuy, where 0 < x < 5 and 0 < y < 3 was examined after reflow, or after reflow on either Cu or Ni/Au metallizations. Heat treatment was conducted in a Differential Scanning Calorimeter (DSC) providing good control of the thermal profile and a quantitative measure of any thermal reactions during the process, including solidification. The effect of peak reflow temperature, cooling rate (0.01 to 3 oC/s), solder composition and metallization on the microstructure of the Pb free solders was examined. The microstructure was viewed with optical microscopy using cross polarizers and by scanning electron microscopy, and the distribution of species within the joint was measured. Grain size and orientations were studied, and related to possible mechanisms of solidification. Support from the National Science Foundation, DM0218129 is gratefully acknowledged.

#### 2:25 PM

WEDNESDAY PM

Microstructure-Based 2D and 3D Modeling of the Deformation of Pb-Free Solders: Rajen S. Sidhu<sup>1</sup>; Xin Deng<sup>1</sup>; Nikhilesh Chawla<sup>1</sup>; <sup>1</sup>Arizona State University, Dept. of Chem. & Matls. Engrg., Tempe, AZ 85287 USA

It is well known that microstructure, as controlled by variations in cooling rate or thermal aging, directly influences the mechanical behavior of Pb-free solders. In this talk, we report on two-dimensional (2D) and three-dimensional (3D) microstructure-based simulations of the deformation in Pb-free solders and solder joints. Representative 2D scanning electron micrographs were used as a basis for the 2D analysis. For the 3D analysis, a serial sectioning approach was used to obtain several 2D sections along the thickness of the solder, followed by 3D reconstruction of the microstructure. The reconstructed 3D volume was then used as an input for modeling using finite element analysis. Several microstructural features of Pb-free solders were modeled. These included: (a) the influence of Ag<sub>3</sub>Sn morphology and distribution on the monotonic behavior of Sn-Ag solder and (b) the influence of Cu<sub>6</sub>Sn<sub>5</sub> intermetallic thickness and morphology on the shear behavior of aged Sn-Ag solder/Cu joints. The effect of these microstructure variables on deformation and damage in Pb-free solders, and the implications for microstructure design of solders with improved mechanical properties will be discussed.

#### 2:45 PM

Effects of Ga Additions on the Microstructure and Properties of Sn-Zn Solder Alloys: Jenn-Ming Song1; Nai-Shuo Liu1; Kwang-Lung Lin1; 1National Cheng Kung University, Dept. of Matls. Sci. & Engrg., Tainan 701 Taiwan

The effects of Ga content on the microstructure, thermal behavior and tensile properties of Sn-Zn eutectic alloy were examined in this study. Results show that Ga was dissolved in both Sn and Zn phases. This gave rise to irregular eutectic structure with misaligned, less distributed massive Zn-rich phase, relatively low melting point, and solid solution strengthening effect. Due to the inhomogeneous dissolution feature of Ga in Sn matrix, Sn-Zn-Ga alloys exhibit a broad melting range and an alternate normal-irregular eutectic structure. Notably, the addition of Ga into the Sn-Zn alloy will improve the tensile strength without reducing the ductility when the Ga content ranges from 0.05 wt% to 1wt%.

#### 3:05 PM

In-Situ Synchrotron X-Ray Diffraction During Melting and Solidification of a Lead-Free Solder Paste: Nick Hoo2; Gavin Jackson<sup>3</sup>; Mike Hendriksen<sup>4</sup>; Hua Lu<sup>1</sup>; Rajkumar Durairaj<sup>5</sup>; Chris Bailey<sup>1</sup>; Ndy Ekere5; Jonathon Wright6; 1University of Greenwich, Computing & Math. Scis., Old Royal Naval College, Greenwich, London SE10 9LS UK; <sup>2</sup>Tin Technology, Unit 3, Curo Park, Frogmore St., St. Albans, Hertfordshire AL2 2NN UK; <sup>3</sup>Henkel Loctite Adhesives, Multicore Solders, Kelsey House, Wood Ln. End, Hemel Hempstead, Hertfordshire HP2 4R UK; 4Celestica Limited, West Ave., Kidsgrove, Stoke on Trent, Staffordshire ST7 1TL UK; 5University of Greenwich, Elect. Mfg. Engrg. Rsch. Grp., Sch. of Engrg., Chatham Maritime, Chatham, Kent ME4 4TB UK; 6European Synchrotron Radiation Facility, Rue Jules Horowitz, Grenoble 38043 France

The intense flux of high-energy X-rays provided by synchrotron radiation sources allows transmission diffraction experiments to be performed. This can be used to gain non-destructive phase and strain data from the bulk of solid materials. The ability to focus the beam of x-rays into a narrow beam or spot of monochromatic x-rays allows 2d and even 3d mapping to be performed. As with all metals and alloys, the properties of a solder alloy are largely dependent on microstructure. The basis of the microstructure is evolved during a reflow operation from the heating and cooling cycle imposed upon the solder paste. This paper will show results from experiments undertaken at the European Synchrotron Radiation Facility. In these experiments, lead-free solder paste was placed onto a printed circuit board and then reflowed to form a solder joint. Time-resolved x-ray diffraction data were collected both from the bulk solder and interfacial regions during the melting and solidification processes. The paper will discuss the formation of microstructure for different pad finishes and cooling rates.

#### 3:25 PM

The Effect of Electroplating Parameters on the Compositions and Morphologies of Sn-Ag Bumps: Jong-Yeon Kim1; Jin Yu1; Jae-Ho Lee2; <sup>1</sup>Korea Advanced Institute of Science and Technology, Ctr. for Elect. Pkgg. Matls., Dept. of Matls. Sci. & Engrg., 373-1 Guseongdong, Yuseong-gu, Daejeon 305-701 Korea; <sup>2</sup>Hongik University, Dept. of Metallurgl. Engrg. & Matls. Sci., 72-1 Sangsu-dong, Mapo-gu, Seoul 121-791 Korea

Eutetic Sn-Ag solder bumps formed by electroplating method have been studied for the flip chip interconnection. The various conditions of electroplating bath were tested to obtain eutectic composition of Sn-Ag alloy. The effect of Ag ion concentration in solution on the morphologies and compositions of the solder bump was analyzed. Pulse plating method was introduced to acquire a level surface and fine microstructure of the solder bump. The surface morphologies and composition of the solder bump were changed with the duty cycle applied for the plating. Surface roughness of the solder bump was enhanced by applying surface active additives in the electroplating bath.

3:45 PM Break

## 3:55 PM Invited

The Microstructure of Sn in Near Eutectic Sn-Ag-Cu Alloy Solder and its Role in Thermomechanical Fatigue: Donald W. Henderson<sup>1</sup>; James J. Woods<sup>1</sup>; Timothy A. Gosselin<sup>1</sup>; Jay Bartelo<sup>1</sup>; Son Tran1; David E. King1; T. M. Korhonen2; M. A. Korhonen2; L. P. Lehman<sup>3</sup>; E. J. Cotts<sup>3</sup>; Sung K. Kang<sup>4</sup>; Paul Lauro<sup>4</sup>; Ismail C. Noyan<sup>4</sup>; Da-Yaun Shih<sup>4</sup>; Charles Goldsmith<sup>5</sup>; Karl J. Puttlitz<sup>5</sup>; <sup>1</sup>IBM Corporation, 1701 North St., Endicott, NY 13760 USA; <sup>2</sup>Cornell University, Dept. of Matls. Sci. & Engrg., Rm. T328 Bard Hall, Ithaca, NY 14853 USA; <sup>3</sup>Binghamton University, Physics Dept., Matl. Sci. Prog., Binghamton, NY 13902-6000 USA; <sup>4</sup>IBM Corporation, T. J. Watson Rsch. Ctr., Yorktown Heights, NY 10598 USA; <sup>5</sup>IBM Corporation, Hopewell Junction, NY 12533 USA

During the solidification of solder joints comprised of near eutectic Sn-Ag-Cu alloys, the Sn phase grows rapidly with a dendritic growth morphology. Notwithstanding the complicated Sn growth topology, the Sn phase demonstrates single crystallographic orientations over large regions. Typical solder Ball Grid Array (BGA) joints, 900 $\mu$  in diameter, are comprised of only 1 to 10 different Sn crystallographic domains. When such solder joints are submitted to cyclic thermomechanical strains, the solder joint fatigue process is characterized by the recrystallization of the Sn phase in the higher deformation regions with the production of a much smaller grain size. Grain boundary sliding is enabled in these recrystallized regions and leads to extensive grain boundary damage, resulting in fatigue crack initiation and growth along the recrystallized Sn grain boundaries.

## 4:20 PM

Quantitative Metallography of β-Sn Dendrites in Sn-3.8Ag-0.7Cu Solder Via Electron Backscatter Diffraction: Daniel Emelander<sup>1</sup>; Jason Jeannette<sup>1</sup>; Aaron LaLonde<sup>1</sup>; Carolyn Larson<sup>1</sup>; Ward Rietz<sup>1</sup>; *Douglas J. Swenson*<sup>1</sup>; Donald W. Henderson<sup>2</sup>; <sup>1</sup>Michigan Technological University, Dept. of Matls. Sci. & Engrg., 1400 Townsend Dr., Houghton, MI 49931 USA; <sup>2</sup>IBM Microelectronics, Dept. U13, Bldg. 022-2, Rm. H007, 1701 North St., Endicott, NY 13761 USA

Near ternary eutectic Sn-Ag-Cu (SAC) alloys are leading candidates for a new microelectronics industry standard lead-free solder. In the solid state, these solders consist of  $\beta$ -Sn, Ag<sub>3</sub>Sn and Cu<sub>6</sub>Sn<sub>5</sub>, where  $\beta$ -Sn comprises the vast majority of microconstituent volume fraction. The β-Sn phase adopts a dendritic morphology, and in a typical micrograph a solder joint appears to contain a large number of fine β-Sn dendrites. In this study, electron backscatter diffraction (EBSD) has been utilized to map the crystallographic orientations of the  $\beta$ -Sn dendrites in more than forty Sn-3.8 wt.%Ag-0.7wt.%Cu solder balls that were cooled at rates ranging from 0.35-3.0°C/s. It was found that at all cooling rates, there are in fact very few (5 ±2) crystallographically independent β-Sn dendrites per solder ball cross section. This suggests that a typical solder joint contains perhaps 10 β-Sn "grains", and as such may not be considered to be "polycrystalline" for purposes of mechanical properties modeling. Possible reasons for the existence of so few β-Sn dendrites are presented, and the utility of polarized light microscopy for identifying independent β-Sn dendrites is also discussed.

## 4:40 PM

**Dissolutive Wetting in the Bi-Sn System**: *Liang Yin*<sup>1</sup>; Timothy J. Singler<sup>1</sup>; Dorel Homentcovschi<sup>1</sup>; <sup>1</sup>SUNY-Binghamton, Dept. of Mech. Engrg., Binghamton, NY 13902-6000 USA

Development of a candidate Pb-free solder alloy requires a fundamental understanding of the alloy's wetting performance. When there is finite solubility of the solid substrate in the liquid alloy, significant dissolution of the substrate can occur. Isothermal sessile drop experiments of seven Bi-Sn alloys wetting Bi substrates were performed in a gaseous reducing atmosphere at 250°C. Meta-stable contact angles and dissolution depths were characterized as functions of alloy composition. Spreading kinetics and dynamic contact angles were also investigated. The coupling of dissolution and wetting are discussed. A partial analytical model is presented that predicts the liquid-solid interface evolution.

#### 5:00 PM

Generation of Low Melting Point Solder and Thermal-Fuse Alloy Wires by Continuous Casting: Zeinab A. Daya<sup>1</sup>; Felix Hong<sup>1</sup>; Hiroshi Soda<sup>1</sup>; Zhiuri Wang<sup>1</sup>; Alexander McLean<sup>1</sup>; Genjiro Motoyasu<sup>2</sup>; <sup>1</sup>University of Toronto, Matls. Sci. & Engrg., 184 College St., Toronto, Ontario M5S 3E4 Canada; <sup>2</sup>Chiba Institute of Technology, Mechanical Science, 2 Tsudanuma, Narashino, Chiba-ken 275-0016 Japan

Because of the brittle nature of bismuth and the strong tendency for segregation, solder and thermal-fuse alloys with high bismuth concentration are not easily produced in the form of small wires by ingot casting and extrusion methods. In this work, an innovative heatedmold continuous casting process, known as the Ohno Continuous Casting (OCC) process has been applied to generate Bi-Sn alloy wires of several compositions. The microstructure was examined and tensile tests performed for wires cast at various speeds. The deformation behavior was investigated by observing the surface structure of wires at various tensile deformation stages, providing insight into the structure-property relationship in low melting point alloys.

# Magnesium Technology 2004: Fundamental Research

Sponsored by: Light Metals Division, LMD-Magnesium Committee Program Organizer: Alan A. Luo, General Motors, Materials and Processes Laboratory, Warren, MI 48090-9055 USA

Wednesday PM	Room: 203B
March 17, 2004	Location: Charlotte Convention Center

Session Chairs: John Hryn, Argonne National Laboratory, Argonne, IL 60439-4815 USA; Zi-Kui Liu, Pennsylvania State University, University Park, PA 16082-5006 USA

#### 2:00 PM

**Diffusion Couple Study of the Mg-Al System**: *Matt Benzio*<sup>1</sup>; Carl Brubaker<sup>1</sup>; Zi-Kui Liu<sup>1</sup>; <sup>1</sup>Pennsylvania State University, Dept. of Matls. Sci. & Engrg., Steidle Bldg., Univ. Park, PA 16802 USA

The Mg-Al system was studied using the diffusion couple technique. The diffusion couples were characterized using light microscopy, electron probe microanalysis, and Vickers hardness. The growth constants, interdiffusion coefficients, activation energies and interdiffusion prefactors for the three intermediate compounds were estimated.

#### 2:20 PM

Ignition Resistance of Various Magnesium Alloys: Jean-Jacques Blandin<sup>1</sup>; Eric Grosjean<sup>2</sup>; Michel Suery<sup>1</sup>; <sup>1</sup>INP Grenoble, Génie Physique et Mécanique des Matériaux (GPM2), ENSPG, BP 46, Saint-Martin d'Hères 38402 France; <sup>2</sup>EADS, Ctr. Commun de Recherches, 12 rue Pasteur, BP 76, (now at AIRBUS), Suresnes 92152 France

The fear of ignition is still today a factor which limits the use of magnesium alloys. The aim of this work is to investigate the ignition resistance of pure magnesium and of two magnesium alloys (AZ91 and WE43) in as-cast conditions. For pure magnesium, continuous heating tests show that ignition generally starts at a temperature lower than the melting point whereas for the AZ 91 alloy, the ignition temperature is between the solidus and the liquidus temperatures, suggesting that liquid phase is needed to initiate burning. For the WE 43 alloy, no ignition is detected up to temperature significantly higher than the liquidus and consequently, this alloy can be considered as an ignition-proof magnesium alloy. The various ignition resistances of the studied materials are discussed in terms of differences in composition and oxidation processes.

## 2:40 PM

Influence of Zinc on the Solubility of Zirconium in Magnesium and the Subsequent Grain Refinement by Zirconium: Zoë C.G. Hildebrand<sup>1</sup>; Ma Qian<sup>1</sup>; David H. StJohn<sup>1</sup>; Malcolm T. Frost<sup>2</sup>; <sup>1</sup>University of Queensland, Div. of Matls., Sch. of Engrg., St Lucia, Brisbane, Queensland 4072 Australia; <sup>2</sup>Australian Magnesium Corporation Limited, PO Box 1364, Milton, Brisbane, Queensland 4064 Australia

Most zirconium-containing commercial magnesium alloys also contain zinc, which varies from ~ 0.5% to ~ 6.5% depending upon the given alloy system. Early work has suggested that the presence of zinc in the range from 3% to 5% could significantly increase the solubility of zirconium in magnesium, therefore enhancing the grain refinement of the final alloy by zirconium. This study investigates the influence of zinc in the range from 0% to 8% on the solubility of zirconium in pure magnesium at three different temperatures 680, 730 and 780°C. The effect of zinc alone as well as the combined effect of zinc and zirconium on the grain refinement of pure magnesium at each of the three temperatures is also investigated. Recommendations are made for the levels of zirconium addition to zinc-containing magnesium alloys as a function of zinc content based on the results obtained from this investigation.

#### 3:00 PM

Metal-Mold Heat Transfer and Solidification of Magnesium Alloys in Belt Casting Processes: J. S. Kim<sup>1</sup>; M. Isac<sup>1</sup>; R. I.L. Guthrie<sup>1</sup>; <sup>1</sup>McGill University, McGill Metals Procg. Ctr., Montreal, PQ Canada

A high speed strip casting simulator has been designed to simulate the casting of magnesium sheet alloys (AM50 and AZ91) on a single belt horizontal caster. Using Inverse Heat Transfer Analysis, temperature-time data from thermocouples inserted in the copper or steel bar

substrates were used to deduce instantaneous heat fluxes between the solidifying strip and the moving mold substrates. Maximum, or peak, heat fluxes were registered downstream of the impact region for metal delivery onto the moving chill mold; for a copper substrate moving at 0.7m/s, peak heat fluxes were recorded after 0.3 seconds of contact, whereas those for a yttria stabilized zirconia coated steel substrate were registered following 2.5 seconds of metal-mold contact. The microstructures of the thin strips (3-4mm thick, 1m long, and 40mm wide) were characterized in terms of SDAS (Secondary Dendrite Arm Spacings) as well as cooling rates. It was found that the major thermal resistance to heat flow from the strip to the substrate resided in an interfacial layer separating the strip from the substrate. This interfacial layer presumably corresponded to the entrainment of a thin gas film, which was manifested in the texture of the bottom surface which was seen to contain numerous small air pockets. Methods to resolve these issues, and to improve thermal contact, are discussed. Results to date suggest that the peaks in the maximum heat fluxes corresponded to maxima in the release of the alloy's latent heat of crystallization during their transformation from the liquid to solid crystalline state.

#### 3:20 PM

Microstructure Controlled Magnesium Alloys Via Cyclically Repeated Plastic Working: Katsuyoshi Kondoh<sup>1</sup>; Tachai Luangvaranunt<sup>2</sup>; Ritsuko Tsuzuki<sup>1</sup>; Shigeharu Kamado<sup>3</sup>; <sup>1</sup>The University of Tokyo, RCAST, 4-6-1, Komaba, Meguro-ku, Tokyo 153-8904 Japan; <sup>2</sup>Chulalongkorn University, Phyathai Rd. Proatumwan, Bangkok 10330 Thailand; <sup>3</sup>Nagaoka University of Technology, 1603-1, Kamitokioka, Nagaoka, Niigata, Japan

Solid-state processing to fabricate high-strengthened magnesium alloys via cyclically repeated plastic working (RPW) and hot extrusion has been developed, in employing magnesium alloy coarse powder as input raw materials. The RPW process, consisting of the compaction and backward extrusion by inserting upper punches alternatively at room temperature, assists the refinement of the magnesium matrix grains by large plastic deformation. In increasing the number of cycles in the RPW, the refined grain size, d is remarkably reduced; for example, d=3-5im of the hot extruded magnesium alloy after RPW process with 200 cycles when using the AZ31 alloy raw powder with that of 120-150im. The RPWed hot extruded alloys show a good correspondence to Hall-Petch's relationship. The ultimate tensile strength of the AZ31 extruded alloy via RPW process with 100 cycles is 330-350MPa, and is much higher than that of the conventional hot extruded alloy without RPW.

3:40 PM Break

#### 3:50 PM

Fatigue Behavior of Thixomolded<sup>®</sup> Magnesium AZ91D Using Ultrasonic Techniques: A. R. Moore<sup>1</sup>; C. J. Torbet<sup>1</sup>; A. Shyam<sup>1</sup>; J. W. Jones<sup>1</sup>; D. M. Walukas<sup>2</sup>; R. F. Decker<sup>2</sup>; <sup>1</sup>University of Michigan, Matls. Sci. & Engrg., Ann Arbor, MI 48109 USA; <sup>2</sup>Thixomat, Inc., Ann Arbor, MI 48108 USA

The fatigue behavior of the Thixomolded® magnesium alloy AZ91D has been examined via ultrasonic fatigue testing techniques at frequencies of approximately 20 kHz and for lifetimes as long as 109 cycles. An apparent endurance limit of approximately 65-70 MPa is observed. Comparison with the fatigue behavior of AZ91 produced by conventional die casting indicates that the Thixomolded® material has an endurance limit substantially higher than that of die cast material. The superior fatigue behavior of Thixomolded® AZ91D is attributed primarily to reduced porosity associated with the thixotropic processing technique. Fractographic analyses indicate that fatigue cracks leading to failure initiate at internal porosity in approximately 75% of tests and at the surface in the remainder of tests. Further fractographic studies illustrate that resulting fatigue lifetimes are greater for associated smaller fracture origination sites, in general. In addition, cumulative life distribution plots are employed in order to analyze apparent dual failure modes.

#### 4:10 PM

Effect of Uniaxial Strain on the Surface Roughness of Pure Mg: Mark R. Stoudt<sup>1</sup>; Abraham Munitz<sup>1</sup>; S. W. Banovic<sup>1</sup>; Richard J. Fields<sup>1</sup>; <sup>1</sup>National Institute of Standards and Technology, Gaithersburg, MD 20899 USA

Pure Mg samples were deformed in uniaxial tension and the concomitant surface topographies were characterized with both scanning laser confocal microscopy (SCLM) and scanning electron microscopy (SEM) techniques. Electron channel patterning analyses were also performed to determine grain orientation. Initial results indicate two principal deformation mechanisms contributing to the development of surface morphology: (i) grain-to-grain interactions and subsequent out-of-plane rotations that produce surface features with low-frequency character (i.e., spanning several hundred microns), and (ii) slip band development within individual grains that produced surface with high frequency character (i.e., spanning one hundred to one thousand nanometers). In addition, slip band evolution was observed to be strongly dependent on grain boundary orientation (Schmid factor) in this materials. The results of this study will be presented and discussed with respect to current theories of plastic deformation and surface roughening.

## 4:30 PM

Fatigue of Die-Cast Magnesium Alloys: Carsten Potzies<sup>1</sup>; Karl Ulrich Kainer<sup>1</sup>; <sup>1</sup>GKSS-Research Center, Ctr. for Magnesium Tech., Max-Planck-Str. 1, Geesthacht 21502 Germany

The magnesium alloy AZ91, which is used in different automotive components, exhibits an excellent castability and is therefore usually fabricated by high pressure die casting. Unfortunately, it reveals only a poor creep resistance, while creep resistant magnesium alloys show a low castability. Alternative magnesium alloys have been developed, which show an acceptable creep resistance as well as a good castability. One of these alloys is a modified magnesium alloy based on AZ. Due to the high casting speeds in high pressure die casting, the melt flow is non-laminar and air can be entrapped causing porosity when the melt solidifies. Porosity highly influences the mechanical properties, reducing significantly the values of elongation, tensile strength and especially fatigue strength. Separately cast test bars of AZ91 and the modified AZ have been examined by rotation beam testing. S-N-curves were displayed to determine and to compare the fatigue lifes and fatigue limits.

# Materials Analysis: Understanding the Columbia Disaster

Sponsored by: TMS Program Organizers: Richard W. Russell, United Space Alliance, Materials & Processes Engineering, Kennedy Space Ctr., FL USA

Wednesday PM	Room: Ballroom B
March 17, 2004	Location: Charlotte Convention Center

Session Chairs: Richard W. Russell, United Space Alliance, Matls. & Processes Engrg., Kennedy Space Ctr., FL USA

#### 2:00 PM Invited

The Materials and Processes Team Role in Columbia's Recovery, Recontruction and Analysis: *Rick Russell*<sup>1</sup>; <sup>1</sup>United Space Alliance, Kennedy Space Ctr., FL USA

An overview of the Columbia investigation, starting from recovery of debris items through the reconstruction and analysis at Kennedy Space Center will be presented. The Materials and Processes (M&P) team's role, including cleaning, field assessment, non-destructive inspection, sampling and analysis, and failure analysis will be discussed.

#### 2:30 PM Invited

Fracture of Aluminum Structural Materials: Robert Piascik<sup>1</sup>; Stephen Smith<sup>1</sup>; <sup>1</sup>NASA Langley Research Center, Hampton, VA USA

During the Columbia reconstruction effort, a delamination fracture mode was observed on much of the orbiter aluminum structure debris. The delamination fracture is characterized by a fiber-like fracture mode similar to that observed in polymer matrix composite fracture. During the Columbia reconstruction effort, the unusual fracture mode was descriptively termed as a "broom straw looking failure". A detailed metallographic study was conducted to understand this first-of-a-kind fracture mode. The aim of this study was to understand this failure mode relative to the high-speed break-up of the orbiter during re-entry.

## 3:00 PM Invited

Failure Analysis of A286 Carrier Panel Fasteners: Tom Collins<sup>1</sup>; Rick Russell<sup>2</sup>; <sup>1</sup>Boeing, Huntington Beach, CA USA; <sup>2</sup>United Space Alliance, Kennedy Space Ctr., FL USA

During field assessment it was note that several A286 carrier panel fasteners had what appeared to be a brittle fracture mode. Results of failure analysis, including chemical, fractographic, metallographic and exemplar testing will be presented.

## 3:30 PM Break

#### 3:50 PM Invited

Analytical Tools and Techniques: Steve McDanels<sup>1</sup>; <sup>1</sup>NASA, Kennedy Space Ctr., FL USA

Several methods of chemical analysis were performed in order to determine the most useful in understanding the slag's depositional characteristics. Techniques included: Scanning Electron Microscopy/ Energy Dispersive Spectroscopy (SEM/EDS), Electron Spectroscopy for Chemical Analysis (ESCA), X-Ray Diffraction (XRD), and Electron MicroProbe Analysis (EMPA). The relative merits and drawbacks of each technique will be explored.

### 4:20 PM Invited

#### Wing Leading Edge Debris Analysis: Sandeep Shah<sup>1</sup>; Greg Jerman<sup>1</sup>; <sup>1</sup>NASA Marshall Space Flight Center, Huntsville, AL USA

Having selected the RCC wing leading edge debris sample analysis techniques, guided by radiography, focused sampling with RCC intact was done for analysis to identify their content, layering, and if possible, hardware of origin. Analysis and Interpretation of this data across the wing leading edge was hoped to answer the high level questions of where did the breach occur? What was the sequence of melting? and What was the plasma flow direction? In sampling, two samples of each feature were taken and emphasis was placed on reproducibility and repeatability. The techniques used were metallography for cross-section, SEM for imaging and x-ray mapping, electron microprobe analysis for pinpoint accurate chemical analysis, x-ray diffraction to identify compounds. The data obtained was able to provide a picture of what happened, consistent with the leading failure scenario based on visual observations.

## 4:50 PM Invited

Failure Analysis Integration: The Materials and Processes Team's Role in the Overall Investigation and Conclusions: Brian Mayeaux<sup>1</sup>; Julie Kramer-White<sup>1</sup>; Rick Russell<sup>2</sup>; <sup>1</sup>NASA Johnson Space Center, Houston, TX USA; <sup>2</sup>United Space Alliance, Kennedy Space Ctr., FL USA

The Materials and Processes team's observations and results are compared and integrated with the findings and conclusions of the reconstruction team, and melded into the overall investigation.

# Materials by Design: Atoms to Applications: Design for Mechanical Functionality II

Sponsored by: Electronic, Magnetic & Photonic Materials Division, EMPMD/SMD-Chemistry & Physics of Materials Committee

*Program Organizers:* Krishna Rajan, Rensselaer Polytechnic Institute, Department of Materials Science and Engineering, Troy, NY 12180-3590 USA; Krishnan K. Sankaran, The Boeing Company, Phantom Works, St. Louis, MO 63166-0516 USA

Wednesday PM	Room: 2	210B
March 17, 2004	Location:	Charlotte Convention Center

Session Chair: M. K. Sunkara, University of Louisville, Louisville, KY 40292-0001 USA

#### 2:00 PM

Characteristic Dimensions in the Fracture and Fatigue of Biomaterials: R. O. Ritchie<sup>1</sup>; <sup>1</sup>Lawrence Berkeley National Laboratory, Matls. Scis. Div., Berkeley, CA 94720 USA

This presentation focuses on the fatigue and fracture toughness properties of human bone and dentin (the major constituent in teeth), in simulated physiological environments, and on how these properties depend upon the hierarchical nature of the nano/microstructure of these mineralized tissues with characteristic microstructural length scales which extend from nanometers to hundreds of micrometers. Although there is substantial clinical interest in their fracture resistance, little mechanistic information is available on how these hard mineralized tissues derive their toughness and how they are specifically affected by cyclic fatigue. Although several toughening mechanisms have been proposed, rarely has their contribution been characterized quantitatively or their origin determined in terms of the salient features of the microstructure. In the present talk, in vitro experiments are described that establish that fracture in dentin and bone is locally strain-controlled. Further, it is shown that toughening is a marked function of orientation and is developed through a variety of extrinsic mechanisms, including crack bridging (from collagen fibrils and uncracked ligaments), crack deflection and diffuse microcracking. These mechanisms provide the means to describe the macroscopic mechanical properties of these biological materials in terms of the nano/microscale features of their structure

#### 2:30 PM

Cellular Control of Toughening Mechanisms in Bone: Bioengineering for Materials Design: *Deepak Vashishth*<sup>1</sup>; <sup>1</sup>Rensselaer Polytechnic Institute, Dept. of Biomed. Engrg., 110 8th St., Jonsson Engrg. Ctr., Rm. 7046, Troy, NY 12180 USA

Bone is a brittle microcracking composite that forms microcracks at several levels of organization during day to day loading. Using a combination of engineering and biological techniques, experimental evidence is presented here to demonstrate how bone utilizes its material and biological characteristics to produce and remove microcracks in order to optimize toughness while remaining physiologically viable. Specifically: (a) Fracture mechanics-based crack growth resistance tests and scanning electron microscopy are utilized to identify the mechanism by which microcrack formation during crack propagation contributes to bone's resistance against fracture or fracture toughness. (b) Histological examination of microdamage and cellular network in aging human bone and statistical techniques are utilized to identify the mechanism by which damaged bone is targeted and eventually replaced by new bone.

#### 3:00 PM

Damage Evolution in Hot Deformation: Nano-Micro- Mesoscale Growth: Amit Ghosh<sup>1</sup>; <sup>1</sup>University of Michigan, Matls. Sci. & Engrg., 2300 Hayward St., Ann Arbor, MI 48109-2136 USA

Engineering alloys exhibit formation of internal voids during large plastic deformation at elevated temperature, a matter of concern in metal forming processes. Typically such void formation occurs at and near grain boundaries, due to grain boundary sliding effects, albeit small at times, which provide an accommodating mechanism for deformation. Thermomechanical processing and casting often leave fine scale damage in materials, particularly at hard second phase particles and grain boundaries. These damages can grow during subsequent deformation primarily by a strain-controlled process. While it is often assumed that recrystallization and homogenization treatments can heal damage and rid material of preexisting damage, research has shown that this notion is only approximately true. "Apparently healed" voids may only represent a weak interface, or nanometer scale voids. As these nanovoids provide free surfaces, they experience deviatoric stresses during deformation and grow by dislocation accumulation at their tips. Gradual, statistical opening of the nanovoids give rise to a "continuous nucleation" phenomenon. In this talk, growth of such voids and the role of healing processes on subsequent damage evolution will be discussed.

## 3:30 PM Break

#### 3:45 PM

## Modeling and Experiments of the Deformation of Ti-Based Alloys at Two Different Length Scales: Clyde L. Briant<sup>1</sup>; <sup>1</sup>Brown University, Engrg., Providence, RI 02912 USA

The two features that most often control the properties of materials are the chemistry of the alloy and the microstructural constituents. Both must be considered carefully if one is going to design the overall properties of a material. The primary example that will be used for this talk are titanium-based materials. First we will consider only monolithic materials, both commercial purity titanium and Ti-6Al-4V, and show the importance of small concentrations of interstitial impurities on the mechanical properties. These changes must be a result of changes in chemical bonding within the alloy and must be modeled with these techniques. We will also present a study of Ti-6Al-4V/TiC composites. It will be shown that the presence of the TiC changes the deformation mode that occurs under some conditions, but once again the strength of the material is controlled by the matrix. Examples of methods to model these microstructures will also be presented and the more general utility of these microstructure-focused methods of modeling will be demonstrated.

## 4:15 PM

Accomplishing Structural Alloy Design Goals Within the Limitations of Bulk Processes: David M. Bowden<sup>1</sup>; Thomas J. Watson<sup>2</sup>; <sup>1</sup>The Boeing Company, MC S245-1003, PO Box 516, St. Louis, MO 63166 USA; <sup>2</sup>Pratt & Whitney, E. Hartford, CT USA

Control of microstructure evolution at the atomic or short-range level to achieve breakthrough material properties is a topic of considerable interest. Computational materials science is emerging as a critical tool to support this level of materials design. And, a variety of methods are being investigated to produce these nanostructured metals, and the advantages of achieving fine microstructures have been clearly demonstrated. However, in order to transition this technology into real products, fine microstructures must be achievable in bulk material forms in an efficient and affordable manner. In this paper, we will discuss the linkage between the scale of design and the scale of production critical to developing nanostructured metals for real applications. This analysis will include a discussion of particular structural applications and the requirements for those applications, both in terms of mechanical properties and cost, and examine the variety of processing approaches available to meet those requirements.

#### 4:45 PM

Materials by Design: Naval Aircraft: *William E. Frazier*<sup>1</sup>; <sup>1</sup>Naval Air Systems Command, 48066 Shaw Rd., Patuxent River, MD 20657 USA

Navy aircraft and weapon systems operate in the world's harshest environments. Navy assets are subjected to extremes in weather conditions, loads (6 times that of land based aircraft), and electromagnetic environments (240v/m). Consequently, virtually every materials technology used on navy aircraft is engineered and tailored for its intended application. This paper discusses the navy's current approach in rapidly developing, qualifying, and transitioning new materials technologies. Aerospace materials programs on engineered materials, accelerated insertion, and collaborative, web-based knowledge management are discussed.

5:15 PM Concluding Remarks K. Rajan and K. K. Sankaran

# Materials Education to Revitalize the Workforce: Session II

Sponsored by: TMS, Public & Governmental Affairs Committee, TMS-Education Committee

*Program Organizers:* Reza Abbaschian, University of Florida, College of Engineering, Gainesville, FL 32611-6400 USA; Iver E. Anderson, Iowa State University, Ames Laboratory, Ames, IA 50011-3020 USA

Wednesday PM	Room: 2	17D
March 17, 2004	Location:	Charlotte Convention Center

Session Chair: TBA

#### 2:00 PM Invited

Meeting the Needs of a Changing Student Population: Rosemary Haggett<sup>1</sup>; <sup>1</sup>National Science Foundation, Washington, DC USA

What can we do to ensure that we have a workforce with the knowledge of science, mathematics and technology needed in our contemporary workplace and community members capable of exercising responsible citizenship in an increasingly technological society? Although our population continues to grow, partly through immigration and partly through birth, the segments of the population that are expanding are less likely to complete a bachelor's degree or an advanced degree and are less likely to be offered educational opportunities by their employers. Furthermore, patterns of college attendance are changing. Although more and more students are enrolled in postsecondary programs, the educational environment is increasing in complexity. Young people and adults have many options for pursuing a degree or for enhancing their employability and opportunity for advancement through credentialing models offered by both traditional educational institutions and new for-profit providers. How can we effectively meet the needs of an increasingly diverse student population?

## 2:30 PM

Materials Science and Engineering Education – Its Continuing Evolution: Carl C. Koch<sup>1</sup>; J. Michael Rigsbee<sup>1</sup>; <sup>1</sup>North Carolina State University, Dept. of Matls. Sci. Engrg., Raleigh, NC 27695 USA

This talk will give a brief history of the coming of materials science and engineering and its present evolution. The program area of materials science developed in the late 1950's as interdisciplinary research in large industrial laboratories such as G.E. and Bell Laboratories. Under the leadership of Morris Fine, the first graduate and undergraduate programs were instituted at Northwestern University in the 1958-1959 period. Materials science and engineering had its roots in physical metallurgy and parts of solid state physics and chemistry. In turn physical metallurgy had grown out of mining and mineral processing programs. The various factors which have influenced its evolution will be considered. These include technological, societal, and accreditation constraints. The present and future trends in the direction of "soft" materials science and engineering will be discussed.

#### 3:00 PM

**The MSE PITCH Program for Graduate Recruiting**: *Kevin S. Jones*<sup>1</sup>; Martha McDonald<sup>1</sup>; <sup>1</sup>University of Florida, Dept. of Matls. Sci. & Engrg., Gainesville, FL 32611 USA

The recruiting of domestic graduate students into Materials Science and Engineering is an ongoing problem nationwide. The Department of Materials Science and Engineering at the University of Florida has developed a new approach to recruiting domestic graduate students. This approach is called the PITCH (Publicize, Identify, Time, Convince, and Host) program. This process is very similar to the methods used to recruit highly sought after student athletes. Using this approach UF-MSE managed the successful recruitment of 75 graduate students over the past two years. The PITCH approach has resulted in over 85% of our last two recruiting classes entering to pursue a PhD. This same group averaged 70% US students and over 20% of the recruits were minority students. In addition the percentage of female students has increase to over 40% in the latest class. This talk will share the critical elements of our recruiting efforts that can assist other engineering schools with improving the quality and diversity of their programs.

## 3:30 PM Break

## 3:50 PM

Towards a New Undergraduate Curriculum in Materials Science and Engineering: Caroline A. Ross<sup>1</sup>; Samuel M. Allen<sup>1</sup>; Subra Suresh<sup>1</sup>; *Donald R. Sadoway*<sup>1</sup>; <sup>1</sup>Massachusetts Institute of Technology, Dept. of Matls. Sci. & Engrg., 77 Mass. Ave., Rm. 8-203, Cambridge, MA 02139-4307 USA

At MIT, wholesale revision of the undergraduate degree program in MSE is underway with the intention of devising a course of study whose aim is to educate specialists in the development and use of materials in technology. The new curriculum comprises core technical knowledge, professional development, and a capstone activity. Pedagogical considerations include integration of subject matter between subjects, reinforcement of theory through applications, and presentation of material on a need-to-know basis, i.e., in time blocks of several weeks as opposed to full semesters. In the junior and senior years students can tailor their course of study by choosing from a large number of restricted electives, each running approximately four weeks, building upon the core and moving towards the frontiers of the field. Professional development is to be embedded in the curriculum in accordance with ABET specifications. Launch of the new program is slated for fall 2003.

## 4:20 PM

Lifelong Learning: The Role of Professional Societies: Michael J. Kenney<sup>1</sup>; <sup>1</sup>ASM International

Professional societies must support and supplement the educational efforts of traditional educational institutions. Pre-college education has become rote in many aspects and standards are mandating a very homogeneous curriculum. College educational programs have diversified to such an extent that graduates lack some of the fundamental knowledge needed to succeed. It is incumbent on professional societies to reach out to both pre-college and college students and to provide development opportunities to working professionals. Without efforts in all these areas, the need for professional societies may disappear completely.

# Materials Processing Fundamentals: Powders, Composites, Coatings and Measurements

Sponsored by: Extraction & Processing Division, Materials Processing & Manufacturing Division, EPD-Process Fundamentals Committee, MPMD/EPD-Process Modeling Analysis & Control Committee

*Program Organizers:* Adam C. Powell, Massachusetts Institute of Technology, Department of Materials Science and Engineering, Cambridge, MA 02139-4307 USA; Princewill N. Anyalebechi, Grand Valley State University, L. V. Eberhard Center, Grand Rapids, MI 49504-6495 USA

 Wednesday PM
 Room: 212B

 March 17, 2004
 Location: Charlotte Convention Center

Session Chair: TBA

#### 2:00 PM

Dense Sintering of Long and Stepped Sample Through Traveling Zone Heating by Means of Electric Power Direct Supplying: *Shuji Tada*<sup>1</sup>; Zheng Ming Sun<sup>1</sup>; Hitoshi Hashimoto<sup>1</sup>; Toshihiko Abe<sup>1</sup>; <sup>1</sup>National Institute of Advanced Industrial Science and Technology, Inst. for Structural & Engrg. Matls., 4-2-1 Nigatake, Miyaginoku, Sendai, Miyagi 983-8551 Japan

A traveling zone heating technique was examined in order to produce long rods or stepped components with high density by means of pressurized pulse discharge sintering. Local heating was enabled by electric power supplied perpendicular to the loading axis. One-direction continuous sintering process was successfully achieved assisted by the unique electrodes which were able to slide along the side wall of the cylinder in the direction of the loading axis while remaining in continuous contact with it. Four successive local heatings over a range 30 mm wide while moving the heating zone distances of 20 mm led to the production of a 55 mm long aluminum rod with a relative density of 99.7%. Also, a 30 mm long round bar with two steps was successfully sintered through this method owing to reducing the stress within thinner part while a thick portion was heated.

#### 2:30 PM

A Study of Particle Size and Velocities Distributions in Centrifugal Atomisation Using Mathematical Regression Techniques: *P. Tsakiropoulos*<sup>1</sup>; Yawei Wang<sup>1</sup>; <sup>1</sup>University of Surrey, Sch. of Engrg., Mech. & Aeros. Engrg., Metall. Rsch. Grp., Guildford, Surrey GU2 7XH UK

A study of the centrifugal atomisation of liquids using a rotating disk was presented at the 2003 annual meeting for the case of the liquid impacting the centre of the rotating disk during atomisation. This year our paper would discuss the atomisation of liquids that impact the disk at off centre positions. The paper would present results on the distribution of particle sizes and velocities in centrifugal atomisation in a purpose-built atomisation chamber. The data was collected using Laser Phase Doppler Anemometry. Mathematical regression analyses were developed for the distributions of particle sizes and velocities for the different operating conditions using the non-dimensional technique of similarity theory. The regressed functions were applied to predict the effect of disk rotating speed, flow rate and disk diameter on the spatial distributions of particle size and velocities for alloy melts. The results of experiments and regression analyses will be presented and discussed.

## 2:50 PM

### Study on the Preparation of Foam Aluminum by Powder Metallurgy Method: L. Wei<sup>1</sup>; G. C. Yao<sup>1</sup>; X. M. Zhang; <sup>1</sup>Northeastern University, Sch. of Matl. & Metall., Liaoning, Shenyang 110004 China

The experiments about process of preparation foam aluminum by powder metallurgy method was carried out in laboratory. The effect of the pressing parameters for making aluminium powder flans, foaming temperature, adding amount of foaming agent and foaming time on the density and porosity and pore morphology of foam aluminum were studied. The aluminium flans were protected in molten salt for isolating from the air. It was found that the hydrogen pressure in the bubble always enlarged along with the increase of time in first stage and make the bubble growing, when the hydrogen pressure was up to a determinate value, the bubble broken and then the hydrogen pressure reduced and expanding drive lack and led to shrinkage. On condition of 300 MPa making flans pressure, 675-680° foaming temperature, foaming time 7 min, adding 1.0%-1.5%TiH2, the foam aluminum specimens with even hole and high porosity were gained. The formation mechanism of forming air bubble was discussed in this work.

#### 3:10 PM

Study on Grain Composition of the Biscuit for Preparing Inert Anode Based on NiFe2O4 Spinel: Y. H. Liu<sup>1</sup>; G. C. Yao<sup>1</sup>; J. H. Xi<sup>1</sup>; J. H. Zhang<sup>1</sup>; <sup>1</sup>Northeastern University, Matl. & Metall., Liaoning, Shenyang 110004 China

In order to obtain the NiFe2O4 spinel based inert anode samples possessing higher volume density and lower porosity, the grain graduation of NiFe2O4 spinel biscuit was studied on the base of the ball arrangement theory by means of vibration entity experiments. Four different main grains were decided according to the different size of products. The packed density was measured to define the optimal grain graduation. The mass ratio and the diameter ratio of main grains to filling grains was find out above all. On the base of it, different quantity of fine powder was added to the sample for the sake of obtaining optimal grain composition. The results validated that the actual stack form of the main grain fit the ball arrangement theory very well, and tend to be in the form of the body centered cubic or hexagonal close-packed, moreover the packed density was the greatest when the ratio of the coarse grains is 42%, medium grains was 18% and fine powder

## 3:30 PM Break

### 4:00 PM

Experimental and Computational Investigations of the Bonding Layer in the CVD Coated WC+Co Cutting Tools: *Zhi-Jie Liu*<sup>1</sup>; Charles McNerny<sup>2</sup>; Pankaj Mehrotra<sup>2</sup>; Aharon Inspektor<sup>2</sup>; *Zi-Kui Liu*<sup>1</sup>; <sup>1</sup>Pennsylvania State University, Matls. Sci. & Engrg., 107 Steidle Bldg., Univ. Park, PA 16802 USA; <sup>2</sup>Kennametal, Inc., Corp. Tech., Latrobe, PA 15650 USA

The effects of processing parameters on the bonding layer structure between tungsten carbide substrate and Al2O3 coating were investigated experimentally and computationally. Bonding layers, considerably thicker than the layers in commercial products, were deposited under industrial production conditions. Different from the belief in the literature that the bonding layer is a cubic Ti(C,N,O) phase, titanium oxides were found. Energy dispersive spectroscopy and X-ray diffraction measurements were used to determine the compositions and structures of the bonding layer and the Al2O3 layer. It was found that the a-Al2O3 phase formed on the oxide bonding layer, and the k-Al2O3 phase formed without the bonding layer. Thermodynamic calculations were conducted to explore the effects of processing parameters on the formation of various oxides. It was concluded that the decomposition efficiency of the gas precursors plays a critical role in the formation of oxides.

## 4:30 PM

The Interface Reaction in Preparation of Aluminum Composite Strengthened by Cenosphere Fly Ash: L. L. Wu<sup>1</sup>; G. C. Yao<sup>1</sup>; Y. H. Liu<sup>1</sup>; 'Northeastern University, Sch. of Matl. & Metall., Liaoning, Shenyang 110004 China

The major constituents of cenosphere fly ash are various oxides such as Al2O3, SiO2, Fe2O3 and their qualities fraction sums surpass 85%. XRD analysis indicates that cenosphere fly ash present in complex glass and ceramic forms. This research adopts liquid stir casting to prepare aluminium composite strengthened by cenosphere fly ash. Cenosphere fly ash preheated at 500° for half an hour was mixed with aluminium at 780° and the composite was prepared. The solidification should be as rapid as possible to prevent floatation of fly ash particles to the top part of the castings. SEM and EDX analysis were carried on to observe the composite. SEM micrograph shows that there was no fly ash particle fall off from section plane of the specimen in the abrading, and the ash particles affixed fast with the aluminium body, and they dispersed uniformity. EDX results show that there were atomic Al, Mg, Fe, Si, C, in the interface of the fly ash particle and aluminium body, it demonstrated that Fe2O3 and SiO2 react with aluminum and produce Fe and Si, MgO react with Al2O3 forming MgO·Al2O3 spinel. These reactions were analysed by thermodynamics calculation also.

## 4:50 PM

**Evaluation of the Initial Residual Stress Distribution and Multiple Pass Grinding Techniques on Final Residual Stress Distribution in D2 Steel:** Olga Petrovna Karabelchtchikova<sup>1</sup>; Iris V. Rivero<sup>1</sup>; <sup>1</sup>Texas Tech University, Dept. of Industrial Engrg., Box 43061, Lubbock, TX 79409-3061 USA

The purpose of this investigation is to correlate the residual stress behavior of D2 steel when subjected to two- and four-passes resulting in equivalent depth during gentle and conventional grinding operations. Single-, double- and triple-tempering were performed on D2 steel samples followed by x-ray diffraction and microstructural material characterization. Hardness, cold work and surface residual stress measurements were collected at this stage of the study. Subsequently the samples were subjected to gentle and conventional grinding conditions to re-evaluate material's properties and surface integrity. Each grinding pass was assessed for its influence on every subsequent pass in terms of residual stresses. Due to non-linearity of the residual stress superposition, the distribution pattern between the samples undergone 2- and 4-pass grinding was shown to be considerably different. Overall, the study identified the optimal combination of treatments, used in D2 thread-rolling die manufacturing, for prolong service life and satisfactory performance.

## 5:10 PM

Characterization of Thermal Lags and Resistances in a Heat-Flux DSC: Gregory E. Osborne<sup>1</sup>; Jay I. Frankel<sup>1</sup>; Adrian S. Sabau<sup>2</sup>; Wallace D. Porter<sup>2</sup>; <sup>1</sup>University of Tennessee, Mech., Aeros. & Biomed. Engrg. Dept., 414 Dougherty Engrg. Bldg., Knoxville, TN 37996-2210 USA; <sup>2</sup>Oak Ridge National Laboratory, 1 Bethel Valley Rd., Oak Ridge, TN 37831-6083 USA

Differential Scanning Calorimetry (DSC) is often used to characterize thermophysical properties associated with phase transformation of metals and alloys. In such devices, however, the practical design of the instrument does not allow for direct temperature measurements of the sample material. As a result, the contact conductances and radiative interactions among system components yield thermal lags between the collected temperature data and sample temperature. Therefore, a direct association of the recorded thermocouple readings to the sample site may produce erroneous results. In order to account for these heat transfer mechanisms, a new parameter estimation method has been developed utilizing a lumped heat transfer model for the key DSC components. Preliminary results using a benchmark numerical problem have been obtained which show accurate recovery of the system parameters and demonstrate the robustness of the new method. Based on these encouraging numerical results, the method is presently being applied to real experimental situations.

## Metals for the Future: Functional Materials

Sponsored by: TMS,

*Program Organizers:* Manfred Wuttig, University of Maryland, Department of Materials & Nuclear Engineering, College Park, MD 20742-2115 USA; Sreeramamurthy Ankem, University of Maryland, Department of Material & Nuclear Engineering, College Park, MD 20742-2115 USA

Wednesday PM	Room: 2	15
March 17, 2004	Location:	Charlotte Convention Center

Session Chair: M. Wuttig, University of Maryland, Dept. of Matls. & Nuclear Engrg., College Park, MD 20742-2115 USA

#### 2:00 PM Opening Remarks by M. Wuttig

#### 2:10 PM Invited

Magnetic Domain Microstructures in Ferromagnetic Shape Memory Alloys: Sai Prasanth Venkateswaran<sup>1</sup>; *Marc De Graef*<sup>1</sup>; <sup>1</sup>Carnegie Mellon University, Matls. Sci. & Engrg., 5000 Forbes Ave., Pittsburgh, PA 15213-3890 USA

Ferromagnetic shape memory alloys, such as Ni<sub>2</sub>MnGa and Co<sub>2</sub>NiGa, have received considerable attention in recent years. These alloys undergo both a paramagnetic to ferromagnetic transition and a martensitic phase transition to a tetragonal structure with a c/a ratio of around 0.96. There is a complex interplay between structural domains (twins) and magnetic domains, and we will present quantitative Lorentz transmission electron microscopy observations of the domain structure in both austenitic and martensitic states. The Lorentz images are analyzed using the Transport-of-Intensity formalism, which allows us to extract quantitative information about the domain structure at the nanometer length scale. We will also present evidence for the existence of a magnetically modulated pre-transformation state, known as "magnetic tweed".

#### 2:40 PM Invited

Self-Assembled Near-Zero-Thickness Nanolayers for Nanodevice Metallization: Interfacial Adhesion and Chemical Isolation: G. Ramanath<sup>1</sup>; P. G. Ganesan<sup>1</sup>; M. J. Frederick<sup>1</sup>; <sup>1</sup>Rensselaer Polytechnic Institute, Dept. of Matls. Sci. & Engrg., Troy, NY 12180 USA

Tailoring near-zero-thickness layers that enhance interfacial adhesion, but inhibit interdiffusion and phase formation, is a critical challenge for future metallization for integrated circuits and MEMS. For instance, <5-nm-thick barriers that can conformally coat sub-100-nm features with aspect-ratios >5:1 are needed to fully realize the potential of Cu metallization. Meeting such exacting requirements necessitates new materials and scalable processing methods based on selfassembly. This talk will describe a completely new approach of using ~0.7 to 5-nm-thick self-assembled molecular layers (SAMs) to inhibit interfacial diffusion and enhance interfacial adhesion. I will first describe the rationale for using SAMs as interface modifiers, and demonstrate that SAMs inhibit Cu diffusion and effect as much as ~5-fold increase in device lifetimes and decrease leakage currents by ~6 orders of magnitude. It will be shown that the SAM molecular length and terminal functional groups are key factors that determine their efficacy as diffusion barriers. Interfacial adhesion of Cu/SAM/silica and Cu/Silica structures measured by a 4-point-bending technique show that interfacial adhesion can be enhanced by more than a factor of 3 for SAMs with terminal groups that bond strongly with Cu (e.g., -SH group) on one end and the dielectric surface (e.g., via Si-O-Si bonds) on another. Electron spectroscopy measurements of fracture surfaces show that delamination occurs at the SAM/Silica interface, leaving the -SH or -COOH groups on the metal side of the interface. The interfacespecific interactions immobilize Cu, and enable very promising barrier properties (factor of 3-4 higher lifetimes) even for sub-nanolayers.

Based on the above, we will present a model to explain important factors that influence interfacial diffusion and adhesion in Cu/SAM/ dielectric structures. If time permits, the strategy of forming self-organized interfacial nanolayers from supersaturated alloy films by solute segregation and phase formation will also be discussed.

#### 3:10 PM Invited

Novel Conductive Oxide Coatings on Metallic Inteconnect for Intermediate-Temperature SOFCs: *Jiahong Zhu*<sup>1</sup>; <sup>1</sup>Tennessee Technological University, Dept. of Mech. Engrg., 115 W. 10th St., Box 5014, Cookeville, TN 38505 USA

This presentation gives a progress overview of the NSF Career Award "Novel Conductive Oxide Coatings on Metallic Inteconnect for Intermediate-Temperature SOFC Application". With the current trends in reducing the SOFC operation temperatures to the range of 500-800°C, ferritic steels are promoted as the candidate materials for the intermediate-temperature SOFC interconnect due to their low cost and ease of manufacture. However, under long-term stack operation, the increase of contact resistance due to the formation of surface oxide layer(s) and Cr migration to other cell components from the interconnects pose serious issues for these otherwise promising materials. Novel conductive spinel phases are investigated in this project as potential coatings to mitigate the current limitations of ferritic steels. Electrical conduction mechanism in substituted spinel phases are being assessed through systematic study of defect structure and electrical conductivity in these oxides. Sol-gel process is used to form the spinel coatings on commercial ferritic steels, while alloy design is explored to develop new-generation ferritic alloys capable of forming the desired spinel layer upon thermal exposure. The integrated educational activities, such as outreach to local high school teachers/students, enhancement of the undergraduate curriculum via familiarizing the students with both bulk material and coating processing, are also discussed.

#### 3:40 PM Invited

**CAREER: Fundamental Micromechanics and Materials Dynamics of Thermal Barrier Coating Systems Containing Multiple Layers:** *Mark L. Weaver*<sup>1</sup>; <sup>1</sup>University of Alabama, Metallurgl. & Matls. Engrg., Box 870202, Tuscaloosa, AL 35487-0202 USA

This research focuses on understanding the fundamental concepts controlling the mechanical properties of thermal barrier coatings (TBC) as a function of thermal exposure, both time and temperature. This program goals are to: (1) Characterize the properties of the macroand micro-constituents of the TBC system as a function of thermal exposure using model TBC systems; (2) Monitor and analyze the displacements of the TBC constituents during thermal cycling and isothermal oxidation coupled with mechanical strain; and (3) Develop models for TBC durability based on microstructural and mechanical evaluations of degradation mechanisms and processes. The goals of the educational plan are: (1) Enhance the undergraduate curriculum by providing students with "hands on" training in the study of commercially viable thick films and coating materials; (2) Encourage undergraduate students to pursue graduate studies in Metallurgical and Materials Engineering; and (3) Increase diversity by attracting underrepresented minority students to undergraduate and graduate study.

### 4:10 PM Break

#### 4:25 PM Invited

Effects of Micro- and Nano-Scale Critical Dimensions on Mechanical Behavior of Model Metals and Alloys: Richard P. Vinci<sup>1</sup>; <sup>1</sup>Lehigh University, Dept. of Matls. Sci. & Engrg., 5 E. Packer Ave., Bethlehem, PA 18015 USA

It is now widely known that the mechanical behavior of metals and alloys can be strongly affected by the reduction of certain critical dimensions (e.g., grain size and film thickness) to the micro- or nanoscale. Furthermore, the techniques used to fabricate materials with these dimensions often introduce characteristics that are not typical of bulk materials. Understanding the ramifications of these phenomena is critical for proper material design and selection for future micro/ nanoelectronic and micro/nanomechanical devices. In this presentation, several examples of these effects in model metals and their alloys will be explored and important open questions will be identified.

4:55 PM Panel Discussion with L. Christodoulou, N. Spaldin, M. Wuttig and Y. Chung

# Multiphase Phenomena in Materials Processing: Session II

Sponsored by: Extraction & Processing Division, Light Metals Division, Materials Processing and Manufacturing Division, EPD-Process Fundamentals Committee, MPMD/EPD-Process Modeling Analysis & Control Committee, MPMD-Solidification Committee Program Organizers: Ben Q. Li, Washington State University, School of Mechanical and Materials Engineering, Pullman, WA 99164-2920 USA; Stavros A. Argyropoulos, University of Toronto, Department of Materials Science and Engineering, Toronto, Ontario M5S 3E4 Canada; Christoph Beckermann, University of Iowa, Department of Mechanical Engineering, Iowa City, IA 52242 USA; Bob Dax, Concurrent Technologies Corporation, Pittsburgh, PA 15219 USA; Hani Henein, University of Alberta, Edmonton, AB T6G 2G6 Canada; Adrian S. Sabau, Oak Ridge National Laboratory, MS-602, Oak Ridge, TN 37831-6083 USA; Brian G. Thomas, University of Illinois, Department of Mechanical and Industrial Engineering, Urbana, IL 61801 USA; Srinath Viswanathan, Sandia National Laboratories, Albuquerque, NM 87185-1134 USA

Wednesday PM	Room: 2	18B		
March 17, 2004	Location:	Charlotte	Convention	Center

Session Chairs: Christoph Beckermann, University of Iowa, Dept. of Mech. Engrg., Iowa City, IA 52242 USA; Bob Dax, Concurrent Technologies Corp, Pittsburgh, PA 15219 USA

## 2:00 PM Invited

The Multi-Fluid Model and its Application to Simulate Multiphase Flows in Materials Processing Systems: Harald Laux<sup>1</sup>; <sup>1</sup>SINTEF Materials Technology, Flow Tech., Alfred Getz vei 2, Trondheim 7465 Norway

Lecture and paper will focus on the derivation of the multi-fluid model, its features and the importance of multi-fluid modeling for multiphase flows in materials processing systems. Examples of CFD simulations from a variety of materials processing systems will be given including bubbly flows, liquid-liquid-gas flows, and granular flows. It will also be shown that multi-fluid models can be used to study solidification problems with complex microstructures. All examples are taken from the work at SINTEF Materials Technology, and are chosen such as to illustrate the salient features of multi-fluid modeling, its limitations, and its present and future usefulness in improving materials processing systems with multiphase flows.

## 2:25 PM Invited

Two-Phase Volume Averaging: Simulation Examples on Phase Separation During Phase Transition with Convection: Andreas Ludwig<sup>1</sup>; Menghuai Wu<sup>1</sup>; <sup>1</sup>University of Leoben, Dept. of Metall., Franz-Josef-Str. 18, Leoben 8700 Austria

Phase separation is frequently occurring during solidification accompanied by phenomena like melt convection, sedimentation or with two liquids Marangoni driven motion. In order to describe these phase separation phenomena a two-phase volume averaging model was designed specially for globular equiaxed solidification of binary alloys and decomposition and solidification of hyper-monotectic alloys. The model considers nucleation and growth of equiaxed grains or second phase droplets, motion and sedimentation of grains or droplet, feeding flow and solute transport by diffusion and convection. It allows the prediction of macrosegregations and the distributions of grain size or droplet size. Evaluations were made by comparing the predictions gained with simulation with experimental results. For example it is shown that the numerically predicted grain size distribution in a plate casting (Al-4wt%Cu) agrees reasonably well with the experimental analyses.

## 2:50 PM

## Phase-Field Modeling of Solidification with Flow Due to Density Change: Ying Sun<sup>1</sup>; Christoph Beckermann<sup>1</sup>; <sup>1</sup>University of Iowa, Dept. Mech. & Industrial Engrg., 2412 SC, Iowa City, IA 52242 USA

A phase-field model is developed that accounts for the effect of density change during solidification as well as for flow. A diffuse interface description of the conservation equations is derived based upon the multiphase averaging method. The phase-field evolution equation is obtained by averaging a sharp-interface condition for the interface temperature that takes into account the effects of density difference between the solid and liquid, interface kinetics, curvature, pressure and stresses. Two different cases are examined: (1) the liquid and solid are both treated as viscous fluids with a single velocity inside the diffuse interface region, and (2) the liquid is a viscous fluid, but the solid is rigid, such that the phase velocities are different. The model is first tested for simple planar and spherical solidification fronts in the presence of a density difference. Then, results for 2-D dendritic growth are presented.

## 3:10 PM

**Development of Microstructure During Sputtering of Polycrystalline Thin Films**: *Max O. Bloomfield*<sup>1</sup>; Yeon Ho Im<sup>1</sup>; Timothy S. Cale<sup>1</sup>; <sup>1</sup>Interconnects for Gigascale Integration, Rensselaer, NY USA

Electrical and mechanical properties of thin films has been a primary interest of the microelectronics manufacturing industry for several decades. In recent years, as the thickness of these films has approached the length scale of the underlying grain structure, qualitative changes in properties of interest have shown up. This size dependence must be understood in the context of the manufacturing processes that produce the microstructure, and how the microstructure evolves during use. We show results of physically based simulations of grain structure development during physical vapor deposition (PVD) of a thin metallic film on a bare substrate. The simulations show how deposited material grows from an initial island stage, until coalescing into a blanket film. In our simulations, the mean free path of atoms in flight is taken to be long compared to the length scale of the grains, and thus the system is in a ballistic transport regime. Transport is solely along lineof-sight paths, and solid-gas collisions dominate over gas phase collisions. The flux of reactive species is calculated from a particle distribution function and a transmission probabilities from a Monte Carlo based transport code. Arriving metals atoms have relatively low energy, and sticking factors are close to unity, so deposition is nonconformal. Shadowing effects of larger, broad grains are accounted for, and the resulting simulation, which does not assume a solid on solid model, exhibits voiding. The grain boundaries that form as islands impinge upon each other are no longer available for deposition from the PVD source, but are allowed to evolve further under curvature driven motion, to minimize grain boundary energies. A finite element based level set code is used to track the resulting changes in geometry and topology, This method allows us to attach arbitrary properties, e.g., orientation and composition, to each grain. Another finite element code can be used to track transport and reaction in the fluid phase above the evolving surface for non-ballistic regime systems. These systems can include electrochemical and electroless plating.

## 3:30 PM Break

## 3:45 PM

Effects of Different Fraction Solids on the Fluidity of Mechanically Stirred A356 Al-Si Alloy: Sh. Nafisi<sup>1</sup>; O. Lashkari<sup>1</sup>; *M. R. Ghomashchi*<sup>1</sup>; A. Charette<sup>1</sup>; <sup>1</sup>University of Quebec, Ctr. for Univ. Rsch. on Aluminum, Dept. of Appl. Scis., 555 Univ. Blvd., Chicoutimi, Quebec G7H-2B1 Canada

One of the main parameters in casting and foundry technology is determination of the molten metal fluidity. This parameter becomes more important in the casting of thin wall parts and thus understanding and controlling fluidity plays an important role in soundness of cast parts. Semi-Solid Metal, SSM, slurry is a mixture of solid and liquid, mushy zone, with solid volume fractions of 0.1-0.5 and apparent viscosity close to oil viscosity at room temperature. It flows easily under pressure and capable of making complicated shapes with high degree of die filling and integrity. In this study, the ability of the semisolid slurry to continue to flow is investigated through the effect of different fraction solids and holding temperatures. The results show that in mechanically stirred semi-solid A356 Al-Si alloy, increasing fraction of solid causes decreasing of fluidity. This critical parameter is also related to different process variables such as stirring speed and time and holding time after stirring. Furthermore, the interrelationship between microstructure evolution and fluidity is discussed.

## 4:05 PM

Multiphase Flow Modeling of Quenching Heat Treatment Process: Mohammed Maniruzzaman<sup>1</sup>; Richard Sisson<sup>1</sup>; <sup>1</sup>Worcester Polytechnic Institute, Ctr. for Heat Treating Excellence, Mech. Engrg. Dept., 100 Inst. Rd., Worcester, MA 01609 USA

The quenching of hot metal parts in a liquid quenchant involves several complex heat and fluid flow processes. Different heat transfer mechanisms occur at different stages of cooling, namely film and nucleate boiling and convection. The heat extraction rate varies by several orders of magnitude over these stages and is a fluid flow parameters (such as Reynolds number, Grashoff's number etc.). The majority of the heat extraction occurs during the boiling stage. Formation of a bubble and its growth and detachment from the hot surface play a major role in the heat-extraction. In this paper, a Computational Fluid Dynamics (CFD) methodology is developed to simulate numerically the boiling heat transfer during quenching heat treatment process. Predicted heat extraction rate is compared with the experimental result.

## 4:25 PM

#### Natural Occurrence of Quasicrystal Shape Found at Nio, Yamaguchi, Japan: Yasunori Miura<sup>1</sup>; <sup>1</sup>Yamaguchi University, Chmst. & Earth Scis., Yoshida 1677-1, Yamaguchi 753-8512 Japan

Natural occurrence of quasicrystal type materials is shown from meteorite shower at Nio, Yamaguchi, Japan. The size of polyhedral shape is varied from 150-400micrometer (in major spherule) and 10-70micrometer (in micro-spherule). The texture is polyhedral shapes (from 10 to 70 micrometer). The composition is Fe-rich (90-96%Fe) mixture with minor Si, Al, Ca (sample No.N1P-3, homogeneous) and Si, Al, Mg, Na, Mn, Ca (No.sp-8, as tweedy texture) by shock wave mixing.

## 4:45 PM

Application of Multiphase Modelling to Hydromet Unit Operation Design: Lanre Oshinowo<sup>1</sup>; Lowy Gunnewiek<sup>1</sup>; Tom Plikas<sup>1</sup>; <sup>1</sup>Hatch Associates Ltd., 2800 Speakman Dr., Mississauga, Ontario L5K 2R7 Canada

The incorporation of advanced analysis tools, such as CFD, into the process plant design process has become possible through advances in commercially available computational fluid dynamics software and faster computers. Multiphase modelling is now typically employed in the design phase of process plant design at Hatch. The additional rigour allows process engineers to come closer to realising true virtual plant design. The objective of this paper is to outline the benefits and pitfalls in the application of multiphase modelling for rigorous design. Several application examples in the hydrometallurgical field will be presented.

# Nanostructured Materials for Biomedical Applications: Session VI

Sponsored by: Electronic, Magnetic & Photonic Materials Division, EMPMD-Thin Films & Interfaces Committee *Program Organizers:* Roger J. Narayan, Georgia Tech, School of Materials Science and Engineering, Atlanta, GA 30332-0245 USA; J. Michael Rigsbee, North Carolina State University, Department of Materials Science and Engineering, Raleigh, NC 27695-7907 USA; Xinghang Zhang, Los Alamos National Laboratory, Los Alamos, NM 87545 USA

Wednesday PM	Room: 2	19A
March 17, 2004	Location:	Charlotte Convention Center

Session Chairs: Andrew Shreve, Los Alamos National Laboratory, Biosci. Div., Los Alamos, NM 87545 USA; Prashant Kumta, Carnegie Mellon University, Dept. of Matls. Sci. & Engrg., Pittsburgh, PA 15213 USA

## 2:00 PM Invited

Polymer/Inorganic Nanocomposites for Biomedical Applications: Evangelos Manias<sup>1</sup>; Ruijian Xu<sup>1</sup>; Alan J. Snyder<sup>2</sup>; James P. Runt<sup>1</sup>; <sup>1</sup>Pennsylvania State University, Matls. Sci. & Engrg., 325-D Steidle Bldg., Univ. Park, PA 16802 USA; <sup>2</sup>Pennsylvania State University, Coll. of Medicine, The Milton S. Hershey Medical Ctr., Hershey, PA 17033 USA

This presentation provides an overview of our activities on polymer/inorganic nanocomposites for biomedical applications. The focus is on polymeric elastomers, in particular poly(urethane urea)s, and our strategies to reduce gas and water permeabilities upon formation of a nanocomposite with organically modified layered silicates (OLS). In contrast with conventional/macroscopic fillers the nanocomposites employing these high-aspect ratio 1nm thin particles can achieve high improvements in permeabilities (up to 400%), without sacrificing the elastomeric character, the strength, and the ductility of the polymer. A discussion tracing the materials properties to the molecular aspects of the nanocomposite structure will also be presented, so as to derive generally applicable design paradigms for polymer nanocomposites with desired properties.

#### 2:35 PM Invited

Nanostructured Conducting Polymer Nanofibers: *Hsing-Lin Wang*<sup>1</sup>; Wenguang Li<sup>1</sup>; <sup>1</sup>Los Alamos National Laboratory, Chmst. Div., MSJ586, C-PCS, Los Alamos, NM 87545 USA

Polyaniline is one of the most promising conducting polymers for commercial applications because it is inexpensive, easy to make, and environmentally stable. In this work, we report the synthesis and characterization of polyaniline chiral nanofibers and their potential applications for chemical separations. Our results show that by varying the experimental parameters, nanofibers can have tunable chirality and can differ by five orders of magnitude. In addition, the thin film cast from the as-synthesized nanofiber solution exhibits micro- and mesoporous features. The as-synthesized chiral, polyaniline nanofibers have a very high surface area and chirality. These characteristics make them extremely attractive candidates for chiral stationary phase in column chromatography, where they separate drugs, amino acids, proteins, and molecules that have asymmetric carbons (chiral centers). This report will discuss the detailed characterization of these nanostructured polyaniline nanofibers by UV-Vis, CD, TEM, and Xray spectroscopy

## 3:10 PM Invited

Temperature-Responsive Polymers and Their Applications in Nanostructures: *Evangelos Manias*<sup>1</sup>; Mindaugas Rackaitis<sup>1</sup>; <sup>1</sup>Pennsylvania State University, Matls. Sci. & Engrg., 325-D Steidle Bldg., Univ. Park, PA 16802 USA

Stimuli responsive materials are central in biomedical applications involving chemical sensing and/or stimuli-driven actuation. A systematic series of temperature-responsive polymers were synthesized and studied, and the onset of their T-response was tailored by design of their monomer. Their T-response was studied both for their water solutions, and when they were end-tethered on a surface. Thermodynamic considerations for the monomer design, afford the possibility to fine-tune the lower critical solution temperature (LCST) point, at values ranging from 5 to  $70^{\circ}$ C, in water. Solubility studies and phase diagrams were done for the solutions, whereas water contact angle, ellipsometry, and atomic force microscopy were carried out for the end-grafted polymers, as a function of grafting density. Model microfluidic devices employing these polymers as T-responsive gates were also realized.

#### 3:45 PM Invited

Peptide-Polymer Conjugates for Surface Modification and Nanoparticle Stabilization: *Phillip B. Messersmith*<sup>1</sup>; <sup>1</sup>Northwestern University, Biomed. Engrg., 2145 Sheridan Rd., TECH E311, Evanston, IL 60208 USA

Certain marine organisms secrete remarkable protein-based adhesive materials for adherence to the mineral, metal, and wood surfaces upon which they reside. For example, mussel adhesive proteins (MAPs) contain L-3,4-dihydroxyphenylalanine (DOPA), an amino acid that is believed to be responsible for the adhesive characteristics of MAPs. In this presentation we will describe our efforts to exploit the adhesive qualities of DOPA containing peptides to control cell behavior at surfaces. We have developed a simple strategy for solution modification of material surfaces utilizing conjugates of DOPA-containing peptides and the nonfouling polymer poly(ethylene glycol) (PEG). Exposure of a variety of material surfaces (e.g. gold, titanium, stainless steel, etc.) to a solution of DOPA-PEG polymer results in deposition of PEG onto the surface and significantly reduced protein and cell adsorption to the surface. Obvious applications of this strategy include protein and cell-resistant surfaces for medical applications, biofunctionalized surfaces, and stabilization of nanoparticles under physiological conditions.

## 4:20 PM

Nanostructured Magnetic Materials for Biomedical Applications: *Raju V. Ramanujan*<sup>1</sup>; <sup>1</sup>Nanyang Technological University, Sch. of Matls. Engrg., Blk. N4.1, Singapore 639798 Singapore

Biodegradable polymer coated magnetic systems, called magnetic carriers, have several important scientific and biomedical applications. The synthesis, by the ball milling process, of magnetic powders of iron oxide, cobalt and iron was carried out. The grain size of the powders following milling was in the nanometer range. The milling time required to form the minimum size of the powders was determined. The biodegradable polymer PLLA and theophyllin was subsequently coated around the powders by the solvent evaporation method. Various parameters such as milling time, agitation speed and polymer concentration were systematically varied to observe the change in magnetic carrier properties. The process parameters to produce magnetic carriers with a small average size, spherical morphology and narrow size distribution were determined. It was found that the agitation speed and polymer viscosity were important parameters to control the size and shape of the carriers. The surface morphology and magnetic properties of the carriers was also analyzed by SEM and VSM, respectively. These results will be presented and their significance will be highlighted.

# 4:55 PM Invited

Nanoengineered Responsive Polymer Surfaces for Micro/ Nanofluidic Bioanalytical Systems: *Qiao Lin*<sup>1</sup>; <sup>1</sup>Carnegie Mellon University, Mech. Engrg., 5000 Forbes Ave., Pittsburgh, PA 15213 USA

Recent advances in macromolecular engineering techniques allow for precisely controlled polymer chain length, uniformity, composition, topology and functionality. We exploit these advances to develop nanoengineered, intelligent polymer nanolayer coatings for surface modification of micro/nanofluidics-based bioanalytical systems. These polymer nanolayers, with a dry thickness ranging from 1 nm to 100 nm, are covalently grafted to the substrate surface with wellcontrolled chain densities and well-ordered chain orientation, and exhibit large changes in swelling and wettability properties in response to temperature changes. We discuss the synthesis and characterization of these polymer nanolayers, and their patterning using microfabrication techniques. The biomedical utility of this innovative surface modification technique is demonstrated by its application to microscale fluid handling. Specifically, we explore thermally responsive polymer nanolayers as a means to manipulate droplets and continuous flow in micro/nanofluidic systems, and to provide an intelligent solid phase for microchip chromatography.

# Phase Transformations and Deformation in Magnesium Alloys: Deformation and Strengthening

Sponsored by: Materials Processing and Manufacturing Division, MPMD-Phase Transformations Committee-(Jt. ASM-MSCTS) Program Organizer: Jian-Feng Nie, Monash University, School of Physics and Materials Engineering, Victoria 3800 Australia

Wednesday PM	Room:	20	)5		
March 17, 2004	Location	1:	Charlotte	Convention	Center

Session Chair: Junichi Koike, Tohoku University, Dept. of Matls. Sci., Sendai 980-8579 Japan

## 2:00 PM Invited

Atomic Mechanisms of Grain Boundary Sliding and Migration in hcp Metals: *Robert C. Pond*<sup>1</sup>; David J. Bacon<sup>1</sup>; Anna Serra<sup>2</sup>; <sup>1</sup>University of Liverpool, Matls. Sci. & Engrg., Liverpool, Merseyside L69 3BX UK; <sup>2</sup>Universitat Politecnica de Catalunya, Matematica Aplicada III, Jordi Girona 1-3, Barcelona, Catalunya 08034 Spain

Atomic scale simulations of grain boundary structures in hcp metals have been investigated using lattice-statics and molecular dynamics. The interaction of crystal dislocations with interfaces, and the response of these structures to applied shear strains have been studied. The boundaries were initially planar, subject to periodic or fixed border conditions, and the number of atoms in each simulation was conserved. Despite these limitations, insights into the fundamental mechanisms of sliding and migration were obtained. These properties were dependent on boundary structure. In twin boundaries for example, impinging crystal dislocations usually decomposed into glissile twinning and sessile dislocations. In response to applied shear strains, twinning dislocations moved readily, while sessile defects acted as sources of twinning dislocations thereby causing local interface migration. On the other hand, the decomposition products of crystal dislocations reaching incommensurate interfaces became partially delocalised. Such interfaces offered very low resistance to sliding.

## 2:35 PM Break

#### 3:10 PM Invited

## Solid Solution Strengthening in Magnesium Alloys: Pavel David Lukac<sup>1</sup>; Zuzanka Trojanova<sup>1</sup>; <sup>1</sup>Charles University, Dept. of Metal Physics, Ke Karlovu 5, Praha 2 12116 Czech Republic

In this paper, the influence of solute atoms on the critical resolved shear stress (CRSS) of both basal and non-basal slip system is presented. The CRSS for the basal slip of Mg alloys increases as  $c^{2/3}$  where c is the solute concentration in atomic fractions. The CRSS for glide in non-basal slip systems exhibits an anomalous temperature dependence and its concentration dependence is more complex. The paper presents an attempt to explain the effect of solute concentration on the deformation behaviour of Mg alloy polycrystals. The increased ductility observed in some Mg alloys may be attributed to the enhanced

activity of pyramidal slip and the double cross slip with the solute concentration. The temperature and concentration dependence of ductility of a Mg alloy should be complex due to a non-monotonic dependence of the CRSS for non basal slip on the test temperature.

## 3:45 PM Invited

Modelling of the Precipitation Processes and Strengthening Mechanisms in Mg-Al-(Zn) Automotive Alloys: Christopher R. Hutchinson<sup>1</sup>; Jian-Feng Nie<sup>1</sup>; Stéphane Gorsse<sup>2</sup>; <sup>1</sup>Monash University, Sch. of Physics & Matls. Engrg., Clayton, Victoria 3800 Australia; <sup>2</sup>Université Bordeaux 1, Inst. de Chimie de la Matière Condensée de Bordeaux, Bordeaux 33608 France

Mg-Al based alloys are the best known Mg alloys and form the basis of the well known precipitation hardened AZ91 series. Precipitation from the supersaturated solid solution is thought to involve the direct formation of lath shaped equilibrium  $Mg_{17}Al_{12}$  phase, predominatly on the basal planes of the matrix. The resulting hardening has been measured by several investigators and the microstructural evolution characterised. In any multi-phase metallic alloy, the strengthening arises from the competition between different hardening modes (peierls, grainsize, solid solution, orowan, composite etc.) In this presentation we report our efforts at modelling the precipitation (mean size and number density) and the hardening resulting from isothermal heat treatments of AZ91. The calculations are compared with experimental data and efforts are made to explain the interesting shape of the Hardness vs. Isothermal ageing time curves for AZ91.

# Roytburd Symposium on Polydomain Structures: Domains in Ferroelectrics and Magnetics

Sponsored by: TMS, MPMD-Phase Transformations Committee-(Jt. ASM-MSCTS)

*Program Organizers:* Julia Slutsker, National Institute of Standards and Technology, CTCMS, Gaithersburg, MD 20899 USA; Greg B. Olson, Northwestern University, Department of Materials Science and Engineering, Evanston, IL 60208 USA

Wednesday PM	Room:	216A
March 17, 2004	Location	: Charlotte Convention Center

Session Chair: Alexander L. Roytburd, University of Maryland, Matls. Sci. & Engrg., College Park, MD 20742 USA

## 2:00 PM Invited

**Domain Formation at Phase Transitions in Ferroelectric Films with Semiconducting and Other Electrodes**: Alexandre M. Bratkovsky<sup>2</sup>; *Arkadi P. Levanyuk*<sup>1</sup>; <sup>1</sup>Universidad Autonoma de Madirid, Depto. de Fisica de la Materia Condensada, C-III, Cantoblanco, Madrid 28049 Spain; <sup>2</sup>Hewlett-Packard Laboratories, 1501 Page Mill Rd., 1L, Palo Alto, CA 94304 USA

A second order phase transition in ideally homogeneous infinite ferroelectric plate with electrodes made of an ideal metal would proceed into a single-domain state. We investigate a realistic situation of a phase transition in a ferroelectric film with real electrodes made of a semiconductor or a metal. The phase transitions in ferroelectrics with semiconductor electrodes have been discussed long ago by Batra et al.<sup>1</sup> and more recently by Watanabe.2 However, previous authors have used an inappropriate thermodynamic potential, based their conclusions on numerical calculations, and neglected or inadequately considered domain formation at the phase transition. They have reached a conclusion that in a ferroelectric with semiconductor electrodes the second order phase transition becomes first order, when the transformation proceeds into a single-domain state. We give a consistent analytical treatment of the problem and conclude that the phase transition remains second order with formation of a domain structure in otherwise ideal samples with practically any realistic electrodes. <sup>1</sup>I.P. Batra, P. Wurfel, and B.D. Silverman, Phys. Rev. B8, 3257 (1973). 2Y. Watanabe, J. Appl. Phys. 56, 527 (1990).

# 2:35 PM Invited

**Energy Minimization and Domain Structure in the Intermediate State of a Type-I Superconductor**: Rustum Choksi<sup>2</sup>; *Robert V. Kohn*<sup>1</sup>; Felix Otto<sup>3</sup>; <sup>1</sup>New York University, Courant Inst., 251 Mercer St., New York, NY 10012 USA; <sup>2</sup>Simon Fraser University, Dept. of Math., Burnaby, BC V5A 1S6 Canada; <sup>3</sup>Universitaet Bonn, Angewandte Mathematik, Bonn 53115 Germany

We often "explain" observed microstructures using arguments based on energy minimization. Usually such arguments minimize the energy within a suitable ansatz; only rarely do they also justify the ansatz. The present work is of the latter type. Our focus is the intermediate state of a type-I superconductor, in the simplest possible case: a plate under a transverse applied field. This is a two-phase problem, involving normal and superconducting domains. The energy, first formulated by Landau, involves a (long-range) magnetic term as well as (local) surface and condensation terms. Landau used energy minimization to predict that flux domains should branch. He missed, however, the problem's remarkable richness when the applied field is near-zero or near-critical. In these regimes there are two small parameters — the normalized surface tension and the volume fraction of one phase — and scaling law of the minimum energy depends on the relation between them.

#### 3:10 PM Break

#### 3:25 PM Invited

Effect of External Mechanical Constraints on Phase Stability and Poly-Domain Structures in Thin Films: S. Choudhury<sup>1</sup>; Y. L. Li<sup>1</sup>; Z. K. Liu<sup>1</sup>; *Long-Qing Chen<sup>1</sup>*; <sup>1</sup>Pennsylvania State University, Matls. Sci. & Engrg., Univ. Park, PA 16802 USA

Many new applications of materials require the growth of thin films on a substrate. It is known that the type of substrate and its crystallographic orientation can have profound effects on the phase transformations and domain structures, and hence properties of thin films as it was shown by Roytburd many years ago. In particular, a substrate can impose a thermal stress due to thermal expansion coefficient difference between the film and substrate or a coherency stress due to the difference in the stress-free lattice parameters of the film and substrate. For phase transformations which produce polydomain structures, we recently developed a phase-field model which can be employed to predict their stability and evolution in thin films. As an example, the phase diagram of a PbZr1-xTixO3 (PZT) film constrained by a much thicker substrate was studied using both thermodynamic calculations and phase-field approach. PZT undergoes a cubic to tetragonal or cubic to rhombohedral transformation in the bulk depending on the composition x. It was found that the ferroelectric transition temperature increases under a substrate constraint regardless the nature of the constraint, i.e., tensile or compressive. It is shown that the orthorhombic phase that does not exist in the bulk becomes stable under a tensile constraint, and the rhombohedral phase in the bulk is distorted in the constrained film. The various ferroelectric polydomain structures produced under different substrate constraints will be discussed.

### 4:00 PM Invited

WEDNESDAY PM

Polydomain Formation in Ferroelectric Films and Thermodynamic Modeling of Polarization-Graded Ferroelectrics: S. Pamir Alpay<sup>1</sup>; Z.-G. Ban<sup>1</sup>; Joseph V. Mantese<sup>2</sup>; <sup>1</sup>University of Connecticut, Dept. of Metall. & Matls. Engrg., Inst. of Matls. Sci., Storrs, CT 06269 USA; <sup>2</sup>Delphi Research Laboratories, Shelby Township, MI 48315 USA

The thermodynamic theory of polydomain structures as applied to an epitaxial film-substrate couple where the film undergoes a cubictetragonal phase transformation is discussed. The parameters of polydomain structures and their dependence on the characteristics of the phase transformation, lattice misfits, the film thickness, and external fields are determined. An effective quantitative theoretical model is provided to explain observed experimental results and to predict and to control the microstructure in epitaxial ferroelectric films. The analysis can be elegantly summarized on a "domain stability map," a phase diagram in the plane of the misfit strain due to the mismatch between the film and the substrate and the tetragonality of the film. The second part of the presentation is concentrated on polarizationgraded ferroelectrics, which exhibit behavior and properties that are not routinely observed from homogenous ferroelectrics. It is shown that the thermodynamic approach is quite general and readily expandable to graded ferromagnets, ferroelastics, and other ferroic systems with proper modifications.

#### 4:35 PM Discussion: Problems and Perspectives of Design and Control of Domain Structures Mediators: G. B. Olson, A. L. Roytburd and J. Slutsker

## Solid and Aqueous Wastes from Non-Ferrous Metal Industry: Session I

Sponsored by: Extraction & Processing Division, EPD-Waste Treatment & Minimization Committee

*Program Organizers:* Junji Shibata, Kansai University, Department of Chemical Engineering, Osaka 564-8680 Japan; Edgar E. Vidal, Colorado School of Mines, Golden, CO 80401-1887 USA

Wednesday PM	Room: 214
March 17, 2004	Location: Charlotte Convention Center

Session Chairs: Mikiya Tanaka, National Institute of Advanced Industrial Science and Technology, Tukuba Japan; Ji-Whan Ahn, Korea Institute Geoscience and Mineral Resources, Teajon Korea

#### 2:00 PM Invited

Production of the High Value Material, Alpha-CaSO<sub>4</sub> Hemihydrate Out of Spent CaCl<sub>2</sub> Solutions by Reaction with H2SO<sub>4</sub>: *Seref Girgin*<sup>1</sup>; George P. Demopoulos<sup>1</sup>; <sup>1</sup>McGill University, Mining, Metals & Matls. Engrg., 3610 Univ. St., Wong Bldg., Montreal, Quebec H3A 2B2 Canada

CaCl<sub>2</sub> can either be found in spent leaching solutions or in waste brines from geothermal fields. One possible treatment option for these solutions is the production of saleable quality gypsum materials by reaction with H<sub>2</sub>SO<sub>4</sub>-an increasingly difficult to sell by-product of the non-ferrous metallurgical industry. One such high-value material is alpha-CaSO<sub>4</sub> hemihydrate (alpha-HH) finding uses in the building industry. Regeneration/production of HCl out of the spent CaCl<sub>2</sub> solutions is another benefit of such treatment process. It is indeed the scope of this work to develop an atmospheric process for the conversion of spent CaCl<sub>2</sub> solutions to high-value alpha-HH and HCl. In this paper, the crystallization of alpha-CaSO<sub>4</sub> hemihydrate out of such chloride solutions is described as a function of various parameters such as solution composition (CaCl<sub>2</sub> and HCl concentration, H<sub>2</sub>SO<sub>4</sub>/CaCl<sub>2</sub> ratio, etc.), method of H<sub>2</sub>SO<sub>4</sub> addition, temperature and seeding.

### 2:30 PM Invited

Removal Treatment of Harmful Materials in Waste Water Using Temperature-Sensitive Polymer Gel: *Hideki Yamamoto*<sup>1</sup>; Akihiro Kushida<sup>1</sup>; Noriyuki Heamot<sup>1</sup>; Yuko Takami<sup>1</sup>; Norihiro Murayama<sup>1</sup>; Junji Shibata<sup>1</sup>; <sup>1</sup>Kansai University, Dept. of Chem. Engrg., Japan

The adsorption removal of harmful organic materials in wastewater has been carried out using the adsorption and desorption characteristics of a temperature -sensitive polymer gel which is synthesized from polyvinylalcohol (PVA). A new adsorption removal process using an air lifting type vessel has been designed and examined for practical use. At higher temperatures, the temperature-sensitive polymer gel shrinks because of discharging water, whereas, in contrast, at lower temperatures, the gel swells as a result of absorbing water. The reversibility of the volume change of the synthesized polymer gel is confirmed by changing temperature. The adsorption behavior of organic materials onto PVA polymer gels in water was investigated at various temperatures. The amount of adsorption of organic materials increases remarkably at temperatures higher than about 305K-320K. The saturated amounts of adsorption are about 0.26mmol/g-gel. The organic material in wastewater could be adsorbed and desorbed reversibly onto PVA polymer gel by the temperature swing. The mechanism of adsorption and desorption of organic materials onto the gel can be explained by the hydration and dehydration of the polymer gel. The driving force of the adsorption is considered to be the hydrophobic interaction between PVA polymer gel and organic compounds.

## 3:00 PM Invited

Treatment of Transition Metal Oxide Wastes by Plasma Driven Electrolysis: Patrick R. Taylor<sup>1</sup>; Wenming Wang<sup>1</sup>; Edgar E. Vidal<sup>1</sup>; <sup>1</sup>Colorado School of Mines, Plasma Procg. Lab., Dept. of Metall. & Matl. Engrg., 1500 Illinois St., Golden, CO 80401-1887 USA

An innovative process to treat transition metal oxide sludge from diverse sources is presented. This technology involves using reversepolarity DC plasma driven electrolysis in molten oxides. The process results in the recovery of the transition metal and other heavy metals from waste. By-products generated throughout the processing will be converted in an environmentally acceptable slag. The significance of this technology is that the treatment of the waste is accomplished in one step which in turn lowers the cost of remediation. Moreover, this process uses high temperature properties of thermal plasmas, which makes it possible to use molten oxides instead of halides as electrolyte. Chromium was successfully reduced from chromite through the plasma driven electro-reduction process. It was shown that the selection of the appropriate ionic conducting oxides was critical for the formation of a slag that would enhance the reduction of chromium oxide.

## 3:30 PM Break

## 3:45 PM

Production of Functional Inorganic Materials, AIPO<sub>4</sub>-5, from Wastes in Aluminum Regeneration Industry: Junji Shibata<sup>1</sup>; Norihiro Murayama<sup>1</sup>; Hideki Yamamoto<sup>1</sup>; <sup>1</sup>Kansai University, Dept. of Chem. Engrg., Osaka 564-8680 Japan

The hydrothermal synthesis of functional inorganic material,  $AIPO_4$ -5, was carried out using aluminum dross as a starting material. The crystalline  $AIPO_4$ -5 was obtained by the hydrothermal reaction conducted in an autoclave. Ay the same time,  $AIPO_4$ -34 and  $AIPO_4$  are formed as a by-product. The product,  $AIPO_4$ -5, has a porous structure comprising of aluminum phosphates, and its pore size is 7 Å. The crystal of  $AIPO_4$ -5 was investigated from the surface property of precursor and the property of tri-ethyl amine as a reaction promoter.

## 4:05 PM

Fluid Bed Destruction of Aqueous and Other Wastes: A Study in Design: Larry M. Southwick<sup>1</sup>; <sup>1</sup>L.M. Southwick & Associates, 992 Marion Ave., Ste. 306, Cincinnati, OH 45229 USA

Much of industry uses fluid beds units to destroy or process waste streams. The beds may be composed of inert solids (such as sand) or of decomposition products (such as iron oxide from the pickling of steel). Feed materials are often aqueous slurries and may contain combustible materials. Such units frequently develop operating problems relating to the smoothness of fluidization, violent pressure disturbances or coarsening of bed material, often to the point of complete loss of operability. Data from one such unit (processing a dissolved air flotation slurry) will be presented and an analysis made which indicates a common source of such problems. The solution was applied and solved the operating problems on the unit. This analysis can also be applied to other types of fluid bed processing, such as roasting of sulfidecontaining feed materials.

## 4:25 PM

Synthesis of Hydrotalcite from the Wastes Discharged in Aluminum Regeneration Process: Norihiro Murayama<sup>1</sup>; Mitsuaki Tanabe<sup>1</sup>; Hideki Yamamoto<sup>1</sup>; Junji Shibata<sup>1</sup>; <sup>1</sup>Kansai University, Dept. of Chem. Engrg., Osaka 564-8680 Japan

The synthesis of hydrotalcite, which is an inorganic anion exchanger and has layer structure of complex hydroxide, is curried out by using aluminum dross and MgCl<sub>2</sub> waste solution discharged from aluminum regeneration process. Various properties such as crystal structure, surface structure, specific surface area, thermal gravity and so on are investigated for the obtained reaction product. Hydrotalcite can be synthesized from the aluminum dross and the waste solution containing MgCl<sub>2</sub> by precipitation reaction. Interlayer distance of the obtained product is about 0.3nm. The obtained hydrotalcite changes to Mg-Al oxide by the calcination at 723K, and then the hydrotalcite is formed again by rehydration operation after the calcination. Physical properties of the hydrotalcate from the above wastes are almost similar to those from reagent.

#### 4:45 PM

Hydrometallurgical Methods for Treating Copper Electrolytic Sludge: N. I. Antipov<sup>1</sup>; A. V. Tarasov<sup>1</sup>; V. M. Paretsky<sup>1</sup>; <sup>1</sup>State Research Center of Russian Federation, State Rsch. Inst. of Nonferrous Metals, 13, Acad. Korolyov St., 129515 Moscow Russia

A hydrometallurgical method developed in the Gintsvetmet Institute for treating anode sludge and based on sulfite leaching (pH 9.2 to 9.6) of gold or hydrochloric acid leaching in the presence of an oxidizing agent permits its efficient quantitative separation from silver at the head of the process, eliminating thereby the need for production of Dore metal and its further electrolytic refining. In the process of sludge treatment, gold and silver are separated into individual highgrade products, i.e., metal powders, and their refining is, therefore, significantly simplified and can be accomplished by the use of sodium sulfite as the main reagent playing the role of a complexing agent and reductant of gold, silver and selenium. Tellurium, lead and antimony are removed from the process circuit in the form of reach intermediate products. Elimination of roasting, sintering and smelting processes improves the environmental performance of the operations and reduces the operating cost for dust recovery and offgas treatment. Investigations conducted have demonstrated that sludge from the Balkhash smelter (Kazakhstan) and Kovoguty Krompahy smelter (Slovakia) can be successfully treated using the proposed technology with recoveries into corresponding metal powders of 99.57% and 95.45% of gold and 99.5% and 98.3% of silver, respectively.

## Solidification of Aluminum Alloys: Gas Porosity/ Micro-Macro Segregation

Sponsored by: Materials Processing & Manufacturing Division, MPMD-Solidification Committee

*Program Organizers:* Men Glenn Chu, Alcoa Inc., Alcoa Technical Center, Alcoa Center, PA 15069 USA; Douglas A. Granger, GRAS, Inc., Murrysville, PA 15668-1332 USA; Qingyou Han, Oak Ridge National Laboratory, Oak Ridge, TN 37831-6083 USA

Wednesday PM	Room: 207B/C
March 17, 2004	Location: Charlotte Convention Center

Session Chairs: Douglas A. Granger, GRAS Inc., Murrysville, PA 15668-1332 USA; Ralph Napolitano, Iowa State University, MSE, Ames, IA 50011 USA

### 2:00 PM Keynote

Hydrogen in Aluminum and its Alloys: D. E.J. Talbot<sup>1</sup>; <sup>1</sup>Consultant, 96 Bury St., Ruislip HA 47TG, Middlesex UK

The effects of hydrogen in aluminum and its alloys are discussed in terms of the occluded forms of hydrogen, kinetics of absorption reactions and control of hydrogen content. Theories of hydrogen solutions and implications for the stability of real solutions are explained. The origins of interdendritic porosity nucleated in the liquid fraction during solidification and secondary porosity nucleated from the solid as microscopic spherical voids are considered in relation to metal composition, hydrogen content, and casting parameters. Residues of ingot porosity survive fabrication as precursors of macroscopic defects whose development depends inter alia on hydrogen absorbed during heat treatments applied in processing. Two potent sources are humid air and surface contamination. Humid air supplies hydrogen by diffusion of OH- ions through the oxidation product to the oxide/ metal interface where they are reduced to hydrogen. Oxidation products offering significant diffusion paths include h-alumina on pure aluminum. MgO with extrinsic OH- cations on aluminum-magnesium alloys and LiOH on aluminum-lithium alloys. Catalysis by sulphur contamination and passivation with fluoride vapours are discussed. A quantitative assessment of pore nuclei as sinks for absorbed hydrogen is given, and precipitation of LiH as an alternative sink in aluminumlithium alloys is explained. Surface contamination implanted by rolling provides a finite source of hydrogen that can diffuse into the metal. Theory and practice of gas purging to reduce hydrogen contents of liquid metal are described with particular reference to in-line treatment with insoluble active gas mixtures. Interdendritic porosity can be avoided by such treatments, but some secondary porosity is inevitable; and its effects are minimized by appropriate onward processing. Facilities to determine hydrogen contents in the liquid by Telegas type instruments and in the solid by vacuum extraction are recommended.

## 2:30 PM

Effect of Hydrogen Porosity and As-Cast Grain Structure on the Mechanical Properties of Cast and Forged Al-1.0%Mg-0.6%Si Alloy: Makoto Morishita<sup>1</sup>; Kiminori Nakayama<sup>2</sup>; Men Glenn Chu<sup>3</sup>; <sup>1</sup>Kobe Steel, Ltd., Matls. Rsch. Lab., 15, Kinugaoka, Moka, Tochigi 321-4367 Japan; <sup>2</sup>Kobelco Research Institute, Inc., Engrg Mech. Div., 1-5-5, Nishi-ku Takatsukadai, Kobe, Hyogo 651-2271 Japan; <sup>3</sup>Alcoa Technical Center, Solidification & Molten Metal Proc. Fundamentals Div., 100 Tech. Dr., Alcoa Ctr., PA 15069 USA

Hydrogen porosity is considered an undesirable feature in aluminum wrought alloy ingots. However, its impact on the mechanical properties of fabricated products is rarely found in the literature. The purpose of this paper is to report the influence of hydrogen porosity and as-cast grain structure on the mechanical properties of an experimental Al-1.0%Mg-0.6%Si alloy. The samples were cast using a bench scale apparatus at the Alcoa Technical Center and subsequently preheated and forged at Kobe Materials Research Laboratory. In this investigation, cast samples were prepared with three different levels of hydrogen and two levels of grain refinement. They were then preheated and forged with three different amounts of reduction. The mechanical properties of both as-cast and forged samples were measured using tensile and toughness tests. The results from these tests will be presented and discussed. Identifying Sources of Gas Causing Porosity Defect in the Lost Foam Aluminum Castings: *Wanliang Sun*<sup>1</sup>; Harry E. Littleton<sup>1</sup>; Charles E. Bates<sup>1</sup>; <sup>1</sup>University of Alabama, Matls. Sci. & Engrg., 917 Bldg., 1530 3rd Ave. S., Birmingham, AL 35294-4480 USA

During the metal filling of the Lost Foam Casting (LFC), existence of the gaseous pyrolysis products around the molten aluminum makes the understanding of the gas porosity defect formation in the lost foam aluminum castings more complicated. In this study, the sources of the gas causing the porosity defects were identified through series of experiments. First, the surfaces of the gas pores in the lost foam aluminum casting, RPT (Reduced Pressure Test) sample and aluminum sand casting were studied visually. Then, the surface of the gas pores in the LFC was studied with SEM (Scanning Electric Microscope) and EDX (Energy Disperse X-ray). Carbon, oxygen and aluminum were detected on the surface of some of the gas pores. Thirdly, the formation of the gas pores in the lost foam casting was visualized using the state-of-art real time X-Ray technology. This experiment provides further evidence that the gas pores in the LFC is predominantly pyrolysis products related.

## 3:10 PM

Association of Hydrogen with Lithium in Aluminum Alloys: Dilys M. Henry<sup>1</sup>; David E.J. Talbot<sup>2</sup>; <sup>1</sup>DuPont Corporate Research & Development, Corp. Failure Analysis, Experimental Sta., E304/C331, Wilmington, DE 19805 USA; <sup>2</sup>Consultant, 96 Bury St., Ruislip HA 47TG, Middlesex UK

The solubilities of hydrogen in the alpha-phase of aluminum alloys containing lithium are an order of magnitude greater than in other alloys. Anomalous values for the solution enthalpy and entropy suggest that the additional solubility is due to special sites at which hydrogen atoms are strongly bound. Support for this view is a marked reduction in the mobility of hydrogen the special sites are intuitively identified as the clusters that are the precursors of lithium-rich precipitates responsible for age-hardening. The present work produced further support for an association of hydrogen with the clusters. Small angle neutron diffraction of AA8090, with and without occluded hydrogen introduced during solutionizing at 450°C and at 500°C, identified a reciprocal constraint on the mobility of lithium. Vant' Hoff Isobars for hydrogen solution in aluminum-lithium alloys exhibit discontinuities at critical temperatures that suggest a change in the association.

# 3:30 PM Break

## 3:50 PM Keynote

Modeling Segregation and Porosity in an Aluminum Casting Alloy: David R. Poirier<sup>1</sup>; Pil K. Sung<sup>1</sup>; <sup>1</sup>University of Arizona, Matls. Sci. & Engrg., Tucson, AZ 85721 USA

The dendritic solidification of an aluminum casting alloy is simulated as a means to study the transport phenomena of alloy elements and hydrogen. The transport is modeled using porous media theory, in which mass, solutal species, energy, and momentum conservations form the underlying set of equations. The set solution is effected by a finite element code. Examples that reveal the formation of macrosegregation and the formation of porosity in castings are presented. These will include the effect of high over-pressures during solidification to suppress porosity.

#### 4:20 PM

Modeling the Effects of Mold Topography on Aluminum Cast Surfaces: *Lijian Tan*<sup>1</sup>; Nicholas Zabaras<sup>1</sup>; <sup>1</sup>Cornell University, Matls. Proc. Design & Control Lab., Sibley Sch. of Mech. & Aeros. Engrg., 188 Frank H. T. Rhodes Hall, Ithaca, NY 14853-3801 USA

A comprehensive review will be provided of recent computational studies for the development of a finite element analysis based design methodology with which casting mold surface topographies can be tuned to produce required surface features and microstructural properties of aluminum ingots. A coupled thermomechanical and melt flow analysis has been developed that together with air-gap nucleation and contact modeling algorithms allows us to study the effects of mold topography on cast surfaces in the early stages of aluminum solidification. A sensitivity analysis to quantify the importance of mold topography on the shell surface morphologies will also be discussed. Mold surface topographies, which consist of unidirectional and bidirectional groove textures, are generated to elicit a radiator-like effect at the mold-casting interface. The rate of heat extraction, the evolution of near-surface cast microstructure, and shell macro morphology can be controlled, once the proper balance between mold surface area extension and the degree of imperfect wetting at the instant solidification starts is determined. A control of the surface features in aluminum

casting is important in minimizing costly post-casting surface milling or scalping.

#### 4:40 PM

Solidification Morphology and Structure of Cast Al-Li 2090 Alloy at Low Superheat: Chandan Mahato<sup>1</sup>; Mohamed Shamsuzzoha<sup>1</sup>; *Nagy El-Kaddah*<sup>1</sup>; <sup>1</sup>University of Alabama, Dept. of Metallurgl. Engrg., Box 870202, Tuscaloosa, AL 35487 USA

The effect of low superheat on solidification morphology and microstructure of Al-Li 2090 alloy has been investigated using the Magnetic Suspension Melting (MSM) process, which is capable of remelting and casting aluminum at superheats as low as 1°C. In this study, the metal was solidified unidirectionally in a cylindrical ceramic mold with a chill stainless steel block at the bottom. The castings were analyzed by microscopic and image analysis techniques. Metallographic examination showed that the cast metal exhibited fine-grained equiaxed structure throughout the ingot, with an average grain size of about 80µm. The average grain size was found to be independent of both the cooling and solidification rates in the mold. TEM examination showed that the matrix exhibits a super lattice type structure of coherent  $\delta$ ' (Al<sub>3</sub>Li) phase with minor amount of T1 (Al<sub>2</sub>CuLi) needles in the matrix. Chemical analysis of the ingots showed typical inverse segregation of Cu in aluminum alloys in the direction of solidification, and very little segregation of Zr.

# Surfaces and Interfaces in Nanostructured Materials: Coatings and Surface Modification

Sponsored by: Materials Processing and Manufacturing Division, MPMD-Surface Engineering Committee *Program Organizers:* Sharmila M. Mukhopadhyay, Wright State University, Department of Mechanical and Materials Engineering, Dayton, OH 45435 USA; Arvind Agarwal, Florida International University, Department of Mechanical and Materials Engineering, Miami, FL 33174 USA; Narendra B. Dahotre, University of Tennessee, Department of Materials Science & Engineering, Knoxville, TN 37932 USA; Sudipta Seal, University of Central Florida, Advanced Materials Processing and Analysis Center and Mechanical, Materials and Aerospace Engineering, Oviedo, FL 32765-7962 USA

Wednesday PM	Room:	217A
March 17, 2004	Location	: Charlotte Convention Center

Session Chair: Narendra B. Dahotre, University of Tenessee, Dept. of Matls. Sci. & Engrg., Knoxville, TN 37932 USA

#### 2:00 PM Invited

Modification of Nanotube-Based Materials by Ion Beam Deposition: Computational Studies: Susan B. Sinnott<sup>1</sup>; <sup>1</sup>University of Florida, Matls. Sci. & Engrg., 154 Rhines Hall, PO Box 116400, Gainesville, FL 32611-6400 USA

Classical molecular dynamics simulations with many-body empirical potentials are used to study the chemical modification of carbon nanotube based materials. Chemical modification of nanotubes is important for controlling their adhesion to polymers in composites. The simulations focus on the use of ion beam deposition to modify the structure of empty nanotubes and of nanotubes filled with buckyballs. The results show that the tube walls can be chemically functionalized and that cross-links can be produced between adjacent nanotubes in a bundle, between nanotube walls within a multi-walled tube structure, and between the nanotube-polymer composites is considered. The simulations show that this approach can produce cross-links between the tubes and polymer chains in situ, but that there are important structural dependencies in the results. The support of the National Science Foundation through grant CHE-0200838 is gratefully acknowledged.

## 2:25 PM

Nanoscale Silver Particle Films for High-Temperature Packaging of Semiconductor Devices: *Zhiye Zhang*<sup>1</sup>; Jesus Noel Calata<sup>2</sup>; John G. Bai<sup>2</sup>; Guo-Quan Lu<sup>3</sup>; Yanjing Liu<sup>4</sup>; <sup>1</sup>Virginia Tech, The Bradley Dept of Elect. & Computer Engrg., Whittemore Hall 618, Blacksburg, VA 24061 USA; <sup>2</sup>Virginia Tech, Dept. of Matls. Sci. & Engrg., 213 Holden Hall, Blacksburg, VA 24061 USA; <sup>3</sup>Virginia Tech, The Bradley Dept. of Elect. & Computer Engrg. & Matls. Sci. & Engrg., Blacksburg, VA 24061 USA; <sup>4</sup>Luna Innovations, Blacksburg, VA 24060 USA

Nanometer-thick silver films were deposited on various substrates (silicon, glass, ceramic, and flexible Kapton<sup>©</sup> films) by dipping in

stable aqueous solutions containing silver nanoparticles using an electrostatic self-assembly technique at room temperature. The silver particles were synthesized by reduction of silver nitrate with sodium borohydride in a solution containing PAA. Characterization of the films using SEM, AFM and XPS shows that the nano-sized silver particles ranging from 30 to 50 nm in diameter are packed closely and homogeneously on the substrates. Silver nanoparticles could lead to significantly lower sintering temperatures with a potential application in high-temperature interconnections of future electronic devices such as SiC. Preliminary sintering tests on the films show widespread neck formation between particles at temperatures as low as 250°C. Further research and investigation of potential applications are ongoing.

## 2:45 PM

Laser Induced In Situ Synthesis of Nanocomposite Carbide Coating on Steel: Anshul K. Singh<sup>1</sup>; Narendra B. Dahotre<sup>1</sup>; <sup>1</sup>University of Tennessee/UTSI, Dept. of Matls. Sci. & Engrg., 10521 Rsch. Dr., Ste. 400, Knoxville, TN 37932 USA

The stress on reducing the size of most contemporary equipments has amplified the importance of nanoscale technology significantly which thus augments the importance of surface properties of materials. With the aim of synthesizing a nano composite carbide coating, a 2.5 KW Nd: YAG laser was employed on the surface of AISI 1010 steel deposited with a precursor powder mixture of Fe, Ti, Cr and C. In-situ formation of ultra hard nanoscale carbide particles (TiC and chromium carbides) dispersed in a Fe-based matrix was observed. The nano composite coating thus achieved has far superior surface properties viz. hardness and wear resistance.

#### 3:05 PM

Chemical Bonding and Morphology of the Thin Carbon Films Created on SiC Surface by the Carbide-Derived Carbon (CDC) Process: Alexander V. Zinovev<sup>1</sup>; Jerry F. Moore<sup>1</sup>; Michael J. Pellin<sup>1</sup>; John A. Carlisle<sup>1</sup>; Orlando H. Auciello<sup>1</sup>; John N. Hryn<sup>1</sup>; <sup>1</sup>Argonne National Laboratory, Matl. Sci. Div., 9700 S. Cass Ave., Argonne, IL 60439 USA

The treatment of silicon carbide ceramic in chlorine contained gas mixture was carried on. Due to the energetically favored reaction of  $Cl_2$  with Si rather than C the selective etching of the SiC can take place, leading to the formation of a carbide-derived carbon (CDC) film. The result of XPS and also Raman spectroscopy, AES and SEM studies of chemical conversion of single crystal SiC and industrial polycrystalline silicon carbide surface treated at different gas concentrations and different temperatures will be presented. XPS analysis of the carbon C1s fundamental peak and the valence band shows that created CDC films are not phase pure but consist of a mixture of sp2 and sp3 bonded carbon. Differences observed in the conversion rate and phases formed on different types of SiC substrates (single crystal or industrial ceramics) will be discussed and are likely due to grain boundary and surface morphology effects.

## 3:25 PM

Nanometer-Scale Coatings for Nano-Structured Solids: Sharmila M. Mukhopadhyay<sup>1</sup>; <sup>1</sup>Wright State University, Mech. & Matls. Engrg., 3640 Colonel Glenn Hwy., Dayton, OH 45435 USA

The concept of surface coatings for property modification is not new, but when the bulk structure to be coated is itself <100 nm in dimension, new challenges emerge. The coating has to be substantially thinner than bulk dimensions, yet be functional. In this presentation, it will be shown that some plasma assisted coatings having thickness in the 1-5 nm range can be very effective for modification of nanofibers, near net shape cellular foams, and other porous materials. Two types of coatings are focused upon initially: (i) those for enhancement surface reactivity and bonding, and (ii) those that make the surface inert. The former has been achieved by a nano-layer of SiO2-type compound, and the latter has been achieved by 1-2 nm layer of -CF2chains. The initial stages of growth of these layers (from atomic clusters to complete mono-layers) have been studied. XPS and AFM results appear to correlate very well with physical properties such as wettability, bond formation and fluid infiltration. Additional aspects of these coatings specific to applications, such as permeability through porous solid, durability, and future possibility of creating multi-layer and multi-functional nano-coatings will be discussed.

## 3:45 PM

Auto-Organized Nanostructures in the Ti-Al-N Thin Film System: Lars Hultman<sup>1</sup>; <sup>1</sup>Linköping University, Thin Film Physics Div., IFM, Linkoping S-581 83 Sweden

The process of age hardening as a means for advanced surface engineering of nanostructured materials has been evidenced in thin film applications. A model system, Ti1-xAlxN, was chosen as such coatings are known for their excellent wear resistance enabling improved machining processes like high-speed and dry cutting. Physical vapour deposition methods with relatively low substrate temperatures are employed to produce supersaturated solid solutions of the material by virtue of the kinetic limitations during synthesis. It is shown using TEM, HREM, XRD, differential scanning calorimetry, and nanoindentation that Ti1-xAlxN coatings with compositions in the miscibility gap initially undergo spinodal decomposition into coherent cubic-phase nanometer-size domains, causing an increase in hardness at elevated temperatures. These intermediate metastable domains transform into their stable phases TiN and AlN during further thermal treatment. Activation energies for the processes indicate defect-assisted segregation of Ti and Al. The findings are corroborated by ab initio calculations of phase stability and molar volume for competing phases. It is inferred that the success of Ti1-xAlxN coatings is not only based on its superior oxidation resistance, but also on its ability for self-adaptation to the thermal load applied during cutting by age hardening. The findings and experimental approach have implications also for other ternary and multinary ceramic systems including the group-III nitride alloys.

#### 4:05 PM

Effect of Processing Parameters on Properties of Nanocrystalline FeCrP Electrodeposits: C. T. Kunioshi<sup>1</sup>; N. B. de Lima<sup>1</sup>; O. V. Correa<sup>1</sup>; L. V. Ramanathan<sup>1</sup>; <sup>1</sup>Cidade Universitaria, Matls. Sci. & Tech. Ctr., Inst. de Pesquisas Energeticas e Nucleares, Av. Prof. Lineu Prestes 2242, São Paulo 05508-000 Brazil

This paper presents the effect of processing parameters such as bath composition, additives to the bath, temperature and current density on the composition, morphology and corrosion resistance of nanocrystalline FeCrP electrodeposits. Deposits with average size of 1.5nm were obtained at current densities up to 150 mA.cm-2 and with bath temperatures up to 50°C. In the presence of formic acid as a complexing agent and aging of the bath, uniform, adherent and nanocrystallline deposits with 9-17%Cr were obtained. The crystallite size decreased with increase in phosphorous content, and this in turn was influenced by the sodium hypophosphite content of the electrolytic bath. Electrochemical measurements revealed overall increase in corrosion resistance with increase in P content.

#### 4:25 PM

Influence of Surface Deposited Nanosized Rare Earth Oxide Gel Morphology on High Temperature Cyclic Oxidation Behavior of Fe20Cr Alloy: S. M.C. Fernandes<sup>1</sup>; L. V. Ramanathan<sup>1</sup>; <sup>1</sup>Cidade Universitária, Matls. Sci. & Tech. Ctr., Inst. de Pesquisas Energéticas e Nucleares (IPEN), Av. Prof. Lineu Prestes 2242, São Paulo 05508-000 Brazil

The use of rare earths to increase the high temperature oxidation resistance of chromia and alumina forming alloys is well known. The rare earths can be added as elements to the alloys or applied on the metal surface as oxides. Several methods have been used to apply rare earth oxide coatings on metal surfaces and the sol-gel technique has been shown to be very efficient. This technique generates nano-sized oxide particles. The influence of sol-gel processing parameters on rare earth (RE) oxide (Y2O3, La2O3, CeO2, Nd2O3, Pr2O3, Dy2O3) morphology has been studied. The influence of RE oxide gel morphology and nature on cyclic oxidation behavior (RT-900°C) of Fe2OCr alloy has also been studied. This paper presents the results of these studies are discusses the role of RE oxide gel morphology (size, shape, distribution) and RE ion radius on cyclic oxidation resistance of the chromia forming alloy.

#### 4:45 PM

A FIB-SIMS Study of Interfaces in TiN/Cu Multilayered Thin Films: Alessio Lamperti<sup>1</sup>; Gregory Abadias<sup>2</sup>; Paolo Maria Ossi<sup>1</sup>; Carlo Enrico Bottani<sup>1</sup>; Riccardo Levi-Setti<sup>3</sup>; <sup>1</sup>Politecnico di Milano, Dipartimento di Ingegneria Nucleare, Via Ponzio, 34-3, Milano I-20133 Italy; <sup>2</sup>Université de Poitiers, Lab. de Métallurgie Physique -UMR CNRS 6630, SP2MI Téléport 2, BP 30179, Futuroscope-Chasseneuil Cedex F-86962 France; <sup>3</sup>University of Chicago, Enrico Fermi Institute, 5514, S. Ellis Ave., Chicago, IL 60637 USA

Among the methods to prepare nanoscale superhard composite coatings the combination of a hard nitride phase (TiN) with a soft metallic phase (Cu) improves coating toughness, while retaining its high hardness. A critical role to obtain a multilayer film with excellent properties is played by the sharpness of its interfaces. Multilayered TiN(1.5-9.1 nm)/Cu(3.4-11.9 nm) superlattices were deposited by dual ion beam sputtering. Previous low-angle XRD and High Resolution TEM showed the presence of several interface defects that could destroy superlattice periodicity. Here Focused Ion Beam - Secondary Ions Mass Spectrometry measurements were performed to study the sharpness and the degree of element intermixing at interfaces as well

as the interface symmetry/asymmetry, with a vertical resolution of few nanometers and 50 nm lateral resolution. The obtained results are critically discussed.

# The Didier de Fontaine Symposium on the Thermodynamics of Alloys: Joint Session with Computational Thermodynamics and Phase Transformations II

Sponsored by: Materials Processing and Manufacturing Division, MPMD-Computational Materials Science & Engineering-(Jt. ASM-MSCTS)

*Program Organizers:* Diana Farkas, Virginia Polytechnic Institute and State University, Department of Materials Science and Engineering, Blacksburg, VA 24061 USA; Mark D. Asta, Northwestern University, Department of Materials Science and Engineering, Evanston, IL 60208-3108 USA; Gerbrand Ceder, Massachusetts Institute of Technology, Department of Materials Science and Engineering, Cambridge, MA 02139 USA; Christopher Mark Wolverton, Ford Motor Company, Scientific Research Laboratory, Dearborn, MI 48121-2053 USA

Wednesday PM	Room: 2	216B
March 17, 2004	Location:	Charlotte Convention Center

Session Chair: TBA

#### 2:00 PM Invited

Modern Computational Materials Science: The Problem of Alloy Phase Stability in Complex Materials: A. J. Freeman<sup>1</sup>; <sup>1</sup>Northwestern University, Dept. of Physics & Astron., 2145 Sheridan Rd., Tech F-269, Evanson, IL 60208 USA

This talk, dedicated to Didier de Fontaine, reviews developments in computational electronic structure theory which have led to the present state of the art determination of alloy phase stability in complex systems, including multi-component aluminide intermetallics made up of transition and rare-earth metals, the prediction of new phases with ternary additions in bulk and at surfaces and interfaces, the dependence of structural phase stability on magnetism, etc. The special problems of treating rare-earth 4f electrons in multi-component intermetallics will be discussed. Illustrative examples will be given on our studies of aerospace materials obtained with our highly precise full-potential first-priniciples methods, which are now capable of treating complex structures with a large number of atoms/cell and to calculate their structural, electronic, magnetic, optical and, more recently, mechanical properties. Currently, the objective of our research is to determine the microscopic mechanisms governing the deformation and fracture behavior of ordered intermetallic aerospace alloys in order to contribute to the development of a fundamental basis for computer-aided alloys design. The most important and challenging goal of our research is to bridge the gap between a microscopic quantum-mechanical description of the chemical bonding and the mesoscopic phenomena which govern the mechanical response of intermetallics. A key feature of the work is our use of a combined approach, which includes firstprinciples calculations of cleavage/shear energetics and analysis of the dislocation structure within the generalized 2D Peierls-Nabarro model with ab-initio parameterization of the restoring forces. This approach was applied to studies of (1) homogeneous intermetallic alloys with emphasis on the role of structural stability on the mechanical properties and the yield stress temperature anomaly, and (2) heterogeneous intermetallic systems, including investigations of eutectic composites and the temperature dependence of the lattice misfit in gamma/gamma superalloys. Work supported by the AFOSR, performed in collaboration with Yu. N. Gornostyrev, O. Yu. Kontsevoi, and N.I. Medvedeva.

#### 2:30 PM Invited

Ab Initio Alloy Thermodynamics: Recent Progress and Future Directions: Axel van de Walle<sup>1</sup>; Mark D. Asta<sup>1</sup>; Gerd Ceder<sup>2</sup>; Christopher Woodward<sup>3</sup>; <sup>1</sup>Northwestern University, Matls. Sci. & Engrg., 2225 N. Campus Dr., Evanston, IL 60208-3108 USA; <sup>2</sup>Massachusetts Institute of Technology, Matls. Sci. & Engrg., Rm. 13-5056, 77 Mass. Ave., Cambridge, MA 02139 USA; <sup>3</sup>Air Force Research Laboratory, Wright-Patterson AFB, OH 45433 USA

Ab initio calculations of the thermodynamic properties of alloys have traditionally suffered from two main shortcomings. First, properly accounting for nonconfigurational sources of entropy is a challenging task. Second, commercial alloys typically consist of numerous components, while first-principles calculations of the properties of multicomponent alloys have rarely been undertaken. Although the paucity of first-principles phase diagrams calculations of multicomponent systems including nonconfigurational entropy contributions has often been attributed to their heavy computational requirements, we show that the development of automated computational tools goes a long way towards making such task practically feasible. We describe recent progress in the development of a software package, the Alloy Theoretic Automated Toolkit (ATAT), which substantially simplifies the tasks necessary for the calculations of thermodynamic properties from first-principles. Examples of applications to the Ti-Al and Ni-Al binary systems as well as multicomponent systems are presented. The calculated properties go beyond the ones typically included in thermodynamic databases. Thanks to the atomistic nature of the calculations, the properties of coherent interfaces as well as short-range order parameters can also be obtained from the same underlying formalism.

#### 3:00 PM

Experimental and Theoretical Evidence for Carbon-Vacancy Binding in Austenite: *Ronald Gibala*<sup>1</sup>; Christopher Wolverton<sup>2</sup>; <sup>1</sup>University of Michigan, Dept. of Matls. Sci. & Engrg., 2300 Hayward, 2026 H.H. Dow Bldg., Ann Arbor, MI 48109-2136 USA; <sup>2</sup>Ford Motor Company, Scientific Rsch. Lab., Dearborn, MI 48121-2053 USA

We have examined several sources of experimental data on facecentered cubic iron-carbon alloys and carbon-containing austenitic alloys which imply that the binding energy between interstitial carbon solutes and vacancies is large, of the order 40-60 kJ/mol, and that vacancies are the more mobile of the point defects. The experimental data include point-defect anelasticity, self diffusion, high-temperature steady-state creep deformation, strain aging and strain-age hardening, and radiation damage. As a complement to these data, we have performed first-principles gradient-corrected density functional calculations to determine directly the binding energy of nearest-neighbor carbon-vacancy pairs. A value of 36 kJ/mol is obtained, and the calculations suggest additional but more modest binding ones for metastable carbides in the iron-carbon system, have been made and will be reported.

#### 3:20 PM

Driving Force for Nanometer-Scale Composition Modulation in Fe-Ag/Mo(110) Alloy Films: Bo Yang<sup>1</sup>; Mark D. Asta<sup>1</sup>; Vidvuds Ozolins<sup>2</sup>; <sup>1</sup>Northwestern University, Dept. of Matls. Sci. & Engrg., 2225 N. Campus Dr., Evanston, IL 60208 USA; <sup>2</sup>University of California, Dept. of Matls. Sci. & Engrg., Los Angeles, CA USA

Compositionally-modulated structures in two-dimensional Fe-Ag/ Mo(110) alloys are studied by first-principles within a recently developed hybrid continuum/atomistic model for the elastic energy (V. Ozolins, M. Asta and J. J. Hoyt, Phys. Rev. Lett. 88, 096101 (2002)). The experimentally observed composition-modulation peridocities of ~2 nm can be understood as arising from a competition between "chemical" contributions to the alloy mixing energy, favoring phase separation, and elastic energy which favors ordering. Monte-Carlo simulations predict that Fe-Ag/Mo(110) stripe structures are thermally stable to disordering up to relatively high temperatures of ~900 K. Simulations are employed to examine the regions of stability of higher-order structures found in a zero-temperature phase diagram featuring a "devil's staircase" of striped phases. We highlight the numerous ways in which our work has been influenced by Prof. de Fontaine's seminal contributions to the theory of size-mismatched alloys and long-period superstructures.

## 3:40 PM Break

#### 3:50 PM Invited

Structure and Dynamics of Light Metal Hydrides: Vidvuds Ozolins<sup>1</sup>; Eric H. Majzoub<sup>2</sup>; David R. Tallant<sup>3</sup>; <sup>1</sup>University of California, Dept. of Matls. Sci. & Engrg., PO Box 951595, BH 6532F, Los Angeles, CA 90095-1595 USA; <sup>2</sup>Sandia National Laboratories, Matls. Chmst., PO Box 969, Livermore, CA 94551-0969 USA; <sup>3</sup>Sandia National Laboratories, PO Box 5800, MS 1411, Albuquerque, NM 87185 USA

Light metal hydrogen compounds represent an interesting new paradigm for reversible hydrogen storage. The recent surge in research has been motivated by the discovery that doping with small amounts of Ti makes enhances the kinetics of hydrogen adsorption and desorption reactions by many orders of magnitude. However, the role that Ti plays in accelerating these processes is poorly understood. We will report on combined first-principles and experimental studies of the structural, dynamical and thermodynamical properties of sodium alanates. Results on the physical properties of stable ordered compounds, lattice defects, hydrogen dynamics, and energetics of Ti substitution sites in bulk alanates will be presented.

#### 4:20 PM Invited

Phase Stability and Instability in Bulk Metallic Glass Forming Systems: Don Nicholson<sup>1</sup>; Miguel Fuentes-Cabrera<sup>1</sup>; Mike Widom<sup>2</sup>; Yang Wang<sup>2</sup>; Marek Mihalkovic<sup>3</sup>; 'Oak Ridge National Laboratory, One Bethel Valley Rd., Oak Ridge, TN 37831 USA; <sup>2</sup>Carnegie Mellon University, PA USA; <sup>3</sup>Slovakia Academy of Sciences, Inst. of Physics

Results of first principles calculations of the energy of compounds, alloys, liquids, and amorphous alloys in glass forming composition ranges are presented. Density functional calculations of the diffusion in the liquid state are compared to embedded atom calculations (EAM). The EAM, which was fit exclusively to first principles results, reproduces well the liquid diffusion and was used to calculate diffusion during quenching of liquids. Chemical, magnetic, and topological contributions to glass formability are discussed. Work supported by DARPA/ONR Grant N00014-01-10961 and DOE Office of Basic Energy Science under subcontract DEAC05-000R22R725464 with UT-Battelle, LLC.

#### 4:50 PM

Impurities Block the Alpha to Omega Martensitic Transformation in Titanium: Dallas R. Trinkle<sup>1</sup>; Richard G. Hennig<sup>1</sup>; Johann Bouchet<sup>2</sup>; Srivilliputhur G. Srinivasan<sup>2</sup>; Robert C. Albers<sup>2</sup>; John W. Wilkins<sup>1</sup>; <sup>1</sup>Ohio State University, Physics, 174 W. 18th Ave., Columbus, OH 43210 USA; <sup>2</sup>Los Alamos National Laboratory, Los Alamos, NM 87544 USA

The pressure driven martensitic phase transition from alpha to omega Ti has not been found in commercial A-70 Ti and Ti-6Al-4V alloys at pressures up to 35 GPa. It is believed to be retarded by O impurities in A-70 Ti and by Al in Ti-6Al-4V alloys. Ab initio calculations determine the energies and sites of interstitial (O, N, C), substitutional impurities (Al, V), and self-defects. Interstitial impurities are preferably located in the octahedral sites of both phases over the hexahedral sites. Nudged elastic band calculations reveal the influence of the impurities on the transition barrier. The octahedral site in alpha transforms into the octahedral or hexahedral sites in omega on a two to one basis. We predict that impurities in A-70 Ti and Ti-6Al-4V shift the omega phase energy relative to alpha, and increase the energy barriers, thus retarding the alpha to omega transition.

#### 5:10 PM

Atomistic and Microstructural Ordering Processes Studied by Hybridized Calculation of Phase Field and Cluster Variation Methods: *Munekazu Ohno*<sup>1</sup>; Tetsuo Mohri<sup>1</sup>; <sup>1</sup>Hokkaido University, Grad. Sch. of Engrg., Div. of Matls. Sci. & Engrg., Kita-13 Nishi-8, Kita-ku, Sapporo 060-8628 Japan

In order to describe the atomistic and the microstructural ordering processes simultaneously, we attempt hybridized calculations of the Phase Field Method (PFM) and the Cluster Variation Method (CVM). The non-uniform chemical free energy in the PFM is obtained based on the atomistic free energy formulated by the CVM. The gradient energy coefficient which determines the spatial scale and controls the anisotropic effects of the interfacial energy is determined within the CVM. Our particular focus is placed on the L10 ordered system. The one-dimensional calculation shows that the anti-phase boundary is necessarily anisotropic in the L10 system when only the neareset neighbor pair interaction is considered. Two-dimensional calculation.

#### 5:30 PM

Shock-Induced Melting and Resolidification of Cu and Si: A Molecular-Dynamics Study: Babak Sadigh<sup>1</sup>; George Gilmer<sup>1</sup>; Jeffrey Colvin<sup>1</sup>; Bryan Reed<sup>1</sup>; Mukul Kumar<sup>1</sup>; <sup>1</sup>Lawrence Livermore National Laboratory, Chmst. & Matls. Sci., 7000 E. Ave., L-353, Livermore, CA 94550 USA

We present a comprehensive study of shock-induced melting and resolidification of Cu and Si, using large-scale molecular-dynamics simulations with supercells containing up to a million atoms. We calculate the nucleation rate of voids upon release of the shock wave and evolution of rarefaction waves. We further study the kinetics of melting/ resolidification by analyzing in detail the motion of solid/liquid interfaces in atomistic systems when the two phases coexist. We study the role of the pressure waves in driving the phase transformation by analyzing the evolution of local stress and temperature in the interfacial regions. Using information from solid-liquid interfacial free energy calculations, we attempt to parametrize a macroscopic phasefield model that can predict the microstructural evolution of shockmelted and resolidified Cu and Si. This work was performed under the auspices of the US Dept. of Energy by University of California Lawrence Livermore National Laboratory under contract No. W-7405-Eng-48.

# The Role of Grain Boundaries in Material Design: Grain Boundary Segregation, Diffusion, Damage

Sponsored by: Materials Processing and Manufacturing Division, ASM/MSCTS-Texture & Anisotropy Committee, MPMD-Computational Materials Science & Engineering-(Jt. ASM-MSCTS) *Program Organizers:* Brent L. Adams, Brigham Young University, Department of Mechanical Engineering, Provo, UT 84602-0001 USA; Thomas R. Bieler, Michigan State University, Department of Chemical Engineering and Materials Science, East Lansing, MI 48824-1226 USA

Wednesday PM	Room: 218A
March 17, 2004	Location: Charlotte Convention Center

Session Chairs: Thomas R. Bieler, Michigan State University, Dept. of Chem. Engrg. Matls. Sci., E. Lansing, MI 48824-1226 USA; David Field, Washington State University, Mech. & Matls. Engrg., Pullman, WA 99164-2920 USA

#### 2:00 PM Invited

Twin Boundary Formation in Thin Copper Films: David P. Field<sup>1</sup>; <sup>1</sup>Washington State University, Mech. & Matls. Engrg., Box 642920, Pullman, WA 99164-2920 USA

In many applications, grain boundary design is aimed at increasing the fraction of special boundaries to improve material properties. In FCC metals, this process typically involves processing techniques that maximize the fraction of twin boundaries in the material. As with bulk materials, thin film microstructures depend upon details of the film processing. For damascene processing of lines the bath chemistry, barrier layer materials and thicknesses, seed layer, line height to width ratio, and annealing temperature and time all play a role in the developing microstructure. This study shows the effects of various processes on grain size and twin boundary fraction. The fraction of twin boundaries is maximized for a particular bath chemistry and annealing temperature by imposing a given line height to width ratio which controls the stress state during annealing.

#### 2:25 PM

Microstructural Engineering of Copper Shaped-Charge Liners: Kerri J.M. Blobaum<sup>1</sup>; James S. Stölken<sup>2</sup>; Mukul Kumar<sup>3</sup>; <sup>1</sup>Lawrence Livermore National Laboratory, Chmst. & Matls. Sci., L-370, 7000 East Ave., Livermore, CA 94550-9234 USA; <sup>2</sup>Lawrence Livermore National Laboratory, Mech. Eng., L-129, 7000 East Ave., Livermore, CA 94550-9234 USA; <sup>3</sup>Lawrence Livermore National Laboratory, Chmst. & Matls. Sci., L-356, 7000 East Ave., Livermore, CA 94550-9234 USA

Using a combination of experiments and modeling, we are developing methods for engineering the microstructure of copper shapedcharge liner cones to improve their performance. It is known that factors such as grain size and morphology, texture, and grain boundary character influence the liner jet break-up time, but their coupled effects are not well understood, particularly at the strain rates experienced by the high explosive-driven liners. The deformation experienced during the expansion of the shaped-charge liner jet is akin to superplastic forming, where the strain rate sensitivity and strain hardening characteristics greatly influence the uniform stretching of the material by delaying the onset of plastic instability. Similarly, it is hoped that increasing the fraction of special boundaries decreases the total interfacial area for void nucleation in the microstructure. Here, we describe a systematic study of the effects of engineered microstructures on mechanical properties. Using finite element analysis, a multistep back-extrusion/annealing process was developed for forming the liners. This process enabled grain boundary engineering of the final microstructure. Results from mechanical testing of these samples, as well as conventionally processed liners, at a range of strain rates and temperatures will be presented. This systematic investigation of the constitutive response of the grain boundary engineered microstructures will be discussed in the context of the performance of shapedcharge liners. This work was performed under the auspices of the U.S. Department of Energy by University of California, Lawrence Livermore National Laboratory under contract No. W-7405-Eng-48.

#### 2:45 PM

The Effect of Grain Boundary Misorientation, Inclination, Crystal Orientation, and Stress State on Microcrack Initiation in Duplex TiAl Grain Boundaries: Alireza Fallahi<sup>1</sup>; Kris Boyapati<sup>1</sup>; *Thomas R. Bieler*<sup>1</sup>; Martin A. Crimp<sup>1</sup>; Amir Zamiri<sup>2</sup>; Farhang Pourboghrat<sup>2</sup>; Darren E. Mason<sup>3</sup>; <sup>1</sup>Michigan State University, Chem. Engrg. Matl. Sci., 2527 Engrg. Bldg., E. Lansing, MI 48824 USA; <sup>2</sup>Michigan State University, Mech. Engrg., E. Lansing, MI 48824 USA; <sup>3</sup>Albion College, Dept. of Math. & Compu. Sci., Albion, MI USA

Prior investigations on microcrack initiation and slip transfer in duplex TiAl by Simkin et al. (Scripta Mater. vol. 49, 149-154, 2003) showed that microcracks nucleate primarily in g-g grain boundaries. Simkin developed a fracture initiation parameter based upon the external stress state, available slip and twinning systems, crystal orientations, and Schmid factors that was able to predict the propensity of a boundary to nucleate microcracks arising from twin interactions with a grain boundary. This parameter did not fully consider the effects of grain boundary inclination with respect to the stress state, nor the effects of local elastic anisotropy on the stress state in the boundary. Serial sectioning on Simkin's specimen has been done to determine grain boundary inclinations. FEM analysis of local microstructure regions that incorporate crystal orientations coupled with tensorial descriptions of elastic stiffness are used to estimate the local stress tensor in the boundary regions. The effect of this additional detailed information on the fracture initiation parameter values and their variability are analyzed and discussed, to determine if a physically based deterministic threshold for microcrack initiation can be identified. Supported by AFRL NO. F49620-01-1-0116 (Craig Hartley).

#### 3:05 PM Break

#### 3:25 PM Cancelled

Impact of Grain Boundary Character on Grain Boundary Dynamics 3-50 PM

Accurate Quantification of Local Boundary Excess by STEM X-Ray Mapping: David B. Williams<sup>1</sup>; Masashi Watanabe<sup>1</sup>; Chunfei Li<sup>2</sup>; <sup>1</sup>Lehigh University, Dept. of Matls. Sci. & Engrg., 5 E. Packer Ave., Bethlehem, PA 18015 USA; <sup>2</sup>Portland State University, Dept. of Physics, 1719 SW 10th Ave., Portland, OR 97201 USA

X-ray mapping in a scanning transmission electron microscope is one of the most useful approaches to characterize boundary segregation with high (nanometer-level) spatial resolution. However, the quantified segregant composition is not always reliable, because the measurement is influenced by the specimen thickness, boundary inclination and other experimental conditions. The boundary excess coverage, which is less sensitive to the specimen and experimental conditions, is a better measure of segregation, but requires knowledge of the specimen thickness. In this study, the local thickness was determined via the ?ê-factor method, which simultaneously provides specimen composition and thickness at the analysis point, using X-ray mapping, and hence the boundary excess is determined locally. In addition, by applying an orientation imaging technique in a transmission electron microscope, the measured values of the local boundary excess can be linked to the crystallographic misorientation across the boundary, thus permitting unique structure-chemistry-property correlations.

#### 4:10 PM

Coalescence of Two Particles with Different Sizes by Surface Diffusion: Joachim H. Schneibel<sup>1</sup>; Pavlo Sachenko<sup>1</sup>; Wen Zhang<sup>2</sup>; <sup>1</sup>Oak Ridge National Laboratory, Metals & Ceram. Div., PO Box 2008, Oak Ridge, TN 37831 USA; <sup>2</sup>Oakland University, Dept. of Math. & Stats., Rochester, MI 48309 USA

Focused ion beam milling was used to drill through polycrystalline 10 mm thick copper foil to machine disc-shaped particles with different sizes that were bonded to each other by a short grain boundary segment, i.e., they formed a neck. During subsequent annealing, sintering of the two particles, i.e., neck growth, was observed. Modeling of the sintering assuming only surface diffusion was in good agreement with the shape evolution observed during annealing. However, once the discs attained a shape close to equilibrium, the numerical computation had difficulty in proceeding further. It will be shown that two particles with different sizes exhibiting only surface diffusion cannot reach equilibrium, and this is the reason why the computation could not proceed. This work was sponsored by the National Science Foundation under grant DMR-9996087, and by the Division of Materials Sciences and Engineering, U.S. Department of Energy, under Contract DE-AC05-000R22725 with UT-Battelle, LLC.

#### 4:30 PM

Effects of Diffusion Induced Recrystallization on Cu-Ni Interdiffusion: Stephen M. Schwarz<sup>2</sup>; Brian W. Kempshall<sup>2</sup>; *Lucille A. Giannuzzi*<sup>1</sup>; <sup>1</sup>FEI Company, One Corp. Way, Peabody, MA 01960-7990 USA; <sup>2</sup>Nanospective Inc., 12565 Rsch. Pkwy., Ste. 300, Orlando, FL 32826 USA

The interdiffusion of epitaxially electrodeposited Ni on single crystal Cu has been studied. Diffusion induced recrystallization (DIR) was observed to occur at the original Cu-Ni interface after diffusion annealing at temperatures between 500 to 650°C for 120 to 200 hours. FIB/TEM techniques were used to compare interdiffusion regions that exhibited DIR versus regions that did exhibit DIR. The DIR regions showed an increase in diffusion lengths and diffusivity by orders of magnitude compared to the non-DIR regions. Diffusivity values obtained for the non-DIR regions from this study are the lowest values for the Cu(Ni) system compared to known literature values, implying that previous values may contain grain boundary contributions. This work was made possible through the support of NSF DMR Award #9703281.

#### 4:50 PM

On the Role of Grain Boundaries in Determining the Rate Process of Deformation of Materials at High Temperatures: D. H. Sastry<sup>1</sup>; <sup>1</sup>Indian Institute of Science, Dept. of Metall., Bangalore 560012 India

At temperatures greater than 0.5 on the homologous temperature scale, the deformation of materials is believed to be controlled by a lattice duffusion mechanism. However, in polycrystals, grain boundaries also play an important role and processes such as grain boundary sliding become dominant. In some cases the rate of grain boundary sliding could be the strain rate (creep rate) controlling step. To understand the exact behavior of grain boundaries, studies on single crystal must be compared with those on polycrystal material. This approach is often laborious. Fortunately, by utilising the 'impression creep' technique, polycrystalline material can be used to understand the deformation behavior of the single crystal also i.e., investigation with as well as without grain boundary influence can be carried out on the same material. The present study describes the results of impression creep testing on some metals at high temperatures. Thermal activation parameters such as activation energy and activation area are evaluated when the interior of grain only is deforming and a comparison is made with those obtained when the grain boundaries are also involved in the creep deformation. The results indicate that, under the experimental conditions employed, grain boundary sliding is not the rate controlling step in high temperature creep of the selected polycrystalline materials. However, it is established that the impression creep technique, applied to polycrystal samples of small size, is capable of giving information on single crystal as well as polycrystal deformation behavior.

# Third International Symposium on Ultrafine Grained Materials: Superplasticity, Creep & Thermal Stability

Sponsored by: Materials Processing & Manufacturing Division, MPMD-Shaping and Forming Committee
Program Organizers: Yuntian Ted Zhu, Los Alamos National Laboratory, Materials Science and Technology Division, Los
Alamos, NM 87545 USA; Terence G. Langdon, University of
Southern California, Departments of Aerospace & Mechanical
Engineering and Materials Engineering, Los Angeles, CA 90089-1453 USA; Terry C. Lowe, Metallicum, Santa Fe, NM 87501 USA;
S. Lee Semiatin, Air Force Research Laboratory, Materials & Manufacturing Directorate, Wright Patterson AFB, OH 45433 USA;
Dong H. Shin, Hanyang University, Department of Metallurgy and
Material Science, Ansan, Kyunggi-Do 425-791 Korea; Ruslan Z.
Valiev, Institute of Physics of Advanced Material, Ufa State Aviation Technology University, Ufa 450000 Russia

Wednesday PM	Room: 2	07A	
March 17, 2004	Location:	Charlotte Convention Cente	r

Session Chairs: Terence G. Langdon, University of Southern California, Aeros. & Mech. Engrg. & Matls. Sci., Los Angeles, CA 90089-1453 USA; Amiya K. Mukherjee, University of California, Chem. Engrg. & Matls. Sci., Davis, CA 95616 USA; Sergey V. Dobatkin, Baikov Institute of Metallurgy & Materials Science, Moscow 119991 Russia

#### 2:00 PM Invited

**Superplasticty in Nanocrystalline Materials**: *Amiya K. Mukherjee*<sup>1</sup>; Nathan A. Mara<sup>1</sup>; Alla V. Sergueeva<sup>1</sup>; <sup>1</sup>University of California, Chem. Engrg. & Matls. Sci., One Shields Ave., Davis, CA 95616 USA

High strain rate and/or low temperature superplasticity was observed in 1420 aluminum alloy and in Ni<sub>3</sub>Al. The enhanced plasticity demonstrated in these materials is attributed to a refinement in grain size to the nano or near-nano range through the use of High Pressure Torsion (HPT). Grain sizes after HPT were approximately 100 nm for the 1420 aluminum alloy, and 50 nm for Ni<sub>3</sub>Al. Tensile testing was carried out at strain rates up to  $10^{-1}$  and temperatures up to  $725^{\circ}$ C. Tensile curves typically exhibit high flow stresses and a degree of strain hardening that cannot be adequately described by conventional recovery mechanisms such as grain growth. Room-temperature TEM in-situ straining experiments reveal little dislocation activity and no evidence of dislocation pile-ups. It is suggested that the dominant deformation mechanism for elevated temperature plasticity in this study is grain boundary sliding and rotation. (NSF-DMR-0240144).

#### 2:20 PM

High Strain Rate Superplasticity in a Spray-Cast Aluminum Alloy Processed by Equal-Channel Angular Pressing: *Cheng* Xu<sup>1</sup>; Terence G. Langdon<sup>1</sup>; <sup>1</sup>University of Southern California, Depts. of Aeros. & Mech. Engrg. & Matls. Sci., Los Angeles, CA 90089-1453 USA

A spray-cast aluminum 7034 alloy, containing 11.5% Zn, 2.5% Mg, 0.9% Cu and 0.20% Zr, was processed by Equal-Channel Angular Pressing (ECAP) at 473 K to produce an ultrafine grain size of ~0.3  $\mu$ m. The mechanical properties of the alloy were investigated using tensile testing at high temperatures over a range of strain rates. The results show that the as-pressed alloy yielded superplastic elongations of >1000% when testing at a temperature of 673 K with strain rates at and above ~10<sup>-2</sup> s<sup>-1</sup>. The strain rate sensitivity was measured as ~0.33, thereby suggesting that dislocation glide may be an important deformation mechanism.

#### 2:35 PM

Structure Formation During High Pressure Torsion and Heating of Low-Carbon Steels With Different Initial States: Sergey Vladimir Dobatkin<sup>1</sup>; Nikolay Alexander Krasilnikov<sup>2</sup>; Kazimir Iosiph Yanushkevich<sup>3</sup>; <sup>1</sup>Russian Academy of Science, Baikov Inst. of Metall. & Matl. Sci., Dept. of Phys.-Mech. Problems of Bulk Nanomatls., Leninky prospekt 49, Moscow 119991 Russia; <sup>2</sup>Ufa State Aviation Technical University, ul. K. Marksa, 12, Ufa 450000 Russia; <sup>3</sup>Institute of Solid State and Semiconductor Physics of the National Academy of Sciences of Belarus, Lab. of Physics of Magnetic Matls., P. Brovki str, Minsk 220072 Belarus

The present work was aimed to study the formation of UFG- ( d < 100 nm) and submicrocrystalline (SMC) structure (100 nm < d < 1000 nm) in 0.12%C-0.85%Mn-0.65%Si and 0.1%C-1.12%Mn-0.08%V-0.07%Ti low carbon steels during severe cold and warm deformation in torsion under high pressure (HPT) and subsequent heating. Steels were either hot rolled or quenched prior to torsion. SPD of these steels at room temperature results in the emerging of nanoscale structure comprised of oriented cell-like fragments and fine grains. SPD of the initially quenched steels leads to a more dispersed nanoscale structure than that of initially hot rolled steels. Changing of microhardness, electrical resistance and structure during heating of SPD steels was studied. Heating on 500°C results in SMC structure with the grain size 300-500 nm.

#### 2:50 PM

High Temperature Deformation Behavior of Ultra-Fine Grained Ti-6Al-4V Alloy: J. H. Kim<sup>1</sup>; Y. G. Ko<sup>1</sup>; S. Y. Han<sup>2</sup>; C. S. Lee<sup>1</sup>; D. H. Shin<sup>2</sup>; S. L. Semiatin<sup>3</sup>; <sup>1</sup>Pohang University Science and Technology, Dept. of Matls. Sci. & Engrg., San 31, Hyoja-dong, Namgu, Pohang, Gyeong-buk 790-784 S. Korea; <sup>2</sup>Hanyang University, Dept. of Metall. & Matls. Sci., Ansan, Gyeong-gi 425-791 S. Korea; <sup>3</sup>Wright-Patterson Air Force Base, AFRL, Wright-Patterson AFB, OH 45433-7817 USA

In this study, high temperature deformation behavior of ultra-fine grained Ti-6Al-4V alloy has been investigated on the basis of the inelastic deformation theory which consists of grain matrix deformation and grain boundary sliding. Microstructure of coarse equiaxed grains (~11 micrometer in diameter) has been significantly refined to 0.3 micrometer with high angle boundaries after 4 times of isothermal equal channel angular (ECA) pressing at 873K. Load relaxation test has been performed at the temperature range of 773K~973K to enlighten the deformation mechanisms operating at specific temperatures and to find optimum superplastic deformation conditions for ultra-fine grained microstructures. Also, main efforts have been devoted to analyze quantitatively the relative amount of each deformation mode, i.e., dislocation glide, dislocation climb and grain boundary sliding operating at specific temperatures. Tensile test of ultra-fine grained specimens has also been carried out to verify the optimum superplastic conditions.

### 3:05 PM

The Mechanical Properties and Microstructure of Equal Channel Angular Pressed Al-Cu-Mg Alloy Fabricated by Spray Deposition: Kyung H. Chung<sup>1</sup>; Dong H. Shin<sup>2</sup>; Enrique J. Lavernia<sup>1</sup>; <sup>1</sup>University of California, Chem. Engrg. & Matls. Sci., One Shields Ave., Davis, CA 95616 USA; <sup>2</sup>Hanyang University, Metall. & Matls. Engrg., Ansan, Kyunggi-do 425-791 Korea

The porous spray deposited Al-4.4Cu-0.8Mg alloy was equal channel angular pressed (ECAPed) to produce fine-grained bulk material without the limitation over cross-sectional dimensions. The ECAP of the spray deposited Al-Cu-Mg alloy is successfully performed at 200°C. After a single pass, the density becomes full and the remaining pore size is reduced to less than 3µm from about 20µm. With repeated ECAP passes, the microstructure becomes more equiaxial and homogeneous. The grain size reduces to the  $100 \sim 250$  nm range after four passes. After ECAP, the room temperature strength is increased up to 110%, and that is attributed to the reduced amount of pore, the increased dislocation density and the reduced grain size. Additionally, the static heat treatments were applied at the spray deposited and ECAPed Al-Cu-Mg alloy. The gging condition will be optimized and the microstructural characteristics will be investigated with focusing on the precipitation behavior. The grain stability also will be examined during the aging process and the relationship between the microstructural features and mechanical properties will be extensively investigated.

#### 3:20 PM

Grain Refinement Mechanisms with Large-Strain Deformation of Zirconium: *M. E. Kassner*<sup>1</sup>; S. A. Barrabes<sup>1</sup>; M.-T. Perez-Prado<sup>2</sup>; <sup>1</sup>University of California, Mech. & Aeros. Engrg., 9500 Gilman Dr., EBU II, La Jolla, CA 92093-0411 USA; <sup>2</sup>CENIM-CSIC, Madrid Spain

Large strain deformation of pure zirconium at elevated temperature in both tension and torsion was studied. POM, TEM and EBSP reveal substantial grain refinement with large strain deformation. The purpose of this work was to address the dynamic restoration and grainrefinement mechanisms in pure \_lpha-zirconium deformed to large strains at 600-800°C. The restoration mechanisms examined included dynamic recovery, grain growth, and various dynamic recrystallization mechanisms. Specifically, the presence of dynamic recrystallization during high temperature mechanical testing (400°C to 750°C) was assessed. This analysis also assisted with the interpretation of the activation energies for creep-plasticity.

#### 3:35 PM

**Grain Growth Inhibition in Nanocrystalline Al-Sc Alloys:** N. Burhan<sup>1</sup>; *M. Ferry*<sup>1</sup>; <sup>1</sup>University of New South Wales, Sch. of Matls. Sci. & Engrg., Sydney, NSW 2052 Australia

An ultrafine-grained microstructure in a range of Al-Sc alloys was produced by Equal Channel Angular Extrusion (ECAE). The alloys were solution treated prior to deformation, deformed by ECAE then aged at low temperature to produce a sub-micron grained microstructure with a high fraction of high angle grain boundaries (HAGB) decorated with nanosized Al<sub>3</sub>Sc particles. General grain stability and particle/grain boundary interactions were studied using electron backscatter diffraction (EBSD) in the scanning electron microscope and transmission electron microscopy. The fine-grained microstructures were found to be highly stable during annealing at elevated temperatures due to Zener pinning from the fine Al<sub>3</sub>Sc particles. The volume fraction and size of fine particles and their rate of coarsening were found to have a strong influence on grain growth. The grain stability in this alloy system was compared with recent models of grain coarsening in particle-containing materials.

### 3:50 PM Break

#### 4:00 PM

Microstructural Evolution During Superplastic Deformation in ECA Pressed Al-Mg-Sc Alloys: *Minoru Furukawa*<sup>1</sup>; Kazuko Furuno<sup>2</sup>; Keiichiro Oh-ishi<sup>2</sup>; Zenji Horita<sup>2</sup>; Terence G. Langdon<sup>3</sup>; <sup>1</sup>Fukuoka University of Education, Dept. of Tech., 1-1, Akama-Bunkyomachi, Munakata, Fukuoka 811-4192 Japan; <sup>2</sup>Kyushu University, Dept. of Matls. Sci. & Engrg., Fukuoka 812-8581 Japan; <sup>3</sup>University of Southern California, Depts. of Aeros. & Mech. Engrg. & Matls. Sci., Los Angeles, CA 90089-1453 USA

ECAP was conducted to achieve grain refinement in Al-0.5%Mg-0.2%Sc and Al-1%Mg-0.2%Sc alloys. The ECAP was performed using dies having internal channel angles of either 60 or 90° where these angles produce equivalent strains of 1.6 and 1.1 for each pass, respectively. Tensile testing at 673K of both alloys showed the elongations to failure increase with increasing equivalent strain. When pressing the Al-0.5%Mg-0.2%Sc and Al-1%Mg-0.2%Sc alloys for 6 passes using a 60° die, the elongations to failure were 340% and 800% at 673K, respectively. Observations using EBSP revealed that, in the as-pressed condition, both alloys had textures and a high fraction of low-angle boundaries. Whereas the texture and a high fraction of low-angle boundaries remained after failure at 340% in the Al-0.5%Mg-0.2%Sc alloy, the texture was removed and there was a large fraction of high-angle boundaries after failure at 800% in the Al-1%Mg-0.2%Sc alloy.

#### 4:15 PM

Neutron Diffraction Study of Super-Plastic Al-Alloy Processed by ECAP: Sven C. Vogel<sup>1</sup>; David J. Alexander<sup>2</sup>; Irene J. Beyerlein<sup>3</sup>; Mark A.M. Bourke<sup>1</sup>; Donald W. Brown<sup>1</sup>; Bjorn Clausen<sup>1</sup>; Saiyi Li<sup>1</sup>; <sup>1</sup>Los Alamos National Laboratory, Los Alamos, NM 87545 USA; <sup>2</sup>Los Alamos National Laboratory, MST-6, MS G770, Los Alamos, NM 87545 USA; <sup>3</sup>Los Alamos National Laboratory, T-3, MS B216, Los Alamos, NM 87545 USA

The use of severe plastic deformation techniques such as equal channel angular pressing, (ECAP) has been shown to refine metal microstructures giving advantageous mechanical properties. In this presentation, we will report results of in-situ neutron diffraction loading measurements on the neutron spectrometer SMARTS at LANSCE performed on an Al-Mg-Sc alloy processed by ECAP. This material was reported to exhibit super-plasticity when deformed in tension at elevated temperatures. In-situ loading experiments provide, among other information, crystal lattice-plane dependent stress-strain curves allowing to understand and predict the macroscopic material performance. Using SMARTS, tensile testing at elevated temperatures is possible simultaneously with the neutron diffraction, providing unique insights into the deformation behavior of the probed material. This experiment is the first application of this technique to a material exhibiting super-plasticity. We will report results from tensile tests of pure Al as a reference material and the Al-Mg-Sc alloy both at roomtemperature and at temperatures for which the alloy was reported to exhibit super-plasticity.

#### 4:30 PM

Influence of Processing Route on Creep of Ultrafine Grained Aluminium Prepared by ECAP: Vaclav Sklenicka<sup>1</sup>; <sup>1</sup>Academy of Sciences of the Czech Republic, Inst. of Physics of Matls., Zizkova 22, Brno CZ-616 62 Czech Republic

Extremely coarse-grained high-purity aluminum was subjected to equal-channel angular pressing (ECAP) and one or repetitive pressing followed either route A,B or C. Creep tests were conducted at 473 K on billets after one pass and after repetitive pressing (up to 12 ECAP passes). In essence, the creep resistance of an ultrafine grained aluminum after ECAP pressing is shown to be considerably improved to an unpressed material. The minimum creep rate for the ECAP material is about one to two orders of magnitude less than that of coarse-grained material. Further, the ECAP material exhibits markedly longer creep life than unpressed material but the creep life of ECAP material decreases with increasing number of ECAP passes. It is suggested that the effect of processing route on creep behaviour may be explained by homogenization of the microstructure and microtexture of the ECAP material.

#### 4:45 PM

Indentation Behavior of Aluminum Prepared by Equal Channel Angular Extrusion: *Fuqian Yang*<sup>1</sup>; Lingling Peng<sup>1</sup>; Kenji Okazaki<sup>1</sup>; <sup>1</sup>University of Kentucky, Chem. & Matls. Engrg., 161 Anderson Hall, Lexington, KY 40506 USA

Equal channel angular extrusion (ECAE) as one of severe plastic deformation methods to produce ultra-fine structure in bulk samples and billets has become a relatively active area. The as-deformed material by the ECAE process is in a non-equilibrium state and displays unique properties, such as high hardening and superplastic behavior. The present work examines the plastic deformation of as-ECAE Al by using indentation technique. The indentation load was found to be proportional to the 3/2 power of the maximum indentation depth. The as-ECAE Al displayed different unloading behavior from the annealed Al due to the large plastic deformation introduced in the ECAE process, which suggests the change of microstructure. A relation between the plastic energy dissipated in the indentation and the indentation load was derived by using dislocation theory - the plastic energy is proportional to the 3/2 power of the indentation load, which was supported by the experimental results.

5:00 PM Award Ceremony

5:15 PM Panel Discussions

# THURSDAY

# Advanced Materials for Energy Conversion II: Thermoelectrics, Superconductors, and Piezoelectric Materials

Sponsored by: Light Metals Division, LMD-Reactive Metals Committee

*Program Organizers:* Dhanesh Chandra, University of Nevada, Metallurgical & Materials Engineering, Reno, NV 89557 USA; Renato G. Bautista, University of Nevada, Department of Chemical and Metal Engineering, Reno, NV 89557-0136 USA; Louis Schlapbach, EMPA Swiss Federal, Laboratory for Materials Testing and Research, Duebendorf CH-8600 Switzerland

Thursday AM	Room: 2	203A	
March 18, 2004	Location:	Charlotte Convention Cent	er

Session Chairs: Jeff Snyder, Jet Propulsion Laboratory-California, Thermoelect. Matls. & Devices Team, Pasadena, CA 91109-8099 USA; James L. Gole, Georgia Institute of Technology, Sch. of Physics, Atlanta, GA 30332-0430 USA; Chandra S. Pande, Naval Research Laboratory, Matls. Sci. & Tech. Div., Washington, DC 20375-5343 USA

### 8:30 AM Keynote

Advances in Thermoelectric Materials Leading to Reliable, Clean Energy Solutions: G. Jeffrey Snyder<sup>1</sup>; <sup>1</sup>Caltech/JPL, Matls. Sci., MS 277, Pasadena, CA 91109 USA

Thermoelectric generators, by converting waste heat into electricity, could be an important solution to today's energy challenges, but their applicability has been limited by the relatively low efficiencies. Solid state thermoelectric cooling devices are rapidly becoming more important for specialty applications. Advances in thermoelectric materials, design and device micro-engineering are rapidly expanding the promise of thermoelectrics. From a phenomenological and microscopic understanding of the thermoelectric effects, improved materials for thermoelectric applications can be engineered, with the ideal material having the electronic structure of a crystalline semiconductor but phonon structure of an amorphous material. The improved thermoelectric properties of many new thermoelectric materials, such as skutterudites and zinc antimonide, can be understood using this principle. Up to 20% thermal to electric conversion efficiency can be achieved by segmenting different materials over a wide temperature range. For segmented devices the compatibility factor, recently derived from the intensive formulation of efficiency, must also be considered for materials selection. Improved cooling performance can be achieved by taking advantage of the time dependence of the Peltier cooling effect or miniaturizing the cooler with MEMS technology.

#### 8:55 AM

Thermoelectric Properties of Several P- and N-Type Half-Heusler Compounds and Effects of Dopants: Yumi Hayashi<sup>1</sup>; Sung Wng Kim<sup>1</sup>; Yoshisato Kimura<sup>1</sup>; Yoshinao Mishima<sup>1</sup>; <sup>1</sup>Tokyo Institute of Technology, Matls. Sci. & Engrg., 4259 Nagatsuta, Midori-ku, Yokohama-shi, Kanagawa-ken 226-8502 Japan

Half-Heusler compounds are attractive Phonon-Glass-Electron-Crystal thermoelectric materials applicable at high temperatures. They exhibit semiconducting properties at Valence Electron Count (VEC) of nearly 18. In the present work, we categorized all the available Half-Heusler compounds by VEC and selected several candidates by preliminary experiments. For instance, n-type HfNiSn and p-type TiFeSb are interesting because of their low thermal conductivity. Additionally, HfNiSn shows excellent seebeck coefficient. Twofold concept of our material design to effectively improve the thermoelectric figure of merit is; to reduce lattice thermal conductivity by alloying heavier elements substituting constitutional elements and to enhance the power factor by doping impurities. We previously reported successful alloy design of TiNiSn by alloying Hf and doping Sb. Sample preparation was conducted using powder metallurgy in order to further reduce thermal conductivity. Thermoelectric properties were evaluated by measuring seebeck coefficient, electrical resistivity and thermal conductivity at temperatures ranging from 300 to 1000 K.

#### 9:15 AM

Thermoelectric Properties and Microstructure of p-Type Bi2Te3-Sb2Te3 Prepared by Powder Consolidation Using Equal Channel Angular Extrusion: *Jae-Taek Im*<sup>1</sup>; K. T. Hartwig<sup>1</sup>; Jeff Sharp<sup>2</sup>; <sup>1</sup>Texas A&M University, Mechl. Engrg., College Sta., TX 77840 USA; <sup>2</sup>Marlow Industries, Inc., 10451 Vista Park Rd., Dallas, TX 75238-1645 USA

Multipass Equal Channel Angular Extrusion (ECAE) was used to consolidate p-type Bi2Te3-Sb2Te3 powder prepared by milling cast material. The sieved powder was vacuum encapsulated and extruded in the temperature range of  $450 \sim 500^{\circ}$ C. The microstructure is characterized by polarized optical microscopy and SEM. The Seebeck coefficient, electrical resistivity, thermal conductivity, and the figure of merit were measured as a function of extrusion temperature and number of extrusion passes. The results are compared with thermoelectric properties and microstructure of cast and extruded material.

#### 9:35 AM

The Enhancement of High Temperature Thermoelectric Properties of TiNiSn Based Half-Heusler Compounds: Sung Wng Kim<sup>1</sup>; Yoshisato Kimura<sup>1</sup>; Yoshinao Mishima<sup>1</sup>; <sup>1</sup>Tokyo Institute of Technology, Interdisplinary Grad. Sch. of Sci. & Engrg., Dept. Matls. Sci. & Engrg., 4259 Nagatsuta Midori-ku, Yokohama, Kanagawa 226-8502 Japan

In order to develop good thermoelectric materials for high temperature thermoelectric applications, a systematic investigation has been conducted on the high temperature thermoelectric properties of TiNiSn based half-Heusler compounds. This study is focused on the optimizing the high temperature thermoelectric properties, especially, reducing the lattice thermal conductivity by fabrication of solid solution and using powder metallurgy techniques. Also, effort to enhance power factor is performed by adding several dopants on TiNiSn-based half-Heusler thermoelectric material. Owing to the reduced lattice thermal conductivity by H alloying and to increased power factor by Sb doping,  $Ti_{0.95}Hf_{0.05}NiSn_{0.99}Sb_{0.01}$  compound prepared by using powder metallurgy technique showed ZT=0.78 at 770K, the highest dimensionless figure of merit for half-Heusler compounds reported so far.

#### 9:55 AM Break

#### 10:10 AM Invited

Recent Developments in Superconducting Materials for Energy Conversion: *Khershed P. Cooper*<sup>1</sup>; Harry N. Jones<sup>1</sup>; Chandra S. Pande<sup>1</sup>; <sup>1</sup>Naval Research Laboratory, Matls. Sci. & Tech. Div., Code 6325, 4555 Overlook Ave. SW, Washington, DC 20375-5343 USA

Superconducting materials are very important for the Energy industry. The promise of superconductors is the transmission of power with no or little loss. Significant progress has been made in the development of high temperature superconductors suitable for use at liquid nitrogen temperature. However, flux pinning problems remain and need better understanding and development of techniques to minimize the adverse effects. A relatively new superconductor, MgB2, was discovered recently. While not a high temperature superconductor, it has many attractive properties such as the absence of a "weak link" effect at the grain boundaries and can operate at liquid hydrogen temperature. However, the synthesis of MgB2 is not trivial and several routes to its fabrication into wire form are being pursued and will be discussed. Many technical problems in the development of these two classes of superconductors remain. The challenges and opportunities in the use of these materials will also be discussed.

#### 10:30 AM

**Piezoelectric Thin Films for Energy Conversion in MEMS**: *D. F. Bahr*<sup>1</sup>; C. D. Richards<sup>1</sup>; R. F. Richards<sup>1</sup>; J. V. Martinez<sup>1</sup>; T. M. Sullivan<sup>1</sup>; <sup>1</sup>Washington State University, Mech. & Matls. Engrg., PO Box 642920, Pullman, WA 99164-2920 USA

Microscale power systems based on MEMS technology offer the possibility to deliver high power densities using batch manufacturing methods. MEMS are particularly attractive for developing structures which flex and bend as opposed to rotate and slide, and piezoelectric materials based on the titanate structure are a good example of how flexing thin film structures can convert mechanical to electrical energy in a small volume package. This presentation will describe the fabrication of thin film based piezoelectrics (such as PZT and a variety of doped derivative compounds) in MEMS and their application in the P3 power system, which utilizes an external combustion engine to covert thermal to mechanical to electrical work. The paper will focus on the control materials properties and their effects on the power production in a prototype device. A path to the optimization of the performance as a function of chemistry, structure, and orientation will be demonstrated. Thermal Energy Storage Investigations in Binary System of Neopentylglycol and Tris(Hydroxymethyl)Aminomethane: Wen-Ming Chien<sup>1</sup>; Dhanesh Chandra<sup>1</sup>; John Hansen<sup>1</sup>; <sup>1</sup>University of Nevada, Metallurgl. & Matls. Engrg., MS 388, Reno, NV 89557 USA

The organic crystalline materials, such as neopentylglycol (NPG) and tris(hydroxymethyl)aminomethane (TRIS), undergo solid-solid phase transitions and store the thermal energy have great potential for the passive solar building application. In this study, the phase diagram of Tris-NPG was constructed using Guinier X-ray diffraction and differential scanning calorimetry (DSC) data. It was found that below ~316 K, there is virtually no solubility of Tris in NPG or visaversa. Between ~316 K to 378 K a wide two-phase region is observed. The maximum solubility of NPG in Tris is 21%NPG at 398 K and that of Tris in NPG is 45% Tris at 413 K. The phase diagram exhibits a peritectic transformation at 423 K and eutectoid transformation at 400 K. The heat capacity measurement of the TRIS-AMPL solid solutions are also performed by using the DSC methods. Thermodynamic and crystal structure of solid solutions and components useful for thermal energy storage will be discussed.

#### 11:10 AM

**An Overview of Piezoelectric Composites**: Michael Arthur Coleman<sup>1</sup>; Renato G. Bautista<sup>1</sup>; <sup>1</sup>University of Nevada, Metallurgl. Engrg., 1664 N. Virginia, MS 388, Reno, NV 89557 USA

Current technological trends have demanded new piezoelectric materials with increased performance capabilities. In order to satisfy these requirements, composite materials consisting of a piezoelectric component and another material have been produced. The secondary phases have been as varied as the potential applications from polymers to metals, glass, and other ceramics. These composite materials have been used to sense and create vibrations, change optical properties for fiber optic applications, activate displacement responses, and sense accelerations. As the uses for piezoelectric composites continue to expand so does the information available on their production and properties. To aid in understanding current trends, this review gives a description of some of the research currently underway in composite design and application.

# Advanced Materials for Energy Conversion II: Metal Hydrides V, Thermal Energy Storage and Containment Materials

Sponsored by: Light Metals Division, LMD-Reactive Metals Committee

*Program Organizers:* Dhanesh Chandra, University of Nevada, Metallurgical & Materials Engineering, Reno, NV 89557 USA; Renato G. Bautista, University of Nevada, Department of Chemical and Metal Engineering, Reno, NV 89557-0136 USA; Louis Schlapbach, EMPA Swiss Federal, Laboratory for Materials Testing and Research, Duebendorf CH-8600 Switzerland

Thursday AMRoom: 204March 18, 2004Location: Charlotte Convention Center

Session Chairs: Stephen N. Paglieri, Los Alamos National Laboratory, Tritium Sci. & Engrg., Los Alamos, NM 87554 USA; Hiroyuki T. Takeshita, Kansai University, Fac. of Engrg., Suita, Osaka 564-8680 Japan; Eric H. Majzoub, Sandia National Laboratories, Analytical Matls. Sci. Dept., Livermore, CA 94550 USA

# 8:30 AM

Methane Cracking Properties of Nitrided Zr-Mn-Fe-Al Getters: Stephen N. Paglieri<sup>1</sup>; Joseph R. Wermer<sup>1</sup>; Erica J. Larson<sup>1</sup>; Hain Oona<sup>1</sup>; John D. Baker<sup>2</sup>; Aleta Hagman<sup>3</sup>; <sup>1</sup>Los Alamos National Laboratory, Tritium Sci. & Engrg., PO Box 1663, MS-C348, Los Alamos, NM 87544 USA; <sup>2</sup>Idaho National Environmental and Engineering Laboratory, ID USA; <sup>3</sup>Northwestern University, Evanston, IL 60208 USA

Methane was decomposed over 5 and 50 g beds of porous Zr-Mn-Fe-Al pellets (SAES St909), retaining carbon on the getter and releasing hydrogen. Steady state methane cracking efficiency varied between 20 and 100% depending on pretreatment conditions, carrier gas (nitrogen or helium), temperature (650-800°C), residence time, and methane concentration (0.25 or 5%). Cracking efficiency declined upon exposure to nitrogen, and increased at higher temperatures and longer residence time. XPS was employed to examine getter utilization and composition while XRD was used to relate performance to structural changes.

# 8:50 AM

Phase Stability and Structure of Zr-Fe SAES St198 Alloy in Hydrogen: Michael Arthur Coleman<sup>1</sup>; Dhanesh Chandra<sup>1</sup>; <sup>1</sup>University of Nevada, Metallurgl. Engrg., 1664 N. Virginia, MS 388, Reno, NV 89557 USA

The Phase stability of the SAES Getter St198, nominally Zr<sub>2</sub>Fe, at elevated temperatures in a hydrogen environment is observed. In addition the susceptibility of Zr<sub>2</sub>Fe and Zr<sub>3</sub>Fe hydrides to disproportionation into Zr<sub>2</sub>H<sub>x</sub> for a range of temperatures is examined. Inelasti Neutron Scattering is used to identify Zr<sub>2</sub>Fe and Zr<sub>3</sub>Fe hydrides and deuterides.

#### 9:10 AM

Heat Capacities and Phase Equilibrium of Pentaglycerine and Neopentylglycol Binary System: *Wen-Ming Chien*<sup>1</sup>; Argenta Price<sup>2</sup>; Dhanesh Chandra<sup>1</sup>; <sup>1</sup>University of Nevada, Metallurgl. & Matls. Engrg., MS 388, Reno, NV 89557 USA; <sup>2</sup>Yale University, New Haven, CT 06520 USA

Polyalcohols, such as pentaglycerine (PG) and neopentylglycol (NPG), are the thermal energy storage materials which reversibly absorb large amounts of heat during solid-state phase transitions and have the potential applications for solar buildings. In this study, the thermal properties of the solid-solid state phase transition for the pentaglycerine and neopentylglycol binary system have been investigated by using differential scanning calorimetry (DSC). The PG-NPG solid solutions have been cycled 5 times between -20°C to 100°C and the different scan rates at 2°C/min, 5°C/min and 10°C/min have been performed. The onset temperatures decease as the %PG composition increases from 10%PG to 25%PG. In the 25%PG to 60%PG composition range, the onset temperatures increase as the %PG compositions increase. The lowest onset temperature occurs at 25%PG-75%NPG solid solution of 8.7°C at 10°C/min rate and 11.7°C at 2°C/min rate. The eutectoid occurs at 20.22°C of 40%PG-60%NPG solid solution. The heat capacity measurement of the PG-NPG solid solutions has also been performed by using the DSC method. The detail phase transitions and heat capacity equations will be presented.

#### 9:30 AM Break

#### 9:45 AM Cancelled

Application of Austenitic Stainless Steels to Hydrogen and Tritium Storage

#### 10:05 AM Cancelled

Thermal Cycling and Creep Studies of AM50+Nd Magnesium Alloy Based Carbon Fiber, SiC Particulate and In-Situ Mg2Si Reinforced Hybrid Composites

#### 10:25 AM

Energy Benefits of Using Nickel Aluminide Intermetallic Alloy Furnace Rolls and New Damper Controls at ISG Burns Harbor Plate's Annealing Furnace: Peter Angelini<sup>1</sup>; Vinod Sikka<sup>1</sup>; Mike Santella<sup>1</sup>; Anthony Martocci<sup>2</sup>; John Mengel<sup>2</sup>; Larry Fabina<sup>2</sup>; <sup>1</sup>Oak Ridge National Laboratories, Metals & Ceram. Div., 1 Bethal Valley Rd., PO Box 2008, MS 6065, Oak Ridge, TN 37831 USA; <sup>2</sup>ISG Burns Harbor Plate Inc. USA

At ISG Burns Harbor Plate Inc.'s, (formerly Bethlehem Steel Burns Harbor Plate Division) annealing furnace, new nickel aluminide intermetallic alloy rolls provide greater high-temperature strength and wear resistance compared to the conventional H series cast austenitic alloys currently used in the industry. This provides energy reduction based on slower roll speeds which allow greater hearth coverage and throughput, longer operating campaigns with fewer furnace light-ups, and improved surface finish of product which allows surface critical product to be processed at this furnace. Two commercial suppliers that followed rigid specifications produced the new alloy rolls. The team of Oak Ridge National Laboratory and ISG personnel developed these specifications. The nickel aluminide rolls are competitively priced with conventional H series alloy rolls. Twenty-nine new automated furnace control dampers have also been installed replacing older design, less effective pressure control dampers. These dampers, along with flame-safety control equipment and new AC motors and control equipment for improved roll speed control, are providing improved furnace control and additional energy efficiency.

#### 10:45 AM Invited

Phase Equilibrium and Thermal Property Studies of Pentaerythritol and 2-Amino-2-Methyl-1,3-Propanediol Binary System: *Wen-Ming Chien*<sup>1</sup>; Dhanesh Chandra<sup>1</sup>; Renee Russell<sup>2</sup>; <sup>1</sup>University of Nevada, Metallurgl. & Matls. Engrg., MS 388, Reno, NV 89557 USA; <sup>2</sup>Pacific Northwest National Laboratory, PO Box 999, MS K6-24, Richland, WA 99352 USA

Thermal energy storage materials, "Plastic Crystals", reversibly absorb large amounts of heat during solid-state phase transitions. These materials have potential applications in thermal energy storage for solar buildings. A binary phase diagram for Pentaerythritol (PE) and 2-amino-2-methyl-1,3- propanediol (AMPL) is proposed. This diagram was determined by high temperature Guinier X-ray diffraction and differential scanning calorimetric (DSC) methods. The low temperature phases of PE and AMPL are in equilibrium between 293 K and 357 K in the composition range of 12 to 98 mol% AMPL. The phase diagram contains two eutectoids at 357 K and 420 K and a peritectic at 457 K. The solubility of AMFL in PE is very high, up to 45 mol% AMFL in PE at 420 K. The solubility of PE in AMFL is very low, only up to 10 mol% PE in AMFL at 357 K. The heat capacities of the PE-AMPL solid solutions are also obtained by using the DSC methods. The detail results obtained by X-ray diffractometry and DSC methods for the phase diagram and heat capacity data will be presented.

# **Aluminum Reduction Technology: Modeling**

Sponsored by: Light Metals Division, LMD-Aluminum Committee Program Organizers: Tom Alcorn, Noranda Aluminum Inc., New Madrid, MO 63869 USA; Jay Bruggeman, Alcoa Inc., Alcoa Center, PA 15069 USA; Alton T. Tabereaux, Alcoa Inc., Process Technology, Muscle Shoals, AL 35661 USA

Thursday AM	Room: 213D	
March 18, 2004	Location: Charlotte Convention Center	

Session Chair: Vinko Potocnik, Vinko Potocnik Consultant, Jonquiere, QC G7S 3C7 Canada

# 8:30 AM

An Improved Equation for the Interelectrode Voltage Drop in Industrial Aluminium Cells: J. Thonstad<sup>1</sup>; H.-D. Kleinschrodt<sup>2</sup>; H. Vogt<sup>2</sup>; <sup>1</sup>Norwegian University of Science and Technology, Dept. of Matls. Tech., 7491 Trondheim Norway; <sup>2</sup>TFH Berlin-University of Applied Sciences, D-13353, Berlin Germany

The interelectrode voltage drop is the largest single component making up the cell voltage in aluminium cells - except during anode effect. The presence of gas bubbles underneath the anode represents an increase in the ohmic resistance, and hence in the voltage drop across the electrolyte. It is common practice to estimate the interelectrode drop by taking into account the enhanced resistance in the gas bubble layer only, whereas the voltage drop in the essentially bubble-free region of the interelectrode space is treated as being unaffected by the presence of bubbles. An analysis shows that this procedure introduces a serious error. The large bubbles underneath the anode exhibit a strong effect on current distribution in the bubble-free region. Application of the finite-element method yields a practical relationship, demonstrating that the conventional procedure gives results for the interelectrode drop that are far too low.

#### 8:55 AM

Numerical Modeling of Heat Exchanges Around an Aluminum Reduction Pot Shell: *Thierry Tomasino*<sup>1</sup>; Celine Martin<sup>1</sup>; Emmanuel Waz<sup>1</sup>; Steeve Renaudier<sup>1</sup>; <sup>1</sup>Pechiney, Ctr. de Recherche de Voreppe, 725, rue Aristide Berges, BP 27, Voreppe Cedex 38341 France

The use of numerical modeling allows evaluation of working conditions and ventilation of electrolytic pots in the aluminum industry. But particular attention has to be paid to the correct analysis of all physical phenomena. A numerical 2D-model which integrates natural convection and radiation in order to describe the heat exchanges around an aluminum reduction pot shell, was developed with the commercial code FLUENT®. The temperature gradient between pot shell walls and ambient air generates a velocity field. The induced turbulent flow necessitates the use of a turbulence model associated to a wall function. The objectives of this work are to determine the best adapted models for both natural convection and radiation, and to consolidate results through different numerical tests. The numerical results are compared to correlations and measurements on pot. A good agreement is found.

#### 9:20 AM

Design Modification of Anode Super-Structure by Finite Element Analysis: M. M. Megahed<sup>1</sup>; H. S. Sayed<sup>1</sup>; F. M. Ahmed<sup>2</sup>; S. A. Mohamed<sup>2</sup>; A. Akhnokh<sup>2</sup>; <sup>1</sup>Cairo University, Fac. of Engrg., Gamaa St., Giza Egypt; <sup>2</sup>Aluminium Company of Egypt, Nag-hammadi Egypt

The Aluminium Company of Egypt (Egyptalum) utilizes pre-baked anode cells with a current of 208 kA. Due to the relatively heavy weight of the existing anode steel structure, R&D at Egyptalum has recently conducted a detailed investigation with the objective of redesigning the anode superstructure to reduce its weight without sacrificing safety. Stress and deformation behaviors of the anode steel structure were investigated by means of finite element technique using shell elements. In addition to self-weight of the structure, weights of busbar, anode carbon, bunkers, lifting and jacking mechanisms, flexibles and crust effect were considered. Temperature variation was also taken into account. The results indicated that the existing anode structure posses a safety factor against yielding of about 7.5 and a safety factor against web buckling of at least 4.2. Thus an attempt was made to reduce anode weight via reducing flanges and web thickness of the anode section as well as the thickness of the trapezoidal gas passage section. Both static, thermal and buckling analysis were conducted by means of the FE model. The final design achieved a weight saving of about 14% with almost the same safety factors against static yielding or web buckling failure. This weight saving amounts to about 1200 kg of steel per anode.

### 9:45 AM

Two-Dimensional Model of Melt Flows and Interface Instability in Hall-Heroult Cells: *Oleg Zikanov*<sup>1</sup>; Haijun Sun<sup>1</sup>; Donald P. Ziegler<sup>2</sup>; <sup>1</sup>University of Michigan, Mech. Engrg., 4901 Evergreen Rd., Dearborn, MI 48128-1491 USA; <sup>2</sup>Alcoa, Primary Metals, Alcoa Techl. Ctr., 100 Techl. Dr., Alcoa Ctr., PA 15069-0001 USA

We derive a two-dimensional model for the melt flows and interface instability in aluminum reduction cells. The model is based on the de St. Venant shallow water equations and incorporates the essential features of the system such as the magnetohydrodynamic instability mechanism and nonlinear coupling between the flows and interfacial waves. The model is applied to verify a recently proposed theory that explains the instability through the interaction between perturbations of horizontal electric currents in the aluminum layer and the imposed vertical magnetic field. We investigate the role of other factors, in particular, background melt flows and magnetic field perturbations.

### 10:10 AM Break

### 10:20 AM

Demonstration Thermo-Electric and MHD Mathematical Models of a 500 kA Al Electrolysis Cell: Part 2: *Marc Dupuis*<sup>1</sup>; Valdis Bojarevics<sup>2</sup>; Janis Freibergs<sup>3</sup>; <sup>1</sup>GeniSim Inc., 3111 Alger St., Jonquiere, Quebec G7S 2M9 Canada; <sup>2</sup>University of Greenwich, Sch. of Computing & Math., 30 Park Row, London SE10 9LS UK; <sup>3</sup>University of Latvia, Inst. of Physics, 32 Miera St., Salaspils 2169 Latvia

In the present study, a full 3D cell thermo-electric model of a 500 kA demonstration cell has been developed and solved. In parallel, a non-linear wave MHD model for the full version of the same 500 kA demonstration cell taking into account the shielding effect of the detailed and optimized geometry of the potshell, is delivered. Preliminary results of the impact of the interactions between the cell thermo-electric and MHD models will be presented.

#### 10:45 AM

**Magnetic Field in Electrolysis Cells and in the Potroom**: *Aureliu Panaitescu*<sup>1</sup>; Augustin Moraru<sup>1</sup>; Ileana Panaitescu<sup>2</sup>; <sup>1</sup>"Politehnica" University of Bucharest, Elect. Engrg. Dept., Splaiul Independentei 313, Bucharest 060032 Romania; <sup>2</sup>Isvor Fiat, Engrg. Processes & ICT, Corso Dante 103, Turin 10126 Italy

The knowledge of the magnetic field is important because its interaction with the current field in the molten media can induce instabilities; it can also affect the operation of electrical devices placed close to the pots. The mapping of the magnetic flux density values allowed the exposure level of the workers in the potroom to be assessed. The determination of stationary magnetic fields in nonhomogenous media with magnetic bodies is considered solved, but only for "local" methods. When the field is described in open domains the use of "integral" formulations is needed. In this area high performance methods of computation are still to be developed. One of them is described in this paper. The magnetic field obtained by our new code is compared with measurements performed inside the whole potroom. The comparisons showed good agreement. We obtained an engineering tool able to analyze the actual configuration and to be used also for the design of other electrolysis cells. The model created, both for complexity and accuracy of results, is a very good one among other known studies.

#### 11:10 AM

**Busbar Optimization of High-Current Reduction Cells**: *Alexander Gusev*<sup>1</sup>; Vassily Krioukovsky<sup>1</sup>; Leonid Krylov<sup>1</sup>; Vitaliy Platonov<sup>2</sup>; Petr Vabishchevich<sup>3</sup>; <sup>1</sup>RUSAL - Management Company, Mfg. Dept., 13/1 Nikoloyamskaya St., Moscow 109240 Russian Federation; <sup>2</sup>Sayanogorsk Aluminium Smelter, Chakassia, Sajanogorsk 662793 Russian Federation; <sup>3</sup>Russian Academy of Science, Inst. of Math. Modlg., 4 Miusskaya sq., Moscow 125047 Russian Federation Busbar design optimization of high-current reduction cells is an important aspect of increasing the amperage. It is related to the fact that the actual busbar design does not provide satisfactory pot stability. For working out of different busbar optimization schemes Russian Aluminium uses a specially developed computer program Arc/@RusAl. Main feature of the program is accurate calculation of magnetohydro-dynamic stability of pots on the basis of mathematic modeling of nonlinear dynamics of electrolyte-metal boundary. The involved mathematical models of the pot stability were verified on working pots by comparing calculated and measured pot stability reserve. On the basis of mathematic modeling we were able to work out several alternatives of busbar optimization. The recommended busbar modifications were implemented on a test group of pots. We obtained increased pot stability that, in turn, allowed achieving a significant reduction in pot voltage and metal level.

#### 11:35 AM

Mathematical Modeling of Aluminum Reduction Cells in "Russian Aluminium" Company: G. V. Arkhipov<sup>1</sup>; <sup>1</sup>Russian Aluminum Company, Engrg. & Tech. Ctr. Russia

To give a comprehensive description of processing running in a cell an Ideal Mathematical Model is to solve interconnected problems of thermo-electric fields, magnetohydrodynamics, aerodynamics, strainedstress state, filtration of the melt and other problems. However, such a comprehensive model does not exist. There are models capable of calculating several fields interrelated with each other or in a certain sequence. The Engineering and Technology Center employs models to assess engineering solutions to retrofit and design cells with self-baking and prebaked anodes. Analysis of cells design involves the following modeling: thermo-electric field; strained-stress state; magnetic field; magnetohydrodynamics; aerodynamics of the air; electrical and heat balance.

#### Bulk Metallic Glasses: Mechanical Behavior

Sponsored by: Structural Materials Division, ASM International: Materials Science Critical Technology Sector, SMD-Mechanical Behavior of Materials-(Jt. ASM-MSCTS)

*Program Organizers:* Peter K. Liaw, University of Tennessee, Department of Materials Science and Engineering, Knoxville, TN 37996-2200 USA; Raymond A. Buchanan, University of Tennessee, Department of Materials Science and Engineering, Knoxville, TN 37996-2200 USA

Thursday AM	Room:	209A
March 18, 2004	Location	: Charlotte Convention Center

Session Chairs: Jinn P. Chu, National Taiwan Ocean University, Matls. Engrg., Keelung, Taiwan 202 China; Christopher A. Schuh, Massachusetts Intitute of Technology, Matls. Sci. & Engrg., Cambridge, MA 02139 USA

#### 8:30 AM Invited

Plastic Flow and Tensile Ductility of a Bulk Amorphous Zr55A110Cu30Ni5 Alloy in the Supercooled Liquid Region: Jinn P. Chu<sup>1</sup>; Chun-Ling Chiang<sup>1</sup>; Chang-Ting Lo<sup>1</sup>; T. G. Nieh<sup>2</sup>; Y. Kawamura<sup>3</sup>; <sup>1</sup>National Taiwan Ocean University, Inst. of Matls. Engrg., 2 Pei-Ning Rd., Keelung 202 Taiwan; <sup>2</sup>Lawrence Livermore National Laboratory, PO Box 808, Livermore, CA 94551 USA; <sup>3</sup>Kumamoto University, Dept. of Mech. Engrg. & Matls. Sci., Kumamoto Japan

Tensile deformation behavior of a cast  $Zr_{55}Al_{10}Cu_{30}Ni_5$  bulk metallic glass in the supercooled liquid region was investigated at strain rates ranging from 10<sup>-4</sup> to 10<sup>-2</sup> sec<sup>-1</sup>. The material exhibited excellent mechanical formability; a maximum tensile elongation of about 800% was recorded in the alloy at an initial strain rate of 10<sup>-2</sup>sec<sup>-1</sup>. The alloy was like a Newtonian behavior at high temperatures but to become non-Newtonian at low temperatures and high strain rates. The strain rate and temperature were found to play an important role in affecting deformation behavior of bulk Zr-based metallic glass in the supercooled liquid region. The strain rate sensitivity, i.e. the m value, was estimated to be ~0.9 under this test condition. Structures of the amorphous material, both before and after deformation, were examined using X-rays diffraction and high resolution transmission electron microscopy.

# 8:55 AM

Containerless Measurement of Thermophysical Properties of Ti-Zr-Ni Alloys: *Robert W. Hyers*<sup>1</sup>; Richard C. Bradshaw<sup>1</sup>; Jan R. Rogers<sup>2</sup>; Thomas J. Rathz<sup>3</sup>; Geun W. Lee<sup>4</sup>; Anup K. Gangopadhyay<sup>4</sup>; Kenneth F. Kelton<sup>4</sup>; <sup>1</sup>University of Massachusetts, Dept. of Mech. & Industrial Engrg., 160 Governors Dr., Amherst, MA 01003 USA; <sup>2</sup>NASA Marshall Space Flight Center, Code SD46, Huntsville, AL 35812 USA; <sup>3</sup>University of Alabama, Huntsville, AL 35899 USA; <sup>4</sup>Washington University, Dept. of Physics, St. Louis, MO 63130 USA

The surface tension, viscosity, density, and thermal expansion of Ti-Zr-Ni alloys were measured for a number of compositions by electrostatic levitation methods. Containerless methods greatly reduce heterogeneous nucleation, increasing access to the undercooled liquid regime at finite cooling rates. The density and thermal expansion are measured optically, while the surface tension and viscosity are measured by the oscillating drop method. The measured alloys include compositions which form a metastable quasicrystal phase from the undercooled liquid, and alloys close to the composition of several multi-component bulk metallic glass-forming alloys. Measurements of surface tension show behavior typical of transition metals at high temperature, but a sudden decrease in the deeply undercooled liquid for alloys near the quasicrystal-forming composition range, but not for compositions which form the solid-solution phase first.

#### 9:20 AM

Enhancement of Plasticity in Ni Based Bulk Metallic Glass Matrix Composites Containing Ductile Brass Phase: Minha Lee<sup>1</sup>; Dong Hyun Bae<sup>1</sup>; Won Tae Kim<sup>2</sup>; Do Hyang Kim<sup>1</sup>; Daniel J. Sordelet<sup>3</sup>; <sup>1</sup>Yonsei University, Metallurgl. Engrg., Ctr. for Noncrystalline Matls., 134 Shinchon-dong, Seodaemun-ku, Seoul 120749 Korea; <sup>2</sup>Chongju University, Physics, Chongju 360-764 Korea; <sup>3</sup>Iowa State University, Matls. Sci. & Engrg., Ames, IA 50014 USA

Centimeter scale Ni-based bulk metallic glass matrix composites were fabricated by warm extrusion of a mixture of gas-atomized fully amorphous powders and ductile brass powders. After consolidation, the composite retained the fully amorphous matrix found in the gas-atomized powder combined with the brass second phase. The confined ductile brass phase enabled the bulk metallic glass matrix composites to deform plastically under uniaxial compression at room temperature. However, control of the volume fraction and distribution of the ductile brass phase was important for the proper combination of the strength and plasticity. Formation of multiple shear bands during compressive straining was investigated to illustrate the enhanced ductility of the bulk metallic glass matrix composite containing ductile brass phase.

### 9:45 AM

**Deformation Behaviours of Bulk Amourphous Alloys During Hot Forming Processes:** *Yong-Shin Lee*<sup>1</sup>; S.-H. Yoon<sup>1</sup>; H.-G. Jeong<sup>2</sup>; <sup>1</sup>Kookmin University, Dept. of Mech. Engrg., 861-1 Chungneung-Dong, Sungbuk-Gu, Seoul 136-702 S. Korea; <sup>2</sup>KITECH, Dept. of Microforming S. Korea

Amorphous alloys are highly useful to realize high performance structural parts due to their excellent characteristics as functional and/ or structural materials, including the isotropic homogeneity free from crystalline anisotropy. Especially, their superior formability from the Newtonian viscous flow behaviour in the super cooled liquid state is very attractive in the view points of high precision forming. Such advantages of amorphous alloys have led researchers to work on manufacturing of highly precise, micro products like MEMS products. In this paper, thermo-mechanical finite element analyses are invoked to examine the deformation behaviours of Zr-based amorphous alloy and Pd-based amorphous alloy during hot forming processes such as hot forging and hot deep drawing. Comparisons of thermo mechanical deformation behaviours of amorphous alloys with those of superplastic materials will be also given.

#### 10:10 AM

High Temperature Deformation and Hardening Associated to Partial Crystallization in Zr Based Bulk Metallic Glasses: Marc Bletry<sup>2</sup>; Qing Wang<sup>1</sup>; Jean-Jacques Blandin<sup>1</sup>; Pierre Guyot<sup>2</sup>; Yves Brechet<sup>2</sup>; Jean-Marc Pelletier<sup>3</sup>; Jean-Louis Soubeyroux<sup>4</sup>; <sup>1</sup>INP Grenoble, Génie Physique et Mécanique des Matériaux (GPM2), BP 46, Saint-Martin d'Hères 38402 France; <sup>2</sup>INP Grenoble, LTPCM, BP 75, Saint-Martin d'Hères 38402 France; <sup>3</sup>INSA de Lyon, GEMPPM; <sup>4</sup>CNRS Grenoble, CRETA

High temperature deformation of various Zr-based BMG were studied mainly in compression in the supercooled liquid region. The effects of temperature and strain rate were investigated, showing a transition from a Newtonian domain at low strain rate and/or high temperature to a non-Newtonian domain at high strain rate and/or low temperature. In the non-Newtonian domain, stress overshoots are generally obtained. The effect of composition on the deviations from the Newtonian behaviour is discussed and the mechanical behaviours of the BMG are interpreted thanks to a model taking into account the variation with experimental conditions of the free volume concentration. Moreover, thermal treatments were also carried out to stimulate partial crystallization in the BMG and the behaviour of the resulting nano-composites was also investigated at high temperature. From such crystallization result important changes in the rheology of the BMG and these mechanical effects of partial crystallization are also discussed.

#### 10:35 AM

**Crystallization Behavior and Mechanical Properties of the Zr63A17.5Cu17.5Ni10B2 Amorphous Alloy**: *Shian Ching Jason Jang*<sup>1</sup>; <sup>1</sup>I-Shou University, Matls. Sci. & Engrg., 1, Sec. 1, Shiuecheng Rd., Dashu Shiang, Kaohsiung County, Taiwan 840 China

The crystallization behavior of Zr63Al7.5Cu17.5Ni10B2 amorphous Alloy was studied by means of scanning and isothermal differential calorimetry (DSC), X-ray diffraction (XRD), and transmission electron microscopy (TEM). A single stage transformation of the amorphous phase forming a Zr2Cu-type crystalline phase was observed. The activation energy for such a single stage crystallization of the amorphous phase was about 360±10 kJ/mole calculated by Kissinger analysis. Kinetics for the crystallization was analyzed by means of Johnson-Mehl-Avrami equation and discussed regarding to the value exponent obtained. The average value of Avrami exponent of 1.99 at the range from 694 to 700 K suggests that the nucleation mechanism is diffusion control with a decreasing nucleation rate. From the TEM analysis, small amount of Zr2Cu-type crystals in the nanoscale dimension (10-20 nm) were observed to precipitate from the amorphous matrix upon the early stage of isothermal heating the amorphous alloy at the temperature between the glass transition temperature and the crystallization. The fracture surface of bending the as-quenched amorphous ribbon 180° presents the typical ductile vein pattern. However, a ductile-brittle transition phenomenon occurs at the amorphous ribbon after 50% crystallization ratio of the isothermal annealing at the temperature between the glass transition temperature and the crystallization.

#### 11:00 AM

Study of the Thermal Properties of Zr61Al7.5Cu17.5Ni10B4 Bulk Amorphous Alloy: *Shian Ching Jason Jang*<sup>1</sup>; L. J. Chang<sup>1</sup>; Y. T. Jiang<sup>1</sup>; T. F. Huang<sup>1</sup>; P. W. Wong<sup>1</sup>; <sup>1</sup>I-Shou University, Matls. Sci. & Engrg., 1, Sec. 1, Shiuecheng Rd., Dashu Shiang, Kaohsiung County, Taiwan 840 China

The ribbons of amorphous Zr61Al7.5Cu17.5Ni10B4 alloys with 0.1 mm thickness were prepared by melt spinning method. The thermal properties and microstructural development during the annealing of amorphous alloy have been investigated by a combination of differential thermal analysis, differential scanning calorimetry, high-temperature optical microscope, X-ray diffractometry and TEM. The glass transition temperature for the Zr61Al7.5Cu17.5Ni10B4 alloys are measured about 627 K (354?). This alloy also obtains a large temperature interval DTx about 86 K. Meanwhile, the calculated Trg for Zr61Al7.5Cu17.5Ni10B4 alloy presents the value of 0.57. The energy of crystallization for the activation alloy Zr61Al7.5Cu17.5Ni10B4 was about 300 kJ/mol., as determined by the Kissinger and Avrami plot, respectively. The average value of the Avrami exponent n were calculated to be 1.99 0.45 for Zr61Al7.5Cu17.5Ni10B4 alloy.

#### 11:25 AM

Research on Fracture Toughness of Fe-Based Bulk Amorphous Alloy: Huaxing Xiao<sup>1</sup>; Guang Chen<sup>2</sup>; <sup>1</sup>Changzhou Institute of Technology, No. 3, Changcheng Rd., Changzhou, Jiangsu 213002 China; <sup>2</sup>Nanjing University of Science and Technology, Jt. Lab. of Nanostructured Matls. & Tech., No. 200, Xiao-ling-wei, Nanjing, Jiangsu China

A plate bulk Fe-Co-Zr-Mo-W-B amorphous alloy with size of  $20 \text{mm} \times 10 \text{mm} \times 1 \text{mm}$  was prepared by arc melting mixtures of pure metals and metalloid B, inductive melting alloy ingots and using copper mold suction casting. The surfaces and fractures of the cast bulk amorphous alloy samples are of typical metallic luster. However, the obvious brittleness of the cast alloy makes it of little practical use. We use Vickers indentation technique to make a research on the amelioration of toughening on brittleness of the Fe-based bulk amorphous alloy. It is found that the fracture toughness of the alloy is raised from 1.6 MPa·m1/2 in the cast state to 4.5 MPa·m1/2 of the current situation. The mechanism of the toughness increase due to toughening in the BMG is discussed.

# Cast Shop Technology: Foundry

Sponsored by: Light Metals Division, LMD-Aluminum Committee Program Organizers: Corleen Chesonis, Alcoa Inc., Alcoa Technical Center, Alcoa Center, PA 15069 USA; Jean-Pierre Martin, Aluminum Technologies Centre, c/o Industrial Materials Institute, Boucherville, QC J4B 6Y4 Canada; Alton T. Tabereaux, Alcoa Inc., Process Technology, Muscle Shoals, AL 35661 USA

Thursday AM	Room: 213B/C
March 18, 2004	Location: Charlotte Convention Center

Session Chair: Ian F. Bainbridge, University of Queensland, Co-op. Rsch. Ctr. for Cast Metals Mfg. (CAST), Brisbane, Qld 4072 Australia

#### 8:30 AM

Monitoring of TiAlSi Particle Formation and Growth in Al-Si Alloys Using LiMCA: *Martin Fortier*<sup>1</sup>; X. Grant Chen<sup>1</sup>; <sup>1</sup>Alcan International Ltd., Arvida R&D Ctr., PO Box 1250, 1955 Blvd. Mellon, Jonquière, Québec G7S 4K8 Canada

The LiMCA (Liquid Metal Cleanliness Analyser) is a well-known equipment in the aluminum industry for the measurement of liquid metal cleanliness. It measures the size and number of particles less conductive than aluminum passing through a calibrated orifice. Titanium aluminides are intermetallic particles that are less conductive than aluminum. They commonly form and grow at high temperatures in Ti-contained aluminum alloys. A LiMCA was thus used inside a crucible of molten Al-Si foundry alloy in order to determine their formation temperature and growth kinetic. Results of the formation temperature are in good agreement with other methods. The growth kinetics of intermetallics is studied in detail in terms of the particle size change with both time and temperature. The use of the LiMCA was thus demonstrated as a tool for rapid evaluation of the formation and growth of intermetallic particles in liquid aluminum.

#### 8:55 AM

Factors Influencing the Modification and Refinement of Hypereutectic Al-Si Alloys for Production of Automotive Pistons: *Shahrooz Nafisi*<sup>1</sup>; Jalal Hedjazi<sup>2</sup>; S. M.A. Boutorabi<sup>2</sup>; Reza Ghomashchi<sup>1</sup>; <sup>1</sup>University of Quebec, 555, Blvd. de l'Université, Chicoutimi, Québec G7H 2B1 Canada; <sup>2</sup>Iran University of Science and Technology, Narmak, Tehran Iran

Al-Si hypereutectic alloys are widely used in auto-industry for applications where wear resistance is of prime concern. Furthermore, their low thermal expansion coefficient and high strength to weight ratio make them the chosen material for fabrication of automotive pistons and engine blocks. Although the primary silicon particles impart adequate wear resistance, the alloy's full potential would only be realized if silicon morphology, size and distribution are optimized and closely controlled. Furthermore, the machining of hypereutectic alloys would be a tool intensive operation if the primary silicon particles are not well distributed and sized. Therefore, the addition of minor amounts of P and/or Sr may be the solution to optimize the primary and eutectic silicon particles within hypereutectic Al-Si alloys. The effects of Cu-P15% and Al-Sr10% master alloys as strong modifiers have been investigated on the microstructure of hypereutectic Al-Si (17-19%) alloys. Thermal analysis has been employed to examine the morphological changes of Si particles and identify the optimum concentration of P and Sr to achieve a fine and well distributed silicon, i.e. eutectic and primary. The results have shown that the temperature for silicon nucleation and the liquidus and solidification temperature range are the important parameters in understanding the refining process.

#### 9:20 AM

Designing a High Quality Molten Aluminum System for the Production of High Volume Engine Block and Head Castings: Venky Srinivasan<sup>1</sup>; <sup>1</sup>GM Powertrain Division, Saginaw, MI USA

The push towards lightweight high performance engines in the automotive world has accelerated the conversion of iron blocks and heads to aluminum. As design engineers drive the requirement of high quality aluminum castings in automotive engines, foundry engineers in the automotive foundry industry are honing in their spotlight on melt quality. Quiescent metal transfer, metal level control, filtration degassing, redundancy during furnace re-lines and just in time liquid metal delivery are some of the key aspects to be considered while designing an integrated melt system for high quality automotive casting operations. This paper describes a systematic approach successfully used to design a cost effective high quality molten aluminum systems Lost Foam automotive block and head castings at GM Powertrain. Quality Piston Made from Hypereutectic Al-21% Si Alloy with Nodular Silicon Grains: *Ru-Yao Wang*<sup>1</sup>; Wei-Hua Lu<sup>1</sup>; Hsien-Yang Yeh<sup>2</sup>; Henry H.E. Yeh<sup>2</sup>; <sup>1</sup>Donghua University, Shanghai 200051 China; <sup>2</sup>California State University, Long Beach, CA 90840 USA

With excellent wear resistance and lower expansion, hypereutectic Al-Si alloy castings are suitable for car engine components, such as piston, cylinder line, engine block and others. As a general thumb, with silicon content wear resistance increases and expansion coefficient decreases. However, this alloy usually has coarse primary silicon with angular shape, which degrades mechanical properties and generates poor machinability, restricting its industry application. Now a procedure has been developed to modify the silicon in hypereutectic Al-Si alloys, in which the eutectic silicon appears with nodular shape and the primary silicon is rounded. The aim of this paper is to study the microstructural features of the piston made from the hypereutectic Al-22%Si alloy and the effect of nodular silicon grains on the mechanical and physical properties of the piston, its machinability and the bench test result.

#### 10:10 AM

**Directional Solidification of Aluminum Matrix Composites:** Alicia Esther Ares<sup>2</sup>; Elvio de Napole Gregolin<sup>3</sup>; Rubens Caram<sup>4</sup>; *Carlos Enrique Schvezov*<sup>1</sup>; <sup>1</sup>University of Misiones, Faculty of Sci., 1552 Azara St., Posadas, Misiones 3300 Argentina; <sup>2</sup>CONICET, 1552 Azara St., Posadas, Misiones 3300 Argentina; <sup>3</sup>Escola Politécnica da USP, Dept. de Engenharia Metalúrgica e de Materiais, Av. Prof. Mello Moraes 2463, Sao Paulo Brazil; <sup>4</sup>State University of Campinas, Matls. Engrg. Dept., CP 6122, Campinas, Sao Paulo Brazil

It has been seen recently a progressive increase in the research of new techniques and processes for the obtention of metal matrix composites (MMC). This paper studies the directional solidification of Al-5SiO<sub>2</sub> fiber composite, due to its excellent mechanical properties and light weight. The columnar-to-equiaxed transition (CET) was observed in the samples directionally solidified from the chill zone in different solidification conditions. The transition occurs when the gradient in the liquid ahead of the columnar dendrites reaches values between -2.70°C/cm and -1.15°C/cm and the growth velocities reach values between 0.04 cm/s and 0.25 cm/s. The microstructure obtained is analyzed taking into account the characteristics of the alloy and the temperature profiles at the solidification interface. The followings tests were carried out on the composite: EDS, Vickers microhardness and optical microscopy. The results of the analysis are compared with those obtained in Al-Si binary alloys.

# Cost-Affordable Titanium Symposium Dedicated to Prof. Harvey Flower: Property Enhancement

Sponsored by: Structural Materials Division, SMD-Titanium Committee

*Program Organizers:* M. Ashraf Imam, Naval Research Laboratory, Washington, DC 20375-5000 USA; Derek J. Fray, University of Cambridge, Department of Materials Science and Metallurgy, Cambridge CB2 3Q2 UK; F. H. (Sam) Froes, University of Idaho, Institute of Materials and Advanced Processes, Moscow, ID 83844-3026 USA

Thursday AM	Room:	206B		
March 18, 2004	Locatior	: Charlotte	Convention	Center

Session Chair: Vladimir A. Duz, ADMA Products Inc., Twinsburg, OH 44087 USA

# 8:30 AM

Applying Laser Powder Deposition for Reducing Costs in Titanium Fabrications: James William Sears<sup>1</sup>; <sup>1</sup>South Dakota School of Mines & Technology, Advd. Matls. Procg. Ctr., 501 E. St. Joseph St., Rapid City, SD 57701 USA

Laser Powder Deposition (LPD) is being evaluated for a variety of applications from aircraft sturctural components to medical implants. This paper will focus on recent work evaluating material response and process developments that are leading this technology towards qualification and acceptance as a manufacturing tool. The concept of using LPD as an Additive Manufacturing tool will be discussed. Basic enconmic models will also be presented.

### 9:00 AM

Ultra-High Pressure Warm Compaction for P/M Titanium Components: Hiroyuki Takamiya<sup>1</sup>; Mikio Kondoh<sup>1</sup>; Takashi Saito<sup>1</sup>; <sup>1</sup>Toyota Central R&D Labs., Inc., Metallic Matls. Lab., 41-1 Yokomichi, Nagakute, Nagakute-cho, Aichi-gun, Aichi 480-1192 Japan

Blended elemental (BE) P/M process is one of an attractive method for obtaining cost affordable titanium components. However, the mechanical properties of the BE titanium products lose out to those of the wrought products mainly due to its residual pores. Furthermore, an excessive dimensional change (shrinkage) is inevitable to the sintering process, which spoils the dimensional precision and requires fatal cost increase in the final machining operation. For overcoming these shortcomings involved in the BE methods, we have developed a new process, ultra-high pressure warm compaction method. The key for the development is a discovery of metal die lubricant. Lithium Stearate shows a surprisingly super lubrication effect restricted at an elevated temperature of around 150°C with higher compacting pressure range from 600 MPa to 2,000 MPa. As a result, we could realize superior mechanical properties comparable to wrought products with an exact shaping (near zero shrinkage) in as sintered condition.

#### 9:30 AM

Light Weight Powder Metallurgy Titanium-Magnesium-Aluminum Composites for Structural Applications: V. S. Moxson<sup>1</sup>; V. A. Duz<sup>1</sup>; J. S. Montgomery<sup>2</sup>; F. H. (Sam) Froes<sup>3</sup>; F. Sun<sup>3</sup>; <sup>1</sup>ADMA Products, Inc., 8180 Boyle Pkwy., Twinsburg, OH 44087 USA; <sup>3</sup>University of Idaho, Inst. for Matls. & Adv. Proc. (IMAP), McClure Hall, Rm. 437, Moscow, ID 83844-3026 USA

This paper describes new high performance and low density titanium alloy ADMATALTM-21 composites produced by innovative and low cost powder metallurgy approach using inexpensive titanium sponge fines, and 90%Mg-10%Al alloy. The ability to produce fully dense components with densities in the range of 2.7 gr/cm3-3.5 gr/cm3 has been demonstrated. Metallographic evaluation and chemical analysis of various phases was performed by scanning electron microscopy and electron probe analysis. Various microstructures of a 50%-75% skeleton of titanium and titanium alloys such as Ti-6Al-4V with a uniform distribution of 90%Mg-10%Al alloy will be presented. Eutectic Mg + All2Mg17 phases with a lamela structure normally exist around the titanium and titanium alloy phase boundaries. These low density composite materials are potential candidates for automotive and aircraft applications as a substitution for aluminum and magnesium alloys.

#### 10:00 AM Cancelled

Properties and Performances of Newly Developed High-Strength Alloy Series "Super-Tix TM"

#### 10:30 AM

A Comparison of Titanium Powders from Various Sources: S. J. Gerdemann<sup>1</sup>; David E. Alman<sup>1</sup>; <sup>1</sup>Albany Research Center, Dept. of Energy, Albany, OR 97321 USA

The sintering behavior of titanium powder compacts made from gas atomized hydride-dehydride (HDH) and sponge powders were examined. Both CP and alloy titanium powders were considered. Compacts were vacuum sintered at 1200, 1275 and 1350°C for up to 960 minutes. The porosity and microstructure of the resulting sintered compacts were examined and the best conditions were used to produce tensile bars for mechanical testing. Some powders were also melted into buttons from which tensile bars were produced for comparison.

#### 11:00 AM

Mechanism of Electrolytic Reduction of Titanium in Solid State in Molten Calcium Chloride Based Salts: S. Bliznyukov<sup>1</sup>; R. Olivares<sup>1</sup>; I. Ratchev<sup>1</sup>; <sup>1</sup>BHP Billiton Minerals Technology, Newcastle, Off Vale S, Shortland, NSW 2307 Australia

Electrolytic reduction of titanium directly from solid TiO2 is a promising alternative to the current Kroll process. This new technology utilises an electrolytic cell, in which molten CaCl2-based salt is used as the electrolyte. A characteristic feature of this process is that the reduction of the feed material takes place in the solid state. Two version of the process have recently become popular, namely FFC and OS, advocated by Prof. D. Fray from Cambridge University and Prof. K. Ono and R. Suzuki from Kyoto University, respectively. The differently perceived mechanism of reduction ultimately may lead to significantly different cell designs and operating parameters. The present work is aimed at understanding the mechanism of titanium reduction as well as the limitations emanating from the process fundamentals.

# Failure of Structural Materials: General

Sponsored by: Structural Materials Division, SMD-Structural Materials Committee

*Program Organizers:* Michael E. Stevenson, Metals and Materials Engineering, Suwanee, GA 30024 USA; Mark L. Weaver, University of Alabama, Metallurgical and Materials Engineering, Tuscaloosa, AL 35487-0202 USA

Thursday AM	Room: 2	11A
March 18, 2004	Location:	Charlotte Convention Center

Session Chairs: Michael E. Stevenson, Metals & Materials Engineers, Suwanee, GA 30024 USA; Mark L. Weaver, University of Alabama, Metallurgl. & Matls. Engrg., Tuscaloosa, AL 35487-0202 USA

### 8:30 AM

Failure Analysis of Structural Metallic Bio-Implants: Michael E. Stevenson<sup>1</sup>; <sup>1</sup>Metals & Materials Engineers, 1039 Industrial Ct., Suwanee, GA 30024 USA

While the usage of advanced polymer compunds for use in structurcal orthopedic implants in increasing tremendously, metal alloys still comprise a substantial portion of the material used in structural biomaterials. This paper will discuss several failure analysis case studies of stainless steel and titanium alloy bio-implants. Topics of discussion will include alloy selection, mechanical design, installation, and usage.

#### 8:50 AM

The Effect of Microstructure on Crack Initiation in Gamma-TiAl Sheet Materials: *Shenavia Wilkerson Howell*<sup>1</sup>; Viola L. Acoff<sup>1</sup>; <sup>1</sup>University of Alabama, Metallurgl. & Matls. Engrg., PO Box 870202, Tuscaloosa, AL 35487 USA

Gamma TiAl sheet materials were investigated to characterize the initiation of cracks as a function of microstructure. The materials used in this study consisted of essentially the same composition, however, one was received in the primary annealed (PA) condition and the other in the designed fully lamellar (DFL) condition. All specimens were subjected to gas tungsten arc welding using a stationary torch (spot welding). For both conditions, all of the specimens cracked catastrophically immediately after welding, however, their mechanism of fracture was different. The fracture that occurred in the PA specimens followed an interdendritic path through regions that did not completely solidify prior to the occurrence of cracking whereas for the DFL specimens, the primary mechanism of fracture was cleavage. For both materials, a preferred growth of columnar grains was observed. The weld structure-property relationship will also be discussed.

#### 9:10 AM

Failure Analysis of a Waste Burning Boiler Flue Gas Scrubber: Lindsey McCall<sup>1</sup>; Michael E. Stevenson<sup>1</sup>; <sup>1</sup>Metals & Materials Engineers, 1039 Industrial Ct., Suwanee, GA 30024 USA

The scrubber tower for a waste burning boiler at a power generation facility suffered a catastrophic failure subsequent to a series of intense storms. While failure had initially been attributed to the weather conditions alone, metallurgical failure anlaysis indicated that severe structural degradation due to corrosion was the root cause. This paper will discuss both the analysis of this failure and the general concepts of metallurgical failure analysis that prevent (or should prevent) arrival at erroneous initial findings pertaining to structural failure.

#### 9:30 AM

#### A Thermal Ablation and Failure Model for Laser Cutting Operations: Ravindra Akarapu<sup>1</sup>; Ben Li<sup>1</sup>; Al Segal<sup>1</sup>; <sup>1</sup>Washington State University, Sch. of Mech. & Matls. Engrg., Pullman, WA 99164 USA

A mathematical model has been developed to perform the failure analysis of ceramic plates during dual laser cutting operations. The model development is based on the finite element simulations of thermal ablation and stress development during laser cutting. The integrated thermal and stress model is further integrated with the failure model to assess the thermal cracking during laser processing. The model development and numerical simulations are discussed and results are presented as a function of various laser cutting conditions.

### 9:50 AM Cancelled

Rheological Modeling of NanoIndentation and Verification of the Fracture Mechanics Principles for Multi-Layered Coatings

### 10:10 AM Break

# 10:40 AM

In-Situ Synchrotron X-Ray Microdiffraction Study of Dislocation Arrangements in Copper-Polycrystals During Uniaxial Deformations: Hyung-Don Joo<sup>1</sup>; Chung-Wung Bark<sup>1</sup>; Nobumichi Tamura<sup>2</sup>; Yang-Mo Koo<sup>1</sup>; <sup>1</sup>Pohang University of Science & Technology, Ctr. for Advd. Aeros. Matls., Hyoja dong, Pohang, KyoungBook 790-784 S. Korea; <sup>2</sup>Lawrence Berkeley National Laboratory, 1 Cyclotron Rd., MS 2-400, Berkeley, CA 94720 USA

The deformation of polycrystalline materials is very heterogeneous both at the intergranular and the intragranular level. Recent experiments have shown that formation of dislocation cell structure and rotation of structural elements at the marcro-level are fundamental to the development of plastic deformation and fracture of solids. However, in-situ study of deformation behavior in polycrystals at mesolevel has not been performed. In-situ measurement of local orientation and strain in Copper-polycrystals during uniaxial Deformations are investigated using synchrotron x-ray microdiffraction method at the Advanced Light Source of which beam size is 1.5micron \*1.5 micron. The intergranular heterogeneities of the deformation-induced microstructure were obtained. The shape of the intensity profile and the direction along elongated streaks in the Laue image are obtained at different positions of grain interior. The differences in the selection of simultaneously acting slip systems and that of dislocation arrangements among the intergranular and the intragranular level are discussed.

#### 11:00 AM Cancelled

Computer Simulation of Rheological Modeling and its Application for Determining the Fracture of Multi-Layered Coatings

#### 11:20 AM

Characterization of Plastic Deformation and Failure of Commercially Pure Titanium Via Disk Bend Testing: *Patrick J. Henry*<sup>1</sup>; Mark L. Weaver<sup>1</sup>; <sup>1</sup>University of Alabama, Metallurgl. & Matls. Engrg., Box 870202, Tuscaloosa, AL 35487-0202 USA

A disk bend test technique has been used to study deformation and failure mechanisms in commercially pure titanium. In the disk bend test, a 4 mm diameter X 0.5 mm thick disk is clamped around its rim in a circular holder and indented to failure with a flat aluminum oxide punch on its back face. The resulting behavior was compared with those from uniaxial compression and ball indentation tests. Differences and similarities in deformation between the disk bend and the compression tests are described.

#### 11:40 AM

Fracture Toughness of Oxide Dispersion Strengthened Chromium Alloys: *Mark L. Weaver*<sup>1</sup>; Patrick J. Henry<sup>1</sup>; Joseph R. Hyde<sup>1</sup>; Jason K. Morgan<sup>1</sup>; <sup>1</sup>University of Alabama, Metallurgl. & Matls. Engrg., Box 870202, Tuscaloosa, AL 35487-0202 USA

This paper presents a study of the mechanical properties of sintered Cr-MgO alloys. The results show that limited room temperature ductility can be obtained in sintered commercial purity chromium by incorporating MgO particles. The results are discussed relative to the deformation of oxide dispersion strengthened metals and alloys.

# **General Abstracts: Session IX**

Sponsored by: TMS

*Program Organizers:* Adrian C. Deneys, Praxair, Inc., Tarrytown, NY 10591-6717 USA; John J. Chen, University of Auckland, Department of Chemical & Materials Engineering, Auckland 00160 New Zealand; Eric M. Taleff, University of Texas, Mechanical Engineering Department, Austin, TX 78712-1063 USA

Thursday AM	Room: 201B
March 18, 2004	Location: Charlotte Convention Center

Session Chair: Eric M. Taleff, University of Texas, Mech. Engrg. Dept., Austin, TX 78712-1063 USA

#### 8:30 AM

Comparison of Metallurgical and Acoustical Issues in Constructing and Tuning Stainless Steel and Brass Drums With a Caribbean Steel Drum Standard: L. E. Murr<sup>1</sup>; E. V. Esquivel<sup>1</sup>; A. C. Somasekharan<sup>1</sup>; C. A.C. Imbert<sup>2</sup>; R. Kerns<sup>3</sup>; S. Irvine<sup>3</sup>; S. Lowrie<sup>3</sup>; <sup>1</sup>University of Texas, Metallurgl. & Matls. Engrg., 500 W. Univ. Ave., El Paso, TX 79968 USA; <sup>2</sup>University of West Indies, Dept. of Mech. Engrg., Trinidad & Tobago, W. Indies; <sup>3</sup>Panyard, Inc., 1216 Calif. Ave., Akron, OH 44314 USA

Stainless steel (316L) and  $\alpha$ -brass drums have been constructed along with a low-carbon (0.06% C) steel drum standard, by welding low-carbon steel sheet skirts (or cylindrical sides) and drum head sheet metal to 9 mm square carbon-steel hoops. The drum heads were all sunk to a depth of roughly 8.8 in. (22.3 cm) by pneumatic hammering to create a hemispherical-like note platform onto which a soprano drum pattern was developed and tuned. These drums are similar to the traditional Caribbean steel drum except the diameter is 23.5 in. (59.7 cm) instead of the standard 22.5 in. (57.2 cm) 55-gallon barrel. Microhardness profiles and drum head deformation features are compared along with optical metallographic and TEM observations of corresponding microstructures. Acoustical spectra for tuned notes common to each drum are examined. The results indicate that drums can be constructed and developed into musical instruments for a variety of metals, including hard aluminum alloys; especially where variations in the sound velocity are accommodated by appropriate alternations of note geometries as in the case of  $\alpha$ -brass.

#### 8:55 AM

Correlation of Microstructure and Thermal Fatigue Properties of Centrifugally Cast High Speed Steel Rolls: Chang Kyu Kim<sup>1</sup>; Jong II Park<sup>2</sup>; Jae Hwa Ryu<sup>2</sup>; Jung Seung Yang<sup>3</sup>; Sunghak Lee<sup>1</sup>; <sup>1</sup>Pohang University of Science and Technology, Ctr. for Advd. Aeros. Matls., San 31, Hyoja-dong, Namgu, Pohang, Kyungbuk 790-784 Korea; <sup>2</sup>Pohang Iron and Steel Co., Ltd., Hot Rolling Dept., 1, Koedong-dong, Nam-gu, Pohang, Kyungbuk 790-600 Korea; <sup>3</sup>INI Steel Company, R&D Dept., 444, Songnae-dong, Namgu, Pohang, Kyungbuk 790-707 Korea

In this study, thermal fatigue life of five different high speed steel rolls whose main composition had been modified were investigated by conducting the constraint thermal fatigue test. Five work roll materials which were manufactured by a centrifugal casting method were investigated quantitatively by microstructures, mechanical properties and thermal fatigue test. The basic microstructures of their shell regions were observed to be composed mainly of coarse primary carbides and tempered martensite matrix, and the cracks of thermal fatigue would initiate on primary carbides located on surface of the specimen and propagate along the primary carbides, and the thermal fatigue life of each roll was decreased with increasing the temperature range of the thermal fatigue cycles. These results were interpreted by the morphology of primary carbides and by cyclic softening phenomena associated with the exposed time at elevated temperatures during the thermal fatigue test.

### 9:20 AM

Morphology, Composition and Size Distribution of Inclusions in Fe-Si-Mn-Ti-Mg-Al-O-S Alloy Steels: Sang-Chae Park<sup>1</sup>; Chul-Ho Chang<sup>1</sup>; Han-Su Kim<sup>1</sup>; Hae-Geon Lee<sup>1</sup>; <sup>1</sup>Pohang University of Science and Technology, Dept. of Matls. Sci. & Engrg., San 31, Hyojadong, Nam-gu, Pohang, Kyungbuk 790-784 Korea

Morphology, composition, size and size distribution of inclusions/ precipitates formed during solidification and heats treating of Fe-Si-Mn-Ti-Mg-Al-O-S alloy steels were studied experimentally and the results were compared with thermodynamic prediction. Composition of the alloy, temperature and cooling rate were varied and the effects of these variables were determined quantitatively. For the Fe-Si-Mn-O-S system, inclusions/precipitates formed during solidification were mostly SiO<sub>2</sub>-MnO oxides having MnS phase in them. Depending on the cooling rate and isothermal holding time and temperature, a Mndepleted zone of the steel matrix was observed around these inclusions/ precipitates. These behaviors could be correctly explained through thermodynamic computation. If Ti was added, the proportion of SiO<sub>2</sub> in the oxide decreased and eventually disappeared to form MnO-TiO<sub>x</sub> compounds, When Ti content exceeded about 100ppm, only titanium oxide phases (Ti2O3 or Ti3O5) formed. In existence of Ti, inclusions/ precipitates became smaller in size and were dispersed more evenly. In most cases, MnS phase were found attached to inclusions/precipitates. Addition of Mg(up to 52ppm) and Al(up to 148ppm) effected the change of composition and size of inclusions/precipitates to a large extent. Addition of Mg led to formation of MgO-TiOx and MgO oxides, depending on Mg content. Addition of Al modified oxides into MgO-Al<sub>2</sub>O<sub>3</sub> type of spinel. From the results of the present study the change of morphology, composition and size of inclusions/precipitates with steel composition and temperature were successfully mapped. Thermodynamic computation was found useful in predicting these changes and hence in designing steel compositions and thermal conditions for obtaining desired inclusions/precipitates.

### 9:45 AM

Thermally and Stress Induced Martensitic Transformation in New CoNiAl Shape Memory Alloys: H. Ersin Karaca<sup>1</sup>; Ibrahim Karaman<sup>1</sup>; Yuriy I. Chumlyakov<sup>2</sup>; <sup>1</sup>Texas A&M University, Dept. of Mech. Engrg., MS 3123, College Sta., TX 77843 USA; <sup>2</sup>Siberian Physical-Technical Institute, Revolution Sq. 1, Tomsk 634050 Russia

In recent years ferromagnetic shape memory alloys have attracted increasing interest because of the ability to obtain one order of magnitude higher recoverable magnetic field induced strain (MFIS) than the other active materials. The main requirements for large magnetic field induced strain are: low twin boundary energy, high strength of matrix, high magnetocrystalline anisotropy energy and saturation magnetization. A recently discovered ferromagnetic shape memory CoNiAl alloy has promising shape memory characteristics for conventional and magnetic shape memory applications. In this study we have demonstrated that these alloys have low pseudoelastic stress hysteresis, high strength for dislocation slip, large pseudoelastic and two way shape memory strain, large pseudoelastic temperature window, and low stress for martensite reorientation. These findings satisfy the thermomechanical requirements to obtain MFIS. Additionally, high melting point, low density, good corrosion and oxidation resistance may result in the replacement of conventional SMAs with CoNiAl in most applications. This work is supported by Army Research Office, Contract No. DAAD 19-02-1-0261.

#### 10:10 AM Break

#### 10:20 AM

Austenite Decomposition in Low-Carbon Fe-C-Mn Steels: *R. E. Hackenberg*<sup>1</sup>; M. C. Gao<sup>2</sup>; D. G. Granada<sup>3</sup>; G. J. Shiflet<sup>2</sup>; <sup>1</sup>Los Alamos National Laboratory, Matls. Sci. & Tech. Div. (MST-6), MS G770, Los Alamos, NM 87545 USA; <sup>2</sup>University of Virginia, Dept. of Matls. Sci. & Engrg., 116 Engineer's Way, Charlottesville, VA 22904-4745 USA; <sup>3</sup>Nacional de Ingenieros Electromecanica, Tegucigalpa Honduras

Previous work on low-carbon Fe-C-Mn and Fe-C-Ni steels has documented kinetic, morphological and Mn partition-no partition transitions as a function of undercooling in the (first-to-appear) ferrite products. To better understand the correlations between these three transitions, the overall transformation kinetics, product morphologies and elemental distributions associated with the isothermal decomposition of austenite in Fe-(0.1, 0.2)C-(3, 4.2)Mn steels were surveyed using optical microscopy, SEM-EDS and TEM. Thermodynamic driving force calculations were done to better understand the undercooling at which these transitions took place. Additionally, the occurrence of carbide-rich products is documented, and similarities are drawn between select Fe-C-Mn steels that exhibit such carbide-rich products and betterknown steels that exhibit a bay on their TTT diagrams, such as Fe-C-Mo.

### 10:45 AM Cancelled

The Aging Behavior of a 24Cr-14Ni-2Mn Stainless Steel Under Nitrogen Atmosphere

#### 11:10 AM

Heat Tinting of MADI(TM): Edward A. Druschitz<sup>1</sup>; Craig Johnson<sup>2</sup>; Alan P. Druschitz<sup>3</sup>; Heinrich Folz<sup>4</sup>; <sup>1</sup>Central Washington University, MET, 1042 Mistwood Place, Forest, VA 24551 USA; <sup>2</sup>Central Washington Unversity, MET, 400 E. 8th Ave., Ellensburg, WA 98926 USA; <sup>3</sup>Intermet Corporation, 939 Airport Rd., Lynchburg, VA 24502 USA; <sup>4</sup>Intermet Neunkirchen Foundry, Postfach 14 18, Neunkirchen Germany

A metallographic technique has been developed to allow for the quantitative determination of the phases present in the microstructure of MADI(TM) (Machinable Austempered Ductile Iron). A correlation between the phases present and mechanical properties has also been determined. This technique and structure-property information are currently being used for production quality control and further material research and development.

# International Laterite Nickel Symposium - 2004: Atmospheric Leaching

Sponsored by: Extraction & Processing Division, EPD-Aqueous Processing Committee, EPD-Copper, Nickel, Cobalt Committee, EPD-Process Fundamentals Committee, EPD-Process Mineralogy Committee, EPD-Pyrometallurgy Committee, EPD-Waste Treatment & Minimization Committee Program Organizer: William P. Imrie, Bechtel Corporation,

Mining and Metals, Englewood, CO 80111 USA

Thursday AM	Room: 217B/C
March 18, 2004	Location: Charlotte Convention Center

*Session Chairs:* Vanessa de Macedo Torres, Companhia Vale do Rio Doce, Base Metals Projects Dept., Santa Luzia, MG 33030-970 Brazil; Roman M. Berezowsky, Dynatec Corporation, Ft. Saskatchewan, Alberta T8L 4K7 Canada

### 8:30 AM

Atmospheric Leaching of Laterites with Iron Precipitation as Goethite: Houyuan Liu<sup>1</sup>; Jim Gillaspie<sup>1</sup>; Coralie Lewis<sup>1</sup>; David A. Neudorf<sup>2</sup>; Steve Barnett<sup>3</sup>; <sup>1</sup>BHP Billiton, Newcastle Tech. Ctr., off Vale St., Shortland, New South Wales NSW 2307 Australia; <sup>2</sup>Hatch Canada, Hydrometall., 2800 Speakman Dr., Mississauga, ON L5K 2R7 Canada; <sup>3</sup>BHP Billiton, Queensland Nickel, 123 Eagle St., Brisbane, Queensland 4000 Australia

A new process was developed to recover nickel and cobalt by leaching laterite ore at atmospheric pressure and 95-105°C. The nickelcontaining goethite in limonite is firstly leached with sulphuric acid to liberate over 90% of nickel, cobalt and iron. The dissolved iron was then precipitated as Ni-free goethite with addition of saprolite. The acid released during iron precipitation is simultaneously used as lixiviant to leach saprolite to recover more nickel. With this process the limonite and saprolite are essentially converted into goethite-, gypsumand silica- containing tailings. Twenty bench tests and two campaigns of pilot plant operation (Capacity: 400 kg dry ore/day) were carried out at the BHP Billiton Newcastle Technology Centre (NTC) from January to August 2002. The overall nickel and cobalt extractions were 81-90% and 91-100% respectively. The average plant availability was 99%. The robustness of this process are most notably the very high plant availability, high consistency and simplicity of the operation.

# 8:55 AM

A Fundamental Study of the Leaching of Pre-Reduced Laterites in Ammoniacal Solutions: Michael J. Nicol<sup>1</sup>; Aleksandar N. Nikoloski<sup>2</sup>; John E. Fittock<sup>3</sup>; <sup>1</sup>Murdoch University, Parker Ctr., South St., Murdoch, Western Australia 6050 Australia; <sup>2</sup>BHP Billiton, QNI Pty Ltd, PMB 5, Mail Ctr., Townsville, Queensland 4818 Australia; <sup>3</sup>BHP Billiton, QNI Pty Ltd, PMB 5, Mail Ctr., Townsville, Queensland 4818 Australia

The recovery of nickel and cobalt by reduction roasting followed by leaching of the metallic iron-alloy grains in ammonia-ammonium carbonate solution remains as a robust, technically advanced process for the treatment of lateritic ores. The chemistry of the leaching of nickel and cobalt is linked closely with the dissolution and precipitation of the iron. Recently published results have shown that iron is prone to passivation in solutions typical of those used in practice and the passivation has been confirmed in actual leaching reactors. This passivation has been shown to be due to the formation of cobalt and nickel sulphide layers as a result of the reduction of thiosulfate present in the leach solutions. This paper will focus on other fundamental aspects of the leaching process such as the role of dissolved oxygen and cobalt(III) ions in the oxidation of the reduced alloy particles. In addition, options for minimizing the extent of passivation and optimising the rate of leaching have been investigated and will be discussed in the light of the fundamental findings.

# 9:20 AM

**Direct Atmospheric Leaching of Saprolitic Nickel Laterite Ores** with Sulphuric Acid: *Walter Curlook*<sup>1</sup>; <sup>1</sup>University of Toronto, Matls. Sci. & Engrg., 184 College St., Toronto, ON M5S 3E4 Canada

An atmospheric acid leaching process for leaching nickel and cobalt from highly-serpentinized saprolitic fractions of nickel laterite deposits has been developed and patented. The process involves leaching the highly-serpentinized saprolitic portion of the nickel laterite ore profile in strong sulphuric acid solutions at atmospheric pressure and temperatures between 80°C and 100°C, essentially autogenously, to extract over 85% of its contained nickel content and a large proportion of its cobalt content after leaching reaction times of about one hour. The amount of sulphuric acid used in the leaching process is between about 80% and 100% by weight of the finely ground highlyserpentinized saprolite ore on a dry weight basis. The metal values are recovered as intermediate products.

9:45 AM Break

# International Laterite Nickel Symposium - 2004: Slurry Rheology, Solution Extraction and Other

Sponsored by: Extraction & Processing Division, EPD-Aqueous Processing Committee, EPD-Copper, Nickel, Cobalt Committee, EPD-Process Fundamentals Committee, EPD-Process Mineralogy Committee, EPD-Pyrometallurgy Committee, EPD-Waste Treatment & Minimization Committee Program Organizer: William P. Imrie, Bechtel Corporation, Mining and Metals, Englewood, CO 80111 USA

Thursday AM	Room: 217B/C
March 18, 2004	Location: Charlotte Convention Center

*Session Chairs:* Larry E. Seeley, President & CEO, SGS Lakefield Research Limited, Lakefield, Ontario K0L 2H0 Canada; Peter G. Mason, Falconbridge (Australia), Toowong, QLD 4066 Australia

### 10:00 AM

A Study Utilising Vane Yield Rheometry to Predict Optimum Thickener Performance Across a Range of Laterite Nickel Ores for the Ravensthorpe Nickel Project: Lincoln Charles McCrabb<sup>1</sup>; Julian Chin<sup>1</sup>; Geoff Miller<sup>2</sup>; <sup>1</sup>Rheochem Ltd/BHP Billiton, 1 Keegan St., O'Connor, Western Australia 6163 Australia; <sup>2</sup>BHP Billiton, Level 12 200 St. Georges Terrace, Perth, Western Australia 6850 Australia

Correct measurement and interpretation of viscosity data is critical for design of any thickening and pumping process that involves a non Newtonian slurry. The nickel laterite pressure acid leach process relies on producing a slurry of maximum achievable solids concentration. Small variations of 1-2% solids concentration can alter economics significantly. For the Ravensthorpe Nickel Project, a rheology protocol has been developed which optimizes the solids concentration across a range of ore types. The vane yield stress technique has been utilized to accurately quantify the flow of thickened slurry in the lower shear range. A yield stress of 100Pa has been used as a benchmark to determine the optimum solids concentration achievable utilizing deep cone thickening. Statistical analysis of the data shows critical rheology distinctions between ore type, particle size, lithology and geochemistry. Linear and power law models have been applied to rheology flow curves to reconcile the material transport properties with the anticipated thickener underflow solids concentration.

# 10:25 AM

Flow Array for Nickel Laterite Slurry: Donald J. Hallbom<sup>1</sup>; Bern Klein<sup>2</sup>; <sup>1</sup>Pipeline Systems Inc., 460 N. Wiget Ln., Walnut Creek, CA 94598-2408 USA; <sup>2</sup>University of British Columbia, Mining Engrg., 5th Floor, 6350 Stores Rd., Vancouver, BC V6t 1Z4 Canada

Limonitic nickel laterite forms time-dependent slurry with complex properties that vary from thixotropy to anti-thixotropy. Stress decay tests indicate that laterite slurry takes roughly two minutes to approach steady state after a step change. As a result, most rheometer measurements are taken at a non-equilibrium state. Two minutes is also long relative to the time that a unit of slurry is at any given shear rate in a processing plant, so the slurry may never reach equilibrium. Chronic problems may occur if designers and operators fail to take this into account. This paper presents the rheology of laterite slurry using a flow array, which describes the rheology using an array of instantaneous flow curves crossed by an equilibrium flow curve along with the structure change rates. This flow array allows the flow behavior of time-dependent slurry to be predicted in non-equilibrium conditions using a simple time-step methodology.

# 10:50 AM

Manganese Separation by Solvent Extraction in Nickel Laterite Processing: *Chu Yong Cheng*<sup>1</sup>; Mark D. Urbani<sup>1</sup>; Martin Houchin<sup>1</sup>; <sup>1</sup>CSIRO, Div. of Minerals, PO Box 90, Bentley, Western Australia 6982 Australia

The separation of manganese from nickel and cobalt is reviewed and new solvent extraction processes for manganese separation are discussed. The use of intermediate precipitation, solids/liquid separation and re-leach in the three WA nickel laterite plants make these processes complicated and costly in capital and operation. By using a new synergistic organic system in semi-continuous tests with a pilot plant leach solution, Ni and Co together with zinc and copper were separated from the Mn, Mg, Ca and Cl) in the first SX circuit by extraction and scrubbing, indicating that manganese can be completely separated from nickel and cobalt using a synergistic solvent extraction approach. Semi-continuous test work with D2EHPA and synthetic and pilot plant leach solutions showed that manganese, together with calcium, copper and zinc can be effectively and efficiently separated from nickel, cobalt and magnesium by extraction, scrubbing and stripping.

#### 11:15 AM

Separation of Ni and Co from Ca, Mg and Mn in Sulphate Laterite Leach Solutions: Erin N. Legault-Seguin<sup>1</sup>; Akram M. Alfantazi<sup>2</sup>; Werner Dresler<sup>1</sup>; <sup>1</sup>Laurentian University, Sch. of Engrg., Ramsey Lake Rd., Sudbury, ON P3E 2C6 Canada; <sup>2</sup>University of British Columbia, Dept. of Metals & Matls. Engrg., Vancouver, BC V6T 1Z4 Canada

The current industrial practice in the processing of nickeliferous laterites involves the precipitation and releaching of Ni and Co to allow separation from the major impurities of Mn, Mg and Ca. A direct solvent extraction process has significant advantages over this practice, which suffers from difficult and costly precipitation steps, lower recovery and inherently complex flowsheets. The present investigation involves the examination of Cyanex 272, Cyanex 301 and Cyanex 302 as extractants for the direct extraction of Ni and Co from major impurities associated with laterite leaching, i.e. Mn, Mg and Ca. For Co extraction, Cyanex 301 and Cyanex 302 are superior to Cyanex 272, because they are able to selectively separate Co from Mn, Mg and Ca. Cyanex 272 offers complete extraction of Co from Ni and Ca, but Mn and Mg pose difficulty. Ni can only be extracted selectively with Cyanex 301, thus another extractant selective for Ni, such as Versatic 10 or Cyanex 301, is needed to recover Ni if Cyanex 302 or Cyanex 272 is used for the initial extraction.

#### 11:35 AM

Solvent Extraction Technology for the Extraction of Nickel Using LIX 84-I. An Update and Circuit Comparisons: J. Murdoch Mackenzie<sup>2</sup>; Michael J. Virnig<sup>1</sup>; <sup>1</sup>Cognis Corporation, Mining Chem. Tech., 2430 N. Huachuca Dr., Tucson, AZ 85745 USA; <sup>2</sup>Cognis Australia, Mining Chem., 284 Victoria Rd., Malaga, Western Australia 6062 Australia

Two commercial nickel solvent extraction plants treating laterite leach solutions and using LIX® 84-I have been operated in Australia. These circuits employ similar extraction chemistry but differ in their leaching and stripping operations. An alternative process involving elements of both can also be conceived. The preparation of the feed solution to solvent extraction plays an important role in nickel extraction using LIX®84-I and the special features of manganese removal and cobalt oxidation in the preparation of the PLS is discussed. This paper compares these three circuit configurations with special reference to the extraction and reductive stripping of cobalt, the advantages and the transfer of zinc and copper to the strip aqueous, ammonia transfer, and sulfur transfer. In addition, the relative advantages and disadvantages of using a mixed hydroxide product as compared to roast reductive leaching approach or mixed sulfide precipitation approach will be considered. The potential degradation of the circuit organic is discussed along with measures to counter the effects of this degradation, such as Co stripping and re-oximation.

# Magnesium Technology 2004: Alloy Development

Sponsored by: Light Metals Division, LMD-Magnesium Committee Program Organizer: Alan A. Luo, General Motors, Materials and Processes Laboratory, Warren, MI 48090-9055 USA

Thursday AM	Room:	203B		
March 18, 2004	Location	n: Charlotte	Convention	Center

Session Chairs: Bob R. Powell, General Motors Corporation, Warren, MI 48090-9055 USA; Mihriban O. Pekguleryuz, McGill University, Montreal, QC H3A 2B2 Canada

#### 8:30 AM

Magnesium Alloys for High Temperature Applications-An Overview: *Mihriban O. Pekguleryuz*<sup>1</sup>; <sup>1</sup>McGill University, Metals & Matls. Engrg., 3610 Univ. St., Wong Bldg., Montreal, Quebec H3A 2B2 Canada New growth area for automotive use of magnesium is nowertrain

New growth area for automotive use of magnesium is powertrain applications such as the transmission case and engine block. These

applications see service conditions in the temperature range of 150-200C under 50-70 MPa of tensile and compressive loads. In addition, metallurgical stability, fatigue resistance, corrosion resistance and castability requirements need to be met. A decade of research and development has resulted in a number of creep-resistant magnesium alloys that are potential candidates for elevated-temperature automotive applications. These alloys are mostly based on rare-erath and alkaline earth elemnt additions to magnesium. This paper gives an overview of the various magnesium alloy systems for use in elevated-temperature applications.

#### 8:50 AM

The Influence of Sb, Si and Sn on the Mechanical Properties of Mg-Al Alloys: *Per Bakke*<sup>1</sup>; Ketil Pettersen<sup>2</sup>; Darryl Albright<sup>3</sup>; <sup>1</sup>Norsk Hydro, CC Magnesium, PO Box 2560, Porsgrunn N-3907 Norway; <sup>2</sup>Norsk Hydro, Corp. Rsch. Ctr., PO Box 2560, Porsgrunn N-3907 Norway; <sup>3</sup>Hydro Magnesium Marketing, 39209 W. Six Mile, Ste. 200, Livonia, MI 48152 USA

Magnesium die casting alloys based on Al as the main alloying element can broadly be grouped into two categories, depending on whether the third element(s) form stable phases with Al or Mg. Alloys with Ca (AX), Sr (AJ) and RE (AE) belongs to the first category, while alloys with Si (AS), Sn (AT) and Sb are examples from the second. This paper addresses alloying additions which form precipitates with magnesium, specifically within the Mg-Al-Sn-(Mn), Mg-Al-Si and Mg-Al-Si-Sb systems. The results show that for some Mg-Al-Sn(-Mn) alloys tensile yield- and ultimate tensile strength better than AZ91 can be obtained. The microstructure of the Mg-Al-Sn alloys consists of an a-Mg matrix with Al and Sn in solid solution, and a grain boundary eutectic of Mg-Mg2Sn. With increasing Al-content, the Mg2Sn phase is pushed into pockets at the grain nodes, and their effect on grain boundary pinning gradually vanishes. The creep resistance increases with increasing Sn or Sb-content, and alloys with creep properties better than AS21X can be obtained. However, with increasing contents of Al, this effect is significantly reduced.

#### 9:10 AM

Nucleation, Precipitation and Strengthening Mechanisms in Mg-Zn-Sn Based Alloys: Alexander Katsman<sup>1</sup>; Shalom Cohen<sup>1</sup>; Ginat R. Goren-Muginstein<sup>1</sup>; *Menahem Bamberger*<sup>1</sup>; <sup>1</sup>Technion, Matls. Engrg., Technion City, Haifa 32000 Israel

This work deals with the development of Mg-Zn-Sn based alloys with enhanced creep properties at elevated temperatures. This is achieved by precipitation of binary phases MgZn and Mg2Sn during the aging of these alloys. Mg-alloys with different amounts of Zn (0.8÷1.7 at.%) and Sn (0.7÷2at.%) were solution treated at 465°C for 96 hours and then water quenched. Aging at 175°C, 200°C, 225°C and 250°C up to 96 hours has led to the precipitation of the binary phases MgZn and Mg<sub>2</sub>Sn. The formation of these phases was studied experimentally (by XRD, SEM and hardness measurements). The Modified Langer-Schwartz approach, taking into account nucleation, growth and coarsening of the new phase precipitations, was used for analysis of the structural changes during aging. Simultaneous formation of the binary MgZn and the Mg<sub>2</sub>Sn phases was considered. Two maxima of hardness during the aging were found to be connected with the formation and coarsening of two types of precipitates. Densities, average size of precipitates and activation energies of the phase formation processes, which determine the strengthening mechanisms, were estimated. A reasonable agreement between the calculations and observations was found.

#### 9:30 AM

Phase Formation, Precipitation and Strengthening Mechanisms in Mg-Zn-Sn and Mg-Zn-Sn-Ca Alloys: Shalom Cohen<sup>1</sup>; Ginat R. Goren-Muginstein<sup>1</sup>; Shaul Avraham<sup>1</sup>; *Menahem Bamberger*<sup>1</sup>; <sup>1</sup>Technion, Matls. Engrg., Technion City, Haifa 32000 Israel

The trend towards weight reduction in transportation equipment has led vehicle manufacturers to produce various components made of Mg alloys. The need for light and strong components that can serve also under relatively elevated temperatures, has led an effort to develop new Mg base alloys. The requirements from the new alloys are a stable structure and good mechanical properties when exposed to elevated temperatures. Based on those demands a new family of Mg-Zn-Sn alloys is been developed. Studying the ternary and quaternary phase diagrams of the above system shows that Mg<sub>2</sub>Sn and several Mg-Zn intermetallics precipitate. An Mg-5%Sn-5%Zn alloy was chosen for a microstructure examination and precipitation hardening study. The addition of Ca to the basic Mg-Zn-Sn alloy was also studied based on the assumption that Mg and Mg-Sn creates stable intermetallics with Ca. The samples were either solution treated at 465°C for 96 hr and then aged in temperatures of 150°C-250°C for 1-96 hr, or thermally exposed at the as-cast condition in temperatures of 150°C-300°C for

long periods of 8-768 hr. The addition of Ca creates MgSnCa during the solidification, however in both alloys, the precipitation of  $Mg_2Sn$  and MgZn is responsible for the hardening during aging and thermal exposure.

#### 9:50 AM

Microstructural Investigations of the Mg-Sn-X and Mg-Sn-Al-X Alloy Systems: Amanda L. Bowles<sup>1</sup>; Carsten Blawert<sup>1</sup>; Norbert Hort<sup>1</sup>; Karl U. Kainer<sup>1</sup>; <sup>1</sup>GKSS Forschungszentrum, Ctr. for Magnesium Tech., Max Planck Str 1, Geesthacht 21502 Germany

In an effort to gain insight into more unusual magnesium casting alloys an investigation of the binary Mg-Sn and ternary Mg-Sn-Al systems has been undertaken. For initial investigations, permanent mould castings have been made. Various elements have been added in minor amounts to the base systems (Mg-Sn and Mg-Sn-Al) and their affect on the microstructure and hardness examined. Specimens were examined in four heat treatment conditions: as-cast (F), solution heat treated (T4), solution heat treated and aged (T6) and artificially aged only (T5) conditions. The microstructures have been examined in both a qualitative manner (optical and electron microscopy) and in a quantitative manner (XRD, EDS).

#### 10:10 AM Break

#### 10:20 AM

# New Aerospace Magnesium Alloy: Paul Lyon<sup>1</sup>; <sup>1</sup>Magnesium Elektron, TSD, PO Box 23, Swinton, Manchester M27 8DD UK

Magnesium based sand casting alloys are used for aerospace applications including helicopter gearboxes and jet engine components. Over the last 20 years, key development goals for new aerospace alloys have included better elevated temperature performance combined with good corrosion resistance. Currently, the alloy with the best property envelope in this field is Elektron WE43B (Mg-Y-Nd-HRE-Zr). The castability of this alloy is however affected by a tendency to oxidation in the molten state. This requires attention to foundry detail if best results are to be achieved. This can impact on cost. Magnesium Elektron have developed a new Magnesium alloy, with significantly improved castability, whilst maintaining a corrosion resistance and mechanical property envelope close to that of Elektron WE43b. This new alloy, currently known as Elektron X, is compared and contrasted with existing Magnesium casting alloys.

#### 10:40 AM

Computational Thermodynamics and Experimental Investigation of Mg-Al-Ca System: Yu Zhong<sup>1</sup>; Jorge O. Sofo<sup>2</sup>; Zi-Kui Liu<sup>3</sup>; <sup>1</sup>Pennsylvania State University, Matls. Sci. & Engrg., 107 Steidle Bldg., Univ. Park, PA 16802 USA; <sup>2</sup>Pennsylvania State University, Matls. Simulation Ctr., Univ. Park, PA 16802 USA; <sup>3</sup>Pennsyvania State University, Matls. Sci. & Engrg., 209 Steidle Bldg., Univ. Park, PA 16802 USA

The laves phases in the Mg-Al-Ca ternary system are the key phases to improve the creep properties at elevated temperatures (>150°C) of Mg-based alloys. Three laves phases i.e. C14, C15 and C36 are investigated by using the Computational Thermodynamics/ First-Principles calculations/experiments combined approaches. Laves phases in Mg-Al-Ca system are modeled as solution phases: (Mg,Al)2Ca. The solubility range of each laves phase is investigated. The ternary Mg-Al-Ca thermodynamic database is thus constructed and used to understand the microstructures and phase relationship of Mg-based alloys. Scheil simulations and equilibrium calculations are performed for the solidification process of the alloys and compared with experimental observations.

### 11:00 AM

The Portevin-Le Chatelier Effect and Creep Behaviour in a Mg-Ca-Zn-Zr Alloy: Suming Zhu<sup>1</sup>; Xiang Gao<sup>1</sup>; Jian-Feng Nie<sup>1</sup>; <sup>1</sup>Monash University, Sch. of Physics & Matls. Engrg., Victoria 3800 Australia

The tensile properties and creep behaviour of Mg-1Ca-0.5Zn-0.6Zr (wt.%) alloy have been studied. Serrated flow (the Portevin-Le Chatelier effect) was observed when the alloy was tensile-tested in an intermediate temperature range (150-200°C). Static strain ageing effect and negative strain rate sensitivity suggested that the serrated flow was related to dynamic strain ageing (DSA) caused by the interaction between dislocations and solute Ca atoms. In creep, the alloy exhibited periodical strain bursts at 150°C. Over-ageing treatment was shown to eliminate the occurrence of strain bursts. The creep deformation mechanism of the alloy was discussed in relation to the DSA effect.

### 11:20 AM

Computational Thermodynamic Modeling of the Al-Mg-Na System: Shengjun Zhang<sup>1</sup>; <sup>1</sup>Pennsylvania State University, Dept. Matl. Sci. & Tech., 107 Steidle Bldg., State College, PA 16801 USA The binary Al-Na and Mg-Na systems were modeled by computational thermodynamics using the Calphad approach. Self-consistent thermodynamic parameters of the binary systems were obtained. Combined with the Al-Mg modeling in the literature with gas phase adding, the phase equilibria of the ternary system were calculated using Thermo-Calc software. Isothermal and isopleth sections of the phase diagram and the projection of the liqudus surface were presented. This present work contributes to the thermodynamic database of aluminum and magnesium alloy systems and can be included in the study of the impurity effects on processing of aluminum and magnesium alloy systems.

## **Metals for the Future: Processing and Bio-Materials** *Sponsored by:* TMS,

*Program Organizers:* Manfred Wuttig, University of Maryland, Department of Materials & Nuclear Engineering, College Park, MD 20742-2115 USA; Sreeramamurthy Ankem, University of Maryland, Department of Material & Nuclear Engineering, College Park, MD 20742-2115 USA

Thursday AM	Room: 2	15
March 18, 2004	Location:	Charlotte Convention Center

Session Chair: S. Ankem, University of Maryland, Dept. of Matl. & Nuclear Engrg., College Park, MD 20742-2115 USA

#### 8:30 AM Opening Remarks by S. Ankem

#### 8:40 AM Invited

Metallic Dental Implants: A Review: Sarit B. Bhaduri<sup>1</sup>; Sutapa Bhaduri<sup>1</sup>; Murali G. Kutty<sup>1</sup>; <sup>1</sup>Clemson University, Sch. of Matls. Sci. & Engrg., 110 Olin Hall, Clemson, SC 29634 USA

The dental implants form a significant share of the rapidly growing medical device market. Among the various implants, the dental implants traditionally enjoyed a high success rate. This review will begin with a brief introduction to the historical perspectives leading to discovery of such implants in Sweden. This will be followed by various classifications of implants and the distinguishing features of each class. The design and materials related issues will be a major portion of the talk. While these implants are traditionally manufactured from titanium, it is important to understand the phenomenon of "Osseointegration" (bonding of bone to the implants). Since osseointegration is a surface phenomenon, it is important to understand how the surface chemistry, morphology and the presence of a coating affect osseointegration. Various processes to obtain the desired surface features will be discussed. The presentation will conclude with some of our results in obtaining the desired surface features.

#### 9:10 AM Invited

Understanding Processing-Microstructure-Property Relationships of High-Temperature Structural Alloys Through Grain Boundary Engineering: C. J. Boehlert<sup>1</sup>; S. Civelekoglu<sup>1</sup>; N. Eisinger<sup>2</sup>; J. F. Bingert<sup>3</sup>; <sup>1</sup>Alfred University, Sch. of Ceram. Engrg. & Matls. Sci., 2 Pine St., Alfred, NY 14802 USA; <sup>2</sup>Special Metals Corporation, Huntington, WV USA; <sup>3</sup>Los Alamos National Laboratory, Los Alamos, NM USA

One goal of this NSF CAREER program (DMR-0134789) is to evaluate the potential of grain boundary engineering for high-temperature structural alloys, including Ni-based superalloys and Ti2AlNb intermetallics. The program involves processing and evaluating microstructures, measuring the grain boundary character distribution (GBCD), performing mechanical testing, and modeling the effects of GBCD on mechanical behavior. Emphasis has been placed on developing a processing methodology which can be used to enhance mechanical behavior and in particular creep resistance. From electron backscattered diffraction (EBSD) analysis, the GBCD of the orthorhombic (O) and body-centered-cubic (BCC) structures of Ti-Al-Nb alloys as well as the FCC-based INCONEL alloy 718 will be presented. For the first time the twin-related O-phase variant interfacial planes, which formed from either the HCP(a2)-O or BCC-O transformation, were quantified for Ti2AlNb alloys. The preferred O-variant boundaries from the HCP-O transformation were near {110} or {130}, while the preferred O-variant boundaries from the BCC-O transformation were near {221}.

#### 9:40 AM Invited

The Effects of Passivation Layers and Film Thickness on the Mechanical Behavior of Freestanding Electroplated Cu Thin Films with Constant Microstructure: Joost Johan Vlassak<sup>1</sup>; <sup>1</sup>Harvard University, DEAS, 311 Pierce Hall, 29 Oxford St., Cambridge, MA 02138 USA

The goal of this paper is to investigate the effects of film thickness and the presence of a passivation layer on the mechanical behavior of electroplated Cu films. Both dislocation dynamics and strain-gradient plasticity models suggest that these factors play important roles in thin film plasticity. To study the effect of passivating layers, freestanding Cu membranes were prepared using silicon micromachining techniques. Some of these membranes were passivated by depositing Ti films with thicknesses ranging from 20 nm to 50 nm on both sides of the membrane. The effect of film thickness was evaluated by preparing freestanding films with varying thickness but constant microstructure, both with and without Ti passivation. The stress-strain curves of the freestanding Cu films were evaluated using the plane-strain bulge test technique. The grain structure and crystallographic texture of the Cu films were determined using EBSD, the dislocation structure through TEM. Yield stress, Young's modulus, residual stress, and work hardening behavior of the films are correlated with film microstructure and thickness.

# 10:10 AM Break

#### 10:25 AM Invited

#### Metals for the Future: Environmentally Benign Pb-Free Solder Alloys: Nik Chawla<sup>1</sup>; <sup>1</sup>Arizona State University, Dept. of Chem. & Matls. Engrg., Ira A. Fulton Sch. of Engrg., Tempe, AZ 85287 USA

Solders are an integral part of electronic packaging. Recently, there has been a significant drive to replace Pb-Sn solders with Pb-free, environmentally-benign solders. Given the widespread use of Pb-Sn solder in the manufacture and assembly of circuit boards, the development and reliability of new Pb-free solders is crucial for the successful substitution of these materials in the electronics industry. In this talk an overview of the thermomechanical behavior and microstructure in Pb-free solders, in bulk form and at small length scales, will be presented. Experiments coupled with microstructure-based simulations have been conducted to further the understanding of deformation in these materials. The challenges and opportunities for metals research in this arena will be explored and discussed.

#### 10:55 AM Invited

The New Renaissance of Biometallic Implants: Otto C. Wilson<sup>1</sup>; <sup>1</sup>Catholic University, BONE/CRAB Lab., Dept. of Biomed. Engrg., Washington, DC USA

Metallic implants have historically served as inactive, structural support systems to repair hard tissue damage. However, a number of advances in bioinorganic chemistry and surface probe techniques have uncovered a whole new world of applications for biometallic implants that range from macroscale to nanoscale implants. New developments in surface modification have been used to transform traditionally inert metal implant surfaces into bioactive surfaces for greatly enhanced integration into the body. The most versatile coatings in this genre include calcium phosphate based minerals (hydroxyapatite), silica based minerals (Bioglass) and even metal oxidation products such as TiO2 which exhibit unique bone bonding behaviors. Nanoscale biometallic implants for treatment of disorders at the cellular and sub cellular level are being developed based on the integral role of metal ions in biological processes such as protein function. An overview of these technologies with respect to current and future advances in metal based orthopedic and vascular implants, shape memory alloy MEMs devices for the assembly of tissue engineering scaffolds, and magnetic nanoparticles for controlled cellular interactions will be presented in this talk.

11:25 AM Panel Discussion with H. Rack, B. B. Rath, B. MacDonald

# Multiphase Phenomena in Materials Processing: Session III

Sponsored by: Extraction & Processing Division, Light Metals Division, Materials Processing and Manufacturing Division, EPD-Process Fundamentals Committee, MPMD/EPD-Process Modeling Analysis & Control Committee, MPMD-Solidification Committee Program Organizers: Ben Q. Li, Washington State University, School of Mechanical and Materials Engineering, Pullman, WA 99164-2920 USA; Stavros A. Argyropoulos, University of Toronto, Department of Materials Science and Engineering, Toronto, Ontario M5S 3E4 Canada; Christoph Beckermann, University of Iowa, Department of Mechanical Engineering, Iowa City, IA 52242 USA; Bob Dax, Concurrent Technologies Corporation, Pittsburgh, PA 15219 USA; Hani Henein, University of Alberta, Edmonton, AB T6G 2G6 Canada; Adrian S. Sabau, Oak Ridge National Laboratory, MS-602, Oak Ridge, TN 37831-6083 USA; Brian G. Thomas, University of Illinois, Department of Mechanical and Industrial Engineering, Urbana, IL 61801 USA; Srinath Viswanathan, Sandia National Laboratories, Albuquerque, NM 87185-1134 USA

Thursday AM	Room:	218B		
March 18, 2004	Location	Charlotte	Convention	Center

Session Chairs: Hani Henein, University of Alberta, Dept. of Chem. & Matls. Engrg., Edmonton, Alberta T6G 2G6 Canada; Adrian S. Sabau, Oak Ridge National Laboratory, Dept. 1835, Oak Ridge, TN 37831-6083 USA

#### 8:30 AM

Effect of Process Variables on Droplet Heat Transfer: Hani Henein<sup>1</sup>; <sup>1</sup>University of Alberta, Advd. Matls. & Procg. Lab., Dept. of Chem. & Matls. Engrg., Edmonton, Alberta T6G 2G6 Canada

Heat transfer between droplets/particles and a gas phase plays an important role in the transport of numerous materials processing operations. These include rapid solidification operations such as gas atomization and spray forming, as well as chemical systems such flash furnaces. Chemical reaction rates and solidification are dependent on the rate of gas-particle or gas-droplet heat transport. Using a heat transport model validated using single fluid atomization of molten droplets; the effect of process variables on heat losses from droplets was examined. In this work, the effect of type of gas, droplet size, gas temperature, gas-droplet relative velocity on the heat transport from AA6061 droplets was examined. The most critical of these process variables to heat transfer is identified and will be presented.

#### 8:50 AM

Separation Characteristics of Gas-Solid Flow in U-Beam Separator: Haigang Wang<sup>1</sup>; S. Liu<sup>1</sup>; Fan Jiang<sup>1</sup>; <sup>1</sup>Chinese Academy of Sciences, Inst. of Engrg. Thermophysics, PO Box 2706, Beijing, Beijing 100080 China

It is difficult to model 3D turbulent flows of a gas containing suspended solid particles through U-beam separators of complex geometry. In this paper, the complex multiphase turbulent flow in U-beam separators is simulated using the standard k-e, RNG k-e and Reynolds stress equation models (DSM) respectively. The gas-phase transport equations coupled with the gas-particle interactions are modified, based on the DSM turbulent models to handle the interaction between the gas and particles, which accounts for both the enhancement and damping of the turbulent energy by the particles. To account the effect of the stochastic characteristic of the instantaneous gas velocity on the particles, the improved Lagrangian stochastic model based on the Reynolds stress was adopted, which attributed to the successful prediction of the turbulence inhomogeniety, turbulence anisotropy, and particle crossing-trajectories effect. The collisions between the particles are also considered in the Hard-Sphere model. To treat the particle-wall collision, the influence of the roughness of the wall on the motion of the solid particles is taken into consideration by imposing random collision angles. To observe the effects of different turbulent models, the flows in a 90° bend with square cross section are simulated firstly. The results are compared with experimental data, which shows that the DSM model is superior to the other two models. It clearly predicts the anisotropic behavior of the Reynolds stresses and the distribution of the velocity in the U-beam separator. Numerical calculations of threedimensional gas-particle flow through a separator with four rows of Ubeam elements show that the particles coarser than 50 mm are mostly separated in the first two rows, particles between 20-50 mm are more likely separated in the third and fourth rows, but with less total efficiency. The collection efficiency increases with the number of U-beam elements, but with raised pressure drop too. Although initially at same starting position, the trajectories of particles of different sizes are different. The results show that the turbulence intensity strongly affects the path of the particle. The calculated results show that the particle separation also rely on particle density, size and free stream velocity. To optimize the effect of a U-beam element should be considered jointly.

### 9:10 AM

#### Multiphase Transitions in Metals Being Electrochemically Deposited: Oleg B. Girin<sup>1</sup>; <sup>1</sup>Ukrainian State University of Chemical Engineering, Dept. of Matls. Sci., Pr. Gagarina, 8, Dnipropetrovsk 49005 Ukraine

There has been experimentally found and theoretically confirmed a change in the aggregate state of the metals being electrochemically deposited wherein while a metal is being electrodeposited on a solid cathode in an aqueous medium, a super-cooled metal liquid is formed that solidifies at the deposition temperature. In general the polymorphous metal being electrodeposited passes in succession through the following phases: metal liquid, intermediate solid modification, and stable solid phase. The fact that in the process of their electrochemical deposition the metals pass via a stage of their liquid state is confirmed by the regular changes of their microstructure, substructure, structural state, structural inhomogeneity and defects in their crystalline structure with the supercooling degree being increased during their electrodeposition. This research project is financed by the Ministry of Education and Science of Ukraine, R&D project No. 0102U001953.

#### 9:30 AM

A Study of Steel Scrap Movement: Diancai Guo<sup>1</sup>; <sup>1</sup>McMaster University, Steel Rsch. Ctr., Hamilton, Ontario L8S 4L7 Canada

Uneven movement of scrap during melting in an Electric Arc Furnace causes operation problems; cave-ins interrupt electric power input. The movement also influences the radiation heat loss to watercooled side panels and roof. An apparatus has been built to simulate the flow of scrap that may be interlocked. It has been observed that flow starts at the point where the suspended length of the pile bottom reaches the average scrap size, and proceeds in the form of cave-ins, but scrap pieces slide with each other as ordinary granules. After a cave-in, the pile angle usually remains much larger than the normally observed angle of repose. The internal stress of a partially suspended scrap pile has been analyzed, and the equivalent cohesion due to interlocking estimated. A numerical model has been developed to simulate the scrap flow. Simulated results agree reasonably with observed phenomena.

#### 9:50 AM Break

#### 10:05 AM Cancelled

#### A Multiphase Solution Algorithm for Microporosity Prediction During Casting

#### 10:25 AM

**Detachment of Bubbles from Their Nucleation Sites**: László I. Kiss<sup>1</sup>; Sándor Poncsák<sup>1</sup>; Alicia Liedtke<sup>1</sup>; Verena Mackowiak<sup>1</sup>; <sup>1</sup>Université du Québec, Ctr. Universitaire de Recherche sur l'Aluminium, 555 boul. de l'Université, Chicoutimi, Québec G7H 2B1 Canada

Bubbles play a very important role in different metallurgical applications like in electrowinning. During heterogeneous nucleation, the maximal size of the bubbles growing at the nucleation sites as well as the nucleation frequency is determined by the so-called detachment condition. Detachment occurs when the external forces acting on the bubble exceed the retaining forces along the solid-gas-liquid triple interface line. The phenomenon depends strongly on the shape and orientation of the solid surface and on the nature and strength of the external buoyancy and drag forces. In the present study the detachment conditions of bubbles from downward facing horizontal and inclined plates were studied experimentally under the effect of gravitational and hydrodynamic forces. The results show the deformation of the bubbles under the effect of the external forces and the detachment conditions as function of the bubble volume.

#### 10:45 AM

Mechanisms and Diffusional Kinetics of the Hard Chromizing Process on Carbon Steels: *Jyh-Wei Lee*<sup>1</sup>; Jenq Gong Duh<sup>2</sup>; <sup>1</sup>Tung Nan Institute of Technology, Dept. Mech. Engrg., #152, Sec. 3, Pei-Shen Rd., Shen-Ken, Taipei Co. Taiwan; <sup>2</sup>National Tsing Hua University, Dept. Matls. Sci. & Engrg., #101, Sec. 2, Kuang-Fu Rd., Hsin Chu Taiwan

Hard chromizing process is a method for developing a surface modified coating providing wear, corrosion resistance and high temperature surface protection. Two carbon steels with 0.45 wt% and 0.95 wt% carbon contents, respectively, were chromized with pack cementation process at 950?• for 1, 4 and 9 hours. The phase transformation and microstructure phenomena of chromized coating layer and matrix of two steels were studied with X-ray diffractometer and electron probe microanalyzer. (Cr,Fe)23C6 and (Cr,Fe)7C3 carbides and (Cr,Fe)2N1-x nitride phases were observed on the chromized surfaces. The thickness of chromized layers obeyed the parabolic rate law. The mechanism and diffusional kinetics of the chromizing process were proposed. The diffusivity of chromium in the (Cr,Fe)7C3 carbide phase was calculated using the moving boundary method.

#### 11:05 AM

A Computational Approach in Obtaining Heat Transfer Dimensionless Correlations: Blas Melissari<sup>1</sup>; *Stavros A. Argyropoulos*<sup>1</sup>; <sup>1</sup>University of Toronto, Dept. of Matls. Sci. & Engrg., 184 College St., Toronto, ON M5S3E4 Canada

There is a paucity of dimensionless convective heat transfer correlations applicable to fluids like liquid metals. The existing correlations cover single Prandtl number metals or at most two different Prandtl number metals. In this paper a computational approach was employed. This approach estimates the melting of solid spheres immersed in different liquid metals and under different convective conditions. The spheres are made from the same material as the liquid metal. The SIMPLER algorithm was implemented in two dimensions axi-symmetrical co-ordinates and three-dimensional Cartesian co-ordinates. Experimental validation of the dimensionless correlation was carried out in two fluids with vastly different Prandtl numbers.

#### 11:25 AM

Mathematical Modeling of Air Gap Phenomena in Squeeze Casting of Aluminum Alloys: *Alfred Yu*<sup>1</sup>; Naiyi Li<sup>2</sup>; Henry Hu<sup>1</sup>; <sup>1</sup>University of Windsor, Mech., Auto. & Matls. Engrg., 401 Sunset Ave., Windsor, Ontario N9B 3P4 Canada; <sup>2</sup>Ford Motor Company, Mfg. Sys. Dept., Ford Rsch. Lab., Dearborn, MI 48121 USA

In the past few years, various squeeze cast aluminum components have been developed and successfully implemented in various vehicles by the automotive industry because of their superior engineering performance. However, fundamental understanding of the formation of air gap during squeeze casting processes is still very limited despite of its significant influence on the extent of heat transfer between the casting and mould. In this paper, a 3-D mathematical model has been developed to simulate phenomena of air gap between the casting and mold during squeeze casting of aluminum alloys. The model considers the effect of process parameters such as applied pressures, initial velocities and mold temperatures on the events of air gap formation. The predication indicates that the occurrence of highly enhanced heat transfer in squeeze casting of aluminum alloys primarily results from the presence of excess applied pressures.

# Nanostructured Materials for Biomedical Applications: Session VII

Sponsored by: Electronic, Magnetic & Photonic Materials Division, EMPMD-Thin Films & Interfaces Committee Program Organizers: Roger J. Narayan, Georgia Tech, School of Materials Science and Engineering, Atlanta, GA 30332-0245 USA; J. Michael Rigsbee, North Carolina State University, Department of Materials Science and Engineering, Raleigh, NC 27695-7907 USA; Xinghang Zhang, Los Alamos National Laboratory, Los Alamos, NM 87545 USA

Thursday AM	Room: 219A
March 18, 2004	Location: Charlotte Convention Center

Session Chairs: Roger J. Narayan, Georgia Institute of Technology, Sch. of Matls. Sci. & Engrg., Atlanta, GA 30332-0245 USA; Marian G. McCord, North Carolina State University, Textile Engrg. Chmst. & Sci., Raleigh, NC 27695-8301 USA; Afsaneh Rabiei, North Carolina State University, Mech. & Aeros. Engrg., Raleigh, NC 27695-7910 USA

# 8:30 AM Invited

Thin-Film Self-Assembled Nanostructured Materials: Andrew P. Shreve<sup>1</sup>; Andrew M. Dattelbaum<sup>1</sup>; James H. Werner<sup>1</sup>; Meri L. Amweg<sup>2</sup>; Chanel E. Yee<sup>2</sup>; Atul N. Parikh<sup>2</sup>; <sup>1</sup>Los Alamos National Laboratory, Biosci. Div., MS G755, Los Alamos, NM 87545 USA; <sup>2</sup>University of California, Dept. of Appl. Sci., Davis, CA USA

Recent studies of thin-film self-assembled nanostructured materials will be discussed. The formation of nanocomposite thin-film silica based materials will be a special emphasis. Such materials can be formed on solid supporting substrates from an evaporation-induced ordered surfactant phase in combination with soluble silica precursors. These structured films can be functionalized, both chemically and biochemically, using various strategies, and representative examples of such functionalization will be presented. The resulting composite materials are active thin-films with tunable responses, and some applications in sensing and molecular recognition will be described. In addition, spatial patterning using uv-processing methods is possible, and results addressing the mechanism of uv-patterning and examples of interactions of patterned functional films with biomolecular assemblies will also be presented.

#### 9:05 AM

Synthesis and Characterization of Nanostructured Inorganic-Organic Composite Biosensor Films: *Tianbao Du*<sup>1</sup>; Olusegun J. Ilegbusi<sup>1</sup>; <sup>1</sup>University of Central Florida, Dept. of Mech., Matls. & Aeros. Engrg., 4000 Univ. Blvd., Orlando, FL 32826 USA

Metal/Semiconductor (M/SC) nanoparticles immobilized in polymer matrices have generated considerable interest in recent years due to their distinct individual and cooperative properties. Such nanostructured composites have exhibited unique physicochemical, electrophysical, magnetic and optical properties. In particular, they have demonstrated potential as chemical sensors for detecting superoxide anion radicals (SOR) in biological fluids. These radicals initiate damage to tissues and biologically active substances in organisms. In this work, various semiconductor-polymer nanocomposite biosensor films for SOR are synthesized by sol-gel technique. The films are deposited from organic solutions on Pt-coated Pyrex glass substrate. They are characterized for surface morphology, chemistry, thickness, and nanocrystallite size using various advanced analytical techniques such as scanning electron microscopy (SEM), X-ray photoelectron spectroscopy (XPS), atomic force microscopy (AFM), and high-resolution transmission electron microscopy (HRTEM) aided by focused ion beam sample preparation. Preliminary results show that the solgel technique could successfully synthesize nanostructured semiconductor-polymer composites with enhanced sensitivity for detection of superoxide radicals.

#### 9:40 AM Cancelled

# **Bicontinuous Nanoporous Pt and Au Electrodes - Processing and Properties**

#### 10:15 AM Invited

Plasma Deposition of Ultrathin Films on Nanoparticles for Bio-Sensor Applications: Donglu Shi<sup>1</sup>; <sup>1</sup>University of Cincinnati, Chem. & Matls. Engrg., 493 Rhodes Hall, Cincinnati, OH 45221-0012 USA

Nanoparticals are used in many applications because of their desirable bulk properties. Unfortunately, the surface of the nanoparticles is often not ideal for the particular application. The ability to deposit well-controlled thin film coatings on nanoparticles would offer a wide range of technological opportunities based on changes to both the bio and physical properties of the nanoparticals. Atomic layer controlled coatings on nanoparticles, for example, would allow them to retain their bulk properties but yield more desirable surface properties. These ultrathin coatings could act to activate, passivate or functionalize the nanoparticles to achieve both desirable bulk and surface properties. This presentation will give an overview of new surface structures by plasma deposition of ultrathin films on various nanoparticle (including nanotubes) for novel engineering applications. The unique properties required in these specific applications could be best achieved by our plasma method. One of the novel applications is in the area of biosensor applications. The fluorescent paramagnetic nanoparticles have been recently developed for various medical diagnostic and environmental applications. These nanoparticles comprise superparamagnetic cores coated or incorporated with spectrally characteristic fluorescent dyes. A thin coating of polymer or silica can be applied to these fluorescent particles to provide various functional groups for passive or covalent coupling to biologicals, such as antigens, antibodies, enzymes, or DNA/RNA hybridization. They can be used as a solid phase for various types of immunoassays and DNA/RNA hybridization probe assays, cell separation, and other diagnostic, medical, and industrial applications.

#### 10:50 AM Invited

Pathogenesis of Vascular Catheter Infections as a Model of Prosthetic Implant Infection: *Robert J. Sheretz*<sup>1</sup>; <sup>1</sup>Wake Forest University, Sch. of Medicine, Med. Ctr. Blvd., Winston-Salem, NC 27157 USA

Prosthetic implants are used increasingly commonly in the care of patients through out the world. The most important complication interfering with their use is infection. Infection of prosthetic devices equals microorganism biofilm formation on the device plus clinical symptoms. Central venous catheters are the best studied example of prosthetic device infection and will be used to illustrate the challenges we must face to improve the outcomes of prosthetic device implantation. Central venous catheters uniformly develop biofilm formation within three days of implantation. Only about half of these biofilms are culture positive. Of those that are culture positive the timing of initial colonization varies by catheter site: subcutaneous segment (average: 5.1 days), tip segment (8.6d), and lumen (13.1d). The greater the number of organisms on a catheter, the greater the likelihood that the catheter will have associated purulence or bloodstream infection. The risk of catheter-related bloodstream infection ranges considerably from £ 2/1000 patient days (peripheral venous catheters, peripherally inserted central catheters (PICC), cuffed central venous catheters, ports), 10/1000 patient days (arterial and Swan-Ganz catheters), to 30-50/1000 patient days (multilumen, hemodialysis). Intrinsic factors that affect the risk of vascular catheter infection include host factors, type of organism, catheter material, and the manufacturing process. Extrinsic factors that can affect the risk of infection primarily involve antiseptic technique such as skin preparation, the use of maximum sterile barriers, and education. New strategies to reduce the risk of catheter-related bloodstream infection target both the internal and external surface of the catheter including anti-infective coatings and anti-infective flush solutions. The importance of these findings to the prevention of infection involving other prosthetic devices will be discussed.

# Solid and Aqueous Wastes from Non-Ferrous Metal Industry: Session II

Sponsored by: Extraction & Processing Division, EPD-Waste Treatment & Minimization Committee

*Program Organizers:* Junji Shibata, Kansai University, Department of Chemical Engineering, Osaka 564-8680 Japan; Edgar E. Vidal, Colorado School of Mines, Golden, CO 80401-1887 USA

Thursday AM	Room: 214
March 18, 2004	Location: Charlotte Convention Center

Session Chairs: Hideki Yamamoto, Kansai University, Dept. of Chem. Engrg. Japan; Edgar E. Vidal, Colorado School of Mines, Dept. of Metallurgl. & Matls. Engrg., Golden, CO 80401-1887 USA

#### 8:30 AM Invited

Selection of Ion-Exchange Resins Suitable for Removing Copper from Aqueous Wastes Generated During Semiconductor Processing Operations: William Ewing<sup>1</sup>; Fanny Darmawan<sup>1</sup>; Fiona M. Doyle<sup>1</sup>; James W. Evans<sup>1</sup>; <sup>1</sup>University of California, Matls. Sci. & Engrg., 210 Hearst Mining Bldg. #1760, Berkeley, CA 94720-1760 USA

Copper is increasingly being adopted for interconnects in semiconductor devices. The aqueous processing techniques used in device manufacture generate copper-bearing wastes, such as spent electrolyte from electroplating, electroplating rinse water, and CMP waste streams. We are examining the use of ion exchange and electrowinning as a means of recovering copper from these streams within the processing plant, to allow recycling of process water and minimize hazardous wastes. Various resins have been tested for their affinity for copper in the presence of plating additives and other organic complexing agents. While chelating resins have a strong affinity for copper, their elution can be problematic. Carboxylate resins do not appear to be capable of removing copper to sufficiently low concentrations. Sulfonate resins, however, appear to be promising, provided there are not high concentrations of competing cations.

#### 9:00 AM Invited

Stability of Hazardous Heavy Metal Waste by Modified Belite Cement Produced from Rolling Sludge: *Ji-Whan Ahn*<sup>1</sup>; Jin-Sang Cho<sup>1</sup>; Hyung-Seok Kim<sup>1</sup>; Ki-Suk Han<sup>1</sup>; Hwan Kim<sup>2</sup>; Choon Han<sup>3</sup>; <sup>1</sup>Korea Institute of Geoscience and Mineral Resources, Matls. & Mineral Procg. Div. Korea; <sup>2</sup>Seoul National University, Sch. of Matls. Sci. & Engrg. Korea; <sup>3</sup>Kwang-Woon University, Dept. of Chem. Engrg. Korea

The Modified belite cement clinker containing  $\beta$ -C<sub>2</sub>S, C<sub>4</sub>A<sub>3</sub>S and C<sub>4</sub>AF was synthesized using industrial by-product, and the solidification/stabilization properties of hazardous heavy metal and organic matter including in industrial wastes by cement produced were investigated. For synthesis of modified belite cement clinker, the raw materials were mainly used rolling sludge, dolomite sludge generated at steel and iron making process, and phosphogypsum generated at soda lime manufacturing process. The mixture of raw materials was sintered at 1250° for 1hr and cooled rapidly in air condition, and properties of the clinker were characterized with XRD, SEM, and EDAX. The Modified belite cement was produced mixing clinker and calcium sulfate ( $CaSO_4$ ). Using XRD, SEM, compressive strength and leaching test of heavy metal, hydration and solidification/stabilization properties of hazard-ous wastes containing heavy metal and organic matter were investigated.

#### 9:30 AM Invited

Solvent Extraction of Nickel in the Spent Electroless Nickel Plating Baths: *Mikiya Tanaka*<sup>1</sup>; Hirokazu Narita<sup>1</sup>; <sup>1</sup>National Institute of Advanced Industrial Science and Technology Japan

With increasing importance of electroless nickel plating technology in many fields such as electronic and automobile industries, the treatment of the spent baths is becoming a serious problem. Although the spent baths are currently treated by conventional precipitation method, a method with no sludge generation is desired. In the EPD Congress 2003, we reported the solvent extraction recovery of nickel from the spent baths by means of solvent extraction using LIX84I as an extractant. A drawback of that method was that the extraction and stripping of nickel were not fast enough to achieve high efficiencies when the continuous extractor was used. We have overcome this difficulty by finding an effective accelerating reagent added into the organic phase of LIX84I. Shaking out tests using a separatory funnel at 240 spm revealed that the extraction and stripping rates of nickel are remarkably enhanced by adding the accelerating reagent: The time to reach equilibria is more than 60 min without additive, but reduced to 10 min by the additive both in the extraction and the stripping with sulfuric acid. Detailed data on the accelerating effects will be presented.

#### 10:00 AM Break

#### 10:15 AM

Recycling Process for Tantalum and Some Other Reactive Metal Scraps: Ryosuke Matsuoka<sup>1</sup>; Kunio Mineta<sup>1</sup>; Toru H. Okabe<sup>1</sup>; <sup>1</sup>University of Tokyo, Inst. of Industrial Sci. Japan

A process of recycling tantalum from capacitor scraps using an oxidation process followed by mechanical separation and chemical treatment was investigated. This study demonstrates that sintered tantalum electrodes inside the capacitor scraps could be collected mechanically after the oxidation of the scraps in air, and high purity  $Ta_2O_5$  powder could be efficiently recovered after chemical treatment. The yield of tantalum from the scraps was approximately 90-92%. By reducing the tantalum oxide obtained by magnesiothermic reduction, tantalum powder with 99 mass% purity was obtained. Chlorination routes for tantalum recovery was also investigated, and the obtained tantalum or tantalum compounds were reacted with chloride scraps such as FeClx. The recycling process by utilizing chloride scrap is extended to other reactive metals (e.g. Ti, RE..).

#### 10:35 AM

Novel Recovering System of Nickel in Waste Water With Solvent Extraction Technique: Yoshinobu Kawano<sup>1</sup>; Sana Takashi<sup>1</sup>; Koichiro Shiomori<sup>1</sup>; <sup>1</sup>Miyazaki University Japan

Novel recovering system of nickel in waste water was developed using solvent extraction technique. Three steps of vibro-mixer type extractors, forward extraction of nickel into the organic solution, back extraction of nickel into the aqueous solution and final purification of nickel in the aqueous solution were connected in series. Waste water was followed and treated with continuously in the system. Optimum condition of the recovering system was determined experimentally in the various operation conditions in each step.

#### 10:55 AM

Removal of Toxic Heavy Metal Ions from Wastewater with Iron-Manganese Compound: *Ruilu Liang*<sup>1</sup>; Eiji Kikuchi<sup>1</sup>; Hiroshi Sakamoto<sup>1</sup>; <sup>1</sup>Akita Prefectural University, Fac. of Sys. Sci. & Tech. Japan

In this paper, adsorption of cadmium, lead, arsenic and selenium ions onto iron-manganese compound adsorbent in aqueous solution was investigated. It was found that the adsorption capacity of the adsorbent is highest under the synthetic conditions: mole ratio of iron to manganese =1:1.5, reacting pH=11 and drying temperature of filter cake =70°. Based on the adsorption isotherms of Cd and Pb ions by the adsorbent, the maximum adsorption amounts were 40 mg Cd and 300 mg Pb per gram adsorbent, respectively. The metal ions were eluted from the iron-manganese compound by adding 0.5 mol/l HNO<sub>3</sub>, and the adsorption capacity of the adsorbent recovered to nearly the previous level. In addition, some fundamental aspects involved in the adsorption are also discussed.

#### 11:15 AM

Hydrometallurgical Method for Treating Special Alloys, Jewelry, Electronic and Electrotechnical Scrap: N. I. Antipov<sup>1</sup>; A. V. Tarasov<sup>1</sup>; V. M. Paretsky<sup>1</sup>; <sup>1</sup>State Research Center of Russian Federation, State Rsch. Inst. of Nonferrous Metals, 13, Acad. Korolyov St., 129515 Moscow Russia

A purely hydrometallurgical flowsheet developed in the Gintsvetmet Institute is based on the use of a versatile acidic technique for recovery of precious and non-ferrous metals into solution. This flowsheet ensures separate recovery of silver and gold, as well as commercial-grade palladium and platinum metal powders. Two alternatives are possible for manufacture of silver metal powder from silver chloride. Depending on the palladium content of solution different alternatives are possible for palladium concentration and refining. Palladium metal powder is produced by aqueous heterogeneous reaction of palladosamine with formic acid. Platinum metal powder is produced by aqueous heterogeneous reaction of ammonium hexachloroplatinate with formic acid at 90°C to 100°C. The proposed flowsheet makes it possible to reliably obtain commercial-grade products of the following quality: bullion gold containing (%%): 99.6-99.9 Au, 0.05-0.2 Ag, 0.007-0.02 Cu, 0.003-0.04 Pd, 0.003-0.005 Fe, 0.005 Pb, 0.005 Sb and 0.005 Bi; - bullion silver containing (%%):99.6-99.9 Ag, 0.07-0.3 Au, 0.01-0.03 Pd, 0.007-0.02 Cu, 0.003-0.005 Fe, 0.005 Pb, 0.005 Sb, 0.005 Bi; platinum and palladium metal powders.

#### Solidification of Aluminum Alloys: Special Effects

Sponsored by: Materials Processing & Manufacturing Division, MPMD-Solidification Committee

*Program Organizers:* Men Glenn Chu, Alcoa Inc., Alcoa Technical Center, Alcoa Center, PA 15069 USA; Douglas A. Granger, GRAS, Inc., Murrysville, PA 15668-1332 USA; Qingyou Han, Oak Ridge National Laboratory, Oak Ridge, TN 37831-6083 USA

Thursday AM	Room: 207B/C
March 18, 2004	Location: Charlotte Convention Center

Session Chairs: Qingyou Han, Oak Ridge National Laboratory, Metals & Ceram. Div., Oak Ridge, TN 37831-6083 USA; Srinath Viswanathan, Sandia National Laboratories, Albuquerque, NM 87185-1134 USA

#### 8:30 AM

Mechanisms of Grain Size Evolution During Aluminum Spray Forming: Yaojun Lin<sup>1</sup>; Yizhang Zhou<sup>1</sup>; Enrique J. Lavernia<sup>1</sup>; <sup>1</sup>University of California, Dept. of Chem. Engrg. & Matls. Sci., Davis, CA 95616-5294 USA

A numerical approach is implemented to analyze the evolution of grain size during spray forming 5083 Al. The evolution of grain size is investigated at the two different thicknesses of the deposit, correspond to 400 and 602°C on the deposit's surfaces. The temperature histories of individual droplets during the flight stage and during impingement onto the two aforementioned deposit's surfaces are calculated. In terms of the calculatd temperature histories, the nucleation behavior and the nuclei growth in individual droplets are computed accordingly. Based on the measured temperature history, nuclei coarsening during the solidification process of remaining liquid phase (applicable to the deposit's surface of 602°C) and grain growth during solid phase cooling are evaluated. The calculated results indicate a bimodal and a relatively uniform grain morphology, corresponding to the deposit's surfaces with the temperature of 400 and 602°C, respectively.

#### 8:50 AM

Prediction of Microstructure and Distribution of Solute in Ternary Al-Zn-Mg Alloys Designed for Cathodic Protection Applications: Julio Alberto Juarez<sup>1</sup>; Carlos Gonzalez<sup>1</sup>; <sup>1</sup>Universidad Nacional Autonoma de Mexico, Inst. de Investigaciones en Materiales, Circuito Exterior S/N, Cd. Universitaria, Mexico, D.F. 04510 Mexico

An analysis of the structure obtained in chill-cast Al-Zn-Mg ingots was carried out. The microstructure consisted of alpha-dendrites, tauintermetallic in solid solution and eutectic in interdendritic regions. The electrochemical behavior of alloys in both cast and heat-treated ingots was investigated in 3% NaCl solution. Results showed that the eutectic and the intermetallic have an impact on the electrochemical efficiency of the alloys, which are designed to be used as sacrificial anodes. To correlate structure with electrochemical efficiency, the Al-Zn-Mg phase diagram for a constant concentration of Zn was analyzed together with growth temperature of phases obtained during solidification. Then, the range of solidification front velocities was predicted, where the alpha-Al and intermetallic phases grew simultaneously. These results, together with the predicted variation with growth velocity of solute concentration in the alpha-Al and the electrochemical efficiency values were used to select an alloy which can be used as Alsacrificial anode.

# 9:10 AM

#### **The Effect of Casting Parameters on the Quality of Thin Gauge Foils**: *Murat Dündar*<sup>1</sup>; Özgül Keles<sup>1</sup>; Bilal Kertý<sup>1</sup>; <sup>1</sup>Assan Aluminum, Tuzla, Istanbul Turkey

In the Aluminum Industry, wrought products with a thickness of 6-200µm are known as foils. Aluminum foil is a preferred material in the packaging industry due to its excellent electrical and heat conductivity, strength, corrosion resistance, cleanliness, compatibility with laminates, impermeability to gas and light, ease of folding, non-toxicity, etc. In today's market, a large percentage of foil production is the result of a combination of conventional ingot casting and hot rolling. The high production costs and time involved in conventional casting has led foil producers to consider continuous casting techniques, especially twin roll casting. One of the challenges of twin roll casting is the solidification process. In this study, the effects of casting parameters on the quality of foil products have been investigated using two different casters. Quality characteristics, such as number of pinholes in the foil, microstructure of the cast product, micro-macro segregation, and grain size, have been examined using mechanical, metallographic, and surface characterization techniques.

#### 9:30 AM

Effect of Mold Vibration on the Solidification Process During Die Casting of AA 356: Numan M. Abu-Dheir<sup>1</sup>; Marwan K. Khraisheh<sup>1</sup>; Kozo Saito<sup>1</sup>; <sup>1</sup>University of Kentucky, Ctr. for Mfg., Mech. Engrg. Dept., 210 CRMS Bldg., Lexington, KY 40506-0108 USA

Mechanical mold vibration using an electromagnetic shaker has been applied to the gravity die casting of AA356. The effect of vibration on the solidification process is being studied through analysis of temperature gradient in the mold. The AA356 is heated to 850°C and then poured into a steel die. The die is then vibrated at different combinations of frequency and amplitude. The mold temperature is measured and analyzed using thermocouples and high resolution images of IR camera. It is shown that the mold vibration alters the temperature profiles. This will have a significant effect on the microstructure and properties of the cast which are currently investigated.

#### 9:50 AM Break

#### 10:10 AM

Correlation of Microstructure and Fluidity in Short Fiber-Aluminum Alloy Matrix Composites-A Comparison With Unreinforced Matrix Alloys: Olga B. Garbellini<sup>1</sup>; Carina N. Morando<sup>2</sup>; Hugo A. Palacio<sup>1</sup>; Heraldo Biloni<sup>1</sup>; <sup>1</sup>University Nacional del Centro de la Provincia de Buenos Aires, IFIMAT-Fac. Cs. Exactas & CICPBA, Pinto 399, Tandil B7000GHG Argentina; <sup>2</sup>University Nacional del Centro de la Provincia de Buenos Aires, IFIMAT-Fac. Cs. Exactas & SeCyT UNCPBA, Pinto 399, Tandil B7000GHG Argentina

This is a study of the fluidity in AlCuSi/Al<sub>2</sub>O<sub>3</sub> composites at the Alrich corner. The fluidity measurements were carried out in terms of a classic foundry practice (i.e., the length the liquid metal flow in a channel packed with an alumina chopped fibers preform while solidifying). The fluidity mechanism was investigated with a focus on microstructure and the fluidity values of eutectics that complete solidification. The results of the fluidity tests indicated that the infiltrated length was best in the alloys and composites situated in the primary Si field, followed by those situated in the primary Al field and close to the the Al-Cu eutectic valley and to the Al-Si eutectic valley respectively. In all cases the results were found to be influenced by the morphology and concentration of constituent phases in the microstructure. They were compared with the results of fluidity tests in unreinforced matrix alloys. Quantitative metallography measurements are presented to substantiate such interpretations.

#### 10:30 AM

Effects of Hot Extrusion Prior to Spheroidization on Al-Si-Cu Alloys: Vjekoslav Franetovic<sup>1</sup>; Jon T. Carter<sup>1</sup>; <sup>1</sup>General Motors, R&D Ctr., Matls. & Processes Lab., MC 480-106-212, 30500 Mound Rd., Warren, MI 48090-9055 USA

The influence of prior hot extrusion of an Al-7%Si-0.5%Mg-3%Cu alloy on the subsequently spheroidized microstructure was studied. Such extrusion promoted a greater degree of spheroidization, smaller alpha globules, and higher levels of entrapped eutectic and entrapped Cu-rich phase, but no net change in copper concentration in the alpha globules (other than the entrapment). The greater degree of spheroidization and the smaller globule size are expected to increase semi-solid formability, but the higher level of entrapped eutectic is expected to slightly reduce semi-solid formability. In samples which were T6 heat treated after spheroidization, the pre-spheroidization extrusion caused an increase of 0.5% Cu in the alpha, but no change in microhardness of either the primary alpha or the eutectic. Data are presented in the forms of optical and scanning electron micrographs, heating curves, and compositional analyses.

#### 10:50 AM

Vacuum-Sealed Aluminum Step Casting: Johnathon Capps<sup>1</sup>; Amit Suryawanshi<sup>1</sup>; *Sayavur I. Bakhtiyarov*<sup>1</sup>; Ruel A. Overfelt<sup>1</sup>; <sup>1</sup>Auburn University, Mech. Engrg. Dept., 202 Ross Hall, Auburn, AL 36849-5341 USA

In this paper experimental data of mold filling and solidification of aluminum alloy A356.2 in V-process casting technique are presented. A vacuum-sealed step pattern (V-process) has been used as a mold. A laboratory apparatus for a gravity filled vacuum-sealed casting was designed and built for an experimental study of the effect of some process parameters on the filling behavior of aluminum alloy in a step-pattern casting. Temperature measurements and "cell-valued discretisation" method has been used to estimate contour maps of the mold filling dynamics. The position of the molten metal front is represented by isochronal lines plotted every 0.2 sec. Solidification rates of an aluminum alloy in sections of different thickness are studied and compared. The experimental results obtained in this study are compared to those predicted by prior numerical simulations.

#### 11:10 AM

Shear Behaviour of a Semi-Solid Al-Cu4.5 Wt.Pct Alloy in Relation to its Microstructure: *P.-D. Grasso*<sup>1</sup>; J.-M. Drezet<sup>1</sup>; J.-D. Wagnière<sup>1</sup>; M. Rappaz<sup>1</sup>; <sup>1</sup>Ecole Polytechnique Fédérale de Lausanne (EPFL), Computational Matls. Lab. (LSMX), MX-G, CH-1015 Lausanne Switzerland

The secondary creep rate for an Al-Cu4.5 wt.pct alloy in the semisolid state has been measured for different microstructures: equiaxed, columnar parallel to the shear plane and columnar perpendicular to the shear plane. These microstructures have been obtained by casting the alloy either with grain refiner to get the equiaxed structure or without to get the columnar one. In the latter case, the cooling has also been adapted in order to obtain the right direction of the columnar grains with regard to the shear plane. From these castings, a sample consisting of an hollow cylinder with a reduced section at mid-height has been machined. The heating of the sample is provided by an induction coil up to a given temperature and the application of the torsion is done by using a pneumatic motor directly fixed on the sample. Different torques and temperatures corresponding to solid fractions higher than 85% are investigated in order to study the different parameters of a classic creep Norton law. Moreover, the influence of the microstructure on the mechanical behaviour of the mushy alloy is discussed. This study was carried out within the framework of the VIR[CAST] project, in which the problem of hot tearing is addressed.

# Surfaces and Interfaces in Nanostructured Materials: Self-Organized and Biological Materials

Sponsored by: Materials Processing and Manufacturing Division, MPMD-Surface Engineering Committee

*Program Organizers:* Sharmila M. Mukhopadhyay, Wright State University, Department of Mechanical and Materials Engineering, Dayton, OH 45435 USA; Arvind Agarwal, Florida International University, Department of Mechanical and Materials Engineering, Miami, FL 33174 USA; Narendra B. Dahotre, University of Tennessee, Department of Materials Science & Engineering, Knoxville, TN 37932 USA; Sudipta Seal, University of Central Florida, Advanced Materials Processing and Analysis Center and Mechanical, Materials and Aerospace Engineering, Oviedo, FL 32765-7962 USA

Thursday AM	Room: 217A
March 18, 2004	Location: Charlotte Convention Center

Session Chair: Sudipta Seal, University of Central Florida, Advd. Matls. Procg. & Analysis Ctr., Oviedo, FL 32765-7962 USA

#### 8:30 AM

**Tribological Properties of Diamondlike Carbon-Metal Nanocomposites:** *Roger Jagdish Narayan*<sup>1</sup>; 'Georgia Institute of Technology, Sch. of Matls. Engrg., Rm. 361, Love Bldg., 771 Ferst St. NW, Atlanta, GA 30332-0245 USA

450

Diamondlike carbon (DLC) consists mainly of sp^3-bonded carbon atoms. DLC coatings possess properties close to diamond in terms of hardness, atomic smoothness, and chemical inertness. Unfortunately, DLC exhibits poor adhesion to metals and polymers. This research involves processing, characterization and modeling of DLC nanocomposite films specifically to improve adhesion and wear properties. A novel target design was adopted to incorporate noncarbon atoms into the DLC films during pulsed laser deposition. STEM-Z contrast and PEELS techniques elucidated atomic structure and bonding characteristics. Wear and adhesion tests demonstrate DLC nanocomposites possess greatly improved mechanical properties. Careful analysis of the Raman data also indicates a significant shift to shorter wavelength with the addition of metal, indicating a reduction in compressive stress. By varying the metal concentration as a function of distance from the interface, it is possible to create a functionally gradient DLC film. These nanocomposite coatings have multiple biomedical applications.

#### 8:55 AM

**DNA-Grafting as a Controlled Nano-Interface**: *Eric Geiss*<sup>1</sup>; Sejong Kim<sup>2</sup>; Fotios Papadimitrakopoulos<sup>2</sup>; Harris L. Marcus<sup>1</sup>; <sup>1</sup>University of Connecticut, Inst. of Matls. Sci., Metall. & Matls. Engrg. Dept., U3136, Storrs, CT 06269-3136 USA; <sup>2</sup>University of Connecticut, IMS Polymer Prog. & Chmst. Dept., U3136, Storrs, CT 06269-3136 USA

Recently, DNA hybridization has been increasingly adopted in materials sciences due to its capability of specific and reversible molecular recognition. These unique properties of DNA have been used for the realization of 2-D assembly of colloidal particles as a precursor to constructing 3-D photonic crystal in a layer-by-layer manner. In order to precisely understand this DNA-assisted assembly of colloidal particles we have quantitatively assessed the surface density of grafted and hybridizing accessible DNA oligomers as the controlled nano-interface on both substrate and colloidal particles. The variations of the concentration of hybridized DNA as a function of parameters such as the number of DNA base pairs, the length of spacer and the size of particle were also investigated to determine the thermal stability and the immobilization strength of colloidal particles on various surfaces.

### 9:20 AM

#### Building Microstructures of Organized Carbon Nanotubes by Chemical Vapor Deposition: *Zhengjun Zhang*<sup>1</sup>; Ye Zhao<sup>1</sup>; Ya Zhou<sup>1</sup>; <sup>1</sup>Tsinghua University, Dept. of Matls. Sci. & Engrg., Beijing 100084 China

Chemical vapor deposition (CVD) using ferrocene (Fe(C5H5)2) and xylene (C8H10) is an economic way to grow carbon nanotubes and is frequently employed to fabricate, and to investigate the growth mechanism of nanotubes on planar substrates. The growth of carbon nanotubes by this approach, as we observed, showed interesting selforganization behaviors at early growth stages, which is closely related to the ratio of catalyst over carbon. Investigation on the very early deposition stages of this CVD means demonstrated that, the selforganization of carbon nanotubes is determined by the way that the catalyst particles adhere to the substrate surface, and the growth kinetics following. This provides ways to control the growth and selforganization of carbon nanotubes. For instance, one might control the adhesion of catalyst particles at the very early deposition stage or the growth kinetics shortly afterwards, to tune the self-organization of nanotubes to build microstructures of organized carbon nanotubes. By adjusting the growth kinetics of carbon nanotubes at the early deposition stages, we successfully fabricated different microstructures of carbon nanotubes on planar silicon substrates.

#### 9:45 AM

HA/DLC Nanocomposite Coatings for Improved Bioactivity and Biocompatibility of Orthopaedic Prostheses: *Bryan F. Bell*<sup>1</sup>; Roger J. Narayan<sup>1</sup>; <sup>1</sup>Georgia Institute of Technology, Sch. of Matls. Engrg., Rm. 361, Love Bldg., Atlanta, GA 30332-0245 USA

Bioactive coatings made of hydroxyapatite (HA) mimic the mineral composition of natural bone. Unfortunately, problems with adhesion, poor chemical and mechanical integrity, and incomplete bone ingrowth limit the use of current hydroxyapatite surfaces. We have developed a novel technique using pulsed laser deposition to produce bioactive hydroxyapatite surfaces on a diamondlike carbon (DLC) interlayer. DLC is an amorphous, hydrogen-free, and primarily sp3bonded form of carbon that exhibits exceptional biocompatibility, wear and corrosion resistance, and mechanical properties. The underlying titanium substrate is first coated with silver-doped DLC using pulsed laser deposition (PLD). The silver dopant aids in adhesion and conveys antimicrobial properties to DLC. The DLC surface is then coated with HA to form the final bilayer material. The films were characterized using SEM, TEM, XRD, Raman spectroscopy, and mechanical testing. HA/DLC bilayers are promising for use in several different orthopaedic implant designs.

# The Role of Grain Boundaries in Material Design: Simulation of Grain Boundary Effects of Properties

Sponsored by: Materials Processing and Manufacturing Division, ASM/MSCTS-Texture & Anisotropy Committee, MPMD-Computational Materials Science & Engineering-(Jt. ASM-MSCTS) *Program Organizers:* Brent L. Adams, Brigham Young University, Department of Mechanical Engineering, Provo, UT 84602-0001 USA; Thomas R. Bieler, Michigan State University, Department of Chemical Engineering and Materials Science, East Lansing, MI 48824-1226 USA

Thursday AM	Room: 2	18A
March 18, 2004	Location:	Charlotte Convention Center

Session Chairs: Christopher A. Schuh, Massachusetts Institute of Technology, Dept. of Matls. Sci. & Engrg., Cambridge, MA 02139 USA; Thomas A. Mason, Los Alamos National Laboratory, Matls. Sci. & Tech., Los Alamos, NM 87545 USA

# 8:30 AM A.D. Rollett Texture Optimization via Grain Growth and Recrystallization

#### 8:55 AM Invited

Insights on Deformation Modes in Hexagonal Metals and Constitutive Modeling: *Thomas A. Mason*<sup>1</sup>; Benjamin L. Hansen<sup>1</sup>; Benjamin L. Henrie<sup>1</sup>; George C. Kaschner<sup>1</sup>; <sup>1</sup>Los Alamos National Laboratory, Matls. Sci. & Tech., MS G755, Los Alamos, NM 87545 USA

The classic works of Kocks, Argon, Ashby and Mecking have used a constitutive model based on internal state variables to model the plastic response of many materials. Difficulty arises when this method is extended to lower symmetry metals where a number of deformation modes contribute to the strain accommodation. Additionally, the activities of the individual modes are strain-rate and temperature dependent and are strongly influenced by the crystallographic texture. This presentation will describe an effort to first quantify and then predict the deformation mode activities in textured hexagonal metals for a variety of deformation rates and temperatures. This is work comprises efforts in quantification of twin area fractions, connection of this information to hardening behaviors and finally to development of a robust, expanded capability to deal with hardening and softening behaviors more complex than the traditional, scalar Voce law.

#### 9:20 AM

Atomic Modeling of the Effects of C and H Impurities on the Grain Boundary Fracture in bcc Fe: Margarita Ruda<sup>1</sup>; Diana Farkas<sup>2</sup>; <sup>1</sup>Centro Atomico Bariloche, CNEA, Bariloche, Rio Negro Argentina; <sup>2</sup>Virginia Tech, Matls. Sci. & Engrg., Blacksburg, VA 24061 USA

We investigated the fracture behavior of a symmetrical tilt [001] (310) grain boundary in bcc iron using atomistic simulation techniques. The effects of interstitial impurities including H and C on grain boundary cohesion and fracture behavior were studied using empirical interatomic potentials. Hydrogen was found to decrease grain boundary cohesion and promote grain boundary fracture, while carbon has the opposite effect.

#### 9:40 AM

Modeling Dislocation Interaction With Grain Boundaries Using Dislocation Dynamics: *Tariq Khraishi*<sup>1</sup>; Yu-Lin Shen<sup>1</sup>; <sup>1</sup>University of New Mexico, Mech. Engrg. Dept., MSC01-1150, Albuquerque, NM 87131 USA

In this work, some preliminary attempts at modeling the dynamic interaction of dislocations with grain boundaries are presented. The modeling technique is that of newly developed dislocation dynamics. The results show interesting micromechanical features of the elastic fields of the boundaries as well as the salient features of their interaction with dislocations. Most importantly, the effect of grain boundaries on the strengthening of crystals is exhibited in a parametric study.

#### 10:00 AM Break

# 10:20 AM Invited

Scaling Laws for Grain Boundary Networks: Megan Frary<sup>1</sup>; *Christopher A. Schuh*<sup>1</sup>; <sup>1</sup>Massachusetts Institute of Technology, Dept. of Matls. Sci. & Engrg., 77 Mass. Ave., Rm. 8-211, Cambridge, MA 02139 USA

Grain boundary networks have frequently been described using concepts from percolation theory, although their topologies are highly nonrandom due to crystallographic constraints. Recent works have identified numerical values for the percolation thresholds of various grain boundary networks, but this value represents only the very beginning of a comprehensive theory of network topology. Here we consider several other aspects of the grain boundary percolation problem using Monte Carlo simulations, including the distribution of boundary cluster sizes, their radii of gyration, and the fractal character of the network. In particular, we focus upon the set of universal scaling laws that link these descriptors, and which are expected to be independent of the shape of the lattice. We compare the scaling laws obeyed for nonrandom grain boundary networks to the "universal" scaling laws usually applicable to random networks, and discuss how crystallography influences these relationships. Finally, we consider the practical relevance of scaling relationships in materials design, especially with regard to small-scale structures.

#### 10:45 AM

Capturing the Role Grain Boundaries in Microstructure-Based Finite Element Models: W. A. Counts<sup>1</sup>; C. C. Battaile<sup>1</sup>; M. V. Braginsky<sup>1</sup>; T. E. Buchheit<sup>1</sup>; <sup>1</sup>Sandia National Laboratories, Albuquerque, NM USA

A microstructure-based finite element model that does not incorporate appropriate length scales cannot capture important experimentally observed phenomena linked to material microstructure. Examples include: grain boundary strengthening and deformation evolution of microstructure that leads to the development of subgrains. To overcome this deficiency, two different approaches have been developed and incorporated into a microstructure-based polycrystal plasticity finite element model: (1) a grain boundary offset model, and (2) a nonlocal integral model. In the grain boundary offset model, the length scale is the result of ad-hoc strengthening of the material near the grain boundary. Conversely, in the nonlocal integral model, a length scale falls out of an integral approximation of the strain gradient and the associated geometrically necessary dislocations (GND's). The results of these two approaches will be compared to each other and to experiments to determine if either or both approaches can provide an accurate and computationally viable method to capture the role of grain boundaries in polycrystalline materials. Sandia is a multiprogram laboratory operated by Sandia Corporation, a Lockheed Martin Company, for the United States DOE under Contract DE-ACO4-94-AL85000.

#### 11:05 AM Invited

Software of Simulation of Oxidation Processes: Jerzy A. Szpunar<sup>1</sup>; Hualong Li<sup>2</sup>; <sup>1</sup>McGill University, Dept. Matls. Sci. & Engrg., 3610 Univ. St., Montreal, Quebec H3A 2B2 Canada; <sup>2</sup>ResMat Corp., 3637 Univ. St., Montreal, Quebec H3A 2B3 Canada

A discrete simulation methodology has been developed that incorporates many structural characteristics of polycrystalline material properties, such as, texture, grain boundary, microstructure, phase composition, chemical composition, stored energy, and residential stress. The computer models developed to study oxidation process is based on quantitative description of oxide and substrate structure. That description allows to simulate the transport of metal and oxygen ions along interfaces and bulk portion of materials. The proposed model help researchers and engineers to understand physical mechanism of oxidation, predict material behaviour, and optimize material processing and properties. In this paper, we will present the results of simulation results of oxidation process on different substrate of Zr-Nb alloys, which are used for manufacturing the pressure tube in CANDU nuclear reactors. The effects of substrate texture, microstructure, grain boundary, and beta phase distribution on oxidation kinetics and hydrogen permeation will be demonstrated.

#### 11:30 AM

**Software of Simulation of Recrystallization Process**: *Hualong Li*<sup>1</sup>; JongTae Park<sup>2</sup>; Jerzy A. Szpunar<sup>3</sup>; <sup>1</sup>ResMat Corp., 3637 Univ. St., Montreal, Quebec H3A 2B3 Canada; <sup>2</sup>POSCO, Tech. Rsch. Lab., PO Box 36, Pohang, Kyoungbuk Korea; <sup>3</sup>McGill University, 3600 Univ. St., Montreal, Quebec H3A 2B2 Canada

A discrete simulation methodology has been developed that incorporates various structural characteristics of polycrystalline materials such as, texture, grain boundary, microstructure, phase composition, chemical composition, stored elastic energy, and residential stress. The computer models developed based on this microstructural description of polycrystalline materials have been used to simulate the processes of oxidation, grain growth, recrystallization, and diffusion. These models can help researchers and engineers to understand physical mechanism, predict material behaviour, and optimize material processing and properties. In this paper, we will present the results of simulation of recrystallization process in 1%Si and 2% Si steel. The deformation texture and microstructure, stored energy and the microstructure prior to deformation are among the major factors in determining the recrystallization texture, and grain growth and kinetics of structure transformation. The comparison of simulation with experimental results is presented.

# **General Poster Session**

Sponsored by: TMS Program Organizer: TMS, Warrendale, PA 15086 USA

Mon PM - Wed PM	Room: Ballroom Foyer
March 15-17, 2004	Location: Charlotte Convention Center

The Application of the Compositional-Spread Approach to the Discovery of Materials for MEMS: Ainissa G. Ramirez<sup>1</sup>; <sup>1</sup>Yale University, Mech. Engrg. Dept., 15 Prospect St., 209 Becton Ctr., New Haven, CT 06520 USA

The rapid growth of MEMS incites the need for the creation of new thin-film materials for these devices. One means of enabling this accelerated pace is through a high-throughput discovery tool called the compositional-spread technique. Using this technique, gold-cobalt thinfilm alloys for contact materials of MEMS microrelays were deposited and subjected to heat treatments for hardening by precipitates. Accordingly, a breadth of precipitation structures are formed in gold using varying cobalt amounts that can be simultaneously synthesized, heattreated, and characterized. These materials are then evaluated for mechanical hardness, conductivity, and composition using four-point probe, nanoindentation, and XPS. The compositional-spread approach was also applied to the development of robust TiNi shape-memory alloys for MEMS. Using MEMS test structures of various compositions, actuation properties can be rapidly mapped. From this method one can trend the material's structure-property relationship.

**The Fabrication of Sintered Metal Fibers for Sound Absorption**: *Bo-Young Hur*<sup>1</sup>; *DongIn Ha*<sup>1</sup>; <sup>1</sup>GyeongSang National University, Div. of Matls. Engrg., Kajoa-dong 900, Chin-ju, GyeongNam 660-701 S. Korea

Porous metals made from sintered particulates are already in widespread use for predominantly functional applications. These materials have low density, an outstanding impact absorption, low conductivity of heat and electrical and superiority sound absorption etc. This study has been purposed for fabrication of sound absorbing materials. In order to making porous structure, firstly the aluminum fibers were fabricated by crucible melt extraction and then sintered. The meltextracted fibers typically show a sickle or kidney shaped cross-section. Mean equivalent fiber diameters and length are 150-350§- and 40-100mm, respectively. The porosity of these materials can be anywhere between 70 and 90%. Pore size is usually between 10-250§-. Depending on the porosity and fiber diameter. The sound absorption of porous structures is prominent on the high frequency region. The acoustic absorption peak tends to move toward low frequency region with the increasing the air gap.

Study on the Characteristics of Bake Hardenable Hot Dip Galvannealed Steel Sheet by the Continuous Galvanizing Line: Sang-hun Cho<sup>1</sup>; Bo-Young Hur<sup>1</sup>; Hiroshi Arai<sup>1</sup>; <sup>1</sup>Gyeongsang National University, Metallurgl. & Matl. Engrg., Kajoa-Dong 900, Chinju, Gyeongnam 660-701 S. Korea

The purpose of this work was to identify the influence of different process variables, such as soaking section temperature (SST), rapid cooling start temperature(RCST), galvannealed temperature(GT), cooling rate(CR), on the morphology, precipitation, BH(Baking hardenable), AI(Aging index), Mechanical properties, and coating layer properties attained changing different processes. The data of these operational variables were reported for each process. TEM/EDS were used to characterize the precipitation in the metallic samples Tensile test was used to measure the BH, AI, and mechanical properties. The amount of interstitial carbon the most important determining value of BH was measured by internal friction test (IFT). also SEM, XRD, and bending tests were performed, in order to evaluate the coating layer.

Foaming Characterization, Rheological, Mechanical Properties of Al Alloy Foam: *Bo-Young Hur*<sup>1</sup>; Soo-Han Park<sup>1</sup>; Arai Hiroshi<sup>1</sup>; Sang-Youl Kim<sup>1</sup>; <sup>1</sup>GyeongSang National University, Div. of Matls. Engrg., Kajoadong, 900, Chinju, Gyeongnam 660-701 S. Korea

Aluminum foam metal was produced by directly Melt Foaming Method. In this foaming process, the surface tension and the viscosity of molten Al that were measured by the ring method and the rotational method, respectively, are the two most important factors. The surface tension and the viscosity were investigated at the temperature range of 933~1223K and the effects of the additional Elements were investigated. The measured surface tension and viscosity of the molten Al alloy decreased with the increasing temperature in Ar(or oxidation) atmosphere and 1atm. Mechanical properties of metal foam depend on cell type, shape, size, homogeneity, surface area and relative density. Deformation of metal foams includes the plastic deformation and collapse and shows a plateau area followed by yielding point.

The Effect of Twinning on the Work Hardening Behavior of Hafnium: Clarissa A. Yablinsky<sup>1</sup>; Ellen K. Ceretta<sup>2</sup>; George T. Gray<sup>2</sup>; Benjamin L. Hansen<sup>2</sup>; <sup>1</sup>Carnegie Mellon University, Matls. Sci. & Engrg. Dept., 3325 Wean Hall, Pittsburgh, PA 15230 USA; <sup>2</sup>Los Alamos National Laboratory, MST-8, MS G755, Los Alamos, NM 87545 USA

The work hardening behavior of HCP metals, such as hafnium, is influenced by slip and twin interactions. While twinning is more likely to occur at low temperatures, high strains, and high strain rates, slip dominates at relatively higher temperatures, lower strains, and lower strain rates. In this study, hafnium was prestrained quasi-statically in compression at liquid nitrogen temperature (77K), creating heavily twinned specimens. The specimens were then reloaded in compression at room temperature. Yield stress, flow stress, and work hardening behaviors of the prestrained specimens were compared to a compression test done at room temperature (298K). The microstructure of each specimen was characterized optically and with the transmission electron microscope. Slip and twinning interactions were examined and the evolution of the microstructure was correlated with the work hardening behavior of the material.

Metallurgical Analysis of Spallation Damage in Copper as a Function of Shock Wave Profile Shape: Clarissa A. Yablinsky<sup>1</sup>; Laura B. Addessio<sup>2</sup>; Ellen K. Cerreta<sup>2</sup>; George T. Gray<sup>2</sup>; Robert S. Hixson<sup>3</sup>; Paulo A. Rigg<sup>3</sup>; Benjamin L. Henrie<sup>2</sup>; <sup>1</sup>Carnegie Mellon University, Matls. Sci. & Engrg. Dept., 3325 Wean Hall, Pittsburgh, PA 15230 USA; <sup>2</sup>Los Alamos National Laboratory, MST-8, MS G755, Los Alamos, NM 87545 USA; <sup>3</sup>Los Alamos National Laboratory, DX-2, MS P952, Los Alamos, NM 87545 USA

Many experimental investigations of dynamic damage (spall) have been done using gun-driven flat top shock waves to generate release waves that interact and cause tension. Such localized tensile pulses can cause damage to occur, and may cause the target to separate into two pieces. Metals that are subjected to shock loading as a result of being in contact with a detonating high explosive are well known to exhibit a triangular ("Taylor-wave") loading/unloading profile. Metallurgical analysis of the damage evolution in shock prestrained samples was conducted to compare the differences in the microstructure caused by each of the profiles. The microstructure of each specimen was characterized optically in an unetched and etched state. EBSD was utilized to quantify the details of damage evolution commensurate with void formation, strain localization, and cracking in the spalled samples.

Electrochemical Evaluation of Diamond-Like Carbon (DLC) Films Deposited on STS 316L and Ti Alloy for Biomedical Application: *Ho-Gun Kim*<sup>1</sup>; Seung-Ho Ahn<sup>1</sup>; Jung-Gu Kim<sup>1</sup>; Se-Jun Park<sup>2</sup>; Kwang-Ryeol Lee<sup>2</sup>; <sup>1</sup>SungKyunKwan University, Dept. of Advd. Matls. Engrg., 300 Chunchun-Dong, Jangan-Gu, Suwon, Kyounggi-Do 440-746 Korea; <sup>2</sup>Korea Institute of Science and Technology, Future Tech. Rsch. Div., PO Box 131, Cheongryang, Sungbuk-Gu, Seoul 130-650 Korea

Diamond-like carbon (DLC) films have several advantages in applications such as high hardness, chemical inertness, low friction and good adhesion properties to several methods. Furthermore, DLC coated STS 316L and Ti alloy (Ti6Al4V) films have been reported to have good biocompatibility, such as the absence of inflammatory response. Thus, corrosion resistance is the first consideration for the biomaterials to be used in the body. DLC films have been deposited onto substrates of STS 316L and Ti alloy using r.f PACVD with  $C_6H_6$  as the process gas. Corrosion behavior of DLC films was investigated by electrochemical techniques (potentiodynamic polarization test, electrochemical impedance spectroscopy) and surface analyses (AFM, SEM, RBS). The electrolyte used in this test was a 0.89% NaCl of pH 7.4 at temperature 37°C. Electrochemical measurements showed that DLC films on STS 316L and Ti alloys with higher bias voltage could improve corrosion resistance in the simulated body fluid environment.

Relationship of Surface Morphology and Electrical Properties of SnO2 Thin Films: Gwang Pyo Choi<sup>2</sup>; Hyun Wook Ryu<sup>2</sup>; Woo Sun Lee<sup>3</sup>; Jin Seong Park<sup>1</sup>; <sup>1</sup>Chosun University, Matls. Engrg., 375 Seosuk Dong, Gwangju 501-759 S. Korea; <sup>2</sup>Chosun University, RIERT, 375 Seosuk Dong, Gwangju 501-759 S. Korea; <sup>3</sup>Chosun University, Elect. Engrg., 375 Seosuk Dong, Gwangju 501-759 S. Korea

#### Thin films of SnO2 with the thickness of 50 to 200nm were deposited by r.f. magnetron sputter to investigate the relationship of a microstructure and an electrical property. The films deposited on SiO2/ Si-substrate were annealed at 500°C and 700°C for 12hr in air and N2 atmosphere to control the microstructure and morphology. XRD, FE-SEM, Ellipsometer, XPS were used to analyze the material properties. I-V characteristics was measured to evaluate the relationship between them and the electrical properties. The morphology and the thickness of the films were varied with the mixing ratios of Ar and O2 during film deposition and with the annealing conditions. Cauliflower-like grain aggregated tiny grains after annealing was decomposed into tiny single grains and the roughness was increased. I-V characteristics was stabilized with air annealing at 500°C. This study was supported by a Korea research foundation grant (KRF-2002-005-D00012).

Influence of the Sputtering Gas on the Preferred Orientation of NiO Thin Films: Hyun Wook Ryu<sup>2</sup>; Gwang Pyo Choi<sup>2</sup>; Woo Sun Lee<sup>3</sup>; Jin Seong Park<sup>1</sup>; <sup>1</sup>Chosun University, Matls. Engrg., 375 Seosuk Dong, Gwangju 501-759 S. Korea; <sup>2</sup>Chosun University, RIERT, 375 Seosuk Dong, Gwangju 501-759 S. Korea; <sup>3</sup>Chosun University, Elect. Engrg., 375 Seosuk Dong, Gwangju S. Korea

Nickel oxide (NiO) thin films were prepared on Si(100) substrates at room temperature by RF magnetron sputtering using a NiO target. The relationship between sputtering gases, and preferred orientation and surface morphology of the NiO films was investigated. (100) and (111) preferred orientations of NiO films were controlled by changing the sputtering gas. Highly crystalline NiO film with (100) orientation was obtained when it deposited in pure Ar gas. For NiO films weages, the origin of the preferred orientation of the films changed from (100) to (111) and their deposition rate decreased. The origin of the preferred orientation of the films with both (100) and (111) orientation had columnar structure. However, the films showed different surface morphologies and roughnesses with the type of sputtering gases. This study was supported by a Korea research foundation grant (KRF-2002-005-D00012).

Mechanical Behavior of Zirconium and Hafnium in Tension and Compression: Laura Beth Addessio<sup>1</sup>; Ellen K. Cerreta<sup>1</sup>; George T. Gray<sup>1</sup>; <sup>1</sup>Los Alamos National Laboratory, MST-8, Bikini Atoll Rd., SM 30, MS G755, Los Alamos, NM 87545 USA

The mechanical behavior of zirconium and hafnium has been examined as a function of stress state. Tests were performed at room temperature in both tension and compression and the resulting microstructure was observed under optical and electron microscopes. The quasi-static work hardening rate as a function of strain for both metals exhibits a compression-tension asymmetry. While both Zr and Hf exhibit a concave down work hardening in tension, they display a parabolic and then linear upward work hardening behavior in compression. The stress-strain and strain hardening curves have been characterized in terms of deformation twinning differences. Further discussion includes the importance of slip and its interaction with twins as it relates to texture.

Analysis of Proposed Binary Eutectic Microstructure Classifications: Guillermo Salas<sup>1</sup>; Saúl Montejano<sup>1</sup>; *Maria Eugenia Noguez*<sup>1</sup>; José Ramírez<sup>1</sup>; <sup>1</sup>Universidad Nacional Autónoma de México, Facultad de Química, Edif. D, Circuito Institutos s/n, Cd. Universitaria, México, D.F. 04510 México

Two important works exist in literature presenting a characterization of eutectics: the one by Kurz and Fisher, where they divide them into regulars and irregulars depending on the entropy of fusion values, allowing a sub-classification based on volume fraction ranges. And the other by Dubey and Ramachandrarao, who focus the importance of the solid phases molar volume ratio, A. They find values for this ratio that determine the eutectic structures for specific ranges of volume fraction, arriving into a division between regular an irregular eutectics. In this work A and the entropies of fusion are calculated for reported classified eutectics. Then the two different proposals are analyzed finding that the thermodynamics is a more accurate factor to divide eutectics into regulars and irregulars, the volume fraction factor should be taken into account for a sub-classification and the molar volume ratio does not determine the microstructures.

Anomalous Nanostructured Titanium Dioxide: Parvesh Sharma<sup>1</sup>; <sup>1</sup>St. Stephen's College, Dept. of Chmst., University of Delhi, Delhi 110060 India

Titanium dioxide nanoparticles prepared in water-in-oil microemulsion droplets by controlled hydrolysis of TiCl4 generated

crystalline nanoparticles of sizes down from 115 nm to 6 nm diameter depending on the size of the aqueous core of the micellar droplets. Powder X-ray diffraction of the vacuum dried product (without sintering) indicated the presence of an unusual type of orthorhombic crystal structure nearly similar to titanium dioxide crystals prepared at high pressure. On gradual heating upto 9000C these metastable crystals are converted into relatively more stable nanorods perhaps through making and breaking of the Ti-O-Ti bonds. It has been concluded that a chemical pressure generated within the constrained volume of aqueous core of the reverse micellar droplets is responsible for the unusual crystal structure of TiO2 nanoparticles.

The Trends of China Alumina Production with Combined Process: *Qingjie Zhao*<sup>1</sup>; <sup>1</sup>Zhengzhou Research Institute Aluminum Corporation of China, Ltd., 82, Jiyuan Rd., Shangjie Dist., Zhengzhou, Henan 450041 China

Most of Chinese bauxite is diasporic bauxite, which has the characteristics of high alumina, high silicon and low iron. Furthermore, the impurity minerals of this bauxite are complex, so most of Chinese alumina is produced by the combined process or the sintering process with high energy consumption. To save energy and reduce costs, it is suggested that the present combined process be reconstructed with a parallel-combined process. Then the bauxite with Al2O3/SiO2 (A/S) weight ratio higher than 10 is dealt with by the Bayer process and the bauxite with A/S 5-8 by the sintering process. The concentration of green liquor in the sintering system is almost the same as that in the Bayer process, and the productivity of both present Bayer and sintering parts can be improved. An economic analysis shows that economic benefit can obviously be obtained. Therefore, the parallel-combined process is a suitable new way for reconstruction of present Chinese alumina production.

A Correlation Between Porosity Enlarged Ratio and Lifetime of Protective Coatings Through Electrochemical Techniques: Seung-Ho Ahn<sup>1</sup>; Jung-Ho Lee<sup>1</sup>; Ho-Gun Kim<sup>1</sup>; Jung-Gu Kim<sup>1</sup>; Ho-Young Lee<sup>1</sup>; Jeon-Gun Han<sup>1</sup>; <sup>1</sup>SungKyunKwan University, Dept. of Advd. Matls. Engrg., 300 Chunchun-Dong, Jangan-Gu, Suwon, Gyounggi-Do 440-746 Korea

The presence of porosity, such as closed pores, open pores and pinholes, in the coatings means that the film density and compactness is lower than that of the bulk materials. It is likely that a porous coated film will give rise to corrosion on the substrate surface through pores or pinholes as a result of attack by some chemicals. Thus, corrosionresistant coatings are mainly controlled by the amount of porosity. In recent literature, various electrochemical methods have been tried to determine through-coating porosity. Especially, the electrochemical impedance spectroscopy (EIS) data were used to predict through-porosity in coatings. The accuracy porosity measurements of coatings are affected by the trend of porosity enlarged ratio (Pe) and charge transfer resistance (R<sub>ct</sub>) as a function of immersion time. In this paper, we are tried to study the quantitative and sensitive methods on the porosity measurement, and to investigate the correlation between porosity enlarged ratio and lifetime of protective coatings using electrochemical techniques.

The Effect of Texture on Deformation Behavior in Zr-2.5%Nb Materials at RT: *SungSoo Kim*<sup>1</sup>; KyungSoo Lim<sup>1</sup>; Yong Moo Cheong<sup>1</sup>; Young Suk Kim<sup>1</sup>; <sup>1</sup>Korea Atomic Energy Research Institute, Reactor Mata.1, PO Box 105, YouSung Post Office, Taejon 305-353 Korea

The deformation behavior was investigated through the tensile tests in the Zr-2.5%Nb material with a different texture in order to understand deformation mechanisms at room temperature. The change in texture and in microstructure with the tensile strain was examined by the inverse pole figure measurement and the TEM, respectively. The results showed that the deformation mechanisms involved in the tensile strain were identified to be both twinning and slip. The degree of change in texture in the direction having a higher basal pole component was appeared to be high due to the operation of twinning. The stress-strain curve varied with texture significantly, since the deformation mechanisms were reflected directly in the curves. It is appeared that the work hardening behavior was affected by both the multiplication of dislocation and the operation of twinning. The contribution and importance of twinning on the tensile deformation of the Zr-2.5%Nb materials were discussed.

**Recycling of Ultra-Fine Fibrous Materials**: Seong Hun Kim<sup>1</sup>; <sup>1</sup>Hanyang University, Fiber & Polymer Engrg., Sung dong gu, Seoul 133-791 S. Korea

Diameter of ultra-fine fiber is smaller than human-hair as single unit micron meter. The ultra-fine fibrous materials has various applications, such as high performance wiping cloths with wiping performance and water absorption, sound proofing materials, and moisture transfer garments, etc. The production expense of the ultra-fine fibers is 5 to 7 times higher than general textile materials. The high value added fibrous materials should not be land filled and re-extrusion process, which are not saving technology of natural resources. The presentation suggests the unique and cost-effective technology of recycling for the ultra-fine fibrous materials. The presented technology withholds long and fine structure of the fibrous materials to save production and labor expenses to prepare the ultra-fine fibrous materials. Newly designed and developed recycling equipments and application of the recycled fibrous materials will be introduced.

Structure and Optical Properites of Zn(1-x)Mg(x)O Thin Film Deposited on Sapphire by Metal Organic Chemical Vapor Deposition: Sun-hong Park<sup>1</sup>; Seon-hyo Kim<sup>1</sup>; Chan-hyuk Park<sup>1</sup>; Ko-gi Lee<sup>1</sup>; <sup>1</sup>Pohang University, Environment Engrg. & Tech., Hyoja-dong, Namgu, Pohang, Kyoung-buk 790-784 S. Korea

High-quality Zn1-xMgxO(0.0; Üx; Ü0.45)thin films were epitaxially growth on (0001)-oriented Al2O3 substrate using metal organic chemical vapor deposition. The optical and structural properties were studied by using transmittance spectrum and XRD measurement. The obtained Zn1-xMgxO films were oriented to (0001) with their crystal property improving with increasing substrate temperature in 300-700; aC range. The band gap of ZnMgO films can be changed between 3.36 and 4.0 eV by adapting the Mg propertion. This result shows a remarkable blueshift. Transmittance spectroscopy was used to characterize to charactrize the excitonic structure of the alloys and photoluminescent properties of the films are also discussed.

Study on Magnetocaloric GdSiGe Thin Films for Microcooling Applications: Senthil N. Sambandam<sup>1</sup>; Shekhar Bhansali<sup>2</sup>; Venkat R. Bhethanabotla<sup>3</sup>; <sup>1</sup>University of South Florida, Elect. Engrg. & Chem. Engrg., ENB 118, 4202 E. Fowler Ave., Tampa, FL 33620 USA; <sup>2</sup>University of South Florida, Elect. Engrg., 4202 E. Fowler Ave., Tampa, FL 33620 USA; <sup>3</sup>University of South Florida, Chem. Engrg., 4202 E. Fowler Ave., Tampa, FL 33620 USA

Microcooling has been the subject of intense research activity recently owing to their potential applications in electronic chip cooling, laser cooling, liquefaction, and in satellites. We present our work towards the development of a magnetocaloric microrefrigerator for the cooling applications. This concept utilizes the adiabatic temperature change of a magnetic alloy upon exposure to a magnetic field resulting from a simultaneous, nearly first order, magnetic and crystallographic phase change. Towards this goal, we prepared thin films of Gd5Si2Ge2 by RF sputtering from a stoichiometric target in an argon atmosphere and studied their properties. Films were prepared at different sputtering pressures in the range of 0.01 to 0.1 Torr and substrate temperatures ranging from 400 to 700°C with subsequent annealing in vacuum at 1300°C. Crystallinity and phase formation in these films were studied by x-ray diffraction and composition by energy dispersive analysis by x-rays. Films prepared at lower substrate temperatures showed a mixture of GdSi and GdGe phases predominantly and upon annealing transformed into the desired Gd5Si2Ge2 phase. Effect of sputtering pressure on the crystallinity was minimal and no significant changes in structure were observed. However, sputtering pressure influenced phase formation. Magnetization and magnetocaloric measurements performed on these films showed a sharp transition near 250 K from paramagnetic to ferromagnetic state and the material exhibited a giant magneto caloric effect. These preliminary studies show that Gd5Si2Ge2 thin films exhibiting the desired magnetocaloric properties for use in MEMS microcoolers.

**Dissolution Kinetics of Fe-Cr Alloys in Molten Aluminum:** *V. I. Dybkov*<sup>1</sup>; K. Barmak<sup>2</sup>; <sup>1</sup>Institute for Problems of Materials Science, Dept. of Phys. Chmst. of Inorganic Matls., Kyiv 03180 Ukraine; <sup>2</sup>Carnegie Mellon University, Dept. of Matls. Sci. & Engrg., 5000 Forbes Ave., Pittsburgh, PA 15213 USA

To evaluate the thickness of dissolved Fe-Cr alloys during their hot-dip aluminizing and the extent of saturation of the aluminum bath with the alloy constituents, experimental data on the dissolution kinetics of the solid-alloy base in the aluminum melt are needed. The dissolution kinetics of Fe-Cr alloys containing up to 25 mass% chromium in an aluminum melt is found by the rotating-disc technique to be non-selective, that is, iron and chromium atoms pass into the bulk of molten aluminum in that ratio in which they are present in the initial alloy. Experimentally determined values of the saturation concentration (solubility) and the dissolution rate-constant of iron and chromium in liquid aluminium for the Fe-Cr alloys are presented. The data obtained can also be employed to evaluate the effect of dissolution on the growth rate of intermetallic layers at the interface between an iron-chromium alloy and molten aluminum. Growth Kinetics of Intermetallic-Compound Layers at the Interface Between Fe-Cr Alloys and Molten Aluminum: V. I. Dybkov<sup>1</sup>; K. Barmak<sup>2</sup>; <sup>1</sup>Institute for Problems of Materials Science, Dept. of Phys. Chmst. of Inorganic Matls., Kyiv 03180 Ukraine; <sup>2</sup>Carnegie Mellon University, Dept. of Matls. Sci. & Engrg., 5000 Forbes Ave., Pittsburgh, PA 15213 USA

Two intermetallic layers  $Fe_2AI_5$  and  $Fe_2AI_7$  are experimentally found to occur between iron-chromium alloys containing up to 25 mass% Cr and a saturated aluminum melt at 700 °C. Under conditions of simultaneous dissolution in pure liquid aluminum, only the  $Fe_2AI_5$  phase forms an adherent layer, whereas the  $Fe_2AI_7$ ,  $FeAI_3$ ,  $FeAI_6$ ,  $CrAI_7$  and other phases exist as inclusions in the aluminum matrix. Dissolution of the Fe-Cr alloy base into molten aluminum causes a many-fold decrease in layer thickness compared with the case where no dissolution occurs. A simple equation for evaluating the  $Fe_2AI_5$  layer thickness during dissolution is proposed. Making the Fe-Cr alloy-to-aluminum transition joints, with the mechanical strength of the joint greater than or equal to that for pure aluminum, appears to be feasible.

The Prevention of Crack Formation at the Interface of Friction Welded TiAl and AISI 4140 Steel: *Won-Bae Lee*<sup>1</sup>; Seung-Boo Jung<sup>1</sup>; *Ja-Myung Koo*<sup>1</sup>; *Jong-Woong Kim*<sup>1</sup>; <sup>1</sup>Sungkyunkwan University, Advd. Matls. Engrg., 300, Cheoncheon-dong, Jangan-gu, Suwon, Kyounggido 440-746 Korea

The microstructural change and mechanical properties of friction welded TiAl alloy/AISI 4140 joint have been investigated with various friction welding conditions for example friction time, friction pressure and upset pressure. At the peripheral side of the joint, crack was observed because of brittle nature of TiAl and internal stress of transformed martensite. This defect cannot be avoidable and deteriorated the mechanical property of the friction welded joint. To prevent the formation of crack at the interface and minimize the brittle martensite phase, ductile copper was to use as stress release buffer layer. TiAl/ AISI 4140 joint was successfully joined using copper buffer layer without crack. The width of martensite structure of AISI 4140 steel side was also minimized.

Measure and Analysis of Copper Vapor in Helium GTA: Xu Chenming<sup>1</sup>; Gao Hongming<sup>1</sup>; Zhang Guangjun<sup>1</sup>; Wu Lin<sup>1</sup>; <sup>1</sup>Harbin Institute of Technology, Satl. Key Lab. of Welding Tech., W. Straight St., Harbin, Heilongjiang 150001 China

In this work, the copper spectrum were acquired in helium GTA by using the spectroscopy method under a variety of current. According to the spectral result, a copper spectral line with less disturbance was decided to obtain Cu single-spectral arc image. After the Abel inversion, the spatial distributions of metal vapor in the arc were obtained. The copper vapour mainly located on the surface of the pool. The vapour amount increased with the current and spread to the top of the arc. The effect of welding current on metal melting speed was evaluated also. This method proved to be effective in the real-time sensing.

Corrosion Characteristics of Copper Pipe in Potable Water System: Yoon Seok Choi<sup>1</sup>; Jae Joo Shim<sup>1</sup>; Dong Ho Shin<sup>1</sup>; Jung Gu Kim<sup>1</sup>; <sup>1</sup>Sung Kyun Kwan University, Advd. Matls. Engrg., 300 Chunchun-Dong, Jangan-Gu, Suwon 440-746 S. Korea

The aqueous corrosion characteristics of a copper were studied in synthetic tap water with velocity(0, 1 m/s), and temperature( $25, 60^{\circ}$ C). The electrochemical properties of specimens were investigated with a potentiodynamic test, potentiostatic test and electrochemical impedance spectroscopy. The corroded surfaces were examined by SEM and XPS. Result of potentiodynamic test showed that the corrosion rate was more sensitive to flow velocity than temperature, which increased with incresing flow velocity. Results of potentiostatic test and EIS measurement also indicated that solution temperature had a small effect on the corrosion resistance, whereas the flow velocity decreased corrosion resistance significantly. This effect can be explained by the increased solubility of copper oxide(Cu2O)at the presence of flow velocity, which is confirmed by SEM and XPS analyses.

Continuous Cooling Transformation Behaviors in Cast Duplex Stainless Steels CD3MN and CD3MWCuN: Yoon-Jun Kim<sup>1</sup>; L. Scott Chumbley<sup>1</sup>; Brian Gleeson<sup>1</sup>; <sup>1</sup>Iowa State University, Dept. of Matls. Sci. & Engrg., Ames, IA 50011 USA

The kinetics of sigma phase transformation in cast duplex stainless steels was investigated under isothermal and continuous cooling conditions. In order to obtain controlled high cooling rates, a furnace equipped to grow crystals by means of the Bridgmann method was used. Samples were soaked at 1100°C for 30 minutes and cooled at different rates by changing the furnace position at various velocities. The velocity of the furnace movement was correlated to a continuous-cooling-temperature profile for the samples. Cooling rates slower than 5°C/min. were obtained using a conventional tube furnace with a pro-

grammable controller. The experimental data were compared to theoretical calculations employing a modified Johnson-Mehl-Avrami (JMA) equation under assumption of the additivity rule. The parameters in the JMA equation were taken from the isothermal heat treatment. Continous-cooling-transformation (CCT) diagrams were constructed based on experimental observations. These are compared to calculated diagrams derived from previously determined isothermal transformation diagrams.

The Effect of Welding Parameters on the Microstructure and Microhardness of Resistance Spot Welded Galvannealed Steel Sheets: Cherqueta R. Claiborn<sup>1</sup>; Viola L. Acoff<sup>1</sup>; 'The University of Alabama, Dept. of Metallurgl. & Matls. Engrg., Box 870202, Tuscaloosa, AL 35487 USA

Galvannealed steel sheets were resistance spot welded to determine the effect of welding parameters on the microstructure and microhardness of galvannealed steel. The specimens were welded at various percent currents while holding all other parameters constant. Light microscopy, microhardness testing, scanning electron microscopy, and x-ray diffraction were used to characterize the welded samples. Microhardness measurements taken across the weld nugget of each sample showed an increase in the microhardness values as the percent current increased. The purpose of this study is to investigate the cause of the increase in microhardness.

# Index

# A

Aaronson, H I		186,	228,
			415
Abadias, G			429
Abbaschian, R 3	15	 277	
			420
Abe, E			295
Abe, T			420
Abedrabbo, S		180,	321
Abiko, T			366
Abinandanan, T A			181
Ablitzer, D			219
Abraham, T			209
Abu-Dheir, N M			450
Abu-Farha, F K			398
Acharjee, S			237
Ackland, G J			222
Acoff, V L 1	90.	237.	255,
			456
Adachi, H			
			314
Adam, G			406
Adamini, P			329
Adams, A N			217
Adams, B L		347,	390,
			451
1			394
			329
Adams, D P			
Adams, D P Adams, M			
Adams, D P Adams, M Adams, T M			321
Adams, D P Adams, M Adams, T M Addessio, L B		453,	
Adams, D P Adams, M Adams, T M Addessio, L B 2 Afshar, S	233,	453,	321
Adams, D P Adams, M Adams, T M Addessio, L B 2 Afshar, S Agarwal, A	233,	453, 301,	321 454
Adams, D P Adams, M Adams, T M Addessio, L B 2 Afshar, S Agarwal, A	233,	453, 301,	321 454 177 346,
Adams, D P Adams, M Adams, T M Addessio, L B 2 Afshar, S Agarwal, A	233,	453, 301, 428,	321 454 177 346, 450
Adams, D P Adams, M Adams, T M Addessio, L B 2 Afshar, S Agarwal, A	233,	453, 301, 428,	321 454 177 346, 450 264
Adams, D P Adams, M Adams, T M Addessio, L B 2 Afshar, S Agarwal, A Agarwal, S Aghion, E	233,	453, 301, 428, 333,	321 454 177 346, 450 264 375
Adams, D P Adams, M Adams, T M Addessio, L B 2 Afshar, S Agarwal, A Agarwal, S Aghion, E Agia, M	233,	453, 301, 428, 333,	321 454 177 346, 450 264 375 331
Adams, D P Adams, M Adams, T M Addessio, L B 2 Afshar, S Agarwal, A Agarwal, A Aghion, E Agia, M Agnew, S R 2	233,	453, 301, 428, 333, 256,	321 454 177 346, 450 264 375 331 287,
Adams, D P Adams, M Adams, T M Addessio, L B 2 Afshar, S Agarwal, A	233,  88,  233, 39,	453, 301, 428, 333, 256, 392,	321 454 177 346, 450 264 375 331
Adams, D P Adams, M Adams, T M Addessio, L B 2 Afshar, S Agarwal, A	233,  88,  233, 39,	453, 301, 428, 333, 256, 392,	321 454 177 346, 450 264 375 331 287,
Adams, D P Adams, M Adams, T M Addessio, L B 2 Afshar, S Agarwal, A	233,  88,  233, 39,	453, 301, 428, 333, 256, 392,	321 454 177 346, 450 264 375 331 287, 410 173
Adams, D P Adams, M Adams, T M Addessio, L B 2 Afshar, S Agarwal, A	233,  88,  233, 39,	453, 301, 428, 333, 256, 392,	321 454 177 346, 450 264 375 331 287, 410 173 437
Adams, D PAdams, MAdams, T MAdams, T MAdams, T MAddessio, L B2 Afshar, SAgarwal, A	233,  888, 233, 39,	453, 301, 428, 333, 256, 392,	321 454 177 346, 450 264 375 331 287, 410 173 437 349
Adams, D PAdams, MAdams, T MAdams, T MAdams, T MAdaessio, L B2 Afshar, SAgarwal, A		453, 301, 428, 333, 256, 392,	321 454 177 346, 450 264 375 331 287, 410 173 437 349 214
Adams, D PAdams, MAdams, T MAdams, T MAdams, T MAdaessio, L B2 Afshar, SAgarwal, A		453, 301, 428, 333, 256, 392, 426,	321 454 177 346, 450 264 375 331 287, 410 173 437 349 214 448
Adams, D PAdams, MAdams, MAdams, T MAdams, T MAdams, T MAdaesio, L B2 Afshar, SAgarwal, A		453, 301, 428, 333, 256, 392, 426,	321 454 177 346, 450 264 375 331 287, 410 173 437 349 214 448 221
Adams, D PAdams, MAdams, T MAdams, T MAdams, T MAdaessio, L B2 Afshar, SAgarwal, A		453, 301, 428, 333, 256, 392, 426,	321 454 177 346, 450 264 375 331 287, 410 173 437 349 214 448
Adams, D PAdams, MAdams, MAdams, T MAdams, T MAdams, T MAdaesio, L B2 Afshar, SAgarwal, A	233, 	453, 301, 428, 333, 256, 392, 426, 426, 453,	321 454 177 346, 450 264 375 331 287, 410 173 437 349 214 448 221
Adams, D P         Adams, M         Adams, T M         Adams, T M         Addessio, L B         Addessio, L B         Agarwal, S         Adams, B         Ahmed, F M         Ahn, J         Ahn, J         Ahn, J         Ahn, S         Ain, S		453, 301, 428, 333, 256, 392, 426, 453,	321 454 177 346, 450 264 375 331 287, 410 173 437 349 214 422 448 221 454 276
Adams, D PAdams, MAdams, T MAdams, T MAdams, T MAdams, T MAdams, T MAdams, T MAdams, SAgarwal, A		453, 301, 428, 333, 256, 392, 426, 453,	321 454 177 346, 450 264 375 331 287, 410 173 437 349 214 448 221 454 221 454 228
Adams, D PAdams, MAdams, T MAdams, T MAdams, T MAdams, T MAdams, T MAdams, T MAdams, SAgarwal, SAgarwal, A	233, 888, 233, 39,	453, 301, 428, 333, 256, 392, 426, 453,	321 454 177 346, 450 264 375 331 287, 410 173 437 349 214 448 221 454 228 381
Adams, D PAdams, MAdams, T MAdams, T MAdams, T MAdams, T MAdams, T MAdams, T MAdams, SAgarwal, A	233, 	453, 301, 428, 333, 256, 392, 426, 453, 380,	321 454 177 346, 450 264 375 331 287, 410 173 437 349 214 448 221 454 228 381 441
Adams, D PAdams, MAdams, T MAdams, T MAdams, T MAdams, T MAdams, T MAdams, T MAdams, SAgarwal, A	233, 	453, 301, 428, 333, 256, 392, 426, 453, 380,	321 454 177 346, 450 264 375 331 287, 410 173 437 349 214 454 221 454 228 381 441 437
Adams, D PAdams, MAdams, T MAdams, T MAdams, T MAdams, T MAdams, T MAdams, T MAdams, SAgarwal, A	233, 888, 233, 39,	453, 301, 428, 333, 256, 392, 426, 453, 380,	321 454 177 346, 450 264 375 331 287, 410 173 437 349 214 448 221 454 228 381 441
Adams, D PAdams, MAdams, T MAdams, T MAdams, T MAdams, T MAdams, T MAdams, T MAdams, SAgarwal, A	233, 888, 233, 39,	453, 301, 428, 333, 256, 392, 426, 453, 380,	321 454 177 346, 450 264 375 331 287, 410 173 437 349 214 454 221 454 228 381 441 437
Adams, D PAdams, MAdams, T MAgarwal, A	233, 	453, 301, 428, 333, 256, 392, 426, 453, 380, 210,	321 454 177 346, 450 264 375 331 287, 410 173 437 349 214 454 221 454 228 381 441 437 360
Adams, D PAdams, MAdams, T MAdams, T MAdams, T MAdams, T MAdams, T MAdams, T MAdams, SAgarwal, A	233, 	453, 301, 428, 333, 256, 392, 426, 453, 380, 210, 175,	321 454 177 346, 450 264 375 331 287, 410 173 437 349 214 448 221 454 228 381 441 437 360 353 215
Adams, D PAdams, MAdams, T MAdams, T MAdams, T MAdams, T MAdams, T MAddessio, L B2 Afshar, SAgarwal, A	233, 	453, 301, 428, 333, 256, 392, 426, 453, 380, 210, 175,	321 454 177 346, 450 264 375 331 287, 410 173 437 349 214 448 221 454 276 228 381 441 437 360 353 215 180
Adams, D PAdams, MAdams, T MAdams, T MAdams, T MAdams, T MAdams, T MAddessio, L B2 Afshar, SAgarwal, A	233, 	453, 301, 428, 333, 256, 392, 426, 453, 380, 210, 175, 	321 454 177 346, 450 264 375 331 287, 410 173 437 349 214 448 221 454 276 228 381 441 437 360 353 215 180 317
Adams, D PAdams, MAdams, MAdams, T MAdams, T MAdams, T MAdams, T MAdams, T MAdams, T MAgarwal, SAgarwal, A	233, 	453, 301, 428, 333, 256, 392, 426, 453, 453, 380, 210, 175, 	321 454 177 346, 450 264 375 331 287, 410 173 437 349 214 448 221 454 276 228 381 441 437 360 353 215 180 317 342
Adams, D PAdams, MAdams, T MAdams, T MAdams, T MAdams, T MAdams, T MAddessio, L B2 Afshar, SAgarwal, A	233, 	453, 301, 428, 333, 256, 392, 426, 453, 380, 210, 175, 	321 454 177 346, 450 264 375 331 287, 410 173 437 349 214 448 221 454 228 381 441 437 360 353 215 180 317 342 431
Adams, D PAdams, MAdams, T MAdams, T MAddessio, L B2Afshar, SAgarwal, A	233, 	453, 301, 428, 333, 256, 392, 426, 453, 453, 210, 175, 380, 375,	321 454 177 346, 450 264 375 331 287, 410 173 437 349 214 448 221 454 276 228 381 441 437 360 353 215 180 317 342 431 444
Adams, D PAdams, MAdams, T MAdams, T MAddessio, L B2Afshar, SAgarwal, A	233, 	453, 301, 428, 333, 256, 392, 426, 453, 453, 210, 175, 380,  3375, 	321 454 177 346, 450 264 375 331 287, 410 173 437 349 214 448 221 454 228 381 441 437 360 353 215 180 317 342 431
Adams, D PAdams, MAdams, T MAdams, T MAddessio, L B2Afshar, SAgarwal, A	233, 	453, 301, 428, 333, 256, 392, 426, 453, 453, 210, 175, 380, 210, 175, 375, 212,	321 454 177 346, 450 264 375 331 287, 410 173 437 349 214 448 221 454 276 228 381 441 437 360 353 215 180 317 342 431 444
Adams, D PAdams, MAdams, T MAdams, T MAdams, T MAdams, T MAdams, T MAdams, T MAdams, SAgarwal, A	233, 	453, 301, 428, 333, 256, 392, 426, 453, 453, 210, 175, 380, 210, 175, 375, 212,	321 454 177 346, 450 264 375 331 287, 410 173 437 349 214 448 221 454 276 228 381 441 437 360 353 215 180 317 342 431 444 230

Alex, T C		171
Alexander, D J	207.	253,
·		434
Alexandrov IV	255,	
Alexandrov, I V	252,	256,
	258,	306
Alfantazi, A M	280,	325,
	409,	444
Algoso, P R		345
Ali, M T		360
	177	
Allaire, C	1//,	178
Allaire, J		177
Allameh, S		308
Allen, S M		420
Allison, J E		375
Allocca, C M		414
Alman, D E		440
Almer, J D	272,	283
Alonso, F		218
Alpas A T	254	413
Alpas, A T Alpay, S P	201,	426
Alpay, 51		
Alsem, D		309
Altenhof, W		313
Altorfer, F		250
Alur, A P		316
Alven, D A		215,
	257	
	357,	400
Aly, I H		403
Amaranti, J		329
Amweg, M L		447
An, K		247
Anand, S		336
Andersen, F B		400
Anderson, A J		341
Anderson, I E	287,	295,
	377.	
	377,	420
	377,	420 408
	377,	420 408 364
	377,	420 408 364 411
	377,	420 408 364 411
	377,	420 408 364 411 213
	377,	420 408 364 411 213 212
	377,	420 408 364 411 213 212 436
	377,	420 408 364 411 213 212 436 271
	377,	420 408 364 411 213 212 436 271 329
	377,	420 408 364 411 213 212 436 271 329
	377,	420 408 364 411 213 212 436 271 329
	377,	420 408 364 411 213 212 436 271 329 247
	377, 	420 408 364 411 213 212 436 271 329 247 296 445
	377, 	420 408 364 411 213 212 436 271 329 247 296 445 449
	377, 	420 408 364 411 213 212 436 271 329 247 296 445 449 361
	377, 	420 408 364 411 213 212 436 271 329 247 296 445 449 361 317
	377, 	420 408 364 411 213 212 436 271 329 247 296 445 449 361 317 236,
	377, 	420 408 364 411 213 212 436 271 329 247 296 445 449 361 317 236,
	377, 295, 422, 427, 194, 378,	420 408 364 411 213 212 436 271 329 247 296 445 449 361 317 236, 420
	377, 295, 422, 427, 194, 378,	420 408 364 411 213 212 436 271 329 247 296 445 449 361 317 236, 420 397
	377, 295, 422, 427, 194, 378,	420 408 364 411 213 212 436 271 329 247 296 445 449 361 317 236, 420 397 359
	377, 295, 422, 427, 194, 378,	420 408 364 411 213 212 436 271 329 247 296 445 449 361 317 236, 420 397 359 222
	377, 295, 422, 427, 194, 378, 369,	420 408 364 411 213 212 436 271 329 247 296 445 449 361 317 236, 420 397 359
	377, 295, 422, 427, 194, 378, 369,	420 408 364 411 213 212 436 271 329 247 296 445 449 361 317 236, 420 397 359 222
	377, 295, 422, 427, 194, 378, 369,	420 408 364 411 213 212 436 271 329 247 296 445 449 361 317 236, 420 397 359 222 414
	377, 295, 422, 427, 194, 378, 369,	420 408 364 411 213 212 436 271 329 247 296 445 449 361 317 236, 420 397 359 222 414 290 258
	377, 295, 422, 427, 194, 378, 369,	420 408 364 411 213 212 436 271 329 247 296 445 449 361 317 236, 420 397 359 222 414 290 258 317
	377, 295, 422, 427, 194, 378, 369, 180,	420 408 364 411 213 212 436 271 329 247 296 445 449 361 317 236, 420 397 359 222 414 290 258 317 321
	377, 295, 422, 427, 194, 378, 369, 180,	420 408 364 411 213 212 436 271 329 247 296 445 449 361 317 236, 420 397 359 222 414 290 258 317 321 453
	377, 295, 422, 427, 194, 378, 369, 180,	420 408 364 411 213 212 436 271 329 247 296 445 449 361 317 236, 420 397 359 222 414 290 258 317 321
	377, 295, 422, 427, 194, 378, 369, 180,	420 408 364 411 213 212 436 271 329 247 296 445 449 361 317 236, 420 397 359 222 414 290 258 317 321 453
	377, 295, 422, 427, 194, 378, 369, 180,	420 408 364 411 213 212 436 271 329 247 296 445 449 361 317 236, 420 397 359 222 414 290 258 317 321 453 243
	377, 295, 422, 427, 194, 378, 369, 180,	420 408 364 411 213 212 436 271 329 247 296 445 449 361 317 236, 420 397 359 222 414 290 258 317 321 453 243 274 314
	377, 295, 422, 427, 194, 378, 369, 180, 250,	420 408 364 411 213 212 436 271 329 247 296 445 449 361 317 236, 420 397 359 222 414 290 258 317 321 453 243 274 314 322
	377, 295, 422, 427, 194, 378, 369, 180, 180, 250, 190.	420 408 364 411 213 212 436 271 329 247 296 445 449 361 317 236, 420 397 359 222 414 290 258 317 321 453 243 274 314 322 362
	377, 295, 422, 427, 194, 378, 369, 180, 180, 250, 190, 344,	420 408 364 411 213 212 436 271 329 247 296 445 449 361 317 236, 420 397 359 222 414 290 258 317 321 453 243 274 314 322 362 440
	377, 295, 422, 427, 194, 378, 369, 180, 180, 250, 190, 344,	420 408 364 411 213 212 436 271 329 247 296 445 449 361 317 236, 420 397 359 222 414 290 258 317 321 453 243 274 314 322 362 440

Argyropoulos, S A 379,	423,
	447
Arif, M	210
Ariza, M P	365
Arjunan, V	397
Arkhipov, G V	438
Arlyuk, B	313
Arroyave, R	363
Artemev, A 334,	384
Arvanitis, A	216
Arya, A	274
Arzt, E	188
Arzt, E 229,	383
Asaro, R	259
Ashida, T	399
Asta, M D 205, 250,	304,
115tu, 111 D 200, 200,	504,
	430 430
	430
	430 386
	430 386 192
	430 386 192 316
	430 386 192 316 172
	430 386 192 316 172 429
	430 386 192 316 172 429 361
	430 386 192 316 172 429 361 403 411
	430 386 192 316 172 429 361 403 411
	430 386 192 316 172 429 361 403 411 .444
	430 386 192 316 172 429 361 403 411 .444 176

# B

Babu, S S	203.	223.	345
Bacchi, D P			319
Backerud, L			403
Backhouse, N			172
Bacon, D J			184.
	224,	226,	425
Bacon, W G			188
Bae, B			246
Bae, D H		287,	438
Bae, J			. 382
Baek, C			352
Baerhold, F			329
Baghbanan, M			308
Bahr, D 224, 262,	275,	394,	435
Bai, G R			238
Bai, J G			428
Baik, S			252
Bailey, C	232,	362,	416
Bailey, R			376
Bainbridge, I	272,	281,	439
Baker, I			281
Baker, J D			436
Bakhtiyarov, S I		375,	450
Bakke, P			444
Balancin, O			237
Balascuta, S			337
Balema, V P			263
Balk, T J			229
Balogh, M P			264
Balooch, M			310
Balsone, S J			204
Bamberger, M			444
Ban, Z			426
Banerjee, D K			319
Bang, J J			395

Bang, W		
	283,	383
Bannuru, T	,	352
Daminuru, 1		
Banovic, S W		418
Barabash, R 279,	324,	394
Barajas, A		214
Barber, M		312
Barber, R E		259
Barbour, J C		352
Barca, B J		399
Bark, C		441
Barmak, K		455
Barnes, A J		264
Barnett, M R		340
Barnett, R S		385
Barnett, S		231,
		443
Baró, M		254
Barrabes, S A		433
Barrie, R L		340
Barron, M F		266
Barseghyan, S A		236
Bartelo, J		416
Bartos, S C		333
Basak, D		247
Baskes, M I 279, 282,	306,	324
Bastaweesy, A		403
Bastawros, A		317
Bates, C E		428
Battaile, C C		452
Battle, T		368
Bautista, R G 169, 210,	202,	309,
		436
Bayuzick, R J		345
Beals, R S		191
Beckermann, C 202,	247,	299,
	423,	446
Behrani, V	175,	215
Bei, H 357,	372,	
	<i>c</i> , <i>-</i> ,	401
Beleggia, M		401 196
Bell, B F	381,	196 451
Bell, B F Bellam, H C	381,	196 451 350
Bell, B F Bellam, H C Bellet, M	381, 203,	196 451 350 404
Bell, B F Bellam, H C Bellet, M 178, Belt, C K	381, 203,	196 451 350 404 177
Bell, B F           Bellam, H C           Bellet, M           Bellet, C K           Ben-Eliyahu, Y	381, 203,	196 451 350 404 177 395
Bell, B F Bellam, H C Bellet, M 178, Belt, C K Ben-Eliyahu, Y Benedikt, B	381, 203,	196 451 350 404 177 395 371
Bell, B F Bellam, H C Bellet, M 178, Belt, C K Ben-Eliyahu, Y Benedikt, B Benedyk, J C	381, 203,	196 451 350 404 177 395 371 237
Bell, B F Bellam, H C Bellet, M 178, Belt, C K Ben-Eliyahu, Y Benedikt, B Benedyk, J C Bennett, B V	381, 203,	196 451 350 404 177 395 371
Bell, B F Bellam, H C Bellet, M 178, Belt, C K Ben-Eliyahu, Y Benedikt, B Benedyk, J C	381, 203,	196 451 350 404 177 395 371 237
Bell, B F Bellam, H C Bellet, M 178, Belt, C K Ben-Eliyahu, Y Benedikt, B Benedyk, J C Bennett, B V	381, 203,  297,	196 451 350 404 177 395 371 237 225
Bell, B FBellam, H CBellet, M178,Belt, C KBen-Eliyahu, YBenedikt, BBenedyk, J CBennett, B VBenson, M L271,Benum, S	381, 203, 297,	196 451 350 404 177 395 371 237 225 411
Bell, B FBellam, H CBellet, M178,Belt, C KBen-Eliyahu, YBenedikt, BBenedyk, J CBennett, B VBenson, M L271,Benzio, M	381, 203, 	196 451 350 404 177 395 371 237 225 411 385 417
Bell, B FBellam, H CBellet, M178,Belt, C KBen-Eliyahu, YBenedikt, BBenedyk, J CBennett, B VBenson, M L271,Benzio, MBerberoglu, H	381, 203, 297,	196 451 350 404 177 395 371 237 225 411 385 417 173
Bell, B FBellam, H CBellet, MBellet, C KBen-Eliyahu, YBenedikt, BBenedyk, J CBennett, B VBenson, M L271,Benzio, MBerberoglu, HBerczik, D	381, 203, 297,	196 451 350 404 177 395 371 237 225 411 385 417 173 215
Bell, B FBellam, H CBellet, MBellt, C KBen-Eliyahu, YBenedikt, BBenedyk, J CBennett, B VBenson, M L271,Benzio, MBerberoglu, HBerczik, DBerezin, A I	381, 203, 297, 212,	196 451 350 404 177 395 371 237 225 411 385 417 173 215 267
Bell, B FBellam, H CBellet, M178,Belt, C KBen-Eliyahu, YBenedikt, BBenedyk, J CBennett, B VBenson, M L271,Benzio, MBerberoglu, HBerczik, DBerezin, A IBerezowsky, R M	381, 203, 297, 297, 212, 284,	196 451 350 404 177 395 371 237 225 411 385 417 173 215 267 443
Bell, B FBellam, H CBellam, H CBellt, M178,Belt, C KBenedikt, BBenedikt, BBenedyk, J CBennett, B VBenson, M L271,Benzio, MBerberoglu, HBerczik, DBerezin, A IBergman, C	381, 203, 297, 297, 212, 284,	196 451 350 404 177 395 371 237 225 411 385 417 173 215 267 443 414
Bell, B FBellam, H CBellam, H CBellt, M178,Belt, C KBeneEliyahu, YBenedikt, BBenedikt, BBenedyk, J CBennett, B VBenson, M L271,Benzio, MBerberoglu, HBerczik, DBerezin, A IBergman, CBergoint, D	381, 203, 297, 212, 284,	196 451 350 404 177 395 371 237 225 411 385 417 173 215 267 443 414 365
Bell, B FBellam, H CBellam, H CBellt, MI78,Belt, C KBenedikt, BBenedikt, BBenedyk, J CBennett, B VBenson, M L271,Benzio, MBerberoglu, HBerczik, DBerezin, A IBergman, CBergoint, DBernard, D	381, 203, 297, 212, 284, 273,	196 451 350 404 177 395 371 237 225 411 385 417 173 215 267 443 414 365 361
Bell, B F Bellam, H C Bellam, H C Bellet, M	381, 203, 297, 212, 284, 273,	196 451 350 404 177 395 371 237 225 411 385 417 173 215 267 443 414 365
Bell, B F Bellam, H C Bellam, H C Bellet, M	381, 203, 297, 212, 284, 273,	196 451 350 404 177 395 371 237 225 411 385 417 173 215 267 443 414 365 361 213 200
Bell, B F Bellam, H C Bellam, H C Bellet, M	381, 203, 297, 212, 284, 273,	196 451 350 404 177 395 371 237 225 411 385 417 173 215 267 443 414 365 361 213
Bell, B F Bellam, H C Bellam, H C Bellet, M	203, 203, 297, 212, 284, 273, 296,	196 451 350 404 177 395 371 237 225 411 385 417 173 215 267 443 414 365 361 213 200
Bell, B FBellam, H CBellam, H CBellt, M178,Belt, C KBen-Eliyahu, YBenedikt, BBenedikt, BBenedyk, J CBennett, B VBenson, M L271,Benzio, MBerberoglu, HBerczik, DBerezowsky, R MBergman, CBergoint, DBernard, DBernueta, L DBesser, A DBesterci, MBewlay, B	381, 203, 297, 212, 284, 273, 296,	196 451 350 404 177 395 371 237 225 411 385 417 173 215 267 443 414 365 361 213 200 311
Bell, B FBellam, H CBellam, H CBellt, M178,Belt, C KBen-Eliyahu, YBenedikt, BBenedikt, BBenedyk, J CBennett, B VBenson, M L271,Benzio, MBerberoglu, HBerczik, DBerezowsky, R MBergman, CBergoint, DBernard, DBernueta, L DBesser, A DBesterci, MBewlay, B	381, 203, 297, 212, 284, 273, 296,	196 451 350 404 177 395 371 237 225 411 385 417 173 215 267 443 414 365 361 213 200 311 358 434
Bell, B FBellam, H CBellam, H CBellt, MBelt, C KBen-Eliyahu, YBenedikt, BBenedikt, BBenedyk, J CBennett, B VBenson, M L271,Benzio, MBerberoglu, HBerczik, DBerezowsky, R MBergman, CBernard, DBernard, DBesser, A DBesterci, MBesterci, MBeyerlein, I J207, 255,Beygelzimer, Y208,	381, 203, 297, 212, 284, 273, 296, 256, 255,	196 451 350 404 177 395 371 237 225 411 385 417 173 215 267 443 414 365 361 213 200 311 358 434 260
Bell, B F Bellam, H C Bellam, H C Bellet, M	381, 203, 297, 212, 284, 273, 296, 255,	196 451 350 404 177 395 371 237 225 411 385 417 173 215 267 443 414 365 361 213 200 311 358 434 260 203
Bell, B F Bellam, H C Bellam, H C Bellet, M	381, 203, 297, 212, 284, 273, 296, 255, 255,	196 451 350 404 177 395 371 237 225 411 385 417 173 215 267 443 414 365 361 213 200 311 358 434 260 203 445
Bell, B F Bellam, H C Bellam, H C Bellet, M	381, 203, 297, 212, 284, 273, 296, 255, 255,	196 451 350 404 177 395 371 237 225 411 385 417 173 215 267 443 414 365 361 213 200 311 358 434 260 203 445 445
Bell, B F Bellam, H C Bellam, H C Bellet, M	381, 203, 297, 212, 284, 273, 296, 255, 255,	196 451 350 404 177 395 371 237 225 411 385 417 173 215 267 443 414 365 361 213 200 311 358 434 260 203 445

Bhansali, S       178, 219, 273,		
$\begin{array}{cccccccccccccccccccccccccccccccccccc$	Bhansali, S 178, 219,	273,
Bhattacharya, P       291         Bhethanabotla, V R       455         Bi, S       265         Bian, Z       217         Biancaniello, F S       372         Bickert, C       177         Bicler, T R       188, 190, 229, 286,		455
Bhethanabotla, V R       455         Bi, S       265         Bian, Z       217         Biancaniello, F S       372         Bickert, C       177         Bieler, T R       188, 190, 229, 286,		
Bi, S       265         Bian, Z       217         Biancaniello, F S       372         Bickert, C       177         Bieler, T R       188, 190, 229, 286,	Bhattacharya, P	
Bian, Z       217         Biancaniello, F S       372         Bickert, C       177         Bieler, T R       188, 190, 229, 286,		
Biancaniello, F S       372         Bickert, C       177         Bieler, T R       188, 190, 229, 286,		
Bickert, C       177         Bieler, T R       188, 190, 229, 286,		
Bieler, T R       188, 190, 229, 286,		
Bilello, J C       176         Bilodeau, J       361         Biloni, H       300, 450         Biner, S B       317, 365         Bing, X       289         Bingert, J F       234, 235, 445         Birdsell, S A       353         Birol, Y       173         Bisen, K B       362         Bittencourt, E       377         Bizos, R       381         Bjerke, W       399         Blakely, K A       209         Blanchard, D       353         Blanchard, P J       287         Blander, A J       356         Blandin, J       417, 438         Blasques, J       M         Blavert, C       445         Bletry, M       438         Blinov, V V       212         Biznyukov, S       440         Blobaum, K J       431         Bloch, J       395         Bloomfield, MO       423         Blue, C A       287, 411         Blum, W       303         Blut, J W       411         Boehlert, C J       391, 445         Boenting, M       358         Boettinger, W J       247, 276, <td></td> <td></td>		
Biloni, H       300, 450         Biner, S B       317, 365         Bing, X       289         Bingert, J F       234, 235, 445         Birdsell, S A       353         Birol, Y       173         Bisen, K B       362         Bittencourt, E       377         Bizios, R       381         Bjerke, W       399         Blakely, K A       209         Blanchard, D       353         Blanchard, P J       287         Blander, A J       356         Blandin, J       417, 438         Blasques, J       M         Blowert, C       445         Bletry, M       438         Bloov, V V       212         Blizonyukov, S       440         Blobaum, K J       431         Bloch, J       395         Bloomfield, M O       423         Blue, C A       287, 411         Blum, W       383         Blust, J W       411         Boehlert, C J       391, 445         Boender, W       219         Boening, M       358         Boettcher, H       403         Boettinger, W J       247, 276,<		
Biner, S B       317, 365         Bing, X       289         Bingert, J F       234, 235, 445         Birdsell, S A       353         Birol, Y       173         Bisen, K B       362         Bittencourt, E       377         Bizios, R       381         Bjerke, W       399         Blakely, K A       209         Blanchard, D       353         Blanchard, P J       287         Blander, A J       356         Blandin, J       417, 438         Blasques, J       M         Blawert, C       445         Bletry, M       438         Blinov, V V       212         Bliznyukov, S       440         Blobaum, K J       431         Bloch, J       395         Bloomfield, M O       423         Blue, C A       287, 411         Blum, W       383         Blust, J W       411         Boehlert, C J       391, 445         Boender, W       219         Boening, M       358         Boettcher, H       403         Boettinger, W J       247, 276,	Bilodeau, J	361
Bing, X       289         Bingert, J F       234, 235, 445         Birdsell, S A       353         Birol, Y       173         Bisen, K B       362         Bittencourt, E       377         Bizios, R       381         Bjerke, W       399         Blakely, K A       209         Blanchard, D       353         Blanchard, P J       287         Blander, A J       356         Blandin, J       417, 438         Blasques, J       M         Blewert, C       445         Bletry, M       438         Blinov, V V       212         Bliznyukov, S       440         Blobaum, K J       431         Bloch, J       395         Bloomfield, M O       423         Blue, C A       287, 411         Bum, V       304         Blum, W       383         Blust, J W       411         Boehert, C J       391, 445         Boettinger, W J       222, 344         Boger, R       214, 314         Bogicevic, A       193         Boileau, J       328         Bojarevics, V       437	Biloni, H 300,	450
Bingert, J F       234, 235, 445         Birdsell, S A       353         Birol, Y       173         Bisen, K B       362         Bittencourt, E       377         Bizios, R       381         Bjerke, W       399         Blakely, K A       209         Blanchard, D       353         Blanchard, P J       287         Blander, A J       356         Blandin, J       417, 438         Blasques, J       M         Blewett, C       445         Bletry, M       438         Blinov, V V       212         Bliznyukov, S       440         Blobaum, K J       431         Bloch, J       395         Bloomfield, M O       423         Blue, C A       287, 411         Bum, V       304         Blum, W       383         Blust, J W       411         Boehert, C J       391, 445         Boettinger, W J       222, 344         Boger, R       214, 314         Bogicevic, A       193         Boileau, J       328         Bojarevics, V       437         Boland, M       415		
Birdsell, S A       353         Birol, Y       173         Bisen, K B       362         Bittencourt, E       377         Bizios, R       381         Bjerke, W       399         Blakely, K A       209         Blanchard, D       353         Blanchard, P J       287         Blander, A J       356         Blandin, J       417, 438         Blasques, J       M         Bletry, M       433         Blinov, V V       212         Bliznyukov, S       440         Blobaum, K J       431         Bloch, J       395         Bloomfield, M O       423         Blue, C A       287, 411         Blum, V       304         Blum, W       383         Blust, J W       411         Boehlert, C J       391, 445         Boender, W       219         Boenting, M       358         Boettcher, H       403         Boettinger, W J       247, 276,		
Birol, Y       173         Bisen, K B       362         Bittencourt, E       377         Bizios, R       381         Bjerke, W       399         Blakely, K A       209         Blanchard, D       353         Blanchard, P J       287         Blander, A J       356         Blandin, J       417, 438         Blasques, J       M         Blawert, C       445         Bletry, M       438         Blinov, V V       212         Bliznyukov, S       440         Blobaum, K J       431         Bloch, J       395         Bloomfield, M O       423         Blue, C A       287, 411         Blum, V       304         Blum, W       383         Blust, J W       411         Boehlert, C J       391, 445         Boender, W       219         Boenting, M       358         Boettcher, H       403         Boettinger, W J       247, 276,		
Bisen, K B       362         Bittencourt, E       377         Bizios, R       381         Bjerke, W       399         Blakely, K A       209         Blanchard, D       353         Blanchard, P J       287         Blander, A J       356         Blandin, J       417, 438         Blasques, J       M         Blawert, C       445         Bletry, M       438         Blinov, V V       212         Bliznyukov, S       440         Blobaum, K J       431         Bloch, J       395         Bloomfield, M O       423         Blue, C A       287, 411         Blum, V       304         Blum, W       383         Blust, J W       411         Boehert, C J       391, 445         Boettinger, W J       247, 276,		
Bittencourt, E       377         Bizios, R       381         Bjerke, W       399         Blakely, K A       209         Blanchard, D       353         Blanchard, P J       287         Blander, A J       356         Blander, A J       356         Blander, A J       417, 438         Blasques, J       M 172         Blawert, C       445         Bletry, M       438         Blinov, V V       212         Bliznyukov, S       440         Blobaum, K J       431         Bloch, J       395         Bloomfield, M O       423         Bluw, V       304         Blum, W       383         Blust, J W       411         Boehert, C J       391, 445         Boettcher, H       403         Boettinger, W J       247, 276,		
Bizios, R       381         Bjerke, W       399         Blakely, K A       209         Blanchard, D       353         Blanchard, P J       287         Blanchard, P J       287         Blanchard, P J       287         Blanchard, P J       287         Blanchard, P J       356         Blandin, J       417, 438         Blasques, J       M         Blawert, C       445         Bletry, M       438         Blinov, V V       212         Bliznyukov, S       440         Blobaum, K J       431         Bloch, J       395         Bloomfield, M O       423         Blue, C A       287, 411         Blum, W       383         Blust, J W       411         Boehlert, C J       391, 445         Boender, W       219         Boening, M       358         Boettcher, H       403         Boettinger, W J       247, 276,		
Bjerke, W       399         Blakely, K A       209         Blanchard, D       353         Blanchard, P J       287         Blander, A J       356         Blandin, J       417, 438         Blasques, J       M         Blawert, C       445         Bletry, M       438         Blinov, V V       212         Bliznyukov, S       440         Blobaum, K J       431         Bloch, J       395         Bloomfield, M O       423         Blue, C A       287, 411         Blum, V       304         Blum, W       383         Blust, J W       411         Boehlert, C J       391, 445         Boender, W       219         Boening, M       358         Boettcher, H       403         Boettinger, W J       247, 276,		
Blakely, K A       209         Blanchard, D       353         Blanchard, P J       287         Blander, A J       356         Blandin, J       417, 438         Blasques, J       M         Blawert, C       445         Bletry, M       438         Blinov, V V       212         Bliznyukov, S       440         Blobaum, K J       431         Bloch, J       395         Bloomfield, M O       423         Blue, C A       287, 411         Blum, V       304         Blum, W       383         Blust, J W       411         Boehlert, C J       391, 445         Boender, W       219         Boening, M       358         Boettcher, H       403         Boettinger, W J       247, 276,		
Blanchard, D       353         Blanchard, P J       287         Blander, A J       356         Blandin, J       417, 438         Blasques, J       M         Blawert, C       445         Bletry, M       438         Blinov, V V       212         Bliznyukov, S       440         Blobaum, K J       431         Bloch, J       395         Bloomfield, M O       423         Blue, C A       287, 411         Blum, V       304         Blum, W       383         Blust, J W       411         Boehlert, C J       391, 445         Boender, W       219         Boening, M       358         Boettcher, H       403         Boettinger, W J       247, 276,		
Blander, A J       356         Blandin, J       417, 438         Blasques, J       M         Blawert, C       445         Bletry, M       438         Blinov, V V       212         Bliznyukov, S       440         Blobaum, K J       431         Bloch, J       395         Bloomfield, M O       423         Blue, C A       287, 411         Blum, V       304         Blum, W       383         Blust, J W       411         Boehlert, C J       391, 445         Boender, W       219         Boening, M       358         Boettcher, H       403         Boettinger, W J       247, 276,	Blanchard, D	353
Blandin, J	Blanchard, P J	287
Blasques, J		
Blawert, C.       445         Bletry, M.       438         Blinov, V V.       212         Bliznyukov, S.       440         Blobaum, K J.       431         Bloch, J.       395         Bloomfield, M O.       423         Blue, C A.       287, 411         Blum, V.       304         Blum, W.       383         Blust, J W.       411         Boehlert, C J.       391, 445         Boender, W.       219         Boening, M.       358         Boetther, H.       403         Boettinger, W J.       247, 276,		
Bletry, M       438         Blinov, V V       212         Bliznyukov, S       440         Blobaum, K J       431         Bloch, J       395         Bloomfield, M O       423         Blue, C A       287, 411         Blum, V       304         Blum, V       304         Blum, W       383         Blust, J W       411         Boehlert, C J       391, 445         Boender, W       219         Boening, M       358         Boettcher, H       403         Boettinger, W J       247, 276,		
Blinov, V V       212         Bliznyukov, S       440         Blobaum, K J       431         Bloch, J       395         Bloomfield, M O       423         Blue, C A       287, 411         Blum, V       304         Blum, W       383         Blust, J W       411         Boehlert, C J       391, 445         Boender, W       219         Boening, M       358         Boettcher, H       403         Boettinger, W J       247, 276,		
Bliznyukov, S       440         Blobaum, K J       431         Bloch, J       395         Bloomfield, M O       423         Blue, C A       287, 411         Blum, V       304         Blum, W       383         Blust, J W       411         Boehlert, C J       391, 445         Boender, W       219         Boening, M       358         Boettcher, H       403         Boettinger, W J       247, 276,		
Blobaum, K J       431         Bloch, J       395         Bloomfield, M O       423         Blue, C A       287, 411         Blum, V       304         Blum, W       383         Blust, J W       411         Boehlert, C J       391, 445         Boender, W       219         Boening, M       358         Boettcher, H       403         Boettinger, W J       247, 276,		
Bloch, J		
Bloomfield, M O       423         Blue, C A       287, 411         Blum, V       304         Blum, W       383         Blust, J W       411         Boehlert, C J       391, 445         Boender, W       219         Boening, M       358         Boettcher, H       403         Boettinger, W J       247, 276,		
Blue, C A       287, 411         Blum, V       304         Blum, W       383         Blust, J W       411         Boehlert, C J       391, 445         Boender, W       219         Boening, M       358         Boettcher, H       403         Boettinger, W J       247, 276,		
Blum, W       383         Blust, J W       411         Boehlert, C J       391, 445         Boender, W       219         Boening, M       358         Boettcher, H       403         Boettinger, W J       247, 276,		
Blust, J W       411         Boehlert, C J       391, 445         Boender, W       219         Boening, M       358         Boettcher, H       403         Boettinger, W J       247, 276,	Blum, V	304
Boehlert, C J       391, 445         Boender, W       219         Boening, M       358         Boettcher, H       403         Boettinger, W J       247, 276,		383
Boender, W       219         Boening, M       358         Boettcher, H       403         Boettinger, WJ       247, 276,		
Boening, M       358         Boettcher, H       403         Boettinger, W J       247, 276,		
Boettcher, H       403         Boettinger, W J       247, 276,		
Boettinger, W J       247, 276, 322, 344         Boger, R       214, 314         Bogicevic, A       193         Boileau, J       328         Bojarevics, V       437         Boland, M       415         Bonacuse, P J       340         Bonsager, M C       198         Bortha, S       281         Borge, G       361         Borjas, N M       230         Bossuyt, S       316         Bottani, C E       429         Bouchet, J       431         Boulianne, R       171         Bourbay, W M       212         Bourham, M       197         Bourgeois, L       295         Bourke, M A       187, 207, 229, 255,		
Boger, R       214, 314         Bogicevic, A       193         Boileau, J       328         Bojarevics, V       437         Boland, M       415         Bonacuse, P J       340         Bonsager, M C       198         Bontha, S       281         Borge, G       361         Borjas, N M       230         Bossuyt, S       316         Bottani, C E       429         Bouchet, J       431         Boulianne, R       171         Bourds, W M       212         Bourham, M       197         Bourgeois, L       295         Bourke, M A       187, 207, 229, 255,	-	
Bogicevic, A       193         Boileau, J       328         Bojarevics, V       437         Boland, M       415         Bonacuse, P J       340         Bonsager, M C       198         Bontha, S       281         Borge, G       361         Borjas, N M       230         Bossuyt, S       316         Bottani, C E       429         Bouchet, J       431         Boulianne, R       171         Bourds, W M       212         Bourham, M       197         Bourgeois, L       295         Bourke, M A       187, 207, 229, 255,		
Boileau, J       328         Bojarevics, V       437         Boland, M       415         Bonacuse, P J       340         Bonsager, M C       198         Bontha, S       281         Borge, G       361         Borjas, N M       230         Bossuyt, S       316         Bottani, C E       429         Bouchet, J       431         Boulianne, R       171         Bourks, W M       212         Bourham, M       197         Bourgeois, L       295         Bourke, M A       187, 207, 229, 255,		
Bojarevics, V       437         Boland, M       415         Bonacuse, P J       340         Bonsager, M C       198         Bontha, S       281         Borge, G       361         Borjas, N M       230         Bossuyt, S       316         Bottani, C E       429         Bouchet, J       431         Boulianne, R       171         Bourds, W M       212         Bourham, M       197         Bourgeois, L       295         Bourke, M A       187, 207, 229, 255,		328
Bonacuse, P J       340         Bonsager, M C       198         Bontha, S       281         Borge, G       361         Borjas, N M       230         Bossuyt, S       316         Bottani, C E       429         Bouchet, J       431         Boulianne, R       171         Bourds, W M       212         Bourham, M       197         Bourgeois, L       295         Bourke, M A       187, 207, 229, 255,		
Bonsager, M C       198         Bontha, S       281         Borge, G       361         Borjas, N M       230         Bossuyt, S       316         Bottani, C E       429         Bouchet, J       431         Boulianne, R       171         Bourds, W M       212         Bourham, M       197         Bourgeois, L       295         Bourke, M A       187, 207, 229, 255,		415
Bontha, S       281         Borge, G       361         Borjas, N M       230         Bossuyt, S       316         Bottani, C E       429         Bouchet, J       431         Boulianne, R       171         Bourds, W M       212         Bourham, M       197         Bourgeois, L       295         Bourke, M A       187, 207, 229, 255,	Bonacuse, P J	
Borge, G       361         Borjas, N M       230         Bossuyt, S       316         Bottani, C E       429         Bouchet, J       431         Boulianne, R       171         Bounds, W M       212         Bourham, M       197         Bourgeois, L       295         Bourke, M A       187, 207, 229, 255,		
Borjas, N M       230         Bossuyt, S       316         Bottani, C E       429         Bouchet, J       431         Boulianne, R       171         Bounds, W M       212         Bourham, M       197         Bourgeois, L       295         Bourke, M A       187, 207, 229, 255,		
Bossuyt, S       316         Bottani, C E       429         Bouchet, J       431         Boulianne, R       171         Bounds, W M       212         Bourham, M       197         Bourgeois, L       295         Bourke, M A       187, 207, 229, 255,		
Bottani, C E       429         Bouchet, J       431         Boulianne, R       171         Bounds, W M       212         Bourham, M       197         Bourgeois, L       295         Bourke, M A       187, 207, 229, 255,		
Bouchet, J       431         Boulianne, R       171         Bounds, W M       212         Bourham, M       197         Bourgeois, L       295         Bourke, M A       187, 207, 229, 255,		
Boulianne, R       171         Bounds, W M       212         Bourham, M       197         Bourgeois, L       295         Bourke, M A       187, 207, 229, 255,		
Bounds, W M       212         Bourham, M       197         Bourgeois, L       295         Bourke, M A       187, 207, 229, 255,		
Bourham, M       197         Bourgeois, L       295         Bourke, M A       187, 207, 229, 255,		
Bourgeois, L         295           Bourke, M A         187, 207, 229, 255,		
Bourke, M A 187, 207, 229, 255, 	Bourgeois, L	295
	Bourke, M A 187, 207, 229,	255,
Bourret, R H 370		
	Bourret, R H	570

Boutorabi, S M	439
Bowden, D M	419
Bowles, A L	445
Bowman, B	. 286
Bowman, R C	210
Boyapati, K	431
Boyce, B L 261, 308,	342
Boydon, J F	264
Boylstein, R E	318
	265
Bradley, J R 264,	
Bradshaw, R C	438
Brady, M P	215
Brady, S	263
Braginsky, M V	452
Brandstaetter, W	404
Bratkovsky, A M	425
Braun, M J	178
Braun, M W 228,	327
Bravman, J C	394
Bray, G	410
Brechet, Y 307,	438
Bretz, G T	287
Briant, C L 264, 347, 418,	419
Brill, M	395
Brinks, H W	353
Brokmeier, H	252
Bronchart, Q	390
Bronfin, B	333
Brooks, C R	271
Brown, D W 207, 255, 283,	296,
	434
Brown, J A	222
Brown, T L 207,	259
Brown, W L	352
Browning, J 172,	399
Browning, P F	411
Brubaker, C	417
Brueck, S R	
	394
Bruggeman, J 212, 267,	394 312,
Bruggeman, J 212, 267,	394 312, 437
Bruggeman, J 212, 267, 	394 312, 437 244
Bruggeman, J 212, 267, 	394 312, 437 244 284
Bruggeman, J	394 312, 437 244 284 270,
Bruggeman, J	394 312, 437 244 284 270, 438
Bruggeman, J	394 312, 437 244 284 270, 438 308,
Bruggeman, J	394 312, 437 244 284 270, 438 308, 452
Bruggeman, J	394 312, 437 244 284 270, 438 308,
Bruggeman, J	394 312, 437 244 284 270, 438 308, 452
Bruggeman, J       212, 267,	394 312, 437 244 284 270, 438 308, 452 256 296 411
Bruggeman, J	394 312, 437 244 284 270, 438 308, 452 256 296 411
Bruggeman, J       212, 267,	394 312, 437 244 284 270, 438 308, 452 256 296 411
Bruggeman, J       212, 267,	394 312, 437 244 284 270, 438 308, 452 256 296 411 .172
Bruggeman, J       212, 267,	394 312, 437 244 284 270, 438 308, 452 256 296 411 .172 318
Bruggeman, J       212, 267,	394 312, 437 244 284 270, 438 308, 452 256 296 411 .172 318 225
Bruggeman, J	394 312, 437 244 284 270, 438 308, 452 256 296 411 .172 318 225 198 346
Bruggeman, J	394 312, 437 244 284 270, 438 308, 452 256 296 411 .172 318 225 198 346 230
Bruggeman, J	394 312, 437 244 284 270, 438 308, 452 256 296 411 .172 318 225 198 346 230 170
Bruggeman, J	394 312, 437 244 284 270, 438 308, 452 256 296 411 .172 318 225 198 346 230 170 219
Bruggeman, J	394 312, 437 244 284 270, 438 308, 452 256 296 411 .172 318 225 198 346 230 170 219 433
Bruggeman, J	394 312, 437 244 284 270, 438 308, 452 256 296 411 .172 318 225 198 346 230 170 219 433 304
Bruggeman, J	394 312, 437 244 284 270, 438 308, 452 256 296 411 .172 318 225 198 346 230 170 219 433 304 262
Bruggeman, J	394 312, 437 244 284 270, 438 308, 452 256 296 411 .172 318 225 198 346 230 170 219 433 304

# С

Cabibbo, M	351
Cady, C M	233
Cahn, J W 205,	384

Calata, J N	428	Chang,
Cale, T S		Chang,
Callahan, P		Chani, V
Calonne, O		Chapell
Campbell, F		Charette
Candy, I		Charit, l
Cantor, B		Chase, I
Cao, F		Chashch
Cao, G		Chatterj
Cao, X		Chaubal
Cao, Y		Chaudh
	257	Chaudh
Capps, J	450	Chawla
Caram, R 195, 344,	440	Chawla.
Caraveo, V		
Carbonneau, A	177	Chen, C
Carlberg, T 218,	298	Chen, C
Carleton, E	354	Chen, C
Carlisle, J A	429	Chen, G
Carlisle, K B	343	Chen, H
Carmo, O A	329	Chen, H
Caro, A	348	Chen, J
Caro, M	348	Chen, J
Caron, Y	273	Chen, J
Carpenter, D A		3
	339	Chen, L
Carsley, J E 211,	265	Chen, L
Carte, S	399	
Carter, E A	274	
Carter, J T 386,	450	Chen, L
Carter, W T 219,	414	Chen, L
Castro, M	273	Chen, L
Castro-Cedeno, M H	273	Chen, L
Caswell, K K	395	Chen, N
Catalina, A V 178, 179,	219,	Chen, P
	404	Chen, Q
Cathey, W K		Chen, Q
Ceder, G 205, 250,		Chen, S
		Chen, S
Cefalu, S A	219	Chen, S
Celanovic, I		Chen, S
Cerreta, E K 233, 303, 453,	454	Chen, S
Cha, P		Chen, T
Chada, S 189,		Chen, T
		Chen, W
Chadha, G	375	Chen, X
Chan, H W		Chen, X
Chan, K S 365,		Chen, Y
Chan, W		Chen, Y
Chandler, R C		Chen, Z
Chandra, D 169, 210, 262,		Chen, Z
	396,	Cheng,
		Cheng,
Chandrasekar, S 207,		Cheng,
Chang, A		Chenmi
Chang, C		Cheong
Chang, C		Cheruku
Chang, C W 199,		Chesoni
Chang, H		
Chang, H		Chiang,
Chang, H J		Chiang,
Chang, I T		Chiang,
Chang, J		Chiang,
Chang, K		Chien, V
Chang, L J		Chiew,
Chang, M S		Childs,
Chang, S 232,	5//	Chin, B

Chang, T	285
Chang, Y A 198,	216
Chani, V	342
Chapelle, P	
Charette, A	423
Charit, I 207,	311
Chase, R	399
Chashchin, O A	212
Chatterjee, A 175,	400
Chaubal, M V	265
Chaudhari, G 237, 255,	259
Chaudhury, P	281
Chawla, K K 293,	343
Chawla, N 286, 293,	331,
	446
	382
Chen, G 260, Chen, G S	439 242
Chen, G Z 182, 199,	242
Chen, H	269
Chen, H	409
Chen, J	243
Chen, J	407
Chen, J J 184, 225, 226,	281.
	441
Chen, L	
Chen, L 181, 277, 294,	305,
	363,
	426
Chen, L J	294
Chen, L J	392
Chen, L J	411
Chen, L Q	277
Chen, L Q	277 374
Chen, M Chen, P	
Chen, M Chen, P Chen, Q 410,	374 409 411
Chen, M Chen, P Chen, Q 410, Chen, Q	374 409 411 312
Chen, M Chen, P Chen, Q	374 409 411 312 382
Chen, M Chen, P Chen, Q	<ul> <li>374</li> <li>409</li> <li>411</li> <li>312</li> <li>382</li> <li>213</li> </ul>
Chen, M Chen, P Chen, Q	<ul> <li>374</li> <li>409</li> <li>411</li> <li>312</li> <li>382</li> <li>213</li> <li>298</li> </ul>
Chen, M	<ul> <li>374</li> <li>409</li> <li>411</li> <li>312</li> <li>382</li> <li>213</li> <li>298</li> <li>330</li> </ul>
Chen, M         Chen, P         Chen, Q         Marcological Action         Chen, S         Chen, S <t< td=""><td><ul> <li>374</li> <li>409</li> <li>411</li> <li>312</li> <li>382</li> <li>213</li> <li>298</li> <li>330</li> <li>367</li> </ul></td></t<>	<ul> <li>374</li> <li>409</li> <li>411</li> <li>312</li> <li>382</li> <li>213</li> <li>298</li> <li>330</li> <li>367</li> </ul>
Chen, M         Chen, P         Chen, Q         410,         Chen, Q         Chen, S         233,         Chen, T	<ul> <li>374</li> <li>409</li> <li>411</li> <li>312</li> <li>382</li> <li>213</li> <li>298</li> <li>330</li> <li>367</li> <li>374</li> </ul>
Chen, M	<ul> <li>374</li> <li>409</li> <li>411</li> <li>312</li> <li>382</li> <li>213</li> <li>298</li> <li>330</li> <li>367</li> <li>374</li> <li>230</li> </ul>
Chen, M       Chen, P         Chen, Q       410,         Chen, Q       410,         Chen, Q       Chen, S         Chen, S       198, 240, 293, 338,         Chen, S       Chen, S         Chen, S       233,         Chen, S       233,         Chen, T       186,         Chen, W       186,	<ul> <li>374</li> <li>409</li> <li>411</li> <li>312</li> <li>382</li> <li>213</li> <li>298</li> <li>330</li> <li>367</li> <li>374</li> <li>230</li> <li>383</li> </ul>
Chen, M         Chen, P         Chen, Q         410,         Chen, Q         Chen, S         Chen, T         Chen, T         Chen, T         Chen, W         Chen, X	<ul> <li>374</li> <li>409</li> <li>411</li> <li>312</li> <li>382</li> <li>213</li> <li>298</li> <li>330</li> <li>367</li> <li>374</li> <li>230</li> <li>383</li> <li>292</li> </ul>
Chen, M         Chen, P         Chen, Q         410,         Chen, Q         Chen, S         Chen, T         Chen, T         Chen, T         Chen, X         Chen, X G	<ul> <li>374</li> <li>409</li> <li>411</li> <li>312</li> <li>382</li> <li>213</li> <li>298</li> <li>330</li> <li>367</li> <li>374</li> <li>230</li> <li>383</li> <li>292</li> <li>439</li> </ul>
Chen, M	<ul> <li>374</li> <li>409</li> <li>411</li> <li>312</li> <li>382</li> <li>213</li> <li>298</li> <li>330</li> <li>367</li> <li>374</li> <li>230</li> <li>383</li> <li>292</li> <li>439</li> <li>389</li> </ul>
Chen, M         Chen, P         Chen, Q         410,         Chen, Q         Chen, S         Chen, T         Chen, T         Chen, T         Chen, T         Chen, X         Chen, X G         Chen, Y	<ul> <li>374</li> <li>409</li> <li>411</li> <li>312</li> <li>382</li> <li>213</li> <li>298</li> <li>330</li> <li>367</li> <li>374</li> <li>230</li> <li>383</li> <li>292</li> <li>439</li> <li>389</li> <li>326</li> </ul>
Chen, M         Chen, P         Chen, Q         410,         Chen, Q         Chen, S         Chen, T         Chen, T         Chen, T         Chen, T         Chen, X         Chen, X G         Chen, Y         304,         Chen, Z	<ul> <li>374</li> <li>409</li> <li>411</li> <li>312</li> <li>382</li> <li>213</li> <li>298</li> <li>330</li> <li>367</li> <li>374</li> <li>230</li> <li>383</li> <li>292</li> <li>439</li> <li>389</li> <li>326</li> <li>238</li> </ul>
Chen, M         Chen, P         Chen, Q         410,         Chen, Q         Chen, S         Chen, T         Chen, T         Chen, T         Chen, T         Chen, T         Chen, X         Chen, X G         Chen, Y         Sold,         Chen, Z	<ul> <li>374</li> <li>409</li> <li>411</li> <li>312</li> <li>382</li> <li>213</li> <li>298</li> <li>330</li> <li>367</li> <li>374</li> <li>230</li> <li>383</li> <li>292</li> <li>439</li> <li>389</li> <li>326</li> <li>238</li> <li>373</li> </ul>
Chen, M         Chen, P         Chen, Q         410,         Chen, Q         Chen, S         Chen, T         Chen, T         Chen, T         Chen, T         Chen, X         Chen, X G         Chen, Y         Sold,         Chen, Z         Chen, Z         Chen, Z	<ul> <li>374</li> <li>409</li> <li>411</li> <li>312</li> <li>382</li> <li>213</li> <li>298</li> <li>330</li> <li>367</li> <li>374</li> <li>230</li> <li>383</li> <li>292</li> <li>439</li> <li>389</li> <li>326</li> <li>238</li> <li>373</li> <li>443</li> </ul>
Chen, M         Chen, P         Chen, Q         410,         Chen, Q         Chen, S         Chen, T         Chen, T         Chen, T         Chen, T         Chen, X         Chen, X G         Chen, Y         Slow, Chen, Z         Chen, C         Chen, L	<ul> <li>374</li> <li>409</li> <li>411</li> <li>312</li> <li>382</li> <li>213</li> <li>298</li> <li>330</li> <li>367</li> <li>374</li> <li>230</li> <li>383</li> <li>292</li> <li>439</li> <li>389</li> <li>326</li> <li>238</li> <li>373</li> </ul>
Chen, M         Chen, P         Chen, Q         410,         Chen, Q         Chen, S         Chen, T         Chen, T         Chen, T         Chen, T         Chen, X         Chen, X G         Chen, Y         Sold,         Chen, Z         Chen, Z         Chen, Z	<ul> <li>374</li> <li>409</li> <li>411</li> <li>312</li> <li>382</li> <li>213</li> <li>298</li> <li>330</li> <li>367</li> <li>374</li> <li>230</li> <li>383</li> <li>292</li> <li>439</li> <li>389</li> <li>326</li> <li>238</li> <li>373</li> <li>443</li> <li>182</li> </ul>
Chen, M	<ul> <li>374</li> <li>409</li> <li>411</li> <li>312</li> <li>382</li> <li>213</li> <li>298</li> <li>330</li> <li>367</li> <li>374</li> <li>230</li> <li>383</li> <li>292</li> <li>439</li> <li>389</li> <li>326</li> <li>238</li> <li>373</li> <li>443</li> <li>182</li> <li>413</li> </ul>
Chen, M	<ul> <li>374</li> <li>409</li> <li>411</li> <li>312</li> <li>382</li> <li>213</li> <li>298</li> <li>330</li> <li>367</li> <li>374</li> <li>230</li> <li>383</li> <li>292</li> <li>439</li> <li>389</li> <li>326</li> <li>238</li> <li>373</li> <li>443</li> <li>182</li> <li>413</li> <li>455</li> <li>454</li> <li>184</li> </ul>
Chen, M	<ul> <li>374</li> <li>409</li> <li>411</li> <li>312</li> <li>382</li> <li>213</li> <li>298</li> <li>330</li> <li>367</li> <li>374</li> <li>230</li> <li>383</li> <li>292</li> <li>439</li> <li>389</li> <li>326</li> <li>238</li> <li>373</li> <li>443</li> <li>182</li> <li>413</li> <li>455</li> <li>454</li> </ul>
Chen, M	<ul> <li>374</li> <li>409</li> <li>411</li> <li>312</li> <li>382</li> <li>213</li> <li>298</li> <li>330</li> <li>367</li> <li>374</li> <li>230</li> <li>383</li> <li>292</li> <li>439</li> <li>389</li> <li>326</li> <li>238</li> <li>373</li> <li>443</li> <li>182</li> <li>413</li> <li>455</li> <li>454</li> <li>184</li> </ul>
Chen, M	<ul> <li>374</li> <li>409</li> <li>411</li> <li>312</li> <li>382</li> <li>213</li> <li>298</li> <li>330</li> <li>367</li> <li>374</li> <li>230</li> <li>383</li> <li>292</li> <li>439</li> <li>389</li> <li>326</li> <li>238</li> <li>373</li> <li>443</li> <li>182</li> <li>413</li> <li>455</li> <li>454</li> <li>184</li> <li>272,</li> </ul>
Chen, M	<ul> <li>374</li> <li>409</li> <li>411</li> <li>312</li> <li>382</li> <li>213</li> <li>298</li> <li>330</li> <li>367</li> <li>374</li> <li>230</li> <li>383</li> <li>292</li> <li>439</li> <li>389</li> <li>326</li> <li>238</li> <li>373</li> <li>443</li> <li>182</li> <li>413</li> <li>455</li> <li>454</li> <li>184</li> <li>272,</li> <li>439</li> <li>438</li> <li>377</li> </ul>
Chen, M         Chen, P         Chen, Q         410,         Chen, Q         Chen, S         Chen, T         Chen, T         Chen, T         Chen, T         Chen, T         Chen, T         Chen, X         Chen, X G         Chen, Y         Chen, Y         Chen, Z         Chen, Z         Chen, Z         Cheng, C Y         Cheng, C Y         Cheng, Y         Cheng, Y         Cheng, Y M         Cheng, Y M         Cheng, Y M         Chensonis, C         177, 218,	<ul> <li>374</li> <li>409</li> <li>411</li> <li>312</li> <li>382</li> <li>213</li> <li>298</li> <li>330</li> <li>367</li> <li>374</li> <li>230</li> <li>383</li> <li>292</li> <li>439</li> <li>389</li> <li>326</li> <li>238</li> <li>373</li> <li>443</li> <li>182</li> <li>413</li> <li>455</li> <li>454</li> <li>184</li> <li>272,</li> <li>439</li> <li>438</li> <li>377</li> <li>374</li> </ul>
Chen, M	<ul> <li>374</li> <li>409</li> <li>411</li> <li>312</li> <li>382</li> <li>213</li> <li>298</li> <li>330</li> <li>367</li> <li>374</li> <li>230</li> <li>383</li> <li>292</li> <li>439</li> <li>326</li> <li>238</li> <li>373</li> <li>443</li> <li>182</li> <li>413</li> <li>455</li> <li>454</li> <li>184</li> <li>272,</li> <li>439</li> <li>438</li> <li>377</li> <li>374</li> <li>232</li> </ul>
Chen, M	<ul> <li>374</li> <li>409</li> <li>411</li> <li>312</li> <li>382</li> <li>213</li> <li>298</li> <li>330</li> <li>367</li> <li>374</li> <li>230</li> <li>383</li> <li>292</li> <li>439</li> <li>326</li> <li>238</li> <li>373</li> <li>443</li> <li>373</li> <li>443</li> <li>182</li> <li>413</li> <li>455</li> <li>454</li> <li>184</li> <li>272,</li> <li>439</li> <li>438</li> <li>377</li> <li>374</li> <li>232</li> <li>436</li> </ul>
Chen, M Chen, P Chen, Q Chen, Q Chen, S Chen, T Chen, T Chen, T Chen, T Chen, T Chen, X Chen, X Chen, X Chen, X Chen, X Chen, X Chen, Y Chen, Z Chen, Z Cheng, C Cheng, X Chenming, X Cheong, Y Cherukuri, B Chesonis, C 177, 218, 	<ul> <li>374</li> <li>409</li> <li>411</li> <li>312</li> <li>382</li> <li>213</li> <li>298</li> <li>330</li> <li>367</li> <li>374</li> <li>230</li> <li>383</li> <li>292</li> <li>439</li> <li>326</li> <li>238</li> <li>373</li> <li>443</li> <li>373</li> <li>443</li> <li>182</li> <li>413</li> <li>455</li> <li>454</li> <li>184</li> <li>272,</li> <li>439</li> <li>438</li> <li>377</li> <li>374</li> <li>232</li> <li>436</li> <li>294</li> </ul>
Chen, M	<ul> <li>374</li> <li>409</li> <li>411</li> <li>312</li> <li>382</li> <li>213</li> <li>298</li> <li>330</li> <li>367</li> <li>374</li> <li>230</li> <li>383</li> <li>292</li> <li>439</li> <li>326</li> <li>238</li> <li>373</li> <li>443</li> <li>373</li> <li>443</li> <li>182</li> <li>413</li> <li>455</li> <li>454</li> <li>184</li> <li>272,</li> <li>439</li> <li>438</li> <li>377</li> <li>374</li> <li>232</li> <li>436</li> </ul>

Chin, J		443
Chin, L A		311
Chinnappan, R		181
Chipara, M		337
Chisholm, M F		225
Chiti, F		318
Chitre, K 2		321
Cho, G		376
Cho, H S		349
Cho, J		221
Cho, J		448
Cho, J		339
Cho, J 2		321
Cho, K H		362
Cho, S		453
Cho, S		189
Cho, W D 2	26,	368
Choate, W T 2	245,	313
Choe, H		356
Choi, B		413
Choi, D		381
Choi, G 4		454
Choi, W K		189
Choi, Y		334
Choi, Y		455
Choksi, R		425
Chao II 202 206 2		
Choo, H 202, 296, 2	.97,	372
Choudhury, S		426
Chown, L H		270
Choy, K		322
Chrisey, D B 1	97,	239
Christakis, N		404
Christie, M A		197
Christodoulou, J		182
Christodoulou, L 1		422
Christopher, W		181
		352
Chromik, R R 2 Chrzan, D 1	.83,	225
Chu, J P 241, 3		438
Cnu, J P 241. 3		4 <del>3</del> X
	00	
Chu, M G 2		343,
Chu, M G 2 	27,	343, 449
Chu, M G 2	27,	343,
Chu, M G 2 	27, 55,	343, 449
Chu, M G	27, 55, 802,	343, 449 456
Chu, M G	27, 55, 802,	343, 449 456 442
Chu, M G	27, 55, 802,	343, 449 456 442 314 433
Chu, M G	27, 55, 802, 	343, 449 456 442 314 433 422
Chu, M G	-27, -55, 802, 	343, 449 456 442 314 433 422 296
Chu, M G       2	-27, -55, 	<ul> <li>343,</li> <li>449</li> <li>456</li> <li>442</li> <li>314</li> <li>433</li> <li>422</li> <li>296</li> <li>321</li> </ul>
Chu, M G	27, 55, 802, 	<ul> <li>343,</li> <li>449</li> <li>456</li> <li>442</li> <li>314</li> <li>433</li> <li>422</li> <li>296</li> <li>321</li> <li>271</li> </ul>
Chu, M G2	27, 55, 802,     	<ul> <li>343,</li> <li>449</li> <li>456</li> <li>442</li> <li>314</li> <li>433</li> <li>422</li> <li>296</li> <li>321</li> <li>271</li> <li>445</li> </ul>
Chu, M G	27, 55, 002,      	343, 449 456 442 314 433 422 296 321 271 445 456
Chu, M G	-27, -55,       	343, 449 456 442 314 433 422 296 321 271 445 456 244
Chu, M G	.27, 55, 602,    	343, 449 456 442 314 433 422 296 321 271 445 456 244 283
Chu, M G	227, 555, 602,  391, 	343, 449 456 442 314 433 422 296 321 271 445 456 244
Chu, M G	227, 555, 602,  391, 	343, 449 456 442 314 433 422 296 321 271 445 456 244 283
Chu, M G       2	27, 55, 802,       	<ul> <li>343,</li> <li>449</li> <li>456</li> <li>442</li> <li>314</li> <li>433</li> <li>422</li> <li>296</li> <li>321</li> <li>271</li> <li>445</li> <li>456</li> <li>244</li> <li>283</li> <li>171</li> </ul>
Chu, M G	227, 1555, 302,  391,  284, 771,	<ul> <li>343,</li> <li>449</li> <li>456</li> <li>442</li> <li>314</li> <li>433</li> <li>422</li> <li>296</li> <li>321</li> <li>271</li> <li>445</li> <li>244</li> <li>283</li> <li>171</li> <li>296,</li> </ul>
Chu, M G	227, 1555, 302,  391,  1884, 771, 	343, 449 456 442 314 433 422 296 321 271 445 456 244 283 171 296, 434 218
Chu, M G	227, 155, 155, 1002,  1002,	343, 449 456 442 314 433 422 296 321 271 445 456 244 283 171 296, 434 218 210
Chu, M G	227, 555, 602,  	343, 449 456 442 314 433 422 296 321 271 445 456 244 283 171 296, 434 218 210 170
Chu, M G	227, 555, 302,  391,  284, 771, 	343, 449 456 442 314 433 422 296 321 271 445 456 244 283 171 296, 434 218 210 170 310
Chu, M G	227, 555, 302,  391,  284, .71, 	343, 449 456 442 314 433 422 296 321 271 445 456 244 283 171 296, 434 218 210 170 310 236
Chu, M G	227, 555, 602,       	343, 449 456 442 314 433 422 296 321 271 445 456 244 283 171 296, 434 218 210 170 310 236 304
Chu, M G	227, 555, 602,       	343, 449 456 442 314 433 422 296 321 271 445 456 244 283 171 296, 434 218 210 170 310 236 304 386
Chu, M G	227, 555, 602,  591,  284, 771,  284, 219, 84,	343, 449 456 442 314 433 422 296 321 271 445 456 244 283 171 296, 434 218 210 170 310 236 304 386 315
Chu, M G	227, 555, 602,  591,  284, 771,  284,  219, 84, 	343, 449 456 442 314 433 422 296 321 271 445 456 244 283 171 296, 434 218 210 170 310 236 304 386
Chu, M G	227, 555, 602,  591,  284, 771,  284,  219, 84, 	343, 449 456 442 314 433 422 296 321 271 445 456 244 283 171 296, 434 218 210 170 310 236 304 386 315

~	10.5
Coleman, M A	436
Colley, L J	386
Collins, P C	358
Collins, T L	319
Collins, T	
Colton, F	329
Colvin, J 406,	431
Combeau, H	248
Compton, C C	
Compton, C.C	303
Compton, W D 207,	259
Conard, B R	244
Conlon, K T	371
Conrad, H 380,	392
Conradi, M	263
Conway-Mortimer, J	230
Cook, B A	287
Cook, R	341
Cooley, J C	253
Cooper, K G	242
Cooper, K P 394,	435
Cooper, R P	191
Copeland, B J	245
Corby, C P	376
Cordes, R	369
Cordill, M J	262
Coriell, S R	247
Cormier, D	197
Cornish, L	270
Correa, O V	429
Corson, R P 396,	397
Costa, M L	329
Cotts, E J 382,	416
Counts, W A	452
Couper, M J	299
Coupez, T	178
Courtenay, J 361,	403
Couturier, G	250
Covert, C	266
Cramb, A W	248
Crimp, M A 324,	
Crist, E M	220
Cristol, B 170, 171,	
Cross, M	
Cruz, E S	
Csontos, A A 199, 200,	226
Cuitino, A M	365
Cunningham, J M	226
Curlook, W 285,	443
Curran, M	316
Curry, M	262
Curtarolo, S 205,	
Czerny, C	329
<i>CL</i> 01111y, C	527

# D

da Cruz, V F	320
Dahle, A 272,	299,
	411
Dahotre, N B 301,	346,
	450
Dai, K	208
Daigle, E O	185
Daimer, J	177
Dalmijn, W L 173,	245
Dalton, R	172
Dalvi, A D 188,	231
Dammers, A J	248

D ( ))D	
Dando, N R 267,	399
Dan'ko, V A	180
Dantzig, J A	386
Dariavach, N	339
Darmawan, F	448
Das, R P	336
Das, R R 195,	237,
	336
Das, S K 172,	213,
	385
Dasari, A	302
Dasgupta, A	192
Dashwood, R J 223,	323
Date, M	294
Dattelbaum, A M	447
Dauskardt, R H 229, 240,	270
David, S A 203, 223,	345
Davies, R W	268
Davis, B R	357
Davis, L J	218
Daw, M 183, 222,	225
Dawson, P R	235
Dax, B 379, 423,	446
Dax, R F	319
Daya, Z A	417
Dayan, D	287
Dayananda, M A 215,	315
Daymond, M R 297, 328,	372
De Angelis, R J	257
de Campos, M F	204
De Fontaine, D R	205
De Graef, M 196,	422
de Groot, J D	273
De Hosson, J T	275
de Jong, R A	362
de Jong, T P 173,	245
de Lima, N B	429
De Messemaeker, J	392
de Napole Gregolin, E	440
de Vasconcelos, P D	172
de Vries, A J	360
Decker, R F	418
Deevi, S C	413
Defendi, G A	320
Dehm, G	229
Dehoff, R R	358
Dejmek, M	387
Del Corso, G	414
Delaire, O	405
Delos-Reyes, M A	279
Demonstration C D 279	
Demopoulos, G P 378,	426
Deneys, A C 184, 225, 226,	281,
	441
Deng, X 286, 293, 331, 341,	416
Denning, J W 276,	332
Dennis, K	296
Derev'yanko, O V	381
Derin, B C	185
Derlet, P M	
Dernedde, E	נער
	305 398
	398
DeRosset, W S	398 182
DeRosset, W S Deryagin, A	398 182 255
DeRosset, W S Deryagin, A Desai, V	398 182 255 410
DeRosset, W S Deryagin, A Desai, V 246, Deshmukh, P V	398 182 255
DeRosset, W S Deryagin, A Desai, V	398 182 255 410
DeRosset, W S Deryagin, A Desai, V 246, Deshmukh, P V	<ul> <li>398</li> <li>182</li> <li>255</li> <li>410</li> <li>398</li> <li>213</li> <li>183</li> </ul>
DeRosset, W S Deryagin, A Desai, V	<ul> <li>398</li> <li>182</li> <li>255</li> <li>410</li> <li>398</li> <li>213</li> </ul>
DeRosset, W S Deryagin, A Desai, V	<ul> <li>398</li> <li>182</li> <li>255</li> <li>410</li> <li>398</li> <li>213</li> <li>183</li> </ul>

Detavernier, C	370
Deveaux, E	415
Deveaux, M	361
	278
Devincre, B	
DeYoung, D H 273,	361
Dias, H P	213
Diaz, L 199,	321
Díaz, R J	171
Dickerson, M B	291
Dickerson, R 342,	411
Dickmann, D	391
Diepers, H	386
Dijkstra, W O	248
Dimiduk, D M 309,	357
Dinda, G	351
Ding, J	243
Ding, R	280
Ding, W	325
Ding, W	288
Dinh, L N	310
Diplas, S	216
Ditenberg, I A	256
Dixon, T W	217
Djambazov, G S	362
Dahadain Q.V. 252 422	
Dobatkin, S V 253, 432,	433
Dogan, N	273
Dogan, O N	401
Doherty, R 204, 250, 302,	303
Dolan, D S	189
Donaldson, A	369
Donaldson, D J	285
Dong, H 278,	406
Dong, S	234
Dong, Y	200
Dong, Z F	241
Dorsam, G	400
Dou, S X	354
Douglas, E	377
Doumanidis, H	209
Dow, J D	276
Downes, S 232,	339
Doyle, C	415
Doyle, F M 280,	448
Drawin, S	358
Drchal, V 192,	304
Dregia, S A	249
Dresler, W	444
Dresselhaus, M S 193,	209
Dreyfus, J	177
Dreysse, H C	348
Drezet, J 203, 218, 385,	450
Dring, K F 223,	323
Driver, J	250
Droste, W E	219
Drouet, M G	245
Drummond, B G	173
Druschitz, A P	442
Druschitz, E A	442
Du, Q 323, 387,	406
Du, T 410,	448
Du, Z 207,	257
Duda, S	373
Dudley, E	230
Dudo, T	259
Dufour, G	171
Dugger, M T	309
1-46601, 141 1	509

460

Duh, J G				332, 447
Dulikravich, G S			193,	288
Dunand, D C	327,	328,	340,	356
Dündar, M			273,	450
Dunham, S N				381
Dunn, J				365
Dunstan, D				262
Duomo, Z				378
Dupuis, M				437
Duquette, D J				413
Durairaj, R			232,	416
Duterque, J				329
Dutrizac, J E		186,	230,	231
Dutta, I	187,	188,	229,	283,
	286,	327,	342,	371
Duval, H				319
Duxbury, P M				391
Duygulu, O				233
Duz, V A	278,	364,	365,	440
Dybkov, V I				455
Dyck, C				394
Dye, D				371
Dyer, T		•••••		370

# E

Earthman, J C	326
Eastman, J A	238
Easton, M 344,	403
Eaton, S	263
Eberl, C	188
Eckert, C E	370
Edelstein, A S	241
Edrisy, A	413
Edwards, B J	317
Edwards, L	217
Efros, B M 255,	260
Efros, N	255
Egami, T	216
Ege, E S	286
Egry, I	380
Eidet, T	272
Eisinger, N 391,	445
Eizenberg, M	198
Ekenes, J M	272
Ekere, N 232,	416
El-Kaddah, N 362,	428
Elder, K R	322
Eliezer, D	192
Elliott, A J	195
Elliott, A L 281,	282
Elmadagli, M	254
Elmer, J W	345
Embury, D 339,	408
Embury, J D 261, 302,	303
Emelander, D	417
Emerson, J A	394
Emura, S	337
Engh, T A	266
England, L G 300,	343
Enikeev, N A 252,	258
Enomoto, M	186
Erasmus, L	330
Erb, A	276
	270 308
Erb, U Erickson, K L	308 338
EIICKSUII, K L	330

Erlebacher, J D	379
Ernst, W	364
Erol, A	290
Esaka, H 184,	301
Escobedo, J	361
Escudero, R	378
Eskin, D	203
Espinoza-Nava, L	399
Esquivel, E V 279, 395,	441
Essadiqi, E	233
Estey, C M	214
Estrin, Y 251, 252,	260
Evangelista, E	351
Evans, G A	292
Evans, J W 280,	319,
	448
Evans, K J	246
Evelin, S S	329
Ewing, W	448
-	

# F

Fabina, L	
Fachinotti, V D	
Fagerlund, K	
Faivre, G P	
Faizan, M	374
Fallahi, A 30	3, 431
Falleiros, I G 20	
Faller, K	
Falticeanu, L C	341
Fan, J	380
Fan, P	368
Fan, W	394
Fang, J S	242
Fang, Q T	318
Farkas, D 205, 224, 25	
	0, 451
Favet, S	
Fazeli, F	
Fecht, H	
Feigl, K	
Feng, F	
Feng, G	
Feng, J C	392
Feng, Q 27	
Feng, Z	-,
Fenton, C	
Fergus, J W	
Fernandes, F	
Fernandes, S M	
Fernandez, F E 19	
Fernandez, J	
Fernández-Flores, R	
Fernández-Serrano, R	
Ferreira, I	
Ferreira, M A	
Ferres, L	
Ferron, C J	
Ferry, M	433
Field, D P 22	
222 279, 320, 34	
	- ) -
Field, R D	
Fielden, D E 202, 23	
Fields, R J	
Finel, A	- )
Fiory, A 180, 27	6, 321

Fiot, L	172
Fischer, B	270
Fischer, C C	348
Fischer, F D	405
Fischer, W K	
	360
Fishman, S G	315
Fiske, M	242
Fiterman, M J	267
Fittock, J E 373,	443
Fitz-Gerald, J	321
Fjaer, H 218,	385
Fjeld, A	319
Fleay, J	230
Fleming, C A	284
Flemings, M C 202, 296,	369
Fleury, D R	230
Flisakowski, P J	361
Florando, J N	309
Flores, A	361
Flores, K H	316
Flores, K M	316
Floro, J A	394
Flower, H M 173, 223,	323
Foecke, T J	268
Foiles, S M	347
Fok, I	285
Folch, R	387
Foley, J C 242, 295,	340
-	
Folz, H	442
Fonseca, M B	230
Foosnaes, T	218
Forbes Jones, R M 219,	414
Fornaro, O	300
Forrest, S	
	180
Forslund, K G	176
Forté, G 170,	311
Fortier, M	439
Fortunier, R	250
Fox, S P 278,	406
Fraczkiewicz, A	225
Franetovic, V 386,	450
Frank, R A	361
Frankel, J I 298,	421
Franklin, J S	296
Frary, M	451
Fraser, H L 309,	358
Fray, D J 182, 199, 223,	
	278,
	440
Frazier, W E 419,	420
Frear, D R 187,	229,
	371
Frederick, M J	422
Free, M L 226, 369,	413
Freels, M	271
Freeman, A J 270,	430
Freibergs, J	437
Frias, J	415
Friedman, L H	408
Friedman, P A 211,	264,
310, 355, 397,	398
Friedrich, H	365
Fries, S G	206
Frisk, K	363
Froes, F H 182, 223,	278,
	440
Frost, H J	204
Frost, M T	
	• ± /

Fu, E K	350
Fu, X	390
Fuentes-Cabrera, M	431
Fujii, H	323
Fujii, H	354
Fujikura, M	315
Fujita, A	396
Fujiyoshi, M	294
Fukamichi, K	396
Fuller, C	226
Fultz, B 206, 354,	405
Furrer, D U 174,	215,
	400
Furu, E	172
Furuhara, T 282,	327
Furukawa, M 206,	251,
	433
Furuno, K	433
Furuya, K	301
Fushen, L	325

# G

Gabb, T P	340
Gable, B M 199,	376
Gabrielyan, T N	312
Gaddis, C S	291
Gagne, J	171
Galarraga, R A	171
Gali, A	185
Galloway, T 170, 212, 265,	311
Gamsjäger, E	405
Ganapathysubramanian, S	235
Gandin, C 202,	248
Ganesan, P G	422
Gang, F	261
Gangloff, R P	410
Gangopadhyay, A K	438
Gao, B	400
Gao, H	395
Gao, J	177
Gao, M C 363,	442
Gao, W	413
Gao, W	241
Gao, X	445
Gao, Y	173
Gararia, S N	312
Garbellini, O B	450
Garcia, A J 240,	291
Gariepy, B	266
Garmestani, H	237
Garner, C M	209
Garratt, M	410
Garud, C	237
Garvin, J W	249
Gatty, D G	399
Gazder, A A	254
Geerpuram, D N	196
Geiss, E	451
Geltmacher, A B 234,	235
Gemeinböck, G	392
Genau, A L	345
Geng, J	359
Gentz, M	371
George, E P 185, 269, 372,	401
George, S	261
Gerberich, W W	261

Gerdemann, S J	
	440
Gerogiorgis, D I	356
Gerritsen, T 330,	331
Gesing, A J 172,	173
Geveci, A	185
Geyrhofer, W	
	336
Ghomashchi, M R	423
Ghomashchi, R	439
	224
Ghoniem, N M	
Ghorbani, H R	331
Ghosh, A K 211, 264,	310,
	419
Ghosh, G 294, 304,	358
Ghosh, S	229
Ghosh, S	328
Giannuzzi, L A	432
Gibala, R 379,	430
Gibson, R	399
Gigliotti, M F	195
Gillaspie, J	443
Gilmer, G	431
	237
Giordani, E J	
Girgin, S	426
Girin, O B 280,	447
Gjestland, H	191
Gladysz, G M	343
Glaner, L	270
Glatzel, U	270
Glavicic, M G	324
Gleeson, B 295, 455,	456
Glicksman, M E 181,	248,
299,	
	409
Gnäupel-Herold, T 268,	372
Go, J	268
Goddard, III, W A	192
Godfrey, A B	407
Goff, A	295
Goldsmith, C	416
	435
Gole, J L 170,	
Golovashchenko, S F 213,	214
Golovashchenko, S F 213,	
Golovashchenko, S F 213, Golumbfskie, W J	243
Golovashchenko, S F 213, Golumbfskie, W J Gomes, A S	243 272
Golovashchenko, S F 213, Golumbfskie, W J Gomes, A S Gomez-Cordobes, J	243 272 412
Golovashchenko, S F 213, Golumbfskie, W J Gomes, A S Gomez-Cordobes, J	243 272 412
Golovashchenko, S F 213, Golumbfskie, W J Gomes, A S Gomez-Cordobes, J Gong, J	243 272 412 237
Golovashchenko, S F 213, Golumbfskie, W J Gomes, A S Gomez-Cordobes, J Gong, J Gonzalez, C	243 272 412 237 449
Golovashchenko, S F 213, Golumbfskie, W J Gomes, A S Gomez-Cordobes, J Gong, J Gonzalez, C Gonzalez Crespo, P A 207,	243 272 412 237 449 258
Golovashchenko, S F 213, Golumbfskie, W J Gomes, A S Gomez-Cordobes, J Gong, J Gonzalez, C	243 272 412 237 449
Golovashchenko, S F 213, Golumbfskie, W J Gomes, A S Gomez-Cordobes, J Gong, J Gonzalez, C Gonzalez Crespo, P A 207, González, M A	243 272 412 237 449 258 361
Golovashchenko, S F 213, Golumbfskie, W J Gomes, A S Gomez-Cordobes, J Gong, J Gonzalez, C Gonzalez Crespo, P A 207, González, M A González-Doncel, G	243 272 412 237 449 258 361 361
Golovashchenko, S F 213, Golumbfskie, W J Gomes, A S Gomez-Cordobes, J Gong, J Gonzalez, C Gonzalez Crespo, P A 207, González, M A González-Doncel, G Goods, S H 209,	243 272 412 237 449 258 361 361 261,
Golovashchenko, S F 213, Golumbfskie, W J Gomes, A S Gomez-Cordobes, J Gong, J Gonzalez, C Gonzalez Crespo, P A 207, González, M A González-Doncel, G	243 272 412 237 449 258 361 361
Golovashchenko, S F 213, Golumbfskie, W J Gomes, A S Gomez-Cordobes, J Gong, J Gonzalez, C Gonzalez, C González, M A González-Doncel, G Goods, S H	243 272 412 237 449 258 361 361 261,
Golovashchenko, S F 213, Golumbfskie, W J Gomes, A S Gong, J Gonzalez, C Gonzalez, C González, M A González-Doncel, G Goods, S H 209, 	243 272 412 237 449 258 361 361 261, 418 244
Golovashchenko, S F 213, Golumbfskie, W J Gomes, A S Gong, J Gonzalez, C Gonzalez, C González, M A González-Doncel, G Goods, S H	243 272 412 237 449 258 361 361 261, 418 244 444
Golovashchenko, S F 213, Golumbfskie, W J Gomes, A S Gomez-Cordobes, J Gonzalez, C Gonzalez, C González, M A González-Doncel, G Goods, S H 209, 	243 272 412 237 449 258 361 361 261, 418 244
Golovashchenko, S F 213, Golumbfskie, W J Gomes, A S Gomez-Cordobes, J Gonzalez, C Gonzalez, C González, M A González-Doncel, G Goods, S H 209, 	243 272 412 237 449 258 361 361 261, 418 244 444
Golovashchenko, S F 213, Golumbfskie, W J Gomes, A S Gomez-Cordobes, J Gonzalez, C Gonzalez, C González, M A González-Doncel, G Goods, S H 209, 	243 272 412 237 449 258 361 361 261, 418 244 444 288 270
Golovashchenko, S F 213, Golumbfskie, W J Gomes, A S Gomez-Cordobes, J Gonzalez, C Gonzalez, C González, M A González-Doncel, G Goods, S H	243 272 412 237 449 258 361 361 261, 418 244 444 288 270 425
Golovashchenko, S F213,Golumbfskie, W JGomes, A SGomez-Cordobes, JGonzalez, CGonzalez, CGonzalez, CGonzález, M A207,González-Doncel, G209,	243 272 412 237 449 258 361 361 261, 418 244 444 288 270 425 416
Golovashchenko, S F 213, Golumbfskie, W J Gomes, A S Gomez-Cordobes, J Gonzalez, C Gonzalez, C González, M A González-Doncel, G Goods, S H	243 272 412 237 449 258 361 361 261, 418 244 444 288 270 425
Golovashchenko, S F213,Golumbfskie, W JGomes, A SGomez-Cordobes, JGonzalez, CGonzalez, CGonzalez, C207,González, M A207,González-Doncel, G209,	243 272 412 237 449 258 361 361 261, 418 244 444 288 270 425 416 395
Golovashchenko, S F213,Golumbfskie, W JGomes, A SGomez-Cordobes, JGong, JGonzalez, CGonzalez, CGonzález, M A207,González-Doncel, G209,	243 272 412 237 449 258 361 361 261, 418 244 444 288 270 425 416 395 266
Golovashchenko, S F213,Golumbfskie, W JGomes, A SGomez-Cordobes, JGonzalez, CGonzalez, CGonzalez, C207,González, M AGonzález-Doncel, GGoods, S H	243 272 412 237 449 258 361 361 261, 418 244 444 288 270 425 416 395 266 203
Golovashchenko, S F213,Golumbfskie, W JGomes, A SGomez-Cordobes, JGong, JGonzalez, CGonzalez, CGonzález, M A207,González-Doncel, G209,	243 272 412 237 449 258 361 361 261, 418 244 444 288 270 425 416 395 266
Golovashchenko, S F213,Golumbfskie, W JGomes, A SGomez-Cordobes, JGong, JGonzalez, CGonzalez, CGonzález, M A207,González-Doncel, G209,	243 272 412 237 449 258 361 361 261, 418 244 444 288 270 425 416 395 266 203 244
Golovashchenko, S F 213, Golumbfskie, W J Gomes, A S Gomez-Cordobes, J Gonzalez, C Gonzalez, C González, M A González-Doncel, G Goods, S H Goods, S H	243 272 412 237 449 258 361 361 261, 418 244 444 288 270 425 416 395 266 203 244 354
Golovashchenko, S F213,Golumbfskie, W JGomes, A SGomez-Cordobes, JGong, JGonzalez, CGonzalez, CGonzález, M AGonzález-Doncel, GGoods, S H	243 272 412 237 449 258 361 361 261, 418 244 444 288 270 425 416 395 266 203 244 354 354
Golovashchenko, S F 213, Golumbfskie, W J Gomes, A S Gomez-Cordobes, J Gonzalez, C Gonzalez, C González, M A González-Doncel, G Goods, S H Goods, S H	243 272 412 237 449 258 361 361 261, 418 244 444 288 270 425 416 395 266 203 244 354
Golovashchenko, S F213,Golumbfskie, W JGomes, A SGomez-Cordobes, JGong, JGonzalez, CGonzalez, CGonzález, M AGonzález-Doncel, GGoods, S H	243 272 412 237 449 258 361 361 261, 418 244 444 288 270 425 416 395 266 203 244 354 354
Golovashchenko, S F213,Golumbfskie, W JGomes, A SGomez-Cordobes, JGong, JGonzalez, CGonzalez, CGonzález, M AGonzález-Doncel, GGoods, S H209,	243 272 412 237 449 258 361 361 261, 418 244 444 288 270 425 416 395 266 203 244 354 354 442 386
Golovashchenko, S F213,Golumbfskie, W JGomes, A SGomez-Cordobes, JGong, JGonzalez, CGonzalez, CGonzález, M AGonzález-Doncel, GGoods, S H209,	243 272 412 237 449 258 361 361 261, 418 244 444 288 270 425 416 395 266 203 244 354 354 442 386 219
Golovashchenko, S F213,Golumbfskie, W JGomes, A SGomez-Cordobes, JGong, JGonzalez, CGonzalez, CGonzález, M AGonzález-Doncel, GGoods, S H209,	243 272 412 237 449 258 361 361 261, 418 244 444 288 270 425 416 395 266 203 244 354 354 442 386 219
Golovashchenko, S F213,Golumbfskie, W JGomes, A SGomez-Cordobes, JGong, JGonzalez, CGonzalez, CGonzález, M AGonzález-Doncel, GGoods, S H	243 272 412 237 449 258 361 361 261, 418 244 444 288 270 425 416 395 266 203 244 354 354 442 386 219

Grant, G J 268,	314
Grasso, P 385,	450
Gratias, D	206
Gray, G T 233,	303,
	454
Grazier, J M	331
Green, B	359
Green, J A	245
Green, W P	264
Greer, A J	276
Greer, A L 298, 316, 344,	403
Greer, J R	261
Gregori, F	366
Gremaud, M	203
Gribb, T T	198
Griese, R 276,	332
Griffin, J V	273
Griffith, M	370
Grimm, T L	303
Grindstaff, Q G	396
Grosjean, E	417
Gross, K J 262,	310
Groza, J R	242
Gruen, G	219
Grugel, R N	247
Grund, G	330
Gschneidner, K A	396
Gu, S	171
Gu, Y 269,	270
Guangjun, Z	455
Guclu, M	365
Guduru, R	393
Guertsman, V	355
Guillemot, G	248
Guillot, J	319
Guinta, R K	394
Guldhav, A	272
Gundakaram, R C	391
Gunderov, D V	260
Gungor, M N 223,	323
Gunnewiek, L 362,	424
Guo, D	447
Guo, F	217
Guo, G	323
Guo, H	282
Guo, T 178,	387
Guo, X	288
Guo, Z X	215
Guozhi, Z	325
Gupta, A K	399
Gupta, M	262
Gupta, P	185
Gurupira, T Z	414
Guruswamy, S 396,	397
Gusev, A	437
Gustafson, T W	173
Guthrie, R I	417
Guven, I	229
Guyer, J E	276
Guyot, P	438
ц	

# H

Ha, D	453
На, Ј	260
Haataja, M	276
Haberling, C	383



Hackenberg, R E	•••••	442
Haeffner, D R		272
Haggett, R		420
Hagiwara, M		337
Hagman, A		436
Hagni, A M		295
Hahn, H W		306
Hakik, M		342
Hakonsen, A		318
Halali, M		369
Halas, N		240
Haldenwanger, H		383
Halikia, I		330
Hall, M G		282
Hallbom, D J		443
Hamadou, H		203
Hamawi, D		395
Hamipikian, J		381
Hammar, R H		211
Hammon, D L		261
Hampikian, J		388
Han, B Q 256, 352,		392
Han, C		448
Han, E		412
Han, G		226
Han, J 301,		388
Han, J		454
Han, K		407
Han, K		392
Han, K		448
Han, L		311
Han, M K		247
Han, Q 227, 266, 281,	298,	299,
		449
Han, S Han, S Y		222 433
Hanada, S		455 315
Hanagan, M J		319
Handtrack, D		315
Hanna, M D		211
Hanrahan, R J		396
Hansen, B L		453
Hansen, J		436
Hansen, N 251, 252,	302	346
Hanson, R		404
Нао, Ү		195
Haouaoui, M	257,	341
Haouaoui, M Harada, H 174,	257, 269,	
Harada, H 174,	269,	341
Harada, H 174, Hardwick, D A	269, 174,	341 270
Harada, H 174, Hardwick, D A 269, 315,	269, 174, 357,	341 270 215,
Harada, H 174, Hardwick, D A	269, 174, 357,	341 270 215, 400
Harada, H 174, Hardwick, D A 269, 315,	269, 174, 357, 	341 270 215, 400 235
Harada, H 174, Hardwick, D A 269, 315, Hardy, J S Hariharaputran, R	269, 174, 357, 	341 270 215, 400 235 181
Harada, H 174, Hardwick, D A	269, 174, 357, 	341 270 215, 400 235 181 287
Harada, H 174, Hardwick, D A 269, 315, Hardy, J S Hariharaputran, R Harringa, J L Harris, B	269, 174, 357, 	341 270 215, 400 235 181 287 230
Harada, H 174, Hardwick, D A	269, 174, 357, 	341 270 215, 400 235 181 287 230 329
Harada, H 174, Hardwick, D A	269, 174, 357, 	341 270 215, 400 235 181 287 230 329 333
Harada, H 174, Hardwick, D A	269, 174, 357, 	341 270 215, 400 235 181 287 230 329 333 328 397 197
Harada, H 174, Hardwick, D A	269, 174, 357,	341 270 215, 400 235 181 287 230 329 333 328 397
Harada, H 174, Hardwick, D A	269, 174, 357, 	341 270 215, 400 235 181 287 230 329 333 328 397 197 276 349
Harada, H 174, Hardwick, D A	269, 174, 357, 	341 270 215, 400 235 181 287 230 329 333 328 397 197 276 349 295
Harada, H 174, Hardwick, D A	269, 174, 357,   288,	341 270 215, 400 235 181 287 230 329 333 328 397 197 276 349 295 324
Harada, H 174, Hardwick, D A	269, 174, 357,	341 270 215, 400 235 181 287 230 329 333 328 397 197 276 349 295 324 435
Harada, H 174, Hardwick, D A	269, 174, 357,	341 270 215, 400 235 181 287 230 329 333 328 397 197 276 349 295 324 435 413
Harada, H 174, Hardwick, D A	269, 174, 357,	341 270 215, 400 235 181 287 230 329 333 328 397 197 276 349 295 324 435

Hashimoto, S		338
Haskel, D		250
Hasnaoui, A		305
Hassan, H		372
Hassan, M I		385
Hata, S		390
Hatch, C		323
Hatsuda, K		206
Hauback, B C		353 318
Haugen, T Hawk, J A	•••••	401
Hayashi, T 215,	315	401
Hayashi, Y		435
Hayes, P C		330
Haywood, R		362
Hazzledine, P M		225
He, G		337
Не, М		373
Heamot, N		426
Hearne, S J		261,
		418
Heason, C P		253
Hebert, R J		253
Hedjazi, J Heilmaier, M		439 355
Hellmig, R		252
Hemker, K J		283
Henager, C H		355
Henderson, D W		286,
		417
Hendriksen, M	232,	416
Henein, H 379,		446
Hennig, R G	183,	431
Henrie, B L	233.	202
		303,
	451,	453
	451,	453 428
	451, 	453 428 441
Henry, D M	451,  344,	453 428 441 380
Henry, D M	451,  344,	453 428 441 380 252
Henry, D M Henry, P J Herlach, D M Herman, G Hermesmann, C	451,  344, 	453 428 441 380 252 214
Henry, D M	451,  344,  408,	453 428 441 380 252
Henry, D M Henry, P J Herlach, D M Herman, G Hermesmann, C Hernández-Morales, J B	451,  344,  408,	453 428 441 380 252 214 409
	451,  344,  408,  340,	<ul> <li>453</li> <li>428</li> <li>441</li> <li>380</li> <li>252</li> <li>214</li> <li>409</li> <li>353</li> </ul>
	451,  344,  408,  340, 	453 428 441 380 252 214 409 353 270 356 390
	451,  344,  408,  340, 	453 428 441 380 252 214 409 353 270 356 390 291
	451,  344,  408,  340, 	<ul> <li>453</li> <li>428</li> <li>441</li> <li>380</li> <li>252</li> <li>214</li> <li>409</li> <li>353</li> <li>270</li> <li>356</li> <li>390</li> <li>291</li> <li>417</li> </ul>
	451,  344,  408,  340, 	453 428 441 380 252 214 409 353 270 356 390 291 417 324
	451,  344,  408,  340, 	453 428 441 380 252 214 409 353 270 356 390 291 417 324 287
	451, 	453 428 441 380 252 214 409 353 270 356 390 291 417 324 287 177
	451, 	453 428 441 380 252 214 409 353 270 356 390 291 417 324 287 177 225
	451,  344,  408,  340,  191, 	453 428 441 380 252 214 409 353 270 356 390 291 417 324 287 177 225 175
	451, 	453 428 441 380 252 214 409 353 270 356 390 291 417 324 287 177 225
	451, 344,  408,  340,  191, 	453 428 441 380 252 214 409 353 270 356 390 291 417 324 287 177 225 175 194
	451, 	453 428 441 380 252 214 409 353 270 356 390 291 417 324 287 177 225 175 194 323
	451, 	453 428 441 380 252 214 409 353 270 356 390 291 417 324 287 175 194 323 453
	451, 	453 428 441 380 252 214 409 353 270 356 390 291 417 324 287 175 194 323 453 269 408 453
	451, 344,  340,  340,  191,  191,  404, 	453 428 441 380 252 214 409 353 270 356 390 291 417 324 287 177 225 175 194 323 453 269 408 453 355
	451, 	453 428 441 380 252 214 409 353 270 356 390 291 417 324 287 175 175 175 175 194 323 453 269 408 453 355 408
	451, 	453 428 441 380 252 214 409 353 270 356 390 291 417 324 287 175 175 175 175 194 323 453 269 408 453 355 408 278
	451,  344,  408,  340,  191,  191,  191,  191,  191,  191,  191, 	453 428 441 380 252 214 409 353 270 356 390 291 417 324 287 175 194 323 453 269 408 453 355 408 278 311
	451,  344,  408,  340,  3340,  191,  191,  191,  191,  394,  394, 	<ul> <li>453</li> <li>428</li> <li>441</li> <li>380</li> <li>252</li> <li>214</li> <li>409</li> <li>353</li> <li>270</li> <li>356</li> <li>390</li> <li>291</li> <li>417</li> <li>324</li> <li>287</li> <li>177</li> <li>225</li> <li>175</li> <li>194</li> <li>323</li> <li>269</li> <li>408</li> <li>453</li> <li>355</li> <li>408</li> <li>278</li> <li>311</li> <li>261</li> </ul>
	451, 	453 428 441 380 252 214 409 353 270 356 390 291 417 324 287 177 225 175 194 323 453 269 408 453 355 408 278 311 261 370
	451, 	<ul> <li>453</li> <li>428</li> <li>441</li> <li>380</li> <li>252</li> <li>214</li> <li>409</li> <li>353</li> <li>270</li> <li>356</li> <li>390</li> <li>291</li> <li>417</li> <li>324</li> <li>287</li> <li>177</li> <li>225</li> <li>175</li> <li>194</li> <li>323</li> <li>453</li> <li>269</li> <li>408</li> <li>453</li> <li>355</li> <li>408</li> <li>278</li> <li>311</li> <li>261</li> <li>370</li> <li>178</li> </ul>
	451, 	453 428 441 380 252 214 409 353 270 356 390 291 417 324 287 177 225 175 194 323 453 269 408 453 355 408 278 311 261 370

Holloway, P H	377
110110 way, 1 11	
Holm, E A 181, 182,	224,
Holm, E A 181, 182,	407
Holmsen, A	398
Holtkamp, D B	303
Homentcovschi, D	417
Hon, M	374
Hong, D	377
Hong, F	417
Hong, J	321
Hong, K	293
6	
Hong, S 214,	350
Hongming, G	455
Hoo, N	416
Hopkins, P L	338
Horita, Z 206,	251,
	433
	356
Horstemeyer, M	
Hort, N	445
Horton, D J	297
Horton, J A 184, 287,	359
Horton, J A 104, 207,	
Horton, W S	286
Hosford, W F	257
Hosking, F M	368
	443
Houchin, M	
House, J W	257
Houston, D Q	191
Howard, D W	395
Howard, S M 214,	314
Howe, J M 371,	384
Howell, S W	441
Hoyt, J J 180,	222,
Hoyt, J J 180,	
	405
Hryn, J 199, 244, 357, 417,	100
$111 \text{ y}_{11}, \text{ J}_{}, 199, 2++, 337, +17,$	429
Hsieh, K	242
Hsieh, K Hsieh, Y Y	242 241
Hsieh, K Hsieh, Y Y Hsiung, L L	242
Hsieh, K Hsieh, Y Y Hsiung, L L	242 241
Hsieh, K Hsieh, Y Y Hsiung, L L Hsu, E	242 241 225 201
Hsieh, K Hsieh, Y Y Hsiung, L L Hsu, E Hsu, S C	242 241 225 201 294
Hsieh, K Hsieh, Y Y Hsiung, L L Hsu, E Hsu, S C Hsu, Y	<ul> <li>242</li> <li>241</li> <li>225</li> <li>201</li> <li>294</li> <li>382</li> </ul>
Hsieh, K Hsieh, Y Y Hsiung, L L Hsu, E Hsu, S C	242 241 225 201 294
Hsieh, K Hsieh, Y Y Hsiung, L L Hsu, E Hsu, S C Hsu, Y	<ul> <li>242</li> <li>241</li> <li>225</li> <li>201</li> <li>294</li> <li>382</li> <li>225</li> </ul>
Hsieh, K Hsieh, Y Y Hsiung, L L Hsu, E Hsu, S C Hsu, Y Hsueh, J Hu, H	<ul> <li>242</li> <li>241</li> <li>225</li> <li>201</li> <li>294</li> <li>382</li> <li>225</li> <li>447</li> </ul>
Hsieh, K Hsieh, Y Y Hsiung, L L Hsu, E Hsu, S C Hsu, Y Hsueh, J Hu, H 311, 313, 376, Hu, S 277,	<ul> <li>242</li> <li>241</li> <li>225</li> <li>201</li> <li>294</li> <li>382</li> <li>225</li> <li>447</li> <li>408</li> </ul>
Hsieh, K         Hsieh, Y Y         Hsiung, L L         Hsu, E         Hsu, S C         Hsu, Y         Hsueh, J         Hu, H         311, 313, 376,         Hu, S         277,         Hu, Y C	<ul> <li>242</li> <li>241</li> <li>225</li> <li>201</li> <li>294</li> <li>382</li> <li>225</li> <li>447</li> <li>408</li> <li>338</li> </ul>
Hsieh, K Hsieh, Y Y Hsiung, L L Hsu, E Hsu, S C Hsu, Y Hsueh, J Hu, H 311, 313, 376, Hu, S 277,	<ul> <li>242</li> <li>241</li> <li>225</li> <li>201</li> <li>294</li> <li>382</li> <li>225</li> <li>447</li> <li>408</li> </ul>
Hsieh, K         Hsieh, Y Y         Hsiung, L L         Hsu, E         Hsu, S C         Hsu, Y         Hsueh, J         Hu, H         Y         Hu, S         Hu, S         Hu, S         Y         Hu, S         Y         Hu, S         Y         <	242 241 225 201 294 382 225 447 408 338 331
Hsieh, K         Hsieh, Y Y         Hsiung, L L         Hsu, E         Hsu, S C         Hsu, Y         Hsueh, J         Hu, H         Mu, S         Hu, H         Mu, S         Hu, S         Hu, S         Hu, S         Hu, S         Hu, S         Mu, S         Mu, S         Mu, S         Huang, C	242 241 225 201 294 382 225 447 408 338 331 269
Hsieh, K         Hsieh, Y Y         Hsiung, L L         Hsu, E         Hsu, S C         Hsu, Y         Hsueh, J         Hu, H         Mu, S         Hu, H         Mu, S         Hu, S         Hu, S         Hu, S         Hu, S         Huag, C         Huang, C	<ul> <li>242</li> <li>241</li> <li>225</li> <li>201</li> <li>294</li> <li>382</li> <li>225</li> <li>447</li> <li>408</li> <li>338</li> <li>331</li> <li>269</li> <li>242</li> </ul>
Hsieh, K         Hsieh, Y Y         Hsiung, L L         Hsu, E         Hsu, S C         Hsu, Y         Hsueh, J         Hu, H         Mu, S         Hu, H         Mu, S         Hu, S         Hu, G         Hu, S         Huag, C         Huang, C S         Muang, C S	<ul> <li>242</li> <li>241</li> <li>225</li> <li>201</li> <li>294</li> <li>382</li> <li>225</li> <li>447</li> <li>408</li> <li>338</li> <li>331</li> <li>269</li> <li>242</li> <li>339</li> </ul>
Hsieh, K         Hsieh, Y Y         Hsiung, L L         Hsu, E         Hsu, S C         Hsu, Y         Hsueh, J         Hu, H         Mu, S         Hu, H         Mu, S         Hu, S         Hu, G         Hu, S         Huag, C         Huang, C S         Muang, C S	<ul> <li>242</li> <li>241</li> <li>225</li> <li>201</li> <li>294</li> <li>382</li> <li>225</li> <li>447</li> <li>408</li> <li>338</li> <li>331</li> <li>269</li> <li>242</li> </ul>
Hsieh, K         Hsieh, Y Y         Hsiung, L L         Hsu, E         Hsu, S C         Hsu, Y         Hsu, Y         Hsueh, J         Hu, H         Mu, S         Hu, Y         Mu, S         Hu, F         294,         Huang, C         Huang, J	242 241 225 201 294 382 225 447 408 338 331 269 242 339 224
Hsieh, K         Hsieh, Y Y         Hsiung, L L         Hsu, E         Hsu, S C         Hsu, Y         Hsueh, J         Hu, H         Mu, S C         Hu, G         Mu, H         Mu, S         Hu, Y C         Mu, Y C         Mu, Y C         Huang, C         Huang, C S         Huang, J	242 241 225 201 294 382 225 447 408 338 331 269 242 339 224 257
Hsieh, K         Hsieh, Y Y         Hsiung, L L         Hsu, S C         Hsu, Y         Hsueh, J         Hu, H         Mu, S C         Hu, H         Mu, S C         Hu, G         Mu, H         Mu, S         Hu, Y C         Mu, Y C         Mu, Y C         Muang, C         Huang, C S         Huang, J         Huang, J G         Muang, J G	242 241 225 201 294 382 225 447 408 338 331 269 242 339 224 257 247
Hsieh, K         Hsieh, Y Y         Hsiung, L L         Hsu, E         Hsu, S C         Hsu, Y         Hsueh, J         Hu, H         Mu, S C         Hu, G         Mu, H         Mu, S         Hu, Y C         Mu, Y C         Mu, Y C         Huang, C         Huang, C S         Huang, J	242 241 225 201 294 382 225 447 408 338 331 269 242 339 224 257
Hsieh, K         Hsieh, Y Y         Hsiung, L L         Hsu, S C         Hsu, Y         Hsu, Y         Hsueh, J         Hu, H         Mu, Y C         Mu, Y C         Mu, F         Huang, C         Huang, C S         Huang, J         Huang, J G         232,         Huang, J Y	242 241 225 201 294 382 225 447 408 338 331 269 242 339 224 257 247
Hsieh, K         Hsieh, Y Y         Hsiung, L L         Hsu, S C         Hsu, Y         Hsu, Y         Hsueh, J         Hu, H         Mu, S         Hu, S         YC         Huang, C         Huang, C S         Huang, J         Huang, J G         Yang, J Y         Yang, J Y	242 241 225 201 294 382 225 447 408 338 331 269 242 339 224 257 247 247 306
Hsieh, K         Hsieh, Y Y         Hsiung, L L         Hsu, S C         Hsu, Y         Hsu, Y         Hsu, Y         Hsu, Y         Mu, H         Mu, S         YC         Huang, C         Huang, C S         Huang, J         Huang, J G         Huang, J Y         Huang, J Y	242 241 225 201 294 382 225 447 408 338 331 269 242 339 224 257 247 247 306 271
Hsieh, K         Hsieh, Y Y         Hsiung, L L         Hsu, S C         Hsu, Y         Hsu, Y         Hsu, Y         Hsu, Y         Hueh, J         Hu, S         YC         Huang, C         Huang, C         Huang, J         Huang, J G         Huang, J Y         Huang, J Y         Huang, J Y         Huang, M	242 241 225 201 294 382 225 447 408 338 331 269 242 339 224 257 247 247 306
Hsieh, K         Hsieh, Y Y         Hsiung, L L         Hsu, S C         Hsu, Y         Hsu, Y         Hsueh, J         Hu, H         Mu, Y C         Mu, F         Poly         Huang, C         Huang, J         Huang, J Y         Huang, J S	242 241 225 201 294 382 225 447 408 338 331 269 242 339 224 257 247 247 306 271
Hsieh, K         Hsieh, Y Y         Hsiung, L L         Hsu, S C         Hsu, Y         Hsu, Y         Hsueh, J         Hu, H         Mu, Y C         Mu, F         Poly         Huang, C         Huang, J         Huang, J Y         Huang, J S	242 241 225 201 294 382 225 447 408 338 331 269 242 2339 224 257 247 247 306 271 271
Hsieh, K         Hsieh, Y Y         Hsiung, L L         Hsu, S C         Hsu, Y         Hsu, Y         Hsu, Y         Hsueh, J         Hu, H         Mu, S         YC         Huang, C         Huang, C S         Huang, J         Huang, J Y         Huang, J Y         Huang, J Y         Huang, J Y         Huang, J T	242 241 225 201 294 382 225 447 408 338 331 269 242 339 224 257 247 247 306 271 271 242 439
Hsieh, K         Hsieh, Y Y         Hsiung, L L         Hsu, S C         Hsu, Y         Hsu, Y         Hsu, Y         Huang, J         Huang, J G         Huang, J Y         Huang, J G         Huang, J Y         Huang, J T         Huang, J T         Huang, J S         Huang, J T         Huang, J Y         Huang,	242 241 225 201 294 382 225 447 408 338 331 269 242 2339 224 257 247 247 306 271 271 242 439 302
Hsieh, K         Hsieh, Y Y         Hsiung, L L         Hsu, S C         Hsu, Y         Hsu, Y         Hsu, Y         Huang, J         Huang, J G         Huang, J Y         Huang, J G         Huang, J Y         Huang, J F         Huang, J Y         Huang,	242 241 225 201 294 382 225 447 408 338 331 269 242 2339 224 257 247 247 306 271 271 242 439 302 261
Hsieh, K         Hsieh, Y Y         Hsiung, L L         Hsu, S C         Hsu, Y         Hsu, Y         Hsu, Y         Huang, J         Huang, J G         Huang, J Y         Huang, J G         Huang, J Y         Huang, J F         Huang, J Y         Huang,	242 241 225 201 294 382 225 447 408 338 331 269 242 2339 224 257 247 247 306 271 271 242 439 302
Hsieh, K         Hsieh, Y Y         Hsiung, L L         Hsu, S C         Hsu, Y         Hsu, Y         Hsu, Y         Mu, H         311, 313, 376,         Hu, S         Y         Hu, H         311, 313, 376,         Hu, S         Y         Huang, Y         Huang, C         Huang, C         Huang, C         Huang, J         Huang, J         Huang, J G         Huang, J Y         Huang, Y	242 241 225 201 294 382 225 447 408 338 331 269 242 339 224 257 247 247 247 247 306 271 247 247 306 271 247 247 247 247 247 247 247 247 247 247
Hsieh, K         Hsieh, Y Y         Hsiung, L L         Hsu, S C         Hsu, Y         Hsu, Y         Hsu, Y         Huang, J         Huang, C         Huang, C         Huang, J         Huang, Y         Huang, Y          Huang, Y	242 241 225 201 294 382 225 447 408 338 331 269 242 339 224 257 247 247 247 247 306 271 247 247 306 271 242 439 302 261 251
Hsieh, K         Hsieh, Y Y         Hsiung, L L         Hsu, S C         Hsu, Y         Hsu, Y         Hsu, Y         Huang, J         Huang, C         Huang, C         Huang, J         Huang, Y         Huang, Y         Huang, Y          Huang, Y	242 241 225 201 294 382 225 447 408 338 331 269 242 339 224 257 247 247 247 247 306 271 271 242 439 302 261 258 374
Hsieh, K         Hsieh, Y Y         Hsiung, L L         Hsu, S C         Hsu, Y         Hsu, Y         Hsu, Y         Mu, H         311, 313, 376,         Hu, Y         Hu, H         311, 313, 376,         Hu, S         Y         Huang, Y         Huang, C         Huang, C S         Huang, C S         Huang, J         Huang, J G         Huang, J G         Huang, J Y         Huang, J Y         Huang, J Y         Huang, S         Huang, T F         Huang, X         251, 252,         Huang, Y         Huang, Y	242 241 225 201 294 382 225 447 408 338 331 269 242 339 224 257 247 247 247 247 247 306 271 271 242 439 302 261 258 374 402
Hsieh, K         Hsieh, Y Y         Hsiung, L L         Hsu, S C         Hsu, Y         Hsu, Y         Hsu, Y         Mu, H         311, 313, 376,         Hu, Y         Hu, H         311, 313, 376,         Hu, S         Y         Huang, Y         Huang, C         Huang, C S         Huang, C S         Huang, J         Huang, J G         Huang, J G         Huang, J Y         Huang, J Y         Huang, J Y         Huang, S         Huang, T F         Huang, X         251, 252,         Huang, Y         Huang, Y	242 241 225 201 294 382 225 447 408 338 331 269 242 339 224 257 247 247 247 247 247 306 271 271 242 439 302 261 258 374 402
Hsieh, K         Hsieh, Y Y         Hsiung, L L         Hsu, S C         Hsu, Y         Hsu, Y         Hsueh, J         Hu, H         311, 313, 376,         Hu, Y         Huaeh, J         Huang, C         Huang, C S         Huang, J         Huang, J Y         Huang, J Y         Huang, J Y         Huang, S         Huang, T F         Huang, Y         Huang, Y         Huang, Y         Huang, Y         Huang, Y         Huang, Y	242 241 225 201 294 382 225 447 408 338 331 269 242 339 224 257 247 247 306 271 271 242 439 302 261 261 258 374 402 189
Hsieh, K         Hsieh, Y Y         Hsiung, L L         Hsu, S C         Hsu, Y       332,         Hsueh, J       311, 313, 376,         Hu, H       311, 313, 376,         Hu, H       311, 313, 376,         Hu, S       277,         Hu, Y C       332,         Huar, S       277,         Hu, Y C       332,         Huar, S       274,         Huang, C       332,         Huang, J       294,         Huang, J       234,         Huang, J Y       234,         Huang, J Y       234,         Huang, J Y       234,         Huang, J Y       234,         Huang, S       Huang, T F         Huang, X       251, 252,         Huang, X       251, 252,         Huang, Y       Huang, Y         Huang, Y       Huang, Y         Huang, Y       271	242 241 225 201 294 382 225 447 408 338 331 269 242 339 224 257 247 247 306 271 271 242 439 302 261 258 374 402 189 346
Hsieh, K         Hsieh, Y Y         Hsiung, L L         Hsu, S C         Hsu, Y         Hsu, Y         Hsueh, J         Hu, H         311, 313, 376,         Hu, Y         Huae, S         Huang, C         Huang, C S         Huang, J         Huang, J, Y         Huang, J Y         Huang, J Y         Huang, J Y         Huang, S         Huang, T F         Huang, Y         Huang, D A         Huang, Y         Huang, Y         Huang, Y         Huang, Y         Huang, Y         Huang, D A         Huang, D A	242 241 225 201 294 382 225 447 408 338 331 269 242 339 224 257 247 247 247 247 306 271 271 242 439 302 261 258 374 402 189 346 384
Hsieh, K         Hsieh, Y Y         Hsiung, L L         Hsu, S C         Hsu, Y       332,         Hsueh, J       311, 313, 376,         Hu, H       311, 313, 376,         Hu, H       311, 313, 376,         Hu, S       277,         Hu, Y C       332,         Huar, S       277,         Hu, Y C       332,         Huar, S       274,         Huang, C       332,         Huang, J       294,         Huang, J       234,         Huang, J Y       234,         Huang, J Y       234,         Huang, J Y       234,         Huang, J Y       234,         Huang, S       Huang, T F         Huang, X       251, 252,         Huang, X       251, 252,         Huang, Y       Huang, Y         Huang, Y       Huang, Y         Huang, Y       271	242 241 225 201 294 382 225 447 408 338 331 269 242 339 224 257 247 247 306 271 271 242 439 302 261 258 374 402 189 346

Hultman, L	429
Hults, W L	283
Hung, C M	375
Hünsche, I	401
Hunt, M	217
Huo, Y	380
Hur, B 214, 404,	453
Hurysz, K M	236
Hutchinson, C R	425
Huzmezan, M	195
Hwang, C 190,	338
Hwang, S	254
Hwang, W	285
Hwang, Y J	197
Hyde, B 224,	
Hyde, J R	441
Hyers, R W 289, 299,	438
Hyland, M 218, 265, 399,	412

# Ι

Ice, G E	279,	324,	394
Ichikawa, T			354
Ichimura, S			220
Ignatenko, L N			258
Ikeda, M			324
Ilegbusi, O J			448
Ilyoukha, N			369
Im, J	259,	341,	435
Im, Y H			423
Imai, T			234
Imam, A			278
Imam, M	182,	223,	278,
			440
			441
Imbert, C A Imrie, W P 188,	, 230,	231,	284,
	372,	415,	443
Indrakanti, S K		227,	281
Indutnyy, I Z			180
Inel, C			173
Inman, D			323
Inoue, A		216,	271
Inoue, H			401
Inspektor, A			421
Ionescu, A			173
Iosub, V			210
Ipser, H		231,	382
Irvine, S			441
Isac, M			417
Ishida, K		191,	242
Ishikawa, K			397
Islam, Z	•••••		250
Itakura, M			390
Itharaju, R R			258
Ito, K 215,	315,	357,	401
Ivan, J			296
Ivanisenko, Y			307
Ivanov, Y F	•••••		255
Iwata, S			304
Iyer, M K			241
Izumi, K	•••••		220

# J

Jablokov, V R		173
Jackson, G		416
Jackson, M	223,	323

Jackson, M R	358
Jackson, S M	413
Jacobsen, L	364
Jacobson, D L	210
Jacot, A 203, 385,	387
Jäger, S	234
Jahnsen, E J	330
Jak, E	330
Jakobsson, A	409
Jalkanen, H	186
Jamey, C	172
Jang, G Y 293,	332
Jang, S J	439
Jankowski, A	406
Janousek, M 174,	215,
	400
Janzen, J 330,	331
Jaouen, O	178
Jaradeh, M	298
Jardy, A 219,	404
Jarry, P P	298
Jayakumar, T	227
Jayaraj, B	410
Jayasekera, S	329
Jeannette, J	417
Jéhanno, P 315,	358
Jensen, C M 263,	353
Jeong, H	438
Jeong, S	286
Jerman, G	
Jha, G	
Jha, M K	171
Jian, X 299,	318
Jiang, C 349,	364
Jiang, F 379,	446
Jiang, H	
Jiang, W	
Jiang, W	316
Jiang, Y T	439
Jiao, H Jiao, W L	228 290
Jiao, w L	
Jin, C	
Jili, M	213
Jin, S 196, 197, Jin, Y M 183, 277,	38/
Jin, Z 349,	350
Jo, H	
Jog, J	
Johnson, C	
Johnson, D D	
Johnson, D R 215,	269.
270, 315,	
Johnson, G L	212
Johnson, J A 284,	318
Johnson, J R	353
Johnson, W C 277,	
Johnson, W L 316,	
Jolly, M R	369
	318
Jonas, J J 201,	318 205
Jonas, J J 201, Jonas, R K	318 205 212
Jonas, J J 201, Jonas, R K Jones, C L	318 205 212 414
Jonas, J J 201, Jonas, R K Jones, C L Jones, H 298,	318 205 212 414
Jonas, J J 201, Jonas, R K Jones, C L Jones, H 298, Jones, H N 392,	<ul> <li>318</li> <li>205</li> <li>212</li> <li>414</li> <li>301</li> </ul>
Jonas, J J	<ul> <li>318</li> <li>205</li> <li>212</li> <li>414</li> <li>301</li> <li>435</li> <li>418</li> </ul>
Jonas, J J	318 205 212 414 301 435 418 420
Jonas, J J	<ul> <li>318</li> <li>205</li> <li>212</li> <li>414</li> <li>301</li> <li>435</li> <li>418</li> <li>420</li> <li>170</li> </ul>

Joo, Y		293
Jörgl, H P		336
Josell, D	220,	229,
	280,	409
Joubert, J		210
Juarez, J A		449
Jung, C		300
Jung, J		383
Jung, J		241
Jung, K	380,	392
Jung, S 198, 338,	374,	455
Jung, Y		362
Jungk, J	261,	308
Juul Jensen, D	204,	390

# K

Kabansky, A E	169
Kabra, S	185
Kaczorowski, J	266
Kad, B 366, 371,	383
Kadolkar, P B	411
Kai, H	378
Kaibyshev, R O	311
Kaikake, A	415
Kainer, K U 418,	445
Kainuma, R 191,	242
Kakegawa, K	296
Kakihira, T	366
Kalantar, D H	366
Kalidindi, S R	303
Kaligotla, A	214
Kalu, P 205,	407
Kamachi, M	206
Kamavaram, V	325
Kammer, D	248
Kamp, N	411
Kampe, S L 223, 295,	296
Kane, J	413
Kaneno, Y 174,	401
Kanert, O	297
Kang, S	258
	198.
Kang, S H 179, 220, 274,	320
Kang, S K 189,	231,
285, 331, 373,	416
Kang, T	382
Kang, Y	309
Kantzos, P T	340
Kao, C R 198, 199, 240,	293,
Kao, C.K 198, 199, 240, 	
	382
Kao, H R	375
Kao, S T	190
Kao, V	233
Kaplan, D I	364
Kaplan, H	332
Kapusta, C	
Kapusta, J	184
Karabasevic, D	180
Karabelchtchikova, O P	421
Karaca, H	442
Karaman, I 207, 216,	257,
	442
Karanjai, M	224
Karma, A S	386
Karner, W	
Karney, G B	195



Kasapoglu, Z	315
Kaschner, G C	451
Kashani-Nejad, S	333
Kashyap, B	224
Kashyap, S C	239
Kaspar, R 259,	350
Kassner, M E 279,	433
Kastebo, J	218
Katgerman, L 203, 220, 248,	385
Katiyar, R S	291
Katsman, A	444
Kaufman, L	192
Kawagoishi, N 410,	411
Kawakami, A	323
Kawamura, Y 295,	438
Kawano, Y	449
Kawasaki, M	258
Kawazoe, Y	390
Kay, N R	229 232
Kay, R Ke, L	292 294
Ke, W	288
Kear, B H	209
Keeskes, L J	254
Keen, L	377
Keist, J	414
Keles, Ö 273,	450
Kelkar, K 219,	362
Keller, J	396
Keller, R	399
Kelly, J J	308
Kelly, P M	228
Kelly, S M	223
Kelly, T F	198
Kelton, K F 289,	438
Kemp, D J 189,	231
Kempshall, B W	432
Kendig, K	175
Kennedy, M S	275
Kenney, M 378,	420
Kepes, A	330
Kerdouss, F	361
Kerns, R	441
Kerr, M	331
Kerstiens, B	330
Kertý, B 273,	450
Kertz Yurko, J E	299
Keskinkilic, E Kestler, H	185 315
Khachaturyan, A 183,	277,
Kilachaturyan, A	277, 384
Khan, Z H	171
Khemelevskaya, I Y	253
Khor, K	411
Khraisheh, M K 258, 398,	450
Khraishi, T 221, 356,	451
Kiese, J	365
Kift, J R	415
Kikuchi, E	449
Kikuchi, K	314
Kikuchi, M	407
Kilmametov, A R	306
Kim, C	180
Kim, C	212
Kim, C 179,	220,
	339
Kim, C	442

Kim, D	374
Kim, D H 217,	438
Kim, D S	287
Kim, H	442
Kim, H 453,	454
Kim, H	448
Kim, H	339
Kim, H	389
Kim, H	448
Kim, H	258
Kim, H J	411
Kim, H S Kim, H Y	252 254
Kim, I J	287
Kim, I S	412
Kim, J	246
Kim, J	175
Kim, J	389
Kim, J	352
Kim, J	455
Kim, J	416
Kim, J 453, 454,	455
Kim, J H	433
Kim, J H 286,	294
Kim, J S	417
Kim, K Kim, K	190 281
Kim, K	309
Kim, N	382
Kim, N J	287
Kim, S 198,	338
Kim, S 214,	453
Kim, S	451
Kim, S	455
Kim, S	264
Kim, S	454
Kim, S 215, Kim, S G	241 387
Kim, S H	387 454
Kim, S K	376
Kim, S S	412
Kim, S W 199,	435
Kim, T	374
Kim, W 321,	358
Kim, W T 217, 387,	438
Kim, Y	287
Kim, Y	352
Kim, Y Kim, Y	260 455
Kim, Y Kim, Y	455 309
Kim, Y H Kim Y S 412	374 454
Kim, Y S 412,	454
Kim, Y S 412, Kimura, T Kimura, T	
Kim, Y S 412, Kimura, T Kimura, T	454 351
Kim, Y S 412,	454 351 384
Kim, Y S       412,         Kimura, T	454 351 384 435
Kim, Y S       412,         Kimura, T	454 351 384 435 191 367 259
Kim, Y S       412,         Kimura, T	454 351 384 435 191 367 259 416
Kim, Y S       412,         Kimura, T	454 351 384 435 191 367 259 416 406
Kim, Y S       412,         Kimura, T	454 351 384 435 191 367 259 416 406 195
Kim, Y S       412,         Kimura, T	454 351 384 435 191 367 259 416 406 195 416
Kim, Y S       412,         Kimura, T	454 351 384 435 191 367 259 416 406 195 416 272
Kim, Y S       412,         Kimura, T	454 351 384 435 191 367 259 416 406 195 416 272 353
Kim, Y S       412,         Kimura, T	454 351 384 435 191 367 259 416 406 195 416 272 353 268
Kim, Y S       412,         Kimura, T	454 351 384 435 191 367 259 416 406 195 416 272 353 268 311

Kiss, L I 213,	
Kissane, J	
Kitahara, H	
Kiyobayashi, T	26
Klarstion, D L	20
Klarstrom, D L 226, 297,	
Kleber, S	35
Klein, B	44
Kleinschrodt, H	43
Kletsky, S V	
Klingbeil, D	36
Klingbeil, N W	28
Klingensmith, M A	31
Klinger, C	36
Klug, K L 223,	32
Klushin, S D	33
Kluthe, C	35
Kmiotek, D S	34
Knabl, W	40
Кпарр, Ј А	26
Knott, S	- 19
Ko, Y G	43
Kobade, R	33
Kobayashi, K	32
Kobayashi, T	27
Kobbeltvedt, O	17
Koch, C C 256, 391,	42
Kogut, D	
Kohlbrecher, J	25
Kohn, A	19
Kohn, R V	42
Kohyama, A	18
Koike, J 199, 340, 384,	42
Koike, K	22
Koike, M	40
Koizumi, Y 259, 351,	38
Kolbe, M	38
Kolobov, Y R	30
Koltun, P	33
Komandur, K	41
Komatsu, S	32
Kommel, L	25
Kompan, Y Y	22
Kondoh, K	41
Kondoh, M	44
Koneva, N A 255,	25
Kongoli, F	18
Konopnicki, M G	21
Konstantinov, K K	35
Kontsevoi, O Y	27
Коо, Н	32
Коо, Ј	45
Коо, Ү	44
Kooistra, G W	32
	38
Kool, P	
Kool, P 293, Koopman, M C 293,	34
Koopman, M C 293, Kopf, S R	41
Koopman, M C 293,	41 19
Koopman, M C 293, Kopf, S R Kopka, L Korb, G	41 19 39
Koopman, M C 293, Kopf, S R Kopka, L Korb, G Korhonen, M A 286,	41 19 39 41
Koopman, M C 293, Kopf, S R Kopka, L Korb, G Korhonen, M A 286, Korhonen, T K	41 19 39 41 28
Koopman, M C 293, Kopf, S R Kopka, L Korb, G Korhonen, M A 286, Korhonen, T K Korhonen, T M	41 19 39 41 28 41
Koopman, M C 293, Kopf, S R Kopka, L Korb, G Korhonen, M A 286, Korhonen, T K Korhonen, T M Korotaev, A D	41 19 39 41 28 41 25
Koopman, M C 293, Kopf, S R Kopka, L Korb, G Korhonen, M A 286, Korhonen, T K Koronen, T M Korotaev, A D Korshunov, A I	41 19 39 41 28 41 25 25
Koopman, M C 293, Kopf, S R Kopka, L Korb, G Korhonen, M A 286, Korhonen, T K Korhonen, T M Korotaev, A D	41 19 39 41 28 41 25 25 25

Kossler, W J	. 276
Koster, E	
Kostika, I	
Kostorz, G	250
Kourov, N I	
Kovar, D	
Kovgan, P A	
Kozeschnik, E	. 405
Kozlov, E V 255	
Kraft, E H	
Kraft, O 188	
Krajewski, P E 211	, 264,
Kral, M V 327	
Krallics, G	
Kramer, M J 175, 215, 238	, 296
Kramer-White, J	419
Vrono M I 105 210 297	400
Krane, M J 195, 219, 387	, 408
Krasilnikov, N A 256	
Krause, A R	214
Krause, E 230	, 231
Krill, C E	
Krioukovsky, V	
Kripesh, V	241
Krishnamurthy, R K	233
<b>2</b>	
Krishnan, A	
Kroupa, A	. 382
Kruger, G A	. 212
Krumdick, G K 200, 244	
Krupakara, P V	226
Kruzic, J J 315	, 316
Krylov, L	. 437
Kuba, M	
Kubat, F	
Kubin, L	
Kudrnovsky, J 192	, 304
Kudrnovsky, J 192 Kulas, M	, 304 . 264
Kudrnovsky, J 192 Kulas, M Kulkarni, A V	, 304 . 264 . 207
Kudrnovsky, J 192 Kulas, M	, 304 . 264 . 207
Kudrnovsky, J 192 Kulas, M Kulkarni, A V Kumar, A	, 304 . 264 . 207 . 227
Kudrnovsky, J 192 Kulas, M Kulkarni, A V Kumar, A Kumar, A	, 304 . 264 . 207 . 227 . 222
Kudrnovsky, J 192 Kulas, M Kulkarni, A V Kumar, A Kumar, A Kumar, D	, 304 . 264 . 207 . 227 . 222 . 336
Kudrnovsky, J 192 Kulas, M Kulkarni, A V Kumar, A Kumar, A	, 304 . 264 . 207 . 227 . 222 . 336 , 431
Kudrnovsky, J 192 Kulas, M Kulkarni, A V Kumar, A Kumar, A Kumar, D Kumar, M 390, 406 Kumar, R	, 304 . 264 . 207 . 227 . 222 . 336 , 431 . 171
Kudrnovsky, J 192 Kulas, M Kulkarni, A V Kumar, A Kumar, A Kumar, D Kumar, M 390, 406 Kumar, R	, 304 . 264 . 207 . 227 . 222 . 336 , 431 . 171
Kudrnovsky, J 192 Kulas, M Kulkarni, A V Kumar, A Kumar, A Kumar, D Kumar, M	, 304 . 264 . 207 . 227 . 222 . 336 , 431 . 171 , 360
Kudrnovsky, J       192         Kulas, M       Kulkarni, A V         Kumar, A       Kumar, A         Kumar, D       Sumar, B         Kumar, R       390, 406         Kumar, S       225, 316         Kumosa, M       225, 316	, 304 . 264 207 . 227 . 222 336 , 431 . 171 , 360 371
Kudrnovsky, J       192         Kulas, M       Kulkarni, A V         Kumar, A       Kumar, A         Kumar, D       Sumar, B         Kumar, R       390, 406         Kumar, S       225, 316         Kumosa, M       Kumta, P	, 304 . 264 207 . 227 . 222 . 336 , 431 . 171 , 360 . 371 . 424
Kudrnovsky, J       192         Kulas, M       Kulkarni, A V         Kumar, A       Kumar, A         Kumar, D       Sumar, B         Kumar, R       390, 406         Kumar, S       225, 316         Kumosa, M       225, 316	, 304 . 264 207 . 227 . 222 . 336 , 431 . 171 , 360 . 371 . 424
Kudrnovsky, J       192         Kulas, M       Kulkarni, A V         Kumar, A       Kumar, A         Kumar, D       Kumar, M         Kumar, R       390, 406         Kumar, S       225, 316         Kumosa, M       Kumta, P         Kumat, P N       Sumar, P	, 304 . 264 207 . 227 . 222 336 , 431 . 171 , 360 371 . 424 . 381
Kudrnovsky, J       192         Kulas, M       Kulkarni, A V         Kumar, A       Kumar, A         Kumar, D       Kumar, M         Kumar, R       390, 406         Kumar, S       225, 316         Kumata, P       Kumta, P         Kumata, C       Kumata, C         Kumar, S       225, 316         Kumata, C       Kumata, C         Kumata, C       Kumata, C         Kumata, C       T	, 304 . 264 207 . 227 . 222 336 , 431 . 171 , 360 371 . 424 . 381 429
Kudrnovsky, J       192         Kulas, M       Kulkarni, A V         Kumar, A       Kumar, A         Kumar, D       Sumar, A         Kumar, M       390, 406         Kumar, R       Sumar, B         Kumar, S       225, 316         Kumta, P       Kumta, P         Kumta, P N       Kunioshi, C T         Kuo, C       201, 227	<ul> <li>, 304</li> <li>, 264</li> <li>207</li> <li>, 227</li> <li>, 336</li> <li>, 431</li> <li>, 171</li> <li>, 360</li> <li>, 371</li> <li>, 424</li> <li>, 381</li> <li>, 429</li> <li>, 280</li> </ul>
Kudrnovsky, J       192         Kulas, M       Kulkarni, A V         Kumar, A       Kumar, A         Kumar, D       Kumar, M         Kumar, R       390, 406         Kumar, S       225, 316         Kumosa, M       Kumta, P         Kumat, P N       Kunioshi, C T         Kuo, C       201, 227         Kuo, R C       234	<ul> <li>, 304</li> <li>, 264</li> <li>, 207</li> <li>, 222</li> <li>, 336</li> <li>, 431</li> <li>, 171</li> <li>, 360</li> <li>, 371</li> <li>, 424</li> <li>, 381</li> <li>, 429</li> <li>, 280</li> <li>, 247</li> </ul>
Kudrnovsky, J       192         Kulas, M       Kulkarni, A V         Kumar, A       Kumar, A         Kumar, D       Kumar, M         Kumar, R       390, 406         Kumar, S       225, 316         Kumosa, M       Kumta, P         Kumat, P N       Kunioshi, C T         Kuo, C       201, 227         Kuo, R C       234	<ul> <li>, 304</li> <li>, 264</li> <li>, 207</li> <li>, 222</li> <li>, 336</li> <li>, 431</li> <li>, 171</li> <li>, 360</li> <li>, 371</li> <li>, 424</li> <li>, 381</li> <li>, 429</li> <li>, 280</li> <li>, 247</li> </ul>
Kudrnovsky, J       192         Kulas, M       Kulkarni, A V         Kumar, A       Kumar, A         Kumar, D       Kumar, B         Kumar, R       390, 406         Kumar, R       225, 316         Kumas, S       225, 316         Kumta, P       Kumta, P         Kunioshi, C T       201, 227         Kuo, R C       234         Kuriyama, N       Sumar, N	<ul> <li>, 304</li> <li>, 264</li> <li>207</li> <li>, 227</li> <li>, 336</li> <li>, 431</li> <li>, 171</li> <li>, 360</li> <li>, 371</li> <li>, 424</li> <li>, 381</li> <li>, 429</li> <li>, 280</li> <li>, 247</li> <li>, 263</li> </ul>
Kudrnovsky, J       192         Kulas, M       Kulkarni, A V         Kumar, A       Kumar, A         Kumar, D       Kumar, B         Kumar, R       390, 406         Kumar, R       225, 316         Kumas, M       225, 316         Kumat, P       Kumas, M         Kumat, P N       Kunioshi, C T         Kuo, C       201, 227         Kuo, R C       234         Kuriyama, N       Kurokawa, A	<ul> <li>, 304</li> <li>, 264</li> <li>, 207</li> <li>, 222</li> <li>, 336</li> <li>, 431</li> <li>, 171</li> <li>, 360</li> <li>, 371</li> <li>, 424</li> <li>, 381</li> <li>, 429</li> <li>, 280</li> <li>, 247</li> <li>, 263</li> <li>, 220</li> </ul>
Kudrnovsky, J       192         Kulas, M       Kulkarni, A V         Kumar, A       Kumar, A         Kumar, D       Kumar, B         Kumar, R       390, 406         Kumar, R       225, 316         Kumas, S       225, 316         Kumat, P       Kumat, P         Kumat, P N       Kunioshi, C T         Kuo, C       201, 227         Kuo, R C       234         Kuriyama, N       Kurokawa, A         Kurtz, R J       Sumosan A	<ul> <li>, 304</li> <li>, 264</li> <li>, 207</li> <li>, 222</li> <li>, 336</li> <li>, 431</li> <li>, 171</li> <li>, 360</li> <li>, 371</li> <li>, 424</li> <li>, 381</li> <li>, 429</li> <li>, 280</li> <li>, 247</li> <li>, 263</li> <li>, 220</li> <li>, 355</li> </ul>
Kudrnovsky, J       192         Kulas, M       Kulkarni, A V         Kumar, A       Kumar, A         Kumar, D       Kumar, B         Kumar, R       225, 316         Kumas, M       225, 316         Kuma, P       Kumar, B         Kuma, P N       Kunioshi, C T         Kuo, C       201, 227         Kuo, R C       234         Kuriyama, N       Kurokawa, A         Kurz, R J       Kurz, G	, 304 . 264 207 . 227 . 222 336 , 431 . 171 , 360 371 . 424 . 381 429 , 280 , 247 . 263 220 355 233
Kudrnovsky, J       192         Kulas, M       Kulkarni, A V         Kumar, A       Kumar, A         Kumar, D       Kumar, B         Kumar, R       225, 316         Kumas, M       225, 316         Kuma, P       Kumar, B         Kuma, P N       Kunioshi, C T         Kuo, C       201, 227         Kuo, R C       234         Kuriyama, N       Kurokawa, A         Kurz, R J       Kurz, G	, 304 . 264 207 . 227 . 222 336 , 431 . 171 , 360 371 . 424 . 381 429 , 280 , 247 . 263 220 355 233
Kudrnovsky, J       192         Kulas, M       Kulkarni, A V         Kulkarni, A V       Kumar, A         Kumar, A       Sumar, A         Kumar, D       Sumar, B         Kumar, R       390, 406         Kumar, R       225, 316         Kumar, S       225, 316         Kumar, P       Kumosa, M         Kumia, P N       Kunioshi, C T         Kuo, C       201, 227         Kuo, R C       234         Kuriyama, N       Kurokawa, A         Kurz, R J       Kurz, G         Kurz, W       203	<ul> <li>, 304</li> <li>, 264</li> <li>, 207</li> <li>, 222</li> <li>, 336</li> <li>, 431</li> <li>, 171</li> <li>, 360</li> <li>, 371</li> <li>, 424</li> <li>, 381</li> <li>, 429</li> <li>, 280</li> <li>, 247</li> <li>, 263</li> <li>, 220</li> <li>, 355</li> <li>, 233</li> <li>, 345</li> </ul>
Kudrnovsky, J       192         Kulas, M       Kulkarni, A V         Kulkarni, A V       Kumar, A         Kumar, A       Sumar, A         Kumar, D       Sumar, B         Kumar, R       390, 406         Kumar, R       225, 316         Kumar, S       225, 316         Kumar, P       Kumosa, M         Kumia, P N       Kunioshi, C T         Kuo, C       201, 227         Kuo, R C       234         Kuriyama, N       Kurokawa, A         Kurz, R J       Kurz, W         Kuz, W       203         Kushida, A       Sushida, A	<ul> <li>, 304</li> <li>, 264</li> <li>, 207</li> <li>, 222</li> <li>, 336</li> <li>, 431</li> <li>, 171</li> <li>, 360</li> <li>, 371</li> <li>, 424</li> <li>, 381</li> <li>, 429</li> <li>, 280</li> <li>, 247</li> <li>, 263</li> <li>, 220</li> <li>, 355</li> <li>, 233</li> <li>, 345</li> <li>, 426</li> </ul>
Kudrnovsky, J       192         Kulas, M       Kulkarni, A V         Kulkarni, A V       Kumar, A         Kumar, A       Sumar, B         Kumar, R       390, 406         Kumar, R       225, 316         Kumar, S       225, 316         Kumar, P       Kumar, B         Kumta, P       201, 227         Kuo, C       201, 227         Kuo, R C       234         Kuriyama, N       Kurokawa, A         Kurz, R J       Kurz, G         Kurz, W       203         Kushida, A       Kushnarev, B	<ul> <li>, 304</li> <li>, 264</li> <li>, 207</li> <li>, 222</li> <li>, 336</li> <li>, 431</li> <li>, 171</li> <li>, 360</li> <li>, 371</li> <li>, 424</li> <li>, 381</li> <li>, 429</li> <li>, 280</li> <li>, 247</li> <li>, 263</li> <li>, 220</li> <li>, 355</li> <li>, 233</li> <li>, 345</li> <li>, 426</li> <li>, 242</li> </ul>
Kudrnovsky, J       192         Kulas, M       Kulkarni, A V         Kulkarni, A V       Kumar, A         Kumar, A       Sumar, A         Kumar, D       Sumar, B         Kumar, R       390, 406         Kumar, R       225, 316         Kumar, S       225, 316         Kumar, S       225, 316         Kumar, P       Kumosa, M         Kumta, P       Kunioshi, C T         Kuo, C       201, 227         Kuo, R C       234         Kuriyama, N       Kurokawa, A         Kurz, R J       Kuz, G         Kuz, W       203         Kushida, A       Kushnarev, B         Kusui, J       Sushida, A	<ul> <li>, 304</li> <li>, 264</li> <li>, 207</li> <li>, 222</li> <li>, 336</li> <li>, 431</li> <li>, 171</li> <li>, 360</li> <li>, 371</li> <li>, 424</li> <li>, 381</li> <li>, 429</li> <li>, 280</li> <li>, 247</li> <li>, 263</li> <li>, 220</li> <li>, 355</li> <li>, 233</li> <li>, 345</li> <li>, 426</li> <li>, 242</li> <li>, 314</li> </ul>
Kudrnovsky, J       192         Kulas, M       Kulkarni, A V         Kulkarni, A V       Kumar, A         Kumar, A       Sumar, A         Kumar, D       Sumar, B         Kumar, R       390, 406         Kumar, R       225, 316         Kumar, S       225, 316         Kumar, S       225, 316         Kumar, P       Kumosa, M         Kumta, P       Kunioshi, C T         Kuo, C       201, 227         Kuo, R C       234         Kuriyama, N       Kurokawa, A         Kurz, R J       Kuz, G         Kuz, W       203         Kushida, A       Kushnarev, B         Kusui, J       Sushida, A	<ul> <li>, 304</li> <li>, 264</li> <li>, 207</li> <li>, 222</li> <li>, 336</li> <li>, 431</li> <li>, 171</li> <li>, 360</li> <li>, 371</li> <li>, 424</li> <li>, 381</li> <li>, 429</li> <li>, 280</li> <li>, 247</li> <li>, 263</li> <li>, 220</li> <li>, 355</li> <li>, 233</li> <li>, 345</li> <li>, 426</li> <li>, 242</li> <li>, 314</li> </ul>
Kudrnovsky, J       192         Kulas, M       Kulkarni, A V         Kulkarni, A V       Kumar, A         Kumar, A       Sumar, A         Kumar, D       Sumar, B         Kumar, R       390, 406         Kumar, R       225, 316         Kumar, S       225, 316         Kumar, P       Kumosa, M         Kumta, P       Kumosa, M         Kunioshi, C T       201, 227         Kuo, R C       204, 227         Kuo, R C       234         Kuriyama, N       Kurokawa, A         Kurz, R J       Kuz, G         Kuz, W       203         Kushida, A       Kushida, A         Kusui, J       Kutty, M G	<ul> <li>, 304</li> <li>, 264</li> <li>, 207</li> <li>, 222</li> <li>, 336</li> <li>, 431</li> <li>, 171</li> <li>, 360</li> <li>, 371</li> <li>, 424</li> <li>, 381</li> <li>, 429</li> <li>, 280</li> <li>, 247</li> <li>, 263</li> <li>, 220</li> <li>, 355</li> <li>, 233</li> <li>, 345</li> <li>, 426</li> <li>, 242</li> <li>, 314</li> <li>, 445</li> </ul>
Kudrnovsky, J       192         Kulas, M       Kulkarni, A V         Kulkarni, A V       Kumar, A         Kumar, A       Sumar, A         Kumar, D       Sumar, B         Kumar, R       390, 406         Kumar, R       225, 316         Kumar, S       225, 316         Kumosa, M       Kumosa, M         Kumta, P       Kumosa, M         Kunioshi, C T       201, 227         Kuo, R C       201, 227         Kuo, R C       234         Kuriyama, N       Kurokawa, A         Kurz, R J       Kurz, G         Kuzz, G       Kushida, A         Kushida, A       Kusui, J         Kusui, J       Kutty, M G         Kutty, T N       Sutty, T N	<ul> <li>, 304</li> <li>, 264</li> <li>, 207</li> <li>, 222</li> <li>, 336</li> <li>, 431</li> <li>, 171</li> <li>, 360</li> <li>, 371</li> <li>, 424</li> <li>, 381</li> <li>, 429</li> <li>, 280</li> <li>, 247</li> <li>, 263</li> <li>, 220</li> <li>, 355</li> <li>, 233</li> <li>, 345</li> <li>, 426</li> <li>, 242</li> <li>, 314</li> <li>, 445</li> <li>, 239</li> </ul>
Kudrnovsky, J       192         Kulas, M       Kulkarni, A V         Kulkarni, A V       Kumar, A         Kumar, A       Sumar, A         Kumar, D       Sumar, B         Kumar, S       225, 316         Kumar, S       225, 316         Kumar, S       225, 316         Kumar, S       225, 316         Kumosa, M       Kumosa, M         Kumta, P       Kumosa, M         Kunioshi, C T       Sunoshi, C T         Kuo, C       201, 227         Kuo, R C       234         Kuriyama, N       Kurokawa, A         Kurz, R J       Kurz, G         Kurz, W       203         Kushida, A       Kushida, A         Kusui, J       Kutty, M G         Kutty, T N       Kuwana, K	<ul> <li>, 304</li> <li>, 264</li> <li>, 207</li> <li>, 222</li> <li>, 336</li> <li>, 431</li> <li>, 171</li> <li>, 360</li> <li>, 371</li> <li>, 424</li> <li>, 381</li> <li>, 429</li> <li>, 280</li> <li>, 247</li> <li>, 263</li> <li>, 220</li> <li>, 355</li> <li>, 233</li> <li>, 345</li> <li>, 426</li> <li>, 242</li> <li>, 314</li> <li>, 445</li> <li>, 239</li> <li>, 218</li> </ul>
Kudrnovsky, J       192         Kulas, M       Kulkarni, A V         Kulkarni, A V       Kumar, A         Kumar, A       Sumar, A         Kumar, D       Sumar, B         Kumar, R       390, 406         Kumar, S       225, 316         Kumosa, M       Kumar, S         Kumar, S       225, 316         Kumosa, M       Kumosa, M         Kumta, P       Kumosa, M         Kunioshi, C T       201, 227         Kuo, R C       201, 227         Kuo, R C       234         Kuriyama, N       Kurokawa, A         Kurz, R J       Kurz, G         Kurz, W       203         Kushida, A       Kushida, A         Kusui, J       Kutty, M G         Kutty, M G       Kutty, T N         Kuwana, K       Kuwano, N	<ul> <li>, 304</li> <li>, 264</li> <li>, 207</li> <li>, 227</li> <li>, 322</li> <li>, 336</li> <li>, 431</li> <li>, 171</li> <li>, 360</li> <li>, 371</li> <li>, 424</li> <li>, 381</li> <li>, 429</li> <li>, 280</li> <li>, 247</li> <li>, 263</li> <li>, 220</li> <li>, 355</li> <li>, 233</li> <li>, 345</li> <li>, 426</li> <li>, 242</li> <li>, 314</li> <li>, 445</li> <li>, 239</li> <li>, 218</li> <li>, 390</li> </ul>
Kudrnovsky, J       192         Kulas, M       Kulkarni, A V         Kulkarni, A V       Kumar, A         Kumar, A       Sumar, A         Kumar, D       Sumar, B         Kumar, R       390, 406         Kumar, S       225, 316         Kumosa, M       Kumar, S         Kumar, S       225, 316         Kumosa, M       Kumosa, M         Kumta, P       Kumosa, M         Kunioshi, C T       201, 227         Kuo, R C       201, 227         Kuo, R C       234         Kuriyama, N       Kurokawa, A         Kurz, R J       Kurz, G         Kurz, W       203         Kushida, A       Kushida, A         Kusui, J       Kutty, M G         Kutty, M G       Kutty, T N         Kuwana, K       Kuwano, N	<ul> <li>, 304</li> <li>, 264</li> <li>, 207</li> <li>, 227</li> <li>, 322</li> <li>, 336</li> <li>, 431</li> <li>, 171</li> <li>, 360</li> <li>, 371</li> <li>, 424</li> <li>, 381</li> <li>, 429</li> <li>, 280</li> <li>, 247</li> <li>, 263</li> <li>, 220</li> <li>, 355</li> <li>, 233</li> <li>, 345</li> <li>, 426</li> <li>, 242</li> <li>, 314</li> <li>, 445</li> <li>, 239</li> <li>, 218</li> <li>, 390</li> </ul>
Kudrnovsky, J       192         Kulas, M       Kumar, A         Kumar, A       Kumar, A         Kumar, D       Sumar, B         Kumar, M       390, 406         Kumar, R       Sumar, S         Kumar, S       225, 316         Kumosa, M       Kumosa, M         Kumita, P       Kumosa, M         Kunosa, M       Kumosa, M         Kumta, P       201, 227         Kuo, C       201, 227         Kuo, R C       234         Kuriyama, N       Kurz, RJ         Kurz, G       Kurz, G         Kurz, W       203         Kushida, A       Kusui, J         Kusui, J       Kusui, J         Kutty, M G       Kutty, M G         Kutty, T N       Kuwana, K         Kuwano, N       Kvande, H	<ul> <li>, 304</li> <li>, 264</li> <li>, 207</li> <li>, 222</li> <li>, 336</li> <li>, 431</li> <li>, 171</li> <li>, 360</li> <li>, 371</li> <li>, 424</li> <li>, 381</li> <li>, 429</li> <li>, 280</li> <li>, 247</li> <li>, 263</li> <li>, 220</li> <li>, 355</li> <li>, 233</li> <li>, 345</li> <li>, 426</li> <li>, 242</li> <li>, 314</li> <li>, 445</li> <li>, 239</li> <li>, 218</li> <li>, 390</li> <li>, 356</li> </ul>
Kudrnovsky, J       192         Kulas, M       Kumar, A         Kumar, A       Kumar, A         Kumar, D       Sumar, B         Kumar, M       390, 406         Kumar, R       Sumar, S         Kumar, S       225, 316         Kumosa, M       Kumosa, M         Kumita, P       Kumosa, M         Kunosa, M       Kumosa, M         Kumta, P       201, 227         Kuo, C       201, 227         Kuo, R C       234         Kuriyama, N       Kurz, R         Kurz, G       Kurz, G         Kurz, W       203         Kushida, A       Kushida, A         Kutty, M G       Kutty, M G         Kutty, T N       Kuwana, K         Kuwano, N       Kvande, H         Kvithyld, A       Kvithyld, A	<ul> <li>, 304</li> <li>, 264</li> <li>, 207</li> <li>, 222</li> <li>, 336</li> <li>, 431</li> <li>, 171</li> <li>, 360</li> <li>, 371</li> <li>, 424</li> <li>, 381</li> <li>, 429</li> <li>, 280</li> <li>, 247</li> <li>, 263</li> <li>, 220</li> <li>, 355</li> <li>, 233</li> <li>, 345</li> <li>, 426</li> <li>, 242</li> <li>, 314</li> <li>, 445</li> <li>, 239</li> <li>, 218</li> <li>, 390</li> <li>, 356</li> <li>, 266</li> </ul>
Kudrnovsky, J       192         Kulas, M       Kumar, A         Kumar, A       Kumar, A         Kumar, D       Sumar, B         Kumar, M       390, 406         Kumar, R       Sumar, S         Kumar, S       225, 316         Kumosa, M       Kumosa, M         Kumita, P       Kumosa, M         Kunosa, M       Kumosa, M         Kumta, P       201, 227         Kuo, C       201, 227         Kuo, R C       234         Kuriyama, N       Kurz, RJ         Kurz, G       Kurz, G         Kurz, W       203         Kushida, A       Kusui, J         Kusui, J       Kusui, J         Kutty, M G       Kutty, M G         Kutty, T N       Kuwana, K         Kuwano, N       Kvande, H	<ul> <li>, 304</li> <li>, 264</li> <li>, 207</li> <li>, 222</li> <li>, 336</li> <li>, 431</li> <li>, 171</li> <li>, 360</li> <li>, 371</li> <li>, 424</li> <li>, 381</li> <li>, 429</li> <li>, 280</li> <li>, 247</li> <li>, 263</li> <li>, 220</li> <li>, 355</li> <li>, 233</li> <li>, 345</li> <li>, 426</li> <li>, 242</li> <li>, 314</li> <li>, 445</li> <li>, 239</li> <li>, 218</li> <li>, 390</li> <li>, 356</li> <li>, 266</li> </ul>

## L

Laberge, C	213
LaCombe, J	395
Lacroix, S	177
Ladeuille, L	202
Ladwig, P F	198
Laha, T	388
Lai, Y	357
Lakshmanan, VI 199, 244,	329
LaLonde, A	417
Lamb, J H	397
Lamérant, J	265
Lamperti, A	429
Landgraf, F J	204
Landis, C	328
Lane, J F	410
Lang, J C	250
Langdon, T G 206, 251, 253,	254,
	340,
	433
Langer, S A	406
Langlais, J	273
Lapovok, R 252, 260, 269,	333
Larocque, J E	311
Larouche, A	273
Larson, C	417
Larson, D J	198
Larson, E J	436
Lashkari, O	423
Latapie, A	301
Latour, R A	240
Latroche, M	210
Latysh, V V	259
Laughlin, D E	371
Lauridsen, E M	204
Lauro, P	416
Laux, H 179,	423
Lavernia, E J 256, 306,	352,
	449
Lavoie, C	370
Laxminarayana, P Lazarz, K A	412 287
Le Bouar, Y M 349,	
Le Boual, 1 M	390 361
Lech-Grega, M	403
Lechevalier, B	252
Lee, C	374
Lee, C P	247
Lee, C S 368,	411
Lee, C S	433
Lee, D 221, 346,	350
Lee, D L	368
Lee, D R	250
Lee, F G	212
Lee, G W	438
Lee, H 325,	442
Lee, H	389
Lee, H	454
Lee, H C	287
Lee, H M 198, 240,	286,
	200.
	280, 382
	382
Lee, I	382 382
Lee, I	382 382 416
Lee, J 382, Lee, J	382 382 416 383

Lee, J	339
Lee, J	247
Lee, J	301
Lee, J	454
Lee, J 293, 409,	447
Lee, J C	374
Lee, J G 188, 285, 286,	293
Lee, J G	287
Lee, J K	277
Lee, J W	293
Lee, K	309
Lee, K	455
Lee, K	453
Lee, K	376 350
Lee, K J 214,	350
Lee, M 214,	438
Lee, M G	314
Lee, P D	173
Lee, S	309
Lee, S 271, 272,	360
Lee, S	293
Lee, S	442
Lee, W	455
Lee, W 453,	454
Lee, Y	309
Lee, Y 236,	438
Lee, Y B	208
Legault-Seguin, E N	444
Lehman, L P 286, 382,	416
Lei, Y	232
Leidl, A	188
LeMay, J D	310
Lenosky, T J	183
Leo, P H	277
Leon Iriarte, J	207
Leonard, D	189
Leonard, F	276
LeSar, R A 182,	224, 407
Lesoult, G	202
Levanyuk, A P	425
Levi-Setti, R	429
Levine, L E	279
Lewandowski, J J 359,	360,
	372
Lewis, A C 234,	235
Lewis, C	443
Lewis, M	371
Lherbier, L	414
Li, B 276, 289,	414
	414 379,
Li, B	379,
Li, B Li, C	379, 446 265 432
Li, B Li, C Li, C	379, 446 265 432 203
Li, B Li, C Li, C Li, D	379, 446 265 432 203 312
Li, B Li, C Li, C Li, D Li, D	379, 446 265 432 203 312 336
Li, B Li, C Li, C Li, D Li, D Li, D	379, 446 265 432 203 312 336 237
Li, B Li, C Li, C Li, D Li, D Li, D Li, F	379, 446 265 432 203 312 336 237 243
Li, B Li, C Li, C Li, D Li, D Li, D Li, F Li, H	379, 446 265 432 203 312 336 237 243 .178
Li, B Li, C Li, C Li, D Li, D Li, D Li, F Li, H	379, 446 265 432 203 312 336 237 243 .178 .238
Li, B Li, C Li, C Li, D Li, D Li, D Li, H Li, H Li, H	379, 446 265 432 203 312 336 237 243 .178 .238 .452
Li, B Li, C Li, C Li, D Li, D Li, D Li, H Li, H Li, H Li, H Li, J	379, 446 265 432 203 312 336 237 243 .178 .238 .452 204
Li, B Li, C Li, C Li, D Li, D Li, D Li, F Li, H Li, H Li, H Li, H Li, J	379, 446 265 432 203 312 336 237 243 .178 .238 .452 204 319
Li, B Li, C Li, C Li, D Li, D Li, D Li, F Li, H Li, H Li, H Li, J Li, J	379, 446 265 432 203 312 336 237 243 .178 .238 .452 204 319 357
Li, B Li, C Li, C Li, D Li, D Li, D Li, F Li, H Li, H Li, H Li, H Li, J	379, 446 265 432 203 312 336 237 243 .178 .238 .452 204 319 357 384



Li, J		334
Li, J C 283,		342
Li, L		368
Li, M Li, N 191, 313,		288 447
Li, N 191, 515, Li, P		
Li, Q		357
Li, S		434
Li, S		374
Li, S X		247
Li, W		312
Li, W		424
Li, X		395
Li, X		262
Li, Y		402
Li, Y		383
Li, Y L	324,	426
Li, Z		268
Liang, B		332
Liang, C C		232
Liang, J		339
Liang, J		413
Liang, R		449
Liang, Y		332
Liang, Z		319
Liao, C		383 350
Liao, X		
Liaw, P K 175, 184, 208, 216, 226,	201,	202, 246,
	234, 271,	240, 296,
	342,	290, 359,
		438
Liedl, G L		377
Liedtke, A		447
Lienert, U 272,		372
Lifen, L		325
Lightle, C	172,	399
Lilleodden, E T		275
Lim, C		201
Lim, K		454
Lim, S		
Limata, L		
Lin, A		291
Lin, C		
Lin, C C		326
Lin, C H		
Lin, C		
Lin, D C		
Lin, H		
Lin, K 189,		
Lin, Q		
Lin, T	326,	337
Lin, W		455
Lin, Y		449
Lin, Y H	332,	338
Lin, Y L		338
Lincoln, J D		326
Lindley, T C		173
Ling, Y		
Lisovskyy, I P		180
Litovchenko, I		257
Little, A L		297
Littleton, H E		428
Liu, B		319 372
L10, C		514

Liu, C T 175, 269, 271,	402
Liu, C Y 294, 332,	375
Liu, H	345
Liu, H	284
Liu, H	443
Liu, H 199,	321
Liu, H J	195
Liu, H K	354
Liu, J	374
Liu, J	292
Liu, N	416
Liu, S	446
Liu, S 299,	300
Liu, S	379
Liu, S	319
Liu, T	374
Liu, W 279,	324
Liu, W J	233
Liu, X J	191
Liu, Y	428
Liu, Y	268
Liu, Y	357
Liu, Y H	421
	269
Liu, Z 181, 192, 194, 221, 277, 294, 305, 322,	349
	445
Liu, Z	304
Liu, Z	313
Liu, Z	421
Livneh, T	395
Lloyd, D J	303
Llubani, S	
Lo, C	
Lo, C C	
Lo, T	337
Loan, M 171,	311
Lofland, S E	291
Loiseau, A	
Lokshin, R G	267
Lomas, R	
Longo, F G	
-	
Looij, J	
Loomis, E	
Lopasso, E	348
Lopez, M F	233
Lorimer, G W 294,	295
Lou, J 261, 308,	377
	225
Louchet, F H	278
Louchet, F H 224,	200
Louchet, F H	399
Louchet, F H	257
Louchet, F H	
Louchet, F H	257 432
Louchet, F H	257 432 441
Louchet, F H	257 432 441 288
Louchet, F H	257 432 441 288 294
Louchet, F H	257 432 441 288 294 428
Louchet, F H	257 432 441 288 294 428 416
Louchet, F H Loutfy, R O	257 432 441 288 294 428 416 411
Louchet, F H Loutfy, R O	257 432 441 288 294 428 416
Louchet, F H Loutfy, R O	257 432 441 288 294 428 416 411
Louchet, F H Loutfy, R O	257 432 441 288 294 428 416 411 332 343
Louchet, F H Loutfy, R O	257 432 441 288 294 428 416 411 332 343 232
Louchet, F H Loutfy, R O	257 432 441 288 294 428 416 411 332 343 232 440
Louchet, F H	257 432 441 288 294 428 416 411 332 343 232 440 409
Louchet, F H Loutfy, R O	257 432 441 288 294 428 416 411 332 343 232 440 409 411
Louchet, F H Loutfy, R O	257 432 441 288 294 428 416 411 332 343 232 440 409 411 265
Louchet, F H	257 432 441 288 294 428 416 411 332 343 232 440 409 411 265 175
Louchet, F H Loutfy, R O	257 432 441 288 294 428 416 411 332 343 232 440 409 411 265 175

Lubarda, V A Lubecka, M	366 321
Lucadamo, G A 308,	347
Lucas, J P 188,	285,
	394
Luckey, S G 397,	398
Ludwig, A 178, 247, 386,	423
Ludwig, L	395
Ludwig, O	218
Ludwig, W	411
Lue, M	242
Lui, T 332,	337
Luis Pérez, C J 207,	258
Lukac, P D	425
Lukashchuk, Y V	256
Lukyanov, I V	312
Lund, A C 234, 236,	317
Luo, A A 191, 233,	287,
	444
Luo, W C 199,	374
Luo, Z 207, 257,	350
Lupulescu, A 248,	409
Lynch, F E	210
Lynn, K	380
Lyon, P	445
Lysczek, E M	198
•	

### Μ

Ma, B M	238
Ma, D	345
Ma, E 176, 305,	391
Ma, H	176
Ma, N	249
Ma, P X	292
Ma, R 313,	332
Ma, S 279,	283
Ma, T	331
Ma, Y	195
Ma, Y	250
Ma, Z Y	311
MacDonald, B	446
MacKay, R A 322,	364
Mackenzie, J M	444
Mackowiak, V	447
MacLaren, I	307
Madenci, E	229
Madshus, S	218
Maeland, A J	353
Magadi, G	248
Magee, T J 230,	329
Magnusson, J H	361
Mahajan, S	193
Mahalingam, T	241
Mahapatra, S P 171,	368
Mahato, C	428
Mahoney, M	226
Maier, H J 257, 302, Maijer, D M 173, 195,	341
Maijer, D M 173, 195,	386
Majetich, S	336
Majkrzak, C F	210
Majumdar, B S 187, 188,	229,
	371
Majzoub, E H 263, 430,	436
Makhlouf, M M 343, 376,	409
Maki, T	282
Maksymowicz, L J	321

Maksyutov, A F	270
Maland, G	318
Malgin, D	256
Mallick, P K	288
Mandal, P	215
Mani, A S	196
Manias, E Manickam, K	424
Maniruzzaman, M 404,	236
Mann, A B	423 197
Mann, V C	267
Manning, C	366
Mannweiler, U	360
Manohar, P A	180
Mantese, J V	426
Mara, N A 317,	432
Marcus, H L	451
Margulies, L 302,	372
Marian, J	183
Marks, J	399
Marks, R A 229,	342
Marshall, D	284
Martchek, K 244,	398
Martens, R L	
Martin, C	
Martin, C	
Martin, E S	266
Martin, G	
Martin, J 177, 218,	272,
	439
Martin, J J	338
Martin, P L 182,	357
Martinent, V	265
Martinez, H	326
Martinez, J V	435
Martinez, R A	202
Martocci, A	436
Maruyama, K	384
Marvin, J	328
Marzari, N	304
Mason, D E	431
Mason, P G 328,	443
Mason, T A 303,	451
Massalski, T B	371
Mast, D	238
Masuda, C 255,	393
Masumura, R A	302
Mathaudhu, S N 216, 259,	341
Mathier, V	
Mathis, A	361
Mathisen, S T	172
Matson, D M 246, 289,	299
Matsuda, T	397
Matsumoto, A	326
Matsuoka, R	449
Matthews, S R	
Matyas, A	330
Maurice, C	250
Maxey, E	297
Mayer, R	411
Mayer, T M	
Mayeaux, B	
Maziarz, W	321
Mazuelas, A	250
Mazumder, J	192
Mazunov, D O	180
Mazzei, Â C	368

McBow, I	185
McCabe, R J 306,	324
McCall, L	441
McCallum, W	296
McClellan, K J	201
McClung, M 213,	399
McComas, E	370
McConaghy, E	
McCord, M G 197, McCoy, R A	447 374
McCrabb, L C	443
McCune, R C 191,	288
McDanels, S	
McDanice, R	202
McDaniels, R L	226
McDonald, M	420
McDonald, N J	300
McDonald, R G	284
McDonald, S D	343
McDougall, J L McDowell, D L	367 289
McFadden, G B 276,	322
McGarrity, E	391
McIntyre, H R	343
McKamey, C G	269
МсКау, В Ј	344
McKay, J	378
McKean, B	
McKenzie, P	
McKillip, J L	381
McLean, A McLean, W	417 310
McNelley, T R 252, 264,	349
10101 (cilcy, 1 it 252, 20-,	
McNerny, C	421 302
	421
McNerny, C	421 302
McNerny, C	421 302 195 300 347
McNerny, C         201,           McQueen, H J         201,           Meade, D	421 302 195 300 347 318
McNerny, C         201,           McQueen, H J         201,           Meade, D	421 302 195 300 347 318 341
McNerny, C         201,           McQueen, H J         201,           Meade, D	421 302 195 300 347 318 341 437
McNerny, C           McQueen, H J         201,           Meade, D	421 302 195 300 347 318 341 437 377
McNerny, C           McQueen, H J         201,           Meade, D	421 302 195 300 347 318 341 437 377 421
McNerny, C           McQueen, H J         201,           Meade, D         201,           Meco, H         308,           Medlin, D L         308,           Meek, T T         299,           Meeks, H S         299,           Mehl, M J         Mehnorra, P           Meier, M         176,	421 302 195 300 347 318 341 437 377
McNerny, C           McQueen, H J         201,           Meade, D	421 302 195 300 347 318 341 437 377 421 217,
McNerny, C         McQueen, H J       201,         Meade, D       201,         Meco, H       308,         Medk, T T       299,         Meeks, H S       299,         Meehl, M J       Mehl, M J         Mehrotra, P       176,         Meier, M H       272, 317,         Meinke, J H       Melcher, S	421 302 195 300 347 318 341 437 377 421 217, 360
McNerny, C         McQueen, H J       201,         Meade, D       201,         Medo, H       308,         Medin, D L       308,         Meek, T T       299,         Meeks, H S       299,         Mehl, M J       100,         Mehrotra, P       176,         Meier, M       176,         Melcher, S       176,         Melcher, S       176,	421 302 195 300 347 318 341 437 377 421 217, 360 391
McNerny, C         McQueen, H J       201,         Meade, D	421 302 195 300 347 318 341 437 377 421 217, 360 391 239 447 317
McNerny, C         McQueen, H J       201,         Meade, D	421 302 195 300 347 318 341 437 377 421 217, 360 391 239 447 317 223
McNerny, C         McQueen, H J       201,         Meade, D	421 302 195 300 347 318 341 437 377 421 217, 360 391 239 447 317 223 357
McNerny, C         McQueen, H J       201,         Meade, D	421 302 195 300 347 318 341 437 377 421 217, 360 391 239 447 317 223 357 322
McNerny, C         McQueen, H J       201,         Meade, D	421 302 195 300 347 318 341 437 377 421 217, 360 391 239 447 317 223 357 322 221
McNerny, C         McQueen, H J       201,         Meade, D	421 302 195 300 347 318 341 437 377 421 217, 360 391 239 447 317 223 357 322 221 203
McNerny, C         McQueen, H J       201,         Meade, D	421 302 195 300 347 318 341 437 377 421 217, 360 391 239 447 317 223 357 322 221
McNerny, C         McQueen, H J       201,         Meade, D	421 302 195 300 347 318 341 437 377 421 217, 360 391 239 447 317 223 357 322 221 203 436
McNerny, C         McQueen, H J       201,         Meade, D	421 302 195 300 347 318 341 437 377 421 217, 360 391 239 447 317 223 357 322 221 203 436 357
McNerny, C         McQueen, H J       201,         Meade, D	421 302 195 300 347 318 341 437 377 421 217, 360 391 239 447 317 223 357 322 221 203 436 357 270 271 180
McNerny, C         McQueen, H J       201,         Meade, D	421 302 195 300 347 318 341 437 377 421 217, 360 391 239 447 317 223 357 322 221 203 436 357 270 271 180 191
McNerny, C         McQueen, H J       201,         Meade, D	421 302 195 300 347 318 341 437 377 421 217, 360 391 239 447 317 223 357 322 221 203 436 357 270 271 180 191 245
McNerny, C         McQueen, H J       201,         Meade, D	421 302 195 300 347 318 341 437 377 421 217, 360 391 239 447 317 223 357 322 221 203 436 357 270 271 180 191 245 424
McNerny, C         McQueen, H J       201,         Meade, D       308,         Medin, D L       308,         Meek, T T       299,         Meeks, H S       99,         Meehl, M J       90,         Mehrotra, P       90,         Meier, M       176,         272, 317,       91,         Melcher, S       90,         Melissari, B       91,         Mello, J M       91,         Mendelev, M I       222,         Mendiratta, M G       174,         Mendoza, R       248,         Meng, D       91,         Menon, S K       174,         Menon, S K       174,         Mercer, C       91,         Mercer, C       91,         Meschter, S J       91,         Mesina, M       92,         Messersmith, P B       92,         Metson, J B       265	421 302 195 300 347 318 341 437 377 421 217, 360 391 239 447 317 223 357 322 221 203 436 357 270 271 180 191 245 424 399
McNerny, C         McQueen, H J       201,         Meade, D       308,         Medin, D L       308,         Meek, T T       299,         Meeks, H S       99,         Mehn M J       90,         Mehn M J       90,         Mehrotra, P       90,         Meier, M       176,         272, 317,       91,         Meloher, S       91,         Meloher, S       91,         Meloher, S       91,         Mello, J M       92,         Mendelev, M I       222,         Mendiratta, M G       174,         Mendoza, R       248,         Meng, D       94,         Mengel, J       94,         Menon, S K       174,         Menzel, B       94,         Mercer, C       94,         Mereteld, D       94,	421 302 195 300 347 318 341 437 377 421 217, 360 391 239 447 317 223 357 322 221 203 436 357 270 271 180 191 245 424 399 250
McNerny, C         McQueen, H J       201,         Meade, D	421 302 195 300 347 318 341 437 377 421 217, 360 391 239 447 317 223 357 322 221 203 436 357 270 271 180 191 245 424 399 250 381
McNerny, C         McQueen, H J       201,         Meade, D       308,         Medin, D L       308,         Meek, T T       299,         Meeks, H S       99,         Mehn M J       90,         Mehn M J       90,         Mehrotra, P       90,         Meier, M       176,         272, 317,       91,         Meloher, S       91,         Meloher, S       91,         Meloher, S       91,         Mello, J M       92,         Mendelev, M I       222,         Mendiratta, M G       174,         Mendoza, R       248,         Meng, D       94,         Mengel, J       94,         Menon, S K       174,         Menzel, B       94,         Mercer, C       94,         Mereteld, D       94,	421 302 195 300 347 318 341 437 377 421 217, 360 391 239 447 317 223 357 322 221 203 436 357 270 271 180 191 245 424 399 250 381 385

Michael, N L	221
Middleton, W J	189
Migchielsen, J	
Mihalkovic, M	431
Mikula, A	
Miles, M P	
Militzer, M 268,	405
Miller, G	443
Miller, G 329,	230
Miller, M	329
Miller, M K 402,	408
Miller, M P	235
Mills, M J 183,	309,
	407
Minamino, Y 259, 351,	388
Mineta, K	449
Minisandram, R S 219,	220
Minor, A 275,	352
Minor, A M	
Mintz, M H	
Miodownik, M A	181
Miracle, D 175,	402
Mirchi, A A 176,	217,
	360
Mirpuri, K	
Mishima, Y 174, 199, 215,	269,
	435
Mishin, Y 222, 346,	377
Mishra, B 193,	199,
	244
Mishra, C R	
Mishra, N C	
Mishra, R K 207, 211,	347 264,
MISHTA, K S 207, 211,	264
210 211 255	
	397
Misra, A 261, 302, 324,	397 408
Misra, A 261, 302, 324, Misra, D K	397 408 302
Misra, A 261, 302, 324, Misra, D K Mistree, F	397 408 302 289
Misra, A	<ul><li>397</li><li>408</li><li>302</li><li>289</li><li>408</li></ul>
Misra, A	<ul> <li>397</li> <li>408</li> <li>302</li> <li>289</li> <li>408</li> <li>408</li> </ul>
Misra, A	<ul> <li>397</li> <li>408</li> <li>302</li> <li>289</li> <li>408</li> <li>408</li> <li>359</li> </ul>
Misra, A	<ul> <li>397</li> <li>408</li> <li>302</li> <li>289</li> <li>408</li> <li>408</li> <li>359</li> <li>424</li> </ul>
Misra, A       261, 302, 324,         Misra, D K	397 408 302 289 408 408 359 424 340
Misra, A       261, 302, 324,         Misra, D K	<ul> <li>397</li> <li>408</li> <li>302</li> <li>289</li> <li>408</li> <li>408</li> <li>359</li> <li>424</li> <li>340</li> <li>253</li> </ul>
Misra, A       261, 302, 324,         Misra, D K       Mistree, F         Mitchell, T E       324,         Mitlin, D       Miura, S         Miura, S       Miura, Y         Miyahara, Y       Miyamoto, H         Mizutani, Y       Mizutani, Y	<ul> <li>397</li> <li>408</li> <li>302</li> <li>289</li> <li>408</li> <li>408</li> <li>359</li> <li>424</li> <li>340</li> <li>253</li> <li>300</li> </ul>
Misra, A       261, 302, 324,         Misra, D K	<ul> <li>397</li> <li>408</li> <li>302</li> <li>289</li> <li>408</li> <li>408</li> <li>359</li> <li>424</li> <li>340</li> <li>253</li> <li>300</li> <li>385</li> </ul>
Misra, A       261, 302, 324,         Misra, D K	<ul> <li>397</li> <li>408</li> <li>302</li> <li>289</li> <li>408</li> <li>408</li> <li>359</li> <li>424</li> <li>340</li> <li>253</li> <li>300</li> <li>385</li> <li>242</li> </ul>
Misra, A       261, 302, 324,         Misra, D K	<ul> <li>397</li> <li>408</li> <li>302</li> <li>289</li> <li>408</li> <li>408</li> <li>359</li> <li>424</li> <li>340</li> <li>253</li> <li>300</li> <li>385</li> <li>242</li> <li>280</li> </ul>
Misra, A       261, 302, 324,         Misra, D K       Mistree, F         Mitchell, T E       324,         Mitlin, D       Miura, S         Miura, S       Miura, Y         Miyahara, Y       Miyamoto, H         Mizutani, Y       Mo, A         Mobasher, A       Moffat, T P         Mohamed, F A       391,	<ul> <li>397</li> <li>408</li> <li>302</li> <li>289</li> <li>408</li> <li>408</li> <li>359</li> <li>424</li> <li>340</li> <li>253</li> <li>300</li> <li>385</li> <li>242</li> <li>280</li> <li>392</li> </ul>
Misra, A	<ul> <li>397</li> <li>408</li> <li>302</li> <li>289</li> <li>408</li> <li>408</li> <li>359</li> <li>424</li> <li>340</li> <li>253</li> <li>300</li> <li>385</li> <li>242</li> <li>280</li> <li>392</li> <li>437</li> </ul>
Misra, A       261, 302, 324,         Misra, D K       Mistree, F         Mitchell, T E       324,         Mitlin, D       Miura, S         Miura, S       Miura, Y         Miyahara, Y       Miyamoto, H         Mizutani, Y       Mobasher, A         Moffat, T P       220,         Mohamed, F A       391,         Mohanty, P S       S	<ul> <li>397</li> <li>408</li> <li>302</li> <li>289</li> <li>408</li> <li>408</li> <li>359</li> <li>424</li> <li>340</li> <li>253</li> <li>300</li> <li>385</li> <li>242</li> <li>280</li> <li>392</li> <li>437</li> <li>288</li> </ul>
Misra, A       261, 302, 324,         Misra, D K       Mistree, F         Mitchell, T E       324,         Mitlin, D       Miura, S         Miura, S       Miura, Y         Miyahara, Y       Miyamoto, H         Mizutani, Y       Mobasher, A         Moffat, T P       220,         Mohamed, F A       391,         Mohanty, P S       198,	397 408 302 289 408 408 359 424 340 253 300 385 242 280 392 437 288 240,
Misra, A       261, 302, 324,         Misra, D K       Mistree, F         Mitchell, T E       324,         Mitlin, D       Miura, S         Miura, S       Miura, Y         Miyahara, Y       Miyamoto, H         Mobasher, A       Moffat, T P         Mohamed, F A       391,         Mohamed, S A       Mohanty, P S         Mohney, S E       198,	397 408 302 289 408 408 359 424 340 253 300 385 242 280 392 437 288 240, 382
Misra, A       261, 302, 324,         Misra, D K       Mistree, F         Mitchell, T E       324,         Mitlin, D       Miura, S         Miura, S       Miura, Y         Miyahara, Y       Miyamoto, H         Mobasher, A       Moffat, T P         Mohamed, F A       391,         Mohamed, S A       Mohanty, P S         Mohney, S E       198,	397 408 302 289 408 408 359 424 340 253 300 385 242 280 392 437 288 240, 382 431
Misra, A       261, 302, 324,         Misra, D K       Mistree, F         Mitchell, T E       324,         Mitlin, D       Miura, S         Miura, S       Miura, Y         Miyahara, Y       Miyamoto, H         Mizutani, Y       Mobasher, A         Moffat, T P       220,         Mohamed, F A       391,         Mohamed, S A       Mohanty, P S         Mohney, S E       198,	397 408 302 289 408 408 359 424 340 253 300 385 242 280 392 437 288 240, 382 431
Misra, A	397 408 302 289 408 408 359 424 340 253 300 385 242 280 392 437 288 240, 382 431 203
Misra, A	397 408 302 289 408 359 424 340 253 300 385 242 280 392 437 288 240, 382 431 203 290
Misra, A	397 408 302 289 408 408 359 424 340 253 300 385 242 280 392 437 288 240, 382 431 203 290 188 228
Misra, A	397 408 302 289 408 408 359 424 340 253 300 385 242 280 392 437 288 240, 382 431 203 290 188 228 197
Misra, A	397 408 302 289 408 408 359 424 340 253 300 385 242 280 392 437 288 240, 382 431 203 290 188 228 197
Misra, A	<ul> <li>397</li> <li>408</li> <li>302</li> <li>289</li> <li>408</li> <li>359</li> <li>424</li> <li>340</li> <li>253</li> <li>300</li> <li>385</li> <li>242</li> <li>280</li> <li>392</li> <li>437</li> <li>288</li> <li>240,</li> <li>382</li> <li>431</li> <li>203</li> <li>290</li> <li>188</li> <li>228</li> <li>197</li> <li>454</li> </ul>
Misra, A	397 408 302 289 408 408 359 424 340 253 300 385 242 280 392 437 288 240, 382 431 203 290 188 228 197 454 398
Misra, A	397 408 302 289 408 408 359 424 340 253 300 385 242 280 392 437 288 240, 382 431 203 290 188 228 197 454 398 364,
Misra, A       261, 302, 324,         Misra, D K       Mistree, F         Mitchell, T E       324,         Mitlin, D       Miura, S         Miura, S       Miura, Y         Miyahara, Y       Miyamoto, H         Mizutani, Y       Mobasher, A         Moffat, T P       220,         Mohamed, F A       391,         Mohaned, S A       391,         Mohaned, S A       293, 338,         Mohri, T       304, 359, 389,         Mokadem, S       Monlevade, E F         Monteiro-Riviere, N       Montejano, S         Montgomery, G P       397,         Montgomery, J S       278,	397 408 302 289 408 408 359 424 340 253 300 385 242 280 392 437 288 240, 382 431 203 290 188 228 197 454 398 364, 440
Misra, A	397 408 302 289 408 359 424 340 253 300 385 242 280 392 437 288 240, 382 431 203 290 188 228 197 454 398 364, 440 252 262,
Misra, A       261, 302, 324,         Misra, D K       Mistree, F         Mitchell, T E       324,         Mitlin, D       Miura, S         Miura, S       Miura, Y         Miyahara, Y       Miyamoto, H         Mizutani, Y       Mo, A         Moffat, T P       220,         Mohamed, F A       391,         Mohamed, S A       391,         Mohaney, S E       198,	397 408 302 289 408 408 359 424 340 253 300 385 242 280 392 437 288 240, 382 431 203 290 188 228 197 454 398 364, 440 252 262, 418

Moore, J F	429
Morales, A T	211
Morando, C N	450
Moraru, A 173,	437
Mordike, B	383
More, K L	215
Morgan, D 205,	289
Morgan, J K	441
Mori, H	301
Mori, T	
Morin, G	
Morishita, M	427
Moriyama, K	
Morral, J E 174,	322
Morris, J G 249,	314
Morris, J R 222, 316, 317,	365
Morris, J W 275, 283,	331
Morrison, M L 271,	359
Morrow, A	415
Morsi, K B 242, 295,	340
Mortensen, D	
Mosher, J	
Moss, S C	250
Mostovoy, S	237
Mota, G E 172,	213
Motahari, S	328
Motoyasu, G	
Moura, R R	
Mourou, G	345
Moxson, V 278, 364, 365,	440
Mucciardi, F 278, 304, 305,	
	380
Muddle, B 371,	415
Mueller-Krumbhaar, H	
Muhlstein, C L	
Muir, D M	284
Mukherjee, A 317, 355,	432
Mukhopadhyay, A 362,	404
Mukhopadhyay, G	194
Mukhopadhyay, P	194
	346,
Mukhopadhyay, S M 301,	450
Mulholland, M	356
Muller, K	
Müller, S	181
Muncy, M	
Mungsantisuk, P 396,	397
Munitz, A 287,	418
Murali, K	397
Murayama, N 426,	427
Murphy, C J	395
Murphy, K	
Murr, L E 192, 279, 395,	
Murray, J	441
	441
Murray, J A	277
	277 188
Murti, V S	277 188 413
Murty, K L 201, 246,	277 188 413 256,
Murty, K L 201, 246,	277 188 413 256, 379
Murty, K L 201, 246, 	277 188 413 256, 379 311
Murty, K L 201, 246,	277 188 413 256, 379 311
Murty, K L 201, 246, 	277 188 413 256, 379 311

## Ν

Na, K	236
Nafisi, S 423,	439
Nagano, T	186
Nagasawa, Y	390
Nah, J	294

Naik, R R	291
Nakagawa, Y	401
Nakamori, Y	263
Nakamura, H	401
Nakamura, N	384
Nakamura, Y	210
Nakano, T	390
Nakano, T	300
Nakayama, K	427
Nam, S	281
Nam, W J	208
Nandy, T	270
Napolitano, R 300, 343, Narayan, J 291, 334,	427
Narayan, J 291, 334,	336
Narayan, R J 197, 239, 291,	337,
	451
Nardi, P	352
Narita, H	449
Narvekar, R N	217
Nash, P 237,	314
Nastac, L 178, 219,	220,
	404
Nastasi, M 302,	408
Navarra, P	380
Nayak, S	334
Nazarov, A A	252
Necker, C T	249
Nedkova, T	184
Needleman, A	377
Neelameggham, R	332
Neilsen, M K	230
Neitzel, G P	404
Nendick, R M	189
Nenkov, K	239
Nerikar, P	302
Nes, E	351
Neudorf, D A 189,	443
Neuschutz, D Ng, K W	404 333
Ngoh, S L	
Nguyen, V	
Ni, H	254
Nibur, K A	224
Nicholson, B K	406
Nicholson, D 359,	431
Nicol, M J	443
Nie, J 187, 228, 294,	295,
	445
Nieh, T G	438
Nielsen, M C	179
Niemczura, W	263
Nienow, A W	318
Nieves, J	291
Nigam, A K	196
Nikandrov, K P	267
Nikoloski, A N	
Nishimura, T	
Nishio, T	
Nishiyama, K	227
Nix, W D 261,	309
Nizovtsev, P N	259
Noakes, R	
Nobile, A	253
Noebe, R D	
Nogita, K	
Noguez, M E	
Norfleet, D M	352

Noronha, S	224
Northwood, D	
Notis, M R 189, 198, 231,	232,
	331,
	416
Novichkov, S B	245
Novotnak, D	414
Nowak, R	177
Noyan, I C	416
Ntakaburimvo, N	178
Nunomura, Y	174
Nurminen, E	186
Nyberg, E	287

### 

O'Brien, J M	257
O'Callaghan, J F	373
Ochoa, F A	331
Oda, T	
	323
Oda, Y	407
Oertel, C	
Ogata, S	
Oh, B	337
Oh, K	383
Oh, K H	283
Oh, S	382
Oh-ishi, K 252, 264,	433
Ohkubo, C	407
Ohkubo, K	359
Ohmori, T	242
Ohnaka, I	
Ohno, M 389,	431
Ohnuma, I	
Okabe, T 366, 407,	449
Okamura, Y	206
Okane, T	299
Okazaki, K	434
Okuno, O	407
Olevsky, E A	242
Olivares, R	440
Oliveira, T	252
Oliver, E C	
Oliver, S R 275,	321
Oliver, W C	308
Olson, D L 192, Olson, G B 192,	210
	358,
	425
Olson, J D	198
Olsvik, A	272
Oltman, E	
Omanovic, S	280
Omran, A M	403
Onderka, B	240
Ooij, W V	238
Oona, H	436
Oosterkamp, L D	191
Oppenheimer, S M	340
Opsahl, T	398
Orimo, S	396
Orlov, D 208, 255,	
Orlova, T S 208, 253, 252,	260
	258
Orth, A	330
Ortiz, A L	346
Ortiz, M	365
Osada, K	211
Osamura, K	314

Osborne, G E	421
Osborne, R C 188, 230,	231
Osetsky, Y N 183, 184, 224,	226
Oshinowo, L 285, 362,	424
Ossi, P M	429
Österle, W	367
Oswald, K	218
Otto, F	425
Ou, S	
Ouimet, L J	191
Ovcharenko, V I	280
Overfelt, R A 375,	450
Oyama, Y	200
Øye, H 176,	218
Oygard, A	318
Ozaki, K 226,	326
Ozcan, A	370
Ozolins, V 263, 305,	430

### P

Padhi, B	368
Paglieri, S N 353,	436
Paik, J	241
Paik, K 294,	339
Pal, U B 280, 325, 366,	409
Palacio, H A 300,	450
Palenik, B P	291
Palumbo, G	308
Pan, D	232
Pan, D 229, 286,	342
Pan, M X	217
Pan, T	191
Panaitescu, A 173,	437
Panaitescu, I 173,	437
Pande, C S 246, 302,	435
Pandya, D K	239
Pang, J H 286, 338,	339
Pang, J W 279,	324
Pang, Y 278,	406
Panov, A V	312
Pant, B B	198
Pao, P S	392
Papaconstantopoulos, D A	377
Papadimitrakopoulos, F	451
Papangelakis, V G	284
Parent, L	361
Paretsky, V M 185,	186,
	449
Parikh, A N	447
Parish, C	395
Parisi, A	387
Park, C	455
Park, C	229
Park, E S	217
Park, H	236
Park, H	241
Park, J	339
Park, J	203
Park, J	452
Park, J I	442
	454
Park, J S 453.	
Park, J S 453, Park, J S	411
Park, J S	411
Park, J S	
Park, J S Park, K S Park, K T	368 349
Park, J S	

<b>D</b> 1 0	
Park, S	
Park, S	455
Park, S S	287
Park, Y	
Parkes, R C	286
Parkin, S	290
Paromova, I V	312
Parrish, E	238
Parsell, D E	359
Parsey, J M 193,	235
Parthasarathy, T A 174, Paserin, V	357
Pasturel, A	
Patankar, S V	
Patel, A D 219,	219
Patel, J	394
Patel, M K 362,	404
Patino, E	378
Pattabiraman, R	236
Pattanaik, G R 239,	291
Patterson, E	399
Patti, A	380
Patzelt, N	330
Paulsen, K	172
Pavio, J	235
Pawaskar, D N	406
Pawlek, R P	313
Paxton, D M	235
Payzant, E A 176, 256,	392
Pecharsky, V K 263,	396
Pedersen, R	272
Peker, A 271,	359
Pekguleryuz, M O	444
Pelletier, J	438
Pellin, M J	429
Pena, J S	
	320
Peng, H	238
Peng, L	238 434
Peng, L Peralta, P D 201, 342,	238 434 411
Peng, L Peralta, P D 201, 342, Percheron-Guégan, A 210,	238 434 411 262
Peng, L Peralta, P D 201, 342, Percheron-Guégan, A 210, Pereloma, E V	238 434 411 262 254
Peng, L	238 434 411 262 254 344
Peng, L	238 434 411 262 254 344 433
Peng, L         Peralta, P D       201, 342,         Percheron-Guégan, A       210,         Pereloma, E V       210,         Perepezko, J H       215, 241, 253,         Perez-Prado, M       Perruchoud, R C	238 434 411 262 254 344 433 360
Peng, L       201, 342,         Peralta, P D       201, 342,         Percheron-Guégan, A       210,         Pereloma, E V       210,         Perepezko, J H       215, 241, 253,         Perez-Prado, M       Perruchoud, R C         Perry, T       Perruchoud, R	238 434 411 262 254 344 433 360 413
Peng, L       201, 342,         Peralta, P D       201, 342,         Percheron-Guégan, A       210,         Pereloma, E V       210,         Perepezko, J H       215, 241, 253,         Perez-Prado, M       Perruchoud, R C         Perry, T       Peter, W       271,	238 434 411 262 254 344 433 360 413 359
Peng, L       201, 342,         Peralta, P D       201, 342,         Percheron-Guégan, A       210,         Pereloma, E V       210,         Perepezko, J H       215, 241, 253,         Perez-Prado, M       Perruchoud, R C         Perry, T       Peter, W         Peterson, L       271,	238 434 411 262 254 344 433 360 413 359 204
Peng, L       201, 342,         Peralta, P D       201, 342,         Percheron-Guégan, A       210,         Pereloma, E V       Pereloma, E V         Perepezko, J H       215, 241, 253,         Perez-Prado, M       Perruchoud, R C         Perry, T       Peter, W         Peterson, L       Peterson, R         244,       244,	238 434 411 262 254 344 433 360 413 359 204 266
Peng, L       201, 342,         Peralta, P D       201, 342,         Percheron-Guégan, A       210,         Pereloma, E V       210,         Perepezko, J H       215, 241, 253,         Perez-Prado, M       Perruchoud, R C         Perry, T       Peter, W         Peterson, L       271,	238 434 411 262 254 344 433 360 413 359 204 266
Peng, L       201, 342,         Peralta, P D       201, 342,         Percheron-Guégan, A       210,         Pereloma, E V       Pereloma, E V         Perepezko, J H       215, 241, 253,         Perez-Prado, M       Perruchoud, R C         Perry, T       Peter, W         Peterson, L       Peterson, R         Peterson, R       244,	238 434 411 262 254 344 433 360 413 359 204 266 358
Peng, L       201, 342,         Peralta, P D       201, 342,         Percheron-Guégan, A       210,         Pereloma, E V       Pereloma, E V         Perepezko, J H       215, 241, 253,         Perez-Prado, M       Perruchoud, R C         Perry, T       Peter, W         Peterson, L       271,         Peterson, R       244,         Petit, P       Petaroli, M         Petraroli, M       Petricca, S         Petrova, R S       S	238 434 411 262 254 344 433 360 413 359 204 266 .358 190
Peng, L       201, 342,         Peralta, P D       201, 342,         Percheron-Guégan, A       210,         Pereloma, E V       Pereloma, E V         Perepezko, J H       215, 241, 253,         Perez-Prado, M       Perruchoud, R C         Perry, T       Peter, W         Peterson, L       271,         Peterson, R       244,         Petit, P       Petraroli, M         Petricca, S       S	238 434 411 262 254 344 433 360 413 359 204 266 .358 190 381
Peng, L       201, 342,         Peralta, P D       201, 342,         Percheron-Guégan, A       210,         Pereloma, E V       Pereloma, E V         Perepezko, J H       215, 241, 253,         Perez-Prado, M       Perruchoud, R C         Perry, T       Peter, W         Peterson, L       271,         Peterson, R       244,         Petit, P       Petaroli, M         Petraroli, M       Petricca, S         Petrova, R S       S	238 434 411 262 254 344 433 360 413 359 204 266 .358 190 381 275
Peng, L       201, 342,         Peralta, P D       201, 342,         Percheron-Guégan, A       210,         Pereloma, E V       215, 241, 253,         Perepezko, J H       215, 241, 253,         Perepezko, J H       215, 241, 253,         Perepezko, J H       215, 241, 253,         Perery, T       Perruchoud, R C         Perry, T       271,         Peterson, L       271,         Peterson, R       244,         Petit, P       244,         Petricca, S       Petrova, R S         Petrova, R S       Pettengill, E C	238 434 411 262 254 344 433 360 413 359 204 266 358 190 381 275 264
Peng, L       201, 342,         Percheron-Guégan, A       210,         Pereloma, E V       210,         Perepezko, J H       215, 241, 253,         Perepezko, J H       215, 241, 253,         Perepezko, J H       215, 241, 253,         Perery, T       Perruchoud, R C         Petry, T       Peterson, L         Peterson, R       244,         Petit, P       Petraroli, M         Petrova, R S       Petrova, R S         Pettersen, K       Pettersen, K	238 434 411 262 254 344 433 360 413 359 204 266 .358 190 381 275 264 444
Peng, L       201, 342,         Percheron-Guégan, A       210,         Pereloma, E V       210,         Perepezko, J H       215, 241, 253,         Perepezko, J H       215, 241, 253,         Perepezko, J H       215, 241, 253,         Perery, T       Perruchoud, R C         Perry, T       Peter, W         Peterson, L       271,         Peterson, R       244,         Petit, P       Petraroli, M         Petrova, R S       Petrova, R S         Pettersen, K       Pettifor, D G         Pharr, G M       372,         Phillion, A       372,	238 434 411 262 254 344 433 360 413 359 204 266 .358 190 381 275 264 444 348
Peng, L       201, 342,         Percheron-Guégan, A       210,         Percepezko, J H       215, 241, 253,         Percepezko, M       Perruchoud, R C         Perry, T       Perruchoud, R C         Perry, T       271,         Peterson, L       271,         Peterson, R       244,         Petit, P       244,         Petit, P       244,         Petrova, R S       Petrova, R S         Petrova, R S       Petrova, R S         Pettersen, K       Pettifor, D G         Pharr, G M       372,         Phillips, E C       372,	238 434 411 262 254 344 433 360 413 359 204 266 .358 190 381 275 264 444 348 401 219 171
Peng, L       201, 342,         Peralta, P D       201, 342,         Percheron-Guégan, A       210,         Pereloma, E V       215, 241, 253,         Perepezko, J H       215, 241, 253,         Perepezko, M       Perruchoud, R C         Perry, T       271,         Peter, W       271,         Peterson, L       244,         Petit, P       244,         Petraroli, M       Petraroli, M         Petrerova, R S       Petrova, R S         Pettengill, E C       Pettersen, K         Pettifor, D G       372,         Phillion, A       Phillips, E C         Phillipot, S R       272,	238 434 411 262 254 344 433 360 413 359 204 266 .358 190 381 275 264 444 348 401 219 171 222
Peng, L       201, 342,         Peralta, P D       201, 342,         Percheron-Guégan, A       210,         Pereloma, E V       215, 241, 253,         Perepezko, J H       215, 241, 253,         Perepezko, M       Perruchoud, R C         Perruchoud, R C       Perruchoud, R C         Perry, T       271,         Peter, W       271,         Peterson, L       244,         Petit, P       244,         Petraroli, M       Petraroli, M         Petrova, R S       Petrova, R S         Pettengill, E C       Pettersen, K         Pettifor, D G       Phar, G M       372,         Phillips, E C       Phillips, E C         Phillpot, S R       Piascik, R	238 434 411 262 254 344 433 360 413 359 204 266 .358 190 381 275 264 444 348 401 219 171 222 418
Peng, L       201, 342,         Peralta, P D       201, 342,         Percheron-Guégan, A       210,         Pereloma, E V       210,         Perepezko, J H       215, 241, 253,         Perepezko, J H       215, 241, 253,         Perez-Prado, M       Perruchoud, R C         Perry, T       Petre, W         Petry, T       271,         Peterson, L       271,         Peterson, R       244,         Petit, P       244,         Petraroli, M       Petraroli, M         Petraroli, M       244,         Petit, P       244,         Petir, P       244,         Petir, P       244,         Petirova, R S       Petrova, R S         Petrova, R S       Petrova, R S         Pettengill, E C       Pettersen, K         Pettifor, D G       Pharr, G M       372,         Phillion, A       Phillips, E C         Phillipot, S R       Piascik, R         Picard, Y N       Picard, Y N	238 434 411 262 254 344 433 360 413 359 204 266 .358 190 381 275 264 444 348 401 219 171 222 418 345
Peng, L       201, 342,         Percheron-Guégan, A       210,         Perrepezko, J H       215, 241, 253,         Perceastriction       Perceastriction         Perceastriction       A         Perceastriction       A         Perceastriction       A         Petroson, L       271,         Peterson, R       244,         Petrit, P       Petraroli, M         Petrova, R S       Petrova, R S         Petrova, R S       Petrova, R S         Pettersen, K       Petrova, R S         Pharr, G M       372,         Phillion, A       Petromon      <	238 434 411 262 254 344 433 360 413 359 204 266 358 190 381 275 264 444 348 401 219 171 222 418 345 365
Peng, L       201, 342,         Percheron-Guégan, A       210,         Percheron-Guégan, A       210,         Pereloma, E V       215, 241, 253,         Perepezko, J H       215, 241, 253,         Perepezko, M       Perruchoud, R C         Perry, T       Petre, W         Petrer, W       271,         Peterson, L       271,         Peterson, R       244,         Petit, P       244,         Petrova, R S       Petrova, R S         Petrova, R S       Pettengill, E C         Pettersen, K       944,         Pettifor, D G       372,         Phillion, A       372,         Phillion, S R       Piascik, R         Picard, Y N       223,         Pickens, J R       223,	238 434 411 262 254 344 433 360 413 359 204 266 358 190 381 275 264 444 348 401 219 171 222 418 345 365 409
Peng, L       201, 342,         Peralta, P D       201, 342,         Percheron-Guégan, A       210,         Pereloma, E V       Pereloma, E V         Perepezko, J H       215, 241, 253,         Perez-Prado, M       Perruchoud, R C         Perry, T       Peter, W         Peter, W       271,         Peterson, L       Peterson, R         Petraroli, M       Petricca, S         Petrova, R S       Petrova, R S         Pettorson, K       9ettifor, D G         Pharr, G M       372,         Phillion, A       Phillipot, S R         Piascik, R       Picard, Y N         Pickens, J R       223,         Pickering, H W       Pillai, V C	238 434 411 262 254 344 433 360 413 359 204 266 358 190 381 275 264 444 348 401 219 171 222 418 345 365 409 399
Peng, L       201, 342,         Peralta, P D       201, 342,         Percheron-Guégan, A       210,         Pereloma, E V       Pereloma, E V         Perepezko, J H       215, 241, 253,         Perez-Prado, M       Perruchoud, R C         Perry, T       Peter, W         Peter, W       271,         Peterson, L       Peterson, R         Petraroli, M       Petricca, S         Petrova, R S       Petrova, R S         Pettorson, K       Pettifor, D G         Pharr, G M       372,         Phillion, A       Phillipot, S R         Picard, Y N       Pickens, J R         Pickens, J R       223,         Pickering, H W       Pillai, V C         Pillis, M F       Pillis, M F	238 434 411 262 254 344 433 360 413 359 204 266 358 190 381 275 264 444 348 401 219 171 222 418 345 365 409 399 243
Peng, L       201, 342,         Percheron-Guégan, A       210,         Pereloma, E V       215, 241, 253,         Perepezko, J H       215, 241, 253,         Perepezko, M       Perruchoud, R C         Perruchoud, R C       Perruchoud, R C         Perry, T       Peter, W         Petrer, W       271,         Peterson, L       271,         Peterson, R       244,         Petit, P       Petraroli, M         Petraroli, M       Petricca, S         Petrova, R S       Petrova, R S         Pettengill, E C       Pettersen, K         Pettifor, D G       Pharr, G M         Phillips, E C       Phillips, E C         Phillpot, S R       Piascik, R         Pickens, J R       223,         Pickering, H W       Pillai, V C         Pillis, M F       Pilon, L	238 434 411 262 254 344 433 360 413 359 204 266 358 190 381 275 264 444 348 401 219 171 222 418 345 365 409 399 243 173
Peng, L       201, 342,         Peralta, P D       201, 342,         Percheron-Guégan, A       210,         Pereloma, E V       Pereloma, E V         Perepezko, J H       215, 241, 253,         Perez-Prado, M       Perruchoud, R C         Perry, T       Peter, W         Peter, W       271,         Peterson, L       Peterson, R         Petraroli, M       Petricca, S         Petrova, R S       Petrova, R S         Pettorson, K       Pettifor, D G         Pharr, G M       372,         Phillion, A       Phillipot, S R         Picard, Y N       Pickens, J R         Pickens, J R       223,         Pickering, H W       Pillai, V C         Pillis, M F       Pillis, M F	238 434 411 262 254 344 433 360 413 359 204 266 358 190 381 275 264 444 348 401 219 171 222 418 345 365 409 399 243

Pineault, J	177
Pinoncely, A 272,	399
Pint, B A	174
Piotrowski, G B	341
Pippan, R 252, 254,	350
D' 1' T	
Pisarkiewicz, T	321
Piskajova, T V	267
Pitchure, D	287
Plapp, M	387
Platek, P	268
Platonov, V	437
Plikas, T 362,	424
Pluth, M J 301,	388
Podey, L	318
Pohar, P	378
Poirier, D R 385,	428
Polasik, S J	309
Poliakov, P V	267
Pollock, T M 195, 270,	345
Pomrenke, G S	179
Pomykala, J A	357
Poncsák, S	447
Pond, R C 228,	425
Ponge, D 259,	350
Pongsaksawad, W	367
Poole, W J 268, 303,	307
Poon, J 216,	217
Popescu, G	290
Popov, V P	381
Popova, N A	258
Portella, P D	367
Folitella, F D	
Porter, W 176, 298,	421
Portmann, M J	250
Posada, T	
	361
Potens, B	388
Potens, B	
Potens, B Potluri, K	388 274
Potens, B Potluri, K Potocnik, V	388 274 437
Potens, B Potluri, K	388 274 437
Potens, B Potluri, K Potocnik, V Potzies, C	388 274 437 418
Potens, B Potluri, K Potocnik, V Potzies, C Poulsen, H	388 274 437 418 372
Potens, B Potluri, K Potocnik, V Potzies, C Poulsen, H	388 274 437 .418 372 431
Potens, B Potluri, K Potocnik, V Potzies, C Poulsen, H	388 274 437 418 372
Potens, B Potluri, K Potocnik, V Potzies, C Poulsen, H	388 274 437 .418 372 431 289,
Potens, B Potluri, K Potocnik, V Potzies, C Poulsen, H	388 274 437 418 372 431 289, 366,
Potens, B Potluri, K Potzies, C Poulsen, H	388 274 437 .418 372 431 289, 366, 420
Potens, B Potluri, K Potocnik, V Potzies, C Poulsen, H	388 274 437 418 372 431 289, 366,
Potens, B Potluri, K Potzies, C Poulsen, H	388 274 437 418 372 431 289, 366, 420 444
Potens, B         Potluri, K         Potocnik, V         Potzies, C         Poulsen, H         Pourboghrat, F         Powell, A C         323, 325, 335,	388 274 437 418 372 431 289, 366, 420 444 396
Potens, B         Potluri, K         Potocnik, V         Potzies, C         Poulsen, H         Pourboghrat, F         Powell, A C         323, 325, 335,	388 274 437 418 372 431 289, 366, 420 444 396 226
Potens, B         Potluri, K         Potocnik, V         Potzies, C         Poulsen, H         Pourboghrat, F         Powell, A C         194, 236, 280,	388 274 437 418 372 431 289, 366, 420 444 396 226 372
Potens, B         Potluri, K         Potocnik, V         Potzies, C         Poulsen, H         Pourboghrat, F         Powell, A C         323, 325, 335,	388 274 437 418 372 431 289, 366, 420 444 396 226
Potens, B         Potluri, K         Potocnik, V         Potzies, C         Poulsen, H         Powell, A C         194, 236, 280,	388 274 437 418 372 431 289, 366, 420 444 396 226 372 372
Potens, B         Potluri, K         Potocnik, V         Potzies, C         Poulsen, H         Powell, A C         323, 325, 335,	388 274 437 .418 372 431 289, 366, 420 444 396 226 372 372 218
Potens, B       Potluri, K         Pottluri, K       Potocnik, V         Potzies, C       Poulsen, H         Pourboghrat, F       302,         Pourboghrat, F       302,         Powell, A C       194, 236, 280,	388 274 437 418 372 431 289, 366, 420 444 396 226 372 372
Potens, B         Potluri, K         Potocnik, V         Potzies, C         Poulsen, H         Powell, A C         323, 325, 335,	388 274 437 .418 372 431 289, 366, 420 444 396 226 372 372 218
Potens, B         Potluri, K         Potocnik, V         Potzies, C         Poulsen, H         Powell, A C         194, 236, 280,	388 274 413 372 431 289, 366, 420 444 396 226 372 218 258 372
Potens, B         Potluri, K         Potocnik, V         Potzies, C         Poulsen, H         Powell, A C         900         323, 325, 335,         323, 325, 335,         367, 378, 408, 409,         Powell, B R         191,         Powell, G         395,         Prabhakaran, R         Prado, F G         Pragnell, P B       253,         Prask, H J       268,         Predecki, P	388 274 437 418 372 431 289, 366, 420 444 396 226 372 218 258 372 218 258 372 371
Potens, B         Potluri, K         Potocnik, V         Potzies, C         Poulsen, H         Powell, A C         194, 236, 280,	388 274 413 372 431 289, 366, 420 444 396 226 372 218 258 372
Potens, B         Potluri, K         Potocnik, V         Potzies, C         Poulsen, H         Powell, A C         194, 236, 280,	388 274 437 418 372 431 289, 366, 420 444 396 372 218 258 372 218 258 372 371 340
Potens, B         Potluri, K         Potocnik, V         Potzies, C         Pourboghrat, F         Powell, A C         323, 325, 335,	388 274 437 418 372 431 289, 366, 420 444 396 372 218 258 372 218 258 372 371 340 436
Potens, B         Potluri, K         Potocnik, V         Potzies, C         Poulsen, H         Powell, A C         194, 236, 280,	388 274 437 418 372 431 289, 366, 420 444 396 226 372 218 258 372 218 258 372 371 340 436 378
Potens, B         Potluri, K         Potocnik, V         Potzies, C         Poulsen, H         Powell, A C         194, 236, 280,	388 274 437 418 372 431 289, 366, 420 444 396 226 372 218 258 372 218 258 372 371 340 436 378 269
Potens, B         Potluri, K         Potocnik, V         Potzies, C         Poulsen, H         Powell, A C         194, 236, 280,	388 274 437 418 372 431 289, 366, 420 444 396 226 372 218 258 372 218 258 372 371 340 436 378 269
Potens, B         Potluri, K         Potocnik, V         Potzies, C         Poulsen, H         Powell, A C         194, 236, 280,	388 274 437 418 372 431 289, 366, 420 444 396 226 372 218 258 372 218 258 372 371 340 436 378 269 360
Potens, B         Potluri, K         Potocnik, V         Potzies, C         Poulsen, H         302,         Pourboghrat, F         Powell, A C         323, 325, 335,	388 274 437 418 372 431 289, 366, 420 444 396 372 218 258 372 218 258 372 371 340 436 378 269 360 253
Potens, B         Potluri, K         Potocnik, V         Potzies, C         Poulsen, H         Powell, A C         194, 236, 280,	388 274 437 418 372 431 289, 366, 420 444 396 226 372 218 258 372 218 258 372 371 340 436 378 269 360
Potens, B         Potluri, K         Potocnik, V         Potzies, C         Pourboghrat, F         Powell, A C         194, 236, 280,	388 274 437 418 372 431 289, 366, 420 444 396 226 372 372 218 258 372 218 258 372 371 340 436 378 269 360 253 223
Potens, B         Potluri, K         Potocnik, V         Potzies, C         Pourboghrat, F         Powell, A C         194, 236, 280,	388 274 437 418 372 431 289, 366, 420 444 396 226 372 372 218 258 372 218 258 372 371 340 436 378 269 360 253 223 361
Potens, B         Potluri, K         Potocnik, V         Potzies, C         Pourboghrat, F         Powell, A C         194, 236, 280,	388 274 437 418 372 431 289, 366, 420 444 396 226 372 372 218 258 372 218 258 372 371 340 436 269 360 253 223 361 195
Potens, B         Potluri, K         Potocnik, V         Potzies, C         Pourboghrat, F         Powell, A C         194, 236, 280,	388 274 437 418 372 431 289, 366, 420 444 396 226 372 372 218 258 372 218 258 372 371 340 436 378 269 360 253 223 361
Potens, B         Potluri, K         Potocnik, V         Potzies, C         Pourboghrat, F         Powell, A C         194, 236, 280,	388 274 437 418 372 431 289, 366, 420 444 226 372 372 218 258 372 218 258 372 371 340 436 378 269 360 253 223 361 195 263
Potens, B         Potluri, K         Potocnik, V         Potzies, C         Poulsen, H         Powell, A C         194, 236, 280,	388 274 437 418 372 431 289, 366, 420 444 396 226 372 372 218 258 372 218 258 372 371 340 436 378 263 253 223 361 195 263 258
Potens, B         Potluri, K         Potocnik, V         Potzies, C         Pourboghrat, F         Powell, A C         194, 236, 280,	388 274 437 418 372 431 289, 366, 420 444 396 226 372 372 218 258 372 218 258 372 218 258 372 371 340 436 253 223 361 195 263 258 339
Potens, B         Potluri, K         Potocnik, V         Potzies, C         Pourboghrat, F         Powell, A C         194, 236, 280,	388 274 437 418 372 431 289, 366, 420 444 396 226 372 372 218 258 372 218 258 372 218 258 372 371 340 436 253 223 361 195 263 258 339
Potens, B         Potluri, K         Potocnik, V         Potzies, C         Poulsen, H         Powell, A C         194, 236, 280,	388 274 437 418 372 431 289, 366, 420 444 396 226 372 372 218 258 372 218 258 372 371 340 436 378 269 360 253 223 361 195 263 258 339 353
Potens, B         Potluri, K         Potocnik, V         Potzies, C         Poulsen, H         Powell, A C         194, 236, 280,	388 274 437 418 372 431 289, 366, 420 444 396 226 372 218 258 372 218 258 372 218 258 372 371 340 436 378 269 360 253 223 361 195 263 258 339 353 282
Potens, B         Potluri, K         Potocnik, V         Potzies, C         Poulsen, H         Powell, A C         194, 236, 280,	388 274 437 418 372 431 289, 366, 420 444 396 226 372 218 258 372 218 258 372 218 258 372 371 340 436 378 269 360 253 223 361 195 263 258 339 353 282

Puttlitz, K J ..... 286, 416

### Q

Qi, G	373
Qi, Y	331
Qian, M 294, 376,	417
Qin, Q	357
Qiu, Z 357,	400
Quan, Z	214
Quatravaux, T	219
Quested, T E	298
Quiroga, A S	300

## R

Raab, G I	255,	256,	257
Raabe, D		259,	350
Rabba, S A			360
Rabeeh, R			308
Rabenberg, J			219
Rabiei, A			447
Rabkin, E			260
Rack, H			446
Rack, H J			350
Rackaitis, M			424
Radmilovic, V			408
Raghavan, P			406
Raghavan, S			387
Rahman, M M			274
Raj, B			227
Raj, I A			236
Rajagopalan, B			288
Rajagopalan, S			342
Rajan, K	102	234	288.
	334	276	419
Rajeev, K P			
Rama Mohan, T R	•••••	190,	239
			224
Ramachandran, V			244
Ramakrishnan, S			333
Ramanath, G			422
Ramanathan, L V	•••••	243,	429
Ramanujan, R V	•••••	238,	424
Ramaswamy, K			256
Ramchandran, R			244
Ramesh, N N			412
Ramesh, R 195,	237,	290,	336
Ramirez, A G			453
Ramirez, J			386
Ramírez, J			454
Ramovic, R			180
Ramsey, L	•••••		172
Rangaswamy, P	•••••	283,	371
Ranieri, S			188
Ranki-Kilpinen, T			186
Rao, S			183
Rao, V N			412
Rapkoch, J M			200
Rappaz, M	202,	247,	299,
	385,	386,	450
Ratchev, I			
Rath, B B	169,	334,	446
Rath, C			336
Rathod, C R			
Rathz, T J			
Ratke, L			
Ratner, B D			

Raty, M 171,	
Ravinder Reddy, N	355
Ravindra, N M 179,	180,
	321
Rawn, C J	400
Ray, K K	227
Ray, L D	318
Raychenko, O I	381
Readey, D W	193
Ready, J 179, 220, 274,	320
Rebak, R B	
Reck, B	244
Reddy, M R	413
Reddy, R G 185, 243,	268,
	357
Redl, C	404
Reed, B 406,	431
Reichert, H	251
Reichman, S H	278
Reid, J G 372,	373
Reilly, E K	
	354
Reilly, J J	353
Rejaee, M	333
Rejent, J A	331
Remhof, A	395
	366
Remington, B A	
Renaudier, S	437
Reny, P	177
Reshetov, A	208
Reuter, M A 200, 232, 245,	362
Reutzel, S	380
Reynier, Y	
Reynolds, T	270
Reynolds, W T 282,	371
Rez, P	354
Reznik, I D	185
Rhee, H 188, 285,	
Rhee, K H	269
Richards, C D 275,	435
Richards, R.F., 275.	435
Richardson, J W 184, 297,	372
Ricker, R	287
Ricketts, N J	376
Rickkets, M S	288
Riddle, R K	330
Riddle, Y W 343, 347,	376
Ried, P P	191
Rieger, L E	326
Riehl, W	230
Rietz, W	417
Rigg, P A	453
Rigopoulos, E	330
Rigsbee, J M 197, 239, 291,	326,
	447
Rijssenbeek, J	263
Riman, R E	197
Ritchie, R O 309, 315, 418,	419
Ritchie, R R	316
Rivard, J D	341
Riverin, G	266
Rivero, I V	
Rivière, C	319
Rivoaland, L	177
Ro, Y	270
Ro, Y J	
1.0, 1 J	410
Dobach I	410
Robach, J	183
Robach, J Robbins, J	183

Robertson, I M	183
Robinson, J A	198
Robinson, M C	275
Robinson, T P	313
Rocha, M S	230
Rodnov, O O 212,	267
Rodrigues, R L	329
Rodriguez Gan, R	373
Rodriguez, P	415
Roesner, H 346,	351
Rogan, R 328,	372
Rogers, J R 289,	438
Rohrer, G 390,	
Rolander, N	
Rolland, K	172
Rollett, A D 180, 204,	249,
	451
Romanov, A E 252,	258
Rong, Z	224
Rosales, I	326
Rosales, P I	175
Rösner, H	307
Ross, C A	
Rossler, U K	239
Rousseaux, J	171
Roven, H J	208
Roy, A	357
Roy, A K	226
Roytburd, A L 322, 334, 384,	425
Rozin, A V	318
Ruban, A V	405
Rubinovich, Z	333
Rubisov, D	284
Ruckebusch, H	173
Ruda, M	451
Rudd, T J	301
Rudin, S P 183,	282
Rudko, G Y	
Rugg, D 182,	
Rühle, M	
Ruile, W	
Runt, J P	
	424
Russell, R	436
Russell, R 418,	419
Ruuskanen, P R	412
Ruzyllo, J	221
Ryan, L	415
Ryu, D	413
Ryu, H 453,	454
Ryu, J	442

## S

Saatci, A		265
Sabau, A S 218, 2	298,	362,
	123,	446
Sachdev, A K	233,	347
Sachenko, P		432
Sadananda, K	348,	366
Sadigh, B	406,	431
Sadler, B A		360
Sadoway, D R 223, 325, 3	366,	420
Saeki, Y		
Saez, E		178
Safi, M		203
Sahling, M		398
Saito, K	218,	450

Saito, N	. 234
Saito, T	440
Saito, Y	206
Sakaguchi, T	. 227
Sakai, T	
Sakamoto, H	449
Sakamoto, M	175
Sakasegawa, H	184
Sakidja, R 215.	
Salami, T O 275.	321
Salas, G	
Saleh, T A	297
Salem, A A 252	
Salimgareyev, H	
Samanta, D	
Sambandam, S N	
Sampson, D	
Samson, S	
Sanchez, J E 187	
Sanders, D G	
Sanders, R E	. 249
Sanders, T H 296	404
Sanders, W S 175, 227,	
Sandhage, K H 291,	337
Sandoz, D	415
Sandrock, G	. 170
Sankar, J	. 337
Sankaran, K K 192	
Santella, M 191,	
Santiago, V R 199	
Sardesai, A S	
Sarihan, V	
Sarikaya, M 292,	
Sastry, D H	
Sato, K	
Sato, M	388
Saunders, T	
Saunders, 1	. 1/2
Coutor I	220
Sauter, L	
Sauvage, X	306
Sauvage, X Savage, M F	306 352
Sauvage, X Savage, M F Savin, I	306 352 322
Sauvage, X Savage, M F Savin, I Saxena, S	306 352 322 288
Sauvage, X Savage, M F Savin, I Saxena, S	306 352 322 288 437
Sauvage, X Savage, M F Savin, I Saxena, S	306 352 322 288 . 437 . 391
Sauvage, X Savage, M F Savin, I Saxena, S Sayed, H S Saylor, D M Saytaeva, K	306 352 322 288 . 437 . 391 . 311
Sauvage, X Savage, M F Savin, I Saxena, S Sayed, H S Saylor, D M Saytaeva, K Scarber, P	306 352 322 288 437 . 391 . 311 . 320
Sauvage, X Savage, M F Savin, I Saxena, S Sayed, H S Saylor, D M Saytaeva, K Scarber, P Scattergood, R O	306 352 322 288 437 391 311 320 393
Sauvage, X Savage, M F Savin, I Saxena, S	306 352 322 288 437 . 391 . 311 . 320
Sauvage, X Savage, M F Savin, I Saxena, S	306 352 322 288 437 391 311 320 393
Sauvage, X Savage, M F Savin, I Saxena, S	306 352 228 288 437 391 311 320 393 381 204 403
Sauvage, X Savage, M F Savin, I Saxena, S	306 352 228 288 437 391 311 320 393 381 204 403
Sauvage, X Savage, M F Savin, I Saxena, S	306 352 322 288 437 391 311 320 393 381 204 403 315
Sauvage, X Savage, M F Savin, I Saxena, S	306 352 228 288 437 391 391 391 320 393 381 204 403 315 310
Sauvage, X Savage, M F Savin, I Saxena, S	306 352 288 437 391 311 320 393 381 204 403 315 310 309,
Sauvage, X Savage, M F Savin, I Saxena, S	306 352 288 437 391 311 320 393 381 204 403 315 310 309,
Sauvage, X Savage, M F Savin, I Saxena, S	306 352 288 437 391 311 320 393 381 204 403 315 310 309, 436
Sauvage, X Savage, M F Savin, I Saxena, S	306 352 288 437 391 311 320 393 381 204 403 315 310 309, 436 240 265
Sauvage, X Savage, M F Savin, I Saxena, S	306 352 288 437 391 311 320 393 381 204 403 315 310 309, 436 240 265 390
Sauvage, X Savage, M F Savin, I Saxena, S	306 352 228 437 391 311 320 393 381 204 403 315 310 309, 436 240 265 390 229
Sauvage, X Savage, M F Savin, I Saxena, S	306 352 288 437 391 311 320 393 381 204 403 315 310 309, 436 240 265 390 229 330
Sauvage, X Savage, M F Savin, I Saxena, S	306 352 288 437 391 311 320 393 381 204 403 315 310 309, 436 240 265 390 229 330 269,
Sauvage, X	306 352 288 437 391 311 320 393 381 204 403 393 381 204 403 309, 436 240 265 390 229 330 229, 432
Sauvage, X	306 352 322 288 437 391 311 320 393 381 204 403 393 381 204 403 309, 436 240 265 390 229 330 269, 432 366
Sauvage, X	306 352 322 288 437 391 311 320 393 381 204 403 393 381 204 403 309, 436 240 265 390 265 390 229 330 269, 432 366 217
Sauvage, X	306 352 322 288 437 391 311 320 393 381 204 403 381 204 403 309, 436 240 265 390 269, 432 330 269, 432 366 217 415

Schönfeld, B	250
Schroth, J G 211,	212,
Schuh, C A 234,	
Schultz, A	191
Schultz, A E	
Schulz, M	238
Schulze, R K	
Schumacher, P Schvezov, C E 195, 344,	344 440
Schwandt, C 195, 544,	
Schwartz, C L	368
Schwarz, R B	353
Schwarz, S M	
Sciammarella, F M	
Seal, S 301,	346,
	450
Searles, M	
Sears, J 341, 406,	440
Sedighy, M	331
Seekely, M J	309
Seel, S C	
Seeley, L	
Seetharaman, S 280,	
Seetharaman, S 248,	
Segal, A Sehitoglu, H	
Seidman, D N 250,	
Sekhar, J A 248, 301,	
Sekido, N	358
Semenova, I P	257
Semiatin, S L 206, 251, 252,	
5000000000000000000000000000000000000	
	433 300 . 366
	433 300 . 366 . 179
	433 300 . 366 . 179 . 320
	433 300 . 366 . 179 . 320 203
	433 300 . 366 . 179 . 320 203 402
	433 300 . 366 . 179 . 320 203 402 402
	433 300 . 366 . 179 . 320 203 402 402 . 350
	433 300 . 366 . 179 . 320 203 402 402 . 350 . 246
	433 300 . 366 . 179 . 320 203 402 402 . 350 . 246 . 277
	433 300 . 366 . 179 . 320 203 402 402 . 350 . 246 . 277 432
	433 300 . 366 . 179 . 320 203 402 402 . 350 . 246 . 277 432 255
	433 300 . 366 . 179 . 320 203 402 402 . 350 . 246 . 277 432 255 425
	433 300 366 179 320 203 402 402 350 246 277 432 255 425 180
	433 300 366 179 320 203 402 402 350 246 277 432 255 425 180 381 412
	433 300 366 179 320 203 402 402 350 246 277 432 255 425 180 381 412 275
	433 300 366 179 320 203 402 402 350 246 277 432 255 425 180 381 412 275 312
	433 300 366 179 320 203 402 402 350 246 277 432 255 425 425 180 381 412 275 312 .419
	433 300 366 179 320 203 402 402 350 246 277 432 255 425 180 381 412 275 312 403
	433 300 366 179 320 203 402 402 350 240 2402 350 246 277 432 255 425 180 381 412 275 312 403 405
	433 300 366 179 320 203 402 402 350 246 277 432 255 425 425 180 381 412 275 312 403 405 428
	433 300 . 366 . 179 . 320 203 402 402 . 350 . 246 . 277 432 255 425 . 180 . 381 . 412 . 275 . 312 . 419 . 403 . 405 . 288
	433 300 366 179 320 203 402 402 350 246 277 432 255 425 180 381 412 275 312 403 403 405 428 313
	433 300 366 179 320 203 402 402 350 240 2402 255 425 425 425 381 412 275 312 403 405 405 428 313 232
	433 300 . 366 . 179 . 320 203 402 402 . 350 . 246 . 277 432 255 425 . 180 . 381 . 412 . 275 . 312 . 419 . 403 . 405 . 428 288 313 232 343
	433 300 366 179 320 203 402 402 350 246 277 432 255 425 180 381 412 275 312 403 405 405 428 288 313 232 343 401
	433 300 . 366 . 179 . 320 203 402 402 . 350 . 246 . 277 432 255 425 . 180 . 381 . 412 . 275 . 312 . 419 . 403 . 405 . 428 288 313 232 343 401 . 195
	433 300 . 366 . 179 . 320 203 402 402 . 350 . 246 . 277 432 255 425 . 180 . 381 . 412 . 275 . 312 . 419 . 403 . 405 . 428 288 313 232 343 401 . 195 . 374
	433 300 366 179 320 203 402 402 350 246 277 432 255 425 180 381 412 275 381 412 275 381 412 275 381 412 275 312 403 403 405 428 288 313 232 343 401 195 374 210 454
	433 300 366 179 320 203 402 402 350 246 277 432 255 425 180 381 412 275 381 412 275 381 412 275 381 412 275 381 412 275 381 403 403 405 428 288 313 232 343 401 195 374 210 374 210 435
	433 300 366 179 320 203 402 402 350 246 277 432 255 425 180 381 412 275 381 412 275 381 412 275 381 412 275 381 412 275 381 403 403 405 428 288 313 232 343 401 195 374 210 374 210 435

Shaw, B A	409
Shaw, L L 202, 208,	346
Shcherbakov, A V	256
She, H	213
Sheen, S R	355
Shen, C	183
Shen, F	290
Shen, H	201
Shen, J Shen, Y	176 408
Shen, Y 221, 286, 356,	451
Shepelyavyj, P E	180
Sheretz, R J	448
Shevade, S S	274
Shi, D 238,	448
Shi, X	179
Shi, X Q	339
Shi, Y	232
Shi, Z	357
Shian, S	291
Shibata, J 426, 427,	448
Shieh, Y C 199,	374
Shield, J E	388
Shields, J A 174,	215,
	400
Shiflet, G J 216,	217,
	442
Shigemastu, I	234
Shih, D 189,	416
Shih, M	179
Shih, P	338
Shiina, S	358
Shim, J	455
Shima, M 234, Shimizu, T	334 358
Shin, D	221
Shin, D H	455
Shin, D H 254, 260,	350
Shin, D H 206, 208, 251,	253,
	433
Shin, E	276
Shin, K S	287
Shinozuka, K 184,	301
Shiomori, K	449
Shizuo, N	269
Shobu, K	175
Shoji, T	294
Shreve, A 424,	447
Shrimpton, J	362
Shu, Y	380
Shuey, M S	364 347
Shuey, R T	395
Shulan, W	367
Shull, R D	195
Shyam, A	418
Sichen, D	409
Sidhu, R	416
Sieck, L V	364
Siegel, R W	381
Siegert, K 234,	398
Siegfried, R M	365
Siekhaus, W J	310
Sikder, A K	222
Sikka, V	436
Sikora, M	321
Siljan, O 312,	400

Sim, G	214
Simak, S I	405
Sinclair, C S	307
Sinclair, I	
Sinclair, K	360
Singh, A K	429
Singh, P 235,	236
Singh, R J	312
Singler, T J 191,	417
Sinha, S K	250
Sinnott, M	218
Sinnott, S B	428
Sisneros, T 296,	297
Sisson, R 404,	423
Sisson, R D	409
Skar, J I	191
Skepper, I G 284,	372
Skibin, A P	318
Sklenicka, V	434
Skoptsov, A M	
Skripnyuk, V	260
· · · · · · · · · · · · · · · · · · ·	405
Skrotzki, W	401
Skyllas-Kazacos, M	267
Sleboda, T	413
Sluiter, M H	390
Slutsker, J 322, 334, 384,	425
Smith, D	273
Smith, F M	
Smith, S	
Smola, B	383
Smugeresky, J E 209,	261,
	418
Show D.C.	
Snow, R C	353
Snugovsky, P	331
Snugovsky, P Snurnitsyna, S S	331 312
Snugovsky, P Snurnitsyna, S S Snyder, A J	331 312 424
Snugovsky, P Snurnitsyna, S S Snyder, A J Snyder, G J	<ul> <li>331</li> <li>312</li> <li>424</li> <li>435</li> </ul>
Snugovsky, P Snurnitsyna, S S Snyder, A J Snyder, G J	<ul> <li>331</li> <li>312</li> <li>424</li> <li>435</li> <li>435</li> </ul>
Snugovsky, P Snurnitsyna, S S Snyder, A J Snyder, G J	<ul> <li>331</li> <li>312</li> <li>424</li> <li>435</li> <li>435</li> <li>214</li> </ul>
Snugovsky, P Snurnitsyna, S S Snyder, A J Snyder, G J Snyder, J So, C Sobkow, Z S	<ul> <li>331</li> <li>312</li> <li>424</li> <li>435</li> <li>435</li> <li>214</li> <li>321</li> </ul>
Snugovsky, P Snurnitsyna, S S Snyder, A J Snyder, G J	<ul> <li>331</li> <li>312</li> <li>424</li> <li>435</li> <li>435</li> <li>214</li> <li>321</li> <li>261,</li> </ul>
Snugovsky, P         Snurnitsyna, S S         Snyder, A J         Snyder, G J         Snyder, J         So, C         Sobkow, Z S         Sobyejo, W	<ul> <li>331</li> <li>312</li> <li>424</li> <li>435</li> <li>435</li> <li>214</li> <li>321</li> <li>261,</li> <li>377</li> </ul>
Snugovsky, P         Snurnitsyna, S S         Snyder, A J         Snyder, G J         Snyder, J         So, C         Sobkow, Z S         Sobyejo, W	<ul> <li>331</li> <li>312</li> <li>424</li> <li>435</li> <li>435</li> <li>214</li> <li>321</li> <li>261,</li> <li>377</li> <li>417</li> </ul>
Snugovsky, P         Snurnitsyna, S S         Snyder, A J         Snyder, G J         So, C         Sobkow, Z S         Soboyejo, W	<ul> <li>331</li> <li>312</li> <li>424</li> <li>435</li> <li>435</li> <li>214</li> <li>321</li> <li>261,</li> <li>377</li> <li>417</li> <li>275</li> </ul>
Snugovsky, P         Snurnitsyna, S S         Snyder, A J         Snyder, G J	<ul> <li>331</li> <li>312</li> <li>424</li> <li>435</li> <li>435</li> <li>214</li> <li>321</li> <li>261,</li> <li>377</li> <li>417</li> <li>275</li> <li>371</li> </ul>
Snugovsky, P         Snurnitsyna, S S         Snyder, A J         Snyder, G J	<ul> <li>331</li> <li>312</li> <li>424</li> <li>435</li> <li>435</li> <li>214</li> <li>321</li> <li>261,</li> <li>377</li> <li>417</li> <li>275</li> <li>371</li> <li>445</li> </ul>
Snugovsky, P         Snurnitsyna, S S         Snyder, A J         Snyder, G J	<ul> <li>331</li> <li>312</li> <li>424</li> <li>435</li> <li>435</li> <li>214</li> <li>321</li> <li>261,</li> <li>377</li> <li>417</li> <li>275</li> <li>371</li> <li>445</li> <li>410</li> </ul>
Snugovsky, P         Snurnitsyna, S S         Snyder, A J         Snyder, G J	331 312 424 435 435 214 321 261, 377 417 275 371 445 410 .382
Snugovsky, P         Snurnitsyna, S S         Snyder, A J         Snyder, G J	331 312 424 435 435 214 321 261, 377 417 275 371 445 410 382 441
Snugovsky, P         Snurnitsyna, S S         Snyder, A J         Snyder, G J	331 312 424 435 435 214 321 261, 377 417 275 371 445 410 .382 441 224
Snugovsky, P         Snurnitsyna, S S         Snyder, A J         Snyder, G J	331 312 424 435 435 214 321 261, 377 417 275 371 445 410 .382 441 224 400
Snugovsky, P         Snurnitsyna, S S         Snyder, A J         Snyder, G J	331 312 424 435 435 214 321 261, 377 417 275 371 445 410 .382 441 224 400 331
Snugovsky, P         Snurnitsyna, S S         Snyder, A J         Snyder, G J	331 312 424 435 435 214 321 261, 377 417 275 371 445 410 .382 441 224 400 331 283
Snugovsky, P	331 312 424 435 435 214 321 261, 377 417 275 371 445 410 .382 441 224 400 331 283 416
Snugovsky, P         Snurnitsyna, S S         Snyder, A J         Snyder, G J	331 312 424 435 435 214 321 261, 377 417 275 371 445 410 .382 441 224 400 331 283 416 318
Snugovsky, P	331 312 424 435 435 214 321 261, 377 417 275 371 445 410 .382 441 224 400 331 283 416 318 382
Snugovsky, P	331 312 424 435 435 214 321 261, 377 417 275 371 445 410 .382 441 224 400 331 283 416 318 382 350
Snugovsky, P	331 312 424 435 435 214 321 261, 377 417 275 371 445 410 .382 441 224 400 331 283 416 318 382
Snugovsky, P	331 312 424 435 435 214 321 261, 377 417 275 371 445 410 377 445 410 331 283 416 318 382 350 380 215
Snugovsky, P	331 312 424 435 435 214 321 261, 377 417 275 371 445 410 377 445 410 331 283 416 318 382 350 380 215
Snugovsky, P	331 312 424 435 425 4261, 321 261, 377 417 275 371 445 410 382 441 224 400 331 283 416 318 382 350 380 215 321 438
Snugovsky, P	331 312 424 435 435 214 321 261, 377 417 275 371 445 410 382 441 224 400 331 283 416 318 382 350 380 215 321 438 272
Snugovsky, P	331 312 424 435 435 214 321 261, 377 417 275 371 445 410 382 441 224 400 331 283 416 318 382 350 380 215 321 438 272 208
Snugovsky, P	331 312 424 435 425 426 435 214 321 261, 377 417 275 371 445 410 382 441 224 400 331 283 416 318 382 350 380 215 321 438 272 208 438 311
Snugovsky, P	331 312 424 435 425 426 435 214 321 261, 377 417 275 371 445 410 382 441 224 400 331 283 416 318 382 350 380 215 321 438 272 208 438 311

Spadafora, F 220, 278,	406	Stree
Spaldin, N 291,		Stroe
Spanos, G 234,	327	Strog
Sparks, C J	185	Stron
Speakman, S		Stucz
Spelt, J K		Stulí
Spencer, D B		Sturn
Spencer, R		Sturn
Speyer, R F		Styre
Spolenak, R 188,		Su, Y
Spreij, M		Subb
Spuskanyuk, A V Srajer, G		Subra
Sridhar, R 244,		 Suda
Srinivasan, R 184, 227,		Suda
Srinivasan, S G 279,		Sudb
		Sudh
Srinivasan, S S		Sudh
Srinivasan, V		Suem
Srivatsan, T S		Suery
Srolovitz, D J 182, 222, 223,	353	Suga
Stach, E A 275,	309	Sugi
Staley, J T		Sui, 2
Stanbery, B J		Suk,
Stanciu, L A		Sulei
Stanton, K T 171,		Sulli
Starke, E A 199, 200,		Sun,
Staudenmann, J		Sun,
Staudhammer, K P 242, 295, Stauffer, E		Sun,
Stauffel, E Stefanescu, D M		Sun, Sun,
Steinbach, I		Sun,
Steiner, C		Sun,
Steiner, J		Sun,
Steingart, D A		Sun,
Stellacci, F		Sund
Stencel, J M	414	Sung
Stephens, C	202	Sung
Stephens, J J		Suni,
Stevens McFadden, F		Sunk
Stevenson, J W 235,		Supa
Stevenson, M E 367, 410,		Surel
Steverson, W B		Sures
Stewart, D L Stierman, R		Surya Suss,
StJohn, D H 294,		Süss,
385, 403,		Sutor
Stober, F 330,		Suyit
Stock, R		Suyit
Stockhausen, W		Suzu
Stoica, A D 184,		Suzu
Stoica, G M 256,	392	Suzu
Stoker, G	230	Suzu
Stölken, J S		Suzu
Stoloff, N S		Suzu
Stolyarov, V 208,		Suzu
Stone, G A		Svob
Stone, I C		Swar
Stone, M O Stone, Z		Swar Swee
Stont, P D 212,		Swee
Storm, D R 212,		
Stoult, M R		Swift
Stout, J		Swift
Stoyanov, S	232	Swis
Straatsma, E N	220	Swyg
Stratton, M		Synk
470		

Street, S C	
Stroeder, M	
Stroganov, A G	245
Stronach, C E	
Stuczynski, T	403
Stulíková, I	383
Sturm, E	398
Sturm, P	265
Styrov, V V	
Su, Y J	241
Subbanna, G N	239
Subramanian, K N 187, 188,	190,
	373
Suda, S	262
Sudakar, C	
Sudbrack, C K	251
Sudhakar, K	
Sudhakar, N 196,	239
Suematsu, H	194
Suery, M	417
Suganuma, K 190,	338
Sugiyama, A	300
Sui, Z	200
Suk, M	299
Suleiman, M	353
Sullivan, T M	435
Sun, D	263
Sun, F 278, 364,	440
Sun, H	437
Sun, W 320,	428
Sun, Y	202
Sun, Y	176
Sun, Y	423
Sun, Z	232
Sun, Z	420
Sundaresan, R	224
Sung, P K	1.00
6	428
Sung, Y	186
Sung, Y Suni, J P	186 347
Sung, Y Suni, J P Sunkara, M K 334,	186 347 419
Sung, Y Suni, J P Sunkara, M K 334, Supatarawanich, V	186 347 419 215
Sung, Y Suni, J P Sunkara, M K 334, Supatarawanich, V Surek, T	186 347 419 215 169
Sung, Y	186 347 419 215 169 420
Sung, Y Suni, J P Sunkara, M K	186 347 419 215 169 420 450
Sung, Y Suni, J P Sunkara, M K 334, Supatarawanich, V Surek, T Suresh, S	186 347 419 215 169 420 450 312
Sung, Y Suni, J P Sunkara, M K	186 347 419 215 169 420 450 312 270
Sung, Y Suni, J P Sunkara, M K	186 347 419 215 169 420 450 312 270 242
Sung, Y Suni, J P Sunkara, M K	186 347 419 215 169 420 450 312 270 242 220
Sung, Y Suni, J P Sunkara, M K	186 347 419 215 169 420 450 312 270 242 220 203
Sung, Y Suni, J P Sunkara, M K	<ul> <li>186</li> <li>347</li> <li>419</li> <li>215</li> <li>169</li> <li>420</li> <li>450</li> <li>312</li> <li>270</li> <li>242</li> <li>220</li> <li>203</li> <li>324</li> </ul>
Sung, YSuni, J PSunkara, M KSuptarawanich, VSurek, TSuresh, SSuresh, SSuss, A GSüss, RSutou, YSuyitnoSuyitno, XSuzuki, ASuzuki, A	186 347 419 215 169 420 450 312 270 242 220 203 324 346
Sung, YSuni, J PSunkara, M KSuptarawanich, VSurek, TSuresh, SSuresh, SSuss, A GSüss, RSutou, YSuyitnoSuyitno, XSuzuki, ASuzuki, ASuzuki, ASuzuki, M	186 347 419 215 169 420 450 312 270 242 220 203 324 346 384
Sung, YSuni, J PSunkara, M KSuptarawanich, VSurek, TSuresh, SSuresh, SSuss, A GSüss, RSutou, YSuyitnoSuyitno, XSuzuki, ASuzuki, ASuzuki, ASuzuki, M	186 347 419 215 169 420 450 312 270 242 220 203 324 346 384
Sung, YSuni, J PSunkara, M KSuptarawanich, VSurek, TSuresh, SSuresh, SSuss, A GSüss, RSutou, YSuyitnoSuyitno, XSuzuki, ASuzuki, ASuzuki, ASuzuki, SSuzuki, SSuzuki, T	186 347 419 215 169 420 450 312 270 242 220 203 324 346 384 194 387
Sung, YSuni, J PSunkara, M KSupatarawanich, VSurek, TSuresh, SSuresh, SSuryawanshi, ASuss, A GSüss, RSutou, YSuyitnoSuyitno, XSuzuki, ASuzuki, ASuzuki, ASuzuki, SSuzuki, TSuzuki, T	186 347 419 215 169 420 450 312 270 242 220 203 324 346 384 194 387 194
Sung, YSuni, J PSunkara, M KSuptarawanich, VSurek, TSuresh, SSuresh, SSuss, A GSüss, RSutou, YSuyitnoSuyitno, XSuzuki, ASuzuki, ASuzuki, ASuzuki, TSuzuki, TSuzuki, Y	186 347 419 215 169 420 450 312 270 242 220 203 324 346 384 194 387 194 291
Sung, YSuni, J PSunkara, M KSuptarawanich, VSurek, TSuresh, SSuresh, SSuss, A GSüss, RSutou, YSuyitnoSuyitno, XSuzuki, ASuzuki, ASuzuki, ASuzuki, TSuzuki, TSuzuki, TSuzuki, Y	186 347 419 215 169 420 450 312 270 242 220 203 324 346 384 194 387 194 291 405
Sung, YSuni, J PSunkara, M KSuptarawanich, VSurek, TSuresh, SSuresh, SSuss, A GSüss, RSutou, YSuyitnoSuyitno, XSuzuki, ASuzuki, ASuzuki, ASuzuki, TSuzuki, TSuzuki, TSuzuki, Y	186 347 419 215 169 420 450 312 270 242 203 324 346 384 194 387 194 291 405 259
Sung, YSuni, J PSunkara, M KSupkarawanich, VSurek, TSuresh, SSuresh, SSuss, A GSüss, RSutou, YSuyitnoSuzuki, ASuzuki, ASuzuki, ASuzuki, SSuzuki, TSuzuki, TSuzuki, YSvoboda, JSwaminathan, S207,Swan-Wood, T	186 347 419 215 169 420 450 312 270 242 220 203 324 346 384 194 387 194 291 405 259 405
Sung, YSuni, J PSunkara, M KSupkarawanich, VSurek, TSuresh, SSuresh, SSuss, A GSuss, RSutou, YSuyitnoSuzuki, ASuzuki, ASuzuki, ASuzuki, TSuzuki, TSuzuki, YSvoboda, JSwaminathan, S207,Sweet, E	186 347 419 215 169 420 450 312 270 242 220 203 324 346 384 194 387 194 291 405 259 405 403
Sung, Y Suni, J P Sunkara, M K	186 347 419 215 169 420 450 312 270 242 220 203 324 346 384 194 387 194 291 405 259 405 403 241,
Sung, Y         Suni, J P         Sunkara, M K       334,         Supatrawanich, V         Surek, T         Suresh, S       334,         Suryawanshi, A         Suss, A G         Süss, R         Sutou, Y         Suyitno         Suyitno, X         Suzuki, A         Suzuki, A         Suzuki, T         Suzuki, T         Suzuki, T         Suzuki, Y         Svoboda, J         Swaminathan, S       207,         Swenson, D J       198, 240,	186 347 419 215 169 420 450 312 270 242 220 203 324 346 384 194 387 194 291 405 259 403 241, 417
Sung, Y         Suni, J P         Sunkara, M K       334,         Supatrawanich, V         Surek, T         Suresh, S       334,         Suryawanshi, A         Suss, A G         Süss, R         Sutou, Y         Suyitno         Suyitno, X         Suzuki, A         Suzuki, A         Suzuki, T         Suzuki, T         Suzuki, T         Suzuki, Y         Svoboda, J         Swaminathan, S       207,         Swenson, D J       198, 240,	186 347 419 215 169 420 450 312 270 242 220 203 324 346 384 194 387 194 291 405 259 403 241, 417 201
Sung, Y         Suni, J P         Sunkara, M K       334,         Supatrawanich, V         Surek, T         Suresh, S       334,         Suryawanshi, A         Suss, A G         Süss, R         Sutou, Y         Suyitno         Suyitno, X         Suzuki, A         Suzuki, A         Suzuki, T         Suzuki, T         Suzuki, T         Suzuki, Y         Svoboda, J         Swaminathan, S       207,         Swenson, D J       198, 240,	186 347 419 215 169 420 450 312 270 242 203 324 346 384 194 387 194 291 405 259 405 403 241, 417 201 284
Sung, Y         Suni, J P         Sunkara, M K       334,         Supatrawanich, V         Surek, T         Suresh, S       334,         Suryawanshi, A         Suss, A G         Süss, R         Sutou, Y         Suyitno         Suyitno, X         Suzuki, A         Suzuki, A         Suzuki, T         Suzuki, T         Suzuki, T         Suzuki, Y         Svoboda, J         Swaminathan, S       207,         Swenson, D J       198, 240,	186 347 419 215 169 420 450 312 270 242 220 203 324 346 384 194 387 194 291 405 259 403 241, 417 201 284 252
Sung, Y         Suni, J P         Sunkara, M K       334,         Supatrawanich, V         Surek, T         Suresh, S       334,         Suryawanshi, A         Suss, A G         Süss, R         Sutou, Y         Suyitno         Suyitno, X         Suzuki, A         Suzuki, A         Suzuki, T         Suzuki, T         Suzuki, T         Suzuki, Y         Svoboda, J         Swaminathan, S       207,         Swenson, D J       198, 240,	186 347 419 215 169 420 450 312 270 242 203 324 346 384 194 387 194 291 405 259 405 403 241, 417 201 284

Szpunar, J A	221,	249,	254,
	281,	356,	452
Szymczak, R			321

# Т

<b>T</b> 1 <b>T</b>		1 7 5
Tabaru, T		175
Tabereaux, A T 170,		176,
	217,	218,
	272,	311,
	356,	360.
		439
Tada, S		420
Taua, 5	•••••	
Taghavi, S M		369
Takahashi, K		323
Takaku, Y		191
Takami, Y		426
Takamiya, H		440
Takano, H		415
Takashi, S		449
Takasugi, T		
	1/4,	401
Takeshita, H T 309,		436
Takeuchi, I		289
Talas, S		290
Talbot, D E       343,         Taleff, E M       184,       211,	427,	428
Taleff, E M 184, 211,	225.	226,
	326,	355,
		441
Talin, A		308
Tallant, D R		430
Tamura, M		301
Tamura, N 372,	394,	441
Tan, H		345
Tan, L		428
	335,	404
Tanabe, M		427
Tanaka, M		449
Tandon, S		196
Tandon, S C		317
Tang, J		380
Tang, W		296
Tarasov, A V		186,
		449
Tatalovich, J		352
Tatyanin, E V		253
Taub, M		240
Tavares, R P		320
Tavera, F J		378
Tawfic, S N		200
Тауа, М		201
Taylor, C		212
Taylor, J A		385
Taylor, M P		212
Taylor, P R		426
Tedstrom, R		222
Teigs, T N		372
Telang, AU 188,		229
Telesman, J		340
Téllez-Martínez, J S	408,	409
Tenhundfeld, G		185
Teramoto, S		401
Teranishi, K		406
Terpstra, R L		295
Teter, D F 233,		396
Tewari, R		400
Tewari, S N		248
Thibault, M		171

Thiel, G H	286
Thirumalai, N	183
Thom, A J 175,	215
Thoma, D J 253,	283
Thomas, B G 203,	218,
	446
Thomas, J	272
Thompson, L J	238
Thompson, S A	411
Thompson, S R	407
Thomson, P F 269,	333
Thonstad, J	437
Thuramalla, N V	398
Thurston, A K	360
Tian, B	254
Tian, H 184, 202, 226,	297
Tian, Z	357
Tikare, V	242
Tilly, D J	278
Timofeeva, V	369
Tin, S	174
Tiryakioglu, M	347
Tiwari, A 195,	237,
	336
Tiwari, R	248
Tizon, E	170
Toda, H	411
Todaka, Y	253
Tokar, V	348
Tokarz, M L	176
Tokimatsu, R C	368
Tomala, J	177
Tomasino, T	437
Tome, C N 207, 255,	339
Tommey, C	172
Tomokiyo, Y	390
Tong, L	243
Tonheim, J	172
Tonti, R T	217
Торро, В	368
Torbet, C J	418
Torek, P	172
Torosyan, A R	236
Torres, V 230, 231, 329,	443
Torsiello, S	171
Tortorelli, P F 174, 215,	269,
	400
Tran, S	416
Tratteberg, O	172
Trebuh, O A	267
Trichy, G R	256
Triessnig, A	404
Trinkle, D R 183,	431
Trivedi, P B	279
Trivedi, R 202, 247,	299,
	386
Trojanova, Z	425
Trubitsyna, I B	253
Trumble, K P 195, 207,	259
Tryon, B	270
Tsai, C M 332,	338
Tsai, D	332
Tsai, J Y 199,	374
Tsai, Y	285
Tsakiropoulos, P 175,	216,
13akiropoulos, 1	421
Tsau, C H	176
1 Jau, U 11	1/0

Tso, C	227
Tsuchida, N	328
Tsuchiya, K	253
Tsuchiyama, A	300
Tsui, F	238
Tsuji, N 207, 259, 351,	388
Tsunekane, M	315
Tsuzuki, R	418
Tszeng, C	314
Tu, K 187, 231,	294
Tuominen, M T	336
Turbini, L J 189,	231,
	416
Turchi, P E 192, 304,	348
Turner, J	329
Turpeinen, P	286
Tyagi, S A	268
Tyumentsev, A N 254, 256,	257

## U

	411
Ubhi, H S	411
Uchic, M D 309,	352
Ucok, I 223, 323,	365
Udaykumar, H S	249
Udovic, T J	210
Ueda, M	324
Ueji, R	259
Uekawa, N	296
Ueshima, M	190
Uesugi, K	300
Uhrig, J R	318
Ulfig, R M	198
Umakoshi, Y	390
Umantsev, A	196
Umeda, T	. 299
Umemoto, M 253,	305
Ungár, T	350
Unland, J	240
Unlu, N	363
Upadhaya, C	336
Upadhyay, V	274
Urbani, M D	443
Ustundag, E 176, 271, 272,	283,
	372
Utigard, T A	313
Utsunomiya, H	206
Utyashev, F Z	255

# $\mathbf{V}$

Vabishchevich, P	437
Vahed, A	329
Vaidyanathan, R 201,	246,
	342
Vainik, R	403
Valek, B C	394
Valiev, R Z 206, 251, 252,	253,
	258,
	307,
	432
Valls, R A	230
van de Walle, A 304, 358,	430
Van Den Avyle, J J	342
van den Broek, B	312
Van der Giesen, E	. 377
van der Merwe, J H 228,	327

van der Meulen, D	329
Van der Ven, A	305
Van Haaften, W	385
Van Humbeek, J	392
van Klaveren, E P	219
Van Schaik, A	200
Van Vliet, K J	334
Van Weert, G	333
Van Wert, J	370
Vandermeer, R A	204
Vanderson, E	261
VanEvery, K J	219
	170
Vanvoren, C	172
Vardill, W	188
Vardill, W	260
Varyukini, V 200,	
Vashishth, D 418,	419
Vasiliev, A L	346
Vasquez, O 199,	321
Vasudevan, A K 347,	348
Vasudevan, V K 175, 238,	301,
	400
Vaudreuil, S	361
Vega, S	215
Velgosova, O 296,	311
Vella, J B	229
Venkatesh, R	289
Venkatesh, V	407
Venkateswaran, S	422
Venskutonis, A 315,	358
Verlinden, B	392
Verma, H C	336
Verma, R	265
Verma, V	233
Vetrano IS	
Vetrano, J S	355
	335 238
Vetrone, J M	238
Vetrone, J M Vetter, R	238 195
Vetrone, J M	238
Vetrone, J M Vetter, R Vianco, P T 331,	238 195
Vetrone, J M Vetter, R Vianco, P T 331, Vidal, E E	238 195 338 448
Vetrone, J M Vetter, R Vianco, P T	238 195 338 448 272
Vetrone, J M Vetter, R Vianco, P T	238 195 338 448 272 384
Vetrone, J M Vetter, R Vianco, P T	238 195 338 448 272 384
Vetrone, J M Vetter, R	238 195 338 448 272 384 361
Vetrone, J M Vetter, R	238 195 338 448 272 384 361 208
Vetrone, J M Vetter, R	238 195 338 448 272 384 361
Vetrone, J M Vetter, R	238 195 338 448 272 384 361 208
Vetrone, J M Vetter, R Vianco, P T	238 195 338 448 272 384 361 208 422 392
Vetrone, J M Vetter, R Vianco, P T	238 195 338 448 272 384 361 208 422 392 444
Vetrone, J M Vetter, R	238 195 338 448 272 384 361 208 422 392 444 410
Vetrone, J M Vetter, R	238 195 338 448 272 384 361 208 422 392 444
Vetrone, J M Vetter, R Vianco, P T	238 195 338 448 272 384 361 208 422 392 444 410 299,
Vetrone, J M Vetter, R Vianco, P T	238 195 338 448 272 384 361 208 422 392 444 410 299, 449
Vetrone, J M Vetter, R Vianco, P T	238 195 338 448 272 384 361 208 422 392 444 410 299, 449 345
Vetrone, J M Vetter, R Vianco, P T	238 195 338 448 272 384 361 208 422 392 444 410 299, 449
Vetrone, J M Vetter, R Vianco, P T	238 195 338 448 272 384 361 208 422 392 444 410 299, 449 345 348
Vetrone, J M Vetter, R Vianco, P T	238 195 338 448 272 384 361 208 422 392 444 410 299, 449 345 348 445
Vetrone, J M Vetter, R Vianco, P T	238 195 338 448 272 384 361 208 422 392 444 410 299, 449 345 348 445 213
Vetrone, J M Vetter, R Vianco, P T	238 195 338 448 272 384 361 208 422 392 444 410 299, 449 345 348 445
Vetrone, J M Vetter, R Vianco, P T	238 195 338 448 272 384 361 208 422 392 444 410 299, 449 345 348 445 213 331
Vetrone, J M Vetter, R Vianco, P T	238 195 338 448 272 384 361 208 422 392 444 410 299, 449 345 348 445 213 331 383
Vetrone, J M Vetter, R Vianco, P T	238 195 338 448 272 384 361 208 422 392 444 410 299, 449 345 348 445 213 331 383 434
Vetrone, J M Vetter, R Vianco, P T	238 195 338 448 272 384 361 208 422 392 444 410 299, 449 345 348 445 213 331 383
Vetrone, J M Vetter, R Vianco, P T	238 195 338 448 272 384 361 208 422 392 444 410 299, 449 345 348 445 213 331 383 434 336
Vetrone, J M Vetter, R Vianco, P T	238 195 338 448 272 384 361 208 422 392 444 410 299, 449 345 348 445 213 331 383 434 336 217
Vetrone, J M Vetter, R Vianco, P T	238 195 338 448 272 384 361 208 422 392 444 410 299, 449 345 348 445 213 331 383 434 336 217 437
Vetrone, J M Vetter, R Vianco, P T	238 195 338 448 272 384 361 208 422 392 444 410 299, 449 345 348 445 213 331 383 434 336 217
Vetrone, J M Vetter, R Vianco, P T	238 195 338 448 272 384 361 208 422 392 444 410 299, 449 345 348 445 213 331 383 434 336 217 437
Vetrone, J M Vetter, R Vianco, P T	238 195 338 448 272 384 361 208 422 392 444 410 299, 449 345 348 445 213 331 383 434 336 217 437 176 188
Vetrone, J M	238 195 338 448 272 384 361 208 422 392 444 410 299, 449 345 348 445 213 331 383 434 336 217 437 176 188 270
Vetrone, J M	238 195 338 448 272 384 361 208 422 392 444 410 299, 449 345 348 445 213 331 383 434 336 217 437 176 188 270 248
Vetrone, J M	238 195 338 448 272 384 361 208 422 392 444 410 299, 449 345 348 445 213 331 383 434 336 217 437 176 188 270 248
Vetrone, J M	238 195 338 448 272 384 361 208 422 392 444 410 299, 449 345 348 445 213 331 383 434 336 217 437 176 188 270 248 383
Vetrone, J M	238 195 338 448 272 384 361 208 422 392 444 410 299, 449 345 348 445 213 331 383 434 336 217 437 176 188 270 248 383 322
Vetrone, J M	238 195 338 448 272 384 361 208 422 392 444 410 299, 449 345 348 445 213 331 383 434 336 217 437 176 188 270 248 383 322 270
Vetrone, J M	238 195 338 448 272 384 361 208 422 392 444 410 299, 449 345 348 445 213 331 383 434 336 217 437 176 188 270 248 383 322 270
Vetrone, J M	238 195 338 448 272 384 361 208 422 392 444 410 299, 449 345 348 445 213 331 383 434 336 217 437 176 188 270 248 383 322 270 350

Vuik, C	248
Vulcan, M	398

## W

Wadley, H N 320	5, 352
Waghmare, U	304
Wagner, G J	
Wagnière, J 203	
Wagoner, R H 214	4, 314
WaKimoto, Y	. 200
Waku, Y	
Waldo, R A	
Waldron, D J	268
Walker, C A	
Walker, M S 235	
Wall, J J	372
Wallace, J P	365
Walters, R T	
Walukas, D M	
Wan, X	276
Wang, C 278	3, 406
Wang, D	
Wang, G 178, 190	), 387
Wang, G 202, 220	5, 271
Wang, G Y 272	1, 411
Wang, H 379	
Wang, H	302
Wang, H	424
Wang, J	
Wang, J	181
Wang, J	242
Wang, J 207, 251, 257, 258	3, 260
Wang, J	356
Wang, J C	
Wang, L	219
Wang, M	
-	
Wang, N	
Wang, P 310	5, 360
Wang, P T	412
Wang, Q	
Wang, Q	
Wang, Q 410	), 411
Wang, R	440
Wang, R J	
Wang, S	
Wang, S	243
Wang, S	. 233
Wang, S F	
Wang, S H	
Wenn CI	275
Wang, S J	. 3/3
Wang, T	322
Wang, T	322 3, 364
Wang, T	322 3, 364 426
Wang, T	322 3, 364 426
Wang, T         363           Wang, T         363           Wang, W         217	322 3, 364 426 7, 402
Wang, T         363           Wang, T         363           Wang, W         217           Wang, X         217	322 3, 364 426 7, 402 410
Wang, T       363         Wang, T       363         Wang, W       217         Wang, X       184, 297	322 3, 364 426 7, 402 410 7, 402
Wang, T       363         Wang, W       363         Wang, W       217         Wang, X       184, 297         Wang, Y       363	322 3, 364 426 7, 402 410 7, 402 197
Wang, T       363         Wang, W       363         Wang, W       217         Wang, X       184, 297         Wang, Y       384, 297	322 3, 364 426 7, 402 410 7, 402 197 291
Wang, T	322 3, 364 426 7, 402 410 7, 402 197 291
Wang, T       363         Wang, W       363         Wang, W       217         Wang, W H       217         Wang, X       184, 297         Wang, Y       184, 297         Wang, Y       184, 297         Wang, Y       184	322 3, 364 426 7, 402 410 7, 402 197 291 4, 297
Wang, T       363         Wang, W       363         Wang, W H       217         Wang, X       363         Wang, X       184, 297         Wang, Y       184, 297         Wang, Y       184, 297         Wang, Y       184, 297         Wang, Y       184         Wang, Y       184         Wang, Y       184	322 3, 364 426 7, 402 410 7, 402 197 291 4, 297 431
Wang, T       363         Wang, T       363         Wang, W       217         Wang, W H       217         Wang, X       184, 297         Wang, Y       184, 297         Wang, Y       184, 297         Wang, Y       184, 297         Wang, Y       184	322 3, 364 426 7, 402 410 7, 402 197 291 4, 297 431 421
Wang, T       363         Wang, T       363         Wang, W       217         Wang, W H       217         Wang, X       184, 297         Wang, Y       184         Wang, Y       305, 322, 363	322 3, 364 426 7, 402 410 7, 402 197 291 4, 297 431 421 3, 364
Wang, T       363         Wang, T       363         Wang, W       217         Wang, W H       217         Wang, X       184, 297         Wang, Y       184         Wang, Y       305, 322, 363	322 3, 364 426 7, 402 410 7, 402 197 291 4, 297 431 421 3, 364
Wang, T       363         Wang, T       363         Wang, W       217         Wang, W H       217         Wang, X       184, 297         Wang, Y       184         Wang, Y       305, 322, 363	322 3, 364 426 7, 402 410 7, 402 197 291 4, 297 431 421 3, 364
Wang, T       363         Wang, T       363         Wang, W       217         Wang, W H       217         Wang, X       184, 297         Wang, Y       184         Wang, Y       305, 322, 363         Wang, Y       174, 182, 183	322 3, 364 426 7, 402 410 7, 402 197 291 4, 297 431 421 3, 364 391 3, 224,
Wang, T       363         Wang, W       363         Wang, W       217         Wang, W H       217         Wang, X       184, 297         Wang, Y       184         Wang, Y       184         Wang, Y       184         Wang, Y       184         Wang, Y       305, 322, 363         Wang, Y       305, 322, 363         Wang, Y       174, 182, 183	322 3, 364 426 7, 402 410 7, 402 197 291 4, 297 431 421 3, 364 391 3, 224, 5, 407
Wang, T       363         Wang, T       363         Wang, W       217         Wang, W H       217         Wang, X       184, 297         Wang, Y       184         Wang, Y       305, 322, 363         Wang, Y       174, 182, 183	322 3, 364 426 7, 402 410 7, 402 197 291 4, 297 431 421 3, 364 391 3, 224, 5, 407
Wang, T       363         Wang, W       363         Wang, W       217         Wang, W H       217         Wang, X       184, 297         Wang, Y       184         Wang, Y       184         Wang, Y       184         Wang, Y       184         Wang, Y       305, 322, 363         Wang, Y       305, 322, 363         Wang, Y       174, 182, 183	322 3, 364 426 7, 402 410 7, 402 197 291 4, 297 431 421 3, 364 391 3, 224, 5, 407

	100
Wang, Z	400
Wang, Z	286
Wang, Z	417
Wang, Z X	188
Wanjale, M	302
5	296
Wannasin, J	
Ward, W G	
Ward-Close, C M	407
Warren, J A 276, 322,	386
Waryoba, D R	205
Watanabe, M	432
Watanabe, T	390
Waterstrat, R M	304
Watkins, T R	400
Watson, T J	419
Watts, J	401
Waz, E	437
Weaver, M L 262,	367,
	441
Webb, D A	220
Webster, T J	197
Wedde, G	. 398
Weertman, J	201
Weertman, J R	349
Wegryzn, J	353
Wei, C	382
Wei, C C	332
Wei, J	
Wei, J H	290
Wei, L	421
Wei, M	243
Wei, W	260
Weil, K	235
Weil, K G	409
Weiland, H	277
Weinan, E	
Weirauch, Jr., D A	273
Weissmueller, J	346
Welch, B	267
Welch, B J 212,	399
Wellnitz, R	214
Wells, M A 268,	386
Welp, U 238,	250
Welsh, G S 271,	272
Wen, S 280,	281
Wen, W	314
Wenderoth, M	270
Weninger, J A	
Wenner, M	233
Wermer, J R 210, 262, 395,	436
Werner, J	
Werner, J H	447
Wetscher, F	
Wetteland, C J	302
Wezyk, W	403
Wheeler, D 220,	
White, B	
White, D	. 329
White, P	267
Whitfield, D S	267
Whiting, M	216
Whittington, B I	
Widjaja, A	
Widom, M	
··· idoiii, ivi	431
Wiench, J	431
	431 263
Wiench, J	431 263 379

Wilkening, S	177
Wilkins, J W 183,	431
Wilkinson, D S	269,
	355
Willander, M	180
Williams, D B	432
Williams, F S	170
Williams, G A	242
	185
Williams, R K	
Wilson, O C	446
Winkelman, G	371
Winterscheidt, D L 278,	406
Winther, G 252,	302
Wirth, B D	183
Wiseman, M	189
	244
Withers, A	
Withers, J C 224,	278
Withers, P J	297
Wittig, J E	327
Wochner, P	250
Wolanski, R 172,	173
Wolf, A	266
	305
Wolf, D	
Wolfe, R C	
Wolverton, C 181, 205, 250,	277,
	430
Wolverton, C C	406
Wong, C K	232
Wong, G C	239
Wong, L L	246
Wong, P W	439
Woo, W	297
Wood, J R	173
Woodard, S	215
Woodman, R H	254
	416
Woods, J J	
Woods, J J Woodward, C	322
Woodward, C	322 430
Woodward, C	430
Woodward, C	430 174
Woodward, C	430 174 416
Woodward, C	430 174 416 354
Woodward, C	430 174 416
Woodward, C	430 174 416 354
Woodward, C	430 174 416 354 338 413
Woodward, C	430 174 416 354 338 413 286
Woodward, C	430 174 416 354 338 413 286 313
Woodward, C       183,         Wright, I G       183,         Wright, J       Wright, P K         Wright, R D       Wright, R N         Wright, W       Wright, W         Wright, W       181, 225, 226,	430 174 416 354 338 413 286 313 281
Woodward, C         Woodward, C       183,         Wright, I G       183,         Wright, J       183,         Wright, P K       183,         Wright, R D       181,         Wright, W       183,         Wright, W       181,         Wu, D T       181,       225,         Wu, E       181,       225,	430 174 416 354 338 413 286 313 281 348
Woodward, C         Woodward, C         183,         Wright, I G         Wright, J         Wright, P K         Wright, R D         Wright, R N         Wright, W         Wuight, W         Wu, B         Wu, D T       181, 225, 226,         Wu, J	430 174 416 354 338 413 286 313 281 348 375
Woodward, C         Woodward, C       183,         Wright, I G       183,         Wright, J       183,         Wright, P K       183,         Wright, R D       181,         Wright, W       183,         Wright, W       181,         Wu, D T       181,       225,         Wu, E       181,       225,	430 174 416 354 338 413 286 313 281 348 375 322
Woodward, C         Woodward, C         183,         Wright, I G         Wright, J         Wright, P K         Wright, R D         Wright, R N         Wright, W         Wright, W         Wu, B         Wu, D T       181, 225, 226,         Wu, J	430 174 416 354 338 413 286 313 281 348 375
Woodward, C         Woodward, C         183,         Wright, I G         Wright, P K         Wright, R D         Wright, R N         Wright, W         Wright, W         Wu, B         Wu, D T         Wu, E         Wu, J         Wu, K	430 174 416 354 338 413 286 313 281 348 375 322
Woodward, C       183,         Wright, I G       183,         Wright, J J       Wright, P K         Wright, R D       Wright, R N         Wright, W       Wright, W         Wu, B       181, 225, 226,         Wu, E       Wu, J         Wu, J       Wu, J         Wu, K       Wu, K	430 174 416 354 338 413 286 313 281 348 375 322 240 421
Woodward, C         Woodward, C         183,         Wright, I G         Wright, P K         Wright, R D         Wright, R N         Wright, W         Wright, W         Wu, B         Wu, D T         Wu, E         Wu, K         Wu, K         Wu, K         Wu, K         Wu, M         Wu, M	430 174 416 354 338 413 286 313 281 348 375 322 240 421 423
Woodward, C         Woodward, C         183,         Wright, I G         Wright, J         Wright, P K         Wright, R D         Wright, R N         Wright, W         Wuight, W         Wu, B         Wu, D T         Wu, B         Wu, Z         Wu, K         Wu, K         Wu, K         Wu, K         Wu, M         178, 247,         Wu, W	<ul> <li>430</li> <li>174</li> <li>416</li> <li>354</li> <li>338</li> <li>413</li> <li>286</li> <li>313</li> <li>281</li> <li>348</li> <li>375</li> <li>322</li> <li>240</li> <li>421</li> <li>423</li> <li>326</li> </ul>
Woodward, C         Woodward, C         183,         Wright, I G         Wright, J         Wright, P K         Wright, R D         Wright, R N         Wright, W         Wu, B         Wu, D T         Wu, B         Wu, U         Wu, Z         Wu, K         Wu, K         Wu, K         Wu, K         Wu, M         178, 247,         Wu, X	<ul> <li>430</li> <li>174</li> <li>416</li> <li>354</li> <li>338</li> <li>413</li> <li>286</li> <li>313</li> <li>281</li> <li>348</li> <li>375</li> <li>322</li> <li>240</li> <li>421</li> <li>423</li> <li>326</li> <li>287</li> </ul>
Woodward, C         Woodward, C         183,         Wright, I G         Wright, J         Wright, P K         Wright, R D         Wright, R N         Wright, W         Wu, B         Wu, D T         Wu, B         Wu, K         Wu, K         Wu, K         Wu, K         Wu, K         Wu, K         Wu, M         178, 247,         Wu, X	<ul> <li>430</li> <li>174</li> <li>416</li> <li>354</li> <li>338</li> <li>413</li> <li>286</li> <li>313</li> <li>281</li> <li>348</li> <li>375</li> <li>322</li> <li>240</li> <li>421</li> <li>423</li> <li>326</li> <li>287</li> <li>233</li> </ul>
Woodward, C         Woodward, C         183,         Wright, I G         Wright, J         Wright, P K         Wright, R D         Wright, R N         Wright, W         Wu, B         Wu, D T         Wu, B         Wu, U T         Wu, K         Wu, J         Wu, K         Wu, K         Wu, K         Wu, M         178, 247,         Wu, X         Wu, X	430 174 416 354 338 413 286 313 281 348 375 322 240 421 423 326 287 233 238
Woodward, C         Woodward, C         183,         Wright, I G         Wright, J         Wright, P K         Wright, R D         Wright, R N         Wright, W         Wu, B         Wu, D T         Wu, B         Wu, K         Wu, K         Wu, K         Wu, K         Wu, K         Wu, K         Wu, M         178, 247,         Wu, X	430 174 416 354 338 413 286 313 281 348 375 322 240 421 423 326 287 233 238

# X

Xi, J H	421
Xia, G 235,	236
Xia, X 276,	332
Xia, Z	232
Xia, Z C 397,	398
Xiang, X	290
Xiang, Y	182

Хіао, Н	439
Xiao, J Q	
Xiao, X	
Xie, F	
Xie, S	
Xie, Y	265
Xihong, Y	269
Xing, Q	302
Xu, C 256, 258, 311, 392,	433
Xu, G	
Xu, H	387
Xu, H 299,	
Xu, J	
Xu, J	
Xu, K	
Xu, O	
Xu, R	
Xu, W	
Xu, Y	
Xu, Y	. 231
Xu, Y B	412
Xue, L	243
Xue, Q 326,	367
Xueyi, G	
•	
Y	

Ya Ping, Y 3	325
	153
	+35 345
	269
	415
	401
	200
	148
	358
,	323
,	315
	95
	298
6,	271
8	130
	382
Yang, D	
Yang, F	
Yang, H4	
Yang, H2	
Yang, J	
Yang, J 4	
Yang, M 1	94
Yang, N Y 3	308
	312
	321
Yang, W 3	328
Yang, W 2	233
	87
	249
Yang, Y 2	265
Yang, Y 2	216
	362
	332
	93
Yang, Z G 235, 2	236
	133
	121
	350
<u> </u>	341
* * *	

Yassar, R S	347
Yasskin, P B	259
Yasuda, H	300
Yatsui, K	194
Yazami, R	
	356
	295
Yee, C E	
Yeh, A	
,	440
,	440
·	358
	173
	283
Yildirim, T	210
Yin, L 191,	417
Yin, Z	171
Yinbiao, Y	234
	291
5.	367
	269
	215
	359
-	204
Yoon, C	
	338
,	251
	293
,	438
	241
/	412
Yoon, Y S	275
Yoshida, S	296
Yoshimi, K 215,	315
Yost, F G	368
	183
	391
	447
	285
V11 K 278	416
· · · · · · · · · · · · · · · · · · ·	406
Yu, L	406 332
Yu, L Yu, O	406 332 182
Yu, L Yu, O Yu, S	406 332 182 254
Yu, L Yu, O Yu, S Yuan, H	406 332 182 254 319
Yu, L Yu, O Yu, S Yuan, H Yuan, L	406 332 182 254 319 354
Yu, L Yu, O Yu, S Yuan, H Yuan, L Yuan, W 202, 226,	406 332 182 254 319 354 271
Yu, L Yu, O Yu, S Yuan, H Yuan, L Yuan, W	406 332 182 254 319 354
Yu, L Yu, O Yu, S Yuan, H Yuan, L Yuan, W 202, 226, Yuan, Z Yuanchi, D	406 332 182 254 319 354 271 401 368
Yu, L Yu, O Yu, S Yuan, H Yuan, L Yuan, W	406 332 182 254 319 354 271 401 368
Yu, L Yu, O Yu, S Yuan, H Yuan, L Yuan, W 202, 226, Yuan, Z Yuanchi, D	406 332 182 254 319 354 271 401 368 185
Yu, L Yu, O Yua, S Yuan, H Yuan, L Yuan, W 202, 226, Yuan, Z Yuanchi, D Yücel, O Yue, S	406 332 182 254 319 354 271 401 368 185
Yu, L Yu, O Yuan, H Yuan, L Yuan, W	406 332 182 254 319 354 271 401 368 185 233
Yu, L Yu, O Yu, S Yuan, H Yuan, L Yuan, W 202, 226, Yuan, Z Yuanchi, D Yücel, O Yue, S Yunyou, Z Yurchenko, L I	406 332 182 254 319 354 271 401 368 185 233 325
Yu, L Yu, O Yuan, H Yuan, L Yuan, W	406 332 182 254 319 354 271 401 368 185 233 325 260 194
Yu, L Yu, O Yuan, H Yuan, L Yuan, W	406 332 182 254 319 354 271 401 368 185 233 325 260 194 202
Yu, L Yu, O Yuan, H Yuan, L Yuan, W	406 332 182 254 319 354 271 401 368 185 233 325 260 194 202 267
Yu, L Yu, O Yuan, H Yuan, L Yuan, W	406 332 182 254 319 354 271 401 368 185 233 325 260 194 202 267 291

# Z

Zabaras, N	235,	237,	319,	428
Zacharia, T				223
Zaitsev, A				342
Zakharov, A E				245
Zakharov, ID				280
Zamiri, A				431

Zamkotowicz, Z	403
Zangari, G	237
Zantye, P	222
Zarembo, S	321
Zavalij, L 382,	416
Zawierucha, R	343
Zeh, J	266
Zehetbauer, M 252, 392, 391,	393
Zeipper, L	392
Zelenitsas, K	175
Zelin, M	355
Zender, G A	
Zeng, K	293
Zeng, X	383
Zerkle, R 213,	399
Zevgolis, E N 330,	373
Zhai, C	288
Zhai, T	410
Zhang, D 323,	413
Zhang, D L	406
Zhang, F	407
Zhang, G	
Zhang, G P	188
Zhang, H	223
Zhang, J	213
Zhang, J H 412,	421
Zhang, K 349,	413
Zhang, L	290
Zhang, M	295
Zhang, M	357
Zhang, M	228
Zhang, Q A	210
Zhang, R	259
Zhang S 200	445
$\Sigma$ mang, $S$ $270$ ,	
Zhang, S 290, Zhang, W	
Zhang, W	
Zhang, W	432 370
Zhang, W 187, 295, Zhang, X 197, 239, 261,	432 370 291,
Zhang, W	432 370 291,
Zhang, W	432 370 291, 447
Zhang, W	432 370 291, 447 421
Zhang, W	432 370 291, 447 421 313
Zhang, W	432 370 291, 447 421 313 345
Zhang, W	432 370 291, 447 421 313
Zhang, W	432 370 291, 447 421 313 345 290
Zhang, W	<ul> <li>432</li> <li>370</li> <li>291,</li> <li>447</li> <li>421</li> <li>313</li> <li>345</li> <li>290</li> <li>375</li> </ul>
Zhang, W	432 370 291, 447 421 313 345 290 375 257
Zhang, W	<ul> <li>432</li> <li>370</li> <li>291,</li> <li>447</li> <li>421</li> <li>313</li> <li>345</li> <li>290</li> <li>375</li> </ul>
Zhang, W	<ul> <li>432</li> <li>370</li> <li>291,</li> <li>447</li> <li>421</li> <li>313</li> <li>345</li> <li>290</li> <li>375</li> <li>257</li> <li>451</li> </ul>
Zhang, W	432 370 291, 447 421 313 345 290 375 257 451 428
Zhang, W	432 370 291, 447 421 313 345 290 375 257 451 428 217
Zhang, W	432 370 291, 447 421 313 345 290 375 257 451 428 217 380
Zhang, W	432 370 291, 447 421 313 345 290 375 257 451 428 217 380
Zhang, W	<ul> <li>432</li> <li>370</li> <li>291,</li> <li>447</li> <li>421</li> <li>313</li> <li>345</li> <li>290</li> <li>375</li> <li>257</li> <li>451</li> <li>428</li> <li>217</li> <li>380</li> <li>322</li> </ul>
Zhang, W	<ul> <li>432</li> <li>370</li> <li>291,</li> <li>447</li> <li>421</li> <li>313</li> <li>345</li> <li>290</li> <li>375</li> <li>257</li> <li>451</li> <li>428</li> <li>217</li> <li>380</li> <li>322</li> <li>402</li> </ul>
Zhang, W	<ul> <li>432</li> <li>370</li> <li>291,</li> <li>447</li> <li>421</li> <li>313</li> <li>345</li> <li>290</li> <li>375</li> <li>257</li> <li>451</li> <li>428</li> <li>217</li> <li>380</li> <li>322</li> <li>402</li> <li>173</li> </ul>
Zhang, W	<ul> <li>432</li> <li>370</li> <li>291,</li> <li>447</li> <li>421</li> <li>313</li> <li>345</li> <li>290</li> <li>375</li> <li>257</li> <li>451</li> <li>428</li> <li>217</li> <li>380</li> <li>322</li> <li>402</li> <li>173</li> <li>454</li> </ul>
Zhang, W	<ul> <li>432</li> <li>370</li> <li>291,</li> <li>447</li> <li>421</li> <li>313</li> <li>345</li> <li>290</li> <li>375</li> <li>257</li> <li>451</li> <li>428</li> <li>217</li> <li>380</li> <li>322</li> <li>402</li> <li>173</li> <li>454</li> </ul>
Zhang, W	<ul> <li>432</li> <li>370</li> <li>291,</li> <li>447</li> <li>421</li> <li>313</li> <li>345</li> <li>290</li> <li>375</li> <li>257</li> <li>451</li> <li>428</li> <li>217</li> <li>380</li> <li>322</li> <li>402</li> <li>173</li> <li>454</li> <li>265</li> </ul>
Zhang, W	<ul> <li>432</li> <li>370</li> <li>291,</li> <li>447</li> <li>421</li> <li>313</li> <li>345</li> <li>290</li> <li>375</li> <li>257</li> <li>451</li> <li>428</li> <li>217</li> <li>380</li> <li>322</li> <li>402</li> <li>173</li> <li>454</li> <li>265</li> <li>257</li> </ul>
Zhang, W	<ul> <li>432</li> <li>370</li> <li>291,</li> <li>447</li> <li>421</li> <li>313</li> <li>345</li> <li>290</li> <li>375</li> <li>257</li> <li>451</li> <li>428</li> <li>217</li> <li>380</li> <li>322</li> <li>402</li> <li>173</li> <li>454</li> <li>265</li> <li>257</li> <li>451</li> </ul>
Zhang, W	<ul> <li>432</li> <li>370</li> <li>291,</li> <li>447</li> <li>421</li> <li>313</li> <li>345</li> <li>290</li> <li>375</li> <li>257</li> <li>451</li> <li>428</li> <li>217</li> <li>380</li> <li>322</li> <li>402</li> <li>173</li> <li>454</li> <li>265</li> <li>257</li> <li>451</li> <li>350</li> </ul>
Zhang, W	<ul> <li>432</li> <li>370</li> <li>291,</li> <li>447</li> <li>421</li> <li>313</li> <li>345</li> <li>290</li> <li>375</li> <li>257</li> <li>451</li> <li>428</li> <li>217</li> <li>380</li> <li>322</li> <li>402</li> <li>173</li> <li>454</li> <li>265</li> <li>257</li> <li>451</li> <li>350</li> </ul>
Zhang, W	<ul> <li>432</li> <li>370</li> <li>291,</li> <li>447</li> <li>421</li> <li>313</li> <li>345</li> <li>290</li> <li>375</li> <li>257</li> <li>451</li> <li>428</li> <li>217</li> <li>380</li> <li>322</li> <li>402</li> <li>173</li> <li>454</li> <li>265</li> <li>257</li> <li>451</li> <li>350</li> <li>249</li> </ul>
Zhang, W	<ul> <li>432</li> <li>370</li> <li>291,</li> <li>447</li> <li>421</li> <li>313</li> <li>345</li> <li>290</li> <li>375</li> <li>257</li> <li>451</li> <li>428</li> <li>217</li> <li>380</li> <li>322</li> <li>402</li> <li>173</li> <li>454</li> <li>265</li> <li>257</li> <li>451</li> <li>350</li> <li>249</li> <li>324</li> </ul>
Zhang, W         Zhang, W         Zhang, X         197, 239, 261,	<ul> <li>432</li> <li>370</li> <li>291,</li> <li>447</li> <li>421</li> <li>313</li> <li>345</li> <li>290</li> <li>375</li> <li>257</li> <li>451</li> <li>428</li> <li>217</li> <li>380</li> <li>322</li> <li>402</li> <li>173</li> <li>454</li> <li>265</li> <li>257</li> <li>451</li> <li>350</li> <li>249</li> <li>324</li> <li>354</li> </ul>
Zhang, W       187, 295,         Zhang, W       197, 239, 261,	<ul> <li>432</li> <li>370</li> <li>291,</li> <li>447</li> <li>421</li> <li>313</li> <li>345</li> <li>290</li> <li>375</li> <li>257</li> <li>451</li> <li>428</li> <li>217</li> <li>380</li> <li>322</li> <li>402</li> <li>173</li> <li>454</li> <li>265</li> <li>257</li> <li>451</li> <li>350</li> <li>249</li> <li>324</li> <li>354</li> <li>258</li> </ul>
Zhang, W       187, 295,         Zhang, W       197, 239, 261,	<ul> <li>432</li> <li>370</li> <li>291,</li> <li>447</li> <li>421</li> <li>313</li> <li>345</li> <li>290</li> <li>375</li> <li>257</li> <li>451</li> <li>428</li> <li>217</li> <li>380</li> <li>322</li> <li>402</li> <li>173</li> <li>454</li> <li>265</li> <li>257</li> <li>451</li> <li>350</li> <li>249</li> <li>324</li> <li>354</li> <li>258</li> </ul>
Zhang, W       187, 295,         Zhang, X       197, 239, 261,	<ul> <li>432</li> <li>370</li> <li>291,</li> <li>447</li> <li>421</li> <li>313</li> <li>345</li> <li>290</li> <li>375</li> <li>257</li> <li>451</li> <li>428</li> <li>217</li> <li>380</li> <li>322</li> <li>402</li> <li>173</li> <li>454</li> <li>265</li> <li>257</li> <li>451</li> <li>350</li> <li>249</li> <li>324</li> <li>354</li> <li>258</li> <li>268</li> </ul>
Zhang, W       187, 295,         Zhang, X       197, 239, 261,	<ul> <li>432</li> <li>370</li> <li>291,</li> <li>447</li> <li>421</li> <li>313</li> <li>345</li> <li>290</li> <li>375</li> <li>257</li> <li>451</li> <li>428</li> <li>217</li> <li>380</li> <li>322</li> <li>402</li> <li>173</li> <li>454</li> <li>265</li> <li>257</li> <li>451</li> <li>350</li> <li>249</li> <li>324</li> <li>354</li> <li>258</li> <li>268</li> <li>256</li> </ul>
Zhang, W       187, 295,         Zhang, X       197, 239, 261,	<ul> <li>432</li> <li>370</li> <li>291,</li> <li>447</li> <li>421</li> <li>313</li> <li>345</li> <li>290</li> <li>375</li> <li>257</li> <li>451</li> <li>428</li> <li>217</li> <li>380</li> <li>322</li> <li>402</li> <li>173</li> <li>454</li> <li>265</li> <li>257</li> <li>451</li> <li>350</li> <li>249</li> <li>324</li> <li>354</li> <li>258</li> <li>268</li> <li>256</li> <li>256</li> </ul>
Zhang, W       187, 295,         Zhang, X       197, 239, 261,	<ul> <li>432</li> <li>370</li> <li>291,</li> <li>447</li> <li>421</li> <li>313</li> <li>345</li> <li>290</li> <li>375</li> <li>257</li> <li>451</li> <li>428</li> <li>217</li> <li>380</li> <li>322</li> <li>402</li> <li>173</li> <li>454</li> <li>265</li> <li>257</li> <li>451</li> <li>350</li> <li>249</li> <li>324</li> <li>354</li> <li>258</li> <li>268</li> <li>256</li> <li>254</li> </ul>
Zhang, W       187, 295,         Zhang, X       197, 239, 261,	<ul> <li>432</li> <li>370</li> <li>291,</li> <li>447</li> <li>421</li> <li>313</li> <li>345</li> <li>290</li> <li>375</li> <li>257</li> <li>451</li> <li>428</li> <li>217</li> <li>380</li> <li>322</li> <li>402</li> <li>173</li> <li>454</li> <li>265</li> <li>257</li> <li>451</li> <li>350</li> <li>249</li> <li>324</li> <li>354</li> <li>258</li> <li>268</li> <li>256</li> <li>254</li> </ul>
Zhang, W         Zhang, W         Zhang, X         197, 239, 261,	<ul> <li>432</li> <li>370</li> <li>291,</li> <li>447</li> <li>421</li> <li>313</li> <li>345</li> <li>290</li> <li>375</li> <li>257</li> <li>451</li> <li>428</li> <li>217</li> <li>380</li> <li>322</li> <li>402</li> <li>173</li> <li>454</li> <li>265</li> <li>257</li> <li>451</li> <li>350</li> <li>249</li> <li>324</li> <li>354</li> <li>258</li> <li>268</li> <li>256</li> <li>254</li> <li>368</li> </ul>
Zhang, W       187, 295,         Zhang, X       197, 239, 261,	<ul> <li>432</li> <li>370</li> <li>291,</li> <li>447</li> <li>421</li> <li>313</li> <li>345</li> <li>290</li> <li>375</li> <li>257</li> <li>451</li> <li>428</li> <li>217</li> <li>380</li> <li>322</li> <li>402</li> <li>173</li> <li>454</li> <li>265</li> <li>257</li> <li>451</li> <li>350</li> <li>249</li> <li>324</li> <li>354</li> <li>258</li> <li>268</li> <li>256</li> <li>254</li> <li>368</li> <li>245</li> </ul>
Zhang, W       187, 295,         Zhang, X       197, 239, 261,	<ul> <li>432</li> <li>370</li> <li>291,</li> <li>447</li> <li>421</li> <li>313</li> <li>345</li> <li>290</li> <li>375</li> <li>257</li> <li>451</li> <li>428</li> <li>217</li> <li>380</li> <li>322</li> <li>402</li> <li>173</li> <li>454</li> <li>265</li> <li>257</li> <li>451</li> <li>350</li> <li>249</li> <li>324</li> <li>354</li> <li>258</li> <li>268</li> <li>256</li> <li>254</li> <li>368</li> <li>245</li> </ul>

Zhou, B	323
Zhou, F	. 306
Zhou, G	325
Zhou, H	336
Zhou, N	383
Zhou, S	364
Zhou, W	339
Zhou, W	288
Zhou, X	352
Zhou, Y	451
Zhou, Y	449
Zhu, A 217,	376
Zhu, J	322
Zhu, J	422
Zhu, J 294,	364
Zhu, J	312
Zhu, S	. 445
Zhu, T	290
Zhu, W	323
Zhu, X	404
Zhu, Y	196
Zhu, Y T 206, 251, 253,	257,
	306,
	432
Zhuo, L	281
Zi, A	252
Ziegler, D P	437
Zikanov, O	437
Zindel, J W	403
Zinovev, A V	429
Zoeller, T	404
Zong, Z 261,	377
Zribi, A 179, 220, 274, 320,	326
Zunger, A 304,	389